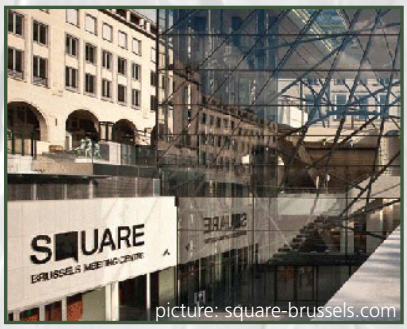
CLAY CONFERENCE

BRUSSELS
March 23-26, 2015

Clays in Natural and Engineered Barriers for Radioactive Waste Confinement





picture: square-brussels.com

6th International conference

SQUARE Brussels Meeting Centre

Background picture: Boom Clay HADES URF, BIB SEM (Desbois et al, 2009)
Responsible editor: Jean-Paul Minon | avenue des Combattants 107 A | 1470 Genappe | Belgium

ONDRAF/NIRAS

ANDRA
French national radioactive waste management agency

COVRA

nagra.

nwmo
NUCLEAR WASTE MANAGEMENT ORGANIZATION
SOCIÉTÉ DE GESTION DES DÉCHETS NUCLÉAIRES

POSIVA

SKB
Svensk Kärnbränslehantering AB

GENERAL TIME TABLE

MONDAY MARCH 23

8.00
Registration

O-00
Opening Ceremony

O-01
Opening Keynotes

13.00
Lunch

14.00 - 15.00
Dedicated poster session

15.00 - 16.20

O-02A Large scale, in situ heater tests - 1	**O-02B** Mass transfer - 1

16.20
Coffee + poster session

16.50 - 18.30

O-03A Large scale, in-situ heater tests - 2	**O-03B** Clay Characterisation - 1 - Nanoscale

18.30
Euridice event

TUESDAY MARCH 24

08.30 | **O-04**
General strategy for clay based disposal systems

10.30
Coffee + poster session

11.00 | **O-05**
Mass transfer - 2

12.45
Lunch

14.00 - 15.00
Dedicated poster session

15.00 - 16.20

O-06A Alterations - 1 - Nitrates, microbiology	**O-06B** Geology

16.20
Coffee + poster session

16.50 - 18.30

O-07A Alterations - 2 - General	**O-07B** Monitoring

19.00
Conference dinner

WEDNESDAY MARCH 25

08:30 | **O-08**
Clay Characterisation - 2 - Multiscale

10.30
Coffee + poster session

11:00 | **O-09**
Bentonite hydro-mechanics

12.45
Lunch

14.00 - 15.00
Dedicated poster session

15.00 - 16.20

O-10A Alterations - 3 - Cement	**O-10B** Gas Transfer

16.20
Coffee + poster session

16.50 - 18.30

O-11A Alterations - 4 - Metal	**O-11B** Clay Rock Mechanical Behavior

18.30
Poster session with beer & cheese evening

THURSDAY MARCH 26

08.30 | **O-12**
Excavation disturbed/damaged zone

10.30
Coffee + poster session

11.00 | **O-13**
Geochemistry

12.40 | **O-14**
Closing ceremony

13.00
Lunch

LEGEND

- Oral session - Copper hall
- Oral session - Silver hall
- Poster session - Grand hall 2
- Conference event

CLAY CONFERENCE

BRUSSELS | March 23-26, 2015

6th International conference | SQUARE Brussels Meeting Centre



TABLE OF CONTENTS

Oral Sessions Programme p. 9

Poster Sessions Programme p. 21

Abstracts Oral Sessions p. 45

- **Session O-00** - Opening Ceremony
- **Session O-01** - Opening Keynotes
- **Session O-02A** - Large scale, in situ heater tests - 1 ..... p. 46
- **Session O-02B** - Mass transfer - 1 ..... p. 54
- **Session O-03A** - Large scale, in situ heater tests - 2 ..... p. 62
- **Session O-03B** - Clay Characterisation - 1 - Nanoscale ..... p. 70
- **Session O-04** - General strategy for clay-based disposal systems ..... p. 80
- **Session O-05** - Mass transfer - 2 ..... p. 92
- **Session O-06A** - Alterations - 1- Nitrates, microbiology ..... p. 101
- **Session O-06B** - Geology ..... p. 108
- **Session O-07A** - Alterations - 2 - General ..... p. 116
- **Session O-07B** - Monitoring ..... p. 126
- **Session O-08** - Clay Characterisation - 2 - Multiscale ..... p. 134
- **Session O-09** - Bentonite hydro-mechanics ..... p. 144
- **Session O-10A** - Alterations - 3 - Cement ..... p. 152
- **Session O-10B** - Gas Transfer ..... p. 160
- **Session O-11A** - Alterations - 4 - Metal ..... p. 168
- **Session O-11B** - Clay Rock Mechanical Behavior ..... p. 178
- **Session O-12** - Excavation disturbed / damaged zone ..... p. 189
- **Session O-13** - Geochemistry ..... p. 201
- **Session O-14** - Closing ceremony

Abstracts poster Sessions p. 211

- **Session P-01 - Alterations** - Metal ..... p. 212
- **Session P-02 - Alterations** - Cement ..... p. 226
- **Session P-03 - Alterations** - General ..... p. 245

• **Session P-04 - Geology and clay characterisation** - 1 ..... p. 274
• **Session P-05 - Geology and clay characterisation** - 2 ..... p. 302
• **Session P-06 - Geochemistry** - 1 ..... p. 328
• **Session P-07 - Geochemistry** - 2 ..... p. 363
• **Session P-08 - Geomechanics** - 1 ..... p. 402
• **Session P-09 - Geomechanics** - 2 ..... p. 463
• **Session P-10 - Geomechanics** -Excavation disturbed / damaged zone ..... p. 512
• **Session P-11 - Large scale in situ heater tests** ..... p. 532
• **Session P-12 - Bentonite hydro-mechanics** ..... p. 554
• **Session P-13 - Gas transfer** ..... p. 591
• **Session P-14 - Mass transfer** - 1 ..... p. 615
• **Session P-15 - Mass transfer** - 2 ..... p. 664
• **Session P-16 - Monitoring** ..... p. 717
• **Session P-17 - General strategy for clay-based disposal systems** ..... p. 739

CLAY CONFERENCE

BRUSSELS | March 23-26, 2015

6th International conference | SQUARE Brussels Meeting Centre



ORAL SESSIONS PROGRAMME

MONDAY MARCH 23, MORNING

Oral Sessions - Copper hall

Session O-00	**Opening Ceremony • J.- P. Minon, P. Lalieux**		
Session O-01	**Opening Keynotes • J.- P. Minon, P. Lalieux**		
	O-01-01 | 35 Years of RD&D on geological disposal in clay rocks: lessons learnt and perspectives	L. Johnson	Nagra, Switzerland
	O-01-02 | Some examples of the importance of clays for the oil industry and opportunities for sharing knowledge	E. Gaucher	Total, France
	O-01-03 | The challenge of managing and sharing big geological datasets	F. Robida	BRGM, France
13.00 - 14.00	**LUNCH**		
14.00 - 15.00	**DEDICATED POSTER SESSION** (P-01, P-04, P-06, P-08, P-11, P-14)		

MONDAY MARCH 23, AFTERNOON
Oral Sessions - Copper hall

Session O-02A	Large scale, in situ heater tests - 1 • M. Van Geet & G. Armand		
15.00 - 15.20	**O-02A-01** | Feasibility of excavation and THM behavior of a full scale disposal cell for nuclear waste in 500 m deep clay formation	J. Morel, F. Bumbieler, N. Conil, G. Armand	Andra, Centre de Meuse/ Haute-Marne, France
15.20 - 15.40	**O-02A-02** | THM analysis of a heating experiment in Callovian-Oxfordian Clay	A. Gens[1], J. Vaunat[1], B. Garitte[3], M. Rostovanyi[1], N. Conil[2], G. Armand[1]	[1]Department of Geotechnical Engineering and Geosciences, Spain / [2]Andra, Centre de Meuse/ Haute-Marne, France / [3]Nagra, Switzerland
15.40 - 16.00	**O-02A-03** | Results to date from the Mock-Up Josef in situ physical model	J. Stastka[1], J. Pacovsky[1], L. Hausmannova[1], R. Vasicek[1], I. Hanusova[2]	[1]Czech Technical University in Prague, Czechia / [2]SÚRAO, Czechia
16.00 - 16.20	**O-02A-04** | 18 Years of heating a full scale EBS at 100°C (FEBEX, Grimsel Test Site) and possible applications at higher temperatures ("hotFEBEX" at > 150°C)	F. Kober[1], I. Gaus[1], S. Birkholzer[1], S. Vomvoris[1]	[1]Nagra, Switzerland / [2]LBNL, USA
16.20 - 16.50	**COFFEE BREAK + POSTER SESSION**		

MONDAY MARCH 23, AFTERNOON
Oral Sessions - Silver hall

Session O-02B	Mass transfer - 1 • K. Koskinen & J.M. Matray		
15.00 - 15.20	**O-02B-01** | Development and validation of a model for smectite clay erosion	I. Neretnieks, L. Moreno, L. Liu	Royal Institute of Technology, Sweden
15.20 - 15.40	**O-02B-02** | Chemical erosion of bentonite buffer – do we observe this in nature?	H.M. Reijonen, N. Marcos	B+Tech Oy, Finland
15.40 - 16.00	**O-02B-03** | Calibrating a 3D numerical model of variably-saturated flow to assess the hydraulic impacts of the future radwaste repository on the Meuse/Haute-Marne site	J. Kerrou[1], G. Deman[1], L. Tacher[2], H. Benabderrahmane[3], P. Perrochet[1]	[1]University of Neuchâtel, Switzerland / [2]EPFL - LMS, Switzerland / [3]Andra, France
16.00 - 16.20	**O-02B-04** | Impact of testing procedure and test analysis methodology on the determination of the hydraulic parameters of low permeability media: In situ hydraulic tests in the Callovo Oxfordian clay	R. Schwarz[1], R. Brauchler[1], M. Pérus[1], J. Croisé[1], R. de la Vaissière[2]	[1]AF Consult, Switzerland / [2]Andra, Centre de Meuse/ Haute-Marne, France
16.20 - 16.50	**COFFEE BREAK + POSTER SESSION**		

MONDAY MARCH 23, AFTERNOON
Oral Sessions - Copper hall

Session O-03A	Large scale, in situ heater tests - 2 • M. Jensen & P. De Preter		
16.50 - 17.30	**O-03A-01** | The Full-Scale Emplacement Experiment – Implementation of a multiple heater experiment at the Mont Terri URL	H.R. Müller, T. Vogt, B. Garitte, S. Köhler, T. Sakaki, H. Weber, T. Vietor	Nagra, Switzerland
17.30 - 17.50	**O-03A-02** | Designing, Commissioning and Monitoring of 40% Scale Bentonite Buffer Test	E. Holt[1], H. Kivikoski[1], P. Marjavaara[2], P. Rantamäki[3]	[1]VTT, Finland / [2]B+Tech Oy, Finland / [3]Posiva Oy, Finland
17.50 - 18.10	**O-03A-03** | The PRACLAY Heater Test at URL HADES: Preparation of the heater switch-on	P. Van Marcke[1], X. Sillen[1], X.L. Li[2], G.J. Chen[2], A. Dizier[2], J. Leysen[2], I. Troullinos[2], J. Verstricht[2], W. Bastiaens[2]	[1]ONDRAF/NIRAS, Belgium / [2]EIG EURIDICE, Belgium
18.10 - 18.30	**O-03A-04** | The PRACLAY Heater Test at URL HADES: First results of the PRACLAY Heater Test	X.L. Li[1], G.J. Chen[1], A. Dizier[1], J. Leysen[1], I. Troullinos[1], J. Verstricht[1], W. Bastiaens[1], P. Van Marcke[2], X. Sillen[2]	[1]EIG EURIDICE, Belgium / [2]ONDRAF/NIRAS, Belgium
18.30 - 21.00	**EURIDICE EVENT**		

MONDAY MARCH 23, AFTERNOON
Oral Sessions - Silver hall

Session O-03B	Clay Characterisation - 1 - Nanoscale • M. Cathelineau & M. De Craen		
16.50 - 17.10	**O-03B-01** | Size and structure – The key to different ratios of edge to face charge for smectite	L. Delavernhe[1,2], A. Steudel[1,2], G.K. Darbha[3], T. Schäfer[3,4], R. Schuhmann[1,2], C. Wöll[1], H. Geckeis[3], K. Emmerich[1,2]	[1]CMM, Germany / [2]IFG, Germany / [3] INE, KIT, Germany / [4]Institute of Geological Sciences, Germany
17.10 - 17.30	**O-03B-02** | Bentonite illitization and its effect on swelling stress: a coupled THMC modeling study on high-temperature effects	L. Zheng, J. Rutqvist, J.T. Birkholzer	LBNL, USA
17.30 - 17.50	**O-03B-03** | Structural defects in layered structures: Their determination and their impact on reactivity	S. Grangeon[1], F. Claret[1], C. Tournassat[1], Y. Linard[2], B. Lanson[3]	[1]BRGM, France / [2]Andra, Centre de Meuse/Haute-Marne, France / [3]University of Grenoble, France
17.50 - 18.10	**O-03B-04** | Thermodynamic properties of hydration of smectites considering the energetic contribution of capillary water	P. Vieillard[1], P. Blanc[2], H. Gailhanou[2], A. Lassin[2], R. Denoyel[3], E. Bloch[3], S. Gaboreau[2], C.I. Fialips[4], B. Madé[5], E. Giffaut[5]	[1]Université de Poitiers / [2]BRGM, France / [3]Aix Marseille Université, France / [4]TOTAL - CSTJF, France / [5]Andra, France
18.10 - 18.30	**O-03B-05** | Ferrous iron uptake on montmorillonites	D. Soltermann[1,2], M. Marques Fernandes[1], R. Dähn[1], C. Gorski[3], B. Baeyens[1]	[1]PSI, Switzerland / [2]Institute of Biogeochemistry and Pollutant Dynamics, Switzerland / [3]Department of Civil and Environmental Engineering, USA
18.30 - 21.00	**EURIDICE EVENT**		

TUESDAY MARCH 24, MORNING

Oral Sessions - Copper hall

Session O-04	**General strategy for clay-based disposal systems • A. Gautschi & T. Jalonen**		
08.30 - 08.50	**O-04-01** | Nagra's RD&D programme on Opalinus Clay - Some recent findings and outlook	I. Gaus, L. Johnson, P. Marschall, T. Vietor, P. Zuidema	Nagra, Switzerland
08.50 - 09.10	**O-04-02** | Geosphere characterization for a DGR in the argillaceous limestone of the Ordovician Cobourg Formation in the Michigan Basin: an integration of field, lab and modelling methods	J.F. Sykes[1], M.R. Jensen[2], S.D. Normani[1], Y. Yin[1], R. Beauheim[3], T. Al[4], I.D. Clark[5]	[1]University of Waterloo, Canada / [2]NWMO, Canada / [3]Intera GeoScience and Engineering Solutions, USA / [4]University of New Brunswick, Canada / [5]University of Ottawa, Canada
09.10 - 09.30	**O-04-03** | Sorption values derived for argillaceous rocks in sorption data bases for safety analysis compared with measured values	B. Baeyens, M. Marques Fernandes, M. Bradbury	PSI, Switzerland
09.30 - 09.50	**O-04-04** | DOPAS Full-Scale Tests – Approach to Compliance Assessment	S. Doudou[1], M.J. White[1], M. Johnson[2], J-M. Bosgiraud[3], P. Grahm[4]	[1]Galson Sciences Ltd, UK / [2]NDA, UK / [3]Andra, France / [4]SKB, Sweden
09.50 - 10.10	**O-04-05** | Approaches to Evaluate and Underpin the Technical Feasibility of the Belgian Disposal Concept	S. Doudou[1], E.J. Harvey[1], P.J. Richardson[1], S.M. Wickham[1], P. Van Marcke[2]	[1]Galson Sciences Ltd, UK / [2]ONDRAF/NIRAS, Belgium
10.10 - 10.30	**O-04-06** | Results and experiences from full scale backfill block manufacturing and installation	E. Jonsson, P. Eriksson	SKB, Sweden
10.30 - 11.00	**COFFEE BREAK + POSTER SESSION**		
Session O-05	**Mass transfer - 2 • E. Gaucher & C. Bruggeman**		
11.00 - 11.20	**O-05-01** | State of the art of the solute diffusion characterisation in the Callovo-Oxfordian formation	J-C. Robinet, D. Coelho, E. Giffaut	Andra, France
11.20 - 11.40	**O-05-02** | Can a macroscopic modeling approach properly describe transport in porous media during mineral precipitation induced clogging?	A. Chagneau[1,2,3], F. Claret[3], F. Enzmann[4], M. Wolf[4], B. Made[5], T. Schäfer[1,2]	[1]INE, KIT, Germany / [2]Freie Universität Berlin, Germany / [3]BRGM, France / [4]Johannes Gutenberg University, Germany / [5]Andra, France
11.40 - 12.00	**O-05-03** | Microscopic modelling of dissolution and surface precipitation of sulfates in granular media: effect on the permeability and effective diffusivity	N.I. Prasianakis[1], T. Gimmi[1,2], G. Kosakowski[1], S.V. Churakov[1]	[1]PSI, Switzerland / [2]University of Bern, Switzerland
12.00 - 12.20	**O-05-04** | Characterization of transport and water retention properties of damaged Callovo-Oxfordian claystone	S. M'Jahad[1], C.A. Davy[2], F. Skoczylas[2], J. Talandier[3]	[1]EDF, France / [2]Ecole Centrale de Lille, France / [3]Andra, France
12.20 - 12.40	**O-05-05** | Combining high resolution two-phase with simplified single-phase simulations in order to significantly reduce computation time for PA/SA simulations for a deep geological repository for radioactive waste	P. Schädle[1], T. Kaempfer[1], G. Pepin[2], J. Wendling[2], J. Brommundt[1]	[1]AF-Consult, Switzerland / [2]Andra, France
12.45 - 13.45	**LUNCH**		
13.45 - 15.00	**DEDICATED POSTER SESSION** (P-02, P-05, P-07, P-09, P-15, P-16)		

TUESDAY MARCH 24, AFTERNOON

Oral Sessions - Copper hall

Session O-06A	Alterations - 1 - Nitrates, microbiology • P. Landais & B. Kalinowski		
15.00 - 15.20	**O-06A-01** | Abiotic and biotic nitrate and nitrite reduction by redox-active Boom Clay components	N. Bleyen[1], M. Vasile[1], C. Bruggeman[1], D. Durce[1], H. Moors[2], E. Valcke[1]	[1]W&D, SCK•CEN, Belgium / [2]MIC, SCK•CEN, Belgium
15.20 - 15.40	**O-06A-02** | Effect of a $NaNO_3$ plume on the diffusion behaviour of HTO, I^-, and HCO_3^-, and on the physico-chemical properties of Boom Clay	E. Valcke[1], M. Aertsens[1], N. Bleyen[1], C. Bruggeman[1], P. De Cannière[2], M. Honty[1], N. Maes[1], A. Mariën[1], H. Moors[3], M. Van Geet[4], M. Van Gompel[1], L. Wang[1]	[1]SCK•CEN, Belgium / [2]FANC/AFCN, Belgium / [3]SCK•CEN, Belgium / [4]ONDRAF/NIRAS, Belgium
15.40 - 16.00	**O-06A-03** | The Bitumen-Nitrate-Clay Interaction Experiment at the Mont Terri Rock Laboratory, Switzerland: Response of Microbial Communities to Additions of Nitrate and Acetate	H. Moors[1], A. Cherkouk[2], M. Mysara[1], N. Bleyen[1], S. Smets[1], B. Schwyn[3], A. Albrecht[4], C. Wittebroodt[5], J. Small[6], P. De Cannière[7], S. Stroes-Gascoyne[8], E. Valcke[1], N. Leys[1]	[1]SCK•CEN, Belgium / [2]HZDR, Germany / [3]Nagra, Switzerland / [4]Andra, France / [5]IRSN, France / [6]National Nuclear Laboratory, UK / [7]FANC/AFCN, Belgium / [8]AECL, Canada
16.00 - 16.20	**O-06A-04** | Modeling of iron/clay interactions coupled to bacteria activity in percolation cells at 60 °C	C. Chautard[1,2], L. De Windt[2], F. Marsal[1], D. Pellegrini[1]	[1]IRSN, France / [2]MINES ParisTech, France
16.20 - 16.50	**COFFEE BREAK + POSTER SESSION**		

TUESDAY MARCH 24, AFTERNOON

Oral Sessions - Silver hall

Session O-06B	Geology • M. Sintubin & M. Mazurek		
15.00 - 15.20	**O-06B-01** | Paleogene marine clays in the southern North Sea Basin (Netherlands): towards a new lithostratigraphic framework	W. Westerhoff, G-J. Vis	TNO, The Netherlands
15.20 - 15.40	**O-06B-02** | 3D stress field sensitivity analysis on the scale of geological siting regions in Northern Switzerland with focus on Opalinus Clay	O. Heidbach[1], T. Hergert[2], K. Reiter1, S.B. Giger[3], P. Marschall[3]	[1]GFZ, Germany / [2]KIT, Germany / [3]Nagra, Switzerland
15.40 - 16.00	**O-06B-03** | Increased confidence in seismic amplitudes by consistent uncertainty quantification	L. Sandjivy[1], A. Shtuka[1], J.L. Mari[2], B. Yven[3], M. Hayet[3]	[1]Seisquare, France / [2]IFP Énergies nouvelles, France / [3]Andra, France
16.00 - 16.20	**O-06B-04** | The origin of strength of Opalinus Clay - phenomenological evidence and conceptual considerations	P. Marschall[1], S. Giger[1], A. Ferrari[2], V. Favero[2], L. Laloui[2], L. Keller[3]	[1]Nagra, Switzerland / [2]École Polytechnique Fédérale de Lausanne, Switzerland / [3]ZHAW/ICP, Switzerland
16.20 - 16.50	**COFFEE BREAK + POSTER SESSION**		

TUESDAY MARCH 24, AFTERNOON

Oral Sessions - Copper hall

Session O-07A	Alterations - 2 - General • J. Bruno & I. Gaus		
16.50 - 17.10	**O-07A-01** | Kinetic experiments in order to determine the rate of oxygen consumption by the Callovian-Oxfordian argillaceous rock	J. Tremosa[1], J. Hadi[1,2], F. Claret[1], C. Tournassat[1], A. Vinsot[3]	[1]BRGM, France / [2]RWI,Switzerland / [3]Andra, Centre de Meuse/Haute-Marne, France
17.10 - 17.30	**O-07A-02** | THC Modelling and Sensitivity Analysis of Bentonite Alteration in a KBS-3 Buffer	S. Benbow[1], J. Wilson[2], R. Metcalfe[1], D. Savage[3], J. Lehikoinen[4]	[1]Quintessa Ltd., The Hub, UK / [2]Quintessa Ltd, UK / [3]Savage Earth Associates Ltd, UK / [4]STUK, Finland
17.30 - 17.50	**O-07A-03** | Evolution of safety-relevant properties of bentonite in crystalline and clay host rock repositories for spent fuel and high level waste	O.X. Leupin[1], P. Sellin[2], L.H. Johnson[1]	[1]Nagra, Switzerland / [2]SKB, Sweden
17.50 - 18.10	**O-07A-04** | A mechanism for bentonite buffer erosion in a fracture with a naturally varying aperture	C. Reid, R. Lunn, G. El Mountassir, A. Tarantino	University of Strathclyde, UK
18.10 - 18.30	**O-07A-05** | Breakdown of the modified Gouy-Chapman model for clay surfaces in equilibrium with a $CaCl^3$ electrolyte: a molecular dynamic study	C. Tournassat[1], I.C. Bourg[2], C.I. Steefel[2]	[1]BRGM, France / [2]LBNL, USA
19.00	**CONFERENCE DINNER**		

TUESDAY MARCH 24, AFTERNOON

Oral Sessions - Silver hall

Session O-07B	Monitoring • E. Verhoef & A. Bergmans		
16.50 - 17.10	**O-07B-01** | Fiber optic sensing methods for monitoring temperature and strain implemented in the FE Experiment	T. Vogt, H.R. Müller, B. Frieg, T. Vietor	Nagra, Switzerland
17.10 - 17.30	**O-07B-02** | Transparent deposition hole mock-up test in 1:3 scale	X. Pintado[1], J. Autio[1], K. Koskinen[2]	[1]B+Tech Oy, Finland / [2]Posiva Oy, Finland
17.30 - 17.50	**O-07B-03** | Long-term strain monitoring in a deep tunnel concrete lining	J. Verstricht[1], A. Dizier[1], X.L. Li[1], A. Van Cotthem[2]	[1]EIG EURIDICE, Belgium / [2]Tractebel Engineering, Belgium
17.50 - 18.10	**O-07B-04** | Monitoring natural and engineered clay in geological repository with optical fiber sensors – lessons learnt from large scale experiments	S. Delepine-Lesoille[1], J. Bertrand[1], G. Pilorget[1], R. Farhoud[1], S. Buschaert[1], T. Vogt[2], J. Verstricht[3]	[1]Andra, France / [2]Nagra, Switzerland / [3]EIG EURIDICE, Belgium
18.10 - 18.30	**O-07B-05** | One-year monitoring of desiccation cracks in Tournemire experimental station using Digital Image Correlation	S. Hedan[1], V. Valle[2], J. Cabrera[3], P. Cosenza[1]	[1]Université de Poitiers, CNRS UMR, France / [2]Université de Poitiers, CNRS UPR, France / [3]DEI-SARG, France
19.00	**CONFERENCE DINNER**		

WEDNESDAY MARCH 25, MORNING

Oral Sessions - Copper hall

Session O-08	**Clay Characterisation - 2 - Multiscale • R. Dohrmann & W. Westerhoff**		
08.30 - 08.50	**O-08-01** | Standardized methodology for quantitative determination of the mineralogy and clay mineralogy in clays and shales	R. Adriaens[1], E. Zeelmaekers[1,2], H. Van Baelen[3], N. Vandenberghe[1], J. Elsen[1]	[1]KU Leuven, Belgium / [2]Shell International Exploration and Production, The Netherlands / [3]ONDRAF/NIRAS, Belgium
08.50 - 09.10	**O-08-02** | The effects of space restriction on microbial activity in final repository clay barrier systems	A. Bengtsson[1], A. Blom[1], K. Pedersen[1,2]	[1]Micans, Sweden / [2]Chalmers University of Technology, Sweden
09.10 - 09.30	**O-08-03** | Pore structure of Boda Claystone Formation, W-Mecsek, Hungary	P. Ács, F. Fedor	GEOCHEM Ltd, Hungary
09.30 - 09.50	**O-08-04** | Investigation of microstructures in naturally and experimentally deformed reference clays from underground research laboratories by using innovative methods in scanning electron microscopy	G. Desbois[1], S. Hemes[1], B. Laurich[1], M. Houben[2], J. Klaver[1], N. Höhne[3], J.L. Urai[1], G. Viggiani[4], P. Bésuelle[4]	[1]RWTH Aachen University, Germany / [2]Utrecht University, The Netherlands / [3]RWTH Aachen University, Germany / [4]Université J. Fourrier, France
09.50 - 10.10	**O-08-05** | Microstructures in tectonically faulted Opalinus Clay: A multi-scale investigation (outcrop mapping, thin sections, BIB-SEM, FIB-TEM)	B. Laurich[1], J.L. Urai[1], G. Desbois[1], C. Vollmer[2], C. Nussbaum[3]	[1]RWTH Aachen University, Germany / [2]University of Münster, Germany / [3]Swisstopo, Switzerland
10.10 - 10.30	**O-08-06** | Hyperspectral imaging for the characterization of clays on large spatial scales	P. Brunner[1], P. Renard[1], J.K. Becker[2]	[1]Univ. Neuchâtel, Switzerland / [2]Nagra, Switzerland
10.30 - 11.00	**COFFEE BREAK + POSTER SESSION**		
Session O-09	**Bentonite hydro-mechanics • P. Sellin & A. Gens**		
11.00 - 11.20	**O-09-01** | DECOVALEX-2015: A THM modelling benchmark based on the performance of heated and hydrated granulated bentonite mixture column tests	B. Garitte[1], C. Lee[2], K. Maekawa[3], C. Manepally[4], P. Pan[5], J. Rutqvist[6], B. Graupner[7], X.R. Wang, H. Shao[8], S. Nguyen[9]	[1]Nagra, Switzerland / [2]KAERI, Republic of Korea / [3]JAEA, Japan / [4]CNWRA, USA / [5]CAS, China / [6]LBNL, USA / [7]ENSI, Switzerland / [8]BGR, Germany / [9]CNSC, Canada
11.20 - 11.40	**O-09-02** | Deformation of compacted bentonite due to highly suctions on various temperatures	T. Nishimura	Ashitech, Japan
11.40 - 12.00	**O-09-03** | Additional repulsive pressures in clays of various mineralogy	W. Baille, T. Schanz	Ruhr-Universität Bochum, Germany
12.00 - 12.20	**O-09-04** | Hydromechanical behaviour of bentonite under in situ conditions	A.C. Dieudonne[1,2], J. Talandier[3], R. Charlier[1]	[1]University of Liege, Belgium / [2]F.R.I.A., Belgium / [3]Andra, France
12.20 - 12.40	**O-09-05** | The role of gas and liquid intrinsic permeability evolutions on resaturation and geomechanical behaviour of heated bentonite	J. Rutqvist, V. Vilarrasa, J. Birkholzer	LBNL, USA
12.45 - 13.45	**LUNCH**		
13.45 - 15.00	**DEDICATED POSTER SESSION** (P-03, P-10, P-12, P-13, P-17)		

WEDNESDAY MARCH 25, AFTERNOON

Oral Sessions - Copper hall

Session O-10A	Alterations - 3 - Cement • E. Gaucher & N. Maes		
15.00 - 15.20	**O-10A-01** | Neutron imaging study of heavy water transport across a cement-clay interface	A. Shafizadeh[1], T. Gimmi[1,3], L. Van Loon[1], S.V. Churakov[1], A.P. Kaestner[2], E. Lehmann[2], U. Maeder[3]	[1]PSI, Switzerland / [2]Neutron Imaging and Activation Group, PSI, Switzerland / [3]University of Bern, Switzerland
15.20 - 15.40	**O-10A-02** | Nature of C-(A)-S-H phases formed from the interaction between concrete and bentonite	R. Fernández, A.I. Ruiz, J. Cuevas	Autonomous University of Madrid, Spain
15.40 - 16.00	**O-10A-03** | Concrete-clay interaction: give-and-take without a loser?	A. Jenni[1], U. Mäder[1], E. Wieland[2], C. Lerouge[3], S. Gaboreau[3], M. Vespa[4], V. Cloet[5]	[1]University of Bern, Switzerland / [2]PSI, Switzerland / [3]BRGM, France / [4]Institute for Nuclear Waste Disposal, Germany / [5]Nagra, Switzerland
16.00 - 16.20	**O-10A-04** | The challenge of analyzing micro-diffraction patterns: From argillaceous rock formations to cement-clay interfaces	R. Dähn[1], J. Osán[2], P. Pattison[3], E. Wieland[1]	[1]PSI, Switzerland / [2]Hungarian Academy of Sciences, Hungary / [3]École Polytechnique Fédérale de Lausanne, Switzerland
16.20 - 16.50	**COFFEE BREAK + POSTER SESSION**		

WEDNESDAY MARCH 25, AFTERNOON

Oral Sessions - Silver hall

Session O-10B	Gas transfer • S. Norris & P. Marschall		
15.00 - 15.20	**O-10B-01** | Physical Modelling of the water-and-gas flow through an Excavation Damaged Zone in the frame of a single porosity model	L-V. Bénet[1], E. Blaud[1], J. Wendling[2]	[1]SOCOTEC SA, France / [2]Andra, France
15.20 - 15.40	**O-10B-02** | Stress coupling in Callovo-Oxfordian claystone during gas and water flow	J.F. Harrington[1], R.J. Cuss[1], D.J. Noy[1], C.C. Graham[1], A.E. Milodowski[1], M. Hall[2], J. Talandier[3]	[1]BGS, UK / [2]University of Nottingham, UK / [3]Andra, France
15.40 - 16.00	**O-10B-03** | Measuring the diffusion coefficient of hydrogen in Boom Clay	E. Jacops[1,2,3], K. Wouters[1], A. Grade[1], N. Maes[1], J. Govaerts[1], E. Weetjens[1]	[1]SCK•CEN, Belgium / [2]KU Leuven, Belgium / [3]RWTH Aachen University, Germany
16.00 - 16.20	**O-10B-04** | Volume change behaviour of Boom Clay during gas injection and dissipation experiments	L. González-Blanco[1], E. Romero[1], X. Li[2], X. Sillen[3]	[1]Universitat Politècnica de Catalunya, Spain / [2]EIG EURIDICE, Belgium / [3]ONDRAF/NIRAS, Belgium
16.20 - 16.50	**COFFEE BREAK + POSTER SESSION**		

WEDNESDAY MARCH 25, AFTERNOON

Oral Sessions - Copper hall

Session O-11A	Alterations - 4 - Metal • M. Cathelineau & J. Wilson		
16.50 - 17.10	**O-11A-01** | Saponite formation in the ABM2 iron-bentonite field experiment at Äspö hard rock laboratory, Sweden	D. Svensson	SKB, Sweden
17.10 - 17.30	**O-11A-02** | Molecular-level insights on Titanium-clay interactions	D. Grolimund[1], P. Wersin[2], L. Kiviranta[3], J. Brendlé[4], M. Snellman[5]	[1]PSI, Switzerland / [2]University of Bern, Switzerland / [3]B+ Tech Oy, Finland / [4]Université de Haute-Alsace, France / [5]Saanio & Riekkola Oy, Finland
17.30 - 17.50	**O-11A-03** | Kinetic modeling of interactions between iron, clay and water: comparison with data from batch experiments	V.V. Ngo[1], A. Clément[1], N. Michau[2], B. Fritz[1]	[1]Université de Strasbourg, CNRS, France / [2]Andra, France
17.50 - 18.10	**O-11A-04** | Gaining insight into corrosion rate and secondary mineral paragenesis from numerical simulations of integrated ironclaystone experiments	O. Bildstein[1], J.E. Lartigue[1], M.L. Schlegel[2], C. Bataillon[3], B. Cochepin[4], I. Munier[4], N. Michau[4]	[1]CEA, DEN, DTN/SMTA/LMTE, France / [2]CEA, DEN, DPC/SEARS/LISL, France / [3]CEA, DEN, DPC/SCCME/LECA, France / [4]Andra, France
18.10 - 18.30	**O-11A-05** | Action of a clay suspension on an iron(0) surface under anoxic conditions: characterization of the neoformed 7 Å iron-rich phyllosilicates	P. Le Pape[1,2], C. Rivard[1,2], M. Pelletier[1,2], I. Bihannic[1,2], R. Gley[1,2], S. Mathieu[3], L. Salsi[3], S. Migot[4], O. Barres[5], C. Carteret[6], F. Villiéras[1,2], N. Michau[7]	[1]Université de Lorraine, LIEC, France / [2]CNRS, LIEC, France / [3]Université de Lorraine, SCMEM, France / [4]Université de Lorraine - CNRS, France / [5]Université de Lorraine - CNRS, GeoRessources, France / [6]CNRS, LCPME, France / [7]Andra, France
19.00	**POSTER SESSION WITH BEER & CHEESE EVENING**		

WEDNESDAY MARCH 25, AFTERNOON

Oral Sessions - Silver hall

Session O-11B	Clay rock mechanical behavior • R. Charlier & P. Delage		
16.50 - 17.10	**O-11B-01** | On the intrinsic properties of shales	V. Favero[1], A. Ferrari[1], P. Marschall[2], L. Laloui[1]	[1]École Polytechnique Fédérale de Lausanne, Switzerland / [2]Nagra, Switzerland
17.10 - 17.30	**O-11B-02** | A micromechanical analysis of clayey rock based on Fast Fourier Transforms method	M. Li, WQ. Shen, JF. Shao	University of Lille, France
17.30 - 17.50	**O-11B-03** | Micro-macro-mechanical study of a clay rock on drying-wetting path	X. Wei[1,6], M. Duc[2], T. Reuschlé[3], H. Souli[4], S. Taibi[5], J-M. Fleureau[1], M. Hattab[6]	[1]Ecole Centrale Paris, France / [2]Université Paris-Est, France / [3]Ecole et Observatoire des Sciences de la Terre, France / [4]Université de Lyon, France / [5]Université du Havre, France / [6]Université de Lorraine, France
17.50 - 18.10	**O-11B-04** | A unified thermo-plastic/viscoplastic constitutive model for geomaterials	S. Raude[1,2], F. Laigle[1], R. Giot[2], R. Fernandes[3]	[1]EDF, CIH, France / [2]Université de Lorraine, France / [3]LaMSID, UMR EDF-CNRS-CEA, France
18.10 - 18.30	**O-11B-05** | Anisotropic swelling behaviour of natural Boom Clay	L-Q. Dao[1], A-M. Tang[1], Y-J. Cui[1], J-M. Pereira[1], X-L. Li[2], X. Sillen[3]	[1]Université Paris-Est, Laboratoire Navier (UMR 8205), France / [2]EIG EURIDICE, Belgium / [3]ONDRAF/NIRAS, Belgium
19.00	**POSTER SESSION WITH BEER & CHEESE EVENING**		

THURSDAY MARCH 26, MORNING

Oral Sessions - Copper hall

Session O-12	**Excavation disturbed / damaged zone • F. Plas & X. Li**		
08.30 - 08.50	**O-12-01** | 10 years of excavation works at the Meuse Haute Marne URL: what have we learn?	A. Noiret, G. Armand, R. de La Vaissière, C. Righini, S. Carraretto, J. Zghondi	Andra, Centre de Meuse/ Haute-Marne, France
08.50 - 09.10	**O-12-02** | A pragmatic methodology to abstract the EDZ around tunnels of a geological radioactive waste repository - Application to the HG-A experiment in Mont Terri	A. Alcolea[1], U. Kuhlmann[1], P. Marschall[2], A. Lisjak[3], G. Grasselli[3], O. Mahabadi[3], R. de La Vaissière[4], H. Leung[5], H. Shao[6]	[1]TK Consult AG, Switzerland / [2]Nagra, Switzerland / [3]Geomechanica Inc., Canada / [4]Andra, Centre de Meuse/ Haute-Marne, France / [5]NWMO, Canada / [6]Federal Institute for Geosciences and Natural Resources, Germany
09.10 - 09.30	**O-12-03** | A numerical analysis of initial damaged zone around underground gallery with a discrete approach	C. Yao[1], A. Poutrel[2], JF. Shao[1]	[1]University of Lille, France / [2]Andra, France
09.30 - 09.50	**O-12-04** | Modelling the excavation damaged zone in Callovo-Oxfordian claystone using shear strain localisation	B. Pardoen[1,2], S. Levasseur[1], F. Collin[1], D. Seyedi[3]	[1]University of Liège, Belgium / [2]F.R.I.A., Belgium / [3]Andra, France
09.50 - 10.10	**O-12-05** | An experimental study of the flow of fluids along faults/fractures and the potential for fault reactivation	R.J. Cuss, J.F. Harrington, A.C. Wiseall, C.C. Graham	BGS, UK
10.10 - 10.30	**O-12-06** | A double scale model for hydro-mechanical coupling in clay rocks; simulation of damage and strain localisation around an excavated gallery	B. van den Eijnden[1,2,3], P. Bésuelle[2,3], F. Collin[4], R. Chambon[2,3], J. Desrues[2,3]	[1]Andra, France / [2]Univ. Grenoble Alpes, France / [3]CNRS, France / [4]University of Liege, Belgium
10.30 - 11.00	**COFFEE BREAK + POSTER SESSION**		
Session O-13	**Geochemistry • J. Bruno & E. Giffaut**		
11.00 - 11.20	**O-13-01** | Conceptual geochemical model analysis of the long-term evolution of the Dutch Boom Clay under conditions with and without disposal of radioactive waste	J. Griffioen[1,2,3], S. Janssen[2], M. Koenen[1], H. Meeussen[4]	[1]TNO Geological Survey, The Netherlands / [2]Deltares, The Netherlands / [3]Faculty of Geosciences, Utrecht University, The Netherlands / [4]NRG, The Netherlands
11.20 - 11.40	**O-13-02** | Characterizing clay pore water composition of Ypresian clays from Doel and Kallo sites, Belgium	A.M. Fernández[1], S. Wilhelm[2], L. Wouters[3], H. Van Baelen[3]	[1]CIEMAT, Spain / [2]AF-Consult, Switzerland / [3]ONDRAF/NIRAS, Belgium
11.40 - 12.00	**O-13-03** | Pitfalls in using the hexammine cobalt method for cation exchange capacity measurements on clay minerals and clay-rocks: redox interferences between the cationic dye and the sample	J. Hadi[1,2], C. Tournassat[1], P. Wersin[2], C. Lerouge[1]	[1]BRGM, France / [2]RWI, Switzerland
12.00 - 12.20	**O-13-04** | A new method for extraction and characterization of porewater chemistry in low-permeability sedimentary rocks	M. Celejewski[1], T. Al[1], I. Clark[2]	[1]University of New Brunswick, Canada / [2]University of Ottawa, Canada
12.20 - 12.40	**O-13-05** | Competitive sorption and sequential reduction of Cr, As and Sb in argillaceous rock suspension under oscillating redox conditions	E. Markelova[1,2], C.T. Parsons[2], R-M. Couture[2,3], D. Tisserand[1], B. Madé[4], P. Van Cappellen[2], L. Charlet[1]	[1]University of Grenoble, France / [2]University of Waterloo, Canada / [3]NIVA, Norway / [4]Andra, France
12.40 - 13.00	**CLOSING CEREMONY • P. Lalieux & A. Gautschi**		
13.00	**LUNCH**		

CLAY CONFERENCE

BRUSSELS | March 23-26, 2015

6th International conference | SQUARE Brussels Meeting Centre



POSTER SESSIONS PROGRAMME

MONDAY MARCH 23TH TO THURSDAY MARCH 26ND

Poster Sessions - Grand hall 2

DEDICATED POSTER SESSIONS - 14.00 - 15.00 - Grand hall 2	
MONDAY MARCH 23th	
P-01	Alterations - Metal
P-04	Geology and clay characterisation - 1
P-06	Geochemistry - 1
P-08	Geomechanics - 1
P-11	Large scale in situ heater tests
P-14	Mass transfer - 1
TUESDAY MARCH 24th	
P-02	Alterations - Cement
P-05	Geology and clay characterisation - 2
P-07	Geochemistry - 2
P-09	Geomechanics - 2
P-15	Mass transfer - 2
P-16	Monitoring
WEDNESDAY MARCH 25th	
P-03	Alterations - General
P-10	Geomechanics - Excavation disturbed / damaged zone
P-12	Bentonite hydro-mechanics
P-13	Gas transfer
P-17	General strategy for clay-based disposal systems

MONDAY MARCH 23TH TO THURSDAY MARCH 26ND

Poster Sessions - Grand hall 2

ALTERATIONS

ALTERATIONS - METAL

P-01-01	Thermodynamic and fully-coupled reactive transport simulations of a steel-bentonite interface	J. Wilson[1], S. Benbow[2], H. Sasamoto[3], D. Savage[4], C. Watson[2]	[1]Quintessa Ltd, UK / [2]Quintessa Ltd, The Hub, UK / [3]JAEA, Japan / [4]Savage Earth Associates Ltd, UK
P-01-02	Instantaneous corrosion rate measurements on carbon steel in Opalinus clay at 90 °C – Bilan after 6 years	S. Necib[1], C. Bataillon[2], S. Daumas[3], D. Crusset[4], S. Dewonck[1]	[1]Andra, Centre de Meuse/ Haute Marne, France / [2]CEA, France / [3]BRGM, France / [4]Andra, France
P-01-03	Modelling in situ experiments of water-iron-claystone interactions and up-scaling to an HLW cell	J. Wilson[1], S. Benbow[2], D. Savage[3], N. Michau[4], S. Necib[4]	[1]Quintessa Ltd, UK / [2]Quintessa Ltd, The Hub, UK / [3]Savage Earth Associates Ltd, UK / [4]Andra, France
P-01-04	How CEC determination can provide information about reactivity between iron powder and clay minerals?	C. Rivard[1,2], P. Le Pape[1,2], A. Razafitianamaharavo[1,2], M. Pelletier[1,2], R. Gley[1,2], M. Mallet[3,4], F. Villiéras[1,2], N. Michau[5]	[1]Université de Lorraine, LIEC, UMR 7360, France / [2]CNRS, LIEC, UMR 7360, France / [3]Université de Lorraine, LCPME, UMR 7564, France / [4]CNRS, LCPME, UMR 7564, France / [5]Andra, France
P-01-05	Carbonates reactivity in temperature and interactions with Fe-minerals	M. Debure[1], S. Grangeon[1], C. Lerouge[1], H. Gailhanou[1], B. Madé[2], C. Tournassat[1]	[1]BRGM, France / [2]Andra, France
P-01-06	Interactions between Fe(0) and Illite-smectite mixed-layer minerals at 90 °C under anoxic conditions - investigation of iron speciation and reaction mechanisms	P. Le Pape[1,2], C. Rivard[1,2], M. Pelletier[1,2], I. Bihannic[1,2], S. Migot[3], J. Ghanbaja[3], M. Abdelmoula[4], F. Villiéras[1,2], N. Michau[5]	[1]Université de Lorraine, LIEC, UMR 7360, France / [2]CNRS, LIEC, UMR 7360, France / [3]Université de Lorraine - CNRS, IJL parc de Saurupt, CC-MEM, France / [4]CNRS, LCPME, UMR 7564, France / [5]Andra, France
P-01-07	Iron/clay/glass interaction in compacted clay at 50°C	S. Necib[1], Y. Linard[1], C. Martin[2], E. Burger[3], P. Jollivet[4], S. Dewonck[1]	[1]Andra, Centre de Meuse/ Haute-Marne, France / [2]Andra, France / [3]EDF les Renardières, France / [4]CEA, DEN/DTCD/SECM, France

ALTERATIONS - CEMENT

P-02-01	Effects of activity of OH^- and temperature on the dissolution rate of compacted montmorillonite under highly alkaline conditions	T. Sawaguchi, M. Tsukada, T. Yamaguchi, M. Mukai	JAEA, Japan
P-02-02	Laboratory experiments on alteration of bentonite-cement interfaces and accompanying changes in diffusivity of solute	T. Yamaguchi, T. Sawaguchi, M. Tsukada, T. Tanaka	JAEA, Japan

P-02-03	Stability of bentonite under high-pH conditions: An experimental approach including modeling	F. Dolder[1], U. Mäder[1], A. Jenni[1], B. Münch[2]	[1]RWI, University of Bern, Geological Sciences, Switzerland / [2]EMPA, Swiss Federal Institute for Materials Testing and Research, Switzerland
P-02-04	Electrolyte-mediated dissolution of montmorillonite in alkaline environments	R. Eriksson, T. Schatz	B+Tech Oy, Finland
P-02-05	THCm numerical models of bentonite heating and hydration tests to study the interactions of compacted bentonite and concrete	J. Samper[1], A. Mon[1], L. Montenegro[1], J. Cuevas[3], R. Fernández[3], M. Jesús Turrero[2], E. Torres[2], A. Naves[1]	[1]University of A Coruña, Spain / [2]Centro de Investigaciones Energéticas, Spain / [3]Universidad Autónoma de Madrid, Spain
P-02-06	Alteration of compacted bentonite contacted with concrete	S. Yokoyama[1], Y. Watanebe[1], A. Jenni[2], U. Mäder[2]	[1]CRIEPI, Japan / [2]RWI, Institute of Geological Sciences, University of Bern, Switzerland
P-02-07	Clay interacting with hardened cement paste at high temperature (70°C): in situ heater tests, lab experiments and reactive transport modelling	P. Lalan[1], A. Dauzères[1], L. De Windt[2], D. Bartier[3], I. Techer[4], V. Detilleux[5]	[1]IRSN, France / [2]Université de Lorraine, France / [4]Université de Nîmes, France / [5]Bel V, Belgium
P-02-08	Erosion Effect Mechanism of Alkaline solution on Compacted GMZ Bentonite	B. Chen[1], J. Guo[1], H. Zhang[2]	[1]Tongji University, China / [2]Shanghai Construction Design & Research Institute Co., Ltd., China
P-02-09	Shear characteristics of Ca-type bentonite immersed in $Ca(OH)_2$ solution	Y. Watanabe, S. Yokoyama, Y. Tanaka	CRIEPI, Japan
P-02-10	Stability of chabazite as cation exchanger in hyper-alkaline media	L. Van Tendeloo, W. Wangermez, A. Maes, C. Kirschhock, J. Martens, E. Breynaert	KU Leuven, Belgium

ALTERATIONS - GENERAL

P-03-01	Porosity Models and Impacts upon Clay Transformations	D. Savage[1], J. Liu[2]	[1]Savage Earth Associates Ltd, UK / [2]Swedish Radiation Safety Authority, Sweden
P-03-02	Controls on Long-Term Transformation of Montmorillonite	D. Savage[1], J. Wilson[2]	[1]Savage Earth Associates Ltd, UK, [2]Quintessa Ltd, UK
P-03-03	Mineralogical-geochemical processes observed in the MX80 bentonite buffer used in deposition holes 5 and 6 of the full scale experiment „prototype repository“ in Äspö, Sweden, after 8 years of operation	R. Dohrmann[1,2], S. Kaufhold[2]	[1]LBEG, Germany / [2]BGR, Germany
P-03-04	THC numerical modelling of the long-term interactions of the corrosion products and the compacted bentonite in a HLW repository in granite	J. Samper, A. Naves, L. Montenegro, A. Mon	University of A Coruña, Spain
P-03-05	Long-term THC simulations of the interactions of the corrosion products, the compacted bentonite, the concrete and the clay in a HLW repository in clay	J. Samper, A. Mon, L. Montenegro, A. Naves	University of A Coruña, Spain
P-03-06	Effect of steam on the swelling capacity of bentonite	O. Karnland	Clay Technology AB, Sweden

P-03-07	MVE – "Rate Drop" experiment: progress report on an in situ glass dissolution test at the Andra's URL	Y. Linard[1], C. Martin[2], M.L. Schlegel[3], P. Jollivet[4]	[1]Andra, Centre de Meuse/ Haute-Marne, France / [2]Andra, France / [3]CEA, DEN/DPC/SEARS [4]CEA, DEN/DTCD/SECM, France
P-03-08	In situ characterization of the Callovian-Oxfordian seepage water composition while exposing the rock to oxygen gas	A. Vinsot[1], M. Lundy[1], Y. Linard[1], S. Wechner[2], J. Trémosa[3], F. Claret[3]	[1]Andra, Centre de Meuse/ Haute-Marne, France / [2]Hydroisotop GmbH, Germany / [3]BRGM, France
P-03-09	Chemical evolution of a HLW cell in Callovo-Oxfordian Claystone: taking into account the oxic transient period	N. C.M. Marty[1], B. Cochepin[2], H. Davarzani[1], C. Tournassat[1], N. Michau[2], I. Munier[2], C. I. Steefel[3], F. Claret[1]	[1]BRGM, France / [2]Andra, France / [3]LBNL, USA
P-03-10	Benchmark for reactive transport codes with application to concrete/clay interaction	N. C.M. Marty[1], O. Bildstein[2], P. Blanc[1], F. Claret[1], B. Cochepin[3], E. C. Gaucher[1], D. Jacques[5], J-E. Lartigue[2], S. Liu[5], K. Ulrich Mayer[4], J. C. L. Meeussen[6], I. Munier[3], I. Pointeau[2], D. Su[4], C.I. Steefel[7]	[1]BRGM, France / [2]CEA Cadarache, France / [3]Andra, France / [4]University of British Columbia, Canada / [5]SCK•CEN, Belgium / [6]NRG, The Netherlands / [7]LBNL, USA
P-03-11	A new view on iron-clay interactions by monitoring pH and H_2 production	F. Bourdelle[1,2], R. Mosser-Ruck[1], L. Truche[1], I. Pignatelli[1], M. Cathelineau[1], N. Michau[3]	[1]Université de Lorraine, France / [2]Université de Lille 1, France / [3]Andra, France
P-03-12	In situ monitoring of gas exchange (O_2, H_2O, CO_2, CH_4) between the Callovian-Oxfordian rock and the atmospheric air in the Bure URL	A. Vinsot[1], M. Lundy[1], Y. Linard[1], Y. Lettry[2], J. Morel[1]	[1]Andra, Centre de Meuse/Haute-Marne, France / [2]Solexperts AG, Switzerland
P-03-13	Corrosion of steel in Toarcian argillite: involvement of microbial metabolisms and biofilms	L. Urios[1], F. Mercier-Bion[4], Y. Leon[4], C. Wittebroodt[3], M. Flachet[2], M. Magot[1], D. Neff[4], P. Dillmann[4]	[1]UPPA, IPREM UMR 5254, IBEAS, France / [2]IRSN, PRP-DGE/SEDRAN/BERIS, France / [3]IRSN, PRP-DGE/SRTG/ LETIS, France / [4]SIS2M/ LAPA, CEA/CNRS UMR 3299, France
P-03-14	Mechanistic and kinetic study of pyrite-hydrogen interaction at low temperature using electrochemical techniques	S. Betelu[1], G. Berger[2], E. Giffaut[3], I. Ignatiadis[1]	[1]BRGM, France / [2]IRAP, France / [3]Andra, France
P-03-15	Modeling of radiolytic leaching of UO_2 pellets in COx clayey water coupled to metallic iron corrosion	M. Odorowski[1,2], L. De Windt[2], C. Jégou[1], V. Broudic[1], C. Martin[3]	[1]CEA, France / [2]MINES ParisTech, Centre de Géosciences, France / [3]Andra, France
P-03-16	Alteration of geological environment condition due to liquid radioactive wastes disposal	V. Krupskaya, S. Zakusin, A. Zhukhlistov	Russian Academy of Sciences, Russian Federation

GEOLOGY AND CLAY CHARACTERISATION

GEOLOGY AND CLAY CHARACTERISATION - 1

P-04-01	A seismic approach to septaria detection in clay deposits	L. Wouters[1], N. Vandenberghe[2], E. Poggiagliolmi[3]	[1]ONDRAF/NIRAS, Belgium / [2]NVDB Consult, Belgium / [3]Entec Integrated Technologies, UK
P-04-02	FE Experiment: Density measurement of granulated bentonite mixture in a 2D pre-test using a dielectric moisture profile probe	T. Sakaki, S. Köhler, H.R. Müller	Nagra, Switzerland
P-04-03	FE Experiment: Density measurement of granulated bentonite mixture in a 3D 1:1 scale mockup test using dielectric tools	T. Sakaki, S. Köhler, M. Hertrich, H.R. Müller	Nagra, Switzerland
P-04-04	Qualitative and quantitative mineral composition of the Rupelian Boom Clay in Belgium	E. Zeelmaekers[1,2], M. Honty[3], A. Derkowski[4], J. Środoń[4], M. DeCraen[3], N. Vandenberghe[1], R. Adriaens[1], L.Wouters[5]	[1]KU Leuven, Belgium / [2]Presently at Shell International Exploration & Production, The Netherlands / [3]SCK•CEN, Belgium / [4]Polish Academy of Sciences, Poland / [5]ONDRAF/NIRAS, Belgium
P-04-05	Structural and mechanical properties of Na rich-montmorillonite:Correlation between XRD analysis and molecular dynamics simulations	W. Oueslati[1,2]	[1]College of Electronics & Communications, Saudi Arabia / [2]Faculté des Sciences de Bizerte, Tunisia
P-04-06	Microstructural characterization of the Ypresian clays at the nm-scale resolution, using broad-ion beam scanning electron microscopy (BIB-SEM) – preliminary results	S. Hemes, G. Desbois, J.L. Urai	RWTH Aachen University, Germany
P-04-07	Multi-scale characterization of pore space connectivity in Boom Clay (HADES-level, Mol, Belgium), using a combination of X-ray µ-CT, BIB-SEM and serial FIB-SEM	S. Hemes[1], G. Desbois[1], J.L. Urai[1], B. Schröppel[2], J-O. Schwarz[3]	[1]RWTH Aachen University, Germany / [2]NMI, University of Tübingen, Germany / [3]Johannes Gutenberg University Mainz, Germany
P-04-08	Microbial diversity, activity and survival in engineered clay barriers	K. Pedersen	Micans, Sweden
P-04-09	Characterization of alternative buffer and backfill materials	P. Keto[1], S. Kumpulainen[1], L. Kiviranta[1], P. Karttunen[1], P. Korkeakoski[2]	[1]B+Tech Oy, Finland / [2]Posiva Oy, Finland
P-04-10	*withdrawn by the author*		
P-04-11	Near-field permeability distribution of FE tunnel in the Mont Terri Rock Laboratory - Influence of shotcrete lining on EDZ development -	H. Shao[1], B. Paul[1], X. Wang[1], J. Hesser[1], J. Becker[2], B. Garitte[2], H. Müller[2]	[1]BGR, Germany / [2]Nagra, Switzerland
P-04-12	Hyperspectral imaging for the characterization of clays: from data acquisition to mineralogical identification	L. Fasnacht[2], D. Malinverni[1], P. Renard[2], L. Marguet[2], P. Brunner[2], J.K. Becker[3]	[1]EPFL, Switzerland / [2]University of Neuchâtel, Switzerland / [3]Nagra, Switzerland
P-04-13	Pore distribution of saturated compacted montmorillonite using NMR relaxometry: effect of salt concentration	T. Ohkubo[1], M. Ibaraki[1], Y. Tachi[2], Y. Iwadate[1]	[1]Chiba University, Japan / [2]JAEA, Japan
P-04-14	Final repository for Denmark's low- and intermediate level radioactive waste	P. Gravesen, B. Nilsson, S. A. Schack Petersen, M. Binderup	GEUS, Denmark
P-04-15	Applying the cosmogenic radionuclide dating technique to estimate rates of landscape development in the Campine area (NE Belgium): first results	K. Beerten[1], V. Vanacker[2]	[1]SCK•CEN, Belgium / [2]Université catholique de Louvain, Belgium

GEOLOGY AND CLAY CHARACTERISATION - 2			
P-05-01	Mineralogical, chemical and mechanical study of potential buffer and backfill materials from alternative buffer material (ABM) test packages 1 and 2	L. Kiviranta[1], S. Kumpulainen[1], P. Korkeakoski[2]	[1]B+Tech Oy, Finland / [2]Posiva Oy, Finland
P-05-02	Hyperspectral imaging for the millimetre-scale characterization of variability in clays	J.K. Becker[2], T.H. Kurz[1], S.J. Buckley[1]	[1]CIPR, Norway / [2]Nagra, Switzerland
P-05-03	Microbial diversity studies of Spanish bentonites: Comparison of clone libraries and Illumina-sequencing based methods	M.L. Merroun[1], M. López-Fernández[1], I. Sánchez-Castro[1], R. Vargas-Vílchez[2], A. Cherkouk[3]	[1]University of Granada, Spain / [2]University of Gent, Belgium / [3]Institute of Resource Ecology, Germany
P-05-04	Understanding the swelling behavior of smectite as a function of temperature and humidity	A.M. Schleicher, B.A. van der Pluijm	University of Michigan, USA
P-05-05	Determination of water retention curve on Czech bentonite	M. Levorova, L. Hausmannova, J. Svoboda	Czech Technical University in Prague, Czech Republic
P-05-06	Clay minerals distribution, textural properties and nano-porosities in hydrothermal dolomites	A. Golreihan, R. Swennen	KU Leuven, Belgium
P-05-07	Variations in microbial community composition in piezometer installations in Boom Clay	K. Wouters[1], M. Mysara[1,2], H. Moors[1], N. Leys[1]	[1]SCK•CEN, Belgium / [2]Vrije Universiteit Brussel, Belgium
P-05-08	Optimization of pore network characterization of compacted clay materials by TEM and FIB/SEM imaging	S. Gaboreau[1], J-C. Robinet[2], D. Prêt[3]	[1]BRGM, France / [2]Andra, France / [3]Université de Poitiers, France
P-05-09	Bentonite Blocks Manufacturing by Uniaxial and Isostatic Methods for Engineering Barrier System Components	E. Holt[1], J. Ritola[1], J. Peura[1], V. Sjöblom[1], K. Haapala[2]	[1]VTT, Finland / [2]Posiva Oy, Finland
P-05-10	Geometry of the Callovo-Oxfordian claystone formation from depth-converted 3D-high resolution seismic data: modeling and spatial uncertainty	B. Yven[1], J-B. Mathieu[2], M. Garcia[2]	[1]Andra, France / [2]KIDOVA, France
P-05-11	Analysis and modeling of spatial trend and spatial uncertainty of physical rock properties in the Callovo-Oxfordian claystone formation from a 3D high resolution impedance cube	M. Garcia[1], J-B. Mathieu[1], B. Yven[2]	[1]KIDOVA, France / [2]Andra, France
P-05-12	DNA isolation from clayey samples: How can you realize this?	H. Moors, K. Wouters, P. Boven, N. Leys	SCK•CEN, Belgium
P-05-13	The influence of sample preparation on the structure of compacted, water saturated MX-80 bentonite	M. Matusewicz, V-M. Pulkkanen, M. Olin	VTT, Finland
P-05-14	Anisotropic features on the thermal conductivity of Ypresian clays	E. Romero[1], A. Lima[2], N. Sau[1], H. Van Baelen[3], X. Sillen[3], X.L. Li[4]	[1]Universitat Politècnica de Catalunya, Spain / [2]Federal University of Pernambuco, Brazil / [3]ONDRAF/NIRAS, Belgium / [4]EIG EURIDICE, Belgium
P-05-15	New paleoseismologic trench accross the Rauw Fault at Mol, Belgium	K. Verbeeck[1], L. Wouters[2], K. Vanneste[1], B. Vleminckx[1], K. Van Noten[1], T. Camelbeeck[1], S. Marco[3], N. Vandenberghe[1]	[1]Royal Observatory of Belgium, Belgium / [2]ONDRAF/NIRAS, Belgium / [3]Samsuffit BVBA, Belgium / [4]KULeuven, Belgium

GEOCHEMISTRY

GEOCHEMISTRY - 1

P-06-01	Influence of Natural Sorbents in Immobilization of Spent Ion Exchange Resins in Cement in Radioactive Waste Management	I. Plecas[1], S. Dimovic[1], D. Arbutina[2]	[1]The "Vinca" Institute of Nuclear Sciences, Serbia / [2]Public Company "Nuclear Facilities of Serbia", Serbia
P-06-02	Preparation and estimation of thermodynamic properties of Fe(II)-, Co(II)-, Ni(II)- and Zr(IV)-containing layered double hydroxides	K. Rozov, H. Curtius, D. Bosbach	Forschungszentrum Jülich GmbH, Germany
P-06-03	Retardation of low-molecular weight organic compounds in clays	Y. Chen[1,2], M.A. Glaus[1], A. Jakob[1], L.R. Van Loon[1], U.K. Mäder[2]	[1]PSI, Switzerland / [2]University of Bern, Switzerland
P-06-04	Constraining porewater chemistry in a clay–rich rock sequence	P. Wersin[1], M. Mazurek[1], H. Niklaus Waber[1], U.K. Mäder[1], T. Gimmi[1,2], D. Rufer[1], C. Lerouge[3], T. Oyama[4], D. Traber[5]	[1]University of Bern, Switzerland / [2]BRGM, France / [3]PSI, Switzerland / [4]CRIEPI, Japan / [5]Nagra, Switzerland
P-06-05	Regional aquifer hydrogeochemistry below the Boom Clay (NE-Belgium): data analysis and modelling	K. Vandersteen, B. Leterme	SCK•CEN, Belgium
P-06-06	The effect of ionic strength on Iodine exclusion in Na-montmorillonite-rich clay rock – a molecular simulations study	F.O. Valega Mackenzie[1], M. Koenen	[1]TNO, The Netherlands
P-06-07	Roles of Interlayer Cation Species and Water Content in Montmorillonite Crystalline Swelling	L. Sun[1], J.T. Hirvi[1], J.T. Tanskanen[1], T. Schatz[2], S. Kasa[3], T.A. Pakkanen[1]	[1]University of Eastern Finland, Finland / [2]B+Tech Oy, Finland / [3]Posiva Oy, Finland
P-06-08	Time evolution of MX-80 bentonite geochemistry under thermo-hydraulic gradients	M.V. Villar, R. Gómez-Espina	CIEMAT, Spain
P-06-09	MOLDATA: A Thermodynamic Database supporting phenomenological studies of the Belgian RD&D programme	S. Salah[1], L. Wang[1], H. De Soete[1], C. Bruggeman[1], S. Brassinnes[2]	[1]SCK•CEN, Belgium / [2]ONDRAF/NIRAS, Belgium
P-06-10	Prediction of R_d values for radionuclides in Boom Clay with an independent multi-surface model	J.C.L. Meeussen[1], T.J. Schröder[1], E. Rosca-Bocancea[1], J.J. Dijkstra[2], C. Bruggeman[3], N. Maes[3]	[1]NRG, The Netherlands / [2]Energy research Centre of the Netherlands, The Netherlands / [3]SCK•CEN, Belgium
P-06-11	Evaluation of waste form behaviour in a geological repository for high-level radioactive waste in Boom Clay in the Netherlands	G. Deissmann[1,2], K. Haneke[2], A. Filby[2], R. Wiegers[3], D. Bosbach[1]	[1]Forschungszentrum Jülich GmbH, Germany / [2]Brenk Systemplanung GmbH, Germany / [3]IBR Consult BV, The Netherlands
P-06-12	Montmorillonite interlamellar surface chemistry: Effect of magnesium ion substitution on cation adsorption	L.P. Lavikainen[1], J.T. Tanskanen[1], T. Schatz[2], S. Kasa[3], T.A. Pakkanen[1]	[1]University of Eastern Finland, Finland / [2]Posiva Oy, Finland / [3]B+Tech Oy, Finland
P-06-13	Evaluation of LILW degradation processes and products in a geological repository for radioactive waste in Boom Clay in the Netherlands	A. Filby[1], G. Deissmann[1,2], R. Wiegers[3]	[1]Brenk Systemplanung GmbH, Germany / [2]Forschungszentrum Jülich GmbH, Germany / [3]IBR Consult BV, The Netherlands

P-06-14	Multi-tracer profile at high spatial resolution across the Opalinus Clay at the Mont Terri URL	H.N. Waber[1], D. Rufer[1], L. Kennell[2], D. Traber[3]	[1]University of Bern, Switzerland / [2]NWMO, Canada / [3]Nagra, Switzerland
P-06-15	Boundary phenomena at the clay solid/liquid interface	R. Eriksson, T. Schatz	B+Tech Oy, Finland
P-06-16	Abiotic and biotic nitrate and nitrite reduction by pyrite	N. Bleyen, M. Vasile, C. Bruggeman, E. Valcke	SCK•CEN, Belgium
P-06-17	Microbial activity in clay porewater containing carbon steel materials, under anoxic conditions at 85°C	M. Labat[1], S. Daumas[2], Z. Ben Ali Gam[1], S. Necib[3]	[1]Université du Sud Toulon-Var, France / [2]BRGM, France / [3]Andra, Centre de Meuse/Haute-Marne, France
P-06-18	Impact of the nature of the electron donor on in situ microbial nitrate reduction processes in Opalinus Clay	N. Bleyen[1], S. Smets[1], H. Moors[1], N. Leys[1], A. Albrecht[2], P. De Cannière[3], B. Schwyn[4], C. Wittebroodt[5], E. Valcke[1]	[1]SCK•CEN, Belgium / [2]Andra, France / [3]FANC/ AFCN, Belgium / [4]Nagra, Switzerland / [5]IRSN, France
P-06-19	Redox capacities of Boom Clay constituents; an electrochemical approach	A.L. Hoving[1], T. Behrends[1], M. Sander[2], N. Maes[3], C. Bruggeman[3]	[1]Utrecht University, The Netherlands / [2]IBP, Switzerland / [3]SCK•CEN, Belgium
P-06-20	Advanced technologies for the investigation of fluids in low-permeable rocks	F. Eichinger, G.D. Lorenz, A. Voropaev, L. Eichinger, S. Wechner	Hydroisotop GmbH, Germany

GEOCHEMISTRY - 2			
P-07-01	Interface equilibrium in bentonite - a general approach to ion diffusion	M. Birgersson	Clay Technology AB, Sweden
P-07-02	Uranium retention by montmorillonite at high ionic strengths	K. Fritsch, K. Schmeide	Institute of Resource Ecology, Germany
P-07-03	Development of the squeezing method for analysing compacted bentonite porewater	J. Järvinen, M. Matusewicz, A. Itälä	VTT Technical Research Center of Finland, Finland
P-07-04	Characterization of porewaters in an aquiclude: challenges of the Bruce DGR formations	I.D. Clark[1], S. Murseli[1], G. St.-Jean[1], T. Al[2], K. Raven[3], L. Kennell[4], M. Hobbs[4], M. Jensen[4]	[1]University of Ottawa, Canada / [2]University of New Brunswick, Canada / [3]Geofirma Engineering Ltd, Canada / [4]NWMO, Canada
P-07-05	Sorption studies of actinides and lanthanides onto clay minerals under saline conditions	A. Schnurr, R. Marsac, T. Rabung, J. Lützenkirchen, H. Geckeis	KIT-INE, Germany
P-07-06	Understanding radionuclide interactions with layered materials	Y. Wang	Sandia National Laboratories, USA
P-07-07	The crystal structure of Magnesium Silicate Hydrate (M-S-H) and its relation with talc-like clay mineral	C. Roosz[1], S. Grangeon[1], S. Gaboreau[1], V. Montouillou[3], P. Blanc[1], B. Lothenbach[4], P. Vieillard[2], P. Henocq[5], E. Giffaut[5]	[1]BRGM, France / [2]Université de Poitiers, France / [3]CNRS, CEMHTI, France / [4]EMPA, Switzerland / [5]Andra, France
P-07-08	Partial pressure of CO^2 in the Boom Clay pore water at 16 and 80°C: Experimental data versus modelling assessment	M. Honty, L. Wang, M. De Craen, N. Maes	SCK•CEN, Belgium

P-07-09	Further understanding of the Boom Clay pore water geochemistry - experiments from the HADES URF, Mol, Belgium	M. Honty, L. Wang, M. De Craen, C. Bruggeman	SCK•CEN, Belgium
P-07-10	Characterization of Dissolved Organic Matter (DOM) derived from Boom Clay, I: Size distribution and element association	M. Bouby[1], U. Kaplan[1], C. Bruggeman[2], D. Durce[2], N. Maes[2], S. Brassinnes[3], T. Schäfer[1]	[1]INE, KIT, Germany / [2]SCK•CEN, Belgium / [3]ONDRAF/NIRAS, Belgium
P-07-11	Characterization of Dissolved Organic Matter /DOM) derived from Boom Clay, II: Organic Functionality	U. Kaplan[1], M. Bouby[1], T. Kupcik[1], D. Schild[1], P. Kaden[1], C. Bruggeman[2], D. Durce[2], N. Maes[2], S. Brassinnes[3], T. Schäfer[1]	[1]INE, KIT, Germany / [2]SCK•CEN, Belgium / [3]ONDRAF/NIRAS, Belgium
P-07-12	Influence of organic cations on clay surfaces and retention capacity -an XPS, FTIR and MD simulation study-	B. Schampera[1], R. Mikutta[1], S.K. Woche[1], D. Tunega[2], R. Solc[2], S. Dultz[1]	[1]Leibniz University Hannover, Germany / [2]BOKU, Austria
P-07-13	Setting up a thermodynamic solid solution model for illites	U.R. Berner	PSI, Switzerland
P-07-14	Study of the surface reactivity of clay mineral phases by isotope exchange	T. Suzuki-Muresan, K. David, K. Perrigaud, C. Landesman, A. Abdelouas, B. Grambow	Université de Nantes, France
P-07-15	Effect of layer charge on the swelling of Na^+, K^+, and Ca^{2+} montmorillonites: DFT and molecular dynamics studies	A. Seppälä, E. Puhakka, M. Olin	VTT, Finland
P-07-16	Geochemistry of Callovo-oxfordian argillite at 80°C: batch experiments and modeling	H. Gailhanou[1], S. Gaboreau[1], M. Debure[1], S. Grangeon[1], P. Blanc[1], N. Marty[1], J.M. Grenèche[2], B. Madé[3], S. Altmann[3], C. Tournassat[1]	[1]BRGM, France / [2]LUNAM–Université du Maine, France / [3]Andra, France
P-07-17	Hydration sequence of swelling clays exchanged with mixed alkali/alkali-earth cations	F. Salles[1], O. Bildstein[2], J-M. Douillard[1], B. Prelot[1], J. Zajac[1], H. Van Damme[3]	[1]Institut Charles Gerhardt Montpellier, France / [2]CEA Cadarache, France / [3]PPMD/ESPCI, France
P-07-18	Zn and Co sorption onto Na-illite – batch sorption study and modelling	V. Montoya[1], T. Kupcik[1], L. Van Laer[3], C. Bruggeman[3], M.A. Glaus[2], B. Baeyens[2], N. Maes[3], T. Schäfer[1], H. Geckeis[1]	[1]INE, KIT, Germany / [2]PSI, Switzerland / [3]SCK•CEN, Belgium
P-07-19	C_s^+ adsorption on hydrated surfaces of illite, smectite, and interstratified illite/smectite clays: Molecular dynamics simulations to test the validity of the additive model	A.G. Kalinichev, N. Loganathan, B.F. Ngouana Wakou, Z. Chen, G. Montavon	Université de Nantes, France
P-07-20	Effect of pore structure of hardened cement paste on C_s^+ diffusion	D. Shitara, H. Takiya, M. Ito, N. Watanabe, T. Kozaki	Hokkaido University, Japan
P-07-21	Uranium adsorption onto bentonite with indigenous sulphate reducing bacteria	S.Y. Lee, J.K. Lee, M.H. Baik, K. Kim	KAERI, Republic of Korea
P-07-22	Anion diffusion in low porosity argillaceous rocks	C. Wigger, L. Van Loon, T. Gimmi	PSI, Switzerland

GEOMECHANICS

GEOMECHANICS - 1

P-08-01	The Stress-Strain-Permeability Behaviour of Clay Rock	C-L. Zhang	GRS, Germany
P-08-02	Laboratory and numerical investigation of the mechanical behaviour of the Tournemire argillite	G. Su[1], T.S. Nguyen[1], E. Haghighat[2], S.Pietruszczak[2], D. Labrie[3], J.D. Barnichon[4], H. Abdi[5]	[1]Canadian Nuclear Safety Commission, Canada / [2]McMaster University, Canada / [3]CANMET, Canada / [4]IRSN, France / [5]University of Ottawa, Canada
P-08-03	Constitutive behaviour of Opalinus Clay and workflow for simplified material laws for engineering purposes	S.B. Giger, P. Marschall	Nagra, Switzerland
P-08-04	Development of a workflow for hydro-mechanical near-field studies – influence of the relative humidity	F. Dedecker[1], D. Billaux[1], A. Papafotiou[2], P. Marschall[3]	[1]ITASCA Consultants S.A.S., France / [2]INTERA, Switzerland / [3]Nagra, Switzerland
P-08-05	Influence of intrinsic material parameters on fluid pressure build-up and two-phase flow phenomena in a deep HLW repository in claystone	V. Shushakova, M. Jobmann, J. Wolf, E. Kuate Simo	DBE TECHNOLOGY GmbH, Germany
P-08-06	Comparative modelling and simulation of selected in situ measurements performed at URL Mont Terri using FLAC-TOUGH and CODE_BRIGHT	R. Seeska[1], O. Czaikowski[2], M. Komischke[2], K.-H. Lux[1], M. Rutenberg[1], K. Wieczorek[2]	[1]TUC, Germany / [2]GRS, Germany
P-08-07	Geomechanical modelling of the Dutch radioactive waste repository accounting for uncertainties	P.J. Vardon[1], P. Arnold[1], M. Milioritsas[1], M.A. Hicks[1], P.A. Fokker[2], J.H. Fokkens[3]	[1]TU Delft, The Netherlands / [2]TNO, The Netherlands / [3]NRG, The Netherlands
P-08-08	3D modeling of the mechanical behavior of liners (segments) placed around the gallery of nuclear waste repository	V. Renaud[1], A. Poutrel[2]	[1]INERIS, France / [2]Andra, France
P-08-09	Hydraulic-mechanically coupled simulation of cyclic deformation processes investigated at the Mont Terri site	G. Ziefle, J. Maßmann	BGR, Germany
P-08-10	Experimental study of the mechanical behavior of a steel casing in a 500 m deep clay formation based on in situ experiments – Analysis of the scale effect	F. Bumbieler, J. Morel, N. Conil, G. Armand	Andra, Centre Meuse/ Haute-Marne, France
P-08-11	Long term behaviour of claystone and its interaction with steel casing – Comparison between continuum/discontinuum 3D models	W. Shiu[1], M. Camusso[1], D. Billaux[1], A. Poutrel[2]	[1]ITASCA Consultants S.A.S., France / [2]Andra, France
P-08-12	Full-scale test of dome plug (Domplu) - design, installation, predictions and results	L. Börgesson[1], T. Sandén[1], M. Åkesson[1], P. Grahm[2]	[1]Clay Technology AB, Sweden / [2]SKB, Sweden
P-08-13	Multiscale modeling of textural and mechanical properties of clays	D. Ebrahimi[1], A.J. Whittle[1], R. J.-M. Pellenq[1,2,3]	[1]Massachusetts Institute of Technology, USA / [2]Aix-Marseille Université, CNRS, France / [3]MSE, USA
P-08-14	Geomechanical characterization of the Opalinus Clay from an analysis of the FE Tunnel excavation at the Mont Terri URL	R. Senger[1], P. Marschall[2], S. Goodarzi[3], D. Walters[3], H.R. Müller[2], T. Vogt[2], B. Garitte[2]	[1]INTERA Incorporated, Swiss Branch, Switzerland / [2]Nagra, Switzerland / [3]TAURUS Reservoir Solutions, Ltd, Canada

P-08-15	Characterization of the damage in Callovo-Orfordian claystone at two scales, strain localisation and micro cracks	P. Bésuelle[1,2], E. Andò[1,2], P. Lanatà[1,2], J. Desrues[1,2], G. Viggiani[1,2], S. Salager[1,2], P. Charrier[1,2]	[1]Univ. Grenoble Alpes, France / [2]CNRS, France
P-08-16	Numerical pre- and post-construction models of the geomechanical behaviour in the FE Experiment at the Mont Terri URL	P. Nater[1], B. Garitte[2], S. Köhler[2], H.R. Müller[2]	[1]Pöyry Switzerland Ltd., Switzerland / [2]Nagra, Switzerland
P-08-17	Insights into the response of a gallery sealing over the entire life of a deep repository	D.F. Ruiz[1], J. Vaunat[1], A. Gens[1], M. Manica[1], A. Pasteau[2]	[1]Universitat Politècnica de Catalunya, Spain / [2]Andra, France
P-08-18	Numerical modelling of drifts excavated in stiff clays	M.A. Mánica[1], A. Gens[1], J. Vaunat[1], D.F. Ruiz[1], D. Seyedi[2], G. Armand[3]	[1]Universitat Politècnica de Catalunya, Spain / [2]Andra, France / [3]Andra, Centre de Meuse/Haute-Marne
P-08-19	Tunnel excavation in a claystone at 500 m deep: Road header under shield with segment emplacement experiment	J. Zghondi, S. Carraretto, A. Noiret, G. Armand	Andra, Centre de Meuse/ Haute-Marne, France
P-08-20	A model benchmark exercise for numerical analysis of the Callovo-Oxfordian claystone hydromechanical response to excavation operations	D. Seyedi[1], G. Armand[2], P. Bésuelle[3], F. Collin[4], S. Cuvilliez[5], J. Desrues[3], G. Duveau[6], A.P. van den Eijnden[1,3], R. Fernandes[5], A. Gens[7], R. Giot[8], D. Hoxa[9], J.B. Kazmierczak[10], B. Pardoen[4], J.C. Robinet[11], J.F. Shao[6], M. Souley[10], T.H. Tran[11], J. Vaunat[7]	[1]Andra, France / [2]Andra, Centre de Meuse/Haute-Marne, France / [3]Univ. Grenoble Alpes–3SR, France / [4]University of Liege, Belgium / [5]EDF R&D, France / [6]LML, UMR 8107 CNRS, France / [7]Universitat Politècnica de Catalunya, Spain / [8]University of Lorraine, France / [9]University of Orléans, France / [10]INERIS, France / [11]EuroGéoMat Consulting, France
P-08-21	Numerical analysis of the stiffness evolution of damaged zone around the drifts under mechanical loading/unloading cycles	M.N. Vu[1], D. Seyedi[1], A. Noiret[2], R. de La Vaissière[2], G. Armand[2]	[1]Andra, France / [2]Andra, Centre de Meuse/Haute-Marne, France
P-08-22	Analytical solution of the post-closure behaviour of an underground cavity excavated in a viscoplastic rock mass	T.A. Bui[1], H. Wong[1], F. Deleruyelle[2], D.K. Tran[3]	[1]Université de Lyon, ENTPE/ LGCB and LTDS UMR CNRS 5513, France / [2]IRSN, PRP-DGE, SEDRAN, BERIS, France / [3]Université de Lyon and ECL, LTDS UMR CNRS 5513, France
P-08-23	Anisotropic convergence analysis in drifts of the Meuse/haute-Marne underground research laboratory	L-M. Guayacán-Carrillo[1,2], J. Sulem[2], D. Seyedi[1], S. Ghabezloo[2], A. Noiret[3], G. Armand[3]	[1]Andra, France / [2]Université Paris-Est, Ecole des Ponts ParisTech, France / [3]Andra, Centre de Meuse/Haute-Marne, France
P-08-24	An anisotropic elastoplastic model for Boom Clay	L-Q. Dao[1], J-M. Pereira[1], Y-J. Cui[1], A-M. Tang[1], X-L. Li[2], X. Sillen[3]	[1]Université Paris-Est, France / [2]EIG EURIDICE, Belgium, [3]ONDRAF/NIRAS, Belgium
P-08-25	Impact of excavation damage on the thermo-hydro-mechanical properties of natural Boom Clay	L-Q. Dao[1], Y-J. Cui[1], A-M. Tang[1], J-M. Pereira[1], P. Delage[1], X-L. Li[2], X. Sillen[3]	[1]Université Paris-Est, France / [2]IEG EURIDICE, Belgium / [3]ONDRAF/NIRAS, Belgium

P-08-26	Temperature effect on the drained creep behavior of Boom clay	Z. Gong[1], W.Z. Chen[1], Y.S. Ma[1], H.D. Yu[1], X-L. Li[2], X. Sillen[3]	[1]Chinese Academy of Science, China / [2]EIG EURIDICE, SCK•CEN, Belgium / [3]ONDRAF/NIRAS, Belgium
P-08-27	Deformation mechanisms of Boom clay during long term consolidation test	H.D. Yu[1], W.Z. Chen, D.S. Yang, Z. Gong, Y.S. Ma, X.L. Li, X. Sillen	[1]Chinese Academy of Science, China / [2]EIG EURIDICE, Belgium / [3]ONDRAF/NIRAS, Belgium
P-08-28	Variation of the hydraulic conductivity of Boom clay under various thermal-hydro-mechanical conditions	Y.S. Ma[1], W.Z. Chen[1], H.D. Yu[1], D.S. Yang[1], Z. Gong[1], X.L. Li[2]	[1]Chinese Academy of Science, China / [2]EIG EURIDICE, SCK•CEN, Belgium
P-08-29	X-ray Computed Tomography Investigation of the Sandy Facies (Opalinus Clay, Mont Terri) Before and After Mechanical Testing	A. Kaufhold[1], W. Gräsle[1], I. Plischke[1], M. Halisch[2], G. Zacher[2]	[1]BGR, Germany / [2]LIAG, Germany / [3]GE Sensing & Inspection Technologies, Germany

GEOMECHANICS - 2			
P-09-01	Hydraulic sealing experiments on Callovo-Oxfordian argillite	C. Imbert[1], P. Sémété[2], G. Touzé[1], J. Delorme[2], B. Février[2], P. Desgrée[2]	[1]CEA, DPC/SECR/LECBA, France / [2]EDF R&D, France
P-09-02	The initial damage/fractured excavation zone around deep underground facilities in Callovo-Oxfordian formation: modelling of fractures network using an anisotropic damage approach funded on shear and extension properties of argilites	R. Robinet[1], F. Plas[2], C. Imbert[3], J.C. Robinet[4]	[1]Tractebel Engineering S.A., Belgium / [2]Andra, France / [3]CEA, France / [4]Euro-Géomat-Consulting, France
P-09-03	Hydro-mechanical simulation in a deep excavation in Boom Clay	P.Y. Hong[1], F. Collin[2], Y. J. Cui[1], X-L. Li[3], X. Sillen[4], J.M. Pereira[1], A.M. Tang[1]	[1]Université Paris-Est, France / [2]University of Liege, Belgium / [3]EIG EURIDICE, Belgium / [4]ONDRAF/NIRAS, Belgium
P-09-04	Multi-scale investigation of the swelling clay material properties	L. Massat[1], O. Cuisinier[1], S. Gaboreau[2], F. Masrouri[1], M. Pelletier[3], I. Bihannic[3], F. Claret[2]	[1]Université de Lorraine, CNRS, France / [2]BRGM, France / [3]Université de Lorraine, France
P-09-05	Study of the long term hydration of the FEBEX mock-up experiment considering four different coupled phenomena	M. Sánchez[1], A. Gens[2], F. Aponte[1], P.L. Martin[3], J.C. Mayor[4]	[1]Texas A&M University, USA / [2]Univ. Politècnica de Catalunya, Spain / [3]CIEMAT, Spain / [4]ENRESA, Spain
P-09-06	Micro scale caracterisation of COX swelling and self-sealing behavior	S. Salager[1,2], D. Takano[3], P. Bésuelle[1,2], E. Andò[1,2], J. Desrues[1,2], G. Viggiani[1,2], P. Charrier[1,2]	[1]Univ. Grenoble Alpes, France / [2]CNRS, Lab 3SR, France / [3]Port and Airport Research Institute, Japan
P-09-07	A two-surface viscoplastic model for saturated clays	P.Y. Hong[1], J.M. Pereira[1], Y.J. Cui[1], A.M. Tang[1], F. Collin[2], X.L. Li[3], X. Sillen[4]	[1]Université Paris-Est, France / [2]University of Liege, Belgium / [3]EIG EURIDICE, Belgium / [4]ONDRAF/NIRAS, Belgium

P-09-08	Microseismicity induced by a gallery excavation in the Mont Terri underground rock laboratory	Y. Le Gonidec[1], J. Sarout[2], J. Wassermann[3], C. Nussbaum[4], P. Bossart[4]	[1]Géosciences Rennes, France / [2]CSIRO, Australia / [3]Géosciences et Environnement Cergy, France / [4]Swisstopo, Switzerland
P-09-09	Swelling pressure behavior of compacted bentonites under controlled suction	Z.G. Yigzaw, O. Cuisinier, F. Masrouri	Université de Lorrraine, France
P-09-10	A model for the swelling of bentonite by lowering salinity	V-M. Pulkkanen	VTT, Finland
P-09-11	Elasto-plastic constitutive law based on evolving soil structure	M. Oualmakran[1,2], B. François[1]	[1]Université Libre de Bruxelles, Belgium / [2]F.R.S.-FNRS, Belgium
P-09-12	Small-strain shear stiffness of compacted MX-80 bentonite	E. Romero[1], J. Suriol[1], A. Lloret[1], X. Pintado[2]	[1]Universitat Politècnica de Catalunya, Spain / [2]B+Tech Oy, Finland
P-09-13	On the hydromechanical behaviour of Ypresian clays	X-P. Nguyen[1], Y-J. Cui[1], A-M. Tang[1], X-L. Li[2], L. Wouters[3]	[1]Université Paris-Est, France / [2]EIG EURIDICE, Belgium / [3]ONDRAF/NIRAS, Belgium
P-09-14	Preliminary comparative study on petrophysical and hydromechanical properties of Boom Clay and Ypresian clays	X-P. Nguyen[1], Y-J. Cui[1], A-M. Tang[1], Y. Deng[2], X. Li[3], L. Wouters[4]	[1]Université Paris-Est, France / [2]Southeast University, China / [3]EIG EURIDICE, Belgium / [4]ONDRAF/NIRAS, Belgium
P-09-15	Investigating the deviatoric behaviour of Boom Clay	X-P. Nguyen[1], Y-J. Cui[1], A-M. Tang[1], X-L. Li[2]	[1]Université Paris-Est, France / [2]EIG EURIDICE, Belgium
P-09-16	The effects of suction and temperature on micro porosity variation in compacted bentonite based on a solid-solution geochemical model	M. Sedighi, H.R. Thomas	Cardiff University, UK
P-09-17	Modelling of large-scale in situ ventilation test in clayey rock	B. Pardoen[1,2], F. Collin[1], J. Talandier[3]	[1]University of Liege, Belgium / [2]F.R.I.A., Belgium / [3]Andra, France
P-09-18	Steel corrosion effects on the thermo-hydro-mechanical process in an underground disposal tunnel for high-level wastes	Y. Jia[2], H. Bian[1], J-F. Shao[2], A. Poutrel[3]	[1]Université de Lorraine, France / [2]Polytech'Lille, France / [3]Andra, France
P-09-19	The concrete interface stability analysis during the hydro-mechanical process in an underground disposal tunnel	H. Bian[1], Y. Jia[2], J-F. Shao[2], A. Pasteau[3]	[1]Université de Lorraine, France / [2]Polytech'Lille, France / [3]Andra, France
P-09-20	Numerical investigation of damage and crack porosity closure effects on the soil-structure interaction around a deep drift at the Meuse/Haute-Marne URL	M. Souley[1], D. Seyedi[2], G. Armand[3], M. Ghoreychi[4]	[1]INERIS, France / [2]Andra, France / [3]Andra, Centre de Meuse/Haute-Marne, France / [4]INERIS, France
P-09-21	Numerical modeling of in situ "PRACLAY seal test"	G. Chen[1], X.L. Li[1], J. Verstricht[1], X. Sillen[2]	[1]EIG EURIDICE, Belgium / [2]ONDRAF/NIRAS, Belgium
P-09-22	Underground storage and its caprock: the good cap / bad cap principle	C. Dietl, H. Baumgartner, E. Jahns	Gesteinslabor Dr. Eberhard Jahns, Germany
P-09-23	Geomechanical model based on the complete description of an UGS caprock: an integrative laboratory study	C. Dietl[1], R. Braun[2], H. Baumgartner[1], E. Jahns[1]	[1]Gesteinslabor Dr. Eberhard Jahns, Germany / [2]Dr. Roland Braun-Consultancy in Rock Mechanics, Germany

P-09-24	Hydromechanical behaviour of technological voids and interfaces: finite element formulation and application	A.C. Dieudonne[1,2], B. Cerfontaine[1], J.P. Radu[1], F. Collin[1], R. Charlier[1]	[1]University of Liege, Belgium / [2]F.R.I.A., Belgium
P-09-25	Experimental evidence and constitutive modelling of desiccation cracks in clayey materials	P. Gerard[1], I. Murray[2], A. Tarantino[2]	[1]Université Libre de Bruxelles (ULB), Batir department, Laboratory of Geomechanics, Belgium / [2]University of Strathclyde, UK
P-09-26	On the thermo-mechanical behaviour of the Callovo-Oxfordian claystone	H. Menaceur[1], P. Delage[1], A.M. Tang[1], N. Conil[2]	[1]Ecole des ponts ParisTech, France / [2]Andra, France
P-09-27	A microstructure investigation of the compression-swelling behaviour of the Callovo-Oxfordian claystone	H. Menaceur[1], P. Delage[1], A.M. Tang[1], J. Talandier[2]	[1]Ecole des ponts ParisTech, France / [2]Andra, France
P-09-28	A poroelastic investigation of the Callovo-Oxfordian claystone	M. Belmokhtar[1], P. Delage[1], S. Ghabezloo[1], H. Menaceur[1], J. Talandier[2]	[1]Ecole des ponts ParisTech, France / [2]Andra, France

EXCAVATION DISTURBED / DAMAGED ZONE

P-10-01	Criteria for demonstrating the integrity of the geological barriers in claystone in Germany	M. Jobmann[1], J. Maßmann[2], A. Meleshyn[3], M. Polster[1]	[1]DBE TECHNOLOGY GmbH, Germany / [2]BGR, Germany / [3]GRS, Germany
P-10-02	Quantitative characterisation of EDZ fracture network in the Meuse/Haute-Marne Underground Research Laboratory - In situ experiment and numerical interpretation of helium injection test -	H. Shao[1], W. Liu[1], S. Göthling[1], J. Hesser[1], J. Morel[2], J. Sönnke[1]	[1]BGR, Germany / [2]Andra, France
P-10-03	Synoptic structural geological analysis of the MB & FE tunnel excavation in the Mont Terri URL: Influences of pre-existing fractures on tunnel stability and EDZ characteristics	J.K. Becker[1], D. Jaeggi[2], D.A.Lisjak[3], H. Madritsch[1], S. Schefer[4], H.R. Müller[1], T. Vietor[4]	[1]Nagra, Switzerland / [2]Swisstopo, Switzerland / [3]Geomechanica Inc., Canada / [4]Geoexplorers Ltd., Switzerland
P-10-04	Ultrasonic and geoelectrical characterization of tunnel near field features within the FE-E experiment (Mont Terri RL)	K. Schuster[1], M. Furche[1], J. Becker[2], F. Schulte[1], H. Albers[1], C. Czora[1], T. Tietz[1]	[1]BGR, Germany / [2]Nagra, Switzerland
P-10-05	High resolution geoelectrical and ultrasonic investigations of EDZ features at the URL Meuse / Haute-Marne	M. Furche[1], K. Schuster[1], J. Morel[2], J. Sönnke[1], H. Albers[1], F. Schulte[1], C. Czora[1], T. Tietz[1]	[1]BGR, Germany / [2]Andra, Centre de Meuse/Haute-Marne
P-10-06	Self-Sealing of Fractures in Clay Rock	C-L. Zhang	GRS, Germany
P-10-07	Strain localization modelling around an underground gallery in Mol with an analysis of the contact pressure on the lining	F. Salehnia[1], A. Dizier[2], X-L. Li[2], X. Sillen[3], R. Charlier[1]	[1]University of Liege, Belgium / [2]EIG EURIDICE, Belgium / [3]ONDRAF/NIRAS, Belgium
P-10-08	Feedback on methods of characterization of damage around underground structures in argillites by analyzing wave propagation	C. Balland[1], P. Côte[2], J. Morel[3]	[1]INERIS, France / [2]IFSTTAR, France / [3]Andra, Centre de Meuse/Haute-Marne, France
P-10-09	EDF contribution to the ANDRA benchmark exercise: "numerical analysis of the Callovo-Oxfordian claystone hydromechanical response to excavation operations"	S. Cuvilliez[1], R. Fernandes[1,2], S. Raude[3]	[1]EDF R&D, France / [2]LaMSID-UMR EDF/CNRS/CEA, France / [3]EDF, France
P-10-10	On the Thermo-Hydro-Mechanical behaviour of a sheared Callovo-Oxfordian claystone sample with respect to the EDZ behaviour	H. Menaceur[1], P. Delage[1], A.M. Tang[1], N. Conil[2]	[1]Ecole des ponts ParisTech, France / [2]Andra, France

HEATER TESTS - GAS TRANSFER - BENTONITE HYDRO-MECHANICS

LARGE SCALE IN SITU HEATER TESTS

P-11-01	The HE-E experiment (Mont Terri): modelling a large in situ heating test	B. Garitte[2], A. Gens[1], R.B. de Vasconcelos[1], J. Vaunat[1], I. Gaus[2]	[1]Universitat Politècnica de Catalunya, Spain / [2]Nagra, Switzerland
P-11-02	Displacement of heater in the THMC China-Mock-up test	Y.M. Liu[1,2], S.F. Cao[1,2], J. Wang[1,2], J.L. Xie[1,2], L.K. Ma[1,2], X.G. Zhao[1,2], L. Chen[1,2]	[1]BRIUG, China / [2]CNNC, China
P-11-03	Results from hydro-mechanical and geochemical analyses of the retrieved buffer material from the Prototype Repository at Äspö Hard Rock Laboratory	L-E. Johannesson, P. Grahm, A. Sjöland	SKB, Sweden
P-11-04	Hydraulic response of Opalinus Clay during excavation and ventilation phases of the 1:1 scale FE Experiment	T. Vogt, H.R. Müller, B. Garitte, T. Sakaki, N. Giroud, T. Vietor	Nagra, Switzerland
P-11-05	THM modeling of the compacted GMZ bentonite in the China-Mock-up test	L. Chen	BRIUG, China
P-11-06	Stability of compacted bentonite blocks and block pedestals under changing climatic conditions in tunnels and long-term loads	B. Garitte, F. Kober, H.R. Müller, S. Köhler, H. Weber, I. Blechschmidt	Nagra, Switzerland
P-11-07	FE experiment/LUCOEX: Production of bentonite based backfill materials	B. Garitte, H.R. Müller, H. Weber	Nagra, Switzerland
P-11-08	FE experiment: THM modelling, predictions, observations and interpretation	B. Garitte, K. Thatcher, T. Vogt, H.R. Müller, T. Vietor	Nagra, Switzerland
P-11-09	3D Numerical simulation on thermo-hydro-mechanical coupled behavior of Boom clay in PRACLAY heating experiment	W.Z. Chen[1], Z. Gong[1], X-L. Li[2], G.J. Chen[2], X. Sillen[3], H.D. Yu[1]	[1]Chinese Academy of Science, China / [2]EIG EURIDICE, SCK•CEN, Belgium / [3]ONDRAF/NIRAS, Belgium
P-11-10	Medium scale ATLAS IV in situ heating test in Boom Clay	G.J. Chen[1], X-L. Li[1], J. Verstricht[1], X. Sillen[2]	[1]EIG EURIDICE, Belgium / [2]ONDRAF/NIRAS, Belgium

BENTONITE HYDRO-MECHANICS

P-12-01	Consequences of water inflow and early water uptake in deposition holes (EVA-project)	L. Börgesson[1], T. Sandén[1], A. Dueck[1], L. Andersson[1], V. Jensen[1], U. Nilsson[1], S. Olsson[1], M. Åkesson[1], O. Kristensson[1], U. Svensson[2], J. Hernelind[3]	[1]Clay Technology AB, Sweden / [2]Computer-aided Fluid Engineering AB, Sweden / [3]5T Engineering AB, Sweden
P-12-02	Modelling of bentonite swelling in complex geometries	L. Börgesson[1], A. Dueck[1], R. Goudarzi[1], J. Hernelind[2]	[1]Clay Technology AB, Sweden / [2]5T Engineering AB, Sweden
P-12-03	Column tests on pellets-based barrier material: analysis and interpretation	A. Gens[1], R.B. de Vasconcelos[1], M.V. Villar[2], J.C. Mayor[3], P.L. Martín[2]	[1]Universitat Politècnica de Catalunya, Spain / [2]CIEMAT, Spain / [3]ENRESA, Spain
P-12-04	Buffer homogenization after loss of bentonite – medium scale laboratory test	A. Dueck, R. Goudarzi, L. Börgesson	Clay Technology AB, Sweden
P-12-05	Theoretical Studies with Density Functional Theory on Ca/ Na Montmorillonite: Structure, Forces and Swelling Properties	L. Liu, G. Yang, I. Neretnieks, L. Moreno	Royal Institute of Technology, Sweden

P-12-06	Different conceptual models for bentonite re-saturation leading to similar mathematical process descriptions	K.-P. Kröhn	GRS, Germany
P-12-07	An extended vapour diffusion model for modelling non-isothermal re-saturation of bentonite buffers	K.-P. Kröhn	GRS, Germany
P-12-08	Wetting Behavior of Bentonite Pellets	J. Martikainen[1], T. Schatz[1], N. Kanerva[1], K. Koskinen[2]	[1]B+Tech Oy, Finland / [2]Posiva Oy, Finland
P-12-09	Testing Backfill Performance in a Pilot-Scale Deposition Tunnel	J. Martikainen[1], T. Schatz[1], J. Autio[1], P. Marjavaara[1], K. Koskinen[2]	[1]B+Tech Oy, Finland / [2]Posiva Oy, Finland
P-12-10	Hydraulic Sealing Ability of Bentonite Pellets at Small, Contact Apertures	J. Martikainen[1], T. Schatz[1], K. Koskinen[2]	[1]B+Tech Oy, Finland / [2]Posiva Oy, Finland
P-12-11	Axial Homogenization of Bentonite: Experiments and Modelling	Md. Mamunul Hassan[1], J. Martikainen[1], K. Koskinen[2]	[1]B+Tech Oy, Finland / [2]Posiva Oy, Finland
P-12-12	The bentonite rock interaction experiment (BRIE) - results from the bentonite parcels	M. Åkesson[1], Å. Fransson[2], A. Sjöland[3]	[1]Clay Technology AB, Sweden / [2]Chalmers University of Technology, Sweden / [3]SKB, Sweden
P-12-13	Dome plug for deposition tunnels – lab tests and design modeling	L. Börgesson, T. Sandén, M. Åkesson	Clay Technology AB, Sweden
P-12-14	The distribution of buffer saturation times in the planned Forsmark Repository	D. Malmberg	Clay Technology AB, Sweden
P-12-15	Coupled hydro-mechanical modelling of bentonite resaturation and swelling for DECOVALEX-2015	K.E. Thatcher[1], A.E. Bond[1], C. McDermott[2], A.P. Fraser-Harris[2], S. Norris[3]	[1]Quintessa Ltd, UK / [2]University of Edinburgh, UK / [3]RWM, UK
P-12-16	Model Development for Thermohydrological-Mechanical (THM) Behavior of Bentonite	R. Fedors[1], C. Manepally[2], S. Stothoff[2], G. Ofoegbu[2], B. Dasgupta[2]	[1]NRC, USA / [2]CNWRA, USA
P-12-17	Characterisation of the volumetric behaviour of MX-80 aggregates using water retention data	V. Navarro[1], L. Asensio[1], Á. Yustres[1], X. Pintado[2]	[1]University of Castilla-La Mancha, Spain / [2]B+Tech Oy, Finland
P-12-18	Variations in unconfined strength results of highly compacted bentonite blocks with respect to various aspects of testing procedures and specimen characteristics	R. Vasicek, M. Levorova, Z. Kaisr	Czech Technical University in Prague, Czech Republic

GAS TRANSFER			
P-13-01	Development of Safety Assessment Scenarios for Gas Behavior in the Bentonite Barrier for TRU Waste Disposal Concepts in Japan	H. Kawamura[1], K. Koga[2], H. Owada[2]	[1]Obayashi Corporation, Japan / [2]RWMC, Japan
P-13-02	Gas migration through a pre-compacted bentonite blocks: in situ demonstration of a gas breakthrough	R. de La Vaissière[1], J. Talandier[2]	[1]Andra, Centre de Meuse/ Haute-Marne, France / [2]Andra, France
P-13-03	Key Achievements of the FORGE Project	R.P. Shaw	BGS, UK
P-13-04	Gas-Permeable Seal Tests at Various Scales at Grimsel Test Site (GTS)	N. Giroud, T. Spillmann, P. Marschall, S. Vomvoris	Nagra, Switzerland
P-13-05	The visualisation of gas pathways in clay-rich materials; initial results from the Fracture Visualisation Rig	A. Wiseall, R. Cuss, C. Graham, J. Harrington	BGS, UK
P-13-06	Evaluation of gas transport phenomena in support of the Full-Scale Emplacement Experiment at the Mont Terri URL	A. Pappafotiou[1], R. Senger[1], P. Marschall[2], B. Garitte[2], H.R. Müller[2]	[1]INTERA Incorporated, Switzerland / [2]Nagra, Switzerland

P-13-07	The gas permeability and self-healing ability of Czech Ca-Mg bentonite	J. Smutek, L. Hausmannova, J. Svoboda	Czech Technical University in Prague, Czech Republic
P-13-08	Scoping calculations of hydrogen generation, transport and consumption in bentonite and Opalinus clay	A. Idiart[1], G. Román Ross[1], O. Silva[1], F. Grandia[1], L. Duro[1], M. Sentís[2]	[1]Amphos 21, Spain / [2]ENSI, Switzerland
P-13-09	Anisotropic diffusion of dissolved gases in Boom Clay	E. Jacops[1,2,3], N. Maes[1], A. Grade[1], J. Govaerts[1], E. Weetjens[1]	[1]SCK•CEN, Belgium / [2]KU Leuven, Belgium / [3]RWTH Aachen University, Germany
P-13-10	Measuring the diffusion coefficient of helium in clay formations envisaged for geological disposal of radioactive waste (Boom Clay, Opalinus Clay and Callovo-Oxfordian Clay)	A. Grade, E. Jacops, N. Maes, J. Govaerts	SCK•CEN, Belgium
P-13-11	Investigating the consequences of uncertainties on gas generation and dissipation for the design and performance of a repository	L.Yu[1], E. Weetjens[1], M. Capouet[2], X. Sillen[2]	[1]SCK•CEN, Belgium / [2]ONDRAF/NIRAS, Belgium
P-13-12	Compressibility properties on loading and on air injection of two deep claystone formations	E. Romero[1], P. Marschall[2], L. González[1], R. Gómez[1]	[1]Universitat Politècnica de Catalunya, Spain / [2]Nagra, Switzerland

MASS TRANSFER

MASS TRANSFER - 1

P-14-01	On the role of "surface diffusion" and competing cations for diffusion of transition metal ions in Opalinus Clay	L.R. Van Loon, W. Pfingsten	PSI, Switzerland
P-14-02	Multispecies random walk simulations in radial symmetry – model concept, benchmark and application to HTO, ^{22}Na & ^{36}Cl diffusion in clay	S. Meng, W. Pfingsten	PSI, Switzerland
P-14-03	Influence of the ionic strength on the diffusion in clay rocks of three sorbing cations: Sr^{2+}, Zn(II) and Eu(III)	S. Savoye, J-L. Lacour, B. Grenut, A. Fayette	CEA, France
P-14-04	Re-saturation and THMC behaviour of bentonite buffers: modelling capabilities, uncertainties and developments	D.G. Bennett[1], S.J. Benbow[2], A.E. Bond[3], M. Shibata[4], K. Ozone[5], H. Takase[5]	[1]TerraSalus, UK / [2]Quintessa Ltd, The Hub, UK / [3]Quintessa Ltd, UK / [4]JAEA, Japan / [5]Quintessa, Japan
P-14-05	Exploring the quantification of groundwater fluxes in the aquifers surrounding a clay host rock	B. Rogiers, M. Gedeon, S. Labat, K. Vandersteen, B. Leterme, K. Beerten, M. De Craen	SCK•CEN, Belgium
P-14-06	Detailed characterisation of borehole cores from deep aquifers surrounding a potential clay host formation, using air permeameter measurements	B. Rogiers[1], K. Vandersteen[1], L. Potums[2], G. Bennett[3,4]	[1]SCK•CEN, Belgium / [2]KU Leuven, Belgium / [3]University of Brussels, Belgium / [4]University of Dodoma, Tanzania
P-14-07	A synthesis of NE-Belgium hydrogeology	K. Vandersteen, M. Gedeon, B. Leterme, B. Rogiers	SCK•CEN, Belgium
P-14-08	Overview of more than 30 years of hydrogeological research in the Belgian nuclear waste disposal programme	K. Vandersteen, M.Gedeon	SCK•CEN, Belgium
P-14-09	A new multiscale approach to modelling the fully coupled hydraulic and thermal evolution of a whole repository throughout its lifetime	A.E. Bond[1], K.E. Thatcher[1], G.H. Towler[1], J. Wendling[2]	[1]Quintessa Ltd, UK / [2]Andra, France

P-14-10	Surface diffusion effects for transition metals in compacted illite	M.A. Glaus[1], M. Aertsens[2], C.A.J. Appelo[3], T. Kupcik[4], N. Maes[2], L. Van Laer[2], L.R. Van Loon[1]	[1]PSI, Switzerland / [2]SCK•CEN, Belgium / [3]Hydrochemical Consultant, The Netherlands / [4]KIT, Germany
P-14-11	Pore network model of electrokinetic transport through charged porous media	B. Rotenberg[2,3], A. Obliger[1,2,3], M. Jardat[2,3], D. Coelho[1], S. Békri[4],	[1]Andra, France / [2]Sorbonne Universités, UPMC Univ. Paris 06, France / [3]CNRS, UMR 8234 PHENIX, France / [4]IFP Energies nouvelles, France
P-14-12	Nature of water diffusion in montmorillonite at different scales: Combination of experimental and modelling approaches	S.V. Churakov[1], T. Gimmi[1,2], L.R. Van Loon[1], F. Juranyi[1]	[1]PSI, Switzerland / [2]University of Bern, Switzerland
P-14-13	Piping and erosion in 1:6 scale tests simulating the saturation of the bentonite buffer in Olkiluoto KBS-3V repository	T. Laurila[1], E. Rautioaho[1], P. Sane[1], X. Pintado[1], K. Koskinen[2]	[1]B+Tech Oy, Finland / [2]Posiva Oy, Finland
P-14-14	The impact of glacial fluid invasion on vertical advective and diffusive processes in the thick Ordovician limestones and shales of the Eastern Michigan Basin	K. Novakowski, O. A. Khader	Queen's University, Canada
P-14-15	Modelling radionuclide transport through a layered porous medium: Analytical analysis to guide simplifications	M. Hayek[1], G. Mayer[1], A. Poller[2]	[1]AF-Consult, Switzerland / [2]Nagra, Switzerland
P-14-16	An improved model for through-diffusion experiments: application to Sr diffusion in Boom Clay and compacted illite	M. Aertsens, L. Van Laer, N. Maes, J. Govaerts	SCK•CEN, Belgium
P-14-17	Study of ^{85}Sr transport through a column filled with crushed granite in presence of bentonite colloids	K. Videnská[1,2], R. Červinka[1], V. Havlová[1]	[1]ÚJV Řež, Czech Republic / [2]Institute of Chemical Technology, Czech Republic
P-14-18	U(VI) diffusion as a function of bentonite bulk density: Results from a 6-year study	C. Joseph[1], J. Mibus[2*], P. Trepte[2§], C. Müller[2], V. Brendler[2], A.B. Kersting[1], M. Zavarin[1]	[1]LLNL, USA / [2]Institute of Resource Ecology, Germany
P-14-19	Helium and argon vertical distribution in porewaters of the Eastern Paris Basin (Bure/Haute-Marne) : constraints on transport processes through the sedimentary sequence	P. Jean-Baptiste[1], B. Lavielle[2], E. Fourré[1], T. Smith[2], M. Pagel[3]	[1]CEA-Saclay, France / [2]Université de Bordeaux, France / [3]Université Paris-Sud, France
P-14-20	THM Modelling of Onkalo - Radioactive Waste Disposal Project	E. Toprak[1], S. Olivella[1], X. Pintado[2]	[1]Escola de Camins, UPC, Spain / [2]B+Tech Oy, Finland
P-14-21	Perturbing a field diffusion experiment: The DR-A test at the Mont Terri Underground Rock Laboratory (Switzerland)	T. Gimmi[1,2], O.X. Leupin[3], J.M. Soler[4], L.R. Van Loon[1], J. Eikenberg[1], M.A. Glaus[1], H.N. Waber[2], W. Pfingsten[1], M. Xie[5], K.U. Mayer[5], C.A.J. Appelo[6], C.I. Steefel[7]	[1]PSI, Switzerland / [2]University of Bern, Switzerland / [3]Nagra, Switzerland / [4]IDAEA-CSIC, Spain / [5]University of British Columbia, Canada / [6]The Netherlands / [7]LBNL, USA
P-14-22	Possibility of using bentonite clay and red clay as a barrier material for sealing of radioactive waste	W. Olszewska, A. Miśkiewicz, G. Zakrzewska - Kołtuniewicz	Institute of Nuclear Chemistry and Technology, Poland
P-14-23	Migration of calcium and bicarbonate ions in water-saturated compacted montmorillonite under electrical potential gradient	S. Tanaka[1], M. Mizuto[1,2], N. Watanabe[1], T. Kozaki[1]	[1]Hokkaido University, Japan / [2]Tokyo Nuclear Services, Japan

P-14-24	Influence of hydraulic gradient on the transport of Dissolved Organic Matter in Boom Clay	D. Durce, C. Bruggeman, N.Maes	SCK•CEN, Belgium
P-14-25	Extrusion and Erosion of Bentonite Buffer Material in Sloped Fracture Environments	T. Schatz, N. Akemati	B+Tech Oy, Finland
P-14-26	The Ypresian clays as a potential host rock for radioactive waste disposal in Belgium: knowledge gaps in the hydrogeology	P.J. Haest[1], Y. Meyus[1], H. Van Baelen[2], L. Wouters[2]	[1]A.G.T. n.v., Belgium / [2]ONDRAF/NIRAS, Belgium

MASS TRANSFER - 2			
P-15-01	Effect of confining pressure on diffusion coefficients: Ordovician shale and limestone, southwest Ontario, Canada and Opalinus clay, Switzerland	T. Al, Y. Xiang	University of New Brunswick, Canada
P-15-02	Diffusion and Sorption of Sr in Compacted Sodium Montmorillonite: Multispecies Modeling	Y. Tachi, K. Yotsuji, T. Ito, T. Suyama	JAEA, Japan
P-15-03	The possibility of salt accumulation due to coupled localized inflow and vapour transport in a KBS-3 repository	M. Birgersson, R. Goudarzi	Clay Technology AB, Sweden
P-15-04	Swelling and erosion of bentonite/montmorillonite in dilute aqueous solutions	M. Hedström[1], E. Hansen[1], N. Kanerva[2], T. Schatz[2]	[1]Clay Technology AB, Sweden / [2]B+Tech Oy, Finland
P-15-05	Homogenisation of a dual density bentonite interface	C.C. Graham[1], J.F. Harrington[1], R.J. Cuss[1], P. Sellin[2]	[1]BGS, UK / [2]SKB, Sweden
P-15-06	Inflow characterization and predicting the TH evolution of a full-scale repository test in Olkiluoto	X. Pintado, E. Rautioaho	B+Tech Oy, Finland
P-15-07	Size distribution of bentonite colloids upon fast disaggregation in lower ionic strength waters	N. Mayordomo[1], C. Degueldre[2], U. Alonso[1], T. Missana[1]	[1]CIEMAT, Spain / [2]PSI, Switzerland
P-15-08	Bentonite erosion and stability of formed colloids	P. Hölttä, V. Suorsa, S. Niemiaho, J. Lehto	University of Helsinki, Finland
P-15-09	Sorption and diffusion behavior of Cs in illite-added compacted montmorillonite	T. Ishidera[1], S. Kurosawa[2], M. Hayashi[2], K. Uchikoshi[2], H. Beppu[2]	[1]JAEA, Japan / [2]Inspection Development Corporation, Japan
P-15-10	Models for ionic diffusion in compacted bentonite. Application to the ABM field test at the Äspö Hard Rock Laboratory	A. Idiart[1], M. Pękala[1], P. Sellin[2]	[1]Amphos 21, Spain / [2]SKB, Sweden
P-15-11	PhreeqcRM: A reaction engine for flow and transport simulators based on the geochemical modelling framework PHREEQC	L. Wissmeier[1], D. L. Parkhurst[2]	[1]AF Consult, Switzerland / [2]U.S. Geological Survey, USA
P-15-12	Large-scale meshing for safety calculations for the planned deep geological repository and its surrounding geological environment in France	N. Hubschwerlen[1], J. Roger[2], L. Tacher[3], B. Vialay[2]	[1]AF Consult, Switzerland / [2]Andra, France / [3]Terre+, Switzerland
P-15-13	Groundwater and thermohaline modelling in the Paris Basin, considering the past geodynamic evolution	J. Holmén[1], H. Benabderrahmane[2]	[1]Golder Associates, Sweden / [2]Andra, France
P-15-14	Acquisition of a permeability profile through the Opalinus Clay at the Mont Terri rock laboratory from a petrophysics-related Poiseuille type law applied to BDB-1 borehole samples	J-M. Matray[1], L. Ould-Bouya[1,2], C. Yu[1]	[1]IRSN, France / [2]University of Paris-Sud 11, France
P-15-15	Process based modelling of Cs transport in Boom Clay	N. Maes, L. Muthwill, L. Van Laer, S. Liu, C. Bruggeman	SCK•CEN, Belgium

P-15-16	Origin of halides (Cl^- and Br^-) and of their stable isotopes ($\delta^{37}Cl$ and $\delta^{81}Br$) at the Tournemire clayrock URL (France) - Experimental and numerical approach	N. Bachirbey[1,2], J-M. Matray[1]	[1]IRSN, France / [2]Université Paris-Sud 11, France
P-15-17	Geochemical evolution and reactive transport of radionuclides in the near-field of a disposal cell for high-level vitrified waste in the Callovo-Oxfordian claystone: the impact of coupled processes on radionuclides retardation	M. Pękala[1], O. Silva[1], D. García[1], J. Molinero[1], M. Grivé[1], A. Idiart[1], I. Munier[2], N. Michau[2], E. Giffaut[2], B. Cochepin[2]	[1]Amphos 21, Spain / [2]Andra, France
P-15-18	Numerical computation of relative permeabilities of argillaceous porous media using Lattice Boltzmann Models and X-ray tomography images	S. Ben Hadj Hassine[1], M. Dymitrowska[1], V. Pot[2], A. Genty[3]	[1]IRSN, France / [2]INRA, France / [3]CEA Saclay, France
P-15-19	The scaling properties of Neretnieks' model for glacial erosion	M. Olin, V-M. Pulkkanen	VTT, Finland
P-15-20	Multitracer (HTO, ^{36}Cl, ^{85}Sr) diffusion in compacted $Cu(en)_2^{2+}$-illite and -montmorillonite	T. Kupcik[1], M.A. Glaus[2], L.R Van Loon[2], B. Baeyens[2], T. Schäfer[1], H. Geckeis[1]	[1]INE, KIT, Germany / [2]PSI, Switzerland
P-15-21	Internal structures of fault zones in low permeability formations and their relationship with fluid flow: insights from the Tournemire URL	P. Dick, C. Courbet, C. Wittebroodt, A. Dauzeres, J-M. Matray	IRSN, France
P-15-22	Characterisation of diffusive transport parameters associated with a secondary fault cross in the Upper Toarcian argillite: FRACTEX project	C. Wittebroodt, J-M. Matray, P. Dick, J. Cabrera, J-D. Barnichon	IRSN, France
P-15-23	Influence of surface conductivity on the apparent zeta potential of homoionic montmorillonite particles	P. Leroy[1], N. Devau[1], C. Tournassat[1], O. Bernard[2], M. Azaroual[1]	[1]BRGM, France / [2]Pierre and Marie Curie University, France
P-15-24	Application of electromigration technique to study radionuclide transport in compacted bentonite	E. Hofmanová[1,2], N. Maes[3]	[1]Czech Technical University in Prague, Czech Republic / [2]Fuel Cycle Chemistry Department, Czech Republic / [3]SCK•CEN, Belgium
P-15-25	Critical insight into methodology of through-diffusion experiments and their evaluation	E. Hofmanová[1,2], D. Vopálka[1], A. Vetešník[1]	[1]Czech Technical University in Prague, Czech Republic / [2]Fuel Cycle Chemistry Department, Czech Republic
P-15-26	Monte-Carlo-based uncertainty propagation in an up-scaled model of solute diffusion in clays	F. Cadini[1], E. Zio[1,2]	[1]Dipartimento di Energia, Politecnico di Milano, Italy / [2]Ecole Centrale Paris and Supelec

MONITORING - GENERAL STRATEGY

MONITORING

P-16-01	FE Experiment: Monitoring of water content in Opalinus Clay using a moisture profile probe and a customized TDR sonde	T. Sakaki[1], T. Vogt[1], H.R. Müller[1], H. Wörsching[2]	[1]Nagra, Switzerland / [2]Solexperts AG, Switzerland
P-16-02	Seismic long-term monitoring in the heater experiment HE-E	K. Schuster	BGR, Germany
P-16-03	Seismic long-term monitoring - characterisation of the 12 years lasting Engineered Barrier Emplacement Experiment (EB/PEBS)	K. Schuster	BGR, Germany
P-16-04	Monitoring system design for Intermediate level long lived radioactive waste cells – Feedback obtained and future demonstrator in Andra's underground laboratory	R. Farhoud, S. Delepine-Lesoille, S. Buschaert, G. Hermand	Andra, France

P-16-05	Downscaled deposition hole simulation in four setups: Transparent, Rigid, Heated and Large scale	X. Pintado[1], K. Koskinen[2]	[1]B+Tech Oy, Finland / [2]Posiva Oy, Finland
P-16-06	Geoelectrical monitoring of dismantling operation within the Engineered Barrier Emplacement Experiment (Mont Terri RL)	M. Furche, K. Schuster, C. Czora, H. Albers	BGR, Germany
P-16-07	High resolution fibre-optic monitoring system for the FE Experiment in Mont Terri	K. Kishida[1], T. Vogt[2], A. Guzik[1], H.R. Müller[2], B. Frieg[2], B. Knüpfer[3]	[1]Neubrex Co., Japan / [2]Nagra, Switzerland / [3]Brugg Kabel AG, Switzerland
P-16-08	FE Experiment: The instrumentation and monitoring concept of a 1:1-scale heater experiment at the Mont Terri URL	T. Vogt, H.R. Müller, T. Sakaki, M. Hertrich, T. Spillmann, B. Garitte, N. Giroud, T. Vietor	Nagra, Switzerland
P-16-09	Safety Indicators and Demonstrators	J.B. Grupa, E. Rosca-Bocancea	NRG, The Netherlands
P-16-10	Electromagnetic techniques for Callovo-Oxfordian Clay Rockwater content measurements	S. Delepine-Lesoille[1], T. Boré[1], J-C. Robinet[1], D. Coelho[1], N. Wagner[3], G. Six[2], F. Taillade	[1]Andra, France / [2]Universite Paris Est, France / [3]Bauhaus-University Weimar, Germany
P-16-11	Ultrasonic monitoring of the concrete block support of a sealing core in Callovo-Oxfordian argilites	C. Balland[1], J. Morel[2], R. de La Vaissière[2]	[1]INERIS, France / [2]Andra, Centre de Meuse/Haute-Marne, France
P-16-12	Data Mining Approach for heavily instrumented repository cells	G. Hermand, N. Gilardi, S. Buschaert, A. Chabiron, N. Stoffels	Andra, France

GENERAL STRATEGY FOR Clay-based DISPOSAL SYSTEMS			
P-17-01	The optimum bentonite for the disposal of high level radioactive waste	S. Kaufhold[1], R. Dohrmann[1,2]	[1]BGR, Germany / [2]LBEG, Germany
P-17-02	Full-Scale Shaft Seal in Granite: Status after 6 Years (2009-2014) of Natural Evolution	D.A. Dixon[1], D.G. Priyanto[2], S. Stroes-Gascoyne[2], P. Korkeakoski[3], R. Farhoud[4]	[1]Golder Associates Limited, Canada / [2]AECL, Canada / [3]Posiva Oy, Finland / [4]Andra, Paris
P-17-03	Perspective of clay-salt slimes using as a sorbent of radionuclide and for safety disposal of radioactive waste	L. N. Maskalchuk, A. A. Baklay, T. G. Leontieva, D. K. Stralenka	Joint Institute for Power and Nuclear Research, Belarus
P-17-04	A Study on the Seismic Response of an Engineered Barrier System	S. Sato[1], Y. Yamamoto[2], S. Suzuki[2], K. Ito[1]	[1]Obayashi Corporation, Japan / [2]NWMO, Japan
P-17-05	SEALEX In situ Experiments-Performance Tests Of Repository Seals: Experimental observations and modelling	N. Mokni, J-D. Barnichon	IRSN, France
P-17-06	Disposal facility for solid low and intermediate level radioactive waste (LILW) intended to be constructed in clay deposits	A. Barinov, A. Tkachenko, S. Speshilov	FSUE, Russian Federation
P-17-07	DOPAS EPSP experiment	J. Svoboda[1], J. Pacovský[1], M. Dvořáková[2], I. Hanusová[2], P. Večerník[3], D. Trpkošová[3]	[1]Czech Technical University in Prague, Czech Republic / [2]SÚRAO, Czech Republic / [3]ÚJV Řež, a. s., Czech Republic
P-17-08	Inflow handling during the emplacement of the backfill in the KBS-3 concept	V. Koskinen[1], T. Sandén[2]	[1]Fortum Power and Heat Oy, Finland / [2]Clay Technology AB, Sweden

P-17-09	EB Experiment: from design to dismantling	M. Rey Mazón[1], J.L. García-Siñeriz[1], B. Palacios[1], J.C. Mayor[2]	[1]AITEMIN, Spain / [2]ENRESA, Spain
P-17-10	Numerical Modelling of 6 Years Natural Saturation of a Full-Scale Shaft Seal in Granite (2009-2014)	D.G. Priyanto[1], D.A. Dixon[2], P. Korkeakoski[3], R. Farhoud[4]	[1]AECL, Canada / [2]Golder Associates Limited, Canada / [3]Posiva Oy, Finland / [4]Andra, France
P-17-11	Geo-scientific Information System Upgrade	M. Gedeon[1], H. De Soete[1], A. Berckmans[2]	[1]SCK•CEN, Belgium / [2]ONDRAF/NIRAS, Belgium
P-17-12	KBS-3H Multi-Purpose test	X. Pintado[1], J. Autio[1], J.L. García-Siñeriz[2], M. Kronberg[3]	[1]B+Tech Oy, Finland / [2]Aitemin, Spain / [3]SKB, Sweden
P-17-13	DOPAS- Full-Scale Demonstration Of Plugs And Seals	J. Hansen	Posiva Oy, Finland
P-17-14	Large-scale sealing experiment in the Meuse/Haute Marne Underground Research Laboratory	R. de La Vaissière, N. Conil, F. Leveau, G. Armand	Andra, Centre de Meuse/ Haute-Marne, France
P-17-15	Material characterisation and laboratory models for EPSP experiment in DOPAS project	P. Večerník[1], D. Trpkošová[1], J. Gondolli[1], J. Svoboda[2], M. Dvořáková[3], V. Havlová[1]	[1]ÚJV Řež, Czech Republic / [2]Czech Technical University in Prague, Czech Republic / [3]SÚRAO, Czech Republic
P-17-16	Approaches to Evaluate and Underpin the Technical Feasibility of the Belgian Disposal Concept	S. Doudou[1], E.J. Harvey[1], P.J. Richardson[1], S.M. Wickham[1], P. Van Marcke[2]	[1]Galson Sciences Ltd, UK / [2]ONDRAF/NIRAS, Belgium
P-17-17	Bentonite buffer design and recognition of risks for Finnish KBS-3V concept	M. Juvankoski[1], E. Holt[1], E. Niemeläinen[1], P. Rantamäki[2]	[1]VTT, Finland / [2]Posiva Oy, Finland
P-17-18	Development of subsurface disposal facility for radioactive wastes in North-West region of Russian Federation (condition and prospects)	D.I. Pavlov, A.V. Demin, V.T. Sorokin, V.V. Kascheev, V.U. Petrov	JSC "ATOMPROEKT", Russian Federation
P-17-19	The monuments of a new kind	C. Massart	Artist-Researcher, Belgium
P-17-20	Andra's scientific knowledge management: an integrated and structured approach to improve data traceability (ISIS project)	A. Chabiron, E. Huret, M. Garcia	Andra, France
P-17-21	Development and application of a safety assessment methodology in preparation for a safety case	M. Capouet[1], C. Depaus[1], E. Weetjens[2], J. Govaerts[2], P. Smith[3]	[1]ONDRAF/NIRAS, Belgium / [2]SCK•CEN, Belgium / [3]Safety Assessment Management GmbH, Switzerland
P-17-22	FE Experiment / LUCOEX: Development of a prototype machine for backfilling horizontal emplacement tunnels with granulated bentonite	H. Jenni[1], S. Köhler[2], H.R. Müller[2]	[1]ROWA, Rowa Tunnelling Logistics AG, Switzerland / [2]Nagra, Switzerland
P-17-23	Support Design of a Large Diameter Gallery for Mid-level Nuclear Waste in Cigéo Project	R. Plassart[1], F. Laigle[1], A. Saitta[2], G. Suzac[2], F. Martin[3], M. Janutolo[3]	[1]EDF, France / [2]EGIS Tunnels, France / [3]BG Ingénieurs-conseils, France
P-17-24	Swiss backfilling concept – Requirements and Approaches for Optimization of the Bentonite Barrier around SF/HLW Disposal Canisters	S. Köhler, T. Fries, H.R. Müller, I. Gaus	Nagra, Switzerland
P-17-25	IGD-TP main achievements to date and role in implementing the European policy on radioactive waste	J. Delay[1], R. Kowe[2], M. Garcia[3]	[1]Andra, Centre de Meuse/ Haute-Marne, France / [2]RWM, UK / [3]Andra, France

CLAY CONFERENCE

BRUSSELS | March 23-26, 2015

6th International conference | SQUARE Brussels Meeting Centre



ABSTRACTS
ORAL SESSIONS

Feasibility of excavation and THM behavior of a full scale disposal cell for nuclear waste in 500 m deep clay formation

J. Morel, **F. Bumbieler, N. Conil, G. Armand**

Andra, Laboratoire de recherche souterrain de Meuse Haute Marne, RD960, 55290 Bure, France

At the Meuse/Haute Marne Underground Research Laboratory, excavated in a 500 m deep clay formation, Andra carries out for several years experiments to study the possibility of disposal for long-lived and intermediate to high level activity waste in deep geological repositories.

The concept of disposal cells studied for high level activity waste (HLW) consists in horizontal micro-tunnels at least 80 m long and about 70 cm in diameter. It comprises a cell body, for waste package disposal, and a cell head, partly backfilled with a swelling-clay plug and then sealed with a concrete plug to provide additional safety. The micro-tunnel is equipped with a casing to allow the emplacement and the retrieval of waste containers. The casing in the head part is slightly larger in diameter in order to absorb the thermal dilation of the body part casing due to heating induced by exothermic packages.

Several campaigns of tests have been carried out since 2009, in order to demonstrate the feasibility of excavation of such micro-tunnels, to study the HM behavior of the rock mass in response to the excavation, and to study the mechanical behavior of the casing. The excavation method uses a guided auger drilling machine, with advance casing.

A full scale demonstrator representative of the benchmark concept has been excavated at the end of 2012, with the objective to study its behaviour under thermal loading (figure 1). The main part of this demonstration experiment is carried out in the framework of the European LUCOEX project. Heat produced by waste packages is simulated using electrical heaters.

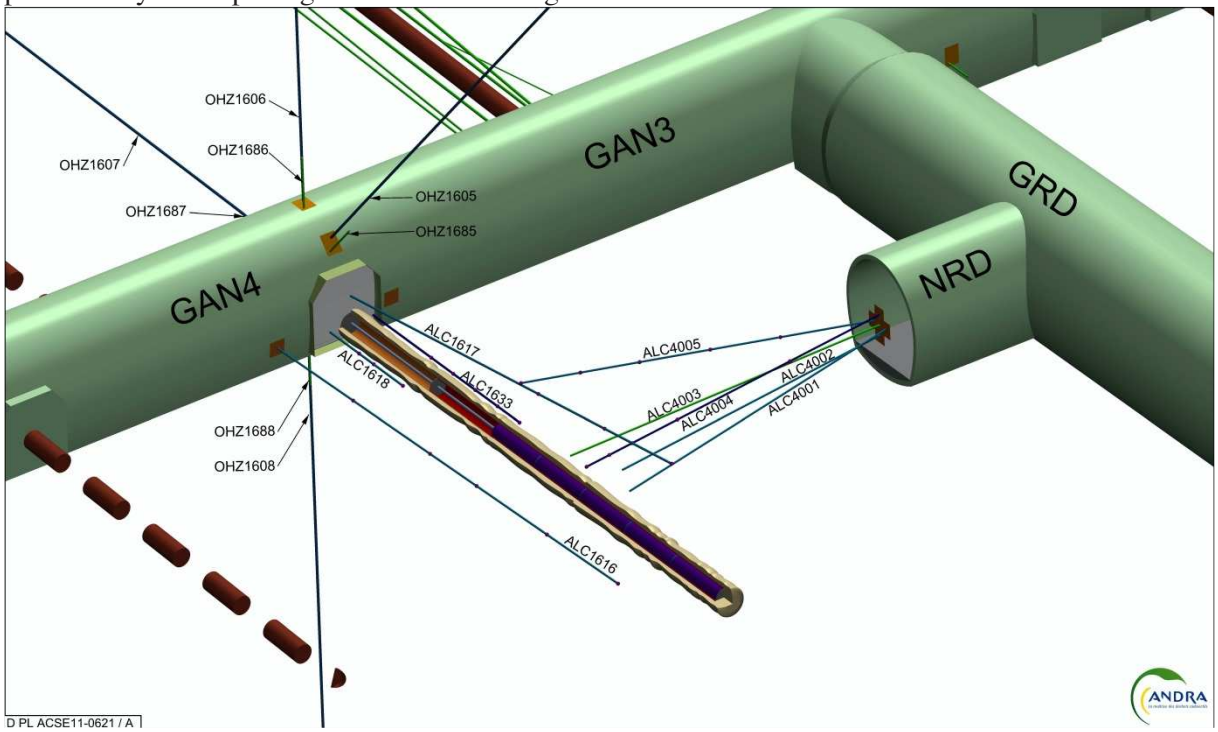


Figure 1 – general view of the HLW cell demonstrator

Casing in head and body parts is instrumented to monitor its thermo mechanical behaviour as well as the rock interface evolution. A surrounding instrumentation has been installed in boreholes and in the access drift to monitor the THM behaviour of the host rock. Heating, performed over a length of 15 m, has started in April 2013 with the goal to reach 90° C at the rock interface in about 2 years.

Monitoring of the excavation showed a HM impact consistent with what was observed in the former phases of the demonstration program, i.e. strong overpressures generated in the near field of the cell horizontal plane.
Mechanical loading of the cell casing starts very quickly after excavation, showing an anisotropic behaviour with a convergence of the casing in the horizontal plane. This mechanism can be directly related to the shape and characteristics of the damaged zone around the cell, and is consistent with what is observed around larger diameter drifts with the same orientation with respect to the natural stress field. It shows also that the annular space between the cell wall and the casing is partly filled with excavation rubbles due to breakouts and spalling, allowing the transmission of the cell wall convergence to the casing.
Heating accelerates cell wall convergence, resulting in an increase in casing loading in the body part (figure 2). However the measured deformations stay small and the local stress measured on the inner face of the casing remains widely below the yield strength of the steel. Sliding of the casing in the insert, due to thermal dilation, is also measured, showing the good operation of the cell head.
THM impact in the near field in the cell horizontal plane is consistent with what was measured with smaller scale THM experiments. Kinetics differences are observed in the cell vertical plane.

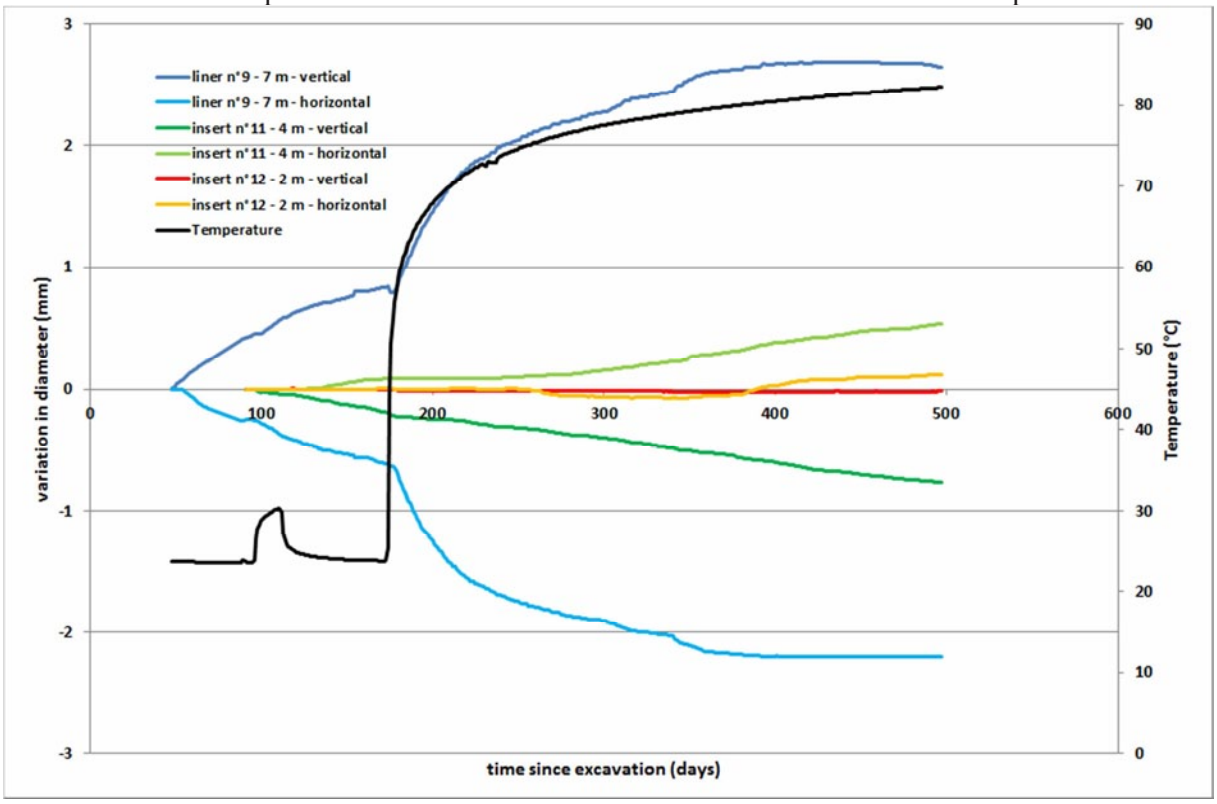


Figure 2 – casing and insert diameter variation

Monitoring is ongoing and numerical modelling is currently being carried out to help in the analysis of these in-situ measurements.

THM analysis of a heating experiment in Callovian-Oxfordian Clay

A. Gens[1*], J. Vaunat[1], B. Garitte[3], M. Rostovanyi[1], N. Conil[2] and G. Armand[2]

1. Department of Geotechnical Engineering and Geosciences, Universitat Politècnica de Catalunya, E-08034 Barcelona, Spain (antonio.gens@upc.edu).
2. Andra, Centre de Meuse/Haute-Marne, Route Départementale 960F. 55290 Bure, France
3. NAGRA, Hardstrasse 73, 5430 Wettingen, Switzerland

(*) corresponding author

The TED experiment is a heating experiment in Callovo-Oxfordian Clay stone that has been performed in the Meuse Haute Marne underground research laboratory. It was developed by Andra to confirm the results obtained in a previous thermal experiment (TER). The main objectives were: characterisation of the thermal properties of intact argillite, identification of the Thermo-Hydro-Mechanical (THM) coupling parameters, improvement of the understanding of THM behaviour and comparison of parameters measured in-situ and in the laboratory. The TED experiment involved three heaters installed in three boreholes at a distance of about 2.7 m. This arrangement was intended to verify the superposition of several temperature fields and study the overpressure generated. This experimental concept "simulate" at a small scale the configuration of high level Long life nuclear wastes cells with parallel micro tunnels.

Three heaters (TED1201, TED1202 and TED1203), each 4 m long, have been installed at the end of a 160 mm diameter and 14 m long boreholes. Scoping calculations were performed with parameters determined in previous experiment TER to design the TED experiment. The nominal power to be applied in each heater has been calculated in order to achieve a maximum temperature of 90ºC on the rock-heater interface when all heaters are simultaneously switched on.

The TED experiment is located in the GED gallery, at the main 490 m deep level (Figure 1). The excavation of the GED gallery started on 21 April 2008, and ended 9 months later, on 22 January 2009. The installation of the instrumentation started six months later, in July 2009, and finished with the installation of the heaters in October 2009. The experiment was heavily instrumented with 116 temperature sensors in the rock mass and 72 in the heater boreholes, 18 piezometers and 2 extensometers and inclinometers in order to observe in detail the in situ THM behaviour of the argillite. The first heating stage started on 25 January 2010 (Figure 1), when the central heater TED1201 was switched on; approximately one year later, on 1 March 2011, the two remaining heaters were also turned on. This second heating stage lasted one year and a half and, on 22 October 2012, the power of all heaters started to decrease step by step and the heating phase ended on 18 July 2013.

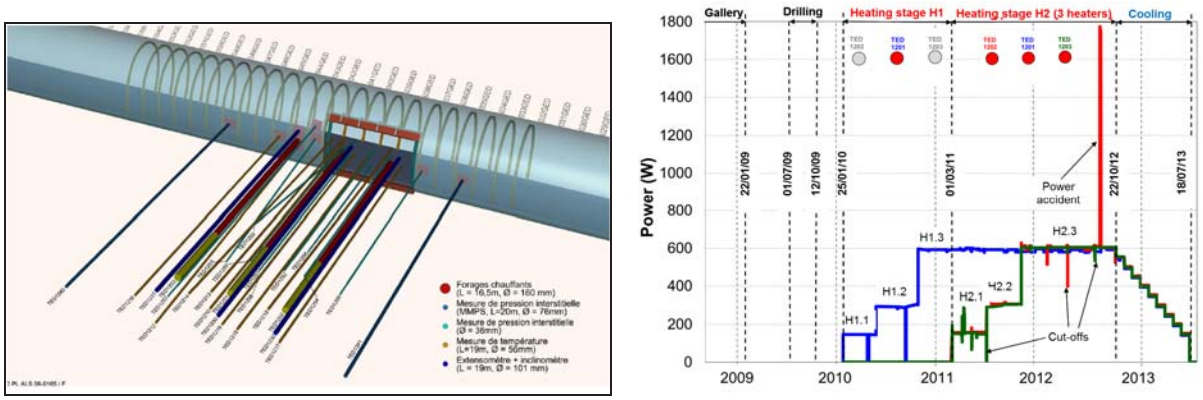


Fig. 1. General lay-out of the TED experiment and sequence of heating/cooling stages.

Interpretation of the test has been assisted by the performance of a suite of analyses simulating the experiment reported in this document. A general coupled THM formulation has been adopted that incorporates the relevant multi-physics phenomena present in the test. Some simplifications are possible due to the fact that the host medium remains unsaturated throughout. In order to incorporate the thermal, hydraulic and mechanical anisotropic properties exhibited by the behaviour of the Callovo-Oxfordian argillite, three-dimensional numerical analyses have been performed. The non-isotropic in situ stress field has also been properly considered.

A very large number of thermal analyses have been performed to obtain the values of anisotropic thermal conductivity that lead to the closest reproduction of the temperatures recorded during the test. As a general rule, a very good reproduction of the temperature field and its variation with time during both heating and cooling has been achieved. Those optimized anisotropic thermal conductivity parameters are subsequently used in the THM computations.

As foreseen, heating of the Callovo-Oxfordian argillite has resulted in significant increases of pore pressures due to the differential thermal expansion of pore water and of soil skeleton and solid phase. The evolution of pore pressures is the result of the interplay of pore pressure generation by heating and pore pressure dissipation. Observations of pore pressures show that the evolution of pore pressures is affected by the anisotropic properties of thermal conductivity, stiffness and permeability.

In addition to the anisotropic properties of the Callovo-Oxfordian argillite the following aspects have been considered: drainage towards the adjacent gallery and some of the test boreholes, variation of permeability with distance to the gallery and the adoption of a more precise variation of water density with temperature. The reference analysis has achieved a satisfactory reproduction of the pore pressure observations in most sensors although some departures can be observed in some individual instances. Anisotropy effects during heating and cooling are adequately captured (Figure 2).

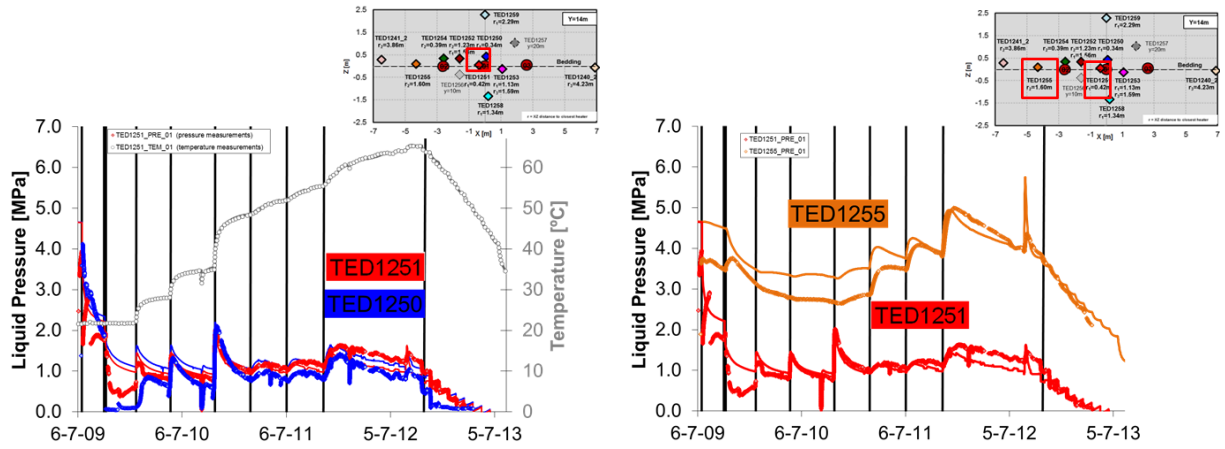


Fig. 2. Comparison of computed and measured pore pressure evolution on various piezometers throughout the duration of the experiment

To enhance the understanding of the test, a programme of sensitivity analysis has been performed varying a number of key parameters: Young's modulus, Biot's coefficient, thermal expansion coefficient and intrinsic permeability. It has been found that the effects of Biot's coefficient and of the thermal expansion coefficient are rather limited. Larger effects are obtained with the variation of the argillite stiffness (Young's modulus) and, especially, of the intrinsic permeability.

The TED experiment has yielded very valuable data on the in situ behaviour of the Callovo-Oxfordian argillite subjected to a cycle of heating and cooling. Interpretation, based on thermal and coupled THM analyses, has proved satisfactory showing that the processes involved are well understood and adequately incorporated in the formulation and associated computer code.

Reference:

- A. Gens, B. Garitte, M. Rostovanyi, J. Vaunat (2014). THM modeling of the TED experiment. Final Report. UPC-CIMNE, 89 p.

Results to date from the Mock-Up Josef in-situ physical model

***J. Stastka*, *J. Pacovsky*, L. Hausmannova, R. Vasicek, *I. Hanusova**
Czech Technical University in Prague, Faculty of Civil Engineering, Centre of Experimental Geotechnics, Thakurova 7, Praha 6, 166 29;
*Radioactive Waste Repository Authority (SÚRAO) Dlážděná 6, Praha 1, 110 00

In 2010 the Centre of Experimental Geotechnics in cooperation with the Czech Radioactive Waste Repository Authority commenced preparations for the first Czech in-situ Mock-up model (Mock-Up Josef) of a bentonite barrier in a granitic rock environment (amphibole-biotite granodiorite/tonalite of the Sázava type, Central Bohemian Pluton) which is currently underway at the Josef Underground Laboratory. Mock-up Josef follows in the footsteps of the Mock-Up-CZ laboratory physical model experiment which was conducted from 2002 to 2006 (Svoboda J. and Vasicek R. 2010). The main aim of the project is to study the stability of bentonite barrier influenced by heating (up to 90°C) when naturally saturated by underground water. Monitoring during the experiment:

- pressure, temperature and relative humidity development (continuous measurement),
- mass and water redistribution (sampling every half year in order to evaluate density and water content),
- changes in hydraulic conductivity and swelling pressure (determined using core samples) and
- mineralogical changes (sampling every half year in order to evaluate phase composition, smectite percentages and cation exchange capacity).

Mock-Up-Josef is made up of bentonite blocks, a heater, a complex monitoring system and additional stainless steel elements (construction for transport, cover, lid etc.). The model was constructed in the Josef facility above-ground laboratory (Figure 1) and subsequently transported to the underground complex in December 2012 in the form of a "supercontainer" with a diameter of 700mm and a height of 2500mm.

Construction and monitoring

The Mock-Up-Josef supercontainer was transported to a short specially-prepared experimental drift at the Josef Underground. The supercontainer was lowered into a vertical disposal hole with a diameter of 750mm and a depth of 2500mm. Czech industrially-produced bentonite "Bentonit 75" (Ca-Mg type; dried, crushed and sieved) was selected as the buffer material. Initial tests of the key geotechnical and geochemical properties and mineralogical composition were based on tried and tested procedures employed in previous projects. The bentonite was compacted in the form of blocks with a dry density of around 1.75Mg/m^3. The target dry density of the whole of the barrier following the sealing of the free spaces was estimated at around 1.5Mg/m^3. A steel heater with a diameter of 320mm was positioned in the central section of the buffer (Figure 1). The heater was then covered with a copper sheet and filled with oil which was subsequently heated to a temperature of 95°C. The variation in temperature between the bottom and top parts was reduced to 1°C with the use of an artificial circulation system. The sensors installed in the model make up an important element of the experiment. Figure 1 shows the positions of the five monitoring profiles each of which houses between 14 and 17 sensors. The hydraulic pressure cells, which monitor swelling pressure development within the bentonite, have already revealed that the evolution of pressure closely follows the saturation of the barrier. The role of the relative humidity sensors is to monitor the redistribution of water content, and the behaviour of the rock mass in the immediate vicinity of the model is being observed by means of strain gauge rock bolts and thermometers.

Evolution of the experiment

The experimental heater was switched on in late December 2012; it is envisaged that the duration of the experiment will be at least three years, i.e. the time period required to achieve full saturation. The model was constructed in such a way as to allow sampling during the course of the experiment. It is planned that sampling will take place twice a year; two samples have been taken to date: 11 and 17 months following the commencement of thermal loading. The sampling process consists of drilling through the lid to pre-determined depths. The first samples were taken from a depth of 320mm following 11 months of operation. The second samples were taken from a depth of 640mm 17 months after the start of operation. It is planned that the next samples will be taken from a depth of 800mm.

Swelling pressure, which is measured on a continuous basis, was observed to increase rapidly in the outer part of the bentonite following the placement of the model in the wet underground disposal hole.

Sampling Results

The density and water content results were assessed in order to determine changes in the development of mass and water transfer at various levels of the experimental buffer. The development of saturation is shown in Figure 2 - increases in water content and degree of saturation over time. The calculated degree of saturation can be seen to be above 80% in all positions. The core samples were also subjected to hydraulic conductivity and swelling pressure testing. The results revealed a slight increase in both parameters compared to initial values. However, no mineralogical changes were observed; smectite content varies from 59.9 to 61.8% ± 0.5% and cation exchange capacity from 68.9 to 71.1 mmol/100g.

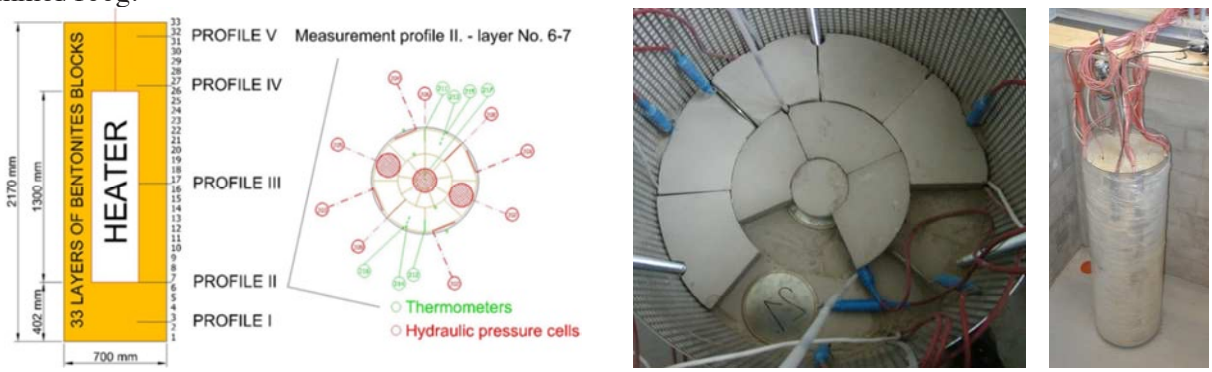


Figure 1 – Cross-sections of the model showing the location of the measurement profiles and sensors (left) and photographs taken during the construction of the model in the above-ground laboratory at the Josef Underground Research Facility (http://ceg.fsv.cvut.cz/)

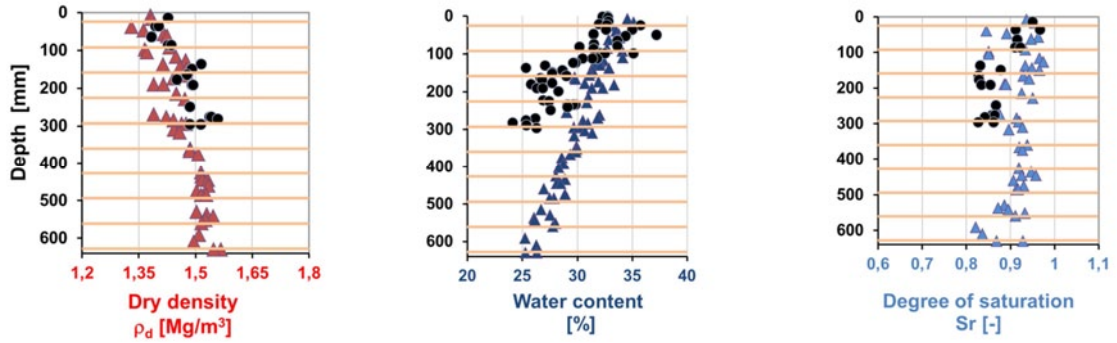


Figure 2 – Results obtained from the sampling of the bentonite at various depths and times. The rings represent the results from the first sampling session - after 11 months at a depth of 320mm below the cover. The triangles represent the results of the second sampling session - after 17 months at a depth of 640mm.

Conclusions

The Mock-Up Josef experiment has been underway since December 2012 at which time both the heating and saturation processes commenced. Swelling pressure, temperature and water content are being measured continuously. The experiment has been subjected to two sampling sessions to date in order to evaluate density, water content, hydraulic conductivity, swelling pressure, cation exchange capacity and mineralogical and chemical composition. The results so far indicate slight changes within the buffer material. The full paper provides a detailed description of the evolution of the various parameters.

References

Svoboda, J. - Vašíček, R. Preliminary geotechnical results from the Mock-Up-CZ experiment In: Applied Clay Science. 2010, vol. 47, no. 1-2, p. 139-146. ISSN 0169-1317

Acknowledgment

The research is being supported by the Czech Radioactive Waste Repository Authority (SÚRAO), number of the project is SO2011-021.

18 Years of heating a full scale EBS at 100°C (FEBEX, Grimsel Test Site) and possible applications at higher temperatures ("hotFEBEX" at > 150°C)

Kober, F.[1], **Gaus, I.**[1], **Birkholzer, S.**[1], **Vomvoris, S.**[1]

[1] Nagra, Hardtsrasse 73, 5430 Wettingen, Switzerland (*florian.kober@nagra.ch*)
[2] LBNL, One Cyclotron Road, Room 308, Mail Stop 74R316C Berkeley, CA 94720, USA

Currently, a number of heating tests have been performed for elucidating repository concepts and programmes that are considering bentonite exposed to temperatures around 100-140°C. Those experiments have been providing valuable information on the performance of various bentonites (e.g., Wyoming, FEBEX). Here we focus on the results obtained from the FEBEX experiment at Nagra's Grimsel Test Site (GTS) that has been dismantled partially in 2002, and will be finally dismantled in 2015 (FEBEX-DP). Based on this information, the knowledge gained from similar experiments (such as SKB – LOT, ANDRA – TBT, Nagra – HE-E and FE) and the objective of extending the knowledge base on bentonite performance beyond the currently tested temperature range, we will also outline potential options for a realization of an in-situ "hotFEBEX" to be conducted at temperatures of 150°C or higher.

The FEBEX experiment consists of an in-situ full-scale engineered barrier system (EBS) test for the disposal of high level waste (HLW). It is performed under natural conditions in crystalline rock in which the canisters are placed horizontally in drifts and are surrounded by a clay barrier constructed of highly compacted bentonite blocks. A partial dismantling and sampling of the EBS was carried out during 2002. Heating started in 1997 and since then a constant temperature of 100°C has been maintained in the remaining heater, while the bentonite buffer has been slowly hydrating in a natural way. A total of 632 sensors in the bentonite barrier, the rock mass, the heaters and the service zone record temperature, water saturation, humidity, total pressure, displacement, and water pressure.

The hydration pattern is relatively symmetric, with no major differences along the axis. Although the host rock is characterized by heterogeneities with zones of higher permeability, the resaturation process is driven by the suction of the bentonite rather than by the availability of water in the rock, especially in the early phase. After 17 years, the water content in the buffer close to the heater still continues to increase slowly. The hydraulic pore pressures in the buffer and the geosphere have practically stabilized. The total pressure in general continues to increase in most points into the buffer, where in some parts pressures of over 6 MPa are registered.

The long monitoring phase and the partial dismantling in 2002 indicate that the EBS has largely performed as expected. Furthermore, the major processes and couplings affecting the buffer saturation during the initial thermal period identified prior to the start of the experiment have been confirmed (Lanyon & Gaus, 2013). After 18 years of operation the experiment will be finally excavated with the following main objectives of the FEBEX-DP:

- Characterization of the key physical properties (e.g., density, water content) of the barrier and their distribution and comparison with results from the partial dismantling and model predictions

- Characterization of corrosion and microbiological processes on heater, instruments and coupons resulting from evolving redox conditions and saturation states, including gas analysis
- Characterization of mineralogical interactions at material interfaces (e.g., cement-bentonite or iron-bentonite, rock-bentonite) by macro- and micro level studies
- Assessment of sensor performance
- Further increasing understanding of the thermo-hydro-mechanical (THM) and thermo-hydro-chemical (THC) processes through integration of monitoring and dismantling results

However, aside from the information gathered from the longest heating test, other repository concepts under development are considering exposure of the bentonite to temperatures of 150°C and beyond. Bentonite performance and parameters for higher temperature are only known from small-scale lab studies, such as the physico-chemical response of materials to high temperatures (changes in mineral chemistry such as smectite to illite and the related decreased swelling capability, mechanical properties, etc.). The complex moisture transport processes and bentonite-rock interactions affecting early disposal system behaviour under natural conditions (pore pressure build-ups, steam generation, vapour diffusion, bentonite saturation etc.) are not well understood. Equally uncertain are other possible impacts such as thermal drying and cracking of the near field rock and the impact on a potentially enlarged excavation damaged zone (EDZ). Furthermore, predictive models for the coupled behaviour of natural and engineered barriers are not tested for these very hot conditions. Their validation will enable to better assess the implications of hot bentonite behavior on the performance of the near-field. Moreover, such an experiment will enable to evaluate different “hot” designs and how they can be optimized in terms of efficient implementation, while ensuring the long-term safety of the repository system.

This contribution will outline the plans of the upcoming FEBEX-DP dismantling and sketch potential options of a “hotFEBEX” test at temperatures >150°C in crystalline host rock. We will sketch potential options of using the well characterized FEBEX drift at the well-equipped GTS and the EBS behaviour knowledge gained from the various experiments for a design of a “hotFEBEX”. Different possibilities for such an experiment are open for discussion, including the type of bentonite, target temperature, duration of heating or the degree of instrumentation.

The support and contributions by the FEBEXe and FEBEX-DP partners is acknowledged.

References

Lanyon G.W., Gaus I. (Ed.)(2013): Main outcomes and review of the FEBEX In Situ Test (GTS) and Mock-Up after 15 years of operation. Nagra Arbeitsbericht. NAB 13-096. Nagra, Wettingen.

Development and validation of a model for smectite clay erosion.

Ivars Neretnieks[1], **Luis Moreno, Longcheng Liu**
Department of Chemical Engineering and Technology
Royal Institute of Technology, KTH
SE 100 44, Stockholm, Sweden.

In nuclear waste repositories of the KBS-3V type used in Sweden and Finland copper canisters, about 1 m in diameter and 5 m tall containing the spent nuclear fuel are emplaced in vertical boreholes at the bottom of tunnels in granitic rock at depths of about 500 m. The canisters are embedded in compacted bentonite clay consisting of around 80 % smectite. When wetted by the groundwater the smectite in the bentonite swells due to the strong repulsive forces between the smectite particles. The bentonite protects the copper canister from corrosive agents carried by the seeping ground water in the fractures as it has a very low hydraulic conductivity and solutes must penetrate the barrier by molecular diffusion, which is a slow process. Should the canister somehow be breached, leaking radionuclides must diffuse through the barrier to reach the seeping groundwater. The plastic bentonite also protects the canister from minor rock movements. If in contact with low ionic strength water, which could reach repository depth e.g. during an ice age when melting glacier water penetrates the rock, the bentonite can release colloidal smectite particles to the seeping water forming a sol. The water can carry away the sol. The main concern is that much bentonite is lost. If a large amount of bentonite leaves the deposition hole important barrier functions can be lost. A secondary concern is that smectite colloids, if they form a sol, could carry attached radionuclides away from a breached canister.

A bentonite erosion model was developed to estimate the loss of smectite in the Swedish KBS-3 repository concept. It was used in performance assessment calculations by SKB and in the modelling of the Finnish repository at Onkalo. The model is based on the dynamic force balance model and gel/sol viscosity models summarised in Neretnieks et al. (2009) and described in more detail in a number of publications (Liu, 2010, 2011 and 2013, Liu et al. 2009a, b, 2011, Moreno et al. 2010, 2011). The swelling of the smectite in the bentonite clay into the fractures with seeping water and the further transport as gel/sol with the water is influenced by the pore water concentration of primarily mono-and divalent cations. The rate of swelling and erosion can be quantitatively described by a set of partial differential equations, PDE's. The system of PDE's to solve is nonlinear and sometimes difficult to solve numerically because of the mutual influence of the evolving chemistry in the smectite gel/sol, the forces acting on the smectite particles and on the viscosity of the gel/sol, which determines when and how it can flow. The numerical difficulties and complex interaction between the various mechanisms involved have led us to explore which mechanisms have a dominating impact on the erosion and how simplifications could be made that will lead to more transparent, faster and more stable calculations.

A two-region model, which avoids some problems in earlier work was developed and tested. The model divides the region of the expanding clay in the fracture in one where the clay behaves like a Bingham solid/fluid that cannot flow but can expand by the repulsive forces between the smectite particles and another, the rim region, surrounding the former where the gel/sol, although highly viscous near the rim border, can flow and carry away the smectite particles that diffuse into this region. This two-region model gives results that are more accurate than those obtained earlier by the fully coupled model because a much higher resolution in the rim region where the erosion loss occurs was implemented by a special technique.

The two-region model is handled by first solving the rim model. This results in a simple expression for a given chemistry and smectite particle size and depends only on the expanding radius to the rim, fracture aperture and water velocity. The equations for the inner region are then solved using a finite difference method with the loss at the rim as a boundary condition. The numerical model follows the expanding grid with fine discretization close to the rim. Time stepping with increasing time steps is

[1] Corresponding author, niquel@kth.se

used. The two-region model is much faster to solve than the fully coupled model and more accurate in the important rim zone.

In some examples covering a wide range of conditions relevant for a repository in crystalline rock it was found that the two-region model gives considerably lower steady state losses of smectite than the earlier results. However, the clay expands much farther out in the fractures, which leads to a larger amount of clay residing in the fractures because the rim expands to a considerably larger distance when the water velocity is small. Then steady state condition may not be reached for very long times. In all, the loss from the source is smaller than previously found. An important finding is that the smectite will expand far out into the fractures even when the seeping water is not very dilute. Bentonite will start to be lost from the deposition hole as soon as the rock around the repository has been resaturated. There is no need for dilute water to intrude for the loss to occur. A positive consequence of the wider intrusion is that as the smectite expands farther from the deposition hole, even in the finest fractures, it creates an extensive stagnant region around the deposition hole and tunnels. This considerably decreases the overall mass transfer rate of solutes to and from the deposition hole.

The two-region model was used to simulate a set of laboratory experiments performed by Schatz et al, (2012) with smectite clay expanding in a 1 mm slit from a cylindrical source. The loss from the source (deposition hole) was fairly well predicted but the rate of sol formation and transport was somtimes underestimated.

References

Liu, L., 2010, Permeability and expansibility of sodium bentonite in dilute solutions. Colloids Surf. A: Physicochem. Eng. Aspects 358 (1–3), 68–78.

Liu L., Neretnieks I., Moreno L., 2011, Permeability and expansibility of natural bentonite MX-80 in distilled water, Physics and Chemistry of the Earth 36, 1783–1791

Liu L., 2011, A model for the viscosity of dilute smectite gels, Physics and chemistry of the earth, 36, 1792-1798

Liu L., 2013, Prediction of swelling pressures of different types of bentonite in dilute solutions, Colloids and Surfaces A: Physicochem. Eng. Aspects 434, 303– 318

Liu, L., Moreno, L., Neretnieks, I., 2009a, A Dynamic force balance model for colloidal expansion and its DLVO-based application, Langmuir 25 (2), 679–687

Liu, L., Moreno, L., Neretnieks, I., 2009b, A novel approach to determine the critical coagulation concentration of a colloidal dispersion with plate-like particles, Langmuir 25 (2), 688–697

Liu L., Neretnieks I., Moreno L., 2011, Permeability and expandability of natural bentonite MX-80 in distilled water, Physics and Chemistry of the Earth, 36, p 1783-1791

Moreno L., Neretnieks I., Liu L., 2010, modelling of bentonite erosion, Swedish Nuclear Fuel and Waste management Co., Technical report, SKB TR-10-64, avalilabe from www.SKB.se

Moreno L., Neretnieks I., Liu L., 2011, Erosion of sodium bentonite by flow and colloid diffusion, Physics and chemistry of the earth, 36, 1600-1606

Neretnieks, I., Liu, L., Moreno, L., 2009. Mechanisms and Models for Bentonite Erosion. Swedish Nuclear Fuel and Waste management Co., Technical report, SKB TR-09-35, avalilabe from www.SKB.se

Schatz, T., Kanerva, N., Martikainen, J., Sane, P., Olin, M., Seppälä, A and Koskinen, K., 2012, Buffer Erosion in Dilute Groundwater. Posiva Report 2012-44 (2012) available from www.POSIVA.fi

Chemical erosion of bentonite buffer – do we observe this in nature?

Reijonen, H.M.[1]* and Marcos, N.[2]
[1,2] Laulukuja 4, 00420 Helsinki, Finland

Bentonites are planned to be used as buffer materials in various types of geological repositories designed to host radioactive waste. Especially in case of HLW/SF disposal, the longevity of compacted bentonite in the repository environment becomes increasingly important due to very long timescales for the safety assessment (up to My). For the bentonite buffer and backfill materials one of the main environmental factors affecting their evolution is the hydrological and hydrogeochemical conditions. Since it is observed in laboratory tests that smectite, esp. montmorillonite forms colloids and dissolves in very dilute conditions, a scenario for chemical erosion has been discussed at lengths especially in relation to geological repositories located at future glaciated terrains and locations otherwise potentially hosting dilute groundwater conditions.

The process of chemical erosion of bentonite is related to fractured host rock systems and it requires dilute groundwater conditions accompanied with sufficient flow rates (see e.g. Neretnieks et al. 2009). Chemical erosion process has been experimentally studied recently in relation to HLW disposal programmes especially in Sweden and in Finland (e.g. Neretnieks et al. 2009 and Schatz et al. 2013). General understanding is that bentonite erosion does not occur when total charge equivalent of cations in groundwater is higher than 4mM, which is reflected in the requirements (SKB 2011, Posiva 2013). Regarding the occurrence of the process of chemical erosion within bentonite EBS, there are two processes to be looked at: 1) infiltration of dilute waters in the bedrock aquifer and related rock-water interaction in the system, and 2) the actual process of erosion of swelling clay in repository conditions assuming that the former produces dilute enough conditions.

In case of crystalline basement areas that have been formerly glaciated, there are two potential evolution paths that may lead to groundwater dilution. One is groundwater recharge during glacial melting periods, and the other, is gradual dilution by meteoric water intrusion in the terrestrial areas due to an interglacial phase. It is known, that melting waters from glaciers gradually dilute the groundwater below, phenomenon that has been observed e.g. in Greenland (Harper et al. 2010). Here however, the duration of glaciation is very different from that of e.g. Fennoscandia, where glacial periods have been intersected with relatively long interglacial periods in between (e.g. Johansson et al. 2011 and references therein).

Montmorillonite and other smectites occur naturally in crystalline basement as fracture filling minerals (e.g. Gehör 2007, Gehör et al. 1997ab) (see Figure 1). Smectites are also observed in e.g. soils, products of hydrothermal alteration in various types of rocks and in paleosols/ancient weathering products of bedrock surfaces. As a matter of fact, smectites are investigated in crystalline basement fractures as a part of standard investigations related to underground construction due to their potential effect on the bedrock mechanical properties. The potential natural analogue for the bentonite buffer longevity in relation to chemical erosion has been acknowledged previously by Arthur & Savage (2011) and Reijonen & Alexander (*in press*).

The occurrence of smectites in various depths and hydrogeochemical environments is investigated here in order to shed light on the discrepancy between the what-if scenarios presented for chemical erosion of bentonite in safety assessments and what is seen in nature. Background is given on the current status of experimental work done as well as briefly refer to most recent modelling done in relation assess the performance of the geological repositories. The main focus will be on reviewing the available data from natural smectite occurrences. The paper will present available data on the occurrence of smectites in relevant geological environments and the boundary conditions with discussion to what extent chemical erosion can be, if possible, observed in nature.

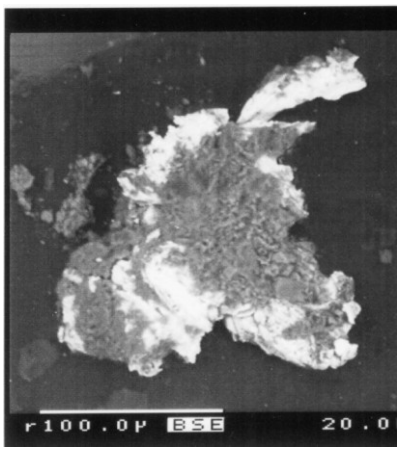


Figure 1. Metallic copper grain (light grey) embedded in smectite (medium gray) from a water-conducting fracture at about 80 m depth (Marcos 2002).

References

Arthur, R., & Savage, D. 2012. Equilibrium constraints on buffer erosion based on the chemistry and chemical evolution of glacial meltwaters. Proc. of 5th International meeting on Clays in Natural and Engineered Barriers for Radioactive Waste Confinement. 22-25 October, 2012, Montpellier, France.

Gehör, S. 2007. Mineralogical Characterization of Gouge Fillings in ONKALO Facility at Olkiluoto. Posiva Working Report 2007-33. Posiva Oy, Olkiluoto, Finland.

Gehör, S., Kärki, A., Taikina-aho, O. 1997a. Loviisa, Hästholmen, Petrology and low temperature fracture minerals in drill core samples HH-KR1, HH-KR2 and HH-KR3. Posiva Working Report 97-40. Posiva Oy, Helsinki, Finland.

Gehör, S., Kärki, A., Suoperä, S., Taikina-aho, O. 1997b. Kivetty, Äänekoski: Petrology and low temperature minerals in the K1-K11 drill core samples. Posiva Working Report 97-16. Posiva Oy, Helsinki, Finland.

Harper J., Hubbard A., Ruskeeniemi T., Claesson Liljedahl L., Lehtinen A., Booth A., Brinkerhoff D., Drake H., Dow C., Doyle S., Engström J., Fitzpatrick A., Frape S., Henkemans E., Humphrey N., Johnson J., Jones G., Joughin I., Klint KE., Kukkonen I., Kulessa B., Landowski C., Lindbäck K., Makahnouk M., Meierbachtol T., Pere T., Pedersen K., Pettersson R., Pimentel S., Quincey D., Tullborg E-L. & van As D. 2010. The Greenland Analogue Project - Yearly Report 2010. Posiva working report 2012-16. Posiva Oy, Eurajoki, Finland.

Johansson, P., Lunkka, J.-P., Sarala, P. 2011. Glaciation of Finland. In: Ehlers, J., Gibbard, P.L. & Hughes, P.D. (eds.). Quaternary Glaciations – Extent and Chronology: A Closer Look. (Developments in Quaternary Science, Vol. 15, p. 105-115). ISBN 978-0-444-53447-7.

Reijonen, H.M. & Alexander, W.R. (in press). Bentonite analogues for geological disposal of radioactive waste – current status and future outlook. Swiss Journal of Geosciences Spec. Publ. Proc 13th NAWG Workshop, Nagoya, Japan, May, 2013.

Marcos N. 2002. Lessons from nature – The behaviour of technical and natural barriers in the geological disposal of spent nuclear fuel. Acta Polytechnica Scandinavica, Espoo, Civil Engineering and Building Construction Series No 124.

Neretnieks, I., Liu, L. & Moreno, L. 2009. Mechanisms and models for bentonite erosion. Stockholm, Sweden: Swedish Nuclear Fuel and Waste Management Co. (SKB). Technical Report TR-09-35. 168 p. ISSN 1404-0344

Posiva 2013. Safety case for the disposal of spent nuclear fuel at Olkiluoto – Performance Assessment 2012. POSIVA Report 2012-04. Posiva, Eurajoki, Finland.

Schatz, T., Kanerva, N., Martikainen, J., Sane, P., Olin, M., Seppälä, A. & Koskinen, K. 2013. Buffer Erosion in Dilute Groundwater. Posiva report 2013-44. Posiva Oy, Eurajoki, Finland. ISBN 978-951-652-226-8, ISSN 1239-3096.

SKB 2011. Long-term safety for the final repository for spent nuclear fuel at Forsmark. Main report of the SR-site project. SKB Report TR-11-01. SKB, Stockholm, Sweden.

Calibrating a 3D numerical model of variably-saturated flow to assess the hydraulic impacts of the future radwaste repository on the Meuse/Haute-Marne site

J. Kerrou[1], G. Deman[1], L. Tacher[2], H. Benabderrahmane[3], P. Perrochet[1]

[1] Centre of Hydrogeology and Geothermics (CHYN), University of Neuchâtel, Rue Emile Argand 11, 2000 Neuchâtel, Switzerland (jaouher.kerrou@unine.ch)

[2] Ecole Polytechnique Fédérale de Lausanne, Laboratoire de Mécanique des Sols (EPFL - LMS), CH - 1015 Lausanne

[3] Andra, 1-7 rue Jean Monnet, 92298 Châtenay-Malabry Cedex, France (hakim.benabderrahmane@andra.fr)

Within the framework of the Andra (French National Agency for Nuclear Waste Management) Cigéo project for a deep geological disposal of intermediate and high-level long lived radioactive waste in low-permeable clay formation a three-dimensional high resolution numerical model of variably-saturated flow was developed. The main objectives of this study were to use the calibrated model: *(i)* to understand the local transient flow behaviour in the Oxfordian aquifer system during and after the construction of the access shafts to the underground Laboratory (URL) in the Callovo-Oxfordian host formation and to evaluate the extension of the unsaturated zones around these structure; *(ii)* to predict the hydraulic perturbation during the construction and the operational period of the future repository infrastructure; and *(iii)* to estimate the repository post-closure resaturation time of the geological/engineered system.

This work is based on Andra 20 years of site investigation campaigns and the associated geological and hydrogeological data and especially the data collected since the construction in 2001 of the shafts of the underground Laboratory in the Callovo-Oxfordian host formation. The conceptual hydrogeological model of the local multi-layered system includes the Oxfordian aquifer, the Kimmeridgian aquitard and the Portlandian aquifer system. The so called aquifers are mainly characterized by sedimentary macro-pores within the Oxfordian limestone formation, and karstic conduits of the Barrois limestone formation. Engineered underground structures to access the URL and the future radwaste repository are integrated into the geological medium. The overall conceptual model was then discretized into 3D finite element mesh with more than 10 million elements and 3.5 million nodes. The mesh was refined around the lineaments of the rivers, and also around the URL and the repository access structures (Shafts and tunnels). The lateral boundary conditions of Dirichlet type were derived from the integrated regional-local hydrogeological model (*Andra, 2012*). Neumann type boundary conditions representing rainwater infiltration are specified on the top of the model. Richard's modified equation of variably saturated flow was solved with the finite element simulator *GroundWater* (*Cornaton*, 2012).

Because of the high cost of the computational time needed for solving nonlinear variably-saturated system with an optimal resolution for large time and space scales, a calibration method was developed. Calibration is the major and challenging issue for matching the times series of the monitoring data (water pressure and water flux measurements) recorded at the URL site.

The method is based on Latin Hypercube Design (LHD) and Response Surface (RS) technics. More precisely, LHD have been used to sample layers parameters (i. e.: hydraulic conductivity and storativity) over their respective possible distributions. A couple of parameters were selected for each of the 16 layers to calibrate. Hundreds of simulations of variably-saturated flow were then solved with

the finite element simulator *GroundWater*. In a second step, a multi-linear regression model was derived from the numerical simulations results to perform statistical tests and to be later used to predict the response of the flow model for other sets of parameters. The target response was an objective function (OF) including measured and computed values of hydraulic heads and discharge rates. This OF represents the misfit of the model to be reduced through the calibration process.

The fairly good matching of measured head and fluxes time series by the model allowed to reproduce the local transient flow patterns. The unsaturated zones around the URL structures extend hundred of meters approximately. After an operational period of 100 years, the repository post-closure re-saturation time is estimated to few thousands of years. The results so far are presented and discussed.

References

F. CORNATON (2012): GroundWater: A 3D Groundwater and Surface-Water Flow, Mass Transport and Heat Transfer Finite Element Simulator. Reference Manual. Neuchâtel, Switzerland: Centre for Hydrogeology and Geothermics.

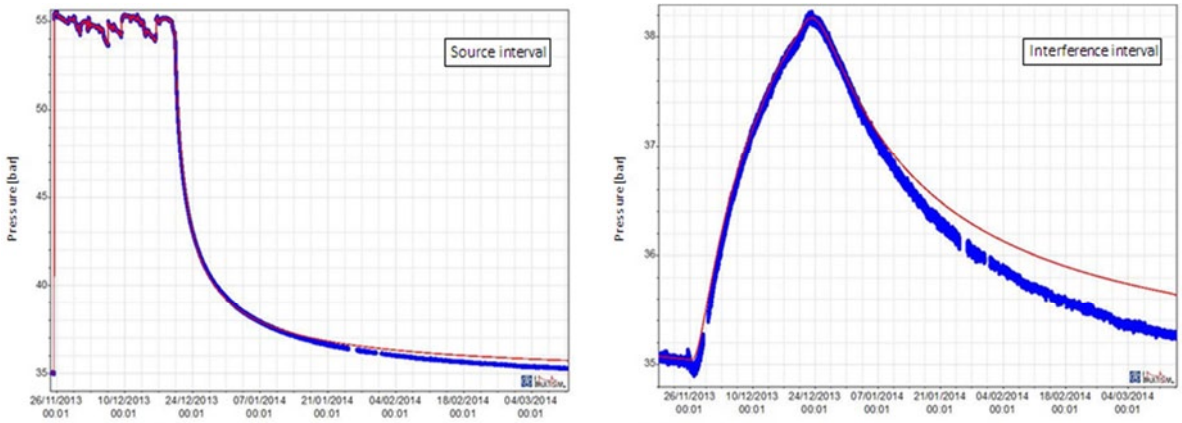
Impact of testing procedure and test analysis methodology on the determination of the hydraulic parameters of low permeability media: In-situ hydraulic tests in the Callovo Oxfordian clay

Rainer Schwarz[1], **Ralf Brauchler**[1], **Marine Pérus**[1], **Jean Croisé**[1], **Rémi de la Vaissière**[2]

[1]AF Consult Switzerland Ltd, Taefernstrasse 26, CH-5405 Baden, Switzerland
[2]Andra CMHM, RD960, F-55290 Bure, France

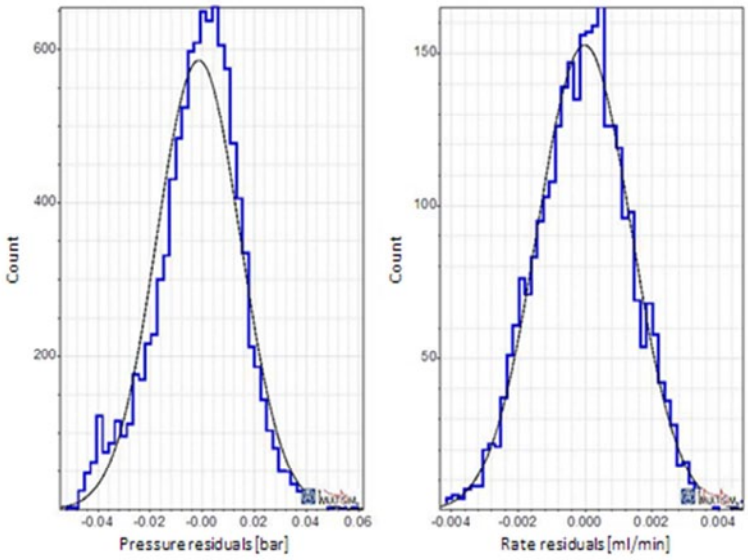
For more than a decade, Andra has performed a large number of hydraulic tests in instrumented boreholes in the Callovo-Oxfordian clay formation at the Underground Research Laboratory of the Centre de Meuse Haute-Marne, France (CMHM URL). In this low-permeability formation, the hydraulic test procedure consists of different test types ranging from pulse withdrawal or injection tests to constant pressure or constant rate injection, followed by shut-in tests. The tests are analysed with state of the art well testing analysis methods comprising diagnostic plots, analytical and numerical solutions, automatic calibration and the determination of confidence ranges for the hydraulic parameters.

In a specific methodological study conducted in 2013/2014, we investigated the impact of test procedure and analysis assumptions on both the best estimate of the determined hydraulic parameters and their corresponding confidence ranges. The study was based on the most common testing procedure applied during the previous 10 years at the CMHM URL: pulse injection and withdrawal tests, with different initial pressure differences, a series of constant pressure injection tests with different pressure levels and observed hydraulic pressure at an observation borehole in ~1 m distance.



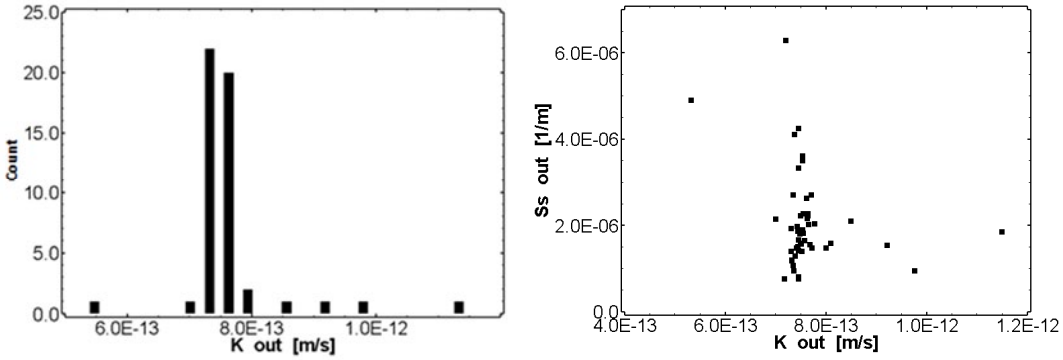
Examples of the measured pressure (blue line) and the simulated pressure based on the best fit hydraulic parameters (red line) for the source interval and an interference interval.

In this methodological study, two series of tests were performed at two different locations at the CMHM URL, selected particularly for covering the natural variability range of the permeability of the undisturbed Callovo-Oxfordian clay. The validity of the radial composite flow model used in the analysis of the hydraulic tests conducted at the two locations was determined by diagnostic plots and checked by fitting residuals between measured and simulated pressures and rates.



Distribution functions for the residuals for the pressures (left) and for the rates (right). Residuals are shown in blue, the associated normal distribution in black.

The hydraulic parameters (permeability, specific storage, radial distance of the interface between inner and outer zone of the radial composite flow model, formation pressure) were estimated following an automated calibration procedure based on a series of repeated numerical flow simulations with varying input parameters (code MULTISIM). The n-dimensional Statistical Inverse Graphical Hydraulic Test Simulator (code nSIGHTs) was used to do a perturbation analysis of selected test sequences and to quantify the influence of the error on non-fitting parameters on the uncertainty range of the hydraulic parameters.



Results of the perturbation analysis: histogram of hydraulic conductivity of the outer zone (left), and linear dependency between the parameters hydraulic conductivity and specific storage (right).

The study showed, as expected intuitively, that variations in the estimated hydraulic parameters as well as their uncertainties decrease as the size of the tested volume of Callovo-Oxfordian clay increases. Therefore, constant pressure injection tests (which typically lead to larger investigation volumes than pulse tests) followed by a shut-in phase are very suitable tests. Furthermore, the constant pressure test may be optimized with respect to the target uncertainty level by adapting the duration of the injection period. The study also confirmed the high quality of the permeability values determined from in-situ hydraulic tests in the Callovo-Oxfordian clay with the test procedures and analysis methods used by Andra during the last decade. These conclusions are derived from the parameter estimations and the rigorous uncertainty analysis which comprised a mathematical uncertainty analysis, a residual analysis, an estimation of joint confidence regions of the calibrated hydraulic parameters, a perturbation analysis and a sampling analysis.

The Full-Scale Emplacement Experiment – Implementation of a multiple heater experiment at the Mont Terri URL

***Herwig R. Müller*, Tobias Vogt, Benoit Garitte, Sven Köhler, Toshihiro Sakaki, Hanspeter Weber, Tim Vietor**

NAGRA, National Cooperative for the Disposal of Radioactive Waste, Hardstrasse 73, CH-5430 Wettingen, Switzerland, herwig.mueller@nagra.ch

Introduction and experimental aims

The Full-Scale Emplacement (FE) Experiment at the Mont Terri underground rock laboratory (URL) is a full-scale multiple heater test in a clay-rich formation ('Opalinus Clay'). It simulates the construction, waste emplacement, backfilling and early post-closure evolution of a spent fuel (SF) / vitrified high-level waste (HLW) repository tunnel as realistically as possible. The main aim of this experiment is to investigate SF / HLW repository-induced thermo-hydro-mechanical (THM) coupled effects onto the host rock at this scale and to validate existing coupled THM models. Further aims are a) the verification of the technical feasibility of constructing a repository tunnel using standard industrial equipment, b) the optimisation of the bentonite buffer material production and c) the investigation of (horizontal) canister and buffer emplacement procedures at underground conditions.

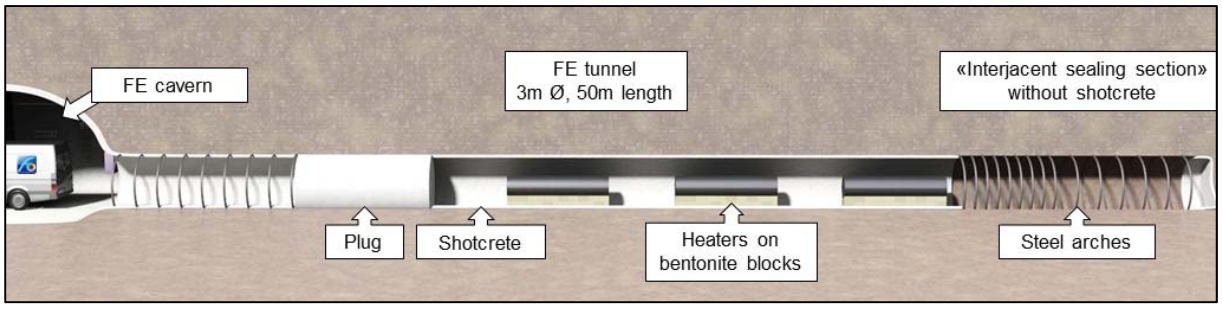


***Figure 1:** Visualization of the general experimental layout of the Full-Scale Emplacement (FE) experiment at the Mont Terri URL; sensors and bentonite backfill are not displayed.*

Experimental layout

The FE experiment is based on the Swiss disposal concept for SF / HLW. The construction of the 50 m long experimental tunnel with a diameter of approx. 3 m was completed in September 2012. At the deep end of the tunnel the so-called "interjacent sealing section" (ISS) was built using only steel arches for rock support whereas the rest of the tunnel is supported by shotcrete. In the FE tunnel three heaters with dimensions similar to those of waste canisters will be emplaced on top of pedestals built of bentonite blocks (see *Figure 1*). The remaining space will be backfilled with granular bentonite. Finally the experiment will be sealed off towards the FE cavern with a concrete plug holding the buffer in place and reducing air and water fluxes.

THM instrumentation

The entire experiment implementation as well as the post-closure THM(C) evolution is monitored using several hundred sensors. The rock in the 'far-field' was instrumented with up to 45 m long boreholes drilled from the FE cavern; this instrumentation was completed in April 2012 before the FE tunnel was built and therefore allowed a 'mine-by' oberservation of the later tunnel construction. Until February 2014 the 'excavation damage zone' (EDZ) was instrumented with radial boreholes drilled from within the FE tunnel. In June 2014 the instrumentation of the tunnel wall was completed for future monitoring of the bentonite buffer. At this stage also many fiber optical cables for distributed temperature and deformation monitoring were installed. More sensors for the observation of the bentonite buffer in close proximity to the heaters will be implemented together with the heaters.

Bentonite buffer production

After re-assessing the range of possibilities for backfilling materials only natural (non-activated) sodium bentonite from Wyoming was used for the FE experiment. Approx. 3'000 highly compacted bentonite blocks, each block with a weight of 25 kg, a dry density of 1.8 g/cm3 and a water content of 20 %, were produced for filling a full 2 m long section in the ISS and for the pedestals below the three heaters. Additionally 350 tons of a highly compacted and granulated bentonite mixture (hcGBM) were produced. With several pre- and mock-up tests it was possible to prove that with highly compacted bentonite granules ("pellets") with an average dry "pellet" density of 2.18 g/cm^3 and with a very broad "pellet" size distribution, a so-called Fuller-type distribution, an overall bulk dry emplacement density of at least 1'450 kg/m^3 (as targeted in the Swiss concept) can be achieved.

Development of a prototype backfilling machine

A challenge was the design and construction of a prototype machine for backfilling horizontal tunnels with hcGBM as dense and homogenous as possible; a visualisation of this machine is shown in *Figure 2*. The machine fits into the small diameter FE tunnel and will transport, emplace and compress the hcGBM using five auger conveyors simultaneously. All relevant parameters such as the backfilling speed and the backfilling pressure can be controlled. The prototype machine was successfully tested in two full-scale pre-tests in May and August 2014 and will be used to backfill the FE tunnel in autumn / winter 2014.



Figure 2: *Visualization of the developed prototype machine with five auger conveyors used for backfilling the FE tunnel with hcGBM. The longest auger is 8.5m long, bringing the machine length (with the hcGBM feeding trolley, which is not shown in this figure) to 17m in total.*

Heating & monitoring

After the heater emplacement and the consequent backfilling, the heating phase will be started. With an initial heat output of 1500 W per heater (according to the Swiss reference case) a temperature of approx. 120-150°C at the heater surface and 60-80°C at the rock surface are expected for the FE experiment at Mont Terri. According to current planning, the heating and monitoring phase of the FE experiment at Mont Terri is envisaged to last at least 10 to 15 years.

Acknowledgments

The FE experiment is implemented in the Mont Terri URL, which is operated by swisstopo. The initiator and lead organisation for the FE experiment is NAGRA; ANDRA (France), BGR (Germany), DOE/LBNL (U.S.A), GRS (Germany) and NWMO (Canada) are participating in the Experiment. The engineering and demonstration components of the FE experiment are also part of NAGRA's participation in the EC co-funded 'Large Underground COncept EXperiments' (LUCOEX) project and therefore receive funding from the European Atomic Energy Community's Seventh Framework Programme (FP7) under grant agreement n269905.

Designing, Commissioning and Monitoring of 40% Scale Bentonite Buffer Test

Erika Holt*, Harri Kivikoski*, Pieti Marjavaara and Pasi Rantamäki*****

* VTT Technical Research Centre of Finland, Espoo, Finland
** B+Tech Oy, Helsinki, Finland
*** Posiva Oy, Eurajoki, Finland

A 40% scale bentonite buffer tests was commissioned to simulate geological disposal of nuclear waste according to the current reference design concept adopted in Finland. Two experimental vertical holes with a diameter of 800 mm were drilled into the tunnel floor at the testing place located 140 m underground. The depth of both of the holes was about 3 m and the distance between the holes was 4 m. The stability of the upper parts of the test holes was secured with anchor bolts into the rock, a concrete structure and two stainless steel collars. The depth of each collar was set to 700 mm to match the thickness of the broken Excavation Disturbance Zone of the host rock. Bentonite buffer blocks and a heating canister simulating nuclear waste were installed in the holes with monitoring equipment. The bentonite buffer blocks were manufactured from MX-80 bentonite by isostatic compression, having an average bulk density of 2094 kg/m^3. The gap between the rock surface and the bentonite blocks was filled with pillow-shaped MX-80-bentonite pellets having an estimated pellet filling density of 1075 kg/m^3. The gap width was 35 mm. The surface temperature of the dummy canister simulating spent fuel was planned to be +90 °C. The heating power of the canisters was calculated to be 900 W.

The goal of the 40% scale bentonite buffer test was to get information about methods and best practices for the installation, the behaviour of sensors and cables in nuclear repository conditions, and the early phase processes in the bentonite buffer. The early phase processes include distribution of the heat, the rate of saturation from the gap to the middle of the buffer block, the effect of watering, the possible piping and erosion, the swelling and the buffer uplifting.

The materials for the buffer systems were preassembled in a laboratory, prior to their use in ONKALO. The instrumentation work included drilling small holes through the bentonite blocks for the installation of the sensors and the cables, including sensors to instrumentation tubes and rock holes. The bentonite blocks were then instrumented so that the vertical holes were first drilled to the bentonite to host sensors and channels were then drilled or cut to the bentonite for cables. The empty spaces around sensors and cables were then filled with bentonite powder.

To fasten the instrumentation to the rock, four stainless steel instrumentation tubes were built to be used as the mounting and housing system for sensors. Total pressure sensors, relative humidity sensors, K-type temperature sensors and water nozzles were fitted to the front faces of the instrumentation tubes. Also the cables from the bottom of the hole containing pore pressure and total pressure sensors were led through the same instrumentation tubes up to the surface tunnel. These instrumentation tubes were installed into the vertical, rock cored, sampling holes, which had been drilled adjacent to the experimental holes. After the installation of the tubes these holes were filled with low-pH cementitious grout.

The assembled and instrumented bentonite block stacks were transported 270 km from VTT Technical Research Center of Finland's laboratories to ONKALO by a large 3-axis truck trailer. The bentonite blocks were wrapped with thin plastic foil and the entire load was then protected with a thicker plastic tarpaulin to minimize any possible moisture changes in the bentonite blocks during the transportation. The bentonite stacks were lowered in the deposition holes.

The overbearing confinement pistons were then moved above the holes by a forklift and the installation was performed in the same way as with the bentonite stacks. Before the final installation, each piston was pre-installed to be sure of its compatibility and proper fit. The pistons were installed carefully on the top of the bentonite block stacks. The final position and required pretension of the piston were achieved by tightening the nuts situated around the piston, to provide the confinement loading simulating backfilling blocks and thus minimizing buffer uplift due to bentonite swelling.

The heating elements of the canisters were turned on in November 2011. The temperature of the canister was raised up stepwise to the target values and then maintained for the test duration.

During the test program one hole was artificially wetted at the start, using salinity water (TDS in the range of 10–12 g/l) representing the ONKALO water composition. A tracer compound, fluoresceine (250 μg/l), was used to mark the water to distinguish it from natural flows. Most of the watering was done at a flow rate of 8–10 litres per minute, while the pressure was monitored to be about 360 kPa. A total of 100 litres of water was injected into the hole over a couple hours during the first wetting phase, approximately one month after installation. During the first phase of water pumping, the water level was monitored with a digital endoscope which was found to be a suitable piece of equipment and that performed well for this task.Two lower nozzles were also used with dosing pumps after the initial load of water. Sixteen water pulses (16 x 400 ml) were delivered through each nozzle thus totalling 12.8 litres of water. The pumping pressure was at first 220 kPa and in the end it was 1200 kPa. After that the artificial watering was stopped.

The duration of the 40% scale buffer test was planned to have continuous monitoring for at least two years, in order to obtain valuable data supporting initial and early stage performance assessments. The following measurements were made in each test hole: The temperature was measured at 30 points (+ six points in the rock between the holes); The total pressure was measured at 10 points, pore water pressure at one point, and relative humidity at eight points; The axial force was measured at four points, and displacements was measured at one point. The temperature readings were also measured by all relative humidity sensors and some pressure sensors. The data acquisition system included three separate loggers from different manufacturers. All data acquisition systems were controlled by using a customized LabView program. The data from the test were collected to the measuring computer and sent from ONKALO over Ethernet to the server aboveground. The measuring computer made local measurement files where the data was recorded in one-minute intervals. From these files a summary file is generated and retrieved hourly to the research result database system, which also makes automatic back-ups of the recorded data. The data are then re-processed and several graphs are drawn automatically.

One experimental test hole was opened and sampled in 2013 after two years of testing. The main goal of the dismantling of the selected hole was to study how to plan, perform and document the actual sampling and removal of the bentonite buffer in underground conditions. The work included studies and testing of the needed equipment, defining what were the best practices of bentonite sampling and how to handle and mark large number of samples in underground conditions and transfer them unchanged to the laboratory for assessments. The laboratory work included the determination of the water content and density distribution of the bentonite buffer blocks and the gap filling pellets.

During dismantling the work methods and practices proved to be efficient and the field work phase was commissioned in the planned four week time window. The removal of the heating canister was found to be challenging. The laboratory assessments of the bentonite buffer and pellet material were also successfully delivered. The used sampling, documenting, packing and marking procedures worked well throughout the sampling chain from ONKALO to laboratory. The results have been used to evaluate the buffer design and safety expectations associated with construction and initial state. The plans and procedures created during this study can be used as a baseline and can be further developed to better serve future demonstration studies and repository operations in ONKALO.

The PRACLAY Heater Test at URL HADES: Preparation of the heater switch-on

P. Van Marcke[1], X. Sillen[1], X.L.Li[2], G.J. Chen[2], A. Dizier[2], J. Leysen[2], I. Troullinos[2], J. Verstricht[2], W. Bastiaens[2]

1: ONDRAF/NIRAS, Kunstlaan 14 Avenue des Arts, 1210 Brussels, Belgium
2: GIE EURIDICE, Boeretang 200, 2400, Mol, Belgium

The PRACLAY Heater Test is a part of the PRACLAY In-Situ Experiment, which also comprises the Gallery&Crossing Test and the Seal Test. The experiment is located in HADES and its layout is shown in Figure 1. The Heater Test is hosted in the PRACLAY Gallery (total length: 45 m; heated length: 30 m; external diameter: 2.5 m) which is constructed perpendicular to the Connecting Gallery.

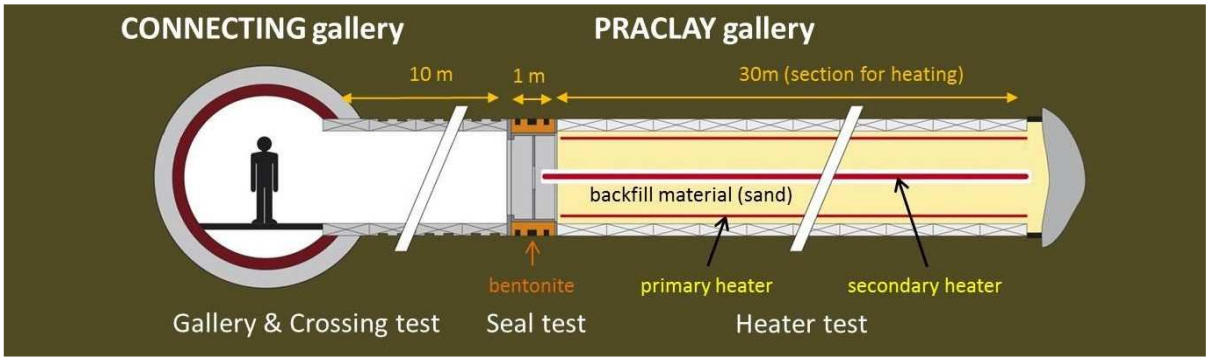


Figure 1: The PRACLAY In-Situ Experiment comprises the Gallery&Crossing Test, the Seal Test and the Heater Test

The aim of the Heater Test is to examine at large scale the impact of a thermal load on the Boom Clay. Such a thermal load leads to perturbations in the clay and can potentially affect its performance as a host rock for geological disposal of radioactive waste.

The Heater Test is intended to be representative of a generic disposal gallery for heat-emitting waste, and not to exactly simulate the current repository design. This is done to make sure that the test remains valid if the design changes in future. It is also not possible to fully reproduce the time scale, the spatial scale and the boundary conditions of a real repository. Therefore the test will be conducted under a reasonably conservative combination of thermal, hydraulic and mechanical conditions.

As for the hydraulic conditions, it is tried to achieve quasi-undrained boundary conditions at the clay-lining interface as these are more penalising than drained boundary conditions. This is realised by backfilling the PRACLAY gallery with water-saturated sand. At the intersection between the heated and the non-heated part of the gallery, a bentonite-based hydraulic seal is installed. The seal has to hydraulically cut off the heated part of the PRACLAY gallery from the rest of the HADES URL.

In 2007 the PRACLAY gallery was constructed to host the test. Subsequently the hydraulic seal was installed in 2010 at the intersection between the heated and the non-heated gallery section. The seal had a central opening to provide access to the heated part of the PRACLAY Gallery This was necessary for the subsequent installation of the heater cables and the backfill sand which was done in 2011-2012. Finally, the central opening in the seal was closed in 2012 completing the set-up of the experiment.

With all test components installed, the decision for switching on the heater depended on:

1. a test set-up state that enables the heater to be switched on, i.e.

   - the hydration of the seal bentonite is sufficient
   - the backfill sand is sufficiently water-saturated
   - the proper functioning of the heater is tested
   - all instrumentation is installed and connected to a data acquisition (DAQ) system with data backup and UPS systems in place

2. the readiness of the EURIDICE team to adequately follow up the test, i.e. verifying that

   - it has the data management tools to archive, analyse, display and report the measurements obtained during the test quickly and in an orderly way
   - the expected evolution of the test is well prepared by numerical simulations of the expected evolution, including a sensitivity analysis, and of various possible scenarios; these analyses will facilitate the interpretation of the measurements during the Heater Test and help to identify the cause where a trend deviates from the expected evolution; they will also inform decisions on whether and how the test set-up needs to be altered;
   - all procedures necessary for the management and steering of the experiment are being prepared and will be completed before starting the test.

A workshop was organised in December 2013 to evaluate remaining work to be done and issues to be addressed in the run-up to the switch-on. The workshop participants agreed that the bentonite hydration and backfill saturation were sufficient for switch-on. Remaining work mainly concerned the testing the heating system (in particular its control system) and preparing the follow-up of the test after switch-on.

By the end of September 2014 the heating system was completely installed and tested and a "PRACLAY Heater Test Management Guide" was established. The guide describes the complete management of the test (i.e. its follow-up, both technically as scientifically, and the steering) by the use of a set of procedures. These procedures aim at:

- describing the follow-up of the test
- defining the action plan in case of unexpected events as to be well prepared for such events
- clearly outlining and assigning the different responsibilities

The procedures will enable EURIDICE to prepare itself for the test, manage the test in a systematic way and avoid or at least minimise improvisation during the test. It also enables the EURIDICE personnel to be well aware of each one's task in the test management by defining the decision and information chains that need to be respected during the test.

In conclusion, by the end of September 2014 EURIDICE considered both the test set-up as its organisation ready for switch-on. The proposed contribution presents the rigorous preparation of the Heater Test by EURIDICE and ONDRAF/NIRAS.

The PRACLAY Heater Test at URL HADES: First results of the PRACLAY Heater Test

X.L. Li[1], G.J. Chen[1], A. Dizier[1], J. Leysen[1], I. Troullinos[1], J. Verstricht[1], W. Bastiaens[1], P. Van Marcke[2], X. Sillen[2]

1: GIE EURIDICE, Boeretang 200, 2400, Mol, Belgium
2: ONDRAF/NIRAS, Kunstlaan 14 Avenue des Arts, 1210 Brussels, Belgium

EURIDICE plans to start the large-scale PRACLAY Heater Test in October 2014. During the test a constant temperature of 80°C will be imposed at the gallery extrados over a 30 m long gallery section for at least 10 years (Figure 1).

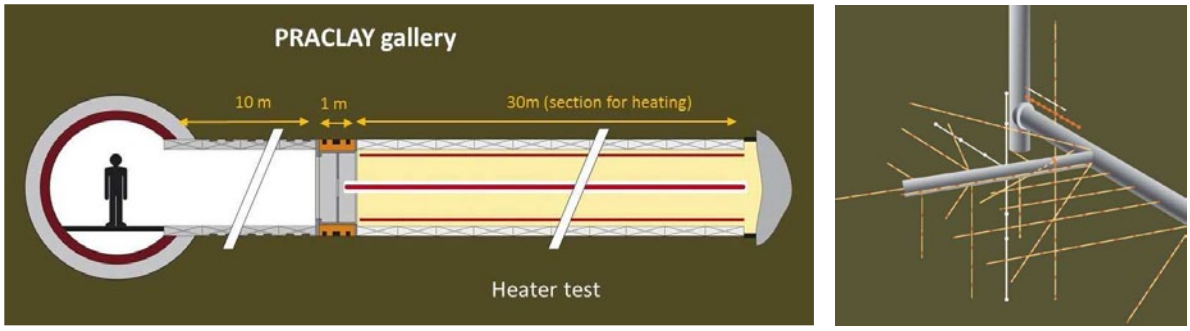


Figure 1: The PRACLAY Heater Test is set-up in the PRACLAY gallery and will heat a 30 m long gallery section during (left), overview of the instrumented boreholes in the clay (right)

The aim of the test is to examine at large scale the impact of a thermal load on the Boom Clay. Such a thermal load leads to perturbations in the clay and can potentially affect its performance as a host rock for geological disposal of radioactive waste. Measurement results from the simple in-situ heater test ATLAS (De Bruyn and Labat, 2002)(Chen et al, 2011) suggest that the performance of the host rock will not be significantly affected by the perturbations resulting from the thermal load. The large-scale Heater Test should allow confirming the small-scale tests and modelling results in repository-representative configurations (Bernier et al, 2007)(Sillen, 2012).

After years of setting up and preparing the PRACLAY Heater Test, EURIDICE considers both the test set-up as its organisation ready for switch-on in October 2014. The preparation of the Heater Test by EURIDICE and ONDRAF/NIRAS is described in "The PRACLAY Heater Test at URL HADES: Preparation of the heater switch-on" (abstract submitted to this conference). In contrast, the present contribution will focus on the main subject of the test, namely the behaviour of the Boom Clay. The measurements obtained in the first months of the test will be presented and compared to the expected evolution of the test. The expected evolution is obtained by numerical simulations.

Modelling has played an important role throughout the design, construction and test preparation stages of the Heater Test as the test conditions have been largely based on numerical simulations. The simulation programme also include a sensitivity analysis and covered various possible scenarios. These analyses will facilitate the interpretation of the measurements during the Heater Test and help to identify the cause should the measurements deviate from the expected evolution. They will also inform decisions on whether and how the test protocol needs to be adapted.

Understanding and predicting the THM response of the clay to the Heater Test requires the complete process to be taken into account: from the hydro-mechanical perturbations induced by the excavation of the PRACLAY gallery to the thermo-hydromechanical perturbations induced by the Heater Test itself. Extensive monitoring of the clay during this process and the continuous analysis of these measurements have enabled to further develop and fine-tune the numerical models.

Figure 2 shows the expected evolution of the radial profile in the horizontal direction of pore water pressure during the first 150 days after switch-on, during which the temperature of the clay in contact with the gallery lining will increase from 16°C (in situ temperature) to about 65°C. The pore water pressure is expected to rapidly increase, essentially as a consequence of a difference in thermal expansion between the water and the clay and the low hydraulic conductivity of the latter.

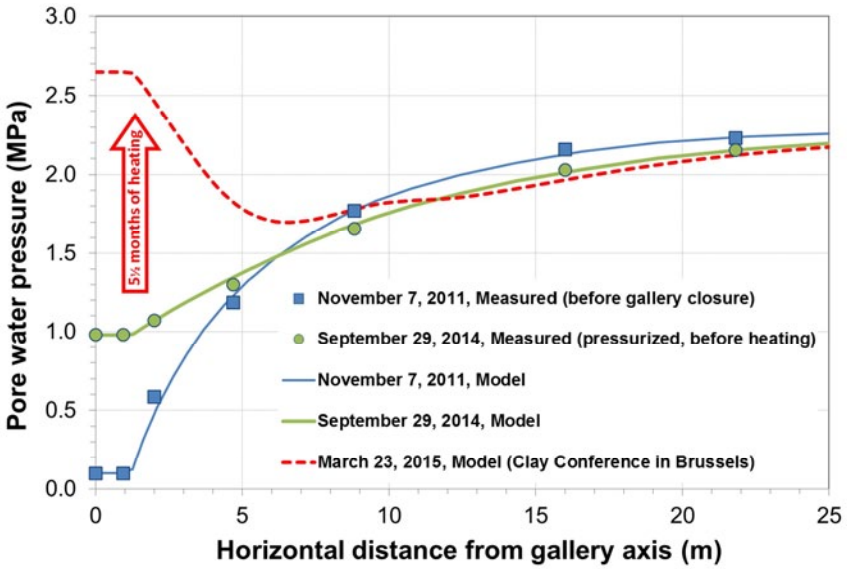


Figure 2: Expected early evolution of the radial profile of pore water pressure into the clay

The numerical simulations have already been challenged, although only to minor extent, during a so-called "dress rehearsal" (final rehearsal) in June 2014. During this short test aiming at verifying the functioning of the heater control system and part of the instrumentation, the system was heated for 2 days while the electric heaters in the gallery delivered about 250 W of heat output per metre of gallery, for a total of 7.5 kW over the length of the heated zone. The (limited) temperature and pore pressure evolutions within and in the immediate vicinity of the gallery were as expected.

The results obtained in the first months are expected to give a good indication on the predictive capacity of the models, as the simulations indicate that the more severe part of the THM transient in the clay should occur early on. This contribution will present those first results and give an evaluation of the predictions.

References:

Chen, G.J., X. Sillen, J. Verstricht, and X.L. Li. 2011. "ATLAS III in Situ Heating Test in Boom Clay: Field Data, Observation and Interpretation." Computers and Geotechnics 38 (5): 683–96. doi:10.1016/j.compgeo.2011.04.001.

De Bruyn, D, and S Labat. 2002. "The Second Phase of ATLAS: The Continuation of a Running THM Test in the HADES Underground Research Facility at Mol." Engineering Geology 64 (2-3): 309–16.

Bernier, F., Li, X.L., Verstrich, J. and Bastiaens, W. 2007. "The In Situ PRACLAY Demonstration and Confirmation Experiments". 11th Congress of the International Society for Rock Mechanics, 8-13 July 2007.

Sillen, X. 2012. "Repository-induced perturbations of the host formation, in the context of the safety case for the geological disposal of VHLW and SF in clay formations." Proceedings of the European Commission TIMODAZ-THERESA Conference, Luxembourg, 2009, EC-Report EUR 25527 EN.

Size and structure – The key to different ratios of edge to face charge for smectite

L. Delavernhe[1,2], A. Steudel[1,2], G.K. Darbha[3], T. Schäfer[3,4], R. Schuhmann[1,2], C. Wöll[1], H. Geckeis[3], *K. Emmerich*[1,2]

[1] Competence Center for Material Moisture (CMM),
[2] Institute of Functional Interfaces (IFG),
[3] Institute for Nuclear Waste Disposal (INE), Karlsruhe Institute of Technology, Hermann-von-Helmholtz-Platz 1, D-76344 Eggenstein-Leopoldshafen, Germany
[4] Institute of Geological Sciences, Department of Earth Sciences, Freie Universität Berlin, 14195 Berlin, Germany

Montmorillonite properties are mainly responsible for bentonite behaviour, and especially interfacial interaction with their environment involving water binding and/or trace element sorption capacity. In order to assess the bentonite performance and predict/control the long-term bentonite behaviour a fundamental understanding of montmorillonite properties is pre-requisite. The montmorillonite mineral general characteristics, structural and chemical heterogeneities are well-known (Emmerich et al., 2009 and references herein). The layer charge properties and the resulting cation exchange capacity behaviour were thoroughly studied in particular by Maes et al. (1979), Wolters et al. (2009), Kaufhold et al. (2011, 2013). However, correlation with morphological parameters was restricted to a few samples (Tournassat et al., 2003), although "edge to face" surface area ratio is a fundamental parameter for their reactivity.

Four purified and Na-saturated montmorillonites < 0.2 μm separated from technical bentonites from different locations (Table) were characterized in particular by their structural composition, layer charge and specific surface area in this study. Statistical AFM measurements on single layers were performed to determine particle size distribution and aspect ratio of these 2:1 layers. Based on the geometrical parameters, the variable charges at the particle edges ($CEC_{V,ES}$) were estimated according to Tournassat et al. (2004). Then, the variable charges were compared to CEC measurements (Cu-trien method) on reduced charge montmorillonites ($CEC_{T,RCM}$) (Li-exchanged montmorillonite followed by heating at 300°C) (Hofmann-Klemen effect).

The low charge dioctahedral montmorillonites exhibited a cation exchange capacity (CEC_T) ranging from 95 to 119 $cmol^+/kg$. CEC_T results both from permanent cation exchange capacity ($CEC_{P,c}$) resulting from isomorphic substitutions and from pH dependent charges lying at the edges surfaces. Influence of structural features and particle morphology on the variable charges were investigated by variable charges quantification following edge site density estimation based on acid-base model surface chemistry (Delavernhe et al., 2014). The particle size distribution, and more precisely the specific edge surface area ($a_{s,edge}$), proved be the determining parameter of variable charges contribution, even of $a_{s,edge}$ represents only 1.2% (Ben_V) to 2.8% (Ben_P) of the total specific surface area. Indeed even if the materials fractionation procedure was identical, distribution heterogeneity of particle size was observed with coarser particles in Ben_V compared to the others materials, with a weighted mean equivalent square length respectively of 245 nm and ~100 nm respectively (Figure 1). The resulting $CEC_{V,ES}$ estimated for a pH of 6 ranged from 6 to 15% (Table 1) resulting from the octahedral sites Me(III)-O, Me(II)-O, Me(III)-O-Me(II) and Me(II)-O-Me(II) (Tournassat et al., 2004). New insights in CEC measurements on RCM materials, i.e. montmorillonite with neutralized contribution of the permanent CEC, revealed good agreements with variable charge quantification by edge site density (Table 1).

Table 1. Total cation exchange capacity (CEC_T) and variable charges contribution (CECv)

Materials	Sources	Layer charge [eq/f.u.]	CEC_T [$cmol^+/kg$]	$CEC_{v\ RCM}$ [%]	$CEC_{v,ES}$ [%]
Ben_C	Bavarian, Germany	0.30	95 ± 2	20 ± 3	15
Ben_V	Wyoming, USA	0.26	96 ± 2	9 ± 1	6
Ben_S	Almería, Spain	0.37	112 ± 7	15 ± 2	13
Ben_P	Commercial product	0.32	119 ± 2	11 ± 1	13

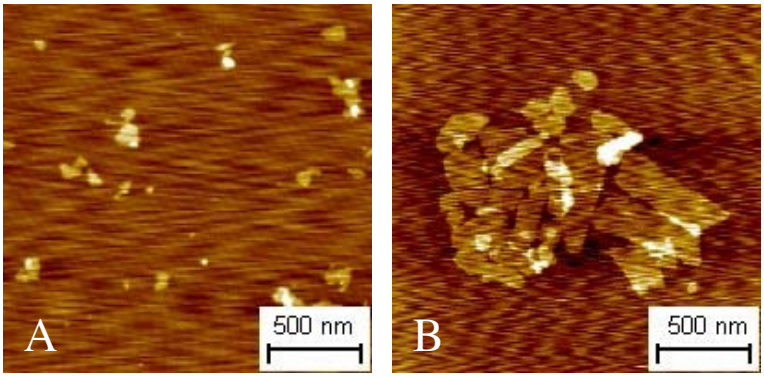


Figure 1. AFM image of Ben_C (A) and Ben_V (B)

Edge sites reactivity of smectite is determining for solute retention, hydration or dissolution process. It is commonly accepted that variables charges ranged between 10-20%, however their accurate quantification is sensitive subject. CEC measurement on RCM materials seems to be a fast alternative method to determine the pH-dependant charge contribution. Permanent cation exchange capacity is function of structural properties, while variables charge are mainly dependant of the edge surface area.

References

Delavernhe, L et al. (2014) in review in Colloids Surf., A
Emmerich, K. et al. (2009). Clay Clay Miner 57(1): 104-114.
Kaufhold, S. and R. Dohrmann (2013). J Colloid Interf Sci 390: 225-233.
Kaufhold, S. et al. (2011). Clay Clay Miner 59(2): 200-211.
Maes, A., et al. (1979). Clay Clay Miner 27(5): 387-392.
Tournassat, C. et al. (2004). J Colloid Interf Sci 273: 234-246.
Wolters, F. et al. (2009). Clay Clay Miner 57(1): 115-133.

Bentonite illitization and its effect on swelling stress: a coupled THMC modeling study on high-temperature effects

***Liange Zheng*, Jonny Rutqvist and Jens T. Birkholzer**

Lawrence Berkeley National Laboratory (LBNL), Berkeley, California 94720, USA, email: lzheng@lbl.gov

Illitization, the transformation of smectite to illite, could compromise the integrity of clays in engineered (bentonite) and natural (clay rock) barriers. It is believed that illitization could be greatly enhanced at temperatures higher than about 100 °C which could significantly lower the sorption and swelling capacity of clays. Thus, understanding this process is very important when designing the maximum temperature radioactive waste repositories. Existing experimental and modeling studies on the occurrence of illitization and related performance impacts are not conclusive, in part because the relevant couplings between the thermal, hydrological, chemical, and mechanical (THMC) processes have not been fully represented in the models. Here we present coupled THMC simulations of a generic nuclear waste repository in a clay formation with a bentonite-backfilled EBS. Two scenarios were simulated for comparison: a case in which the temperature in the bentonite near the waste canister can reach about 200 °C and a case in which the temperature in the bentonite near the waste canister peaks at about 100 °C.

Our model results indicate that some degree of illitization occurs both in the clay host rock (as previously revealed by natural analogue studies) and in the EBS bentonite. Other chemical alterations include the dissolution of K-feldspar and calcite, and the precipitation of quartz, chlorite, and kaolinite. However, the quantity of illitization, expressed as the smectite volume fraction change, is affected by many chemical factors and therefore varies a great deal. The most important chemical factors are the concentration of K in the pore water as well as the abundance and dissolution rate of K-feldspar. Less important are the concentration of Na and the quartz precipitation rate. We also compared the chemical changes and the resulting swelling stress change for two types of bentonite: Kunigel-VI and FEBEX bentonite. For Kunigel-VI bentonite, the decrease in smectite volume fraction ranges from 0.004 to a maximum of 0.085 (about 27% of the initial volume fraction of smectite) in 1000 years for the 200°C scenario. For FEBEX bentonite, the decrease in smectite volume fraction ranges from 0.01 to a maximum of 0.04 (7% of the initial amount) in 1000 years. The smectite volume fraction in the clay formation decreases moderately in some cases, but in other cases it decreases by as much as 0.035, fully depleting the initial smectite.

Higher temperatures also lead to much higher stresses in the near field, caused by thermal pressurization and vapor pressure buildup in the EBS bentonite and clay host rock. During the period of strongly elevated thermal stress, the contribution of smectite dissolution to changes in total stress is minimal. Chemical changes including changes in pore water ion concentration and smectite volume fraction, however, lead to a reduction in swelling stress, which is more pronounced for Kunigel-VI bentonite than for FEBEX bentonite. For Kunigel-VI bentonite, a reduction in swelling stress is up to 16–18% for the 200°C scenario, whereas for FEBEX bentonite, the model shows only about 1.5–3.6% reduction in swelling stress. The reasons are (1) that FEBEX bentonite exhibits less illitization, and (2) that FEBEX bentonite has a higher swelling capacity so that the relative reduction in swelling stress is fairly small.

The modeling work leads to a tentative conclusion that an argillite repository with bentonite EBS could sustain higher than 100°C as far as illitization concerns, with the following reasons:

1. Despite illitization in the bentonite is enhanced at higher temperature, such enhancement is fairly limited even at 200 °C due to other constrains of illitization such as the supply of K and Al.

2. Illitization causes only moderate decrease of swelling pressure and thus compromises insignificantly the functionality of EBS such as sealing the gap. Although for the bentonite having low swelling capacity (e.g., Kunigel-VI bentonite), chemical changes could results in relatively large reduction in swelling pressure in the worst scenario, for bentonite with high swelling capacity (e.g., FEBEX bentonite) chemical changes could only lead to about a few percent reduction of swelling pressure in 1000 years. Using bentonite with high swelling capacity could diminish the undesirable consequence (if there is any) of illitization.
3. Illitization in EBS could be suppressed by relatively easy engineering methods such as increasing the concentration of Na in the pore water of bentonite.

Structural defects in layered structures: Their determination and their impact on reactivity

Sylvain Grangeon[1,*], Francis Claret[1], Christophe Tournassat[1], Yannick Linard[2] and Bruno Lanson[3]

[1] BRGM, 3 avenue Claude Guillemin, 45060 Orléans cedex 2, France.
[2] Andra, Centre de Meuse/Haute Marne, 55290, France.
[3] CNRS and Univ. Grenoble Alpes, ISTerre, F-38041, Grenoble, France.
* Corresponding author. E-mail address: s.grangeon@brgm.fr

Clay minerals are layered structures that suffer from various and frequent crystallization faults, including point defects (e.g. layer vacancies and/or isomorphic cationic and anionic substitutions) and stacking defects (e.g. interstratification, well-defined or random stacking faults) that complicate the study of their structure, compared to most of other minerals. Determination of their crystal-structure is even further complicated by the small size of these minerals that possibly result from a "poisoning effect" induced by the presence of foreign cations in their layers.

The determination of the actual crystal structure of clay minerals, in particular the nature and density of structural defects, is however of paramount importance to understand and model clay minerals reactivity[1]. X-ray diffraction patterns of clay minerals often only exhibit 00*l* reflections and a few asymmetrical *hk* bands, while the *hkl* reflections are absent owing to the systematic occurrence of random stacking faults[2] (i.e. turbostratism; random translations in the layer plane and/or random rotation about the normal). To overcome this problem, a mathematical formalism was developed that allows the calculation of X-ray diffraction patterns from structures affected by various density and nature of structural defects, including turbostratism[3]. This development led to a better understanding of the structure from many clay minerals, including layer structure (e.g. nontronite[4]) and, using a complementary analysis of 00*l* reflections, of interlayer water and cations organization [5, 6].

It is however obvious that not only clays suffers from the here above mentioned crystallization defects. Rather, nanocrystalline (i.e. particles smaller than 100 nm) and defective lamellar structures affected by turbostratism are ubiquitous in natural and man-made environments. One can for example cite manganese[7] and iron oxides[8] or nanocrystalline calcium silicate hydrates[9] (C-S-H). The former two are reported to control the fate of many trace elements in the environment, including metals and actinides (in the case of vernadite, a manganese oxide) or oxyanions (in the case of fougèrite, an iron hydroxide). These minerals also often exhibit redox properties (e.g. Mn^{3+}/Mn^{4+} or Fe^{2+}/Fe^{3+}) that enables for the degradation of organic compounds[10,11]. Contrastingly, C-S-H is not found in natural environments, but is the main hydration product from various types of cement, including ordinary Portland cement, controls main cement chemical and physical properties[12, 13], and exerts a strong control on trace elements mobility. All these minerals and phases have close structural similarities with clays, as already noticed decades ago[14], and thus methods used for the analysis of clay mineral structure are transposable to these phases. As for clays, a sound understanding of the crystal structure from these minerals and phases is a fundamental basis for many applications. First, the nature of point defects determines the type of elements that can be sorbed (typically, in the case of oxides, isomorphic substitutions create a limited layer charge deficit and favour the sorption of alkali and alkali-Earth elements as hydrated outer-sphere complexes, whereas layer vacancies favour the sorption of multivalent elements as inner-sphere complexes) and, second, the density of these defects dictate the overall reactivity.

The present work will review recent applications of the specific method used to model X-ray diffraction patterns from nanocrystalline and defective lamellar structures, and will demonstrate that modelling can be used to retrieve accurate structural information, such as crystallite sizes and interlayer and layer structure, including nature and density of structural defects (Figure 1). The consistency between this method and other spectroscopic (e.g. synchrotron X-ray absorption spectrometry) or microscopic (e.g. transmission electron microscopy) techniques will be illustrated on nanocrystalline manganese (vernadite) and iron (fougèrite) oxides and nanocrystalline calcium silicate hydrates (C-S-H).

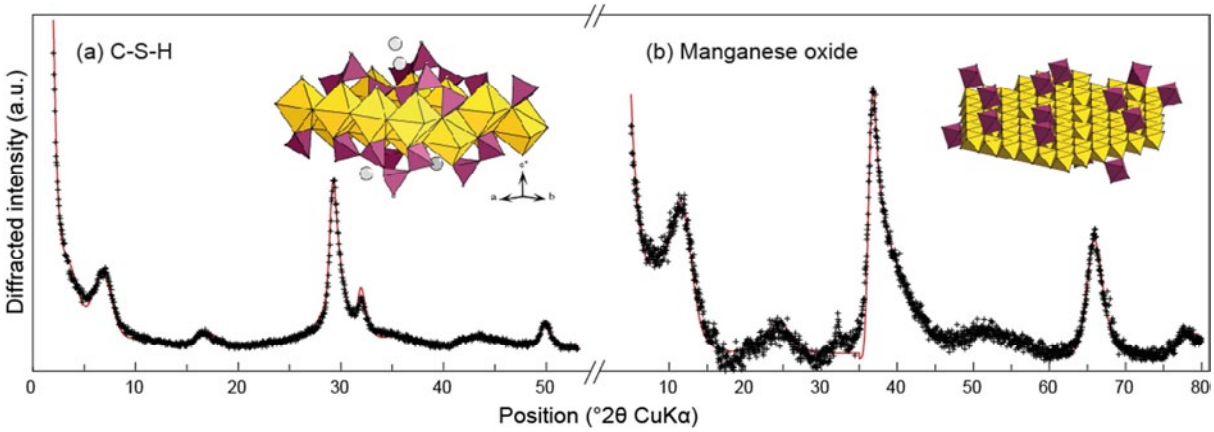


Figure 1. Exemple of refined X-ray diffraction patterns from two nanocrystalline and turbostratic structures: C-S-H[8] (a) and a biogenic manganese oxide[15] (b). In both patterns, crosses are the experimental points and solid lines the calculated patterns. The two insets at the top right of each pattern are sketches of refined layer structures. In C-S-H, layers are built of Ca polyhedra (yellow) with ribbons of wollastonite-like Si tetrahedra (purple) running at the surface. In the manganese oxide, layers are built of Mn octahedra (yellow) and layer vacancies capped by interlayer Mn sorbed as inner-sphere complexes (purple). In both cases, typical crystallite size is 10 nm in the layer plane and 3 to 5 nm perpendicular.

References

1. Lanson, B., Modelling of X-ray diffraction profiles: Investigation of defective lamellar structure crystal chemistry. In *Layered Mineral Structures and their application in Advanced Technologies*, Brigatti, M. F.; Mottana, A., Eds. The European Mineralogical Union and the Mineralogical Society of Great-Britain & Ireland: London, 2011; Vol. 11.
2. Warren, B. E., X-Ray Diffraction in Random Layer Lattices. *Physical Review* **1941,** 59, (9), 693.
3. Drits, V. A.; Tchoubar, C., *X-ray diffraction by disordered lamellar structures : theory and applications to microdivided silicates and carbons*. Springer-Verlag: Berlin, 1990; p 371.
4. Gates, W. P.; Slade, P. G.; Manceau, A.; Lanson, B., Site occupancies by iron in nontronites. *Clays and Clay Minerals* **2002,** 50, (2), 223-239.
5. Ferrage, E.; Lanson, B.; Michot, L. J.; Robert, J. L., Hydration Properties and Interlayer Organization of Water and Ions in Synthetic Na-Smectite with Tetrahedral Layer Charge. Part 1. Results from X-ray Diffraction Profile Modeling. *Journal of Physical Chemistry C* **2010,** 114, (10), 4515-4526.
6. Claret, F.; Sakharov, B. A.; Drits, V. A.; Velde, B.; Meunier, A.; Griffault, L.; Lanson, B., Clay minerals in the Meuse-Haute marne underground laboratory (France): Possible influence of organic matter on clay mineral evolution. *Clays and Clay Minerals* **2004,** 52, (5), 515-532.
7. Bargar, J. R.; Fuller, C. C.; Marcus, M. A.; Brearley, A. J.; Perez De la Rosa, M.; Webb, S. M.; Caldwell, W. A., Structural characterization of terrestrial microbial Mn oxides from Pinal Creek, AZ. *Geochimica et Cosmochimica Acta* **2009,** 73, (4), 889-910.
8. Trolard, F.; Bourrié, G.; Abdelmoula, M.; Refait, P.; Feder, F., Fougerite, a new mineral of the pyroaurite-iowaite group: description and crystal structure. *Clays and Clay Minerals* **2007,** 55, (3), 323-334.
9. Grangeon, S.; Claret, F.; Lerouge, C.; Warmont, F.; Sato, T.; Anraku, S.; Numako, C.; Linard, Y.; Lanson, B., On the nature of structural disorder in calcium silicate hydrates with a calcium/silicon ratio similar to tobermorite. *Cement and Concrete Research* **2013,** 52, 31-37.
10. Ruby, C.; Upadhyay, C.; Géhin, A.; Ona-Nguema, G.; Génin, J.-M. R., In Situ Redox Flexibility of Fe^{II-III} Oxyhydroxycarbonate Green Rust and Fougerite. *Environmental Science & Technology* **2006,** 40, (15), 4696-4702.
11. Nasser, A.; Buchanovsky, N.; Gerstl, Z.; Mingelgrin, U., Mineral induced mechanochemical degradation: The imazaquin case. *Chemosphere* **2009,** 75, (1), 20-27.
12. Blanc, P.; Bourbon, X.; Lassin, A.; Gaucher, E. C., Chemical model for cement-based materials: Temperature dependence of thermodynamic functions for nanocrystalline and crystalline C–S–H phases. *Cement and Concrete Research* **2010,** 40, (6), 851-866.
13. Manzano, H.; Dolado, J. S.; Guerrero, A.; Ayuela, A., Mechanical properties of crystalline calcium-silicate-hydrates: comparison with cementitious C-S-H gels. *physica status solidi (a)* **2007,** 204, (6), 1775-1780.
14. Brunauer, S.; Greenberg, S. A. In *The Hydration of Tricalcium Silicate and 8-Dicalcium Silicate at Room Temperature*, Chemistry of Cement: Proceedings of the Fourth International Symposium, Washington, 1960; US National Bureau of Standards, Ed. Washington, 1960.
15. Grangeon, S.; Lanson, B.; Miyata, N.; Tani, Y.; Manceau, A., Structure of nanocrystalline phyllomanganates produced by freshwater fungi. *American Mineralogist* **2010,** 95, (11-12), 1608-1616.

Thermodynamic properties of hydration of smectites considering the energetic contribution of capillary water.

P. Vieillard[1], P. Blanc[2], H. Gailhanou[2], A. Lassin[2], R. Denoyel[3], E. Bloch[3], S. Gaboreau[2], C.I. Fialips[4], B. Madé[5] & E. Giffaut[5]

1. CNRS-IC2MP-UMR7285, HydrASA, 5 Ave Albert Turpain, F-86022 Poitiers Cedex (philippe.vieillard @univ-poitiers.fr)
2. BRGM 3 av. Claude Guillemin, BP 6009, F-45060 Orléans Cedex 2 (pblanc@brgm.fr)
3. Aix Marseille Université, CNRS, MADIREL UMR 7246, 13397, Marseille, France,
4 TOTAL - CSTJF, Av. Larribau, 64018 Pau Cedex, France
5- Andra, F-92298 Châtenay-Malabry Cedex, France

In the framework of radioactive waste repository within natural clayey formations (Callovo-Oxfordian clayrock) or using engineered clayey barriers, the prediction of the long-term behavior of clay materials requires the thermodynamic properties of clay minerals in order to model the evolution of primary clay minerals in response to potential chemical perturbations. These data sets can be merged in a thermodynamic database "Thermochimie" (Giffaut et al. 2014), initially created by Andra in 1996.

Hydration properties of swelling clay minerals may be very variable depending on the chemical composition of the clay, on the nature of the interlayer cations and on the interlayer charge (Cases et al., 1997; Bérend et al., 1995; Vieillard et al., 2011). The Wyoming smectite has been largely studied, notably for assessing its hydration behavior as a function of the interlayer cations, in connection with its structural characteristics (Ferrage et al., 2005; Salles et al., 2010).

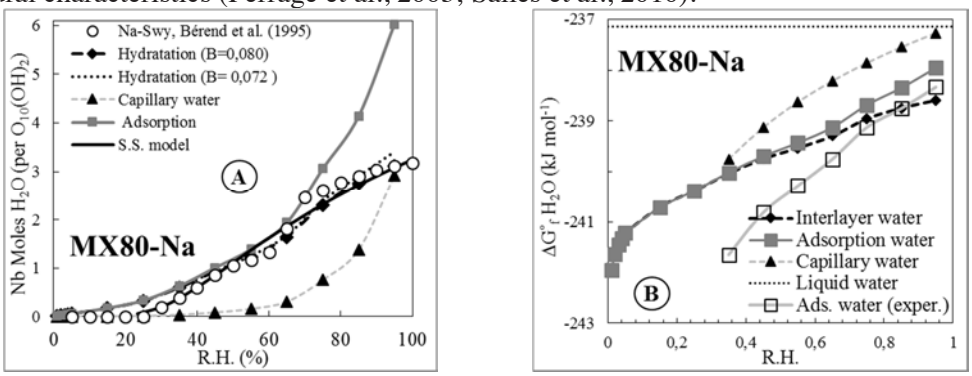


Figure 1 – Adsorption isotherms of interlayer water and free energy of formation of water in different states (sorbed, hydration, capillary) versus relative humidity

The purpose of the present study was to parameterize a predictive model of consistent thermodynamic data of hydration and the amount of effective interlayer water for all di-octahedral and tri-octahedral smectites with different structural charges (interlayer, tetrahedral or octahedral) in a large range of relative humidity close to saturation. Five natural 2:1 clay minerals: Smectite MX-80, Beidellite, Nontronite, Saponite and Vermiculite have been used in this work and are conditioned into nine homoionic clays minerals, for which adsorption-desorption isotherms are measured at two temperatures 25°C and 45°C.

The thermodynamic parameters ($\Delta H°_{ads}$, $\Delta G°_{ads}$ and $S°_{ads}$) are extracted from the adsorption-desorption isotherms performed at two temperatures done on nine samples. In order to extract the thermodynamic parameters of interlayer water sensu stricto from adsorption-desorption isotherms, the capillary water contribution is considered (Lassin et al. 2005) (Fig. 1) and dissociated from the hydration thermodynamic contribution. The latter are retrieved by using the solid solution model of Ransom and Helgeson, (1994) and provide a set of 4 thermodynamic parameters $\Delta\overline{H}^{\circ}_{Hyd}$, $\Delta\overline{S}^{\circ}_{Hyd}$, W_H et W_S characterizing the theoretical mechanisms of adsorption of the interlayer water versus the relative humidity in the 35%-100% relative humidity range.

From the nine different samples, the set of thermodynamic parameters of the solid solution between interlayer water and anhydrous clay are regressed depending on the nature of the clay

(interlayer cation, interlayer, tetrahedral and octahedral charges, nature of the cations in the octahedral sites). For the same tetrahedral and interlayer charges, a linear relationships is observed between the four thermodynamic parameters and the nature of the interlayer cation defined by its electronegativity and its entropy of hydration. Two different sets of parameters are developed for di-octahedral and tri-octahedral smectites respectively, allowing to model the hydration isotherm versus the relative humidity in the first hand and, in the second hand, to provide the formation properties of the interlayer water for a given relative humidity. To validate this model, results of prediction are compared with other experimental adsorption isotherms performed on natural dioctahedral and trioctahedral smectites, showing a good agreement for the relative humidity domain higher than 60%. Solubility products from experimental measurements on natural clays compiled by Vieillard, (2000) and calculated Log K from calorimetric measurements of some natural clays given by Blanc et al., (2014) are compared with predicted solubility products calculated by combining the model for the anhydrous phases (Blanc et al., 2014) and the hydration model from the present work, displaying a good agreement (Fig. 2).

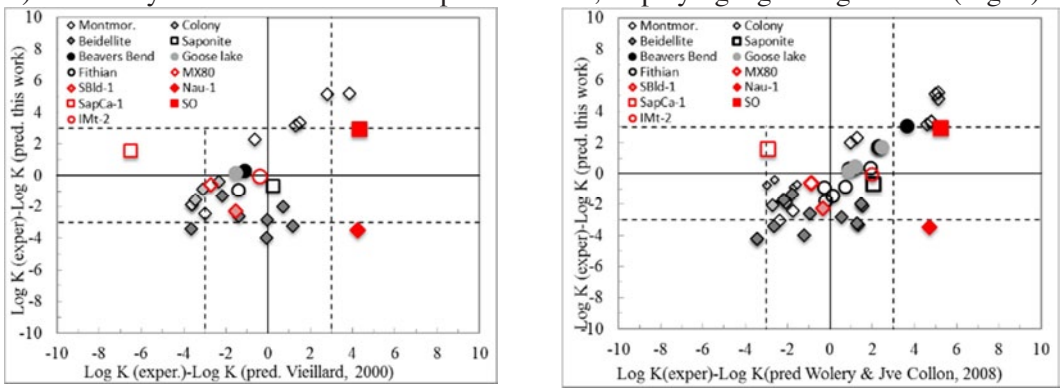


Figure 2 – Comparison of experimental log K of some natural clays (Vieillard, 2000, Blanc et al. 2014) with predicted values (see text).

Références:

Bérend, I., Cases, J.M., François, M., Uriot, J.P., Michot, L., Masion, A., Thomas, F., 1995. Mechanism of adsorption and desorptionof water vaporby homoionic montmorillonites:2. The Li^+, Na^+, K^+, Rb^+ and Cs^+ exchanged forms. Clays and Clay Minerals 43, 324-336.

Blanc, P., Vieillard, P., Gailhanou, H., Gaboreau, S., Claret, F., Gaucher, E.C., Fialips, C.I., Made, B., Giffaut, E., 2014. A generalized model for predicting the thermodynamic properties of clay minerals. American Journal of Science (in press)

Cases, J.M., Bérend, I., François, M., Uriot, J.P., Michot, L., Thomas, F., 1997. Mechanism of adsorption and desorption of water vapor by homoionic montmorillonite: 3. the Mg^{2+}, Ca^{2+},Sr^{2+} and Ba^{2+} exchanged forms. Clay and clays minerals 45, 8-22.

Ferrage, E., Lanson, B., Sakharov, B.A., Drits, V.A., 2005. Investigation of smectite hydration properties by modeling experimental X-ray diffraction patterns: Part I. Montmorillonite hydration properties. American Mineralogist 90, 1358-1374.

Giffaut, E., Grivé, M., Blanc, P., Vieillard, P., Colas, E., Gailhanou, H., Gaboreau, S., Marty, N., Madé, B., 2014. Andra Thermodynamic database for performance assessment: Thermochimie. Applied Geochemistry.

Lassin, A., Azaroual, M., Mercury, L., 2005. Geochemistry of unsaturated soil systems: Aqueous speciation and solubility of minerals and gases in capillary solutions. Geochimica et Cosmochimica Acta 69, 5187-5201.

Ransom, B., Helgeson, H.C., 1994. A Chemical and Thermodynamic Model of Aluminous Dioctahedral-2/1 Layer Clay Minerals in Diagenetic Processes - Regular Solution Representation of Interlayer Dehydration in Smectite. Amer J Sci, 294, 4, 449-484.

Salles, F., Bildstein, O., Douillard, J.M., Jullien, M., Raynal, J., Van Damme, H., 2010. On the Cation Dependence of Interlamellar and Interparticular Water and Swelling in Smectite Clays. Langmuir 26, 5028-5037.

Vieillard, P., 2000. A new method for the prediction of Gibbs free energies of formation of hydrated clay minerals based on the electronegativity scale. Clays Clay Minerals 48, 459-473.

Vieillard, P., Blanc, P., Fialips, C.I., Gailhanou, H., Gaboreau, S., 2011. Hydration thermodynamics of the SWy-1 montmorillonite saturated with alkali and alkaline-earth cations: a predictive model. Geochimica Cosmochimica Acta 75, 5664-5685.

Ferrous iron uptake on montmorillonites

D. Soltermann[1,2], *M. Marques Fernandes*[1], R. Dähn[1] , C. Gorski[3] and B. Baeyens[1]

[1]Laboratory for Waste Management, Paul Scherrer Institut, Villigen PSI, Switzerland, (*maria.marques@psi.ch).
[2]Institute of Biogeochemistry and Pollutant Dynamics, ETH Zürich, Zürich, Switzerland.
[3]Department of Civil and Environmental Engineering, Pennsylvania State University, Pennsylvania, United States.

In the near-field of a deep underground high-level radioactive waste repository the production of H_2 and the corrosion of iron canisters will release large amounts of ferrous iron (Fe(II)) into the interstitial porewater of the engineered barrier (bentonite). The presence of high Fe(II) concentrations in the porewater might have a significant influence on the sorption behaviour of radionuclides through competitive sorption but might also influence the redox state of the radionuclides through various associated redox reactions. An improved knowledge of the Fe(II) uptake behaviour on natural clay minerals is therefore essential for understanding the fate of radiocontaminants.

In this study the uptake of Fe(II) by several montmorillonites was investigated by batch sorption experiments, surface complexation modelling, Moessbauer spectroscopy and X-ray absorption spectroscopy (XAS). The choice of montmorillonite as sorbent is highly relevant since this clay mineral is foreseen as a backfill material in the concept for radioactive waste repositories in many countries.

Four different montmorillonite samples were used, a synthetic montmorillonite with no structural Fe(III), two natural montmorillonites with 0.5 wt.% (STx) and 2.9 wt.% (SWy) structural Fe(III), and a dithionite-treated SWy where all structural Fe(III) was reduced to Fe(II). For all these montmorillonites Fe(II) sorption edges and isotherms were measured. All sorption experiments were carried out under anoxic (O_2 <0.1 ppm) conditions. The sorption of Fe(II) on STx and SWy was also measured under electrochemically controlled reducing conditions.

The Fe(II) sorption behaviour under anoxic conditions on the Fe-free, Fe-low (STx) and dithionite treated SWy is similar and comparable to that of other divalent metals, e.g. Zn(II). The data could be successfully modelled with the two-site protolysis non-electrostatic surface complexation and cation exchange (2SPNE SC/CE) sorption model [1-2]. In contrast, the uptake of Fe(II) on SWy with 2.9 wt.% structural Fe(III), was much more pronounced, and could be quantitatively described only after introducing an additional surface reaction involving an electron transfer from the surface-bound ferrous iron to the structural ferric iron [3].

Mössbauer spectroscopy on ^{57}Fe loaded samples prepared under anoxic conditions confirmed that on the Fe-low and dithionite-reduced clays iron is predominantly sorbed as Fe(II) whereas as on SWy iron is predominantly oxidized to surface-bound Fe(III) and Fe(III) oxides. This surface induced Fe oxidation and formation of Fe(III) was also observed by Schaeffer et al. on nontronite [4]. ^{57}Fe Mössbauer spectroscopy was also performed on ^{56}Fe loaded clays to probe the oxidation state of structural iron upon sorption of Fe(II). The observed reduction of structural Fe(III) in SWy unambiguously evidences the role of structural Fe(III) as an e^- acceptor. These results were supported by XAS [2].

Sorption experiments on STx and SWy carried out under electrochemically reducing conditions (Eh = -0.640 V) were in agreement with the data obtained under anoxic conditions on the iron free and low iron montmorillonite (STx) i.e. iron is mainly present as a Fe(II) surface complex [4]. The extended 2SPNE SC/CE sorption model is capable to quantitatively describe sorption edges and isotherms for different montmorillonites with low and high iron contents over a wide range of redox conditions ($-0.64\ V \leq Eh \leq +0.28\ V$) and Fe(II) equilibrium concentrations.

This study showed that the uptake of Fe(II) on clay minerals is controlled by the clay properties (i.e. oxidation state and availability of structural iron) and/or aqueous redox conditions

References:

1. Soltermann, D., Marques Fernandes, M., Bradbury, M. H., Dähn, R., Brendlé, J. and Baeyens, B. (2012). Fe(II) sorption on a synthetic montmorillonite. A combined macroscopic and spectrosocpic study. Environ. Sci. & Technol. 47(13), 6978-5168.

2. Soltermann, D., Marques Fernandes, M., Baeyens, B., Dähn, D., Josh, P. A., Scheinost, A. C. and Gorski, C. A. (2014). Fe(II) uptake on natural montmorillonites. I. Macroscopic and spectroscopic characterization Environ. Sci. & Technol. 48(15), 8698-705.

3. Soltermann, D.; Baeyens, B.; Bradbury, M. H. and Marques Fernandes, M. (2014). Fe(II) uptake on natural montmorillonites. II. Surface complexation modeling. Environ. Sci. & Technol. 48(15), 8688-97.

4. Schaefer, M. V.; Gorski, C. A.; Scherer, M. M. (2011). Spectroscopic Evidence for Interfacial Fe(II)-Fe(III) Electron Transfer in a Clay Mineral. EnvironSci. & Technol. 45 (2), 540-545.

Nagra's RD&D programme on Opalinus Clay - Some recent findings and outlook

I. Gaus[1], L. Johnson, P. Marschall, T. Vietor, P. Zuidema

Nagra, Hardstrasse 73, 5430 Wettingen, Switzerland

Nagra's mission is to develop safe geological repositories in Switzerland for all radioactive wastes arising in Switzerland. The procedure for site selection in Switzerland foresees application within the next 7 to 8 years for general (site) licences for two repositories, one for low and intermediate level waste (L/ILW) and one for spent fuel, vitrified high level waste (HLW) and long-lived ILW (referred to hereafter as the HLW repository). The proposed disposal siting regions are located in sedimentary rocks in Northern Switzerland, except for one region in Central Switzerland for L/ILW. Repository implementation involves a stepwise process that takes several decades, thus a comprehensive planning base for the scientific and engineering work is needed. The RD&D plan focuses on planning the work needed to support the general site licence applications, with a view to also ensuring that long-term in situ studies supporting the future construction stage are planned and initiated. Nagra's most recent RD&D plan was published in 2009, while the next version is foreseen for 2016.

An important part of the RD&D activities is targeting the Opalinus Clay formation, the host rock selected for the HLW repository and a possible host rock candidate for the L/ILW repository (Nagra, 2008). The Opalinus Clay has a low hydraulic conductivity in the range of 10^{-12} to 10^{-14} m s^{-1} and a porosity of 0.12 and 0.15 in the siting regions. The Opalinus Clay formation is generally 100 m thick and is surrounded by clay-rich confining units. The Opalinus Clay formation has the following favourable characteristics (Nagra, 2002):

- The Opalinus Clay has such a low hydraulic conductivity that solute movement through the formation is predominantly by diffusion rather than advection.
- The geochemical conditions in the Opalinus Clay are reducing, slightly alkaline and moderately saline and favour the preservation of the engineered barriers and radionuclide retention.
- The geochemical environment in the Opalinus Clay and surrounding formations is expected to remain effectively stable for several million years.
- The properties of the Opalinus Clay ensure that repository-induced and natural fractures will be of very low hydraulic conductivity due to the self-sealing capacity of the Opalinus Clay; i.e. their effect on the hydraulic properties of the Opalinus Clay will be negligible.
- The Opalinus Clay is an indurated claystone (clay shale) with reasonable engineering properties, allowing tunnels to be constructed at depths of several hundred metres.

The presentation provides an overview of Nagra's most recent and planned RD&D activities.

In the first part the activities related to the structural, geological, geochemical, hydrogeological and hydromechanical characterisation of the Opalinus Clay from the microscale to the regional scale are discussed. Natural tracer profiles have been instrumental for demonstrating the extremely low transport capacity of the Opalinus Clay and further refinement of the argumentation in the next years is foreseen. At the large scale 3D seismics (starting 2015) and deep drilling (starting 2017) are planned at the proposed repository sites to refine the geosphere models. At the very small scale hyperspectral scans are contributing to the mineralogical characterisation. Further efforts will aim to enhance the correlation between mineralogy and petrophysical parameters. While these elements contribute to the development of accurate static geomodels, several activities are already anticipating the development

[1] Corresponding author: irina.gaus@nagra.ch

of the dynamic models for the proposed sites. The understanding of the constitutive behaviour of the Opalinus Clay will be enhanced (e.g. using novel large strain experiments and adequately assessing the role of the hydraulic state of the samples). Detailed geochemical analysis and modelling are accurately assessing the pore water compositions in support of the long-term safety assessment.

In the second part, the focus is on the impact of the repository on the Opalinus Clay from a long term safety point of view. This includes gas migration and thermo-hydro-mechanical impacts as well as excavation damaged zone (EDZ) characterisation and clay interface reactions. With the results of large-scale gas related experiments (HG-A and HG-D) available and the FORGE 7th Framework project now complete, the conceptual picture on how gas is transported in the EDZ and the disturbed OPA can be refined while advanced numerical models (FEM-DEM) provide insight into the formation of the EDZ. A series of increasingly complex heater tests (HE-D, HE-E, FE) are significantly contributing to the understanding of thermally induced effects in the Opalinus Clay and the bounding of induced overpressures. Important observations to confirm these bounding assumptions are expected in the years to come.

Finally, in the third part, activities supporting engineering and planning of repository construction are highlighted. As the plans for the repository are targeted to be at the concept stage at the time of the licence application, these activities will remain mainly desk-based (e.g. modelling studies). The 1:1 scale multiple heater test at Mont Terri (FE-experiment), for which the construction was finalised in December 2014, had a strong demonstration component (as part of the DOPAS 7th Framework project) regarding the feasibility of the horizontal emplacement concept as proposed by Nagra and accepted by the Swiss Government (Nagra, 2002).

In all of these activities the Mont Terri Rock laboratory, where Nagra is running an extensive experimental programme, plays a crucial role. The Mont Terri Rock laboratory, located in the north-eastern part of Switzerland, at significant distance from the potential repository sites, provides direct access to Opalinus Clay. However, boundary conditions at Mont Terri (stress regime, temperature) and certain properties (the Opalinus Clay at Mont Terri is faulted and shows a significant anisotropy in mechanical, hydraulic and thermal properties) are different from those anticipated at the potential repository sites, which are characterised by less faulting, stronger rocks, higher temperatures and stresses. A transferability approach needs to be developed and substantiated with the help of data from boreholes at the planned repository sites. Direct access to the underground at the site is foreseen only after the site license application, when the on-site underground research laboratories will be constructed.

Considerations regarding the anticipated geological and tectonic evolution of the Opalinus Clay, taking into account an assessment time of 1 Mio years and the location of the sites close to the Alps, are a further important aspect of the RD&D programme.

References

Nagra (2002): Project Opalinus Clay: Safety report: Demonstration of disposal feasibility for spent fuel, vitrified high-level waste and long-lived intermediate-level waste (Entsorgungsnachweis). Nagra Technischer Bericht. NTB 02-05. Nagra, Wettingen.

Nagra (2008): Vorschlag geologischer Standortgebiete für ein SMA- und ein HAA-Lager: Geologische Grundlagen (Bericht zur Geologie). Nagra Technischer Bericht. NTB 08-04. Nagra, Wettingen.

Geosphere characterization for a DGR in the argillaceous limestone of the Ordovician Cobourg Formation in the Michigan Basin: an integration of field, lab and modelling methods

***J.F. Sykes*[1], M.R. Jensen[2], S.D. Normani[1], Y. Yin[1], R. Beauheim[3], T. Al[4] and I.D. Clark[5]**

[1]University of Waterloo, Dept of Civil and Environmental Engineering, Waterloo Ontario Canada N2L3G1
[2]Nuclear Waste Management Organization, 22 St. Clair Ave. East, Toronto Ontario Canada M4T2S3
[3]Intera GeoScience and Engineering Solutions, 1812 Centre Creek Drive, Suite 300, Austin Texas 78754
[4]University of New Brunswick, Department of Earth Sciences, Fredericton New Brunswick Canada E3B5AB
[5]University of Ottawa, Department of Earth Sciences, Ottawa Ontario Canada K1N6N5

A Deep Geologic Repository (DGR) for low and intermediate level radioactive waste has been proposed by Ontario Power Generation for the Bruce site near Tiverton, Ontario, Canada. Situated on the eastern flank of the Michigan Basin, the DGR concept envisions a repository excavated at a depth of 680m within the near horizontally bedded argillaceous limestone Cobourg Formation beneath 200m of Ordovician age shale. The attributes of the host Cobourg Formation and enclosing bedrock formations were determined using a multi-disciplinary approach in which complimentary evidence from field, laboratory, self-analogue and illustrative numerical modelling methods were integrated to establish groundwater system behaviour over extended time and space scales. A key component of this approach was hypothesis testing and numerical experiments that were used to instil confidence in the host and enclosing rock properties and behaviour including the potential for solute transport from a repository. Computational codes for the work included the three-dimensional saturated density-dependent flow model FRAC3DVS-OPG, the two-phase gas and water flow model TOUGH2-MP and the reactive transport model MIN3P-NWMO.

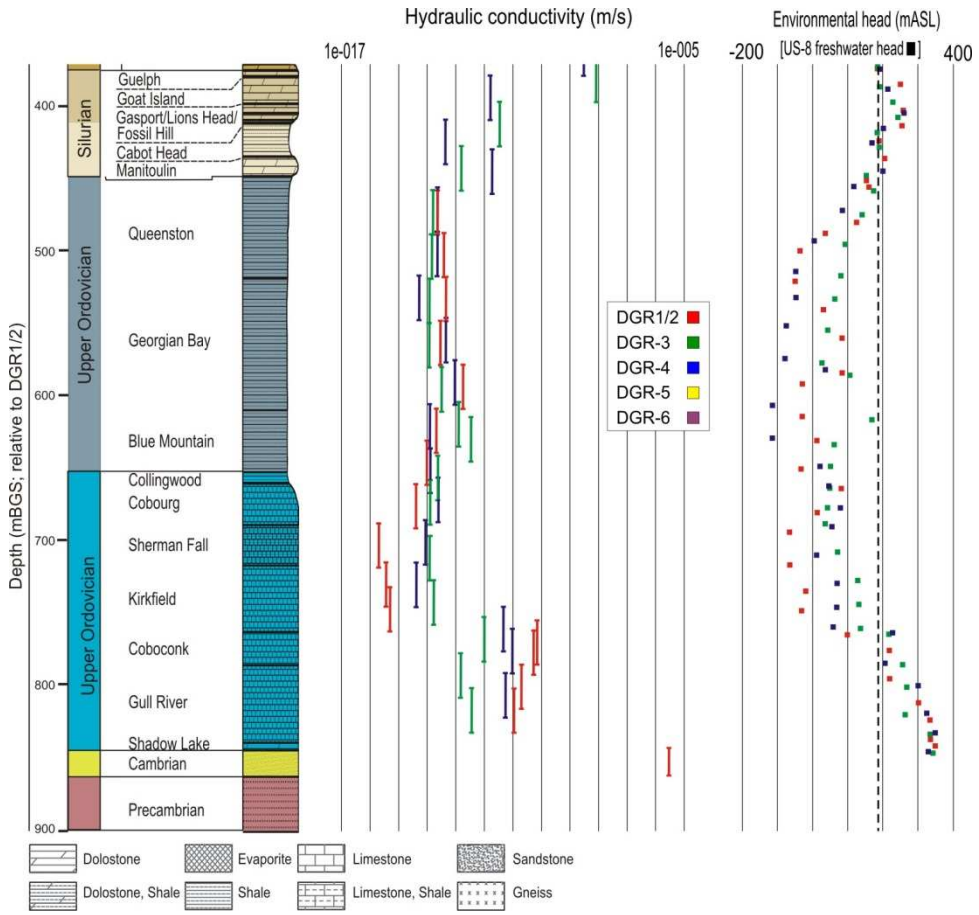


Figure 1: Hydraulic conductivity and environmental heads from DGR borehole data

A program of hydraulic borehole testing was performed using a custom-designed straddle-packer (30 m interval) testing tool in six DGR boreholes intersecting the Ordovician strata. Data inversion of obtained pressures yielded estimates of horizontal hydraulic conductivity (K_H) less than 10^{-14} m/s within the Cobourg Formation. These estimated K_H values were consistent with laboratory derived values. Estimated horizontal hydraulic conductivities within the overlying shale and underlying carbonate Ordovician formations ranged between 10^{-14} and 10^{-11} m/sec (Figure 1). The laboratory testing of rock specimens provided values of porosity and mechanical properties for the estimation of storage coefficients (10^{-7} to 10^{-6} m^{-1}); the porosity of the argillaceous limestone is less than 2%.

The distribution of hydraulic formation pressures within the Ordovician sedimentary sequence was measured using a Westbay MP-55 multi-level casing system installed in four boreholes encompassing the proposed repository footprint (i.e., 3.5 km^2). Pressure data from these multi-level installations has revealed that the Cambrian sandstone and the Guelph Formation in the Silurian are over-pressured relative to fluid density corrected hydrostatic levels while the Ordovician limestone and shale are significantly under-pressured (refer to Figure 1). The abnormal pressure data have provided a self-analogue to assess the formation scale low permeability of the Ordovician sediments and to yield estimates of vertical hydraulic conductivity (K_V). A key element included an assessment of several phenomena capable of generating the abnormal formation pressures and, in particular, the strong under-pressures. Hypotheses developed in this regard included glacial ice-sheet loading and unloading, the burial history of the post Devonian sediments and the presence of an immiscible gas phase in the rock. The glaciation hypothesis was tested assuming multiple 120 ka glacial cycles over a 1 Ma period. The possible ice loading was developed using the University of Toronto Glacial Systems Model (GSM). Using the computational models FRAC3DVS-OPG and TOUGH2-MP, the parameter estimation model PEST, and a one-dimensional conceptual model, all three cited hypotheses were able to generate the under-pressures although in several cases required formation scale K_V values were orders-of-magnitude lower than the horizontal conductivities estimated from borehole and laboratory testing.

The geochemical and isotopic compositions of pore fluids and gases in the Ordovician sediments were determined by vacuum distillation of crushed and sieved rock at 150°C. Rock samples were obtained from the recovery of approximately 3800 m of high-quality, 75 mm diameter core from the 6 boreholes drilled to depths between approximately 450 and 860 m below ground surface at the Bruce nuclear site. Porewater throughout the upper 240 m of the Ordovician shale and carbonate aquiclude at the site has uniformly high salinity with strong Bromide enrichment consistent with a primary brine source generated through seawater evaporation to halite saturation. The profile of the stable water isotopes is consistent with a basin brine of evaporative origin. Preservation of the brine signature in the Ordovician sediments suggests that migration has been minimal since the Silurian.

The interpretation of the abnormal pressures together with porewater geochemical evolution and vertical environmental tracer distributions through the sedimentary sequence such as Cl and $\delta^{18}O$, the occurrence of juxtaposed zones of biogenic and thermogenic methane and helium ($^3He/^4He$) accumulations, amongst other metrics, provide evidence that pore fluids residing within the low permeability Ordovician sediments have long residence times and are essentially stagnant. Evidence strongly points to a diffusion dominated transport regime unaffected by geologic perturbations. Numerically estimated Peclet numbers for a broad range of normal evolution and sensitivity cases are less than 0.004 for a characteristic length of unity. Mean Life Expectancy (MLE), which is a measure of the average time for particles at a given point to exit a steady-state groundwater flow system, is estimated to be greater than 44 Ma for the proposed location of the DGR. An MLE of 164 Ma was estimated for the base-case scenario that used the hydraulic conductivities derived from the borehole straddle-packer tests and lab developed effective diffusion coefficients for the rock estimated from data obtained using X-ray radiography. Numerical experiments to describe the evolution of the pressures and chemistry of the rock indicate that the formation scale diffusion coefficients may be lower than the lab-based values. Multiple lines of evidence, including in-situ hydraulic testing, geochemical analyses, and numerical modelling, support the conclusion that the Cobourg Formation and the shales of the Ordovician age sediments have very low permeabilities and diffusion properties with these characteristics being sustained over geologic time.

Sorption values derived for argillaceous rocks in sorption data bases for safety analysis compared with measured values

Bart Baeyens, **Maria Marques Fernandes, Michael Bradbury**

Paul Scherrer Institut, Laboratory for Waste Management, 5232 Villigen PSI, Switzerland

In the Sectoral Plan for Deep Geological Repositories, Nagra has proposed six regions which are suitable for hosting a repository for low- and intermediate-level (L/ILW) and high-level (HLW) radioactive waste (Nagra 2008). Provisional safety analyses for all siting regions are part of the procedure, and support the evaluation and selection process. The host rocks being considered are all classified as argillaceous rocks in which released radionuclides will migrate mainly by diffusion. A state-of-the-art sorption data base (SDB) is one of the key parameter sets needed to quantify the radionuclide retardation in the host rocks and the bentonite buffer.

In order to derive sorption values for argillaceous rocks under a wide range of porewater and mineralogical compositions, a detailed procedure was developed by Bradbury et al. (2010). The methodology was based on sorption edge measurements on illite and montmorillonite, the hypothesis that 2:1 type clay minerals are the dominant sorbents, and so-called conversion factors which take into account the clay mineral content of the argillaceous rocks and radionuclide speciation in the different porewaters. All of the host rocks selected by Nagra: Opalinus Clay, 'Brauner Dogger', Effingen Member and Helvetic Marls, and, MX-80 bentonite, contain significant fractions of 2:1 clay minerals such as illite, illite-smectite mixed layers and montmorillonite.

Since this procedure for generating sorption values for SDBs is relatively new, verifications on the validity of the methodology were required. The aim of the study reported here was to measure sorption isotherms for representative radionuclides under realistic chemical conditions on the host rocks being considered, and to compare measured and calculated sorption values at trace concentrations. Co(II) and Ni(II) were chosen as being representative for divalent transition metals, Eu(III) for trivalent lanthanides and actinides, and Th(IV) for tetravalent actinides. Sorption isotherms for U(VI) were also measured. The quality of the selection procedures was then judged by level of correspondence between measured and calculated values for each rock type and the associated water chemistries.

A vast amount of sorption data on various argillaceous host rocks and MX-80 bentonite is presented and compared with blind predictions. In all, a total of 53 sorption isotherms with the elements Cs(I), Co(II), Ni(II), Eu(III), Th(IV) and U(VI) on Opalinus Clay, 'Brauner Dogger', Effingen Member, Helvetic Marls and MX-80 bentonite have been measured.

The sorption data at trace concentrations are presented by plotting the “measured R_d values” against the “calculated R_d values”, Figure 1. The continuous line represents a 1:1 correspondence between the measured and calculated sorption values. Points falling below this line indicate under predicted values whereas those above the line indicate over predicted values. The dashed lines encompass almost all of the measured data and illustrate that the maximum difference between the calculated and measured R_d values is generally at most a factor of ±6, i.e. ±0.8 log units. Based on this, it is concluded that the methodology applied to derive sorption values in the SDBs for a wide range of host rock mineralogy and water chemistry combinations has a high degree of reliability and captures the sorption in real systems within the uncertainty bounds given.

From the information presented here, and other studies carried out (Bradbury and Baeyens 2010, 2011), there is now a substantial body of evidence which strongly supports the approach and methodology for developing SDBs for argillaceous rocks and bentonite as applied in Baeyens et al. (2014).

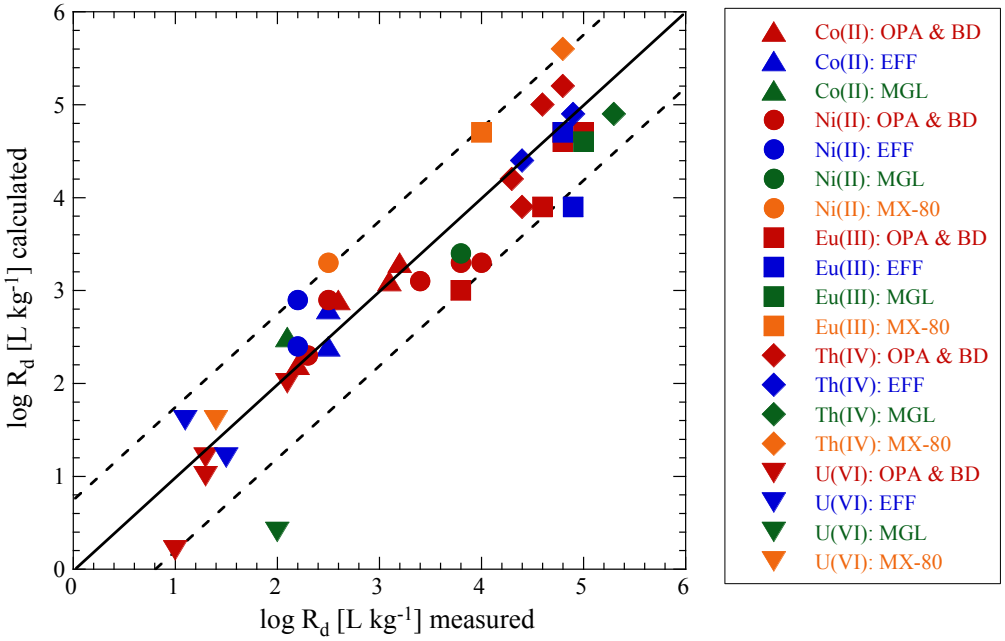


Figure 1: Overview of the comparison of measured and calculated sorption data at trace concentrations for Co(II), Ni(II), Eu(III), Th(IV) and U(VI) on Opalinus Clay (OPA), 'Brauner Dogger' (BD), Effingen Member (EFF), Helvetic Marls (MGL) and MX-80 bentonite (MX-80). The broken lines represent a band width of ± 0.8 log units.

References:

Baeyens, B., Thoenen, T., Bradbury, M.H. and Marques Fernandes, M. (2014): Sorption data bases for the host rocks and lower confining units and bentonite for provisional safety analyses for SGT-E2. Nagra Technical Report NTB 12-04. Nagra, Wettingen.

Bradbury, M.H., Baeyens, B. and Thoenen, T. (2010): Sorption data bases for generic Swiss argillaceous rock systems. Nagra Technical Report NTB 09-03. Nagra, Wettingen.

Bradbury, M.H. and Baeyens, B. (2010): Comparison of the reference Opalinus Clay and MX-80 bentonite sorption data bases used in the Entsorgungsnachweis with sorption data bases predicted from sorption measurements on illite and montmorillonite. PSI Report No. 10-09 and Nagra Technical Report NTB 09-07.

Bradbury, M.H. and Baeyens, B. (2011): Predictive sorption modelling of Ni(II), Co(II), Eu(III), Th(IV) and U(VI) on MX-80 bentonite and Opalinus Clay: A "bottom-up" approach. Appl. Clay Sci. 52, 27-33.

Nagra (2008): Begründung der Abfallzuteilung, der Barrierensysteme und der Anforderungen an die Geologie. Bericht zur Sicherheit und technischen Machbarkeit. Nagra Technical Report NTB 08-05. Nagra, Wettingen.

DOPAS Full-Scale Tests – Approach to Compliance Assessment

S. Doudou[1], M.J. White[1], M. Johnson[2], J-M. Bosgiraud[3] and Pär Grahm[4]

1 Galson Sciences Ltd, 5 Grosvenor House, Melton Road, Oakham, LE15 6AX, United Kingdom
2 Nuclear Decommissioning Authority, Curie Avenue, Harwell, Oxfordshire, OX11 0RH, United Kingdom
3 National Radioactive Waste Management Agency (Andra), 92298 Chatenay-Malabry, France
4 Swedish Nuclear Fuel and Waste Management Co, Oskarshamn, Sweden

The Full-Scale **D**emonstration **O**f **P**lugs **A**nd **S**eals (DOPAS) Project is a European Commission (EC) programme of work jointly funded by the Euratom Seventh Framework Programme and European nuclear waste management organisations (WMOs). The DOPAS Project is running in the period September 2012 – August 2016. Fourteen European waste management organisations (WMOs), and research and consultancy institutions, from eight European countries are participating in DOPAS. A set of full-scale tests, laboratory experiments, and performance assessment studies of plugs and seals in geological repositories will be carried out in the course of the project.

DOPAS aims to improve the industrial feasibility of plugs and seals, the measurement of their characteristics, the control of their behaviour over time in repository conditions and their hydraulic performance with respect to safety objectives.

The DOPAS Project focuses on tunnel, drift and shaft plugs and seals for crystalline, clay and salt rock. This paper focuses on two tests one in both a clay rock and crystalline rock:

- *Clay rock*: the Full-scale Seal (FSS) test being undertaken by ANDRA in a surface facility at St Dizier. FSS is a full-scale test of the reference drift and intermediate-level waste (ILW) disposal vault seal for the French Cigéo repository concept. The seal itself consists of a cast concrete containment wall, a swelling clay core and a shotcrete containment plug. The design also includes recesses that represent breakouts generated by the removal of the concrete lining used to support drifts and vaults during operations; the linings are removed to ensure that the seal meets hydraulic requirements.
- *Crystalline rock*: the Dome Plug (DOMPLU) test related to plugs in horizontal tunnels. DOMPLU is a full-scale test of the reference deposition tunnel plug in SKB's repository design. The plug consists of a dome-shaped, unreinforced concrete plug, a watertight seal and a filter zone. The function of the concrete plug is to resist deformation and to keep the watertight seal, filter and backfill in place. The watertight seal is made of bentonite blocks and pellets. Its function is to seal water leakage paths and to ensure an even pressure on the concrete. The filter is made of sand or gravel. Its function is to collect water draining from the deposition tunnel so that no water pressure is applied on the concrete plug before it has cured and gained full strength. The plug also contains concrete beams to aid construction, drainage, cooling and grouting pipes.

This paper describes the approach followed to assess the compliance of DOMPLU and FSS to their design bases. The initial learning gained from the installation and commissioning of the

two tests is summarised, and the construction methodologies and technologies are briefly assessed.

The starting point for compliance assessment was the design basis. The design basis is the set of requirements, conditions and needs that are taken into account in the design process. The design basis specifies the required performance of a component of a repository and the conditions under which the component has to provide the specified performance.

For each test design basis, a review was undertaken, and for each requirement (or condition) the approach to demonstrating compliance was described. The development of the compliance strategy statements in this way allowed for a reconsideration of the design statements, and in certain cases suggestions for rewording or other types of feedback related to the design basis statements. This is part of the iterative development of the design basis. The requirement-by-requirement (or condition-by-condition) review of the design basis allows generic methods for demonstrating compliance to be identified. This approach allows feedback to the specification of the design basis to be captured and the methodologies and technologies used to during each test to be evaluated and assessed.

Approaches to Evaluate and Underpin the Technical Feasibility of the Belgian Disposal Concept

S. Doudou[1], E.J. Harvey[1], P.J. Richardson[1], S.M. Wickham[1] and P. Van Marcke[2]

1 Galson Sciences Ltd, 5 Grosvenor House, Melton Road, Oakham, LE15 6AX, United Kingdom
2 ONDRAF/NIRAS, Avenue des Arts 14, 1210 Brussels, Belgium

In 2009, ONDRAF/NIRAS, the Belgian Agency for Radioactive Waste and Enriched Fissile Materials, established a six-year research, development and demonstration (RD&D) programme to explore the feasibility of its concept for the geological disposal of category B&C radioactive waste in Belgium. This programme, generally referred to as "Project B&C Techno", aims to acquire evidence and build arguments in order to demonstrate that the proposed disposal system can be constructed, operated and progressively closed, taking into account long-term safety requirements and operational safety requirements, at a cost that is commensurate with available funding. In particular, it aims to demonstrate that there are no fundamental flaws or "showstoppers" relating to plans for construction and operation of the disposal facilities. The developments in understanding gained through the programme will support ONDRAF/NIRAS' first Safety and Feasibility Case (SFC1).

Project B&C Techno brings together international experts from a range of waste management organisations and supporting research and consultancy organisations, to explore, at the conceptual design level, the anticipated feasibility of activities in three distinct areas:

- Waste post-conditioning in monoliths (category B) and supercontainers (category C).
- Repository construction.
- Repository operation and closure.

Selected main outcomes from the programme include:

- Determination of the performance of the category B monolith under various accident scenarios, through simulation of impact damage resulting from various drop configurations.
- Design of a device to tilt the supercontainer from a vertical to a horizontal orientation following assembly and prior to transfer.
- Development of a concrete composition for the supercontainer concrete buffer and testing of its construction feasibility and performance in half-scale tests.
- Design of a repository ventilation system for repository construction and operation.
- Development of a shaft hoisting system and an underground transport system for transporting the supercontainers and monoliths from the surface to their disposal positions in the repository.
- Development of functional requirements for the repository backfill, and research to develop the backfill formulation to fulfil these requirements.

Galson Sciences Ltd has been supporting coordination of activities under Project B&C Techno. This support has included synthesis of research outputs and development of various tools and methods to demonstrate that the Belgian geological disposal concept is feasible to implement. RD&D activities undertaken to substantiate feasibility focus on issues of particular relevance to the Belgian concept, and aim to avoid repeating work where transferable evidence is available from elsewhere.

Two examples of tools developed by Galson Sciences Ltd for ONDRAF/NIRAS under Project B&C Techno to substantiate feasibility are:

- A review of other national geological disposal concepts to identify transferable experience relating to the feasibility of constructing and assembling comparable disposal system components. This enables identification of key gaps in knowledge, and hence, prioritisation of ONDRAF/NIRAS' ongoing RD&D activities.
- Development of a storyboard illustrating the steps involved in disposing of category B&C waste, from retrieval from interim storage, through transport to the disposal site, to backfilling and closure of the repository.

This paper describes the outcomes from development of both substantiation tools.

Review of Disposal Concepts

The objective of this study was to review the designs and concepts for geological disposal under consideration by waste management organisations in nine countries, and focus on the engineering and technical feasibility of fabricating or constructing components similar to those envisaged in the Belgian geological disposal concept for category B&C wastes, with a view to identifying the extent to which RD&D work in those countries helps to substantiate the feasibility of implementing the Belgian concept.

Disposal concepts in the following nine countries have been reviewed: Canada, Finland, France, Germany, Japan, Sweden, Switzerland, the UK and the US. The specific components of the disposal concepts covered are: the Spent Nuclear Fuel (SNF) canister, SNF overpack insert, overpack, concrete container for Long-Lived Low and Intermediate-Level Waste (LILW-LL – equivalent to category B waste in Belgium), repository layout, waste transport methods, ventilation approach, backfilling concept, and sealing method.

The study concluded that transferrable experience from the countries reviewed can be used for all the disposal concept components considered, except for the backfilling concept used in Belgium for category C waste. No other country reviewed uses cement-based materials for backfilling High-Level Waste (HLW) and SNF disposal galleries. However, many countries use such materials for backfilling LILW-LL disposal galleries.

Storyboard

A series of diagrams, referred to as the "B&C Techno Storyboard", have been produced illustrating, at a high level, the sequence of activities involved in constructing and operating a repository for category B&C waste, from the initial retrieval of the wastes from interim storage through transport and emplacement in the repository, through to final closure of the repository.

The storyboard provides a completeness check on activities under Project B&C Techno, informs consideration of operational safety, highlights any remaining open questions, and also acts as a communication tool.

Results and experiences from full scale backfill block manufacturing and installation

Esther Jonsson, *Peter Eriksson*

Swedish Nuclear Fuel and Waste Management Company (SKB), Box 250, SE-10124 Stockholm, Sweden

Introduction

SKB's method for disposal of spent nuclear fuel is the KBS-3 method where the spent nuclear fuel is placed in copper canisters which are deposited in vertical deposition holes in crystalline rock. The canisters are surrounded by a bentonite buffer, after deposition the deposition tunnels are filled with backfill material. The reference concept for backfill involves use of pre-compacted bentonite blocks and pellets as shown in Figure 1.

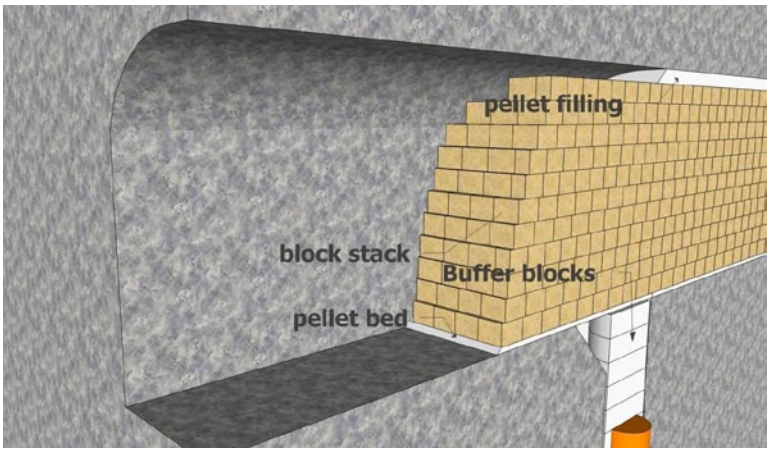


Figure 1. *Illustration of backfill components in a deposition tunnel*

The concept for production and installation of backfill in deposition tunnels has been further developed in SKB's project "System design of backfill" during 2010 – 2014. The main objective with this project was to ensure that the method selected for backfill works as intended with reasonable efficiency.The project was ended with a full scale underground test at Äspö Hard Rock Laboratory where 12 meters of backfill was installed in a tunnel located at a level of -450 meters.

Backfill design

The main function of the backfill is to limit flow of water (advective transport) in deposition tunnels and restrict upwards buffer swelling/expansion. In order for the backfill to fulfil its function it must be installed with a certain density which will set requirements on the deposition tunnel geometry and the backfill installation.

Backfill block manufacturing

Approximately 400 tonnes of backfills blocks were needed to perform the installation test at Äspö. The bentonite material used was a 2012 delivery of Asha NW BFL-L. The material was delivered in bigbags.The dry density of the blocks should be 1,650 – 1,750 kg/m^3. The backfill blocks should have the required dimensions and be possible to handle with a vacuum tool.
The bentonite was mixed to 20 % water content and then compacted in a press from SACMI.
The press is similar to what could be expected to be used in a future production facility.

Backfill installation test
This test was the first underground installation test of backfill at SKB. An industrial robot was purchased and developed for installation of backfill, which included development of a gripper, a platform, a measurement and control system. Since the test was performed with prototype equipment and also included manual operations which will not take place in the real repository, the installation time cannot be taken as the actual installation time for the real case. The test included installation of a 10 cm foundation bed of bentonite pellets, installation of bentonite blocks according to a certain stacking pattern (Figure 2) and installation of bentonite pellets in the gap between the stack and the rock walls.



***Figure 2**. Underground backfill block installation*

Results and experiences
In total 1820 blocks with the size 500x571x400 mm were manufactured with the average dry density of 1642 kg/m^3, this is a bit less than required, but the density can probably be increased by small adjustments in the process.
Some problems connected to the backfill material were discovered during the backfill manufacturing. One problem was that the granule size distribution varied between the bags. Different granule size distributions give different bulk densities. Since the mould filling was controlled by a filling height and not by mass it was hard to get an even density and height measurement. Another problem was the presences of stones in the backfill material. These stones got stuck in the mould filling equipment causing it to overheat, which resulted in extended production time.

During the installation test 1684 blocks or 12.3 meters of backfill were installed in the tunnel. 71% of the tunnel volume was filled with blocks and the rest with pellets. The installed dry density was about 1,420 kg/m^3. For this particular material 1230 kg /m^3 is the minimum density needed to reach the required hydraulic conductivity and swelling pressure, hence there are some margins in the installed backfill.
The robot had problems gripping 40 of the blocks due to cracks, inhomogeneities and larger pores. Only one block was dropped during the entire installation.

Conclusions
- A production system for backfill components can be built based on available standard equipment.
- Good control of the ingoing material regarding foreign materials and granule size distribution is essential for manufacturing with good quality and repeatability.
- The underground test showed that the installation of backfill can be carried out as intended, but further development of the equipment is needed to speed up the process.

State of the art of the solute diffusion characterisation in the Callovo-Oxfordian formation

Robinet Jean-Charles, Coelho Daniel & Giffaut Eric

Andra, 1-7 rue Jean-Monnet, F92298 Châtenay-Malabry, France (jean-charles.robinet@andra.fr).

For more than 15 years, the Callovo-Oxfordian formation is studied by Andra as a potential host formation for the deep disposal of high and intermediate level long life radioactive wastes in France (www.Cigéo.com). This presentation aims to show how a generalized model of diffusion of radionuclides is deducted from the overall work carried out over this period characterizing and understanding the diffusion-driven transport in the Callovo-Oxfordian formation. This research has been developed based on specific programs and European projects (Funmig, Catclay, and Recosy).

The following issues will be addressed as regards to the up-to-date results:

- The general strategy is based on a multi-scale approach combining laboratory studies on cm-scale clayrock samples (the main source of quantitative data) with more focused studies carried out at smaller scales and/or on analogous materials (mainly for understanding underlying phenomena), large scale (dm-m) *in-situ* and *ex-situ* studies (for validation of cm-scale results). This multi-scale strategy aims to consolidate the diffusion data and models.

- The variability of diffusion properties through the Callovo-Oxfordian formation. Effective diffusion coefficients and accessible porosity for HTO and a non sorbing anion (Cl^-) were determined by means of through diffusion experiments on cm thick samples taken from several boreholes distributed in the studied area. Based on statistical analysis, general trends will be proposed and discussed as regards to mineralogy and porosity.

- Anion exclusion and cation enhanced diffusion is specific to clay-rich materials. Their occurrence in the Callovo-Oxfordian formation is now established from different studies. From this statement, we propose an operational diffusion model to predict the effective diffusion coefficient of radionuclides in COx. This model is based on a predicted speciation for radionuclides in the Callovo-Oxfordian pore water, the bulk diffusion coefficient of species and the diffusion behavior of reference tracers (HTO, Cs^+ and Cl^-) in Callovo-Oxfordian formation.

- The use of R_d values extracted from batch and diffusion experiments in the objective to assess and predict *in-situ* migration of interacting species (Cs, Sr, Ni, Eu…).

Finally, we will set out the current research program mainly intended to determine the influence of thermal, hydraulical, mechanical and chemical disturbances in the near field of disposal vaults on the transfer properties in COx.

Can a macroscopic modeling approach properly describe transport in porous media during mineral precipitation induced clogging?

Chagneau, A [a,b,c]; *Claret, F* [c,*] ; Enzmann, F [d]; Wolf, M [d]; Made, B[e]; Schäfer, T [a,b,*]

[*] **corresponding authors: f.claret@brgm.fr ; thorsten.schaefer@kit.edu**

[a] Institute for Nuclear Waste Disposal (INE), Karlsruhe Institute of Technology (KIT), Karlsruhe, Germany
[b] Department of Geosciences, Freie Universität Berlin, Berlin, Germany
[c] Water and Environment division, French Geological Survey (BRGM), Orléans, France
[d] Department of Geosciences, Johannes Gutenberg University, Mainz, Germany
[e]Andra, 7 rue Jean Monnet, 92298 Chatenay-Malabry Cedex.

The understanding of permeability and tortuosity evolution due to porosity changes is of paramount importance for the description of various hydrogeological processes, such as fluid circulation in acid mine drainage remediation or hydrothermal systems, management of aquifer recharge, efficiency of permeable reactive barrier and the long-term geochemical evolution of host rock considered for high-level nuclear waste repositories. The description of clogging phenomena in a reactive transport code is challenging, particularly over the long time periods (1000 to 1,000,000 years) that are of interest in most safety assessment cases. In addition to the validation of numerical scheme, experiments to validate the implemented laws used for the coupling of geochemistry (e.g. dissolution-precipitation reactions) to the transport parameters (induced porosity changes) and overall fluid flow processes (e.g. Carman-Kozeny relationship or Archie's law) are required.
The so-called Archie's law (Archie, 1942) is widely used in reactive transport models (Navarre-Sitchler et al., 2009) and describes the relationship between the effective diffusivity (D_e, in m^2s^{-1}) of a dissolved species in a porous media and the diffusion coefficient of that same species in pure water (D_w, in m^2s^{-1}). The D_e/D_w ratio is a function of the tortuosity of the material (τ) and its constrictivity (δ) and therefore on the accessible porosity of the material (ε_a). As both the tortuosity and the constrictivity are difficult to measure experimentally, their ratio is often described as the geometrical factor, G. The relationship can be written as follows:

$$\frac{D_e}{D_w} = \frac{\delta}{\tau} = \frac{1}{G} = \varepsilon_a^n$$

where m is a called the cementation exponent. Though this empirical power law can accurately describe simple porous natural systems such as poorly compacted sands and sandstones, its applicability to more complex, low porosity and heterogeneous systems is questionable (Navarre-Sitchler et al., 2009)

In order to tackle this issue and to check the domain of validity of Archie's law, X-Ray transparent diffusion column experiments have been performed. Different porous media (clay, sand) have been used. In the present paper the focus is given on poorly compacted sand. Reduction of the pore space was induced by diffusion controlled precipitation of a simple salt, celestite ($SrSO_4$). A multi-scale and multi-technique approach has been used in order to characterize the transport properties before, during and after the reduction of the porosity as well as the amount of material that has precipitated. In this manner, (i) conservative tracer experiments (HTO) before and during the formation of a precipitation front, (ii) computed micro-tomography (μ-CT) coupled to pore-morphology modeling before and after the formation of a precipitation front, and (iii) post mortem analysis of the precipitate (dissolution, SEM-EDX) have been performed.

The conducted experiments are reproducible and after approximately 15 days the measured flux of through diffusing tracer HTO was constant and seemed to indicate that a steady state was reached, and that the pore space within the precipitation front was not fully clogged. Indeed, it was found that the

reduced pore space in the precipitation zone remained fully connected (no isolated pores) under the resolution of CT (~6 μm), allowing for the migration of the tracer. The porosity and transport parameters prior to clogging estimated by the first 2 methods were consistent, as was the mass of precipitate estimated by the last two methods.

However, the reactive transport model built upon the experimental results underestimated the remaining connected porosity in the precipitation zone and overestimated the amount of precipitate. The results presented demonstrate that 1D continuum models might fail in the long-term prediction of transport in geochemically disturbed systems and argue for more complex 2D pore-scale reactive transport and/or a modified diffusivity/porosity relationship.

References

Archie, G.E., 1942. Electrical Resistivity Log as an Aid in Determining Some Reservoir Characteristics. T Am I Min Met Eng 146, 54-62.

Navarre-Sitchler, A., Steefel, C.I., Yang, L., Tomutsa, L., Brantley, S.L., 2009. Evolution of porosity and diffusivity associated with chemical weathering of a basalt clast. J Geophys Res-Earth 114.

Microscopic modelling of dissolution and surface precipitation of sulfates in granular media: effect on the permeability and effective diffusivity.

N.I. Prasianakis[1], **T. Gimmi**[1,2], **G. Kosakowski**[1], **S.V. Churakov**[1]

[1]Laboratory for Waste Management LES, Nuclear Energy and Safety Department, Paul Scherrer Institut, CH-5232 Villigen, Switzerland.
[2]University of Bern, Institute of Geological Sciences, CH-3012 Bern, Switzerland.

Recent advances in microstructure modelling [1] and in X-ray tomographic techniques [2,3] facilitate on one hand the statistical geometric description of realistic geometrical structures of the materials of interest, and on the other hand their acquisition. These models and experimental techniques have been successfully applied to various highly porous materials such as clays and concrete. At the same time advancements in numerical algorithms and computer technology allow the simulation of 3D transport phenomena in conditions that it is either impossible to measure with a fully experimental technique [4,5] or where the evolution of the system occurs at geological relevant time scales.

Of great interest is the study of dissolution and precipitation phenomena and their effect on the porous media mass transport properties. For example, when a mineral precipitates/dissolves on the reactive porous surface, the overall porosity decreases/increases leading to a subsequent decrease/increase in permeability and effective diffusivity. At the same time the connectivity of the pores can also change in a way to block or to facilitate the mass diffusion processes.

In order to better understand the processes, a numerical tool is established using the lattice Boltzmann modeling framework. The lattice Boltzmann algorithms are based upon the solution of the Boltzmann BGK equation on a square/cubic lattice discretized space. The kinetic origin, the statistical description of populations of particles and the locality of the numerical operations, facilitate the modeling and simulation of transport phenomena in realistic complex geometries e.g. X-ray tomography output of porous media.

More specific a multicomponent LB mixture model, which takes into account dissolution-precipitation processes is created, benchmarked against well-defined simple simulation setups [6] and is further applied to simulate laboratory experiments on dissolution-precipitation of sulfates in granular media. The pore scale modelling results are compared with the experimentally observed evolution of porosity and corresponding changes in transport parameters [7]. The ability of pore scale simulation approach to provide effective transport and kinetic parameters for continuum scale reactive transport simulations is discussed.

References

[1] Tyagi M., Gimmi Th., Churakov S.V., "Multi-scale micro-structure generation strategy for up-scaling transport in clays", Advances in Water Resources 59, 181-195 (2013)
[2] Zhang M., Xu K., He Y., Jivkovt A.P, "Pore-scale modelling of 3D moisture distribution and critical saturation in cementitious materials.", Construction and Building Materials 64: 222–230 (2014).
[3] Holzer L., Münch B., Rizzi M., Wepf R., Marschall P., Graule T., "3D-microstructure analysis of hydrated bentonite with cryo- stabilized pore water." Applied Clay Science 3-4: 330-342 (2009).
[4] Prasianakis N.I., Rosén T., Kang J., Eller J., Mantzaras J., Büchi F.N., "Simulation of 3D porous media flows with application to polymer electrolyte fuel cells", Communications in Computational Physics 13, 851-866 (2013).

[5] Rosén T., Eller J., Kang J., Prasianakis N.I., Mantzaras J., Büchi F.N., "Saturation dependent effective transport properties of PEFC gas diffusion layers", Journal of Electrochemical Society 159, F536-F544 (2012).
[6] Tartakovsky A. M., Meakin P., Scheibe T.D., Eichler West R.M, "Simulations of reactive transport and precipitation with smoothed particle hydrodynamics.", Journal of Computational Physics 222: 654–672 (2007).
[7] Poonoosamy, J., Kosakowski, G., Van Loon, L., Mäder U. "Dissolution-Precipitation Processes in Tank Experiments for Testing Numerical Models for Reactive Transport Calculations". (to be subm.)

Characterization of transport and water retention properties of damaged Callovo-Oxfordian claystone

S. M'Jahad *(1), **C. A. Davy** (2), **F. Skoczylas** (2), **J. Talandier** (3)
*Corresponding author: sofia.m-jahad@edf.fr
(1) EDF R&D, Département AMA, 1 avenue du général de Gaulle, 92140 Clamart, France
(2) Ecole Centrale de Lille and LML UMR CNRS 8107, 59650 Villeneuve d'Ascq, France
(3) Andra, 1-7 rue Jean Monnet, 92298 Châtenay-Malabry Cedex, France

Aims and Scopes

In France, the French National Radioactive Waste Management Agency (Andra) designs an underground repository for high-level and long-lived nuclear waste. This repository will be located in east of France (Meuse/Haute-Marne). It will be built within an argillaceous formation (Callovo-Oxfordian claystone - COx) at 500 meters depth, which has favorable properties such as low permeability and is seismically stable. The excavation of repository induces damages locally around tunnels. This excavated damaged zone (EDZ) could be schematically divided into two parts: a zone close to the wall with a dense connected fractures network, a zone farther with isolated fractures and diffusive damage. In any case, EDZ could be potentially preferential pathways for fluid transport and radionuclides migration.
For performance and safety assessment, it is important to characterize the impact of such damage on the behavior of the host rock. The aim of this study is to investigate the influence of damage on the hydraulic properties of Cox claystone, partially or completely saturated, such as water retention properties, gas permeability and gas breakthrough pressure (GBP).

Sample preparation and induced damage protocol

Samples are prepared from different cores of COx claystone, obtained by drilling with given *in situ* orientation: vertical, horizontal and inclined. Samples are cylinders of 37.7 mm diameter and 10 mm height for water retention isotherms and gas permeability tests, and cylinders of 20 mm diameter and 40 mm height for water retention isotherms only. Previous studies ([2],[4]) show that there is no impact of sample dimensions on water retention properties and permeability results. A damaged procedure, which consists in one imbibition/drying cycle, has been conducted on so-called "damaged claystone" samples, in order to induce a small diffusive damage, representative of the EDZ zone. However, in practice, this damage procedure provides similar damage to the spontaneous damage (and cracking) of COx when it is subjected to ambient humidity and temperature conditions under free volume and no mechanical loading. The main difficulty of the study was to prepare "intact" samples because a lot of samples were initially damaged or damaged during the preparation and testing phases. Therefore, results of this experimental campaign on intact claystone were very few compared to the number of samples initially prepared. Also, it is difficult to develop a repeatable cracking methodology on claystone and to obtain "intact" samples: a sorting methodology is developed instead. To allow for this sorting, relative gas permeability results are compared with those of previous LML studies [4].

Experimental methods

For water retention experiments, samples are placed in hermetic chambers, above salt-saturated solutions, each at a fixed relative humidity (RH) value of 100%, or 98, 92, 85, 75, 70, 59, 43 or 11% at 20°C. Mass evolution is recorded continuously (1) under constant RH until mass stabilization, and then (2) by placing the samples in an oven at 65°C until the so-called dry mass stabilization is reached. The mass recorded at RH=100% corresponds to the sample saturated mass. Water saturation level Sw is calculated at each RH using the following definition, where m_{RH} is the stabilized mass at given RH, m_{dry} is sample dry mass, and $m_{saturated}$ is water-saturated mass, i.e. at RH=100%:

$$S_w = \frac{m_{RH} - S_{dry}}{m_{saturated} - S_{dry}}$$

For gas transport experiments, gas permeability K_{gas} is measured for each sample at given RH (or S_W) after mass stabilization, under a fixed confinement P_c (6 or 12MPa). Gas relative permeability is defined as:

$$K_{rg} = \frac{K_{gas}(RH)}{K_{dry}} = \frac{K_{gas}(S_w)}{K_{dry}}$$

where K_{dry} is the dry gas permeability (after 65°C oven-drying) of the same sample as the one tested at given RH. All permeability tests are performed with the quasi-static technique, see e.g. [3] for details.
For an initially fully water-saturated porous medium, gas breakthrough pressure (GBP) is defined as the gas injection pressure (applied on the sample upstream side) at which gas is expelled on the downstream sample side. Prior to GBP test, the sample is fully water saturated in a hydrotatic cell at a confinement of 5, 6 or 12MPa, by applying 4MPa water pressure gradient until liquid permeability reaches 10^{-20}-10^{-21}m^2. Then, upstream and downstream pipes are emptied from water and the sample is kept at a constant confining pressure P_c=5, 6 or 12MPa. The 2cl downstream chamber is closed by a dedicated valve, and its pressure is recorded with a pressure transducer. Argon gas pressure is increased very slowly on the upstream side (at a rate of 1 to 10 days between two ΔP_{gas}=0.5 MPa steps), until gas presence is detected in the downstream chamber. Gas detection is performed using both the downstream pressure transducer (±100 Pa) and a dedicated argon gas detector (±0.1μl/sec). Fluid movement towards the sample downstream side is detected via downstream pressure increase. Every 24h, the valve connected to the downstream chamber is opened. Whenever it is actually present, argon is expelled and identified with the gas detector.

Results and discussion

Almost all of the samples of our study are damaged, either initially or due to the laboratory protocol. The damage procedure increases the mean gas permeability by a factor 5, but these mean values vary hugely from one sample to the other (no reproducibility of the damage protocol). Also, COx samples have different degrees of damage within the same core. Mass stabilization under different RH is relatively fast (a few days) except at RH=100%, at which the claystone continues its water uptake, over very long periods (~100 days). This is observed by [2] for COx claystone and Opalinus clay: continuous water uptake results from the coupling between hydration and clay mineral swelling, and generates damage (cracking) under free volume boundary conditions. This damage increases the apparent porosity of the sample from 14-19%, value usually observed on intact Cox to 20-25% after swelling. The influence of damaged on capillary pressure/water saturation relationship and on gas relative permeability has been explored. Hysteresis effect between adsorption and desorption has been highlighted by taking several initial sample hydric states. Based on our sorting methodology which distinguishes three types of COx samples, main categories for water retention and gas transport assessment are:

- The so-called “intact” claystone is characterized by dry gas permeability below 1. 10^{-18}m^2: a good correlation is obtained between effective permeability and water saturation degree.
- “Micro-cracked” claystone presents a greater effective permeability, by about one order of magnitude than the intact claystone, and a low correlation between effective permeability and water saturation degree.
- The highly fractured claystone displays atypical results, and in particular dry and effective permeabilities above 1. 10^{-17}m^2, even at high confinement (12 MPa), no correlation between effective permeability and saturation.

In addition, GBP displays low values: from 0.3 to 1.4 MPa for samples oriented horizontally or inclined to the bedding plane, while GBP of vertically-oriented samples of the same dimensions may be higher, between 1.4 and 2.2 MPa (LML results [5]), and about 5-6 MPa for intact claystone (BGS results) [1]. Campaigns of GPB measures show clearly that GBP are a good indicator to indicate the degree of damage for the clay material which is in some cases more sensible to damage than gas permeability.

REFERENCES

[1] Harrington J.F., Cuss R.J., Noy D.J. and Talandier J., Processes governing advective gas flow in the Callovo Oxfordian Claystone (COx), 4th EAGE Shale Workshop Shales: “What do they have in common?”, 6-9 April 2014, Porto, Portugal.
[2]: Zhang C.L., Czaikowski O., Rothfuchs T.: Thermo-Hydro-Mechanical Behaviour of the Callovo-Oxfordian Clay Rock – Final report of the BURE-HAUPT / EC-TIMODAZ project, GRS-266, 2010.
[3]: Loosveldt H., Lafhaj Z., Skoczylas F., Experimental study of gas and liquid permeability of a mortar, Cement and Concrete Research, Vol 32, pp. 1357-1363, 2002.
[4]: M’Jahad S., Impact de la fissuration sur les propriétés de rétention d’eau et de transport des géomatériaux. Application au stockage des déchets radioactifs, PhD thesis, Ecole Centrale de Lille, 2012.
[5]: C. A. Davy, S. M'Jahad, F. Skocylas, J. Talandier, M. Ghayaza, "Evidence of discontinuous and continuous gas migration through undisturbed and self-sealed COx claystone", oral presentation at a plenary session of the 5th International Meeting on Clays in Natural and Engineered Barriers for Radioactive Waste Management, Montpellier, 22-25th October, 2012.

Combining high resolution two-phase with simplified single-phase simulations in order to significantly reduce computation time for PA/SA simulations for a deep geological repository for radioactive waste

Philipp Schaedle[1], **Thomas Kaempfer**[1], **Guillaume Pepin**[2], **Jacques Wendling**[2], **Juergen Brommundt**[1]

[1] AF-Consult Switzerland Ltd, Groundwater Protection and Waste Disposal, Taefernstrasse 26, CH-5405 Baden, Switzerland, *Philipp.Schaedle@afconsult.com*

[2] Andra, 1-7 rue Jean Monnet, F-92298 Châtenay-Malabry Cedex, France

For the performance analysis and safety assessment (PA/SA) of a planned deep geological repository for high-level long-lived radioactive waste (HLW-LL) and intermediate-level long-lived radioactive waste (ILW-LL), it is international standard to develop models which are capable to simulate two-phase flow and radionuclide transport through the repository and its host rock formation.

The models for PA/SA must have a high resolution and include all structures and features, and all relevant physical flow and transport processes should be parameterized and represented as accurately as possible. Because of these requirements, the models include nonlinearities and the resulting discretized mathematical equations have to be solved iteratively; hence the computational effort is large. Additional challenges are posed by both the spatial and temporal scales. The planned repository considered here consists of thousands of emplacement cells with relevant details on the decimeter-scale, and several kilometers of access tunnels and shafts. The potential radionuclide release in and from the repository and transport to the biosphere must be simulated for up to one million years. Finally, any modern PA/SA includes probabilistic studies to assess uncertainties. These may involve several hundred or even thousands of model runs. All these factors combined suggest that fundamental optimizations of the model are essential for computation times which allow for the required number of simulations to be conducted within a reasonable study duration, whereas the simulation quality in terms of results shall remain high.

Here we test an approach to increase the efficiency of the simulations by decoupling the flow and transport computations. The idea is to perform the time consuming two-phase flow simulations only once, followed by many less demanding single-phase unsaturated transport simulations that reuse the two-phase flow results. The main limitations of this are that the considered radionuclides need to be completely soluble in water, and their influence on flow has to be negligible. These requirements are fulfilled by many radionuclides in a repository. In addition, various optimizations of the spatial discretization have been tested to further reduce the computational effort.

The combination of these simplifications and optimizations is tested with the radionuclide iodine-129 (^{129}I). Numerical simulations with TOUGH2 are developed to model the migration of ^{129}I that is released from both HLW-LL and ILW-LL in a deep geological repository situated in the Callovo-Oxfordian clay formation in France. In a first step, a reference model is built using a detailed representation of geometry and accounting for all relevant physical processes governing the radionuclide transport from the time of closure of the repository up to one million years. This reference model considers, in particular, the two-phase physics explicitly. The second step involves our specifically devised transition methodology with the step by step implementation of simplifications and optimizations on the reference model until a single-phase model for radionuclide transport results, in which the two-phase physics are considered implicitly through spatiotemporal adjustments of the hydraulic parameters. The step by step implementation is actually an iteration of two processes: The first process is a simplification of the spatial discretization, and based on this the

second process leads to the corresponding single-phase model. After each process in each step the quality of the simulation results is evaluated with benchmarking criteria that compare radionuclide fluxes across a set of benchmarking surfaces to the fluxes in the reference results. These two processes are repeated until the final stage of simplifications and optimizations is reached, i.e. the benchmark criteria are no longer satisfied.

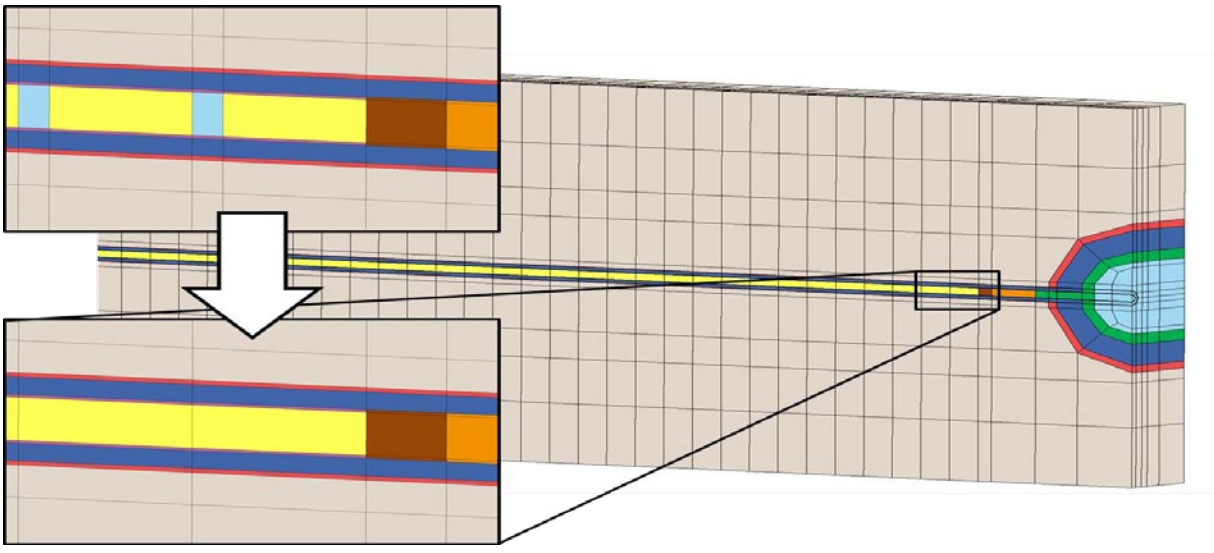
To investigate this approach two different studies are carried out, considering an emplacement drift with surrounding host rock 1) in the HLW-LL and 2) in the ILW-LL parts of the repository. First the spatial discretization is simplified for each model. For the HLW-LL model, different materials are merged and their parameters are lumped together to get an adequate physical representation. For the ILW-LL model drastic simplifications are possible; the more than 400 m long drift with several hundred waste canisters is represented by a few elements without breaching the benchmark criteria.

The decoupling of the two-phase and the single-phase computation is realized using our newly developed methodology implemented in the TOUGH2 modules eos75r and eos9nT. While running the two-phase flow and transport simulations in eos75r specific hydraulic results are stored in every computation time step. Later on these data are read by module eos9nT to compute transport results. Using this methodology it is possible to consider specific needs of each model in terms of temporal discretization, whereas the maximum temporal resolution is constrained by the eos75r simulations.

Our results show that as long as the numerical discretization remains the same, the applied method for going from two-phase to single-phase physics is very accurate. Radionuclide fluxes across all the benchmarking surfaces are identical, except where minor rounding errors occur due to numerically caused discrepancies in the output time-steps. This implies that our methodology may be applied successfully as long as none of the simplifications of the reference model violate benchmarking criteria.

Various sensitivity studies demonstrate that the approach is quite robust in the sense that most of the simplifications lead to results which fulfill the benchmarking criteria independently of the parameter values chosen for the sensitivities. This especially holds for the two-phase to single-phase transfer.

We conclude that the developed approach leads to a significant reduction of the computational effort while the results are very accurate. Furthermore, it is shown that it is possible to reduce the spatial resolution drastically and still produce results of very good quality in terms of satisfying the benchmark criteria. The developed approach continues to be used and pursued in the PA/SA program of Andra.



Example of one simplification step for spatial discretization.

Abiotic and biotic nitrate and nitrite reduction by redox-active Boom Clay components

N. Bleyen* [1], M. Vasile[1], C. Bruggeman[1], D. Durce[1], H. Moors[2] and E. Valcke[1]

[1] W&D Expert Group, SCK•CEN, Boeretang 200, 2400 Mol, Belgium
[2] MIC Expert Group, SCK•CEN, Boeretang 200, 2400 Mol, Belgium

In Belgium, Boom Clay is studied as a potential host rock for the deep geological disposal of Eurobitum, an intermediate-level long-lived bituminised radioactive waste form. This clay formation possesses favourable physico-chemical characteristics, which will limit and delay the migration of leached radionuclides to the biosphere over extended periods of time. Eurobitum consists of ~60 wt% hard bitumen (Mexphalt R85/40), in which the radioactive waste and high amounts of $NaNO_3$ (20 to 30 wt%) and other salts and (hydr)oxides (10 to 20 wt%) are homogeneously dispersed [1, 2]. During and after saturation of the filled and closed disposal gallery, this bituminised waste will take up water, resulting in the dissolution of $NaNO_3$ crystals and the subsequent leaching of significant amounts of nitrate, as well as of soluble organic bitumen degradation products, into the clay pore water [3]. Owing to the importance of the clay formation in the overall repository safety concept, it is necessary to assess the effect of the leached $NaNO_3$ (and nitrite formed by radiolysis) on the physico-chemical properties of the clay.

To assess a possible oxidation of redox-active Boom Clay components (*e.g.* dissolved organic matter and pyrite) by nitrate and/or nitrite and the impact of these reactions on the barrier function of the Boom Clay (e.g. possible decrease in reducing capacity, or mechanical disturbance by gas generation), long-term (up to 2.5 years) abiotic and biotic batch tests have been performed. In these tests, dissolved organic matter (DOM; 100-150 mg C/l) and pyrite (0.5 g/l) were each incubated with nitrate (0 to 0.1 M $NaNO_3$) or nitrite (0 to 0.05 M $NaNO_2$) in respectively clay water (collected from the EG/BS piezometer installed in the HADES URL, Mol, Belgium) or a bicarbonate solution (simulating the bicarbonate concentration in Boom Clay pore water, *i.e.* 15 mM $NaHCO_3$). Abiotic clay water solutions were obtained by addition of NaN_3 (0.1 wt%) or by filter sterilisation. In contrast to clay water, microbes were not present in the prepared pyrite suspensions. To study microbial pyrite oxidation, the suspensions were therefore inoculated with *Thiobacillus denitrificans,* a known nitrate-dependent autotrophic pyrite oxidiser [4]. Microbiological analyses confirmed the presence or absence of nitrate or nitrite reducing microorganisms in respectively the biotic and abiotic tests. To assess the nitrate and nitrite reduction by DOM or pyrite in time, the chemical composition of the solutions was analysed regularly. Furthermore, the impact of nitrate or nitrite on the reducing capacity of DOM was investigated using ferric citrate according to an in-house optimised protocol [5].

Based on the results of these long-term batch tests, an abiotic reaction between the studied redox-active components of Boom Clay (*i.e.* pyrite and DOM) and nitrate does not occur or is characterised by very slow kinetics (reaction not observed after 2.5 years). On the other hand, a slow microbial nitrate reduction does occur using either pyrite or DOM as electron donor. In these tests, reduced N species (mainly nitrite) and in case of pyrite oxidation also sulphate (and thiosulphate as intermediate product), were produced. Microbial nitrate reduction rates of ~14 µM NO_3^- per gC per day and ~0.2 µmol NO_3^- per m² pyrite per day were observed using respectively DOM and pyrite as electron donor.
While no decrease in reducing capacity of DOM was observed in the abiotic clay water solutions with nitrate (in agreement with the lack of nitrate reduction), microbially mediated nitrate reduction by DOM did result in a decrease in the reducing capacity of DOM (decrease observed over 1 year). However, the results of size exclusion chromatography showed no significant shifts in the molecular weight distribution of the DOM after microbial nitrate reduction after 1 year or after 2.5 years. This is in contrast to the shift in the size profile that was observed when DOM was oxidised aerobically (*i.e.* using O_2 as oxidant) for 3 months. These results suggest that the DOM was not oxidised extensively during the observed microbial nitrate reduction.

To investigate the reason why microbial nitrate reduction by DOM in Boom Clay pore water is only a slow process, the bioavailability of the DOM in clay water was examined. For this, the impact of acetate, an easily biodegradable organic compound and one of the main radiolytic and chemical degradation products of bitumen, on the microbial nitrate reduction process in Boom Clay pore water was investigated. The results of these batch tests indicate that microbial nitrate reduction in Boom Clay pore water from the EG/BS piezometer occurs with and without additional acetate, although the latter causes a significant increase (~200 times) in reduction rate. In all of the test solutions, nitrate was mainly reduced to nitrite, although some denitrification was also observed (20 to 30% of all reduced nitrate) when acetate was introduced to the system. The difference in metabolism in the presence or in the absence of acetate is most likely due to the lower bioavailable C/N ratio found in the test solutions without acetate [6]. Based on these results, the DOM in Boom Clay pore water can be considered as poorly bioavailable for microbial nitrate reducers.

In contrast to nitrate, nitrite is able to oxidise DOM and pyrite, both abiotically and biotically, although also here only rather slow rates were observed (similar to the observed microbial nitrate reduction rates). Under all test conditions, denitrification was observed, resulting in the formation of gaseous N species. When pyrite was incubated abiotically with nitrite for 2.5 years, both thiosulphate and sulphate were produced. The reaction rate seems to slow down after the first few months, suggesting some passivation of pyrite due to the formation of an oxidation layer on the surface of pyrite. XRD (X-ray diffraction) and XPS (X-ray photoelectron spectroscopy) analyses are on-going to investigate this further. In the biotic batch tests, nitrite-dependent oxidation of pyrite by *T. denitrificans* was observed for 1 year, resulting in the formation of sulphate. Similar to what was observed in the biotic tests with nitrate, thiosulphate was only found as an intermediate product in the microbial pyrite oxidation.

The results of the tests described above indicate that an abiotic reaction between the studied redox-active components of Boom Clay (*i.e.* pyrite and DOM) and nitrate does not occur or is characterised by very slow kinetics. A slow microbial nitrate reduction (mainly to nitrite) was however observed both with DOM and pyrite as electron donor. The low reaction rate has been attributed to the low bioavailability of DOM in the Boom Clay pore water (sampled from the EG/BS piezometer). On the other hand, nitrite was shown to oxidise both DOM and pyrite, although also at a rather slow rate. This reaction can occur both abiotically and mediated by microbes.

Acknowledgements
This work is undertaken in close co-operation with, and also with the financial support of ONDRAF/NIRAS, the Belgian Agency for the Management of Radioactive Waste and Enriched Fissile Materials, as part of its programme on the geological disposal of intermediate-level long-lived radioactive waste.

References
[1] Demonie M. (1996). Chemische samenstelling van het gebitumineerd product van de fluxen E1 tot en met EX. Note Belgoprocess reference AFB-96-390, 21/10/96.
[2] Boulanger D. (2011). Source term for the Safety and Feasibility Case 1. NIROND TR-2011-68. ONDRAF/NIRAS, Brussels, Belgium.
[3] Valcke E., Mariën A., Van Geet M. (2009). The methodology followed in Belgium to investigate the compatibility with geological disposal of Eurobitum bituminized intermediate-level radioactive waste. MRS Proceedings 1193: 105-116.
[4] Bosch J., Lee K-J, Jordan G., Kim K-W, Meckenstock R.U. (2012). Anaerobic, nitrate-dependent oxidation of pyrite nanoparticles by *Thiobacillus denitrificans*. Environ. Sci. Technol. 46: 2095-2101.
[5] Bleyen N., Vasile M., Mariën A., Valcke E. (2015). Methods for determination of the redox capacity of DOM in RBCW. External Report SCK•CEN-ER-283, SCK•CEN, MOL, Belgium.
[6] Oh J., Silverstein J. (1999). Acetate limitation and nitrite accumulation during denitrification. J. Environ. Eng. 125: 234-242.

Effect of a $NaNO_3$ plume on the diffusion behaviour of HTO, I^-, and HCO_3^-, and on the physico-chemical properties of Boom Clay

E. Valcke*[1], M. Aertsens[1], N. Bleyen[1], C. Bruggeman[1], Pierre De Cannière[2], M. Honty[1], N. Maes[1], A. Mariën[1], H. Moors[3], M. Van Geet[4], M. Van Gompel[1], and L. Wang[1].

[1] Waste and Disposal Expert Group, SCK•CEN, Boeretang 200, 2400 Mol, Belgium
[2] present address: FANC/AFCN, Ravensteinstraat / Rue Ravenstein 36, 1000 Brussels, Belgium
[3] present address: Microbiology Research Unit, SCK•CEN, Boeretang 200, 2400 Mol, Belgium
[4] present address: ONDRAF/NIRAS, Avenue des Arts / Kunstlaan 14, 1210 Brussels, Belgium

In Belgium, Boom Clay is studied as a potential host formation for the geological disposal of Eurobitum, an intermediate-level long-lived bituminised radioactive waste form. Boom Clay possesses favourable physico-chemical characteristics to limit and delay the migration of the leached radionuclides towards the biosphere over extended periods of time. Eurobitum contains high amounts of $NaNO_3$ (20 to 30 wt%), which upon contact with water will dissolve and leach out from the waste, and migrate into the surrounding clay. The concomitant increase of the ionic strength (IS) of the pore water and the subsequent compression of the electrical double layer (EDL), the ion exchange reactions with Na^+, and possibly redox reactions with nitrate will induce a cascade of partly coupled processes that will affect the physico-chemical and radionuclide migration properties of the clay [1,2].

As part of the studies on the effect of a $NaNO_3$ plume, 10 year lasting percolation tests were performed with four Boom Clay cores (∅ 38 mm; height 30 mm) placed in oedometers under a constant load of 2.75 MPa, injecting sequentially Boom Clay pore Water (BCW; IS = 0.016 M), BCW with 0.1 M (IS ~0.12 M), 0.5 M (IS ~0.5 M), and 1 M (IS ~1 M) $NaNO_3$, at a hydraulic pressure of ~0.8 MPa. For two cores, named 'vertical' or V-cores, the percolation direction was perpendicular to the clay bedding plane; for the other two 'horizontal' or H-cores, it was parallel to this plane. The following parameters were monitored: volumetric deformation of the clay, electrical conductivity (EC) and hydraulic conductivity (K), pH, dissolved organic matter (DOM) content, and concentration of key ions in the percolate. When for a given percolation solution the HC was more or less stable, tracer pulse injection tests were performed with tritiated water (HTO), iodide (I^-), and $H^{14}CO_3^-$. For each test, the dispersion coefficient D and the product ηR, with η the diffusion accessible porosity and R the retardation factor, were determined by fitting the tracer concentration in the percolate as a function of time.

Although subject to large uncertainties, the results suggest a small compression (~1 vol%) of the clay cores after 10 years of percolation. For all cores, the results on EC, K, pH, DOM content, and ionic composition are very similar when expressed as a function of the percolated volume (given the ~2.8 times higher K for the H-cores, parameter values evolved more slowly for the V-cores). After each switch to a higher IS, about four pore volumes of solution were needed to reach a steady state EC. The hydraulic conductivity increased quickly but moderately (< 25%) after each switch, and then decreased slowly to a value close to or smaller than the HC before the switch. This behaviour is explained respectively by the rapid decrease of the thickness of the clay minerals EDL caused by the rapid IS increase after a switch, and by the slow re-increase of the EDL thickness upon ion exchange of bivalent cations (Ca^{2+} and Mg^{2+}) with the monovalent Na^+ ion, and by the clay consolidation. After 10 years, K was slightly lower than its value before the start of the percolation tests.

After every switch to a higher IS, the cation concentration profiles showed a sharp rise, followed by a slow decrease. Reactive transport modeling with the PHREEQC code using cation exchange parameters determined on non-perturbed Boom Clay [3] could describe well the experimental results (improvements are necessary for higher IS), confirming that ion exchange is the dominant mechanism regulating the cation elution in these tests [4]. The pH and DOM content showed trends opposite to those of the cations: a sharp decrease of 0.5-0.7 pH units was followed by a slower re-increase to more or less the initial value. The pH decrease is attributed to the precipitation of $CaCO_3$, liberating protons from bicarbonate, upon Ca^{2+} displacement from the clay by Na^+. The re-increase is most likely due to

the re-decrease of the Ca^{2+} concentration, and due to the pH buffering effect of the clay. The DOM content first decreased sharply. This is attributed to the increased concentration of bivalent bridging cations and the DOM sorption on the clay minerals, and to a smaller extent to the compression of the EDL of humic acids and their subsequent coagulation induced by the increased IS. The concentrations of sulphate, nitrite and ammonium remained mostly below the detection limit, indicating that in absence of microbial activity no important reactions occurred between nitrate and redox active Boom Clay components. This is confirmed by the results of dedicated abiotic batch tests [5,6].

For HTO the values of ηR were independent of the IS: for each IS an average value (four cores) between 0.38 and 0.40 was observed. The average ηR value of the anions increased with IS: for I^- from 0.17 at 0.016 M to 0.28 at 1.0 M, for $H^{14}CO_3^-$ from 0.26 at 0.016 M to 0.49 at ~0.5 M and 0.56 at ~1.0 M. The ηR values for $H^{14}CO_3^-$, being higher than for HTO, suggest a slight retardation ($R > 1$). For I^-, extrapolation of ηR to higher IS yields a value of ~0.3. This value can be considered as the interparticle pore space [7], which for the(se) Boom Clay (cores) makes up ~75% of the total porosity (under the studied conditions). The high value of the interparticle pore space explains the rapid effect of changing IS on hydraulic conductivity. Under the high pressure gradient applied to the percolation solutions, and using radionuclide and Boom Clay specific values for the longitudinal dispersivity [8], the contribution of the hydrodynamic dispersion was estimated at ~5%–7% for HTO, 8%–15% for I^-, and 25%-50% for $H^{14}CO_3^-$. The effective diffusion coefficient D_{eff} remained stable for HTO (1.5×10^{-10} m²/s for the H-cores and 0.5×10^{-10} m²/s for the V-cores), whereas for I^- it increased with ~50% between 0.016 M and 1 M (at 0.016 M, D_{eff} was 0.5×10^{-10} m²/s for the H-cores and 0.2×10^{-10} m²/s for the V-cores). For $H^{14}CO_3^-$ in the H-cores, D_{eff} increased from 0.2×10^{-10} m²/s at 0.016 M to ~0.48×10^{-10} m²/s at 0.5 and 1 M. The anisotropy of the dispersion and diffusion coefficients is ~2.8.

Considering that a high IS increase will only affect a few metres of clay around the galleries hosting Eurobitum waste [9], the results of these percolation and pulse injection experiments suggest that the consequences of a $NaNO_3$ plume on the physic-chemical properties of, and the behaviour of anionic radionuclides in Boom Clay would be limited, even with higher D_{eff} values [10].

Acknowledgements
This work is undertaken in close co-operation with, and also with the financial support of ONDRAF/NIRAS, the Belgian agency for the management of radioactive waste.

References

[1] Boulanger D. (2011). Source term for the Safety and Feasibility Case 1. NIROND TR-2011-68. ONDRAF/NIRAS, Brussels, Belgium.
[2] Valcke E., Mariën A., Van Geet M. (2009). The methodology followed in Belgium to investigate the compatibility with geological disposal of Eurobitum bituminized intermediate-level radioactive waste. Mat. Res. Soc. Symp. Proc. 1193, 105-116.
[3] De Craen, M., Wang, L., Van Geet, M., Moors, H. (2004). Geochemistry of Boom Clay pore water at the Mol site. SCK•CEN-BLG-990, SCK•CEN, Mol, Belgium.
[4] Martens, E., *et al*. (2011). Modelling of cation concentrations in the outflow of $NaNO_3$ percolation experiments through Boom Clay cores. J. Phys. Chem. Earth 36, 1693-1699.
[5] Mariën, A., *et al*. (2011). The study of abiotic reduction of nitrate and nitrite in Boom Clay. Phys. Chem. Earth, Parts A/B/C 36, 1639-1647.
[6] Bleyen, N., *et al*. (in preparation). Abiotic nitrate and nitrite reduction by pyrite.
[7] Van Loon, L., Glaus, M., Müller, W. (2007). Anion exclusion effects in compacted bentonites: towards a better understanding of anion diffusion. Appl. Geochem. 22, 2536-2552.
[8] Aertsens, M., *et al*. (2009). Effect of ionic strength on the transport parameters of tritiated water, iodide and $H^{14}CO_3^-$ in Boom Clay. Mat. Res. Soc. Symp. Proc. 1193, 497-504.
[9] Weetjens, E., Valcke, E., Mariën, A. (2014). Sodium nitrate release from Eurobitum bituminised radioactive waste. SCK•CEN-ER-146, SCK•CEN, Mol, Belgium.
[10] Weetjens, E. (2014). Safety Assessment calculations for geological disposal of Eurobitum bituminised waste in Boom Clay. In preparation. SCK•CEN, Mol, Belgium.

The Bitumen-Nitrate-Clay Interaction Experiment at the Mont Terri Rock Laboratory, Switzerland: Response of Microbial Communities to Additions of Nitrate and Acetate

Hugo Moors[(1)], **Andrea Cherkouk**[(2)], **Mohamed Mysara**[(1)], **Nele Bleyen**[(1)], **Steven Smets**[(1)], **Bernhard Schwyn**[(3)], **Achim Albrecht**[(4)], **Charles Wittebroodt**[(5)], **Joe Small**[(6)], **Pierre De Cannière**[(7)], **Simcha Stroes-Gascoyne**[(8)], **Elie Valcke**[(1)] **and Natalie Leys**[(1)]

[1]SCK•CEN, Boeretang 200, BE-2400 Mol (Belgium)
[2]HZDR, Bautzner Landstraße 400, DE-01328 Dresden (Germany)
[3]NAGRA, Hardstrasse 73, CH-5430 Wettingen (Switzerland)
[4]Andra, 1-7 rue Jean-Monnet, FR-92298 Châtenay-Malabry Cedex (France)
[5]IRSN, Bâtiment 76/2, B.P. 17, FR-92262 Fontenay-aux-Roses (France)
[6]National Nuclear Laboratory, Birchwood Park, Warrington WA3 6AE (United Kingdom)
[7]FANC-AFCN, Ravensteinstraat 36, BE-1000 Brussel (Belgium)
[8]AECL, Whiteshell Laboratories, Pinawa, Manitoba R0E 1L0 (Canada)

Clay deposits such as the Opalinus Clay formation are studied as host rocks for geological disposal of high- and intermediate-level long-lived radioactive waste in several European countries. Bituminized intermediate-level long-lived radioactive waste contains, besides bitumen and radionuclides, also large amounts of nitrates and sulphates. Over time, these salts will dissolve, leach and diffuse into the surrounding clay host rock, together with water soluble organic substances. The presence of these compounds will induce several processes (*e.g.* ionic strength changes, ion exchange reactions with Na^+, redox reactions with NO_3^-, …) that may affect the barrier properties of the clay host rock.

To study the fate of such inorganic– and organic leachates, an *in situ* experiment, called Bitumen-Nitrate-Clay interaction (BN) experiment, was installed in the Opalinus Clay at the Mont Terri underground research laboratory (St. Ursanne, Switzerland). The BN experiment aims to investigate the impact of a nitrate plume, with or without acetate, on the biogeochemistry of the near-field host rock. Acetate is used as representative of the organic water soluble fraction of bitumen degradation products. At a later stage, the BN experiment also aims to investigate the impact of nitrate and acetate on radionuclide reactivity and transport, especially for the redox sensitive radionuclides (e.g. ^{79}Se, ^{99}Tc, ^{23x}U, …). The microbial analyses of the BN experiment intend to elucidate if and how currently present microbial communities are affected, and if and how microbes are involved in the observed biogeochemical processes. In this respect it is noteworthy to mention that the current BN set-up does not take into account any cement matrix or backfill, and offers the microbes only a pure aquatic environment, at almost neutral pH, in the form of a water-filled borehole. Such set-up allows free movement of nutrients, energy sources and dissolved electron donors and – acceptors, and does not impose any physical and/or chemical restriction on the microorganisms. In a real radioactive waste repository, the conditions will mostly deviate from the ones present in the BN experiment. Therefore, the *in situ* BN experiment can only be considered as a well engineered disposal 'test case'.

The downhole equipment of the BN experiment consists of three packed-off intervals, each lined with a filter screen in which Artificial Pore Water (APW) is circulating. All metal parts of the experiment are stainless steel. A series of perturbation tests was performed, in which nitrate with or without acetate was injected into the circulating borehole solutions. Different concentrations and concentration ratios of nitrate and acetate were tested. Microbial analyses were performed on samples taken at pivotal moments (*e.g.* before, during and after initiating the perturbation tests). Microbial investigations, included Scanning Electron Microscopy (SEM), DNA-based molecular biology methods, ATP measurements, and cultivation-based techniques. Priority was given to DNA-based molecular biology analysis methods, as these methods can provide very accurate information on the composition and possible evolution of bacterial communities in response to the geochemical

perturbations. During interval installation and the first experiment manipulations, no precautions were taken to guarantee full sterile working conditions, since this will not be the case either during the excavation and operational phase in a future repository. In later manipulations, the injection solutions were sterilized, to facilitate the interpretation of the microbial analyses.

The genetic analyses indicated that a considerable number of microbial species were introduced during the course of the experiments, as many species detected in the borehole solutions were also present in the various batches of APW solutions. A number of microbial species disappeared from the borehole solutions, probably due to the lack of nutrients or unsuitable physico-chemical conditions. However, the species that did remain and survive typically represent species that are versatile towards respiration type, carbon– and energy source (*i.e.* they can easily switch from oxic to anoxic conditions, use of different organic or inorganic carbon sources, ...) and are capable of thriving in an oligotrophic clay environment. Nevertheless, whether introduced or indigenous, all test results indicated that an active microbial community was present at all times in all the borehole solutions.

The shifts observed in bacterial populations appeared to correlate well with the imposed physico-chemical changes. Under what is referred to as "unperturbed borehole solution conditions" (no nitrate or acetate additions), the most abundant microbes detected by genetic analyses are oligotrophic heterotrophs. Amongst these oligotrophic heterotrophs are species that are specialized in degrading complex carbon sources. In each solution sampled before geochemically perturbing the interval solutions with nitrate or acetate, microorganisms were found that are capable of using sulphate as electron acceptor. Each interval harbored also a population that is capable of autotrophic metabolism. This means that the microbial community would have the capacity to convert inorganic carbon molecules (*e.g.* bicarbonate) into organic carbon molecules (*e.g.* carbohydrates). The latter could possibly be used as carbon source by organotrophs. Besides, every interval community harbored also bacterial species that are capable of fixing N_2 gas and reducing nitrogen further into its most reduced form, ammonia.

As soon as nitrate was added, *i.e.*, an electron acceptor that renders more chemical redox energy than the naturally present sulphate, an overwhelming community shift appeared to nitrate reducing bacteria. If in parallel acetate, an easily oxidizable carbon source, was offered, the community composition did not alter that much, but the speed of nitrate reduction was increased twentyfold. This high speed was maintained as long as the easily consumable carbon source was abundant. When the energetic carbon source (*i.e.* acetate) was used up or the easily accessible electron acceptor (*i.e.* nitrate) became exhausted, the microbial communities of the intervals gradually shift towards a community which harbored again some sulphate reducing prokaryotes and many microbial species primarily characterized as oligotrophic heterotrophs of which some are also able to switch to autotrophic metabolism.

Acknowledgements

This work has been undertaken in close co-operation with Swisstopo, the operator of the rock laboratory and the project management team at Mont Terri, in particular Christophe Nussbaum and Thierry Theurillat. Financial support was provided by the Mont Terri Consortium. Technical assistance of Wim Verwimp and Patrick Boven (SCK•CEN) is also greatly appreciated.

Modeling of iron/clay interactions coupled to bacteria activity in percolation cells at 60 °C

C. Chautard[a,b], L. De Windt[b], F. Marsal[a], D. Pellegrini[a]

[a] IRSN, PRP-DGE/SEDRAN/BERIS, B.P. 17, 92262 Fontenay-aux-Roses Cedex, France
[b] MINES ParisTech, Centre de Géosciences, 35 rue St Honoré, 77305 Fontainebleau Cedex, France

The introduction of microbial species in a radioactive waste repository during the operational phase and the survival of bacteria after its closure cannot be presently excluded. Firstly, the presence of microorganisms has recently been evidenced in deep clayey environment. Secondly, electron donors such as hydrogen gas produced by anoxic metallic corrosion or biodegradable organic matter contained in argillite may be available for bacterial development.

This work aims at modeling iron/clay chemical interactions coupled to bacterial activity at the laboratory. Two percolation cell experiments were conducted during 13 months at 60°C. Synthetic clayey pore water circulated under a pressure gradient through a metallic iron powder and an artificially cracked Toarcian argillite from the Tournemire research facility. A metallic iron rod was also placed into the argillite. A mix of sulfate reducing bacteria (SRB) and iron reducing bacteria (IRB) was introduced at the iron/clay interface in the first cell, whereas the second cell was maintained under strictly abiotic conditions. The chemistry of the aqueous solutions at the outlet of the cells was monitored over time and solid characterizations were carried out at the end of the experiments. Bacteria activity during the experiment was evidenced by population monitoring, a significant decrease of aqueous sulfate concentrations, and the precipitation of iron sulfide minerals.

Reactive transport modeling of the experiments was performed with the HYTEC code considering aqueous reactions, mineral dissolution/precipitation and cation exchanges at thermodynamic equilibrium. The thermodynamic constants were selected from the EQ3/6 and Thermoddem databases. Additional kinetic constraints were set for the anoxic corrosion of metallic iron, for the precipitation of corrosion products, and for the SRB-controlled reactivity between hydrogen, produced by iron corrosion, and aqueous sulfates. The kinetic rate constants were adjusted onto the experimental results. Attention was paid to the aqueous chemistry as well as the mineralogy and spatial localization of the corrosion products. Both magnetite (Fe_3O_4) and chukanovite ($FeCO_3(OH)_2$) precipitated inside the iron powder, though chukanovite was more preferentially located close to the argillite. At the iron rod/argillite interface, chukanovite precipitated in the inner layer in contact with iron and siderite ($FeCO_3$) in an outermost layer. An additional precipitation of mackinawite (FeS) and greigite (Fe_3S_4) occurred with bacteria only. The depth of argillite perturbation was small (10 – 30 µm in the experiments) at both interfaces, although overestimated in the modeling. The local pH value, carbonate diffusion and BSR activity were key factors controlling the mineralogical evolution.

Paleogene marine clays in the in the southern North Sea Basin (Netherlands): towards a new lithostratigraphic framework

Wim Westerhoff & Geert-Jan Vis

TNO – Geological Survey of the Netherlands, PO box 80015, 3508TA Utrecht, The Netherlands

In the search for a suitable host rock for long-term storage of radioactive waste, the Oligocene Rupel Clay Member (Boom Clay in Belgium) is the main focus in several applied geoscientific studies. A recent update of the geological and geohydrological characteristics of the Rupel Clay Member in the Netherlands has shown that the deposit is more than 100 m thick and present in the larger part of the onshore Netherlands up to a depth of 1500 m. The grain size distribution demonstrates both vertical and lateral variations and shows a relatively high percentage of silt. This may indicate that the deposit is less homogeneous than previously thought. At a regional scale, the clay deposit shows a remarkable variability of the calculated permeability with lowest values in the northern part of the country and higher but more variable values towards the south and southeast. In addition, permeability shows a decreasing trend with increasing depth.

The Rupel Clay Member, is not the only massive clay deposit preserved in the Cenozoic sedimentary sequences of the Dutch subsurface. Three main clay deposits are known to occur underneath the Rupel Clay Member: the Asse (1) and Ieper (2) Members of the Dongen Formation show a maximum thickness of respectively 170 and 140 m. The deeper situated Paleocene Landen Clay Member (3) has a mean thickness ranging between 30 – 70 m. These Paleogene deposits were formed in lagoonal and shallow marine environments with relative little influx of sediments derived from bordering land surfaces to the south and southeast .

A major clay deposit on top of the Rupel Clay Member is the so-called Veldhoven Clay Member. Due to erosion in the Early Miocene the Veldhoven Clay member has a restricted spatial distribution, limited to the Roer Valley Graben (SE Netherlands). The thickness reaches nearly 100 m. The Paleogene deposits are overlain by the Miocene Breda Formation which in general shows a marked unconformity at its base. In the northern part of the country thick clay deposits from part of the Breda Formation but they are not ranked in a formal lithostratigraphical hierarchy.

No major river systems influenced the sediment supply to the area (onshore Netherlands) during the Paleogene. It's assumed that through longshore drift the larger part of the sediments originated from the northwest and northern part of the North Sea Basin. On the contrary, during the Neogene sedimentation was strongly controlled by input from major river systems originating in the Baltic area (Eridanos) and the Rhenish Massif and Alps (Rhine-Meuse system). As a result, Paleogene sediment often show a smaller mean grain size when compared to the Neogene deposits. However, such general trends fade towards the centre of the basin.

This study focuses on two research questions: the first is focussed on the confusing lithostratigraphical nomenclature applied in the Netherlands and neighbouring countries. Therefore a detailed cross-border correlation scheme is set up, and suggestions to simplify the system are made. The second question concerns the problem of gradually changing facies

following a transect from the margin towards the centre of the basin and how to reconcile that with a lithostratigraphic approach. Lithostratigraphical units are often defined on well-recognisable lithological differences that can be discerned easily in a vertical sequence. However, resulting from lateral changes in facies it is often hard to define laterally the boundaries of a strictly defined lithostratigraphical unit. To define such units in the Lower Paleogene sequences is severely hampered by the lack of reliable lithological data. If there are samples, they are mostly from cuttings while the bulk of the lithological information has to be interpreted from seismic and well-logging data. The combined information from lithological observations and geophysical data form the preferred ingredients for defining the marine Cenozoic deposits in the Dutch subsurface.

3D stress field sensitivity analysis on the scale of geological siting regions in Northern Switzerland with focus on Opalinus Clay

Oliver Heidbach[1], **Tobias Hergert**[2], **Karsten Reiter**[1], **Silvio B. Giger**[3] **and Paul Marschall**[3]

[1] GFZ German Research Centre for Geosciences, Section 2.6 Seismic Hazard and Stress Field, Telegrafenberg, 14473 Potsdam, Germany

[2] Karlsruhe Institute of Technology, Institut für Angewandte Geowissenschaften, Adenauerring 20b, 76131 Karlsruhe, Germany

[3] National Cooperative for the Disposal of Radioactive Waste, 5430 Wettingen, Switzerland

As part of the "Sectoral Plan of Deep Geological Repositories" three different candidate geological siting areas were selected for high-level waste (HLW) repositories in Northern Switzerland (BFE 2011, Fig.1). The in situ stress field is an important state variable to assess the engineering feasibility of underground structures in these areas, but direct stress measurements at the depth of potential repositories are very scarce (Fig.1).

To investigate the range of contemporary stress conditions we conducted sensitivity analyses using 3D geomechanical-numerical modelling covering the areas of the geological siting regions. The focus of the parametric study was on the impact of mechanical properties of sedimentary layers and fault structures on the stress field in the Opalinus Clay host rock. Effects of current topography and future ice cover were also investigated. The models are semi-generic in the sense that they are based on existing geological models, but geomechanical units and in particular fault structures were simplified, or complemented by hypothesized fault structures to explore the effect on the local stress field. The goal of this study is on the relative impact of structural and rheological features rather than a precise estimation of the absolute stress state.

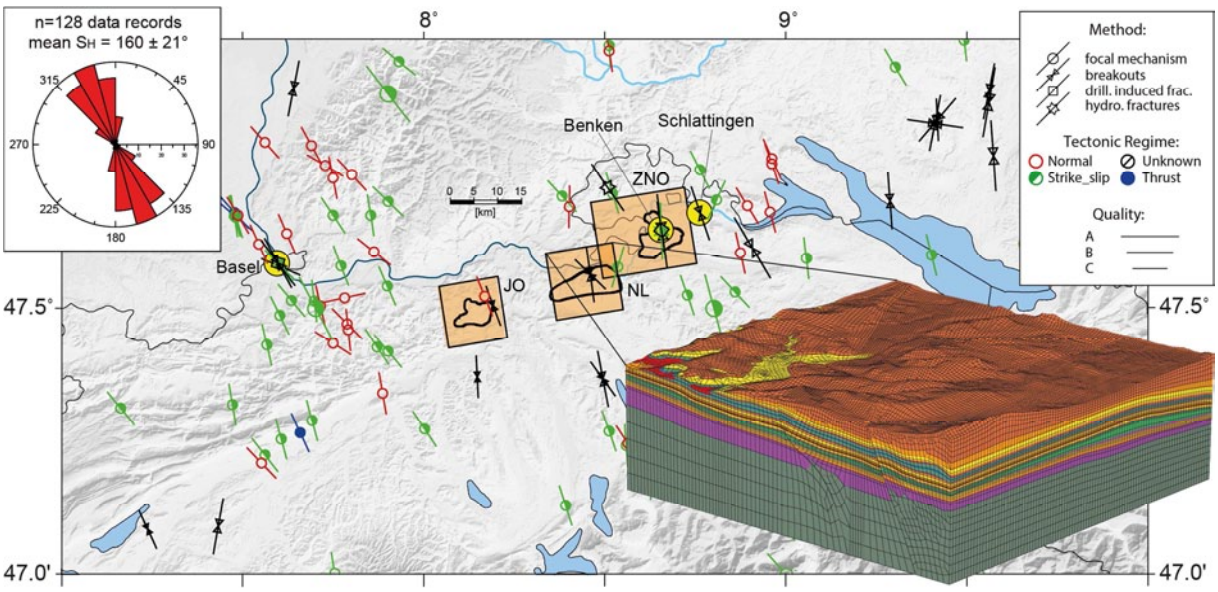


Fig. 1. Stress map of Northern Switzerland based on the revised World Stress Map release 2008 (Heidbach et al. 2010, Nagra 2013). Lines show the orientation of maximum horizontal stress S_{Hmax}. Orange rectangles mark model areas; thick black lines within the model areas encircle the geological siting regions for HLW: Jura Ost (JO), Nördlich Lägern (NL) and Zürich Nordost (ZNO). Yellow circles show the sites where stress magnitude data are available in the depth range of potential repositories (Basel, Benken, Schlattingen). For the NL model area the discretized model volume is presented as an example; colour-code shows the stratification (see Fig. 2).

The incorporated 3D geological models contain fault surfaces, topography from a digital elevation model and 12 stratigraphic units with different linear elasto-plastic rock properties. To constrain the initial and boundary conditions for a base model we use orientations of maximum horizontal stress (S_{Hmax}), stress regime information (Fig. 1), magnitudes of the minimum horizontal stress (S_{hmin}) from

hydraulic fracturing and a semi-empirical relationship of the stress ratio S_h/S_V with S_V as the vertical stress for overconsolidated, argillaceous sediments.

The model runs demonstrate that the stress ratios S_{Hmac}/S_V, S_{hmin}/S_V and S_{Hmax}/S_{hmin} are considerably reduced in the argillaceous formations with respect to the stiffer formations of e.g. the Malm and the upper and lower Muschelkalk (Heidbach et al. 2014). The stiffer formations are characterized by higher stress ratios, higher differential stresses and greater horizontal stress anisotropy than the softer argillaceous formations. It can be concluded that the stiffer formations carry the main load of the lateral tectonic push in the far field.

Major fault structures also impact on the stress field in the area of potential repositories, although to a lesser extent than the mechanical stratigraphy (i.e. the stiffness contrast in the sediment formations). The E-W and NW-SE striking faults reduce the lateral push by thrust faulting and lateral displacements. Higher fault friction increases stress ratios, particularly horizontal stress anisotropy is increased. Topography influences the stress state due to the spatially varying weight acting on the subsurface, but the impact on the Opalinus Clay layer is small except for the uppermost 300-400 m (true vertical depth). An ice cover of 500-1000 m lowers the stress ratios and their lateral variability.

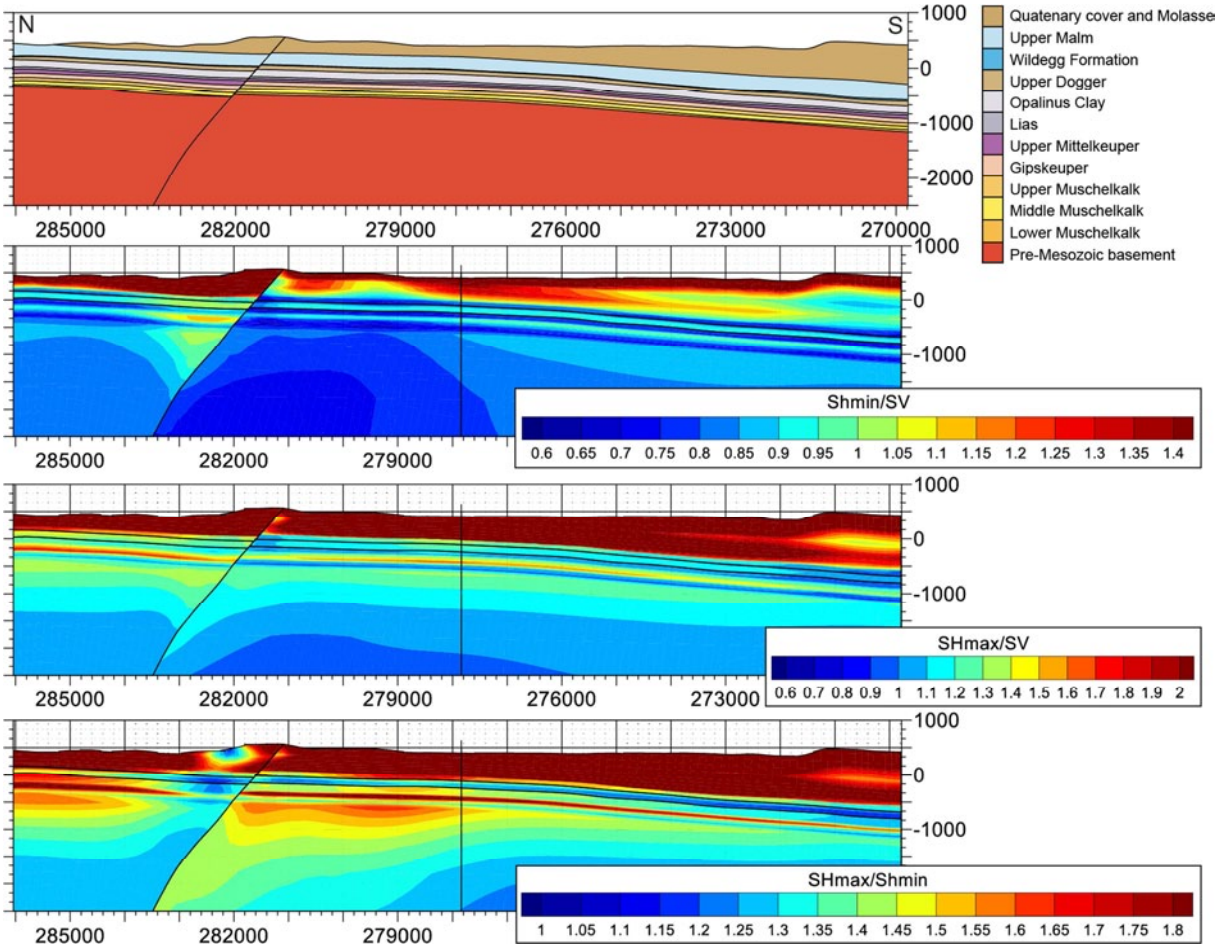


Fig. 2. Resulting stress ratios on NS sections of the model ZNO through the Benken borehole. Thin black lines in the model results show top and bottom of Opalinus Clay; vertical black line shows the borehole Benken.

References

BFE (2011), Sachplan geologische Tiefenlager – Ergebnisbericht zu Etappe 1: Festlegungen und Objektblätter. Bundesamt für Energie BFE, Bern.

Heidbach, O., Tingay, M., Barth, A., Reinecker, J., Kurfeß, D. & Müller, B. (2010), Global crustal stress pattern based on the World Stress Map database release 2008, Tectonophysics 482, 3-15, doi:10.1016/j.tecto.2009.07.023.

Heidbach, O. & Reinecker, J. (2013), Analyse des rezenten Spannungsfeldes der Nordschweiz, Nagra Arb. Ber. NAB 12-05. Nagra, Wettingen, Switzerland.

Heidbach, O., Hergert, T., Reiter, K. & Giger, S.B. (2014), Local stress field sensitivity analysis - case study Nördlich Lägern, Nagra Arb. Ber. NAB 13-88. Nagra, Wettingen, Switzerland.

Increased confidence in seismic amplitudes by consistent uncertainty quantification

***L. Sandjivy*(Seisquare) A. Shtuka (Seisquare) J.L. Mari (IFP Énergies nouvelles) B.Yven (Andra) M. Hayet (Andra)**

Seisquare,30, Avenue du General De Gaulle 77210 - Avon, France
IFP Énergies nouvelles, IFP school, 1 et 4 avenue de Bois-Préau, 92852, Rueil Malmaison Cedex, France
Andra 1/7 Rue Jean Monnet, 92298 Châtenay-Malabry Cedex, France.

Within its mission to design and build an engineered storage facility for thehigh level radioactive wastes in the eastern Paris Basin, the French National Radioactive Waste Management Agency (Andra) is conducting innovative and extensive characterization of the Callovo-Oxfordian claystone formation (Cox) and surrounding Middle and Upper Jurassic shallow-marine carbonate formations. High resolution 3D seismic data are used to model the distribution of mechanical and hydrogeological propertiesof the geological formations [1]. Assessing the reliability of the modelling is crucial for making decision on the design of the radioactive waste facility. We show how first assessing the reliability of seismic stacked amplitudes that are input to the geophysical inversion is the cornerstone of the whole model reliability assessment process. Stochastic processing of the pre-stack amplitude gathers enables to compute Stochastic Quality Indexes (SQI) attached to stacked amplitude data.
The input to characterize the Callovo-Oxfordian claystone formation (Cox) and neighbouring Oxfordian and Dogger limestones are pre-stack time migrated (PSTM) seismic sections that have been used for inversion into elastic impedance sections. Measured amplitudes were monitored and analyzed closely throughout processing to ensure that true amplitudes were preserved.
A Stochastic Quality Assessment (SQA) wokflow has been designed to assess the reliablity of the stacked amplitudes and to optimize further modelling of mechanical and hydrogeological properties.SQA processing of seismic data works under a mathematical framework known as Geostatistics or topo-probability models, where the observed (measured) seismic amplitude is considered as a unique realization of a random function (RF) defined in space and time ([2], [3]). The added value of using this type of theoretical framework is that it takes into account the spatial correlation between measured seismic amplitudes at different locations using variograms or spatial covariance.

The estimation variance is normalized and expressed as a percentage of the stacked amplitude called the Spatial Quality Index (SQI). Small SQI means good confidence in the stacked amplitude (Figure 1).

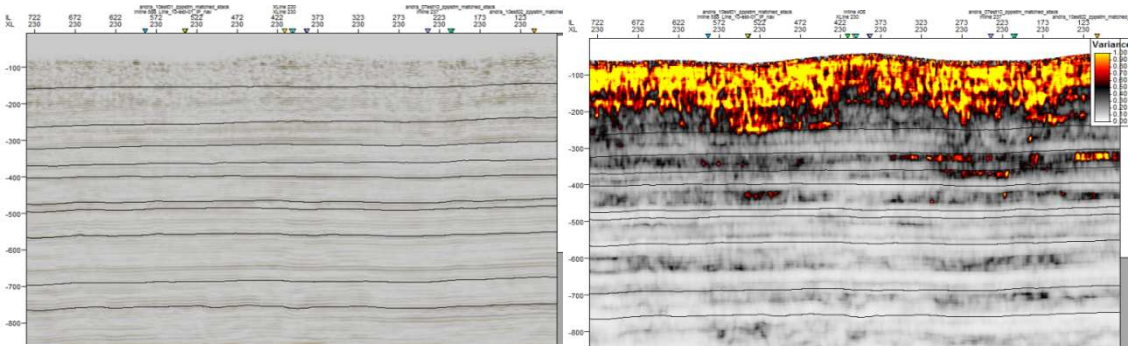


Figure 1: Stacked amplitude section (right) and SQI indicator of the reliability of the stacked amplitude values (left).White SQI areas (near 0% error) indicate reliable amplitude values. Dark to red SQI areas (above 50% error) indicate non reliable amplitude values. Horizons (black lines) interpreted on the stacked section (left) can be checked on the SQI section (right).

The present work is part of anextensivecharacterization of the Callovo-Oxfordianclaystoneformation (Cox) and neighbouringOxfordian and Dogger limestonesconductedby the French National RadioactiveWaste Management Agency (Andra). Innovativemodelling of a pseudo Gamma Ray and of permeability index (Ik-Seis) at the seismicscaleaims at verifying the homogeneity of the Callovo-Oxfordianclaystoneformation and identifyingporous and permeablelayers in the surroundingMiddle and Upper Jurassic shallow-marine carbonateformations.

The results shown here are obtained on the XL217 cross line on the seismic cube. Figure 2 shows the instantaneous amplitude section (left), its associated SQI factor (center), and pseudo gamma ray attribute (right) in depth. The quality of seismic instantaneous amplitudes is quantified by their attached SQI values that enables in turn to attach confidence on the result of the modelling of the pseudo gamma ray attribute. Blue SQI areas on the seismic section (low SQI values) indicate reliable amplitudes (80% to 90% reliability), green SQI areas indicate less reliable amplitudes (50 to 70% reliability).

The high values of the pseudo gamma ray (yellow to brown areas) are associated with the Callovo–Oxfordian (550-720 m depth interval). We can notice lateral variation of the shale content in the Callovo Oxfordian that are partly related to corresponding variations of the SQI factor that is to the quality of the seismic amplitudes.

A significant lateral variation of the seismic amplitude is also visible inside the 700 – 750m depth window that corresponds to the presence of a porous layer, between CMP 600 and CMP 400 at the top of the Dogger formation. This interpretation in confirmed by a very low value of the pseudo gamma attributes and is reliable as shown by a low SQI factor.

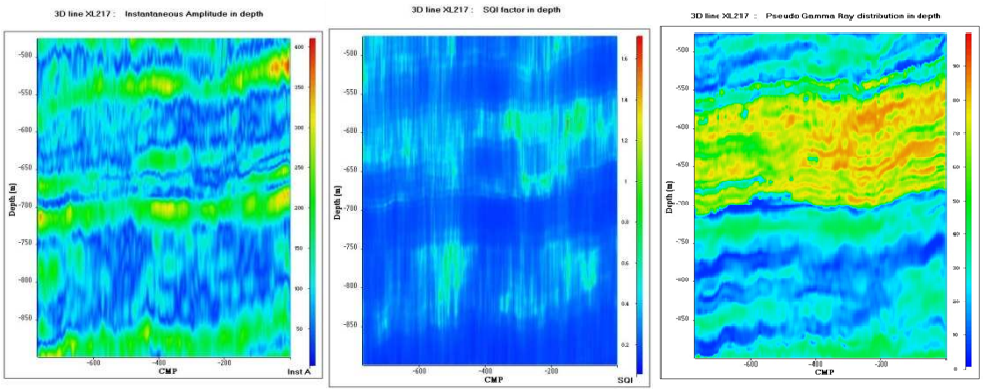


Figure 2: *Instantaneous amplitude (left), SQI factor (center), and pseudo gamma ray distribution in depth.*

We show how stochastic processing of pre stack seismic data benefits to quantify the quality of the seismic amplitudes. The computation of a SQI factor specific to the stacking process quantifies the reliability of the stacked amplitude and can be considered as a reliable indicator of the preservation of true amplitude by the processing sequence. In this case study, SQI helps to validate the identification of lateral variation of shale content inside the target layer and of a porous and permeable layer in the limestone just below.

References

[1] Mari J.L, Yven B., The application of high resolution 3D seismic data to model the distribution of mechanical and hydrogeological properties of a potential host rock for the deep storage of radioactive waste in France, Marine and Petroleum Geology, 2013, DOI: 10.1016/j.marpetgeo.2013.10.014.

[2] A. Shtuka (Seisquare), L. Sandjivy (Seisquare), J.L. Mari (IFP School), J.F.Dutzer (GDF Suez), F. Piriac (Seisquare) & R. Gil (Seisquare) Geostatistical Seismic Data Processing:Equivalent to Classical Seismic Processing +Uncertainties! EAGE 2011 BarcelonaExpanded Abstracts.

[3] Shtuka, A., Gronnwald, T., Piriac, F. 2009, A generalized probabilistic approach for processing seismic data, 79th annual SEG meeting, Expanded Abstracts.

The origin of strength of Opalinus Clay - phenomenological evidence and conceptual considerations

P. Marschall[1], ***S. Giger***[1], ***A. Ferrari***[2], ***V. Favero***[2], ***L. Laloui***[2], ***L. Keller***[3]

(1) National Cooperative for the Disposal of Radioactive Waste, 5430 Wettingen, Switzerland
(2) Soil Mechanics Laboratory, École Polytechnique Fédérale de Lausanne, CH-1015 Lausanne, Switzerland
(3) ZHAW/ICP, Wildbachstrasse 21, 8401 Winterthur, Switzerland

Indurated clays, such as claystones and shales represent a category of fine grained sedimentary geomaterials which exhibit transitional deformation behaviour between hard soils and weak rocks (Gens 2013). After deposition and depending on the experienced stress history, the the geomaterial undergoes diagenetic processes, forming its peculiar structure and affecting its hydro-mechanical behaviour. In this context, the term "structure" is used according to Lambe & Whitman (1969), characterising the combined effect of fabric (geometric arrangement of soil particles) and bonding (interparticle forces, chemico-physical bonds). Bonding is usually dominant in rocks while fabric controls the strength in soils. According to Horsrud et al. (1998) claystones and shales are characterised by well-marked bedding-plane fissility and low plasticity, i.e. they do not form a plastic mass when wet, although they may disintegrate when immersed with water. With increasing depth, effects of compaction and diagenesis cause the shale to deviate more and more from typical properties and behaviour of a clay-rich soil. In this sense, Horsrud et al. (1998) propose to describe shales as a rock, which may be conceptualised in the well-established constitutive frameworks of soil mechanics, if certain limiting conditions are met.

The Opalinus Clay in the Molasse Basin and in the Jura Fold and Thrust Belt of Northern Switzerland is a moderately to heavily overconsolidated claystone ($1.5 \leq OCR \leq 5$) with a clay mineral content between 40 and 75%, quartz content between 10 and 30% and a carbonate content between 5 and 35 %. Based on grain size distribution the Opalinus Clay classifies as a clayey (and sandy) siltstone (Fig. 1a). A shortcoming of classifications based only on grain size distributions is that they give no information on the intensity of bonding or lithification (Gens 2009). In this perspective the consistency behaviour (Atterberg limits) provides additional insight in the intrinsic properties of the destructured geomaterial, substantiating the tendency of the grain surfaces to attract water and to form the so-called "adsorbed water films" (e.g. Schmertmann 2012). The water films on the particle surfaces are thought to contribute to the shear resistance of soils on the macroscopic scale in terms of cohesion and friction angle. The determination of the Atterberg limits of the Opalinus Clay is therefore a valuable qualitative indicator for the friction angle. As shown in Figure 1b the plasticity index plots broadly along the A-line of the plasticity chart, which separates clayey from silty soils. The reported values for liquid limit w_L and plasticity index P_I range from approximately 30 to 50 % and approximately 10 to 25 %, respectively. Drawing on empirical correlations by Terzaghi et al. (1996) and Stark&Eid (1994), the friction angle of the Opalinus Clay can be bracketed in the range between 20 and 35°.

Studies on reconstituted specimens are capable of distinguishing between the intrinsic properties of unstructured (i.e. remoulded) geomaterial and the diagenetically evolved properties, corresponding to the natural state of the material. A comprehensive study has been conducted at the Laboratory of Soils Mechanics of the Swiss Federal Institute of Technology in Lausanne (EPFL) to evaluate the role of bonding and cementation in Opalinus Clay (ongoing PhD thesis of V. Favero). For this, oedometric tests and permeability measuremements were conducted on remoulded Opalinus Clay samples from the deep geothermal well Schlattingen-1 in the Molasse Basin of Northern Switzerland. The results were compared with tests on intact samples both from Schlattingen and from the Mont Terri URL (located in the Jura Fold and Thrust Belt). The interpretation of the results indicates that the void ratio/ porosity of the natural material is related not only to the mechanical compaction and fabric evolution but also to the diagenetic phenomena (bonding). The stiffness of the natural material was higher due the effect of the structure (cementation and bonding). Furthermore, characteristic changes were observed in the porosity-permeability relationship (Figure 2a), indicating a marked difference in the connectivity of the pore space. Increased swelling upon stress release of the reconstituted material (i.e. high swelling sensitivity) can be explained with bond breakage during reconstitution of the material.

Horsrud et al. (1998) indicate that Terzaghi's principle of effective stress is not assured in stiff claystones due to their low porosity and the high proportion of bound porewater. Biot's poromechanical theory offers a convenient framework, introducing the Biot coefficient to express effective stress in terms of total stress and pore pressure. Evidence was found for a distinct dependence of the Biot coefficient on mean effective stress. Quantitative investigations of the microscopic pore connectivity, based on FIB naotomography and TEM provide additional insight on the role of pore pressure. Figure 2b indicates, that only a limited a limited fraction of the pores in Opalinus Clay forms a connected pore network. Geostatistical annalyses of the pore connectivity exhibit, that the fraction of connected pores decreases significantly with inreasing mean stress, which explains the observed stress-dependence of the Biot coefficent.

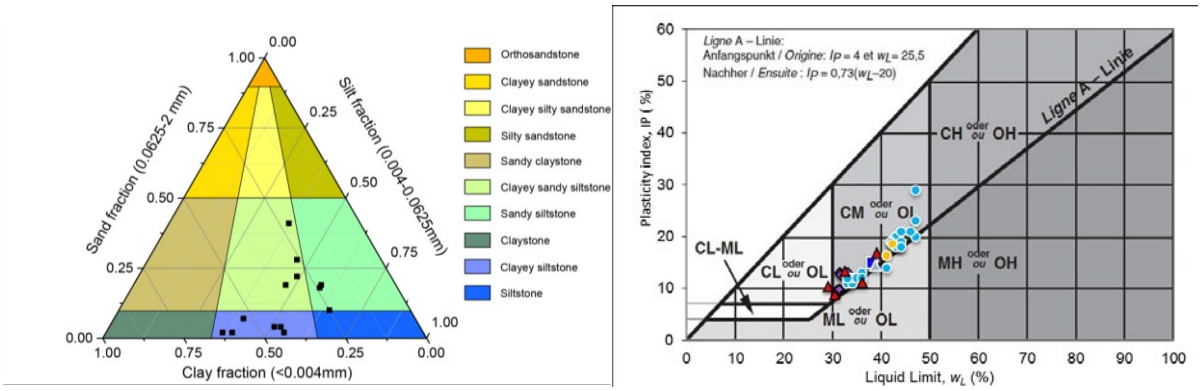


Figure 1: Classification of the Opalinus Clay in terms of grain size and consistency: (a) USCS classification of fine-grained sedimentary rocks and (b) Plasticity chart (SN 670 004-2a).

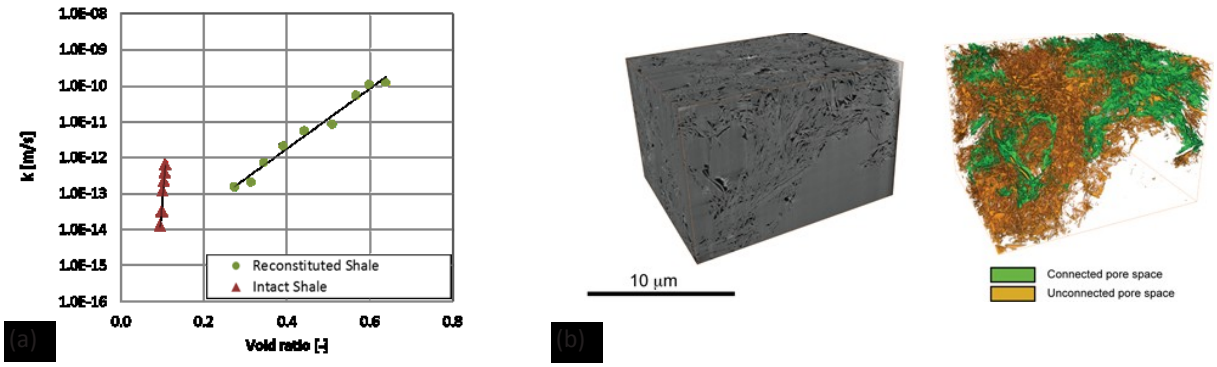


Figure 2: (a) Permeability-porosity relationship of Opalinus Clay: comparison of specimen in reconstituted / natural state and (b) Visualization of FIB-nt data (green - connected pore space; orange – unconnected pores)

Gens, A. (2013): On the hydromechanical behaviour of argillaceous hard soils-weak rocks. Proceedings of the 15th European Conference on Soil Mechanics and Geotechnical Engineering. Geotechnics of Hard Soils – Weak Rocks (Part 4).

Horsrud, P., Sonstebo, E.F., Boe, R. (1998): Mechanical and petrophysical Properties of the North Sea Shlaes. Int. Rock Mech. Min. Sci, vol. 35, 8, pp1009-1020.

Lambe, R. & Whitman, V. (1969): Soil mechanics. Wiley.

Schmertmann, J.H. (2012): New concepts for the mobilization of the components of shear resistance in clay. Norwegian Geotechnical Institute, Oslo. Publication 208. 48p.

Stark, T.D. & Eid, H.T. (1994): Drained residual strength of cohesive soils. Journal of Geotechnical Engineering 120/5, 856–871.

Terzaghi, K., Peck, R.B. & Mesri, G. (1996): Soil mechanics in engineering practice. Third edition. John Wiley & Sons, New York.

Kinetic experiments in order to determine the rate of oxygen consumption by the Callovian-Oxfordian argillaceous rock

Joachim Tremosa[1], **Jebril Hadi**[1,2], **Francis Claret**[1], **Christophe Tournassat**[1] **and Agnes Vinsot**[3]

[1]BRGM, 3 avenue Claude Guillemin, 45060 Orléans, France
[2]Now at: Rock-Water Interaction (RWI), Institute of Geological Sciences, CH-3012 BERN Switzerland
[3]Andra, Centre de Meuse/Haute-Marne, RD 960, 55290 Bure, France

Deep argillaceous rocks expected to host nuclear waste disposal are reducing environments. In such sedimentary formation some iron bearing minerals exist and Fe may be present as both sorbed and structural species in smectite and illite (in both oxidation state Fe^{II} and Fe^{III}) and in pyrite or siderite as well (Fe^{II}) [1]. Air will be introduced within the repository facilities in the deep geological disposal during the exploitation period. In addition, ventilation of the galleries will occur during this period. Hence, the prevailing reducing condition will be perturbed and the redox sensitive minerals will react. This phenomena is well known and has been observed for example in mining environment when pyrite reacts under oxidative condition and leads to acid mine drainage. In the case of argillaceous rock, the pH buffer capacity is much higher and this should not happen as the pH decrease will be compensated by calcite dissolution. Associated to pyrite dissolution, sulfate concentration will increase in the pore water, the clay exchanger population will also be modified and mineral dissolution/precipitation will occur. A complete description of the relevant mineral pathways induced by oxidation of argillaceous rock can be found in Vinsot et al. [2]. Some uncertainties remain concerning both the identification of all the species involved in the oxygen reduction and the reaction kinetics. An in situ experiment was designed by Andra to tackle those issues [3] and it was launched 5 years ago. The experimental setup is based on gas circulation in a borehole and the seepage water chemistry could be monitored as a function of time. Although, the experimental observations are consistent with the fact that pyrite is probably one of the main oxygen reducer, first reactive transport modeling indicates that reproducing accurately the pore water evolution is difficult, particularly regarding the sulfate behavior (Figure 1).

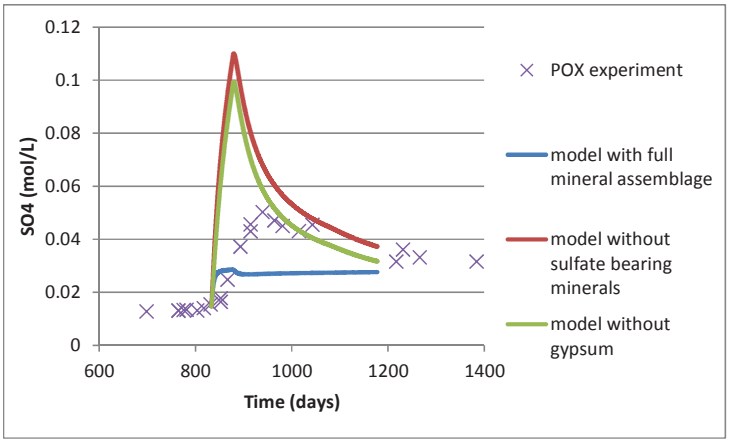
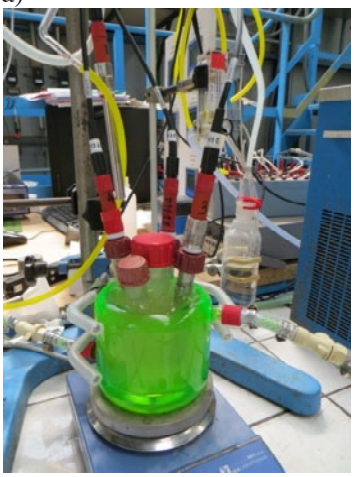


Figure 1. Sulfate evolution due to an injection of O_2 in the POX in-situ experiment. Models considering different mineral assemblages were tested to simulate the experimental data but pointed a lack in the control of the sulfate system in the Callovian-Oxfordian rock under oxidative conditions.

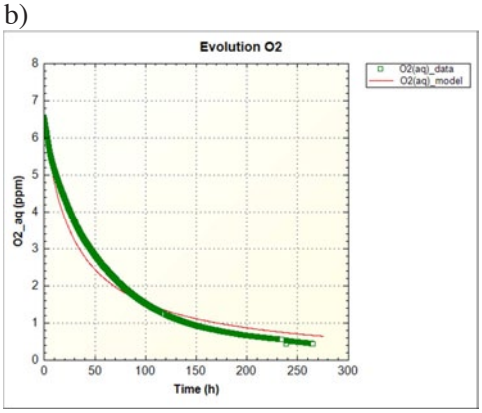
In order to improve our understanding and better constrain the built models, laboratory experiments allowing measurements of rate of oxygen consumption by Callovian-Oxfordian (COx) sample suspended in a synthetic porewater solution [4] have been set up. The designed experimental setup allows monitoring some of the solution's electrochemical parameters (Eh, pH and conductivity) along with dissolved O_2 concentration (Figure 2a). A first series of experiments was conducted in a solution prepared in atmospheric conditions (21% O_2). However, CO_2 partial pressure of the Callovian-Oxfordian formation can be more than 10-100 times greater than atmospheric pressure of CO_2 (Gaucher [5]). A second series of experiments was therefore conducted in presence of a O_2-CO_2 (20%-1%) gas mixture in order to be as close as possible to in situ conditions. In comparison to

experiments performed under O_2 condition only, the pH remains stable (figure 2b&c).Since a part of Fe^{II} present in COx is contained in the smectite structure, a series of experiments have also been carried out with a partially dithionite reduced Fe-bearing reference montmorillonite (UPM).

a)



b)



c)

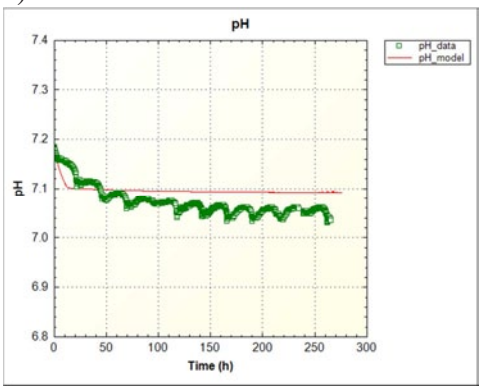


Figure 2. a) Picture of the experimental device allowing to measure the O_2 consumption by the COx rock under controlled conditions; b) and c) Measured and modeled O_2 content in solution and pH during one of the oxidation experiment.

In the future other minerals will be used (siderite, different clay) in order to determine if pyrite is really the main oxygen reducer or if other minerals have also to be considered in our modeling assumptions. Organic matter could also contribute but it is not part of the current study.
The determined oxygen consumption rates will be used in the reactive transport modeling in order to test if it improves the reproduction of the experimental data and our global understanding of the ongoing mechanisms.

1. Tournassat, C., et al., *Cation exchanged Fe(II) and Sr compared to other divalent cations (Ca, Mg) in the bure Callovian-Oxfordian formation: Implications for porewater composition modelling*. Applied Geochemistry, 2008. **23**(4): p. 641-654.
2. Vinsot, A., et al., *Oxidation front and oxygen transfer in the fractured zone surrounding the Meuse/Haute-Marne URL drifts in the Callovian–Oxfordian argillaceous rock*. Geological Society, London, Special Publications, 2014. **400**.
3. Vinsot, A., et al. *In situ characterization of the Callovian-Oxfordian seepage water composition while exposing the rock to oxygen gas*. Submitted
4. Vinsot, A., S. Mettler, and S. Wechner, *In situ characterization of the Callovo-Oxfordian pore water composition*. Physics and Chemistry of the Earth, 2008. **33**: p. S75-S86.
5. Gaucher, E.C., et al., *A robust model for pore-water chemistry of clayrock*. Geochimica et Cosmochimica Acta, 2009. **73**(21): p. 6470-6487.

THC Modelling and Sensitivity Analysis of Bentonite Alteration in a KBS-3 Buffer

S Benbow[1]*, J Wilson[2], R Metcalfe[1], D Savage[3], J Lehikoinen[4]

1. Quintessa Ltd., The Hub, 14 Station Road, Henley-on-Thames, Oxfordshire RG9 1AY, United Kingdom.
2. Quintessa Ltd., 633-635 Birchwood Boulevard, Warrington WA3 7QU, United Kingdom.
3. Savage Earth Associates Ltd, 32 St Albans Avenue, Bournemouth BH8 9EE, UK
4. STUK - Radiation and Nuclear Safety Authority, P.O.Box 14, FI-00881 Helsinki, Finland.

* corresponding author: stevenbenbow@quintessa.org

Chemical interactions between repository barriers (engineered and natural) are driven by chemical, thermal, and hydraulic gradients, which evolve in space and time in the repository system. The use of contrasting materials, such as clay, cement/concrete, and copper/steel leads to sharp chemical gradients at interfaces. Their interactions are influenced by various chemical and transport processes and moreover, will be strongly coupled in a non-linear fashion. From a chemical point of view, dissolution and precipitation processes, as well as ion exchange reactions, might alter the pore space with accompanying changes in material characteristics (transport, flow, and mechanical properties). In terms of transport, the saturation state, water flow and the diffusion of solutes across the various material interfaces will strongly influence the extent and timescale over which chemical processes occur. The thermal pulse originating from radioactive decay may also accelerate chemical transformations, change the stability of minerals, and accelerate diffusive transport. Last but not least, mechanical processes might result in porosity changes and the associated transport parameters.

Illitization and cation exchange are considered as the main potential modes of montmorillonite alteration in most safety assessments, and can impact negatively upon the swelling capacity of barriers. The illite reaction is usually argued to be unlikely at in situ conditions. These reactions are only two of a number of chemical processes that could occur, depending upon the composition of the groundwater intruding from the host rock and the design of the Engineered Barrier System (EBS). For example, conversions of montmorillonite to a range of other smectites (e.g. saponite, beidellite), or other clay minerals (e.g. vermiculite), are possible depending upon the groundwater composition. Alternatively, zeolites/feldspathoids could form if it is possible that leachates from cement grouts might access the buffer. Furthermore, the possibility of the ingress of dilute glacial meltwaters cannot be entirely excluded for some proposed repository locations for HLW/SF, in which case the potential for montmorillonite dissolution and buffer erosion must be considered. Consequently, models based on illitization and cation exchange alone do not necessarily capture the key controls on changes in physicochemical properties of the evolving buffer and may therefore be neither conservative nor realistic. The relative importance of the alternative potential transformation processes needs to be assessed in order to determine the extent of and controls on the alteration.

To this end, a range of reactive transport models has been developed and applied to Posiva's implementation of the KBS-3 EBS design (Posiva, 2012). Various modelling options were included to allow the sensitivity to alternative processes and parameterisations, including:

- Montmorillonite behaviour modelled assuming either cation exchange or dissolution/precipitation kinetics;
- Four groundwater compositions (brackish; saline; highly saline; and glacial meltwater);
- Two buffer compositions with different montmorillonite contents (75 and 90 %);
- Two thermodynamic databases: the Geochemist's Workbench® database 'thermo.com.v8.r6+' (Bethke, 2008); and Andra's Thermochimie v7b (Andra, 2014); and
- Alternative temperature parameterisations based on bounding and realistic assumptions: fixed uniform low temperature (11 °C); fixed uniform high temperature (95 °C); or a spatially and temporally evolving temperature field calculated with a coupled TH calculation that simulates the evolution through the thermal period and into the long-term (to 100,000 y).

Secondary mineral precipitation within the EBS depends on both thermodynamic stability and the rate of precipitation of the mineral, for which there is considerable uncertainty. Different sets of minerals are included in each of the thermodynamic databases considered. Further alternative models were therefore developed in some cases to assess the sensitivity to the choice of potential secondary minerals, in particular:

- In some instances specific secondary minerals were suppressed in order to investigate uncertainties in kinetic rates; and
- Vermiculite minerals were considered with the Thermochimie TDB in some instances.

The envelope of calculations performed encompasses a wide range of possible scenarios. In contrast to the typical assumptions of illitization and cation exchange, models based on kinetic assumptions suggest that some montmorillonite dissolution and alteration is possible where the buffer is in contact with the host rock (e.g. neighbouring a transmissive feature - Figure 1). Alternative databases predict different compositions and extents of secondary minerals and different long-term stable montmorillonite end members (Na-dominated in some cases and Ca- or Mg-dominated in others). In many scenarios, a reduction in porosity is predicted near flowing features, with porosity clogging occurring in some cases on timescales between 200 and 100,000 y. In all cases only relatively small regions of the buffer undergo significant alteration, but the proportions of the montmorillonite cation end-members can vary greatly and could impact upon the swelling capacity of the buffer. The results highlight the role of secondary minerals in determining the potential buffer evolution. In particular the possibility (or not) of saponite or vermiculite precipitation in the buffer is seen to lead to different potential evolutions in some cases, but does not lead to any situations in which a large proportion of the montmorillonite might be lost or transformed.

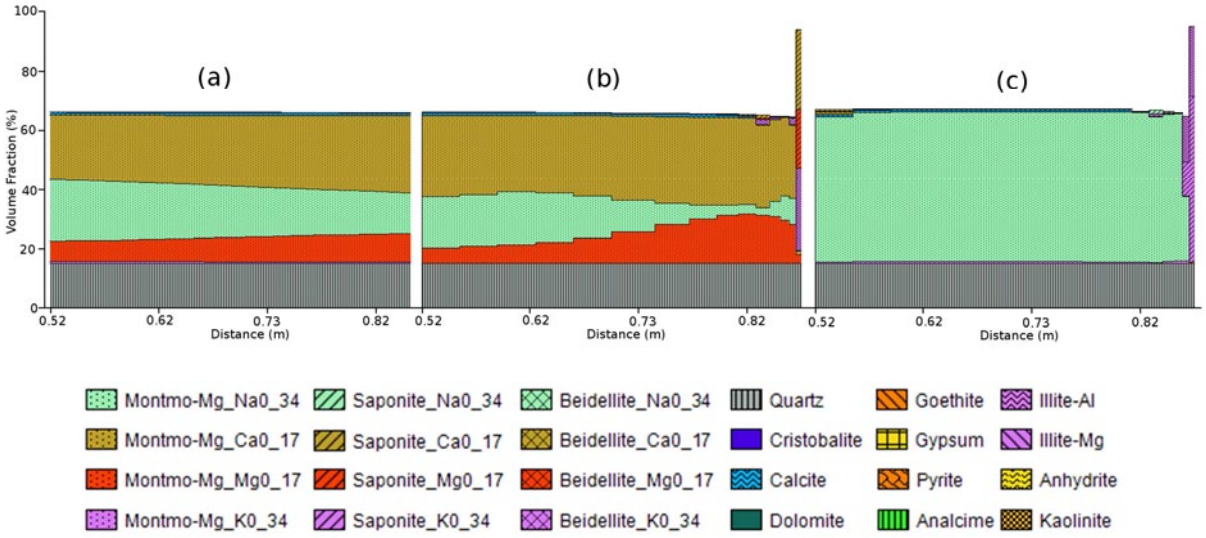


Figure 1. Buffer alteration 140 years after emplacement for the case of an intruding brackish water with spatially and temporally evolving thermal conditions: (a) when only cation exchange alteration is assumed; (b) when only montmorillonite dissolution/precipitation kinetics are assumed (TDB=thermo.com.v8.r6+);and (c) when only montmorillonite dissolution/precipitation kinetics are assumed (TDB=Thermochimie v7b). Kinetic treatments lead to porespace reduction near the contact with the groundwater; alternative databases lead to different secondary mineral assemblages and different dominant cation species

References:

Andra (2014), "Thermochimie", http://www.Thermochimie-tdb.com

Bethke, C. M. (2008) Geochemical and Biogeochemical Reaction Modeling. Cambridge University Press, Cambridge, UK.

Posiva (2012) Safety Case for the Disposal of Spent Nuclear Fuel at Olkiluoto -Description of the Disposal System 2012. Posiva Report 2012-05

Evolution of safety-relevant properties of bentonite in crystalline and clay host rock repositories for spent fuel and high level waste

Author(s) *Olivier X. Leupin*[1], Patrik Sellin[2], and Lawrence H. Johnson[1]

1 Hardstrasse 73, 5430 Wettingen, Switzerland

2 Blekholmstorget 30, SE-101 24 Stockholm

Bentonite has been proposed as buffer material to surround canisters of spent fuel and high-level waste in crystalline rock KBS-3 repositories and in the Swiss clay rock repository. Desired properties of bentonite used as buffer are to some degree independent of the nature of the host rock and include (i) low hydraulic conductivity/permeability, (ii) swelling and self-sealing (and healing) ability and (iii) durability of these properties. These properties are needed to fulfil safety functions which in turn allow for evaluating the performance of a repository. These include: limitation of the advective flow in the near field, minimizing microbial activity so as to limit microbial-induced corrosion, preventing canister sinking, providing a suitable swelling force against the host rock, damping rock-shear movements that might damage the canisters and limiting radionuclide transport after canister breaching. The relative importance of these safety functions and the quantitative requirements on the buffer to achieve them are somewhat different for crystalline and clay rock repositories. For example, the ability of buffer to limit stresses on canisters during potential rock shear events is more important for crystalline rock repositories as compared to clay rock repositories. In addition, the importance of radionuclide retention might be somewhat lower for buffer in clay rock compared to crystalline rock. Nonetheless, for both repositories, a bentonite buffer provides important contributions to repository safety related to providing the above safety functions as well as system robustness for various potential repository evolution scenarios.

The perturbations during the construction of the tunnels / emplacement boreholes and after the emplacement of the canisters will result in a high temperatures and hydraulic- and chemical gradients after closure of the repository that will affect the performance of the bentonite.

In a clay host rock the bentonite buffer, emplaced with relatively low moisture content, is expected to be resaturated by inward flow from the low permeability host rock. Depending on the overburden and structural strength of the clay rock, tunnel supporting structures such as a concrete liner or steel anchors and arches will be needed for the construction. The potential interactions of bentonite with engineered components (canister metals, concrete tunnel liner, steel support mesh, and arches, plus transport rails) are likely to be strongly non-linear, with a complex interplay between fluid transport, clay ion exchange and dissolution, secondary mineral growth, and consequent changes in physical properties (porosity, permeability, swelling pressure) of the clay. An initially high temperature gradient, a result of the initially low thermal conductivity of bentonite, might result in a zone of precipitated minerals around the canister increasing the brittleness and locally reducing the porosity of the bentonite. Despite the initially high temperature at the canister surface, possibly up to 150°C, little mineral alteration of the montmorillonite is expected.

In a crystalline rock the compacted bentonite rings are emplaced with high moisture content thus the higher thermal conductivity of high moisture content bentonite and the low rock temperatures ensure that canister surface temperature does not exceed 100°C. A few field tests have shown an increase in magnesium content in the bentonite close to the heater after excavation. The reason for this could be either an alteration or a neo-formation process.

In a crystalline rock, like the Forsmark site in Sweden, a large variability of resaturation time for different canister positions can be expected. While a few deposition holes will be saturated within a few tens of years, the majority will remain partly saturated for thousands of years. A long saturation time introduces some additional aspects about the performance of the repository that needs to be resolved:

- Will a slow saturation lead to heterogeneous conditions in the buffer (by mass redistribution)?

- Will a long term exposure to unsaturated conditions (vapour) affect the properties of the bentonite?
- Can the safety functions be considered upheld in a partially saturated buffer?
- Are the current THM-models suitable in a case with very slow resaturation?

This paper highlights the expected evolution of the bentonite buffer and its properties in clay-rock and in crystalline - rock repositories and discusses differences and common issues. It further provides a synthesis of information from experimental and modelling studies obtained during national and international projects (e.g. PEBS, ABM, LOT, FEBEX etc.) to assess to what degree the bentonite performance might be impaired and how the changes over the transient period may impact the overall repository performance.

Bentonite properties were assessed over a wide range of conditions and based on today's process understanding it can be concluded that the investigated bentonite is expected to fulfil the required safety functions over geological timescales and that the repository system robustness is greatly improved by using bentonite as buffer material.

A mechanism for bentonite buffer erosion in a fracture with a naturally varying aperture

***Christopher Reid*, Rebecca Lunn, Gráinne El Mountassir & Alessandro Tarantino**

Christopher Reid
christopher.reid@strath.ac.uk
PhD Student
Department of Civil and Environmental Engineering
University of Strathclyde
Level 5
James Weir Building
75 Montrose Street
Glasgow
G1 1XJ

< This research was undertaken in the context of deep geological nuclear waste disposal, with a view to examining the mechanism through which bentonite buffer extrudes into and erodes from a rock fracture intersecting a deposition hole. A phenomenon likely to occur during periods of glaciation. Previous researchers have examined the mechanism for, and rates of bentonite erosion, using purified montmorillonite in planar fractures (Schatz et al 2013). Here, we explore the effects of using as delivered MX-80 bentonite and a naturally variable aperture designed to mimic a rock fracture, constructed by taking a cast of a natural fracture present in a core of microgranite from Ailsa Craig, Scotland.

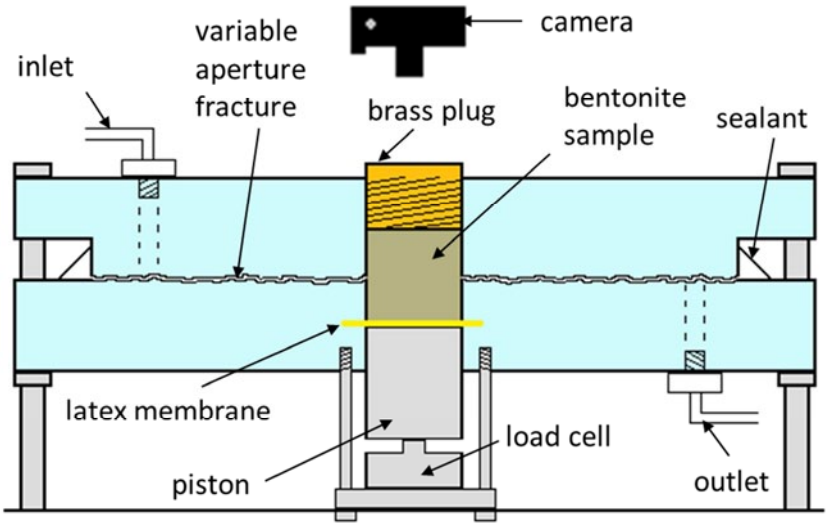


Figure 1. Schematic cross section of flow cell.

The cell, depicted in figure 1, was subject to flow through with deionised water. Gravimetric analysis was undertaken on the effluent and the swelling pressure of the bentonite monitored throughout. Image analysis of the extrusion process and accessory mineral ring formation was also undertaken. Erosion rate, swelling pressure and image analysis data correlated to reveal a previously undiscovered mechanism governing the erosion process. The erosion rate of buffer material exhibits a distinct cyclical nature, governed by increases/ decreases in the swelling pressure generated by the bentonite material and the affect this has on the presence of a ring of apparently non-erosive accessory minerals at the periphery of the extruded material as depicted in figure 2. This supports a theory put forward by previous researchers that the accessory minerals, accounting for up to 25% of the buffer, may provide

some mitigating effect against buffer erosion by way of filtration effects (Richards and Neretnieks 2010)

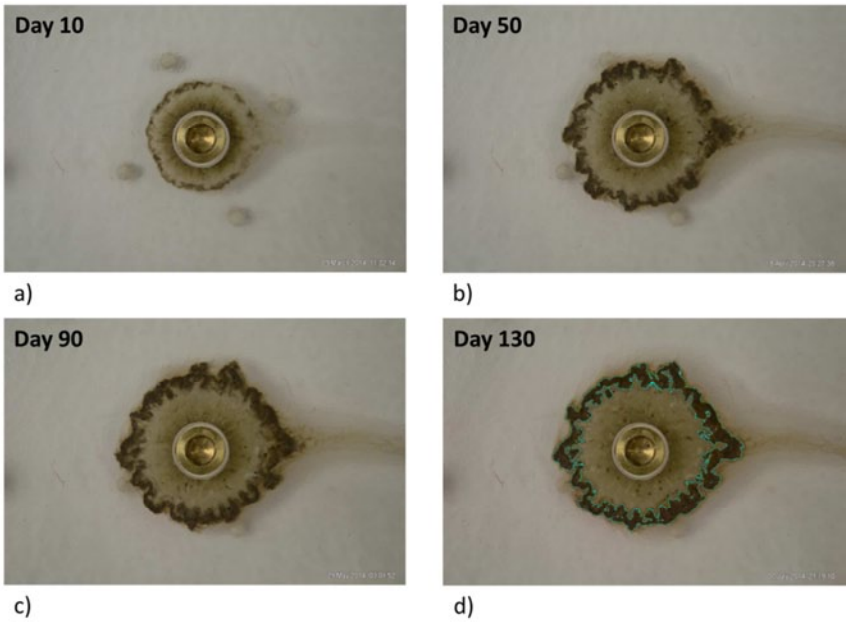


Figure 2: a) Extrusion into fracture after day 10 b) Extrusion into fracture after day 50 c) Extrusion into fracture after day 90 d) Extrusion into fracture after day 130 with evaluated accessory mineral ring area highlighted.

During non-erosive periods the swelling pressure increases and the thickness of the accessory mineral ring is relatively stable. It is proposed the swelling pressure increases to the point where the accessory mineral ring is perturbed, resulting in an erosive period. During erosive periods the swelling pressure concomitantly decreases as a consequence of mass loss and the accessory mineral ring increases in thickness, attenuating the erosion rate. This cycle appears to repeat until such time when the accessory mineral ring is sufficiently robust to prevent further periods of erosion. >

References:

Richards, T. & Neretnieks, I. (2010) *Filtering of clay colloids in bentonite detritus material*. Chem. Eng. Technol. 2010, 33, No. 8, 1303–1310

Schatz, T., Kanerva, N., Martikainen, J., & Sane, P. (2013) *Buffer erosion in dilute groundwater*. Posiva report 2012-44

Breakdown of the modified Gouy-Chapman model for clay surfaces in equilibrium with a $CaCl_2$ electrolyte: a molecular dynamic study.

Christophe Tournassat[a*], Ian C. Bourg[b], Carl I. Steefel[b]

[a]Water and Environment division, French Geological Survey (BRGM), Orléans, France

[b]Earth Sciences Division, Lawrence Berkeley National Laboratory, Berkeley, CA, 94720 USA

*corresponding author: c.tournassat@brgm.fr

Clay minerals have a high specific surface area that enhances their ability to influence water in their vicinity. Their surface charge, which varies as a function of physical-chemical conditions of the surrounding water, results in a complex organization of solute ions as a function of distance from the surface. This organization is known as the electrical double layer where counter-ions are electrostatically attracted to the surface whereas co-ions are repelled from it. Abundant and convincing spectroscopic evidence has emerged of a complex layering of water molecules and ionic species adsorbed at specific distances from the charged surfaces, a feature that can be captured by surface complexation models derived from Stern theory. The modified Gouy-Chapman model (MGC), or its modified version based on the resolution of the full Poisson-Boltzmann equation, is often used to calculate the electrostatic potential value in the diffuse region between the Stern layer and the bulk solution. Based on a comparison of the MGC model with Monte-Carlo simulations of discrete hard-sphere ions immersed in an implicit solvent, it was demonstrated long ago that the resolution of the full Poisson-Boltzmann equations can give accurate results for cations and anions distribution in the vicinity of a charged surface if both anions and cations are monovalent, if their total concentration does not exceed 0.1 mol/dm^3 and if the surface charge is not too high. When divalent (or multivalent) ionic species are present, the MGC model fails at reproducing Monte-Carlo simulations results in most conditions, because the MGC model neglects ion-ion interactions. For example, for 2:1 electrolytes the MGC model is thought to be inaccurate at salt concentrations greater than 0.005 mol/dm^3 (Torrie and Valleau, 1982; Carnie and Torrie, 1984; Boda et al., 2004).

Deviations from Poisson-Boltzmann model predictions probed by spectroscopic tools are now also available. Bu et al. (2006) demonstrated, using anomalous X-ray reflectivity data, that the MGC model is strikingly accurate at a highly charged interface in contact with a homovalent monovalent salt background up to a concentration of 10^{-2} mol dm^{-3}. Another study performed in similar conditions found that while accurate at 0.01 mol dm^{-3}, the Poisson-Boltzmann model failed to reproduce X-ray reflectivity data at higher concentrations (Luo et al., 2006). Molecular dynamics (MD) calculation studies have provided broadly similar results to those obtained by X-ray reflectivity (Wang and Chen, 2007; Lima et al., 2008; Lee et al., 2012). However, these studies were performed using homovalent monovalent electrolytes that are not generally representative of environments that are rich in clay minerals, whose surface sites tend to be occupied by divalent cations in natural clay formations.

In the present study, we evaluated the accuracy of MGC model predictions in a clay/water system in the presence of divalent cations and monovalent anions using MD calculations. Clay surfaces present several advantages with regards to molecular simulations owing to the 2D pseudo-periodicity of the clay particles. This system is particularly well suited to enabling accurate comparison between the MGC model prediction and the actual distribution of ions at the solid-water interface. Amongst clay minerals, montmorillonite has been the matter of multiple of MD simulation studies, but the vast majority of them involved only monovalent cations in interlayer spaces without the presence of anions. Few studies have been focused on divalent cations and/or charged surfaces in contact with large pores where the diffuse layer can fully extend without overlapping (Tournassat et al., 2009; Bourg and Sposito, 2011). We will

show that the MGC model prediction of the electrostatic potential value at the surface as well as the charge compensation over the distance from the surface are considerably more accurate than previously inferred from its comparison with Monte-Carlo simulations of discrete hard-sphere ions immersed in an implicit solvent.

References

Boda, D., Henderson, D., Plaschko, P., Fawcett, R.W., 2004. Monte Carlo and density functional theory study of the electrical double layer: the dependence of the charge/voltage relation on the diameter of the ions. *Molecular simulation* 30, 137–141.

Bourg, I.C., Sposito, G., 2011. Molecular dynamics simulations of the electrical double layer on smectite surfaces contacting concentrated mixed electrolyte (NaCl-CaCl2) solutions. *Journal of Colloid and Interface Science* 360, 701–715.

Bu, W., Vaknin, D., Travesset, A., 2006. How accurate is Poisson-Boltzmann theory for monovalent ions near highly charged interfaces? *Langmuir* 22, 5673–5681.

Carnie, S.L., Torrie, G.M., 1984. Advance in Chemical Physics. In: Prigogine, I., A., R.S. (Eds.), *Advances in chemical physics*. John Wiley & Sons, Inc., pp. 141–253.

Lee, J.W., Nilson, R.H., Templeton, J.A., Griffiths, S.K., Kung, A., Wong, B.M., 2012. Comparison of Molecular Dynamics with Classical Density Functional and Poisson–Boltzmann Theories of the Electric Double Layer in Nanochannels. *Journal of chemical theory and computation* 8, 2012–2022.

Lima, E., Horinek, D., Netz, R., Biscaia, E., Tavares, F., Kunz, W., Boström, M., 2008. Specific ion adsorption and surface forces in colloid science. *The Journal of Physical Chemistry B* 112, 1580–1585.

Luo, G., Malkova, S., Yoon, J., Schultz, D.G., Lin, B., Meron, M., Benjamin, I., Vansek, P., Schlossman, M.L., 2006. Ion distributions near a liquid-liquid interface. *Science* 311, 216–218.

Torrie, G., Valleau, J., 1982. Electrical double layers. 4. Limitations of the Gouy-Chapman theory. *The Journal of Physical Chemistry* 86, 3251–3257.

Tournassat, C., Chapron, Y., Leroy, P., Boulahya, F., 2009. Comparison of molecular dynamics simulations with Triple Layer and modified Gouy-Chapman models in a 0.1 M NaCl - montmorillonite system. *Journal of Colloid and Interface Science* 339, 533–541.

Wang, M., Chen, S., 2007. Electroosmosis in homogeneously charged micro- and nanoscale random porous media. *Journal of Colloid and Interface Science* 314, 264–273.

Fiber optic sensing methods for monitoring temperature and strain implemented in the FE Experiment

***Tobias Vogt*[1], Herwig R. Müller[1], Bernd Frieg[1], Tim Vietor[1]**

[1] Nagra, Hardstr. 73, 5430 Wettingen, Switzerland (tobias.vogt@nagra.ch)

The Full-Scale Emplacement (FE) Experiment at the Mont Terri underground research laboratory in Switzerland is a 1:1-scale multiple heater test in a clay-rich formation (Opalinus Clay). Based on the Swiss repository concept it simulates the construction, emplacement, backfilling, and post-closure thermo-hydro-mechanical (THM) evolution of a spent fuel (SF) / vitrified high-level waste (HLW) repository tunnel in a realistic manner. The main aim of this experiment is to investigate SF / HLW repository-induced THM coupled effects mainly in the host rock but also in the engineered barrier system (EBS), which consists of bentonite pellets and blocks.

The entire experiment implementation (in a 50 m long gallery with approx. 3 m diameter) as well as the post-closure THM evolution will be monitored using a network of several hundred sensors (state-of-the-art sensors and measurement systems as well as novel fiber-optic sensor technologies). The sensors are distributed in the host rock near- and far-field, the tunnel lining, the EBS, and on the heaters.

The fiber-optic instrumentation concept and first monitoring data with focus on distributed temperature and strain sensing are presented. Distributed fiber-optic sensing is a suitable monitoring technique for the application in large scale heater tests, because the sensor (fiber-optic cable) is heat and corrosion resistant due to the lack of electronics at the measurement location. In addition, the distributed sensing method provides a spatial resolution in the dm-m range along the fiber-optic cable.

In the FE Experiment fiber-optic cables for distributed sensing are installed in boreholes and at the tunnel wall. Measurements are performed by sensing the Raman (temperature measurements only) and Brillouin (temperature and strain measurements) backscattering. The objectives of the implemented distributed fiber-optic sensors are to investigate spatiotemporal variations of heat transport into the host-rock as well as tunnel wall displacements. In addition, different sensing cables, light reading units, installation techniques and calibration methods will be evaluated. Special attention will be paid to the cross-sensitivity of temperature and strain for using Brillouin sensing. Due to the dense instrumentation of conventional sensors (PT1000, thermocouples, LVDT) a direct in-situ comparison and evaluation of the different measurement systems is possible. Besides the technical aspects first data from the experimental heating phase will be shown.

Transparent deposition hole mock-up test in 1:3 scale

Xavier Pintado[1], **Jorma Autio**[1], **Kari Koskinen**[2]

[1] B+Tech Oy, Laulukuja 4, 00420 Helsinki, Finland
[2] Posiva Oy, Olkiluoto, Finland
Correspondence: xavier.pintado@btech.fi

The buffer design in a KBS-3 type repository for spent nuclear fuel in Finland is simulated and investigated experimentally in a transparent test set-up to ensure the safety and performance of the design. The fully instrumented transparent test system unfolds the key features that affect water transport and buffer performance. The stepwise progress from small to large scale tests side by side with modelling has been carried out in Finland as part of the integration of THM-experimental work and modelling (Pintado et al., 2010) to undertand the processes that affect buffer performance.

The test setup (Figure 1a) is a modular system of tubes manufactured from acrylic (PMMA) plastic reinforced with metal bands made in carbon steel painted for protection against corrosion. The inner diameter is 800 mm and the height is 2000 mm (ten blocks 200 mm thickness). The sample has 700 mm diameter and the 50 mm gap between the wall and the sample is filled with pellets (Figure 1b). The axial swelling load is measured with a load cell on top and the radial swelling pressure is measured with pressure sensors with a diameter of 50 mm. There are six sensors in two sections. The test setup has five wireless transmitters developed by AITEMIN (www.aitemin.es) which send the signal from three total pressure sensors and three capacitive hygrometers each other (Figure 1c). The position of the sections with wireless data transmission is in Figure 1d.

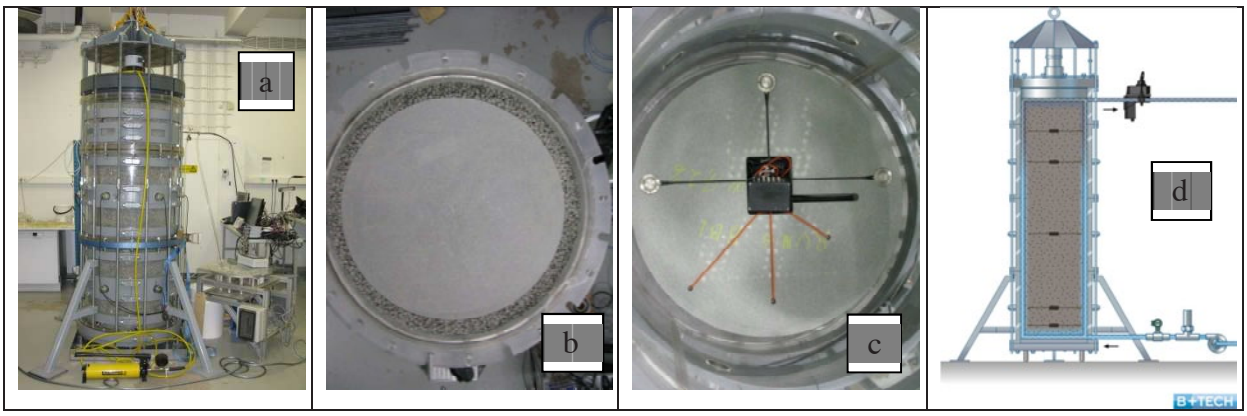


Figure 1. *Test setup (a). Sample and gap filled with pellets (b). Transmitter and sensors (c). Test setup schematic image (d) with the wireless sections.*

The test was done pumping water at flow rate of 0.1 L/min and a TDS (total dissolved content of solids) of 10 g/L (mixture of NaCl and $CaCl_2$) through a water inlet at the bottom of the cell. The water flows out through a water outlet at the top of the cell. The effluent is collected in flasks for measuring the content of effluents and calculates the erosion rate. The water was pumped during 1180 hours and the pump was stopped because of cracks appeared in the flanges between plastic tubes. The test was ongoing 1870 hours more without flow and finally dismantled. After the test, a post-mortem analysis was done measuring the final water content and the final bulk density. The dry density distribution and the degree of saturation can be calculated from these measures. The suction in these samples was also measured with a chilled-mirror dew point psychrometer.

The swelling pressure measured with the sensors outside the cell is presented in Figure 2.

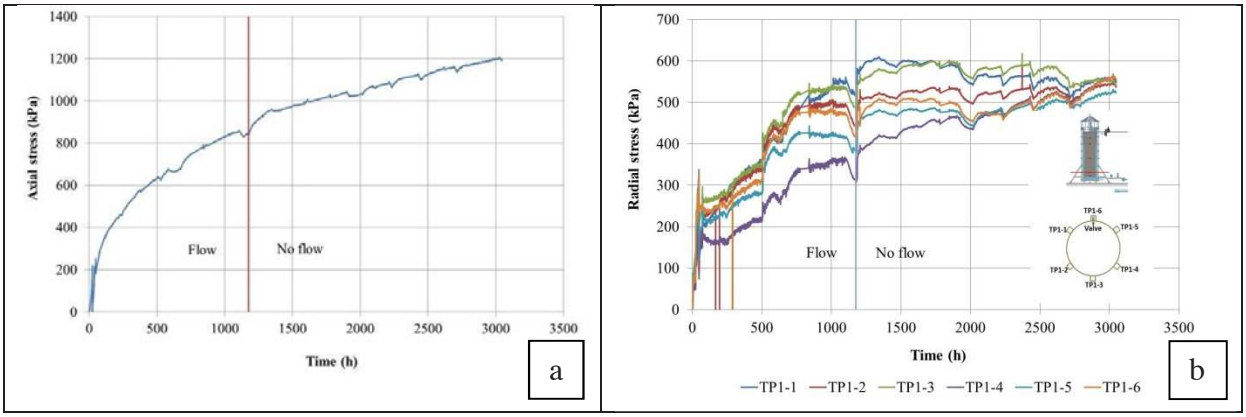


Figure 2. *Axial swelling pressure vs time (a). Radial swelling pressure vs time (b).*

The swelling pressure and the relative humidity measured with the wireless transmitter sensors are presented in Figure 3.

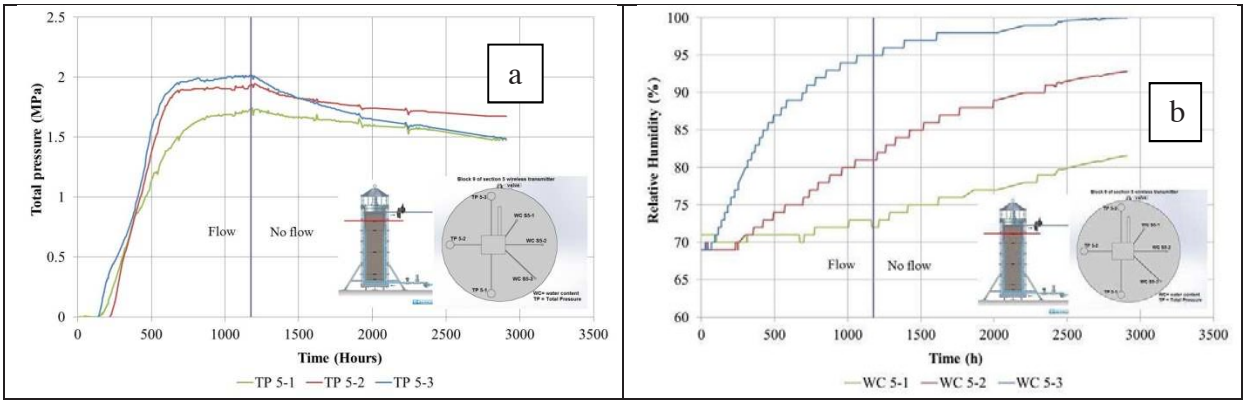


Figure 3. *Swelling pressure vs time (a) measured with the wireless transmitters sensors. Relative humidity vs time (b) measured with the wireless transmitters sensors.*

The erosion evolution and the average final density in the flow channel section is presented in Figure 4.

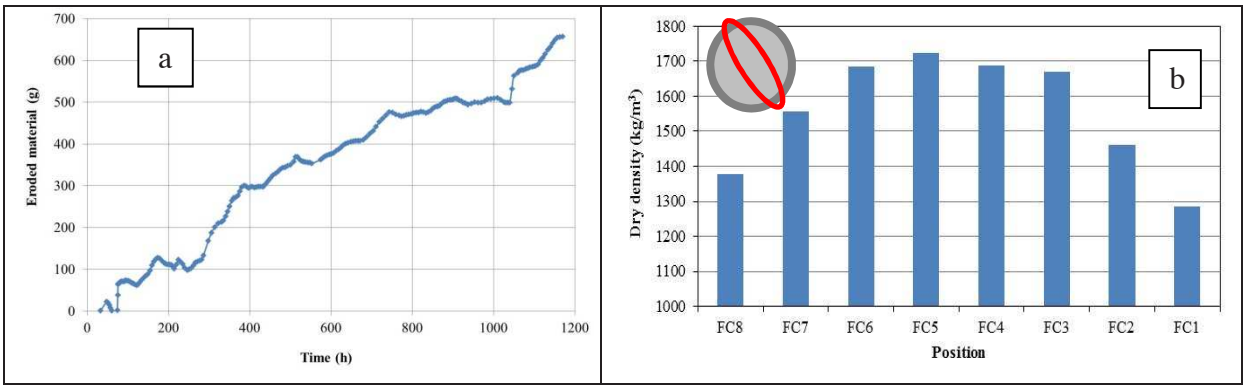


Figure 4. *Eroded material vs time (a). Dry density distribution measured in the post-mortem analysis at the end of the test (b) measured at the flow channel section. FC1 means the left bottom position and FC8 the right upper position in the insert.*

References

Pintado, X., Autio, J., Koskinen, K. (2010). Integration of THM-experimental work and modelling to design. Proceedings of the Meeting "Nantes 2010". Clay in Natural and Engineered Barriers for Radioactive Waste Confinement. Andra. France

Long-term strain monitoring in a deep tunnel concrete lining

Jan Verstricht[1], Arnaud Dizier[1], Xiangling Li[1], Alain Van Cotthem[2]

[1]*EIG EURIDICE, Boeretang 200, 2400 Mol (Belgium) [jan.verstricht@euridice.be]*

[2]*Tractebel Engineering, Avenue Ariane 7, 1200 Brussels (Belgium)*

Abstract: A safe long-term management of radioactive waste requires the isolation of this waste from humans and the environment. Currently, the most favoured strategy consists of disposal in geological stable layers. In Belgium, deep – poorly indurated - clay formations are considered (pending government approval), and disposal in such formations require a structural support of the host rock excavations, typically by lining of the underground galleries. This lining allows not only for operational safety, it also minimizes the perturbation (or excavation damaged/disturbed zone) of the host formation. Furthermore, it is essential if reversibility would be a requirement in the phased development of a repository. An important boundary condition for the design of such a support is the time dependant stress state of the clay formation around the lining. In Belgium, the feasibility and safety of waste disposal in clay is investigated at real scale since 1980 in the "HADES" underground research facility, situated at the site of the SCK•CEN Nuclear Research Centre in Mol, at a depth of 220 m depth in the Boom Clay formation. Initially consisting of a single shaft with manually excavated galleries, it was extended in 2002 and 2007 with additional galleries, constructed by industrial techniques (tunnel boring machine and wedge-block lining with unreinforced precast concrete segments). The first extension was the construction of the Connecting Gallery (connecting the existing part with a newly excavated access shaft) in 2002. To verify the design of these linings, routinely used at tunnelling projects at shallow depths (such as the London underground), but which were applied here for a first time at these depths, several segments were instrumented with embedded vibrating wire strain gauges during casting. Strains have been monitored since then (Fig. 1) and allow assessing the stresses inside the lining, as well as deriving the stress state of the host formation around it. Based on this monitoring set-up, a similar approach was performed for the construction of the PRACLAY Gallery (2007), where, in addition to the strains, the contact pressure between the lining and host formation and the load between the segments is also being monitored directly. The measurements have shown that the wedge-block lining method, in which the segments are expanded against the host rock during lining construction, results in a rapid increase in stress. Also the anisotropy of the stress state (horizontal – vertical) of the surrounding host formation can be clearly acknowledged by the strains observed. With strain gauges installed both near the inside and the outside of the lining, bending moments can be clearly derived. Further, the symmetry inside each ring (similar behaviour of the segments at similar positions), and the consistency between the different instrumented rings, are a good quality indicator of the monitoring results. To explain the long-term strain observations, some of which exhibit a continuous strain increase, a visco-elastic model has to be assumed. A correct interpretation of the long-term lining response further requires a thorough understanding of both the concrete and host formation behaviour (in particular creep), which is the subject of additional investigations. Ten years after the construction of the Connecting Gallery, all 250 strain gauges are still functional and monitoring the lining strains. They show an interesting potential for long-term monitoring of underground structures in a real repository.

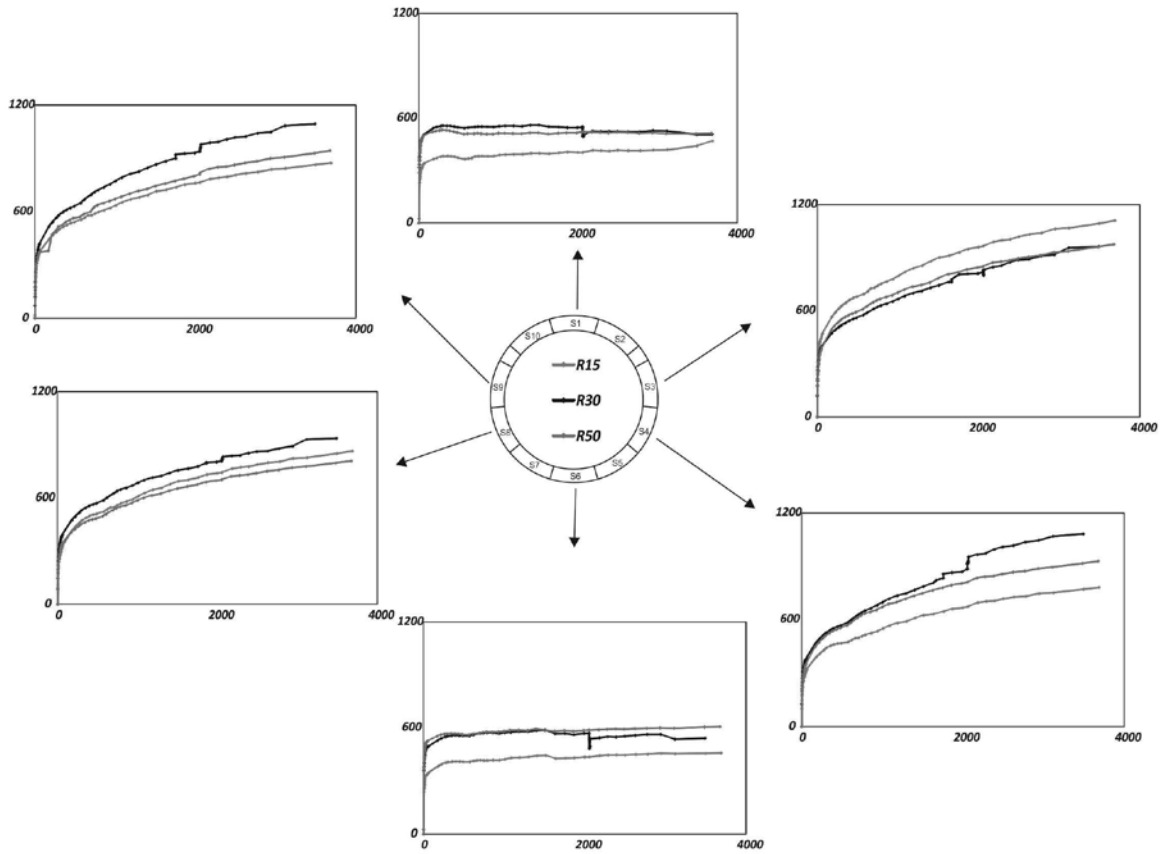


Figure 1 – *The strain evolution in three rings - over more than 10 years – shows a remarkable symmetry and are quite consistent with each other.*

Monitoring natural and engineered clay in geological repository with optical fiber sensors – lessons learnt from large scale experiments

S. Delepine-Lesoille, J. Bertrand, G. Pilorget, R. Farhoud, S. Buschaert, T. Vogt*, J. Verstricht**

Andra, 1-7 rue Jean Monnet 92298 Chatenay-Malabry, France
* Nagra, Hardstr. 73, 5430 Wettingen, Switzerland
**EIG EURIDICE, c/o SCK•CEN, Boeretang 200, 2400 Mol, Belgium

Within 40 years developments, optical fiber sensors have reached technological maturity and are now deployed on numerous civil-engineering structures. They also demonstrated compatibility with harsh environments. We review possibilities and limits of optical fiber monitoring systems for structure made of clay, based on lessons learnt from geological repository mock-ups.

Among existing monitoring technologies, optical fibers offer outstanding advantages such as resistance to harsh environments (heat, corrosion and radiations), ability to perform remote sensing, placing electronic parts kilometres away from the area to monitor, reduced intrusivity thanks to mm-sized sensing cable with large choice of materials. In the EU project Modern, we provided an extensive review of optical fiber sensors as a function of the spatial resolution, the optical principle implemented inside the system, the sensing parameter etc.. However, their applications to monitor structure made of clay were not addressed. This paper summarizes the performances and limits of optical fiber sensing systems implemented in clay materials, with a focus on distributed and long-base sensors (punctual sensors such as Bragg gratings are not considered).

In the monitoring systems of nuclear waste underground repositories, optical fiber sensors should enable mechanical and thermal monitoring of surface dykes, rock evolution surrounding disposal cells, sealings and remote boreholes for global monitoring of sites. In such geo-structure instrumentation optical fiber sensor systems will be exposed to large construction operations and dusty atmospheres. These challenges can be successfully met, paying large attention to various implementation details which have been tested in three experiments in different underground research laboratories (URL), PRACLAY in Hades (Belgium), the Full scale emplacement (FE) experiment in Mont Terri (Switzerland), GCR (Stiff design) gallery in Bure (France).

Temperature measurements

In the GCR and the FE Experiment, fiber-optic Raman temperature monitoring systems were installed (i) in boreholes (see fig.1) and (ii) at the interface between the shotcrete liner and the bentonite backfill.

Special tools were designed to limit the puncturing of the optical fiber, at both extremities of the borehole, that is to say the sealing and the far extremity. To enable high-quality measurement provided by loop configurations, the sensing fiber was installed with a U-shape; Since borehole diameter (8cm and 13cm) was smaller than the minimum curvature radius of the optical fiber, a curvature guide was successfully implemented. Distributed Raman systems produced good quality data over several hundred meters.

Resolution and accuracy are satisfactory and in the same range as standard point temperature sensors (0.1°C). The

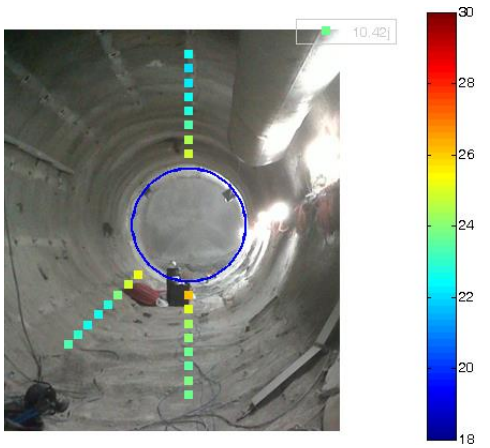


Figure 1 Distributed temperature measurement obtained with Raman OFS in Bure during concrete liner pouring.

distributed temperature measurements along the fiber-optic cable reveal detailed insights into the spatio-temporal varying temperature field in the rock around the gallery. However, in the FE Experiment, the dust protection had to be improved after failure of the Raman device during tunnel construction.

Strain sensing

Tests were performed on long-base extensometers and distributed sensing systems.

Interferometric sensors allow strain monitoring with long measurement bases (typically 10 m) and high resolution, in the order of 2μm; they are useful when a global value for the deformation is needed – e.g. installing such a sensor (or chain of sensors) in a borehole allows to obtain the functionality of an extensometer. In Hades, one sensor (over 9) was broken during installation. The inherent simplicity of such a system (compared with traditional borehole extensometers with anchors, connecting rods and displacement transducers) allowed for installations which were previously not possible. Temperature compensation is ensured thanks to internal reference sensors; its efficiency will be evaluated with the heating phase of PRACLAY.

Truly distributed strain sensing systems are based on Rayleigh and/or Brillouin scatterings. Strain resolution is degraded down to 30μm/m for most Brillouin sensing systems, but this performance can be reached over several kilometres with a meter spatial resolution. One Rayleigh device offers truly distributed strain sensing with few μm/m sensitivity, at the expense of short distance range, in the order of 100m. Their prices (in the order of 70k€ to 120k€) and the necessary competences needed to perform and interpret these measurements refrain their installation in HADES, where only intermittent measuring campaigns are performed.

In Bure, a Brillouin device is running continuously since October 2011. It stores the whole measured scattering profile along the entire optical line (raw data) and provides some interpreted strain data to the remote acquisition system. One return to supplier revealed mandatory over the last three years, due to the hard disk's breakdown. Despite a cabinet, a thick clay layer covers the instrument and fiber connections. The Rayleigh device test failed three times in Bure (opposite to several successful laboratory experiments and tests in HADES). We suspect the instrument to be totally incompatible with vibrations, created by permanent digging in several galleries of the Bure URL.

Whatever the selected measuring device, temperature compensation has to be implemented separately. Loose tubes were evaluated; a disappointing outdoor test showed that a more advanced design is mandatory to limit friction inside the tube over the entire temperature variation range. In Bure, the association of Raman (for temperature) and Brillouin (temperature and strain) sensing chains has been implemented. It works well but faces an implementation difficulty: to localize very accurately the measuring points along the two different sensing lines (Raman –resp. Brillouin- scattering is measured into multimode –resp. singlemode- fibers). It has been solved by creating artificial events, (i) thermal excitation during the construction step (ii) permanent reference points along the sensing lines. Such systems are also able to quantify possible drift of the measuring systems over decades. In the FE Experiment, temperature compensation will rely not only on Raman and Brillouin sensing chains, but also on a new hybrid Brillouin-Rayleigh backscattering instrument. This single device performs two scattering measurements in a single optical fiber, which should solve the map fusion difficulty.

On top of measuring principle, selection of the sensing cable is important. At this stage, optical fiber connectors are a weak point and splicing operations underground are a bit more delicate than soldering copper cables. The external sheath ensures protection of the optical fiber and also drives the strain transfer from the structure to the optical fiber where sensing is performed. The influence of the external sheath and the selected filling material is under evaluation. At this stage we showed that in the natural hard-clay of Bure, in the engineered bentonite in Mont-Terri, the several tested optical fiber cables were sufficiently robust to tolerate construction conditions.

Although strain distributed sensing systems are not as mature as Raman distributed temperature monitoring systems, results are promising. Next step of the qualification process is to implement on site special fibers meant to handle radiations.

One-year monitoring of desiccation cracks in Tournemire experimental station using Digital Image Correlation

Stephen HEDAN[a*], Valéry VALLE[b], Justo CABRERA[c], Philippe COSENZA[a]

[a] - Université de Poitiers, CNRS UMR 7285 IC2MP, HydrASA
Ecole Nationale Supérieure d'Ingénieurs de POITIERS
1 rue Marcel Doré, 86022 Poitiers Cedex
stephen.hedan@univ-poitiers.fr
[b] - Université de Poitiers, CNRS UPR 3346 Institut PPRIME
S.P. 2 M.I., Bd. M. et P. Curie, Téléport 2, B.P. 30179
86962 Futuroscope Chasseneuil Cedex
[c] - DEI-SARG Department, Institute for Radiological Protection and Nuclear Safety,
B.P. 17, 92262 Fontenay-aux-Roses Cedex
*stephen.hedan@univ-poitiers.fr

Digital image correlation (DIC) was used for the first time in an underground gallery to monitor desiccation cracks during an annual climatic cycle. This experimental *in situ* investigation was carried out on a study area of 344×275 mm², located on a gallery at the Tournemire experimental station, during which the relative humidity (RH) and temperature (T) were continuously measured for more than one year.

Our results demonstrate the ability of the non-invasive DIC method to monitor (a) clay-rock strains for at least four months and (b) the opening and closure of desiccation cracks for more than one year. Moreover, our study provides the following phenomenological results. First, as observed in the laboratory, the hydric strains were anisotropic; the strains perpendicular to the desiccation cracks were almost homogeneous and much larger than those parallel to the same cracks. Second, the changes in crack apertures calculated from the displacement fields (at an accuracy of approximately 26.9 μm) and the strain fields were clearly correlated with changes in RH and T (with 25%<RH<99% and 6°C<T<14°C). Third, contrary to direct measurements acquired at the Mont-Terri site (Möri et al., 2010), the crack apertures of the desiccation cracks were reversible after one year of data acquisition.

Moreover, although the main desiccation cracks were sub-horizontal and associated with the direction of bedding planes, our work demonstrated the existence of sub-vertical cracks. Finally, the qualitative interpretation of our entire dataset has emphasized the need for a multi-scale approach to understand the desiccation cracking mechanisms at the scale of an underground facility.

Références

Hédan S, Cosenza P, Valle V, Fauchille AL, Dudoignon P, Cabrera J, Investigation of the damage induced by desiccation and heating of Tournemire argillite using digital image correlation, , Int. J. Rock Mech. Min. Sci. 2012; 51: 64-75.

Hédan, S., Fauchille, A. L., Valle, V., Cabrera, J., & Cosenza, P. (2014). One-year monitoring of desiccation cracks in Tournemire argillite using digital image correlation. Int. J. Rock Mech. Min. Sci. 68, 22-35.

Möri A., Bossart P., Matray JM, Franck E, Fatmi H, Ababou R, Mont Terri Project: cyclic deformations in the Opalinus Clay, In: proceedings of the International Meeting of Clay in Natural and Engineered Barriers for Radioactive Waste Confinements, Nantes; 2010. p. 103-124

Standardized methodology for quantitative determination of the mineralogy and clay mineralogy in clays and shales

***Adriaens, R.*[1,*], Zeelmaekers, E.[1,2], Van Baelen, H.[3], Vandenberghe, N.[1], Elsen, J.[1]**

[1]Department Earth & Environmental Sciences, Katholieke Universiteit Leuven, Celestijnenlaan 200E, 3001 Heverlee
[2] Shell International Exploration and Production, The Hague, The Netherlands
[3] ONDRAF/NIRAS, Kunstlaan 14, 1210 Brussels
*corresponding author: rieko.adriaens@kuleuven.be

The mineralogy and detailed clay mineralogy of clays and shales are basic rock properties influencing the characteristics for which they are considered as host rock barrier in geological disposal of radioactive waste. Particularly the amount and composition of expandable minerals is of interest, especially for the Boom Clay and Ypresian clays in Belgium, as these are the youngest of the currently investigated potential host rocks in Europe and therefore are expected to contain the largest amount of expandable layers. Experience has learned that when samples are analyzed for quantitative clay mineralogy by different laboratories, reported results are often highly variable. This demands for the standardization of preparation procedures. Here, we present an outline of such a standardized procedure which allows for reliable and reproducible clay mineralogical data. This methodology is constantly being updated in the framework of a comparative mineralogical project study of the Boom Clay and Ypresian clays carried out by KULeuven and ONDRAF/NIRAS.

A full clay mineralogical characterization involves studying minerals at two levels: (1) at the bulk level on random oriented powders and (2) at the level of separate clay-sized fractions which are studied on oriented clay slides. Both powders and clay slides are studied using X-ray diffraction methods to characterize and quantify the different components in detail. Although mineral and clay mineral identification on X-ray diffraction patterns is relatively straight-forward, quantification is susceptible to much more ambiguity and absolute quantification errors are often greatly underestimated. With the introduction of standardized preparation procedures and highly-specialized quantification software however, the reliability of clay mineral quantification has been greatly improved.

Preparation for bulk measurements on random oriented powders involves the addition of an internal standard and wet grinding using a McCrone micronizing mill (after *Środoń et al., 2001*). In order to ensure perfect random orientation of mineral crystallites for measurement, samples are subsequently processed by a spray-drying equipment, which produces spherical aggregates, suitable for XRD measurement (after *Hillier, 1999*). Quantification is based on the summation of diffraction patterns of pure mineral standards using the QUANTA software (© Chevron ETC). Clay minerals are hereby quantified in groups, rather than on species level. This implies that some of the most common clay minerals, such illite, smectite and mixed-layer illite-smectite are quantified all together. Micas on the other hand can be quantified separately. Quantification of clay minerals down to species level is nevertheless possible when studying oriented clay slides.

Preparation of oriented clay slides is completed after an intensive chemical treatment to remove all aggregate-forming particles such carbonate cements, organic matter and free Fe-(hydr)oxides (modified after *Jackson, 1975*). Size separation is established by centrifugation on a chosen cut-off value, <2μm is often used. The <2μm clay fraction is subsequently Ca-saturated by which all exchangeable cation positions are occupied with Ca^{2+} allowing for objective mineralogical comparison between samples with naturally different exchangeable cation occupancies. Oriented clay slides are prepared by sedimenting a clay slurry on a glass slide prior to XRD measurement. Samples are

recorded in air-dry, ethylene glycolated and heated to 500°C conditions. Clay modelling and quantification of diffraction patterns is established using the SYBILLA software (© Chevron ETC) following the multispecimen approach (*Sakharov et al., 1999*). Following this approach, clay minerals are quantified down to species level.

In order to increase the reliability of the clay modelling and reveal more specific research questions, XRD-methods are complemented by Cation Exchange Capacity measurements, microscopical methods (SEM) and major element analysis by ICP-OES. The functionality of this working method is demonstrated for the Boom Clay in which expandable layers mainly occur as interstratified illite-smectite (R0) whereas the clay fraction <2μm of Ypresian clays is characterized by large amounts of discrete smectite. Detailed results for the Boom Clay are available on the related poster presentation "*Qualitative and quantitative mineral composition of the Rupelian Boom Clay in Belgium*".

References

Hillier, S. (1999). Use of an air brush to spray dry samples for X-ray powder diffraction. *Clay Minerals*, **34**, 127-135.

Sakharov BA, Lindgreen H, Salyn AL, Drits VA (1999) Determination of illite-smectite structures using multispecimen XRD profile fitting. *Clays and Clays Minerals*, **47**, 555-566.

Środoń, J., Drits, V.A., McCarty, D.K., Hsieh, J.C.C., Eberl, D.D. (2001). Quantitative XRD analysis of clay-rich rocks from random preparations. *Clays & Clay Minerals*, **49**, 514-528.

The effects of space restriction on microbial activity in final repository clay barrier systems

Andreas Bengtsson[1], **Anders Blom**[1] **and Karsten Pedersen**[1,2]

[1]Microbial Analytics Sweden AB, Mölnlycke Fabriker 9, 435 35, Mölnlycke, Sweden. [2]Department of Civil and Environmental Engineering, Chalmers University of Technology, Göteborg, 412 96, Sweden. Corresponding author e-mail: abe@micans.se

In most models for geodisposal of spent nuclear fuel, bentonite and other clays has an important barrier function in maintaining the integrity of the spent fuel canisters. The clay is intended to hinder inward and outward transport of radionuclides and groundwater, and also act as a buffer against rock movements. Sulfate-reducing bacteria (SRB) in the surrounding groundwater and naturally residing in the clay could harm the canister by production of corrosive sulfide by reduction of sulfate. A strong limiting factor for microbial activity is the density of the clay. Several experiments with the aim of finding the density threshold for microbial activity in repository clays have been carried out. In this report results from three of recently performed space restriction experiments on Wyoming MX-80 bentonite and Boom clay are presented.

In one experiment ten identical test cells which consisted of a titanium cylinder with a piston inside were used. The cells were filled with MX-80 bentonite clay powder with an addition of a bacterial cocktail consisting of three different species of SRB (except sterile controls). By tightening screws running through a lid on top of the piston and thereby forcing the piston downwards the amount of pressure acting on the clay could be regulated and also monitored by a load cell connected to a data collection system. Five of the test cells were adjusted to a density of 1750 kg m^{-3} and the other five test cells were adjusted to 2000 kg m^{-3} during simultaneous water saturation with a salt solution without carbon source through an inlet at the bottom. In contrast to previous experiment, no free aqueous phase was used in this experiment to avoid microbial activity outside the clay core. After approximately 70 days when the clay had reached the desired densities and was fully water saturated, the piston and bottom lid were removed. A 40 µm titanium filter that was attached to the bottom lid and kept the clay from swelling out into the inlet hole was replaced with a copper disc that simulated a copper canister. On the top side $^{35}SO_4^{2-}$ together with lactate was added. The test cells were then closed again and the load cell, piston and top lid were refitted. After 47, 77 and 123 days from the addition of sulfate and lactate test cell 3 and 8, test cell 4 and 9 and test cell 1, 2, 5, 6, 7 and 10 were sampled, respectively. The radioactivity of the $Cu_x{}^{35}S$ that had formed on the copper discs was localized and quantified using electronic autoradiography. Bentonite samples were taken from different layers of the clay and analyzed for distribution of ^{35}S, most probable number of SRB and distribution of SO_4^{2-}.

Approximately 7000 times higher surface radioactivity was measured on the 1750 kg m^{-3} discs compared to the 2000 kg m^{-3} discs. The rate of sulfate to sulfide conversion was also much higher in the 1750 kg m^{-3} cells. Heat treatment of the clay did not have any significant sterilization effect in the 1750 kg m^{-3} cells where cells with addition of microbes showed similar levels of radioactivity on the discs compared to the discs in 1750 kg m^{-3} cells with heat treated clay. In the 2000 kg m^{-3} case the cells with added microbes showed a low level of sulfate-reducing activity and the heat treated cells did not show any measurable radioactivity on their discs. Results from MPN analysis matched results from radioactivity measurements on the copper discs to some extent. In the 1750 cases (added microbes or not) an increasing trend was found, with relatively high bacterial numbers from the latest sampling at 123 days compared to day 47. For the 2000 case, low numbers or values below detection of cultivable SRB were found in the test cells. An uneven sulfate distribution through the clay was observed with lower values closest to the copper disc, probably due to a wash out effect during water saturation. This effect was more profound in the 2000 kg m^{-3} test cells. To avoid this in future

experiments the water saturation media could be added from the opposite side of the clay core. The added radioactive sulfate on the other hand diffused readily through the all test cells. A slight increase of ^{35}S could be seen in the clay closest to the copper disc.

The experiment above was repeated with Boom clay instead of MX-80 bentonite with the following modifications. Water from the underground laboratory HADES in Mol, Belgium was sampled and inoculated in SRB-medium with different carbon sources to select for different SRB species. These cultures were then used as microbial additions to the Boom clay cores in the test cells. Three different densities were investigated; 1800, 1900 and 2000 kg m^{-3}. Preliminary results shows that a cut off in microbial activity lies between 1800 and 1900 kg m^{-3} with approxiamtely three times higher surface radioactivity was measured on the 1800 kg m^{-3} discs compared to the 1900 kg m^{-3} discs.

An additional experiment with four different densities (1850, 1900, 1950 and 2000 kg m^{-3}) with the intended backfill material Asha bentonite of the Swedish KBS-3 repository model is ongoing. To further pinpoint the microbial activity threshold in MX-80 bentonite, this experiment also contains test cells with MX-80 bentonite compacted to 1900 kg m^{-3}. No results can however be reported from this experiment in the time of writing.

These experiments shows that bacteria truly are opportunistic life forms that can take advantage of seemingly small density decreases and are able to proliferate in an otherwise harsh environments. However, how an elevated temperature in a real repository affect the microbial activity remains uncertain.

Pore structure of Boda Claystone Formation, W-Mecsek, Hungary

Péter Ács[1], *Ferenc Fedor*[1]

[1]GEOCHEM Ltd, H-7614 Pécs, P.O.Box 35., acs.peter@geochem-ltd.eu

The pore character of Upper Permian Boda Claystone Formation (BCF), which is a potential host rock for the deep geological disposal of HLW in Hungary, were investigated as a part of a complex BCF study of Gorica Block (GB) accomplished between 2009-2013. Observing and describing the pore structure of a given rock is significant to understand the main transport mechanism, and hence, to understand the real behavior of the rock.

The BCF is characterized by diagenetically altered monotonous cycles of relatively homogeneous sediments that could be accumulated in a long time shallow-water lacustrine environment under semi-arid to arid climatic conditions (playa). The albite and analcim-bearing claystone layers consist of illite and/or muscovite (30-40 %), chlorite (5-10%), authigenic albite (25-40%) and analcime (in GB), quartz (5-10%), carbonates (5-10%, generally calcite or dolomite), hematite (5-10%) and other inconsiderable amount of phyllosilicates (Varga et al, 2005, Fedor et al, 2012, 2014). However, some papers have been published (Fedor et al, 2008, Osán et al, 2014, Breitner et al, 2014) in connection with petrophysical behavior and metal uptake of BCF, so far relatively small amount of data are available in relation to pore structure. In order to obtain detailed information about the pore structure and porosity, three different methods were used such as He-pycnometry, mercury intrusion porosimetry (MIP) and physisorption analysis. During the measurements 55 segments of a 10 m long BCF core and 1 m of overlaying sandstone from Ib-4 borehole were analyzed. Axial and radial plugs were drilled from core with 1,5" and 1" diameter, and fragments were used during the Hg-porosimetry and physisorption tests. Before measurements the samples and fragments were dryed at 105 ^{o}C to reach constant weight.

The skeletal volumes of the plugs were measured at 25 °C by He-pycnometry, then helium porosity (Φ_{He}) skeletal density ($\rho_{skeletal}$) and bulk density (ρ_{bulk}) were calculated. Both BCF and covering sandstone samples have low helium porosity (2,14±1,15 %, 4,91±0,70 % respectively) and radial cores have lower values which is indicating anisotropy. Higher skeletal density was found for BCF plugs than for fragments (2,655±0,056 g/cm^3, 2,714±0,014 g/cm^3 respectively).

MIP was used to investigate the pore size distribution in macro- and mesopore region and the mercury porosity (Φ_{Hg}), surface area (S_{Hg}) and fractal dimension (D_Z) of the samples, the contact angle was also measured. During the MIP tests lower porosity values are obtained than in He-pycnometry mesurement, which is explained by the fact that the pores are not accessible below 3,5 nm pore diameter for mercury. In the case of BCF there was no mercury intrusion into the macropore region, pore size distribution show peaks below 20 nm. So the calculated surface area is related to the mesopores although the MIP measurement does not cover the full range of mesoporous region (2 nm – 50 nm). The overlaying sandstone samples have peaks below 50 nm but wide peaks between 5 µm-60 nm were also obtained, so samples show macroporous and mesoporous characteristics. The fractal dimension, which is related to the roughness of the pore surface, was determined by the Zhang method (Zhang et al, 2006) and realistic values were calculated only at low pressure range (0,055 - 0,324 bar).

N_2 (77 K) and CO_2 (273 K) gases were applied during the physisorption tests. In the case of N_2 gas BET surface area (S_{BET}), pore size distribution (BJH method), fractal dimension (D_F, FHH method), and total pore volume (V_{tot}) were calculated. The CO_2 gas is very useful to explore the micropore structure of samples. The micropore surface area (S_{mic}) and micropore volume (V_{mic}) were calculated with the Dubinin-Radushkevich method in this case. Isotherms of BCF and covering sandstone samples show similarity to the type IV according to the IUPAC classification. This is a characteristic of mesoporous material with high energy of adsorption. Hysteresis can be observed on all isotherms

due to the capillary condensation, but the shape of the hysteresis loops are different. The results show that BCF samples have pores with narrow and wide sections and possible interconnecting channels. In contrast, the hysteresis loops of the overlaying sandstone samples are typical for the slit-like pores (Condon 2006). According to the pore size distribution, sharp peaks below 20 nm in BCF samples and below 100 nm in case of sandstone were observed. These peaks can be related to the microjoints opened during drying. The calculated S_{BET} and S_{mic} values are higher of the BCF (16,3±2,3 m^2/g, 14,7±2,3 m^2/g respectively) than of the sandstone (5,5±0,9 m^2/g, 3,9±0,6 m^2/g respectively). The effect of the outgassing process on three BCF samples within 105 °C-300 °C range using 50 °C temperature steps was also studied. The results suggest that the temperature caused no significant change in the pore structure during the degassing process. In both cases of BCF and sandstone two fractal regions between 0,10-0,40 and 0,48-0,90 relative pressure range were found. The samples have rough and heterogeneous surface, the calculated higher value of BCF fractal dimension may be related to the higher micropore volume.

On the basis of the pore structure analyses, the BCF is an extremely tight, micro- and mesoporous rock with relatively small pore surface but good pressure controlled self-healing capability. According to the pore range, and on the basis of reservoir state water permeability measurements (Fedor et al, 2008, 2012, 2014), different diffusion types could be the main transport mechanism in the rock. Water, which saturated the pores is trapped in capillaries or irreducible water on pore surface. The real amount of crystalline, irreducible, capillary and movable water, description of transport mechanism, origin and synthesis of movable water and the effect of temperature and pressure to the different processes are in the focus of future projects.

References

BREITNER, D., OSÁN, J., FÁBIÁN, M., ZAGYVAI, P., SZABÓ, CS:, DÄHN, R., MARQUES, FERNANDES, M., SAJÓ, I. E., MÁTHÉ, Z., TÖRÖK, SZ.: ***Characteristics of uranium uptake of Boda Claystone Formation as the candidate host rock of high level radioactive waste repository in Hungary***, Environ Earth Sci (2014), DOI 10.1007/s12665-014-3413-4.

CONDON J. B.: ***Surface area and porosity determinations by physisorption,*** Elsevier, (2006), pp. 6-14.

FEDOR, F., MÁTHÉ, Z., HÁMOS, G., SOMODI, G, JOBBIK, A., SZŰCS, I.: ***Laboratory Pressure Pulse Decay permeability measurement of Boda Claystone, Mecsek Mts., SW Hungary,*** Physics and Chemistry of the Earth (2008), pp. S45-S53.

FEDOR, F. (ed).: ***Special Petrophysical and Geophysical Examinations to Compare the Laboratory and Field Measurements – Final Report***., Hungarian manuscript, (2012).

FEDOR, F. (ed).: ***Final report of laboratory measurements for complex transport modelling in W-Mecsek Mts, Hungary***, Hungarian manuscript, (2014).

OSÁN, J., KÉRI, A., BREITNER, D., FÁBIÁN, M., DÄHN, R., SIMON, R., TÖRÖK, SZ.: ***Microscale analysis of metal uptake by argillaceous rocks using positive matrix factorization of microscopic X-ray fluorescence elemental maps***, Spectrochimica Acta Part B: Atomic Spectroscopy 91, (2014), pp. 12-23.

VARGA, A., SZAKMÁNY, GY., RAUCSIK, B., MÁTHÉ, Z.: ***Chemical composition, provenance and early diagenetic processes of playa lake deposits from the Boda Siltstone Formation (Upper Permian), SW Hungary***, Acta Geol. Hung., 48, (2005), pp. 49–68.

ZHANG, B., LIU, W., LIU, X.: ***Scale-dependent nature of the surface fractal dimension for bi- and multi-disperse porous solids by mercury porosimetry***, Applied Surface Science, 253 (2006), pp. 1349-1355.

Investigation of microstructures in naturally and experimentally deformed reference clays from underground research laboratories by using innovative methods in scanning electron microscopy

Guillaume Desbois[1)], **Susanne Hemes**[1)], **Ben Laurich**[1)], **Maartje Houben**[2)], **Jop Klaver**[1)], **Nadine Höhne**[3)], **Janos L. Urai**[1)], **Gioacchino. Viggiani**[4)] **& Pierre Bésuelle**[4)]

[1)] Structural Geology, Tectonics and Geomechanics, EMR, RWTH Aachen University, Lochnerstr. 4-20, D-52056 Aachen, Germany
[2)] Structural geology and tectonics, Utrecht University, Postbus 80021, 3508 TA Utrecht, The Netherlands
[3)] Institut für Bauforschung der RWTH Aachen, Schinkelstraße 3, 52062 Aachen
[4)] Laboratoire 3SR, Université J. Fourrier, BP53, 38041 Grenoble Cedex 9

Due to their low permeability and possible self-sealing properties in natural conditions, clays are of major importance for nuclear waste disposal in deep geological formations and for reservoir development in unconventional resources. In clays, porosity at grain boundaries is one of the fundamental parameters, defining the fluid transfer properties of the material. Unfortunately, most traditional methods fail to directly image both the porosity in a representative area (or volume) down to the resolution of pore scale and the nature of the pore filling fluid.
The application of ion beam milling techniques to fine-grained clays allows investigating porosity with unprecedented clarity at nm-resolution within representative areas under SEM. SEM pore imaging on Broad Ion Beam (BIB) prepared surface gives both qualitative and quantitative insights of porosity in 2D cross-sections. The combination of cryogenic techniques with ion beam milling preparation allow studying pore fluids in preserved clay-rich samples. The characterization of pore network in volume was done by using Focussed Ion Beam coupled with SEM (FIB-SEM) in order to image 3D pore network and try to find complementarities with 2D porosity analysis (BIB-SEM) and correlation with bulk porosity measurement (e.g. mercury injection porosimetry (MIP). Effective pore connectivity is currently investigated with an analogue of MIP based on Wood's metal, which is solid at room temperature and allows microstructural investigation of Wood' metal filled pores with BIB-SEM after the injection.
More recently, we are developing the combination of conventional stress-strain data (bi-axial and triaxial deformation tests), strain localization characterized by strain fields measurement (DIC – Digital Image Correlation) and microstructural investigations below micrometre scales (BIB-SEM) on a same sample, which offers the unique opportunity to answer to the fundamental questions: (1) "When", (2) "Where" and (3) "How" the sample were deformed in laboratory. The preliminary results, compared to microstructures recorded in naturally deformed clays, indicate that ductile behaviour of the clay matrix may be underestimated in the extrapolation of constitutive laws derived from deformation experiments in laboratory.

Microstructures in tectonically faulted Opalinus Clay: A multi-scale investigation (outcrop mapping, thin sections, BIB-SEM, FIB-TEM).

Ben Laurich[1], Janos L. Urai[1], Guillaume Desbois[1], Christian Vollmer[2] and Christophe Nussbaum[3]

[1] RWTH Aachen, Institute for Structural Geology, Tectonics and Geomechanics, Lochnerstr. 4-20, 52056 Aachen, Germany.
[2] University of Münster, Institut for Mineralogy, Correnstr. 24, 48149 Münster, Germany.
[3] Swiss Geological Survey, Federal Office of Topography Swisstopo, Seftigenstr. 264, 3084 Wabern, Switzerland.

Fault movement in clay can be highly localized in thin shear zones only a few microns wide. The microstructure of these thin zones can significantly influence the hydrological and mechanical properties of a formation and can thus control its mass transport properties and seismic stability. Usually the underlying deformation mechanisms remain speculative as investigating the internal structure of the thin shear zones is complicated and as the microstructure can be rather similar for a wide range of deformation mechanisms.
We use a multi-scale approach (outcrop mapping, thin-section analysis, ion beam electron microscopy) to describe the microstructure in tectonically sheared, overconsolidated Opalinus Clay (OPA) from the Mont Terri Underground Research Laboratory (CH), a site to evaluate the long-term safety of radioactive waste disposal.
We identified five structural elements: (1) slickensides, which are in cross-sectional view associated to (2) a μm thin zone of slickenside parallel oriented particles, (3) gouge, (4) calcite and celestite veins and (5) scaly clay. Moreover, we found a significant loss in porosity for gouge, veins and the thin shear zone compared to the protolith.
From these elements we infer interacting deformation mechanisms that hold the key to understand the evolution of the found observed microstructure. Therein, the strength of OPA might not only be controlled by cataclastic processes and friction between clay particles, but as well by pressure solution as slickensides show isolated veins and patches of calcite in releasing bands associated to risers and calcite free areas in restraining bands. Moreover, first results indicate that ductile behaviour has occurred at different scales: Scaly clay forms microfolds and crenulation cleavage on the dm to mm scale, however comprise thin shear zones with slickensides indicating frictional sliding on the μm scale. On the other hand, gouge shows a strong fabric intensity and a strict P-orientation of particles that indicates a ductile deformation of the gouge internal structure in the mm-μm range.

We discuss processes of localization during incipient faulting in mudrocks at about 1.5 km depth, episodic fluid flow and resealing, and the formation of slickensided surfaces in deformed mudstones. Further we compare the tectonically sheared samples to synthetically deformed samples in order to evaluate the influence of more rapid deformation mechanisms.

Hyperspectral imaging for the characterization of clays on large spatial scales

P. Brunner[1], P. Renard[1], *J. K. Becker*[2]

1 Centre d'hydrogeologie, Univ. Neuchâtel, Rue Emil-Argand 11, CH-2007 Neuchâtel
2 Nagra, Hardstrasse 73, CH-5430 Wettingen, jens.becker@nagra.ch

Hyperspectral imaging has been widely used to estimate the mineral content of rocks. However, most applications of this technique have been in air-borne data acquisition systems. The use of ground-borne hyperspectral data is more recent and subject to some methodological differences. The main differences appear in the scale of the acquired pixels, which for ground borne data can be below a square-millimeter, compared to several square decameters or more for airborne data. The spectral analysis of pixels in ground borne data, where scans are often performed over rather similar materials (e.g. different types of clays) is challenging compared to the spectrally more discriminable pixels acquired over larger areas in airborne data (typically vegetation, water, rock formations). Therefore, the post-processing of the hyperspectral scans, including the reconstruction, classification and upscaling, are important steps and require rigorous (geo)statistical procedures.

One important step of the post-processing of hyperspectral scans is the classification of the scans. In this step, each pixel of the scan is compared to an end-member spectrum for a certain mineral and, if the probability of a match is higher than a certain threshold, the pixel is classified using this mineral. Especially on larger scale scans, where each pixel represents a mixture of several minerals, a varying amount of pixels of the scan will not be classified because no accurate fit of this pixels spectrum with one of the end-member spectra can be found. In this case, the only partially classified image may be reconstructed using multiple-point statistical methods. The approach is stochastic and builds on the classified pixels of the scan, resulting in an ensemble of equiprobable, exhaustive 2D images. This step may be applied at different resolutions because the data acquisition typically is conducted at different resolutions. If a low and high resolution data set overlap, multiple-point statistics can be trained and then used to simulate the unresolved high resolution variability within the low resolution pixels at other locations. This technique can also be used to determine upscaling/downscaling laws.

The principles and methods briefly summarized above have been applied to several scans of outcrops in the underground lab in Mont Terri, Switzerland. The underground lab is situated within the Opalinus Clay, one of the proposed host rocks for the storage of radioactive waste in Switzerland. Several so called niches and tunnel walls in different orientations (with respect to the bedding planes of the Opalinus Clay) have been scanned and processed covering areas ranging from 1-5 m^2 (see Fig. 1).

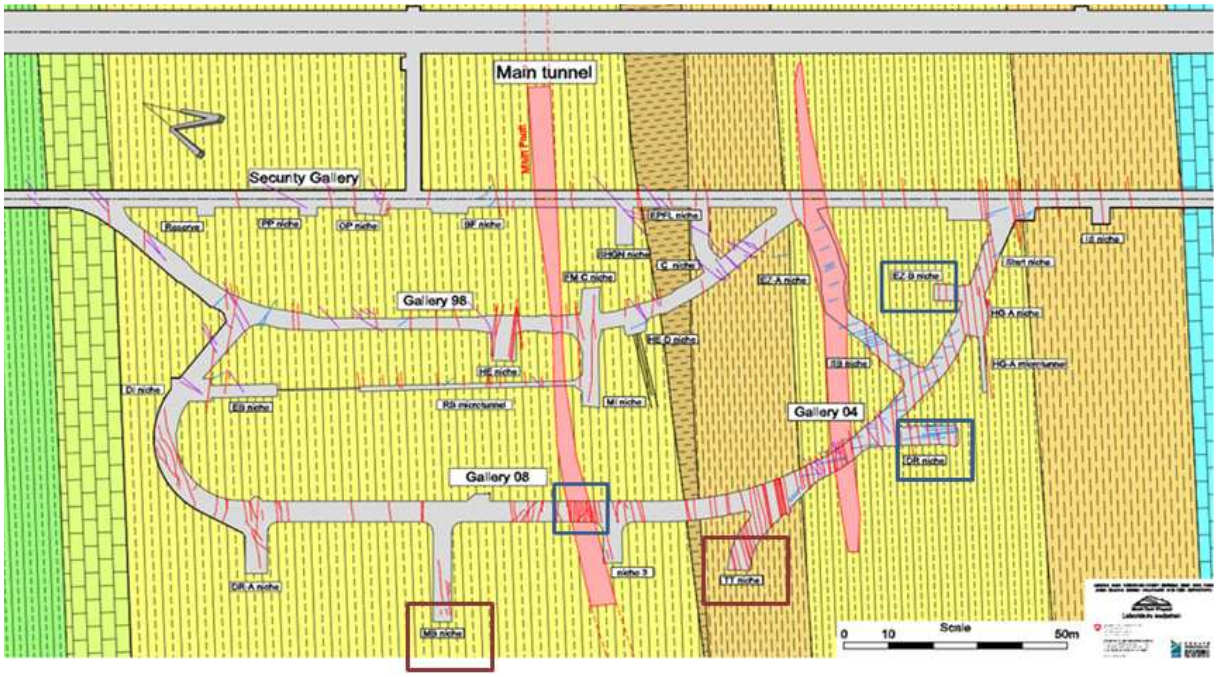


Fig. 1: Floor plan of the underground laboratory Mont Terri. Blue frames indicate outcrop scans, red frames indicate locations where additional core scans have been performed.

The next step will be to use all of these scans to simulate the heterogeneity in 3D. For that purpose, additional information such as borehole data (e.g. geophysical logs) or lab analyses (such as mineralogical analyses) must be integrated in the analysis.

DECOVALEX-2015: A THM modelling benchmark based on the performance of heated and hydrated granulated bentonite mixture column tests

Garitte B. (Nagra), Lee C. (KAERI), Maekawa K. (JAEA), Manepally C. (CNWRA), Pan P. (CAS), Rutqvist J. (LBNL), Graupner B. (ENSI), Wang X.R., Shao H. (BGR), Nguyen S. (CNSC)

NAGRA, National Cooperative for the Disposal of Radioactive Waste, Hardstrasse 73, CH-5430 Wettingen, Switzerland, benoit.garitte@nagra.ch

Introduction

In this paper, a modelling benchmark exercise from the DECOVALEX-2015 project is presented. The benchmark exercise presented is part of a task geared towards the understanding of Thermo-Hydro-Mechanical (THM) processes in a bentonite buffer and an argillaceous host rock of a repository for high level radioactive waste. The task is based on the performance and analysis of 1) the HE-D heating test at Mont Terri (rock only), 2) laboratory column tests on bentonite pellets and 3) the HE-E heating experiment at Mont Terri (integrating buffer materials and host rock). The focus of the paper is on the modelling of the bentonite pellets column tests that were carried out at CIEMAT (Villar et al., 2012 and 2014) to mimic the radial heat and water flow around the HE-E heater.

Experimental set-up

The columns of pellets are 50 cm high which corresponds to the distance between the rock and the heater in the HE-E experiment. The walls of the columns where isolated to simulate 1D-flow conditions. Several heating stages were applied from the bottom of the column: the bottom temperature was set to 100 °C for the first 3500 hours and then increased to 140 °C until the end of the experiment. 140°C corresponds to the heater surface temperature in the HE-E experiment. This temperature was kept constant during the last phase of the experiment (still on-going) during which the column was hydrated from the top by applying a water pressure of 0.1 MPa. The column itself is equipped with three pairs of relative humidity sensors and temperature sensors that allow for comparison with the numerical models. Water intake and axial pressure on the top of the cell were also measured.

Modelling results

The modelling results from 8 modelling teams are discussed and compared to the experimental data. This exercise enables a detailed evaluation of the strengths, weaknesses, and adequacies of the various approaches and computer codes used by the various modelling teams. Although the power loss through the lateral and bottom boundaries had to be estimated, the analysis allowed to gain insights into the complex coupled THM behaviour and the thermal parameters of the bentonite pellets.

References

Villar M.V., Martín P.L., Gómez-Espina R., Romero F.J., Barcala J.M.. 2012. THM cells for the HE-E test: setup and first results. PEBS Report D2.2.7a. CIEMAT Technical Report CIEMAT/DMA/2G210/02/2012. Madrid, 34 pp.

Villar, M.V., P.L. Martin, R. Gomez-Espina, and F.J. Romero. "Long-term THM Tests Reports: THM Cells for the HE-Test: Update of Results Until February 2014." PEBS Report D2.2-7.3. Madrid, Spain: Long-Term Performance of Engineered Barriers Systems Project. 2014.

Titles Deformation of compacted bentonite due to highly suctions on various temperatures

Author(s) Prof. Tomoyoshi NISHIMURA, Ashikaga Institute of Technology, JAPAN

Address(es) 268 Omae Ashikaga Tochigi, JAPAN 326-8558
E-mail tomo@ashitech.ac.jp

Abstract: Swelling properties of compacted bentonite such as deformation, swelling pressures and shear strength associated to hydration resulting from either water adsorption or vapor pressure changes are important for radioactive waste disposal system. It was certain that hydration-induced macro-structure or micro structure had significant effect on potential at double layer system in the compacted bentonite. Geotechnical and geo-environmental engineers focus on swelling mechanism of compacted bentonite for a decade ago. These days the measurement of both swelling deformation and swelling pressures of the unsaturated bentonite are conducted. Considering volume deformation and shear strength due to hydration potential changes, it is necessary to establish a safety framework for compacted bentonite barrier system. Nowamooz and Masrouri (2012) presented soil-water characteristic curve for bentonite using osmotic method or vapor pressure technique, and MIP (Mercury Intrusion Porosimeter) technique appeared the pore size distribution in the double structural level. Romero et al. (1999) gave understanding be-tween MIP data and predicted soil-water characteristic curve. Morodome and Kawamura (2009) investigated the swelling behaviour of Na- and Ca-montmorillonite at various temperatures greater than 50 ℃, up to 150 ℃ using in situ X-ray diffraction (XRD) analysis. They could explain the increasing basal spacing (Å) with increasing of relative humidity.

This study focused on the influence of temperature on deformation of compacted, unsaturated bentonite, and investigated volume deformation of compacted bentonite under various temperatures. The bentonite used in this test program were Na-montmorillonite, that it was statically compacted to approach to a dry density of 1.6Mg/m3 as target value. All specimens were applied highly suction more than 2.8 MPa using vapour pressure technique (i.e. controlling of relative humidity), and the temperature increased from 20 ℃ to 60 ℃ under a constant relative humidity. The deformation due to both changes of suction and basal spacing was measured over a period of one year that indicated swelling behaviour under unsaturated condition for compacted bentonite. Also, the test results described elastic-plastic deformation of compacted bentonite in the range from 33 % to 98 % in relative humidity.

Additional repulsive pressures in clays of various mineralogy

Wiebke Baille **and Tom Schanz**

Ruhr-Universität Bochum, Chair of Foundation Engineering, Soil and Rock Mechanics, 44780 Bochum, Germany, wiebke.baille@rub.de

In the past years, compacted bentonites have been proposed as suitable barrier and backfilling materials in the toxic waste repositories due to their low permeability and developement of swelling pressures to fulfill the sealing requirements (Pusch, 1977; Dixon and Gray, 1985; Pusch and Yong, 2006). Net repulsive physicochemical forces are known to be responsible for the swelling pressure development in saturated bentonites (Bolt, 1956; van Olphen, 1977; Mitchell, 1993). For a given interlayer distance, the net physicochemical forces correspond to the sum of the above repulsive diffuse-double-layer forces, attractive van der Waal's forces and repulsive short range forces within the clay-water system. Some recent studies attempted to evaluate the swelling pressures of compacted bentonites on the basis of diffuse double-layer repulsive pressures (Komine and Ogata, 1996; Tripathy et al., 2004; Schanz & Tripathy, 2009). A comparison of experimental and theoretical results showed that the experimental swelling pressures are either smaller or greater than their theoretical counterparts within different dry density ranges. At close interlayer distance smaller than 2 nm, the hydration energy due to surface and ion hydration and the Born repulsion are the major components contributing to the swelling pressure (Verwey and Overbeek, 1948; van Olphen, 1977; Kjellander et al., 1988; Yong, 1999). The Born component of the repulsive pressure strictly corresponds to the overlapping of electron clouds of adjacent atoms. Born repulsion increases sharply with decreasing interlayer distance. In most cases, the nature of these repulsive pressures is presented as exponential functions, power laws, and steep linear relations (Anderson & Lu 2001, Santamarina 2001). For example, the Born repulsion F_B can be calculated using eq. 1, where B and n are constants, and 2*d* is the distance between the layers.

$$F_B = B / (2d)^n \quad (1)$$

However, direct quantification of the net physicochemical forces is difficult. Therefore, no attempt was made to compute the Born repulsion alone from eq. 1, rather, an attempt was made to account for the theoretical double layer repulsive and the attractive pressures separately and the net pressures were then deducted from the experimental swelling pressures of the clays studied to obtain the additional repulsive pressures R_{add} at close interparticle distances (Tripathy et al. 2006). This procedure is illustrated in Fig. 1, where the vertical lines correspond to the magnitude of R_{add} at a given interlayer distance 2d or respective dry density. The diffuse double layer repulsive pressures for the compacted clays were determined using the equations for the diffuse double layer theory of interacting platelets (van Olphen, 1977). The attractive pressures for the same range of interlayer distances were calculated using the van der Waals-Hamaker equation (eq. 2),

$$A = A_h/48\pi\,[1/d^3+1/(d+\delta)^3-2/(d+0.5*\delta)^3] \quad (2)$$

where *d* is half of the interlayer distance, δ is the thickness of the clay particle, and A_h is the Hamaker constant (= 6.11 10^{17} kNm for water as the bulk fluid). The theoretical net interparticle pressure (i.e., repulsive minus attractive, R - A) was thus calculated. Finally, the additional repulsive pressure was calculated as difference between the experimental swelling pressures and the theoretical net interparticle pressures R – A at given interlayer distance 2*d*.

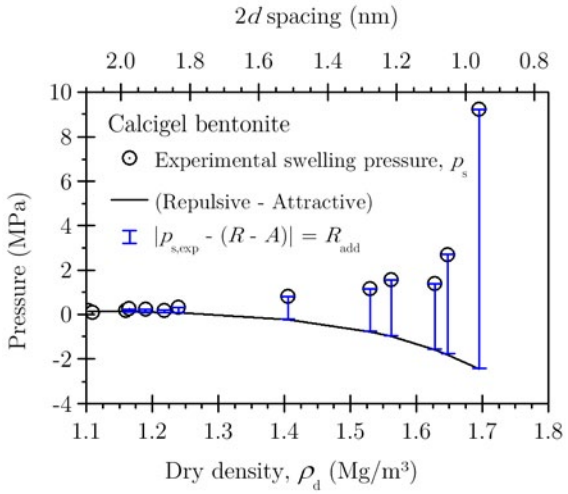


Fig. 1: Illustration of the determination of additional repulsive pressures R_{add}

The evaluation of the additional repulsive pressures R_{add} was performed for Calcigel bentonite, NX illite and Spergau kaolin using own experimental swelling pressure data (Baille et al. 2010, Baille, 2014) and for several highly plastic bentonites reported in literature (MX 80, Febex, Bentonite S2, Kunigel, Kunigel V1).

A unique correlation was obtained between the spacing between the bentonite platelets and the additional repulsive pressures below a bentonite platelet spacing of about 1.5 nm for the bentonites studied (Fig. 2 (a)). For NX illite and Spergau kaolin, correlations differed significantly from that of the bentonites. For all three clays, additional repulsive pressures became significant for dry densities greater than the respective Proctor dry density of the clay (Fig. 2 (b)).

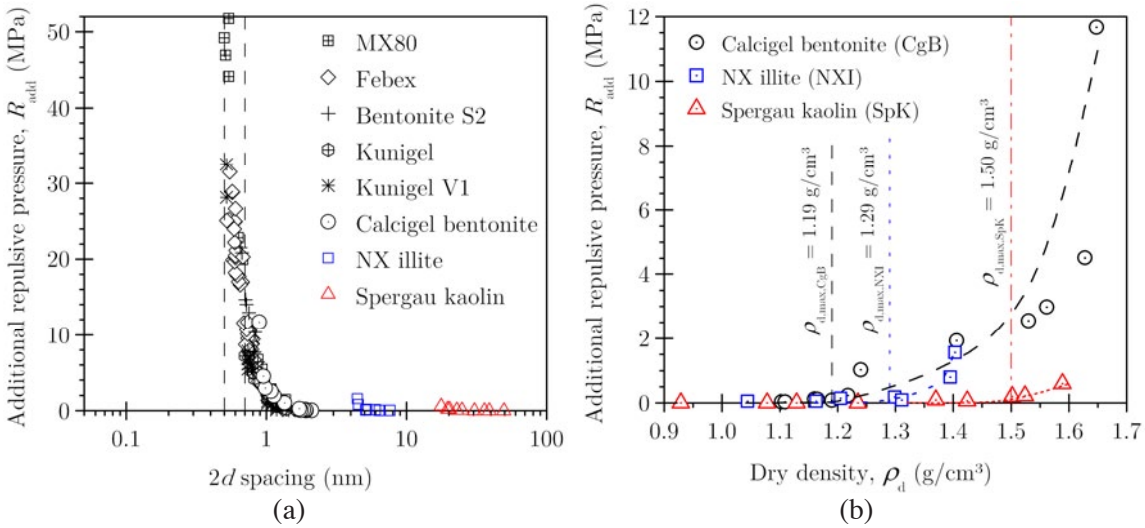


Fig. 2: Additional repulsive pressures R_{add} versus (a) 2*d* spacing and (b) dry density of the clays

References:

Baille, W., Tripathy, S., and Schanz, T. 2010. Swelling pressures and one-dimensional compressibility behaviour of bentonite at large pressures, *Applied Clay Science* 48, 324– 333.

Baille, W. Hydro-mechanical behaviour of clays - significance of mineralogy. Phd-thesis, Ruhr-Universität Bochum, 2014.

Dixon, D.A., Gray, M.N. 1985. The engineering properties of buffer material. Technical report TR-350, Underground Research Laboratory, Atomic Energy of Canada Limited, Pinawa MB, Canada.

Pusch R. 1977. Highly compacted sodium bentonite for isolating rock-deposited radioactive waste products. *Nuclear Tech*. 45, 153 157.

Pusch, R., Yong, R.N., 2006. Microstructure of Smectite Clays and Engineering Performance. SPON Research, Taylor & Francis, London and New York.

Anderson, M. T. & Lu, N. 2001. Role of microscopic physicochemical forces in large volumetric strains for clay sediments. *Journal of Engineering Mechanics* 127(7), 710–719.

Bolt, G., 1956. Physico-chemical analysis of the compressibility of pure clays. *Géotechnique* 6(2), 86–93.

Kjellander, R., Marcelja, S., Pashley, R. & Quirk, J. 1988. Double-layer correlation forces restrict calcium-clay swelling. *Journal of Physical Chemistry* 92, 6489–6492.

Komine, H. & Ogata, N. 1996. Prediction for swelling characteristics of compacted bentonite. *Canadian Geotechnical Journal* 33, 11–22.

Mitchell, J. K. 1993. Fundamentals of Soil Behaviour. 2 edn, John Wiley & Sons, Inc.

Santamarina, J. C. 2001. Soils and waves. John Wiley & Sons.

Schanz, T. & Tripathy, S. 2009. Swelling pressure of a divalent-rich bentonite: Diffuse double-layer theory revisited. Water Resources Research 45(2), W00C12.

Tripathy, S., Sridharan, A. & Schanz, T. 2004. Swelling pressures of compacted bentonites from diffuse double layer theory. Canadian Geotechnical Journal 41, 437–450.

Tripathy, S., Kessler, W. & Schanz, T. 2006. Determination of interparticle repulsive pressures in clays, in G. Miller, C. Zapata, S. Houston & D. Fredlund, eds, 'Proceedings of the Fourth International Conference on Unsaturated Soils', Carefree, Arizona, USA, pp. 2198–2209.

van Olphen, H. 1977. An introduction to clay colloid chemistry, 2nd edn, John Wiley & Sons, New York London Sydney Toronto.

Verwey, E. & Overbeek, J. 1948. Theory of the stability of lyophobic colloids, Elsevier, Amsterdam.

Yong, R. 1999. Soil suction and soil-water potentials in swelling clays in engineered clay barriers. *Engineering Geology* 54, 3–13.

Hydromechanical behaviour of bentonite under in situ conditions

A.C. Dieudonne[1,2], **J. Talandier**[3] **and R. Charlier**[1]

[1] University of Liege, ArGEnCo Department, Chemin des Chevreuils 1, 4000 Liege, Belgium (ac.dieudonne@ulg.ac.be, robert.charlier@ulg.ac.be)
[2] F.R.I.A., Fonds de la Recherche Scientifique – FNRS, Rue d'Egmont 5, 1000 Brussels, Belgium
[3] Agence nationale pour la gestion des déchets radioactifs (Andra), Châtenay-Malabry, France (jean.talandier@andra.fr)

In recent years, particular attention has been paid to the behaviour of bentonite-based materials in relation to their use as engineered barriers in deep geological repositories for nuclear waste. In this context, the engineered barrier aims at creating a zone of low permeability that is able to reduce water flow coming from the host rock, hence the release of radionuclides into the environment. Therefore bentonite-based materials have generally been selected for their high swelling capacity, their low permeability and their important radionuclides retardation capacities.

However, the placement of a bentonite buffer within a gallery involves unavoidable technological voids between the engineered barrier and the host rock. While most researches have traditionally focused on the behaviour of the buffer and the host rock separately, little attention has been paid to the role and influence of technological voids and interfaces between materials. However, several laboratory experiments have put into evidence the influence of technological voids on the final swelling pressure developed by a bentonite buffer and the role of interfaces on water flow and gas migration. Still, the existence of technological voids is generally neglected in numerical modelling and perfect contact is assumed between the different materials. This strong hypothesis assumes continuity of both mechanical displacements and pore pressures between materials, which is not true, especially during the first years of the disposal life. Therefore the behaviour of interfaces should be considered and special numerical tools should be developed.

In this paper, the hydromechanical behaviour of a bentonite buffer submitted to hydration under in situ conditions is studied numerically using the finite element code Lagamine, developed at the University of Liege. The problem studied is directly related to the set of experiments PGZ2 developed in Andra's underground research laboratory where different types of bentonite are tested. The objective of those experiments is to characterize the water saturation of bentonite seals firstly under natural conditions and secondly in presence of gas.

More precisely, the test modelled consists in the excavation of a small-diameter gallery (diameter = 101.3 mm) within the Callovo-Oxfordian claystone (France). During this stage, pore water pressure at the wall of the borehole progressively decreases due to gallery drainage. Then, a block of compacted bentonite with a diameter of 94.0 mm is placed in the gallery and hydration from the host rock is allowed. The difference in diameters between the gallery and the bentonite plug yields some technological voids concentrated above the plug. Indeed, due to gravity effects, contact between the plug and host rock initially occurs at the bottom of the gallery. The existence of this technological void rock is explicitly taken into account and modelled using an interface finite element. This interface finite element is able to reproduce the behaviour of technological voids before contact between materials, as well as the hydromechanical behaviour of interfaces when contact occurs. The hydromechanical behaviour of the buffer is modelled using the so-called Barcelona Basic Model, coupled with a two-phase flow law accounting for the double-structure character of bentonite-based materials. In particular, the evolution of permeability with macroporosity is considered. In addition, a double-structure water retention curve has been developed to model the water retention properties of expansive bentonite under different conditions ranging from constant volume to free-swelling conditions.

Numerical results of the problem show that the bentonite plug first exhibits swelling under almost free-swelling conditions. During this stage, technological voids are progressively filled by bentonite which effective density decreases. Furthermore, since contact between the host rock and the bentonite buffer initially occurs over a limited surface area, the hydration kinetics of the buffer appears to be slower than in the absence of gaps between the materials, when perfect contact between the materials is assumed.

Contact between the bentonite buffer and the host rock is progressively reached, from bottom to top. At that moment, the swelling pressure starts to develop against the gallery wall. The final swelling pressure reached after full saturation of the engineered barrier appears to be smaller than the one computed in the absence of technological voids between the buffer and the host rock. Indeed, the swelling pressure of bentonite is directly associated with its effective density. In addition the time required to reach full saturation appears to be considerably higher when technological voids are considered.

The role of gas and liquid intrinsic permeability evolutions on resaturation and geomechanical behaviour of heated bentonite

Jonny Rutqvist, Victor Vilarrasa, Jens Birkholzer

Lawrence Berkeley National Laboratory, Berkeley, CA 947 20, U.S.A., Jrutqvist@lbl.gov

Numerical modelling of coupled thermal-hydro-mechanical (THM) processes and resaturation of bentonite-based buffer material is usually conducted using Phillip and de Vries' approach for heat and moisture flow in soils, assuming infinitely high gas mobility, whereas the liquid mobility changes as a result of relative permeability effects. Material parameters such as diffusion coefficients, retentions curves, intrinsic and liquid relative permeability are usually determined by model calibration against a suite of laboratory experiments. Because the Phillip and de Vries' approach has been successfully applied to reproduce experimental results, it is generally assumed that it provides an adequate approximation of the full multiphase coupled THM processes.

In this study we use multiphase flow coupled THM modelling to investigate the role of gas and liquid intrinsic and relatively permeability evolutions on buffer resaturation and geomechanical behaviour. We conduct numerical modelling at several scale: (1) laboratory column experiments on various types of bentonite samples, (2) in situ heater experiments at Mont Terri, Switzerland and Horonobe Japan, and (3) a generic repository to evaluate long-term performance implications. Multiphase flow modelling results show that the intrinsic gas permeability must be several orders of magnitude higher than the intrinsic permeability for liquid flow, in order to model the typical saturation evolution observed in a bentonite buffer surrounding a heat source, including the thermally driven drying in the hot inner parts. Otherwise, the gas pressure will increase and this in turn will suppress vapour diffusion along the thermal gradient. As a result, drying in the inner parts of the buffer would be prevented. This lack of drying strongly affects the saturation evolution in relatively short-term laboratory and in situ heater experiments, whereas the effect may not be as significant in the longer term. However, regarding long-term behavior, we found that the evolution of intrinsic permeability for liquid flow significantly impacts the time to full resaturation of the buffer. In particular, we show the importance of considering dual-structure behaviour of the bentonite, including the evolution of micro- and macro-structural changes, and the evolution of macro-porosity that is the connected porosity accessible to liquid flow. Considering the delay of buffer resaturation that has been observed in large-scale multiyear experiments and was linked to dual-structure behaviour, we found that such phenomena could delay the time to full resaturation in a repository setting from tens of years to thousands of years. However, despite such a delay, our model results show that the buffer would still be functioning as a barrier since sufficient swelling can develop even when the buffer is not fully saturated.

Nevertheless, it is important to consider gas and liquid permeability and their changes with mechanical deformations, both when calibrating THM properties from laboratory experiments and when applying the models to in situ experiments and for predicting of long-term repository performance.

Neutron imaging study of heavy water transport across a cement-clay interface

A. Shafizadeh[1], T. Gimmi[1,3], L. Van Loon[1], S. V. Churakov[1], A. P. Kaestner[2], E. Lehmann[2], and U. Maeder[3]

[1]Laboratory for Waste Management, Paul Scherrer Institut, Villigen, Switzerland
[2]Neutron Imaging and Activation Group, Paul Scherrer Institut, Villigen, Switzerland
[3]Rock-Water Interaction, Institute of Geological Sciences, University of Bern, Bern, Switzerland

Cement and concrete materials are in direct contact with clays in most designs of geological repositories for nuclear waste. The geochemical contrast between clay and cement pore waters will promote geochemical reactions that alter pore structure of the cement-clay interface. This alteration in the long term can lead to modifications of local transport parameters and influence some processes considered in repository's performance assessment.

We set up laboratory experiments with small cement-clay interface samples. The laboratory experiments aim at simultaneous monitoring of the mineralogical (e.g. dissolution/precipitation) and structural evolution (e.g. porosity changes) expected to occur at the cement-clay interface. Neutron imaging and through diffusion experiments are the main experimental techniques used to characterize any changes in transport parameters. Mineralogical changes will be investigated later by X-ray diffraction, X-ray fluorescence and SEM/FIB techniques. Here we only report the results of diffusion experiments.

Several experimental cells have been built to contain an interface consisting of a small clay plug (Na-Montmorillonite, around 40 percent porosity, 5 mm diameter and 5 mm length) and a small hardened cement plug (OPC, around 60 percent porosity) of the same size. The cell design allows investigating the porosity (i.e., water content) evolution in the alteration zone near the interface by neutron radiography, a method which is highly sensitivity to the water content of a sample. Simultaneously, it allows performing through-diffusion experiments and thus investigating the spatial dependency of transport parameters (diffusion coefficients, accessible porosities) across the interface.

Advancement of a D_2O front, resolved in time and space, across an aged interface sample (273 days old) and two fresh ones (1 day old) was measured using cold neutrons at ICON facility in SINQ, PSI. Heavy water (D_2O) was introduced to diffuse into the normal pore water (H_2O) present in the cement and clay pore space. The difference in neutron scattering properties of these two types of water makes it possible to observe the spatially resolved dynamics of the D_2O diffusion. Obtained images were geometrically aligned and black and white spots due to γ- radiation or pixel failures were filtered (gamma filter). The images were corrected then for dark current (image with closed shutter), for spatial heterogeneity of the beam and the detector (open beam correction), and for average beam intensity (dose correction with internal standard). Finally, the corrected images obtained at different times were normalised with a reference image to obtain the transmission images.

Diffusion through the fresh interface samples occurred as expected from the original diffusion parameters of these materials. In contrast, the D_2O front merely stopped at the interface of the aged sample (Figure 1). This may be the result of mineralogical changes at the interface, for instance, a porosity reduction by mineral precipitation known as clogging.

Imaging the interface on these samples will continue for six more months before cutting the sample to prepare a cross section for more detailed investigation of the mineralogical changes. Combined results from these characterisation techniques together with neutron imaging and through diffusion experiments will provide adequate information to derive the relation between porosity, local and macroscopic diffusion parameter changes that are required for reactive transport simulations.

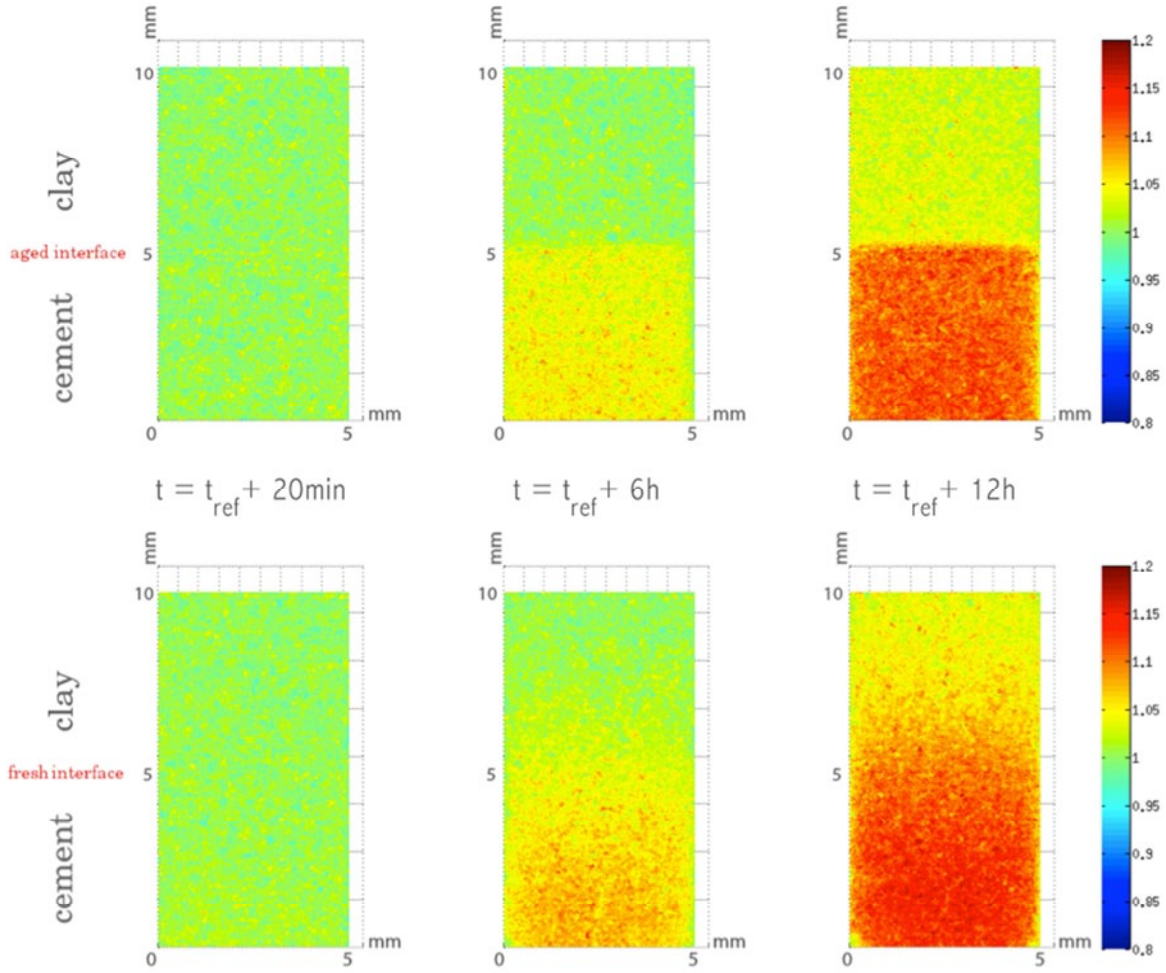


Figure 1: Selected transmission image time series of D_2O advancement (normalised to t_{ref}) across an aged interface (top row) and a fresh one (bottom row) measured using a neutron beam. Higher values (in red) indicate higher D_2O content. The D_2O was introduced to the cement part of the sample (bottom)

Nature of C-(A)-S-H phases formed from the interaction between concrete and bentonite

Raúl Fernández, **Ana Isabel Ruiz and Jaime Cuevas**

Department of Geology and Geochemistry, Faculty of Sciences, Autonomous University of Madrid, 28049, Madrid, Spain.

Concrete and compacted bentonite are considered as engineered barriers for the deep geological disposal of spent fuel and high-level radioactive waste in argillaceous rock. The mineralogical interactions and geochemical processes of these two materials have been studied by means of laboratory experiments in transport cells performed under the European PEBS project (long-term Performance of Engineered Barrier System). The diffusive transport of solutes across the concrete/bentonite interface leads to sharp gradients in pH that enhances the dissolution of montmorillonite and accessory minerals in bentonite and precipitation of carbonates, hydroxides and C-(A)-S-H phases at the interface, decreasing the porosity and modifying the initial geochemical properties of the system.

The transport experiments consisted in a cylindrical 30 mm length upper concrete piece in contact with a 70 mm length compacted FEBEX bentonite block at the bottom, inserted in a cylindrical 70 mm inner diameter Teflon cell. The cell was hydrated with a saline solution from the concrete side and heated at a constant temperature of 100 ºC from the bottom side. HB4 and HB5 experiments were dismantled after 4.7 and 6.5 years of operation and the geochemical and mineralogical alteration was studied in different sections all across the columns. The present investigation is focused on the study of the nature of the new-formed C-(A)-S-H phases at the concrete/bentonite interfaces.

The examination of the C-(A)-S-H is not easy because they are observed covering the surface of clay aggregates and cannot be isolated. Determination of identity, composition and morphology of C-(A)-S-H was performed by XRD and SEM-EDX analyses of samples at the concrete/bentonite interface. Carbonates (calcite and aragonite), ettringite and gypsum were identified along with C-(A)-S-H phases with different fibrous morphologies and Ca/Si ratios. Substitution of Ca for Mg and Na, and Si for Al, S and Fe in C-S-H structures was observed offering a quite variable composition. A statistic calculation based on frequency indicated that the most repeated Ca/Si ratio lie between 0.5 and 0.6, decreasing the frequency with the increasing Ca/Si ratio.

In order to produce less variable C-S-H or C-A-S-H phases under more specific conditions and favour the interpretation of the experimental data, additional experiments were performed using portlandite as a simplified source of Ca and hydroxides from concrete degradation. Eight hydrothermal batch experiments were performed in closed reactor at 60 and 120 ºC, using the same FEBEX bentonite or a extracted < 2 μm size fraction of this bentonite, which corresponds to almost 100% montmorillonite. Two montmorillonite/portlandite molar ratios were considered: 2:1 and 3:1, and the experiments were run for a reaction time close to 2 months. Manipulation of samples was performed in a globe chamber, free of atmospheric water and CO_2, in order to inhibit the carbonation of samples.

Precipitation of C-A-S-H was produced in the batch experiments with limited substitution of Al for Si and negligible substitution of Mg and Na for Ca. Carbonates, ettringite or other secondary phases were not produced. The morphology and composition of the formed C-A-S-H phases depends on the reaction conditions. Acicular and fibrous morphologies with certain laminar character was observed by SEM and EDX analyses showed that lower Ca/Si and higher Al/Si ratios were achieved with the increase in temperature and lack of accessory minerals. It was clearly distinguished by XRD the formation of orthorhombic 11Å-tobermorite in experiments performed at 120 ºC and a more disordered monoclinic tobermorite at 60 ºC.

Interestingly, a broad reflection at 13.2-13.3Å was observed at 60 and 120 ºC, either with bentonite or its < 2 μm size fraction. This reflection, which is not characteristic of a Ca-montmorillonite (typically identified at 15Å) neither a 11Å-tobermorite, could suggest an intercalation or association at the structural scale of tobermorite and montmorillonite. These reflections were also observed in samples taken from the interface from the transport experiments.

A compositional representation Al/Ca vs Si/Ca (Figure 1) obtained by EDX analyses performed on C-(A)-S-H phases found in both types of experiments is useful to discriminate the trends in composition that will be dominated from portlandite dissolution in concrete and its interaction with bentonite (and montmorillonite). A quite linear increasing trend is observed for the analyses performed in batch experiments, and it is confirmed, at least at low Si/Ca ratios in the transport. These data support the existence of the association tobermorite-like/montmorillonite phases (Si/Ca >1.5), which has to be further confirmed. All other spots may not correspond strictly to C-(A)-S-H.

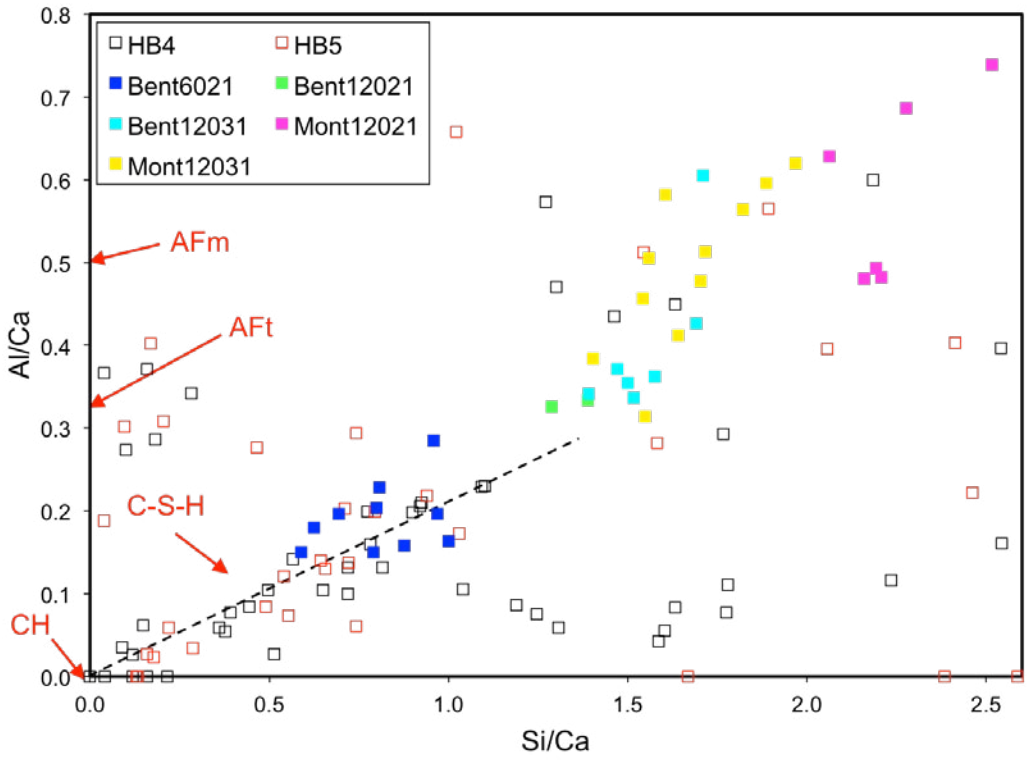


Figure 1: Composition plots (Al/Ca versus Si/Ca) for individual EDX analyses of C-(A)-S-H in transport experiments (HB4 and HB5) and batch experiments. Notations: Bent and Mont for bentonite and < 2 μm size fraction (montmorillonite), respectively; 60 and 120 for temperatures of reaction; 21 and 31 for the 2:1 and 3:1 montmorillonite/portlandite ratio; CH = portlandite; AFt = ettringite; AFm = hydrated calcium aluminate.

Acknowledgements

The research leading to these results has received funding form the European Atomic Energy Community's Seventh Framework Programme (FP7/2007-2011) under grant agreement 249681.

Concrete-clay interaction: give-and-take without a loser?

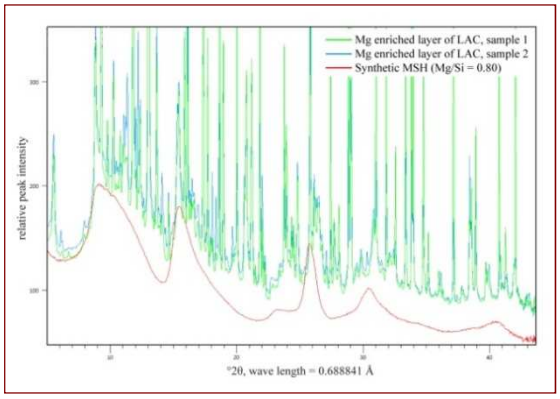
Andreas Jenni[1], **Urs Mäder**[1], **Erich Wieland**[2], **Catherine Lerouge**[3], **Stéphane Gaboreau**[3], Marika Vespa[4], **Veerle Cloet**[5]

[1] RWI, Institute of Geological Sciences, University of Bern, CH-3012 Bern, Switzerland (andreas.jenni@geo.unibe.ch)
[2] Laboratory for Waste Management, Paul Scherrer Institute, CH-5232 Villigen PSI, Switzerland
[3] BRGM, F-45060 Orléans Cedex 2, France
[4] Karlsruhe Institute of Technology, Institute for Nuclear Waste Disposal, D-76021 Karlsruhe, Germany
[5] Nagra, CH-5430 Wettingen, Switzerland

Deep geological waste repositories rely on engineered structural elements regardless of host rocks considered. The use of cementitious materials is obvious for this purpose, although the material contrast between cement and any host rock leads to chemical and mineralogical interactions. These are mainly driven by chemical gradients in pore water, and might influence host rock properties like permeability, swelling pressure, or specific retention in case of clay rocks.
Extensive investigations on concrete-Opalinus Clay (OPA) interfaces recovered after 2.2 y of interaction from the Cement-Clay Interaction (CI) experiment at the Mont Terri Underground Laboratory (St. Ursanne, Switzerland) revealed significant alteration in the different cements within a couple of millimetres, but minor changes in OPA [1].
Owing to the especially developed drilling technique for coring undisturbed interfaces [1], a larger number of high-quality samples could be retrieved from the same interfaces after 4.85 y of interaction, allowing for more extensive investigations. These include

- standard optical and scanning electron microscopy with energy dispersive spectroscopy, resulting in element maps and semi-quantitative chemical data (SEM EDX)
- synchrotron micro x-ray diffraction spectroscopy (μXRD), resulting in spatially resolved phase information [2]
- synchrotron x-ray absorption near edge structure (μXANES), resulting in spatially resolved phase and elemental coordination information
- μRaman and infrared spectroscopy, both supporting spatially resolved phase identification and phase structure information
- autoradiography, resulting in spatially resolved porosity information [3]
- determination of cation exchange occupancy and aqueous leaching of the clay [3]

The thin interaction layers in both cement and OPA, the multi-mineral concrete aggregates that disturb investigations on the cement in between, and the presence of poorly crystalline and/or solid-solution phases (partly little investigated so far, e.g. [4]), necessitate this comprehensive suite of spatially resolved expensive techniques.
The results presented here come from three concrete-OPA interfaces, whose concretes contain 1) Portland cement (OPC), 2) ESDRED cement especially designed for repository applications (40% of cement substituted with silica fume), and 3) low alkali cement (LAC, containing slag and nanosilica). In general, the chemical zonation and the thicknesses of the zones did not change from 2.2 y to 4.85 y of interaction, but strongly depend on the type of cement. The striking Mg enrichment close to OPA occurs only in the low-pH cements LAC and ESDRED, where the OPA is also enriched close to the interface. Only a fraction of this Mg enrichment can be attributed to the observed increase of Mg on the clay exchanger (at the expense of Ca and Na), but μXRD indicates the presence of a poorly crystalline magnesium silicate hydrate (MSH, [4]). The same phase is present in the Mg enriched cement, as shown by μXRD (Figure) and μXANES, both spectra are compared with measurements on pure synthesised MSH [5]. Structure and thermodynamic property investigations are ongoing, first results indicate similarities to talc [5], supported by [6]. Further characteristics of the interaction zone are a decalcification in all three cements close to OPA (found in many studies, e.g. [7, 8]), and a sulphur depletion, followed by a layer enriched in S further away. Thicknesses of observed carbonation layers mainly depend on the water/binder ratio of the cement. Decalcification decreases, carbonation increases porosity in the cements.



Synchrotron XRD spectrum of synthetic MSH [5], compared with spectra of Mg enriched zone of LAC adjacent to OPA. The latter show peaks from cement and aggregate phases, but the underlying background matches the spectrum of synthetic MSH. This agrees with [4, 6].

Data from 2.2 y and 4.85 y samples both suggest diffusion of CO_2/HCO_3^-, SO_4^{2-}, and Mg species, from OPA into cement. pH decrease in the cement next to the interface leads to instability of sulphur-bearing cement hydrates, the S in solution diffuses towards higher pH (away from the interface), where ettringite can form and incorporate S. In turn, the cement releases Ca, which is mainly found in short calcite veins extending into the OPA.
Ongoing modelling studies of several groups deal with the data presented here [9, 10]. The presence of swelling clays might require a multi-porosity reactive transport code to account for the interlayer region explicitly [11, 12]. First results from CrunchFlowMC calculations support the formation of a Mg hydrate, and indicate a rapid formation of interaction layers followed by an early decrease of intergranular porosity. Lab experiments investigate the interaction of clay with cementitious pore fluids corresponding with the cements used here (Dolder et al., this conference). During the duration of the CI experiment of at least 20 y, further sampling is foreseen resulting in more data, which will better define timescales of mechanisms, and provide a sounder basis for more reliable model predictions.

Acknowledgement
The CI Project is funded by ANDRA, CRIEPI, IRSN, Nagra, Obayashi, and SCK•CEN. The on-site team operating the Mont Terri facility (Swisstopo) is acknowledged for field support.

References

[1] Jenni, A., et al., *In situ interaction between different concretes and Opalinus Clay*. Phys. Chem. Earth, Parts A/B/C, 2014. **70–71**: p. 71-83.
[2] Dähn, R., et al., *X-ray micro-diffraction studies of heterogeneous interfaces between cementitious materials and geological formations*. Phys. Chem. Earth, Parts A/B/C, 2014. **70–71**: p. 96-103.
[3] Lerouge, C., et al., *CI Experiment Phase 18: Geochemical characterization of CI core samples*. Mont Terri Project, 2013. TN 2013-79.
[4] Brew, D.R.M. and F.P. Glasser, *Synthesis and characterisation of magnesium silicate hydrate gels*. Cem. Concr. Res., 2005. **35**(1): p. 85-98.
[5] Lothenbach, B., et al. *Calcium and magnesium silicate hydrates*. *NUWCEM 2nd International Symposium on Cement-Based Materials for Nuclear Wastes*. 2014. Avignon, France.
[6] Mitsuda, T. and H. Taguchi, *Formation of magnesium silicate hydrate and its crystallization to talc*. Cem. Concr. Res., 1977. **7**(3): p. 223-230.
[7] Dauzères, A., et al., *Physico-chemical investigation of clayey/cement-based materials interaction in the context of geological waste disposal: Experimental approach and results*. Cem. Concr. Res., 2010. **40**(8): p. 1327-1340.
[8] Gaboreau, S., et al., *In-situ interaction of cement paste and shotcrete with claystones in a deep disposal context*. Am. J. Sci., 2012. **312**(3): p. 314-356.
[9] Berner, U., D.A. Kulik, and G. Kosakowski, *Geochemical impact of a low-pH cement liner on the near field of a repository for spent fuel and high-level radioactive waste*. Phys. Chem. Earth, 2013. **64**: p. 46-56.
[10] Kosakowski, G. and U. Berner, *The evolution of clay rock/cement interfaces in a cementitious repository for low- and intermediate level radioactive waste*. Phys. Chem. Earth, 2013. **64**: p. 65-86.
[11] Alt-Epping, P., et al., *Benchmark reactive transport simulations of a column experiment in compacted bentonite with multi-species diffusion and explicit treatment of electrostatic effects*. submitted.
[12] Appelo, J.A.C. and P. Wersin, *Multicomponent diffusion modeling in clay systems with application to the diffusion of tritium, iodide, and sodium in opalinus clay*. Environ Sci Technol, 2007. **41**(14): p. 5002-5007.

The challenge of analyzing micro-diffraction patterns: From argillaceous rock formations to cement-clay interfaces

Rainer Dähn[1], János Osán[2], Phil Pattison[3], and Erich Wieland[1]

[1]Laboratory for Waste Management, Paul Scherrer Institut, 5232 Villigen Switzerland
[2]Centre for Energy Research, Hungarian Academy of Sciences, 1525 Budapest, Hungary
[3]Laboratoire de Cristallographie, École Polytechnique Fédérale de Lausanne, 1015 Lausanne, Switzerland

Synchrotron-based micro X-ray fluorescence (microXRF), micro X-ray absorption spectroscopy (microXAS) and micro X-ray diffraction (microXRD) are powerful tools for spatially resolved micro-scale investigations of retention processes in heterogeneous systems. The simultaneous registration of the diffraction signal using an area detector can yield a wealth of crystallographic information on mineral assemblages, which is complementary to that of microXRF/XAS. The interpretation of the diffraction patterns produced by "real" samples such as polymineralic aggregates, soil nodules or cements is still a challenging task since they represent an integral signal in which many crystal grains from different structures can contribute. The challenge of analyzing these complex diffraction patterns will be highlighted exemplarily on the study of the metal uptake by argillaceous rock samples and cement-clay interfaces.

Argillaceous rocks and cement-based materials play an important role in multi-barrier concepts developed worldwide for the safe disposal of radioactive wastes in deep geological repositories. An approximately 180 million year old marine clay-rich sediment (Opalinus Clay, OPA) was identified and selected as the first-priority host-rock for the disposal of high-level radioactive waste in Switzerland. Both materials, i.e. OPA and cement used for construction of the repository, are heterogeneous mineral assemblages with discrete nano- to micro-scale particles. Hardened cement paste (HCP) consists of mainly calcium (aluminium) silicate hydrates, portlandite, calcium aluminates, and some minor phases such as calcite and hydrotalcite, in hyper-alkaline environment (pH > 11), while OPA is a mineral assemblage consisting mainly of illite, illite-smectite mixed layers, kaolinite, quartz and calcite in near neutral conditions.

The identification of mineral phases in argillaceous rock samples with microXRD can yield important information on the mineral phases responsible for heavy metal uptake [e.g. 1, 2]. The data analysis is normally straightforward, since the XRD patterns are mostly powder-like and well documented in databases. For example the 060 reflection can be used to distinguish between aluminous (1.501 Å) and ferric smectites (1.52 Å) [3, 4]. In a study on the uptake of Ni by a Hungarian argillaceous rock formation (Boda Claystone Formation, BCF) it was possible to unambiguously demonstrate with microXRD that Ni enrichment correlate with the spatial distribution of illite and montmorillonite clay minerals [2].

The diffraction patterns produced with micro-scale resolution by cement samples are usually complex images, in which many crystal grains from different structures may contribute. The quality of the diffraction data ranges from almost perfect individual single crystals to microfine powders or even non-crystalline materials depending on crystal size. In a conventional single crystal diffraction experiment, usually only one (or, predominantly only one) crystal will be probed. The unknown parameters are the orientation of the crystal relative to the coordinate frame of the diffractometer, and possibly also the crystal space group itself (i.e. when solving a new structure). In the case of micro-diffraction on a polycrystalline sample, however, it is more likely to have several crystallites diffracting in the beam on a single image. In some cases, the crystallites probed are so small compared to the size of the X-ray beam that only a powder pattern can be registered. Further, it should be noted that many hundreds of diffraction images can be produced using synchrotron-based microXRD as the beam is scanned over the sample, and each image may have contributions from many crystallites, in different (and unknown) orientations and be made up from a mixture of various mineral species.

At present, the standard method to overcome the difficulties in analyzing complex diffraction pattern is to reduce the wealth of crystallographic information by performing an angular averaging of the

diffraction image into a 1-D pattern. This procedure effectively reduces the diffraction image made up of individual spots to a spherically averaged powder pattern. This obviously represents a serious loss of information contained in the original images, but it does allow a comparison to be made with data in standard crystallographic databases for powder patterns, which contain a series of d-spacings for a given space group and their respective intensities as recorded in conventional powder diffraction. It is then possible to look for a high number of "hits" for those d-spacings expected on the basis of some prior knowledge of the sample and hence the likely crystal structures expected for this type of sample. Therefore, in order to extract the maximum information an approach has been developed in which microXRD was applied to thin sections which were rotated in the X-ray beam [5]. This approach was applied to cement-clay interfaces samples, both from a natural analogue (Maqarin, Jordan) and samples from a long-term Cement/OPA-Interaction experiment ("CI-project") in the Mont Terri Rock Laboratory (St-Ursanne, Switzerland). Obviously the approach to search for references in databases must fail if an unknown newly formed phase has formed. Furthermore, despite the fact that the principal structures of most rock-forming minerals are well known, many of their polymorphs are not known because these polymorphs may only form in micron- and submicron-sized. These limitations can be overcome by analysing the single-crystal 2-D diffraction data obtained with a micro-focus X-ray beam. For example high resolution X-ray diffraction data were collected on selected tobermorite crystals found in the thin section of the Maqarin sample using a beam size of 1x1 μm^2. The refined unit cell was found to correspond to 11 Å tobermorite [6].

This newly developed microXRD approach on rotating thin sections with micrometer precision can give important insights on the formation of mineral phases in geological settings. Finally, the results of this state-of-the-art study can be an essential step in further constraining and, consequently, improving reactive transport models, which are currently being used for long-term predictions of the evolution of the interfaces between cement and OPA and the release of radionuclides from a deep geological radioactive waste repository into the environment.

1. Vespa, M., A. Manceau and M. Lanson (2010). "Natural attenuation of zinc pollution in smelter-affected soil." Environmental Science & Technology 44(20): 7814-7820.

2. Osán, J., A. Kéri, D. Breitner, M. Fábián, R. Dähn, R. Simon and S. Török (2014). "Microscale analysis of metal uptake by argillaceous rocks using positive matrix factorization of microscopic X-ray fluorescence elemental maps." Spectrochimica Acta Part B: Atomic Spectroscopy 91: 12-23.

3. Brindley, G. W. and G. Brown (1980). Crystal structures of clay minerals and their X-ray identification. London, Mineralogical Society.

4. Srodon, J., V. A. Drits, D. K. McCarty, J. C. C. Hsieh and D. D. Eberl (2001). "Quantitative X-ray diffraction analysis of clay-bearing rocks from random preparations." Clays and Clay Minerals 49: 514-528.

5. Dähn, R., D. Popov, P. Schaub, P. Pattison, D. Grolimund, U. Mäder, A. Jenni and E. Wieland (2014). "X-ray micro-diffraction studies of heterogeneous interfaces between cementitious materials and geological formations." Physics and Chemistry of the Earth 70-71: 96-103.

6. Merlino, S., E. Bonaccorsi and T. Armbruster (2001). "The real structure of tobermorite 11Å: normal and anomalous forms, OD character and polytypic modifications" European Journal of Mineralogy 13(3): 577-590.

Acknowledgement
The research leading to the results of heavy metal uptake by argillaceous rocks has received funding from the Swiss-Hungarian Cooperation Programme through Project n° SH/7/2/11. The courtesy of the Public Limited Company for Radioactive Waste Management (PURAM, Hungary) for providing the BCF samples for analysis is also appreciated. The sample preparation and SEM analysis of the cement-clay interfaces performed by Urs Mäder and Andreas Jenni from the University of Bern is kindly acknowledged. The corresponding diffraction measurements and analyses were performed by Dmitry Popov and Philippe Schaub, who are grateful for a grant of the Paul Scherrer Institut (PSI), and of the PSI department ''Nuclear Energy and Safety'', respectively. The beamline scientists Rolf Simon (FLUO, ANKA, Germany) and Daniel Grolimund (MicroXAS, SLS, Switzerland) are gratefully acknowledged for their help at the beamline. Partial financial support was provided by the National Cooperative for the Disposal of Radioactive Waste (Nagra).

Physical Modelling of the water-and-gas flow through an Excavation Damaged Zone in the frame of a single porosity model

Luc-Vincent Bénet [1], Étienne Blaud [1], Jacques Wendling [2]

[1] SOCOTEC SA / Projets Industriels / AME, 1 Avenue du Parc 78640 Montigny-le-Bretonneux, France (luc-vincent.benet@socotec.com)
[2] Andra, 92298 Châtenay-Malabry Cedex, France (jacques.wendling@andra.fr)

Introduction

The Excavation Damaged Zone (EDZ) can be regarded as a double-porosity porous media consisting of blocks of argillite crossed by cracks generated by shear stresses or traction stresses. However, most of the hydraulic-gas simulations that Andra had undertaken are based on a single-porosity model of the EDZ. The aim of this study is to make the current simple-porosity hydraulic model of the EDZ more representative of the real double-porosity porous media of the EDZ as assessed by the *in situ* measurements performed Bure URL.

Methodological approach

The new simple-porosity model of the EDZ has been developed in several stages: first of all a review of data describing the EDZ has been achieved in order to build a double-porosity model representative of the actual geometrical and hydraulical understanding of the EDZ. Then, this numerical model has been used to perform several sets of numerical simulations to calculate the response to different hydraulic loads: transversal or longitudinal flow of water and gas flow over a large range of capillary pressure (i.e. level of saturation). Finally, the physical properties of a single-porosity model have been calibrated to reproduce the hydraulic responses of the double-porosity model

Geometrical and physical modeling

The simple-porosity model describes the EDZ as composed of two cylindrical zones in which the hydraulic properties (gas-and-water permeabilities, porosity, and capillary parameters) are uniform. The inner zone represents the more hydraulically conductive part composed of highly connected cracks which have been mainly generated by traction stress. The outer zone represents the part composed of weakly connected micro-cracks which have been mainly generated by shear stress.

The geometry of the double-porosity model is based on the geomechanical conceptual model build from the *in situ* measurements. In the double-porosity model, the spacing, the orientation, the extension and the thickness of cracks is based of mean values of measurements. The extensions of the traction cracks zone and the shear cracks zone are both oblong. The crack hydraulic thickness is defined as uniform in each part of the EDZ. This hydraulic thickness has been calibrated by simulation of longitudinal water flow in saturated media to be consistent with the *in situ* measurements of the water permeability. The capillary properties of cracks have been established by using the hydraulic diameter to define the surface tension between gas and water.

Main results

The physical parameters of the single-porosity model of the EDZ have been modified to take into account the hydraulic-gas behaviour of the double-porosity model that has been meant to be geometrically and hydraulically representative of the real EDZ. The new single-porosity model differs, in particular, on four points :

- The anisotropy of the permeability, particularly for the inner EDZ zone, because the shear stress are mainly oriented longitudinally and weakly connected transversally ;
- The drastic reduction of potential gas content, because the overall section area of the cracks is very low compared to the section area of the EDZ ;
- The high conductivity to gas flow in low unsaturated EDZ, because of the relatively high thickness of cracks compared to the mean porous diameter of the argillite;
- The anisotropy of the water relative conductivity of the outer EDZ zone.

Stress coupling in Callovo-Oxfordian claystone during gas and water flow

J.F. Harrington[1], R.J. Cuss[1], D.J. Noy[1], C.C. Graham[1], , A.E. Milodowski[1]
M. Hall[2] & J. Talandier[3]

[1]British Geological Survey, Nottingham, NG2 5AN, UK; [2]University of Nottingham, NG7 2RD, UK; [3]Andra, 1-7, rue Jean Monnet, 92298 Chatenay-Malabry, France,.

To predict the evolution of a Geological Disposal Facility (GDF), it is first necessary to understand the interaction between a number of key features and processes and the impact they may have on the long-term performance of specific system components. Central to these issues is an understanding of the mechanisms and processes governing the movement of repository gases and the role of groundwater as a medium for the transportation of contaminants and resaturation and self-sealing of system components. Recent studies on clay-based systems have shown that the advective movement of gas is accompanied by the formation of pressure-induced pathways leading to a dilatant response within the host material. The localised nature of these features results in little if any desaturation of the clay. However, the increase in pore volume during pathway formation and propagation creates a spatial constraint, and as such, an interaction with the local stress field. In contrast, significant desiccation of the host rock and key engineered components (backfills, gallery seals, and borehole plugs) will occur during construction and operation of the GDF. This combined with accompanying ground movements caused by destressing and convergence of the rock mass, result in the development of an engineered damaged zone (EDZ), the evolution of which will also be strongly influenced by the prevailing stress field and availability of water to aide self-sealing.

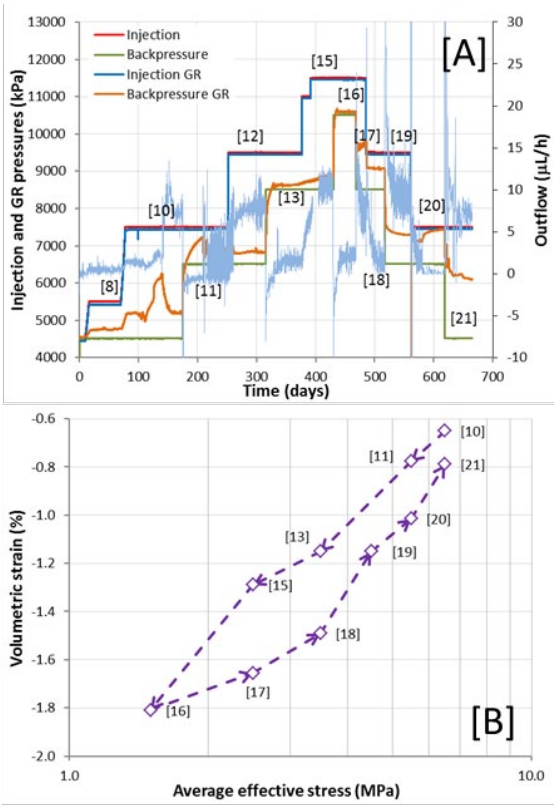


Figure 1 [A] *Gas flow rates at the injection and backpressure filters during gas injection test COx-3. [B] Cross-plot of volumetric strain versus average effective stress for COx-3 data. The negative strain response is symptomatic of an increase in sample volume.*

Understanding the couple between stress field and flow is therefore of paramount importance in describing the long-term behaviour of such repository systems. To explore these issues a number of laboratory based tests on intact and fractured samples of Callovo-Oxfordian claystone (COx) were undertaken. These employed a range of experimental geometries from conventional isotropic permeameters to custom-designed heavy duty shear rigs.

The coupling between volume change and gas flow for intact host rock was explored in a number of tests, in particular COx-3, an intact isotropically stressed sample which examined the relationship between steady state flow rate, gas and porewater pressure gradient and its coupling to volumetric strain (the latter derived from changes in confining system volume). In this test, consecutive increments in gas pressure gradient of 3 MPa and 1 MPa were systematically applied to the sample by increasing either injection or backpressure values (Figure 1A). This was followed by decrements in pressure remapping the original 'drainage' curve. Analysis of the data, Figure 1B, clearly shows that volume change is an integral component in the development of flow (and therefore gas permeability)

and is clearly coupled to the effective stress state. The data suggests that most if not all of the strain associated with gas flow is recovered (in this example) as the internal gas pressure within the pathways declines. Post-test X-ray CT imaging (Figure 2) alludes to the presence of a small network of microcracks. While the origin of these features remains unclear its seems reasonable to assume they represent pre-existing planes of weakness and therefore potential sites for gas migration.

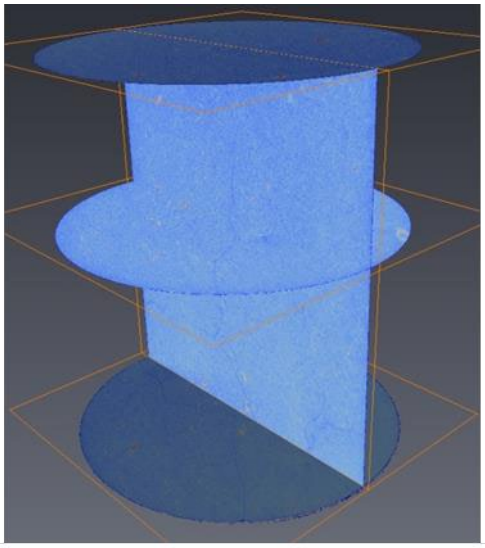


Figure 2 X-ray CT image of core Cox-3 showing a localised network of cracks.

To examine self-sealing processes within the EDZ a sample of COx containing a natural transverse fracture (Figure 3B) was subject to an unloading/loading confining pressure history. Inspection of the data suggests a subtle, continued reduction in permeability with time which showed little apparent sensitivity to the initial reduction in confining pressure (Figure 3B). However, at an average effective stress of 3.2 MPa, stage [9], permeability began to increase. This continued through stages [10] and [11] reaching a maximum value of 5.3×10^{-20} m^2, and while low, this value remains around one order of magnitude above that expected for intact COx. Under these conditions it seems reasonable to assume that such features may act as focal points for future flow events.

By tracking net flow during this phase of testing, it was possible to construct a soil mechanics plot of void ratio against average effective stress (commonly referred to as an e log P plot), Figure 3[B]. Inspection of the data clearly shows an increase in sample volume as the effective stress decreased in a linear manner. Initially this swelling induced increase in porosity resulted in a small decrease in bulk permeability, which then increased as porosity continued to increase as the confining stress on the fractured sample reduced. As the confining pressure was increased at the end of the unloading cycle, permeability followed an almost identical path to reach a final value of 1.8×10^{-20} m^2.

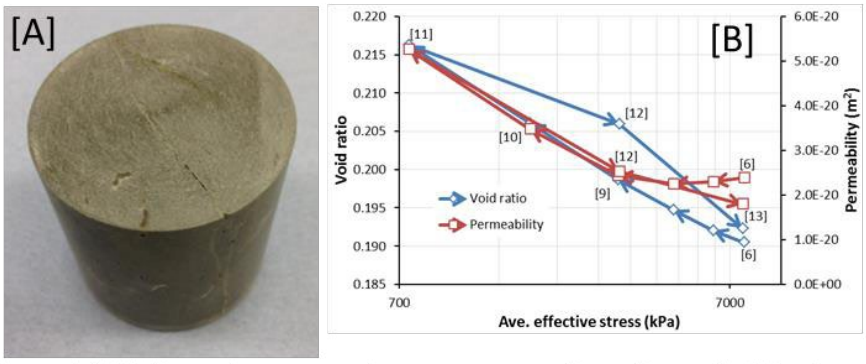


Figure 3 [A] *Photo of transverse fracture running through sample COx-4. [B] Cross-plot of void ratio and permeability versus average effective stress.*

Changes in fracture flow have been investigated using the bespoke Direct Shear Rig (DSR) during tests DSR_COx-1 and DSR_COx-2. The experimental geometry means that pore pressure is delivered directly to the fracture plane and allows transmissivity to be investigated as normal load is changed. During a loading cycle the flow along the fracture was seen to initially decrease from ~ 25 to 12×10^{-14} $m^2.s^{-1}$ as normal load increased from 2 to 2.5 MPa. Following this a linear relationship between fracture transsmivity ($m^2.s^{-1}$) and normal stress (MPa) was noted with the form $-4.3\sigma_N + 23$. During unloading, considerable hysteresis was also observed with flow not recovering during this history.

These results combined with those from tests COx-3 and COx-4 illustrate the importance of stress coupling and its potential impact on flow. For conductive fractures stress history is clearly important and the current stress field is not necessarily the dominant factor governing fluid flow.

Measuring the diffusion coefficient of hydrogen in Boom Clay

E. Jacops [1,2,3], K. Wouters [1], A. Grade [1], N. Maes [1], J. Govaerts [1], E. Weetjens [1]

[1] SCK•CEN, Insitute for Environment, Health and Safety, Boeretang 200, 2400 Mol, Belgium (ejacops@sckcen.be)
[2] KU Leuven, Earth and Environmental Sciences, Celestijnenlaan 200E, 3001 Heverlee, Belgium
[3] RWTH Aachen University, Institute of Geology and Geochemistry of Petroleum and Coal, Lochnerstr. 4-20, 52056 Aachen, Germany

Boom Clay has been studied since 1974 as a potential host formation for the disposal of high-and intermediate level long-lived radioactive waste in Belgium. In such a geological repository, generation of gases by different processes like anaerobic corrosion, microbial activity, radiolysis,… is unavoidable. The generated gases (mainly H_2 from anaerobic corrosion) will dissolve in the ground water and dissipate from the repository by diffusion. If the rate of gas generation is larger than the diffusive flux into Boom Clay, the pore water within the disposal gallery will become oversaturated, a free gas phase will form within the porous space of the engineered barrier system and free gas ingress into the Boom Clay may eventually occur. In order to make a correct evaluation of the balance between gas generation versus gas dissipation, a reliable estimate for gas diffusion coefficient of dissolved hydrogen is essential.

The currently available gas diffusion parameters for hydrogen in Boom Clay were obtained from the MEGAS project (Modelling and Experiments on Gas Migration in Repository Host Rocks) carried out some 20 years ago (Volckaert et al., 1994). Due to experimental problems, only estimations of D_{app} (apparent diffusion coefficient) could be made and re-evaluation of these MEGAS data by Aertsens (2009) lead to estimated D_{app} values varying over a wide range (5×10^{-12} m²/s to 4×10^{-10} m²/s). In order to obtain more accurate calculations on the formation of a free gas phase, an accurate diffusion coefficient for dissolved hydrogen is needed (Weetjens and Sillen, 2006).

In 2008 SCK•CEN (Mol, Belgium) developed a new method to measure the diffusion coefficient of dissolved gases in low-permeability materials with high precision (Jacops et al., 2013). The technique consists of a double through-diffusion test. A saturated Boom Clay test core (diameter 80 mm, length 30 mm) is placed between two reservoirs filled with 500 ml water and 500 ml probe gas at 1 MPa. The gases dissolve in the water (Henry's law) and due to the concentration gradient, the dissolved gases diffuse from the high-concentration compartment through the clay core to the low-concentration compartment. The change in gas composition in the low-concentration compartments is followed by GC. By using a diffusive transport model (based on the 1st and 2nd law of Fick for diffusive transport in porous media), the diffusion coefficient is calculated from the breakthrough curve.

When performing diffusion experiments with H_2 on Boom Clay samples, the results can be affected by the conversion of H_2 into CH_4 by methanogenic micro-organisms as described by Ortiz et al. (2002) and Volckaert et al. (1994). Microbial activity is expected to be low or non-existent within the Boom Clay samples but activity can clearly take place in filters next to the sample and in reservoirs. To avoid microbe-induced experimental artifacts, appropriate sterilization measures are needed in order to obtain an accurate diffusion coefficient for hydrogen in Boom Clay.

Different sterilization protocols were tested. A first protocol used $SnCl_2$ and Triclosan as microbial inhibitor (for 1 experiment). A second protocol used gamma irradiation of the compete set-up with a received dose of ca. 40 kGy (for 2 experiments). A third protocol combined heat sterilization, gamma irradiation, gas sterilization over a filter and the use of an inhibitor (for 3 experiments). Microbial activity was assessed by measurement of ATP (adenosinetriphosphate) in the recovered water.

Sterilization protocols 1 and 2 were not successful: CH_4 was measured in the gas phases in all experiments and microbial analyses of the water recovered from the experiments executed with protocol 2 (γ-irradiation) points to the presence of active micro-organisms. This clearly indicates that

methanogenic micro-organisms were actively converting H_2 into CH_4. The three diffusion experiments with sterilization protocol 3 were successful. No CH_4 was measured in the gas phases and microbial analyses of the waters indicated no microbial activity. The obtained results (D_{eff}: effective diffusion coefficient) are summarized in Table 1.

Table 1: Identification of the samples (taken from the cores from the Mol-1 drilling, a drilling campaign in Mol, north-east Belgium), measured D_{eff} and 95% confidence interval

Sample n°	95b	96b	127b
Depth (m BDT*)	243.96-244.06	244.76-244.87	275.62-275.72
Orientation with respect to bedding planes	⊥	//	//
D_{eff} H_2 (x 10^{-10} m^2/s)	2.64	7.14	5.51
95% confidence interval (x 10^{-10} m^2/s)	2.43-2.86	6.77 – 7.55	5.40 – 5.62

* reference depth is expressed as "m below drilling table" (m BDT). The drilling table was located at 29.73 m T.A.W. (Tweede Algemene Waterpassing).

The obtained values for D_{eff} are in line with values obtained for other gases (Jacops et al., 2013). Also the anisotropy ratio is in line with data obtained for other tracers (I, HTO).

Different attempts to measure the diffusion coefficient of dissolved hydrogen gas (H_2) were made, but despite the use of different types of microbial inhibition/sterilization procedures, recurrent conversion of H_2 into CH_4 by micro-organisms was observed. Only by using a complex sterilization procedure, microbial activity was successfully inhibited. Three successful diffusion experiments were performed leading to reliable diffusion coefficients perpendicular and parallel to the bedding plane with a narrow 95% confidence interval. As the Boom Clay cores are taken from the Putte member which is the most clayey and homogeneous part of the Boom Clay layer and thus the most relevant part of the Boom Clay for a future geological repository, the obtained diffusion coefficients should allow a more accurate assessment of the capacity of Boom Clay for dissipating H_2 by molecular diffusion of the dissolved gas. A good estimate of that capacity is essential to determine for which waste and engineered barrier designs combinations a free, pressurized gas phase may appear in the near field of the disposal galleries.

Acknowledgements
This work is undertaken in close co-operation with, and also with the financial support of ONDRAF/NIRAS, the Belgian Agency for the Management of Radioactive Waste and Enriched Fissile Materials, as part of its programme on the geological disposal of intermediate-level long-lived radioactive waste.

Aertsens, M. (2009) Re-evaluation of the experimental data of the MEGAS experiment on gas migration through Boom Clay. SCK•CEN ER-100, Mol.
Jacops, E., Volckaert, G., Maes, N., Weetjens, E., Govaerts, J., 2013. Determination of gas diffusion coefficients in saturated porous media: He and CH4 diffusion in Boom Clay. Applied Clay Science, 83-84(0): 217-223.
Ortiz, L., Volckaert, G., Mallants, D., 2002. Gas generation and migration in Boom Clay, a potential host rock formation for nuclear waste storage. Engineering Geology, 64: 287-296.
Volckaert, G. et al., 1994. MEGAS Modelling and experiments on gas migration in repository host rocks. Final Report Phase 1. EUR16235, Luxembourg.
Weetjens, E., Sillen, X., 2006. Gas Generation and Migration in the Near Field of a Supercontainer-based Disposal System for Vitrified High-Level Radioactive Waste, 11th International High-level Radioactive Waste Management Conference (IHLRWM), Montpellier.

Volume change behaviour of Boom Clay during gas injection and dissipation experiments

L. González-Blanco[1], *E. Romero*[1], X. Li[2], X. Sillen[3]

[1] Department of Geotechnical Engineering and Geosciences, Universitat Politècnica de Catalunya, Barcelona, Spain. enrique.romero-morales@upc.edu
[2]EIG EURIDICE, Mol, Belgium.
[3]ONDRAF/NIRAS, Brussels, Belgium.

Introduction

An experimental study on Boom Clay –one of the potential deep clay formations in Belgium for the geological disposal of long-living and heat-emitting radioactive waste– has been performed using controlled volume-rate gas injection tests on high-pressure oedometer cells. These gas injection tests intend to analyse the influence of the stress state and the anisotropic flow conditions (flows parallel or orthogonal to bedding), as well as to study the interaction between deformation and gas migration process. Results of selected tests on two sample orientations are presented, paying particular attention to sample deformation on gas injection and dissipation stages. The gas pressurisation process at constant vertical stress acts as an unloading stage, which may induce expansion and degradation (opening of fissures) on the clay and that could have important consequences on gas transport process (González-Blanco et al, 2014).

Equipment and experimental methods

An instrumented high-pressure oedometer cell (50 mm in diameter and 20 mm high) was used, which was specifically designed to apply vertical stresses up to a maximum of 10 MPa, while injecting air at controlled volume rate. Undisturbed Boom Clay cores recovered at a depth of 223 m from the URL at Mol (Belgium) were trimmed at two orientations (flows parallel and orthogonal to bedding). For the air injection tests, the upstream water line at the bottom of the sample was drained and the top recovery system filled with water to better ensure sample saturation and detect sample outflow volumes (air or water) at constant downstream pressure (0.5 MPa). Air injection tests at controlled volume rates (2 and 100 mL/min) and constant vertical stress of 6 MPa were performed on saturated samples. After reaching maximum air pressure (4 MPa), slightly below the air entry value (around 5 MPa), the upstream piston was stopped (shut-in) and air pressure was let to decay at constant air volume. The difference between the vertical stress and maximum air pressure was kept close to the *in situ* vertical effective stress (around 2.3 MPa). After the air tests, samples were unloaded under undrained conditions to prevent further expansion and degradation of the material, and to retain the pore size distribution attained after the air tests. Mercury intrusion porosimetry tests were performed on samples after the air injection tests and on samples that followed equivalent mechanical stress paths without air injection to detect changes in the pore size distributions.

Experimental results and interpretation

Figure 1 presents the evolution of volumetric strain with constitutive stress (vertical stress σ_v minus air pressure at the bottom injection point u_a^{bottom}) along the air injection and dissipation stages of four selected tests at different sample orientations and two volume rates for air injection. Compression strains are positive. The samples at $\sigma_v = 6$ MPa displayed some expansion at the early air injection stage (A to B), which was slightly larger at the slower air injection rate and when bedding planes were not confined by the oedometer condition (bedding planes orthogonal to flow). After shut-in (point B), expansion continued in the samples subjected to fast air injection (B to B') as the air pressure front propagated into the sample, inducing the fluid pressure to increase and the constitutive stress to decrease. This expansion was also affected by air dissolved in pore water during the injection phase and the consequent increase in water compressibility. Again, the expansion was larger in the case of flow orthogonal to bedding planes, where the material was less constrained to expand. This expansion after shut-in was not observed on samples subjected to slow air injection rate, since pore pressure was nearly equilibrated during air injection.

Some elapsed time later after shut-in, the air injection pressure started to decline along the dissipation stage towards point C. This dissipation stage induced the constitutive stress to increase leading to the progressive compression of the material. The two samples with bedding planes orthogonal to flow underwent the largest compressions, which were very similar in magnitude. The sample subjected to slow injection rate with bedding planes parallel to air flow showed a quasi-reversible volume change response along the dissipation stage. The first air outflow detection also depended on the injection rate. In samples tested at fast rate, this outflow was consistently detected during the dissipation stage, whereas in samples tested at slow rate, it occurred during the injection stage. Figure 2 shows the intrinsic (air) permeability using dissipation data plotted against the maximum expansion underwent by the samples during injection/dissipation stages. Higher permeability values were detected at larger expansions, which suggest the role played by clay deformation on gas transport process.

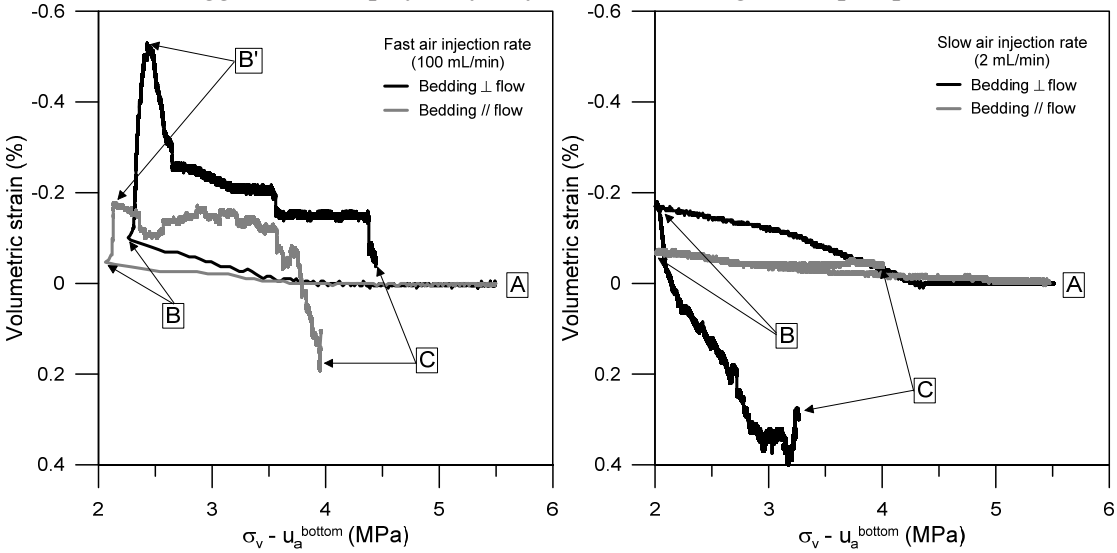


Figure 1. Evolution of volumetric strains during air injection (A to B) and dissipation (B to C) stages.

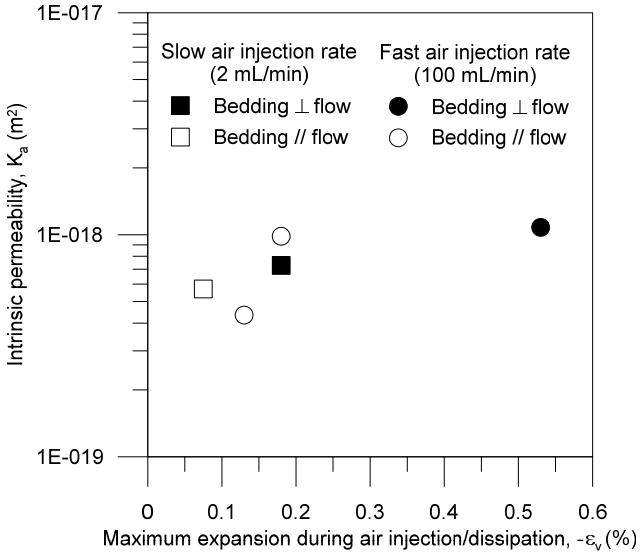


Figure 2. Intrinsic permeability (air) versus maximum expansion during air injection/dissipation.

Acknowledgements

Financial support of ONDRAF/NIRAS (Belgium) through a PhD collaboration agreement with CIMNE (Spain) 'Laboratory investigation of the gas transport process in a repository located in Boom Clay' (2012-2016) is greatly acknowledged.

References

González-Blanco, L., Romero, E., Li, X., Sillen, X. 2014. Importance of sample volume changes and material degradation on gas transport properties in Boom Clay. 7th International Congress on Enviromental Geotechnics, Melbourne, Australia, 10-14 November 2014.

Saponite formation in the ABM2 iron-bentonite field experiment at Äspö hard rock laboratory, Sweden

Daniel Svensson

Department of Research and Safety Assessment, Swedish Nuclear Fuel and Waste Management Co (SKB), Äspö Hard Rock Laboratory, Box 929, SE-572 29, Oskarshamn, Sweden. daniel.svensson@skb.se

The Alternative Buffer Material field experiment started at Äspö Hard Rock Laboratory, Sweden in 2006 at 450 m depth underground. Twelve different compacted clays (3 dm diameter discs) were placed in direct contact with each other, onto a heated iron cylinder with a target temperature of approximately 130 ºC. The first package (ABM1) was excavated in 2009, 2½ years after installation, and was analyzed extensively regarding chemistry (including Fe-redox chemistry), mineralogy, hydromechanical properties and microbiology (*e.g.* Svensson *et al.,* 2011; Svensson and Hansen, 2013). In late 2012 three new modified experiments were installed (ABM45) in order to provide several long-term experiments for the future. In April 2013 the second package (ABM2) was excavated, 6½ years after the installation.

In ABM2 visual observations indicated a strong interaction between the clay and the iron heater, seen as a dark discoloration of the iron-bentonite interface. The amount and/or type of corrosion on the iron heater were visually very different between the various types of bentonite. In several blocks centrosymmetrical precipitates such as anhydrite was found (Figure 1, left).

Many samples have been analysed to different extent at Äspö Hard Rock Laboratory. We have focused on one clay and one sample more than the others (the one with the so far highest level of newly formed tri-smectite). A sample was collected by scraping directly from iron heater at Febex clay block number 9 (similar to Figure 1, right). This sample was a mixture of corrosion product (magnetite) and of what seems to be a newly formed trioctahedral smectite (saponite), together with the original dioctahedral smectite and accessory minerals. After dispersion and magnetic separation (to remove the magnetite) the sample was Ca-exchanged to distinguish Mg^{2+} in octahedral layer from interlayer. In the XRD data a new reflection at 1.55 Å was observed, corresponding to a trioctahedral phase, in addition to the original reflection at 1.50 Å from the dioctahedral smectite. Upon ethylene glycol solvation a 17 Å basal spacing was observed, which is typical for a smectite. No other basal reflections were observed.

The intensity relation of the 060 reflections indicated an approximate relation of 35:65 between trioctahedral to dioctahedral smectite. A linear combination of FT IR data using the original smectite and a German ferrous saponite (supplied from BGR, Germany) supported a 40:60 distribution. μ-RAMAN spectra were collected on 20 random ~10x10 μm spots and all had a similar appearance, indicating that the sample was very homogenous. Small amounts of dark very small particles (~5x5μm) were observed and RAMAN data indicated these as likely magnetite remainings not removed by the magnet, however to low in content to be observed by XRD. The identified phases from quantitative XRD analysis using the Siroquant software (minor amounts of albite and quartz) were subtracted from the chemical content of the purified sample (as determined by XRF), together with the approximative amount of dioctahedral smectite from the 060 intensity relation (empirical data was used from the original clay). The proportion of di:tri smectite was varied somewhat to optimize the calculated stuctural formula based on what is known of ideal trioctahedral smectites. The chemical composition obtained agreed with what was expected from a saponite. The molar content of Mg was somewhat larger than Fe suggesting a ferrous saponite and not a ferrosaponite where Fe>Mg. The thermal stability of the phase was investigated by consecutive heating of the sample in furnace (500-750 C, totally 74 h) and XRD data was measured at 4 different times in between the temperature

increased. The newly formed phase was found to have greater or similar thermal stability as the original dioctahedral smectite, which separated it from a stevensite (pure Mg-tri smectite) that has a lower thermal stability. The saponite may have formed by (1) solid state transformation of montmorillonite by substitution/rearrangement, or by (2) dissolution of montmorillonite and/or accessory minerals followed by reaction with corrosion products and saponite precipitation. There are a number of published studies were trioctahedral smectites such as saponite and stevensite are synthesized rapidly and easily in the laboratory in similar conditions (*e.g.* Vogels *et al.*, 2005). Hover *et al.* (1999) states that formation of authigenic trioctahedral smectite is common in evaporative lake sediments, and their data indicates that dioctahedral smectite may transform to trioctahdedral Mg-smectite in hypersaline porewaters with a high Mg^{2+}/Ca^{2+} ratio. Mg-has been found to be enriched towards the heater in a number of bentonite field experiments, possibly causing somewhat similar conditions.

The combination of experimental data, observations from laboratory synthesis and field studies indicates that formation of saponite in heated bentonite is reasonable to occur, at least to some extent and at least in some types of bentonites during specific conditions such as high temperature and iron-heater. No impact on the bentonite performance is expected at the very low level of formation observed. Saponite has actually been proposed as a possible alternative buffer material candidate, as it has rather similar properties as bentonite. No trioctahedral smectites have been observed in experiments using copper heaters, which is the target canister material in the SKB KBS-3 concept.



Figure 1. Left: In several bentonite blocks centrosymmetrical white precipitates and significant corrosion at the iron heater interface could be seen. Right: At some locations on the heater a thin layer was found loosely bound to the heater associated with corrosion products and clay minerals.

References

Hover, V. C., Walter, L., M., Peacor, D. R., Martini, A. M. (1999) Mg-smectite authigenesis in marine evaporative environment, Salina Ometepec, Baja California. *Clays and Clay Minerals*, **47**, 252-268.

Svensson, D., Dueck, A., Nilsson, U., Olsson, S., Sandén, T., Eriksson, S., Jägervall, S., and Hansen, S. (2011) Alternative Buffer Material. Status of the ongoing laboratory investigation of reference materials and test package 1. SKB Technical Report, TR-11-06, SKB, Stockholm.

Svensson, P. D., Hansen, S. (2013) Redox chemistry in two iron-bentonite field experiments at Äspö hard rock laboratory, Sweden: An XRD and Fe K –edge XA NES study. Clays and Clay Minerals, 61, 566-579.

Vogels, R.J.M.J., Kloprogge, J.T., Geus, J.W., Beers, A.W.F. (2005) Synthesis and characterization of saponite clays: Part 2. Thermal stability. *American Mineralogist*, **90**, 945-953.

Molecular-level insights on Titanium-clay interactions

D. Grolimund[1], **P. Wersin**[2], **L. Kiviranta**[3], **J. Brendlé**[4], **M. Snellman**[5]

1. Paul Scherrer Institute, CH-5232 Villigen, Switzerland (daniel.grolimund@psi.ch)
2. University of Bern, Institute of Geological Sciences, CH-3012 Bern, Switzerland (paul.wersin@geo.unibe.ch)
3. B+ Tech Oy, FIN-00420 Helsinki, Finland (leena.kiviranta@btech.fi)
4. Université de Haute-Alsace (Mulhouse), F-68093 Mulhouse, France (jocelyne.brendle@uha.fr)
5. Saanio & Riekkola Oy, FIN-00420 Helsinki, Finland (margit.snellman@sroy.fi)

Posiva and SKB are developing a design alternative of the KBS-3 method, termed KBS-3H, in which several spent fuel canisters are emplaced horizontally in deposition drifts (SKB/Posiva 2013). In this design, an assembly of a Cu-waste canister surrounded by bentonite blocks is placed in a perforated shell, a so-called supercontainer (SC), before emplacement in the deposition drift. The currently selected material for the SC is titanium rather than steel. This selection is based on the distinguished properties of titanium, such as its inert geochemical behaviour (Schutz (2005). Unfortunately, the physical-chemical behaviour of titanium under geochemical conditions relevant for the deposition drift is not known in detail, and it is important to analyze potentially adverse effects of titanium and its corrosion products on the overall performance of the barrier system. In particular, the interaction of titanium with clay minerals needs to be assessed.

Obviously, the impact of Ti corrosion products on the physical and chemical properties of the clay barriers does not solely depend on the absolute corrosion rates and corresponding amounts of Ti loading in the clay materials. Of fundamental importance is the chemical nature of the species formed after the Ti corrosion products have reacted with clay barrier materials. Possible molecular interaction mechanisms of Ti with clays include: i) sorption by cation exchange, ii) specific (inner-sphere) sorption to clay edge sites, iii) substitution of Al and Si by Ti in octahedral or tetrahedral clay sites and iv) precipitation of secondary phases such as TiO_2, Ti-Fe oxides or Ti silicate phases. Sorption processes and the formation of nano-crystalline or amorphous ('gel-like,') Ti-oxide phases may influence the retention characteristics and the swelling properties of the clay barrier. Identifying the predominant molecular interaction processes is crucial in order to assess potential impacts on safety functions of the clay barrier. Consequently, there is need for analytical investigations capable in providing molecular level information. However, two main obstacles turn molecular-level investigations on the Ti clay interaction into a real challenge. First, based on the extremely low corrosion rates and low solubility of Ti^{4+} only small amounts of reaction products can be expected to be formed during experimentally accessible timescales. Second, the considerable levels of geogenic Ti present even in 'purified' natural clay samples generally mask the molecular characteristics of the Ti reaction products. In this study, an advanced experimental strategy involving the use of synthetic, Ti-free montmorillonite combined with elevated reaction temperatures allowed to overcome these experimental challenges.

An extended series of batch-type investigation has been conducted to shed more light on Ti-clay interaction processes and on the Ti species resulting from these interactions. Corrosion of metallic Ti and the interaction of resulting corrosion products with clay were proceeding simultaneously in the same experimental system. Metallic Ti foil coupons and coarse grained Ti powder were employed as Ti corrosion source terms. Ti corrosion and concurrent reaction of the products with synthetic Ti-free montmorillonite took place in 0.1 M NaCl solutions at different pH and temperature conditions. After different time intervals (each several months), Ti metal and clay materials were separated and analysed by wet chemistry and spectroscopic methods.

Synchrotron-based X-ray techniques have been employed to analyse the interaction of the released Ti with the clay material. First, X-ray Fluorescence (XRF) served to quantify the association of Ti with the clay. After measureable quantities being observed, X-ray Absorption Spectroscopy (XAS) techniques were applied to obtain molecular-level information of the Ti reaction products. X-ray Absorption Near Edge Spectroscopy (XANES) at the Ti K-edge is exceedingly sensitive to the electronic state, site coordination (tetrahedral vs octahedral) and site symmetry, as well as site distortions. Complementary, Extended X-ray Absorption Fine Structure (EXAFS) analysis can provide

measures of the identity and quantity of coordinating atoms and related local interatomic distances with good accuracy. XAS measurements have been recorded at the microXAS beamline at the Swiss Light Source. Due to the trace levels of Ti present in the reacted clay, data had to be collected in fluorescence mode.

Selected XANES results are depicted in Figure 1. The three samples (different in reaction times) exhibit distinct and nearly identical pre-edge signatures (Fig. 1, bottom). Comparing with reference compounds (Fig. 1 top), the pre-edge features of the Ti reacted clay samples are in close agreement with the first shell coordination of Ti in titanite, indicating an octahedrally coordinated, low-distortion site. Based on this observation, the formation of nano-crystalline or amorphous ('gel-like') Ti-oxide phases as well as Ti-Fe oxides phases and the Ti substitution in tetrahedral clay sites can be round out. Similar, interfacial species due to cation exchange appear unlikely as such complex would exhibit a considerable degree of distortion. To be noted are the post-edge differences as compared to the titanite spectrum. This points towards differences in the first shell Ti-O distances and to disparities regarding the type of coordinating atoms in higher order shells.

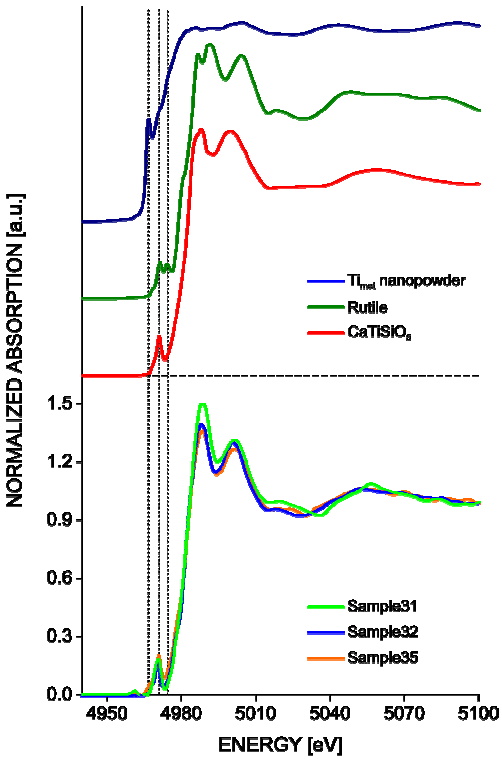


Figure 1. XANES analysis of reference compounds (top) and reacted synthetic montmorillonite samples (bottom). After reacting with the clay, the Ti corrosion product exhibit a first molecular coordination shell similar to Ti in titanite (octahedrally coordinated, low-distortion site).

Despite the trace amount of Ti associated with the clay, good quality EXAFS data could be obtained (Figure 2). Preliminary analysis conclusions are consistent with a structural incorporation of Ti into octahedral sites of the clay framework. Refined structural analysis based on the EXAFS data and structural simulations as well as ^{19}F solid state NMR data are currently underway.

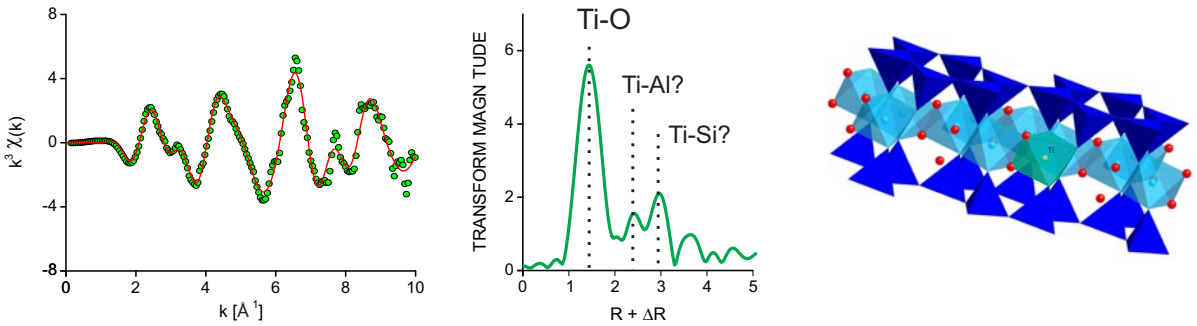


Figure 2. EXAFS spectrum (left), corresponding Fourier Transform (middle), and structural model (right) of Ti reacted with synthetic montmorillonite. Preliminary analysis points strongly towards the structural incorporation of Ti in the clay framework.

The employed innovative strategy based on the use of synthetic, Ti-free clay material combined with the application of advanced analytical tools (synchrotron-based spectroscopic techniques, solid state NMR) allows developing – experimentally supported - a molecular-level understanding of clay barrier modifications induced by the corrosive release of Ti.

References:

Schutz R.W. (2005): Corrosion of titanium and titanium alloys. In Handbook, Volume 13B Corrosion. Materials. ASM International (Materials Park OH), pp. 252-299.

SKB / Posiva, 2013. KBS-3H Complementary Studies 2008-210. SKB Technical Report TR-12-01. POSIVA Report 2013-03.

Kinetic modeling of interactions between iron, clay and water: comparison with data from batch experiments

Viet V. Ngo[1], Alain Clément[1], Nicolas Michau[2], *Bertrand Fritz[1,*]*

[1]Laboratoire d'Hydrologie et de Géochimie de Strasbourg, Université de Strasbourg/EOST, CNRS, 1 rue Blessig, F-67084 Strasbourg Cedex, France
[2]Andra, Parc de la Croix Blanche, 1/7 rue Jean Monnet, F-92298 Châtenay-Malabry Cedex, France

*Corresponding author: Bertrand Fritz
Email addresses: bfritz@unistra.fr

The use of carbon steel overpack is studied in the framework of the concept of deep geological disposal developed by Andra. The direct contact of the iron with the geological environment creates potential physical and chemical changes in the near field environment of the repository. Therefore, a thorough understanding of the mechanisms and mineralogical/chemical evolutions caused by the interactions of iron with clay via a modeling tool is necessary to the assessment of the performance of the geological disposal. The batch experiments being modeled in the current study consist of powders of iron and Callovo-Oxfordian (COx) claystone, and water. These experiments were carried out at a constant temperature of 90°C for 90 days (Bourdelle et al., 2014). The simulations were carried out by means of the kinetic reaction code, called Kindis (Madé et al., 1994). The overall objective of this modeling work aims at an enhanced mechanistic understanding of reaction pathways and controlling parameters in using the batch experiments.

The experimental observations are successfully reproduced by the model regarding geochemical evolution and mineralogical transformations (Ngo et al., revision being processed). For example, the stability of pH around 7 and the total dissolved carbon in the aqueous solution (Figure 1), which are controlled by saturation state of carbonates in the system, are predicted accurately. In addition, the model predicts that during the interactions between iron and clays, greenalite, chukanovite, and saponite form as the main secondary minerals (Figure 2). Moreover, the destabilization of some important primary minerals in the claystone such as quartz, illite, and smectite are also predicted by the numerical simulations. The consistency of the predictions with the experimental observations can be shown in activity diagrams of these secondary minerals, which represent the relation of H_4SiO_4 activity and CO_2 partial pressure or Ca^{2+} activity (Figure 3). Another important result is that both the model and experimental data indicated that magnetite is not formed in the experiments.

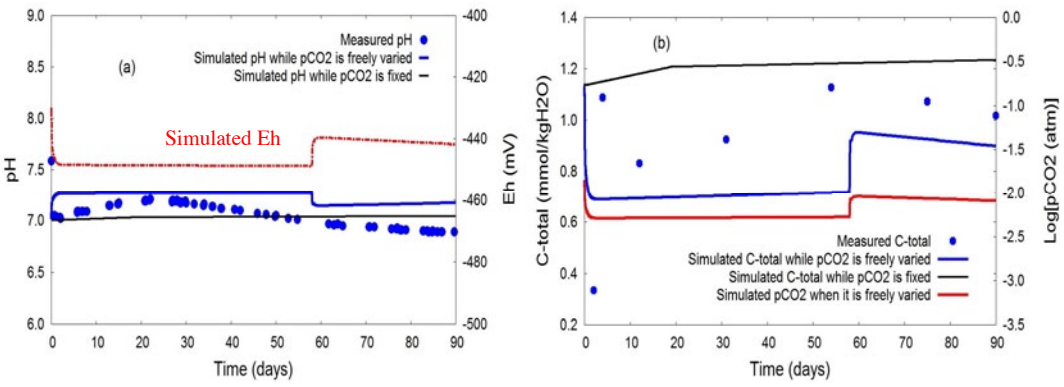


Figure 1. *(a) Evolution of pH and Eh in the aqueous solution. (b) Evolution of total dissolved carbon in the experimental system.*

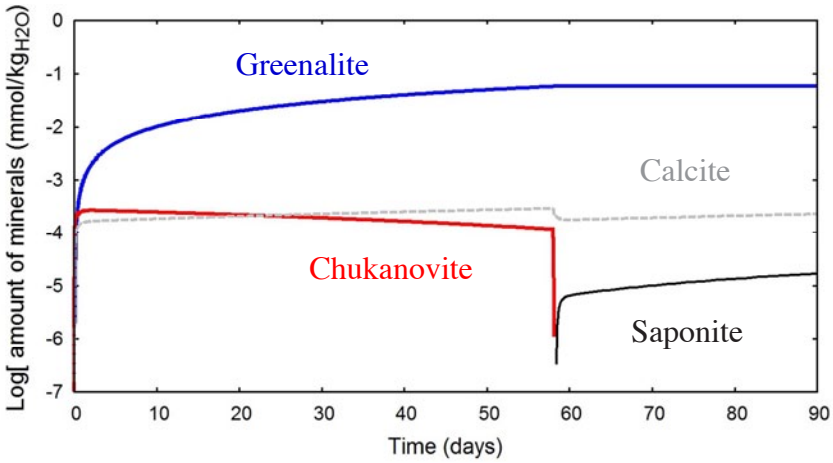


Figure 2. *Simulated concentrations of the secondary minerals precipitated in the experimental system. Calcite is a primary mineral but precipitated as well.*

The analysis of three sensitivity cases made clear that the uncertainty in corrosion and dissolution rates for iron, quartz, and illite plays an important role on the predicted evolution of pH in the aqueous solution and the formation of secondary minerals. Through this modeling work, the controlling mechanism of the interactions of iron, clay, and water at the specific conditions is fairly well understood. However, the robustness of the geochemical code Kindis should also be tested against other experiments with different experimental conditions.

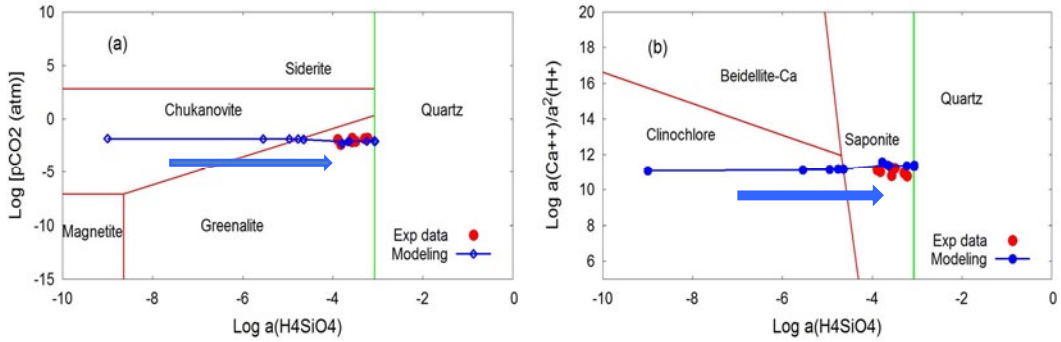


Figure 3. *Phase diagrams of quartz and different minerals that potentially precipitated at 90°C in the experimental system: (a) when fixing log[pO2 (atm)] = -60, (b) when fixing log[a(Mg^{2+})/a^2(H^+)] = 9. The red points are determined from the measured concentrations of Si, C_{total}, Ca^{2+}, and H^+. The green line is the equilibrium saturation of quartz at 90°C.*

References

Bourdelle, F., Truche, L., Pignatelli, I., Mosser-Ruck, R., Lorgeoux, C., Roszypal, C., Michau, N., 2014. Iron–clay interactions under hydrothermal conditions: Impact of specific surface area of metallic iron on reaction pathway. *Chemical Geology* 381(0), 194-205

Madé, B., Clément, A., Fritz, B., 1994. Modeling mineral/solution interactions: The thermodynamic and kinetic code KINDISP. *Computers & Geosciences* 20(9), 1347-1363

Ngo, V.V., Clément, A., Michau, N., Fritz, B. (Revision being processed). "Kinetic modeling of interactions between iron, clay and water: comparison with data from batch experiments". *Applied Geochemistry*.

Gaining insight into corrosion rate and secondary mineral paragenesis from numerical simulations of integrated iron-claystone experiments

O. Bildstein[1,*], J.E. Lartigue[1], M.L. Schlegel[2], Ch. Bataillon[3], B. Cochepin[4], I. Munier[4], N. Michau[4]

1. CEA, DEN, DTN/SMTA/LMTE, Cadarache, 13108 Saint Paul lez Durance, France (olivier.bildstein@cea.fr)
2. CEA, DEN, DPC/SEARS/LISL, 91191 Gif-sur-Yvette, France (michel.schlegel@cea.fr)
3. CEA, DEN, DPC/SCCME/LECA, 91191 Gif-sur-Yvette, France (christian.bataillon@cea.fr)
4. Andra, DRD/EAP, 92298 Châtenay-Malabry Cedex, France (benoit.cochepin@andra.fr, isabelle.munier@andra.fr, nicolas.michau@andra.fr)

* corresponding author

The understanding of iron-clay systems is based on results from batch experiments dedicated to dissolution and transformation kinetics of clay minerals in the presence of iron and steel, and from integrated experiments with massive claystone and iron/steel components. The following step consists in modelling these experiments in order to validate the models and determine the set of parameters. The results are confronted with observations of metallic archaeological analogues that evolved for 100s to 1,000s of years buried in soils, in order to extend the validity of the parameters determined in the experiments over such period of time. These parameters are then integrated into numerical simulations in order to predict the evolution of such systems on the time scale of the repository (e.g. Bildstein et al., 2006).

In this study, a series of calculations were performed to simulate iron corrosion in contact with claystone in the conditions of the integrated experiment "Arcorr2008" conducted at the CEA (Schlegel *et al.*, 2014): the purpose was to adjust the mineral paragenesis predicted by the model with the sequence of minerals observed in the experiment.
The experimental setup consisted in a brick of Callovo-Oxfordian claystone (COx) from Bure (France) in which three probes were inserted. The probe of interest for the monitoring of the corrosion rate (by in situ electrochemical impedance spectroscopy) and the identification of secondary minerals was a massive Armco iron rod. The experiment was conducted in anoxic conditions with the massive COx brick fully saturated with synthetic porewater at 90°C. After 2 years of corrosion, the average thickness of oxidized iron was about 13 μm (with a maximal corrosion rate of 90 μm/year in the first month, decreasing to less than 1 μm/year at the end of the experiment). A discontinuous layer of magnetite was identified directly at the contact with iron, followed by a layer of a Fe-silicate mineral in the corrosion zone and a layer of Fe-Ca-Mg-carbonate mineral in the transformed claystone (Fig. 1). The thickness of the alteration zone was less than 0.1 mm.

The numerical simulations were performed in the same conditions (temperature, initial water and claystone composition) considering, in a first step, the corrosion rate measured in the experiments. The selection of potential secondary minerals is crucial for the evolution of the geochemical system: a series of minerals were therefore tested (montmorillonite, vermiculite, nontronite, saponite, as well as Fe-silicates, oxides, and carbonates including chukanovite). The other adjusted parameters include the kinetics constant and reactive surface area for primary and secondary minerals: a base case was built with the data from Palandri and Kharaka (2004) and BET surface areas. The best fit was obtained by increasing the dissolution kinetics of quartz by two orders of magnitude in order to provide enough silica for the precipitation of greenalite (Fig. 2). Magnetite precipitates at the beginning of the simulation when the corrosion rate is high, and persists throughout the simulation. The precipitation of chukanovite is never predicted in these conditions.

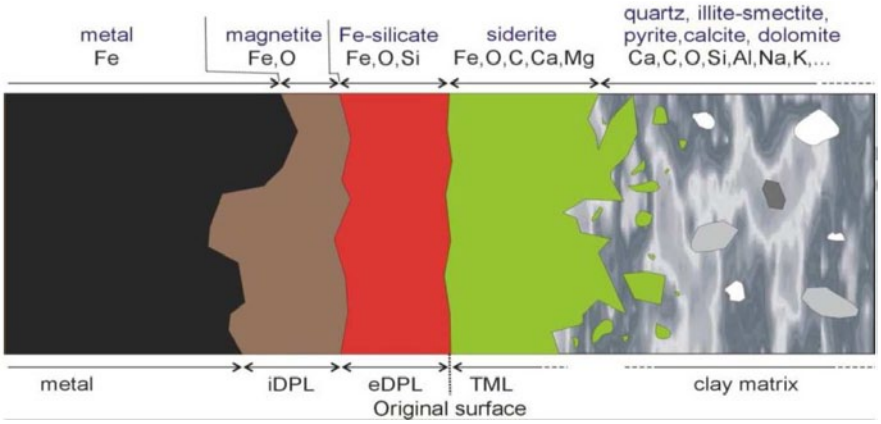


Figure 1. Observed corrosion products in the internal and external dense product layer (DPL) and in the transformed clay matrix layer (TML) after 2 years (ArCorr2008 experiment; Schlegel et al. 2014).

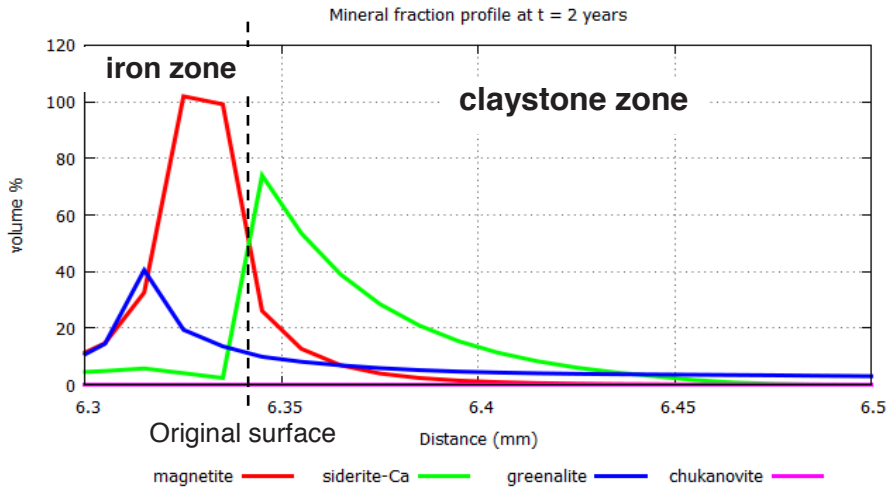


Figure 2. Corrosion products and secondary minerals predicted by the simulations after 2 years.

Nevertheless, these modelling results are not consistent with the experimental observations especially concerning the location where magnetite is forming. At the interface with corroding iron and dissolves on the other side in favour of Fe-silicate and Fe-carbonate precipitation. This process is confirmed by electrochemical corrosion models at the nanometric scale in the internal dense product layer (Bataillon *et al*., 2010), which also attribute the decrease of the corrosion rate to limited diffusion of oxygen in the magnetite dense layer.

This hypothesis has been tested with simulations containing an initial layer of magnetite (simulating a pre-corroded iron layer) with a low diffusivity. In this test case, the migration of iron in solution is dramatically decreased but the magnetite layer does not dissolve. New simulations are therefore being performed focusing on diffusivity and reactivity in the magnetite layer.

References

Bataillon, C., F. Bouchon, C. Chainais-Hillairet, C. Desgranges, E. Hoarau, F. Martin, S. Perrin, M. Tupin and J. Talandier (2010) Corrosion modelling of iron based alloy in nuclear waste repository. Electrochimica Acta 55(15): 4451-4467

Bildstein O., Trotignon L., Perronnet M., Jullien M. (2006) Modelling iron-clay interactions in deep geological disposal conditions. Physics and Chemistry of the Earth 31(10-14): 618-625

Palandri J.L., Kharaka Y.K. (2004) A compilation of rate parameters of water–mineral interaction kinetics for application to geochemical modeling. U.S. Geological Survey Water-Resources Investigations Report 04-1068

Schlegel M.L., Bataillon C., Brucker F., Blanc C., Prêt D., Foy E., Chorro M. (2014). Corrosion of metal iron in contact with anoxic clay at 90°C: Characterization of the corrosion products after two years of interaction. Appl. Geochem. http://dx.doi.org/10.1016/j.apgeochem.2014.09.002.

Action of a clay suspension on an iron(0) surface under anoxic conditions: characterization of the neoformed 7 Å iron-rich phyllosilicates

Pierre Le Pape[1,2], **Camille Rivard**[1,2], **Manuel Pelletier**[1,2], **Isabelle Bihannic**[1,2], **Renaud Gley**[1,2], **Sandrine Mathieu**[3], **Lise Salsi**[3], **Sylvie Migot**[4], **Odile Barres**[5], **Cédric Carteret**[6], **Frédéric Villiéras**[1,2], **and Nicolas Michau**[7]

[1] Université de Lorraine, LIEC, UMR7360, Vandœuvre-lès-Nancy, F-54500, France
[2] CNRS, LIEC, UMR7360, Vandœuvre-lès-Nancy, F-54500, France
[3] Université de Lorraine, SCMEM, Vandœuvre-lès-Nancy, F-54500, France
[4] Université de Lorraine - CNRS, IJL parc de Saurupt, CC-MEM, Nancy, F-54011 Cedex, France
[5] Université de Lorraine – CNRS, GeoRessources, UMR7359, Vandœuvre-lès-Nancy, F-54500, France
[6] CNRS, LCPME, UMR7564, Villers-lès-Nancy, France F-54600, France
[7] Andra, Châtenay-Malabry, F-92298, France

In the context of the underground disposal of radioactive waste, many experiments were recently achieved to assess the reactivity of iron/clay interfaces. Despite the variety of experimental setups developed during the last decade, from *in situ* large scale experiments to laboratory batch studies, the proper characterization of iron-rich phyllosilicates at the iron/clay interface still remains challenging. Indeed, in *in situ* experiments that respect the final design of the repository, the quantities of newly formed products are generally low and are limited in space to a very thin interface region. In batch experiments with iron and clay/rock materials brought as powders, iron-rich phyllosilicates are difficult to isolate from the initial mixture and from the other newly formed phases to obtain good experimental observations and reproducible results. We here present results obtained from a "mesoscopic" experimental setup which allowed both an accurate characterization of 7 Å iron-rich phyllosilicates and a better understanding of their formation mechanisms.

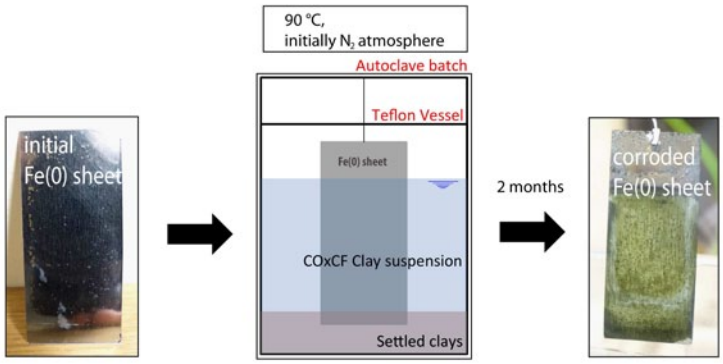


Figure 1 : Experimental setup with the two domains of interaction, and global evolution of the iron sheet surface before and after batch experiment.

Batches experiments were carried out at 90°C and under anoxic conditions. A Fe(0) sheet was placed in an autoclave so that the lower part of the sheet bathes in the clay suspension and the upper part contacts the

atmosphere of the experimental setup (Fig. 1). This experimental set-up allows both to reproduce reactive conditions as those obtained with previous experiments with Fe(0) powder and diluted suspension of clay minerals (Rivard et al., 2011), and to materialize an extended iron surface to analyze. Moreover, the choice of such geometry (Fe(0) sheet/clay suspension) appears to be more representative of what could be expected in disposal conditions than batch experiments performed with Fe(0) powder.

After two months of experiment, the mineralogical products at the surface of the Fe(0) sheet were observed using multiple techniques, namely XRD, SEM/TEM-EDXS, μ-FTIR and μ-Raman. Such caracterizations showed that both parts of the Fe(0) sheet reacted, with magnetite as the main resulting mineral on the atmospheric part and 7 Å iron-rich serpentines as main end-products on the clay suspension part associated with additional magnetite in small amounts. A spatial heterogeneity in both serpentine crystallochemistry and morphology was observed, from the Fe(0) contact towards the clay suspension. Indeed, a pure Fe-Si phyllosilicate was observed at the direct contact with the Fe(0) sheet with a progressive incorporation of Al instead of Fe in the clay phases observed closer to the solution interface. Finally, our system allowed to collect for the first time a set of infrared spectra in double reflexion mode of the pure 7 Å Fe-phyllosilicate newly formed at the Fe(0) surface. The shape of the two main regions around 3550 - 3395 cm^{-1} and 986 – 1097 cm^{-1} could be assigned to a berthierine/odinite signature.

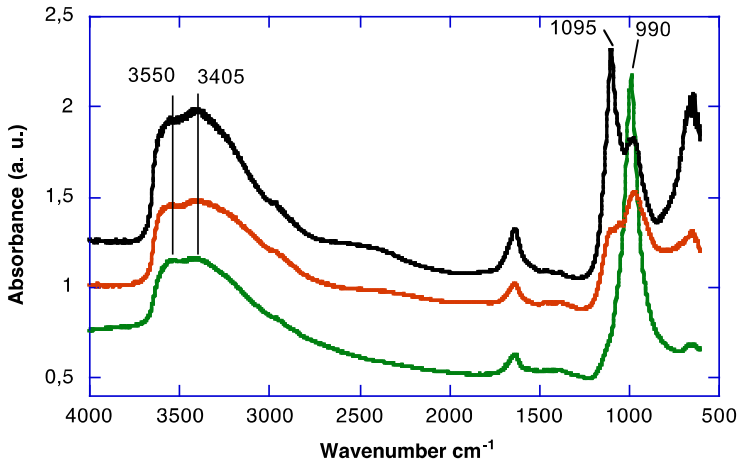


Figure 2 : Example of FTIR spectra collected at the Fe(0) sheet surface on aggregates of different thickness and attributed to berthierine.

Rivard C. (2011) Contribution à l'étude de la stabilité des minéraux constitutifs de l'argilite du Callovo-Oxfordien en présence de fer à 90°C. Thèse de l'Institut National Polytechnique de Lorraine, Vandoeuvre-lès-Nancy, France, 331 p.

On the intrinsic properties of shales

V. Favero[1], *A. Ferrari*[1], *P. Marschall*[2] *and L. Laloui*[1]

(1) Soil Mechanics Laboratory, École Polytechnique Fédérale de Lausanne, CH-1015 Lausanne, Switzerland
(2) National Cooperative for the Disposal of Radioactive Waste, 5430 Wettingen, Switzerland

Shales are natural sedimentary geomaterial which manifest an intermediate behaviour between a soil and a rock. Due to their peculiar features they appear suitable geomaterials for the nuclear waste storage. The material tested in this study is the Opalinus Clay shale from the Northern region of Switzerland. Opalinus clay samples coming from different depths have been considered: the Opalinus Clay shaly facies from the Mont Terri Underground Laboratory consists of a dark grey silty, calcarerous shale with a typical content of 25-30% carbonate, 5-10% quartz and 10-15% biodetritus. The Opalinus Clay from a deep geothermal well (depth of 837.44 - 891.25 m) near the village of Schlattingen in the Molasse Basin consists mainly of claystone with a carbonate content of 10-20% and a quartz content in the range of 15-32%. The performance of Opalinus Clay as part of the engineering barrier for the high-level nuclear waste storage is closely related to the hydro-mechanical properties of the material. Such properties are strongly affected by the geological history: indeed, a natural sedimentary geomaterial undergoes diagenetic processes and cementation after deposition, and such phenomena are responsible for its peculiar structure, which in turn affects its hydro-mechanical behaviour. The definition of "structure" considered in this work is the one proposed by Lambe & Whitman (1969), that is the combination of fabric (arrangement of soil particles) and bonding (inter-particle forces, chemical-physical bonds). Bonding is usually dominant in rocks while the influence of fabric is more important in soils. Many studies related to reconstituted clayey materials are available in the literature (Burland, 1990;Cotecchia and Chandler, 2000;Chandler, 2010) where the influence of the structure of a clayey material on the mechanical response is analysed. However, very limited investigations have been carried out on reconstituted shales. In order to study the intrinsic properties of Opalinus Clay, i.e. properties that are independent from its natural state (Burland, 1990), a series of low pressure (1-1000 kPa) and high pressure (1-100MPa) oedometric tests have been carried out. The results on the reconstituted material have been compared to those of the intact one and the major aspects related to the effect of structure on the geomechanical behaviour have been highlighted. Particular attention is given to the compressibility, swelling response and permeability of the material at the reconstituted and intact states. The low pressure oedometric tests have been conducted using a standard apparatus, while the high pressure oedometric tests have been carried out using an advanced oedometric apparatus, designed and manufactured at the Swiss Federal Institute of Technology of Lausanne (EPFL). As a consequence a wide range of stresses was covered, which was needed to observe significant variation of porosity for the reconstituted and intact shales. In order to prepare the intact samples for the high pressure oedometric testing, a systematic procedure was developed and applied (Ferrari and Laloui (2012). As to the reconstituted shale specimens' preparation, the definition of reconstituted material given by Burland (1990) has been considered. According to Burland (1990) a reconstituted soil is a soil that has been thoroughly mixed with water at a water content between the liquid limit (w_L) and 1.5 w_L, without air drying and without oven drying, and then consolidated in one-dimensional conditions. The specimens' preparation procedures are described in detail. The oedometric tests are run by incremental loading both at low and high pressures. Each incremental loading is kept constant until complete dissipation of the excess pore water pressure is observed by the analysis of the settlement versus time curves. The results of the oedometric tests in terms of void ratio versus vertical effective stress are reported in Figure 1. The normal compression line (NCL) for the reconstituted shale samples is called intrinsic compression line (ICL) (Burland, 1990). The comparison between the ICL and the natural material NCL provides information about the lower compressibility of the natural material, which is considered to be the result of the effect of the structure (fabric and bonding). At the maximum considered effective stress level, the void ratio of the reconstituted material is still far from that of the intact shale leading to the conclusion that the porosity of

the natural material being related not only to the mechanical compaction and fabric configuration but also to the diagenetic phenomena (bonding). A greater swelling behaviour during unloading is systematically observed for the reconstituted material compared to the intact one; these phenomena are likely to be related to the bond breakage during the reconstitution of the material. The oedometric modulus of the intact material has been compared to the one of the reconstituted shale as a function of the vertical effective stress and of the void ratio: considerably lower values of the oedometric modulus for the same vertical effective stress or for the same void ratio are in general highlighted for the reconstituted material compared to the intact one. The analysis of the time-settlements curves during the loading-unloading steps of the oedometric tests, allows back calculating the permeability of the tested samples (Ferrari and Laloui, 2012). The results of the intact and reconstituted samples are compared as a function of the void ratio: greater values of permeability are in general observed for the reconstituted material due to the greater range of void ratio variation involved.

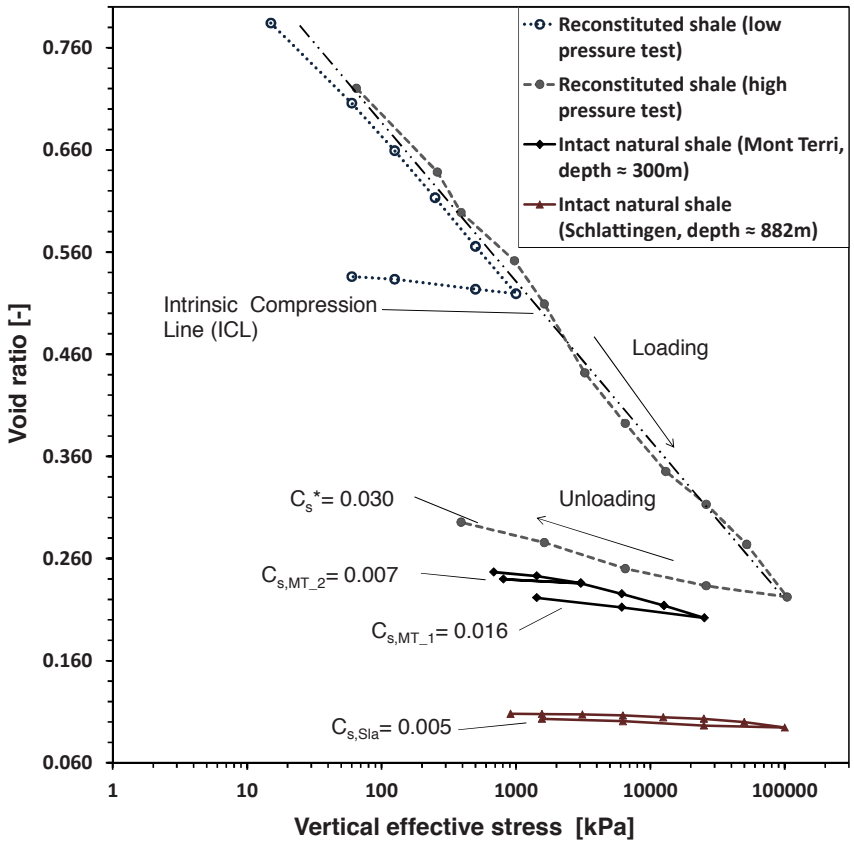


Figure 1: Oedometric tests results on reconstituted and intact Opalinus Clay shales

Burland, J. (1990) On the compressibility and shear strength of natural clays. *Géotechnique* 40(3):329-378.

Chandler, R. (2010) Stiff sedimentary clays: geological origins and engineering properties. *Géotechnique* 60(12):891-902.

Cotecchia, F. & Chandler, R. (2000) A general framework for the mechanical behaviour of clays. *Géotechnique* 50(4):431-447.

Ferrari, A. & Laloui, L. (2012) Advances in the Testing of the Hydro-mechanical Behaviour of Shales. In *Multiphysical Testing of Soils and Shales*.) Springer, pp. 57-68.

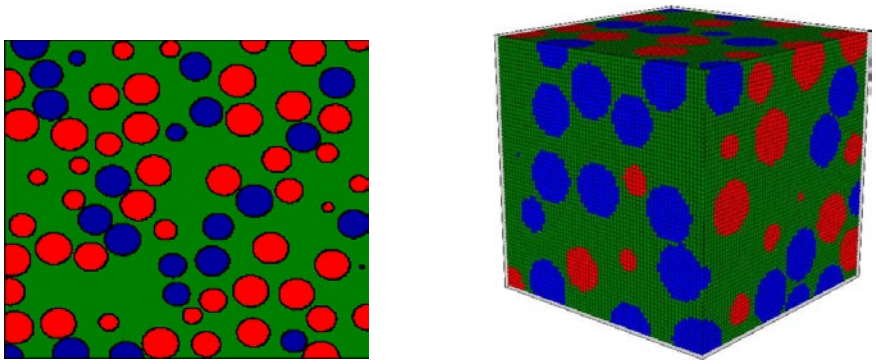
Lambe, T. & Whitman, R. (1969) *Soil Mechanics*, 553 pp. John Wiley, New York.

A micromechanical analysis of clayey rock based on Fast Fourier Transforms method

Author(s) (Times New Roman 12, bold),
MY Li, WQ Shen, *JF Shao*

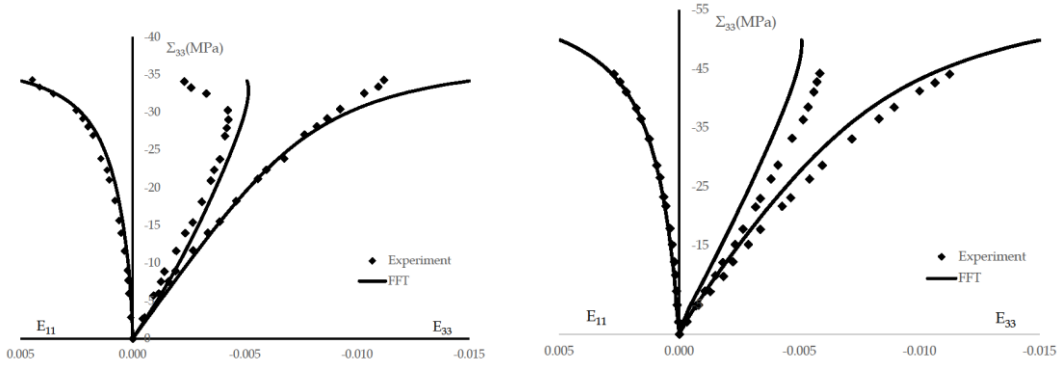
Address(es) (Times New Roman 10)
LML, University of Lille, Cité scientifique, 59655 Villeneuve d'Ascq, France
Email : jian-fu.shao@polytech-lille.fr

Clayey rocks are heterogeneous materials with complex structures at different material scales. In view of modelling thermo-hydromechanical behaviour for engineering application such as geological disposal of radioactive waste, two materials scales are particularly relevant. At the mesoscopic scale, clayey rocks can be seen as a composite material composed of a clay matrix and mineral inclusions, mainly quartz and calcite grains. At the microscopic scale, the clay matrix itself is a polycrystalline aggregate constituted by clay plates of different orientations and inter-particular pores. The macroscopic behaviour of clayey rocks is inherently depending on the local behaviour of each constituent and the evolution of microstructures. A number of phenomenological models have been proposed, providing a descriptive modelling of macroscopic responses observed in laboratory tests, but generally fails to establish relationships between macroscopic responses and microscopic behaviours and structures. Micromechanical models, based on nonlinear homogenization techniques, provide a promising way to develop physical based constitutive models for heterogeneous rocks, for instance (Abou-Chakra Guery et al., 2008; Shen et al., 2012, 2013). However, in these models, strong assumptions are generally introduced to simply the real microstructure of clayey rocks, for example, periodic distribution of spherical inclusions and pores. Further, size effects of heterogeneities cannot be taken into account. In order to estimate the macroscopic behaviour of such materials considering a microstructure as close possible as that obtained from microscopic observations, full field simulations have being developed recently on the representative volume element (RVE), using various numerical solutions. In the present work, we propose to study the macroscopic elastoplastic behaviour of Callovo-Oxfordian argillites (Cox), using the Fast Fourier Transforms (FFT) method initially proposed by Moulinec and Suquet (1994, 1998) for composite materials. At this stage, we consider the Cox argillites at the mesoscopic scale, seen as a three-phase composite composed of the clay matrix and two families of mineral grains, quarts and calcite. The clay matrix is described by a pressure sensitive elastoplastic model with a non-associated flow rule. The spherical quartz and calcite grains verify a linear elastic behaviour. Two families of mineral grains are randomly distributed inside the clay matrix, as shown in Figure 1, respectively for two and three dimensional representation of RVE. Note that the choice of a random distribution of spherical grains is presented here as an example. It is possible to consider other kinds of distributions and other forms of grains without any fundamental difficulties. After the identification of local parameters of each constituent, a series of FFT simulations have been performed. In particular, triaxial compression tests with different confining pressures and on samples with different mineralogical compositions have been simulated. Some examples are illustrated in Figure 2. One can see the good agreement between numerical results and experimental data. The proposed micromechanical analysis is able to capture the main features of mechanical behaviours of Cox argillite as well as the effects of mineralogical compositions. This works opens a new way for modelling the nonlinear behaviour of clayey rocks with complex microstructures and physical mechanisms such as interface debonding, effects of pores and size effects of constituents.



(a) 2D microstructure with resolution: 256×256 *(b) 3D microstructure with resolution:64×64×64*

Figure 1: Representation of Cox argillite microstructure: Green: clay matrix; Blue: quartz; Red: Calcite



(a) Depth 466.8m, f_0 = 51%, f_1 = 26%, f_2 =23% *(b) Depth 451.4m, f_0 =47%, f_1 =31%, f_2 =22%*

Figure 2: Comparisons between numerical results and experimental data: (a) Uniaxial compression, (b) Triaxial compression under 10MPa confining pressure

Acknowledgement:

This work has been partially supported by Andra which is gratefully acknowledged.

References

Abou-Chakra Guery, A., Cormery, F., Shao, J. F., and Kondo, D. (2008). *A micromechanical model of elastoplastic and damage behavior of a cohesive geomaterial*. International Journal of Solids and Structures, 45:1406–1429.

Moulinec, H. and Suquet, P. (1994). *A fast numerical method for computing the linear and nonlinear mechanical properties of composites*. Comptes Rendus de l'Academie des Sciences, t.318:1417–1423.

Moulinec, H. and Suquet, P. (1998). *A numerical method for computing the overall response of nonlinear composites with complex microstructure*. Computer Methods in Applied Mechanics and Engineering, 157:69–94.

Shen WQ, Shao* JF, Kondo D, Gatmiri B (2012), A micro-macro model for clayey rocks with a plastic compressible porous matrix, International Journal of Plasticity 36, 64–85

Shen WQ, Kondo D, Dormieux L, Shao JF (2013), A closed-form three scale model for ductile rocks with a plastically compressible porous matrix, Mechanics of Materials 59 (2013),73–86

Micro-macro-mechanical study of a clay rock on drying-wetting path

Xin Wei[1,6], Myriam Duc[2,], Thierry Reuschlé[3], Hanene Souli[4], Said Taibi[5], Jean-Marie Fleureau[1], *Mahdia Hattab*[6]

1. Laboratoire de Mécanique des Sols, Structures et Matériaux, Ecole Centrale Paris - CNRS UMR 8579, Châtenay-Malabry, France
2. Université Paris-Est, Institut Français des Sciences et Technologies des Transports, de l'aménagement et des réseaux, Département Géotechnique, Environnement, Risques Naturels et Sciences de la Terre, Marne-la-Vallée, France
3. Ecole et Observatoire des Sciences de la Terre, Institut de Physique du Globe de Strasbourg (CNRS/UdS UMR 7516), 5 rue René Descartes, 67084 Strasbourg Cedex, France
4. Université de Lyon, Ecole Nationale d'Ingénieurs de Saint Etienne, Laboratoire de Tribologie et Dynamique des Systèmes, UMR5513 CNRS, 58 rue Jean Parot, 42023 Saint-Etienne, Cedex2, France
5. Laboratoire Ondes et Milieux complexes, Université du Havre - CNRS UMR 6294, Le Havre, France
6. Laboratoire d'Étude des Microstructures et de Mécanique des Matériaux, Université de Lorraine - CNRS UMR 7239, Metz, France

In order to better understand the conditions in which fissures may appear in a nuclear waste storage site and the mechanisms involved in their formation, tests were carried out on the clayey rock of the French potential storage site in Bure. The samples were taken from the site at approximately 500 m depth and kept under stress and isolated from the atmosphere until they were tested. These tests involved macroscopic indirect traction tests, ultrasound wave propagation measurements, permeability and electrical conductivity tests, drying-wetting tests and porosimetry analyses, as well as observations by SEM and ESEM of the microfabric of the rock, performed one month and one year after decompression of the rock and under several values of suction.

Concerning the effect of creep after decompression of the rock, it appears very limited, both at the macro and micro scales.

On the contrary, the effect of hydric conditions is very important. Starting from the initial state of the material, corresponding to a suction of approximately 100 MPa and to a water content close to the shrinkage limit, the clayey rock experiences little volume change on drying path, but the change is much more important on wetting path. Accordingly, practically no fissures are observed during drying whereas fissures become very obvious on wetting path, especially when the suction becomes lower than 10 MPa.

The results of the indirect traction (Brazilian) tests highlight the non-linear increase in strength of the rock with suction similar to what is observed in other clayey materials. At the same time, mercury intrusion porosimetry reveals that there is a slight increase in the cumulated pore volume, but with little change in the size of the pores. These results are confirmed by the observations by SEM of freeze-dried specimens prepared at different suctions. Under high suction, the pictures show a dense

clay matrix with the presence of closed fissures formed by clay particles assembled face to face. When the suction decreases, the orientation of the layers does not change but the arrangement of clay particles becomes less dense. Moreover, fissures, sometimes open, are observed. In the wettest state, the fissures become more numerous, always oriented parallel to the layers.

This study at different scales gives a precise picture of the mechanisms involved in the formation of fissures in an overconsolidated clayey rock, both as the result of creep and changes in the hydric conditions. It clearly establishes the relative effect of suction and fissures on the behaviour of the material.

A unified thermo-plastic/viscoplastic constitutive model for geomaterials

S. Raude[1,2], **F. Laigle**[1], **R. Giot**[2], **R. Fernandes**[3]

[1]EDF, Centre d'Ingénierie Hydraulique (CIH), Savoie Technolac, Le Bourget-du-lac, France.

[2] GeoRessources, UMR 7359 – ENSG – Université de Lorraine, Vandoeuvre-lès-nancy, France.

[3] LaMSID, UMR EDF-CNRS-CEA 8193, Clamart, France.

The effect of temperature on the behaviour of geomaterials is a crucial issue in geotechnical and underground engineering. The literature on the thermo-mechanical behaviour of rocks and soils contains many applications in the fields of high-level nuclear waste disposal (Laloui & Modaressi (2002), Gens & Olivella (2001), Hueckel & Peano (1987), Delage et al. (2010)), heat storage (Burger et. al (1985)), geothermal structures (Laloui et al. (2006), Dupray et al. (2014)), petroleum drilling, zones around buried high-voltage cables (Mitchell et al. (1982)), bituminous materials (Darabi (2012)), and geological research. In the context of nuclear waste disposal at great depths, the thermo-mechanical behaviour of Boom clay (Baldi et al. (1988), Hueckel & Baldi (1990), Sultan & Cui (2002), Fançois et al. (2009)), Opalinus clay (Tsang et al. (2012), Jobmann & Polster (2007), Zhang et al. (2007)), Callovo-Oxfordian argillite (Zhang et al. (2007), Gasc-Barbier et al. (2004), Jia et al. (2009)) and Äspö diorite (Pan & Feng (2013), Koyama et al. (2013)) has recently received special attention in Europe.

Research in these areas has demonstrated that rocks and soils may suffer from changes in their mechanical properties during short-to long-term exposure to an elevated temperature. These changes include effects on the friction angle, permeability/porosity, elastic moduli, shear strength, dilatancy, softening, brittle-to-ductile transition, and creep.

Since Prager's first works on the modelling of non-isothermal plastic deformation, many constitutive models have been developed to include these phenomena in computational inelasticity. Most models generalise the critical-state model to include the effects of temperature on the short-term behaviour of clays and rocks. However, except for the models that were developed by Modaressi & Laloui (1997) and Zhou et al. (2011), the effect of time on the thermo-mechanical behaviour is often not coupled to the rate-independent plasticity even if the long-term behaviour appears essential for ensuring the safety and stability during the design and construction analysis in many fields, such as the storage of nuclear waste. Thus, it appears important to combine both instantaneous and delayed thermo-mechanical effects to obtain appropriate constitutive equations to model such problems.

A unified thermo-plastic/viscoplastic constitutive model has been developed for this purpose. The two mechanisms follow the classical theories of plasticity and Perzyna viscoplasticity. The mathematical expression of two yield surfaces is based on a generalised Hoek-Brown failure criterion (Equation (1)). The model includes the evolutions of the two yield limits (Figure 1) and the fluidity coefficient with temperature. The direction of the inelastic strain rates depends on the evolution of the dilation angle, which varies according to the stress and a state variable, i.e., the flow rules are non-associated.

$$F^p(\boldsymbol{\sigma}, \xi^p, T) = \frac{qr(\theta)}{r_c^0} - \sigma_c \left(\frac{m^p}{\sigma_c} \left(p - \frac{qr(\theta)}{3r_0^c} \right) + s^p \right)^{a^p} \quad (1)$$

The model was validated under several thermo-mechanical conditions on two clayey rocks (Figure 2). The typical features of the thermo-mechanical behaviour of geomaterials were well reproduced. The numerical predictions of the triaxial compression tests and creep tests clearly indicate that the model can predict the overall behaviour of geomaterials under deviatoric and non-isothermal stress paths.

The model is going to be applied to large-scale boundary value problems including the modeling of the *in-situ* experiment TER (Jia et al. 2009) (Figure 3).

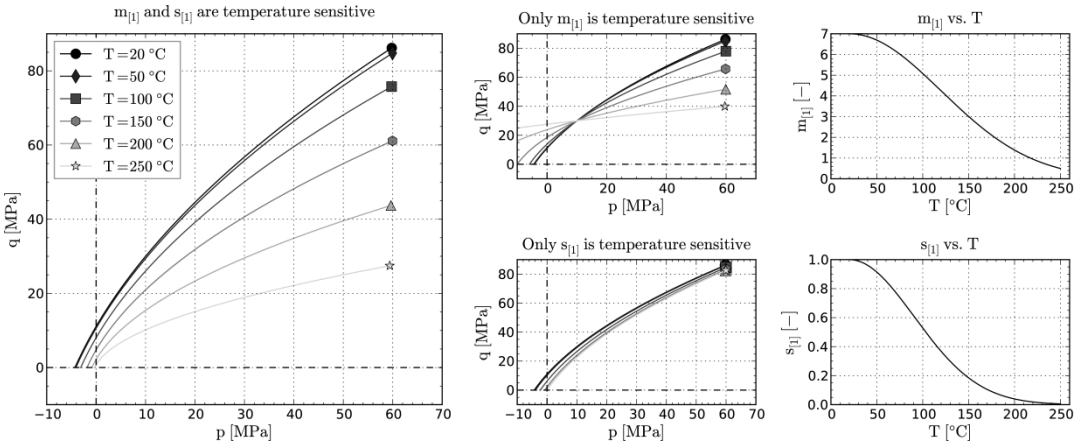


Figure 1: Temperature effects on the two material parameters m_1 and s_1 and their consequences on the maximum strength surface in the stress space.

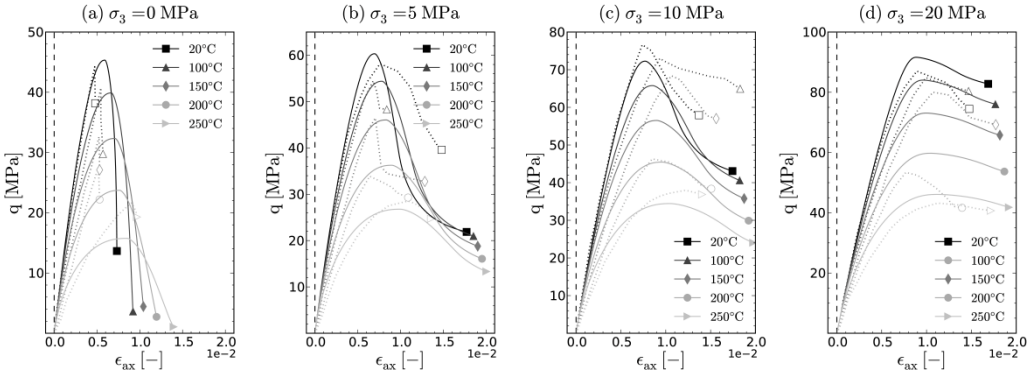


Figure 2: Numerical predictions for triaxial compression tests that were performed at confining pressures between 0 and 20 MPa and temperatures between 20°C and 250 °C on Tournemire argillite. Experimental data are from Masri (2010). The dotted lines refer to the experimental data, whereas the solid lines refer to the numerical predictions.

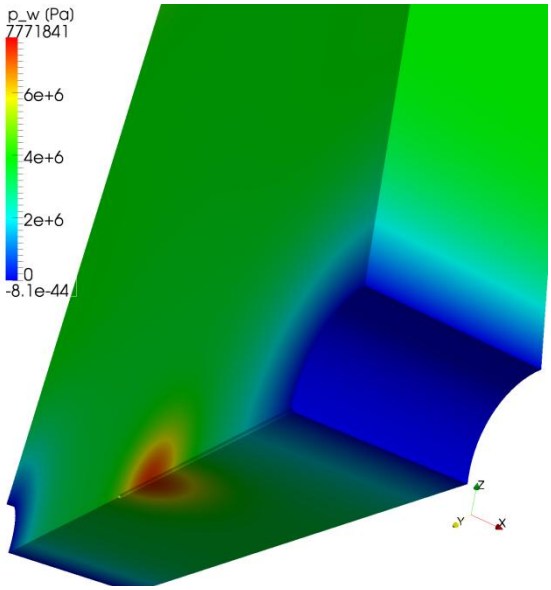


Figure 3: Numerical modeling of *in-situ* TER experiment. Map of pore water pressures during the heating phase.

References

Laloui, L. Modaressi, H. 2002. Modelling of the thermo-hydro-plastic behaviour of clays. *In: Hoteit N, editor. Hydromechanical and thermohydromechanical behaviour of deep argillaceous rock. Balkema*. 161-70.
Gens, A. Olivella, S. 2001. Clay barrier in radioactive waste disposal. *Revue Française de Génie Civil* 5(6):845-56.
Hueckel, T. Peano, A. 1987. Some geotechnical aspects of radioactive waste isolation in continental clays. *Comput Geotech*. 3(2,3):157-82.
Delage, P. Cui, YJ. Tang, M. 2010. Clays in radioactive waste disposal. *J Rock Mech Geotech Engin* 2(2):111-23.
Burger, A. Recordon, E. Bovet, D. Cotton, L. Saugy, B. 1985 Thermique des nappes souterraines. *Presse Polytechniques Universitaires Romandes*.
Laloui, L. Nuth, M. Vulliet, L. 2006. Experimental and numerical investigations of the behaviour of a heat exchanged pile. *Int J Numer Anal Meth Geomech*. 30:763-81.
Dupray, F. Laloui, L. Kazangda, A. 2014. Numerical analysis of seasonal heat storage in an energy pile foundation. *Comput Geotech*. 55:67-77.
Mitchell, JK. McMillan, JC. Green, SL. Sisson, RC. 1982. Field testing of cable backfill systems. *In: Boogs SA, et al., editors. Underground cable backfill. New York: Pergamon Press*. 19-33.
Darabi, MK. Abu Al-Rub, RK. Masad, EA. Little, DN. 2012. Thermodynamic-based model for coupling temperature-dependent viscoelastic, viscoplastic, and viscodamage constitutive behavior of asphalt mixtures. *Int J Numer Anal Meth Geomech*. 36:817-54.
Baldi, G. Hueckel, T. Pellegrini, R 1988. Thermal volume changes on the mineral-water system in low porosity clay soils. *Can Geotech J*. 25:807-25.
Hueckel, T. Baldi, G. 1990. Thermoplasticity of saturated clays: experimental constitutive study. *J Geotech Eng-ASCE*. 116(12):1778-96.
Sultan, N. Delage, P. Cui, YJ. 2002. Temperature effects on the volume changes behaviour of Boom clay. *Eng Geol*. 64:135-45.
François, B. Laloui, L. Laurent, C. 2009. Thermo-hydro-mechanical simulation of ATLAS in situ large scale test in Boom clay. *Comput Geotech*. 36:626-40.
Tsang, CF. Barnichon, JD. Birkholzer, J. Li, XL. Liu, HH. Sillen, X. 2012. Coupled thermo-hydro-mechanical processes in the near field of high-level radioactive waste repository in clay formations. *Int J Rock Mech Min Sci*. 49:31-44.
Jobmann, M. Polster, M. 2007 The response of Opalinus clay due to heating: a combined analysis of in situ measurements, laboratory investigations and numerical calculations. *Phys Chem Earth*. 32:929-36.
Zhang, CL. Rothfuchs, T. Su, K. Hoteit, N. 2007. Experimental study of the thermo-hydro-mechanical behaviour of indurated clays. *Phys Chem Earth*. 32:957-65.
Gasc-Barbier, M. Chanchole, S. Bérest, P. 2004. Creep behavior of Bure clayey rock. *Appl Clay Sci* 26:449-58.
Jia, Y. Bian, HB. Duveau, G. Su, K. Shao, JF. 2009. Numerical modelling of in situ behaviour of the Callovo-Oxfordian argillite subjected to the thermal loading. *Eng Geol*. 109:262-72.
Pan, P. Feng, X. 2013. Numerical study on coupled thermo-mechanical processes in Äspö pillar stability experiment. *J Mech Geotech Eng*. 2:136-44.
Koyama, T. Chijimatsu, M. Shimizu, H. Nakama, S. Fujita, T. Kobayashi, A. Ohnishi, Y. 2013. Numerical modeling for the coupled thermo-mechanical processes and spalling phenomena in Äspö pillar stability experiment (APSE). *J Mech Geotech Eng*. 5:58-72.
Modaressi, H. Laloui, L. 1997. A thermo-viscoplastic constitutive model for clays. *Int J Numer Anal Meth Geomech*. 21:313-35.
Zhou, H. Hu, D. Zhang, F. Shao, JF. 2011. A thermo-plastic/viscoplastic damage model for geomaterials. *Acta Mech Solida Sin*. 24:195-208.
Masri, M. 2010. Etude expérimentale et modélisation numérique du comportement thermomécanique à haute température de l'argilite de Tournemire. Doctoral Thesis, Université Lille 1 des sciences et technologies.

Anisotropic swelling behaviour of natural Boom Clay

Linh-Quyen DAO [1], Anh-Minh TANG [1], *Yu-Jun CUI* [1], Jean-Michel PEREIRA[1], Xiang-Ling LI [2], Xavier SILLEN [3]

[1] Université Paris-Est, Laboratoire Navier (UMR 8205), 6-8, av. Blaise Pascal, Cité Descartes, 77455 Marne-la-Vallée, France.
[2] European Underground Research Infrastructure for Disposal of nuclear waste in Clay Environment (EURIDICE, Mol, Belgium)
[3] Belgian Agency for Radioactive Waste and Enriched Fissile Materials (ONDRAF/NIRAS, Brussels, Belgium)

Boom Clay, situated between depths of about 185 m and 287 m at the Mol-Dessel nuclear site in Belgium, has been considered as one of potential host-rocks for the geological disposal of radioactive waste. Several studies on hydraulic conductivity, solute diffusion, thermal conductivity and small-strain shear modulus showed that this clay has anisotropic properties due to its natural deposition. Boom Clay exhibits a swelling behavior due to its clay mineralogy, and it can be expected that material anisotropy similarly affects the swelling characteristics. In this study, the swelling of Boom Clay samples along different orientations was studied through swelling tests in oedometer cell and in triaxial cell (free swelling under constant confining pressure). From these tests, the anisotropy of swelling pressure is analyzed and compared with a different approach proposed by Cui et al. (2013).

EXPERIMENTAL RESULTS

In this study, swelling tests were performed in a standard oedometer cell (without lateral pressure measurements) in accordance with three conventional methods: (1) zero-swell under low pressure (sample saturated at 0.1 MPa), (2) zero-swell under high pressure (sample saturated at σ_v = 2.4 MPa) and (3) pre-swell under high pressure (sample saturated at σ_v = 2.4 MPa). The principle of each method is presented in Figure 1. Samples were tested along different orientations with respect to the axis of the oedometer cell: perpendicular ($\theta = 0°$), inclined 45° ($\theta = 45°$), and parallel ($\theta = 90°$) to the bedding plane (where θ is the angle between the vector normal to planes of bedding and the axis of the cell, which is also the direction of the major principal stress during the tests).

The results evidence the anisotropy of swelling pressure σ_s of Boom Clay: $\sigma_s(\theta = 45°) < \sigma_s(\theta = 90°) < \sigma_s(\theta = 0°)$. In other words, the swelling pressure in the direction perpendicular to the bedding plane is the highest. It appears also that the swelling pressure depends strongly on the method applied. By method (1), the values of σ_s vary between 0.7 – 1.2 MPa which are in good agreement with some values proposed for natural Boom Clay by others authors (Horseman et al., 1987). Method (2) & (3) give higher values of σ_s which vary between 2.75 – 5.1 MPa. The anisotropy of σ_s is more visible in the tests at high pressure (method (2) & (3)) than at low pressure (method 1) (see Figure 2). This suggests that at low pressure the soil swelling could, to some extent, erase the material anisotropy.

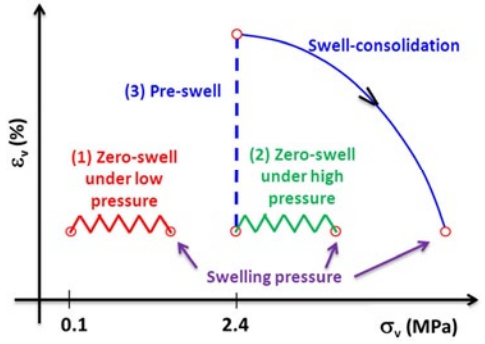


Figure 1: Three conventional methods for determining the swelling pressure.

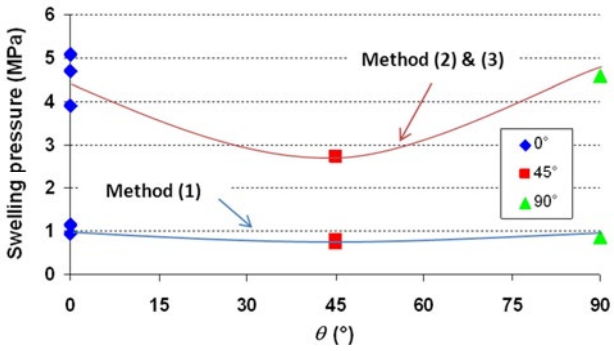


Figure 2: Swelling pressure of natural Boom Clay along different orientations with respect to the normal to the planes of bedding.

The swelling under constant volume was also investigated using an oedometer cell with lateral pressure σ_h measurement. The values of σ_s in two directions were measured at the same time using a lateral pressure sensor (in horizontal direction) and a force sensor (in vertical direction). Two sample orientations were tested: $\theta = 0°$, $\theta = 90°$. Several tests were performed for each orientation, starting from different initial vertical stress σ_v (before the saturation). The lateral pressure after the saturation was presented versus the initial one (before the saturation) in Figure 3. From these results, the anisotropy was identified: the swelling pressure perpendicular to the bedding plane is higher than that parallel to the bedding plane. The lateral swelling pressure under constant vertical stress (condition $\Delta\varepsilon_h = 0$) was also studied in order to better understand the effect of initial vertical stress. These results of σ_s were in good agreement with those obtained by constant volume method (see Figure 3, 4). When the initial σ_v increases, the lateral swelling pressure parallel and perpendicular to bedding also increases (Figure 4).

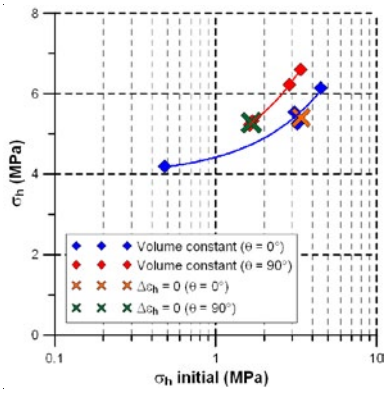


Figure 3: Lateral pressure before and after the saturation in modified oedometer cell

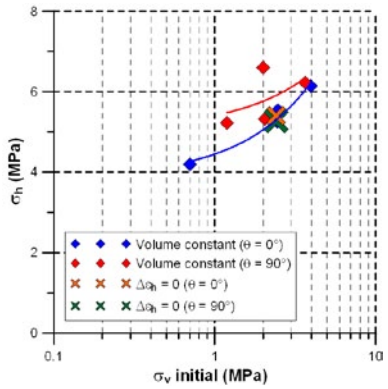


Figure 4: Lateral pressure after the saturation versus initial vertical stress in modified oedometer cell

Finally, the anisotropy of swelling behaviour was also confirmed by considering the free swelling under constant confining pressure in the triaxial cell, in which larger sample expansion was observed in the direction perpendicular to the bedding planes.

DISCUSSIONS

Another method for determining the swelling pressures proposed by Cui et al. (2013) for the stiff clays was chosen to make a comparison. Following this method, the compression oedometer curves with several loading/unloading cycles on Boom Clay of three types of samples (θ = 0°,θ = 45°, θ = 90°) were revisited. The swelling pressures were then interpreted versus the initial voids ratio (before swelling). This interpretation leads to the conclusion that the degree of anisotropy on swelling pressure of Boom Clay becomes significant at low initial voids ratio e (between 0.25-0.4) (see Figure 5). At the void ratio close to that in-situ (around 0.6), the effect of anisotropy on σ_s is not significant.

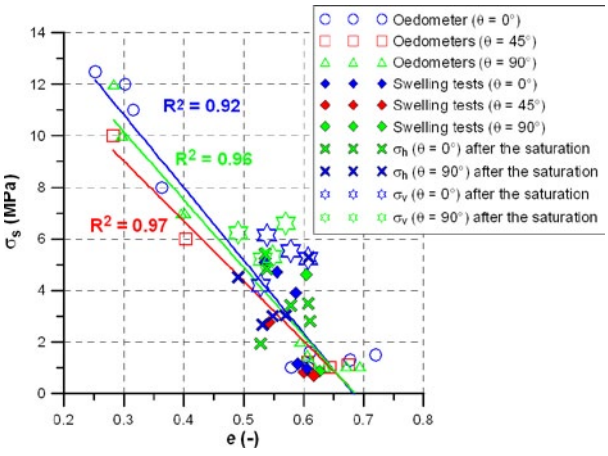


Figure 5: Swelling pressure of natural Boom Clay versus the initial void ratios.

All the values of swelling pressures obtained from the conventional swelling tests and from the direct measurements (by two sensors) were compared with the values obtained from the oedometer tests (Figure 5). A linear trend between the swelling pressure and initial void ratio was found, which is in good agreement with the observation of Cui et al. (2013).

REFERENCES

Cui, Y.J., Nguyen, X.P., Tang, a. M., Li, X.L., 2013. An insight into the unloading/reloading loops on the compression curve of natural stiff clays. Appl. Clay Sci. 83-84, 343–348.

Horseman, S.T., Winter, M.., Entwistle, D.C., 1987. Geotechnical characterization of Boom Clay in relation to the dlsposal of radioactive waste. Report.Luxembourg, Brussels.

10 years of excavation works at the Meuse Haute Marne URL: what have we learn?

A. Noiret[1,*], G. Armand[1], R. de La Vaissière[1], C. Righini[1], S. Carraretto[1], J. Zghondi[1]

[1]Andra R&D, Meuse/Haute-Marne Underground Research Laboratory, 55290 Bure, France
[*]aurelien.noiret@andra.fr

From the year 2000, the French national radioactive waste management agency (Andra) started to build the Meuse/Haute-Marne underground research laboratory (M/H-M URL) at Bure at nearly 300 km East of Paris. The technology demonstration, performance and safety assessment are main objectives of the research program, as a crusader for feasibility studies for deep geological repository. The host formation consists of a claystone (Callovo-Oxfordian argillaceous rock) lying between 420 m and 550 m in depth, which is overlain and underlain by poorly permeable carbonate formations.

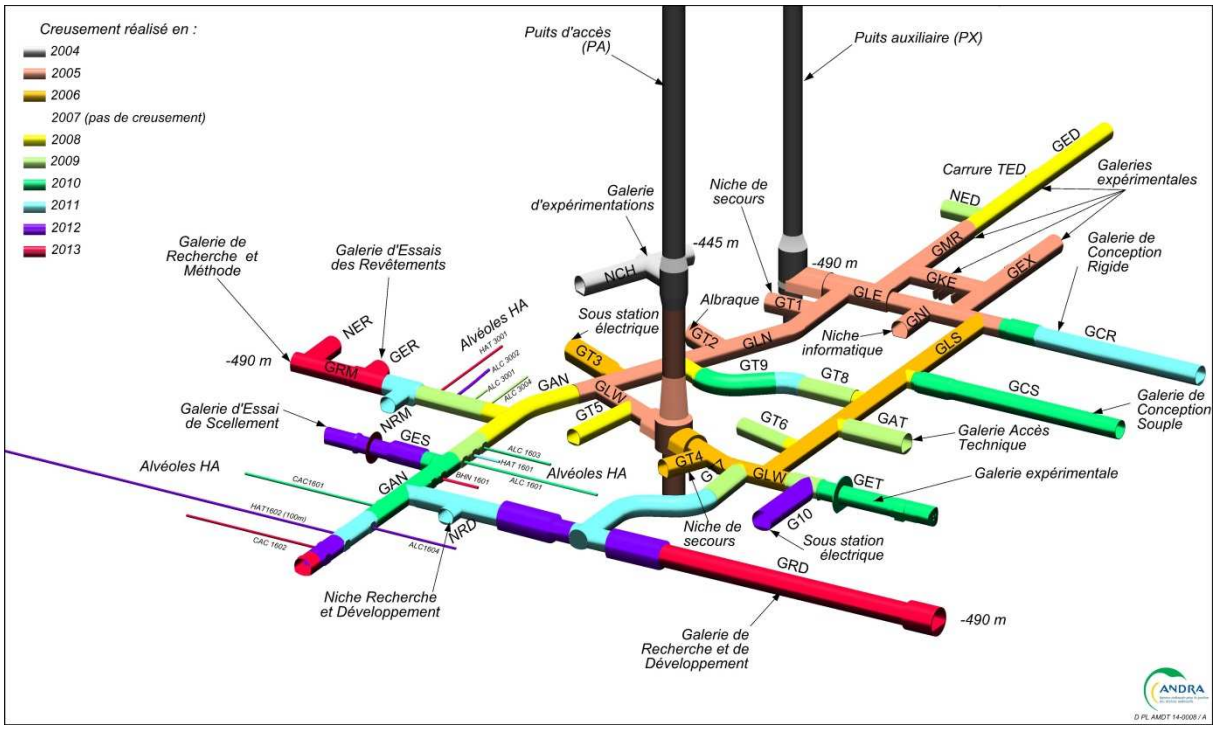


Figure 1: General view of the Meuse/Haute-Marne underground research laboratory and dates of construction of the different shafts and drifts

It is of first importance to well understand the impact of the excavation and support methods on the induced fractures and the hydro-mechanical behaviour of the claystone around the drift. The discontinuities formed within the EDZ (excavation damaged zone) represent one of the possible pathways for the migration of radionuclide towards the surface. The knowledge of the mechanisms of their creation and the control of their evolution will built confidence in the performance assessment. A better understanding of the hydromechanical behaviour of the rock mass and the interaction with the support give important data to optimize the design of nuclear waste repositories in claystone host rocks. A scientific study on the hydromechanical behaviour has been performed at the main level of the URL (-490m) for the last 10 years (Figure 1). An overview of these works is resumed in this paper.

The orientation of the experimental drifts has been determined according to the orientation of in situ stress field which was determined by Wileveau et al. (2007). Depending on the orientation of drifts to

in situ stress, host rock exhibits different responses to digging. Different methods of excavation and support had been tested at the main level. Excavations were carried out hydraulic rock breaker (GED, GAN, GRM…), road header (GET, GCS, GCR) and tunneling machine (GRD4). Different supports, from soft to stiff, emplaced with more or less delay were also tested:

- radial rock bolts, sliding ribs and thick layer of shotcrete,
- radial rock bolts with reinforced shotcrete shell interrupted by yieldable concrete called soft support,
- soft support with concrete lining poured with 7 month delay,
- segment emplacement technic.

All these experimental drifts are instrumented in order to measure the short and long term hydro-mechanical behaviour (Armand et al. 2013). For example, network of instrumented bores are used to follow the host rock response during digging. These measurements give impressive data base which could be used to compare field data to numerical models and are really useful to develop and validate reliable models. Different kind of observations such as structural analysis on core, geological survey of the drift face and sidewalls, were made to achieve an understanding of the fracture network characteristics, generation and extent (Armand et al. 2014). Hydraulic conductivity measurements (pulse and constant head test) were carried out with multi packer systems to estimate the extension of the EDZ. Near the wall, fractures exhibited high transmissivity, but further deep in the rock the shear fractures show a lower permeability of the undisturbed or slightly disturbed rock mass.

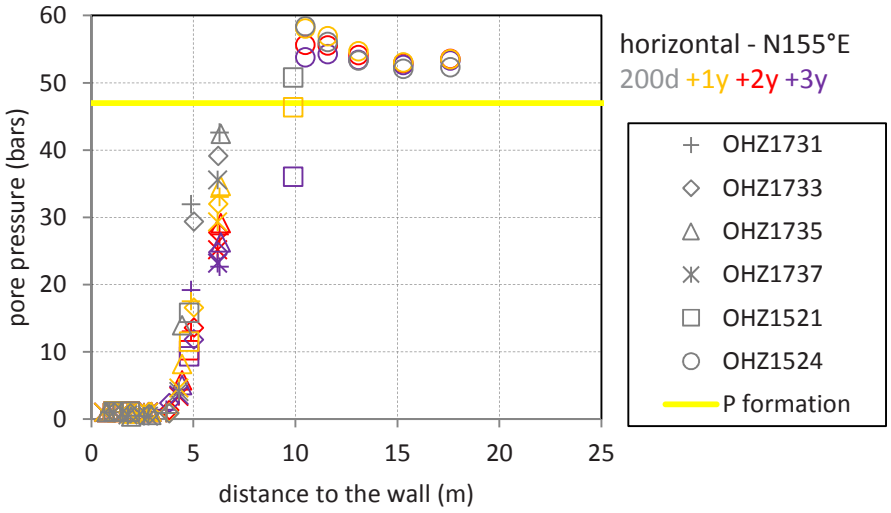


Figure 2: Horizontal pore pressure profile for a drift parallel to the major stress (N155°E)

These measurements and observations showed that shear and tensile induced fractures appear during the digging. Their patterns and extension depend on the size and orientation of the drifts, and distance to the front of the support set up and its stiffness. This induced fracture network has a strong effect on the long term hydromechanical behavior (convergence, permeability, pore pressure gradient).

References

Armand, G., Leveau, F., Nussbaum, C., de La Vaissiere, R., Noiret, A., Jaeggi, D., Landrein, P. & Righini, C. 2014), Geometry and properties of the excavation induced fractures at the Meuse/Haute-Marne URL drifts, Rock Mech. Rock Eng. 47 , p. 21-41. Doi:10.1007/s00603-012-0339-6

G. Armand, A. Noiret, J. Zghondi, D.M. Seyedi,2013, Short- and long-term behaviors of drifts in the Callovo-Oxfordian claystone at the Meuse/Haute-Marne Underground Research Laboratory, Journal of Rock Mechanics and Geotechnical Engineering 5,pp 221–230

Wileveau, Y., Cornet, F.H., Desroches, J. and Blumling, P. 2007. Complete in situ stress determination in an argillite sedimentary formation, Phys. & Chem. of the Earth, 32, 866-878.

A pragmatic methodology to abstract the EDZ around tunnels of a geological radioactive waste repository - Application to the HG-A experiment in Mont Terri.

Andrés Alcolea[1], *Uli Kuhlmann*[1], *Paul Marschall*[2], *Andrea Lisjak*[3], *Giovanni Grasselli*[3], *Omid Mahabadi*[3], *Rémi de La Vaissière*[4], *Helen Leung*[5], *Hua Shao*[6]

[1] TK Consult AG, Hallenstrasse 10, 8008 Zürich
[2] National Cooperative for the Disposal of Radioactive Waste, 5430 Wettingen, Switzerland
[3] Geomechanica Inc., 36 Nesbitt drive, Toronto, ON, M4W 2G3, Canada
[4] French National Agency for Radioactive Waste Management, 55290 Bure, France
[5] Nuclear Waste Management Organisation, Toronto, Ontario, Canada
[6] Federal Institute for Geosciences and Natural Resources, 30655 Hannover, Germany

In indurated clays such as the Opalinus Clay, the Excavation Damaged Zone (EDZ) around underground structures is a zone of brittle failure, associated with significant changes in flow and transport properties. These property changes can include an increase in hydraulic conductivity of one or more orders of magnitude. In the long-term, the EDZ fractures are expected to re-seal in response to the resaturation process and pore pressure recovery.

Safety Assessment studies are often based upon simplified representations of the EDZ, assuming concentric shells (single shell or double shell, respectively) with enhanced hydraulic conductivity. The radius of the EDZ shell typically depends on the local tunnel radius and on the orientation of the tunnel axis to the principal horizontal stress direction. Various numerical EDZ abstraction approaches have been proposed in recent years for the abstraction of complex EDZ fracture networks to simplified representations with equivalent flow and transport characteristics. In the present approach, explicit use is made of geological and hydraulic data, associated with the in-situ characterization of EDZ fracture networks in open tunnels. A versatile workflow for EDZ abstraction is developed with the following goals: (i) to cope with a wide range of geological, hydrogeological and geomechanical conditions and the associated conceptual and parametric uncertainties, (ii) to cover the relevant geomechanical phenomena and processes that are associated with the creation of the EDZ during construction and its evolution during operational times and after backfilling of the underground structures (Figure 1), and (iii) to capture in a consistent way the experimental evidence of the EDZ self-sealing, which has been gained as part of in-situ experiments in underground rock laboratories (e.g., Mont Terri / HG-A experiment).

The methodology presented here consists of three main steps (Figure 2). First, a hybrid finite/discrete element method (FDEM) is used to simulate the geometry and geomechanical conditions of the discrete fracture networks forming the EDZ (Figure 2a). Second, the geometry and hydro-geomechanical properties simulated by the FDEM are mapped onto a finite element mesh (Figure 2b), which allows to solve the fluid motion equations in the excavation near-field. A prominent feature of the suggested methodology is that hydraulic parameters of both fracture and matrix evolve with time as a response to resaturation of the tunnel surroundings. Finally, an abstraction of the complex model is made upon the late time behavior (after full resaturation) of the system (Figure 2c). The main outcomes are:

- Spatio-temporal distributions of hydraulic parameters and corresponding specific fluxes towards the tunnel, with special emphasis on the late time behavior.
- The abstraction of the EDZ at late times. Finally, a piece-wise homogeneous model with hydraulic behavior identical to that of the complex model is defined.

The present study focuses on the temporal evolution of hydraulic parameters of the EDZ around the tunnel. For illustration purposes, the methodology is applied to the HG-A experiment at the Mont Terri URL.

Specific objectives of this study are:

1) To quantify the temporal evolution of hydraulic properties in response to pressure variations caused by the resaturation of the EDZ after excavation and emplacement.
2) To quantify the temporal evolution of the specific axial flux through the EDZ.
3) To quantify the total time required for a full resaturation of the EDZ.

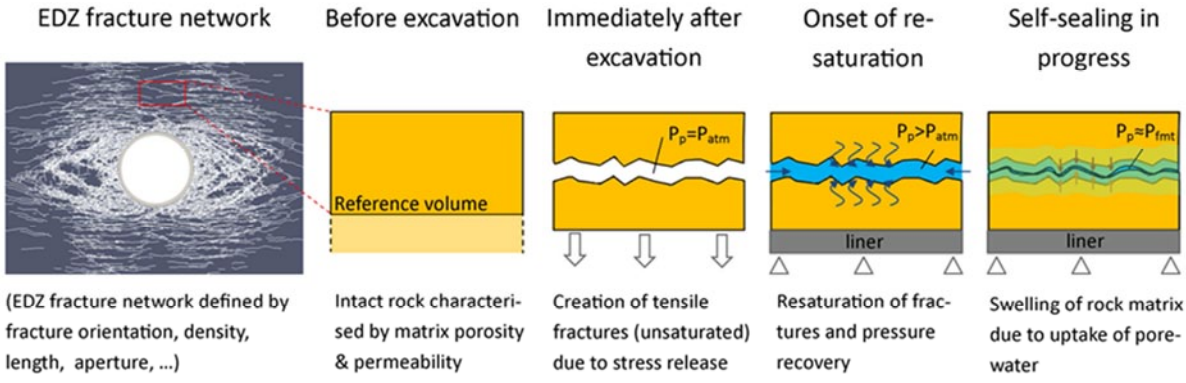


Figure 1: Schematic sketch of the conceptual framework for EDZ fracture closure in Opalinus Clay, covering the key phenomena and features from the early post excavation phase until static formation pressure recovery.

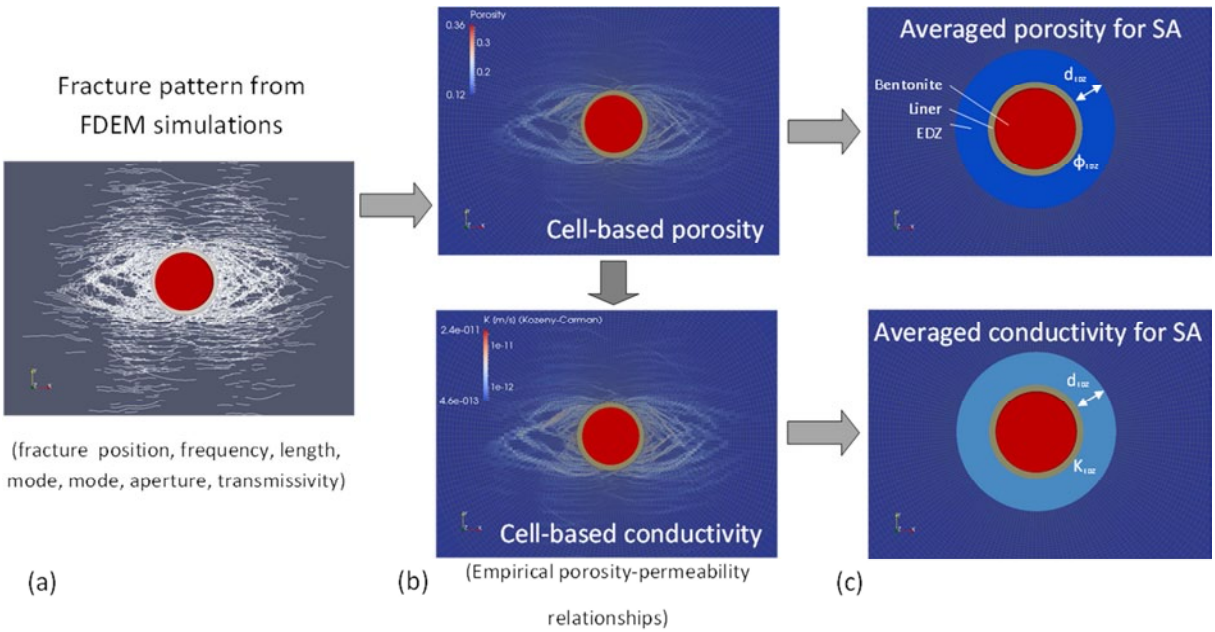


Figure 2: Concept of the EDZ abstraction process for Safety Assessment (SA) applicable for a circular tunnel: (a) Representative fracture patterns are simulated for relevant repository configurations with a discrete element model (FDEM); (b) The discrete fracture patterns are converted in heterogeneous porosity and conductivity distributions; (c) In a final abstraction process, the heterogeneous porosity / conductivity distributions are converted in a shell defined by a radius and homogeneous porosity / conductivity.

A numerical analysis of initial damaged zone around underground gallery with a discrete approach

Author(s) (Times New Roman 12, bold),
Chi YAO[1], Adrien POUTREL[2], *Jianfu SHAO*[1]

Address(es) (Times New Roman 10)
[1]LML, University of Lille, Cité scientifique, 59655 Villeneuve d'Ascq, France
Email: jian-fu.shao@polytech-lille.fr
[2]Andra, Chatenay-Malabry, France

This work is devoted to numerical modelling of excavation induced initial damaged zone around underground gallery in Callovo-Oxfordian (Cox) claystone. Extensive laboratory investigations have shown that plastic deformation and microcrack induced damage are two essential mechanisms of the mechanical behaviour of the Cox claystone. The failure process is inherently related to the transition from diffuse microcracks to localized macroscopic fractures. In situ experiments realized in the underground research laboratory (URL) at Bure have also revealed fractured and damage zones around different kinds of galleries. The overall hydromechanical behaviours of galleries are strongly controlled by the initiation and propagation of such zones. Therefore, the dimensional of disposal facilities is related to the proper description of the initial damaged zone then of its evolution. From a theoretical point of view, the transition from diffuse damage to localized fracture is still an open issue for numerical modelling of full failure process in various clay porous materials. Different kinds of methods have been so far developed, for instance, extended finite element method (XFEM), enriched finite element method (EFEM), description of strain localization bands and cohesion zones, discrete element methods (DEM) etc. Without giving here detailed comparisons between all these methods, the modelling of cohesive materials with multiple cracks is a common delicate challenge deeding further efforts. In the present work, we propose an extension of Rigid Block Spring Method (RBSM) (Kawai, 1977; Nagai et al., 2004) for modelling the initiation and propagation of damaged zone in Cox claystone. In this method, the cohesive rock sample is replaced by an equivalent assembly of rigid blocks which are linked each other by spring type interfaces. Compared with the classical RBSM, we have introduced a non-uniform distribution of stress and strain along each interface allowing the description of progressive damage and failure of the interface. The macroscopic elastic property of the rock is described by the local elastic moduli of interfaces. Also, the macroscopic failure process is controlled by the progressive failure of interfaces, which is described by a specific failure criterion. The parameters of interfaces can be identified from the macroscopic stress-strain responses in triaxial compression tests. Further, by assuming a specific spatial distribution of local properties of interfaces, it is possible to account for the material anisotropy of Cox. Both anisotropic elastic properties and mechanical strength have been described by the proposed method. A series of 2D simulations have been performed. We have considered the excavation of two representative galleries in the underground research laboratory (URL), oriented respectively along the minor and major horizontal principal stress. The distributions of stresses and displacements have been obtained. In particular, the initiation and propagation of macroscopic fracture zones around the galleries have been analysed. Some examples are shown in Figure 1. It is found that for the gallery parallel to the minor horizontal stress, an important fracture zone is obtained along the vertical axis (roof point). When the initial anisotropy of claystone is considered, the damaged zone can propagate until the horizontal axis (foot point). On the other hand, for the gallery parallel to the major horizontal stress, only diffuse microcracks are obtained in the isotropic material. However, when we take into account the material initial anisotropy, localized fractures are found along the horizontal axis. Further, the obtained displacements are also quite close to the measured values. This work has been shown that the RBSM is an efficient tool for the numerical modelling of fracture process in cohesive rocks. This method can also be extended to 3D simulations and hydromechanical modelling. However, the parameters of the model used at this stage were determined only from a limited number of laboratory tests and need to be verified with respect to additional experimental data. Also, only a first phase of validation of the proposed model has been

performed with the in situ observations of two selected galleries, and a deeper phase of validation is still necessary in view of predictive modelling of other structures.

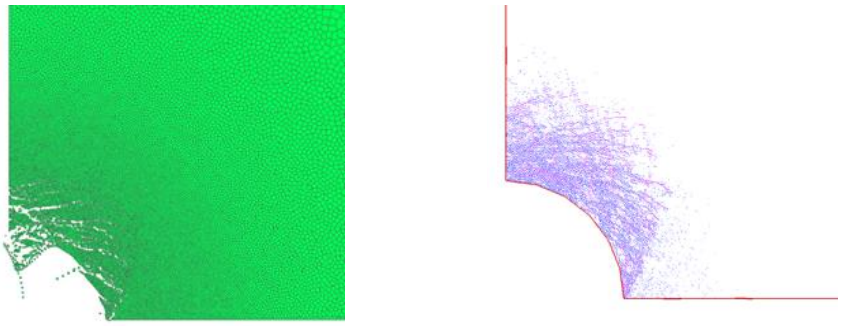


Figure 1: Illustration of fractured zone and cracks distribution around the gallery parallel to the minor horizontal stress

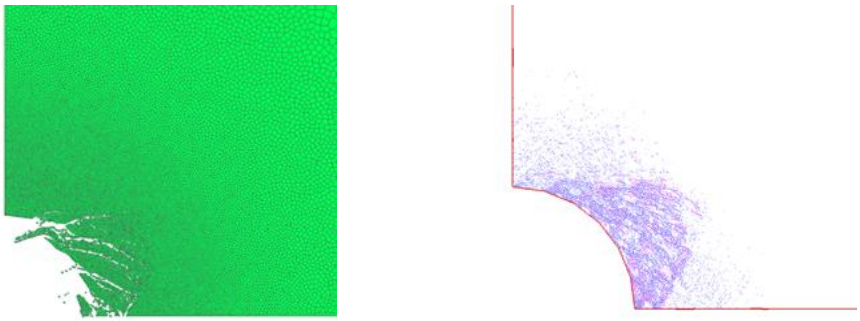


Figure 2: Illustration of fractured zone and cracks distribution around the gallery parallel to the major horizontal stress

Acknowledgement:

This work has been supported by Andra which is gratefully acknowledged.

References

Kawai T. New Element Models in Discrete Structural Analysis. Journal of the Society of Naval Architects of Japan 1977:174-180.

Nagai K, Sato Y, Ueda T. Mesoscopic Simulation of Failure of Mortar and Concrete by 2D RBSM. Journal of Advanced Concrete Technology 2004, 2: 359-374

Modelling the excavation damaged zone in Callovo-Oxfordian claystone using shear strain localisation

***B. Pardoen*[1,2], S. Levasseur[1], F. Collin[1], D. Seyedi[3]**

[1] ArGEnCo Department, University of Liège, Liège, 4000, Belgium,
[2] FRIA, F.R.S.-FNRS scholarship holder. E-mail: b.pardoen@ulg.ac.be
[3] Andra, R&D Division, 92298 Chatenay-Malabery, France.

The solution currently studied for long-term management of radioactive waste is the repository in deep argillaceous geological media with low permeability. The drilling of underground galleries in these clayey rocks induces damage propagation in the surrounding medium. This excavation process creates a damaged zones in which the material properties are modified (Blümling et al. 2007). The prediction of the fracture structure and material properties evolution within this zone is a major issue especially in the context of underground disposal.

Experimental works have highlighted that the damage around galleries in Callovo-Oxfordian claystone is localised and develops mainly as extensional and shear fractures (Armand et al. 2014). We propose to represent these shear fractures with strain localisation in shear band mode. In order to properly represent the shear strain localisation behaviour, an enhanced model introducing a regularization method and an internal length scale is needed. Among the different regularization methods, the coupled second gradient local model is chosen (Collin et al. 2006).

The constitutive mechanical law used for the clayey rock is an elasto-viscoplastic model. Due to their mode of deposition, argillaceous rocks are anisotropic materials with a stratified structure. These materials are therefore characterised by a cross-anisotropy, with an isotropic behaviour in the stratification planes. This cross-anisotropy is taken into account both in the elastic (Graham and Houlsby 1983) and plastic behaviours of the material. The material plasticity is defined by a non-associated Van Eeckelen yield surface including friction angle hardening, cohesion softening as well as cohesion anisotropy. The latter is modelled by introducing a microstructure fabric tensor (Pietruszczak et al. 2002). The creep deformation of the material is described by a viscoplastic process that corresponds to a delayed plastic deformation (Zhou et al. 2008). Furthermore, a flow model is used to reproduce transfers in partially saturated porous media. The different parameters used in the model are obtained from the literature and from experimental data fitting. The experimental data are provided by the French national radioactive waste management agency, Andra.

To illustrate the development of the damaged zone, a two-dimensional plane strain state hydro-mechanical modelling of a gallery excavation is performed (Lagamine code, ULg) for two orientations of the gallery in the Callovo-Oxfordian claystone. Firstly, a gallery oriented along the minor horizontal principal stress is considered. In this direction, the anisotropy of the stress state in the plane perpendicular to the gallery is the predominant factor leading to the elliptical shape of the damaged zone, with a significantly larger extent in the vertical direction. Secondly, a gallery oriented along the major horizontal principal stress is modelled. The stress state in the plane perpendicular to the gallery is quasi-isotropic and does not lead to shear strain localisation unless the material anisotropy is considered. This material anisotropy seems to be the predominant factor leading to the elliptical shape of the damaged zone, with a larger extent in the horizontal direction. Moreover, the modelling provides information about the fracture structure and evolution around the gallery. It exhibits a chevron fracture pattern corresponding to *in situ* experimental measurements of shear fractures for both considered gallery orientations (Armand et al. 2014).

References :

Armand G, Leveau F, Nussbaum C, de La Vaissiere R, Noiret A, Jaeggi D, Landrein P, Righini C (2014) Geometry and properties of the excavation-induced fractures at the Meuse/Haute-Marne URL drifts. Rock Mech Rock Eng 47(1):21–41

Blümling P, Bernier F, Lebon P, Martin CD (2007) The excavation damaged zone in clay formations time-dependent behaviour and influence on performance assessment. Phys Chem Earth 32(8–14):588–599

Collin F, Chambon R, Charlier R (2006) A finite element method for poro mechanical modelling of geotechnical problems using local second gradient models. Int J Numer Meth Eng 65(11):1749–1772

Graham J, Houlsby GT (1983) Anisotropic elasticity of a natural clay. Geotechnique 33(2):165–180

Pietruszczak S, Lydzba D, Shao JF (2002) Modelling of inherent anisotropy in sedimentary rocks. Int J Solids Struct 39:637–648

Zhou H, Jia Y, Shao JF (2008) A unified elastic-plastic and viscoplastic damage model for quasi-brittle rocks. Int J Rock Mech Min, 45:1237–1251

An experimental study of the flow of fluids along faults/fractures and the potential for fault reactivation

R.J. Cuss, **J.F. Harrington, A.C. Wiseall, and C.C. Graham**

British Geological Survey, Keyworth, Nottingham, NG12 5GG

Understanding flow along fractures and faults is of importance to the Performance Assessment (PA) of a Geological Disposal Facility (GDF) for radioactive waste. Flow can occur along pre-existing fractures in the host-rock or along fractures created during the construction of the GDF within the Excavation Damage Zone (EDZ). The complex fracture network will have a range of orientations and will exist within a complex stress regime that will vary over time. With this in mind, a programme of experiments has been performed using two bespoke direct-shear rigs in order to understand fluid flow along fractures and faults.

The Direct Shear Rig (DSR) was designed to investigate multi-phase flow in fractured rock. The apparatus has the capability to achieve 10 MPa normal load on samples of 60 × 60 mm. Pore fluid is introduced to the centre of the top section of the fractured material which ensures fluid is introduced directly to the fracture plane. This apparatus has been used to investigate gas and water flow along fractures in Opalinus Clay and Callovo-Oxfordian Claystone. The Angled Shear Rig (ASR) is similar to the DSR with several specific modifications. Instead of testing of rock samples, the apparatus measures flow parameters of clay gouge material between two-steel platens. The lower platen allows the fracture plane to be angled to the direction of shear and can be 0 °, 15 °, 30 ° and 45° to the shear direction. To date, experiments have been conducted on fully saturated kaolinite and Ball Clay gouge material.

Gas injection testing was performed by compressing a known volume of helium by means of a constant injection of water into an interface vessel. Assuming the ideal gas law, this should achieve the black curve shown in Figure 1. As seen, following gas entry the resultant pressure curve is different for three tests conducted on a 30° fault gouge. The gas entry pressure (i.e. the pressure at which gas first starts to flow) is similar for the three tests. However, permeability differences post-gas entry resulted in different pressure curves. This is seen at all fault angles investigated.

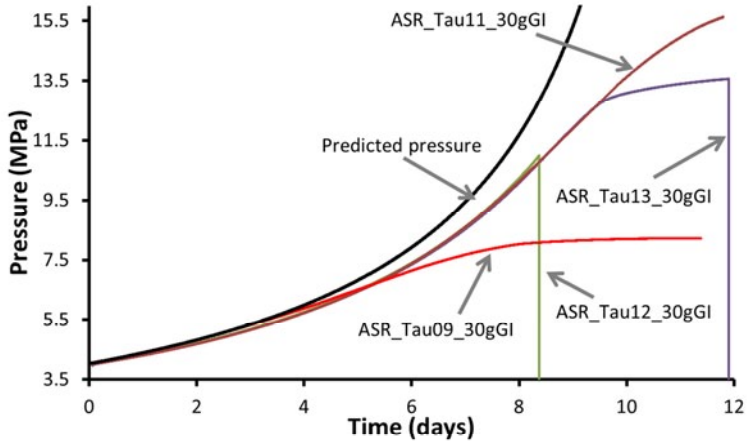


Figure 1 Repeat gas injection testing under identical conditions showing differences in permeability following a repeatable gas injection pressure.

One test was performed for a prolonged period of time to investigate the likelihood of repeat gas entry. This showed multiple gas breakthrough events, with the "form" of the breakthrough changing as well as the magnitude of the breakthrough pressure. This demonstrated that fault-valve behaviour does occur and faults are likely to show episodic flow over geological timescales.

Figure 2 shows a test conducted simulating cycles of increased and decreased vertical load on a fault gouge of Ball Clay angled 30° to the shear direction. Flow initially decreased as vertical load was increased. On the unloading cycle flow is not recovered and hysteresis is seen. This "stress memory" is also observed in kaolinite, Opalinus Clay and Callovo-Oxfordian Claystone. On reloading flow follows a similar path to that seen during unloading, until a stress greater than previously experienced,

when flow then continues to decrease. Similarities of stress history dependence have been seen between water and gas flow in kaolinite, although differences exist during the initial test history during gas flow tests. These observations show the importance of stress history on fracture flow. Consideration of just the current stress acting upon a fracture may result in inaccuracies of predicted gas or water flow.

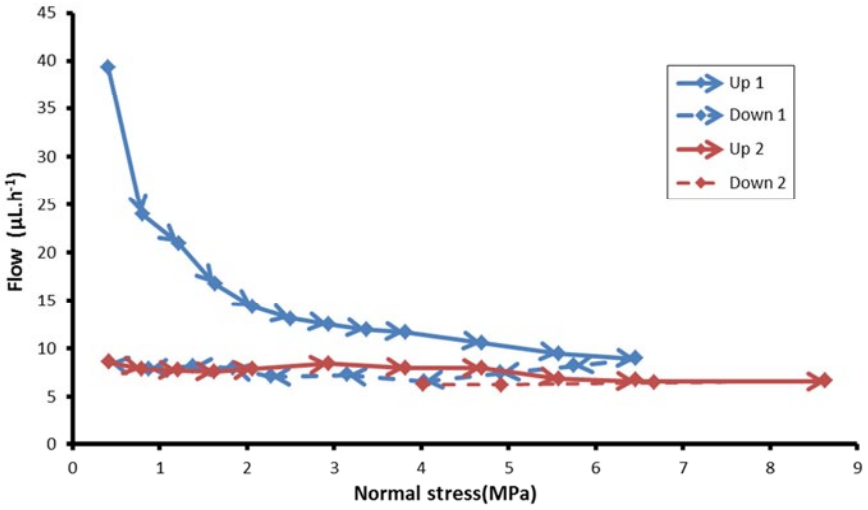


Figure 2 Flow history seen during a repeat cycle of loading and unloading of a Ball Clay fault gouge

An experimental study has been conducted investigating fault reactivation in kaolinite and Ball Clay fault gouge material oriented 30° to the shear direction. The test history consists of a shearing phase followed by a constant flow experiment to increase pore pressure within the fault gouge. The shear part of the experiment gives information on initial shear stress, yield stress and peak shear stress, with the flow part of the experiment giving the pore pressure at reactivation. Changes in vertical displacement and shear stress identify the shear movement of the gouge material during reactivation. Figure 3 shows that initial shear stress, yield stress and peak stress all increased linearly with increasing vertical stress. Additionally, the pressure observed during injection generally increases with increased.

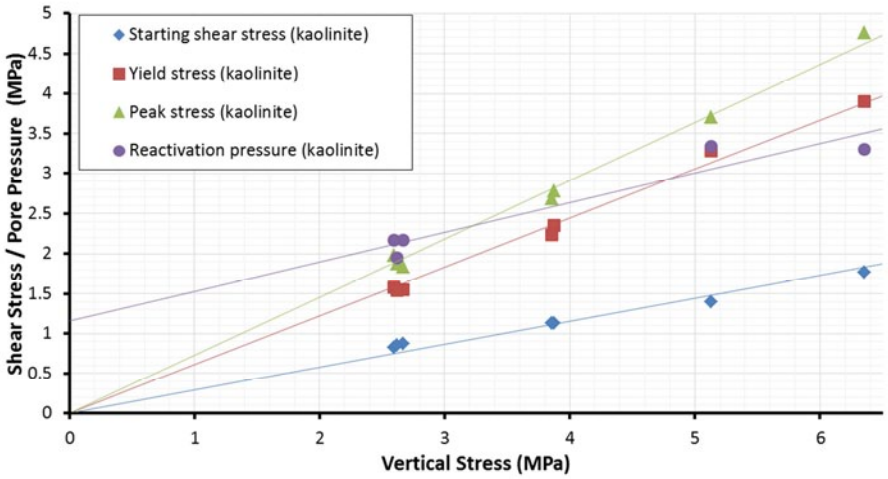


Figure 3 Initial shear stress, yield stress, peak stress and pore pressure at reactivation for a kaolinite fault gouge oriented 30° to the shear direction.

Experimental studies have increased our knowledge of multi-phase flow along fractures and faults. Considerable stress history is seen during loading / unloading of fractures, episodic flow, and fault reactivation has been observed at a stress dependent on the vertical load.

A double scale model for hydro-mechanical coupling in clay rocks; simulation of damage and strain localisation around an excavated gallery

Author(s)
B. van den Eijnden[1,2,3], *P. Bésuelle*[2,3], F. Collin[4], R. Chambon[2,3], J. Desrues[2,3]

[1] Andra, F-92810, Chatenay-Malabry, France
[2] Univ. Grenoble Alpes, Lab. 3SR, France
[3] CNRS, Lab 3SR, France
[4] Univ. Liège, ArGenCo, Belgium

The principle of deep geological repositories for the disposal of radioactive waste relies among others on the low permeability of the host rock. As the permeability is influenced by mechanical damage of the material, the coupling between hydraulic and mechanical behaviour of the host rock is of importance in the study of radioactive waste repositories.

In this context an approach is investigated for the modelling hydro-mechanical coupled behaviour of Callovo-Oxfordian claystone, a potential host rock for repositories in France. The approach presented is a double-scale finite element method (FEM^2) using a representative elementary volume (REV) to model the material behaviour at the micro scale. The global response of this REV serves as a homogenised numerical constitutive law for the macro scale.

On the macro-scale, a poro-mechanical continuum is defined with fully coupled hydro-mechanical behaviour. On the micro scale, the micro structure of the material in the REV contains elastic deformable solids separated by cohesive interfaces. Cohesive forces are described by a damage law, allowing softening of the material due to deformation. Additionally, the interfaces form a porous network allowing fluid transport prescribed by the variation in interface opening. With fluid pressure acting on the solid parts, this gives a coupled hydro-mechanical system at the micro level.

To obtain objective computation of strain localisation, the proposed model is coupled with a local second gradient frame that introduces implicitly an internal length at the macro scale. This demonstrates the ability of this regularization method to be coupled with any constitutive equation.

Computational homogenization by static condensation, commonly used for homogenization in purely mechanical problems, is used to retrieve the macro tangent stiffness from the micro level. The extension of this homogenization approach for hydro-mechanical coupling is discussed and results of the homogenization are presented.

The developed double scale approach is applied in the simulation of a gallery excavation with a 2D boundary values problem, to model damage and strain localisation in the damage zone. The influence of the microstructure is studied in term of onset and pattern of localisation. Results illustrate the ability of the double-scale approach to take into account the anisotropy of the material.

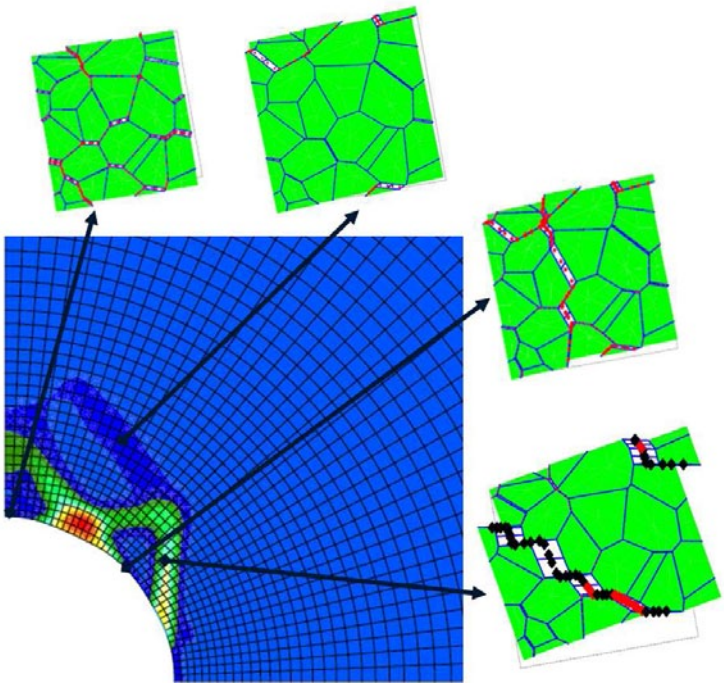


Figure 1: Gallery excavation modelling using the double scale model. Microscopically damaged REVs are concentrated in macroscale strain localization bands.

Conceptual geochemical model analysis of the long-term evolution of the Dutch Boom Clay under conditions with and without disposal of radioactive waste

***Jasper Griffioen*[123], Stefan Janssen[2], Mariëlle Koenen[1] & Hans Meeussen[4]**

[1] TNO Geological Survey, P.O. Box 80 015, 3508 TA Utrecht, the Netherlands, [2] Deltares, Utrecht, the Netherlands, [3] Faculty of Geosciences, Utrecht University, Utrecht, the Netherlands, [4] NRG, Petten, the Netherlands

The Boom Clay in the Netherlands is considered as a potential formation for future geological disposal of radioactive waste. Within the current Dutch research programme on geological disposal of radioactive waste OPERA, the feasibility and post-closure safety of a repository in this formation is investigated. An important aspect in this post-closure safety assessment is the geochemical evolution of the Boom Clay at geological time scale both under autonomous condition and under the potential influence of corrosion and degradation products released from the engineered barrier system (EBS). The objective of this study is to determine what geochemical development of the Boom Clay may be expected over a time scale of 1 million years. As input for this, the current geological situation, the nation-wide variability in geochemical composition of the Boom Clay, the variability in release of products from the EBS as well as future geological and hydrological scenarios are considered. Further, attention is paid to the conceptual uncertainty in the geochemical and hydrogeological processes that may happen at the geological time scale. Conceptual uncertainties in geochemical processes refer to penetration of oxygen and related redox processes, the extent of silicate weathering or the role of microbially mediated redox processes. Conceptual uncertainties in hydrogeological processes refer to, amongst others, the presence of deep subglacial tunnel valleys and the act of advection due to compaction/decompaction of the Boom Clay following glacial cycles. Model scenarios are established that combine the uncertainty in the controlling processes with the variability in geochemical properties of the clay. Quantitative prognosis modelling at the core scale is performed based on these scenarios. The focus in the interpretation is on the size of the reaction zone and the cyclic versus linear nature of the controlling processes. The latter refers, for example, to the cyclic nature of glaciations versus the continuity of kinetically controlled geochemical processes. The first results for diffusive controlled transport suggest that the reaction zones are limited to several meters. New results for scenarios with advective control will be presented.

The research leading to these results has received funding from the Dutch research programme on geological disposal OPERA.

Characterizing clay pore water composition of Ypresian clays from Doel and Kallo sites, Belgium

Ana María Fernández, Stefan Wilhelm, Laurent Wouters, Hervé Van Baelen

CIEMAT, Dpto. Medio Ambiente, E-28040 Madrid, Spain, anamaria.fernandez@ciemat.es
AF-Consult Switzerland Ltd., Taefernstrasse 26, CH-5405 Baden, Switzerland, stefan.wilhelm@afconsult.com
ONDRAF/NIRAS, Avenue des Arts 14, 1210 Bruxelles, Belgium, l.wouters@nirond.be, h.vanbaelen@nirond.be

Following the recommendations of the SAFIR Evaluation Commission, ONDRAF/NIRAS is currently undertaking studies on the Ypresian clays as a potential host rock for the long-term management of high-level radioactive wastes in Belgium. The study on the hydrochemistry of the Ypresian clays will provide necessary information for characterising the geological barrier ability. It also will form the base line chemistry of the undisturbed system.

The term Ypresian clays refers to those clays deposited during the Ypresian period 56-48 Ma ago, a nearly continuous sequence of soft or poorly indurated clayey layers deposited early in the Eocene in an open marine basin (Van Marcke and Laenen, 2005). The formation can be defined as a consolidated plastic clayrock. A geological and hydrogeological survey on the Ypresian clays was started in the mid-1990s below the Doel nuclear zone, in order to assess their potential as host formation. Meanwhile additional data from a second borehole at Kallo, situated about 7 km south of Doel, have become available. Evidently, there are some differences between Doel and Kallo sites. The overall salinity at Kallo is lower compared to Doel, but the mineralogical composition, grain size, porosity and water content (and its variability) seem to be comparable between these two sites. Apart for the difference in salinity between both locations, which is difficult to explain by the stratigraphic offset of approximately 40 m only, also a high vertical variability has been observed at both locations, which deserves an explanation. For clarification of the observed discrepancies and data deficiencies (sample alteration by pyrite oxidation, problems with CO_2 outgassing and some high TDS values compared to the overall trend), further studies of the hydrochemistry and pore water characterization of the Ypresian clays were initiated. The selected method for analyzing the pore water composition was the squeezing technique. This technique was successfully applied for determining the pore water composition in low-porosity, low water content and highly consolidated clayrocks, such as Opalinus Clay (Fernández et al., in press), or Callovo-Oxfordian clay-rock (Fernández et al., 2009). However, as recommended in these works, a threshold squeezing pressure must be selected for each specific clayey formation for avoiding membrane effects (ionic ultrafiltration, chemical fractionation or anion exclusion processes). The validity of the squeezing technique depends on the experimental conditions, the physical properties of the clayrock (e.g., water content, burial compaction) and the type of clay minerals involved. For this reason, prior to measuring the pore water composition of the selected core samples, it was necessary to define a uniform procedure with optimized conditions for pore water extraction. Hence, several squeezing tests have been performed for evaluating the ion pore water concentration as a function of squeezing pressure and time. Other tests, such as leaching, CEC, mineralogy, water content and dry density determinations, basal spacings, etc. have been performed for a complete understanding the physico-chemical properties and geochemical processes in the Ypresian clays.

In this study seven core samples were analysed, which belong to the Kallo-1 well drilled in 2008/2009 and to the Doel-1 well drilled 1997/1998 (Kern 26, Kern 40). The value ranges for dry density, water content and total porosity are 1.44–1.71 g/cm^3, 21.9– 32.8% and 37.9–47.9%, respectively (Figure 1a). The cation exchange capacity values between 24 and 45 meq/100g (Figure 1b), with sodium being the main cation at exchange sites. Naturally, the Ypresian clays are mainly composed of clay minerals (35-65 wt%) and, in second order, of quartz (25–45 wt%). Calcite/dolomite, feldspars, pyrite and organic matter are found at much lower quantities varying throughout the investigated formations. The clay fraction is dominated by smectite (27–56 wt%) and illite (I/S ML) with much minor amounts of kaolinite. CEC values show the trend of the smectite content in the samples (Figure 1b).

The pore water composition was extracted by squeezing at different pressures (from 5 to 100 MPa in one test and from 5 to 30 MPa in other ones). In this plastic clayrock, pore water (NaCl water-type with chloride contents of 0.24 M and 0.14 M in the Doel and Kallo wells, respectively) could be collected at a pressure of 5 MPa. Successive aliquots taken at different pressure steps indicate that the ion concentration vary significantly (Figure 2a and Figure 2b), showing a significant drop at pressures higher than 30 MPa. The pressure has, without doubt, an influence on the measured pore water compositions and thus a pressure as close as possible to the formation pressure should be applied. Different tests show reproducibility in the data. However, sometimes successive aliquots at the same pressure show decreasing concentrations, especially at high pressures. Taking care about these variations but also about the amount of pore water needed for a full analysis, at the present only an upper threshold squeezing pressure of 20 MPa has been defined for extracting the pore water in the Ypresian clays (Na-smectitic-rich Formation). Further constrictions will be defined based on supplementary tests and the analysis of the rest of the selected drill cores. On the other hand, values of anion-accessible porosity fractions of about 0.63 have been found in this clayey formation.

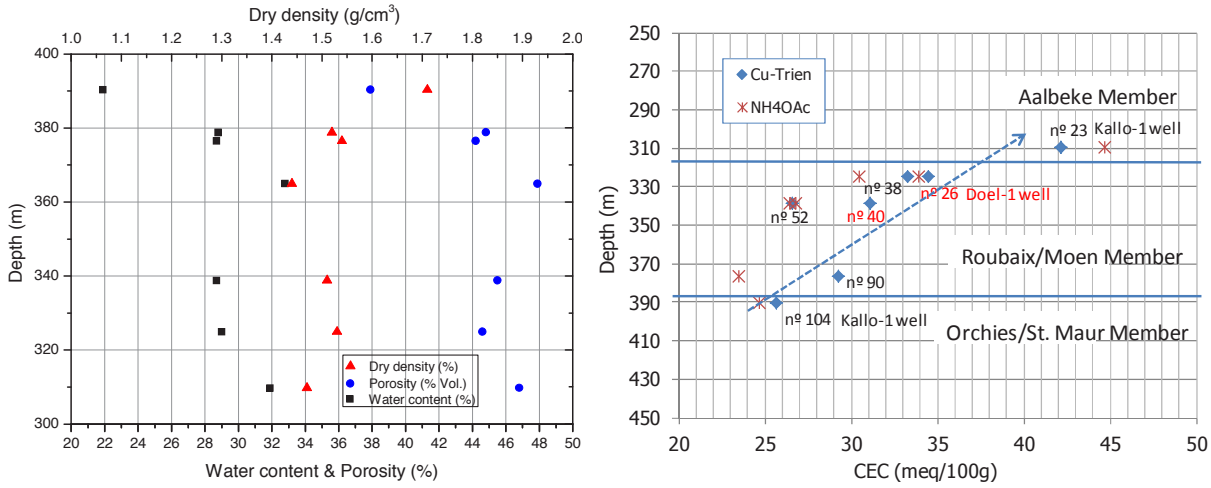


Figure 1. a) Physical properties of the core material analysed from Ypresian clays, and b) CEC data

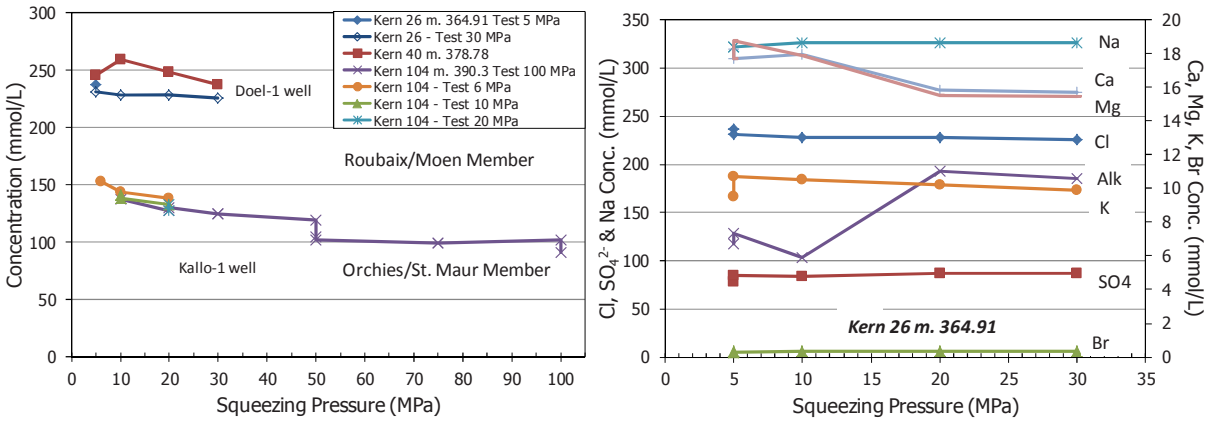


Figure 2. a) Chloride concentration as a function of squeezing pressure, and b) Pore water composition as a function of squeezing pressure in the core sample Kern 26 m. 364.91 from the Doel-1 well

References:

Fernández, A. M., Sánchez-Ledesma, D. M., Tournassat, C., Melón, A., Gaucher, E. C., Astudillo, J., Vinsot, A., 2014. Applying the Squeezing Technique to Highly Consolidated Clayrocks for Pore Water Characterisation: Lessons Learned from Experiments at the Mont Terri Rock Laboratory. *Applied Geochemistry*, 49, 2-21.

Fernández, A.M., Melón, A., Sánchez-Ledesma, Gaucher, E., Tournassat, C., Altmann, S., Vinsot, A., Maes, N., De Craen, M., Leupin, O., Wersin, P., Astudillo, J., 2009. Study of different Argillaceous Formations performed in the context of the FUNMIG Project. Publicación Técnica de Enresa 05/2009, 214 pp.

Van Marcke, P, Laenen, B., 2005. The Ypresian clays as possible host rock for radioactive waste disposal: an evaluation. ONDRAF/NIRAS Technical Report, Publication NIROND 2005-01.

Pitfalls in using the hexammine cobalt method for cation exchange capacity measurements on clay minerals and clay-rocks: redox interferences between the cationic dye and the sample.

Jebril Hadi[1,2], Christophe Tournassat[1], Paul Wersin[2] and Catherine Lerouge[1]

[1]BRGM, D3E/SVP, 3 avenue Claude Guillemin, 45060 Orléans, France
[2]Rock-Water Interaction (RWI), Institute of Geological Sciences, CH-3012 Bern, Switzerland

Cation exchange capacity (CEC) is an important property of clay minerals, indicating their ability to exchange cations with a surrounding solution. The CEC originates from the negative charge of the structural layers of clay particles, which is compensated by the adsorption of cations on the clay surface. CEC is usually measured through the use of index cations which replace those from the clay exchanger. Among the various existing index cations, cationic dyes, such as copper triethylenetetramine (Cu-Trien) or hexammine cobalt trichloride (CoHex), are popular in clay chemistry because a short single extraction followed by colorimetric measurements is sufficient to measure accurately the CEC with those cationic dyes. In addition, the analysis of extracted cations provides an additional control on the CEC measurement.

The methodology related to these cationic dyes and their applications are relatively well documented (e.g. [1-5]). However, these cationic dyes are redox sensitive species [6-8] and, surprisingly, the existing literature does not contain any information on possible biases to the method in relation to this redox reactivity. The present study focuses on the application of CoHex method on three kinds of clay samples: (i) oxidized smectites (in their pristine state), (ii) chemically reduced smectites and (iii) preserved clay rock samples originating from various deep formations. Results obtained with chemically reduced samples show unambiguously that redox reactions occur between the clays' structural Fe(II) and Co(III) from the cationic dye, leading to a great overestimation of the CEC values calculated from the colorimetric assays (Figure 1). However, our results show that in those conditions, the CEC can still be correctly determined from the analysis of extracted cations, provided that information on soluble salts present in the sample are also known. Moreover, a reduction of the cationic dyes leads to a large release of ammonia in solution, originating from the coordination sphere of Co(III) in the CoHex. In that case, a correct determination of the CEC based on the colorimetric method is made difficult if not impossible.

The interaction of the cationic dye with aqueous Fe(II) in anoxic conditions has also been investigated in parallel. All aqueous iron is removed rapidly from the solution through oxidation and co-precipitation in a layered double hydroxide phase mixed to magnetic oxides [9]. Consequently, the CoHex method is not reliable for measurement of exchangeable Fe(II) in clay samples.

Samples from deep underground clay formations such as Opalinus Clay and Callovian-Oxfordian clay-rocks contain reductive chemical species such as Fe(II) in various minerals (*e.g.* clays, pyrite, carbonates). Redox interactions between such species and the cationic dye can impede a correct interpretation of CEC colorimetric measurements, and also comparison of those values with CEC values determined from extracted cations assays. For instance, our results explain the anomalously high exchanged ammonia concentration that was measured on Opalinus Clay samples using the CoHex method ([10]), a result that was not understood until now.

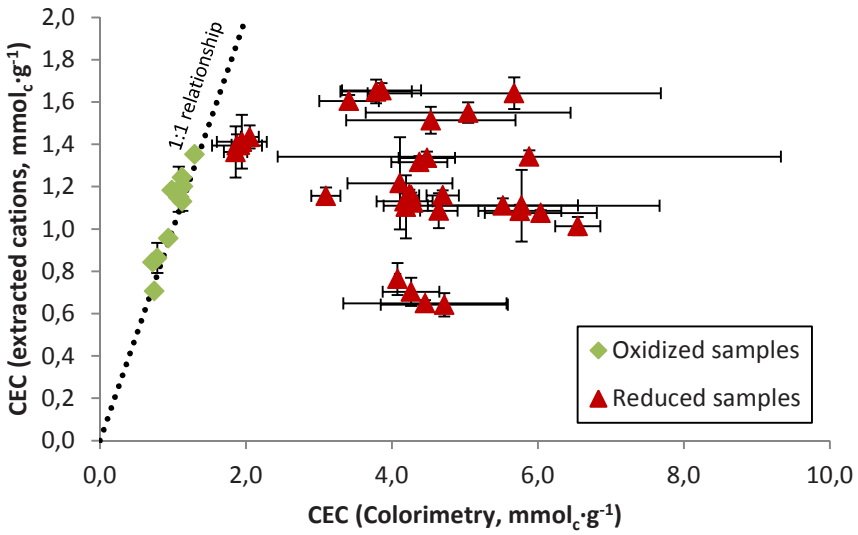


Figure 1. Comparison between two approches for CEC determination (raw colorimetric measurements vs. raw extracted cation analysis) on two series of samples: oxidised (green diamonds) and reduced (red triangles) pure smectites. CEC measurements from the two approaches compare well on oxidized samples but strongly disagree on reduced samples. In this case, colorimetric CEC values are obviously incorrect. Error bars reflect two times the standard deviation of triplicate measurments.

References

[1] R. Morel, *Etude expérimentale des phénomènes d'échange sur différents minéraux argileux*, Annales Agronomiques (Paris) 8 (1957) 5.
[2] J.C. Rémy, L. Orsini, *Utilisation du chlorure de cobaltihéxamine pour la détermination simultanée de la capacité d'échange et des bases échangeables dans les sols*, Sciences du Sol 4 (1976) 269.
[3] L.P. Meier, G. Kahr, *Determination of the cation exchange capacity (CEC) of clay minerals using the complexes of copper(II) ion with triethylenetetramine and tetraethylenepentamine*, Clays Clay Miner. 47 (1999) 386.
[4] Afnor, in: *Détermination de la capacité d'échange cationique (CEC) effective et des cations échangeables à l'aide d'une solution de trichlorure de cobaltihéxamine*. 2007.
[5] R. Dohrmann, S. Kaufhold, *Three new, quick CEC methods for determining the amounts of exchangeable calcium cations in calcareous clays*, Clays Clay Miner. 57 (2009) 338.
[6] I.M. Kolthoff, S.E. Khalafalla, *The composition and reactivity of the precipitate formed at the dropping mercury electrode upon one-electron reduction of hexaamminecobalt(III)*, Inorg. Chem. 2 (1963) 133.
[7] A. Yamada, T. Yoshikuni, Y. Kato, N. Tanaka, *Computer-aided measurement of kinetic parameters of electrode reactions of cobalt(III)—ammine complexes at mercury electrodes*, Analytica Chimica Acta-Computer Techniques and Optimization 5 (1981) 421.
[8] X.B. Ji, M.C. Buzzeo, C.E. Banks, R.G. Compton, *Electrochemical response of cobalt(II) in the presence of ammonia*, Electroanalysis 18 (2006) 44.
[9] J. Hadi, S. Grangeon, F. Warmont, A. Seron, J.M. Greneche, *A novel and easy chemical-clock synthesis of nanocrystalline iron-cobalt bearing layered double hydroxides*, J. Colloid Interface Sci. 433 (2014) 130.
[10] F.J. Pearson, D. Arcos, J.-Y. Boisson, A.M. Fernandez, H.-E. Gäbler, E. Gaucher, A. Gautschi, L. Griffault, P. Hernan, H.N. Waber, in: *Mont Terri project - Geochemistry of water in the Opalinus clay formation at the Mont Terri Rock Laboratory.*, Bern, 2003.

A new method for extraction and characterization of porewater chemistry in low-permeability sedimentary rocks

Magda Celejewski[a], **Tom Al**[a], **Ian Clark**[b]

[a] Department of Earth Sciences, University of New Brunswick, Fredericton, New Brunswick, E3B 5A3, Canada
[b] Department of Earth Sciences, University of Ottawa, Ottawa, Ontario, K1N 6N5, Canada

Measurements of spatial variability of naturally-occurring tracers in porewater from low-permeability rocks can provide insight into porewater residence time and the nature of solute transport. These system characteristics, in turn, are required to assess the long-term stability of geologic systems for waste management. However, the measurement of porewater chemistry in low-permeability rocks is challenging because of small fluid volumes and the difficulty of extracting representative samples. Several techniques for porewater characterization are available, but the results they provide can be affected by ion exchange and mineral dissolution, and they may require independent porosity measurements.
The objectives of this work are to develop and test a method of extracting representative samples of *in-situ* porewater from low-permeability rocks, and to accurately quantify solute concentrations in the extracted porewater. The method involves extraction of porewater by absorption into hydrophilic cellulosic membranes. The mass of extracted water is measured by near infrared (NIR) spectrometry, and the masses of solutes extracted with the porewater are quantified by inductively coupled mass spectrometry (ICP-MS). *In-situ* porewater solute concentrations are obtained by normalizing solute mass to water mass. Laboratory experiments using controlled additions of brine to cellulosic membranes confirm that the method is capable of providing porewater solute concentrations with precision and accuracy that are within the limits suggested by USEPA Method 6020A for analysis of saline water samples by ICP-MS (Figure 1).

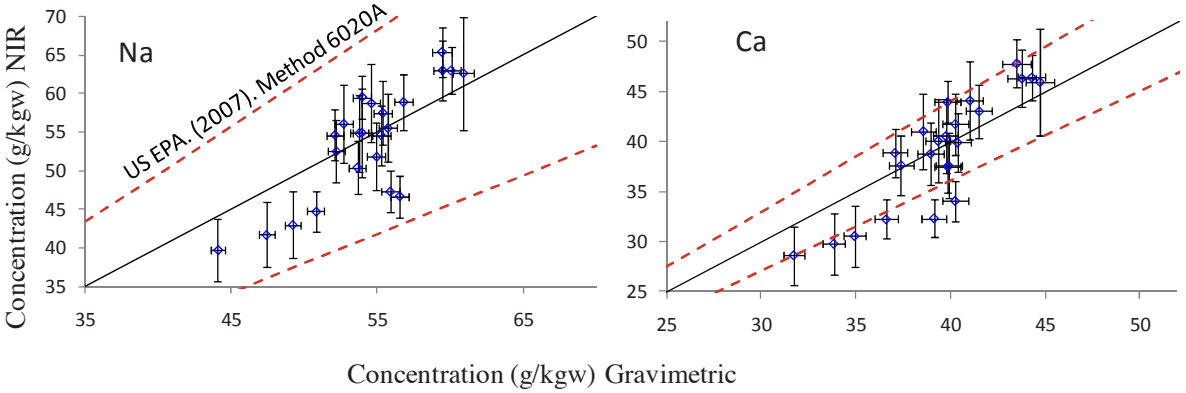


Figure 1. Examples of Na and Ca concentrations (g/kgw) calculated from water masses measured gravimetrically and by NIR spectrometry. The dashed lines correspond to a relative error margin accepted by US EPA method 6020a. Error bars depict the propagated instrumental error from NIR spectrometric and gravimetric water measurements and ICP-MS solute analysis

Field trials were conducted on paired samples of low-permeability ($K < 10^{-12}$ m/s, porosity < 10 %) shale drill cores from the Michigan Basin in Kincardine, Ontario using the absorption method and an established crush and leach method. A direct comparison of major ion (Na^+, K^+, Mg^{2+}, Ca^{2+}, Sr^{2+}, Cl^-, Br^-) ratios demonstrates that the absorption method provides precise porewater chemistry data that are independent of porosity, and should be free of ion exchange and mineral precipitation/dissolution artefacts (Figure 2).

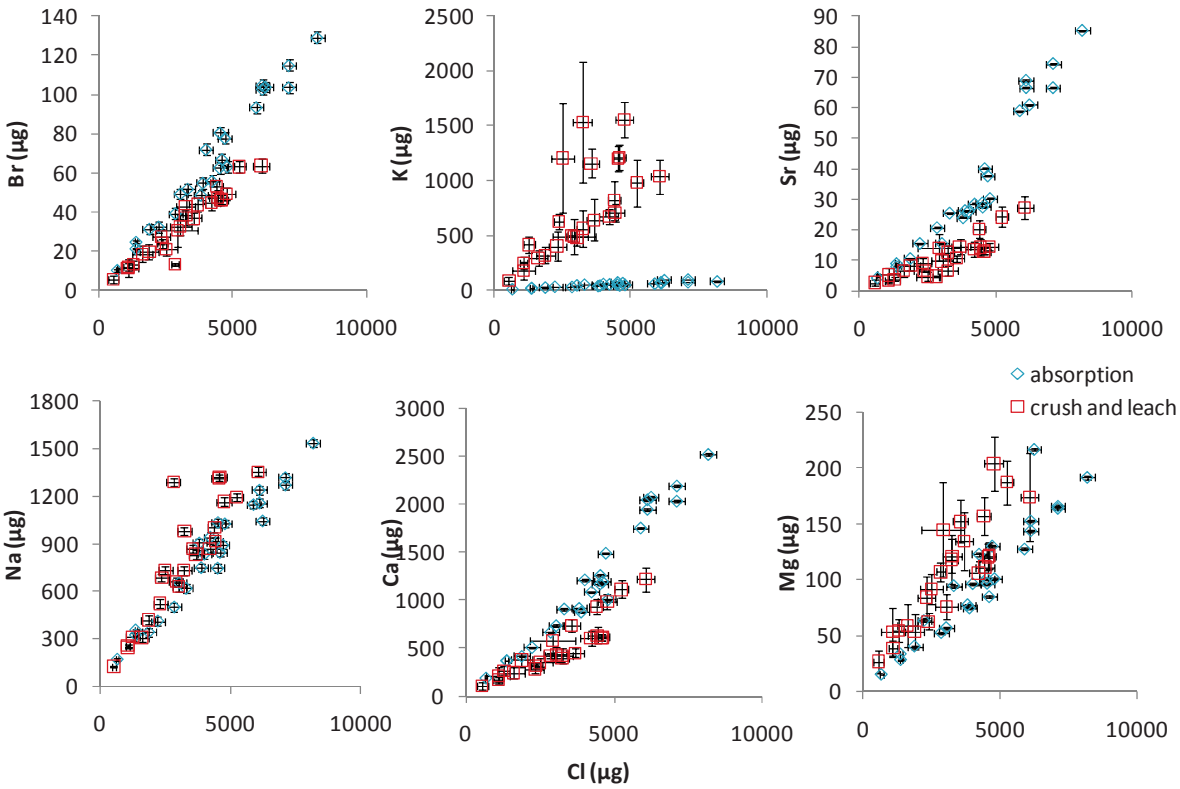


Figure 2. Solute ratio comparisons depicting the porewater solute masses obtained using the absorption method (◊) and a crush and leach method (□).

A detailed description of the absorption method will be provided, followed by the results of porewater extractions from Opalinus Clay ($K < 10^{-12}$ m/s, porosity < 22 %) obtained from a deep borehole at the Mont Terri Laboratory, Switzerland. Concentrations of major ions will be quantified and compared to results from other methods.

Competitive sorption and sequential reduction of Cr, As and Sb in argillaceous rock suspension under oscillating redox conditions

***Ekaterina Markelova*[1,2*], Christopher T. Parsons[2], Raoul-Marie Couture[2,3], Delphine Tisserand[1], Benoit Madé[4], Philippe Van Cappellen[2], Laurent Charlet[1]**

[1]ISTerre, University of Grenoble (38041 Grenoble CEDEX 9, France);
[2]Ecohydrology, University of Waterloo (N2L3G1 Waterloo 200 University Av W, Canada);
[3]NIVA (NO-0349 Oslo Gaustadalleen 21, Norway);
[4]Andra (92298 Chatenay-Malabry Cedex, Parc de la Croix-Blanche, 1-7 rue Jean-Monnet, France);
[*]corresponding author: ekaterina.markelova@uwaterloo.ca

Introduction. Storage of radioactive waste containing radionuclides and toxic chemicals require understanding of the potential release of highly toxic non-radioactive inorganic contaminants, such as Cr, As and Sb in a clayrock surface environment. Once contaminants are released from engineered barriers, their mobility and toxicity will be controlled by their speciation and restricted by the argillaceous geological barrier in place. That is, contaminant fate will ultimately depend on the environmental conditions (abiotic, biotic, redox state) and on the sorption capacity of the surrounding matrix, including the clay minerals present in it.

Methods. Batch experiments in bioreactors were conducted to investigate the mobility of aqueous Cr(VI), As(V) and Sb(V) under a variety of possible subsurface conditions and leakage scenarios, resulting in contact of these redox-sensitive contaminants with clay rock (50 g L^{-1}), pore water (synthetic media) and microorganisms, both under anoxic and oxic conditions. The fate of contaminants in clay/soil suspensions under redox oscillating conditions has previously been investigated individually (Parsons et al., 2013; Hockmann et al., 2014; Ilgen et al., 2014). The research presented here is focused on the behavior of the combination of multiple aqueous contaminants to better mimic diverse waste conditions and examine the competitive sorption and sequential reduction of the above-mentioned oxyanions.

Redox oscillations were induced by alternate sparging of gas mixtures for periods of 7 days: 1% CO_2 + 99% N_2 and 1% CO_2 + 79% N_2 + 20% O_2. This resulted in quite small redox potential (E_H) fluctuations in a range from +254±9 mV to +338±2 mV (*vs*. SHE) with no decrease to negative values at pH 6.87, T = 25°C, I = 0.05 M. Abiotic conditions were ensured by high-temperature sterilization of clay and the use of microbial inhibitors (sodium azide, streptomycin, kanamycin sulfate). Biotic conditions were initiated by the injection of soil inoculum in the beginning of the experiment followed by regular additions of organic carbon (ethanol) every 14 days at the beginning of each anoxic phase. Microbial activity was monitored in terms of adenosine triphosphate (ATP) concentrations. Solid phase elemental concentrations were determined using X-ray fluorescence spectrometry (XRF), while aqueous concentrations were analyzed by Inductively Coupled Plasma Atomic Emission Spectrometry (ICP-AES). Speciation analyses have been performed using HPLC coupled to hydride generation and atomic absorption spectroscopy (HG-AAS).

Results. Total aqueous concentrations demonstrate that the removal of the contaminants occurs the fastest and to the greatest extent in the biotic experiment under anoxic conditions (fig. 1). The immobilization percentages were 100% for Cr, 83% for As and 44% for Sb after 7 successive redox-oscillating phases. The Cr depletion by the end of the first anoxic phase suggests the complete reduction of soluble Cr(VI) (0.5 mmol L^{-1}) to insoluble Cr(III) compounds. Arsenic speciation analyses indicate the reduction of As(V) (0.5 mmol L^{-1}) to As(III) at a slower rate, but concurrent with chromium reduction coupled to ethanol oxidation at E_H = 255 mV. Upon reduction of Cr and As, an increase in the removal rate of total aqueous Sb was observed. Antimony speciation analyzes will be conducted to verify the proposed microbial reduction sequence of the contaminant oxyanions:
$CrO_4^{2-} + HAsO_4^{2-} \rightarrow Sb(OH)_6^-$.

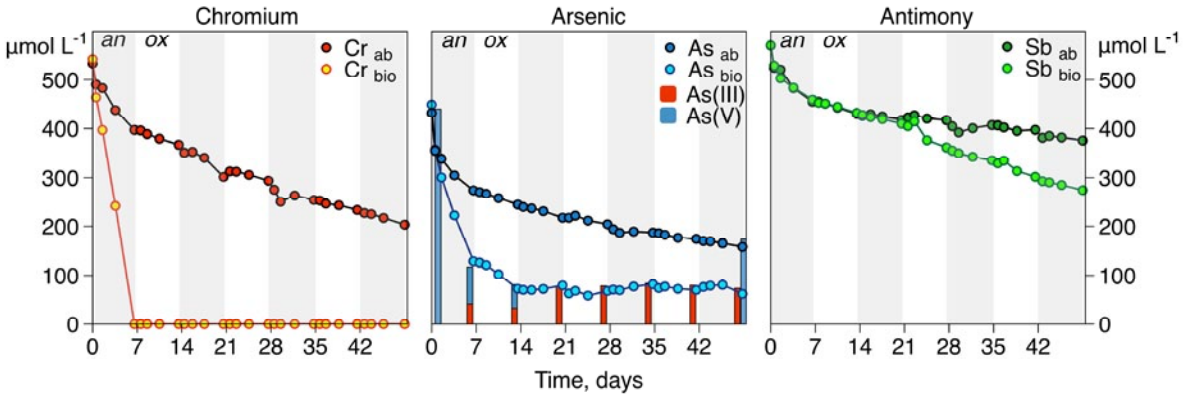


Figure 1. Retention behavior of Cr, As, Sb within argillaceous rock suspension under anoxic (an) and oxic (ox) conditions in abiotic (ab) and biotic (bio) environments.

Discussion. The weak sorption behaviour observed in this study is interpreted in terms of electrostatic repulsion between the deprotonated clay surface and the negatively charged oxyanions at neutral pH. Additionally, the presence of competing ligands in pore water, such as sulfate (SO_4^{2-}, 4.4 mmol L^{-1}) and bicarbonate (HCO_3^-, mmol L^{-1}), that were introduced to the clay suspension along with the synthetic media and with the gaseous phase, respectively, may compete with the contaminant and reduce sorption capacity (Appelo, 2005).

Sb is found to be the most mobile contaminant compared to Cr and As under all experimental conditions. In the abiotic scenario the immobilization of dissolved oxyanions is attributed to competitive sorption to matrix minerals. The highest binding affinity belonged to arsenate (Kd = 42.63 L kg^{-1}), followed by chromate (Kd = 31.75 L kg^{-1}) and antimonate (Kd = 10.13 L kg^{-1}) at pH 7. The stronger adsorption of arsenate can be ascribed to the fact that surface hydroxyl groups can be protonated by the proton of $HAsO_4^{2-}$. In contrast, CrO_4^{2-} is deprotonated and, therefore, less adsorbing, while $Sb(OH)_6^-$ contains hydroxyl group, which is even more resisting adsorption. The relative solid concentrations revealed an accumulation of As and Cr in the solid phase in proportion to their removal from the solution by the end of the experiments.

At neutral pH, stimulation of reduction reactions leads to the decrease of aqueous contaminant concentrations likely via formation of precipitates ($Cr(OH)_3°$ or Cr_2O_3) or soluble neutrally charged complexes ($H_3AsO_3°$, $Sb(OH)_3°$). The interaction between PZC of matrix minerals (34% of kaolinite with pzc = 4.6 and 25.5% of SiO_2 with pzc = 2.0) and pKa of arsenite and antimonite determine the adsorption envelope, that is, larger pKa values of reduced species (pKa_1 ($H_3AsO_3°$) = 9.22 and pKa_1 ($Sb(OH)_3°$) = 11.8) have relatively higher affinity with negatively charged surfaces as compared to their oxidized species (pKa_1 ($HAsO_4^{2-}$ = 2.3 and pKa_1 ($Sb(OH)_6^-$) = 2.7) at pH 7.

Implications. Despite greater removal of reduced species under redox-oscillating conditions, toxic As and Sb compounds are persistent in solution and can be volatilized (Feldmann, 1995; Vriens et al., 2013). This could increase the risk for the environment and suggests that the mobility of these contaminants in reducing clays is of concern.

References

Appelo, C. (2005). Geochemistry, groundwater and pollution, 2nd ed. Balkema, Leiden ;;New York.
Feldmann, J., Hirner, A.V. (1995). *Int. J. Environ. Anal. Chem.* 60, 339–359.
Hockmann, K., Lenz, M., Tandy, S., Nachtegaal, M., Janousch, M., & Schulin, R. (2014). *J. Hazard. Mater.*, *275*, 215–21.
Ilgen, A. G., Majs, F., Barker, A. J., Douglas, T. A., & Trainor, T. P. (2014). *Geochim. Cosmochim. Acta*, *132*, 16–30. doi:10.1016/j.gca.2014.01.019
Parsons, C. T., Couture, R.-M., Omoregie, E. O., Bardelli, F., Greneche, J.-M., Roman-Ross, G., & Charlet, L. (2013). *Environ. Pollut. (Barking, Essex : 1987)*, *178*, 254–63.
Vriens, B., Lenz, M., Charlet, L., Berg, M., Winkel, L.H.E. (2013). *Nature Comm.*, 3035, doi:10.1038/ncomms4035.

CLAY CONFERENCE

BRUSSELS | March 23-26, 2015

6th International conference | SQUARE Brussels Meeting Centre



ABSTRACTS
POSTER SESSIONS

Thermodynamic and fully-coupled reactive transport simulations of a steel-bentonite interface

***James Wilson*[1]*, Steven Benbow[2], Hiroshi Sasamoto[3], David Savage[4], Claire Watson[2]**

1. Quintessa Ltd., 633-635 Birchwood Boulevard, Warrington WA3 7QU, United Kingdom.
2. Quintessa Ltd., The Hub, 14 Station Road, Henley-on-Thames, Oxfordshire RG9 1AY, United Kingdom.
3. Japan Atomic Energy Agency (JAEA) 432-2 Hokushin, Horonobe, Teshio-gun, Hokkaido 098-3224, Japan.
4. Savage Earth Associates Ltd. 32 St Albans Avenue, Bournemouth, BH8 9EE, United Kingdom.

*corresponding author: jameswilson@quintessa.org

Engineered barrier system (EBS) designs for the geological disposal of high-level radioactive waste often include a bentonite buffer. One potentially deleterious process that could occur in the buffer is the alteration of swelling clay to iron-rich minerals, some of which have a limited capacity to swell. There is a lack of relevant natural analogues of iron-bentonite interactions and experimental data do not provide an unequivocal indication of the conditions that will promote non-swelling clay minerals (such as berthierine or cronstedtite) to form rather than swelling clays (such as iron-rich saponite). In addition, many of the previously-published reactive transport models of iron-bentonite or iron-claystone interfaces have not considered how the evolution of mineral-fluid equilibria in the bentonite buffer could affect the nature and rate of steel corrosion. In this study, new thermodynamic models of iron-rich clay minerals are presented which suggest that the activities of major ions, especially Fe^{2+}, Fe^{3+}, Al^{3+}, H^+ and $SiO_{2(aq)}$, act as key controls on the relative stabilities of Fe-rich clay minerals. In particular, they suggest that Fe-saponite is stabilised under low $f\ O_{2(g)}$ conditions when $SiO_{2(aq)}$ activities are buffered by quartz or more soluble silica polymorphs (e.g. chalcedony). Iron (II)-rich 1:1 clay minerals (such as berthierine) tend to be stabilised in fluids that are quartz under-saturated (Figure 1).

The thermodynamic models were used to inform the development of fully-coupled reactive transport simulations of the Japanese 'H-12' HLW concept that includes a steel overpack surrounded by a cylindrical 70 cm-thick bentonite/sand buffer. Three models were constructed: (1) steel corrosion reaction applied on a boundary directly in contact with bentonite at a fixed rate; (2) steel corrosion reaction applied on a boundary directly in contact with bentonite at a diffusion-limited rate; and (3) a 'corrosion cell' representation with a fixed steel corrosion rate. The simulations were run at a temperature of 70 °C. The extent and nature of the alteration predicted by the models was found to be sensitive to model conceptualisation. The 'corrosion cell' assumption leads to steel corrosion products including magnetite and siderite and the alteration of primary minerals to berthierine (~2 cm thick layer forming over 100 000 years, with partial loss of montmorillonite to a depth of ~9 cm). In contrast, the boundary corrosion assumption with a fixed steel corrosion rate leads to faster alteration to swelling and non-swelling iron-rich clay minerals (with loss of bentonite porosity next to the steel occurring after 2100 years, Figure 2). In the diffusion-limited corrosion rate model, the steel corrosion rate varies over time as the bentonite porewater composition evolves and there is a strong coupling of steel corrosion rate to porewater pH. Depending on model assumptions, the steel corrosion rate may be up to 2 or 3 orders of magnitude lower than is typically assumed in performance assessment models and the spatial extent of alteration is much more limited (millimetre rather than centimetre scale, Figure 2).

Although much progress has been made in understanding iron-bentonite interactions, a number of uncertainties associated with modelling bentonite evolution remain, especially with regard to ion transport through smectite interlayers and the potential for complex couplings between chemical and physical processes.

This study was conducted as part of H22 'The project for Assessment Methodology Development of Chemical Effects on Geological Disposal System' funded by the Ministry of Economy, Trade and Industry of Japan.

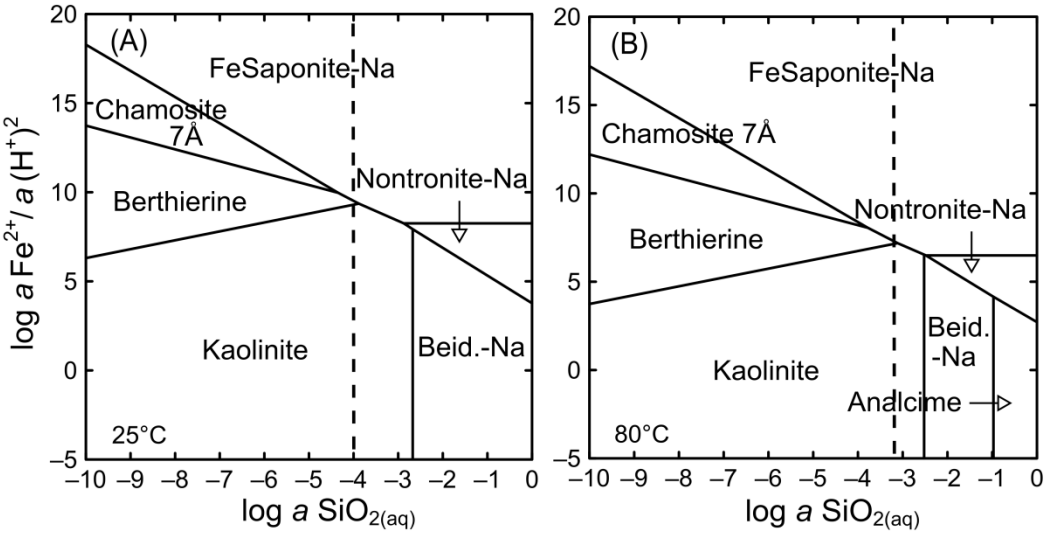


Figure 1: Activity diagrams showing smectite and 1:1 layer silicate stability fields in the system Al_2O_3- FeO-Fe_2O_3-H_2O- SiO_2 at 25 °C (left) and 80 °C (right) with $f\,O_{2(g)}$ set at magnetite-hematite equilibrium (log a Na^+ / a H^+ = 5). The dashed line corresponds to quartz equilibrium. Note that iron(II)-rich 1:1 clay minerals (such as berthierine) tend to be stabilised in fluids that are quartz under-saturated.

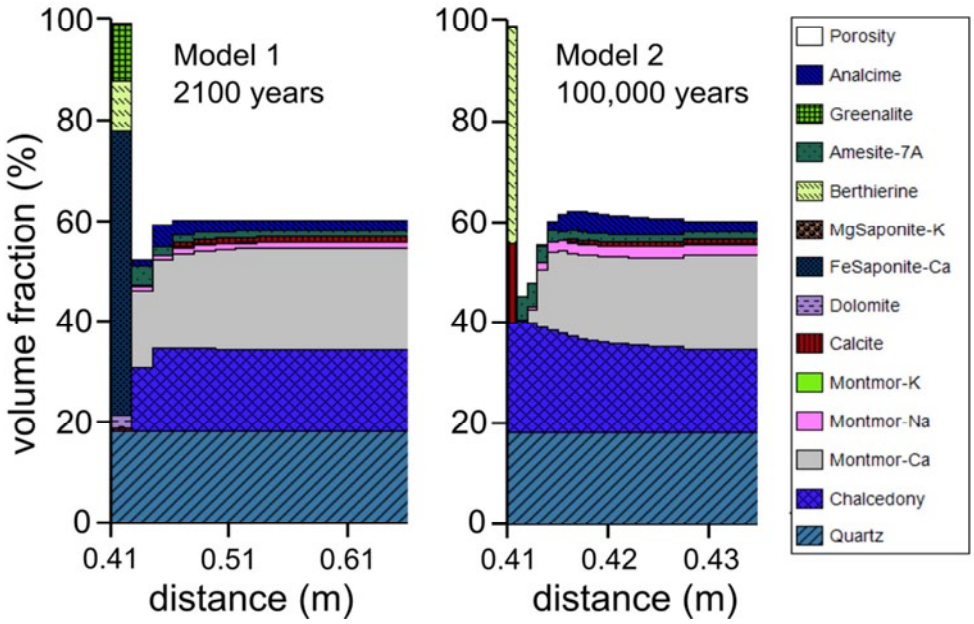


Figure 2: Volume fraction plots for Model 1 (fixed steel corrosion rate of 1µm/yr) and Model 2 (diffusion-limited corrosion rate) iron-bentonite simulations. The cylindrical steel overpack has a radius of 0.41m (note different length scales in the plots).

Instantaneous corrosion rate measurements on carbon steel in Opalinus clay at 90 °C – Bilan after 6 years

S.Necib[1], C.Bataillon[2], S.Daumas[3], D.Crusset[4], S.Dewonck[1]

1.Andra, Meuse/Haute Marne Center, 52290 Bure, France 2. CEA, Saclay ; 3. CFG Services, Marseille, France,4. Andra, 92290 Châtenay-Malabry, France

Carbon steel (C-steel) is studied to be the reference material for the metallic components in the high level waste (HLW) repository concepts of several European countries such as France, Switzerland, Belgium. Initially, oxygen is expected to be present and rapidly consumed by the host rock and corrosion processes. Therefore anoxic conditions will prevail afterwards. Moreover, temperature will increase up to 90°C due to radioactive decay.

In order to measure the instantaneous corrosion rate (CR) of C-steel under anoxic conditions at 90°C, an *in situ* experiment has been conducted in the Mont-Terri underground rock laboratory (URL) based in Switzerland.

The test chamber located in a vertical borehole 8 m deep (see Figure 1), contained a three electrochemical cell to perform electrochemical impedance spectroscopy (EIS) and therefore determine the instantaneous CR of C-steel in contact with porewater with a significant S/V ratio (surface area of the material/volume of the electrolyte). All the electrodes were connected to a potentiostat located in a surface cabinet in the gallery.

After six years of experiment, carbon steel materials have shown a decrease of the corrosion rate over time followed by a steady state of the CR at less than 2 μm/year (see Figure 2). The last measurements revealed that it was not possible to extrapolate the transfer resistor anymore, and the EIS diagrams imply the presence of a blocking passive film at the metal/electrolyte interface.

Further to dismantling, it will be possible to characterise the corrosion products formed at the metal/surface interface.

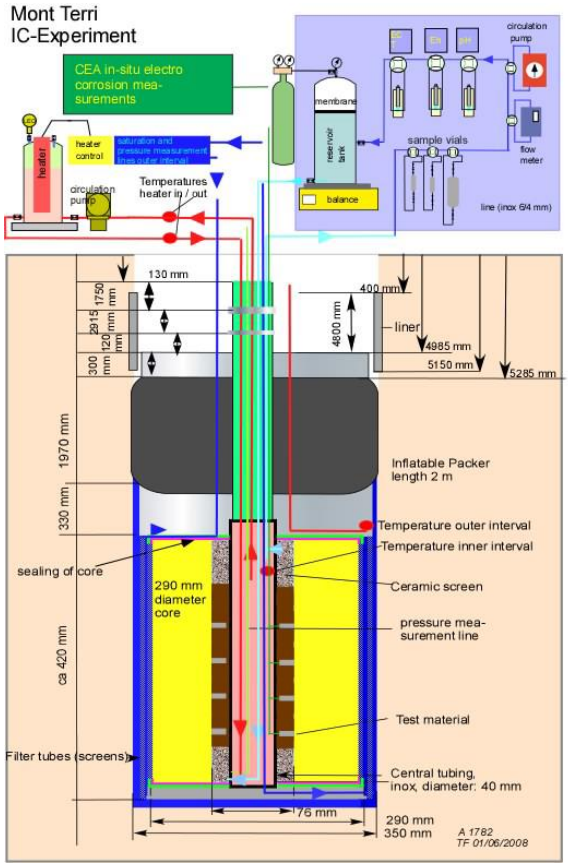


Figure 1: Schematic diagram of the experimental setup

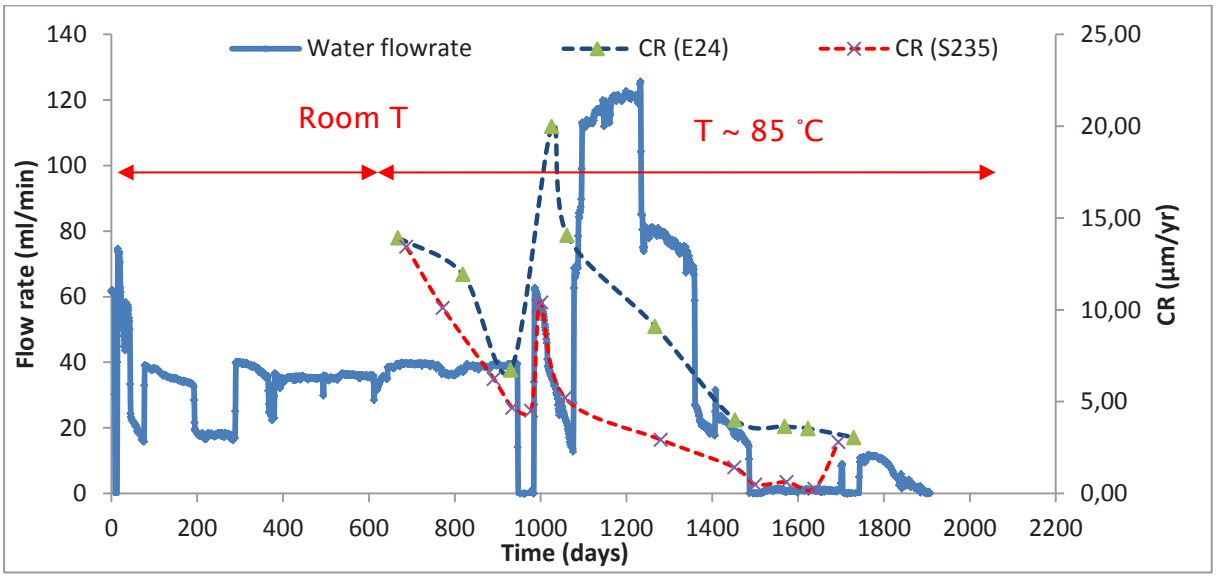


Figure 2: Evolution of the corrosion rate (CR) of C-steel materials over time in Opalinus clay

Modelling *in-situ* experiments of water-iron-claystone interactions and up-scaling to an HLW cell

James C. Wilson[1]*, Steven Benbow[2], David Savage[3], Nicolas Michau[4], Sophia Necib-Ammour[4]

1. Quintessa Ltd., 633-635 Birchwood Boulevard, Warrington WA3 7QU, United Kingdom.
2. Quintessa Ltd., The Hub, 14 Station Road, Henley-on-Thames, Oxfordshire RG9 1AY, United Kingdom.
3. Savage Earth Associates Ltd. 32 St Albans Avenue, Bournemouth, BH8 9EE, United Kingdom.
4. ANDRA, 1/7 rue Jean Monnet, 92298 Châtenay-Malabry Cedrex, France.

* corresponding author: jameswilson@quintessa.org

Engineered barrier system (EBS) designs for the geological disposal of high-level radioactive waste often include steel components and clay minerals. The French HLW cell design includes a steel liner emplaced within the Callovo-Oxfordian (COx) claystone. To explore possible rates of steel corrosion in such a system, the 'MCO1202' in situ experiment was set up in the underground laboratory at Bure to explore the rate and nature of steel corrosion in the presence of Callovo-Oxfordian (COx) claystone porewater. Geochemical (reactive-transport) models of the experiment were constructed in order to explore controls on steel corrosion rates and inform models of the long-term evolution of the HLW cell. Experimental results were not made available to the modellers during the model development stage; however, it was made clear that heterogeneous damaged thicknesses of corrosion products had been observed and that it had been hypothesised that measured corrosion rates may have been influenced by factors such as the initial oxidation of the claystone followed by an acidic pH transient.

Geochemical models were constructed using the Quintessa code 'QPAC'. Given the complexity associated with the MCO experiment, the approach taken in developing the models was to start with a simple representation of the experiment, and then incrementally increase the complexity of the models. This would allow factors having a strong influence on the rate of corrosion to be clearly identified. Two conceptual models were developed, the first assumed water-saturated conditions in the experimental region and claystone (Figure 1), the second was more complex and included multiphase flow. A number of fully-coupled reactive-transport simulations were developed to explore the effect of assuming either no oxidation of the COx in contact with the experiment vessel, or partial oxidation during emplacement of the experiment. Mineral dissolution-precipitation processes were modelled using a Transition-State-Theory expression with terms for pH and T dependency of reaction rates. The simulations included steel corrosion products and iron-rich clays.

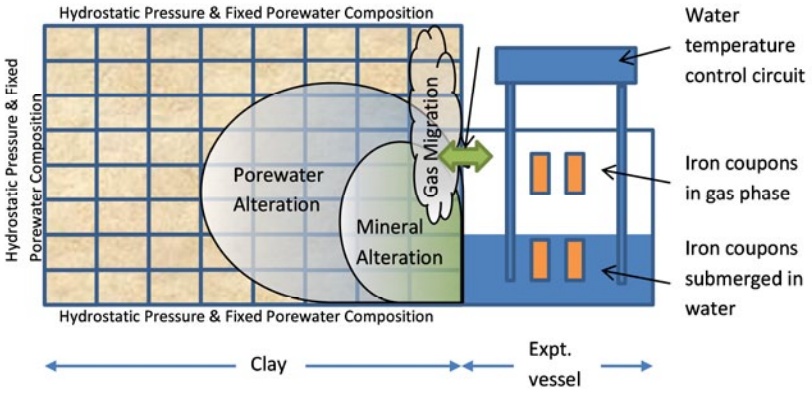


Figure 1: Schematic diagram showing the features and processes included in the MCO1202 experiment simulations constructed using QPAC.

Although there were some differences between the models and the experimental data, the broad evolution was successfully simulated. The models suggest that there may have been partial oxidation of the COx or a source of O_2 present in the MCO experiment that resulted in a reduction of pH which enhanced rates of steel corrosion. The 'expected evolution' simulation resulted in minor corrosion of steel samples (loss of 1.3 % of initial mass after 2 years), whereas in the worst-case 'partial oxidation' cases with a pH-dependent corrosion rate, and where elevated $f\,O_{2(g)}$ conditions were applied through the simulation, only 3.5 % of the initial mass of steel remained after 2 years. Different model assumptions led to the formation of different steel corrosion products, which included pyrite, magnetite, goethite, greenalite, siderite and mackinawaite.

The scale of the MCO experiment simulations was increased to that of a HLW cell (steel liner emplaced in COx) to investigate the impact of the corrosion models at full scale. The HLW geometry assumed that an Excavated Damaged Zone (EDZ) is created during the drilling, with a 'technological gap' being present between the steel HLW liner and COx. It was assumed that during the construction and/or operational period, 50% of the pyrite present throughout the EDZ is oxidised prior to the liner being able to react with the COx porewater. Although the technological gap will close with time, it was assumed in the conceptual model that this stays open. This is a conservative assumption which maximises the ratio of water volume to steel surface area. A thermal gradient was applied across the HLW cell (~80 ºC close to the steel liner). A number of cases were developed to explore different modelling assumptions (e.g. steel corrosion rate, possible steel corrosion products).

The processes observed in the MCO experiment simulations were also predicted in the up-scaled HLW cell models (initial pH reduction due to partial COx oxidation, potential for enhanced steel corrosion rate, formation of typical steel corrosion products and iron-rich clays, Figure 2). However, the simulations suggest that extensive corrosion phenomena seen in the MCO experiments and replicated by the MCO models are not necessarily expected to be possible in the up-scaled HLW geometry, due to the differences in the ratio of water to steel surface area. In considering the implications for the simulations for HLW cell performance, it must be remembered that the models are arguably somewhat conservative in nature, due to the fact that half of the pyrite present in the EDZ was assumed to have been oxidised during the early stages of repository evolution, and that the whole surface of the steel was allowed to react with the water volume present in the technological gap. It may be the case that if pyrite did oxidise in the COx, the alteration may be much less extensive than that assumed in the computer models.

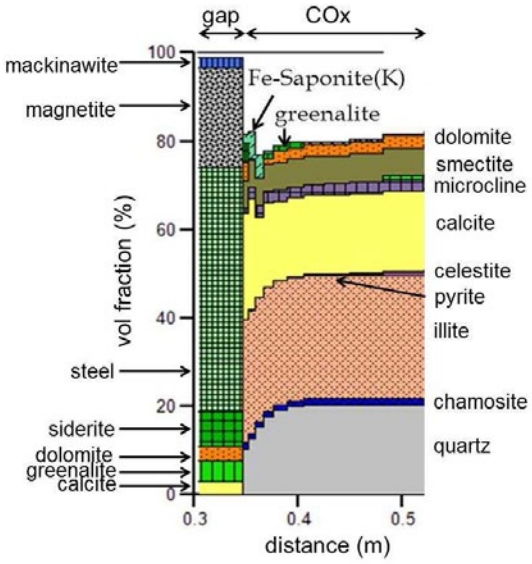


Figure 2: Volume fraction plot for HLW Concept 1 'An1' simulation (temperature-dependent steel corrosion rate, 3 µm/year at 25 ºC) after 1259 years, by which time the gap between the claystone and the steel liner (pessimistically assumed to stay open) became full of steel corrosion products.

How CEC determination can provide information about reactivity between iron powder and clay minerals?

Camille Rivard[1,2*], Pierre Le Pape[1,2], Angelina Razafitianamaharavo[1,2], *Manuel Pelletier*[1,2], Renaud Gley[1,2], Martine Mallet[3,4], Frédéric Villiéras[1,2], Nicolas Michau[5].

[1] Université de Lorraine, LIEC, UMR7360, Vandœuvre-lès-Nancy, F-54500, France
[2] CNRS, LIEC, UMR7360, Vandœuvre-lès-Nancy, F-54500, France
[3] Université de Lorraine, LCPME, UMR7564, Villers-lès-Nancy, France F-54600, France
[4] CNRS, LCPME, UMR7564, Villers-lès-Nancy, France F-54600, France
[5]Andra, Châtenay-Malabry, F-92298, France
* Current address: European Synchrotron Radiation Facility, Grenoble, F-38000, France

In the context of French geological repository of radioactive waste, a large series of studies were undertaken in order to better understand the interaction between metallic iron and clay minerals. Among these studies, batch experiments were performed to show how the nature of the pristine clay influences the formation mechanisms and the properties of newly formed mineral phases. Our experimental strategy was based on the use of iron (Fe0) powder (35 microns diameter) in a diluted suspension of purified clay minerals (liquid:solid ratio of 1:20), components of the Callovo-Oxfordian rocks, i.e. kaolinite, illite, montmorillonite, interlayered illite/smectite. Experiments with Callovo Oxfordian rock (COx) and extracted clay fraction of COx (COxCF) were also conducted. Samples were kept under anoxic atmosphere and at stable temperature of 90°C during durations from 1 to 9 months (Rivard 2011).

In order to characterize the newly formed products and to follow the evolution of clay mineral properties, a set of characterizations, included Cation Exchange Capacity (CEC) determination of initial and newly formed minerals, was used (Rivard et al. 2013a and b). CEC was obtained after cobaltihexamine exchange, using two distinct measurements (i) the cobaltihexamine ions concentration remaining in the exchange solution determined by UV spectrophotometry (referred to as CEC_{CoHex}), and (ii) the exchanged-cations concentration determined by atomic absorption spectroscopy (referred to as CEC_{Cat}).

For Fe0 free experiments the CEC_{CoHex} and CEC_{Cat} values were similar. However, in the case of iron/clay samples, a gap between the two values was systematically observed, as shown by results obtained after 1 month experiment (Table 1).

Table 1: CEC values and differences between CEC_{CoHex} and CEC_{Cat} measured on different purified clays in suspension with or without metallic iron, after one month interaction (clay purification and Na-saturation procedures described in Rivard 2011 and Rivard et al. 2013a).

samples		CEC_{CoHex} (meq/100 g)	CEC_{Cat} (meq/100 g)	ΔCEC (meq/100 g)
KGa-2 [1]	1m no Fe	2	4	-2
	1m Fe	26	3	23
Ill [2]	1m no Fe	26	25	1
	1m Fe	50	23	27
SWy-2 [1]	1m no Fe	96	94	2
	1m Fe	152	77	75
GB [3]	1m no Fe	93	93	1
	1m Fe	202	70	132
ISCz-1 [1]	1m no Fe	37	37	0
	1m Fe	63	23	40

[1] .From The Clay Mineral Society, [2] .From Socodis, Haute-Loire, France (Bardot et al. 1998), [3] .From IKO

To understand the specific interaction occurring between metallic iron surface and the cobaltihexamine, experiments involving magnetite and/or metallic iron powder in variable amounts were conducted. Those experiments provided a difference between measured CEC_{CoHex} and CEC_{Cat}

(ΔCEC), but only in the case of Fe0. Indeed, we could show that the presence of free metallic iron surface was affecting the cobaltihexamine concentration. SEM and XPS investigations of the iron grains surface unravelled the reduction of Co(III) to Co(II), as well as the formation of a surface product mainly identified as Co(II)-hydroxide. From CEC measurements, a linear relation could be established between Fe0 surface area (from 0.01 to 0.12 m^2/g) and CEC_{CoHex} value (Figure 1).

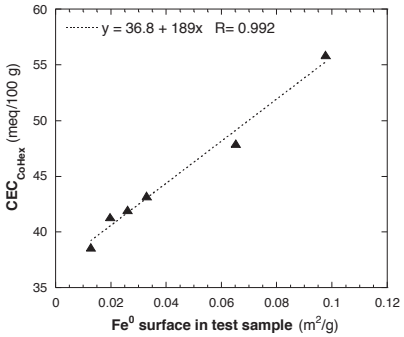


Figure 1. CEC_{CoHex} value as a function of the surface of Fe0 in the test sample, obtained by UV spectrophotometry.

To check the validity of our approach, we applied the ΔCEC proxy to a set of mixtures including COxCF and Fe0 powder displaying different grain sizes (from 20 μm to 1.5 mm). Knowing the introduced amount of Fe0 in each experiment, the ΔCEC could be used to estimate the Fe0 specific surface area (SSA). ΔCEC values suggest that for all experiments, the final Fe0 SSA is (i) generally higher than the initial one, (ii) higher than the theoretical value obtained by applying calculation considering a uniform surface corrosion model, and (iii) strongly higher in the presence of clays.
As the robustness of the ΔCEC proxy had been demonstrated, this proxy was also measured for the experiments involving purified clay minerals (Rivard C, 2011). ΔCEC values were shown to be higher for smectite clays (GB and SWy2), suggesting an increase of the Fe0 surface area with this kind of clay minerals.

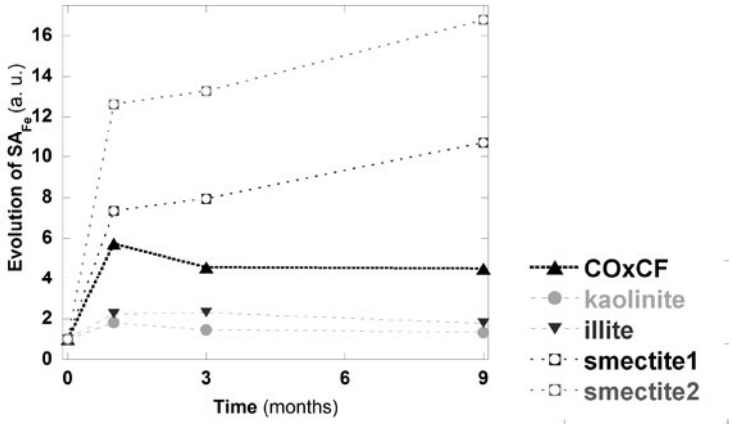


Figure 2: Evolution of the SSA_{Fe} as a function of time and type of clays (SSA Fe is determined from the ΔCEC measurement).

Rivard C. (2011) Contribution à l'étude de la stabilité des minéraux constitutifs de l'argilite du Callovo-Oxfordien en présence de fer à 90°C. Thèse de l'Institut National Polytechnique de Lorraine, Vandoeuvre-lès-Nancy, France, 331 p.

Rivard C., Montarges-Pelletier E., Vantelon D., Pelletier M., Karunakaran C., Michot L. J., Villieras F. and Michau N. (2013a) Combination of multi-scale and multi-edge X-ray spectroscopy for investigating the products obtained from the interaction between kaolinite and metallic iron in anoxic conditions at 90°C. *Physics and Chemistry of Minerals*, 40, 2, 115-132.

Rivard C., Pelletier M., Michau N., Razafitianamaharavo A., Bihannic I., Abdelmoula M., Ghanbaja J. and Villiéras F. (2013b) Berthierine-like mineral formation and stability during the interaction of kaolinite with metallic iron at 90°C under anoxic and oxic conditions. *American Mineralogist*, 98, 1, 163-180.

Carbonates reactivity in temperature and interactions with Fe-minerals

M. Debure[1,*], S. Grangeon[1], C. Lerouge[1], H. Gailhanou[1], B. Madé[2], C. Tournassat[1]
1. BRGM, French Geological Survey, D3E/SVP, 3, avenue Claude Guillemin - BP 36009, 45060 Orléans Cedex 2, France
(m.debure@brgm.fr, s.grangeon@brgm.fr, c.lerouge@brgm.fr, h.gailhanou@brgm.fr, c.tournassat@brgm.fr)
2. Andra, 1 – 7 rue Jean Monnet, 92298 Châtenay-Malabry, France (benoit.made@andra.fr)
*Corresponding author

The carbonate system is the one of most reactive in the mineralogical assemblages of clay-rocks. Consequently, pristine clay-rocks pore water compositions are expected to be at equilibrium with carbonate minerals. However, it is difficult to fully reconcile the concentration data obtained from seepage water sampled in equipped *in situ* boreholes with the equilibrium concentrations obtained from pore water modeling (Pearson et al., 2011). It is especially true for dolomite whose solubility spans a large range of values in thermodynamic database as a function of crystallinity considerations, and for siderite/ankerite or other Fe-bearing carbonates whose compositions influence their solubility. The understanding of the carbonate system in clay-rock is necessary for a number of predictions including the effect of an increase of temperature on the pore water chemistry. In this respect, experiments were conducted to study the kinetics of equilibration of carbonate mineral assemblages as a function of temperature (25-80°C) in chemical conditions otherwise similar to those encountered in the Callovian-Oxfordian clay-rock.

Several authors reported higher Ca releases than Mg releases in solution during dolomite dissolution (*e.g.* Pokrowsky and Schott, 2001, Gautelier et al., 2007; Urosevic et al., 2012; Debure et al., 2013). However, others authors observed in their studies some experiments that displayed higher Ca release than Mg and some others that exhibited only small differences between Ca and Mg concentrations in solution (e.g. Pokrowsky et al., 2005; Zhang et al., 2007). Dolomite incongruent dissolution has been explained by the lower hydration energy of Ca^{2+} compared to Mg^{2+} and leading to a lower stability of Ca^{2+} at the dolomite/water interface and to a Ca-depleted layer at the dolomite surface (Busenberg and Plummer; 1982; Pokrowsky and Schott, 2001; Zhang et al., 2007). More recently, Urosevic et al; (2012) evidence the formation of an $MgCO_3$ phase at the dolomite surface. However, the experimental data do not allow to quantitatively characterizing that phase. Such contradictory results underline the complexity of dolomite dissolution. In this study, dolomite dissolution in pure water was investigated. Solution composition was monitored as a function of time and the mineralogy and surface chemistry was characterized before and after reaction (XRD, SEM, TEM and Raman analyses). Experiments were performed with powders (< 12 μm) and with monocrystals. Mixed system such as dolomite/calcite and dolomite/calcite/goethite were investigated to quantify the Mg incorporation in calcite and the Fe incorporation in calcite and dolomite. Goethite was selected for those experiments in agreement with the presence of nanogoethite detected in COx samples (Gailhanou et al., 2012). These experiments were performed in a glove box with a 99%N_2/1%CO_2 atmosphere that is representative of the *in-situ* conditions (Gaucher et al., 2009) in order to preserve the systems from oxidizing perturbation and to buffer the pH.

For all the systems, high temperatures promoted high kinetic rate of dissolution and high concentrations in solution. Solution analyses did not evidence a large difference between Ca and Mg released in solution in the case of dolomite dissolution in pure water at 25°C and at 80°C. Nevertheless, TEM-EDX measurements showed the presence of incongruent Mg/Ca phases after reaction. SEM, Raman analyses did not evidence Mg-bearing minerals

precipitation but reveal the formation of hematite on the dolomite surface due to Fe impurities incorporated inside the crystals. In the calcite/dolomite systems, steady-state conditions were quickly reached if solutions with composition closed to the expected equilibrium conditions were used as initial bulk electrolytes.
In the dolomite/calcite/goethite systems, steady state conditions were quickly reached in solution as well (see Figure 1). TEM-EDX chemical analyses indicated a possible Fe incorporation in calcite and in dolomite. Further characterizations are in progress.

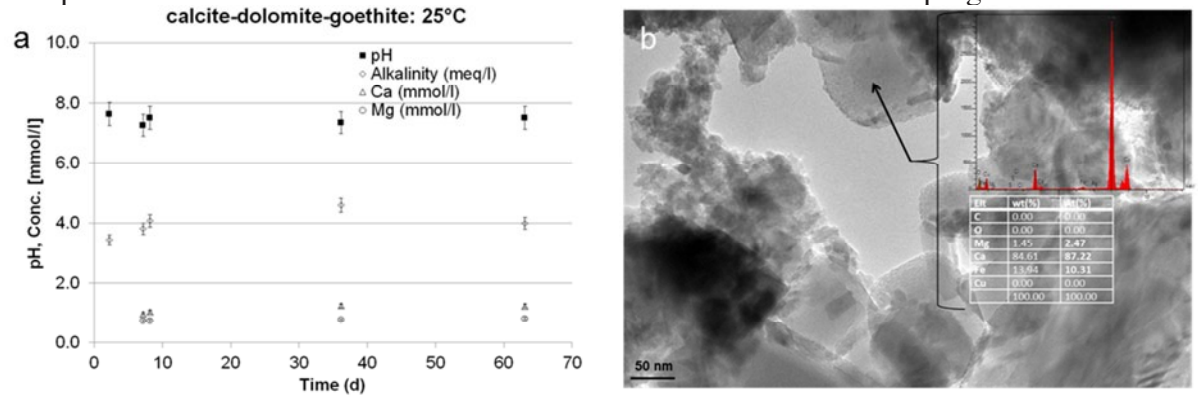


Figure 1. *Left :* evolution of pH in the batch solution and elements concentrations in solution over the time; *right:* TEM micrography showing a potential Fe incorporation in calcite in the case of calcite-dolomite-goethite experiment after 8 days of reaction at 80°C.

Finally, solution compositions at steady-state are mostly consistent with equilibrium calculations. The initially under-saturated solutions approach equilibrium with dolomite, calcite and/or magnesite, suggesting secondary phase's formation as observed by Urosevic et al. (2012). Additional analyses (*e.g.* Small-angle X-ray scattering) are foreseen to investigate dolomite crystal surface and to characterize secondary carbonates minerals.

References

Busenberg, E., Plummer, L.N., 1982. Am. J. Sci. 282, 45–78.

Debure, M., Frugier, P., De Windt, L., Gin, S., 2013. Appl. Geochem. 33, 237–251.

Gailhanou H., Tournassat C., Laperche V., Grangeon S., Blanc P., Marty N., Crouzet C., Henry B., Grenèche J.M., Kars M., Madé B., Altmann S. and Gaucher E.C., 2012. International meeting "Clays in Natural and Engineered Barriers for Radioactive Waste Confinement", Montpellier, France

Gaucher, E.C., Tournassat, C., Pearson, F.J., Blanc, P., Crouzet, C., Lerouge, C., Altmann, S., 2009. Geochim. Cosmochim. Acta 73, 6470–6487.

Gautelier, M., Schott, J., Oelkers, E.H., 2007. Chem. Geol. 242, 509–517.

Mettler, S., Wolthers, M., Charlet, L., von Gunten, U., 2009. Geochim. Cosmochim. Acta 73, 1826-1840.

Pearson, F. J., Tournassat, C. & Gaucher, E. C. 2011. Applied Geochemistry, 26, 990-1008

Pokrovsky, O.S., Schott, J., 2001. Am. J. Sci. 301, 597–626.

Pokrovsky, O.S., Golubev, S.V., Schott, J., 2005. Chem. Geol. 217, 239–255.

Urosevic, M., Rodriguez-Navarro, C., Putnis, C.V., Cardell, C., Putnis, A., Ruiz-Agudo, E.N., 2012. Geochim. Cosmochim. Acta 80, 1–13.

Zhang, R., Hu, S., Zhang, X., Yu, W., 2007. Aquat. Geochem. 13, 309–338

Interactions between Fe(0) and Illite-smectite mixed-layer minerals at 90 °C under anoxic conditions - investigation of iron speciation and reaction mechanisms

Pierre Le Pape[1,2], **Camille Rivard**[1,2]*, **Manuel Pelletier**[1,2], **Isabelle Bihannic**[1,2], **Sylvie Migot**[3], **Jaafar Ghanbaja**[3], **Mostapha Abdelmoula**[4], **Frédéric Villiéras**[1,2], **and Nicolas Michau**[5]

1 Université de Lorraine, LIEC, UMR7360 Vandoeuvre-lès-Nancy, F-54500, France
2 CNRS, LIEC, UMR7360Vandoeuvre-lès-Nancy, F-54500, France
3 Université de Lorraine - CNRS, IJL parc de Saurupt, CC-MEM, Nancy, F-54011 Cedex, France
4 CNRS, LCPME, UMR7564, Villers-lès-Nancy, France F-54600, France
5 Andra, Châtenay-Malabry, F-92298, France
* Current address: European Synchrotron Radiation Facility, Grenoble, F-38000, France

In France, the high level radioactive wastes resulting from the activity of nuclear power plants are planned to be deeply buried into the Callovo-oxfordian (COx) claystone formation. This rock contains a variety of clay minerals, namely kaolinite, illite, smectite, chlorite and mixed-layer Illite-Smectite minerals (IS), the latter representing at least 50 % of the clayey phases of COx. During the last decade, many studies were conducted to document the interactions between clay minerals previously mentioned and iron. However, only a few studies were dedicated to the specific investigation of iron/IS interactions.

We here present the results of iron/IS interactions in batch experiments performed at 90° and under anoxic conditions. We use powder metallic iron with mean diameter of 35μm, and purified I/S (ISCz-1) from Clay Mineral Society. Batch contents consisting in mixing of iron powder and an IS suspension with liquid/solid ratio of 1/20 and iron/clay ratio of 1/3, were sampled at different time step from two day to three months to observe the evolution in time of the reaction products (solid and aqueous solution). The powder samples resulting from the batch experiments were characterized using a wide range of microscopic methods (TEM/SEM-EDXS, HRTEM), spectroscopic methods (FTIR, Mossbauer), and by X-Ray Diffraction. Major cation concentrations were also measured in solution for each time step.

Results indicate that the system reactivity is not much different compared to experiments involving other clay phases, particularly illite or smectite (Rivard C., 2011). Indeed, iron dissolution leads to a fast pH increase (within the first days of the experiment), which itself leads to IS dissolution, attested by the evolution of cation concentrations in solution. As well as in the smectite case, the elements provided by the IS dissolution are used to precipitate 7 Å iron rich serpentine and magnetite minerals.

However, particularities were noticed for this specific IS/iron system. Indeed, our XRD investigations revealed that in presence of iron the IS superstructure is dramatically damaged in time, which attest of its dissolution. Moreover, XRD data indicate that the smectite layers of the IS structure are dissolved prior and/or faster than the illite ones, and that a new diffraction peak appears, characterized by a 8.7 Å distance. HRTEM imaging not only confirmed the presence of 7 Å serpentines but also revealed the presence of 10 Å/7 Å mixed-layer minerals. Mossbauer results indicate that more than 70 % of initial iron is consumed after three months, and confirmed the classic scheme in which serpentine minerals containing Fe(II) and Fe(III) are produced as well as magnetite at a lesser extent. These results are in agreement with data obtained in similar conditions by Pignatelli et al. (2014) on Callovo-Oxfordian samples. However, data analysis pointed out the existence of another clay-like mineral containing Fe(II), which amount can reach 20 % of the total iron.

Altogether, our results suggest that IS display a specific behavior compared to the other clay minerals, certainly due to the interlayered character. Our study shed the light on several specific iron/IS reaction pathways, and further investigations including XRD modeling are needed to better understand the full processes involved in Iron/IS interactions.

Rivard C. (2011) Contribution à l'étude de la stabilité des minéraux constitutifs de l'argilite du Callovo-Oxfordien en présence de fer à 90°C. Thèse de l'Institut National Polytechnique de Lorraine, Vandoeuvre-lès-Nancy, France, 331 p.

Pignatelli I., Bourdelle F., Bartier D., Mosser-Ruck R., Truche L., Mugnaiolli E. and Michau N. (2014) Iron-clay interactions : detailed study of the mineralogical transformation of claystone with emphasis on the formation of iron-rich T-O phyllosilicates in a step-by-step cooling experiment from 90°C to 40°C. Chemical Geology, 387, pp 1-11.

Iron/clay/glass interaction in compacted clay at 50°C

S.Necib[1], Y.Linard[1], C. Martin[2], E.Burger[3], P. Jollivet[4], S.Dewonck[1]
1- Andra, Centre Meuse/Haute-Marne, RD 960, 55290 Bure
2- Andra, Siège, Parc de la Croix Blanche - 1/7 rue Jean Monnet, 92298 Châtenay-Malabry
3- EDF les Renardières
4- CEA, DEN/DTCD/SECM/Laboratoire d'étude du Comportement à Long Terme, F-30207 Bagnols-sur-Cèze

In the context of geological disposal nuclear waste repository, multi-engineered barriers will be emplaced in the Callovo-Oxfordian claystone (COx). Therefore it is necessary to investigate the interactions between iron, glass and clay, which are the main components of said barriers.

Recently an experiment that contains five boreholes with an identical setup has been launched in the Underground Research Laboratory (URL) developed by Andra (The National Radioactive Waste Management Agency of France) at Bure (East of the Paris Basin, France) to study the evolutions of the interactions between iron, glass and clay. Each vertical descending borehole is seven meters deep and contains a two meters high test chamber with a series of stacked clay blocks (see Figure 1 and Figure 2). In each one of them there are four holes filled with a mixture of iron and/or glass, iron and/or clay, glass and/or clay. The temperature was set at 50°C and the intervals were all closed with a packer in order to maintain anoxic conditions.

After two years, the first borehole was dismantled. Water sampling revealed partial water resaturation in the test chamber. At – 7 meters the samples were fully resaturated, while at – 5 meters resaturation was minimal.
From a corrosion point of view, all of the metallic samples were not significantly affected. Gravimetric measurements have been carried out to measure metal loss and determine the mean average corrosion rate (CR). The samples made of C-steel grade P275 revealed a mean average CR comprised between 2 and 9 μm/yr. Some samples were emplaced in a way simulating a potential "crevice corrosion effect", which slightly increased the CR up to 12 μm/yr. The samples made of stainless steel grade 309 and 316 revealed very low CR below 0.2 μm/yr.
Scanning electron microscopy (SEM) was conducted on C-rings specimen grade P275, commonly used to assess stress corrosion cracking (SCC) and more particularly crack initiation. The results showed the absence of cracks, even in the area under tensile stress. General corrosion was the main corrosion type, however a few pits were observed.
X-Ray Dispersive (XRD) analyses were carried out on P275 grade sample. The results revealed the presence of α-FeOOH Goethit, $FeCO_3$ Siderite and Fe_3S_4 Greigite.

Regarding the glass, six altered glass-iron samples have been characterized by SEM-EDX, TEM and EPMA to provide information on the composition and morphology of the alteration layer and corrosion products. The alteration products of glass are made of a gel layer, a newly formed layer, and loose precipitates associated with the corrosion products of iron. The gel thickness, corresponding to the amount of altered glass and assuming a constant glass dissolution rate suggests a mean alteration rate similar to the initial rate measured for the SON68 glass in synthetic COx porewater at 50°C in conventional laboratory. … In the alteration layer, there is the presence of crystalline phases and precipitates of many different chemical compositions: rare earth compounds associated with calcium and silicon (apatite phase) or borates, presence of ZnS and FeS that could possibly be related to bacterial activity. There is a wide variation in Si / Fe and Al / Fe in the newly formed layer. The gel incorporates varying Fe contents and, in many cases, there is a significant retention of boron in the newly formed layer.

After three years, water sampling revealed a full resaturation of the test chamber. The next borehole installation to be dismantled has been forecasted to take place five years following the initial start date.

This will give new results on the evolution between iron, clay and glass under resaturated conditions at 50°C in direct contact with compacted clay.

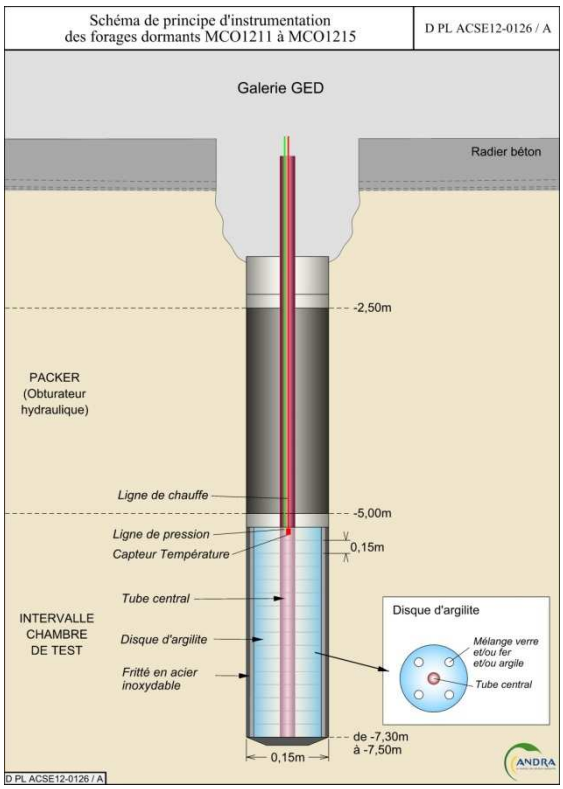


Figure 1 Experimental set-up


Figure 2: Top view of a clay block showing the four holes containing the samples (iron and/or clay and/or glass)

Effects of activity of OH^- and temperature on the dissolution rate of compacted montmorillonite under highly alkaline conditions

Takuma Sawaguchi[1,*], Manabu Tsukada[1], Tetsuji Yamaguchi[1], Masayuki Mukai[1]

Part of this research is funded by the Secretariat of Nuclear Regulation Authority, Nuclear Regulation Authority, Japan (formerly the Nuclear and Industrial Safety Agency, Ministry of Economy, Trade and Industry, Japan).

1. Waste Disposal Safety Research Group, Nuclear Safety Research Center, Sector of Nuclear Safety Research and Emergency Preparedness, Japan Atomic Energy Agency, Tokai, Ibaraki 319-1195, Japan
* Corresponding author: sawaguchi.takuma@jaea.go.jp

Introduction

Highly alkaline groundwater induced by cementitious materials in a deep geological isolation system of high-level radioactive waste is likely to alter bentonite buffer materials and to cause the physical and/or chemical barrier functions of the buffer materials to deteriorate. In order to evaluate the long-term alteration behavior, the dissolution rate of montmorillonite in compacted sand-bentonite mixtures was formulized [1]. Furthermore, we showed that the dissolution rate of montmorillonite was higher in compacted pure montmorillonite than in compacted sand-bentonite mixtures at 130 °C. The difference was explained as that the dissolution of montmorillonite in the compacted mixtures was inhibited by decreasing the activity of hydroxide ions (a_{OH^-}) with the dissolution of accessory minerals such as silica in the mixtures [2]. In this study, the dependences of the dissolution rate of compacted montmorillonite on a_{OH^-} and temperature were experimentally investigated.

Experimental

The montmorillonite (Kunipia F, from Kunimine Industries Co. Ltd.) were compacted in specimen holders (20 mm in diameter by 10 mm in thickness) to obtain dry density of 1,060 kg m^{-3}. Three simulated groundwaters were provided with NaCl-NaOH mixed solutions of the total Na concentration of 1 mol dm^{-3} and OH^- concentration 0.1, 0.3 and 1 mol dm^{-3}. The holders were soaked in the simulated groundwaters at room temperature under vacuum to saturate the specimen. Then, the holders were placed in Teflon® containers of 0.065 dm^3 of the simulated groundwater and kept at 50, 70 and 90 °C in ovens to observe montmorillonite dissolution over a reasonable time period. Schematic image of the specimen in container assembly was shown in Fig. 1. Each of the assembly was taken from the oven at the fixed sampling time. The compacted montmorillonite specimen was pushed out from the holder frame 2 mm at a time by using a screw presser and sliced with a steel blade. Each sliced piece was weighed, freeze-dried at -110 °C, and analysed for the amount of remained montmorillonite by the methylene-blue adsorption titration method [3, 4].

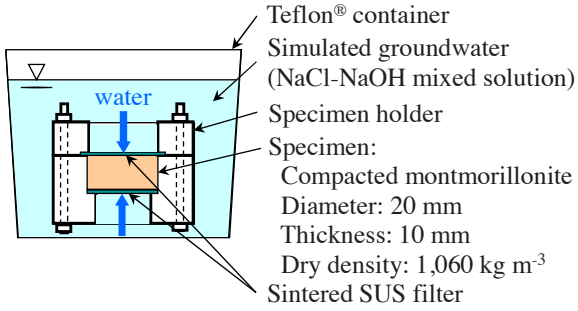


Fig .1 Schematic drawing of the experimental configuration for the alteration experiment.

Results and discussion

The amount of montmorillonite in the compacted montmorillonite decreased in several months under the employed conditions of temperature and pH, as seen in Fig. 2. The higher concentration of OH^- in external solution and/or temperature results in the faster decrease in the amount of montmorillonite. The decreases are approximately linear with time, and can be expressed as $W(t) = W(0) - R_A t$, where $W(t)$ denotes the density of compacted montmorillonite (kg m^{-3}), $W(0)$ the initial

density (kg m^{-3}), R_A the dissolution rate of montmorillonite (kg m^{-3} s^{-1}) and t the time after the contact with the simulated groundwater. The R_A is a function of a_{OH^-} (mol dm^{-3}) and temperature (K) as shown in Fig. 3, and can be expressed as

$$R_A = 30000\ (a_{OH^-})^{1.3}\ e^{-55000/RT} \qquad (1)$$

by multiple regression analysis including R_A data at 130 °C [2] where R is the gas constant (8.314 J mol^{-1} K^{-1}). The dissolution rate in compacted montmorillonite: equation (1), was higher than that in the compacted mixtures: $R_A = 3500\ (a_{OH^-})^{1.4} e^{-51000/RT}$ [1]. The above-mentioned consideration that the dissolution of montmorillonite in the mixtures was inhibited by that of accessory minerals at 130 °C would be applicable to the temperature range of 50-130 °C. Whether accessory minerals exist together with montmorillonite or do not showed little effect on the dependence of the montmorillonite dissolution rate on a_{OH^-} and/or temperature.

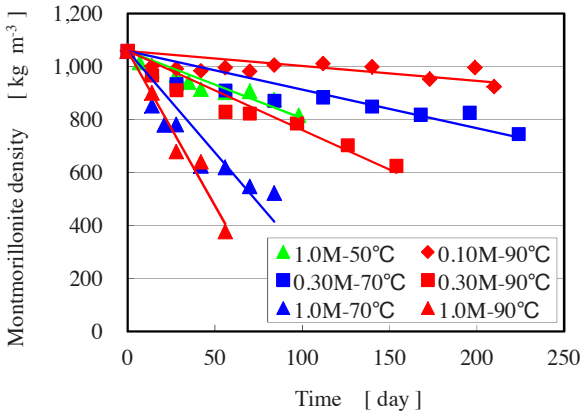


Fig.2 Time courses of montmorillonite densities in compacted montmorillonite under highly alkaline conditions. The straight lines were obtained by the least squares method.

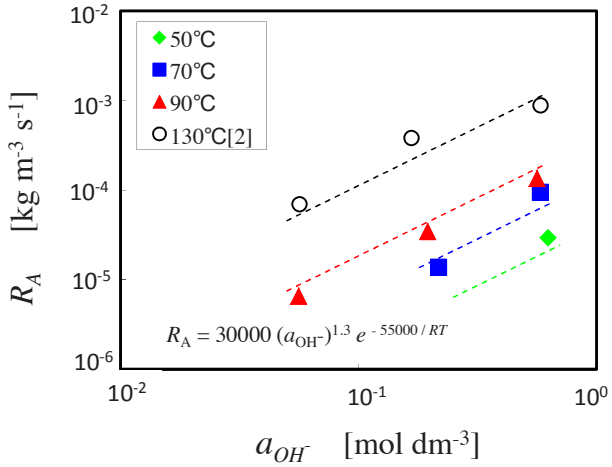


Fig.3 Dependence of the montmorillonite dissolution rate, R_A (kg m^{-3} s^{-1}), on activity of OH^-, a_{OH^-} (mol dm^{-3}) and temperature.

References

[1] Yamaguchi, T. et al., Physics and Chemistry of the Earth, 32, 298-310 (2007).
[2] Sawaguchi, T. et al., Journal of Nuclear Fuel Cycle and Environment, 20, 71-77 (2013). [in Japanese]
[3] Hang, P. T., Brindley, G. W., Clays Clay Minerals, 18, 203-212 (1970).
[4] Brindley, G. W., Thompson, T. D., Israel Journal of Chemistry, 8, 409-415 (1970).

Laboratory experiments on alteration of bentonite-cement interfaces and accompanying changes in diffusivity of solute

Tetsuji Yamaguchi, Takuma Sawaguchi, Manabu Tsukada, Tadao Tanaka

Part of this research is funded by the Secretariat of Nuclear Regulation Authority, Nuclear Regulation Authority, Japan (formerly the Nuclear and Industrial Safety Agency, Ministry of Economy, Trade and Industry, Japan).

Nuclear Safety Research Center, Sector of Nuclear Safety Research and Emergency Preparedness, Japan Atomic Energy Agency, Tokai, Ibaraki 319-1195, Japan

Introduction

Highly alkaline groundwater induced by cementitious materials in a deep geological isolation system of high-level radioactive waste is likely to alter bentonite buffer materials and to cause the physical and/or chemical barrier functions of the buffer materials to deteriorate. In order to evaluate the long-term alteration behavior, understanding of the phaenomena occurring at the interface between bentonite and cementitious materials is essential, especially changes in transport properties through the interface accompanying mineralogical alterations. Hoshino et al. (2009) [1] studied diffusivity of tritiated water through mixed specimens of granulated hardened cement and bentonite, and suggested that the diffusivity decreased with aging down to 20% of the initial value over 180 days. The relationship between such significant change in diffusivity and the ones occurring at interfaces between bentonite and intact cementitious materials, however, has not been clarified. In this study, alteration of bentonite-cement interfaces and accompanying changes in diffusivity of tritiated water was experimentally investigated using intact hardened cement specimens.

Experimental

Two types of experiments were performed. The first one simulated alteration of hardened cement paste with carbonate / bicarbonate anions supplied from bentonite as shown in Fig. 1(a). In this experiment, carbonate anions were supplied from aqueous solution without using bentonite. The second experiment simulated alteration of hardened cement with silicates supplied from bentonite by contacting hardened cement and compacted bentonite as shown in Fig. 1(b).

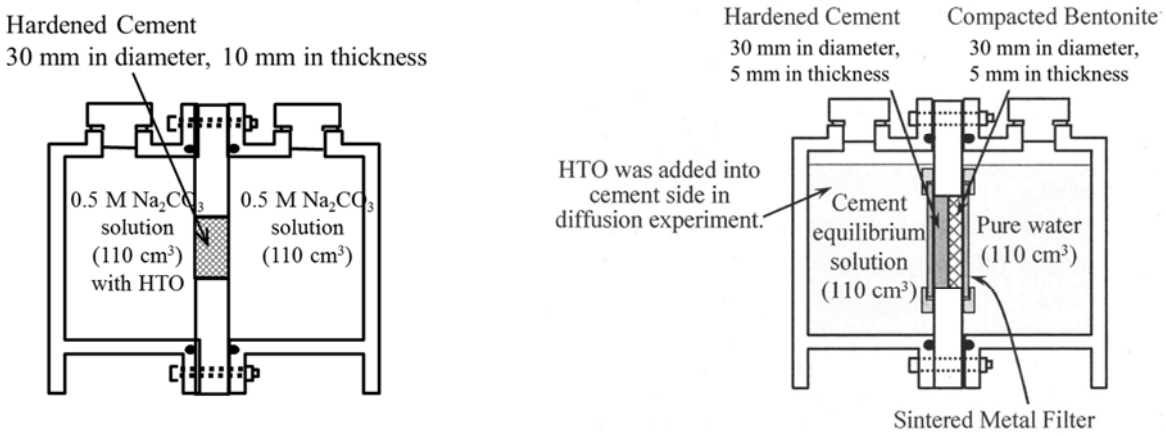


Fig. 1 Experimental configuration of alteration and diffusion experiment of bentonite-cement interfaces for carbonate system (a) and for silicate system (b).

Results and discussion

The first experiment for carbonate system showed dissolution of $Ca(OH)_2$ and ettringite and formation calcite at the interface. The effective diffusivity of tritiated water decreased to 70% of the initial value after 180-day period. The second experiment for silicate system showed dissolution of $Ca(OH)_2$ and formation of calcite and katoite. The effective diffusivity decreased to 71 % of the initial value after 600-day period. The changes in the diffusivity were much less than that observed by Hoshino et al. (2009) [1]. More alteration of interfaces occurred at the experiment using granulated hardened cement [1] than the present experiments because of more reactive surface areas: 14.13 cm^2 for the experiment for carbonate system, 7.065 cm^2 for silicate system and 104 cm^2 for the experiment using granulated hardened cement [1]. The range of mineralogical alteration and changes in diffusivity were limited at the interface in the present experiments. Assuming that the diffusivity decreased to 20% of the initial value at the limited altered ranges at the interfaces, the equivalent diffusivity ($D_{e,equiv}$) of the specimens can be evaluated as;

$$1/D_{e,equiv} = x/(0.2D_{e,0}) + (1-x)/D_{e,0} \quad \text{or} \quad D_{e,equiv}/D_{e,0} = 1/(4x+1)$$

where $D_{e,0}$ is the initial diffusivity (m^2/s), x the ration of the range of alteration to the total thickness. This equation gives an x value of 0.11 for carbonate system, which means the range of alteration is 1.1 mm for two reactive surfaces, 0.55 mm for each surface for 180 days. The x value of 0.1 is estimated for the silicate system, which means the 0.5 mm range was altered over 600 days.

The range of alteration L (mm) would be proportional to the square root of time because the alteration was driven by the diffusive transport of solute:

$$L = a\sqrt{t}$$

where a is the proportional constant (mm $y^{-0.5}$), t the period of alteration (y). The proportional constant was determined for carbonate system and silicate system as shown in Table 1.

Table 1 The range of alteration L and the proportional constant a estimated for the experiments for carbonate and silicate systems.

	Carbonate system	Silicate system
t (y)	0.492	1.643
L (mm)	0.55	0.50
a (mm $y^{-0.5}$)	0.783	0.390

The ranges of alteration over 15 years are estimated to be 3.03 mm for carbonate system and 1.5 mm for silicate system by using the a values. Mineralogical characterization of a concrete / argillite interface that experienced 15 years of interaction at Tournemire URL [2-4] showed formation of calcite and changes in grain densities within the first centimeter [2,3]. On the other hand, dissolution of quartz and formation of CSH was observed only in the first millimeters of the interface [2,4]. Our estimation of the ranges of alteration for carbonate and silicate systems agree with those observed at the cement-argillite interface at Tournemire. A consistent explanation was given to the results from the alteration experiment using bentonite and granulated hardened cement [1], the alteration experiment of hardened cement with carbonate / bicarbonate anions, the alteration experiment of bentonite and hardened cement and the observation of the cement-argillite interactions over 15 years at Tournemire URL. Such an explanation enhances our confidence in our assessment of alteration of cement-bentonite systems and can be a base for using our data and models in long term assessment of radioactive waste disposal.

Acknowledgement

Mr. Seiichi Hoshino of Taiheiyo Cement Corp. is greatly acknowledged for his contribution to the experiments and data analyses.

References

[1] Hoshino, S. et al., Mater. Res. Soc. Proc. Vol. 1193, 445-452 (2009).
[2] Tinseau, E. et al., *Waste Management*, 26, 789-800 (2006).
[3] Gaboreau, S. et al., Appl. Geochem. 26, 2159-2171 (2011).
[4] De Windt, L. et al., Phys. Chem. Earth 33, S295-S305 (2008).

Stability of bentonite under high-pH conditions: An experimental approach including modeling

Florian Dolder[1], Urs Mäder[1], Andreas Jenni[1], Beat Münch[2]

[1]RWI, University of Bern, Geological Sciences, Bern 3012, Switzerland
[2]EMPA, Swiss Federal Institute for Materials Testing and Research, Dübendorf, Switzerland

The Swiss concept for geological disposal of high-level radioactive waste foresees bentonite as buffer between canister and hostrock, as backfill material and for tunnel sealing. Shotcrete is proposed as tunnel supporting material. The emplacement of high-pH cementitious material next to clay generates a chemical gradient that drives diffusive transport. Both laboratory studies and reactive transport modeling predict significant mineral alteration near the interfaces [1, 2].

We aim at characterizing and quantifying the cement/bentonite interfaces both spatially and temporally by focusing on the advective-diffusive transport domain resolved at intermediate spatial scales. The core infiltration equipment, made of carbon fiber and plastics, that is used for these investigations holds a cylindrical bentonite sample under confining pressure and imposes a constant hydraulic gradient to drive a small advective flux [3]. Compacted and pre-saturated MX-80 bentonite is exposed to high-pH cementitious pore-fluids which are expected to alter the mineral assemblage over time. The related change in phase densities, porosity and local bulk density is tracked at an intermediate scale by computed tomography (CT) during ongoing infiltration.

In addition, the obtained data will be modelled, using the multicomponent reactive flow and transport code CrunchFlow [4]. The code includes a double porosity concept (micro- and macroporosity) along with surface complexation (Stern layer), all meant to simulate a realistic clay mineral behaviour [5]. The thermodynamic data set includes cement phases (CEMDATA database; [6] and [7]).

In one set-up a potassium, sodium and hydroxide based infiltration fluid (0.28 molal), simulating an OPC pore-fluid (ordinary Portland cement) with a pH of 13.4, was used. The MX-80 bentonite sample had an initial saturated density of 1.92 g/cm^3 and a water content of 25 wt.% and these values shifted to 1.89 – 1.93 g/cm^3 and 31 – 33 wt.% within 760 days. The hydraulic conductivity decreased after switching from artificial pore-water to a high-pH pore-fluid from ~1.1*10^{-13} m/s to ~1.3*10^{-14} m/s. A decrease in all ion concentrations with the exception of sulphate, silica and potassium was observed, while pH just slightly increased from ~7.5 to ~8.

CT scans tracked a progressing, hemispherical reaction front from the filter into the first mm of the bentonite sample, revealing two distinguishable zones of bulk density increase. The reaction front was analyzed post-mortem in a longitudinal section and a zone of Mg and Ca enrichment was found (Fig. 1). The region enriched in Ca consisted of two zones characterized by various amounts of precipitated calcite, confirmed by XRD and Raman spectroscopy measurements. The Mg enriched zone showed an increased concentration in the central parts of the core (up to 1.5 mm) and passed into a zone of single clay package enrichment (1.5 – 2.5 mm). The link between Mg enrichment and new mineral formation is in the XRD spectra not clear. In the same area dissolution of cristobalite (polymorph of silica) could be observed in the XRD spectra and in SEM morphology.

First attempts of reactive transport modeling showed good agreement with the measured aquatic chemistry while the newly occurring mineral assemblage has to be still improved.

Further investigation are planned to resolve the newly formed Mg phase with more detailed investigations, and a more detailed modelling interpretation.

Related information on this topic will be presented from the CI experiment (Cement-Clay-Interaction) by Jenni et al. (this conference).

Acknowledgement
Financial support from Nagra is gratefully acknowledged. The Department of Forensic Medicine at Uni Bern is acknowledged for providing time and technical support on their scanner.

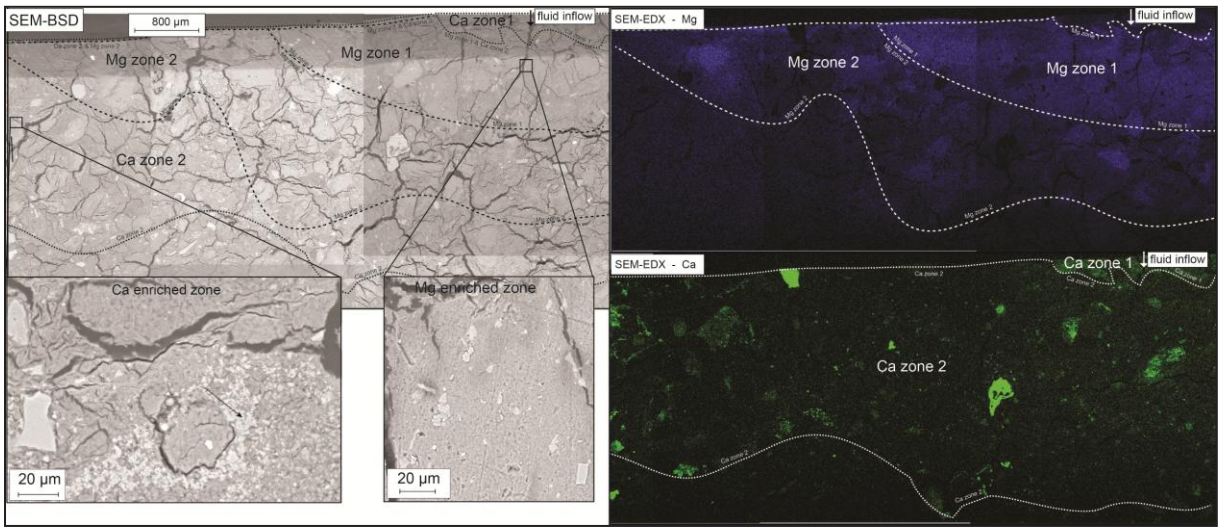


Fig. 1: SEM-BSD image of a trans-section taken at the inlet of the bentonite sample along with the corresponding element mapping for magnesium and calcium.

References

1. Dauzeres, A., et al., *Physico-chemical investigation of clayey/cement-based materials interaction in the context of geological waste disposal: Experimental approach and results*. Cement and Concrete Research, 2010. **40**(8): p. 1327-1340.
2. Jenni, A., et al., *In situ interaction between different concretes and Opalinus Clay*. Physics and Chemistry of the Earth, Parts A/B/C, 2014. **70–71**(0): p. 71-83.
3. Dolder, F., et al., *Experimental characterization of cement–bentonite interaction using core infiltration techniques and 4D computed tomography*. Physics and Chemistry of the Earth, Parts A/B/C, 2014. **70–71**(0): p. 104-113.
4. Steefel, C.I., *CrunchFlow. Software for Modeling Multicomponent Reactive Flow and Transport, User's manual*, 2006, E. S. Division Ed. Lawrence Berkeley National Laboratory: Berkeley, CA.
5. Steefel, C.I., *Development of an explicit diffuse layer model for CrunchFlow*, 2010: Update. E. S. Division Ed. Lawrence Berkeley National Laboratory: Berkeley, CA.
6. Jacques, D., *Benchmarking of the cement model and detrimental chemical reactions including temperature dependent parameters. Project near surface disposal of catergory A waste at Dessel*. NIRAS-MP5-03 DATA-LT(NF) Version 1 NIROND-TR 2008-30 E, 2009.
7. Lothenbach, B. and F. Winnefeld, *Thermodynamic modelling of the hydration of Portland cement*. Cement and Concrete Research, 2006. **36**(2): p. 209-226.

Electrolyte-mediated dissolution of montmorillonite in alkaline environments

Rasmus Eriksson **and Tim Schatz**

B+Tech Oy, Laulukuja 4, Helsinki, Finland

Dissolution and mineralogical alteration of bentonite material are interrelated processes and may, under certain circumstances, affect the performance of buffer or backfill material in a spent nuclear fuel repository. Mineralogical alteration could, for example, lead to decreased swelling pressure due to reduced swelling clay fraction, while dissolution may lead to loss of buffer (or backfill) material. At full saturation, dissolution is mainly a concern at rock fracture/buffer or rock fracture/backfill interfaces, where material can extrude into the fracture and therefore become diluted. Dissolution is not expected to occur to a significant amount in the compacted and fully saturated buffer or backfill matrices because the amount of pore water is small, and the pore water is to a large degree bound to surfaces (interlayers) and ions, which reduces its capacity to accommodate dissolved species.

We have performed a series of potentiometric and conductometric titrations on dilute Na-montmorillonite suspensions and corresponding supernatants at NaCl and $CaCl_2$ concentrations between 0.0001 – 1 mol/L. The samples were allowed to equilibrate for 30 minutes under gentle stirring prior to analysis. The titrations were performed by first titrating the sample with 1 M NaOH to pH 11, and thereafter immediately continuing by titrating the sample with 1 M HCl to pH 4. The maximum equilibration time between titrant additions was set to 30 seconds in order to minimize the accumulated leakage from the pH electrode (a Metrohm gel electrode), which would otherwise affect the conductivity data.

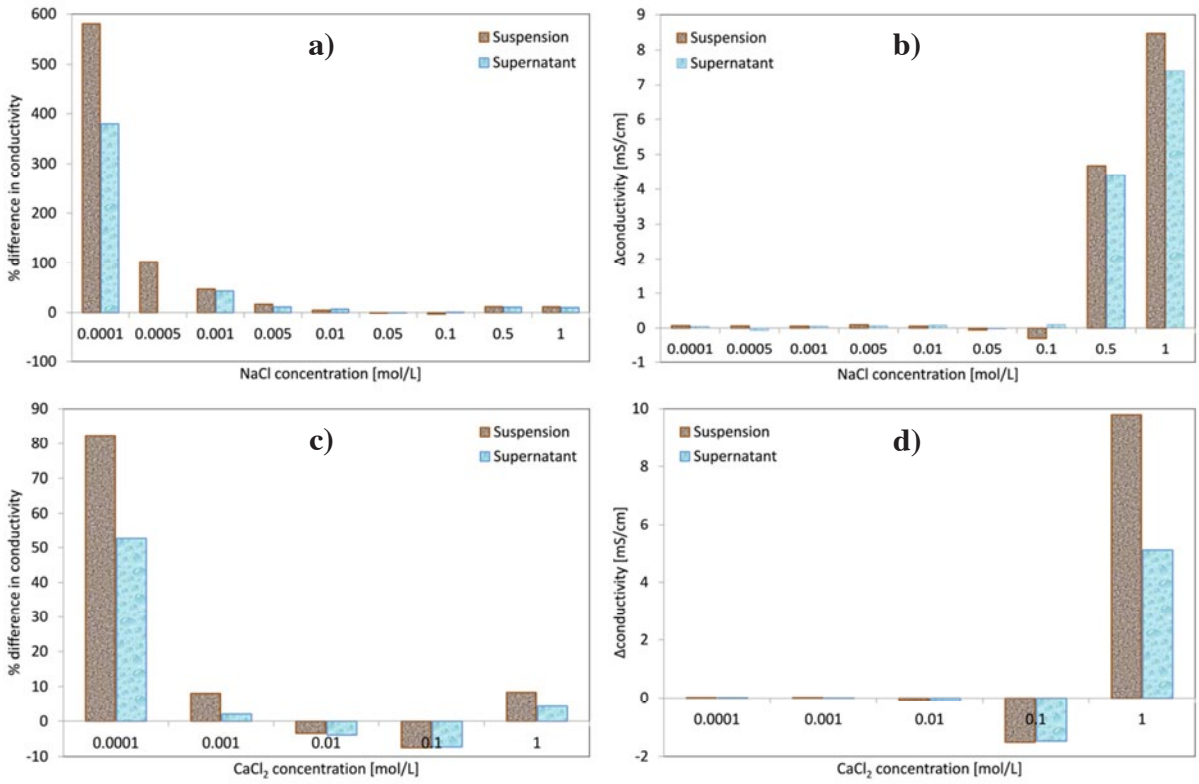


Figure 1. The difference in conductivity between 1.5 g/L Na-montmorillonite samples and an aqueous solution at the same background electrolyte concentration. a,c) The relative difference (in %) for NaCl (a) and $CaCl_2$ (c) as background electrolyte. b,d) The absolute difference (in mS/cm) for NaCl (b) and $CaCl_2$ (d) as background electrolyte.

A comparison of initial sample conductivities (before any titrant addition) to conductivities of electrolyte solutions of equivalent concentrations (at 25 °C) reveals that montmorillonite particles are not inert materials, especially in the presence of high electrolyte concentrations (Fig. 1). The conductivity values of the samples have been normalized to 25 °C assuming a 2% change per °C. In general, the *relative* difference in conductivity is largest at the lowest electrolyte concentrations (≤ 0.001 M, Fig. 1a,c), and the *absolute* difference is largest at the highest electrolyte concentrations (≥ 0.5 M, Fig. 1b,d). At the highest electrolyte concentrations the difference in conductivity is on the order of several mS/cm, which implies a significant increase in the electrolyte concentration of the aqueous phase (several tens of mM in concentration) as compared to the conductivity of the background electrolyte. Montmorillonite is the only source material available, and therefore the increase in conductivity is due to dissolving montmorillonite.

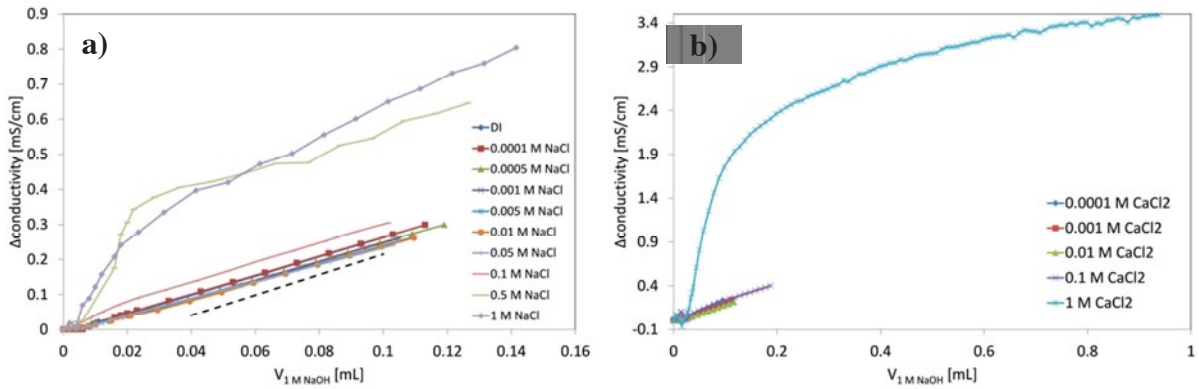


Figure 2. Conductometric titrations of 1.5 g/L Na-montmorillonite samples at different a) NaCl concentrations and b) $CaCl_2$ concentrations. The y-axis shows the change in sample conductivity relative to the initial conductivity.

Titrating the samples up to pH 11 shows that further dissolution is more pronounced at higher electrolyte concentrations (Fig. 2). Below an electrolyte concentration of 0.5 M, no significant dissolution is observed, while above 0.5 M, the conductivity increase is much larger than what would be expected due to NaOH addition (Fig. 2). Montmorillonite dissolution involves reactions with water along the edge surface, but the reaction mechanism and the dissolution products have not been precisely determined. Our study suggests that the presence of electrolytes accelerates montmorillonite dissolution to a significant degree, perhaps even to a larger degree than the effect of elevated pH. As suggested by Kubicki *et al*. [1], electrolytes may facilitate the formation of metastable surface groups that are believed to act as precursors to the actual dissolution reaction.

[1] Kubicki, J. D.; Sofo, J. O.; Skelton, A. A.; Bandura, A. V. *J. Phys. Chem. C* **2012**, 116, 17479-17491.

THCm numerical models of bentonite heating and hydration tests to study the interactions of compacted bentonite and concrete

Javier Samper [(1)], Alba Mon [(1)], Luis Montenegro [(1)], Jaime Cuevas[(3)], Raúl Fernández [(3)], María Jesús Turrero[(2)], Elena Torres[(2)] & Acacia Naves [(1)]

[(1)] University of A Coruña, 15071 La Coruña, Spain, jsamper@udc.es
[(2)] Centro de Investigaciones Energéticas, Medio Ambientales y Tecnológicas, Av. Complutense, 28040 Madrid, Spain
[(3)] Universidad Autónoma de Madrid. Facultad de Ciencias, 28049 Madrid, Spain

Coupled thermal (T), hydrodynamic (H) and chemical (C) models which account for mechanical (m) deformation have been developed within the PEBS Project for modeling the time evolution of the engineered barrier system (EBS) of a HLW repository. Here we present the numerical model of a heating and hydration experiment performed by Ciemat on compacted FEBEX bentonite to study the interactions of concrete and bentonite under repository conditions and analyze how such interactions affect the bentonite properties. The experiment was modelled with INVERSE-FADES-CORE (Zheng et al., 2010). Here we report the model of the test HB4 that lasted for 4.5 years.

The test was performed on a cell containing a 7.15 cm thick bentonite sample in contact with a 3 cm thick piece of concrete. The cell was hydrated at a constant pressure at the top of the cell through the concrete at ambient temperature while the temperature was maintained constant at 100ºC at the bottom of the cell. The cell was placed in a Teflon coverture to prevent the lateral heat conduction and bentonite swelling. The test was modeled with a 1D grid. Bentonite parameters were taken from the model of the CT23 heating and hydration experiment (Zheng et al., 2010). The parameters for the concrete of the HB4 test were derived from laboratory experiments (Villar et al., 2012; Villar, 2013). The initial porosity of the bentonite is 0.4 and the initial gravimetric water content is 13.3%, which corresponds to a saturation of 57% and a suction of $1.27 \cdot 10^8$ Pa. The concrete of the HB4 test has a porosity of 0.125 and a gravimetric water content of 2.2%. The initial temperature is 22ºC. The gas pressure is assumed equal to the atmospheric pressure during the test. The initial stress is uniform, isotropic and equal to $2.5 \cdot 10^5$ Pa. A liquid pressure of 100 kPa is specified at the hydration boundary of the HB4 test. The cells were hydrated with a synthetic Spanish Reference Clay porewater (Turrero et al., 2011). The porewater composition of the bentonite at a water content of 13.3% was derived from Fernández et al. (2001). The initial chemical composition of the concrete porewater for the HB4 test was derived from Yang et al. (2008) by assuming that the concentration of dissolved Ca^{2+} is controlled by local chemical equilibrium with respect to portlandite, HCO_3^- with calcite, Mg^{2+} with brucite, Al^{3+} with ettringite and SiO_2 with C1.8SH. The hydration water has the composition of the synthetic Spanish Reference Clay porewater (Turrero et al., 2011). The considered initial mineral volume fractions in the bentonite were: 0.36% of calcite, 0.08% of gypsum and 1.19% of cristobalite while in the concrete were: 7.4% of portlandite, 2.2% of ettringite, 14.6% of C1.8SH, 1% of brucite, 0.1% of calcite and 62.2% of quartz. Secondary minerals considered in the model were anhydrite, sepiolite, anorthite and C0.8SH. The dissolution/precipitation of portlandite, ettringite, C1.8SH, C0.8SH, quartz and cristobalite was simulated with the kinetic formulation of Fernández et al. (2009). Cation exchange and surface complexation were also considered.

The experimental data show an altered layer of bentonite (< 5 mm) which is cemented by mineral precipitation. A second layer (< 3 cm) is affected by changes in the concentrations of exchanged cations. Table 1 shows the summary of the main experimental observations of the mineral patterns at the end of the HB4 test. The computed values of dissolved/precipitated mineral phases were compared to these observations. For the most part, the numerical models capture the main trends of mineral dissolution-precipitation. However, there are discrepancies for ettringite and CSH precipitation for which the model predicts much less precipitation than the observed values. In the hydration zone the

porosity decreases mainly due to brucite precipitation. Here calcite, ettringite, C1.8SH and C0.8SH precipitate but at a much smaller rate. In the concrete near the bentonite, the porosity increases due to the dissolution of C1.8SH, portlandite and ettringite. In the bentonite in contact with the concrete, the porosity decreases due to brucite, calcite and sepiolite precipitation. The lack of thermodynamic data for CASH phases prevented us to account for them in the models.

Table 1. Experimental observations and model predictions of mineral dissolution/precipitation at the end of the HB4 test after 1610 days.

		Observations	Model results
Concrete	Hydration interface	- **Brucite** precipitates - **Calcite** precipitates	- **Brucite** precipitates (2.8 % volume) - **Calcite** precipitates (0.1 % volume)
Concrete	Concrete	- **Calcite** precipitates everywhere - **C0.8SH** precipitates - **Ettringite** precipitates everywhere - **Portlandite** is nearly absent	- **Calcite** precipitates everywhere - **C0.8SH** precipitates ($8{\cdot}10^{-9}$ % volume) - **Ettringite** precipitates near the hydration (less than 1% in 1cm thickness) and dissolves in the rest (max of 2% volume in 2 cm thickness) - **Portlandite** dissolves everywhere (max of 1.6% volume in the interface)
Concrete	Contact concrete-bentonite	-**Calcite** precipitates more than in the rest of the concrete - **Ettringite** precipitates more than in the rest of the concrete	- **Calcite** precipitates more than in the rest of the concrete (3% volume) - **Ettringite** dissolves near the interface
Bentonite	Contact bentonite-concrete (< 2 mm)	- **Calcite**/aragonite precipitates - **Mg-silicates** (sepiolite or saponite) - **C0.8SH** (very low) precipitation - No **ettringite** precipitation - No **anorthite** precipitation	-**Calcite** precipitation - A front of **sepiolite** precipitation (max of 0.3% volume in 0.2 cm from the interface) - A front of **brucite** precipitation (max of 11% volume in the interface) - No **C0.8SH** precipitation - No **ettringite** precipitation - No **anorthite** precipitation
Bentonite	Bentonite	-**Calcite** dissolves (not clear)	-**Calcite** dissolves (0.35% volume in 30 cm thickness)
Bentonite	Heating interface	- **Gypsum** and **chloride** precipitation	- **Anhydrite** precipitates (1% volume)

References

Fernández A.M., Cuevas, J., Rivas, P., 2001. Pore water chemistry of the FEBEX bentonite. Mat. Res. Soc. Symp. Proc. 663, 573-588.

Fernández, R., J. Cuevas, U. K. Mäder (2009) Modelling concrete interaction with a bentonite barrier. Eur. J. Mineral., 21, 177-191.

Turrero, M. J., M. V. Villar, E. Torres, A. Escribano, J. Cuevas, R. Fernández, A. I. Ruiz, R. Vigil de la Villa, I. del Soto (2011). Deliverable 2.3-3-1 of PEBS Project. Laboratory tests at the interfaces, Final results of the dismantling of the tests FB3 and HB4. CIEMAT

Villar, M. V., P. L. Martín, F. J. Romero, V. Gutiérrez-Rodrigo, J. M. Barcala (2012). Gas and Water Permeability of Concrete. Informes técnicos CIEMAT.

Villar, M. V., (2013). Long-term Performance of Engineered Barrier Systems PEBS. Summary of concrete hydraulic properties determined at CIEMAT. Technical Note CIEMAT/DMA/2G210/01/13.

Yang, C., J. Samper, L. Montenegro (2008) A coupled non-isothermal reactive transport model for long-term geochemical evolution of a HLW repository in clay, Environmental Geology, 53:1627–1638. DOI 10.1007/s00254-007-0770-2.

Zheng, L., J. Samper, L. Montenegro, A.M. Fernández, (2010). A coupled model of heating and hydration laboratory experiment in unsaturated compacted FEBEX bentonite. Journal of Hydrology 386, 80-94.

Acknowledgements. The research leading to these results has received funding from the European Atomic Energy Community's Seventh Framework Programme (FP7/2007-2011) under grant agreement 249681. This work was partly funded by ENRESA (Spain) and from the Regional Government of Galicia (Project 10MDS118028PR and Fund 2012/181 from "*Consolidación e estruturación de unidades de investigación competitivas*", Grupos de referencia competitiva).

Alteration of compacted bentonite contacted with concrete

Shingo Yokoyama[†,*], **Yasutaka Watanebe**[†], **Andreas Jenni**[‡] **and Urs Mäder**[‡]

† Nuclear Fuel Cycle Backend Research Center, Central Research Institute of Electric Power Industry, 1646 Abiko, Chiba, Japan
‡ RWI, Institute of Geological Sciences, University of Bern, Baltzerstrasse 3, CH-3012 Bern, Switzerland
* Corresponding author, e-mail: shingo@criepi.denken.or.jp

INTRODUCTION

The engineered barrier of a radioactive waste disposal facility has been required to have suitable physicochemical properties and long-term stability. Bentonite and cementitious materials that have the potential to be used in the engineered barriers for the radioactive waste disposal facility might be gradually altered by reactions with groundwater. Especially, the bentonite barrier might be altered by alkaline solutions which arise from leaching of the cementitious materials. Consequently, the suitable properties of the bentonite barrier might be changed. Therefore, understanding of the interaction between bentonite and cementitious materials is important for the long-term safety assessment of the radioactive waste disposal.

The Cement-Clay Interaction (CI) experiment at Mont Terri underground laboratory was started in 2007 to reduce uncertainties in process understanding related to cement-clay interfaces[1)]. In the CI experiment, three different types of concrete and the mixture of highly compacted MX-80 bentonite pellets and fines were installed in two vertical boreholes in Opalinus Clay at 2007[1)]. Core samples including the bentonite-concretes interfaces were successfully collected by drilling campaigns in 2012. In this study, the core samples collected in 2012 were investigated to estimate the mineralogical alteration of bentonite reacted with concretes for about five years.

SAMPLES AND METHODS

Two different core samples (BCI-12 and BCI-15) were investigated in this study. BCI-12 included the low alkali concrete (LAC)-bentonite interface, while BCI-15 included the ordinary portland cement (OPC)-bentonite interface. The inner structure of core samples were observed by X-ray CT analyses. The core samples were then cut by the dry-type cutting machine for the following analyses. Furthermore, the compacted bentonites were separated into ten parts in the depth direction from the interface as shown in Fig.1. Mineral composition of the bentonites was estimated by XRD analyses. Chemical compositions of the bentonites and the montmorillonites were analysed by SEM-EDS and EPMA. The montmorillonite contents and the compositons of the exchangeable cations in the bentonites were estimented by the methylene blue (MB) adsorption experiment and the extraction experiments using 1M NH_4Cl solution, respectively. The changes of mineralogical nature of the montmorillonite were estimated by XRD analyses after EG treatment (for estimation of illitization), Green-Kelly test (for estimation of beidellitization), and alkylammonium exchange treatment (for estimation of mean layer charge).

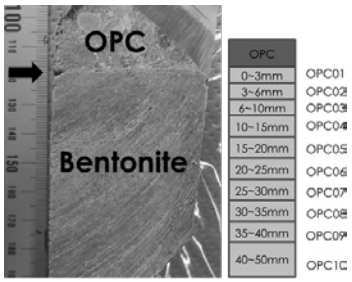


Fig.1 photograph of BCI-15 after cutting.

RESULTS AND DISCUSSION

Characterization of bentonite.

Since the mixture of highly compacted bentonite pellets and fines was used in the CI experiment, initial density of the bentonite was heterogeneous. However, the bentonite of both core samples in X-ray CT images shows homogeneous grey value. This indicates that the density of the bentonite of the both core samples is homogenized by the swelling of bentonite pellets and fines.

The mineral composition of bentonites is montmorillonite, quartz, cristobalite and feldspar. In both BCI-12 and BCI-15, the cristobalite near the interface was dissolved due to the reaction with cementitious pore water. The montmorillonite content of bentonite in BCI-12 is constant in the depth direction from the interface (Fig.2). In the case of BCI-15, the montmorillonite content near the interface is decreased and stays constant from a depth of 6 mm (Fig.2). This reduction of the montmorillonite content is caused by the dissolution of montmorillonite under alkaline condition.

In both core samples, the total amount of extracted cations near the interface is increased due to the enrichment of Mg and Ca phases. . This is caused by new precipitates (e.g. calcite) dissolving during five times extraction processing. In fact, increase of Ca and Mg in montmorillonite and some minerals high in Ca or Mg were observed by SEM-EDS analyses.

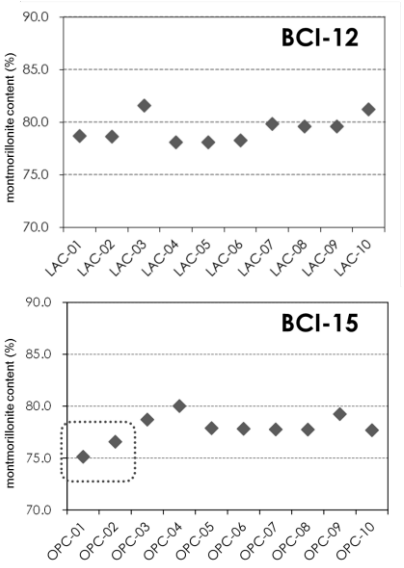


Fig.2 Montomorillonite content (%) in each bentonite.

Characterization of montmorillonite.

The chemical compositions of the montmorillonite in BCI-12 analyzed by point analysis using SEM-EDS indicate that the concentration of Mg near the interface is higher than that at 60 mm distance from the interface. In case of BCI-15, the concentration of Ca and Mg near the interface is slightly higher than that at 60 mm distance from the interface. These results are consistent with the results of extracted cations composition analysis.

The illitization of montmorillonite was estimated using Watanabe's diagram"[2] based on XRD patterns after EG treatment. From the results, the illitization did not occur since all samples in both BCI-12 and BCI-15 were plotted 100%-smectite on Watanabe's diagram. The beidellitization of montmorillonite was estimated by Green-Kelly test. In both BCI-12 and BCI-15, the montmorillonite is the dominant phase in bentonite since d-value of all samples shows 9.3 Å. However, PCI01 shows a weak shoulder at around 18 Å (Fig.3). This indicates that the beidellitization of montmorillonite in OPC01 occurred slightly. Therefore, it is necessary to investigate the older samples in contact with OPC. The mean layer charge of the montmorillonite was estimated by alkylammonium exchange treatment[3]. Although the mean layer charge of the montmorillonite near the interface seems to have increased slightly, it is within the error of this method. Therefore, the mean layer charge of samples is unchanged. However, if bentonite reacts with OPC for a longer period, the mean layer charge of montmorillonite might changed. Therefore, it is necessary to investigate samples from the next drilling campaign.

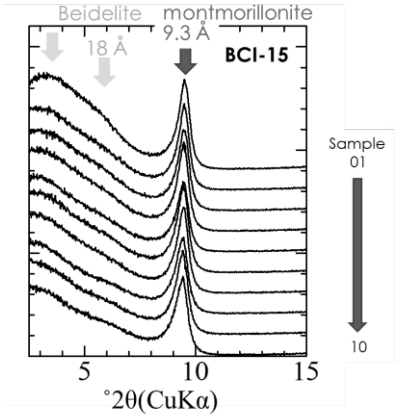


Fig.3 XRD patterns of montmorillonite after Green-Kelly test.

CONCLUSION

The bentonite in two different core samples in the CI experiment was analysed to understand the mineralogical alteration of bentonite close to concrete. High alkali cement, i.e OPC, is more likely to cause alteration of the compacted bentonite compared with LAC (low alkali cement).

REFERENCES

1) Jenni et al. (2014) Phys. Chem. Earth, 70-71, 71-83. 2) Watanabe (1988) Clay Science, 7, 97-114.
3) Olis et al. (1990) Clay Minerals, 25, 39-50.

Clay interacting with hardened cement paste at high temperature (70°C): in situ heater tests, lab experiments and reactive transport modelling

Philippines Lalan[1, 2 *], Alexandre Dauzères[1], Laurent De Windt[2], Danièle Bartier[3], Isabelle Techer[4], Valéry Detilleux[5]

[1] Institute of Radiation Protection and Nuclear Safety (IRSN) PRP-DGE/SRTG/LETIS, BP 17, 92262 Fontenay-aux-Roses cedex, France
[2] Mines-ParisTech, Centre de Géosciences, 35 Rue St-Honoré, 77300 Fontainebleau, France
[3] CNRS UMR 7566, Université de Lorraine, BP 70239, 54506 Vandœuvre-lès-Nancy, France
[4] CNRS UMR 7330, Université de Nîmes, 30 000 Nîmes, France
[5] Bel V, 148 Rue Walcourt, 1070 Anderlecht, Belgium

* Corresponding author

In several countries the recommended option for long term management of intermediate-level long-lived or high-level radioactive wastes is deep geological disposal. The current geological disposal facility design developed by the French National Radioactive Waste Management Agency (Andra) is located in a thick argillaceous layer of Callovo-Oxfordian age (argillite from Bure, France). Nevertheless, use of cementitious materials for radioactive waste containers, facility vaults and sealing could disturb argillite properties of radionuclides containment. In fact, argillite and cementitious materials have contrasting chemical properties triggering perturbations in each material around their contact. Two types of cementitious materials are considered: OPC binder and low-pH binder. The first one has an alkaline-rich pore solution with a very high pH (>13 at 25°C) which causes an aggressive alkaline plume within the argillite and the second one has been created in order to decrease this perturbation by limiting the pore solution pH under 11 at 25°C. Presence of radioactive wastes in the facilities will induce a temperature increase in the radioactive waste storage cells. At the interface between the host-rock and the cementitious materials the temperature may rise until 70°C during decades. Under these conditions of temperature and environment, the clay / concrete behaviour remains actually little-known, especially under representative contact conditions.

The present study focused on the argillite / OPC hardened cement paste and argillite / low-pH hardened cement paste interfaces at 70°C. Two, six and twelve month experiments in dedicated diffusion cells and one year experiments under in situ conditions at the Tournemire underground research laboratory (IRSN) were carried out. Both experimental devices were designed to perform the experiments at 70°C. In each case, cement paste was poured directly on the argillite surface. Multiple analyses were used to characterise samples: SEM-EDS, TEM, μ-tomography, Sr isotopy and TGA for solid samples; ICP-OES, chromatography, pH-metry and TOC-metry for aqueous samples. In a second time, reactive transport modelling with HYTEC was performed in order to better understand the impact of a high temperature on the physico-chemical behaviour of clay / cement paste interfaces. A special emphasis was put on evolution understanding of the diffusion properties within the materials around their contact.

The experimental results of argillite / OPC interface showed a cohesive interface whatever the experimental duration. After one-year interaction, a continuous ribbon of C-S-H was set up within the argillite in retreat from the interface. Tobermorite and phillipsite was clearly characterized by XRD and SEM in this area which also presented a loss of cohesive properties where the samples broke systematically. Further investigations are still needed to analyse dissolution-precipitation processes of clay phases. In the cement paste side, already well-known processes were shown: decalcification, diffuse carbonation, ettringite precipitation and porosity opening. Extension of the mineralogical perturbation was about hundreds of micrometres. Experiments in dedicated diffusion cells indicated a

good reproducibility of the results according to solution analyses. First results of argillite / low-pH hardened cement paste interfaces after one year of interaction showed gypsum precipitation at the interface and also within argillite cracks.

Temperature imprints on the system were taken into account in modelling through thermodynamics constants and through Arrhenius activation energies for kinetic reaction rate and aqueous species diffusion coefficients. Cation exchanges were introduced within the model. Modelling results reproduced quite correctly mineralogical processes but alteration depths were too wide. Work on reaction kinetics, on impact of temperature on parameters and on porosity evolution feedbacks has been still on-going.

In contrary to bulk experiments, it should be note that in our devices where both materials are in contact a diffuse carbonation was favoured and thus no clogging has been seen at the interface. Phillipsite and tobermorite precipitation was already described in this range of temperature but never under representative in situ conditions. Precipitation of phillipsite or other zeolites are often predicted by modelling but never observed at low temperature. This discrepancy stays a point to shed light on.

Erosion Effect Mechanism of Alkaline solution on Compacted GMZ Bentonite

CHEN Bao[1], GUO Jiaxing[1], *ZHANG Huixin*[2]

1. Key Laboratory of Geotechnical and Underground Engineering of Ministry of Education, Tongji University, Shanghai 200092, China;
2. Shanghai Construction Design & Research Institute Co., Ltd., Shanghai 200050, China;

Gaomiaozi(GMZ) bentonite has been selected as potential buffer/backfill material of the deep geological repository for high-level nuclear waste disposal in China. Highly alkaline environment induced by cementitious materials in radioactive waste repositories are likely to alter montmorillonite, the main constituent of bentonite buffer materials. Over long time periods, the alteration may cause the physical and/or chemical properties of the buffer to deteriorate.

For the purpose of acquiring quantitative data to determine the effect of alteration on the permeability and absorbability of a bentonite buffer, dissolution rates of montmorillonite and diffusivity of hydroxide ions in compacted bentonite, some experimental studies were conducted on compacted GMZ bentonite with dry density of 1.7g/cm^3 , under highly alkaline, simulated groundwater conditions, where NaOH solutions and $Ca(OH)_2$ solutions with various pH values with a multifuctional swelling-permeameter (Fig.1). The methylene blue (MB) absorption was measured with the combination of fluorescent detection method and spectrophotometer method, to obtain the effects of alkaline solution on bentonite absorbability. The porosity of bentonite samples after solution erosion was detected by the experiment of mercury intrusion porosimetry (MIP). Then the microscopic characteristics of specimens corroded by alkaline solution were studied by scanning electron microscope (SEM), transmission electron microscope (TEM), energy dispersive spectroscopy (EDS) and X-ray diffraction (XRD) tests, and the erosion mechanism was analyzed based on the results, Moreover, diffusivity of OH^- and dissolution of montmorillonite experiments were designed to get the possible erosion degree by alkaline solution on bentonite.

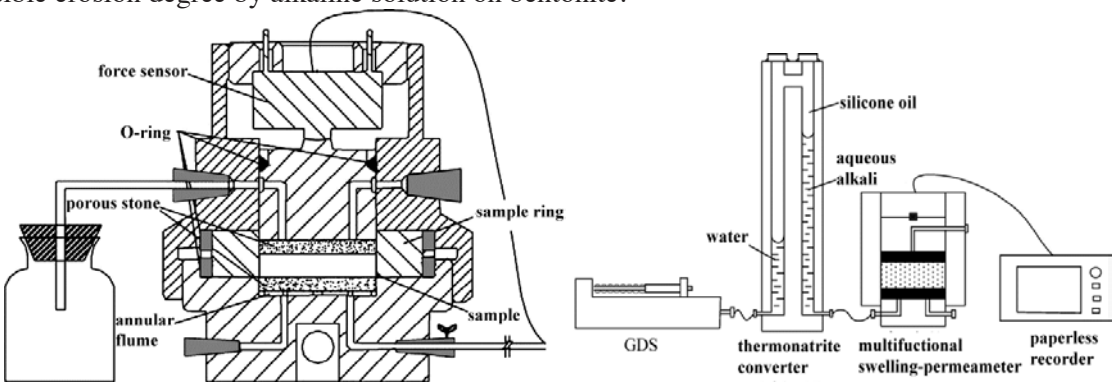


Fig.1 Multifuctional swelling-permeameter suitable to hyper-alkaline infiltration

The results show that $Ca(OH)_2$ solutions have little effect on the permeability and swelling potential of bentonite, so as NaOH solution with pH value no more than 12. While the pH value of NaOH solution is more than 13, the permeability of specimens will be enhanced evidently, and the swelling potential will decrease with the increase of pH values (Fig.2). Furthermore, the pore volume and pore diameter of GMZ bentonite exposed to alkaline solution were changed (Fig.3). At the micro aspect, the CEC, special surface and montmorillonite in bentonite decrease with the infiltration of alkaline solution, and then it results in the reduction of absorbability, an increase of bentonite's porosity and permeability. Therefore, the dissolution and structure destruction of montmorillonite by the erosion of hyper-alkaline solution is the main effect of hyper-alkaline solution on bentonite. The objective of this study is to make the link among the mineralogical transformations (Fig.4), the textural and mechanical changes produced in the compacted bentonite as a consequence of the alkaline solution erosion.

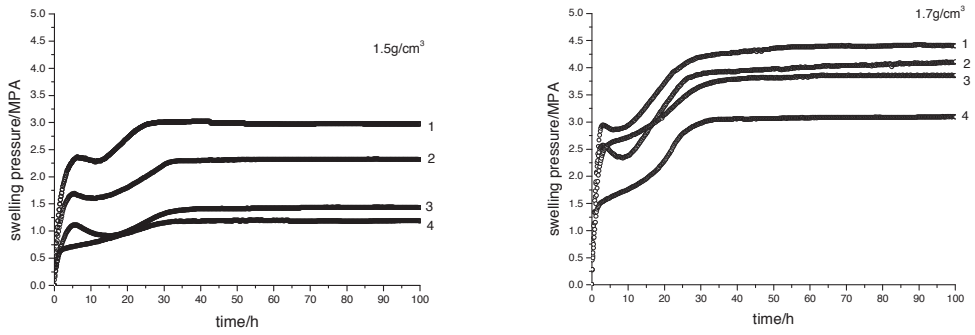


Fig.2 Swelling pressure vs. time for samples with dry densities from 1.50g/cm^3 and 1.70g/cm^3

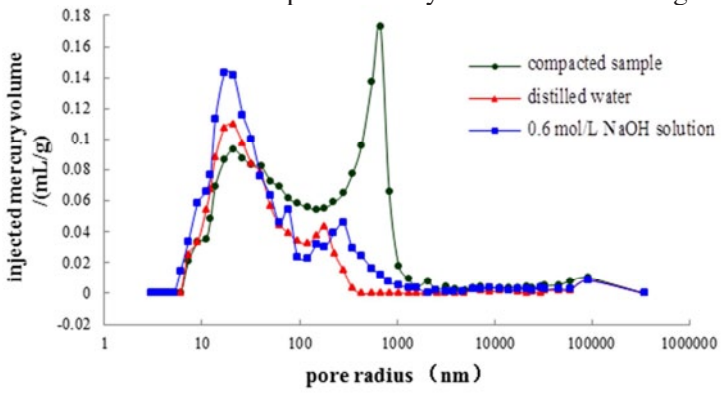


Fig.3 Relationship between injected mercury volume and entrance pore radius of samples with 1.70 g/cm^3 dry density

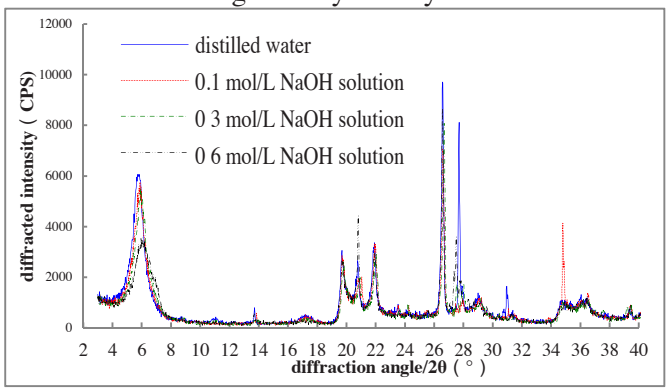


Fig.4 XRD results of samples submitted to the NaOH solutions with different concentration

Key words:
bentonite; swelling pressure; permeability; hyper-alkaline; dry density; methylene blue (MB) absorption ; dissolution; mercury intrusion porosimetry (MIP)

Shear characteristics of Ca-type bentonite immersed in $Ca(OH)_2$ solution

Yasutaka Watanabe, Shingo Yokoyama and Yukihisa Tanaka

Central Research Institute of Electric Power Industry
1646 Abiko, Abiko-shi, Chiba-ken, Japan
Corresponding author, e-mail: yasutaka@criepi.denken.or.jp

For the engineered barrier in radioactive waste disposal facilities, alteration of the bentonite will occur through reactions with alkaline solution as a leachate of the cementatious materials. It is required for long-term safety of the facilities to understand chemical-mechanical behavior of the bentonite. The objective in this paper is to investigate shear characteristics of Ca-type bentonite immersed in $Ca(OH)_2$ solution.

Triaxial compression tests have been conducted using two kinds of specimens, i.e. a bentonite and a bentonite-sand mixture. Ca-type bentonite has been used. Montmorillonite content of the bentonite estimated by methylene blue absorption was approximately 84 %. Approximately 66 % of cation exchangeable capacity was occupied by Ca ion. Each specimen size has been 40 mm in height and 20 mm in diameter. The specimens have been produced by applying axial loading statically. Effective bentonite density of the specimens has been 1.0 Mg/m^3. The specimens were immersed in 5 mmol/L-$Ca(OH)_2$ solution because the leachate of the cementatious materials will be controlled by $Ca(OH)_2$ in future. The outer solution has been exchanged once every two weeks to keep unsaturation in solubility of the solution. The immersed specimens have been stored in a vacuumed desiccator at 40 degrees Celsius to accelerate alteration.

pH and Si, Al, Ca, Na ions of the exchanged outer solution have been measured for 711 days. pH has been almost constant around 12.1. Ca ion concentration has been also constant throughout experiments. The highest concentrations of Si ion and Na ion have been detected at the beginning, and the concentrations gradually decreased. Al ion has not been detected. Because montmorillonite is composed by Si, Al and so on, no release of Al ion implied that most of montmorillonite has not been dissolved in 5 mmol/L-$Ca(OH)_2$ solution.

The triaxial compression tests in a consolidated and un-drained condition have been conducted using the specimens immersed in $Ca(OH)_2$ solution. For basic cases, the specimens have been just saturated by deionized water and $Ca(OH)_2$ solution at room temperature. Deviator stress has been increased along with axial strain, and deviator stress reached at residual stress at 10% of axial strain. In comparison with the basic cases, a different shear behaviour has been observed in the specimen after immersion in $Ca(OH)_2$ solution for 580 – 711 days at 40 degrees Celsius. The specimen immersed for 580 days, deviator stress has been gradually increased, and the maximum deviator stress has been obtained at 1 – 2 % of axial strain. After the peak, deviator stress has been drastically decreased. For the specimen immersed for 711 days, the maximum deviator stress has been larger than that of the specimen immerged for 580 days. Then, the axial strain at the maximum deviator stress has been also 1 – 2 %. Internal friction angle of the specimens has been decreased after the immersion, while cohesion has been increased. Especially, for the bentonite immersed in $Ca(OH)_2$ solution, the friction angle has changed from 26.6° to 23.2°, and the cohesion intercept from 0 kPa to 250 kPa during 580 days.

As a result of X-ray diffraction, changes of mineral composition of the bentonite and the bentonite-sand mixture immersed in $Ca(OH)_2$ solution have not been observed. Mean layer charge of montmorillonite has not changed after the immersion. The montmorillonite content of the bentonite after the immersion have not been decreased. Therefore, dissolution and mineralogical change of the montmorillonite have not almost occurred. Amount of the leachable cation of the bentonite by 1 mol/L-NH_4Cl solution has increased after immersion. These experimental results implied that some amorphous material containing Ca precipitated inside the specimen through the reaction between the bentonite and $Ca(OH)_2$ solution. The precipitation presumably influenced to the cohesion of the specimens.

In conclusion, this study obtained that the shear strength of the Ca-type bentonite immersed in $Ca(OH)_2$ solution increased, but the axial strain at failure decreased. It is further study to investigate the relation between the brittle failure and the precipitation.

Stability of chabazite as cation exchanger in hyper-alkaline media

Leen Van Tendeloo, Wauter Wangermez, André Maes, Christine Kirschhock, Johan Martens and Eric Breynaert*

Centre for Surface Chemistry and Catalysis, KU Leuven, Kasteelpark Arenberg 23, 3001 Heverlee.
*e-mail: eric.breynaert@biw.kuleuven.be

Despite all efforts towards selective waste collection and consequent recycling, non-reusable and highly toxic waste fractions remaining at the end of the revalorization chain, require permanent disposal. One example is the low- and medium-level, short-lived conditioned radioactive waste that has to be stored safely for several decades up to centuries. As for chemotoxic waste, a feasible scenario for this waste fraction involves immobilization and isolation in concrete-based surface disposal facilities. The concrete acts as a first barrier in preventing the radionuclides from entering the biosphere. The use of a second, redundant engineered barrier in the inspection room of the disposal facility complementing the primary concrete barrier is considered by ONDRAF/NIRAS as a defence in depth option to minimise the concentration levels of toxic elements. To fulfill its role, this second barrier should be capable of adsorbing radionuclides in the long-term and under the alkaline conditions arising from the leaching of the repository. Zeolites are considered as a promising material to fulfill these requirements. However, more insight is needed in their exchange properties and stability in hyper alkaline conditions.

The first cement degradation stage generates hyper alkaline, saline pore water (pH 13.5, 0.25 M alkaline cations), with K^+ as the main cation. Alkaline cations have a strong structure directing effect on the formation and stability of zeolites. A zeolite type typically occurring in K^+ systems is CHA (chabazite). The synthesis of chabazite in 1 M KOH solution, and its excellent cation exchange properties, already indicate this zeolite as a potentially suitable material for this application.
Since the Cs isotopes (^{137}Cs and ^{134}Cs) present in the radioactive waste of the Cat A disposal facility have been indicated as the isotopes predominantly contributing to the final dose to man of such a facility, this element was chosen as a chemical probe to study possible hydroxyl induced changes to the CHA framework. Comparison of the Cs^+ cation exchange properties of chabazite in K^+ and Na^+ containing solutions at pH 8 and pH 13, revealed a slight increase of the K_D with increasing pH.
Further, insight is gained in the formation process of chabazite in pure KOH, using zeolite Y as a source of Si and Al. The most important characterization techniques used in this work are XRD, SEM, TEM, ^{27}Al and ^{29}Si MAS NMR.
Next to pure KOH, chabazite formation was also demonstrated in simulated young concrete pore water (YCW). The crystallization of chabazite and other zeolite products in this medium were evaluated as function of temperature (60 and 85°C) over a timeframe of more than 2 years. At both temperatures a fraction of MER (merlinoite) type zeolite was obtained in the product mixture. Although the MER framework structure is known to provide ideal coordination sites for K^+ cations, the formation of this zeolite at low temperatures and K^+ concentrations was rather unexpected.

The sorption behavior of chabazite, in combination with its crystallization and stability in young concrete porewater, confirm this zeolite as a valid candidate material for inclusion in engineered barriers installed around concrete based waste storage facilities. However, further research is needed to elucidate the mechanisms of the hydroxyl induced changes to the framework indicated by ^{137}Cs, and to reveal which parameter of the YCW facilitated the formation of merlinoite next to chabazite.

Acknowledgements

This work was supported by long-term structural funding by the Flemish Government (Methusalem) and by ONDRAF/NIRAS, the Belgian Agency for Radioactive Waste and Fissile Materials, as part of the program on surface disposal of Belgian Category A waste. L.V.T. and E.B. acknowledge a mandate as, respectively, an aspirant and a postdoctoral fellow of FWO Vlaanderen.

Porosity Models and Impacts upon Clay Transformations

David Savage[1*] and Jinsong Liu[2]

[1]Savage Earth Associates Ltd, 32 St Albans Avenue, Bournemouth BH8 9EE, UK
[2]Swedish Radiation Safety Authority, 171 16 Stockholm, Sweden
[*]Corresponding author

The understanding of clay structure and porosity at different water/clay ratios and compaction densities is fundamental to the role of compacted clay as a buffer and backfill in a geological repository for HLW. Currently there are two types of model available to describe porosity: a concept involving different types of pore; and that which focuses on a single type of pore.

Considerable analytical (e.g. Likos and Wayllace, 2010) and theoretical (e.g. Muurinen et al., 2004) evidence exists for the presence of different pore types in compacted bentonite, even at densities considered for a clay buffer. Despite this evidence, some key processes (e.g. swelling, freezing) have been interpreted using a model which considers the existence of a single pore type, whereas others (e.g. colloidal properties, pore fluid evolution) are interpreted using a multiple-porosity concept. Moreover, in some activities (e.g. pore-fluid evolution, clay alteration), there is a confusion of the two models, with in some instances, initial pore fluid compositions calculated using a multiple porosity model and subsequent calculations employing a single (total porosity) model. Consequently, there is scope for an improvement in the consistency in the use of porosity models, not only between, but also within, different topic areas. In some topic areas (e.g. ionic transport), there are different interpretive models using conflicting porosity concepts. It is not clear that these differences will be resolved in the short-term so that these models need to be tested against laboratory-derived datasets.

Here, the effect of different porosity models upon clay mineral transformations is evaluated. Intrinsic to alteration reactions is the role of water/solid ratio, defined in a bentonite-pore fluid system by (the inverse of) porosity. In other words, the greater the porosity (according to which porosity model is adopted), the greater the role of pore water composition in the alteration process. As described in seminal papers of water-rock interaction in the 1980s (e.g. Giggenbach, 1984), if porosity is low, alteration is controlled by an effective isochemical recrystallization, termed 'rock-dominated alteration', whereas the opposite would be termed 'fluid-dominated alteration'. So for example, if bentonite is altered by a cement-derived $Ca(OH)_2$-rich fluid then alteration under a high porosity (high water/solid ratio) would produce alteration dominated by the fluid composition, i.e. solids dominated by Ca^{2+} and OH^-, such as high Ca/Si ratio C-(A)-S-H and/or zeolites with high Ca/Si. By contrast, under a low porosity (low water/solid ratio), alteration would be dominated by the composition of the clay, so that Si and Al would dominate the alteration, leading to the growth of zeolites with low Ca/Si ratios and feldspars.

As an example of this hypothesis, calculations have been carried out using the 'Geochemists Workbench' (GWB) computer code to react Na-montmorillonite with synthetic cement pore fluids. These reactions were carried out at different water/(water + clay) mass ratios to investigate the impact of water/clay ratio (porosity) upon the magnitude and style of alteration. The results of these calculations are expressed in terms of volume percentage of mineral versus water/(water + clay) ratio in Figure 1. For an 'evolved' pore fluid composition (pH = 12.45; portlandite saturated) it can be seen that at low water/(water + clay) ratios (< 0.5) alteration of Na-montmorillonite is minor (> 98 % montmorillonite is preserved), whereas at high water/(water + clay) ratio (> 0.95), Na-montmorillonite is removed[1]. At water/(water + clay) ≤ 0.95, alteration is 'clay-dominated' and is characterised by an assemblage of albite + quartz + Na-saponite + scolecite (high Si Ca-zeolite), but at 0.95 < water/(water + clay) < 1.0, alteration is 'fluid-dominated' and consists of jennite (high Ca/Si C-S-H mineral) + gismondine (low Si Ca-zeolite) + katoite (Ca-aluminate hydrate) + Ca-saponite.

[1] The calculations carried out here do not consider reaction kinetics which would slow the alteration process.

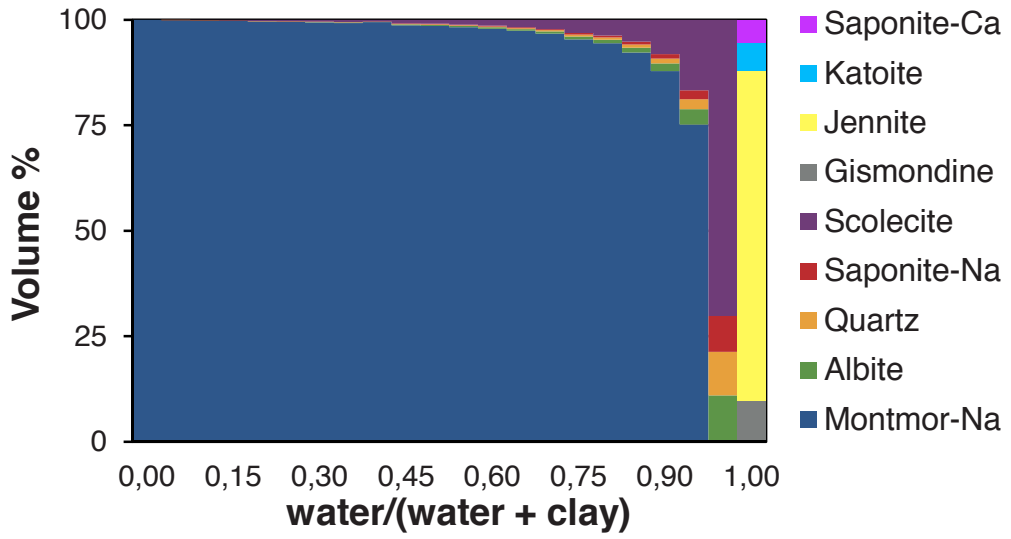


Figure 1. Alteration of Na-montmorillonite (volume % of mineral) by a $Ca(OH)_2$-saturated solution at 25 °C using GWB (Bethke, 2008) with the LLNL database 'thermo.com.V8.R6.230' (amended to include cement mineral data such as jennite from Lothenbach and Winnefeld, 2006) versus water/(water + clay) ratio.

In this particular simulation (but not in others), there is little difference in the magnitude and style of alteration at water/(water + clay) ratios typical of compacted bentonite (≤ 0.4). However, it does highlight that in laboratory experiments which use dispersed clay samples and a 'batch' equilibration system to characterise clay alteration, the high water/clay ratio in such experiments (e.g. 0.995 in the experiments of Savage et al., 1992; ~0.85 in the experiments of Fernández et al., 2009; 0.91 in the experiments of Kaufhold and Dohrmann, 2011) may induce a different reaction path from that which might be associated with compacted samples. In other words, these experimental systems produce a fluid-dominated alteration style rather than the clay-dominated alteration that would be expected in a compacted clay system.

These calculations illustrate that the fluid/clay ratio can have an important impact not only upon the magnitude of alteration, but also upon the nature of the reaction path. Consequently, it is of key importance that the most relevant ratio ('porosity') is used not only in geochemical calculations, but also in experimental systems.

References:

Bethke, C. M., Geochemical and Biogeochemical Reaction Modeling, Cambridge University Press, 2008.

Fernández, R., Rodríguez, M., Vigil de la Villa, R., and Cuevas, J., *Geochemical constraints on the stability of zeolites and C-S-H in the high pH reaction of bentonite*. Geochim Cosmochim Acta 74**:** 890-906, 2009.

Giggenbach, W. F., *Mass transfer in hydrothermal alteration systems*. Geochim Cosmochim Acta 48**:** 2693-2711, 1984.

Kaufhold, S., and Dohrmann, R., *Stability of bentonites in salt solutions III - Calcium hydroxide*. Appl Clay Sci 51**:** 300-307, 2011.

Likos, W. J., and Wayllace, A., *Porosity evolution of free and confined bentonites during interlayer hydration*. Clays Clay Mins 58**:** 399-414, 2010.

Lothenbach, B., and Winnefeld, F., *Thermodynamic modelling of the hydration of Portland cement*. Cem Conc Res 36**:** 209-226., 2006.

Muurinen, A., Karnland, O., and Lehikoinen, J., *Ion concentration caused by external solution into the porewater of compacted bentonite*. Phys Chem Earth 29**:** 119-127, 2004.

Savage, D., Bateman, K., Hill, P., Hughes, C., Milodowski, A., Pearce, J., Rae, E., and Rochelle, C., *Rate and mechanism of the reaction of silicates with cement pore fluids*. Appl Clay Sci 7**:** 33-45, 1992.

Controls on Long-Term Transformation of Montmorillonite

David Savage[1*] and James Wilson[2]

[1]Savage Earth Associates Ltd, 32 St Albans Avenue, Bournemouth BH8 9EE, UK
[2]Quintessa Ltd., 633/635 Birchwood Boulevard, Birchwood, Warrington, WA3 7QU, UK
[*]Corresponding author

A number of safety functions for the buffer and backfill in a geological repository for HLW/SF are fulfilled if the presence of montmorillonite can be maintained in the long-term. The transformation of montmorillonite to non-swelling minerals is addressed in most safety assessments by evaluating the potential for the smectite to illite reaction to occur. This reaction is usually shown to be unfavourable on the grounds of mass balance (limited supply of K^+) and kinetics (temperatures < 100 °C are too low for significant reaction under near-neutral pH conditions). Although this may (superficially) demonstrate system robustness, this type of calculation may be neither conservative nor realistic.

lllitisation is only one of a number of montmorillonite transformation reactions that could occur, depending upon the design of the EBS and the composition of the ambient groundwater in the host rock. For example, conversions of montmorillonite to zeolite, and/or a range of non-swelling Fe-silicates are possible depending upon the amounts of cementitious sealing materials and steel waste package and structural elements employed in repository construction. Consequently, the relative importance of potential transformations needs to be assessed from the following perspectives: mass balance (is there enough of a key reactant?); mass action (is the reaction thermodynamically favourable?); and kinetics (is the reaction fast enough to be significant?).

All potential clay mineral transformations are complex, non-linear reactions, driven in turn (principally) by activities of SiO_2, OH^-, Al^{3+} and temperature. Because of the juxtaposition of chemically-incompatible materials and evolving temperature in the EBS during the first few hundred years after closure, activities of these key species will vary spatially and temporally across the buffer and backfill, such that patterns of alteration may be complex and heterogeneous. For example, it is likely that different alteration reactions will occur in the buffer at the separate interfaces with waste package and rock (e.g., Marty et al., 2010). Moreover, eventual perforation of waste packages may lead to significant changes in pore fluids due to exposure of their contents (e.g. waste glass, spent fuel, cast iron canister insert), leading to 'spikes' in SiO_2 and Fe^{2+} in pore fluids.

To illustrate the time-dependent aspects of long-term transformation reactions and also the role of silica activity, a schematic reaction-path for a bentonite buffer in fractured hard rocks is shown in Figure 1 (left). Initial post-closure conditions are represented by point A, where silica activity is defined by chalcedony solubility at 15 °C and the activities of other chemical species by albite (Na^+), microcline (K^+), kaolinite (Al^{3+}), Ca-saponite (Mg^{2+}), and calcite (Ca^{2+}). Silica activity and $f\,CO_2(g)$ were fixed at that for chalcedony solubility ($SiO_{2(aq)}$) and 10^{-5} bars ($CO_2(g)$), typical of deep groundwaters in fractured hard rocks (e.g. Savage et al., 1999; Coudrain-Ribstein et al., 1998). It can be seen that sodium montmorillonite is stable under such conditions. The thermal pulse from emplaced waste packages is described by the reaction-path from points A to B, where it can be seen that this would initially stabilise muscovite (a proxy for illite) and then laumontite (Ca-zeolite) relative to montmorillonite. Point B is defined by equilibration of quartz at a temperature of 100 °C, reflecting the greater rate of growth of quartz at this higher temperature. This thermal pulse is anticipated to last for a few hundred years at most for most disposal concepts studied and would thus limit the potential for conversion of montmorillonite to zeolite (kinetic constraint).

Waning temperatures over hundreds of years would lead to potential de-stabilisation of zeolite minerals such as laumontite, a consequent release of Ca^{2+} and $SiO_2(aq)$, and thus eventual equilibration of pore fluids with Ca-montmorillonite, the ion-exchanged form of Na-montmorillonite ('montmor-Ca' in Figure 1, left) and is reflected in the reaction path from points B to C.

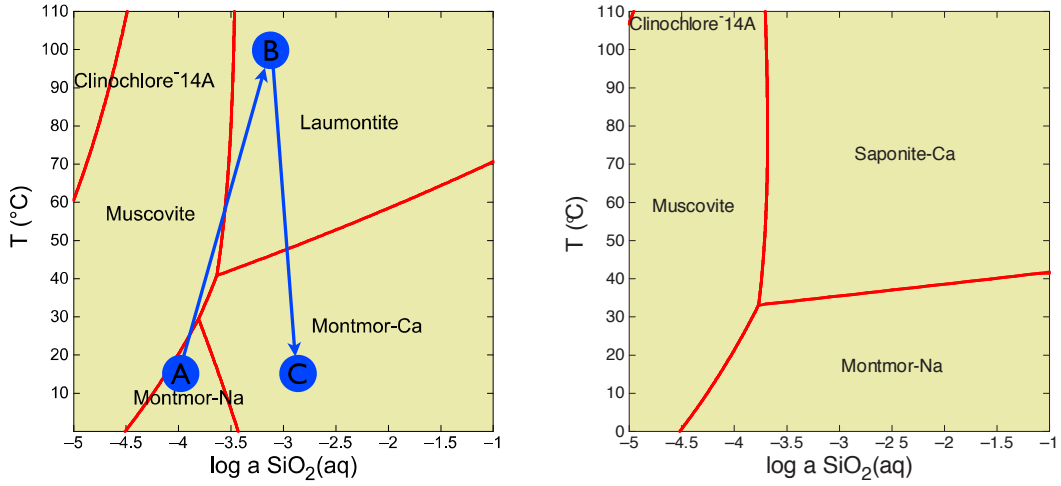


Figure 1. Possible reaction-path for pore fluids in a bentonite buffer in fractured hard rocks (left) shown on a SiO_2(aq) versus temperature activity diagram for the system Na_2O-K_2O-CaO-MgO-Al_2O_3-SiO_2-CO_2-H_2O, constructed using 'Geochemist's Workbench' and LLNL database 'thermo.com.V8.R6.230'. Alternative mineral stabilities for this system where Mg^{2+} is defined by Na-saponite are shown in the right-hand figure.

Point C is defined by the solubility of amorphous silica at 15 °C, reflecting the likely prolonged supersaturation of pore fluids with respect to quartz and chalcedony at low temperature after the thermal pulse.

The precise nature of mineral stability in this system is dependent upon the assumed mineral buffers for aqueous species, so that if Ca-saponite is replaced by Na-saponite as a control upon Mg^{2+}, the laumontite stability field is replaced by that for Ca-saponite and the stability of Na-montmorillonite extends across a wide range of $SiO_{2(aq)}$ at low temperature (Figure 1, right). This emphasises the need not only to determine groundwater compositions during site characterisation activities, but also to understand the controls of key chemical components (e.g. Savage et al., 1999).

Due to the inherent uncertainties of thermodynamic data for clay and zeolite minerals especially, such calculations are illustrative only, but serve to highlight that simple scoping calculations cannot capture the potentially complex clay mineral transformations accompanying long-term evolution of near-field pore fluids. Models aimed at simulating near-field evolution need to address the key controls of mass balance, mass action and kinetics in a spatially-, temporally-, and thermally-variable framework.

References:

Coudrain-Ribstein, A., Gouze, P., and de Marsily, G., *Temperature-carbon dioxide partial pressure trends in confined aquifers*. Chemical Geology 145**:** 73-89, 1998.

Marty, N. C. M., Fritz, B., Clément, A., and Michau, N., *Modelling the long term alteration of the engineered bentonite barrier in an underground radioactive waste repository*. Applied Clay Science 47**:** 82-90, 2010.

Savage, D., Arthur, R. C., and Saito, S., *Geochemical factors in the selection and assessment of sites for the deep disposal of radioactive wastes*. *In* Chemical Containment of Wastes, Geol. Soc. London Spec. Pub. 157, pp. 27-45, 1999.

Mineralogical-geochemical processes observed in the MX80 bentonite buffer used in deposition holes 5 and 6 of the full scale experiment „prototype repository“ in Äspö, Sweden, after 8 years of operation

[1,2] *Dohrmann, Reiner*, [2]Kaufhold, Stephan

1 LBEG, Stilleweg 2, D-30655 Hannover, Germany
2 BGR, Stilleweg 2, D-30655 Hannover, Germany

Bentonites are candidate materials for High-Level Radioactive Waste (HLRW) repositories and, therefore, are investigated with respect to long term stability. In order to identify possible bentonite alteration processes long term in-situ tests are conducted in rock laboratories. The prototype repository *in-situ* experiment (PR) is one of the outstanding tests due to the size of the installation as well as the duration. The poster will show results of chemical and mineralogical analysis and highlight alteration processes of the bentonite MX 80. Cation exchange was observed in the bentonite buffer materials. This was most likely caused by inflowing Na-Ca-Cl-type granitic groundwater. The MgO concentration increased at the bentonite–Cu canister interface, the Mg sink however could not be detected. Ca-carbonate and Ca-sulfate were also found at this interface. Chemical analysis, scanning electron microscopy, and differential thermal analysis were used to detect Cu corrosion products at the bentonite-canister interface. Up to 0.5 mm into the bentonites Cu could be detected by SEM-EDX. The CEC dropped in the MX80 buffer compared to the CECs of the reference samples, particularly in the warmer deposition hole 5 compared to the colder deposition hole 6. Overall the prototype repository in-situ experiment proved that cation exchange reactions occurred in full scale bentonite buffer experiments in all bentonite blocks but structural degradation of smectite could not be identified.

THC numerical modelling of the long-term interactions of the corrosion products and the compacted bentonite in a HLW repository in granite

Javier Samper, **Acacia Naves, Luis Montenegro, Alba Mon**

University of A Coruña, 15071 La Coruña, Spain, jsamper@udc.es

A THC numerical model of the long-term geochemical evolution of the bentonite barrier of a spent-fuel carbon-steel canister repository in granite is presented. The model accounts for canister corrosion, the chemical interactions of corrosion products and bentonite, mineral dissolution precipitation, surface complexation, of Fe^{2+} and H^{+} on three types of sorption sites and cation exchange reactions of Ca^{2+}, Mg^{2+}, Na^{+}, K^{+} and Fe^{2+}. The model considers the generation of H_2(aq) which is allowed to diffuse through bentonite and the flow through granite which flushes the bentonite/granite interface. Numerical simulations are performed for 1 Ma for a reference scenario at a constant temperature of 25ºC and assuming anoxic corrosion at a constant rate of 2 μm/y. Model results indicate that canister corrosion causes a marked increase in pH and the concentration of dissolved Fe^{2+}. Most of the released Fe^{2+} diffuses from canister into the bentonite where it precipitates mainly as magnetite. Dissolved Fe^{2+} sorbs by surface complexation and undergoes cation exchange. Sorption plays a relevant role in the geochemical evolution of bentonite. The competition of Fe^{2+} and H^{+} for the sorption sites near the canister/bentonite interface causes several sorption fronts which induce fronts on pH, Eh, dissolved Fe^{2+} and mineral dissolution/precipitation. The precipitation of corrosion products takes place in a 7-8 cm thick band of bentonite near the canister/bentonite interface and leads to a severe decrease of bentonite porosity.

The numerical predictions contain uncertainties due to simplification in the geometric model and the model structure (dimensionality) and uncertainties in the conceptual model (processes) and the model parameters. A systematic sensitivity analysis of the model results to changes in the following parameters was performed: 1) The corrosion rate; 2) The effective diffusion coefficient, D_e, of the dissolved species in the bentonite; 3) The water flow through the granite at the bentonite/granite interface; 4) The cation selectivities and 5) The chemical compositions of the bentonite and granite porewater (Samper et al., 2013). Long term simulations were performed for a set of variant scenarios to evaluate the effect of the simplifications of the conceptual model. These scenarios account for: 1) The thermal field in the bentonite barrier which may last for thousands of years; 2) The dependence of the corrosion rate on temperature; 3) The dependence of the corrosion rate on the chemical conditions; 4) The kinetics of magnetite precipitation and 5) The kinetic dissolution of smectite and the neoformation of Fe-clay minerals and zeolites.

The thermal transient stage was taken into account by solving for the heat transport through the bentonite buffer. The time evolution of temperature was prescribed at the canister/bentonite interface. The temperature increases up to 97 ºC after 24 years and decreases smoothly afterwards. The computed temperatures are used for updating the equilibrium constants, the activity coefficients and the rate constants. The thickness of the bentonite affected by a decrease of porosity increases 1 cm when the thermal gradient was considered. The corrosion rate increases and afterwards decreases with temperature reaching a maximum value of 4.8 μ/y when the thermal transient and the temperature-dependence of the corrosion rate are taken into account. In this scenario the computed pH and the concentration of dissolved Fe^{2+} increase faster and the fronts of pH, Eh, sorption, dissolved Fe^{2+}, and mineral dissolution/precipitation occur before than the reference scenario. The thickness of the bentonite affected by a decrease of porosity is of 6-7 cm in this scenario. The dependence of the corrosion rate on the chemical conditions (pH, Eh, Fe^{2+} concentration) was analyzed by performing an

isothermal sensitivity run accounting for a variable corrosion rate, which depends on the ratio between the ion activity product and the equilibrium constant for iron dissolution. Model results show that canister corrosion slows down leading to significant changes in the patterns of pH, Eh, iron sorption and mineral dissolution/precipitation after 1000 years. Magnetite and siderite precipitation after 1 Ma is significantly lower than that of the reference scenario near the canister, but iron precipitation takes place in the entire bentonite buffer.

Model results show that the penetration of magnetite precipitation into the bentonite and, therefore, the zone of bentonite affected by the reduction of porosity decreases significantly when kinetically-controlled magnetite precipitation was considered. Model results are very sensitive to changes in the magnetite reactive surface area. The larger the reactive surface area, the thinner the zone of bentonite affected by canister corrosion.

The long-term relevance of kinetically-controlled smectite dissolution and its influence on the thickness of altered bentonite was evaluated with a sensitivity run. The Al^{3+} released by smectite dissolution precipitates as analcime. Smectite dissolves and analcime precipitates in the entire bentonite barrier after 10^4 years in very small concentrations. Only 0.2% (volume) of the smectite is dissolved after 1 Ma. Therefore, smectite dissolution is not a relevant reaction in the long-term geochemical evolution of the repository. The scenario which considers the neoformation of cronstedite in addition of smectite dissolution and analcime precipitation shows that cronstedite precipitates near the canister/bentonite interface reducing slightly the precipitation of analcime. The precipitation of cronstedite does not affect significantly the smectite dissolution but it influences the precipitation of the corrosion products. The penetration of the corrosion products and the thickness of bentonite affected by porosity reduction are similar to those of the reference scenario.

Numerical simulations were performed with 1D and 2D axisymmetric models. The results of the 2D model which accounts for canister border effects and the flow and solute transport through the granite are similar to those of the 1D axisymmetric model. Models results show that the penetration of the geochemical perturbations caused by the corrosion products into the granitic rock formation is significantly smaller than the separation between galleries. Therefore, the assumption of the 1D axisymmetric model that the galleries do not interact is valid.

The conclusions of our numerical model of the interactions of bentonite and corrosion products are largely consistent with those reported by Bildstein et al. (2006), Wersin et al. (2007), Savage et al. (2010) and Marty et al. (2010) for bentonites.

References

Bildstein, O., Trotignon, L., Perronnet, M., Jullien, M., 2006. Modelling iron-clay interactions in deep geological disposal. Physics and Chemistry of the Earth 31, 618–625.

Marty, N.C.M, Fritz, B., Clément, A., Michau, N., 2010. Modelling the long term alteration of the engineered bentonite barrier in an underground radioactive waste repository. Applied Clay Science, 47, 82-90.

Samper et al. (2013). Report on long-term THC(m) predictions of a HLW repository in granite. PEBS Project Deliverable 3.5-3. Available on-line: http://www.pebs-eu.de.

Savage, D., Watson, C., Benbow, S., Wilson, J., 2010. Modelling iron/bentonite interactions. Applied Clay Science 47, 91-98.

Wersin, P., Birgersson, M., Olsson, S., Karnland, O., Snellman, M., 2007. Impact of corrosion-derived iron on the bentonite buffer within the KBS-3H disposal concept – the Olkiluoto site as case study. Posiva Report 2007-11.

***Acknowledgements**: The research leading to these results has received funding from the European Atomic Energy Community's Seventh Framework Programme (FP7/2007-2011) under grant agreement 232598. This work was partly funded by ENRESA (Spain), the Spanish Ministry of Economy and Competitiveness (Project CGL2012-36560) and Galicia Regional Government (Fund 2012/181 from "Consolidación e estruturación de unidades de investigación competitivas").*

Long-term THC simulations of the interactions of the corrosion products, the compacted bentonite, the concrete and the clay in a HLW repository in clay

Javier Samper, **Alba Mon, Luis Montenegro & Acacia Naves**

University of A Coruña, 15071 La Coruña, Spain, jsamper@udc.es

The evaluation of the long-term geochemical evolution of the engineered barrier system of a high-level radioactive waste repository requires the use of reactive transport models. Here we present a non-isothermal unsaturated/saturated water flow and multicomponent reactive solute transport model of a HLW repository in clay according to the Spanish Reference Concept (Enresa, 2004). The model has been constructed by extending and improving the model performed previously by our group within the NFPRO Project (Yang et al. 2008). The model of 2008 focused on the interactions of the bentonite buffer, the concrete liner and the clay formation. The updated model performed within the PEBS Project considers simultaneously the interactions of the corrosion products and the bentonite and the interactions of the bentonite buffer, the concrete liner and the clay formation. The reactive transport model has been improved also by: 1) Considering the kinetic dissolution of smectite and the precipitation of secondary mineral phases; 2) Updating the bentonite selectivity coefficients; and 3) Taking into account proton and iron sorption by surface complexation on three types of protolysis sites.

The model domain was discretized with a 1-D axisymmetric grid which includes 4 material zones: the canister, the bentonite buffer, the concrete liner and the clay formation with a total length of 25 m. Simulations were run for 1 Ma. The model was performed in two stages. The first one lasts until the bentonite barrier becomes almost saturated. The second one extends to 1 Ma. In the first stage of bentonite saturation, water flows from the clay formation through the concrete to the bentonite and controls the solute transport in the system. The second stage starts once the bentonite buffer is saturated. Then, water flow is negligible and solute transport occurs entirely by molecular diffusion. The model accounts for the thermal field in the bentonite barrier by prescribing a time-varying temperature function at the inner boundary to simulate the cooling of the radioactive waste and solving the heat transport. The reference model accounts for homogeneous reactions (acid-base, aqueous complexation and redox reactions) and heterogeneous reactions such as mineral dissolution/precipitation, cation exchange and surface complexation.

The chemical system is defined in terms of the following primary species: H_2O, H^+, Ca^{2+}, Mg^{2+}, Na^+, K^+, Cl^-, SO_4^{2-}, HCO_3^-, $SiO_2(aq)$, $O_2(aq)$, Fe^{2+} and Al^{3+}. The model considers the following initial minerals: 1) iron in the canister; 2) smectite, calcite, gypsum and quartz in the bentonite; 3) tobermorite, portlandite, brucite and calcite in the concrete; and 4) calcite, gypsum, quartz, and dolomite in the clay formation (Enresa, 2004). The secondary minerals considered in the model which can precipitates include: magnetite, siderite, goethite, gyrolite and analcime. The model considers the kinetic dissolution of smectite and the precipitation of analcime. A constant corrosion rate of 2 μ/year is considered in the updated model. The model accounts for cation exchange reactions involving Na^+, Ca^{2+}, Mg^{2+}, K^+ and Fe^{2+}. Cation exchange was modelled with the Gaines-Thomas convention. Surface complexation reactions were considered in the bentonite. They were modelled with the triple sorption site model of Bradbury and Baeyens (1997; 2005).

The parameters for the model were taken from the previous model of Yang et al. (2008). The initial pore water chemical compositions and the mineral volume fractions in the bentonite barrier, the concrete liner and the clay formation were taken from Enresa (2004). The initial porewater of the canister is assumed to be the same as that of the bentonite porewater.

The pH front affects the entire bentonite buffer after t = 10,000 years and penetrates 0.95 m in the clay formation after 100,000 years. The time evolution of the pH computed with the updated and the previous models is generally similar. The pH is slightly different in the bentonite due to canister corrosion and smectite dissolution. The penetration of the high pH front into clay for the updated model (0.95 m) is slightly larger than for the previous model (0.70 m). The general patterns of the mineral dissolution/precipitation of the previous model are similar to those of the updated model. However, there are differences due to canister corrosion, the smectite dissolution and the role of surface complexation.

Portlandite and tobermorite dissolve in the concrete. Brucite, gypsum and sepiolite precipitate in the concrete and at the bentonite-concrete and clay-concrete interfaces. The updated model predicts more intense alterations in the bentonite and in the clay. At t = 1 Ma, pore clogging affects all the concrete; 1 cm thick zone at the bentonite-concrete interface and a 2.5 cm zone at the clay-concrete interface (Figure 1). The sensitivity analysis shows that the final pH distribution is more sensitive to smectite dissolution than to the surface complexation. Magnetite precipitation is sensitive to the surface complexation. Pore clogging is sensitive to ettringite dissolution in the concrete and Mg-saponite precipitation in the bentonite. The conclusions of our numerical model are consistent for the most part with those reported by others for similar systems.

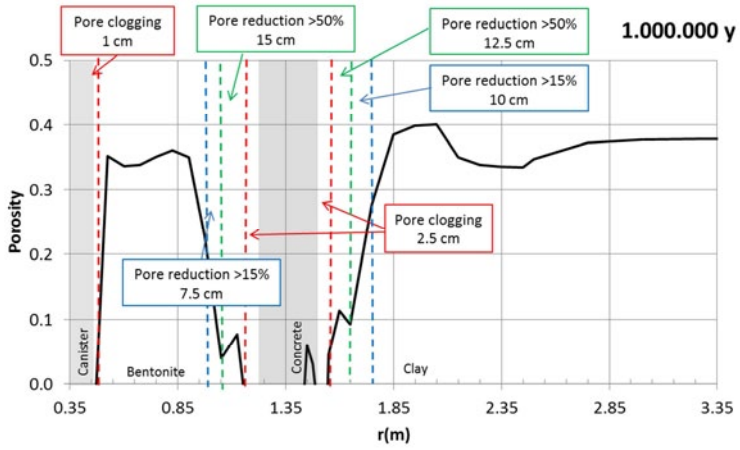


Figure 1. Spatial distribution of the computed porosity at t = 1Ma. Porosity changes due to mineral dissolution/precipitation reactions. The blue lines indicate the zones where the porosity reduction is higher than 15%. The green lines indicate the zones where the porosity reduction is higher than 50%.The red line indicates the zone where the zones with pore clogging.

References

Enresa (2004). Evaluación del comportamiento y de la seguridad de un almacén geo-lógico profundo de residuos radiactivos en arcilla. Clave: 49-1PP-M-A1-01. Enresa (In Spanish).

Bradbury, M.H., Baeyens, B. (1997). A mechanistic description of Ni and Zn sorption on Na-montmorillonite. Part II: Modelling. Journal of Contaminant Hydrology 27, 223-248.

Bradbury, M.H., Baeyens, B. (2005). Modelling the sorption of Mn(II), Co(II), Ni(II), Zn(II), Cd(II), Eu(III), Am(III), Sn(IV), Th(IV), Np(V) and U(VI) on montmoril-lonite: Linear free energy relationships and estimates of surface binding constants for some selected heavy metals and actinides. Geochimica et Cosmochimica Acta 69, 875-892.

Yang, C., J. Samper, L. Montenegro (2008) A coupled non-isothermal reactive transport model for long-term geochemical evolution of a HLW repository in clay, Environmental Geology, 53:1627–1638. DOI 10.1007/s00254-007-0770-2.

***Acknowledgements**: The research leading to these results has received funding from the European Atomic Energy Community's Seventh Framework Programme (FP7/2007-2011) under grant agreement 232598. This work was partly funded by ENRESA (Spain), the Spanish Ministry of Economy and Competitiveness (Project CGL2012-36560) and Galicia Regional Government (Fund 2012/181 from "Consolidación e estruturación de unidades de investigación competitivas").*

Effect of steam on the swelling capacity of bentonite

Ola Karnland

Clay Technology AB, Ideon Science Park, SE-223 70 Lund, Sweden, (ok@claytech.se)

Couture (1985) presented experimental results concerning the effects of steam on bentonite at temperatures between 150 and 250°C. The effect was studied by varying the water-to-solid ratio in a systematic way in a closed system, and subsequently measure the clay/water volume after mixing with water, dispersion and settlement. A rapid irreversible reduction of the volume of the bentonite was claimed to be the result after only 7 days of exposure to steam. The largest reduction was found at relatively low water-to-solid ratios during heating, and no or only minor effects were found if the clay was completely dry, or if the water-to-solid ratio was high enough during heating. Since a repository may be partially water saturated during a substantial period of time, the results have led to persisting uncertainty for the safety assessment, since swelling ability of montmorillonite is fundamental for a bentonite buffer with respect to almost all of the buffer functions. As a consequence, some additional studies have been performed concerning the effects of steam on bentonite and possible implications for a repository (Oscarson & Dixon 1990, Haas et al. 1999). Fortunately, these studies have not shown the dramatic changes reported by Couture (1985), especially with respect to the irreversibility.

The present work, had the basic ambition to repeat the experiments by Couture and expand the tests and analyses enough to understand the discrepancy between the available studies, and thereby remove, or at least reduce, the uncertainty concerning the effects steam on bentonite. Totally nine different bentonites brands, including e.g. MX-80, FEBEX and Kunigel V1, were used in the experiments representing a broad range of different qualities with respect to exchangeable ion, accessory minerals and production techniques. The materials were tested as delivered, and in some cases also after purification and exchange to Na^+, K^+ and Ca^{2+}-form. In addition to the basically commercial products, the Clay Mineralogical Society standard bentonite SWy-1 was used, which was of special interest since this material was also used in the study by Couture (1985).

The basic testing principle was to expose the various clay materials to 150 or 200°C at different water-to-solid ratios for one week, and thereafter measure the water containing capacity initially after passive water uptake and secondly after active dispersion and settlement. Small clay samples were confined in containers made of PEEK and titanium in series of five individual samples. The water-to-liquid ratio in each sample was controlled by mixing in water before heating, or by controlling the water pressure through a titanium filter in contact with the clay. In the latter case, the pressure was chosen to give a defined relative humidity, corresponding to a specific water-to-solid ratio in the clay. After the heating phase, the clay samples were allowed to cool in the test cells, and the water-to-solid ratios were determined by drying at low pressure at room temperature. The samples were ground to a similar grain size as the specific reference material, and 0.1 gram of dry material was placed in 5 mL sized test tubes, and deionised water was added. The tubes were sealed and placed to rest for several weeks until no further change in clay volume was observed. In most cases, the upper surface of the clay was distinct and the clay/water volume was determined for each sample. The tubes were thereafter shaken and the clays were dispersed ultrasonically for 15 minutes, and allowed to settle and the clay/water volumes were again measured. The dispersion of the reference material resulted in formation of voluminous sols and gels with much larger volume than what was formed after passive swelling in pure water in these materials. The ability to form such voluminous structures by dispersion and subsequent sedimentation was reduced by exposure to steam in these materials, but not the ability to swell. Some results are illustrated as in Figure 1. In general, sedimentation and sol/gel formations are a delicate processes, which are sensitive to small changes in ionic strength, pH etc. (Birgersson et al. 2009). There are consequently no significant experimental results showing negative effects of steam on the passive uptake of water in bentonite, usually termed swelling capacity, and there are no indications that steam should change the physical properties of a bentonite buffer in a long-term

perspective except for the statements presented by Couture. Couture defined the swelling capacity of a clay as the maximum specific volume in water, and according to the tests procedure given by Couture (1985), all samples were actively dispersed ultrasonically and then allowed to settle. The statement by Couture (1985) that "the reduced swelling capacity corresponds to reduced uptake of water by hydrated layers of the montmorillonite" is consequently questioned. Not only based on the above discussion, but also on the statement that "montmorillonite altered by water vapour at 250°C expands only to a maximum basal spacing of 19 Å, which corresponds to three water layers per 10 Å silicate layers in the structure". No reference or experimental results which supported such a statement were provided. On the contrary, the lowest reported clay volume was 4 cm^3/g clay, which corresponds to a mean interlayer distance of approximately ten times the stated distance of 9 Å.

In the present study, large differences in final volume after active dispersion were found between reference and steam exposed material in some of the examined bentonites. These results were qualitatively similar to those found in (Couture, 1985), who used the term "swelling capacity", although the results clearly relates to sedimentation properties rather than to swelling properties.
The term "swelling capacity" is normally used to describe the maximum volume after passive water uptake (free swelling or unconfined swelling). No such tests were performed in the study by Couture, and results from the present study show no significant effect of steam at the examined temperatures (up to 200°C). There are consequently no experimental indications in the two studies that short term exposure to steam impair the swelling properties of bentonite.

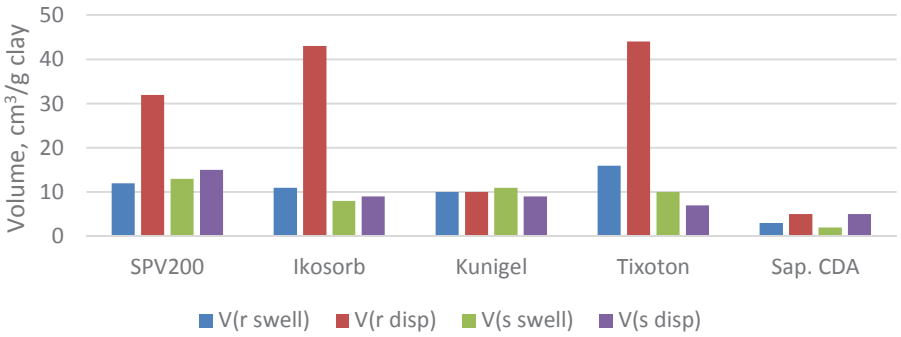


Figure 1 Clay/water volumes for five materials. V(r swell) represents the volume of passive water uptake in reference materials, V(r disp) represents the volume after settlement of actively dispersed material, and V(s swell) and V(s disp) represents the corresponding volumes for materials exposed to steam.

References

Birgersson, M., Börgesson, L., Hedström, M., Karnland, O. & Nilsson, U. (2009): Bentonite erosion – Final report. SKB Technical Report TR-09-34. SKB Svensk Kärnbränslehantering AB, Stockholm, Sweden.

Couture, R.A (1985): Steam rapidly reduces the swelling capacity of bentonite. Nature 318, 50-52.

Haas, R., Teysseire, Ph. & Bucher, F. (1999): Einfluss von Wasserdampf auf Quellpotential von Bentonit. Unpubl. Nagra Internal Report. Nagra, Wettingen, Switzerland.

Oscarson, D.W. & Dixon, D.A. (1990): Effect of heating unsaturated bentonite on the swelling and hydraulic properties of subsequently saturated clay. *In:* Proc. of the Annual Conf. and 1st Bienial Environmental Speciality Conf. of the Canadian Soc. of Civil Engineering II-1, 312-223. Hamilton, Ontario.

MVE – "Rate Drop" experiment: progress report on an in situ glass dissolution test at the Andra's URL.

Yannick Linard[1], Christelle Martin[2], Michel L. Schlegel[3], Patrick Jollivet[4]

1- *Andra, Centre Meuse/Haute-Marne, RD 960, 55290 Bure*
2- *Andra, Siège, Parc de la Croix Blanche - 1/7 rue Jean Monnet, 92298 Châtenay-Malabry*
3- *CEA, DEN/DPC/SEARS/Laboratoire d'Ingénierie des Surfaces et Lasers, 91191 Gif-sur-Yvette*
4- *CEA, DEN/DTCD/SECM/Laboratoire d'étude du Comportement à Long Terme, F-30207 Bagnols-sur-Cèze*

Introduction

As part of the evaluation of the safety of the geologic disposal of high-level long-lived vitrified radioactive waste, an integrated *in situ* experiment, named MVE-Rate Drop, is being performed in the Andra's underground research laboratory (Bure, France). In this *in situ* experiment, the long-term performance of SON68 glass – inactive surrogate of the French R7T7 HLW glass – is studied in realistic disposal conditions. We report on our present progress and we compare our latest experimental results with findings from surface laboratory experiments and modelling predictions.

Experimental concept

The experimental setup is made of an interval of a vertical descending borehole filled by a mixture of glass powder and iron filings (Figure 1a). The test interval is then closed, saturated with a synthetic water simulating the porewater chemistry of the surrounding Callovo-Oxfordian argillaceous rock (COx) and the pressure raised to 40 bars (close to the pressure of the rock surrounding the sealed interval). Due to the lack of hydraulic pressure difference between the interval and the surrounding rock, the transport of dissolved elements is mainly diffusive. In contact of the same water, four cells fixed at the extremity of rods are filled with the same glass/iron mixture to allow us to sample at four times the solid phases. Around the vessel, a heater system maintains a temperature of 50° C. A closed water circulation is maintained at flow rate equal to 5 mL/minute between the interval and a module located in the drift. This module is made of a circulation pump, a flowmeter, several sampling cells used to get samples of the leachate and monitor its chemical evolution, and different sensors to measure inline pH, Eh and electrical conductivity.

Progress report

The MVE-Rate drop test has been installed and the test interval has been resaturated with water on July 2, 2010. Thus, the test provides a 5-year survey that can be exploited to understand the kinetics of in situ SON68 glass alteration. The first sampling rod was extracted on June 18, 2012, i.e. 713 days after the water saturation. At the time of this writing, the other rods are still in place in the borehole.

Water chemistry

The pH values are mainly neutral (6.8 – 7.5) along five years at 50°C. Redox potentials are clearly negative. Initial decrease in sulphate concentration and increase in chloride content reflect a bacterial activity (which has been confirmed by microbiological analysis) and the impact of drilling operations (including the drying of the borehole wall), respectively.

The evolution of the boron concentration, present only at trace levels in the rock and its porewater, reflects the progress of the dissolution reaction of the glass. However, measured boron concentration has to be corrected for losses due to diffusive transport in the geological formation. The normalized mass loss values (NL) calculated from the measured concentrations of boron in solution are shown in Figure 1b. After 120 days, the rate of boron release slows down, reflecting a decrease of the alteration rate. Initial rate (r_0) is estimated at 1.10^{-2} $g.m^{-2}.d^{-1}$, close to most r_0 values measured in pure water in conventional laboratory and slightly inferior to the r_0 measured in synthetic COx porewater at 50°C (about 9.10^{-2} $g.m^{-2}.d^{-1}$).

In longer term, the rate is about 6 10^{-5} $g.m^{-2}.d^{-1}$, similar in magnitude to the residual rate observed for classical experiments in pure water with the same S/V (glass-surface-area-to-solution-volume) ratio (about 400 cm^{-1}) at 50 ° C. This is surprising because the dissolved concentrations of silicon do not indicate that a steady state is reached. Tests carried out by conventional laboratory with COx porewater indicate larger differences in the kinetics with pure water tests. Interpretation of the results of conventional laboratories concerning the comparison of SON68 glass dissolution in pure water and in COx porewater highlights the role of magnesium: a strong anti-correlation was found between the

amount of altered glass in COx porewater and magnesium concentrations in the leaching solution. The decrease in the concentration of magnesium in the leachate is explained by the precipitation of magnesium silicates at the surface of glass altered layers. In our test, this anti-correlation is also present (Figure 1b) without result in high kinetic difference with pure water tests.

Solid phase characterization

The characterizations by SEM-EDX, TEM and EPMA performed on the glass-iron sample altered during 713 days in the first extracted rod provide information on the composition and morphology of the alteration layer and corrosion products. The alteration products of glass are made of a gel layer, a newly formed layer, and loose precipitates associated with the corrosion products of iron. The gel thickness, corresponding to the amount of altered glass and assuming a constant glass dissolution rate during the 713 days of leaching, suggests a mean alteration rate of 2.7 10^{-2} $g.m^{-2}.d^{-1}$, different from that calculated from NL(B). The alteration layer contains crystalline phases and precipitates of many different chemical compositions: rare earth compounds associated with calcium and silicon (apatite phase) or borates, presence of ZnS and FeS that could possibly be related to bacterial activity. There is a wide variation in Si / Fe and Al / Fe ratios in the newly formed layer. The gel incorporates Fe at various amounts, there is a significant retention of boron in the newly formed layer, that could, at least partially, explain the difference between the glass dissolution rates calculated from NL(B) and derived from the measurement of gel thickness.

Corrosion products are made of siderite and chukanovite, hydrated Fe-silicate phases, and locally some Fe sulfide (mackinawite). The Fe-silicate had a highly disordered structure, probably with silicate groups forming embryonic sheets acting as precursors of larger phyllosilicate particles. The scarcity of corrosion products in the middle of the sample probably reflects the occurrence of gradients in Fe and/or ligands (carbonate, silicate) concentration. Iron was however present in the alteration layers of glass everywhere in the sample, suggesting that local corrosion was significant, but that dissolved oxidized Fe was scavenged by these layers. No passive layer in contact with metal iron was observed, hence any layer, if present, would be no thicker than a few nm, meaning that they would be extremely prone to dissolution.

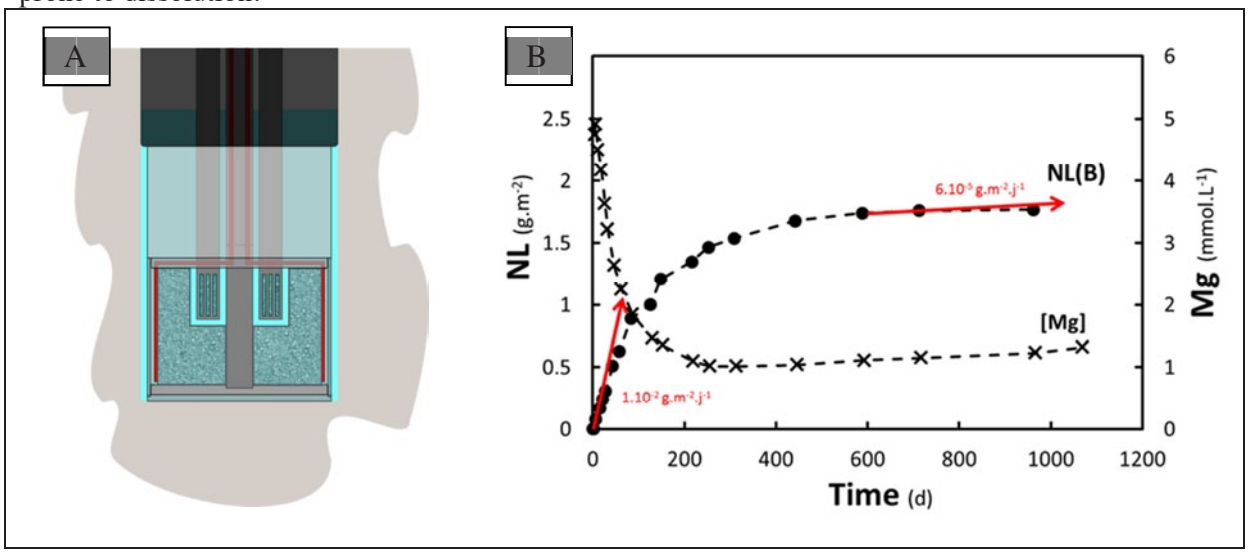


Figure 1: A. Test interval layout. B. Normalized mass loss (NL) calculated for boron and magnesium concentration versus time during the leaching of SON68 glass powder mixed with iron powder at 50 ° C.

In situ characterization of the Callovian-Oxfordian seepage water composition while exposing the rock to oxygen gas

A. Vinsot[1], M. Lundy[1], Y. Linard[1], S. Wechner[2], J. Trémosa[3], F. Claret[3]

1 Andra, CMHM, F-55290 Bure, France
2 Hydroisotop GmbH, D-85301 Schweitenkirchen, Germany
3 BRGM, F-45060 Orléans, France

Excavation of the Andra's Underground Research Laboratory (URL) drifts at a depth of 490 meters in the Callovian-Oxfordian argillaceous rock induces water evaporation and rock forming minerals (especially pyrite) oxidation at the rock surfaces exposed to air. Drift ventilation keeps extracting water from the rock and oxidizing rock components. These processes lead to the formation of new minerals like gypsum on the rock surfaces exposed to air. If ventilation stops, resaturation of the previously desaturated zones would take place and liquid water is expected to flow out from the rock into the drifts after a while. The composition of this water would differ from the pristine rock pore water composition especially because of its chemical interactions with the newly formed minerals. It is necessary to characterize this modified water composition in order to evaluate how the various materials (*e.g.* concrete and steel) would evolve in the drifts and vaults of a radioactive waste disposal installed in such a rock.

The "POX experiment"[1], which was implemented in a borehole in the Andra's URL, addresses an aspect of this objective. Indeed, this experiment is dedicated to the quantitative study of oxygen consumption by the Callovian-Oxfordian argillaceous rock. Furthermore, it aims at studying the consequences of the oxygen consumption on the seepage water composition. Over a two-year long initial phase launched in 2009, the rock natural gases and pore water at the test location were observed. Afterwards, oxygen injection was started and is currently underway.

Experimental setup

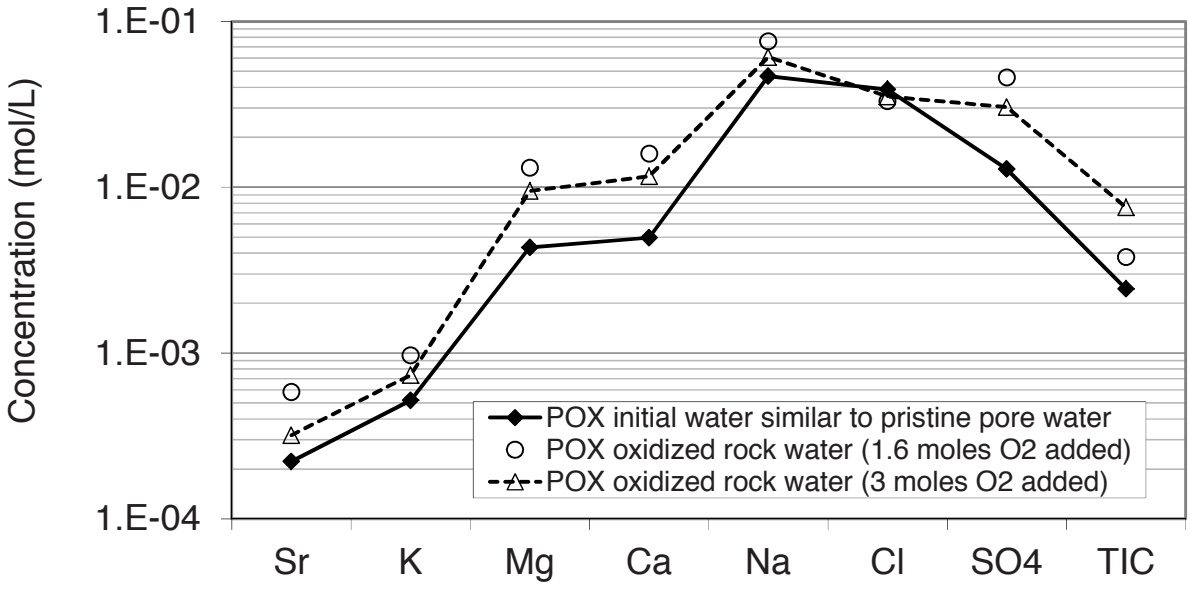
The experimental setup is based on gas circulation within a borehole. It consists of a 15 m-long and 76 mm-diameter ascending borehole, from which the last 5 m constitute the test interval. The rock surface in the test interval is close to 1 m^2. The last 6 m of the borehole were cored with argon as a drilling fluid in order to protect the rock from any contact with air. The borehole equipment was installed just after the drilling and isolated the test interval with a packer. The equipment includes several lines, which link the test interval to the drift, and make it possible to circulate gas and collect the seepage water flowing from the rock into the test interval. In the drift, a gas circulation module allows to circulate the gas and to monitor its composition. This module includes a circulation pump, an oxygen specific probe and cylinders which can be disconnected to perform gas sample analyses. In addition, the gas circulation module makes it possible to inject pure oxygen at a controlled flow rate. Another module is dedicated to water extraction at a controlled flow rate and permits water composition monitoring.

Chronology and results

Preceding the oxygen injection phase, a stable water production flow rate between 30 and 40 mL/day was obtained in the borehole. The extracted water composition was similar to those previously obtained in the URL (Vinsot et al. 2008), with pH = 7.1, ionic strength = 0.08 mol/L, total dissolved species content (TDS) close to 4 g/L and electrical conductivity = 6.3 mS/cm.

[1] POX for "Perturbation OXydante" in french

Oxygen injection was started in 2011. Since then, thanks to continuous injection of pure oxygen at regulated flow rate, oxygen partial pressure in the borehole test interval has been maintained at a value close to 0.2 bars (air value) over 650 days. Oxygen injection was stopped twice during 150 and 200 days, respectively. While oxygen partial pressure was 0.2 bar, the oxygen consumption rate by the Callovian-Oxfordian rock was between 0.003 and 0.009 moles of $O_2/m^2/day$. After about 1 mole of oxygen had been injected, seepage water composition started to change. Within the following months, as a total of 1.6 moles of O_2 had been injected, the sulfate concentration increased by up to a factor of 3.6 leading this species to become the second major one; calcium, magnesium and strontium concentrations also increased by up to a factor of three; the water electrical conductivity increased by up to 70%, the ionic strength by up to 95%, reaching 0.15 mol/L and the TDS increased by up to 100%. At that time, the pH measured was 6.1. About 16 months later, during which oxygen injection was interrupted twice and after a total of 3 moles of oxygen had been injected, the seepage water composition had the concentration values shown on the figure below; its pH was 7.4, its ionic strength was 0.12 mol/L; its TDS was 6.4 g/L and its electrical conductivity was 8.7 mS/cm. One year later, as a total of 5 moles of oxygen had been injected, the seepage water composition was in the range defined by the 2 oxidized rock water compositions described above and shown on the figure below.



Next experimental and modeling steps will aim at clarifying the secondary mineral species which are involved in the oxygen consumption and the reaction kinetics (Trémosa et al., submitted). It should lead to an updated description of the consequences of oxygen consumption by the Callovian-Oxfordian argillaceous rock on the composition of the water that will fill the drifts after their closure. Specific impact of water evaporation on the composition of this water will also need to be unraveled.

References

Trémosa J., Hadi J., Claret F., Tournassat C., Vinsot A. (submitted). Kinetic experiments in order to determine the rate of oxygen consumption by the Callovo-Oxfordian Argillaceous rock. *Clays in natural and engineered barriers for radioactive waste confinement, 6th international conference, Bruxelles 2015*.

Vinsot A., Mettler S., Wechner S. (2008). In-situ characterization of the Callovo-Oxfordian pore water composition. *Physics and Chemistry of the Earth* 33, S75-S86.

Chemical evolution of a HLW cell in Callovo-Oxfordian Claystone: taking into account the oxic transient period

Nicolas C.M. Marty[1], **Benoit Cochepin**[2], **Hossein Davarzani**[1], **Christophe Tournassat**[1], **Nicolas Michau**[2], **Isabelle Munier**[2], **Carl I. Steefel**[3], **Francis Claret**[1]

1. BRGM – 3 avenue. Claude Guillemin, BP6009 45060 Orléans Cedex 2, France
2. Andra – Parc de la Croix Blanche, 1-7 rue Jean Monnet, 92298 Châtenay-Malabry Cedex
3. Lawrence Berkeley National Laboratory, Berkeley, CA 94720, USA

Corresponding author: n.marty@brgm.fr

Numerous calculations have been performed to represent the long-term chemical evolution of the autochthonous (e.g. argillaceous rock) and allochthonous (e.g. cement based materials, carbon steel) materials that may interact within the French underground radioactive waste repository concept. The oxic transient related to the operating period (due to the access drift ventilation) in High-Level and long-lived Waste (HLW) repository facilities is often neglected in the simulation of their long-term chemical evolution. However the initial oxidation of the reduced environment prevailing in the claystone and the oxic corrosion of the carbon steel in the HLW cell head combined with the anoxic corrosion of the carbon steel and H_2 production in the using part of the cell may lead to a complex oxidizing/reducing front (De Windt *et al.*, 2014). The present study intends to simulate the transition phase between the periods with oxidative and reductive conditions in order to determine:

- how the chemical compositions of the metallic materials, clay and cement in the HLW cell are altered by atmospheric oxygen and carbon dioxide during the operating period;
- and how these alterations affect the long term chemical evolution of the system after closure of disposal cell.

The modelling strategy relies on a two steps procedure. Two phases flow simulations were carried out with Comsol Multiphysics, in order to obtain the temperature and water saturation profiles as a function of the different operating steps. The chemical evolution of the HLW cell was then simulated with the reactive transport code CrunchFlow (Steefel *et al.*, 2014) with fixed water saturation and temperature profiles derived from the thermal-hydrology simulations. The code flexibility enabled the simultaneous consideration of the irreversible reaction describing the pyrite oxidation by O_2, and subsequent sulphates release, and the reversible reaction of pyrite dissolution/precipitation under anoxic conditions. The simulation of the oxic period led to pyrite oxidative dissolution together with iron oxi(hydr)oxides and gypsum precipitations (Fig. 1). As a result of pyrite dissolution, the pH value in the pore water decreased, but is rapidly buffered by carbonate dissolution at the wall of the drift. After the sealing of the disposal cell by addition of 3 meters of bentonite and 4 meters of concrete (2009 version of Andra's concept), iron canister corrosion consumes the O_2, which leads to the establishment of reducing conditions. Once O_2 is depleted, the canister corrosion then produces H_2. Magnetite and siderite were simulated as being the main corrosion products. The alteration of the clay-minerals under reducing conditions was characterised primarily by a transformation of pyrite into pyrrhotite. In addition, formation of greenalite was simulated at the interface between the claystone and the metallic material. Those two predictions are in agreement with results obtained on short term experiments (Truche *et al.*, 2009; Bourdelle *et al.*, 2014). Simulation results indicated also a destabilization of the illite–smectite and quartz minerals of the claystone (Fig. 2).

Bourdelle F., Truche L., Pignatelli I., Mosser-Ruck R., Lorgeoux C., Roszypal C., Michau N. (2014) Iron–clay interactions under hydrothermal conditions: Impact of specific surface area of metallic iron on reaction pathway. *Chemical Geology* 381, 194-205

Steefel, C.I., Appelo, C.A.J., Arora, B., Jacques, D., Kalbacher, T., Kolditz, O., Lagneau, V., Lichtner, P.C., Mayer, K.U., Meeussen, J.C.L., Molins, S., Moulton, D., Shao, H., Šimůnek, J., Spycher, N., Yabusaki, S.B., Yeh, G.T. (2014) Reactive transport codes for subsurface environmental simulation, *Computational Geosciences,* DOI: 10.1007/s10596-014-9443-x

Truche L., Berger G., Destrigneville C., Guillaume D., Giffaut E. (2009) Kinetics of pyrite to pyrrhotite reduction by hydrogen in calcite buffered solutions between 90 and 180 °C: Implications for nuclear waste disposal. *Geochimica et Cosmochimica Acta* 74 (10), 2894-2914

De Windt L., Marsal F., Corvisier J., Pellegrini D. (2004) Modeling of oxygen gas diffusion and consumption during the oxic transient in a disposal cell of radioactive waste. *Applied Geochemistry* 41, 115-127

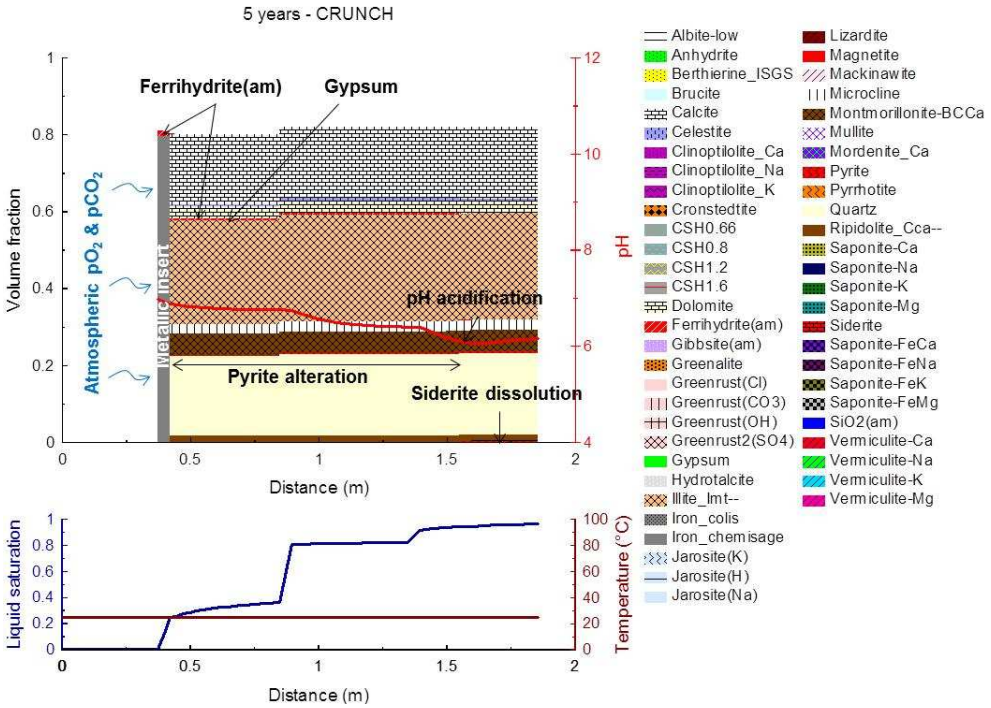


Fig 1. 5 years of oxydative period simulated using CrucnFlow.

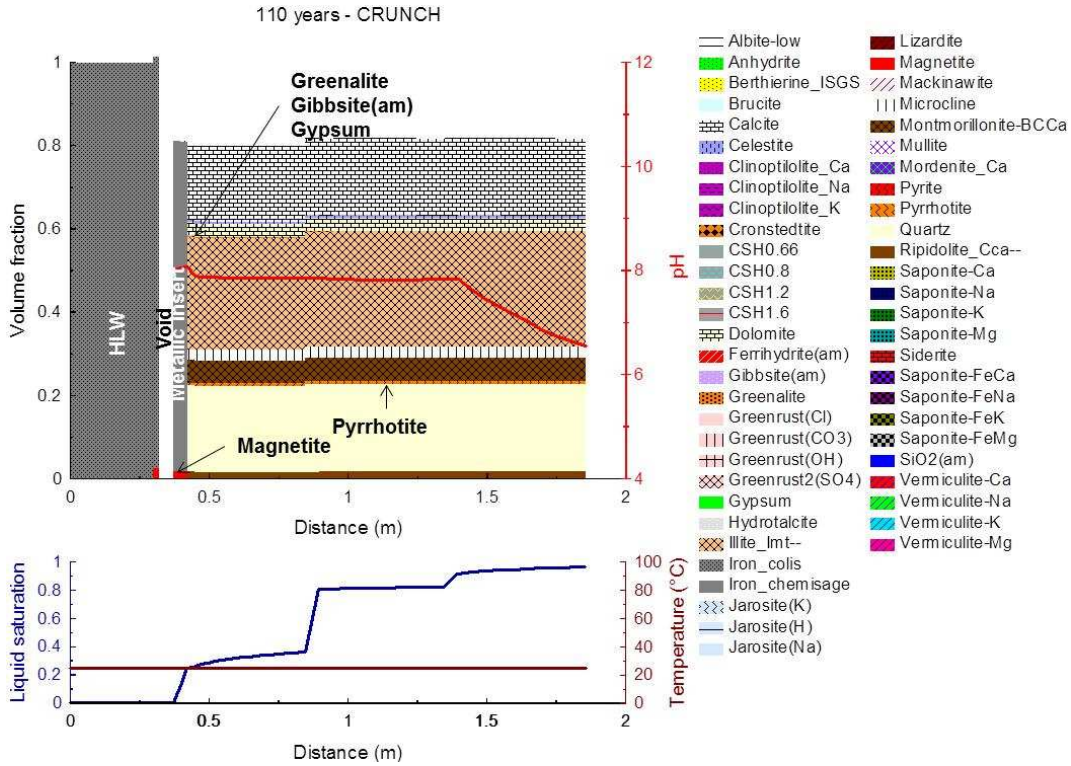


Fig 2. 105 years of reductive period simulated using CrucnFlow.

Benchmark for reactive transport codes with application to concrete/clay interaction

Nicolas C.M. Marty[1], Olivier Bildstein[2], Philippe Blanc[1], *Francis Claret*[1], Benoit Cochepin[3], Eric C. Gaucher[1], Diederik Jacques[5], Jean-Eric Lartigue[2], Sanheng Liu[5], K. Ulrich Mayer[4], Johannes C. L. Meeussen[6], Isabelle Munier[3], Ingmar Pointeau[2], Danyang Su[4] and Carl I. Steefel[7]

1 BRGM, 45060 Orleans Cedex, France
2 CEA, Cadarache, 13108 Saint-Paul-lez-Durance, France
3 Andra, 1/7 Rue Jean Monnet, 92298 Châtenay-Malabry Cedex, France
4 Department of Earth, Ocean and Atmospheric Sciences. University of British Columbia, 2207 Main Mall, Vancouver BC, Canada.
5 Belgian Nuclear Research Centre SCK.CEN, Boeretang 200, Mol, 2400 Belgium
6 Nuclear Research and Consultancy Group, PO Box 25, 1755 ZG Petten, The Netherlands
7 Lawrence Berkeley National Laboratory, Berkeley, CA 94720, USA
Corresponding author: f.claret@brgm.fr

Nuclear waste repositories will use a significant quantity of cement: for the construction of access drifts, disposal cells and concrete plugs, and as containment material for low- to intermediate-level waste. Several European countries have chosen claystone formations as possible host rocks (Landais, 2006). Numerous cement/clay interfaces will thus be present in a radioactive-waste repository.

Due to contrasting geochemical conditions (including Eh, pH, solution composition), these interfaces are subjected to steep concentration gradients and are highly reactive. Predicting long-term changes (1,000 to 100,000 years) in these cementitious and clayey materials is thus crucial for assessing the behaviour of such infrastructures. Experiments cannot provide sufficiently reliable information over such long time scale. Although natural and archaeological analogues can be very helpful, modelling is the unique tool to analyse and test different evolution scenarios. In order to build a better confidence in such calculations, it is of paramount importance to demonstrate that the results obtained are not dependent on the choice of the numerical reactive transport code to perform the simulation. In order to address this issue, a benchmark problem, divided into three steps with increasing geochemical refinement, has been set up (Marty *et al.*, submitted).

In all cases, the solutes transport across the interface between clayey host rock and concrete is diffusion driven and a 1D radial geometry and isothermal conditions (25°C) have been both considered. Both materials are full saturated. The first step of the benchmark only considers porewater solutions and the clayed host rock which is only modelled by an exchanger. The second step introduces the full mineralogy for both the concrete and the claystone considering slow kinetics rates for mineral dissolution-precipitation reactions, whereas the third one focuses on fast reaction rates.

Seven international teams have been involved in this benchmarking exercise. All reactive transport codes used (TOUGHREACT, PHREEQC with two different ways of handling transport, CRUNCHFLOW, HYTEC, ORCHESTRA, MIN3P-THCm) gave very similar patterns in terms of predicted solute concentrations and of minerals distribution evolution (Fig. 1). The benchmarking exercise demonstrates that reactive transport tools have reached such a level of maturity as to be confidently used in support of long-term performance assessments.

Landais, P. (2006) Advances in geochemical research for the underground disposal of high-level, long-lived radioactive waste in a clay formation. *Journal of Geochemical Exploration* 88(1–3), 32-36

Marty N.C.M, Bildstein O., Blanc Ph., Claret F., Cochepin B., Gaucher E.C., Jacques D., Lartigue J.E., Liu S., Mayer K.U.,. Meeussen J.C.L., Munier I., Pointeau I., Su D. and Steefel C.I. (submitted) Benchmarks for multicomponent reactive transport across a cement/clay interface. *Computational Geosciences*.

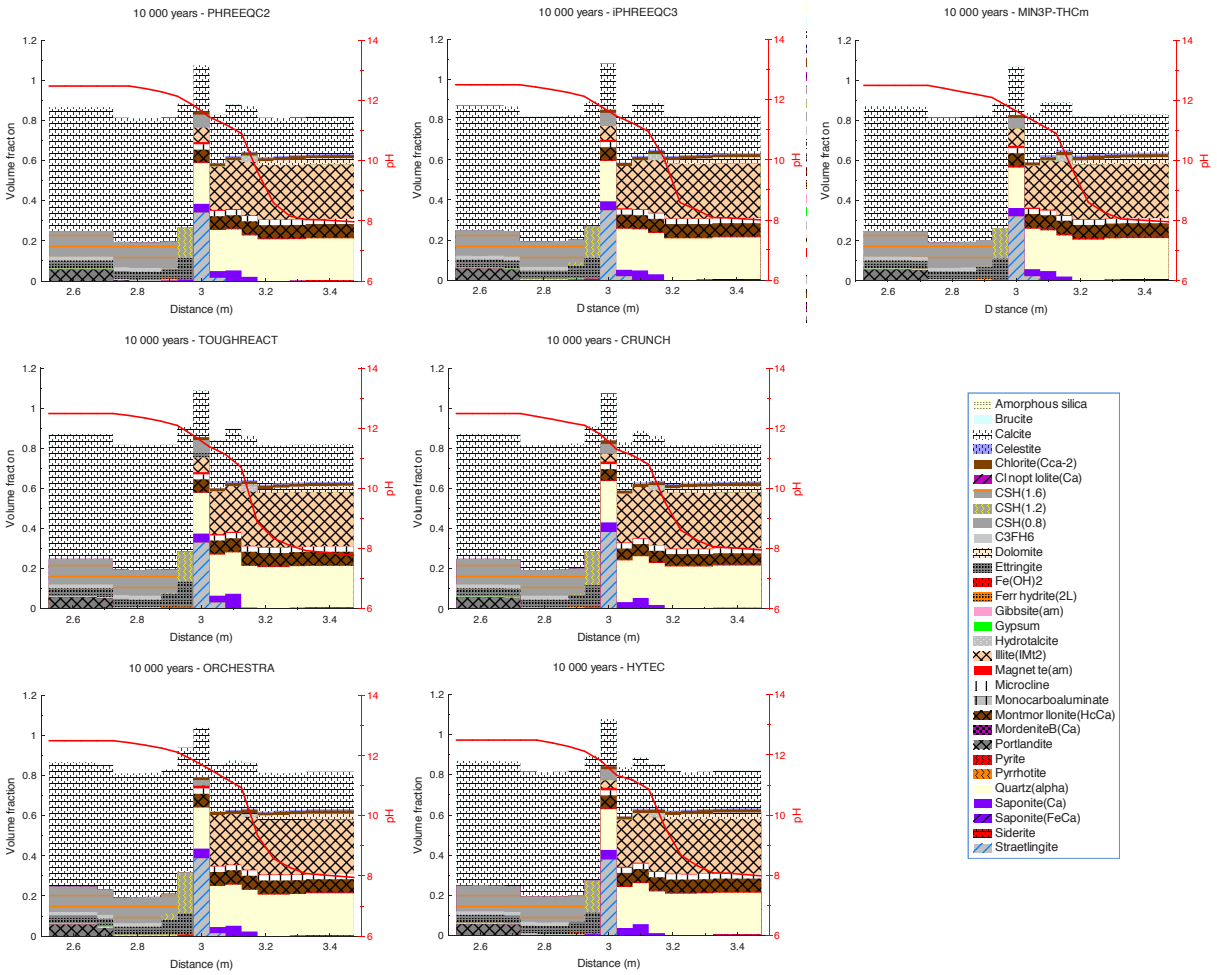


Figure 1: Mineralogical and pH changes obtained with TOUGHREACT, PHREEQC2, iPHREEQC2 (external transport module), CRUNCH, HYTEC, ORCHESTRA and MIN3P-THCm after 10,000 years of concrete/claystone interaction. The initial volume fraction value for t=0 is the value far from the interface (2.5 m for concrete and 3.5 m for claystone)

A new view on iron-clay interactions by monitoring pH and H_2 production

Franck Bourdelle[1,2,*], **Régine Mosser-Ruck**[1], **Laurent Truche**[1], **Isabella Pignatelli**[1], **Michel Cathelineau**[1], **Nicolas Michau**[3].

[1] GeoRessources, UMR 7359, Université de Lorraine, Campus Aiguillettes, 54506 Vandoeuvre-lès-Nancy, France.
[2] LGCgE, Université de Lille 1, Cité Scientifique, SN5, 59655 Villeneuve d'Ascq Cedex, France.
[3] Andra, Direction Recherche et Développement/Service Colis et Matériaux, Parc de la Croix Blanche, 1/7 rue Jean Monnet, 92298 Châtenay-Malabry cedex, France.
* Corresponding author: franck.bourdelle@univ-lille1.fr

Iron-clay interactions are one of the most significant perturbations impacting the evolution of a deep geological waste repository in claystone formation. Indeed, several research programs (e.g. OECD-NEA, 2012) envisage the association of natural (claystone) and engineered (glass, steel canisters, bentonite, re-enforced concrete structures) barriers to confine radioactive wastes. According to this concept, Andra (the French National Radioactive Waste Management Agency) has identified the Callovo-Oxfordian claystone (COx) of the Paris Basin, a complex low-permeability clayey rock, as a potential host-rock for the French repository program at Bure (Meuse/Haute-Marne, France).

In order to evaluate and predict the evolution of repository conditions, especially those related to interactions between the host rock and the exothermic steel canisters under anoxic conditions, numerous experimental investigations have been focused on iron-clay interactions these last 15 years (e.g. Lantenois, 2003; de Combarieu et al., 2011; among others). These studies have shown that: (i) clay minerals are destabilized and become very reactive, (ii) new-Fe rich phases crystallize, as chukanovite and cronstedtite (Pignatelli et al., 2014a and b), (iii) the pH of run solutions, which contains high concentration of potassium and low contents of iron, varies according to the physico-chemical parameters of the medium (e.g. the specific surface area of the metallic iron used; Bourdelle et al., 2014) and (iv) the iron corrosion process can be probed through H_2 degassing (Bourdelle et al., 2014). However, the reaction kinetic and mechanism are still poorly constrained, because of the lack of self-consistent experimental approach and coupled monitoring of the chemical and mineralogical evolutions.

To fill this gap, a parametric kinetic investigation of iron-claystone interaction at 90°C in a water saturated-anoxic medium has been carried out. A series of original continuous monitoring experiments with various Fe/COx ratios were performed to measure pH and H_2 partial pressure evolution in real-time (Figure 1), while the gas and solution compositions were analyzed, and the solid run products were finely characterized. Through this approach, H_2 production and time-variation of pH can be used together for the first time to precisely investigate the reaction rate and chemical changes induced by the mineralogical transformations. The results confirm that COx claystone is a very reactive material - much more reactive than a bentonite alone or any combination of silicates, clay minerals, carbonates and oxides. But above all, this series of experiments demonstrates the strong control of the mineralogical changes on the physical-chemical parameters. Therefore, by monitoring *in situ* the pH (Figure 2), we highlight a competition between the rock alteration and the iron corrosion process, which deeply depends on Fe/COx ratio. Similarly, by monitoring the H_2 degassing, we demonstrate that the mass of COx in the experiment controls the dynamics of H_2 production and therefore the iron corrosion rate (Figure 3a). As an illustration, the comparison of two experiments with the same iron content but different starting COx contents shows that the H_2 production rate decreases with the Fe/COx ratio, while the pH is increased at high Fe/COx ratio. All these results allow to conclude that COx in contact with metallic iron accelerates the iron corrosion process (Figure 3b), by controlling the medium parameters (as pH) and by acting as a Fe-pump, incorporating the released iron in newly-crystallized clays minerals (Fe-serpentine like).

Figure 1
Experimental set-up

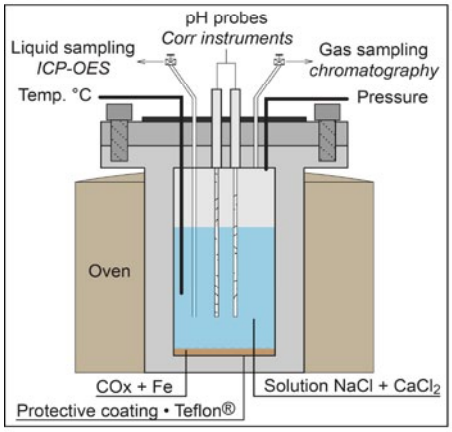


Figure 2
pH - 90°C

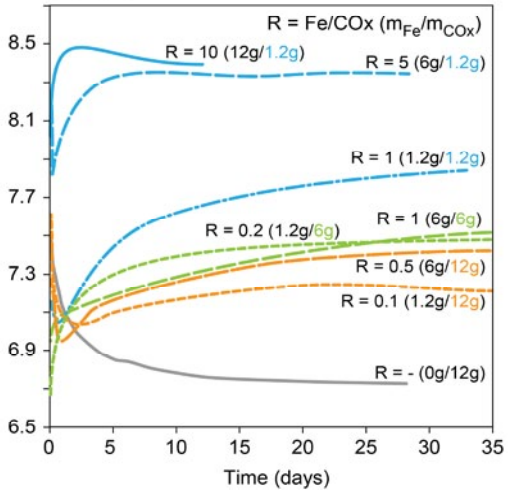


Figure 3a
nH_2 released
after 30 days ($\times 10^{-3}$ mol)

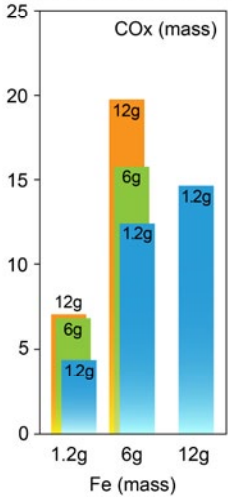
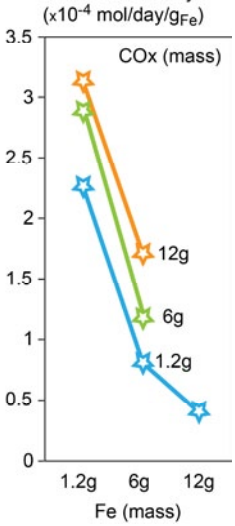


Figure 3b
H_2 degasing rate
on the first 15 days
($\times 10^{-4}$ mol/day/g_{Fe})



Bourdelle, F., Truche, L., Pignatelli, I., Mosser-Ruck, R., Lorgeoux, C., Roszypal, C., Michau, N., 2014. Iron-clay interactions under hydrothermal conditions : impact of the specific surface area of metallic iron on reaction pathway. Chem. Geol., 381, 194-205.

de Combarieu, G., Schlegel, M.L., Neff, D., Foy, E., Vantelon, D., Barboux, P., Gin, S., 2011. Glass-iron-clay interactions in a radioactive waste geological disposal: An integrated laboratory-scale experiment. Appl. Geochem., 26, 65-79.

Lantenois, S., 2003. Réactivité fer métal/smectites en milieu hydraté à 80°C. Thesis, Orléans, Orléans University, France.

OECD, 2012. Geological Disposal of Radioactive Waste: National Commitment, Local and Regional Involvement. A Collective Statement of the OECD Nuclear Energy Agency Radioactive Waste Management Committee Adopted March 2012, pp. 24.

Pignatelli, I., Mugnaioli, E., Mosser-Ruck, R., Barres, O., Kolb, U., Michau, N., 2014a, A multi-technique, micrometer- to atomic-scale description of a synthetic analogue of chukanovite, $Fe_2(CO_3)(OH)_2$. Europ. J. Miner., 26, 221-229.

Pignatelli, I., Bourdelle, F., Bartier, D., Mosser-Ruck, R., Truche, L., Mugnaioli, E., Michau, N., 2014b. Iron-clay interactions : detailed study of the mineralogical transformation of claystone with emphasis on the formation of iron-rich T-O phyllosilicates in a step-by-step cooling experiment from 90°C to 40°C. Chem. Geol., 387, 1-11.

In situ monitoring of gas exchange (O_2, H_2O, CO_2, CH_4) between the Callovian-Oxfordian rock and the atmospheric air in the Bure URL

A. Vinsot[1], **M. Lundy**[1], **Y. Linard**[1], **Y. Lettry**[2], **J. Morel**[1]

1 Andra, CMHM, F-55290 Bure, France
2 Solexperts AG, CH-8617 Mönchaltorf, Switzerland

Excavation and ventilation of underground drifts in the Callovian-Oxfordian argillaceous rock induce gas exchanges between atmospheric air and rock pore water on the rock surfaces exposed to air. The principal gases concerned are water vapor, nitrogen (N_2), oxygen (O_2), carbon dioxide (CO_2) and light alkanes (CH_4, C_2H_6). Furthermore, oxygen from atmospheric air reacts with several rock components, the most important being pyrite; these components are oxidized while oxygen is consumed. In a radioactive waste disposal installed in such a rock, similar gas exchanges would happen for the duration of the time that the drifts and cells are open to air circulation. When the drifts and cells will be closed to air circulation, seeping water from the rock will fill them back. In order to better evaluate how fast the water will fill back the drifts and cells after their closure, it is interesting to quantify the water evaporation fluxes extracted from the rock during the ventilation phase. Moreover, it is necessary to evaluate the consequences of the gas exchanges that occur during the ventilation phase on the composition of the water that will fill the drifts after their closure. Indeed, further evolution of the various materials (*e.g.* cement, steel) present in the drifts will be influenced by their interactions with this water.

Experiments regarding gas exchanges between the Callovian-Oxfordian rock and air have been performed at several scales in the Bure Underground Research Laboratory (URL) at 490 m-depth: in 7 cm-diameter boreholes, in 70 cm-diameter cells and in a >4 m-diameter section of a drift.

Gas circulation experiments performed in boreholes make it possible to show that Callovian-Oxfordian pore water contains dissolved N_2 and light alkanes in addition to dissolved CO_2 already known to be present (Cailteau et al., 2011) and to evaluate their concentrations.

At the cell scale, the content of several gases, including water vapor, was monitored over a period of one year at several locations in the gaseous atmosphere of a 21 m-length horizontal cell (Figure 1). The cell's equipment included steel-casing and a packer that prevents the drift air to circulate directly into the cell. The casing annulus was closed with expanding foam over a length of several tens of cm. The gas content was monitored at depths of 4, 12 and 21 m into the cell casing. After the cell had been closed, oxygen content decreased (Figure 2), while water vapor, CO_2 and CH_4 increased. A few months later, the content of each gas became more or less stable. Oxygen content stabilized at a value between 11 and 13 vol% (Figure 2). This value is explained by the stationary state in which the flux of oxygen consumed by the rock has been compensated by an inflowing flux of fresh air. The inflowing air flux was expected to circulate through the fractured zone induced by the drift excavation (Armand et al., 2014).

It is possible to propose for each gas an estimated value of the flux exchanged between the gaseous phase and the rock, based upon the data measured. It should also be possible to quantify the inflowing flux of fresh air. These results will be useful when interpreting the data obtained at the drift scale later on.

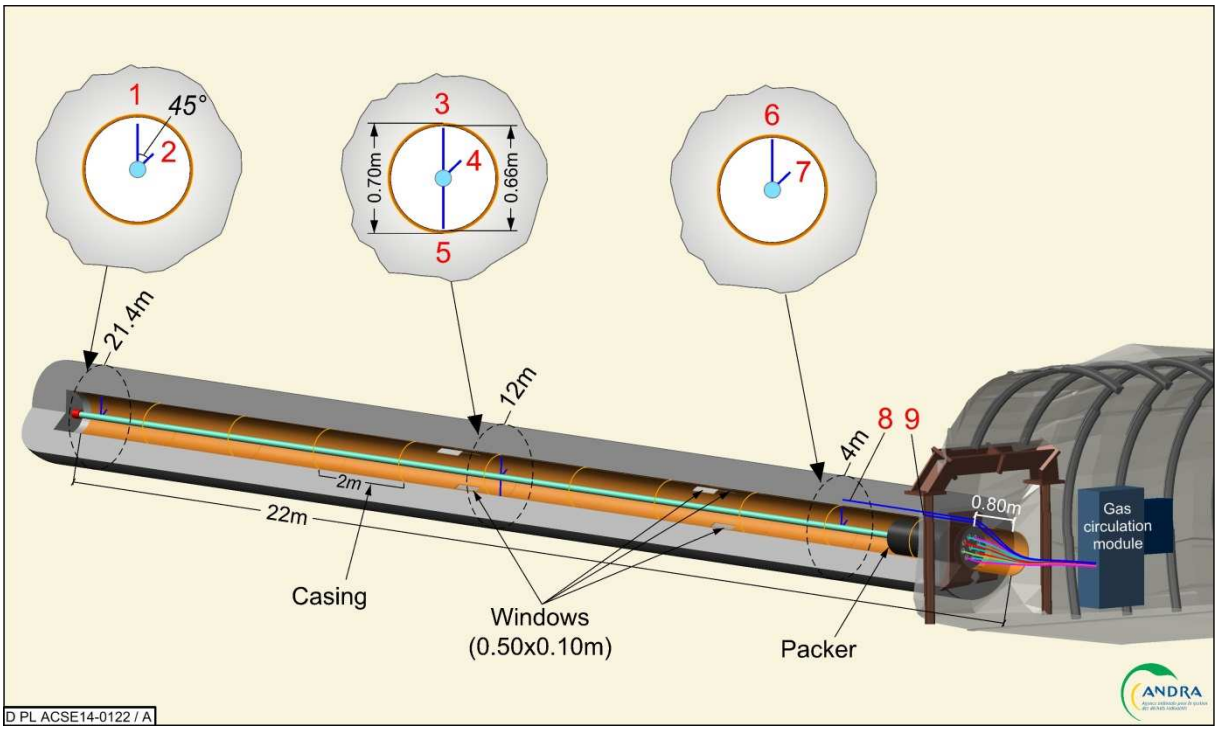


Figure 1 *Schematic view of the experimental setup making it possible to monitor the gas composition in the ALC3004 closed cell.*

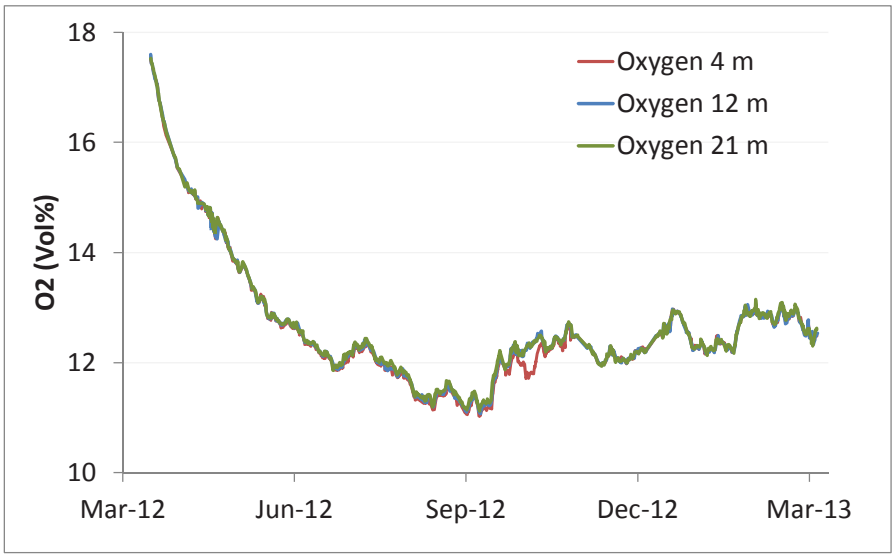


Figure 2 *Oxygen content measured values at three depths in the ALC3004 closed cell.*

References

Armand, G., Leveau, F., Nussbaum, C., Vaissiere, R., Noiret, A., Jaeggi, D., Landrein, P., Righini, C., 2014. Geometry and Properties of the Excavation-Induced Fractures at the Meuse/Haute-Marne URL Drifts. *Rock Mech Rock Eng* 47, 21-41.

Cailteau, C., Pironon, J., de Donato, P., Vinsot, A., Fierz, T., Garnier, C., Barres, O., 2011. FT-IR metrology aspects for on-line monitoring of CO_2 and CH_4 in underground laboratory conditions. *Analytical Methods* 3, 877-887.

Corrosion of steel in Toarcian argillite: involvement of microbial metabolisms and biofilms

L. Urios[1,*], F. Mercier-Bion[4], Y. Leon[4], C. Wittebroodt[3], M. Flachet[2], M. Magot[1], D. Neff[4], P. Dillmann[4]

1. UPPA, IPREM UMR 5254, Equipe Environnement et Microbiologie, IBEAS, F-64013 PAU, France
2. IRSN, PRP-DGE/SEDRAN/BERIS, B.P. 17, 92262 Fontenay aux Roses Cedex, France
3. IRSN, PRP-DGE/SRTG/LETIS, B.P. 17, 92262 Fontenay aux Roses Cedex, France
4. SIS2M/LAPA, CEA/CNRS UMR3299, 91191 Gif-sur-Yvette Cedex, France
*Corresponding author: laurent.urios@univ-pau.fr

Context

According to the French design developed by Andra for deep geological disposal, high level radioactive waste would be emplaced in carbon steel overpacks in the Callovo-Oxfordian clayey formation surrounded by a carbon steel liner. The metallic components have to ensure containment and mechanical support respectively, for several hundreds years. During the first stage of disposal, they would be in unsaturated and oxic conditions, while an anoxic and saturated environment should prevail after the hydraulic transient. Thus, it is important to well understand the short and long term behavior of these metallic materials, considering the corrosion mechanisms in oxic and anoxic conditions, for assessing the safety of such a disposal. In this context, the French Institute for Radiological Protection and Nuclear Safety (IRSN) has been conducting research programs since 1991 in the Tournemire Underground Research Laboratory (URL), consisting in a tunnel and galleries crossing a Toarcian Argillaceous formation (Aveyron, France) which is particularly interesting for its properties close to those of the Callovo-Oxfordian argillite.

The existence of microbial processes in this formation was first shown by the study of time evolution of the chemical and isotopic compositions of fracture groundwaters collected in several boreholes. These investigations suggested that aqueous sulphates and their isotopic composition were controlled by bacterial sulphate reduction (Beaucaire *et al.*, 2008). In addition, the presence of microorganisms has been evidenced in the Toarcian formation as well as on the wall of a gallery and in the excavation damaged zone (EDZ) (Urios *et al.*, 2012). These observations indicated that clayey rocks do not prevent bacterial development and that exogenous microorganisms, introduced, which will be in a disposal facility during the operational phase, may colonize the EDZ. Sulphate-reducing (SRB) and iron-reducing bacteria (IRB), able to develop at high temperature at the interfaces between steel and Toarcian argillite, have been detected (Urios *et al.*, 2013). Localized corrosion can be favored by SRB in anoxic conditions (Campaignole and Crolet, 1997, Liu *et al.*, 2009) and IRB could promote corrosion by interacting with corrosion products formed previously (Videla, 1996, Herrera and Videla, 2009). Recently, the characterization of the microbial diversity at interfaces between steel coupons and argillite in boreholes filled with re-compacted argillite after 10 years of interaction has been investigated (Urios *et al.*, 2014). The biodiversities differed depending on the steel type and the borehole considered, indicating the influence of both iron-clay interactions and *in situ* environmental conditions.

Experiments

An original study has been launched on steel coupons emplaced in Toarcian argillite core samples from the Tournemire URL in contact with a synthetic solution, representative of the pore water, percolating through the set-up, in absence and in presence of a mix of different bacterial strains. Several environmental conditions are tested: two temperatures (25°C and 50°C), anoxic or oxic atmospheres, and contact times from one to nine months. The bacterial mix, representative of those encountered in the geological layer (Urios *et al.*, 2012) included SRB, sulfur-oxidizing bacteria (SOB), IRB, and biofilm forming strains. This mix had been chosen to follow possible synergy between the different types of metabolisms and their relative effect on steel corrosion. After 1, 4 and 9 months, the coupons were studied with FESEM to evidence the surface biofilms morphology, by Energy Dispersive Spectroscopy for the chemical composition and by μRaman spectroscopy, and XRD to

identify the phases constituting the corrosion products. A characterization of the bacterial diversity on coupons and in the outgoing solution has been realized using qPCR and high-throughput sequencing.

Results

FESEM evidenced the presence of bacteria on the external surface of corrosion products formed on the steel surfaces. Indeed, corrosion product growth already occurred for one month experiments concomitantly to the presence of bacteria and increased for four months with the localized apparition of bacterial morphologies. Carbon-rich products with bacterial shapes were observed on the corrosion layer, indicating the development of biofilms. Moreover, the nature of the corrosion products is typical of each medium: for the aerated one, lepidocrocite, goethite and magnetite were evidenced whereas for deaerated conditions, siderite, chukanovite and magnetite were observed. Nevertheless it seems that coupons in aerated conditions show the predominance of magnetite when bacteria are added, whereas the same coupons without bacteria only exhibited lepidocrocite and goethite. In aerated conditions, carbonate-containing phases detection associated to biofilms suggests the formation of oxygen-poor areas allowing sulphate-reduction. The characterization of the microbial diversity indicates which introduced species survived all along the experiment. Corrosion rates after 1 and 4 months have been calculated and show effects of both experiment duration, globally slowing down them, and the presence of the initial bacterial mix. All the results and also corrosion rates after 9 months will be presented and discussed.

References

Beaucaire, C., Michelot, J.L., Savoye, S. & Cabrera, J. (2008) Groundwater characterisation and modelling of water rock equilibria in the Tournemire argillaceous formation (Aveyron, France). *Appl. Geochem.* **23**, 2182-2197.

Campaignole, X. & Crolet, J.L. (1997) Method for studying stabilization of localized corrosion on carbonsteel by sulphate-reducing bacteria. *Corrosion* **53**, 440-447.

Herrera, L.K. & Videla, H.A. (2009). Role of iron-reducing bacteria in corrosion and protection of carbon steel. *Int. Biodeter. Biodegrad.* **63**, 891-895.

Liu, T., Liu, H., Hu, Y., Zhou, L. & Zheng, B. (2009) Growth of thermophile sulphate-reducing bacteria and its effect on carbon steel. *Mater. Corr.* **60**, 218-224.

Urios, L., Marsal, F., Pellegrini, D. & Magot, M. (2012). Microbial diversity of the 180 million-year-old Toarcian argillite from Tournemire, France. *Appl. Geochem.* **27**, 1442-1450.

Urios, L., Marsal, F., Pellegrini, D. & Magot, M. (2013). Microbial diversity at iron-clay interfaces after 10 years of interaction inside a deep argillite geological formation (Tournemire, France). *Geomicrobiol. J.* **30**, 442-453.

Urios, L., Maillet, A., Dauzères, A., Flachet, M. and Magot, M. (2014). Tournemire argillite/carbon steel evolution under bacterial influence after 10 years of *in situ* interaction. *Corr. Eng. Sci. Tech.* **49**: 554-561.

Videla, H.A. (1996). Corrosion inhibition by bacteria. In: *Manual of Biocorrosion*. CRC Lewis Publishers, Boca Raton, Florida, pp. 121–135.

Mechanistic and kinetic study of pyrite-hydrogen interaction at low temperature using electrochemical techniques

***S. Betelu*[1], G. Berger[2], E. Giffaut[3] and *I. Ignatiadis*[1]**

[1]BRGM, Water, Environment and Ecotechnologies Division, 3 Avenue Claude Guillemin, BP 36009, 45060 Orléans Cedex, France (s.betelu@brgm.fr; i.ignatiadis@brgm.fr)
[2]IRAP, Observatoire Midi-Pyrénées 14 av. E. Belin, 31400 Toulouse, France
[3]ANDRA, Head of the Transfer and Migration Department, R&D Division, 1-7, rue Jean-Monnet, 92298 Châtenay-Malabry, France

Within the context of the investigation of the impact of the geochemical evolutions of the nuclear waste storages on the surrounding material, the objective of the work presented here was the characterization of pyrite interaction with hydrogen at low temperature (25-90°C). The emphasis was put on the understanding in depth of both phenomenology and kinetics.

For this purpose, the use of electrochemical techniques in combination with pyrite mineral electrodes has constituted a novel experimental and complementary approach in comparison with the geochemical research realized by Truche et al. (2010) under hyper-thermal temperatures, from 90 to 180°C and under H_2 partial pressures pH_2 ranging from 8 to 18 bars.

Experiments were conducted in a wide range of conditions (pH, temperature, ionic composition, gaseous environment) close to the expected evolution of the repository groundwater chemistry.
More specifically, after pyrite electrodes had been designed and assembled (figure 1A), various electrochemical disturbances were applied to FeS_2 electrode (and to platinum electrode (Pt) for comparison) while it was submerged in a partially reconstituted COx pore water solution, enclosed in a **H**igh **P**ressure **T**hermo-**R**eactor (**HPTR**) at 90°C (figure 1A) or in a **L**ow **P**ressure **T**hermo-**R**eactor (**LPTR**) (figure 1B) at 25°C, in the absence and in the presence of (i) pyrite grains (particle size ranging from 40 to 63 μm) and (ii) H_2 (pH_2 ranging from 0 or 1 bar).

Experiments that were performed in carbonaceous buffers (HCO_3^-/CO_3^{2-} buffer, pH 8.6 and 10.0) in **the HPTR** (at 90°C, which is the maximal temperature expected in the repository) with or without hydrogen led us to determine mechanism and estimate pyrite corrosion rates.

Experiments that were performed in anoxic environment (N_2 and/or H_2) in carbonaceous buffer in **the LPTR** (at 25°C) in which hydrogen was produced *in situ* by electrolysis led to comfort phenomenology at higher pH, from 9.3 to 11.2. Indeed polarization provided H_2 and OH^- formation in the solution, and thus its progressive alkalization.

Mechanism was established by using potentiometric measurements, linear sweep polarization **(LSP)** and Electrochemical Impedance Spectrometry (**EIS**).
Both electrochemical (Tafel plots and Polarisation Resistance (R_p)) and gravimetric (mass loss) approaches were used as complementary methodologies to estimate pyrite corrosion rates.

In addition to the electrochemical behaviour of platinum and pyrite electrodes, pH, temperature and pressure of the liquid medium were monitored. FeS_2 morphological and chemical characterizations were realized by *Scanning Electron Microscopy* **(SEM)** and Energy-dispersive X-ray spectroscopy **(EDS)**.

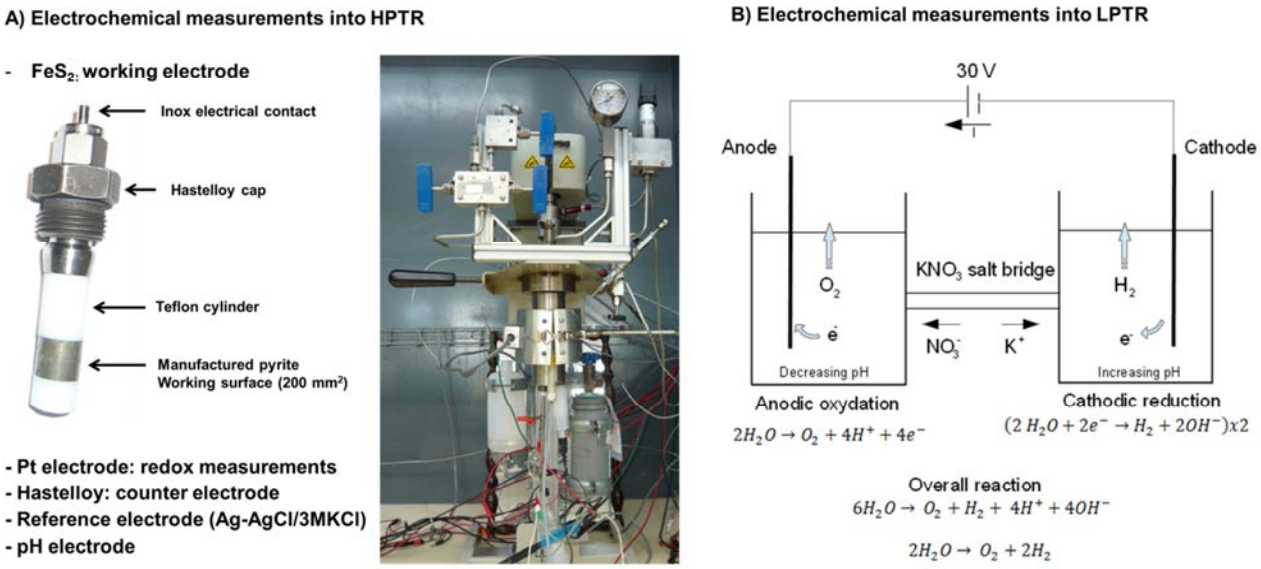


Figure 1: A) FeS_2 electrode made with "pure" Peruvian pyrite for experiments realized in a Hastelloy High Pressure Thermo-Reactor (HPTR)
B) Electrolysis scheme experiment of the Low Pressure Thermo-Reactor (LPTR).

The elucidation of the mechanism governing the reduction of the sulphur S° of the FeS_2 was the first challenge we answered. Indeed, the S° is reduced to sulphide (HS^-/S^{2-}), which is freed in solution, whereas the pyrite turns superficially into pyrrhotite (FeS_{1+x} with $0<x<0.125$), forming a layer that slows down the reduction process. Experiments conducted into HPTR and LPTR lead to approach phenomenology (which will be discussed) versus pH.

Investigations conducted by electrochemistry (at 90°C in high pressure thermo-reactor) allowed us to provide Pyrite corrosion rates in the absence and in the presence of hydrogen. It is worth noting that they are of the same order of magnitude 10^{-3} mm.year^{-1} whatever the pH (in the range 0.5 mm.year^{-1} - 3.6 10^{-3} mm.year^{-1}). In parallel, experiments conducted by gravimetric measurements were of prime importance. Both electrochemical and gravimetric measurements allow us to identify and distinguish the following phenomena on pyrite: (i) corrosion and corrosion-scaling measurable by electrochemistry, (ii) corrosion and chemical dissolution measurable by gravimetric measurements.

Results provided by electrochemical and gravimetric measurements will be discussed and compared to the calculated corrosion rates using the rate law determined by Truche *et al*. (2010).

Acknowledgement

The research has received funding from i) the European Union's European Atomic Energy Community's (Euratom) FP7/2007-2011 under grant agreement n° 212287 (RECOSY project) and ii) the ANDRA under the BRGM-ANDRA partnership (TRANSFERT and CAPTANDRA projects).

References

Betelu S., Lerouge C., Berger G. Ignatiadis I. (2012) - Mechanistic study of pyrite reduction by hydrogen in NaCl 0.1 M at 90 °C using electrochemical techniques. Scientific and Technical contribution in the 4AWS of RECOSY in Karlsruhe (Germany), 23rd – 26th January 2012.

Ignatiadis I., Betelu S., Lerouge C., Berger G. (2012) - Mechanistic and kinetic study of pyrite reduction by hydrogen gas produced in situ by water electrolysis in NaCl 0.1 M at 25°C using electrochemical techniques. Oral presentation during the 4AWS of RECOSY in Karlsruhe (Germany), 23rd – 26th January 2012.

Truche L., Berger G., Destrigneville C., Guillaume D., Giffaut E. (2010) - Kinetics of pyrite to pyrrhotite reduction by hydrogen in calcite buffered solutions between 90 and 180°C: implication for the nuclear waste disposal. Geochim. Cosmochim. Acta 74, 2894-2914.

Modeling of radiolytic leaching of UO_2 pellets in COx clayey water coupled to metallic iron corrosion

M. Odorowski[a,b], L. De Windt[b], C. Jégou[a], V. Broudic[a], C. Martin[c]

[a] Commissariat à l'Energie Atomique et aux Energies Alternatives, Centre de Marcoule, DEN/MAR/DTCD/SECM/LMPA, 30207 Bagnols-sur-Cèze Cedex, France
[b] MINES ParisTech, Centre de Géosciences, 35 rue St Honoré, 77305 Fontainebleau Cedex, France
[c] Agence Nationale pour la gestion des Déchets Radioactifs, 1/7 rue Jean Monnet, 92298 Chatenay-Malabry Cedex, France

In the event of direct disposal of spent fuel in a nuclear waste repository, the chemical reactions between the fuel and its environment, including the clay and the pore water, must be understood and the resulting radionuclide release must be quantified. The French nuclear waste management agency (Andra) has selected a Callovo-Oxfordian (COx) clay formation for the nuclear waste repository. This anoxic and reducing environment is interesting regarding the low solubility of uranium and plutonium in these conditions. However, the disposal of spent fuel may locally disrupt these reducing conditions. Indeed, the alpha activity of the fuel may induce the alpha radiolysis of the pore water producing oxidizing species like H_2O_2. These species may cause the oxidizing dissolution of the spent fuel matrix, thus releasing the radionuclides in the environment.

In order to quantify the influence of environmental parameters including the clayey water chemistry, the redox properties of the environment, the presence of iron, leaching experiments of different UO_2 pellets (as a proxy for the spent fuel matrix) have been carried out. The UO_2 pellets were doped with alpha-emitters ($^{238/239}Pu$) to reproduce the alpha activity of a spent fuel (with a burnup of 47 GWd/T_{iHM}) after 50 years or 10 000 years of radioactive decay. The system has been gradually complicated: the first leaching were realized in carbonated water (Muzeau, Ph.D. thesis, 2007), then in synthetic clayey water, and finally synthetic clayey water in the presence of metallic iron. The clayey water is synthetized to reproduce the composition of the COx clay pore water. The experiments were conducted in a glove box during one year.

Reactive transport modeling is a key step in the assessment of the long-term performance of radioactive waste disposals due to its ability to couple the geochemical evolution of the waste forms and the engineered barriers, the migration of radionuclides and the chemical buffering of the host-rock. Water radiolysis and corrosion of metallic components can be further introduced in such modeling at the expense of some basic simplifications. Modern reactive transport codes can technically cope with several hundreds of chemical reactions but the global and coupled effect of all these reactions still remains uncertain, demanding for experiment/modeling comparison.

The set of cell experiments were modeled with the HYTEC code incorporating the main mechanisms involved. That is to say H_2O_2 production at the pellet surface, congruent dissolution of the $U_{1-x}Pu_xO_2$ matrix, generalized corrosion of metallic iron coupon (with hydrogen generation), complexation and redox aqueous chemistry, precipitation of secondary phases (carbonates, hydroxides and silicates) were simultaneously modeled as well as the gas phase composition and species diffusion in the experimental cells. The thermodynamic constants were selected from the EQ3/6 and Thermochimie databases with kinetic constraints on the oxidative and anoxic dissolution of Fe(0) and UO_2. H_2O_2 yield versus α-activity was estimated by preliminary modeling with Chemsimul.

The model was in good agreement with the experiments. Results showed a significant influence of clayey water compared to carbonated water on the dissolution of UO_2. The concentration of uranium severely decreased in the synthetic clayey water. The model approached these experimental concentrations provided that Ca-Si-U minerals can precipitate. When iron was introduced in the system, uranium concentrations became very low compared to simpler systems. The modeling also correctly led to the precipitation of carbonates onto the iron coupon as well as of Fe(III) hydroxides and silicates onto the UO_2 surface. Following a Fenton-like reaction, the coupling or competition between the rate of radiolytic H_2O_2 production at the pellet surface and the rate of Fe(II) diffusion towards the pellet, induced by iron corrosion, is the key factor controlling plutonium and uranium releases in the modeling.

Alteration of geological environment condition due to liquid radioactive wastes disposal

V. Krupskaya, **S. Zakusin, A. Zhukhlistov (s)**

Institute of Geology, Mineralogy and Petrography of Ore Deposits of the Russian Academy of Sciences, Moscow, Russia

One example of so called "historical' kind of sites of low- and middle-active waste disposal which was used in some countries in 50-60's is their isolation in deep layers of geological environment. In this case specially prepared wastes are injected via the system of wells in sand layers of syncline structure. It is very important to avoid tectonic dislocations and have isolating clay layer of an appropriate thickness above and below the reservoir layer.
Depths of injection are usually 350-550 m, which is significantly deeper than aquifers that are used for water supply and thus, the risk of drinking water and river systems contamination is reduced to a minimum. This approach is based on the oil and gas development technology.
Liquid radioactive wastes (LRW) are thermodynamically unstable, weakly alkaline (pH = 8-10.5) or acidic (pH = 2-3) solutions with a total dissolved solids (TDS) amount up to 30 g / l. The solutions are rich with Na+, NH4+ and alkaline earth metals and anions:NO3-, SO42-, Cl-, HCO3-. Also, solutions contain dissolved corrosion products, small amounts of phosphorus-compounds, silicon in the form of orthosilicic acid and decay products, in addition, acidic solutions contain acetic acid.
The method of LRW isolation into the deep layers poses a potential risk of long-term use, however the risk water supply systems contamination with radionuclides and heavy metals can appear not only just a "potential". Currently in Russian Federation at a time of so called "final repository" construction the method described above is still being used for a disposal of significantly reduced amounts of LRW. Continuous monitoring of the geological environment, aquifers and river systems has shown no evidence of contamination so far.
However, the burial has been carrying out for several years and the scope of the study was to assess the degree of alteration of the geological environment as a result of long-term LRW influence. The results of research can be used in the simulation of possible emergency impacts on the geological environment.
Samples were collected from the sand reservoir layer at a distance of 110-150 m from injection wells to avoid the influence of radioactivity. Thus, in the target range of reservoir layers there is no influence of radioactive decay, and the impact on the reservoir can be narrowed down to the influence of highly reactive solutions.
The study revealed alteration of host rocks as a result of geological and technological processes. Such processes as formation of H-smectites and kaolinite to smectite transformation through series of kaolinite-smectite were revealed in the reservoir layers as a result of a long-term injection of highly reactive wastes generated. Herewith, neoformed smectite and natural diagenetic smectite are significantly different.
Thus it may be counterintuitive but as a result of long-term exposure to the LRW there is smectitic phase synthesized and its high sorption capacity can increase isolating properties of the geological environment. However, the study have shown preservation and even increase of isolating properties of the geological environment at the moment. Peculiarities of the mineral transformation processes that appears in "historical" waste sites certainly need additional studies.

A seismic approach to septaria detection in clay deposits

L. Wouters[1] , N. Vandenberghe[2] and E. Poggiagliolmi[3]

[1]Ondraf-Niras , Kunstlaan 14, 1210 Brussel

[2] NVDB Consult , Wijgmaalse stwg 170, 3150 Haacht

[3]Entec Integrated Technologies, Titchfield House, 68/85 Tabernacle Street, London EC2A 4RR.

During several upward directed drillings in the HADES-Underground Research Facility at Mol, a water influx occurred when a particular level of septaria in the Boom Clay was crossed. Septaria are hard calcareous concretions in clay known to possibly contain water in their septae. However the volume of water encountered during the drilling was unexpectedly high in comparison with the sizes of the concretions and their septae volume known from previous direct observations. The implication seems that septaria at this specific level are larger or numerous enough to have grown together, horizontally and maybe vertically as at this particular level two septaria horizons occur closely superposed. Therefore the question arises how to detect and image such intergrowth of septaria to better prove the origin of the water influxes observed and to avoid drilling or excavating such zones during future developments in the Boom Clay.

At this stage a seismic imaging approach is being tested. This is inspired by the good septaria images, including diffractions, obtained at shallow depths in the Boom Clay during river surveys by the UGent (Henriet et al.,1992; Missiaen et al.,2002). This justified to investigate under which conditions seismic methods could successfully be applied in land conditions, in underground conditions and in more deeply buried Boom Clay. Using a stepwise approach, the objective is to find out the instrumentation requirements together with acquisition and processing conditions necessary to locate septaria, estimate their dimensions and their separation distances.Sensitivity analyses based on forward modelling are an obvious initial step for optimising seismic acquisition and processing parameters. However, to be of practical use as an interpretation tool, the results of modelling must be made to agree with real seismic images. The very high resolution required to resolve seismically the separation and coalescence among the septaria bodies, implies to first test the available high resolution acquisition equipment by means of a field experiment at an overburden free Boom Clay site. This approach was also justified by the need to acquire information on the attenuation of high frequencies over distance in the clay, for which no reliable and precise enough information could be found.

The experiment was set up at the Argex clay pit in Kruibeke where the clay is 48 m thick and where the excavation front allowed a good control over the depth and the nature of at least 6 well-known septaria levels. Moreover, this site is located very closely to the river where, as mentioned above, two seismic surveys successfully showed diffractions corresponding to septaria levels in the Boom Clay. From the clay pit's working floor, a 50m deep borehole was drilled through the Boom Clay, lined with PVC and the annulus filled with bentonite. In addition, 9 shotholes were drilled inline, the nearest one to the deep borehole being separated by only a few meters. Each shothole was 2m deep, their separation was 10m and they were lined with PVC but without annulus filling. Parallel to the line of shotholes, a shallow ditch was excavated and kept water filled during the experiment. The purpose of the ditch was for the deployment of a string array composed of 72 hydrophones with an interspace of 1m. During the experiment the string position was shifted along the inline direction by 50 cm, to effectively double the number of receivers in the shot records and thereby halving their separation and increasing the overall spatial resolution of the acquisition setup. The same hydrophone string was also employed for receiving seismic signals emanated by a sparker source placed at regular intervals in the

deep borehole. The choice of hydrophones instead of high frequency geophones was made because the latter were affected by spurious responses in the high frequency range of interest. The P-wave sparker source, Geotomographie SBS-42, was chosen because of its relatively high output power (1000 Joules) over a frequency range spanning several kHz. The field set up, consisting of hydrophone receivers and sparker source, was used to produce three sets of data: sparker source in the shallow holes with the hydrophone string array in the deep hole (OVSP), sparker shots at 1m interval in the deep borehole with the hydrophone string array in the trench (RVSP) and finally the sparker source in the shallow holes with the hydrophone string array in the trench (SR). The field experiment was carried out by Fugro Aperio.

The pre-migration processing included the attenuation of unwanted events such as tube waves, in addition to velocity and spectral analysis. The velocities obtained in the clay are 1600 m/sec at the top increasing to 1800 m/sec at its base. These velocities are not unlike those measured in the Boom Clay at a few hundred meters burial depth probably because of the uplift history of the Boom Clay at Kruibeke. The spectral analysis of the shot records shows that most of the signal down to an amplitude threshold of -20db is contained within 100 to 3000 Hz range with a maximum peak occurring at approximately 500 Hz. The overall shape of the spectra is variable, probably because no editing of noisy traces was done prior to the computation of the spectra. Some of the better quality shot records exhibit signal at frequencies in excess of 4000 Hz, giving a range of wavelengths in the clay between 0.6 to 0.45m. Using the Rayleigh criterion applied to a thin layer and with appropriate data processing for reducing noise and taking account of the propagating wavelet bandwidth and phase rather than a single dominant frequency, the vertical resolution of a thin clay layer bounded between two septaria bodies could approach 15 cm. Similarly, assuming a propagation velocity through the septaria carbonate of 4000 m/s, a thickness resolution of 0.3m could be achieved. The spatial resolution, using the first Fresnel zone radius criterion, is about 1.2m at a depth of 10m. Again, with the appropriate data processing which should include diffraction imaging and wavelet deconvolution, spatial resolutions in the order of few tens centimetres can be achieved. Migration imaging produced from the OVSP and RVSP showed some reflection events in the subhorizontal Boom Clay. The RVSP configuration, having more source points compared to the OVSP, produced a higher S/N ratio. The velocity profile derived from the processed VSP's was used to depth migrate the SR data. Because of the geometry of the field set up, most of the energy received from reflectors within the clay is above critical angle. Future reprocessing must include the appropriate amplitude and phase corrections to transform above critical angle reflected energy into narrow angle equivalent. Although the fold average for the SR data is low, about 7, CMP processing without migration was applied to the data. Again reflections clearly appear within the Boom Clay but in addition, diffraction-like hyperbolic features can also be seen. Although no final correlation could yet be made between the septaria horizons in the clay and the more pronounced internal Boom Clay reflections, the inference can be made that the clay embedding the concretions in the septaria horizons still contains enough carbonate to cause acoustic impedance contrasts. This seems to be supported in some cases by field observations and by sharp increases in sonic transit time over short depth intervals in borehole logs of the Boom Clay.

Future work will involve additional processing to further reduce the deleterious effect of noise, to stabilise high end frequency response, to investigate diffractions, to transform wide angle reflections into their narrow angle equivalent, and to use instantaneous frequency methods rather than spectral ratios to measure vertical and horizontal attenuation. Different source options and the possible use of accelerometers will be assessed. A very important objective for a future field experiment is to measure reliably both horizontal and vertical attenuation in the clay as a function of frequency. Further field experiments will be steered by forward modelling based on the results of the experiment discussed in this study.

In conclusion, seismic data collected in the Boom clay with a bandwidth of up to 3000 to 4000 Hz, could produce septaria images with centimetres resolution both in the vertical and horizontal directions. This means that individual septaria and their separation can be potentially resolved.

Henriet, J.P., Verschuren, M., Versteeg, W. ,1992. Very high resolution 3D seismic reflection imaging of small-scale structural deformation. First Break 10, 81-88.

Missiaen, T., Versteeg, W., Henriet, J.P., 2002. A new 3D seismic acquisition system for very high and ultra high resolution shallow water studies. First Break 20, 227-232.

FE Experiment: Density measurement of granulated bentonite mixture in a 2D pre-test using a dielectric moisture profile probe

Toshihiro Sakaki, Sven Köhler and Herwig R. Müller

Nagra, Hardstrasse 73, 5430 Wettingen, Switzerland

1. Introduction

In the Full-Scale Emplacement (FE) Experiment at the Mont Terri Rock Laboratory, Nagra has constructed a 5-arm auger system to emplace granulated bentonite mixture (GBM) around three heaters that are to be placed horizontally on bentonite block pedestals. The target dry density of the bulk GBM as emplaced is 1.45 Mg/m^3 or more.

In order to verify and optimize the density of the emplaced GBM, a series of pre-tests has been performed in a 2D intermediate-scale tank with only one auger. This study presents the results from this pre-test, particularly the achieved bulk dry density of the GBM which was monitored using a dielectric moisture profile probe.

2. Material, tools and calibration

The GBM is produced to meet a number of strict requirements such as the pellet density, particle size distribution and water content. For the FE experiment, pellets of compressed bentonite with an average density of 2.18 Mg/m^3 were produced. The compressed pellets were then milled and mixed to have a particle size distribution similar to the "Fuller curve". The particles of the GBM ranged up to ~10 mm. The water content of the GBM after production was about 5 % by mass.

For measuring the density of the filled GBM, a commercial tool based on the dielectric method was examined. The tool tested was originally designed for measuring soil moisture profiles. As noted earlier, because the GBM is produced to have consistent properties including water content, the moisture sensor detects more moisture when the density is higher. In other words, the density of the GBM can be inferred from the measured moisture. In this study, we present the results obtained using a 1 m-long profile probe. The profile probe was first calibrated for density and was shown to have a sufficient sensitivity to dry density, as in **Figure 1**.

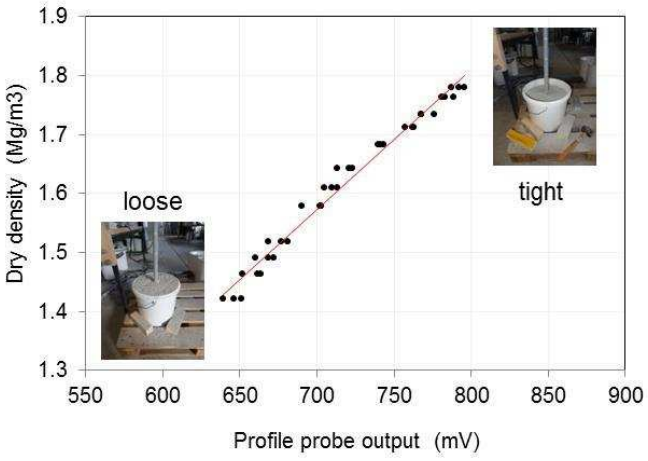


Figure 1. Profile probe mV output vs dry density. The profile probe was placed in the middle of a bucket filled with GBM. Photographs show the initial loose packing and final tight packing.

3. GBM filling in intermediate-scale two-dimensional tank

The filling test was performed on March 17, 2014 at an underground industrial testing facility Versuchsstollen Hagerbach (VSH) in Switzerland. A single auger was used to fill an intermediate-scale vertical two-dimensional tank with dimensions of 1 m (H) x 5 m (L) x 0.8 m (W) as shown in **Figure 2**. The front side of the tank is a glass wall to allow visual observation. The auger was positioned along the center line of the tank and the auger tip was about 40 cm below the top ceiling. The GBM was filled as smoothly as possible at the rate of ~170 kg/min, except when a new bag of bentonite had to be loaded. The auger was pushed back when the emplacement force reached 5 to 6 kN.

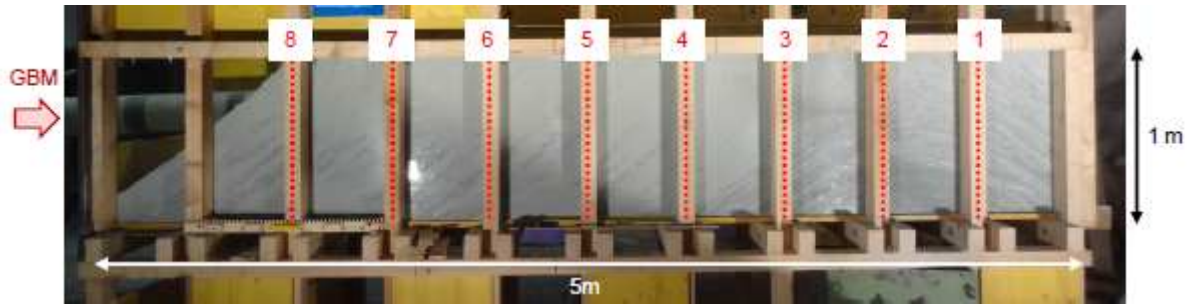


Figure 2. Intermediate-scale 2D tank and measurement locations. The auger tip was initially positioned between profiles 1 and 2 and moved left as filling proceeded.

In this test, the density of the emplaced GBM was monitored with the profile probe along eight vertical profiles distributed over the entire tank length (**Figure 2**). The access tubes for the probe were pre-installed at the locations shown in the figure, 15 cm away from the wooden back wall so that the sample volume (approx. 6~10 cm radius around the access tube) of the profile probe is contained within the GBM. The profile probe measurement along a profile was taken with a vertical spatial resolution of 5 cm. All the profile probe measurements were taken after the emplacement was completed. The raw sensor readings in mV were converted into dry density according to the calibration in **Figure 1**. The density values measured with the sensors were compared to the average density obtained from the mass balance.

4. Results and discussion

The bulk dry density along the eight profiles was calculated using the calibration in **Figure 1** and the profile probe outputs for a filling without any additional densification or homogenization measures (such as a use of vibratory devices). Profiles 1 and 8 were partially affected by the boundary effects, whereas profiles 2 through 7 were very similar. It was also seen in the results that the bulk dry density tends to show low values near the ceiling, the highest values near the auger and the average along each profile is around 1.5 Mg/m^3. The average dry density estimated by mass balance was 1.52 Mg/m^3, while the average of the PR2 measured values for the entire domain was 1.51 Mg/m^3. Despite the visually observable heterogeneity, the mean dry density was found to be higher than the target dry density of 1.45 Mg/m^3. It was shown that the dielectric profile probe is a powerful tool for monitoring GBM if the installation of the access tubes is possible.

References

Müller, H. R. et al. (2015) Müller et al. (2015), The Full-Scale Emplacement Experiment – Implementation of a multiple heater experiment at the Mont Terri URL, this conference.

FE Experiment: Density measurement of granulated bentonite mixture in a 3D 1:1 scale mockup test using dielectric tools

Toshihiro Sakaki, Sven Köhler, Marian Hertrich and Herwig R. Müller

Nagra, Hardstrasse 73, 5430 Wettingen, Switzerland

1. Introduction

The Full-Scale Emplacement (FE) Experiment is a 1:1 scale heater experiment being constructed at the Mont Terri Rock Laboratory in order to demonstrate feasibility of the Swiss repository concept of high-level radioactive waste and/or spent fuel and to investigate thermal-hydraulic-mechanical (THM) effect onto the host rock (Müller et al., 2015). Three heaters are used to mimic waste canisters and to be horizontally placed on bentonite block pedestals. For emplacing the granulated bentonite mixtures (GBM) to fill the space around the heaters, Nagra has constructed a prototype 5-arm auger system. The target dry density of the bulk GBM as emplaced is 1.45 Mg/m^3. In order to test the newly built prototype backfilling machine and to verify the achievable density of the emplaced GBM, a 3D 1:1 scale mock-up tunnel with a dummy waste canister and pedestal was constructed and filled with the GBM. This study presents results of bulk dry density of the GBM measured during the mock-up test using different dielectric tools.

2. Material and methods

2.1 Granulated bentonite mixture

The GBM used in this test was produced so that its particle size distribution follows the Fuller curve as close as possible. The particles of the GBM were produced by milling highly compacted bentonite briquettes with an average density of 2.18 Mg/m^3 and their size ranged up to ~10 mm. Other conditions such as the initial water content of about 5% by mass remain the same as those used in the previous pre-tests.

2.2 Three-dimensional 1:1 scale mockup setup

The 1:1 mockup tunnel has dimensions of 8 m in length and 2.5 m in diameter. Since the five augers of the backfilling machine are aligned in a staggered manner referring to the expected repose angle of the GBM, the back end of the mockup tunnel was built at an angle of 45 degrees in order to reduce the amount of the GBM to be used. A dummy heater (4.6 m in length, 1.05 m in diameter) was placed on a metal pedestal near the tunnel entrance. After completing the installation of monitoring tools described below, the space between the tunnel wall and the dummy heater was filled with the GBM using the 5-arm auger system.

2.3 Monitoring tools

For measuring the density of the filled GBM, three dielectric tools were tested and distributed within the GBM. These tools were originally designed mainly for measuring soil moisture. Because the GBM was produced to have consistent properties including the water content, the moisture sensors yield a higher total moisture value when the density is higher. All the sensors and access tubes were pre-installed prior to the GBM emplacement.

1) Moisture profile probe. A total of 22 access tubes were installed radially at sections with and without the dummy heater. Each yielded a profile along 65~70 cm from the tunnel wall.

2) PICO TDR sensor. Four 3 m-long access tubes were vertically installed behind the dummy heater to monitor the density over the entire vertical diameter. In the horizontal direction, one was installed perpendicular to the tunnel axis and two were parallel to the tunnel axis.

3) ECH_2O moisture sensors. Seven in the lower half vertical profile where the access tubes for the profile probe could not be installed, 10 along the tunnel wall, five on the tip of the augers. All ECH_2O sensors were configured to take data every one minute whereas the profile probe and PICO sensor were only for post-emplacement measurement.

3. Preliminary results

The sensors are currently being calibrated for density using the GBM used in this filling test. Although the final density values have not yet been obtained, the general trend observed in the raw readings from the sensors during the mock-up test indicate the following.

- The readings from the sensors showed that the density distribution has some small-scale heterogeneity. Such heterogeneity was also observed in the 2D tank filling test. In the case of the 3D mockup tunnel with a dummy canister, the distribution seemed more complex.
- The top half portion seemed to be filled with somewhat higher density as compared to the bottom half.
- The horizontal profile perpendicular to the tunnel axis showed a lower density region near the tunnel center (behind the heater dummy).

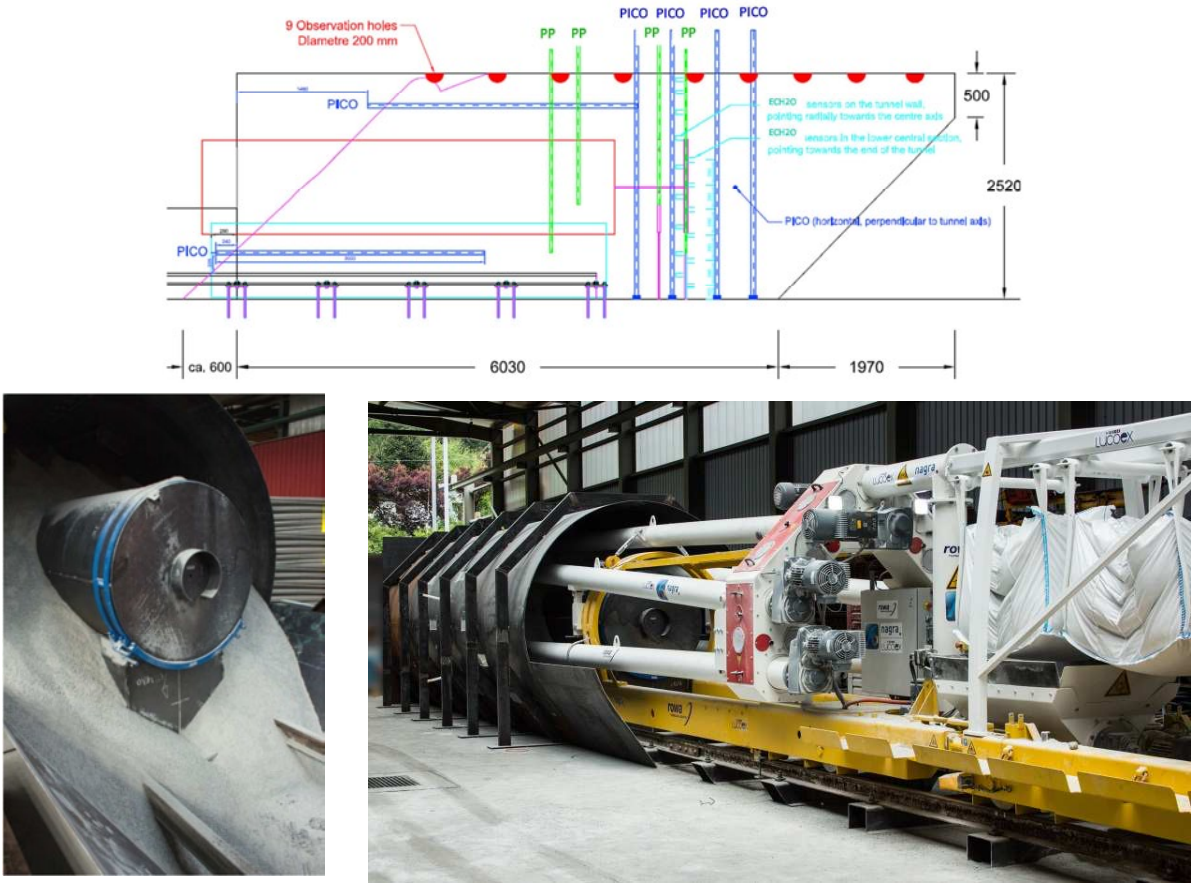


Figure 1. Schematic view of the 8 m-long 1:1 scale mock-up tunnel with a dummy heater. Top) Side view of sensor locations, Bottom left) Slope of the GBM upon completion of the emplacement. Bottom right) The mockup setup with backfill machine.

4. Conclusions

The dielectric tools for monitoring soil moisture showed high potential for estimating the density of the GBM filled with an auger system if the pre-installation of the access tubes is possible. The heterogeneous density field was found out to be more complex than that observed in a 2D tank. In addition, it is our intention to further investigate possible measurement artefacts such as the effect of the metal tunnel wall and the spacing of the emplaced access tubes. Additional measurements based on RI and cone penetration were also performed and the results will be compared with those obtained by the dielectric tools.

References

Müller, H. R. et al. (2015), The Full-Scale Emplacement Experiment – Implementation of a multiple heater experiment at the Mont Terri URL, this conference.

Qualitative and quantitative mineral composition of the Rupelian Boom Clay in Belgium

E. Zeelmaekers[1 2], M. Honty[3], A. Derkowski[4], J. Środoń[4], M. DeCraen[3], N. Vandenberghe[1], R. Adriaens[1] and L.Wouters[5]

[1] Laboratory for Applied Geology and Mineralogy, University of Leuven, Celestijnenlaan 200E, 3001 Leuven-Heverlee, Belgium

[2] Presently at Shell International Exploration & Production, The Hague, The Netherlands
edwin.zeelmaekers@shell.com

[3] Institute of Environment, Health and Safety, Belgian Nuclear Research Centre(SCK-CEN), Boeretang 200, 2400 Mol, Belgium

[4] Institute of Geological Sciences, Polish Academy of Sciences, Research Centre in Kraków, ul. Senacka 1, PL-31002 Kraków, Poland

[5] NIRAS-ONDRAF, Kunstlaan 14, 1210 Brussels, Belgium

The Boom Clay Formation is an Early Oligocene deposit found in the underground of northern Belgium, which has been intensely studied for decades in the frame of the disposal of nuclear waste at the research site of Mol. Thus far however, no reference mineral composition for the Boom Clay existed and widely varying results are reported in numerous studies. All of these studies had in common that they were done using non-standardized sample pretreatments and analysis methods that could be considered semi-quantitative at best. The goal of the presented study was to determine a reference composition for the Boom Clay using proven high accuracy methods on 20 samples carefully selected to represent the vertical lithological variability of the formation.

For bulk mineralogical analysis, air-dried samples were hand-ground <0.5 mm and milled in methanol during 5 min in a McCrone Micronizing Mill together with 10 wt % of a zincite internal standard. The resultant powder was side-loaded into a diffractometer holder. After an initial phase identification, the quantitative composition was determined using a set of prerecorded standards, using the Quanta software (Chevron ETC proprietary). The method (Środoń *et al*., 2001) combines the advantages of both full pattern summation and single peak quantification methods. In this method clays and micas are quantified based on their *060* reflections and are reported in groups. Both the method and the software have been demonstrated to be highly accurate and repeatable (e.g. see reports on the *Reynolds Cup* results in Kleeberg, 2005; Omotoso *et al*., 2006). In the bulk rock, siliciclastics were found to vary from 27 to 72wt%, clay minerals and micas from 25 to 71wt%, carbonates from 0 to 4wt%, accessory minerals (mainly pyrite and anatase) from 2 to 4wt% and organic matter from 0.5 to 3.5wt%. This bulk rock composition was independently validated by major element chemical analysis. Structural formulae of the variable composition minerals present are calculated and combined with a statistical distribution of the trace elements over all the present minerals to calculate petrophysical properties useful for well log analysis in the clay (Derkowski *et al*., 2008; Środoń and Kawiak, 2012).

The hand-ground <0.5mm material was also used to extract the clay fractions (<2μm and <0.2μm). The extraction techniques involve carbonates removal, organic matter mild oxidation, and Fe-(oxy-) hydroxides removal followed by grain size fractionation by centrifugation, as described in detail by Jackson (1975). The extracted clays were converted to their Ca-form as in this cation state clay minerals are least susceptible to ambient humidity variations. In addition, cation saturations with Mg and K were prepared for specific identification purposes. Only small differences in clay mineral ratios were observed between the diffraction patterns of smear mounts and sedimentation slides, but the

sedimentation slides produced stronger intensities and less noise because of a better preferred orientation of the clay minerals and, therefore, they were chosen as the preferred preparation method, for both the <2μm and <0.2μm size fractions. The qualitative and quantitative composition of the clay fractions was determined by modeling diffraction patterns of oriented slides of the extracted clay fractions using the Sybilla software (Chevron ETC proprietary). Sybilla combines the formalism for calculating the diffraction patterns of mixed-layered clay minerals presented by Drits and Sakharov (1976) with a user-friendly graphical interface. Modeling was performed with the "multispecimen" method, as proposed by Sakharov *et al*. (1999). Modeled layer type parameters include: mean crystal size thickness, d-spacing, Fe-content, K-content (illitic layer types) and water and glycol contents for swelling layer types. The detailed composition of the clay-sized fraction was determined by modeling of oriented diffraction patterns, using a higher sigma star value for smectite than for the other clay minerals. This last parameter describes the degree of preferred orientation. It was found that the <2μm clay mineralogy of the Boom Clay is qualitatively homogeneous, it contains 14 to 25wt% of illite, 19 to 39wt% of smectite, 19 to 42wt% of randomly interstratified mixed-layered illite-smectite (with about 65% illite layers), 5 to 12wt% of kaolinite, 4 to 17wt% of randomly interstratified mixed-layered kaolinite-expandables (with about 17 to 19 % expandables) and 2 to 7wt% of chloritic minerals including chlorite, "defective" chlorite and mixed-layered chlorite-expandables. The determined illitic content was independently validated using a comparison of calculated and measured K_2O contents; the smectitic content was independently validated using cation exchange capacity measurements; kaolinitic and chloritic contents were independently validated by applying the bulk quantification method on the extracted clay fractions.

In a final step, bulk rock and clay analysis results were then combined to obtain the overall detailed qualitative and quantitative composition of the Boom Clay. Knowing the detailed mineralogical composition will help to further understand the thermal, hydraulic, mechanical and chemical behavior of the Formation. In particular the nature and the content of the swelling minerals and their corresponding exchange capacity are significant properties for a potential nuclear waste clay host rock.

References

Derkowski, A., McCarty, D.K., Środoń, J., Eberl, D.D., 2008. BestRock-mineralogy, chemistry, and mineral surface property optimization to calculate petrophysical properties of the mineral matrix. Mineralogia-Special Papers, 33, 53

Drits, V.A. & Sakharov, B.A., 1976. X-ray Structural Analysis of Mixed-Layer Minerals. Nauka, Moscow. *(in Russian)*

Jackson, M.L., 1975. Soil chemical analysis - Advanced course, 2nd edition. Published by the author, Madison, Wisconsin, 895pp.

Kleeberg, R., 2005. Results of the second Reynolds Cup contest in quantitative mineral analysis. International Union of Crystallography. Commission on Powder Diffraction Newsletter, 30, 22-24.

Omotoso, O., McCarty, D.K., Hillier, S., Kleeberg, R., 2006. Some successful approaches to quantitative mineral analysis as revealed by the 3rd Reynolds Cup Contest. Clays and Clay Minerals, 54, 748-760.

Sakharov, B.A., Lindgreen, H., Salyn, A.L. &Drits, V.A., 1999. Determination of illite-smectite structures using multispecimen X-ray diffraction profile fitting. Clays and Clay Minerals, 47, 555-566.

Środoń, J., Drits, V.A., McCarty, D.K., Hsieh, J.C.C. & Eberl, D.D. (2001): Quantitative X-ray diffraction analysis of clay-bearing rocks from random preparations. Clays and Clay Minerals, 49, 514-528.

Środoń, J. and Kawiak, T., 2012. Mineral compositional trends and their correlations with petrophysical and well-logging parameters revealed by Quanta + Bestmin analysis: Miocene of the Carpathian Foredeep, Poland. Clays and Clay Minerals, 60, 1, 63-75.

Structural and mechanical properties of Na rich-montmorillonite:Correlation between XRD analysis and molecular dynamics simulations

Walid Oueslati[a,b]

[a]General Studies Department, College of Electronics & Communications, Technical and Vocational Training Corporation, TV Street, P.O. Box 2816, Jeddah 21461, Saudi Arabia
[b]Departement de physique, Faculté des Sciences de Bizerte, Zarzouna 7021, Tunisia
E-mail: walidoueslati@ymail.com

A study of structural and mechanical properties of montmorillonite using Molecular Dynamics Simulations based on energy minimization technique was investigated, in order to determine The velocity anisotropy parameters and elastic constants which play a very important role to estimate Young's modulus and Poisson's ratios accurately. Indeed, the experimental prediction of the mechanical properties of minerals remains difficult because of their small particle size (typically < 2 micrometers). This work aims at examining, the effect of an applied mechanical constraint on the structural changes in the case of Na rich-montmorillonite and its relation with the elastic properties.
The mechanical constraint is created, at the laboratory scale, by applying a monoaxial pressure for unstressed host material (i.e. Na rich montmorillonite). The structural analysis before and after stress is achieved using an XRD profile modeling approach[1]. This investigation allowed us to determine several structural parameters related to the nature, abundance, size, position and organization of exchangeable cation and water molecule in the interlamellar space along the c* axis.
In order to evaluate the affected elastic properties, the GULP [2] code have been used to study the structure and the interlamellar organization. Indeed, Several mechanical properties have been calculated, such as the full elastic constants tensors, shear modulus, bulk modulus, Young modulus along a, b and c directions. The S- and P-wave velocities as well as Poisson ratio were also evaluated.
the bulk modulus and elastic constants of montmorilonite have been calculated from first principles within density functional theory (DFT). The obtained elastic constant shows that $C_{11}\approx C_{22}$ and higher than C_{33},indicating that stressed montmorillonite is more flexible in a and b direction than c one. The predicted bulk and shear modulus are respectively equal to 49.38 and 19.31 GPa. The Poisson's ratios exhibit prominent anisotropy, with values ranging from 0.04 to 0.49. The Young's modulus in the [100] and [010] directions is larger than E_3 (Young moduli in[001] direction) it varies from 4.8 GPa to 14.9 GPa. According to the interlamellar space configuration the calculated elastic constant tensors indicate that the a direction is slightly more flexible than the b direction.

Keywords : Elastic properties; montmorillonite; GULP code; Quantitative XRD analysis.

[1]. W. Oueslati, H. Ben Rhaiem, A. Ben Haj Amara, 2011. *XRD investigations of hydrated homoionic montmorillonite saturated by several heavy metal cations*. Desalination. 271:139-149.

[2]. J. D. Gale, 1997. *GULP: A Computer Program for the Symmetry-Adapted Simulation of Solids* J. Chem. Society- Faraday Transactions. 93, 629-637.

Microstructural characterization of the Ypresian clays at the nm-scale resolution, using broad-ion beam scanning electron microscopy (BIB-SEM) – preliminary results

Susanne Hemes, **Guillaume Desbois, Janos L. Urai**

Structural Geology, Tectonics and Geomechanics, Geological Institute, RWTH Aachen University, Lochnerstrasse 4-20, 52062 Aachen, Germany.

Abstract:

Besides the Boom Clay Formation (Oligocene), the Ypresian clays, part of the Eocene Ieper Group (Kortrijk Formation and Kortemark Member), are currently considered and investigated as an alternative, for the research on deep geological disposal of radioactive waste (ONDRAF/NIRAS, 2001). However, the microstructures of Ypresian clays are so far not extensively characterized.

In the present contribution, a combination of broad-ion beam milling and scanning electron microscopy (BIB-SEM), was applied to analyze the microstrucure – in particular the porosity – of six representative samples of the Ypresian clays, originating from different depth of the Kallo-1 (2008) borehole and comprising different mineralogical compositions (clay contents ranging between 30 to 71 dry wt.-%), as well as grain-size distributions, from clayey to fine-sand sized material. Analyses were carried out within representative elementary areas (REAs) of BIB cross-sections of several hundred μm^2 and at resolutions down to several hundred nm^2 (pixel-size).

Preliminary results show significant differences to microstructures observed in the Boom Clay Formation, from a previous study by Hemes et al. (2013):

1.) The Ypresian clay samples investigated show much larger average grain-sizes, a more heterogeneous and wider grain-size distribution as well as a higher contribution of silt-sized particles to the overall observed microstructures.
2.) Total observed porosities are between 7-17 % of the analyzed areas, but show significantly different pore-size distributions, compared to the Boom Clay Formation (Hemes et al., 2013).
3.) Whereas pore-size distributions in Boom Clay are clearly unimodal – with either very small pores (< 1E+06 nm^2) within the clay-matrix, or larger inter-aggregate pores (> 1E+07 to 1E+08 nm^2) contributing to the major fraction of the observed porosity, in the Ypresian clays, both porosity regimes (small pores within the clay-matrix as well as large inter-aggregate pores) contribute to major fractions of the total observed porosities.
4.) Peaks in total porosity contributions are located below 1E+06 nm^2 for the small pore-size regime and > 1E+07 nm^2 for the large, inter-aggregate pores.
5.) Qualitative analysis of pore morphologies shows very roundish pores, described as “flower-like” (compared to much more elongated pores in the Boom Clay); large pores at clay – non-clay mineral interfaces do also show mostly rounded pore boundaries, significantly different from typical morphologies of drying artifacts.
6.) Quantitative pore shape analysis corroborate the bullet point (5), by providing much lower axial ratios, lower elongation factors and higher roundness values as well as higher circularities – compared to the Boom Clay; indicating more roundish pore morphologies in the Ypresian clays.
7.) Power-law analyses of pore-size distributions suggest two distinct pore-size regimes, by showing clear changes in the power-law exponents of pore-size distributions, often located ~ 3E+04 nm^2 pore area, as well as around 1E+06 nm^2.

Multi-scale characterization of pore space connectivity in Boom Clay (HADES-level, Mol, Belgium), using a combination of X-ray μ-CT, BIB-SEM and serial FIB-SEM

***Susanne Hemes*[1], Guillaume Desbois[1], Janos L. Urai[1], Birgit Schröppel[2], Jens-Oliver Schwarz[3]**

1: Structural Geology, Tectonics and Geomechanics, Geological Institute, RWTH Aachen University, Lochnerstrasse 4-20, 52056 Aachen, Germany.
2: Natural and Medical Sciences Institute (NMI) at the University of Tübingen, Markwiesenstrasse 55, 72770 Reutlingen, Germany.
3: Institute of Geosciences, Johannes Gutenberg University Mainz, J.-J.-Becher-Weg 21, D-55128 Mainz, Germany.

Abstract:

The Boom Clay (Rupelian, Oligocene) is besides the Ypresian clays, one of the potential host rock materials for radioactive waste disposal in Belgium (Gens et al., 2003; Van Marcke et al., 2005; Verhoef et al., 2011). To access parameters, relevant for the better understanding of transport mechanisms of radionuclides and to identify potential anisotropies of the material, it is crucial to characterize the pore space and its connectivity at high resolution (down to the nm-scale) and in 3D. In the present contribution, X-ray μ-CT imaging, 2D BIB-SEM porosity investigations, FIB-SEM serial cross-sectioning and pore network extraction (PNE) modelling (after Dong and Blunt, 2009) were combined to show a high connectivity of the pore space in fine-grained ON-Mol-1-196 (HADES-level) Boom Clay, over several orders of magnitude. Moreover, results were compared to bulk sample Mercury injection Porosimetry (MIP) data and 2D BIB-SEM porosities, obtained within representative elementary areas (REAs; Hemes et al., 2013).

A high complexity of the 3D pore morphologies and pore space connectivity was observed and resolved by FIB-SEM, showing high pore body coordination numbers and ~ 87 % of the total pore space connected. Pore throat orientation analyses on both X-ray μ-CT and FIB-SEM data, suggest preferred pore throat orientations parallel to the sample bedding, possibly enhancing the permeability of the material in this direction.
Comparison of pore network extraction results from X-ray μ-CT and FIB-SEM to MIP data, indicates a high connectivity of the pore space in fine-grained Boom Clay over several orders of magnitude in pore throat diameter, mainly controlled by two pore space connectivity regimes; 1) within the fine-grained clay-matrix of the sample – with pore throat diameters mostly between 20-100 nm, resolved by FIB-SEM and 2.), with pore throat diameters mainly between 2-7 μm, controlling the connectivity of larger inter-aggregate pores or fracture related porosity, resolved by X-ray μ-CT.

Pore-size distribution analyses on segmented 2D pore areas and 3D pore body and pore throat volumes equivalent cross-sectional areas, suggest power-law behaviours of pore-sizes over ~ 6 orders of magnitude, with power-law exponents between 2.2-2.4, which is in good agreement with previous results of power-law analysis on MIP data (Hemes et al., 2013). This seemingly scale-invariance of the results was interpreted as self-similarity of the observed pore space microstructural features, possibly relating to larger scale characteristics of the Boom Clay Formation and hinting towards the possibility of up-scaling of the results.
The good agreements of pore-size distributions obtained from 2D and 3D data, as well as between the number fraction distribution of pore bodies and pore throats from PNE on X-ray μ-CT and FIB-SEM data, and bulk sample Mercury intrusion curve (Hemes et al., 2013) on the same reference sample, suggest representativeness of investigations.

A combination of X-ray μ-CT, with 2D BIB-SEM and 3D serial FIB-SEM allows for the direct investigation and observation of pore space connectivity, within representative volume elements, and over nearly the entire relevant pore throat diameter range, controlling the major connectivity of the pore space in fine-grained HADES-level Boom Clay.

Microbial diversity, activity and survival in engineered clay barriers

Karsten Pedersen
Microbial Analytics Sweden AB, Mölnlycke Fabriker 9, 43535 Mölnlycke Sweden

Microbial processes can under certain conditions result in the formation of gas and sulphide [1]. Gas formation can give rise to pore pressure and mechanical effects in the engineered barriers, and sulphide from sulphate reducing bacteria (SRB) can corrode the metal canister [2]. Sulphide formation must take place in the buffer barrier, near the canister, and be of considerable extent for corrosion to be a threat to the canister integrity, mainly due to the fact that sulphide is commonly precipitated with ferrous iron and, therefore, sulphide concentrations do not show up as high concentrations in groundwater and thereby its diffusive transport capacity is very low. In order for the above-described processes to take place, the bacteria must be present in clays, be active and have access to water, nutrients and space. The presence of microorganisms in various clays intended for engineered barriers have been documented repeatedly. A large diversity and numbers of bacteria were found in Asha 505, Calcigel, Callovo Oxfordian, Deponit CA-N, Friedland, Ibeco Seal M-90, Ikosorb, Kunigel V1, MX-80 and Rokle bentonites. Most of these clays contained SRB and iron-reducing bacteria [3, 4].

Several investigations of long-term survival of introduced and naturally present microorganisms with different relevant characteristics have been performed in the Äspö Hard Rock Laboratory (HRL). Mesophilic, thermophilic and spore-forming sulfate reducing bacteria, together with desiccation resistant, chemo-organotrophic or chemolithotrophic spore- and non-spore forming bacteria were mixed with bentonite clay to give approximately 100 million bacteria per gram (dry weight) of clay and exposed to 20–70°C temperatures for 15 months [5, 6]. The major outcome was elimination, to below detection limits, of all bacteria except the spore-forming ones. In other full scale experiments surviving microorganisms could be cultivated from the buffer after several years of exposure [7, 8].

The worst-case scenario in metal canister corrosion would be if SRB formed biofilms on the canisters or grew intensively in the buffer close to the canister. To mimic this situation, several experiments have been executed and evaluated [9]. The SRB used were very active at a saturated bentonite density of 1,500 kg/m^3, but that sulphide production decreased at higher densities [10]. This experiment indicated that SRB probably cannot be active at the canister surface at a repository bentonite density of 2,000 kg/m^3 at full water saturation. However, the experiment was run with two laboratory species and it may be possible that species naturally present in bentonites could survive better. Therefore, additional experiments were carried out using natural groundwater under *in situ* conditions including a hydrostatic pressure of 25 bars at a depth of 450 m in the Äspö HRL [11, 12]. That groundwater contained many hundreds of different microbial species, including many naturally occurring species of SRB. Radioactive hydrogen sulphide formed by the SRB reacted with introduced copper surfaces and formed radioactive copper sulphide, which was measured by electronic radiography. The results showed that SRB were active and produced hydrogen sulphide over the range of tested densities, i.e. 1500 to 2000 kg m^3. However, the sulphide producing activity at the highest density was hardly detectable.

It seems safe to conclude that microbial sulphide production will diminish in bentonites with increasing density and swelling pressure and approach nil when the density is above 1900 - 2000 kg m^3. If this density decreases below this level, for instance due to buffer erosion or illitization, or due to irregularities (contaminant materials, large pores or gaps) in the bentonite density, microbial sulphide production may commence. The concentration of sulphate in bentonite pore water can be substantial and reach 0.1 M which, if electron donors such as organic material or hydrogen are available, can be reduced to sulphide. Further, all experiments on microbial activity in bentonites referred to in this abstract have been done with MX-80. Because the composition and the natural content of microorganisms of commercial bentonite vary significantly, the cut off density for microbial activity

may also vary. A proper safety case requires that the bentonite finally selected as material for engineered barriers is tested for the potential risk of microbial sulphide production and concomitant canister corrosion.

References

1. Lydmark, S. and J. Persson, Production of gas and sulphide by bacteria in Boom Clay, in ONDRAF/NIRAS NIROND-TR REPORT 2010-16 E. 2010, ONDRAF/NIRA. p. 40.
2. Smart, N.R., et al., In situ evaluation of model copper-cast iron canisters for spent nuclear fuel: a case of microbiologically influenced corrosion (MIC). Corrosion Engineering, Science and Technology, 2014. **49**(6): p. 548-553.
3. Svensson, D., et al., Alternative buffer material. Status of the ongoing laboratory investigation of reference materials and test package 1, in SKB Technical Report TR-11-06. 2011. p. 146.
4. Masurat, P., S. Eriksson, and K. Pedersen, Evidence of indigenous sulphate-reducing bacteria in commercial Wyoming bentonite MX-80. Applied Clay Science, 2010. **47**(1-2): p. 51-57.
5. Motamedi, M., O. Karland, and K. Pedersen, Survival of sulfate reducing bacteria at different water activities in compacted bentonite. FEMS Microbiology Letters, 1996. **141**(1): p. 83-87.
6. Pedersen, K., et al., Cultivability of microorganisms introduced into a compacted bentonite clay buffer under high-level radioactive waste repository conditions. Engineering Geology, 2000. **58**(2): p. 149-161.
7. Arlinger, J., et al., Prototype repository - Microbes in the retrieved outer section, in SKB Report P-13-16. 2013. p. 44.
8. Lydmark, S. and K. Pedersen, Äspö hard rock laboratory canister retrieval test microorganisms in buffer from the canister retrieval test – numbers and metabolic diversity, in SKB Report P-11-06. 2011. p. 35.
9. Persson, J., et al., Microbial incidence on copper and titanium embedded in compacted bentonite clay, in SKB Report R-11-22. 2011.
10. Pedersen, K., et al., Mixing and sulphate-reducing activity of bacteria in swelling, compacted bentonite clay under high-level radioactive waste repository conditions. Journal of Applied Microbiology, 2000. **89**(6): p. 1038-1047.
11. Masurat, P., S. Eriksson, and K. Pedersen, Microbial sulphide production in compacted Wyoming bentonite MX-80 under in situ conditions relevant to a repository for high-level radioactive waste. Applied Clay Science, 2010. **47**(1-2): p. 58-64.
12. Pedersen, K., Analysis of copper corrosion in compacted bentonite clay as a function of clay density and growth conditions for sulfate-reducing bacteria. Journal of Applied Microbiology, 2010. **108**(3): p. 1094-104.

Characterization of alternative buffer and backfill materials

Keto Paula[1], Kumpulainen Sirpa[1], *Kiviranta Leena[1]*, Karttunen Petriikka[1] and Korkeakoski Petri[2]

B+Tech Oy, Laulukuja 4, 00420 Helsinki, Finland (paula.keto@btech.fi, sirpa.kumpulainen@btech.fi, leena.kiviranta@btech.fi, petriikka.karttunen@btech.fi)
Posiva Oy, Olkiluoto, 27160 Eurajoki, Finland (petri.korkeakoski@posiva.fi)

The aim of this work was to search alternative buffer and backfill materials for current design of Posiva Oy (MX-80, Friedland clay, high grade Milos bentonite) (Juvankoski et al. 2013, Keto et al. 2013), to assess the factors affecting the acquisition, to determine chemical, hydraulic, swelling, and mechanical properties of alternative materials, and to compare alternative material properties with the current reference materials.

Altogether 22 alternative materials were received from eleven different bentonite producers initially from Azerbaijan, China, Cyprus, India, Italy, Spain, United States and Turkey. 11 of materials were in powdered form and the rest 11 were granular products. Montmorillonite contents given by suppliers varied between 20 – 85%.

All bentonites were tested with index tests. Water ratio was determined gravimetrically after heating the sample at 105°C for 24h. The swelling index was determined as a volume of swelled material (ml/2g) after period of 24h (ASTM D 5890-06). Granule size distribution of samples was determined by dry sieving (CEN ISO/TS 17892-4: 2004). Chemical composition of alternative materials was determined with ICP-AES, Leco (total S, total C, sulphate and inorganic C) and LOI. In addition, ferrous iron was determined titrimetrically. The analyses were done by AcmeLabs (Acme Analytical Laboratories (Vancouver) Ltd.). Cation exchange capacity (CEC) was measured using Cu(II)-triethylenetetramine method (Meier and Kahr 1999, Ammann et al. 2005).

Three alternative materials were selected for further studies. Original exchangeable cations were extracted using solution of NH_4Cl in 80% ethanol (Belyayeva 1967, Jackson 1975). Mineralogical composition was defined after identifying minerals with x-ray diffraction (XRD) and optical microscopy, and quantifying mineralogical composition with Rietveld refinement using Siroquant software. Grain density was determined in 1 M NaCl solution (Karnland et al. 2006). Swelling pressure and hydraulic conductivity were determined using de-aired 1%-salt solution, which had Na:Ca-ratio of 2:1, as saturant and permeant (e.g. Kiviranta and Kumpulainen 2011). Unconfined compressive strength tests were done by electromechanical uniaxial press using axial strain rate of 0.8 mm/min following ASTM D2166-06 for samples with similar initial water content of 10% and similar dry density of 2000 kg/m^3.

All studied alternative materials fulfilled the design specifications set by Posiva Oy (see Juvankoski et al. 2013, Keto et al. 2013) for chemical composition of buffer and backfill materials (<1% $C_{org.}$, <1%S_{total} and <50%$S_{sulphidic}$ from the S_{total}). Considering the backfill these design specifications are currently under discussion due to the high amount of backfill placed in the repository. Based on the measured data new screening limits for the raw materials potential as backfill materials were suggested aiming at decreasing the amount of potentially harmful substances in the repository. From the mineralogical point of view, the three materials studied in more detail were in the pre-determined range for smectite/montmorillonite content for backfill use (30-75%). Also the desired range of smectite/montomorillonite content for backfill is under discussion due to quality, cost and long-term performance related reasons. From the buffer and backfill production point of view, most of the purchased alternative materials were too fine, too coarse, or too wet for use for manufacturing of compacted buffer and backfill components as such. In the future, technical material specifications such as granule size distribution and water ratio must be defined better before asking quotations from the

bentonite producers in order to get materials, which have more suitable technical properties for buffer and backfill purposes. The work will be continued in 2014-2015.

References

Ammann L., Bergaya F., Lagaly G. 2005. Determination of the cation exchange capacity of clays with copper complexes revisited. Clay Minerals, 40, 441-453.
ASTM D2166-06. Standard Test Method for Unconfined Compressive Strength of Cohesive Soil.
ASTM D5890-06. Standard Test Method for Swell Index of Clay Mineral Component of Geosynthetic Clay Liners.
Belyayeva N.I. 1967. Rapid method for the simultaneous determination of the exchange capacity and content of exchangeable cations in solonetzic soils. Soviet Soil Science, 1409-1413.
Finnish Standard CEN ISO/TS 17892-4: 2004. Geotechnical investigation and testing. Laboratory testing of soil. Part 4: Determination of particle size distribution.
Jackson M.L. 1975. Soil chemical analysis – advanced course. 2nd edition. Madison, Wisconsin.
Juvankoski M., Ikonen K., Jalonen T. 2013. Buffer Production Line 2012. Design, production and initial state of the buffer. POSIVA 2012-17. Posiva Oy, Olkiluoto, Finland.
Karnland O., Ohlsson S., Nilsson U. 2006. Mineralogy and sealing properties of various bentonites and smectite-rich materials. SKB TR-06-30. Swedish Nuclear Fuel and Waste Management Company (SKB), Stockholm, Sweden.
Keto P. (ed.), Hassan Md.M., Karttunen P., Kiviranta L., Kumpulainen S., Korkiala-Tanttu L., Koskinen V., Jalonen T., Koho P., Sievänen U. 2013. Backfill Production Line 2012. Design, Production and Initial State of the Deposition Tunnel Backfill and Plug. POSIVA 2012-18. Posiva Oy, Olkiluoto, Finland.
Kiviranta L., Kumpulainen S. 2011. Quality control and characterization of bentonite materials. Working Report 2011-84. Posiva Oy, Olkiluoto, Finland.
Meier L.P., Kahr G. 1999. Determination of the cation exchange capacity (CEC) of clay minerals using the complexes of copper(II) ion with triethylenetetramine and tetraethylenepentamine. Clays and Clay Minerals, 47, 386-388.

WITHDRAWN BY AUTHOR

WITHDRAWN BY AUTHOR

Near-field permeability distribution of FE tunnel in the Mont Terri Rock Laboratory - Influence of shotcrete lining on EDZ development -

Shao, Hua[1,*]; Paul, Benjamin[1]; Wang, Xuerui[1]; Hesser, Jürgen[1];
Becker, Jens[2]; Garitte, Benoit[2] & Müller, Herwig[2]

1. Federal Institute for Geosciences and Natural Resources (BGR), 30655 Hannover, Germany
2. National Cooperative for the Disposal of Radioactive Waste, 5430 Wettingen, Switzerland

* Contact person: Corresponding author (e-mail: shao@bgr.de)

Abstract

Permeability and its spatial distribution around an underground opening in the geological formation are important for the interpretation of thermal, hydraulic and mechanical findings from an in-situ demonstration experiment. Within the site characterisation program of the FE project permeability measurements have been conducted in six short boreholes. Four of them are located in a section without shotcrete support (GM 40 m) and the other two in a section with a three-layers-shotcrete lining (GM 14.7m).

The measurements were carried out about one year after excavation, using a double piston mechanical packer with a short interval of 10 cm. Because of the high amount of short interval tests, a precise distribution of permeability along boreholes is ensured (Fig. 1). Different orientations of the boreholes were designed for the investigation of the bedding plane dependency due to the transversal isotropic properties of Opalinus Clay. As expected, the extension of an increased permeability is larger (to 2 m) in the section without shotcrete support than that in the section with a shotcrete lining (< 1.5 m).

The water contents in the sections with or without shotcrete linings show in the long-term monitoring also different behaviour. The water content in the section with shotcrete lining keeps almost constant, while the water content in the section without shotcrete tends to continuously decreasing (Fig. 2). Generally, the water contents close to the tunnel react with the change of tunnel temperature and relative humidity, especially in the section without shotcrete lining.

The analysis of the abovementiond observations/findings were done by FEM calculations with OpenGeoSys using a 2D coupled hydromecahnical model. The mechanical and hydraulic anisotropic properties as well as the swelling/shrinkage behaviour of the Opalinus clay were considered in the model. As boundary condition on the tunnel surface suction pressure was calculated by Kelvin's equation based on measured temperature and relative humidity. Sensitivity studies were done by variating parameters, e.g. permeability, specific storage of Opalinus clay and shotcrete. Special attention was paied to the effect of the retention curves of Opalinus clay and shotcrete.

Due to higher stiffness of the shotcrete in comparison with that of Opalinus clay the displacement in the section with shotcrete lining is smaller than in the section without shotcrete. This leads to a smaller EDZ extension in the section with shotcrete lining. This is more obvious in the direction perpendicular to the bedding, where the E-modulus of clay is only half of that parallel to the bedding. In the direction parallel to the bedding, desaturation induced shrinkage deformation may dominate the EDZ development.

The shotcrete has a relatively high suction capacity and a high initial water content, the interface between shotcrete and Opalinus clay will become more saturated. Thus, the excavation induced fracture can be sealed. The continuous decrease of the water content is reduced to the desaturation process because of the change of pore water pressure during the operating phase.

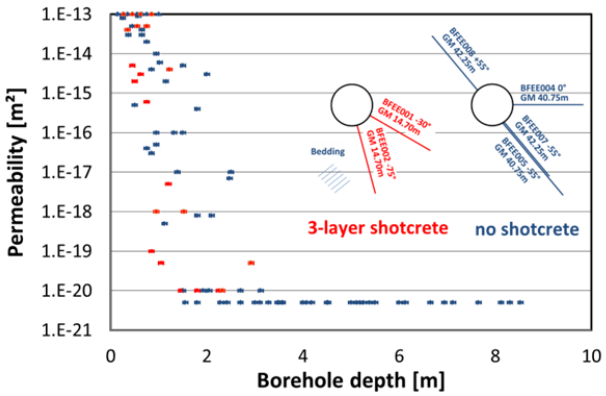


Figure 1: Permeability distribution.

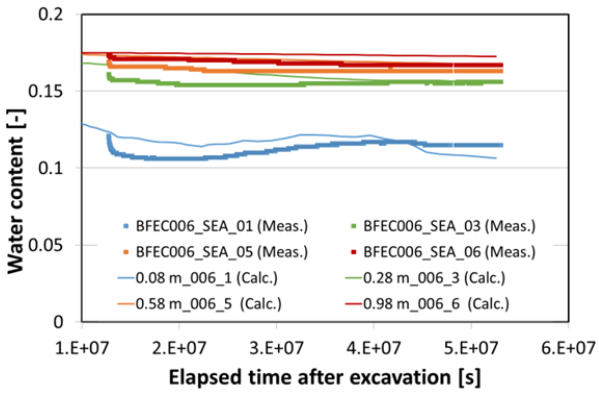


Figure 2: Measured and modelled water content.

Reference

Jeoung, J. Y., Lee, S., Leet, G. (2008): Evaluation of hydraulic conductivity of shotcrete lining samples, World Tunnel Congress 2008 - Underground Facilities for Better Environment and Safety, India

Schneider, S., Mallants, D. & Jacques, D. (2012): Determining hydraulic properties of concrete and mortar by inverse modelling, Mater. Res. Soc. Symp. Proc. Vol. 1475 © 2012 Materials Research Society, doi: 10.1557/ opl.2012.601

Shao, H., Schuster, K., Sönnke, J. & Bräuer, V. (2008): EDZ development in indurated clay formations - In-situ borehole measurements and coupled HM-modelling, Physics and Chemistry of the Earth, 2008; Elsevier, doi: 10.1016 / j.pce.2008.10.031

Hyperspectral imaging for the characterization of clays: from data acquisition to mineralogical identification

Duccio Malinverni[1], Philippe Renard[2], Laurent Marguet[2], *Laurent Fasnacht*[2], Philip Brunner[2], Jens K. Becker[3]

[1] Laboratory of Statistical Biophysics, EPFL, Switzerland
[2] CHYN, University of Neuchâtel, Switzerland
[3] NAGRA, Hardstrasse 73, 5430 Wettingen, Switzerland

Hyperspectral imaging is a promising technique for the characterization of clay formations by non-invasive imaging. The method allows for rapid acquisition of surface data, with applications to mineralogical classification, and characterization of spatial distribution of minerals. The underlying paradigm is the acquisition of full reflectance spectra for each image pixel (in a given wavelength range). Comparison of the spectra with reference mineral spectra and unmixing algorithms allows mapping the mineralogical composition of the acquired samples.
Initially applied to airborne data, hyperspectral imaging was first used to perform surveys of land coverage and evolution, effectively discriminating different soil coverage [1]. More recently [2], it has been applied in ground based geological studies. The application of hyperspectral imaging to the identification of minerals at ground level presents new challenges, mainly due to the higher resolution of the acquired images, as well as the higher similarity between mineral spectra, compared to spectrally more heterogeneous media present in air borne data (e.g. discrimination of water, vegetation or rock coverage).
In the present study, we present a workflow for the acquisition and processing of geological data based on ground borne hyperspectral imaging. Our method is developed based on borehole samples and field measures of outcrops in the Opalinus Clay, one of the proposed host rocks for the storage of radioactive waste in Switzerland.

Images are acquired with a Specim SWIR camera, allowing the acquisition of 256 wavelengths per pixel, in the near infrared spectrum. The raw radiance data is converted in reflectance values by calibration of the measures based on the acquisition of a white reference using a 99% reflective white target (Spectralon) and measuring the baseline black level of the camera. This results in a reflectance spectrum for each image pixel. The samples and outcrops are illuminated using multiple halogen bulbs setups, in order to achieve a homogenous illumination of the target samples.
We propose a three-step process to classify the image pixels:

1. Image derived classes are extracted from the hyperspectral image. These classes capture the majority of the spectral variability of the data and represent the basis into which all image pixels are classified.
2. All pixels are subsequently assigned to one of these basis classes by a spectral similarity method.
3. Each basis class is decomposed as a superposition of pure spectra, obtained from a reference library of known reflectance spectra of pure minerals. This allows to estimate the total fraction of minerals present in the surface layer of the sample, as well as to assess the spatial distribution of the minerals (Figure 1).

The obtained mineralogical estimates on core samples are in reasonable agreement with geo-chemical determination techniques.

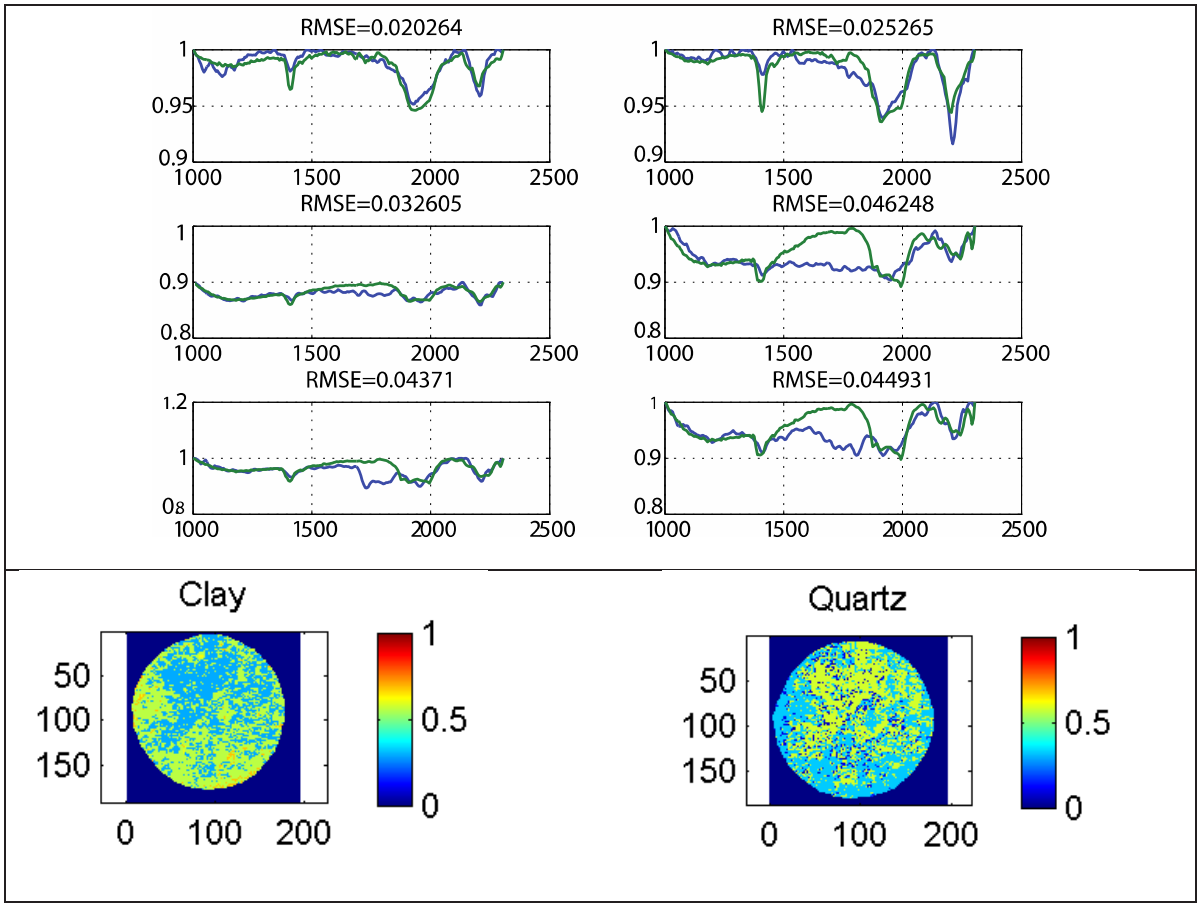


Fig. 1: Top - Decomposition of the base classes into 15 pure mineral spectra. Green: the classes spectra. Blue: the fit based by linear composition. Bottom - Spatial distribution of clay and quartz in a sample (as fraction of pixels).

Ongoing work on the application of this workflow on outcrop imaging presents promising results. New challenges, mainly with respect to the control of illumination in outcrop imaging, are currently being investigated. The characterization of spatial distribution of mineralogy in clay samples opens exciting possibilities to the three dimensional reconstruction of clay formations. With the characterization of multiple outcrops of apparent facies of a clay formation, the stochastic simulation of the body of the formation can be tackled using multiple point statistics simulations [3]. The reconstructed mineralogical distributions on the outcrops can be used as partial training images for the simulation of internal heterogeneity within clay formations. In particular, combining the spatial distribution of mineralogy with known physical properties of the composing minerals allows the construction of geological models of porosity and permeability, which is of crucial importance in the characterisation of potential waste disposal sites.

References

[1] Camps-valls, G., Tuia, D. & Bruzzone, L., 2014. Advances in hyperspectral image classification. IEEE Signal Processing Magazine.
[2] Kurz, T.H. et al., 2012. Close Range Hyperspectral Imaging Integrated with Terrestrial Lidar Scanning Applied To Rock Characterisation at Centimetre Scale. International Archives of the Photogrammetry, Remote Sensing and Spatial Information Sciences, XXXIX(September), pp.417–422.
[3] J. Straubhaar, P. Renard, G. Mariethoz, R. Froidevaux, O. Besson (2011) An Improved Parallel Multiple-Point Algorithm Using a List Approach. Math Geosci 43 (3), 305-328, DOI: 10.1007/s11004-011-9328-7

Pore distribution of saturated compacted montmorillonite using NMR relaxometry: effect of salt concentration

Takahiro Ohkubo[1], **Moe Ibaraki**[1], **Yukio Tachi**[2], **Yasuhiko Iwadate**[1]

1 Faculty of Engineering, Chiba University, 1-33 Yayoi-cho Inage-ku, Chiba 263-8522, Japan
2 Japan Atomic Energy Agency, Muramatsu 4-33, Tokai, Ibaraki, 319-1194, Japan

^{1}H NMR relaxometry was applied for investigation of pore structure in compacted saturated montmorillonite with different salt concentration. We used the same methodology to characterize pore structure saturated by water as our previous study,[1] thus, ^{1}H longitudinal relaxation time (T_1) distribution was mathematically obtained from recovery magnetization resulting from inversion recovery pulse sequence The compacted samples were prepared by use of Kunipia-F (Na-montmorillonite contents >98 wt%) without further purification, which was provided by Kunimine Industries Co., Ltd. The compaction of samples was achieved that the mass of powder Kunipa-F corresponding to desired dry density, ρ_d, was to transferred to a stainless cylinder (10 mm diameter), compacted to a height of 15 mm in an uniaxial press. Dry densities were 0.8 and 1.2 g/cm^3. Compacted samples were displaced to PCTFE (polychloro-trifluoroethylen) cylinders and they were sandwiched between ceramics filters to suppress expansion during saturation. The samples were saturated with pure water 0.05, 0.10, 0.50, and 1.0 mol/L NaCl concentration for 1 month at least. After saturation, both ends of a PCTFE cylinder were sealed with PCTFE screw caps to avoid water evaporation during NMR measurement. All NMR measurements were conducted at 23.5 MHz resonant frequency for protons The sample temperature for the NMR measurements was kept at 30°C. NMR signal intensity resulting from inversion recovery sequence was analyzed by a continuous relaxation distribution,

$$M(\infty) - M(\tau) = \int_0^\infty P(T_1) \exp\left(-\frac{\tau}{T_1}\right) dT_1$$

where, $M(\tau)$ was signal intensity measured at 40 different recovery time (τ), and $M(\infty)$ is FID signal (equivalent to a measurement at infinite τ), and $P(T_1)$ is T_1 distribution We assume three T_1 thresholds to identify hydrated space corresponding to 1-, 2-, and 3 hydrated layers, which are 1 2, 2.3, and 3.5 ms, respectively.[1] These thresholds were set up on the bases of XRD profile of saturated compacted montmorillonite with well controlled water contents.

Figure 1 shows T_1 distribution of compacted saturated montmorillonite with ρ_d =1.2 g/cm^3 saturated by different NaCl concentration, dotted vertical lines are guides for thresholds of 1-, 2-, and 3 hydrated layers. A single symmetrical peak was observed for all conditions. Its peak position slightly shifted to shorter relaxation times, when the NaCl concentration was increased. Population of water in different hydrated layer was estimated from summation of $P(T_1)$ in the range corresponding to 1-, 2-, and 3 hydrated layer. Figure 2 shows population of water in 1-, 2-, and 3 hydrated layers as a function of NaCl concentration. The threshold to discriminate between inter- and intra-layer (intrapartilce pore) water is 3 hydrated layer, which is questionable from existence of 4 hydrated layer revealed by modelling of X-ray profile[2], but we use this threshold to compare with our previous study. The amounts of water in 1- and intra-layer were negligible small for all conditions at ρ_d=1.2 g/cm^3. On the other hand, water in 2-hydrated layer was decreased instead of increment of water in 3-hydrated layer. It is expected that aggregation of negatively charged montmorillonite layers are shrunk with increasing NaCl concentration to compensate positively charged Na.

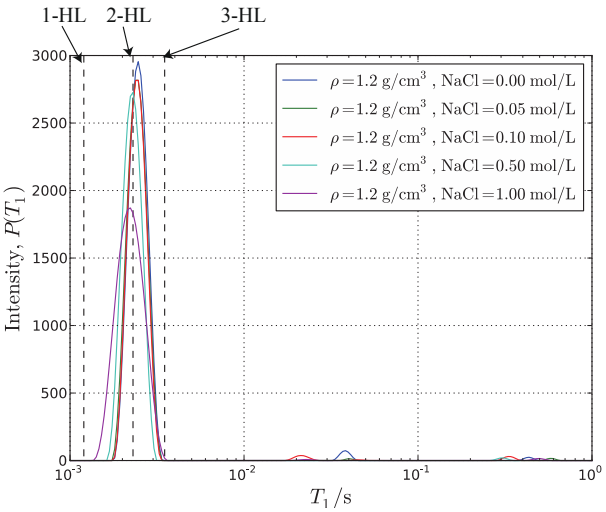


Figure 1 T_1 distributions of compacted saturated Kunipia-F. Broken lines of 1-, 2- and 3-HL mean thresholds of 1-, 2- and 3-hydrated layer, respectively.

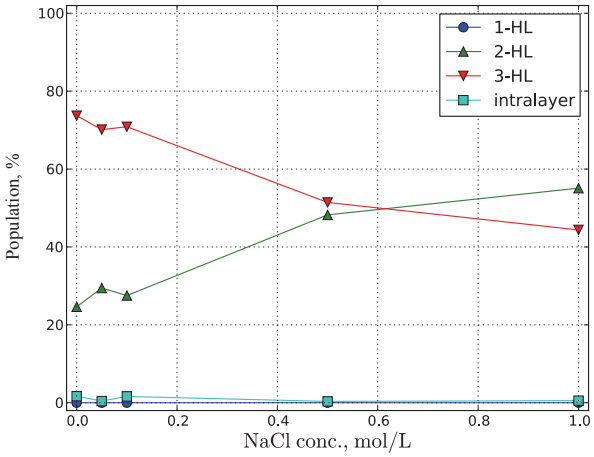


Figure 2 Proportion of 1-, 2, 3-hydrated layer and intralayer water.

*This study was partly funded by the Ministry of Economy, Trade and Industry of Japan.

References

1. T. Ohkubo H Kikuchi and M Yamaguchi, "An approach of NMR relaxometry for understanding water in saturated compacted bentonite" *Phys. Chem Earch* **33** S169-S176 (2008)
2. M. Holmboe, S Wold and M Jonsson, "Porosity investigation of compacted bentonite using XRD profile modelling" *J. Cont Hydro*. **128** 19-32 (2012)

Final repository for Denmark's low- and intermediate level radioactive waste.

Peter Gravesen *, **Bertel Nilsson, Stig A. Schack Petersen, Merete Binderup**
Geological Survey of Denmark and Greenland (GEUS), Øster Voldgade 10, 1350 Copenhagen, Denmark
* email address pg@geus.dk

The Danish Parliament decided in 2003 that the temporal disposal of the low- and intermediate level radioactive waste at the nuclear facilities at Risø should find another location for a final repository. The Danish radioactive waste must be stored on Danish land territory (exclusive Greenland) and must hold the entire existing radioactive waste, consisting of the waste from the decommissioning of the nuclear facilities at Risø, and the radioactive waste produced in Denmark from hospitals, universities and industry. The radioactive waste is estimated to a total amount of up to 10,000 m^3.

The Geological Survey of Denmark and Greenland, GEUS, is responsible for the geological studies of suitable areas for the repository. The task has been to locate and recognize non-fractured Quaternary meltwater clays, Tertiary clays or Precambrian bedrocks with low permeability which can isolate the radioactive waste from the surroundings the coming more than 300 years. Twenty two potential areas have been located and sequential reduced to the most favorable two locations taking into consideration geology, hydrogeology, nature protection and climate change conditions. Further detailed environmental and geology investigations is planned to be undertaken at the two potential localities from 2015. This study together with other studies of safe transport of the radioactive waste; an investigation of appropriate repository concepts, and a strategic environmental assessment carried out in 2014 will constitute the basis upon which the final decision can be taken by the Danish Parliament on repository concept and repository location. The final repository is planned to be established and in operation at the earliest 2020.

Applying the cosmogenic radionuclide dating technique to estimate rates of landscape development in the Campine area (NE Belgium): first results

K. Beerten[1,*] and V. Vanacker[2]

[1]Institute Environment-Health-Safety, Belgian Nuclear Research Centre (SCK•CEN), Boeretang 200, 2400 Mol, Belgium
[2]Georges Lemaître Centre for Earth and Climate Research, Université catholique de Louvain, 1348 Louvain-la-Neuve, Belgium
*Corresponding author: kbeerten@sckcen.be

High-level and/or long-lived radioactive waste is a major radiological hazard to man and environment. ONDRAF/NIRAS, the Belgian agency for radioactive waste management entitled to manage these materials in the long-term, currently investigates the safety and feasibility of geological disposal in poorly indurated plastic clays such as the Boom Clay and Ypresian clays.

An important requirement for geological formations hosting a repository for radioactive waste is sufficient depth to ensure isolation of the waste from potential receptors (humans, animals, plants) and to protect it from potential detrimental processes occurring at the surface, for a very long time period, up to 1 Ma. Over such long timescales, the repository depth and the thickness of the overburden may vary significantly due to various geodynamic processes.

The past evolution of the overburden and depth of a potential host formation is usually analysed using burial graphs, where the evolution of depth is depicted against time. These inaccurate graphs give insight in the past geological and geomorphological stability of a specific area when integrated alltogether. The Boom Clay burial graph in Mol has proven to be inaccurate for the last 1 Ma given the fact that a considerably amount of erosion, ca. 25 m, must have occurred since (Beerten et al., 2013). This implies that at present Boom Clay is not at its deepest burial depth at the Mol site, as has been suggested by previously compiled burial graphs (Mertens, 2005). In general, age control on burial and erosion events is poor, given the lack of datable material and/or the difficulty to quantify amounts and rates of erosion. The question arose whether the Pleistocene erosion event documented in the Mol area could be more accurately constrained in time.

East of the Mol site, the aforementioned erosion event is thought to be inhibited by an erosion-resistant landform, i.e., the Campine Plateau. It originally represented a river valley in which sediments from the river Rhine, and further to the south from the Meuse, were deposited and thus represents a classic case of relief inversion. Current estimates for the plateau age range between 0.6 Ma and 1 Ma, based on chronostratigraphical correlations with other fluvial sediments, either in the Roer Valley Graben or upstream in the Meuse Valley (see references in Beerten et al., 2013). The area west of the plateau, the region around the Mol site, has thus been lowered by 25 m since deposition of the fluvial sands on top of the plateau.

Cosmogenic radionuclides (CRN) allow us to quantify geomorphological processes over timespans up to the last 1 Ma. By measuring depth profiles of in-situ produced CRN (such as 10Be and 26Al) in fluvial terraces, we can constrain their age, the erosion since burial and the average erosion rate in the upstream catchment at that time. In this study, we use the CRN profile technique developed by Hancock et al. (1999) to constrain erosion of the terrace deposits given the current constraints on the

terrace age. Here we use 10Be ($t_{1/2}$ = 1.50 My) that is produced in situ at the surface, primarily via target nuclei bombardment by secondary cosmic ray particles.

The sampled sequence, reaching up to 3.6 m in thickness, consists of relatively coarse fluvial sand on top of the plateau, about 1-2 m below the crest. The upper 45 cm of the sequence is composed of another sediment type, namely aeolian sands, that cover the region as a blanket in a somewhat irregular manner (with respect to both shape and thickness). A large amount of sediment was taken for each sample, usually around 1.5 kg, in order to ensure a sufficient amount of the desired grain size fraction for cosmogenic radionuclide analyses. Ten samples were taken from which 7 were analysed.

The CRN results show that there is a clear decrease in 10Be concentration with depth. The concentrations range between $1.5 \times 10^5 \pm 0.02 \times 10^5$ at/g (atoms per gram) for the uppermost sample to $9.0 \times 10^4 \pm 0.2 \times 10^4$ at/g for the lowermost sample. Based on these samples, we can say that at 45 cm depth about $6.4 \pm 0.2 \times 10^4$ at/g of 10Be was produced in-situ after deposition of the fluvial sediments. As such, under the hypothesis of no erosion, we obtain an apparent exposure age of 21,500 ± 1,500 year. This is in strong contradiction with chronostratigraphical age estimates of the fluvial deposits that cover the Campine Plateau, that range between 0.6 Ma and 1 Ma. The logical explanation for this discrepancy is that the long-lasting assumption of no or limited erosion here is violated, and that a significant amount of erosion has taken place after deposition of the Sterksel Formation.

In order to check the hypothesis of significant post-depositional erosion at the sampling location, several scenarios combining the age of the Sterksel Formation and the erosion rate are put forward. Estimates of the 10Be concentration for the uppermost sample can thus be obtained for these different scenarios. Comparison with the measured 10Be concentration then allows to identify plausible scenarios that lead to an accurate description of the erosional history and age of the Campine Plateau. Given the current age estimates for the Campine Plateau (between 0.6 Ma and 1 Ma), an erosion rate of 10-20 m/Ma yields calculated 10Be concentrations that are in fair agreement with the measured ones.

So far, 7 out of 10 samples were analysed. In the next step, the three remaining samples will be analysed for their 10Be content, in order to confirm the observed concentration profile. Furthermore, these samples will be prepared for 26Al analysis as well. Combining 10Be and 26Al concentrations provides a better estimate of the burial age of the sediments, such that the scenarios derived in this study can be further constrained in order to accurately describe the erosional history of the area. We conclude that the CRN profile technique has proven to be a useful tool to determine the rate of geomorphological processes in the Campine area over the last 1 Ma.

References

Beerten, K., De Craen, M., Wouters, L., 2013. Patterns and estimates of post-Rupelian erosion in the Campine area, north-eastern Belgium. Physics and Chemistry of the Earth 64, 12-20.

Hancock, G.S., Anderson, B.S., Chadwick, O.A., Finkel, R.C. (2001). Dating fluvial terraces with 10Be and 26Al profiles: Application to the Wind River, Wyoming. Geomorphology 27: 41-60.

Mertens, J., 2005. Burial history of the two potential host formations (Boom Clay; Ypresian Clays). ONDRAF/NIRAS Technical note 2005-006.

Mineralogical, chemical and mechanical study of potential buffer and backfill materials from alternative buffer material (ABM) test packages 1 and 2

Kiviranta Leena[1], Kumpulainen Sirpa[1] and Korkeakoski Petri[2]

[1] B+Tech Oy, Laulukuja 4, 00420 Helsinki, Finland (sirpa.kumpulainen@btech.fi, leena.kiviranta@btech.fi)
[2] Posiva Oy, Olkiluoto, 27160 Eurajoki, Finland (petri.korkeakoski@posiva.fi)

In a large-scale alternative buffer material (ABM) experiment conducted by SKB (Swedish Nuclear Fuel and Waste Management Co) (Eng et al., 2007), three test packages with centrally located steel heaters surrounded by stacks of compacted bentonite rings of various clay materials were placed in boreholes in Äspö underground test laboratory in Sweden. The first parcel (ABM1) was saturated with Äspö groundwater and the heater was turned on simultaneously at the start of the saturation. Also the second parcel (ABM2) was saturated with Äspö groundwater, but in this case, heating was started after the bentonite was estimated to be fully saturated. The ABM1 package was left equilibrating for approximately 30 months in total and it was exposed to a maximum temperature of 130 °C for approximately 18 months before dismantling. The ABM2 package was left equilibrating for approximately 6.5 years in total. It was exposed to heating for a total of 5 years, of which approximately 3 – 4 years was at maximum temperature (130 °C) before dismantling the package.

Chemical, mineralogical and mechanical properties of the MX-80, Dep-CaN, Asha and Friedland clay samples from the ABM1 package were previously analysed and compared to reference samples by Kumpulainen and Kiviranta (2010, 2011). Chemical analyses (ICP-AES, C, CO_3, S, water soluble SO_4, Fe^{2+}/Fe^{3+}), exchangeable cation analyses, mineralogical analyses (XRD, FTIR) and selective CBD-extraction were used to determine changes in the chemistry and mineralogy of the ABM materials. Swelling pressure and hydraulic conductivity measurements were performed both for core-drilled samples and for ground and re-compacted samples.

Equilibration of exchangeable cation composition with Äspö groundwater was observed in all ABM1 samples (Kumpulainen and Kiviranta, 2011). Increases in soluble sulphate content in the vicinity of the heater were believed to originate from precipitation of sulphate salts. Increased total iron and CBD-extractable iron concentration was observed in a few ABM1 samples within a thin layer of material (a few mm) next to the heater. In addition, a slight decrease was observed in swelling pressure of some core-drilled ABM1 samples. However, when the material was ground, compacted and analyzed again, the swelling pressure was fully recovered. Svensson et al. (2011) performed similar tests for ABM1 package and observed similar decreases in swelling pressure, changes in exchangeable cation composition, and accumulation of iron near the heater. In addition, Svensson et al. (2011) observed increases in cation exchange capacity towards the heater and reduced failure strains. Further, Kaufhold et al. (2013) observed indications of the formation of trioctahedral clay minerals at the heater-bentonite contact in a few clays of the ABM1 package.

Almost the same set of materials were studied in the ABM2 package (MX80, Dep-CaN and Friedland clay) as compared to the ABM1 package in order to detect possible differences between the packages. Also, approximately the same set of tests, with minor improvements, was performed for the ABM2

samples in order to compare the results to ABM1 samples. The improvements included a more focused analysis of the parameters that were subject to change in the ABM1 test (based on studies by Kumpulainen and Kiviranta (2010, 2011), Svensson et al. (2011) and Kaufhold et al. (2013)), revised sampling and sampling frequency (e.g. thinner sample slices at the heater contact), and improved methodology (e.g. more detailed analyses of water soluble species, separation of clay fraction). As the three studied material samples from ABM2 package were located side by side at the bottom of the package, possible interactions between these materials were also studied.

Preliminary results from studies of the ABM2 samples indicate that similar, and in some cases more pronounced, changes occur in the ABM2 materials as compared to the ABM1 package. The analysis of samples from the ABM2 package is ongoing and will be finalized by the beginning of 2015.

References

Eng A., Nilsson U., Svensson D. 2007. Äspö Hard Rock Laboratory. Alternative Buffer Material. Installation report. IPR-07-15. Swedish Nuclear Fuel and Waste Management Co, Stockholm, Sweden.

Kaufhold S., Dohrmann R., Sandén T., Sellin P., Svensson D. 2013. Mineralogical investigations of the first package of the alternative buffer material test – I. Alteration of bentonites. Clay Minerals, 48, 199-213.

Kumpulainen S., Kiviranta L. 2010. Mineralogical and chemical characterization of various bentonite and smectite-rich clay materials. Posiva Working report 2010-52. Posiva Oy, Olkiluoto, Finland.

Kumpulainen S., Kiviranta L. 2011. Mineralogical, chemical and physical study of potential buffer and backfill materials from ABM test package 1. Posiva Working report 2011-41. Posiva Oy, Olkiluoto, Finland.

Hyperspectral imaging for the millimetre-scale characterization of variability in clays

T. H. Kurz[1], S. J. Buckley[1], *J. K. Becker*[2]

[1] Uni Research CIPR, Allégaten 41, N-5007 Bergen, Norway
[2] Nagra, Hardstrasse 73, CH-5430 Wettingen, Switzerland, jens.becker@nagra.ch

Hyperspectral imaging is an established technique for remotely analysing the mineral content of rock surfaces. However, most applications have used airborne or spaceborne acquisition systems, such as in mineral exploration at regional scales, where pixel sizes on the ground cover relatively large areas. Recently, new technology has become available that allows applications from the ground, of exposed rock outcrops, cut tunnels and in laboratory settings. Consequently, detailed analysis of mineral content and distribution is now possible in applications addressing clay characterisation. In this research, we present mm-scale hyperspectral image analysis of drill cores taken from an underground laboratory (Mont Terri, Switzerland). The core samples were extracted from the Opalinus Clay, one of the proposed host rocks for the disposal of radioactive wastes in Switzerland. The data acquisition, processing and results of the method are discussed, as well as the use of the identified mineral end-members for improving understanding of larger scale (hyperspectral scans of a cut tunnel face in the same host rock; 5 m-scale) clay variability.

Four cores were taken from the TT Niche in the Mont Terri underground laboratory, and these were cut to give a flat surface. A scanning system covering the short-wave infrared (SWIR) region of the electromagnetic spectrum was chosen to allow identification of different clay types, images were captured with a pixel size of ca. one millimetre. The spectral sampling was 5 nm across 240 bands in the SWIR wavelengths, allowing subtle material differences to be evaluated.

Data pre-processing followed a general workflow of 1) correction and calibration of the measured reflectance to achieve high quality reflectance input; 2) data volume and noise reduction; 3) variability analysis. Subsequently, the properties of profiles through the wavelength measurements (spectral curves) were inspected and processed to identify end-members for the mineralogy present in the core sections. The ultimate goal of this stage is a set of unique end-members, which can be then input to classification schemes to map and quantify the content and distribution of minerals in the scanned core surfaces. As the grain size of the clay minerals is still several orders of magnitude finer than the resolution of the hyperspectral images, each pixel is likely to represent a mixture of different minerals. To address this, the spectral end-members were compared with supplementary analysis methods, as well as using sub-pixel classification algorithms. X-ray fluorescence (XRF) and X-ray diffraction (XRD) were both carried out on samples taken at points in the hyperspectral data indicating representative mineral differences.

Images of the cut TT Niche were acquired, from several ranges (1m and 12 m). As scanning conditions are less controlled than in the laboratory core scanning setting, spectral data are influenced by e.g. lighting conditions and adjacency effects, and spatial resolution is lower meaning that in longer range images material mixture effects are more apparent, and the end-member identification more uncertain. The end-members from the cut tunnel face were compared to the spectral data from the core imagery, as well the XRF and XRD results.

Even though the Opalinus Clay is considered as relatively homogenous, the hyperspectral imaging identifies mineral differentiation on a small scale (Fig. 1). The end-member spectra show diagnostic spectral properties which allow identifying minerals such as kaolinite, illite, calcite, quartz and feldspar. These mineral compositions of the end-members have been confirmed by the XRD analysis. As a final result, hyperspectral classifications allow mapping the distribution of different clay types such as kaolinite, illite, carbonate and quartz-feldspar dominated clay.

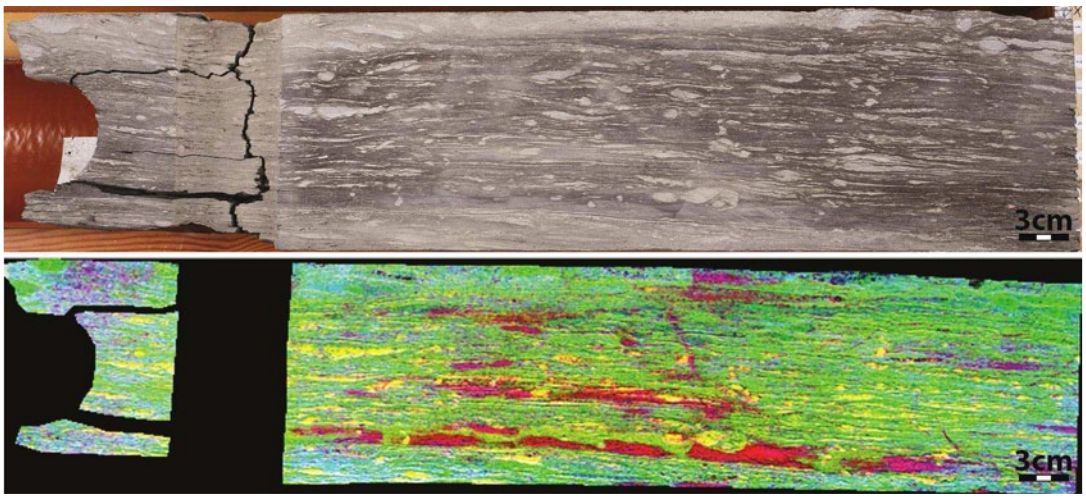


Fig. 1. Conventional digital image (above) and hyperspectral variability analysis (below) of a cut core.

The results suggest that hyperspectral imaging can be used to quickly and efficiently identify the mineral composition of a rock, even of clays, and its variability. One of the main advantages of this method is that, due to the nature of the measurement, 2D areas at different scales (mm to m) can be processed. This measurement method is also a great tool to understand the correlation between mineralogical and geophysical parameters across multiple scales and spatial extents, if the necessary geophysical parameters exist, and for the population of geostatistical models at the repository scale.

Microbial diversity studies of Spanish bentonites: Comparison of clone libraries and Illumina-sequencing based methods

***M.L. Merroun*[1],** M. López-Fernández[1], I. Sánchez-Castro[1], R. Vargas-Vílchez[2], A. Cherkouk[3]

[1]Department of Microbiology, University of Granada, Spain,
[2]Laboratory of Microbial Ecology and Technology, University of Gent, Belgium
[3]Institute of Resource Ecology, Helmholtz-Zentrum Dresden Rossendorf, Dresden, Germany

The long-term disposal of radioactive wastes in a deep geological repository (DGR) is the accepted international solution for the treatment and management of these special residues, mainly produced by the nuclear energy industry. The present work describes the structure and composition of microbial communities in Spanish bentonites, considered as natural analogue of the bentonite-engineered barrier, by two different culture- independent approaches based on the 16S ribosomal RNA gene analysis: clone libraries and Illumina sequencing platform. These two techniques showed a high microbial diversity of the bentonite samples studied. The microbial community was dominated by Proteobacteria and Bacteroidetes, and contained bacteria potentially involved in the possible microbial deterioration processes of DGR safety case including transformations of clay minerals, mobilization/immobilization of radionuclides, etc. When analysing all of the datasets from the samples *en masse* we observed high similarity between the clone libraries and Illumina datasets in terms of dominant groups and the community profiles at the phylum level, while significant differences in the proportion of some phyla and class between the samples were observed. Illumina-sequencing was more sensitive to Bacteroidetes, while in the case of Gammaproteobacteria class, the traditional clone library was much more efficient. The structure and composition of the microbial communities present in the bentonites samples will be discussed in term of geochemistry and mineralogy of the clays, and also on their impact in the safety case of DGR. The results obtained indicate that the combination of both molecular techniques provide an accurate and boarder view of the microbial communities present in complex environmental samples.

Understanding the swelling behavior of smectite as a function of temperature and humidity

Anja M. Schleicher, ***Ben A. van der Pluijm***

Department of Earth and Environmental Sciences, University of Michigan, Ann Arbor, MI 48109, USA

Investigating the nature of clay minerals is fundamental to understanding rock alteration, with direct implications for the nuclear waste deposit industry. Especially the sensitivity of smectite clay minerals can provide information about the temperature history and processes in near-surface environments. Using a range of analytical methods, which include X-ray diffractometry with an attached humidity chamber or high-temperature stage, as well as X-ray goniometry, elemental analysis and electron microscopy (SEM/TEM), we determined the properties of smectite clay minerals in several borehole samples from the Japan Trench subduction zone, to assess the extent of smectitic phases in space and depth, fabric development, and, especially, the swelling characteristics of smectitic phases.

In order to investigate the changing properties of smectite, a humidity chamber connected to an X-ray diffractometer allows determining the in-situ absorption of water onto and/or into the crystal structure of smectite by direct measurement of the hydration state at controlled fluid and temperature conditions. Based on experiments on clay-rich samples from drill core of the Nankai Trough in Japan, we determined that smectite is abundant and forms easily at temperatures occurring at near-surface conditions. We observe that smectite is stable at temperatures where the rocks were situated, and that swelling is not significantly affected by alteration due to temperatures up to 75°C/90°C. This detailed characterization of the hydration state of smectite in its original setting is critical for the understanding of clay-fluid interaction and mechanical properties during crustal displacement.

In a second step, using a high temperature stage connected to an X-ray diffractometer, the behavior of smectite during fast (5 minutes) and slow (5 hours) heating sequences was examined in samples from the Japan Trench. Pelagic-sourced smectite is the most abundant clay mineral that is incorporated into a fault zone at ~820 mbsf. Eight measurement sets were analyzed, taken at 25° C pre-heating, increasing maximum temperatures in the range 50-220° C, and 25° C post-heating. We observe that (i) both slow and fast heating causes reduction of water interlayers in smectite between 50-200°C, with a delay of water-release during quick heating at temperatures up to 150° C, (ii) smectite recovers more quickly to the original hydration state after fast heating than slow heating between 50-150°C, and (iii) non-recoverable collapse of all smectite occurs at ~200°C, for fast and slow heating, respectively.

Based on the results with the humidity chamber and the high-temperature stage, we conclude that if smectite is present in a sample, distributed heating can be calibrated. In case of the problem concerning claystone as nuclear waste disposal, heat generated by nuclear waste does not cause the formation temperature to exceed a maximum of 150- 200° C, because of the possible changes this may cause to the physical properties of clay minerals. Temperature related research on clay minerals is an important aspect and needs to be taken into consideration in nuclear waste storage investigations.

Determination of water retention curve on Czech bentonite

Marketa Levorova, **Lucie Hausmannova, Jiri Svoboda**

Czech Technical University in Prague, Faculty of Civil Engineering, Centre of Experimental Geotechnics, Thakurova 7, 166 29 Prague 6

Water retention curve (WRC) is the relationship between the water content (θ) and the soil water potential (ψ). This characteristic is one of the essential characteristics governing water and gas transfer under unsaturated conditions. Moreover on the basis of this relationship the relative permeability for gas and water is possible to predict for different materials. As such it is commonly used in many engineering industries occupied with geotechnics and soil science.

In many repository concepts the swelling and non-swelling clay based materials are used as sealing. The WRC is fundamental relation to estimate the evolution of the water content in the barrier (especially when swelling clays are used) and prediction of the time needed for full saturation (Villar, 2005).

This paper describes procedure and results of the determination of WRC of Czech bentonite named B75. It is industrially dried and milled natural Ca-Mg bentonite mainly from the North Bohemian mining sites. For the retention curve determinations of bentonites is necessary to cover a large range of suction. Measurement for bentonite is usually done in range of suction from 100kPa to 300MPa. More than one method of determining individual WRC points is usually used to cover of the whole range. Following methods are usually used to determining WRC for bentonites: vapour equilibrium method (salt solution method and sensor method), osmotic method, filter paper method and method based on grain size distribution. The results obtained from the different methods of determining of points WRC are compatible (Noguchi 2011; Villar 2005). In this project the first mentioned method, which covers the widest range of suction, was used for a basic description of the WRC.

The WRC evaluation is made on powder and compacted samples of bentonite. The specimens of loose powder bentonite were dispersed on the Petri dishes; the specimens form compacted material were placed inside cells from stainless steel with perforated covers in order to prevent swelling and volumetric changes of samples.

Both types of specimens were then placed in the desiccators with salt solutions that control the relative humidity of the atmosphere of desiccators. Once the weight of samples is stabilised the water content of samples is evaluated. The following salts are used in the measurement of WRC points: CuSO4.5H2O, NaCl, NaNO2, Mg(NO3)2, K2CO3, LiCl. The WRC points are determined in both a saturation path as well in a desaturation path – in total 11 equilibrium points is obtained for each sample and suction range from 10 to 160MPa covered.

The authors would like to express their thanks for assistance provided by project GA14-19655S which is funded by the Czech Science Foundation (GACR).

References

VILLAR, Maria Victoria a A. LLORET. Determination of water retention curves of two bentonites at high temperature. *Advanced experimental unsaturated soil mechanics*. London: Taylor&Francis Group, 2005, s. 77-82. ISBN 0415383374.

NOGUCHI, T., J. MENDES a D.G. TOLL Comparison of soil water retention curves obtained by filter paper capacity suction probe and pressure plate. EDITORS, Apiniti Jotisankasa. *Unsaturated soils: theory and practice : proceedings of the 5th Asia-Pacific Conference on Unsaturated Soils, Pattaya, Thailand, 14-16 November 2011*. Bangkok, Thailand: Geotechnical Engineering Research and Development Centre, Department of Civil Engineering, Faculty of Engineering, Kasetsart University, 2012, s. 409-414. ISBN 9786167522777.

Clay minerals distribution, textural properties and nano-porosities in hydrothermal dolomites

Asefeh Golreihan, **Rudy Swennen**

Geodynamics and Geofluids Research Group, Geology Section, Department of Earth and Environmental Sciences, KU Leuven, Celestijnenlaan 200E, 3001 Heverlee – Belgium
asefeh.golreihan@ees.kuleuven.be, rudy.swennen@ees.kuleuven.be

Authigenic clay minerals have been reported in several studies of structurally controlled hydrothermal dolomites (HTD). Since several HTD bodies form petroleum reservoirs worldwide, understanding reservoir properties of these hydrothermal dolomites is fundamental. This issue is not possible without considering clay minerals as intercrystalline pore filling minerals. The formation of authigenic clay minerals even in small volumes (less than 2%) in the pore space can remarkably influence reservoir properties of these carbonates. Clays have variable mineralogy, textural properties, and micro- nano porosity in studied samples.
In the current study Quantitative XRD analysis on bulk and the clay fraction together with FEG-EPMA, SEM and micro-CT are used to investigate mineralogy, identify and quantify mineral micro and nano-porosity and geochemistry.
Clay minerals in the studied samples are mainly chlorite and kaolinite. Illite and several mixed layer clay minerals (corrensite, chlorite-smectite and smectite-illite) occur in small quantities. Iron (hydr) oxides as well as organic matter and some non-carbonate constituents present in the samples. Based on the current examinations, clay rich dolomites are formed in different paragenetic phases of dolomitization from clay- lime cave filling precursors. Micro and nano porosities in samples varie based on composition, structure, pressure, and compaction history.

Variations in microbial community composition in piezometer installations in Boom Clay

Katinka Wouters[1], **Mohamed Mysara**[1,2], **Hugo Moors**[1], **Natalie Leys**[1]

[1] Unit of Microbiology, Belgian Nuclear Research Centre (SCK•CEN), Mol, Belgium
[2] Department of Bioscience Engineering, Vrije Universiteit Brussel, Brussels, Belgium

Introduction

The Boom Clay layer is presently investigated as a potential host rock for geodisposal of nuclear waste in Belgium. The HADES underground research facility (EIG Euridice c/o SCK•CEN), located at 230 m depth under the site of SCK•CEN (Mol, Belgium), provides access to this clay layer for *in situ* geological, geochemical and geomicrobiological testing. In order to predict how microbiology will affect the biogeochemical processes in a disposal scenario, the resident microbial communities of Boom Clay and the man-made structures within this clay are being characterised.

Objectives and Methods

In this study, water samples were collected from Boom Clay via various existing HADES piezometers (diverse in depth, orientation, location, age, materials used, etc., Table 1), including some of the PRACLAY piezometers used for geochemical follow-up along the large scale heater test (Fig. 1). Microbial cells from these samples were concentrated on a 0.45 μm filter membrane, followed by DNA extraction, PCR amplification of the V1-V3 region of bacterial 16S rDNA, automated sequencing and an in-house developed bio-informatics analysis.

The aim was to assess differences or shared features of the microbial communities residing in piezometer boreholes, supplementary to the previous screening of a single, vertical piezometer [1], and to correlate variations to geochemical analyses.

Results

Along the five piezometers, bacterial communities of the filters within one piezometer seem more similar to each other compared to those in other piezometers, despite a variety of filter materials (TD-116W) or Boom Clay layers sampled (TD-11D, [1]) within one piezometer. While the boreholes of piezometers TD-116W and TD-116E seem highly enriched in one family of *Betaproteobacteria* (*Rhodocyclaceae*), the other piezometers, TD-11D, CG-35E and CG30E, seem to balance dominance between members of the *Chloroflexi, Proteobacteria, Actinobacteria, Firmicutes, Bacteroidetes* and *Chlorobi*, although in different ratios and with variations in overall diversity (Fig. 2 and Table 2).

Conclusion

The observed variability in bacterial community composition suggests enrichment of certain members of the community in preference, according to the engineering properties and characteristics of the piezometer installation, above the geology of clay layer sampled or the piezometer materials used. Although such local enriched microbial community might not be representative for the total (engineered) clay environment, it shows that technical installations (such as piezometers) can introduce and promote local variations in the clay environment and the associated bioprocesses. Further studies of other piezometers and of clay samples are needed, to pinpoint the source bacterial community underlying *in situ* enrichment, to unravel the mechanism that shapes such microbial community in different repository conditions and to outline the relevance of the (dominant) microbial classes in defining borehole water (and gas) chemistry.

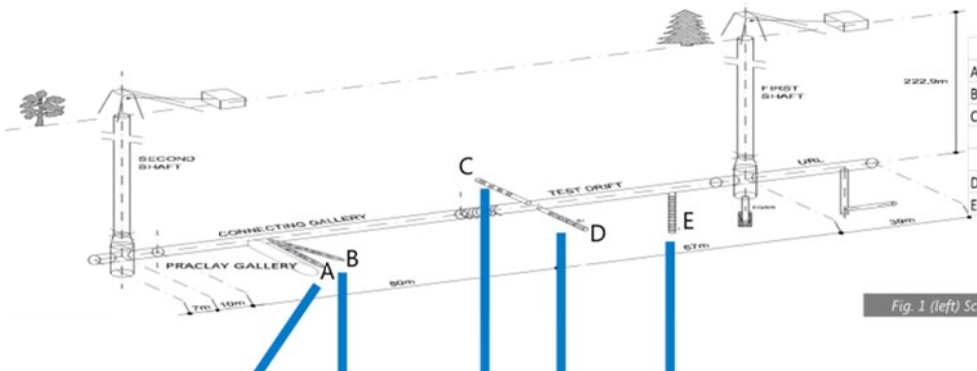


Table 1 Properties of the five piezometers (A-E) sampled for microbiology

	Piezometer	Tubing	Filter composition	Number of filters	Filter Pore Size	Installation
A	CG-35E	Stainless Steel	Krebsöge	3	7-16 µm	2007
B	CG-30E	Stainless Steel	Krebsöge	3	7-16 µm	2007
C	TD-116W	PEEK	Carbon	1	90 µm	2000
			Glass	1	10-16 µm	2000
			Shumatherm	1	60 µm	2000
D	TD-116E	Stainless Steel	Krebsöge	4 (of which 1 sampled)	7-16 µm	1999
E	TD-11D	Nylon	Shumatherm	12 (of which 6 analyzed)	60 µm	2001

Fig. 1 (left) Schematic view of the HADES URF, indicating position and orientation of five piezometers (A-E)

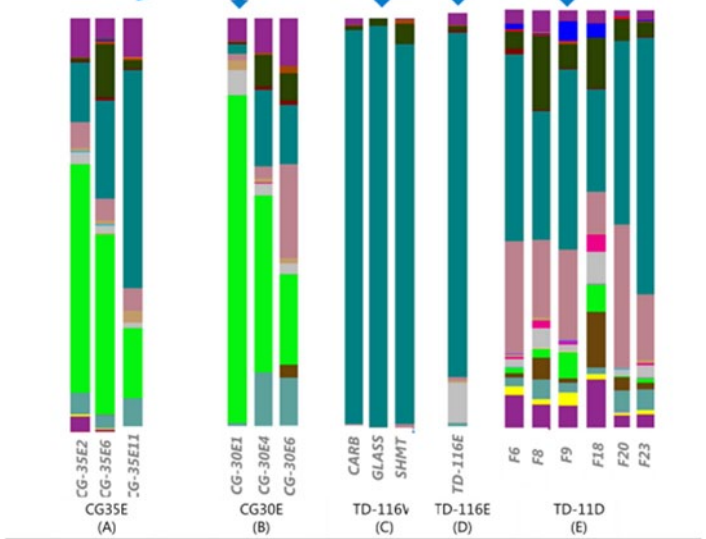


Fig. 2 Composition of bacterial communities in each filter of the five piezometers (legend to the right)

Phylum	Class	CG-35E (3)	CG-30E (3)	TD-116W (3)	TD-116E (1)	TD-11D (6)
unclassified	unclassified					
unclassified	unclassified	5.1 - 9.3 %	5.5 - 11.4 %	0.1 - 1.6 %	2.80%	1.5 - 5.1 %
Verrucomicrobia	Subdivision3					
Verrucomicrobia	Opitutae					
Tenericutes	Mollicutes					
Spirochaetes	Spirochaetes					
Proteobacteria	unclassified					
Proteobacteria	Gammaproteobacteria					
Proteobacteria	Deltaproteobacteria					
Proteobacteria	Betaproteobacteria	21.2 - 60.1 %	4.1 - 43.4 %	96.5 - 97.6 %	84.10%	46.4 - 83 %
Proteobacteria	Alphaproteobacteria					
Gemmatimonadetes	Gemmatimonadetes					
Fusobacteria	Fusobacteria					
Firmicutes	unclassified					
Firmicutes	Negativicutes					
Firmicutes	Erysipelotrichia					
Firmicutes	Clostridia	1.2 - 3.0 %	2.5 - 6 %	0.1 - 0.7 %	9.60%	1.5 - 7.7 %
Firmicutes	Bacillus					
Deinococcus-Thermus	Deinococci					
Cyanobacteria	Chloroplast					
Chloroflexi	unclassified					
Chloroflexi	Thermomicrobia					
Chloroflexi	Dehalococcoidetes					
Chloroflexi	Anaerolineae	16.9 - 55.3 %	21.9 - 79.2 %	0.0 -0.0 %	0.00%	0.4 - 6.5 %
Chlorobi	unclassified					
Chlorobi	Ignavibacteria	0.0 - 0.1 %	0.0 - 3.1 %	0.0 - 0.1 %	0.00%	0.9 - 13.2 %
Bacteroidetes	unclassified					
Bacteroidetes	Sphingobacteria					
Bacteroidetes	Flavobacteria	3.3 - 7.9 %	1.5 - 13.9 %	0.0 - 0.9 %	1.10%	3.0 - 6.0 %
Bacteroidetes	Bacteroidia					
Actinobacteria	Actinobacteria	0.4 - 3.8 %	0.4 - 0.9 %	0.0 - 0.1 %	0.90%	3.4 - 11.9 %
Acidobacteria	Acidobacteria_Gp7					
Acidobacteria	Acidobacteria_Gp6					
Acidobacteria	Acidobacteria_Gp3					
Acidobacteria	Acidobacteria_Gp16					

Table 2 (above) Range of percentual representations of bacterial phyla in the five piezometer boreholes

Optimization of pore network characterization of compacted clay materials by TEM and FIB/SEM imaging

Stéphane Gaboreau[a, 1], Jean-Charles Robinet[b], Dimitri Prêt[c]

[a] BRGM, Environment and Process Division, 3, avenue Claude Guillemin, F-45060 Orléans Cedex 2, France
[b] Andra, 1/7 rue Jean Monnet, Parc de la Croix Blanche, 92298 Châtenay-Malabry Cedex, France
[c] UMR CNRS 7285 IC2MP, Université de Poitiers, Equipe HydrASA, rue Albert Turpain, Bat B8, 86022 Poitiers, France

The transport properties of clay-rocks are controlled by their complex pore network and the reactive and negatively charged clay mineral surfaces. The Pore Size Distribution (PSD) and the geometrical features of the pore network constitute key parameters governing the migration of solvate elements through the clay formations. Upon the last few years, some works have contributed to improve the knowledge of some clay-rich rock pore networks by using innovative microscopic imaging techniques (FIB-nt, BIB, X-ray…). Even if these techniques allow imaging the mesostructure scale organization of clay-rocks and clay materials, these studies have however highlighted several limitations to fully represent the spatial distribution of pores in terms of PSD, geometry and connectivity. In the present work, we demonstrate that a multi-scale characterization of pore network of clay materials based on FIB-nt and TEM techniques is feasible and could be robustly achieved for providing some useful input data in order to assess a future modeling task. The studied material was a compacted clay materials composed of illite, a non-swelling mineral. Illite was chosen in order to represent an analog system mimicking the clay matrix of the clay-rocks. This compacted clay plug allows working on homogeneous system with a controlled porosity, facilitating the comparison between different methods. All the techniques used in the present work whether bulk or microscopic methods show that all results converge to a similar and entire PSD (figure 1). The main improvement of this work was to demonstrate how the usual resolution limitations and the data handling of the FIB-nt techniques could be improved in order to recognize a fully connected pore network.

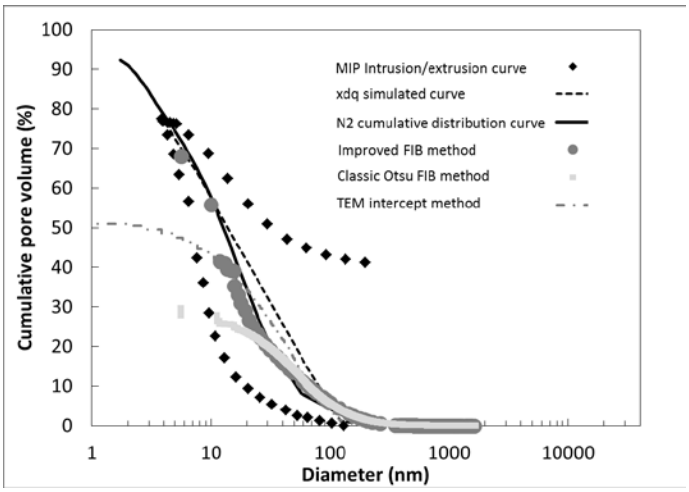


Figure 1 – Pore size distribution (PSD) of the compacted IDP. PSD calculated with the different methods (bulk and microscopic) are illustrating. The PSD calculated from the 3D FIB-nt volume is given according the two discussed method (the present work and Otsu thresholding).

Bentonite Blocks Manufacturing by Uniaxial and Isostatic Methods for Engineering Barrier System Components

Holt, Erika[1], Ritola, Jouko[1], Peura, Jutta[1], Sjöblom, Ville[1], Haapala, Keijo[2]

1) VTT Technical Research Centre of Finland, Espoo, Finland
2) Posiva, Eurajoki, Finland

Introduction

Posiva Oy is currently planning the ONKALO facility, a spent nuclear fuel repository in Olkiluoto. The repository will consist of deposition holes deep in the bedrock where the copper canisters containing the spent fuel will be surrounded by a bentonite buffer. The KBS-3V design calls for the horizontal deposition tunnels containing the vertical deposition buffer and canister holes to be backfilled with highly compacted bentonite blocks. Compacted bentonite pellets are also used around the circumference of both the buffer and backfill, to ensure thermal and hydro stability with the surrounding bedrock. The function of the bentonite buffer and backfill materials is to restrict groundwater flow and to protect the canister. The bentonite components of the Engineering Barrier System (EBS) have to fulfil certain density and homogeneity requirements to ensure safe functional performance for thousands of years.

Bentonite components used in the EBS of a nuclear waste repository can be manufactured using various methods. The size of the buffer blocks in the final repository will be 1650 mm in diameter and at least 400 mm in height. In some cases ring-shaped blocks are produced to surround the canister. The dimensions of the backfill blocks are specified to be 550 mm in length, 470 mm in width and 330 mm in height. Manufacturing tolerances are typically around 1 mm. The manufacturing of these components has been developed in Finland during the past five years, from small-scale laboratory pressing through full-scale factory production. This presentation summarizes some of the key results from the component manufacturing process, with specific attention to the impact of bentonite clay parameters on the initial state of the manufactured components.

Methods and material properties

There are two main methods of producing bentonite buffer or backfill components: by uniaxial or isostatic compression. In the *uniaxial method*, bentonite powder is poured into a rigid form and a piston is pushed by a pressing device so the bentonite is compacted at a certain pressure along the vertical axis. In the *isostatic method*, bentonite is enclosed in a flexible membrane surrounded by a pressurized liquid medium, generating simultaneous compression from all directions. Bentonite pellets are typically roller-compacted or extrusion pressed to achieve a target density.

Posiva's reference material for buffer blocks is MX-80 type bentonite, having a water content of 17 % ±1 %. The target density of the saturated buffer is 2000 kg/m^3 ±50 kg/m^3 in a deposition hole. For the backfill blocks the reference material is Friedland clay having a target dry density of 2030 ± 40kg/m^3 at 10 % water content. The reference material for backfill blocks is Friedland clay, with the alternative being Ibeco RWC-BF. Pellets can be either MX-80 or lower-quality bentonite, and the water content is usually similar to the levels used in the corresponding buffer or backfill. In all manufacturing cases, the loading level and rate are adjusted to obtain the best products. For instance, in uniaxial compaction the pressure is often in the range of 25-100 MPa. Removal of the blocks from moulds can prove challenging, especially for uniaxial when trying to avoid the use of lubricants or coatings. The components must be homogenous, with minimal cracks or defects. The tensile strength capacity needs to be sufficient to handle vacuum lifting during handling and emplacement. Large components made by isostatic compressions are typically manufactured with 5-10% greater dimensions, then machined down by dry-cutting and polishing to obtain the actual specific dimensions.

Upscaling and manufactory

Manufacturing of buffer and block components by the isostatic and uniaxial compression methods have been studied and developed by Posiva at VTT for over 5 years. The development of the manufacturing technique and testing methods has advanced from small-scale laboratory scale blocks to full scale factory blocks in both methods. Modeling has been done to evaluate the compaction process and optimal mould designs.

The results have shown that during block compaction there is a clear relation between density and bentonite water content, at all pressure levels. The density is often independent of the size or shape of the compressed blocks. During isostatic pressing, the filling with vibration results in about 20% higher initial bentonite density, which can be helpful for achieving certain dimensions. For both uniaxial and isostatic large scale blocks, there has been very little difference in properties (such as strength, bulk density and water content) across the block when the optimal water content has been used. Non-destructive testing, such as X-ray and ultrasound, has not proven sufficient to detect variations in properties of the high compacted blocks.

During manufacturing of pellets, it was possible to achieve uniform pellets with sufficient crush strength and abrasion resistance, which are important parameters needed to avoid breaking during placement. It was possible to produce pellets with higher water contents, for instance to 21% with MX-80, when making extrusion pellets compared to roller-compaction. The amount of void space between pellets, when placed as gap filling, was sufficient to allow for rapid water infiltration during artificial wetting.

During manufacturing and storage of EBS components, the relative humidity of the production environment has proven to be important. Raw materials and compacted samples must be protected against moisture at all stages. The suitable relative humidity has been found to be 60-75% to prevent defects in the blocks.

The results of these studies are being used in Posiva's buffer and backfill design work and in preparation for full-scale in-situ demonstrations at ONKALO.

References

Holt, Erika. Peura, Jutta. (2011). Buffer component manufacturing by uniaxial compression method – Small scale. Posiva Working report 2011-42. 91 p.

Holt, Erika. Sjöblom, Ville. Fortino, Stefania. Koskinen, Ville. (2014). Uniaxial Compression of Bentonite Backfill Blocks, from Lab to Factory Scale. Posiva Working Report 2014-xx, 105 p. (draft)

Laaksonen, Rainer. (2010). MANU – Isostatic compression of buffer blocks – Small scale. Posiva Working Report 2009-134. 40 p.

Marjavaara, Pieti. Holt, Erika. Sjöblom, Ville. (2013). Customized Bentonite Pellets: Manufacturing, Performance and Gap Filling Properties. Posiva Working Report 2012-62, 76 p.

Ritola, Jouko. Pyy, Erkko. (2012). Isostatic compression of buffer blocks – Middle scale. Posiva Working Report 2011-62. 61 p.

Ritola, Jouko. Sjöblom, Ville. (2014). Manufacturing of Buffer Components by Isostatic Compression Method. Posiva Working Report 2014-xx (draft).

Geometry of the Callovo-Oxfordian claystone formation from depth-converted 3D-high resolution seismic data: modeling and spatial uncertainty

Béatrice Yven (Andra), **Jean-Baptiste Mathieu (KIDOVA), Michel Garcia (KIDOVA)**

Andra 1/7 Rue Jean Monnet, 92298 Châtenay-Malabry Cedex, France
KIDOVA, 155, avenue R. Salengro, 92370 Chaville, France

The research conducted by the French Radioactive Waste Management Agency over the past 20 years has served to demonstrate the feasibility and safety of deep disposal of high-level wastes and intermediate-level long-lived wastes. Today, this research is helping prepare for industrial disposal centre's construction and operation. The Callovo-Oxfordian claystones (COX) have been selected as a potential host formation. Therefore, the geometry of this formation is required to position the repository, design its shape and numerically simulate its behaviour.

This article will present the structural model of the COX formation, estimated from a depth-converted 3D-high resolution seismic cube acquired in the contemplated repository area (ZIRA). As no borehole is located inside this area, the calibration process was performed using three 2D-seismic lines passing through the 3D seismic cube and three boreholes located 2-3km away from the ZIRA. Three strong reflection events were picked on the seismic data within the COX. The deepest event is correlated with the base of the COX (LS0), whereas the two other events represent the limits of the third-order depositional sequences (LS1, LS2) (Figure 1). The primary aim of structural modelling was to estimate the top of the claystone formation (SNC). Furthermore, the limits of the main petrophysical units, defined in a previous study from borehole log data and cores [1], also had to be estimated within the ZIRA. The petrophysical units are the Clayey unit (UA), the Transitional unit (UT) and the silto-carbonated unit (USC) as shown in Figure 1. They are essential to better understand and characterize the spatial variability of rock properties within the COX formation. The associated article of Garcia *et al*. (2015) shows how the petrophysical units were taken into account to quantify the spatial variability of rocks properties within the seismic cube [2].

The estimation of the different key horizons relies on marker data from boreholes where all the horizons are identified. They were used to establish relationships between non-seismic and seismic (reflecting) horizons in terms of (smoothed) bivariate histograms between either unit thicknesses or horizon elevations (Figure 2). The bivariate histograms were then used to estimate and quantify the spatial uncertainty of the non-seismic horizons within the ZIRA. A seismic facies analysis was eventually carried out to verify that the estimated horizons were matching the facies changes. This analysis proved to be efficient to confirm the major transitions from the Dogger to the COX, and from the COX to the Oxfordian limestones platform. As expected, however, it showed that there is no clear transition between the two units UA2 and UA3 at the seismic scale within the ZIRA (Figure 1). Figure 3 represents the elevation map of the base (LS0) and thickness of the COX formation in the ZIRA. These results confirm that the thickness increases in the north-east direction and that the dip is low (1°) and oriented nord-west.

An important challenge of this study was to quantify spatial uncertainty associated with estimated horizons. The article will detail the method used to quantify overall spatial uncertainty and will present results for different estimated horizons.

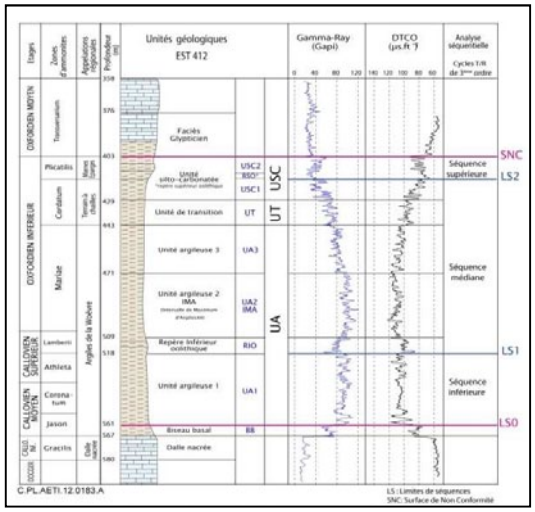


***Figure 1**: Geological units and stratigraphic sequence of the Callovo-Oxfordian formation: Clayey unit (UA), Transitional unit (UT), silto-carbonated unit (USC), top and base of the formation (SNC, LS0 respectively), 3rd-order T-R sequences limits (LS1, LS2).*

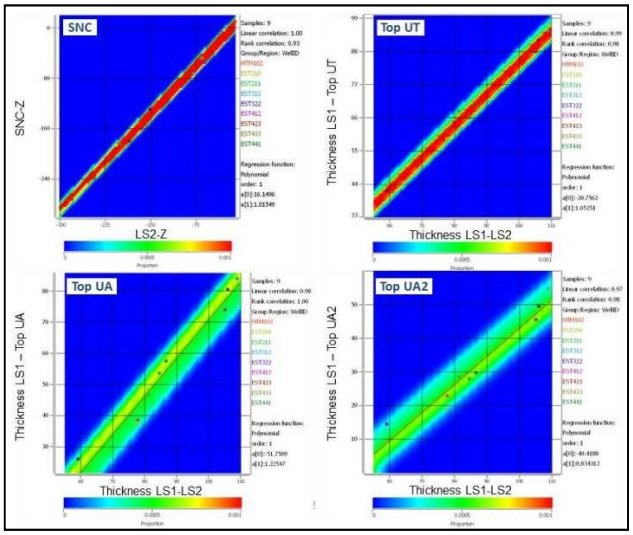


***Figure 2**: Scatterplots and associated smoothed bivariate histograms (density maps), between horizons (top left) or thicknesses, allowing to estimate SNC and the top of UT, UA and UA2 units.*

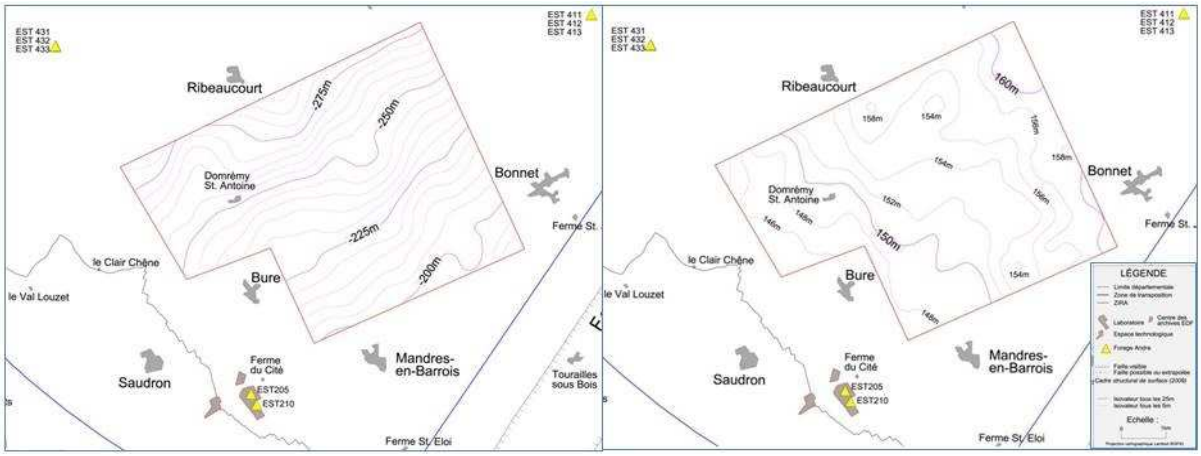


***Figure 3:** Elevation map of the base (LS0) and thickness of the COX formation in the ZIRA.*

References

[1] Garcia M.H., Rabaute A., Yven B. and Guillemot D., 2011. Multivariate and spatial statistical analysis of Callovo-Oxfordian physical properties from lab and borehole logs data: Towards a characterization of lateral and vertical spatial trends in the Meuse/Haute-Marne Transposition Zone, Physics and Chemistry of the Earth, Vol. 36, Issues 17–18, 1469–1485.

[2] Garcia M.H., Mathieu J.B. and Yven B., 2015. Analysis and modeling of spatial trend and spatial uncertainty of physical rock properties in the Callovo-Oxfordian claystone formation from a 3D high resolution impedance cube. Submitted at the 6th conference on Clays in Natural and Engineered Barriers for Radioactive Waste Confinement, Brussels, Belgium.

Analysis and modeling of spatial trend and spatial uncertainty of physical rock properties in the Callovo-Oxfordian claystone formation from a 3D high resolution impedance cube

Michel Garcia **(KIDOVA), Jean-Baptiste Mathieu (KIDOVA), Béatrice Yven (Andra)**

KIDOVA, 155, avenue R. Salengro, 92370 Chaville, France
Andra 1/7 Rue Jean Monnet, 92298 Châtenay-Malabry Cedex, France.

The geological exploration of the Meuse/Haute-Marne area began in 1994. Several boreholes were drilled, and the Callovo-Oxfordian argillite, thought to become a potential storage formation, were cored and logged. 2D seismic surveys were completed, as well as geological field observations, and an underground research laboratory was created. A 250 km^2-wide Transposition Zone was delimited, which was subject to further investigations in 2007 and 2008, including another series of coring and logging in four additional boreholes, and a tighter 2D seismic survey. From this work, a restricted 28 km^2 wide zone of interest (ZIRA) was identified as possible future repository area (Figure 1). In 2010, a 3D seismic survey was carried out to derive from it depth-converted seismic horizons and a 3D high resolution impedance cube that is 37 km^2 wide and covers the ZIRA. They were used to build a structural and geological model of the 3D seismic survey area that is suitable for safety assessment. The structural model is presented in the associated article of Yven *et al*. (2015) [1]. This article focuses on the geological model with the estimation of flow and transport rock properties.

Safety assessment studies require rock properties of the Callovo-Oxfordian claystone formation (COX) as input to simulate THM phenomena that should result from the implementation of a geological repository in the ZIRA. Up to eight types of flow and transport rock properties must be characterized and modelled in the COX: clay content, total porosity, bulk density, thermal conductivity, specific heat, diffusion coefficient, accessible porosity for different components and permeability. The intended repository being the source of all the physical phenomena to simulate, the geological model must be precise enough in and around the ZIRA to capture the spatial distribution and the heterogeneity of rock properties that are consequential for safety assessment. The particularity of this study is that no borehole, hence no rock data, are available within the 3D seismic survey area where the rock properties must be estimated. Consequently, relationships had to be inferred, between the seismic impedances (P-wave and S-wave impedances IP and IS) and the rock properties, from faraway wells where both types of data are present. These relationships were then used to estimate the spatial trends and spatial uncertainty of rock properties from 3D seismic data in the COX. Not all rock properties were successfully estimated this way. Only clay content, total porosity, bulk density and thermal conductivity were correlated with IP and IS, the clay content being best correlated.

The proposed approach required to address several issues.

- Change of support issues to relate at best rock property data representative of a small scale (30 cm for well-logs data, less for lab data), to 3D seismic impedance data corresponding to 7.5 m high support. The way to proceed to upscale rock properties depends on the available data (regularly spaced logs data vs. sparse lab data on cores) and the additive nature or not of the property (arithmetic vs. nonlinear averaging).

- Data integration issues to combine strongly correlated IP and IS data as spatial trend information on rock properties. Multivariate polynomial regression was used to derive and extrapolate "geophysical" estimates of the rock properties from IP and IS. The latter being known everywhere within and around the ZIRA, the "geophysical" estimates were used as spatial trend information about the corresponding rock properties.
- Bivariate statistical issues to infer and extrapolate bivariate distribution models that fully and properly describe the nonlinear relationships between "geophysical" estimates and rock properties. An innovative regression-based bivariate histogram smoothing method was used (Figure 1).
- Uncertainty estimation issues to quantify local uncertainty about rock properties from previously inferred bivariate distribution models. The smoothed bivariate histograms fully defining the relationships between "geophysical" estimates and rock properties, they were used to derive confidence intervals.

This approach allowed to estimate rock properties of the COX everywhere within the 3D seismic survey area and to quantify local uncertainty (Figure 2). The article will detail the approach and will present results obtained for different rock properties.

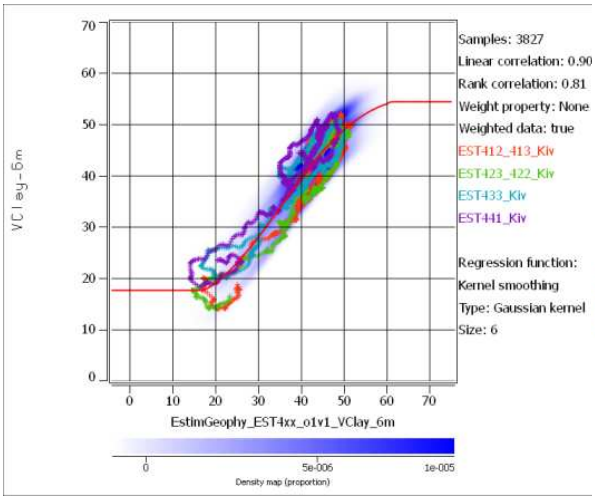


Figure 1: *Scatterplot and associated smoothed bivariate histogram (density map) of clay content vs. its "geophysical" estimate.*

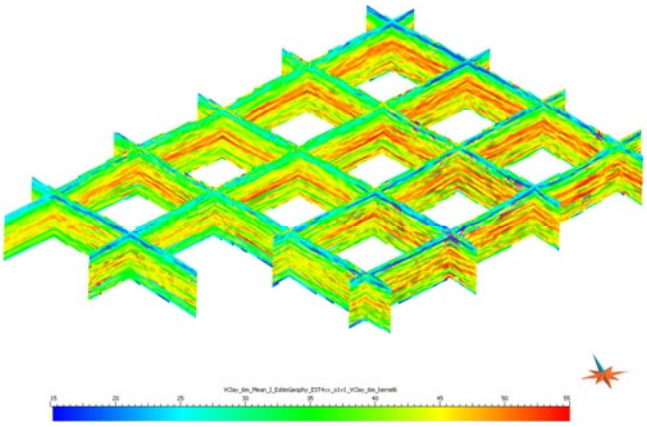


Figure 2: *3D view of mean clay content estimated at the 3D seismic grid scale (6 m high).*

References

[1] Yven B., Mathieu J.-B. and Garcia M.H., 2015. Geometry of the Callovo-Oxfordian claystone formation from depth-converted 3D-high resolution seismic data: modelling and spatial uncertainty. Submitted at the 6th conference on Clays in Natural and Engineered Barriers for Radioactive Waste Confinement, Brussels, Belgium.

DNA isolation from clayey samples: How can you realize this?

Hugo Moors, **Katinka Wouters, Patrick Boven and Natalie Leys**

SCK•CEN, Institute for Environment, Health and Safety, Laboratory for Molecular & Cellular Biology, Boeretang 200, B-2400 MOL (Belgium)

The starting point of any molecular biology study is DNA. It is still a technological challenge, to obtain sufficient amounts of DNA from complex soil or environmental samples. Several factors, like mineralogy, organic or inorganic contaminants and the diversity of structural materials (e.g. composition of cell layers, presence of nucleases, …) of living creatures protecting and confining their DNA, may seriously jeopardize the quantitative and qualitative isolation of DNA from soil or environmental samples. At present, a huge variety of soil DNA isolation methods exist, either as protocol described in literature or either as commercially available kits. However, many isolation methods are designed to isolate DNA from very specific environments or microbial species, while commercially available kits are often black-boxes which contain solutions or materials of which the composition or construction is not revealed by the kit producers.

Finding a workable protocol for the extraction of DNA from soil samples can be a very demanding, expensive, time consuming or even a non feasible task. Two of the major obstacles are the presence of (re)active clay minerals (*e.g.* smectites, illites, silicates, …) and the presence of aqueous Dissolved Organic Material (DOM), like humic– and fulvic acids or humus. Clay minerals are especially a quantitative problem during DNA extraction due to their strong molecular interaction capacity which is associated to the small sizes of the minerals, and, consequently their very high specific surfaces (over 100 [$m^2.g^{-1}$]). Furthermore, due to isomorphic substitution inside the crystal lattices (*e.g.* Accidental crystallization of Al^{3+} into a Si^{4+} lattice position), the surfaces of clay minerals carry almost always substantial negative charge densities. To counteract the thus generated charge imbalance of the crystal lattices, clay minerals surround themselves with positively charged ions, cations, originating from the interstitial mineral solution. These layers of cations are capable of electrostatically binding anionic species through a mechanism called cation bridging. Besides, the frayed edges of the clay minerals are known to be very active sorption sites. Above pH 5, which is the isoelectrical point of nucleic acids, DNA is a polyanionic polymer prone to interact with active sorption sites or present cations.

Humic– and fulvic acids, that are the main constituents of DOM, are organic molecules with very complex structures. Because DOM has many DNA like chemical characteristics, it will normally co-extract with DNA, rendering impure and low quality DNA. Furthermore, it is known that DOM can form strong covalent bounds with DNA which causes severe substrate inhibition, thereby making the DNA unsuitable for further enzymatic downstream applications. One experimental study even indicates that obtaining inhibitor-free DNA is the major limitation of any soil molecular biological analyse. Co-extracted DOM may also cause problems during optical DNA quantification measurements as it absorbs UV-light, exactly at the same wave lengths as DNA does i.e., between 230 and 280 nm. As a consequence, a substantial overestimation of the DNA quantity is made when using standard spectrophotometric techniques to quantify the amount of extracted DNA. Such overestimation may lead to the unsuccessful application (e.g. template concentration calculation for PCR analysis) of downstream processing, thereby rendering false negative results.

Before developing our own DNA extraction protocol, we attempted and tried to extract soil DNA from pristine and from inoculated clay samples with at least seven different commercially available soil or water DNA extraction kits. From MO BIO Laboratories, Inc we tested: PowerMax™, PowerSoil™, UltraClean® Soil, UltraClean® Water and the UltraClean® Microbial (all UltraClean® kits were tested with and without additional PowerClean™ DNA Clean-Up Kit). From Zymo Research we evaluated the ZR Soil Microbe DNA Kit™. From Epicentre Biotechnologies we tested the SoilMaster™ DNA Extraction. All kits were tested according the manufacturer's protocols. When variations of the protocols were documented, all of them were also tested. None of the commercial tested kits was able to extract any spectrophotometric quantifiable or PCR amplifiable DNA out of samples containing Boom Clay. Even 200 mg of Boom Clay was inoculated with a substantial amount

of bacteria (= one billion bacteria), no detectable DNA could be extracted with any of the tested commercial kits. As a consequence we stopped buying expensive kits and decided to develop our own DNA isolation protocol.

Two possible strategies exits to isolate DNA form environmental samples. The first strategy is known as the indirect extraction method. The idea of the indirect DNA extraction method is to firstly separate the microorganisms from the soil, and, subsequently extract the DNA from the liberated microorganisms. The second strategy, known as the direct extraction method, is to try to extract the DNA directly from the soil sample, so without any microbe soil separation step. Based on a profound literature survey, it became evident that the direct method has the highest change to be successful and the highest level of reproducibility. The two major problems to solve when developing a direct extraction method is firstly, to find a cell lysis procedure that functions in the presence of all category of soil particles, and secondly, to maintain the integrity of DNA once it is liberated from cell and soil. Potassium O-ethylcarbonodithioate, also known as Potassium Ethyl Xanthogenate (PEX), proved to have excellent physico-chemical characteristics to lyse almost all types of cells, even in the presence of soil samples containing clay, and to maintain the integrity of the liberated DNA by neutralizing active sorption sites of clay minerals and deactivating DNAse activity by scavenging almost all divalent cations. The latter are needed by nucleases as co-factors, without divalent cations nucleases cannot destroy free floating DNA. The cell lysis and DNA stabilizing strengths of PEX, are supported by adding sodium dodecyl sulfate (SDS), 2,2′,2″-Nitrilotriacetic acid (NTA) and ammonium acetate. Along with the development of an efficient way to liberate and maintain DNA from clay minerals, we also developed a novel way to minimize the interference of DOM. The simple addition of two vitamin B complexes to DNA solutions contaminated with DOM, allowed to effectively eliminate the inhibitory activity of DOM during downstream DNA processing.

The efficacy of the newly developed PEX-protocol was tested using different types of cultivated reference bacterial strains which were mixed with reference DOM and/or different kinds of environmental– , soil– , sediment– , geological and even clay containing samples. The extraction yield surpassed the performance of most commercial DNA extraction procedures. The purity of the isolated DNA was suited for most common downstream molecular biology applications including PCR amplification (from as little as 0.4 [pg.μl-1] DNA) and metagenomic analysis.

The influence of sample preparation on the structure of compacted, water saturated MX-80 bentonite

Michał Matusewicz, **Veli-Matti Pulkkanen, Markus Olin**

VTT Technical Research Centre of Finland, P.O. Box 1000, FI-02044 VTT, Finland
michal.matusewicz@vtt.fi

MX-80 bentonite is a reference clay material in the KBS-3 concept of spent nuclear fuel repository. The clay buffer plays an important safety role protecting the copper canister and retarding radionuclide transport should a leak occur. Therefore it is crucial to deeply understand the properties and behaviour of MX-80 bentonite at the repository conditions. Long life time of the repository poses a big challenge to experimental investigation of the bentonite properties as it is impossible to conduct laboratory experiments of comparable duration. For this reason the preparation of short experiments should be done very carefully.

In this work we investigate the influence of different ways of sample preparation on the structure of compacted, water saturated bentonite. The samples are either:

- compacted air-dry to the target density
- compacted air-dry to 1.6 g/cm^3 dry density and let to swell to the target density
- compacted air-dry to 1.6 g/cm^3 dry density, water saturated in confine condition and let to swell to the target density.

We use Small Angle X-Ray Scattering (SAXS) to analyse the structural changes in the samples. We observe different spectra for the samples of the same densities but prepared according to different procedures.

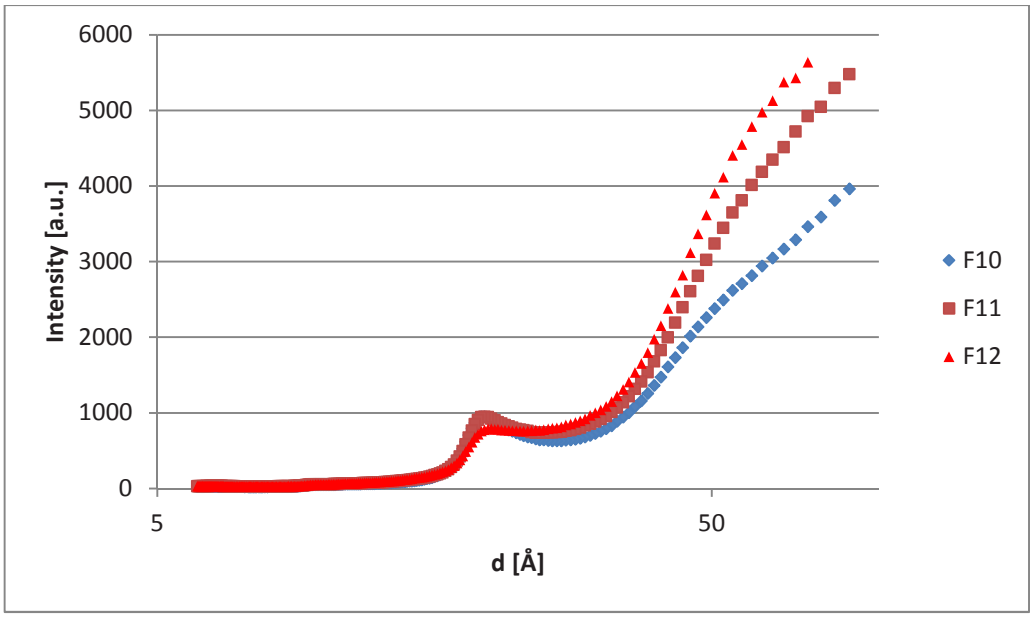


Figure 1: Example comparison of samples of dry density 0.7 g/cm^3. Sample F10 was compacted to target density, F11 was swelling from dry compacted state, F12 was swelling from wet compacted state.

Acknowledgements

The research leading to these results has received funding from the European Atomic Energy Community's Seventh Framework Programme (FP7/2007-2011) under Grant Agreement n°295487, the BELBaR project.

References

Delage, P., Marcial, D., Cui, Y. J., & Ruiz, X. (2006). Ageing effects in a compacted bentonite: a microstructure approach. Géotechnique, 56(5), 291-304.

Muurinen, A., Karnland, O., & Lehikoinen, J. (2007). Effect of homogenization on the microstructure and exclusion of chloride in compacted bentonite. Physics and Chemistry of the Earth, Parts A/B/C, 32(1), 485-490.

Anisotropic features on the thermal conductivity of Ypresian clays

***E. Romero*[1], A. Lima[2], N. Sau[1], H. Van Baelen[3], X. Sillen[3], X. Li[4]**

[1] Department of Geotechnical Engineering and Geosciences, Universitat Politècnica de Catalunya, Barcelona, Spain. enrique.romero-morales@upc.edu
[2]Civil Engineering Department, Federal University of Pernambuco, Brazil
[3]ONDRAF/NIRAS, Brussels, Belgium
[4]EIG EURIDICE, Mol, Belgium

Introduction

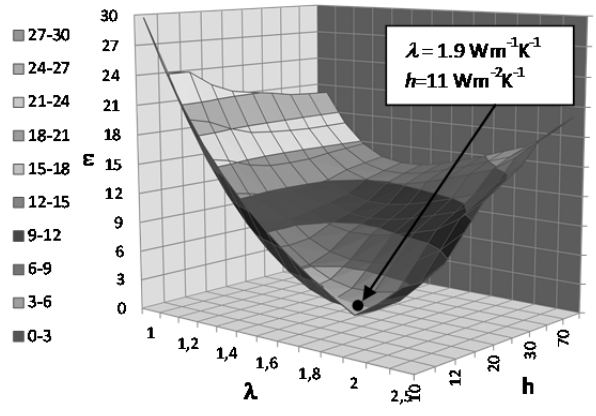
An experimental study on Ypresian clays –one of the potential deep clay formations in Belgium for the geological disposal of long-living and heat-emitting radioactive waste– has been undertaken to systematically study anisotropic features on the thermal conductivity using different experimental techniques and protocols. A clear influence of bedding planes on the anisotropic heat conduction has been identified by Garitte *et al*. (2014), when using back-analysis methodology on *in situ* heating tests in three argillaceous host formations. Nevertheless, exploring thermal conductivity features at laboratory scale on this type of rocks with bedding planes is not straightforward. One of the main drawbacks when laboratory tests are performed under unstressed conditions refers to the possibility of opening of fissures and gaps along bedding planes that affect its correct determination. The present study is aimed at exploring this thermal parameter with different techniques (back-analysis and direct measurement) and sample pre-conditioning procedures to have a more consistent determination at laboratory scale. Two main directions have been studied: heat flow parallel and orthogonal to bedding planes.

Experimental methods and results

Reported values on Ypresian clays for depths between 370 to 374 m (the depth of interest of the present study) in the direction orthogonal to bedding planes have indicated relatively low values between 0.62 and 1.12 $Wm^{-1}K^{-1}$ (I.N.I.S.Ma 1998). These values were consistently measured with a thermal conductivity tester under null lateral stress and under a low vertical stress applied. These low values were affected by the inherent anisotropy of the material (smaller values have been measured when flow is orthogonal to bedding planes) and mainly by open and partially saturated fissures along the bedding planes. Degrees of saturation between 0.94 and 0.98 have been measured after retrieval due to the difficulty of this clay to sustain the negative pore water pressure induced on total stress relief (maximum suction is limited to 2 MPa at the in situ porosity 0.43).

A first series of tests was carried out using the constant volume and axi-symmetric heating cell described in Romero *et al*. (2013), in which the material was tested under fully saturated conditions and under a constant water back-pressure of 1.2 MPa. A controlled-power heater (40 mm in height) was installed along the axis of the sample (75 mm in diameter and 100 mm in high) in the lower part of the cell and three thermocouples at different heights monitored the sample response during heating and cooling. This way, bedding planes, which were positioned parallel to the vertical axis, did not undergo any volume change during the heating/cooling paths (lateral contact was ensured during cooling, as detected by lateral strain gauges attached to the cell). In the interpretation of the results, it was assumed that temperatures and heat flux were not influenced by water pressure and flow, which means that heat convection was assumed to be negligible (conduction was the driving process). A back-analysis of temperature measurements was carried out by performing uncoupled thermal simulations using a finite element program. Heat exchanged by the highly conductive stainless steel cell with the controlled water bath was accounted for as a convection-type boundary condition of the problem through a convection coefficient h. Optimization was aimed at identifying the values of the saturated thermal conductivity λ and the convection coefficient h, in which least squares differences ε between temperature simulations and readings were computed for different elapsed times. Figure 1 shows these differences and the best agreement for parameters. The high value of the thermal conductivity (1.9 $Wm^{-1}K^{-1}$) was explained as a consequence of the high quartz content of the clay (43-45%) at the depth of interest and to the fact that it was measured along a preferential direction parallel to bedding planes.

Nevertheless, the suggested procedure is not free of drawbacks, since a certain degree of judgment must be always put in interpreting the data. For this reason, a second series of tests was carried out to determine anisotropic features with direct measurements of thermal conductivity. A careful pre-conditioning protocol was followed to define the initial state of the material and to ensure its saturation before measuring thermal conductivity. Two different initial states were considered, which are referred as protocols 1 and 2 in Figure 2. In the first protocol, samples (40 mm in diameter and height) with two different orientations of bedding planes were installed in a triaxial cell and isotropically loaded to a total mean stress equivalent to the geostatic condition (4 MPa). This process was carried out under constant water content and using controlled stress rate. The samples were put in contact with synthetic Ypresian clay water (YCSW in Figure 2) and then allowed equalising. Afterwards, the saturated samples were isotropically unloaded under water undrained conditions (top and bottom valves closed). Once unloaded, the saturated samples were placed in the thermal conductivity measurement setup. Protocol 2 only differed in the final drained unloading stage. An equivalent steady-state setup to that described in Barry-Macaulay *et al*. (2013) was used with two controlled-temperature caps and two heat flux sensors at the top and bottom of the sample that allowed detecting heat losses from the sample (samples were insulated to minimise radial heat losses). Temperature gradients across the specimen were measured with two additional thermocouples placed inside the sample. An axial load was applied on the sample to ensure a good contact between thermal caps and the sample.
Tests results using direct measurements displayed higher values than those reported by I.N.I.S.Ma (1998) and consistent with the higher value reported when using back-analysis methodology in the constant volume heating cell. Clear anisotropic features were detected, with higher thermal conductivity when flow was parallel to bedding planes. The results also highlighted the need to follow strict protocols to pre-condition argillaceous materials with bedding planes to minimise opening of fissures during thermal conductivity tests.



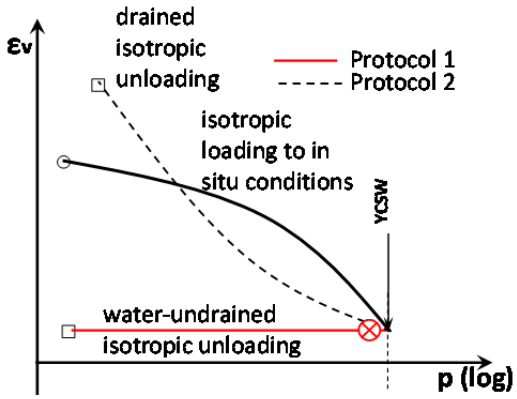


Figure 1 (left). Three-dimensional graph showing the differences in temperature between measurements and simulations in the back-analysis of the heating pulse test. Determination of thermal conductivity λ and convection coefficient h.
Figure 2 (right). Protocols 1 and 2 to apply controlled initial states under fully saturated conditions for the thermal tests.

Acknowledgements
Financial support of ONDRAF/NIRAS (Belgium) through a collaboration agreement with CIMNE (Spain) 'Complementary tests on thermal anisotropy of the Ypresian clays'' (2014-2015) is greatly acknowledged.

References

Barry-Macaulay D., Bouazza A., Singh R.M., Wang B. and Ranjith P.G. (2013). Thermal conductivity of soils and rocks from the Melbourne (Australia) region. Engineering Geology 164: 131–138.
Garitte, B., Gens, A., Vaunat, J. and Armand, G. (2014). Thermal conductivity of argillaceous rocks: Determination methodology using in situ heating tests. Rock Mechanics and Rock Engineering 47(1): 111-129.
I.N.I.S.Ma. (1998). Technical report n° 74252. Mons, Belgium.
Romero, E., Lima, A., Gens, A., Vaunat, J. and Li, X.L. (2013). Determination of the thermal parameters of a clay from heating cell tests. Proc. 18th Int. Conf. on Soil Mechanics and Geotechnical Engineering. Presses des Ponts, Paris: 3403-3406.

New paleoseismologic trench accross the Rauw Fault at Mol, Belgium

Verbeeck Koen[1], *Wouters Laurent [2], Vanneste Kris[1], Vleminckx Bart[1], Van Noten Koen[1], Camelbeeck Thierry[1], Marco Schiltz[3] and Vandenberghe Noël[4]*

1. Royal Observatory of Belgium, Seismology, Avenue Circulaire 3, BE-1180 Uccle, Belgium Email: koen.verbeeck@oma.be
2. ONDRAF/NIRAS – Belgian agency for radioactive waste and enriched fissile materials, Avenue des Arts 14, BE-1210 Brussels, Belgium
3. Samsuffit BVBA, Eggelstraat 8, BE-2530 Boechout
4. KULeuven, Earth and Environmental Sciences, Celestijnenlaan 200^{E}, BE-3001 Heverlee, Belgium

The Rauw Fault is the closest fault to the nuclear zone of Mol-Dessel (Figure 1A) with some indirect evidence for Quaternary movement. The 'De Maat' lignite layer situated in the ± 2 to 3 million years old sands of the Mol Formation is displaced 15 m vertically by this fault, observed between the lignite extraction front ending against the fault and a borehole (Gullentops et al., 1974). Part of this displacement probably dates to the Quaternary, indicated by the alluvial Lommel sand with gravel (1000 – 700 kyr) which was only deposited on the downthrown block, east of the fault (Pannekoek, 1924 and Vandenberghe, 1982 and 1990). The differential erosion between gravelly Lommel sand in the east versus pure Mol sand in the west caused relief inversion (Gullentops & Vandenberghe, 1995). The present-day topographical expression is therefore opposite to the fault movement. This suggests that fault movement occurred in the early Quaternary and that the long-term deformation rate is low. But how about the Rauw Fault's most recent movement and its potential to generate earthquakes? We conducted a targeted geomorphological & geophysical survey consisting of electrical resistivity tomography, electromagnetic resistivity, ground-penetrating radar, cone penetration tests (CPT), hand augering and two 10-m-deep cored boreholes (Verbeeck et al., 2001). With this information, a first 90-m-long and 3-m-deep trench was opened in 2003. Based mainly on the CPT profile, we expected to find 2 faults in the trench. The westernmost minor fault, with about 1 m offset, was observed in the trench as a deformed layer of peat blocks within white Mol sands but without Quaternary offset. However, the easternmost main fault with 6 m offset on the CPT profile was not observed in the trench, because we misinterpreted one of the CPT's and the geophysical signal of a large ice-wedge cast at that location looked like a fault. After a new geophysical survey in a wide area around this trench, other possible fault branches were identified. Using advanced interpretation techniques on a new CPT-E profile, the expected 6-m-offset fault was localised 30 m east of the 2003 trench. On the basis of these results a new trench was opened during summer 2014.
The trenches revealed intensely cryoturbated Pleistocene sediments overlying Pliocene Mol sand (Figure 1 A,B and C). The narrow fault zone juxtaposes white Mol sands overlain by a black lignite-rich sand layer followed by brown-coloured Mol sand on the footwall against the upper part of the brown-coloured Mol sand in the hanging wall. The average base of the cryoturbated late Pleistocene sediments (OSL dated younger than 20 kyr BP) does not show displacement. Furthermore, the fault itself is bent downslope due to periglacial soil creep and it is crosscut by frost cracks/wedges. This places an upper bound of ± 20 kyr on the fault movement. It is well possible that the last activity is much older, but a long erosional hiatus in the sediments makes more precise impossible. The Lommel sands are not observed in the trench, but the gravel with ventifacts in the Pleistocene sands was most probably reworked from this deposit, suggesting that it was present in the vicinity. On the CPT-E profile the base and the internal layers within the Mol sands all show the same displacement and thus all of the 6 m movement post-dates this deposition. Furthermore the brown staining due to organic coating around the sand grains in the top of the Mol sands indicates soil formation. This process would have required a considerable amount of time after the retreat of the sea, in a climate that was not too cold. The fault displacement also clearly postdates this brown staining. The fault movement is therefore episodic in nature and most of it occurred during the early Quaternary but, without possibility for more precise dating.

Due to the limited Quaternary thickness and long erosional hiatus at the Mol, Postel trench site and along most of the fault, future efforts should concentrate further northward where the Quaternary is thicker and possibly has better stratigraphic resolution.

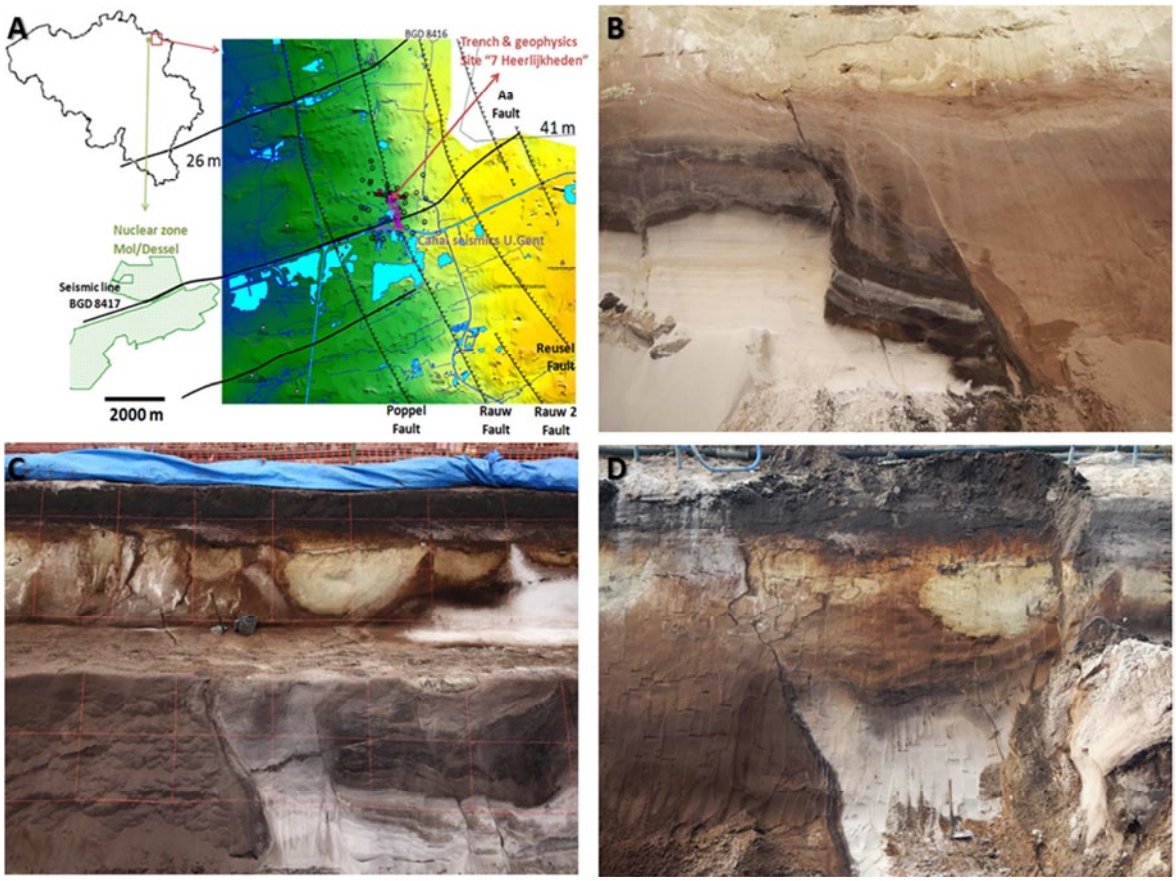


Figure 1: A: DEM of the investigated area with indication of faults and seismic lines by Belgian Geological Survey and Ghent University, B, C and D: pictures of the Rauw fault on the 60°inclined walls of the 2014 trench. B: fa ult zone on the northern trench wall, C: fault zone on the benched southern trench wall, D:fault zone on the southern trench wall after further excavation, removing the bench shown in C.

References:

De Batist, M., J. Van Lint, W. Versteeg, and P., Van Rensbergen, (1992). Structureel ondiepwater seismisch onderzoek: R.C.M.G. Gent, Ministerie van de Vlaamse Gemeenschap, Brussel.

Gullentops, F., Huyghebaert, Wittewrongel & Dricot, (1974). Verslag van de buitengewone vergadering op 21 tot 23 juni: Belgische Vereniging voor Geologie en Société Géologique de Belgique.

Gullentops, F. & N. Vandenberghe, (1995). Toelichtingen bij de Geologische kaart van België: Kaartblad 17 Mol: Belgische Geologische Dienst & Anre, 64p.

Pannekoek, A.J., (1924). Einigen Notizien über die Terrassen in Mittel- und Nord-Limburg: Natuurhistorisch Maandblad 13, p. 305-336.

Vandenberghe, J., (1982). Geoelectric investigation of a fault system in Quaternary deposits: Geophysical Prospecting 30, p. 879-897.

Vandenberghe, J., (1990). Morphological effects of Pleistocene faulting in unconsolidated sediments (Central Graben, Netherlands): Zeitschrift für Geomorphologie N.F. 34/1: p. 113-124.

Verbeeck, K., T. Camelbeeck, K. Vanneste, L. Wouters & M. Dusar, (2001). Studie van de tektonische activiteit van de breuken van Rauw en Poppel: Report for convention CCHO 2000-508/00/00 between the Royal Observatory of Belgium and NIRAS, 138p.

Influence of Natural Sorbents in Immobilization of Spent Ion Exchange Resins in Cement in Radioactive Waste Management

*I. Plecas**, S. Dimovic* and D. Arbutina**

*The "Vinca" Institute of Nuclear Sciences, P.O. Box 522, 11001 Belgrade, Serbia
** Public Company "Nuclear Facilities of Serbia", P.O. Box 4, 11001 Belgrade , Serbia

Abstract

Leach characteristics of ^{137}Cs and ^{60}Co radionuclides from spent mix bead ion exchange resins and both ordinary Portland cement and cement mixed with two kind of natural sorbents, (bentonite and clinoptilolite) have been studied using International Atomic Energy's (IAEA) standard leach method.
A study is undertaken to determine the waste immobilization performance of low-level wastes in cement-natural sorbents mixtures. The solidification matrix was a standard Portland cement mixed with 290-350 (kg/m^3) spent mix bead exchange resins, with or without 1-10 % of bentonite or/and clinoptilolite The leaching rates from the cement-bentonite matrix as ^{60}Co: $(1.20\text{-}9.72)x10^{-5}$(cm/d) and for ^{137}Cs: $(1.00\text{-}9.22)x10^{-4}$(cm/d), after 300 days were measured. From the leaching data the apparent diffusivity of cobalt and cesium in cement-bentonite or/and clinoptilolite matrix with a waste load of 350 (kg/m^3) spent mix bead exchange resins was measured as ^{60}Co: $(1.0\text{-}5.9)x10^{-6}$(cm^2/d) and for ^{137}Cs: $(0.48\text{-}2.4)x10^{-4}$ (cm^2/d) after 300 days. These results are part of a 30-year mortar and concrete testing project which will influence the design of radioactive waste management for a future Serbian radioactive waste disposal center.

Preparation and estimation of thermodynamic properties of Fe(II)-, Co(II)-, Ni(II)- and Zr(IV)-containing layered double hydroxides

Konstantin Rozov, **Hilde Curtius, Dirk Bosbach**

Forschungszentrum Jülich GmbH, Institute for Nuclear Waste Management and Reactor Safety (IEK-6), Wilhelm-Johnen-Str., 52425 Jülich, Germany, k.rozov@fz-juelich.de

The investigation of layered double hydroxides (LDHs) was performed because they and similar "green rust" phases were identified as specific secondary phases forming during the evolution of the disposed research reactor fuel elements under nuclear repository relevant conditions [1]. LDHs or "hydrotalcite-like" solids are of interest in environmental geochemistry because they can substitute various cations and especially due to the anion-exchange properties and, therefore, can be considered as buffer materials for retention of mobile and hazardous radionuclides (like, ^{14}C, ^{129}I, ^{36}Cl, ^{79}Se *etc*.). In our study Fe^{2+}-, Co^{2+}-, Ni^{2+}- and Zr^{4+}-containing LDHs have been synthesized by co-precipitation method and characterized (PXRD, FT-IR, SEM-EDX, TGA-DSC) in order to investigate the effect of substitution of 2- and 4-valent cations on the stability of LDHs. PXRD measurements demonstrated that: (1) pure Mg-Al-Fe(II) LDHs are existing in the range of the mole fraction of iron x_{Fe} = Fe/(Mg+Fe) between 0 and 0.13. Unit-cell parameters (a_o=b_o) as a function of x_{Fe} follow Vegard's law corroborating the existence of a solid solution when x_{Fe} = 0 - 0.13. Products of syntheses with $x_{Fe} \geq$ 0.13 contain detectable amounts ($\geq$1-2 wt%) of additional phases (like, magnetite, maghemite, lepidocrocite); (2) pure Ni^{2+}- and Co^{2+}-containing LDHs (mole fractions of Ni and Co were equal to 0.1) have been synthesized successfully; (3) Mg-Al-Zr(IV) precipitates with mole fraction of zirconium x_{Zr} = Zr/(Zr+Al) = 0.0 - 0.5 show PXRD patterns attributed to pure LDHs and the variation of lattice parameters a_o=b_o as a function of x_{Zr} is in agreement with Vegard's law demonstrating the presence of solid solution. In contrast, PXRD analyses of precipitates with $x_{Zr} \geq 0.5$ have shown the presence of additional X-ray reflexes typical for brucite. The stoichiometry of LDHs has been established by ICP-OES and SEM-EDX analyses and reveals that (Mg+Fe)/Al, (Mg+Co)/Al and (Mg+Ni)/Al ratios in Fe^{2+}-, Co^{2+}- and Ni^{2+}- containing solids are remarkably close to desired 3:1 for the whole range of solid compositions. However, in Mg-Al-Zr(IV) LDHs the increase of x_{Zr} in co-precipitating synthesis solutions leads to the formation of solids with significantly reduced Mg/(Al+Zr) ratios. This fact and results of thermodynamic calculations with GEM-Selektor software [2] indicate that the incorporation of Zr into the LDH structure increases significantly the aqueous solubility of LDHs due to the preferred localization of $Zr(OH)_5^-$-ligands in the interlayer space of brucite-like layers. On the other hand esimates of molar Gibbs free energies shown that the substitution of Fe^{2+}, Co^{2+} and Ni^{2+} into the LDHs does not affect so significantly on the stability of LDHs. Finally, reliable estimate of standard Gibbs free energy of formation for pure Mg-Al hydrotalcite composition (-3619.04±15.27 kJ/mol) has been provided. For the first time, by applying Calvet-type solution calorimetry values of standard entlhalpy (-4013.89±13.27 kJ/mol) and absolute molar entropy (254.63±25.34 J/mol·K) of pure Mg-Al-Cl LDH have been determined.

References

H.Curtius, G.Kaiser, Z.Paparigas, B.Hansen, A.Neumann, M.Klinkenberg, E.Müller, H.Brücher, D.Bosbach. Wechselwirkung mobilisierter Radionuklide mit sekundären Phasen in endlagerrelevalnten Formationswässern. Berichte des Forschungszentrums Jülich; 4333, ISSN 0944-2952.

D.A.Kulik, T.Wagner, S.V.Dmytrieva, G.Kosakowski, F.Hingerl, K.V.Chudnenko, U.Berner (2013) GEM-Selektor geochemical modeling package: revised algorithm and GEMS3K numerical kernel for coupled simulation codes. Comput. Geosci. 17, 1–24.

Retardation of low-molecular weight organic compounds in clays

***Yanhua Chen*[ab], Martin A. Glaus[a], Andreas Jakob[a], Luc R. Van Loon[a], Urs K. Mäder[b]**

[a]Laboratory for Waste Management, Paul Scherrer Institut, CH-5232 Villigen PSI, Switzerland
[b]Institut für Geologie, University of Bern, Baltzerstrasse 3, CH-3012 Bern, Switzerland

Carbon-14 is an important contributor to the annual radioactive dose predicted in performance assessment of low- and intermediate-level radioactive waste repository in Switzerland. ^{14}C is assumed to be mainly released to the biosphere as organic compounds, yielding from the corrosion of activated steel (Nagra, 2008). To date, performance assessment is based on the assumption that the transport of organic compounds is unretarded. However, if a weak retardation can be robustly demonstrated, this would lead to a larger extent of decay of ^{14}C within the barriers and to a significant reduction of its maximum dose. Possible interactions of the organic model compounds with clay are still poorly known, they are presumed rather weak. The main tasks of this project are: (i) to investigate the transport behaviour of organic model compounds with different structure in argillaceous media, and (ii) to derive the quantitative relationships (Schwarzenbach et al., 2006) between the sorption properties and structural elements of organic compounds.

The batch sorption technique is not ideally suited to measure low sorption distribution ratios (R_d). R_d values less than 5×10^{-4} m^3/kg are an approximate lower limit for the measurements. In contrast the infiltration technique with compacted clays allows a much more sensitive determination of R_d values. Porosity of compacted clay affects the detection limit of R_d in an infiltration experiment. For a porosity of 0.3, an R_d value of 5×10^{-5} m^3/kg is an approximate detection limit, and the sensitivity for low R_d values can be increased by one order of magnitude compared to conventional batch sorption technique. Opalinus Clay is one of the preferred host rock options for the disposal of radioactive waste in Switzerland. Thus, illite and kaolinite, important clay minerals present in Opalinus Clay, were used in this project as model clay minerals.

In the infiltration experiments, a constant advective flow through a column of compacted clay sample was generated by pressurised helium. The breakthrough of a pulse of tracers (Na-propanoate, Na-2-hydroxypropanoate (Na-lactate), Na-3-hydroxypropanoate, Na-d-gluconate; structural formulas are shown in Figure 1) was monitored. A non-sorbing tracer, tritiated water (HTO), was used as a conservative reference. The effluent concentrations were measured with ion chromatography and the activity of HTO was measured by liquid scintillation counting. The breakthrough of individual tracer was modelled with a 1D advection/diffusion approach model implemented in COMSOL Multiphysics.

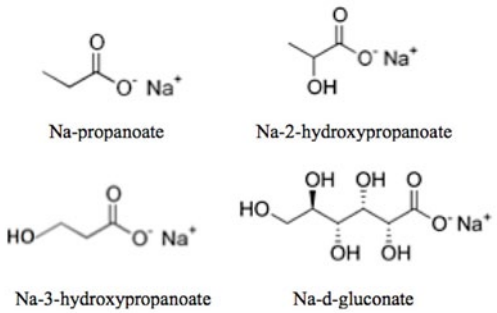
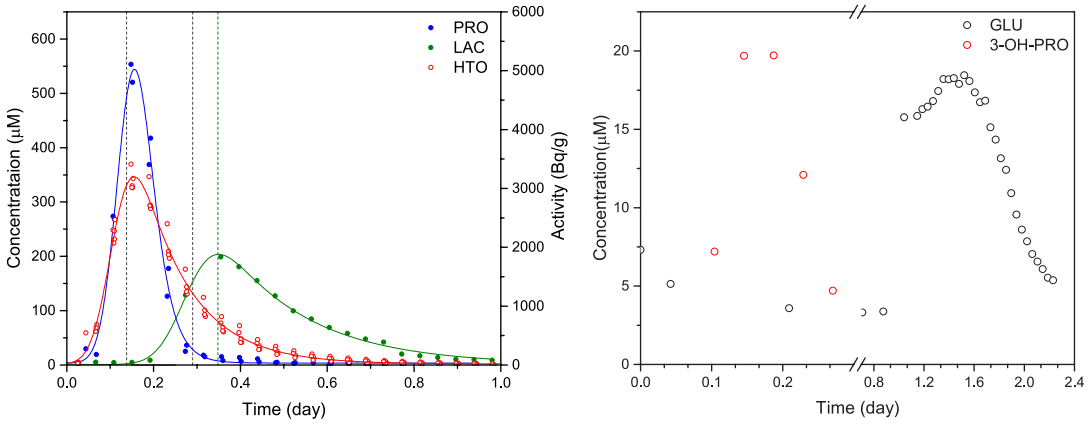


Figure 1. Structural fomulas of investigated organic compounds

Breakthrough curves are shown in Figure 2. Within the given limits for peak resolution, the breakthroughs of propanoate and HTO were identical. Similar behaviour was observed for 3-



hydroxypropanoate. Lactate, however, was significantly retarded with an R_d value of 4×10^{-4} m^3/kg, and gluconate had the most significant retardation. Mass balance was calculated and all compounds were almost completely recovered in the effluents except gluconate and 3-hydroxypropanoate.

Figure 2. Breakthrough curves for HTO, propanoate, lactate on the left, and gluconate, 3-hydroxypropanoate on the right. Concentrations/activity of tracers were plotted in dots as a function of time. Solid curves were only shown for visualization purpose.

Chromatographic behavior of organic compounds is often used to characterise their physico-chemical behavior in the environment (Tülp et al., 2008). In ion-exclusion chromatography (Dionex IonPac ICE-AS6 column, negatively charged), lactate eluted earlier than propanoate due to a much stronger electrostatic exclusion. The elution order resulting from the retention times coincided with the order of the pK_a-values of the acids. A lower pK_a value indicated an earlier elution of the acid. However, this order was the opposite for illite (negatively surface charged) as shown above. A pure electrostatic interaction could rather be excluded for explaining such behaviour with illite. The retardation behaviour of lactate might be explained by a specific chelation of the alpha-hydroxo group with coordination metalcenters of illite. Further experiments (e.g. with butanoate, 2-hydroxybutanoate) and spectroscopic investigations will be done to substantiate such an interpretation.

References

Bradbury, M.H., Baeyens, B. (2009): Sorption modelling on illite Part I: Titration measurements and the sorption of Ni, Co, Eu and Sn. Geochimica et Cosmochimica Acta, 73, 990-1003.

Fischer, K., Kotalik, J., Kettrup. A. (1999): Chromatographic properties of the ion-exclusion column IonPac ICE-AS6 and application in environmental analysis, Part I: chromatographic properties. J. Chromatogr. Sci. 37, 477–85.

Nagra (2008): Begründung der Abfallzuteilung, der Barrierensysteme und der Anforderungen an die Geologie: Bericht zur Sicherheit und Machbarkeit. Nagra Technischer Bericht. NTB 08-05. Nagra, Wettingen.

Schwarzenbach, R.P., Escher, B.I., Fenner, K., Hofstetter, T.B., Johnson, C.A., von Gunten, U., Wehrli, B. (2006): The challenge of micropollutants in aquatic system. Science, 313, 1072-1077.

Tülp, H.C., Goss, K.-U., Schwarzenbach, R.P., Fenner, K. (2008): Experimental determination of LSER parameters for a set of 76 diverse pesticides and pharmaceuticals. Environmental Science and Technology, 42, 2034-2040.

Constraining porewater chemistry in a clay–rich rock sequence

Paul Wersin[1], Martin Mazurek[1], H. Niklaus Waber[1], Urs K. Mäder[1], Thomas Gimmi[1,2], Daniel Rufer[1], Catherine Lerouge[3], Takahiro Oyama[4], Daniel Traber[5]

1. University of Bern, Institute of Geological Sciences, CH-3012 Bern, Switzerland (paul.wersin@geo.unibe.ch)
2. BRGM-ISTO-UMR 7327, 3 av. C. Guillemin, B.P. 36009, Orléans, 45060, France
3. LES, Paul Scherrer Institut, 5232 Villigen, Switzerland
4. CRIEPI, 1646 Abiko, Abiko-Shi, Chiba-ken 270-1194, Japan
5. NAGRA, Hardstrasse 73, CH-5430 Wettingen, Switzerland

It is important to evaluate the porewater chemistry of argillaceous host rocks for safety assessment because it affects radionuclide migration. The nanometric pore-space architecture and the resulting very low hydraulic conductivity, however, make the sampling and characterisation of porewater chemistry a difficult task. Thus, in order to understand and reduce uncertainties induced by sampling and experimental disturbances, a multi-method strategy is generally required. Here a combined experimental and modelling approach is presented for the analysis of the porewater chemistry in a rock sequence comprising Opalinus Clay and so-called "confining units" 'Brown Dogger' and Staffelegg Fm. (Liassic).

The data was obtained from analyses on drillcores of a deep borehole at Schlattingen (NE Switzerland). The studied rock sequence can be roughly divided into four units: The top unit (~25 m thick) corresponds to the lower part of the Effingen Member (Malm) and is made up of silty to sandy calcareous marls. The underlying unit (~77 m thick), termed 'Brown Dogger', exhibits rather variable lithology. It consists predominantly of clayrocks and marls with variable contents of calcite and quartz. The third unit is the ~120 m thick Opalinus Clay, which is characterized by fairly homogeneous silty to fine sandy clayrocks. The lowest unit (Staffelegg Fm., ~53 m thick) is also rather rich in clay minerals and consists of a variable sequence of marls, clayrocks and few limestone beds. Only the three lower units were considered for porewater chemistry modelling.

Experimental: Rock core samples representative for the overall lithology of the corresponding stratigraphic unit were taken about every 5 m, sealed on-site according to a standardized protocol to protect them from oxidation and evaporation, stored cool and sent to the laboratory for subsequent analyses. *Mineralogical compositions, water contents and density measurements* were obtained for 30 samples. From water contents and grain density, water-loss porosity was derived. *Aqueous leachates* were prepared at a solid/liquid (S/L) ratio of 1, with contact times of 48 h. *Cation exchange properties* were studied using the Ni eythylenediamine method at S/L = 1. All procedures, except for milling, were carried out under N_2 atmosphere in a glovebox. *Squeezing tests* were conducted on 12 selected clay-rich samples. Porewaters were extracted at 200 to 500 MPa, but only data from the lowest squeezing pressure of 200 MPa are reported here. Porewater was also extracted with the *advective displacement technique* from a core sample of the 'Brown Dogger' unit. CO_2 partial pressure measurements were carried out on well-preserved cores in gas cells.

Model setup: The aim of the modelling was to simulate porewater compositions using primarily chloride data from leachates and exchangeable cation data and to compare these with the data from squeezing and advective displacement. Leachate chloride data was re-calculated to in-situ porosity by considering water contents and a uniform anion-accessible porosity of 0.5. The latter was based on the comparison of leachate and squeezing data (Wersin et al. 2012). Furthermore, pCO_2 as obtained from pCO_2 measurements was considered as input. The applied thermodynamic model was based on the studies of Pearson et al. (2011) and Gaucher et al. (2009). A base case and several variant cases were defined, all of which assumed equilibrium with calcite, omnipresent in the rock sequence. Further, sulphate equilibrium with respect to celestite or a $CaSO_4$ phase was considered. The uncertainty in pCO_2 was addressed by variation in pCO_2 in a specific model case.

Results and conclusions: In general, comparison between data obtained from squeezing and advective displacement analyses with the modelling results (base case) yields agreement within a factor of two for the modelled samples along the rock sequence. This is illustrated in Figure 1 for the solute ions Cl^-, SO_4^{2-}, Na^+, Ca^{2+}, Mg^{2+}, K^+ and Sr^{2+}. The sulphate data tend to support the assumption of celestite equilibrium, showing agreement between measured and modelled values within 10–60%. Assuming equilibrium with a $CaSO_4$ phase, the agreement is worse, suggesting that the latter phase is less likely to control sulphate composition in the porewater. The agreement of measured and modelled data for the exchangeable cations Na^+, K^+, Ca^{2+}, Mg^{2+}, and Sr^{2+} indicates the validity of the cation exchange model and of the calcite equilibrium constraint as well as the correct determination of the exchangeable cation inventory. For the squeezing data, only a limited set of pH and alkalinity data could be obtained. In the modelling a constant pCO_2, as determined from pCO_2 measurements (i.e. $10^{-2.2}$–$10^{-2.5}$ bar), was considered. Applying a lower pCO_2 of $10^{-3.1}$ bar, yields nearly identical results for the solute ions mentioned above, and therefore only affecting pH and alkalinity (not shown). This highlights the strong buffering effect of cation exchange in spite of shifted carbonate equilibrium.

Overall, our multi-method approach supports earlier findings on anion-accessible porosity and porewater chemistry for a clay-rich rock sequence with variable lithology and mineralogy.

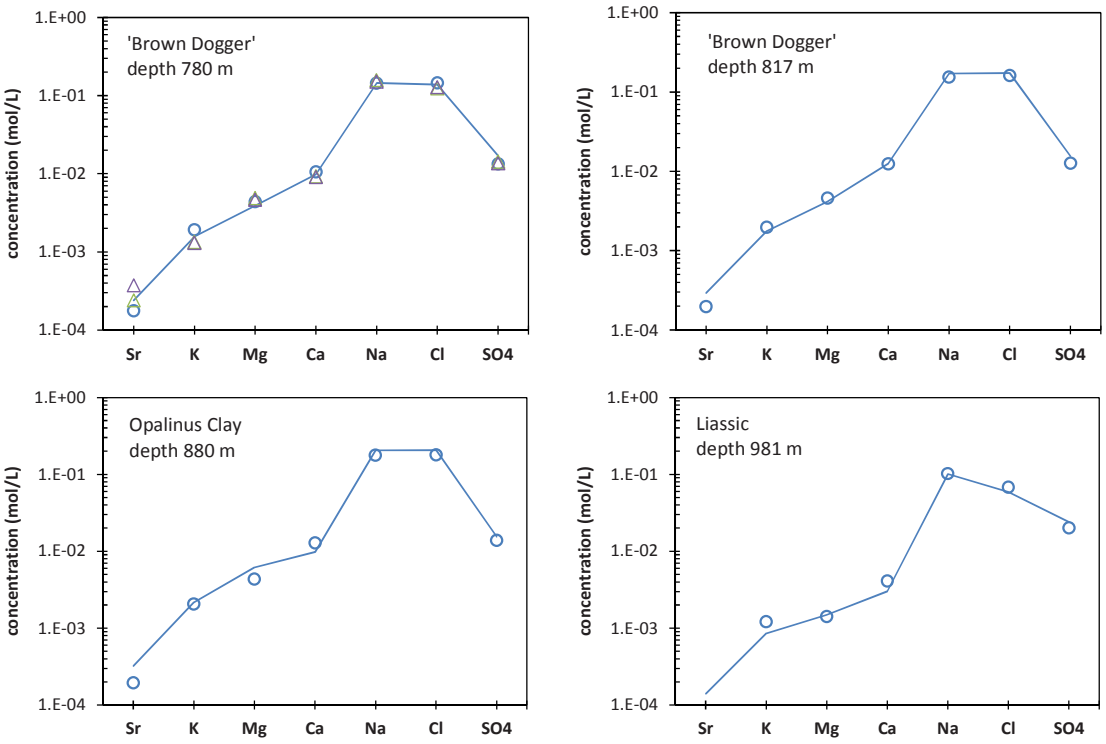


Figure 1: Schoeller diagram comparing ion compositions from squeezing (circles) and advective displacement (triangles) with modelled data (lines). Modelled data corresponds to base case (see text).

References:

Gaucher, E.C., Tournassat, C., Pearson, F.J., Blanc, P., Crouzet, C., Lerouge, C. & Altmann, S. 2009. A robust model for pore-water chemistry of clayrock. Geochim. Cosmochim. Acta 73, 6470–6487.

Pearson, F.J., Tournassat, C. & Gaucher, E.C. 2011. Biogeochemical processes in a clay formation in situ experiment: Part E – Equilibrium controls on chemistry of pore water from the Opalinus Clay, Mont Terri Underground Research Laboratory, Switzerland. Applied Geochemistry 26, 990–1008.

Wersin, P., Waber, H.N., Mazurek, M., Mäder, U.K., Gimmi, T., Rufer, D. & Traber, D. 2013. Resolving Cl and SO4 profiles in a clay-rich rock sequence. Procedia Earth and Planetary Science 7, 892 – 895.

Regional aquifer hydrogeochemistry below the Boom Clay (NE-Belgium): data analysis and modelling

K.Vandersteen* **and B. Leterme**

Institute Environment-Health-Safety, Belgian Nuclear Research Centre (SCK•CEN), Boeretang 200, 2400 Mol, Belgium
*Corresponding author: katrijn.vandersteen@sckcen.be

SCK•CEN has been involved for more than 30 years in the Belgian research programme on the long term management of high-level and/or long-lived radioactive (B&C) waste coordinated by ONDRAF/NIRAS. One aspect of the research is the study of the regional hydrogeology and geochemistry of the aquifer systems surrounding the Boom Clay.
This study presents the analysis and modeling of groundwater geochemistry in the confined aquifers below the Boom Clay in NE-Belgium. This so-called deep aquifer system includes, with increasing depth, parts of the Oligocene Aquifer System, The Bartoon Aquitard System and the Ledo-Paniselian-Brusselian Aquifer System.

During the Neogene (24 to 2.5 million years ago), several marine transgressions and regressions took place in NE-Belgium. At the end of the Neogene, the sea drew back from this area after having deposited shallow marine and estuarine sands and some clay. From then on, the seawater in the aquifers (both above and below the Boom Clay) gradually diluted as the aquifers were flushed with fresh recharge water. Afterwards, water-rock interactions, including cation exchange, began to play a role in the deep aquifer system. This led to changes in groundwater composition over time.

Geochemical data (major ions, stable isotopes, radioactive isotopes, dissolved gases) have been collected at a regional scale from the piezometric network in the deep aquifer system in NE-Belgium. Several measurement campaigns have been performed between 1980 and 2014.

Currently, groundwater in the deep aquifer system is mainly of the Na-HCO_3 to Na-Cl type. Because of the low groundwater velocity, re-equilibration with the host formations generally occurs. The main geochemical indicators (salinity, stable isotopes $\delta^{18}O$ and $\delta^{2}H$) point to a mixture between saline water (to the NW) and fresh recharge water (from the SE). SE-NW gradients of ion concentrations are observed and can be explained in agreement with the pattern of natural groundwater flow (Figure 1).
The ratio of sulphate to chloride concentrations in the deep aquifers increases from SE to NW and is consistently lower than the seawater ratio. The low sulphate content can be explained by sulphate reduction associated with organic matter degradation.
Variations in HCO_3^- content along the flow path are visible: there is an increase in HCO_3^- content towards the centre and then again a decrease towards the NW. Calcite dissolution as a result of cation exchange (more Na^+ in solution and Ca^{2+} on the exchanger leads to more calcite dissolution) can explain these variations in HCO_3^- content.
The $\delta^{13}C$ values are close to or higher than –12‰, which is the common value for systems closed to CO_2. Higher values for $\delta^{13}C$ might point to renewed dissolution of calcite due to the presence of cation exchange.

Mineralogical data on the deep aquifers in NE-Belgium are scarce. In the Oligocene Aquifer System, the most abundant minerals are quartz, clay, and feldspar. Some carbonates are also present. The Ledo-Paniselian-Brusselian Aquifer System mainly consists of fine to coarse glauconitic and calcareous sands, containing limestone benches and locally thin marl and clay lenses. High carbonate concentrations are present in the Brussels and Lede Sands, attributed to the abundance of calcareous microfossils and other skeletal grains.

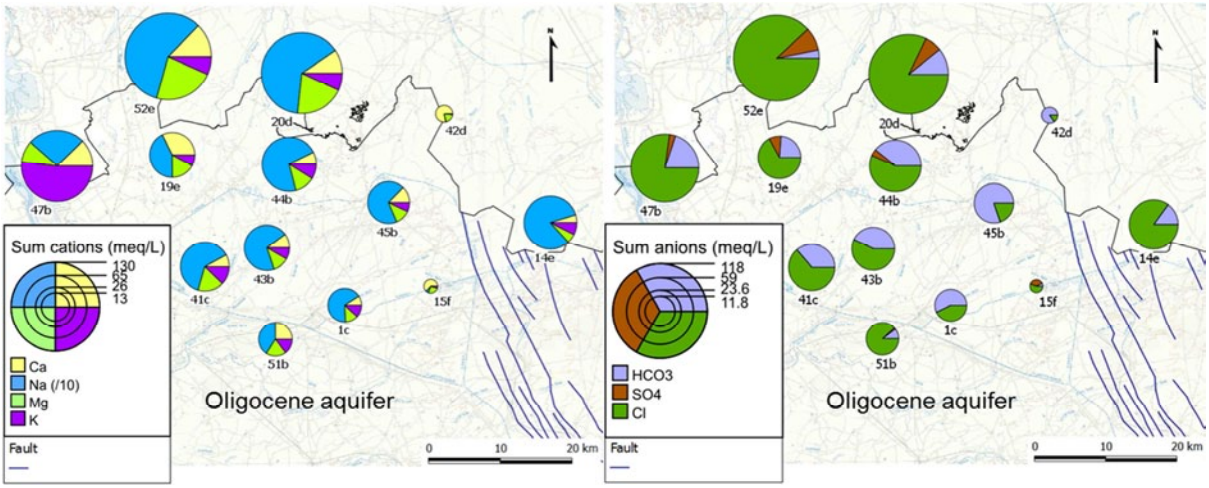


Figure 1. Total cation (a) and anion (b) content in the Oligocene aquifer in NE-Belgium (sampling campaign of 2008).

Building on the concepts emerging from the geochemical data analysis and recent groundwater flow modeling (Vandersteen *et al*., 2014), a geochemical model was developed in PhreeqC (Parkhurst and Appelo, 1999). Calculations were done for several locations in the deep aquifer system, using geochemical and mineralogical data and the PhreeqC thermodynamical database.
The geochemical modelling indicates that most water samples in the deep aquifer system are close to saturation or are supersaturated for carbonates and quartz, which is in accordance with the low flow rates in this aquifer system as calculated by the groundwater model.

The inverse modelling tool of PhreeqC was used, which aims at deciphering the reactions and mixtures which have led to a given water quality. The mineral composition and water end members are required input. We assume as end members sea water, recharge water and reference Boom Clay water (De Craen et al., 2004). Following the results of the $\delta^{13}C$ data analysis, we assume the system is closed with respect to CO_2. As mineral phases, we include the cation exchange complexes, calcite, quartz, K-feldspar, albite, kaolinite and organic matter, in line with the measured mineralogical composition.Results of the inverse geochemical modelling confirm that the current geochemical composition of the deep aquifer system is a result of mixing different waters in combination with different water-rock interactions. Dilution of seawater increases from NW to SE (from 20% in the NW to 1% in the SE for the Oligocene aquifer system). Concerning water-rock interactions, there is consistency in cation exchange, calcite dissolution, silicate dissolution and sulphate reduction throughout the study area.

The main conclusion of the study is that the patterns derived from the data analysis could be confirmed by geochemical modelling. More accurate data, e.g. on mineralogy and CEC, however, are required to improve further (inverse) geochemical and reactive transport modelling.

References

De Craen, M., Wang, L., Van Geet, M., Moors, H., 2004. *Geochemistry of Boom Clay porewater at the Mol site*. Scientific Report, SCK•CEN-BLG-990, 180 pp.

Parkhurst, D.L., and Appelo, C.A.J., 1999, *User's guide to PHREEQC (Version 2)--A computer program for speciation, batch-reaction, one-dimensional transport, and inverse geochemical calculations*: U.S. Geological Survey Water-Resources Investigations Report 99-4259, 312 p.

Vandersteen, K., Gedeon, M., Marivoet, J. and L. Wouters, 2014. *Regional groundwater modelling of the confined aquifers below the Boom Clay in NE-Belgium*. Geological Society, London, Special Publications. doi:10.1144/SP400.22

The effect of ionic strength on Iodine exclusion in Na-montmorillonite-rich clay rock – a molecular simulations study

F. O. Valega Mackenzie[1], Mariëlle Koenen

[1]TNO, De Rondom 1, P.O. Box 6235, Eindhoven 5600HE, The Netherlands

The Boom Clay is currently investigated in the Dutch research programme on geological disposal of radioactive waste (OPERA) as potential host rock in the Netherlands. The slow migration of radionuclides through the host rock is the most relevant safety function of the clay. Diffusion of radionuclides through the pore space of a clay rock is affected by processes such as anion exclusion, cation surface diffusion, and intra-particle diffusion [1]. These processes, which are ion specific, not only affect diffusion fluxes but also the diffusion path length (tortuosity). The importance of the individual contribution of the different processes to the diffusion rate is still unclear. Within the RANMIG project of the OPERA programme these individual processes are further investigated. Molecular simulations are used to assess the role of anion exclusion on iodine diffusion under varying brine compositions prevailing in the Dutch Boom Clay. The clay molecular model adopted was a Na-montmorillonite (Figure 1, left image) such as introduced by Greathouse and Cygan [2]. Interatomic potential and parameters for the atomic interactions was described using the ClayFF [3] force field. Force field parameters for Iodine were adopted from Reiser et al. [4]. The NaCl concentration in the Dutch Boom Clay formation water varies significantly, between 0.02M and 2.0M. The concentration is systematically changed in the model to assess its effect on iodine exclusion. In addition, an increasing amount of Cl^- ions within the solution is replaced by I^- ions to assess the effect of iodine concentration on its exclusion behavior, thereby always maintaining electroneutrality of the system. We examine how the density profiles change for each ionic species (Figure 1, right image) under the presence of varying NaCl and I^- concentrations. These profiles result in thicknesses of the anion exclusion zone and require further translation to ion specific, effective diffusion coefficients to be used in reactive transport models. For this purpose, the link will be made with actual clay rock characteristics such as multicomponent (clay) mineralogy and pore space architecture.

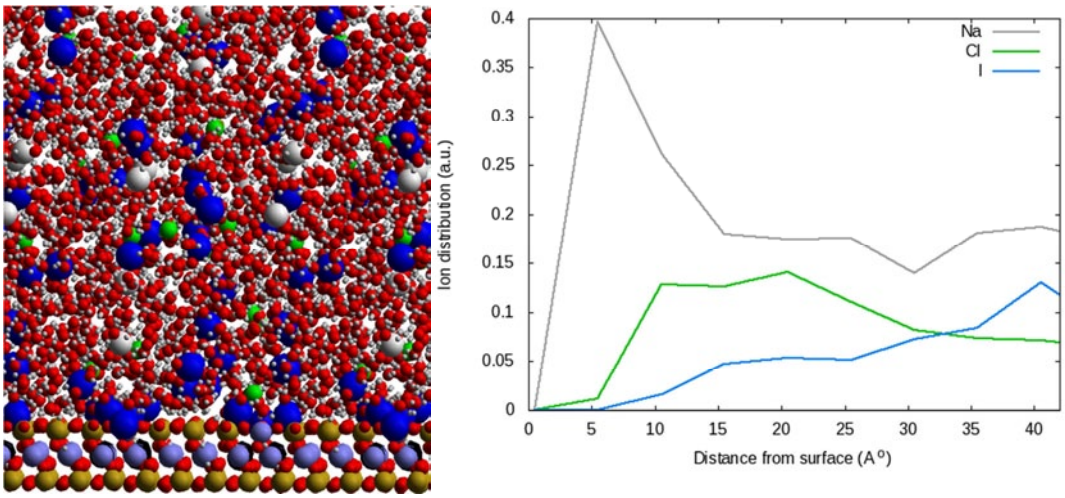


Figure 1. Depiction of the Na-montmorillonite and brine molecular system considered at a NaCl concentration of 1.6M (left). Concentration profile for Na, Cl and I with distance from the clay mineral surface after a 5ns simulation (right).

[1]

[1] Appelo C. A. J., Van Loon L. R. and Wersin P. (2010). Multicomponent diffusion of a suite of tracers (HTO, Cl, Br, I, Na, Sr, Cs) in a single sample of Opalinus Clay. Geochimica et Cosmochimica Acta 74, 1201-1219. doi:10.1016/j.gca.2009.11.013

[2] Greathouse, J. A., & Cygan, R. T. (2005). Molecular dynamics simulation of uranyl(VI) adsorption equilibria onto an external montmorillonite surface. *Physical chemistry chemical physics : PCCP*, *7*(20), 3580–6. doi:10.1039/b509307d

[3] Cygan, R. T., Liang, J.-J., & Kalinichev, A. G. (2004). Molecular Models of Hydroxide, Oxyhydroxide, and Clay Phases and the Development of a General Force Field. *The Journal of Physical Chemistry B*, *108*(4), 1255–1266. doi:10.1021/jp0363287

[4] Reiser, S., Deublein, S., Vrabec, J., & Hasse, H. (2014). Molecular dispersion energy parameters for alkali and halide ions in aqueous solution. *The Journal of Chemical Physics*, *140*(4), 044504. doi:10.1063/1.4858392

Roles of Interlayer Cation Species and Water Content in Montmorillonite Crystalline Swelling

Linlin Sun[1], Janne T. Hirvi[1], Jukka T. Tanskanen, Tim Schatz[2], Seppo Kasa[3], *Tapani A. Pakkanen*[1]

[1] Department of Chemistry, University of Eastern Finland P.O.Box 111, FI80101, Joensuu, Finland
[2] B+Tech Oy, Laulukuja 4, FI00420, Helsinki, Finland
[3] Posiva Oy, Olkiluoto, FI27160, Eurajoki, Finland

Montmorillonite, as the main mineral component of bentonite buffer MX-80, is well known for its distinct swelling properties.[1] The swelling potential largely depends on the interlayer cations and the water environment.[2,3] In this work, molecular dynamic simulations were employed to study the crystalline swelling behaviour of montmorillonites with four different interlayer cation compositions: sodium ions, calcium ions, and mixed sodium/calcium ions with molar ratios of 2:1 and 1:1. Our model includes two clay layers (**Figure 1**) into which cations and stepwise increasing amount of water molecules were evenly positioned to mimic the swelling. The molecular dynamic simulations were performed with the CLAYFF force field[4] using SPC water model.[5] The effect of temperature and pressure was also considered.

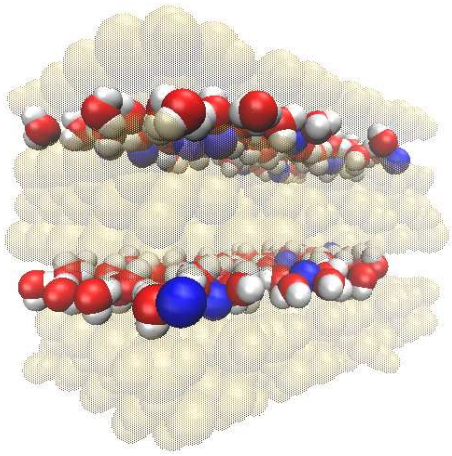


Figure 1. Structure of the sodium montmorillonite supercell.

Our simulations demonstrate that the *d*-spacings increase non-linearly with the increase in water content. In the sodium montmorillonite, the increase levels off around the *d*-spacing values of 12 Å and 15 Å, implying the formation of 1- and 2-layer water hydrates. The transition from 1-layer hydrate to 2-layer hydrate and the layer expansion takes place at lower water contents in calcium and mixed sodium-calcium montmorillonites than in sodium montmorillonite. This is due to the higher hydration energy of calcium than sodium ions, which promotes association of water molecules with calcium ions, leading uneven water distribution in the interlayer space and increased *d*-spacing (**Figure 2**). The corresponding structures are sensitive to temperature and pressure changes as water molecules may migrate between 1- and 2-layer hydrate structures. The influence of the interlayer ion composition was weak for hydrates consisting of more than two water layers.

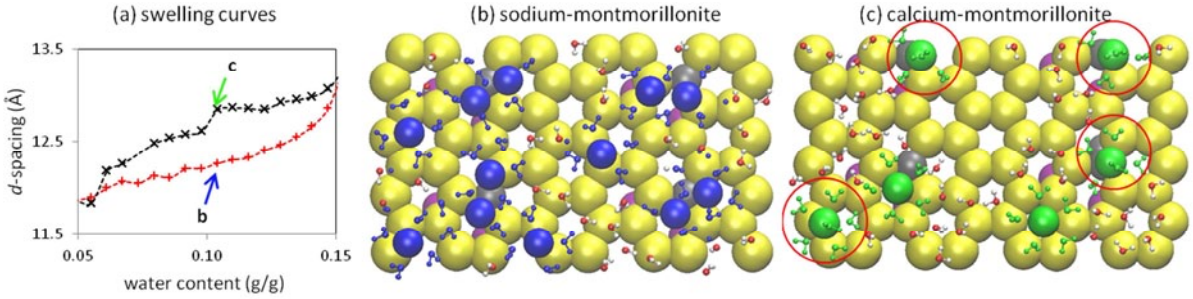


Figure 2. (a) The swelling curves for sodium montmorillonite and calcium montmorillonite are shown in dotted red and black curves, respectively. The final geometries at water contents of 0.11 g/g are also shown in (b) and (c). The red circles indicate strong water association to calcium ions and the formation of outer-sphere complexes.

The understanding of crystalline swelling is important for evaluating the feasibility and optimizing the performance of the bentonite buffer for geo-disposal of nuclear waste. The present work hopes to provide insight into the crystalline swelling behavior of bentonite clay at atomic level and also into interactions between structural units in montmorillonite.

References

1. Pusch, R. Use of bentonite for isolation of radioactive waste products. *Clay Miner*. 1992, 27, 353-361.
2. Young, D. A.; Smith, D. E. Simulations of clay mineral swelling and hydration: dependence upon interlayer ion size and charge. *The Journal of Physical Chemistry B*. 2000, 104, 9163-9170.
3. Marry, V.; Turq, P.; Cartailler, T.; Levesque, D. Microscopic simulation of structure and dynamics of water and counterions in a monohydrated montmorillonite. *J. Chem. Phys*. 2002, 117, 3454-3463.
4. Cygan, R. T.; Liang, J.; Kalinichev, A. G. Molecular models of hydroxide, oxyhydroxide, and clay phases and the development of a general force field. *The Journal of Physical Chemistry B*. 2004, 108, 1255-1266.
5. Berendsen, H. J.; Postma, J.; Van Gunsteren, W.; Hermans, J. Interaction models for water in relation to protein hydration. *Intermolecular forces*. *Springer*. 1981, 331-342.

Time evolution of MX-80 bentonite geochemistry under thermo-hydraulic gradients

Gómez-Espina, R., *Villar, M.V*

CIEMAT, Avd. Complutense 40, 28040 Madrid

The thermo-hydraulic (TH) tests reproduce in the laboratory the thermal and hydraulic conditions to which bentonite is subjected in the engineered barrier of a deep geological repository of radioactive waste. The Temperature Buffer Test (TBT project) was a full-scale test for HLW disposal that aimed at improving the understanding of the thermo-hydro-mechanical behaviour of buffers with a temperature around and above 100°C during the water saturation transient. ANDRA run this test at the Äspö HRL in cooperation with SKB (Svensk Kärnbränslehantering AB 2005). To simulate the conditions of the field test in the laboratory, 20-cm high columns of MX80 bentonite compacted at dry density 1.70 g/cm^3 with an initial water content of 16 percent were submitted in TH cells to heating and hydration by opposite ends. The temperature at the bottom of the columns was set at 140°C and on top at 30°C, and deionised water was injected on top at a pressure of 0.01 MPa. The tests were running for 496 (test TBT500, Gómez-Espina & Villar 2010) and 1510 days (test TBT1500, Gómez-Espina & Villar 2013). Upon dismantling water content, dry density, physical properties, geochemistry and mineralogy were determined in different positions along the bentonite columns.

At the end of the test a sharp water content gradient was observed along the columns, as well as an inverse dry density gradient. Hydration modified also the bentonite microstructure (Villar et al. 2012). An overall decrease of the smectite content with respect to the initial value took place, especially in the most hydrated areas –where the percentage of interestratified illite increased– and in the longer test. Towards the heater, the content of magnesium in the octahedral layer of the smectite increased. On the other hand, the content of cristobalite, feldspars and calcite increased. Smectite dissolution processes (probably colloidal) occurred, particularly in the more hydrated areas and in the longer test. The fact that deionised water was used for hydration could have favoured this process.

The cationic exchange complex was also modified as a consequence of the TH treatment, with a loss of exchangeable positions towards the heater. The content of exchangeable sodium decreased in both tests towards the heater, whereas the content of exchangeable magnesium in the proximity to the heater changed over time. Overall, the average calcium content in the interlayer increased over time. The calcium content increased also as a soluble salt, which could be related to gypsum dissolution, since the content of soluble sulphate also increased. Calcite precipitation processes could have taken place near the heater, accompanied by a decrease in alkalinity.

The content of soluble salts was determined by performing aqueous extracts. The composition of the pore water was then deduced thorough geochemical modelling from the aqueous extracts results (Figure 1). Due to the dissolution of low-solubility species and to the loss of exchangeable positions in the smectite, the content of soluble salts in the pore water increased with respect to the original one, especially in the longer test and in the more hydrated areas. The solubilized ions were transported; sodium, calcium, magnesium and sulphate having a similar mobility, which was in turn lower than that of potassium and chloride. Overall the pore water evolved from sodium bicarbonate type to sodium sulphate type in the hydrated areas and to sodium chloride type in the proximity to the heater, due to the low degree of water saturation.

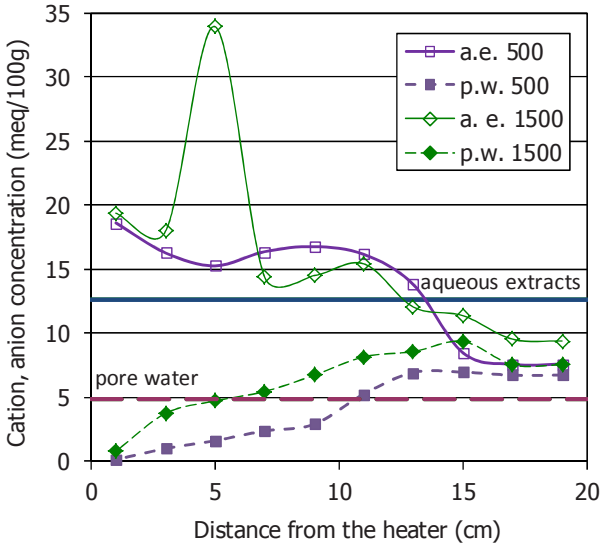


Figure 1: Ion concentration along the bentonite column as measured in the aqueous extracts (a.e.) and in the pore water (p.w., computed with Phreeqc) for the two tests (the horizontal lines indicate the values for the original sample)

When extrapolating these data to real repository conditions, the experimental constraints of this kind of tests must be taken into account, in particular, the fact that deionised water – instead of groundwater– was used for saturation and that evaporation through the base of the cell took place, which probably made desiccation more intense than in the real case.

Gómez-Espina, R. & Villar, M.V. 2010. Geochemical and mineralogical changes in compacted MX-80 bentonite submitted to heat and water gradients. Applied Clay Science 47: 400-408.

Gómez-Espina, R. and Villar, M.V., 2013. Modificaciones en la bentonita MX-80 compactada sometida a tratamiento termo-hidráulico. 1290, CIEMAT, Madrid.

Svensk Kärnbränslehantering AB. 2005. Äspö Hard Rock Laboratory. Annual Report 2004. SKB Technical Report TR-05-10. Stockholm, Sweden. 211 pp.

Villar, M. V., Gómez-Espina, R., Gutiérrez-Nebot, L., Campos, R., Barrios, I. 2012. Physical changes in MX-80 bentonite saturated under thermal gradient. ANDRA 5th International Meeting Clays in Natural and Engineered Barriers for Radioactive Waste Confinement, Montpellier, October 2012. Abstracts, pp 312-313, AP/PTO/10.

The research leading to these results received funding from ENRESA (Spanish Agency for Nuclear Waste Management) and the European Atomic Energy Community's Seventh Framework Programme (FP7/2007-2011) under Grant Agreement n°249681, the PEBS project.

MOLDATA: A Thermodynamic Database supporting phenomenological studies of the Belgian RD&D programme

S. Salah[1], L. Wang[1], H. De Soete[1], C. Bruggeman[1], and S. Brassinnes[2]

[1] Belgian Nuclear Research Centre (SCK•CEN), Boeretang 200, B-2400 Mol, Belgium
(Corresponding author: ssalah@sckcen.be)
[2] Belgian Agency for Radioactive Waste and Enriched Fissile Materials (ONDRAF/NIRAS), Avenue des Arts 14, B-1210 Brussels, Belgium

In Belgium, ONDRAF/NIRAS (Belgian Agency for Radioactive Waste and Enriched Fissile Materials – O/N) represents the authority responsible for the management of all types of radioactive waste. The long-term management solution proposed by ONDRAF/NIRAS for category B&C waste, corresponding to high-level and/or long-lived radioactive waste and spent fuel is deep geological disposal in poorly indurated clay (i.e. Boom Clay or Ypresian Clays). As a preliminary step to the siting process, O/N is currently preparing its first Safety and Feasibility Case (SFC1). In Belgium, the safety concept for geological disposal of B&C waste considers the installation of a multi-barrier repository system within poorly indurated clays (i.e. Ypresian clays, Boom Clay).

MOLDATA has been mainly developed by SCK•CEN within the frame of the current RD&D programme of O/N. The main objective of O/N to initiate the MOLDATA project together with SCK•CEN was the need for a unique, high-quality and internally consistent thermodynamic database able to be used for all geochemical and reactive transport calculations performed in the frame of the phenomenological studies and supporting the safety assessment studies.

Such calculations are indispensable to evaluate geochemical processes (e.g., sorption, solubilities…) affecting the migration/retention behaviour of radionuclides under laboratory (short-term) and/or in-situ conditions (e.g., pH, pCO_2,…), but also to enable predictions about their long-term behaviour in a disposal facility under evolving conditions.

The reliability of such calculations is however highly depending on the quality of the used thermodynamic data. With respect to thermodynamic database development, quality means that the data must be correctly implemented, numerically accurate, traceable, internally consistent, up-to-date and well documented. Another objective in database compilation is to strive for completeness, meaning that the solid, aqueous and gas species comprised in the database should enable the adequate representation of the different repository constituents, such as the waste forms (e.g. glass and SF), the engineered barrier materials (e.g. bentonite, cement…), as well as the host rock, but also the assessment of the geochemical conditions prevailing and evolving in the near-field and far-field of a repository.

In contrast to other approaches (i.e. Swiss, German), the compilation strategy chosen for MOLDATA has been rather focused on data completeness than on data review. It was considered that sufficient sources of high quality data are available and that the data for MOLDATA could be extracted from these without further verification. With respect to radioactive waste relevant radionuclides, the review books published by the Nuclear Energy Agency (OECD/NEA) represent probably the most esteemed sources comprising data of very high quality. Besides these data, MOLDATA comprises data from the ANDRA TDB (Thermochimie v. 5), the LLNL TDB (thermo.com.v8.r6+.dat) and the NAGRA/PSI TDB (Database 01/01). In order to incorporate as much as possible the most up-to date data, also literature data were screened during the compilation procedure.

It should be mentioned, that for the major elements Si, Al and Fe, a thorough review of the thermodynamic data was considered to be needed. It is well known, that large discrepancies between

the available thermodynamic data for these elements exist. Therefore, special effort was put into the evaluation and consistency verification of these elements.

The extraction, selection and consistency verification of the data from the above mentioned sources were done by using the in-house developed software, i.e. the Geochemical Database Processor GDP (De Soete et al., 2010). The so-called Central Database represents the "core" of the GDP, into which the datasets from the different sources are uploaded (via import filters) and stored in a standardized format. The data selected to be downloaded can be exported via specific filters enabling the generation of output files in different formats (i.e. GWB or PHREEQC).

If available, all standard state properties (i.e. the standard molar Gibbs free energy of formation $\Delta_f Gm°$, the standard molar enthalpy of formation $\Delta_f Hm°$, the standard molar entropy of formation $\Delta_f Sm°$ and the standard molar heat capacity $\Delta_f Cp,m$) of the species are extracted from the different sources. Based on the selected basis species for MOLDATA and the free energy of formation data ($\Delta_f Gm°$), the molar Gibbs energy of reaction and reaction constants ($\Delta G_r m°$/logβ/logK° values) are calculated (during data export) for the equilibrium under consideration. In this way, internal consistency of the reaction constants can be ensured. At the current stage, MOLDATA comprises only reaction constants for 25°C, but it is foreseen to incorporate temperature dependency in future versions. During data export, it is possible to choose between three activity coefficient models, i.e. the Davies model, the WATEQ DH convention, and the B-dot model.

The current MOLDATA release (MOLDATA_R2) comprises in total ~4000 species (84 basis species, 74 redox species, 1505 aqueous species, 1446 minerals and 190 gases) and is available in two formats, i.e. GWB and PHREEQC.

As mentioned before, the application of MOLDATA within the frame of SFC1 is expected to support the assessment of the long-term evolution of the disposal components, the pore water geochemistry, as well as the geochemical processes influencing the retention and migration of the waste relevant radionuclides. These processes include mainly the speciation, solubility and sorption of the radionuclides under the different near-field and far-field conditions, as well as alteration, corrosion and perturbation phenomena.

The reliability of a thermodynamic database is generally evaluated by performing so-called benchmark calculations revealing the capability to reproduce independent experimental data gathered from literature, laboratory experiments and/or field observations. MOLDATA was shown to be able to successfully reproduce such data, but also in-house obtained experimental data. In this contribution some results of these calculations will be presented and discussed with respect to other TDBs (notably the source databases used to compile MOLDATA).

ACKNOWLEDGEMENT
This study was performed in cooperation with, and with the financial support of the Belgian Agency for Radioactive Waste and Fissile Materials (ONDRAF/NIRAS), as part of its programme on geological disposal of high-level/long-lived waste.

References

De Soete H. (2010): The Geochemical Data Processor. User's Manual and Functions Library. Internal SCK-CEN document.

Wang L., Salah S. and De Soete H., MOLDATA: A thermochemical database for phenomenological and safety assessment studies for disposal of radioactive waste in Belgium – Data compilation strategy. External Report SCK•CEN ER-121, 2011.

Prediction of R_d values for radionuclides in Boom Clay with an independent multi-surface model

J.C.L. Meeussen[1], T.J. Schröder[1], E. Rosca-Bocancea[1] J.J. Dijkstra[2], C. Bruggeman[3], and N. Maes[3]

1) Nuclear Research and Consultancy Group, Westerduinweg 3, 1755 LE, Petten, The Netherlands. 2) Energy research Centre of the Netherlands, Westerduinweg 3, 1755 LE, Petten, The Netherlands. 3) Belgian Nuclear Research Centre, Boeretang 200, 2400 Mol, Belgium. Corresponding author: meeussen@nrg.eu

Introduction

A number of European countries currently consider argillaceous rock formations as host rock for deep geological radioactive waste storage (Altmann et al. 2012). The main advantage of clay rock formations is the combination of a very low hydraulic conductivity with a high sorption capacity which strongly reduces and delays the migration of radionuclides towards the biosphere. Furthermore, the plasticity and swelling behaviour of clay rocks cause self-healing of cracks and ensure that the low hydraulic conductivity is maintained in the long-term.
The long-term safety of a repository depends on the capacity of the host formation to delay radionuclide fluxes towards the biosphere. Due to the low hydraulic conductivity of clay rock formations, diffusion is generally assumed to be the main mechanism for radionuclide migration. For each nuclide, the retardation effect of sorption may be summarized by a retardation factor (R_d). This is a conditional constant which is valid for a specific host rock material and geochemical conditions and is commonly derived from laboratory experiments (Miller and Wang 2012). Empirically determined retardation factors unfortunately do not give insight into the sensitivity of the measured values for varying conditions in space and /or time. This kind of insight requires a basic level of understanding the underlying processes. Sufficient understanding of these processes is also necessary to extrapolate short term laboratory values to long term field values.

The aim of the present work, which is carried out as part of OPERA, the Dutch national research programme on geological disposal of radioactive waste, therefore is to:

- Evaluate the current level of process understanding by verifying to what extend state-of-the-art sorption models are able to independently predict empirical retardation values for Boom Clay formations in the Netherlands.

- Evaluate the sensitivity of the calculated retardation values for a number of important input parameters (such as pH, pe, salt concentration, dissolved organic matter, iron oxide and clay content)

Modelling approach

One way to evaluate the current level of understanding of the underlying sorption processes is to test to what extend the observed sorption behaviour can be explained by independent prediction of sorption using current multi-surface sorption models. For that purpose we

implemented a multi-surface model for Boom Clay within the geochemical modelling framework ORCHESTRA (Meeussen, 2003), using distinct sorption models for iron oxides, clay, organic matter (dissolved and particulate) in a similar way as described by Dijkstra et al. (2009). Additionally a number of relevant precipitates were included (e.g. Pyrite, Calcite). Data of the physical and chemical composition of Boom Clay were taken from literature. With the resulting geochemical "Boom Clay Model", the distribution of a number of safety-relevant radionuclides with contrasting chemical behaviour (including Se, U, Tc, Th, I) over the solid and dissolved phase, and the resulting retardation factor R_d, can be calculated for a wide range of environmental conditions. To evaluate the sensitivity of the calculated R_d for different environmental settings, a Monte Carlo simulation was carried out (10.000 realizations) for the following input parameters: pH, pe, element concentrations, salt concentration, clay content, organic matter content, dissolved organic matter content, iron oxide content, porosity.
The calculation results are compared with retardation data provided in literature, and it is analysed whether the proposed processes can explain the observed migration behaviour. Subsequently, the consequence of parameter variation for long-term safety assessment calculations is evaluated.

Results

The results of this work make clear:

- To what extend independently predicted retardation factors R_d are in agreement with empirical retardation values
- What the sensitivities of the calculated R_d-values are for a number of important input parameters

Acknowledgement

This research has received funding from the Dutch research programme on geological disposal OPERA. OPERA is financed by the Dutch Ministry of Economic Affairs, Agriculture and Innovation and the public limited liability company Elektriciteits-Produktiemaatschappij Zuid-Nederland (EPZ) and coordinated by COVRA".

References

Altmann, S., Tournassat, C., Goutelard, F., Parneix, J.C., Gimmi, T. and Maes, N., 2012. Diffusion-driven transport in clayrock formations. Applied Geochemistry, 27, p.463-478.

Meeussen, J.C.L., 2003. ORCHESTRA: An Object-Oriented Framework for Implementing Chemical Equilibrium Models. Environmental Science &Technology, 37 (6), p.1175-1182.

Miller, A.W., and Wang, Y, 2012. Radionuclide interaction with clays in dilute and heavily compacted systems: a critical review. Environmental Science &Technology, 46, p.1981-1994.

Dijkstra, J. J., Meeussen J.C.L., Comans R.N.J., 2009, Evaluation of a generic multisurface sorption model for inorganic soil contaminants, Environmental science & technology, 43 (16) p. 6196-6201.

Evaluation of waste form behaviour in a geological repository for high-level radioactive waste in Boom Clay in the Netherlands

Guido Deissmann[1,2], **Kirsten Haneke**[2], **André Filby**[2], **Rob Wiegers**[3], **Dirk Bosbach**[1]

[1]Forschungszentrum Jülich GmbH, Institute for Energy and Climate Research: Nuclear Waste Management and Reactor Safety (IEK-6), 52425 Jülich, Germany (g.deissmann@fz-juelich.de); [2]Brenk Systemplanung GmbH, 52080 Aachen, Germany; [3]IBR Consult BV, 6081PH Haelen, The Netherlands

The primary objective of the Dutch research programme into geological disposal of radioactive waste (OPERA - OnderzoeksProgramma Eindberging Radioactief Afval) is the development of initial conditional safety cases for generic repositories in the Tertiary Boom Clay and Zechstein rocksalt formations in the Netherlands. The generic disposal concept for high-level radioactive waste (HLW) in Boom Clay pursued within this context is based on the Belgian supercontainer concept [1]. In this concept, cementitious materials are extensively used in the engineered barrier system (i) as buffer within the waste container, (ii) as backfilling grout, and (iii) in the construction material for the disposal gallery linings. Thus the post closure conditions in the near-field will be governed by the interaction of Boom Clay porewaters with cementitious materials, leading to highly alkaline conditions in the vicinity of the emplaced wastes. The HLW inventory for the OPERA safety case comprises in particular vitrified wastes (HLW glass) from the reprocessing of light water reactor (LWR) fuels from commercial nuclear reactors and spent research reactor fuels, besides spent uranium targets from molybdenum isotope production, and non-heat generating wastes such as compacted hulls and ends from fuel assemblies.

In this paper we present and discuss initial results of the evaluation of the corrosion behaviour of and the radionuclide release from vitrified HLW and spent fuel from research reactors under the disposal conditions encountered in a geological repository in Boom Clay in the Netherlands. The overall aim of this project is (i) to provide a coherent picture of the radionuclide release from HLW disposed in a generic repository in Boom Clay, (ii) to increase the understanding of waste form evolution (i.e. leaching and dissolution behaviour with time) and the radionuclide migration behaviour in the near-field, and finally (iii) to develop source terms for relevant radionuclides that are the main contributors to dose in the long-term in support of the post closure safety assessments. The results derived address directly the safety function "delay and attenuation of releases" relevant after the failure of the waste canisters when the waste forms come into contact with the near-field water. Due to the variability of the porewater composition encountered in the Boom Clay in the Netherlands and the generic nature of the OPERA safety case (i.e. without selection of a repository site), various scenarios regarding the composition of the near-field water resulting from the interaction of Boom Clay porewater with the cementitious materials and their evolution with time will be discussed.

Vitrified HLW within the OPERA inventory comprise predominantly R7T7 glasses from spent fuel reprocessing in La Hague, France, and, to a lesser extent, glasses from the reprocessing of fuels from the Dodewaard NPP in Sellafield, UK. The dissolution behaviour of the glasses depends on their composition (e.g. Mg-bearing glasses such as MW produced in the Sellafield vitrification plant exhibit generally a lower durability than the French R7T7 glasses) as well as on the post closure conditions in the near-field. In general, HLW glass dissolution is expected to be more rapid at high pH in alkali-rich waters compared to waste emplacement in a non-cementitious, clay-based repository, leading to the formation of altered glass and secondary silicate phases, some of which may retain certain radionuclides (e.g. [2]). However, the presence of elevated calcium concentrations such as in evolved cement porewaters buffered by portlandite appears to reduce the glass dissolution rate (e.g. [3]), suggesting a favourable effect on HLW glass durability under high pH conditions. Thus the evolution of near-field chemistry and the extent of cement alteration resulting from the exchange with Boom

Clay porewaters will directly impact the glass corrosion rates, the formation of glass alteration layers and secondary phases as well as radionuclide release with time.

Research reactor fuels relevant within the OPERA safety case are plate-shaped dispersion type fuels consisting of uranium-aluminide (UAl_x) or uranium-silicide (e.g. U_3Si_2) fuel particles dispersed in an aluminium matrix that is metallurgicaly bonded to aluminium cladding, employing either high-enriched uranium (HEU, up to 80 to 95 wt.% ^{235}U) or low-enriched uranium (LEU, up to 20 wt.% ^{235}U). Corrosion data obtained for these types of fuels in salt brines, granite waters, or clay waters indicate a – with respect to the time scales relevant for geological disposal – practically instantaneous corrosion after coming into contact with groundwater (i.e. after failure of the waste canisters) [4, 5]. A similar behaviour is suggested under disposal conditions in a cementitious repository in Boom Clay, due to high aluminium corrosion rates under alkaline conditions leading to a fast disintegration of the fuels. The amount, nature and stability of potential secondary phases formed during the corrosion process (e.g. layered double hydroxide phases (LDH)) that may retain certain radionuclides depend on the near field conditions and is as such the degree of interaction of the Boom Clay pore waters with the cementitious materials and the stage of cement degradation at the time of the failure of the waste canisters. Uranium and some actinides are assumed to be solubility limited under the expected near-field conditions.

References

[1] Verhoef, E., Neeft, E., Grupa, J., Poley, A. 2011. Outline of a disposal concept in clay. OPERA-PG-COV008. COVRA, Vlissingen, 1–17.
[2] Lemmens, K., Cachoir, C., Ferrand, K., Mennecart, T., Gielen, B., Vercauter, R. 2012. Interaction of cementitious materials with high-level waste matrices. In: Cementitious materials in safety cases for geological repositories for radioactive waste: role, evolution and interaction, NEA/RWM/R(2012)3, 129–130.
[3] Utton, C.A., Hand, R.J., Bingham, P.A., Hyatt, N.C., Swanton, S.W., Williams, S.J. 2013. Dissolution of vitrified wastes in a high-pH calcium-rich solution. Jour. Nucl. Mat. 435, 112–122.
[4] Brücher, H., Curtius, H. 2007. Investigations into the behaviour of research reactor fuel elements in repository relevant aquatic phases. Transactions 11th International Topical Meeting Research Reactor Fuel Management (RRFM), Lyon, France, 11– 15 March 2007, 5 p.
[5] Curtius, H., Kaiser, G., Müller, E., Bosbach, D. 2011. Radionuclide release from research reactor spent fuel. Jour. Nucl. Mat., 416, 211–215.

Acknowledgements

The research leading to these results has received funding from the Dutch research programme on geological disposal, OPERA. OPERA is financed by the Dutch Ministry of Economic Affairs and the public limited liability company Elektriciteits-Produktiemaatschappij Zuid-Nederland (EPZ), and is coordinated by COVRA.

Montmorillonite interlamellar surface chemistry: Effect of magnesium ion substitution on cation adsorption

Lasse P. Lavikainen*[1], Jukka T. Tanskanen[1], Timothy Schatz[2], Seppo Kasa[3], Tapani A. Pakkanen[1]

[1]Department of Chemistry, University of Eastern Finland, P.O. Box 111, FI-80101, Joensuu, Finland
[2]Posiva Oy, FI-27160, Olkiluoto, Eurajoki, Finland
[3]B+Tech Oy, FI-00420, Laulukuja 4, Helsinki, Finland

Montmorillonite structure and its interlamellar surfaces were studied on molecular level by quantum chemical methods. Positions of Mg-substitutions in the octahedral sheet of the layer structure and their effect on interlamellar cation-surface interaction were investigated by utilizing dry periodic Na- and Ca-montmorillonite models. It was found that Mg-substitutions may occur in several configurations in the octahedral sheet and that cation-surface interaction strength is linearly correlated with the inverse distances between cations and Mg-substitutions in the periodic lattice (figure 1). The results were rationalized by examining surface charge density and atomic partial charges in the system, which indicated that surface charge density is most negative near the Mg-substitutions due to lower partial charge of substituting Mg(II) in comparison to unsubstituted Al(III). Therefore adsorption sites close to Mg-substitutions attract cations most strongly. Montmorillonite clay mineral is the main component in bentonite clay, which is the candidate buffer material for long-term nuclear waste disposal among many other applications.

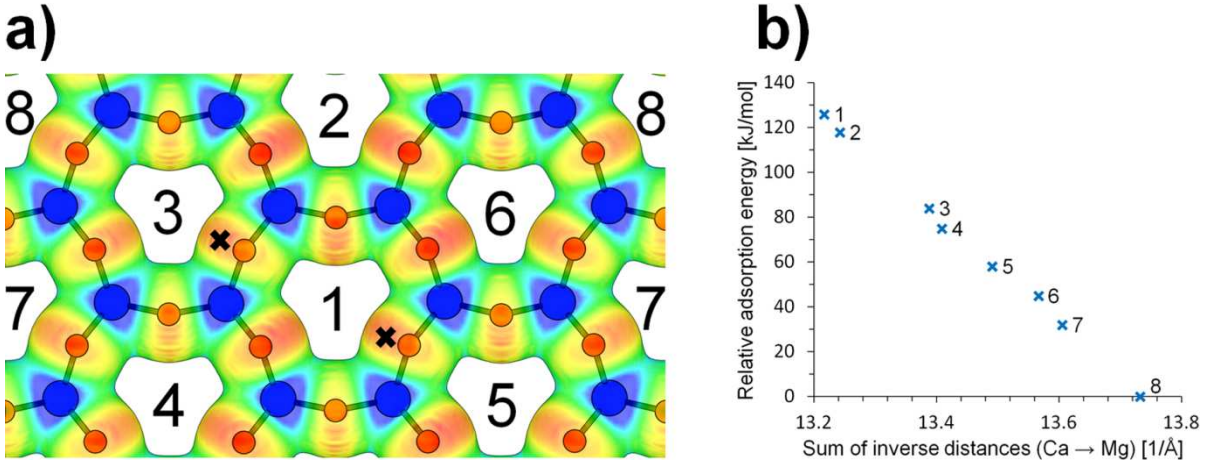


Figure 1. a) Electrostatic potential mapped on montmorillonite electron density isosurface. The most negative areas are indicated by red color and positive areas by blue color. The potential is most negative near Mg-substitutions, whose position in the octahedral layer is indicated by black crosses. Cation adsorption sites are numbered in the order of decreasing adsorption energy. **b)** Ca-cation adsorption energies against sum of inverse distances between Ca^{2+} and Mg-substitutions in the periodic lattice. The adsorption energies are reported in relation to site with lowest adsorption energy, which is set to zero. Since the sum of inverse distances runs over infinity, the sum was limited on the basis of ~99% convergence, which corresponds to 32 Å radius.

Evaluation of LILW degradation processes and products in a geological repository for radioactive waste in Boom Clay in the Netherlands

André Filby[1], **Guido Deissmann**[1,2], **Rob Wiegers**[3]

[1]Brenk Systemplanung GmbH, Heider-Hof-Weg 23, 52080 Aachen, Germany (a.filby@brenk.com),
[2]Forschungszentrum Jülich GmbH, Institute for Energy and Climate Research: Nuclear Waste Management and Reactor Safety (IEK-6), 52425 Jülich, Germany; [3]IBR Consult BV, 6081PH Haelen, The Netherlands

OPERA is the Dutch acronym for research programme for geological disposal of radioactive waste which focusses on the development of initial conditional safety cases for generic repositories for high-level and low-intermediate level (LILW) radioactive waste in the Boom Clay and Zechstein rocksalt formations in the Netherlands.
In the disposal concept aspired in this context, cementitious materials are extensively used, e.g. as buffer within the waste containers, as backfill material and also as construction material. Thus, highly alkaline conditions are expected in the vicinity of the emplaced wastes.

LILW arises mainly from activities with radioactive materials or radioisotopes in the industry, research institutions and hospitals. It includes lowly contaminated materials, such as plastics, cellulose or metal and is stored in containers with volumes of 200, 400, 600, 1.000 or 1.500 litres at COVRA.

According to [1],

- the waste is likely to contain a significant fraction of solid organic/degradable material,
- the waste may contain a significant fraction of NaOH/KOH and is processed by COVRA into a stable solid cementitious waste form for storage.

In this study, the initial results of the evaluation of degradation processes and products (e.g. gas generation) of the LILW matrix are presented. Several chemical and physical processes relevant for the LILW degradation and the formation of degradation products are investigated, whereas focussing on the investigation of the chemical and physical behaviour of the degradation products and their interaction with the host rock and the engineered barrier system, respectively.
Due to the expected high amount of organic materials in the LILW, emphasis is laid in this paper on the degradation processes of cellulose and hemicellulose under alkaline (repository) conditions, rate and extent of degradation with time and the identification of degradation products (e.g. isosaccharinic acid, xylosaccharinic acid and small chain fatty acids [2]) under near-field conditions. Furthermore, the results regarding the investigation on the degradation processes and degradation products of plastics, polystyerene and PVC under repository conditions are discussed.

Due to the variability of the porewater composition encountered in the Boom Clay in the Netherlands and the generic nature of the OPERA safety case (i.e. without selection of even a potential repository site), various scenarios regarding the composition of the near-field water resulting from the interaction of Boom Clay porewater with the cementitious materials and their evolution with time will also be discussed.

References

[1] Meeussen, J.C.L., Rosca-Bocancea, E. 2014. Determination of the inventory, Part B: Matrix composition. OPERA-IR-NRG1112B. COVRA, Vlissingen.

[2] Humphreys, P. N., Laws, A., Swanton, S.W. 2010. A Review of Cellulose Degradation and the Fate of Degradation Products Under Repository Conditions. Serco/TAS/002274/001, Issue 2. SERCO, Oxfordshire, UK.

Multi-tracer profile at high spatial resolution across the Opalinus Clay at the Mont Terri URL

H.N. Waber[1], D. Rufer[1], L. Kennell[2], D. Traber[3]

[1] Rock-Water Interaction, Inst. of Geological Sciences, University of Bern, Switzerland (*waber@geo.unibe.ch)
[2] NWMO, 22 St. Clair Avenue East, M4T 2S3 Toronto, Ontario, Canada
[3] Nagra, Hardstrasse 73, Wettingen, Switzerland

Understanding solute transport on a large scale is important when assessing the performance of natural barrier systems such as a clay-rich sedimentary rock sequence. Testing of laboratory-derived transport and chemical parameters is conducted by modelling solute transport on the scale of the host rock formation. The results of the modelling need to be consistent with field observations, such as porewater tracers determined across the lithology of interest and palaeo-hydrogeological evolution of the site. With regard to the distribution of natural porewater tracers, field observations require the appropriate degree of spatial resolution in order to unequivocally detect modifications induced by changes in the boundary conditions over the time period of interest.

At the Mont Terri URL, a 250 m long borehole was recently core-drilled across the entire Opalinus Clay including its hanging wall and footwall as part of the DB and DB-A Experiments. The inclined borehole, BDB-1, encountered variably composed limestone and calcareous marls of the Hauptrogenstein (0–37 m borehole length, BHL) and the Passwang Formation (37–106 m BHL) followed by the intercalation of different facies of the Opalinus Clay (106–238 m BHL) and the underlying argillaceous marls of the Staffelegg Formation (238–248 m BHL, former Liassic). It was drilled using limestone groundwater as drilling fluid down to ~90 m BHL followed by air-flushed drilling down to the end of the borehole. The design of the drilling allowed, for the first time, the collection of samples for porewater chemical, isotopic and noble gas tracers along a borehole profile at a high spatial resolution across the entire sedimentary sequence. A groundwater sample was collected from a packer interval at 51–59.7 m BHL within the Passwang Formation, ~45 m from the top of the Opalinus Clay. Borehole logging indicated no other water inflows across the entire profile, though some moist zones were encountered during drilling between 97 m and 105 m BHL.

The core samples (~30 cm in length) reveal significant differences in clay content and water-loss porosity between the individual stratigraphic units and less so between the different facies in the Opalinus Clay (Figure 1). This renders the application of a uniform geochemical porosity across the entire profile questionable.

Across the Opalinus Clay the spatial distribution of chemical, isotopic and noble gas tracers generally confirms results previously obtained from individual, short boreholes drilled at different locations along the Mont Terri URL (e.g. Pearson et al., 2003). Adopting for the Opalinus Clay samples the well established Cl-accessible porosity of 0.54, an asymmetric concentration profile is obtained with minimum Cl^- and Br^- porewater concentrations of about 2 g/kg_{H2O} and 7 mg/kg_{H2O}, respectively, at the interface with the overlying Passwang Formation and maximum concentrations of about 12.6 g/kg_{H2O} and 40 mg/kg_{H2O}, respectively, at the interface with the underlying Staffelegg Formation. The shape of the chemical tracer profiles is nicely reflected by those of the porewater $\delta^{18}O$ and $\delta^{2}H$-values, which range from –8.84‰ to –7.44‰ VSMOW and –64.4 to –49.2‰ VSMOW, respectively (Figure 2). In contrast, noble gas concentrations show relatively stable values across the Opalinus Clay, are enriched in the radiogenic isotopes and vary only within a factor of about 2–4.

At the interfaces between shaly and sandy facies, excursions from the generally smooth profile shape are observed for chemical tracer concentrations, which are not resolved outside the analytical uncertainty in isotope tracers. In spite of a rather small distance between samples (<3 m), it cannot currently be resolved if these differences are due to differences in the Cl-accessible porosity (so that the assumption of a homogenous Cl-accessible porosity becomes invalid) or due to a geologically young perturbation of the porewater system in the Opalinus Clay. In the Staffelegg Formation, a decrease is suggested for all tracer concentrations based on the limited number of samples. The lower boundary of the system, however, was not intersected by the BDB-1 borehole. From the interface Passwang For-

mation–Opalinus Clay towards shallower depth, several small-scale fluctuations occur in the porewater $\delta^{18}O$- and $\delta^{2}H$-values indicating the superposition of different signals transferred from the groundwater into the porewater and vice versa over the more recent past. Over the same section, the apparent porewater Cl^- and Br^- concentrations display a highly heterogeneous behaviour when a homogenous Cl-accessible porosity is applied. Similar profile shapes – as could be expected from the palaeohydrogeologic evolution of the site – are, however, only obtained if the fraction of the Cl-accessible porosity is varied between about 0.65 and 1 according to the clay content of the samples.
Porewater concentrations of Cl^-, Br^-, He, Ar, ^{18}O and ^{2}H adjacent to the water-conducting zone are different from that of the collected groundwater in spite of the groundwater's rather long residence time as indicated by its low ^{14}C content (1.10±0.12 pmc). Until independent estimates of Cl-accessible porosity are available for the rock samples in the Passwang Formation, exchange between the groundwater and porewater and their time dependence cannot be further assessed because absolute concentrations of the chemical tracers are required.

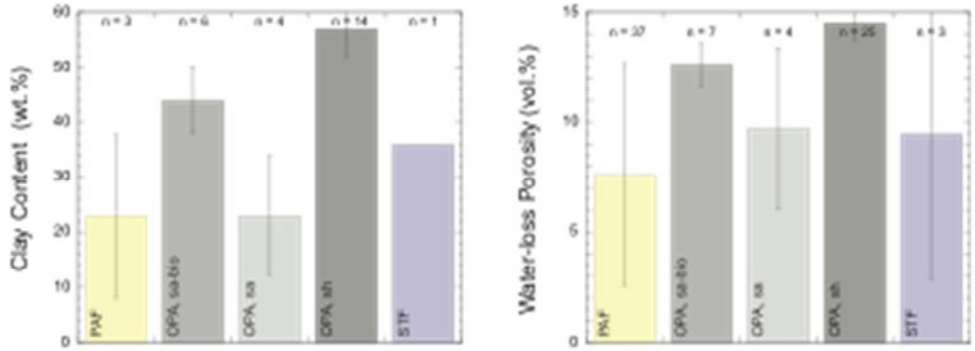


Figure 1: Average values and standard deviation of clay content and water-loss porosity of different stratigraphic units (PAF: Passwang Formation, OPA: Opalinus Clay with sa-bio = sandy-bioclastic, sa = sandy and sh = shaly facies, STF: Staffelegg Formation; n= number of samples).

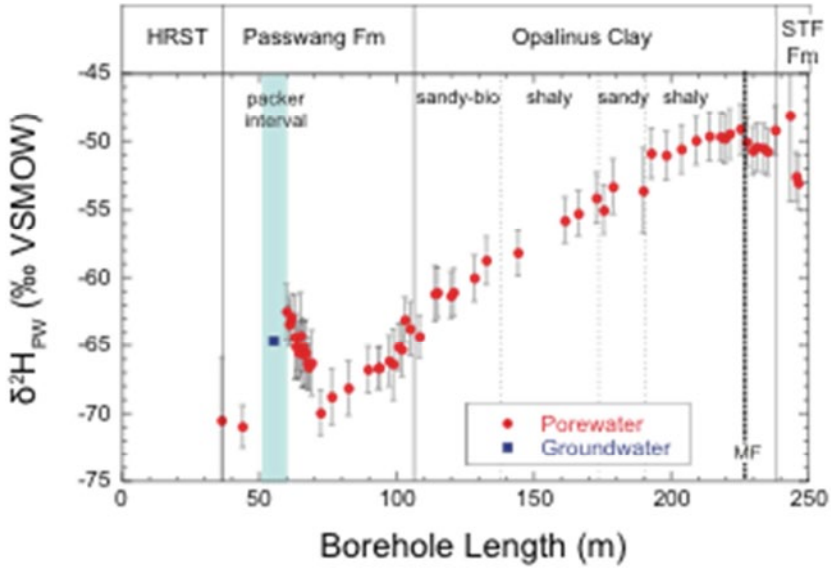


Figure 2: Distribution of $\delta^{2}H$ in samples from borehole BDB1 across the Opalinus Clay at the Mont Terri URL (HRST = Hauptrogenstein, STF = Staffelegg Formation; MF = Main Fault).

References

Pearson, F.J., Arcos D., Bath, A., Boisson, J.Y., Fernandez, A.M., Gaebler, H.E., Gaucher, E.C., Gautschi, A., Griffault, L., Hernan, P. & Waber, H.N. (2003). Mont Terri Project - Geochemistry of Water in the Opalinus Clay Formation at the Mont Terri Rock Laboratory. Swiss Federal Office of Water and Geology (FOWG), Geology Series No. 5, Bern, Switzerland.

Boundary phenomena at the clay solid/liquid interface

Rasmus Eriksson **and Tim Schatz**

B+Tech Oy, Laulukuja 4, Helsinki, Finland

One scenario of interest for the long-term safety assessment of a spent nuclear fuel repository involves the loss of bentonite barrier material through contact with dilute groundwater at a transmissive fracture interface. Small-scale, flow-through, artificial fracture experiments demonstrated that the quasi-free swelling of compacted montmorillonite into thin, horizontal fractures in the presence of dilute aqueous solutions leads to the formation of an inner, rigid gel phase and an outer, colloidal phase, with a distinct interface separating these two phases [1]. However, the exact mechanism leading to the formation of the colloidal phase, followed by erosive loss of material due to flowing (ground)water, has not been determined.

Optical Coherence Tomography (OCT) imaging of the interface between the inner and the outer phase of swelling clay material inside an artificial fracture revealed that a domain of sedimented colloidal material extends radially outwards from the perimeter of the inner gel phase (see Figure 1).

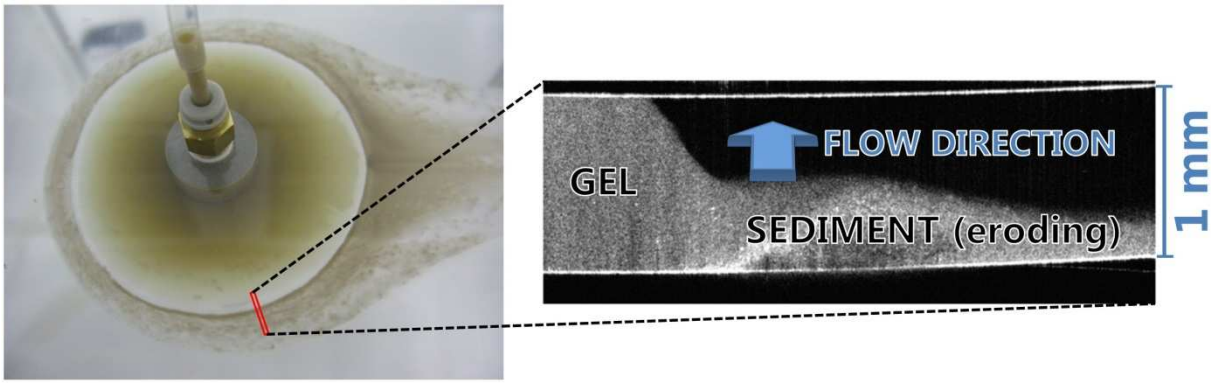


Figure 1. On the left: Montmorillonite expanding and eroding into an artificial fracture under dilute conditions. On the right: OCT image of the interfacial zone between the gel-like, inner body of material and the outer, colloidal phase (as indicated in red on the left).

OCT imaging was also performed in the presence of imposed flow through the artificial fracture system. At volumetric flow rates ranging between 1 - 10 ml/min only small perturbations could be observed to occur in or around the sedimented zone, but overall, the sediment appears to remain structurally intact. Even at flow rates of 200 mL/min the sedimented zone remains mostly intact, although large flocs can be seen to move over the sedimented zone at this flow rate. It is likely that the strongly deposited sediment originates from colloidal material which is initially generated at the gel/sol interface and which later aggregates, downstream of the source, leading to the formation of the sedimented zone.

The mechanism behind particle detachment from the inner, rigid body is not precisely known, but may be due to either mechanical or chemical processes (or both). We have investigated the rheological properties of batch montmorillonite suspensions of differing composition (in terms of solids content and electrolyte concentration) designed to cover a range of predicted physicochemical states of the swelling clay inside an artificial fracture. Based on these results we have determined that for Na clay and 50/50 mixtures of Na and Ca clay, the solids content near the outer perimeter of the inner, rigid body lies between 2 - 4 vol %. In this range the clay suspensions exhibit a distinct jump from predominantly viscous character to predominantly gel-like character (see Figure 2a). By contrast, Ca clay displays no gel-like character, even at 4 vol% (Fig. 2b). Furthermore, at high electrolyte

concentrations (170 mM NaCl) the gel-like response for any clay is significantly reduced or disappears entirely (Fig. 2b).

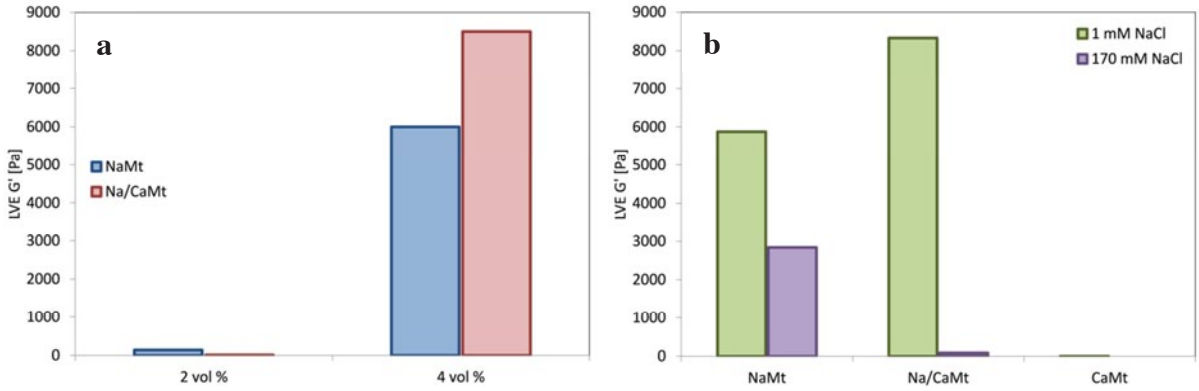


Figure 2. The average elastic modulus (G') of montmorillonite suspensions in the linear viscoelastic region (LVE). a) Comparison of solids contents at 1 mM NaCl. b) Effect of electrolyte concentration.

Frequency sweeps demonstrate that the viscous character of the suspensions increases at low frequencies, which is a typical response for a Maxwell viscoelastic material (Fig. 3). Clay suspensions relax very slowly though, which is probably related to limitations in the rotational and translational freedom of movement caused by the irregular shape of clay particles.

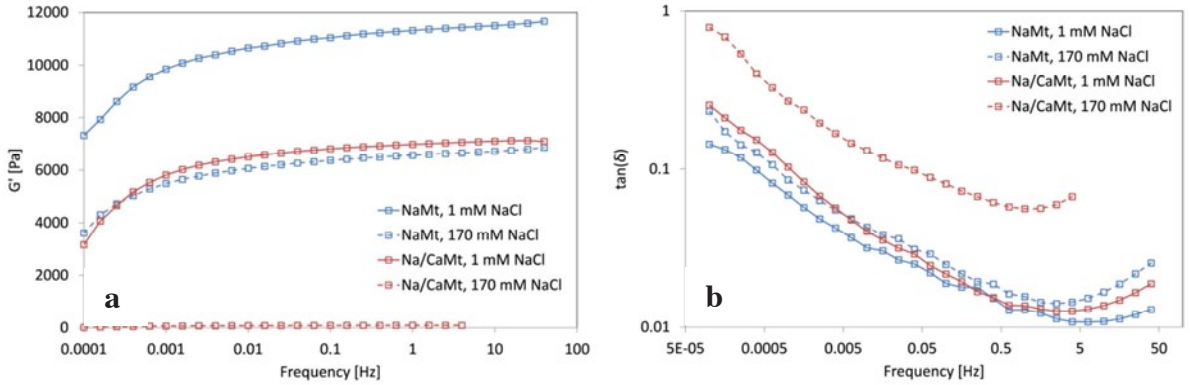


Figure 3. The elastic modulus (a) and corresponding loss factor (b) as a function of frequency for 4 vol % montmorillonite suspensions (, i.e. a larger loss factor corresponds to an increasingly viscous character of the material).

An analysis of the expected shear stresses (due to flowing groundwater) at the perimeter of the inner (gel-like) body of material strongly suggests that mechanical forces cannot overcome the yield stress of the material, and consequently, cannot detach particles at the interface. However, the increasingly viscous nature of the material at low frequencies leads us to believe that clay suspensions (at least at low solids contents) do not continually behave like gels over long time-scales, but will, when subject to strain (including gravitational load), deform and relax. From a mechanical point of view, the long term fate of material extruding into a fracture will therefore depend on whether a continuous, low intensity strain can stretch the material to such a degree as to allow for detachment of particles (due to e.g. shear or chemical processes). Alternatively, the material may expand "infinitely", albeit at an extremely slow rate. Unfortunately, the present analysis does not allow for these assessments to be made.

[1] *Buffer erosion in dilute groundwater*. Posiva report 2012-44; Posiva Oy: Olkiluoto, 2012.

Abiotic and biotic nitrate and nitrite reduction by pyrite

N. Bleyen* [1], **M. Vasile**[1], **C. Bruggeman**[1] **and E. Valcke**[1]

[1] W&D Expert Group, SCK•CEN, Boeretang 200, 2400 Mol, Belgium

Eurobitum is an intermediate-level long-lived bituminised radioactive waste form that consists of ~60 wt% hard bitumen (Mexphalt R85/40), in which the radioactive waste and high amounts of $NaNO_3$ (20 to 30 wt%) and other salts and (hydr)oxides (10 to 20 wt%) are homogeneously dispersed [1, 2]. In the Belgian deep geological disposal concept for Eurobitum, a poorly indurated clay formation would serve as the main barrier against the dispersion of radionuclides. The Boom Clay is currently studied as a potential host rock for the final repository for Eurobitum, because of its favourable physico-chemical characteristics, (*a.o.* its reducing capacity), which would limit and delay the migration of leached radionuclides to the biosphere over extended periods of time. During and after saturation of the disposal gallery, Eurobitum will take up water, resulting in the dissolution of $NaNO_3$ crystals and the subsequent leaching of significant amounts of nitrate and to a lesser extent also nitrite (formed by radiolysis of nitrate) into the clay pore water [3].

As the reducing conditions in the Boom Clay are important to its overall barrier function, it is necessary to assess the possible chemical interactions between nitrate and/or nitrite and one of the main redox-active components of the clay formation, *i.e.* pyrite. To study this, long-term abiotic batch tests were performed in anaerobic conditions, in which commercial pyrite (grain size < 150 µm; SA = 1.53 m²/g) was exposed to different concentrations of nitrate (0 to 0.1 M $NaNO_3$) or nitrite (0 to 0.005 M $NaNO_2$) in a bicarbonate solution (simulating the bicarbonate concentration in Boom Clay pore water, *i.e.* 15 mM $NaHCO_3$) at pH~9. The chemical composition of the solutions was analysed regularly to assess the nitrate and nitrite reduction by pyrite. Microbiological analyses (MPN or Most Probable Number tests) confirmed that all tests were performed in absence of sulphur-oxidising microorganisms. As a positive control, biotic tests were also performed, assessing microbial pyrite oxidation at neutral pH with nitrate or nitrite as electron acceptor by *Thiobacillus denitrificans*, a known nitrate-dependent autotrophic pyrite oxidiser [4].

After incubation of a pyrite suspension with nitrate for 2.5 years (under abiotic conditions), no significant decrease in nitrate nor an increase in reduced N species (NO_2^-, NH_4^+ or N_2O) or in sulphate or thiosulphate was detected. These results indicate that nitrate is not reduced abiotically by pyrite, at least not within this experimental time frame. When *T. denitrificans* was present and active in pyrite suspensions with nitrate, a significant nitrate reduction to nitrite and a formation of sulphate (and thiosulphate as intermediate product) was observed over ~4 months, indicating that microbial nitrate-dependent pyrite oxidation did occur, in contrast to abiotic nitrate reduction by pyrite.

When pyrite was incubated abiotically with nitrite for 2.5 years, nitrogenous gasses were formed, as well as both thiosulphate and sulphate (Figure 1), indicating that pyrite can be oxidised abiotically by nitrite. During the first month, both thiosulphate and sulphate were produced in more or less equal quantities, while afterwards ~80% of the total dissolved S was thiosulphate. This suggests that thiosulphate was not an intermediate product in this process, but rather one of the end products. The reaction rate seems to slow down after the first few months, suggesting some passivation of pyrite due to the formation of an oxidation layer (possibly siderite or goethite) on the surface of pyrite, which is in agreement with the results described in [5]. XRD (X-ray diffraction) and XPS (X-ray photoelectron spectroscopy) analyses are on-going to investigate this further. In the biotic batch tests, nitrite-dependent oxidation of pyrite by *T. denitrificans* was observed over 1 year, resulting in the formation of sulphate. Similar to what was observed in the biotic tests with nitrate, thiosulphate was only observed as an intermediate product in the microbial pyrite oxidation. The microbial pyrite oxidation rate was ~5 times higher than the abiotic reaction rate.

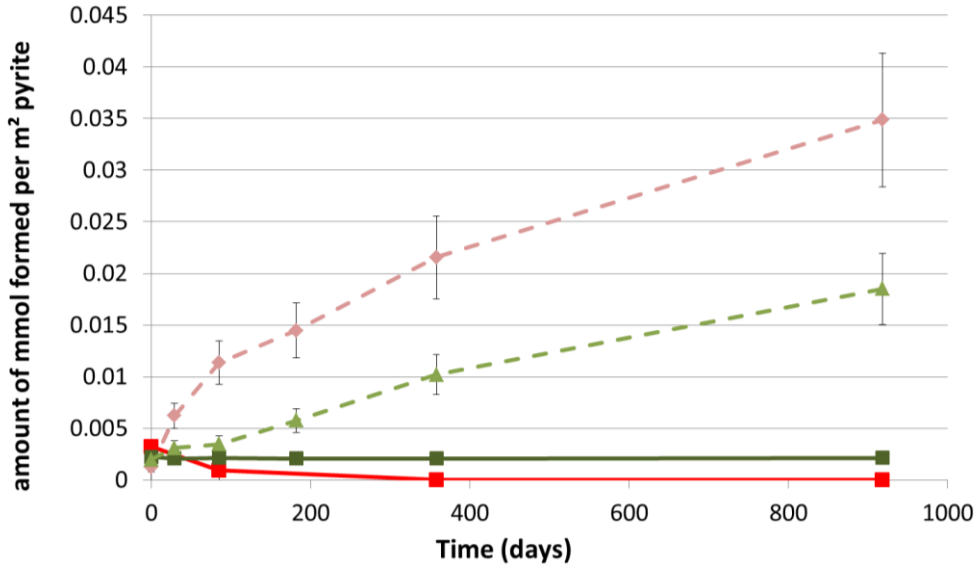


Figure 1: *Evolution of sulphate (green lines) and thiosulphate (red lines) in the pyrite suspensions containing no (full lines) or 0.005 M $NaNO_2$ (interrupted lines). All concentrations are normalised to the specific surface area of the pyrite. The error bars present the 95% confidence intervals for all values.*

The results of the batch tests described above suggest that chemical reduction of nitrate by pyrite is not possible or is characterised by very slow kinetics. Nitrite on the other hand, can oxidise pyrite abiotically and might therefore have a more significant impact on the reducing capacity of the Boom Clay. In the presence of pyrite-oxidising microorganisms, both nitrate and nitrite can be reduced microbially with pyrite as electron donor.

Acknowledgements
This work is undertaken in close co-operation with, and also with the financial support of ONDRAF/NIRAS, the Belgian Agency for the Management of Radioactive Waste and Enriched Fissile Materials, as part of its programme on the geological disposal of intermediate-level long-lived radioactive waste.

References

[1] Demonie M. (1996). Chemische samenstelling van het gebitumineerd product van de fluxen E1 tot en met EX. Note Belgoprocess reference AFB-96-390, 21/10/96.
[2] Boulanger D. (2011). Source term for the Safety and Feasibility Case 1. NIROND TR-2011-68. ONDRAF/NIRAS, Brussels, Belgium.
[3] Valcke E., Mariën A., Van Geet M. (2009). The methodology followed in Belgium to investigate the compatibility with geological disposal of Eurobitum bituminized intermediate-level radioactive waste. MRS Proceedings 1193: 105-116.
[4] Bosch J., Lee K-J, Jordan G., Kim K-W, Meckenstock R.U. (2012). Anaerobic, nitrate-dependent oxidation of pyrite nanoparticles by *Thiobacillus denitrificans*. Environ. Sci. Technol. 46: 2095-2101.
[5] Descostes M., Beaucaire C., Mercier F., Savoye S., Sow J., Zuddas P. (2002). Effect of carbonate ions on pyrite (FeS_2) dissolution. Bull. Soc. Géol. France 173: 265-270.

Microbial activity in clay porewater containing carbon steel materials, under anoxic conditions at 85°C

Marc Labat[1], Sylvie Daumas[2], Zouhaier Ben Ali Gam[1], *Sophia Necib*[3]

[1] Laboratoire de Microbiologie IRD, Aix-Marseille Université, Université du Sud Toulon-Var, CNRS/INSU, IRD, MI0 UM110, 163 avenue de Luminy, case 925, F-13288 Marseille cedex 9, France

[2] CFG Services Groupe BRGM, 117 avenue de Luminy 13009 Marseille, France

[3] Agence nationale pour la gestion des déchets radioactifs (Andra), Centre de Meuse/Haute-Marne, F-55290 Bure, France.

Micro-organisms are known to be present in soils under various environmental conditions. Their adaptability to the temperature, chemistry and pH changes can often be surprising.
In the context of geological repository concepts, metallic components made of carbon steel will be used as structural barriers. Therefore they will be in contact with clay porewater, which contains microbial activity.
The purpose of this study is to investigate the microbial activity in clay porewater containing carbon steel materials in order to understand their potential role on the corrosion processes.

The investigations have been performed over 6 years, by sampling porewater coming from the test chamber of IC experiment in the Mont-Terri Laboratory, containing 4 metallic samples with a surface area of 64 cm^2 each. Furthermore, microbiological studies by classical culture techniques and biomolecular studies have both been carried out to determine either the different bacterial groups or the different species present.
For microbiological studies, culture based enumeration of bacterial groups with the potential for aftergrowth were counted on various culture media via the most probable number (MPN) technique. Each seeding stage took place under sterile conditions and to avoid disturbing in-sample redox potential. The incubations were performed in mesophilic and thermophilic conditions.

For biomolecular studies, all amplifications were performed by polymerase chain reaction (PCR). The PCR used in this study is a PCR targeting the V3 region of 16S rDNA. The reason V3 is the region of interest in this gene is that (i) it is highly conserved over the geologic time scale (the V3 region is conserved in both ancestral and present-day bacteria) and (ii) it produces a functional RNA that is not translated into a protein yet possesses standout secondary structures critical to the functionalization of this RNA. More highly-conserved target sequences makes it possible to differentiate more individual organisms.Whether the molecular analysis technique used is double-strand (denaturating gradient gel electrophoresis or DGGE) or single-strand (single strand conformation polymorphism or SSCP), both hinge on first completing the steps outlined above, i.e. extraction of either *Bacteria*-specific or *Archaea*-specific DNA followed by DNA amplification. There are two techniques that use electrophoresis to quickly get a snapshot of the microbial communities present in an ecosystem.

The results by classical culture techniques (MPN) have revealed low concentration of strict aerobic and/or facultative anaerobic mesophilic bacteria counted from 2.5 up to 60 bacteria/mL, whereas thermophile counts were at or under the limit of detection in the inner-ring pore water. Mesophilic strict anaerobes were either absent from the water samples or counted around just 25 bacteria/mL. But IC samples also count mesophilic sulphate-reducing bacteria (SRB) and thiosulphate-reducing bacteria (TRB) in concentration ranges of 250–6000 bacterial/mL and 25–6000 bacteria/mL, respectively. The mesophilic TRB decline over time whereas the mesophilic SRB still count around 6000 bacterial/mL at 18 months after the initial sample time. Some were hydrogenophiles.

Thermophilic sulphur-reducing bacteria survive but at relatively low concentrations. Only these thermophilic bacteria present in the inner ring of the IC–ex are likely to be active *in situ* under the temperature conditions of the test platform.

For biomolecular studies, the results by quantitative PCR (qPCR) put the estimated total in-sample bacteria concentrations at 2.5 10^6 *Bacteria*/mL and 1.3 10^3 *Archaea*/mL. After DNA extraction, PCR amplification then 16S rDNA cloning–sequencing of the dominant and minor *Bacteria* and *Archaea*, a number of different bacterial species were phylogenetically identified.
The metabolic potentials—both anabolic and catabolic—of the bacteria found in this IC–experiment were then evaluated, factoring in only the dominant *Bacteria* and *Archaea* identified with over 97% sequence homology. On this basis, there are 7 mesophilic metabolisms and 4 thermophilic metabolisms liable to play a role *in situ*, with the thermophiles being the only likely active metabolisms in the inner-ring IC–ex pore water where water temperature is 85°C.

Ten species display a strict anaerobic metabolism adapted to the deep-minus redox potential conditions of this ecosystem. Of these species, three are members of the same SRB group that was also evidenced by indirect-method counts after incubation on selective pro-mesophile and pro-thermophile culture media. As an example, *Geobacter bremensis* is known as a strictly anaerobic, dissimilatory ferric-iron-reducing bacteria with ferrihydrite as electron acceptor. This species also grows by reducing Mn(IV), elemental sulfur and fumarate. But its role is not clearly established in this IC–experiment as it is a mesophilic species. Only the thermophilic species *Desulfotomaculum geothermicum* is liable to thrive under the high-temperature conditions of the IC–experiment trial. This species is known to grow chemolithoautotrophically with hydrogen plus sulfate as energy source and carbon dioxide as carbon source without requirement of additional organic carbon like acetate. Its *in situ* activity is potentially capable of promoting accelerated corrosion by creating strongly localized corrosion that can ultimately perforate electrodes installed in the bore chamber. The corrosion rates measured by electrochemical impedance suggest localized corrosion is unlikely to be an issue. A post-stripdown characterization of the electrode surface will confirm or disconfirm this type of corrosion attack. Thiosulphate-reducers were found by the microbial culture techniques but not picked up by the molecular biology techniques.
Cross-comparison between the two techniques showed that PCR–DGGE/cloning outperformed PCR–SSCP/cloning by yielding more exhaustive information on bacterial community composition in the water circulating in the Iron Corrosion Experiment inner ring.
To conclude, PCR–SSCP without cloning/sequencing can be used to compare several profiles of time-series samples taken from the same environment in order to capture whether modified physical–chemical or other ecosystem parameters trigger structural or diversity changes in dominant and minor *Bacteria* or *Archaea* communities. A parallel investigation of bacterial community composition can also be led by focusing PCR–DGGE/cloning–sequencing on the major *Bacteria* and *Archaea* species liable to have ecosystem–niche impact and on the minor *Bacteria* and *Archaea* species identified with over 97% sequence homology.

Impact of the nature of the electron donor on *in situ* microbial nitrate reduction processes in Opalinus Clay

N. Bleyen[1], S. Smets[1], H. Moors[1], N. Leys[1], A. Albrecht[2], P. De Cannière[3], B. Schwyn[4], C. Wittebroodt[5] and E. Valcke[1]

[1] SCK•CEN, Boeretang 200, BE-2400 Mol, Belgium; [2] ANDRA, 1-7 rue Jean-Monnet, FR-92298 Châtenay-Malabry Cedex, France; [3] FANC, Ravensteinstraat 36, BE-1000 Brussel, Belgium; [4] NAGRA, Hardstrasse 73, CH-5430 Wettingen, Switzerland; [5] IRSN, Bâtiment 76/2, B.P. 17, FR-92262 Fontenay-aux-Roses, France.

In several countries, such as Belgium and France, deep clay formations are foreseen as the host rock for geological disposal of bituminised low-level and intermediate-level long-lived radioactive waste. Suitable clay formations such as Boom Clay, Callovo-Oxfordian Clay and Opalinus Clay exhibit favourable hydromechanical and geochemical characteristics (*e.g.* self-sealing capacity, low permeability, reducing conditions), which are expected to retard the migration of radionuclides [1, 2, 3]. Along with radionuclides, certain classes of bituminised radioactive waste also contain (high concentrations of) $NaNO_3$, dispersed in the bitumen matrix. After waste cell closure, and during and after saturation the disposal gallery, this bituminised waste will take up water, ultimately resulting in the dissolution and leaching of significant amounts of $NaNO_3$ into the near field [4]. This nitrate plume could induce several geochemical and biochemical processes in the concrete and clay barriers of the repository. The phenomenology of these nitrate-related processes in the host rock will be the subject of this presentation.

To study these processes, an *in situ* experiment in the Opalinus Clay, named the Bitumen-Nitrate-clay interaction (BN) experiment is being performed at the Mont Terri Rock Laboratory (Switzerland). The experiment consists of a vertical borehole rigged with a downhole equipment containing three packed-off intervals, each lined with a cylindrical sintered stainless steel filter screen to allow contact with the surrounding clay. The intervals were saturated with artificial Opalinus Clay pore water (APW), containing all major ions at site-specific concentrations but no organic matter, and were equilibrated with the surrounding clay for ~8 months. Each interval is connected to a stainless steel water circulation unit, equipped with a circulation pump, a flow meter and water sampling containers, to ensure a chemically well mixed solution, a constant water flow and an easy sampling procedure. A gas trap is placed in the circulation to sample the gas produced by microbial activity. Water samples are regularly taken to assess the chemical composition and the microbial population in the intervals. To continuously monitor the nitrate and nitrite concentrations, pH and E_h, an on-line UV spectrophotometer as well as pH and redox electrodes are installed in the water circuit of two of the intervals [5, 6]. During the tests of the BN experiment, the intervals are injected with APW containing $NaNO_3$ with or without additional electron donors (acetate, H_2), expected to be present in and around a repository for bituminised radioactive waste.

In the first series of tests [7], the biogeochemical evolution of the pore water in the intervals was investigated after injection with low concentrations of nitrate (up to 1.5 mM NO_3^-) with or without acetate (C/N ratio 0.4:1 or 0.8:1). More recently, a second series of tests was performed with higher nitrate concentrations (15, 25 and 50 mM). In the test with 25 mM nitrate, acetate was added ~3 months after nitrate addition (*i.e.* 'pulse injection'; C/N ratio = 0.4:1), to investigate the effect of this electron donor on the microbial nitrate reduction rate and metabolism. A similar experiment with a pulse injection of H_2 is currently being performed.

For higher concentrations of nitrate (25 mM or 50 mM) without addition of electron donors, denitrification (*i.e.* nitrate reduction to gaseous nitrogen species) using clay components (*e.g.* dissolved organic matter, pyrite) as electron donor occurred as seen by the presence of N_2O and N_2 in the gas trap. However, a more significant fraction of the added nitrate diffused into the surrounding clay. The microbial nitrate reduction rate (based on the production rate of nitrite, N_2O and N_2) after injection with an initial concentration of 50 mM NO_3^- is comparable to the rate when only ~1.5 mM NO_3^- was injected in the borehole [7], *i.e.* 0.02-0.04 mM NO_3^-/day.

When acetate was added to an interval that was initially injected with nitrate (~25 mM NO_3^-), the microbial population responded quickly, triggering a strong increase in microbial activity: a fast nitrate reduction to nitrite dominated (~90% of total decrease in nitrate) while only some denitrification (~10% of total decrease in nitrate) occurred. The fast nitrate reduction rate after pulse injection with acetate agrees well with a previously reported rate observed in the BN experiment [7] (~1 mM NO_3^-/ day), when nitrate and acetate were added with a similar C/N ratio of ~0.4:1, but with much lower concentrations (~20x less). When all acetate was consumed, the produced nitrite seemed to disappear quite rapidly, suggesting both diffusion and reduction (microbially and/or chemically) using clay components as electron donor.

The microbial nitrate reduction rates observed in the BN experiment do not seem to be dependent on the nitrate concentration, but rather on the availability and energy producing capacity of the electron donor. Indeed, in the absence of acetate, the microbial activity seemed to be limited by the availability of the electron donors and the rate at which electrons can be provided by the clay. Addition of an energetically favourable electron donor like acetate resulted in a severe increase of the microbial nitrate reduction rate. However, as a higher C/N ratio did not induce a faster microbial reaction [7], the rate might also be limited by other microbial nutrients obtained from the clay.

The results of our experiments indicate that in case of microbial growth and activity in the near field of a geological repository for bituminised radioactive waste, microbial nitrate reduction using clay components can occur. In the presence of easily degradable compounds leached from the bituminised waste, the microbial nitrate reduction rate would significantly increase. This rate will therefore be highly dependent on the availability and the nature of the electron donors present in the near field of the repository.

Acknowledgements

This work is undertaken in close co-operation with Swisstopo, the operator of the rock laboratory and the project management team at Mont Terri, in particular Christophe Nussbaum and Thierry Theurillat. Financial support was provided by the Mont Terri Consortium. The authors wish to thank Sonia Selenska-Pobell (HZDR), Andrea Geissler (HZDR) and Simcha Stroess-Gascoyne (AECL) for their help in performing and/or interpreting the microbiological analyses, and Joe Small (NNL) for modelling the biogeochemical processes in the BN experiment. Technical assistance of Wim Verwimp and Patrick Boven (SCK•CEN) is also greatly appreciated.

References

[1] Andra (2005). Dossier 2005 Argile – Référentiel du site de Meuse/Haute Marne. C.R.P.ADS.04.0022, Andra, Paris, France.
[2] Nagra (2002). Project Opalinus Clay – safety report: demonstration of disposal feasibility for spent fuel, vitrified high-level waste and long-lived intermediate-level waste (Entsorgungsnachweis). Nagra Technical Report NTB 02-05, Nagra, Wettingen, Switzerland.
[3] ONDRAF/NIRAS (2009). The long-term safety assessment methodology for the geological disposal of radioactive waste. ONDRAF/NIRAS Report NIROND TR- 2009-14 E.
[4] Valcke, E. *et al*. (2009). The methodology followed in Belgium to investigate the compatibility with geological disposal of Eurobitum bituminized intermediate-level radioactive waste. Mater. Res. Soc. Symp. Proc., 1193, 105-116.
[5] Bleyen, N. *et al*. (2011). Bitumen-Nitrate-clay interaction (BN) experiment: Testing and installation of the on-line measurement of the nitrate and nitrite concentration in artificial pore water. Technical Note 2010-73, Mont Terri Project.
[6] Bleyen, N. *et al*. (2013). Bitumen-Nitrate-clay interaction (BN) experiment: Evaluation of the on-line measurements of the chemical composition of artificial pore water: part 2. Technical Note 2013-45, Mont Terri Project.
[7] Bleyen, N. *et al*. (2012). *In situ* analysis of microbial reduction of a nitrate plume in Opalinus Clay. Clays in Natural and Engineered Barriers for Radioactive Waste Confinement, Montpellier, France, 22-25 October 2012.

Redox capacities of Boom Clay constituents; an electrochemical approach

A.L. Hoving[a], **T. Behrends**[a], **M. Sander**[b], **N. Maes**[c], **C. Bruggeman**[c]

[a] Faculty of Geosciences, Department of Earth Sciences - Geochemistry, Utrecht University, P.O. box 80021, 3508 TA Utrecht, Netherlands
[b] Institute of Biogeochemistry and Pollutant Dynamics (IBP), ETH Zurich, Zurich, Switzerland
[c] SCK●CEN, Expert Group Waste Disposal, Boeretang 200, B-2400 Mol, Belgium

Deep underground disposal is currently considered to be the best long-term solution to isolate long-lived radioactive waste from the biosphere. Although multiple engineered barriers will isolate the waste from the geological surroundings for an extended period of time, eventually spreading of radionuclides beyond the engineered barriers is expected. This will expose long-lived radionuclides to the surrounding sediment. Due to their low permeability and their possibility to retain radionuclides, clay-rich formations, like the Boom Formation in Belgium and in the Netherlands, are considered as possible host rocks for radioactive waste repositories.

Mobility of radionuclides in clay depends, among other factors, on their solubility and their tendency to adsorb to the solid phase. For some long-lived radionuclides, like uranium and selenium, these properties are highly dependent on their redox state. Several constituents in the Boom Clay, such as pyrite, siderite, organic matter and Fe-bearing clay minerals, are expected to be redox active and may be able to participate in redox reactions with radionuclides (Bruggeman *et al*., 2005; Bruggeman *et al*., 2007; Bruggeman and Maes, 2010). Although chemical analyses can give information about the amount of present redox-active substances, their reduction and oxidation capacities cannot be derived from chemical analyses alone. Particularly, neither the amount of Fe in the clay structure accessible to redox reactions, nor the redox reactivity of organic matter can simply be quantified by mineralogical or elemental analyses. Here, we investigate the redox properties of Boom Clay with the eventual goal to predict the equilibrium speciation of redox sensitive radionuclides in this geological formation.

A novel electrochemical technique, using electron mediators (Aeschbacher *et al*., 2010; Gorski *et al*., 2012), was used to determine the redox reactivity of the Boom Clay by monitoring the current over time at a constant electrode potential. By integrating current over time the electron donating and accepting capacities of the samples could be determined. Besides natural, fresh Boom Clay samples, chemically altered Boom Clay and various minerals, such as pyrite, siderite, illite and smectite were analyzed. The electrochemical characterization was complemented by chemical analyses of the samples and Mössbauer spectroscopy.

The electrochemical results show that the electron donating capacities of Boom Clay samples from different depths and locations were much larger than the electron accepting capacities. Upon electrochemical oxidation of the Boom Clay, the time evolution of the oxidative current showed two phases: high electron transfer rates occurred at the beginning of the measurement, which was followed by a second phase with lower rates. Comparison with electrochemical properties of reference materials revealed that the fast rates can be ascribed to redox transformations of Fe in clay minerals, while the slow rates can be attributed to the oxidation of pyrite. Within the group of possible electrochemically active constituents in the Boom Clay, both pyrite and Fe in clay minerals are dominating the electron fluxes in the electrochemical experiments and might therefore be the most important phases to react with radionuclides.

Acknowledgements

The research leading to these results has received funding from the Dutch research programme on geological disposal, OPERA. OPERA is financed by the Dutch Ministry of Economic Affairs and the public limited liability company Elektriciteits-Produktiemaatschappij Zuid-Nederland (EPZ), and is coordinated by COVRA.

References

Bruggeman, C.; Maes, A.; Vancluysen, J.; Vandemussele, P. (2005). Selenite reduction in Boom Clay: effect of FeS_2, clay minerals and dissolved organic matter, *Environmental Pollution*, **137** (2), 209-221

Bruggeman, C.; Maes, A.; Vancluysen, J. (2007). The interaction of dissolved Boom Clay and Gorleben humic substances with selenium oxyanions (SeO_3^{2-} and SeO_4^{2-}), *Applied Geochemistry*, **22**, 1371-1379

Bruggeman, C.; Maes, N. (2010). Uptake of Uranium(VI) by pyrite under Boom Clay conditions: Influence of dissolved organic carbon, *Environmental Science & Technology*, **44** (11), 4210-4216

Aeschbacher, M.; Sander, M.; Schwarzenbach, R. P. (2010). Novel electrochemical approach to assess the redox properties of humic substances. *Environmental Science & Technology*, **44**, 87-93

Gorski, C. A.; Aeschbacher, M.; Soltermann, D.; Voegelin, A.; Baeyens, B.; Marques, M.; Hofstetter, T. B.; Sander, M. (2012). Redox properties of structural Fe in smectites: 1. Electrochemical quantification of electron donating and accepting capacities. *Environmental Science & Technology*. **46** (17), 9360-9368

Advanced technologies for the investigation of fluids in low-permeable rocks

F. Eichinger, G.D. Lorenz, A. Voropaev, L. Eichinger, S. Wechner
Hydroisotop GmbH, Woelkestrasse 9, 85301 Schweitenkirchen, Germany, info@hydroisotop.de

The investigation of fluid circulation and processes within sediments and rocks as well as artificial barriers (bentonite) of low permeability requires progressive, specialized and innovative methods of analysis, sample preparation and sampling.

The in-situ fluids exist in different aggregate states depending on different factors, e.g. temperature, pressure, salinity, and microbial activities.

The extraction/sampling of those fluids from low permeable bedrock is sensitive against artefacts, which include for example evaporation, interaction with installation equipment, and deterioration of gas contents due to a co-trapping at water traps.

One of the main challenges is to develop and apply analytical methods to determine the fluid chemistry, gas concentrations, isotope signatures of the water, and dissolved or free gases on low to very low sample volumes.

Isotope and physical-chemical analysis of pore water and pore gases require coupled sophisticated methods to obtain enough material for the detectors. The isotope composition of water and the dissolved constituents of pore fluids can be either investigated using exchange experiments both for rock fragments from core samples or from hydraulic tests in borehole segments, or it can be investigated by the retrieval of the water phases with siccatives. Experiments for the investigation of the water origin have been successfully carried out using bags filled with siccative and placing within boreholes of the rocks or artificial walls in question. The measurement of the isotope composition of the water molecule (Oxygen-18 and Deuterium) can be done using the method of cavity ring down spectrometer which requires very low volumes. If only the water molecule is investigated this method is very useful for profiles of water migration and the origin of water, even for tracer experiments using Deuterium as tracer. If the rock moisture is very low and the siccative had not deposited long enough, then the isotope signature may not have reached the originary state. This can lead to significant misinterpretation. A special issue of this method is the observation of CO_2 migration through rock and barriers. As the oxygen of CO_2 exchanges with the H_2O, significant amounts of CO_2 can be observed by the isotope signature of the pore water.

A further challenge is to analyse and evaluate the origin and evolution of hydrogen, which can be present in hydrological bedrock systems geogenic or formed due to artefacts induced by microbial processes or interaction with metal devices. The only possibility to evaluate the origin is the determination of the δ^2H-H_2 values, which is done by advanced mass spectrometric methods on small scale samples. Hydrogen can also be formed by the disaggregation of organic material present in low and intermediate level radioactive waste. The formation of hydrogen in the first 60 years after repository can be evaluated by determination of tritium.

Interface equilibrium in bentonite – a general approach to ion diffusion

Martin Birgersson

Clay Technology AB, Ideon Science Park, S-223 70 Lund, Sweden

Previous results strongly suggests that ion diffusion in compacted bentonite may be successfully described by solely accounting for accurately treated montmorillonite interlayers (Birgersson and Karnland, 2009). The modelling approached outlined in (Birgersson and Karnland, 2009) conceives water saturated bentonite as a homogeneous assemblage of interlayers, and the rather complicated diffusive behaviour of ions in bentonite was demonstrated to fully stem from processes of maintaining chemical equilibrium at all interfaces between the bentonite and external solutions. The present work generalizes this ion equilibrium treatment to any kind of chemical specie, explicitly including activity coefficient corrections.

The requirement of chemical equilibrium for an aqueous specie i across an interface between an external solution and bentonite gives a Nernst type of equation

$$\frac{c_i^{int}}{c_i^{ext}} = \Xi_i = \Gamma_i \cdot f_D^{-z_i}$$

where Ξ_i is the ion equilibrium coefficient as defined in (Birgersson and Karnland, 2009) and where a Donnan factor has been defined

$$f_D = e^{\frac{\phi^* F}{RT}}$$

as well as an activity coefficient ratio

$$\Gamma_i = \frac{\gamma_i^{ext}}{\gamma_i^{int}}$$

In the expressions above, superscripts "ext" and "int" labels quantities on the external and internal (clay) side of the interface, respectively. Furthermore, F is Faraday's constant, RT the product of absolute temperature and the universal gas constant, and ϕ^* denotes the electrostatic potential across the interface (Donnan potential).

The combination of the Nernst type equation with the equation describing charge neutrality in the clay gives the main equation in the present approach for calculating interface equilibrium (i.e. calculating f_D)

$$\sum_i z_i \cdot \Gamma_i \cdot f_D^{-z_i} \cdot c_i^{ext} = c_{IL}$$

Here c_{IL} is a clay specific parameter quantifying the surface charge on the smectite in the bentonite. It may be related to the cation exchange capacity (CEC) e.g. as

$$c_{IL} = \frac{CEC \cdot \rho_w}{F \cdot w}$$

where ρ_w is water density and w is the water-to-solid mass ratio. Note that c_{IL} equals the mean interlayer concentration of mono-valent cations required to precisely compensate the structural smectite surface charge.

This approach has been used to model several experiments involving ionic diffusion in bentonite or pure montmorillonite. As an example is here shown the ion equilibrium approach applied to the "uphill" diffusion set-up (Glaus et al., 2013). This experiment demonstrates transport of a tracer from a compartment of lower to a compartment of higher concentration, while a concentration difference spontaneously develops across a compacted montmorillonite sample. As shown in figure 1, with the

application of interface equilibrium, this type of tests are very accurately modelled by the presented approach.

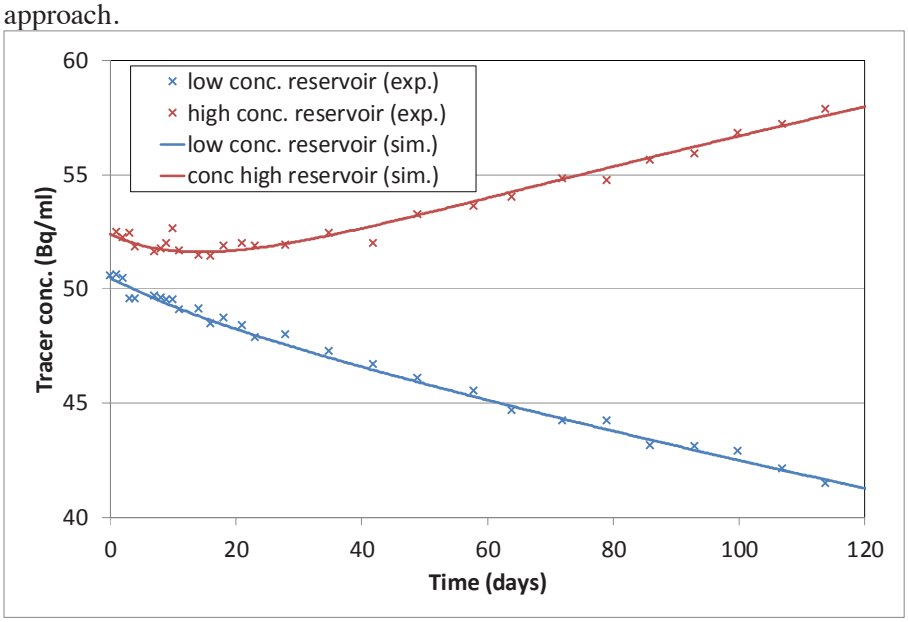


Figure 1:Modeling (full lines) of the uphill phenomenon (Glaus et al., 2013) using the presented approach to ion diffusion in bentonite.

A key challenge for an adequate application of the presented approach is the calculation of activity coefficients in the interlayer environment. Here is suggested an "equivalent salt solution" approximation, in which the smectite charge of the bentonite is conceived of as an equivalent amount of mono-valent anions situated in the interlayer. With this assumption, the bentonite ionic strength is given by

$$I_{int} = \frac{1}{2}\left(\sum_i z_i^2 \cdot c_i^{int} + c_{IL}\right)$$

Activity coefficient corrections for several ions are discussed.

References:

Birgersson, M., Karnland, O., 2009. Ion equilibrium between montmorillonite interlayer space and an external solution—Consequences for diffusional transport. Geochim. Cosmochim. Acta 73, 1908–1923.

Glaus, M.A., Birgersson, M., Karnland, O., Van Loon, L.R., 2013. Seeming Steady-State Uphill Diffusion of $^{22}Na^{+}$ in Compacted Montmorillonite. Environ. Sci. Technol. 47, 11522–11527

Uranium retention by montmorillonite at high ionic strengths

Katharina Fritsch, **Katja Schmeide**

Institute of Resource Ecology, Helmholtz-Zentrum Dresden-Rossendorf e.V., Bautzner Landstrasse 400, 01328 Dresden, Germany

Clay and clay minerals are viewed as potential host rock as well as backfill material for nuclear waste disposal in deep geological formations. While South German clay deposits have pore waters with ionic strengths below 0.5 mol l^{-1}, North German clay deposits exhibit high ionic strengths up to 4 mol l^{-1} in the depth relevant for repositories.[1] Such high ionic strength conditions are rarely investigated and are therefore in the focus of the present work. Montmorillonite is used as model clay for uranium sorption experiments in sodium and calcium chloride. Additionally, a mixed electrolyte was prepared that resembles the groundwater composition at the Konrad site, which serves as a reference site. Surface complexation modelling is employed to gain thermodynamic data from the sorption experiments.

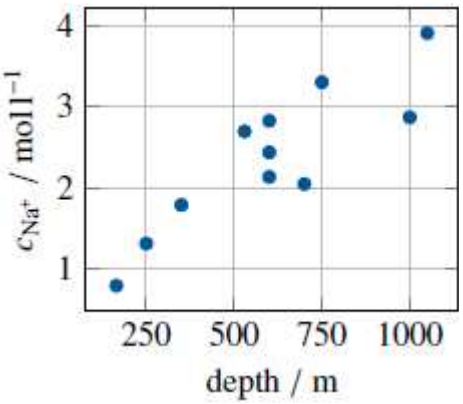


Figure 1: Na^+ content in the groundwaters of the Konrad site depending on depth.

Sorption experiments were conducted with Na montmorillonite SWy-2, which was purified according to Poinssot et al. [2] and Bradbury et al. [3]. Sorption edges were determined with an initial U(VI) concentration of 1 10^{-6} mol kg^{-1} and a solid-liquid ratio of 4 g kg^{-1} in a pH range of 4 to 10 with electrolyte concentrations from 0.1 to 3 mol kg^{-1}. The U(VI) concentration for sorption isotherms ranged from 1 10^{-8} to 1 10^{-5} mol kg^{-1}. The mixed electrolyte was composed of c_{NaCl} = 2.52 mol kg^{-1}, c_{CaCl2} = 0.12 mol kg^{-1} and c_{MgCl2} = 0.048 mol kg^{-1} (overall I = 3.02 mol kg^{-1}).

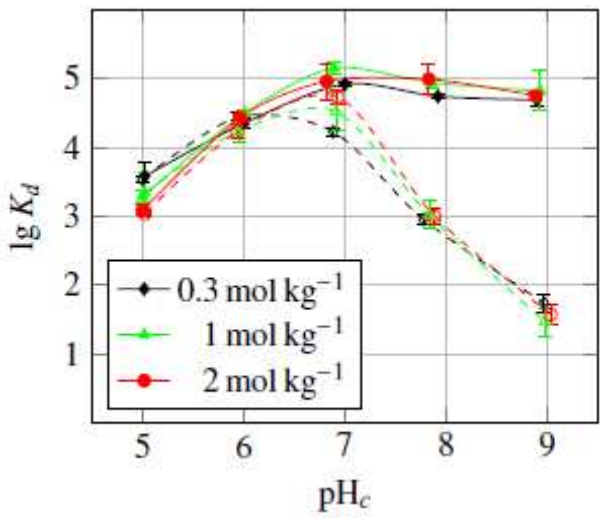


Figure 2: pH and ionic strength dependence of U(VI) (c_U = 10^{-6} mol kg^{-1}) sorption onto montmorillonite in NaCl in absence (continuous lines) and presence (dashed lines) of CO_2

The classic ionic strength effect describes the decrease of sorption with increasing ionic strength and is generally only observed in the acidic pH range, where cation exchange is the predominant sorption mechanism. Natural groundwaters at the Konrad site have pH values above 5.5, where cation exchange is not the dominant sorption mechanism anymore, which in turn causes a smaller influence of ionic strength on sorption. The sorption maxima in the different salt systems usually lie just below the neutral point and well within the pH range of groundwaters at the reference site. The sorption edge in NaCl is observed at pH 4.1. In the mixed electrolyte, sorption is increased in the alkaline pH range when compared to pure electrolytes. This is due to the magnesium content in this electrolyte, which forms hydroxide precipitates that influence uranium retention by co-precipitation.

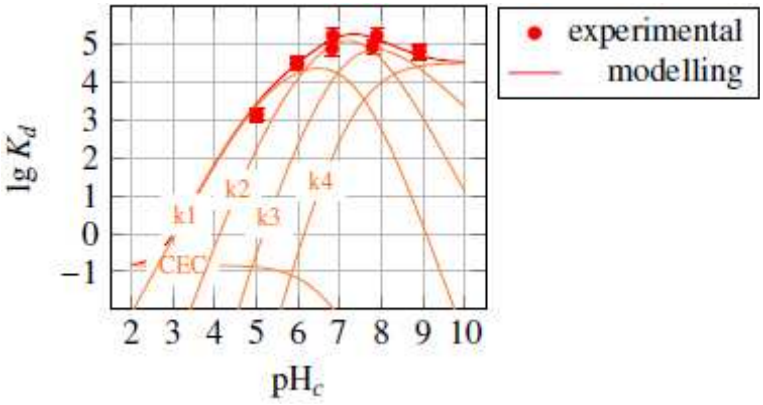


Figure 3: U(VI) sorption onto montmorillonite in NaCl (3 mol kg^{-1}) in absence of CO_2. Modelling of strong sorption sites.

	Surface complex	log k
CEC	Cation exchange	0.47
k1	$\equiv SOUO_2^+$	1.7
k2	$\equiv SOUO_2(OH)$	-3.8
k3	$\equiv SOUO_2(OH)_2^-$	-11.4
k4	$\equiv SOUO_2(OH)_3^{2-}$	-19.7

Surface complexation modelling with the 2 site protolysis non-electrostatic surface complexation and cation exchange model (2SPNE SC/CE)[4] in conjunction with spectroscopic investigation of the sorption phenomena can be used to identify the surface species involved. The results show that $\equiv SOUO_2^+$ is the dominant surface complex below pH 6. Uranium hydroxide complexes become the dominant surface complexes above pH 7 in absence of CO_2. In presence of CO_2, sorption above pH 7 is decreased due to aqueous uranium carbonate complexes.

In general, there is no influence of ionic strength on U(VI) retention by montmorillonite at environmentally relevant pH values. The classic ionic strength effect can only be observed in the acidic pH range, and only up to a sodium chloride concentration of 2 mol kg^{-1}. However, in the presence of calcium or magnesium chloride, uranium retention is promoted by secondary phase formation which leads to partial irreversibility of immobilisation at high ionic strengths in the alkaline pH range.

[1] Brewitz, W. et al. Eignungsprüfung der Schachtanlage Konrad für die Endlagerung radioaktiver Abfälle. GSF-T 136; **1982**.
[2] Poinssot, C. et al. Experimental studies of Cs, Sr, Ni, and Eu sorption on Na-illite and the modelling of Cs sorption. NTB 99-04; **1999.**
[3] Bradbury, M.; Baeyens, B. *Geochim Cosmochim Acta* **2009**, 73, 990–1003.
[4] Bradbury, M.; Baeyens, B. *J Contam Hydrol* **1997**, 27, 223–248.

Development of the squeezing method for analysing compacted bentonite porewater

JÄRVINEN JOONAS[1], MATUSEWICZ MICHAŁ[1] AND ITÄLÄ AKU [1]

VTT Technical Research Center of Finland, Otakaari 3, Espoo, Finland, P.O.Box 1000, 02044 VTT. Joonas.Jarvinen@vtt.fi

Many safety functions set for the bentonite buffer in KBS-3 concept are based on processes which are related to the composition of porewater. Important safety-relevant prosecces are e.g. swelling, precipitation and dissolution reactions, transport of the water, colloids and ions. One of the methods used for analyzing porewater in compacted bentonite is squeezing. In this technique, the mixing of the different water types, dissolution of accessory minerals and cation exchange need special attention, however.

This work describes the method for studying composition of the porewater by combining squeezing methods, chemical analyses, microstructure measurements and modelling. MX-80 bentonite porewater is squeezed out with four different maximum pressures, the origin of the water is studied by measuring bentonite microstructure before and after squeezing by SAXS and NMR, and the cation exchange and dissolution reactions are studied by chemical analyses and geochemical modelling. The preliminary squeezing results are presented in table 1.

Table 1. maximum squeezing pressure and chemical composition of the squeezed porewaters. Pw-%=percent of squeezed porewater, w_lost-%=percent of the porewater lost during squeezing and CBE-%=charge balance error.

Phase		Squeezing pressure [MPa]			
[mmol/L]	0	60	80	104	120
Na		239	240	237	217
K		2,1	2,2	1,8	1,6
Ca		62	62	67	59
Mg		25	24	25	25
Cl		381	375	384	355
SO4		7	7	6	7
HCO3		3,6	3,9	3,3	3,4
pw-%		31,4	36,6	39,8	46,9
w_lost-%		5,6	5,2	8	5,4
CBE-%		2,1	2,6	2,9	2,0

The average distance of the interlamellar space was observed to decrease from 18.6 Å to 16.6 Å according to SAXS measurements when 60 MPa pressure was used. This indicates mixing of different water types. The results are not so clear for ions which could be the concequence of constant mixing of interlamellar and non-interlamellar waters during squeezing.

Characterization of porewaters in an aquiclude: challenges of the Bruce DGR formations

Clark, Ian Douglas[1], Murseli, Sarah[1], St.-Jean, Gilles[1], Al, Tom[2], Raven Ken[3], Kennell Laura[4], Hobbs Monique[4] and Jensen Mark[4]

[1] University of Ottawa, 25 Templeton, Ottawa, Ontario, Canada
[2] University of New Brunswick, 3 Bailey Dr, Fredericton, New Brunswick, Canada
[3] Geofirma Engineering Ltd, 1 Raymond St #200, Ottawa, Ontario, Canada
[4] Nuclear Waste Management Organization, 22 St. Clair Avenue East, Toronto ON, Canada

The low-permeability Ordovician shales and argillaceous limestone formations on the eastern flank of the Michigan Basin in southern Ontario, Canada, are being considered for construction of a deep geological repository (DGR) for low- and intermediate-level radioactive waste. The lithology in the vicinity of the proposed DGR is characterized by the presence of a 200+ m shale sequence that overlies the proposed repository horizon. Hydraulic conductivities as low as 10^{-14} ms^{-1} and low volumetric water contents (down to 0.5% in the Ordovician carbonates) in the sedimentary formations have greatly limited options for extraction and analysis of porewaters, solutes and gases. High-temperature vacuum-distillation (6 hours at 150°C) was found consistently to yield reproducible measurements during geochemical characterization activities and currently is being further tested and adapted for application in additional rock types (crystalline rock, clays).

Prior to its application, the vacuum-distillation method was thoroughly evaluated and adapted at the University of Ottawa for use on the shales and carbonates that underlie southern Ontario. The method was tested at a variety of temperatures (50 to 200°C) and durations of extraction under static vacuum (2 to 8 hours) to establish the protocol for extraction at 150°C for 6 hours from 40 g of crushed and sieved (2 to 4 mm grain size) core samples. Produced water and CO_2 were trapped cryogenically for measurement of $\delta^{13}C_{CO_2}$, gravimetric water content, $\delta^{18}O_{H_2O}$ and δD_{H_2O}. Following vacuum-distillation, the baked rock was leached for a 60 day period under anaerobic conditions for solute yields that were normalized to recovered porewater for molal porewater concentrations. All core samples are run as a set of four replicates to ensure reproducibility.

Coherent profiles for conservative solutes and isotopes show the shale aquiclude porewaters to be ~5.8 molal Na-Ca-Cl-Br brine (Figure 1), interpreted as a highly evaporated, post-dolomitization brine that infiltrated the section during Silurian time. Stable isotope profiles of water, with $\delta^{18}O = -3.2 \pm 0.6‰$ and $\delta D = -48 \pm 2‰$, from six deep boreholes, using the vacuum-distillation method, yield consistent results (Figure 1). In addition, for those formations from which groundwater samples could be obtained (Salina A1 Unit, Guelph Formation and Cambrian), vacuum-distillation results are consistent with measured groundwater isotopic values (Figure 1). The contribution of clay hydration waters is considered to be minor given that these are largely illite-bearing shales, and that the isotopic fractionation between clay hydration water and the porewater reservoir is insufficient to impart a significant error on the measurements; although, in smectite-bearing materials the effect of clay hydration waters would require evaluation.

CH_4 and He were sampled in separate experiments, using microcores for He and outgassing from broken core in sealed containers for CH_4. Their concentrations and isotopes provide age constraints, showing little to no diffusive transport into or out of the shale section since Paleozoic time. Isotopes for CH_4 and CO_2 ($\delta^{13}C_{CH_4}$, δD_{CH_4} and $\delta^{13}C_{CO_2}$) define a zone of in-situ biogenic methane interpreted to have been generated prior to infiltration of Silurian hypersaline brine and trapped in the shale aquiclude since that

time. He is shown by $^{3}He/^{4}He$ to have ingrown in these shales over a minimum of 260 million years. Below the aquiclude, both CH_4 and He are allochthonous. The transition between the two zones of only a few tens of meters demonstrates little to no evidence of mixing over geological time.

Refinements to the vacuum-distillation method now allow for the analysis of 10 g micro-samples, crushed and vacuum extracted at 150°C for 1 hour (micro vacuum-distillation, µVD), which reduces extraction time and increases through-put. Currently, work on OPA cores from Mont Terri is being undertaken using µVD and a modified micro-coring method for He concentration and isotopes.

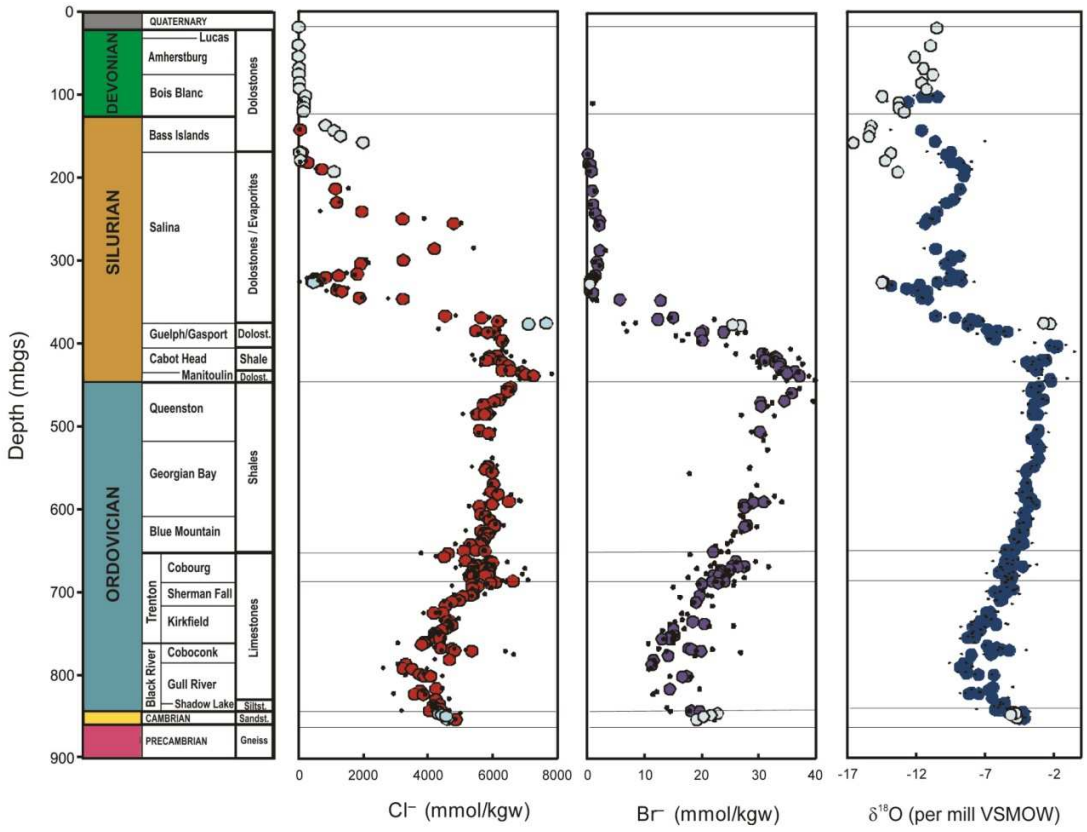


Figure 1: Composite porewater profiles for Cl^-, Br^- and $\delta^{18}O$ from six deep boreholes at the Bruce site in the Paleozoic formations of the Michigan Basin southwestern Ontario, Canada. Free-flowing groundwaters sampled from the section are shown as light blue discs in the Devonian strata from surface to 180 m depth, in the Silurian strata at 330 m and 380 m depth, and in the Cambrian at the base of the profile at 850 m. Coloured discs represent a 3 point running mean of porewater data to highlight primary and secondary features of the profiles. Each point is the mean of four replicate extractions and analysis.

Sorption studies of actinides and lanthanides onto clay minerals under saline conditions

Andreas Schnurr, **Rémi Marsac, Thomas Rabung, Johannes Lützenkirchen, Horst Geckeis**

Karlsruhe Institute of Technology, Institute of Nuclear Waste Disposal (KIT-INE). P. O. Box 3640, 76021 Karlsruhe, Germany. E-mail: *andreas.schnurr@kit.edu*

Abstract

Actinide retention at clay mineral surfaces is a well established process, which has been intensely investigated in the context of nuclear waste disposal (e.g. Bradbury and Baeyens, 2009). Up to now, however, no mechanistic sorption model exists that reliably describe actinide uptake under ionic strength conditions in groundwater upto high salinity (~ 5 mol/kg). Such conditions are to be expected e.g. in the vicinity of a repository in rock salt formations, in the Jurassic and lower Cretaceous clay rock layers in Northern Germany (Brewitz, 1980) or in sedimentary rocks in Canada (Fritz and Frape, 1982), all identified as potential host rocks for high level nuclear waste disposal.

Within the present study lanthanide/actinide ion (Eu(III), Cm(III), U(VI)) interactions with montmorillonite and illite in aqueous solution ($I \leq 4$ mol/L NaCl, $CaCl_2$ and $MgCl_2$) in the absence of carbonate are investigated. Batch sorption and time-resolved laser fluorescence spectroscopy (TRLFS) experiments are carried out for a given ionic strength at fixed metal concentration and constant solid to liquid ratio for $3 < pH_c < 12$ (for $MgCl_2$ solutions up to $pH_c = 9$). Highly saline conditions have a surprisingly small impact on K_D - values in the NaCl system (Fig. 1, left). A significant decrease in sorption extent is observed in solutions with elevated Mg/$CaCl_2$ concentrations (Fig. 1, right), notably for the trivalent cations. Nonetheless, K_D values remain high ($\log K_D \geq 4.5$) for all systems in the pH_c range 7 - 11. TRLFS studies using Cm(III) as a fluorescent probe do not display any in the metal ions first coordination sphere at a given pH_c if ionic strength is increased. As a consequence, we do not expect any change in the surface speciation of Cm(III) at elevated ionic strength compared to a previous study (Rabung et al., 2005). The same surface species are assumed and uptake data are described using the non-electrostatic 2SPNE/SC CE approach (Bradbury and Baeyens, 2002). The impact of elevated ionic strength on the activities of solutes and of water is taken into account by applying the Pitzer approach.

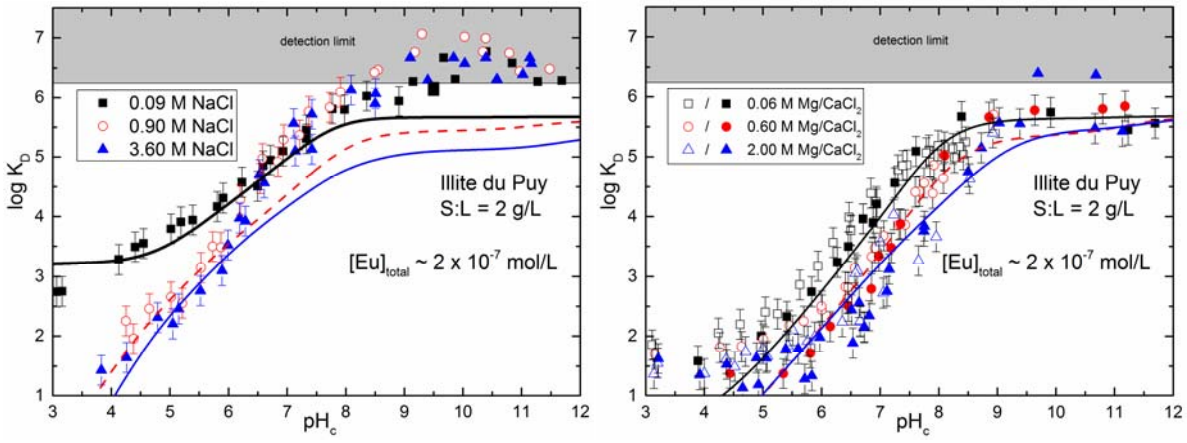


Figure 1: Sorption edges for Eu ($m_{Eu,total} \sim 2.0 \times 10^{-7}$ mol/L), S:L 2 g/L, on Na-illite as a function of pH_c and at different NaCl (left) and Mg/$CaCl_2$ (right) concentrations. Sorption data (symbols) are presented as logarithm of distribution ratio ($\log K_D$). Curves represent blind predictions using the 2 SPNE SC/CE model and Pitzer equations (for the Mg/$CaCl_2$ system data from the Ca-SWy-1 (Bradbury and Baeyens, 2006) system have been used and adaped).

Acknowledgments

We are grateful to Maria Marques Fernandes (Laboratory for Waste Management (LES) Paul-Scherrer-Institute Switzerland) for providing the purified Illite du Puy and Na-SWy-2. The research has received partially funding from the German Federal Ministry of Economics and Technology (BMWi) under contract no. 02 E 10961.

References

Brewitz W. (1980) Zusammenfassender Zwischenbericht, GSF T 114.

Bradbury M. H. and Baeyens B. (2002) Sorption of Eu on Na- and Ca-montmorillonites: Experimental investigations and modeling with cation exchange and surface complexation. *Geochim. Cosmochim. Acta* **66**, 2325-2334.

Bradbury M. H. and Baeyens B. (2006) Modeling sorption data for the actinides Am(III), Np(V) and Pa(V) on montmorillonite. *Radiochim. Acta* **94**, 619-625.

Bradbury M. H. and Baeyens B. (2009) Sorption modeling on illite. Part I: Titration measurements and the sorption of Ni, Co, Eu and Sn. *Geochim. Cosmochim. Acta* **73**, 990-1003.

Fritz P. and Frape S. K. (1982). Saline Groundwaters in the Canadian shield – a first overview. *Chemical Geology* **36**, 179-190.

Rabung Th., Pierret M. C., Bauer A., Geckeis H., Bradbury M. H. and Baeyens B. (2005) Sorption of Eu(III)/Cm(III) on Ca-montmorillonite and Na-illite. Part 1: Batch sorption and time-resolved laser fluorescence spectroscopy experiments. *Geochim. Cosmochim. Acta* **69**, 5393-5402.

Understanding radionuclide interactions with layered materials

Yifeng Wang

Sandia National Laboratories, Department of Nuclear Waste Disposal Research & Analysis, P. O. Box 5800, MS0779, Albuquerque, New Mexico 87185-0779, USA; ywang@sandia.gov

Layered materials play an important role in nuclear waste management and environmental cleanup. Better understanding of radionuclide interactions with those materials is critical for engineering high-performance materials for various applications. This presentation will provide an overview on radionuclide interactions with two general categories of layered materials – cationic clays and anionic clays – from a perspective of nanopore confinement. Nanopores are widely present in layered materials, either as the interlayers or as inter-particle space. Nanopore confinement can significantly modify chemical reactions in those materials. This effect may cause the preferential enrichment of radionuclides in nanopores and therefore directly impact the mobility of the radionuclides. This effect also implies that conventional sorption measurements using disaggregated samples may not represent chemical conditions in actual systems. The control of material structures on ion exchange, surface complexation, and diffusion in layered materials will be systematically examined, and the related modeling approaches will be discussed.

This work was performed at Sandia National Laboratories, which is a multiprogram laboratory operated by Sandia Corporation, a Lockheed-Martin Company, for the DOE under contract DE-AC04-94AL8500.

.

The crystal structure of Magnesium Silicate Hydrate (M-S-H) and its relation with talc-like clay mineral

Roosz C.[a], Grangeon S.[a], Gaboreau S.[a], Montouillou V[c]., Blanc P.[a], Lothenbach B.[d], Vieillard P.[b], Henocq P.[e] and Giffaut E.[e]

[a]BRGM, 45060 Orleans Cedex, France, croosz@brgm.fr
[b]CNRS-IC2MP-UMR-7285 -Hydrasa, 5 Av. Albert Turpain, 86022 POITIERS-Cedex, France
[c]CNRS, CEMHTI, UPR 3079, 45071, Orléans, France
[d]EMPA, Swiss Federal Laboratories for Materials Science and Technology, Laboratory for Concrete and Construction Chemistry, Überlandstrasse 129, 8600 Dübendorf, Switzerland
[e]Andra, F-92298 Châtenay-Malabry Cedex, France.

In the framework of a geological disposal of radioactive waste, cement-based materials will be highly used; the deep geological disposal facility will imply large amounts of concrete in the clay rock formation. In this context, low pH cementitious materials are considered, especially for sealing requirements, in order to minimize chemical interactions at the interfaces between cementitious materials and the clay surrounding rock formations and/or engineered clay materials. The target is to reach a concrete pore solution pH more compatible with the clay materials or rock formation (pH ~7-7.5) for reducing the detrimental impact of the alkali plume from the cement-based materials. Recent studies[1–3] have proposed low-pH formulations based on ternary and quaternary mixes of Portland cement with supplementary cementitious materials (SCMs) such as blast furnace slag (BFS) and fly ash (FA). For these formulations, the pH is controlled by low C/S C-S-H.

However, if for Ordinary Portland Cement (OPC) concrete formulations, the hydration products are well characterized with suitable constrained kinetic/thermodynamic models[4] [4], , the mineralogical control of elements in solution have to be discussed for low pH formulations because of their higher aluminum and magnesium contents[5]. In particular, for the hydration of MgO, which is mainly introduced by the BFS, Zhang et al.[6] have mentioned the precipitation of brucite ($MgOH_2$) which reacted with the silica fume to produce a magnesium silicate hydrate (M-S-H). The calculated pH in equilibrium with this mineralogical assemblage is around 10.5 and satisfies the requirement of low pH condition.

The occurrence of M-S-H has been mentioned in many environments[6–9], and was described as low crystalline phases according to the low intensity and broad peaks signals. Despite this abundance of M-S-H evidences and characterizations, the structure of M-S-H is not well known. Some authors have explained the precipitation of such Mg-silicate hydrates according to Ca/Mg isomorphic substitution in the calcium silicate hydrates (C-S-H). The present study aims to determine this crystal structure and to define their nature (cement phase or phyllosilicate). Two low temperature synthesis of M-S-H have been made, with Mg/Si ratios of 0.6 and 1.2, close to the talc composition ($Mg_3Si_4O_{10}OH_2$) and consistent to the Ca/Si ratio of the C-S-H phases. Crystal chemistry of M-S-H was determined by combining TGA, electron probe micro-analysis (EPMA), TEM, NMR and powder X-ray diffraction. These experimental investigations of poorly crystalline Mg-silicates showed a 2:1 magnesium phyllosilicate-like structure with short range stacking order, identified as a talc-like structure. All the talc structure crystallographic evidences described in previous studies are in agreement with the characterization of the talc synthesis performed for short synthesis time[10]. In that case, the M-S-H particles display a low crystallinity and a small size. XRD patterns were successfully modelled according to the modelling approach developed by Plançon[12,13] and used by Grangeon et al[11], providing

meaningful and accurate structural information, including structure defects, despite the weak modulation of the profiles. A full structure model is then proposed for M-S-H.

(1) García Calvo, J. L.; Alonso, M. C.; Hidalgo, A.; Fernández Luco, L.; Flor-Laguna, V. Development of Low-pH Cementitious Materials Based on CAC for HLW Repositories: Long-Term Hydration and Resistance against Groundwater Aggression. *Cem. Concr. Res.* **2013**, *51*, 67–77.

(2) García Calvo, J. L.; Hidalgo, A.; Alonso, C.; Fernández Luco, L. Development of Low-pH Cementitious Materials for HLRW Repositories. *Cem. Concr. Res.* **2010**, *40*, 1290–1297.

(3) Cau Dit Coumes, C.; Courtois, S.; Nectoux, D.; Leclercq, S.; Bourbon, X. Formulating a Low-Alkalinity, High-Resistance and Low-Heat Concrete for Radioactive Waste Repositories. *Cem. Concr. Res.* **2006**, *36*, 2152–2163.

(4) Matschei, T.; Damidot, D.; Marchand, J.; Lothenbach, B. Thermodynamic Modelling: State of Knowledge and Challenges. *Adv. Cem. Res.* **2010**, *22*, 211–223.

(5) Lothenbach, B.; Le Saout, G.; Ben Haha, M.; Figi, R.; Wieland, E. Hydration of a Low-Alkali CEM III/B–SiO2 Cement (LAC). *Cem. Concr. Res.* **2012**, *42*, 410–423.

(6) Zhang, T.; Cheeseman, C. R.; Vandeperre, L. J. Development of Low pH Cement Systems Forming Magnesium Silicate Hydrate (M-S-H). *Cem. Concr. Res.* **2011**, *41*, 439–442.

(7) Ono, H.; Wada, S. I. Properties of Layer Silicates Formed from MgO-SiO2-H2O Mixtures at 25 Degree C. *J. Fac. Agric. Kyushu Univ.* **2007**, *52*, 159–162.

(8) Dumas, A.; Martin, F.; Le Roux, C.; Micoud, P.; Petit, S.; Ferrage, E.; Brendlé, J.; Grauby, O.; Greenhill-Hooper, M. Phyllosilicates Synthesis: A Way of Accessing Edges Contributions in NMR and FTIR Spectroscopies. Example of Synthetic Talc. *Phys. Chem. Miner.* **2013**, *40*, 361–373.

(9) Brew, D. R. M.; Glasser, F. P. Synthesis and Characterisation of Magnesium Silicate Hydrate Gels. *Cem. Concr. Res.* **2005**, *35*, 85–98.

(10) Dumas, A.; Martin, F.; Ferrage, E.; Micoud, P.; Le Roux, C.; Petit, S. Synthetic Talc Advances: Coming Closer to Nature, Added Value, and Industrial Requirements. *Appl. Clay Sci.* **2013**, *85*, 8–18.

(11) Grangeon, S.; Claret, F.; Lerouge, C.; Warmont, F.; Sato, T.; Anraku, S.; Numako, C.; Linard, Y.; Lanson, B. On the Nature of Structural Disorder in Calcium Silicate Hydrates with a Calcium/silicon Ratio Similar to Tobermorite. *Cem. Concr. Res.* **2013**, *52*, 31–37.

(12) Plançon, A. Diffraction by Layer Structures Containing Different Kinds of Layers and Stacking Faults. *J. Appl. Crystallogr.* **1981**, *14*, 300–304.

(13) Plancon, A. New Modeling of X-Ray Diffraction by Disordered Lamellar Structures, such as Phyllosilicates. *Am. Mineral.* **2002**, *87*, 1672–1677.

Partial pressure of CO_2 in the Boom Clay pore water at 16 and 80°C: Experimental data versus modelling assessment.

***Honty M.*, Wang L., De Craen M., Maes N.**[1]

[1] Belgian Nuclear Research Centre (SCK•CEN), Waste and Disposal Expert Group, Boeretang 200, 2400 Mol, Belgium

The partial pressure of CO_2 is an important parameter affecting the solubility and speciation of radionuclides in the pore waters of candidate host rocks for geological radioactive waste disposal. Under undisturbed conditions, the dissolved CO_2 gas is in equilibrium with the minerals present in the Boom Clay. The disposal of high activity, heat-emitting waste will subject the host rockto a thermal stress that will change the mineral solubilities as well as the stability of natural organic matter and thus affect the pCO_2 of the system. Calculations performed for the current Belgian disposal concept indicate that the temperature in the near field of the Boom Clay may reach up to 80°C (Sillen and Marivoet, 2007), depending on the waste type, cooling time and distance between galleries. Importantly, thermal degradation of Boom Clay kerogen may serve as an additional source of CO_2 when exposed to heat (Deniau et al., 2005; Lorant et al., 2008).

In preparation of the large scale *in-situ* PRACLAY heater test (to be started in the near future), an experimental programme was developed to enable monitoring of the pore water chemistry during heating. Firstly, the pCO_2 representative of *in-situ* conditions at 16°C needed to be determined. The circulation system installed on the piezometers CG-30E and CG-35E around the PRACLAY gallery allows for the simultaneous sampling of gas and pore water and in-situ pH measurement at 16°C *(see also poster presentation on the Boom Clay pore water geochemistry, Honty et al., this conference)*. In addition, laboratory batch tests were set up to study the pCO_2 evolution up to 80°C. The batch tests run inside reaction vessels placed in an oven kept at a constant temperature of 80°C. Gas analysis are performed at SCK•CEN using a VARIAN CP-4900 Micro Gas Chromatograph. The geochemical model assuming an equilibrium between: pH, pCO_2 & calcite and the mineral assemblage model to buffer pCO_2 in the system (as proposed by Coudrain-Ribstein and Gouze (1993) and Coudrain-Ribstein et al. (1998)), is tested in the light of the experimental data.

At 16°C, 81 measurements of log pCO_2 lead to a range of values between -3.14 to -2.41 atm (95% confidence interval) with the mean value of -2.68 atm. The pCO_2 data do not show any significant correlation with the pH (Figure 1), Ca or alkalinity, suggesting that calcite equilibium may not be the only controlling mechanism. An alternative model (mineral assemblage model, cf. above) assuming the reaction

(1) Clinochlore + 5 CO_2(g) + 5 Calcite = Kaolinite + Quartz + 2 H_2O + 5 Dolomite

with thermodynamic parameter values from the Thermoddem 2011 (Blanc et al., 2012) database leads to a value of pCO2 = $10^{-2.62}$ at temperature of 16 °C which is in a good agreement with the average value of $10^{-2.68}$ mentioned above.

At 80°C, the pCO_2 reaches a plateau around 0.175 ($10^{-0.75}$) atm after 90 days of the experiment (Figure 2). The initial data point (t0) corresponds to pCO_2 as measured at ~20°C prior to heating. It is concluded that both pCO_2 at 16°C and pCO_2 generated at 80°C agree reasonably well with the mineral assemblage model and related equilibrium reaction (1). Using this model, it is assumed that any CO2 production due to decomposition of kerogen will be buffered as long as the buffering minerals are present. In general, the proposed model is able to predict the evolution of pCO_2 (g), but lightly and systematically overestimates the total CO_2 yields. The more frequent sampling in the course of the stepwise heating is planned in order to dwell on the kinetics of the CO_2 production. In the near future, the large scale PRACLAY heater test will serve, among others, to further validate lab measured pCO_2 at 80°C under *in-situ* conditions.

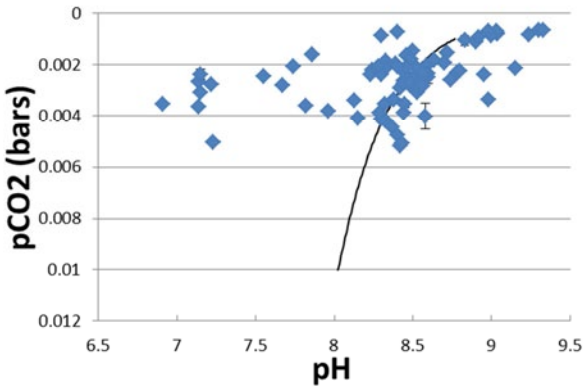


Figure 1. In-situ pCO_2 and pH measured in the filters of the piezometers CG-30E and CG-35E around PRACLAY gallery. Solid line – model assuming reaction $CO_2(g) + H_2O = HCO_3^- + H^+$ as the control mechanism.

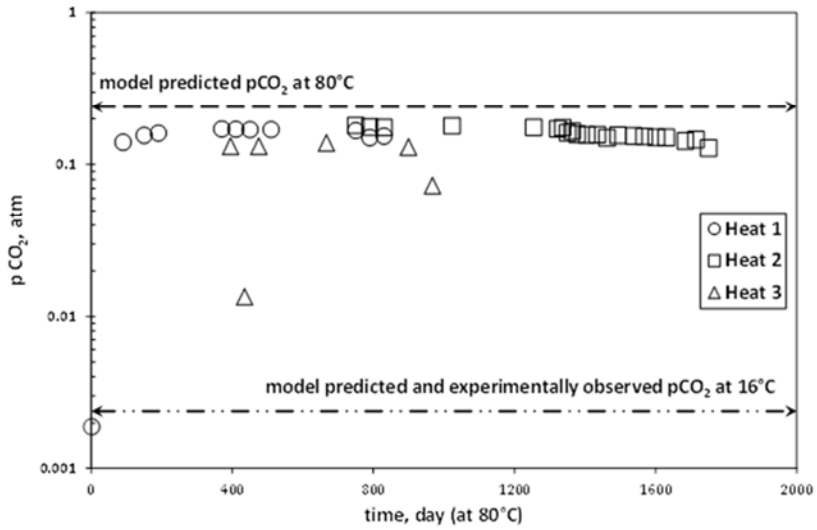


Figure 2. Evolution of pCO2 at 80°C as a function of time. Model calculated partial pressures of CO2 (g) at 16 and 80°C are also shown for comparison (using the mineral assemblage model).

References:

Blanc, P., Lassin, A., Piantone, P., Azaroual, M., Jacquemet, N., Fabbri, A., and Gaucher, E. (2012) Thermoddem: A geochemical database focused on low temperature water/rock interactions and waste materials, Applied Geochemistry, 27: 2107-2116.

Coudrain-Ribstein, A. and Gouze, P. (1993) Quantitative study of geochemical processes in the Dogger aquifer, Paris Basin, France, Applied Geochemistry, 8: 495-506.

Sillen, X. and Marivoet, J., 2007. Thermal impact of a HLW repository in clay. Deep disposal of vitrified high-level waste and spent fuel. SCK•CEN-ER 38, Mol, Belgium.

Deniau, I., Behar, F., Largeau, C., De Canniere, P., Beaucaire, C., and Pitsch, H., 2005. Determination of kinetic parameters and simulation of early CO_2 production from the Boom Clay kerogen under low thermal stress. Applied Geochemistry 20, 2097-2107.

Lorant, F., Largeau, C., Behar, F., and De Canniere, P., 2008. Improved kinetic modeling of the early generation of CO_2 from the Boom Clay kerogen. Implications for simulation of CO_2 production upon disposal of high activity nuclear waste. Organic Geochemistry 39, 1294-1301.

Further understanding of the Boom Clay pore water geochemistry - experiments from the HADES URF, Mol, Belgium.

Miroslav Honty*, Lian Wang, Mieke De Craen and Christophe Bruggeman

Belgian Nuclear Research Centre (SCK•CEN), Waste and Disposal Expert Group, Boeretang 200, 2400 Mol, Belgium
*Corresponding author: miroslav.honty@sckcen.be

As the Boom Clay in the Campine subcrop is considered as a potential host rock for the geological disposal of radioactive waste, a good understanding of the Boom Clay geochemical conditions is essential. This is because the geochemical environment determines, among others, the speciation and solubility of radionuclides.

In 2004, a state of the art report on the Boom Clay pore water chemistry and the understanding of the Boom Clay geochemical environment for the Mol site was presented by De Craen et al. (De Craen et al., 2004). In this report, a reference range was given for the Boom Clay pore water composition, which was based on the TD-11D piezometer, covering a limited depth range (~40 m) of the Boom Clay. The theoretical pH and pCO_2 were calculated from the measured pore water composition of this piezometer due to the lack of the *in situ* measured pH and pCO_2.

The major achievements presented here relate to the use of *in-situ* pore water data from several piezometers around the HADES URF, and covering more or less the entire thickness of the Boom Clay Formation at the Mol site. In addition, the improved methodology for borehole drilling and installation of piezometers, the improved methodology for *in-situ* sampling of pore water and dissolved gasses, and the new methodology for *in situ* pH measurements, led to an integrated data set of pore water chemistry, pH and pCO_2, representative of *in situ* conditions.

The new data confirmed the general statements about the Boom Clay pore water chemistry reported earlier. The Boom Clay pore water in Mol is characterised by an overall homogeneous composition, although small variations can be recognised. The latter mainly reflect natural variation within the Boom Clay (e.g. more DOC in pore waters obtained from organic-rich black layers) and slightly increasing concentrations of major anions and cations towards the HADES gallery. In general, the Boom Clay pore water in Mol is a $NaHCO_3$ solution of 15 mM, containing an important amount of dissolved organic matter (average of 104 mg C / L). It is characterised by its slightly alkaline pH of 8.3 and redox potential around -300 mV. The mean partial pressure of CO_2 reaches the value of log pCO_2 = -2.68, which is in agreement with both calcite equilibrium and the mineral assemblage model. However, the observed pore water chemistry and pH variations are more in favour of the mineral assemblage model (Coudrain-Ribstein et al., 1998) than considering purely calcite and pH as controlling factors affecting the pCO_2 of the system (see below).

Geochemical modelling explained the observed major cation concentrations by cation exchange and mineral dissolution/precipitation mechanisms. The geochemical model assumed the equilibrium of calcite, siderite, pyrite, and chalcedony, and the cation exchange between Ca, Na, K, and Mg. Note that in the past model, only calculated pH and pCO_2 values were used because of the lack of reliable measurements. Today, we show that the 2004-geochemical model is still valid, but based on the new experimental data, some significant improvements in understanding of the Boom Clay geochemistry were achieved:

- Experimental measurements on pCO_2 indicate that the *in situ* value is constant despite the variation of pH and the chemical composition in the pore waters. The constant pCO_2 is in line with the well-known phenomena that, under the control of a specific mineral assemblage, pCO_2 depends only on temperature. This changes the existing notion that pH and pCO_2 are always correlated and it is a big step further in understanding the geochemistry of Boom Clay. More experimental data is desirable to further demonstrate the finding however.

- Representative measured *in situ* pH values are available now. However, the controlling mechanism on the pore water pH is still to be understood. We know now that pH is likely independent of pCO_2 and may be controlled by the original pore water composition and sampling artifacts.

- The cation exchange property of Boom Clay is not homogeneous throughout the Boom Clay. There is an observable trend that the ratio (with respect to Na^+) of cation exchangeable cations (K^+, Mg^{2+}, Ca^{2+}) decreases with depth towards the more saline waters. At a certain stratigraphic level, the constant cation ratio seems to represent the feature of cation exchange and can be used as a model parameter to constrain cation exchange when the detailed selectivity parameters are not available.

- Concerning mineral solubility mechanisms, the previous assumptions on calcite, siderite, pyrite, and kaolinite are still valid. The quartz instead of chalcedony is used as a proxy mineral to account for the measured Si concentrations in the pore water. There is a possibility that dolomite and Mg-chlorite are also in chemical equilibrium with the pore water.

Based on the experimental results, a reference range is given for the Boom Clay pore water composition in Mol. Such reference range stems from the natural variability of the Boom Clay pore water as measured in the piezometers installed around the HADES URF. It reflects a range of values which are most likely to be measured if pore water is sampled and analysed from this site. Although we prefer to give a reference range of values, modellers and experimentalists often need one single reference composition of Boom Clay pore water. In this respect, the modelled reference composition of Boom Clay pore water at the Mol site, given in De Craen et al. (2004), is still valid.

De Craen M., Wang L., Van Geet, M. & Moors H. (2004) The geochemistry of Boom Clay pore water at the Mol site, status 2004. SCK•CEN Scientific Report. BLG 990.

Coudrain-Ribstein, A., Gouze, P., and de Marsily, G. (1998) Temperature-carbon dioxide partial pressure trends in confined aquifers, Chemical Geology, 145: 73-89.

Characterization of Dissolved Organic Matter (DOM) derived from Boom Clay, I: Size distribution and element association

M. Bouby[1], U. Kaplan[1], C. Bruggeman[2], D. Durce[2], N. Maes[2], S. Brassinnes[3], T. Schäfer[1]*

* **corresponding author: thorsten.schaefer@kit.edu**

[1] Institute for Nuclear Waste Disposal (INE), Karlsruhe Institute of Technology, D-76021 Karlsruhe, Germany
[2] Belgian Nuclear Research Centre SCK·CEN, Boeretang 200, 2400 Mol, Belgium
[3] ONDRAF/NIRAS, Belgian Agency for Radioactive Waste and Enriched Fissile materials, Geological Disposal, R&D, Avenue des Arts, 14, 1210 Bruxelles, Belgium

In Belgium, deep geological disposal of nuclear waste is envisaged by ONDRAF/NIRAS, the Belgian Agency for Radioactive Waste and enriched Fissile Material, in poorly indurated clay formations like the Boom Clay (BC) or Ypresian clays (http://www.ondraf-plandechets.be). These host rocks have favourable intrinsic properties promoting the retention of radionuclides (low hydraulic conductivity, reducing redox capacity, slightly alkaline character, high specific surface area, cationic exchange capacity and plasticity). Organic material (OM) is present in 1 to 5% wt in BC [1]. Knowing the possible interactions with radionuclides (RNs), this organic material has to be properly characterized. Accordingly, to complement the Belgian research program conducted so far, this research focuses on a better determination and characterization of the mobile size fraction of dissolved organic matter (DOM) currently present and to be expected within the lifespan of the repository (i.e., taking into account the possible geochemical evolution).
Practically, this work concentrates on the size distribution and natural metal association determination of 1) current pore water DOM and 2) DOM released from solid clay samples. The pore waters and solid clay samples are representative of different horizons of the Boom Clay formation in Mol under present-day conditions (i.e., 15 mM $NaHCO_3$).

Boom Clay pore waters are sampled from three piezometers: Spring (1 sample), Morpheus (4 samples), EG/BS (1 sample) located in the HADES underground research facility at Mol. Spring is representative of a given layer (horizontal drilling). EG/BS represents several layers as a bulk (vertical drilling over ~15m). The pore water samples obtained from the Morpheus piezometer come from different levels representing the geological variation; F4: bulk clay with low DOC, F8: bulk double-band silt, F12: bulk silt, F20: bulk clay with high DOC. The pore waters are directly sampled in Swagelok containers under anoxic conditions and kept closed until sample measurements.
Solid clay discs originate from a core drilled vertically down the HADES gallery (perpendicular to bedding plane). The outer rim (~ 2 mm) is removed with a knife and then some pieces are suspended during 1 week up to 1 year in synthetic Boom Clay water (SBCW) consisting of 15 mM $NaHCO_3$ at a solid/liquid ratio of 0.2 kg/L. The suspension obtained from this leaching experiment is then ultra-centrifuged at 15,000 rpm during 90 min. For reproducibility tests, the OM mobilized from three clay discs is collected and stored in glass vials into the fridge before use.

Detailed investigations were carried out by DOC analysis and Asymmetrical Flow Field-Flow Fractionation coupled to a UV-Visible spectrophotometer and an ICPMS detector (AsFlFFF/UV-Vis/ICP-MS; for details see e.g. [2]) before or after (sequential) ultra-filtration (UF). Complementary analyses were done by High Pressure Size Exclusion Chromatography coupled to a UV-Visible spectrophotometer (HPSEC/UV-Vis.). Sequential UF consists of using UF cartridges rinsed before use with ultra-pure water 3 times at 3,500 rpm during 35 min. The cut-offs used are 100 kDa, 30 kDa, 10 kDa and 1 kDa. All the BC pore waters and the leachate suspensions from the solid clay disc samples are sequentially ultra-filtrated as indicated. The different filtrates are placed in glass vials and stored at 4°C in a fridge.

Boom Clay pore water. DOM size distributions obtained by UF, AsFlFFF/UV-Vis./ICP-MS and HPSEC/UV-Vis are consistent with each other. Results agree with DOC analysis on the different isolated fractions.
The analyses show that the OM present in all the BC pore waters analyzed is smaller than 70 kDa or ~ 11 nm. It presents several fractions differing in size. A rather good homogeneity is found between pore water samples originating from different piezometers but at the same geological horizon.The inorganic element analysis reveals the OM-association of several elements like Mg, Mn, Sr and traces of lanthanides (Lns) and actinides (e.g. U, Th). Fe was presently only detected in EG/BS pore water.

OM leachates from clay discs. DOM size distributions obtained by UF, AsFlFFF/UV-Vis./ICP-MS (see Figure 1 and 2) and HPSEC/UV-Vis are consistent. Results agree with DOC analysis on the different isolated fractions.
The samples consist of four OM fractions: 2 fractions are smaller than ~16 kDa or ~ 6 nm and represent 15-25 % ; the 2 other fractions (representing 75-85 %) of the DOC are greater than ~ 6 nm and goes up to ~ 100 nm. Interestingly, the bigger sized OM fractions are those containing mainly the lanthanides and actinides (Th, U) elements, as seen from a direct comparison of the Figures 1 and 2.

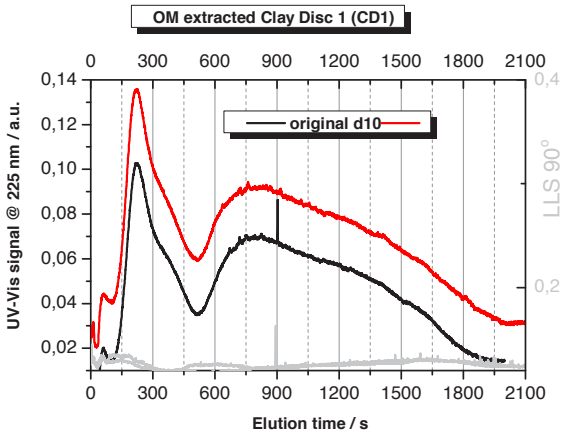


Figure 1: AsFlFFF/UV-Vis fractograms

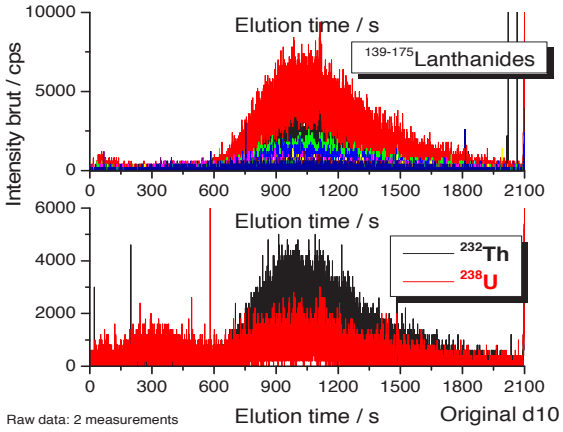


Figure 2: AsFlFFF/ICP-MS fractograms

These results are consistent with the results on the BC pore waters which have been naturally filtered.

Through samples taken at the HADES site, different horizons of the Boom Clay formation were investigated. The present results show an OM size homogeneity: small size fractions (< 70 kDa) are found in all natural pore water samples but with various relative quantities. OM leached from clay disc in laboratory experiments present in addition bigger size fractions.

References:

[1] C. Bruggeman, M de Craen, "Boom Clay natural organic matter", Status report 2011, SCK.CEN-ER.206, External Report, June 2012.
[2] Bouby, M.; Geckeis, H.; Lützenkirchen, J.; Mihai, S.; Schäfer, T., Interaction of bentonite colloids with Cs, Eu, Th and U in presence of humic acid: A flow field-flow fractionation study. Geochim. Cosmochim. Acta 2011, 75, (13), 3866-3880.

This work is entirely financed by ONDRAF/NIRAS.

Characterization of Dissolved Organic Matter /DOM) derived from Boom Clay, II: Organic Functionality

U. Kaplan[1]*, M. Bouby[1], T. Kupcik[1], D. Schild[1], P. Kaden[1], C. Bruggeman[2], D. Durce[2], N. Maes[2], S. Brassinnes[3], T. Schäfer[1]*

[1] Institute for Nuclear Waste Disposal (INE), Karlsruhe Institute of Technology, D-76021 Karlsruhe, Germany
[2] Belgian Nuclear Research Centre SCK·CEN, Boeretang 200, 2400 Mol, Belgium
[3] ONDRAF/NIRAS, Belgian Agency for Radioactive Waste and Enriched Fissile materials, Geological Disposal, R&D, Avenue des Arts, 14, 1210 Bruxelles, Belgium

Dissolved organic matter (DOM) is a complex heterogeneous mixture composed generally of humic substances and non- humic fractions (e.g. carbohydrates, lipids, amino- and fatty acids) [1,2]. Boom Clay DOM is considered to consist solely of humic substances (the non-humic fraction being negligible). Research has shown that DOM plays an important role in controlling the speciation and toxicity of trace metals in aquatic environments [e.g. 3]. In Belgium, deep geological disposal of nuclear waste is envisaged by ONDRAF/NIRAS, the Belgian Agency for Radioactive Waste and enriched Fissile Material, in poorly indurated clay formations like the Boom Clay (BC) or Ypresian clays (http://www.ondraf-plandechets.be). The Boom Clay has favourable properties promoting the retention of radionuclides (RNs) within the host formation, like a low hydraulic conductivity and high sorption capacity. However, the Boom Clay (BC) pore water also contains DOM, which may potentially influence the mobility of RNs within the formation and therefore has to be properly characterized. In this study, we will present an approach of DOM functionality characterization of different size fraction isolated from BC pore water using various spectroscopic techniques (UV-Vis, XPS, STXM and NMR). The information obtained on the structural characterization of DOM can be used to provide a mechanistic understanding of RN complexation behaviour and the reversibility of RN sorption processes on organic colloids in order to reliably predict the long-term contaminant mobility in deep geological formations. Exemplarily, results are presented for Boom Clay pore water sampled from SPRING 116 piezometer of the HADES underground laboratory. The SPRING 116 piezometer is equipped with a large filter screen with a pore size distribution of 7 to 16µm giving no size exclusion to pore water organic matter. The piezometer is installed horizontally into the Boom Clay [4]. All sampling and preparation steps are performed under anoxic conditions (< 1ppm O_2).

UV-Vis. The UV/VIS spectra of the humic substances are dependent on the pH, the ionic strength, and the presence of complex formation with higher-valent metal ions [5]. For the evaluation of the UV-Vis spectra the absorption ratio at two wavelengths (300 and 400 nm or E3 and E4, respectively) for different fractions (<1 kDa, 1-10 kDa, 10-100 kDa and unfiltered SPRING 116 pore water) is calculated. This value can be used for a qualitative classification of HA and FA [6]. UV/Vis results for show in comparison to [6] for all size fractions measured a dominance of fulvic acid type material.

XPS. XPS was used to describe the elemental composition and to study the C, O, N, and S functional groups (see table 1). DOC extracted was separated by 1kDa ultrafiltration (filter material: modified polyethersulfone on polyethylene substrate). The filter cakes were washed by adding 1 mL of Milli-Q water to remove the salt content followed by subsequent ultrafiltration using the same filtration units. The suspension was deposited on an aluminium foil and dried at room temperature under Ar atmosphere. XPS results show the photoelectron lines of carbon at ~ 286 eV (C1s), of nitrogen at ~ 400 eV (N1s), and of sulfur at ~164 eV (S2p) and ~ 229 eV (S2s). Narrow spectral scans were used for speciation. The O/C ratio of SPRING porewater > 1kDa was measured to be ~0.48 which is nearly identical to the results obtained for Boom Clay Fulvic Acid (0.46) published in [7].

Table 1: Atomic Concentration Table (at-%), relative error ± (10-20) %

Sample	C	N	O	Na	Mg	Al	S	Cl	K	Ca	Fe	O/C
Spring	58.8	4.1	28.5	3.1	-	1.2	0.4	0.6	2.2	0.8	0.3	**0.48**

* **corresponding authors: ugras.kaplan@kit.edu; thorsten.schaefer@kit.edu**

Furthermore, inorganic impurities of the elements Al, Ca, K and Fe could be detected. As the SPRING piezometer has a large filter diameter the possibility of organic matter associated clay colloids cannot be ruled out at the present stage of investigations.

STXM. STXM investigations were carried out at the Canadian Light Source (CLS), beamline 10ID-1_STXM. Sample preparation was performed by using 1μL of pore water directly dried on Si_3N_4 windows under Ar atmosphere (glove box) and measurements on different element absorption edges including the carbon K-edge, potassium L-edge, nitrogen K-edge and Fe L-edge were performed. Principal component and cluster analysis [8] revealed only one significant cluster in the SPRING sample investigated, whereas in other pore waters examined at least two clusters could be identified.

Table 2: Semi-quantitative analysis of the average carbon K-edge by spectra de-convolution

Sample	Red shift area	C_{arom}	Phenol-type	C_{aliph}	Carboxyl-type	O-alkyl-type
COx (447) HA isolate (ref. [9])	5	22	16	17	27	14
COx (447) FA isolate (ref. [9])	3	23	14	19	30	10
Gorleben FA (ref. [10])						
Recharge (GoHy-421)	0	12	12	10	41	25
Enhanced DOC (GoHy-2227)	4	18	19	7	40	12
Boom Clay (Spring porewater)	**1**	**15**	**10**	**14**	**43**	**17**

The Spring porewater DOC spectra (Table 2) are clearly different from the organic matter extracted from Callovo-Oxfordian (COx) and lies in the range of groundwater FAs from the Gorleben site. In a further step we used a sulphur embedded microtome section of the Boom Clay sediment (sample code TD25-26/06-52) (Figure 1) to locate potential source regions of the pore water organic matter via target spectra analysis and inorganic mineral correlation. In the microtome under the spectral resolution measured, organic matter associated to illite (K L-edge measured simultaneously and Al K-edge) and pure organic matter could be identified. Target spectra analysis showed a good correlation between the pore water DOC and the solid organic matter (SOM) characterised in the microtome. The SPRING porewater DOC analysis by UV/Vis, XPS and STXM gives a consistent picture and comparison to SOM by STXM reveals strong spectral similarities, although the oxygen containing functional groups are enriched in the porewater, which is expected for hydrophilic compounds. Furthermore, NMR results on Boom Clay organic material will be presented to give more details on organic functionality and structure.

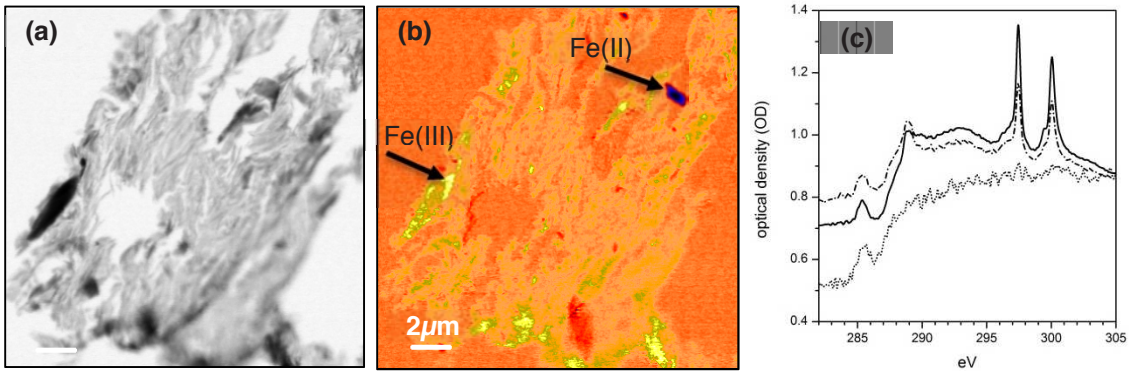


Figure 1. STXM absorption image of the Boom Clay microtome showing the resolution for spectral analysis (a); Fe(II)/Fe(III) distribution map with high Fe(II) and high Fe(III) regions as indicated by the arrows (b), and carbon K-edge cluster spectra found in the microtome (c).

References:

[1] Chin, Y. P.; Aiken, G.; Oloughlin, E. (1994) *Environ. Sci. Technol.* 28(11), 1853-1858.; [2] Bouby et al. (2015) this abstract volume.; [3] Ma et al. (1999) *Environ. Toxicol. Chem.* 18(5), 828-837.; [4] De Craen et al. (2004) Scientific Report SCK•CEN- BLG-990.; [5] Buckau, G. (1991) PhD thesis. Freie Universität Berlin, Berlin.; [6] Claret et al. (2003) *Sci. Total Environ.* 317(1-3), 189-200. [7] Bruggeman, C.; De Craen, M. (2011) External Report SCK•CEN-ER-206, 12/CBr/P-37. ; [8] Lerotic, M. et al. (2004) *Ultramicroscopy* 100(1-2), 35-57.; [9] Schäfer et al. (2009) *J. Electron Spectrosc. Relat. Phenom.* 170, 49-56. [10] Schäfer, T. et al. (2005) *Org. Geochem.* 36(4), 567-582.

Influence of organic cations on clay surfaces and retention capacity -an XPS, FTIR and MD simulation study-

Schampera, B.[1], **Mikutta, R.**[1], **Woche, S.K.**[1], **Tunega, D.**[2], **Solc, R.**[2], **Dultz, S.**[1]
[1] Institute of Soil Science, Leibniz University Hannover, Germany
[2] Institute for Soil Research, University of Natural Resources and Life Sciences (BOKU), Austria

Clays and clay minerals in natural or engineered barriers prevent migration of toxic species to the environment. Especially bentonites (main constituent montmorillonite) are frequently examined for the use in barrier systems to reduce pollutant discharge due to their high permeability, ductility and cation exchange capacity (CEC). A challenge is the improvement of the low retardation capacity for anions and non-polar compounds, which can be obtained by modification with specific organic cations. Such organoclay material may have (i) the capability to adsorb anions in high amounts, (ii) the ability to sorb anions and cations simultaneously, and (iii) the capacity for adsorption of non-polar compounds. Chemical modification induces changes of material properties including surface characteristics. As transport mechanisms at solid-liquid interface are generally affected by material surface properties, knowledge on altered surface properties of clays is required. The arrangement of the organic cations in the montmorillonite interlayer space as a function of the applied amount of organic cations was studied in detail (e.g., [1], [2]) in contrast to the modification of physicochemical properties of the external surfaces.

In this study, the effect of increasing loadings (up to 3.5 times of the CEC) of two organic cations [hexadecylpyridinium- (HDPyCl) and hexadecyltrimethylammonium-chlorid (HDTMACl)] on the external montmorillonite surface has been investigated. X-ray photoelectron spectroscopy (XPS) combined with molecular dynamic (MD) simulations were used to characterize the arrangement of the organic cations on the external surfaces of montmorillonite. To examine the diffusion of conservative solutes (D_2O), anions (NO_3^-, SeO_3^{2-}), cations (NH_4^+) and non-polar compounds (phenanthrene) as a significant indicator of retention properties of clays, evaluations of transport by infrared spectroscopy (IR) was combined with MD simulations.

Quantification of elements assigned to the clay and organic compound by XPS clearly showed an increasing coverage of the clay surface by organic cations with increasing applied amount (Fig. 1, trend in atom-% of O, N, C, Si, Al).

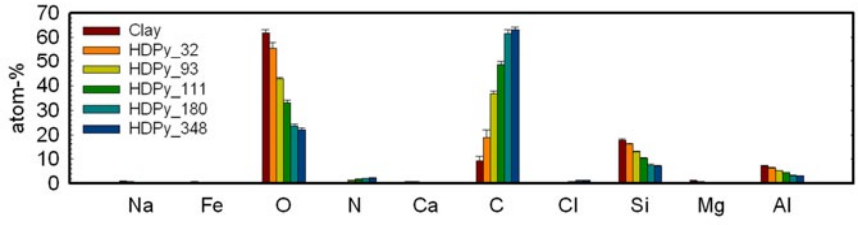


Fig. 1 XPS quantification of elements contained in the clay structure (e.g. O, Si and Al) and organic cation (e.g. N and C). (HDPy_32, _93, _111, _180, _348 = $HDPy^+$ amount adsorbed corresponding to 32, 93, 111, 180, 348 % of the CEC).

Further changes of surface properties have been evaluated by determination of surface charge and wettability. Classical force-field MD simulations were performed on organoclay-water slab models with a surface coverage range from 0.125 to 1.5 $HDTMA^+$ ions/A_{uc} (unit cell area) using the LAMMPS package [3]. Findings by XPS and MD confirmed the formation of mono- to bilayers parallel or in an angled arrangement of the cations on the clay surface (Fig. 2b, c). This was supported by an increase of surface charge with the amount of organic

cations applied (-119 to +55 $mmol_c/kg$) and varying wettability (hydrophilic/hydrophobic). The arrangement of the organic cations at the surface differed from the arrangement in the interlayer space. Our results indicate that the varying surface arrangement will inevitably affect the transport behavior at the solid-liquid interface of the modified clays.

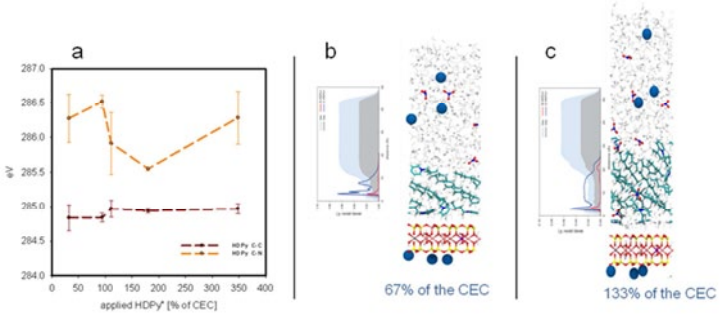


Fig. 2a-c Variation of the surface arrangement of the organic cations with respect to the applied and adsorbed amount; a: Dependence of XPS C1s high resolution spectra of C-C and C-N binding energy (eV) on adsorbed amount; b: one-dimensional density profiles of atoms from the adsorbed surface layer (left) and a snapshot from MD showing an arrangement of $HDPy^+$ cations for an adsorbed amount of 67% CEC (right); c: the same as in b) for an adsorbed amount of 133% CEC.

IR-Diffusion experiments conducted for D_2O, 1M anion and cation solution as well as solution of non-polar compounds (in pure water, original clay and organoclay samples) and MD-simulations provided comparable results and trends for free solution, effective or apparent diffusion. For example, the diffusion coefficient for the NO_3^- anion in free solution is 1.2 x $10^{-9}m^2/s$ (experiment) and 1.5 x $10^{-9}m^2/s$ (MD simulation), respectively. Calculated rock capacity factors, tracing specific material retardation capacity, showed the impact of surface property changes on the retention. While high retention of conservative solutes was traceable for the analyzed clay and organoclays (except hydrophobic $HDPy^+$-montmorillonite), natural clay exhibited low retardation for monovalent anions and hydrophobic $HDTMA^+$-montmorillonite for bivalent anions. The lowest rock capacity factor for cations prevailed for hydrophobic $HDPy^+$-montmorillonite. In contrast the largest retention capacity for non-polar compounds was analyzed for hydrophobic $HDTMA^+$-montmorillonite.

Combined experimental and MD studies proved to be powerful tools in the characterization of the arrangement of organic cations on the external clay surfaces and diffusion and transport processes at the solid-liquid interface of organoclays.

References

[1] Meleshyn, A. & Bunnenberg C. *J. Phys. Chem. B* 2006, 110, 2271-2277.
[2] Park, Y., Ayoko, G.A., Frost, R.L. *J. Coll. Int. Sci.* 2011, 354, 292–305.
[3] Plimpton, S. *J. Comp. Phys.* (1995), 117, 1-19.

Setting up a thermodynamic solid solution model for illites

U.R. Berner
Paul Scherrer Institut, CH-5232 Villigen PSI

Very recently we presented a thermodynamic model for montmorillonite, essentially designed for the use in reactive transport simulations (Berner et al., 2013) and for modelling the composition of clay pore waters (bentonite, Opalinus Clay). This model was based on a stoichiometric unit $Na^+[Mont^-].4.84H_2O$ where $[Mont^-]$ consists of 2:1 TOT layers, intercalated with about 2 layers of water including the counter-ion Na^+. The interlayer water was formulated as chemically bound water, in order to control and facilitate mass balance calculations in cases where the montmorillonite phase may dissolve (i.e., under elevated pH-conditions) in the reactive transport simulations. Based on selectivity coefficients evaluated by Bradbury and Baeyens (2002, 2005), the thermodynamic properties (Δ_fG^0-values) of other end-members (e.g., $K^+[Mont^-].4.84H_2O$, $Ca^{2+}[Mont^-]_2.9.68H_2O$, $Mg^{2+}[Mont^-]_2.9.68H_2O$, etc.) were derived. The final set of seven end-members (Na, K, Ca, Mg, Sr, Fe(II), Ba) was regarded as an ideal montmorillonite solid solution. This solid solution was calibrated against solution/solubility data obtained by Bradbury and Baeyens (1995) during purification and conditioning of MX-80 Na-montmorillonite. The resulting phase also includes surface-dependent S≡OH-groups whose acidity constants were also taken from Bradbury and Baeyens (2002, 2005). The montmorillonite model was successfully applied to reactive transport modelling in clay rock/cement systems (Kosakowski and Berner 2013) and was used to model clay pore water compositions in ongoing safety assessments for a deep geological repository.

Besides montmorillonites clay host rocks contain illite and illite/smectite mixed layers, phases that may be even more important when considering mass fraction-, cation exchange-, sorption- and pH-control properties of host rocks for deep geological repositories. The present work therefore aims at setting-up a thermodynamic model for illite, based on the approach previously applied to montmorillonite.
According to present opinions illites and particularly illite/smectite mixed layers are comprised of basic units similar to the TOT layers of the montmorillonite. A key difference is given by the fact that in pure illite two TOT layers are interconnected solely by K^+-ions and do not contain interlayer water. Since illites may exhibit substantial cation exchange properties (about 20 % of montmorillonite) they must include substantial parts of smectite-type interlayers including accessible interlayers. This forms the conceptual basis of our set-up.
We rely on composition and characteristics of Na-illite du Puy, evaluated by Bradbury and Baeyens (2009). The illite consists of staples of about 50 to 100 TOT layers, interconnected by either K^+-ions or by $[Na^+, xH_2O]$. Elementary analysis of the illite phase is compatible with 77 % of TOT-TOT units occupied by K^+ and 23 % TOT-TOT units occupied by $[Na^+, xH_2O]$. Vertical stacking of TOT layers would therefore mean that about each fifth interlayer is comprised by hydrated sodium $[Na^+, xH_2O]$, all other interlayers do not include water but solely K^+.
In this study we adopt a horizontal arrangement of illite- and smectite type units as outlined in Figure 1. We assume that all TOT layers have the same stoichiometric composition, independent of the interlayer cation. Hence, the central part of the pile of individual TOT-TOT pairs (right side in Fig. 1) is occupied by K^+ ions, the TOT pairs in the outer rim of the pile (left side) are occupied by hydrated Na^+ ions (~ 2 layers of water). This set-up leads to a rather complex basic stoichiometric unit:

$$\{K[Si_{4-x}Al_x][Al_{2-p-s-t}Mg_pFe_s^{2+}Fe_t^{3+}]O_{10}(OH)_2\}_y\{Na[Si_{4-x}Al_x][Al_{2-p-s-t}Mg_pFe_s^{2+}Fe_t^{3+}]O_{10}(OH)_2.4.84H_2O\}_z\,,$$

where the stoichiometric coefficients x, p, s, t, y, z=f(CEC) will be selected according to and compatible with the detailed elementary analysis of the Na-illite de Puy and the measured cation exchange capacity (CEC) reported by Bradbury and Baeyens (2009) and Baeyens (2014). The stoichiometric ratio Fe^{2+}/Fe^{3+} may be critical for system Eh in thermodynamic model calculations.

Hence, selecting a ratio identical to the ratio previously used in the montmorillonite model appears to be a consistent and sensible initial value.
Detailed equilibrium solution data including Na-, K-, Mg-, Ca-, Sr-, Al-, Si- and Fe concentrations as well as pH and ionic strength from Baeyens (2014) are used to calibrate the free energy of formation ($\Delta_f G^0$) of the presented stoichiometric unit for use in thermodynamic geochemical equilibrium models. Similar to the montmorillonite model, selectivity constants for cations reported by Bradbury and Baeyens (2009) are used to construct a corresponding illite solid solution model for describing cation exchange properties. Reported surface site capacities and protolysis constants are used to describe the amphoteric and potentially the sorption properties of the illite type phase.
First results of this calibration process will be presented and consistency with the existing model for the montmorillonite phase will be discussed.

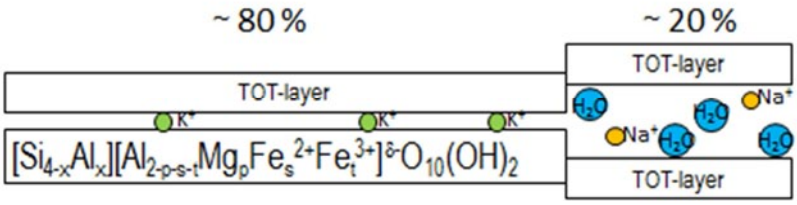


Fig. 1: Simplified operational representation of illite-smectite mixed layers. An alternative would be a vertical stacking where about each fifth TOT-TOT unit would be intercalated with hydrated Na^+ ions (~ 2 layers of water). In the present study a horizontal arrangement is adapted. The sketch represents one half of a vertical cut through the pile of TOT layers (only one TOT-TOT pair is shown for simplicity). The central part of the pile of individual TOT-TOT units (right side, no interlayer water) is occupied by K^+ ions, the TOT units in the outer rim of the pile (left side) are occupied by hydrated Na^+ ions (~ 2 layers of water).

References

Baeyens, B. (2014), Paul Scherrer Institute, Villigen, Switzerland, unpublished internal reports.

Berner, U., Kulik, D.A., Kosakowski, G. (2013). Geochemical impact of a low-pH cement liner on the near field of a repository for spent fuel and high-level radioactive waste. Phys. Chem. Earth 64, 46-56.

Bradbury, M.H., Baeyens, B. (1995). A quantitative mechanistic description of Ni, Zn and Ca sorption on Na-montmorillonite. Part I: Physico-chemical characterisation and titration. PSI Report 95-10, Paul Scherrer Institute, Villigen, Switzerland, and Nagra Technical Report 95-04, Nagra, Wettingen, Switzerland.

Bradbury, M.H., Baeyens, B. (2002). Porewater chemistry in compacted re-saturated MX-80 bentonite. In: Physico-Chemical Characterisation and Geochemical Modelling, PSI Report 02-10. Paul Scherrer Institute, Villigen, Switzerland.

Bradbury, M.H., Baeyens, B. (2005). Modelling the sorption of Mn(II), Co(II), Ni(II),Zn(II), Cd(II), Eu(III), Am(III), Sn(IV), Th(IV), Np(V) and U(VI) on montmorillonite: Linear freee energy relationships and estimates of surface binding constants for some selected heavy metals and actinide. Geochim. Cosmochim. Acta 69, 875-892.

Bradbury, M.H., Baeyens, B. (2009). Sorption modelling on illite Part I: Titration measurements and the sorption of Ni, Co, Eu and Sn. Geochim. Cosmochim. Acta 73, 990-1003.

Kosakowski, G., Berner, U. (2013). The evolution of clay rock/cement interfaces in a cementitious repository for low-and intermediate level radioactive waste. Phys. Chem. Earth 64, 65-86.

Study of the surface reactivity of clay mineral phases by isotope exchange

Suzuki-Muresan T., David K., Perrigaud K., Landesman C., Abdelouas A., Grambow B.

SUBATECH, Unité Mixte de Recherche 6457, Ecole des Mines de Nantes, CNRS/IN2P3, Université de Nantes, 4 rue Alfred Kastler, BP 20722, 44307 Nantes cedex 03, France

Corresponding author: tomo.suzuki@subatech.in2p3.fr

The Callovo Oxfordian argillite was chosen as a potential host rock to store future long life intermediate level waste and high level waste. The argillite was chosen for its properties adapted to store these waste packages in terms of strengths coefficients radionuclide retention properties, low water permeability, a large specific surface [1 2]. The argillite is composed mainly of clay (illite, illite interlayer / smectite 45-55%), carbonates 30-40%, tectosilicates 20-30% and pyrite 1-2% [3]. The aim of our study was to better understand the reactivity of clay mineral phases, especially in the conditions close to equilibrium expected when pore water saturates the geological formation thousands of years after the site closure.

In this work, we studied the individual major components of Callovo Oxfordian argillite namely illite, illite/smectite and calcite. The argillite was treated to recover the fine clay fraction (<2μm). The surface reactivity of these phases was evaluated by following the isotope ratio in solution of element constituting the matrices such as silicon ($^{29}Si/^{28}Si$) for argillaceous phases and calcium ($^{42}Ca/^{44}Ca$) for calcite. The isotopic tracer was added when solid/solution equilibrium has been reached. Under these conditions, the natural isotope ratio is modified so as to obtain a mix (=natural + tracer) isotope ratio whose variations can be analyzed precisely. Different experimental conditions were imposed: pH, temperature, composition of the solution, m/V. The isotope ratio measurement of calcium and silicon has been performed by mass spectrometry plasma source and double focusing monocollection (HR-ICP-MS).
The results show that the reactivity of the clay phase highly depends on temperature. In the near-equilibrium conditions, we have identified and confirmed that a mechanism of dissolution/precipitation controls the equilibrium [4]: (i) 90°C the variation of the mix isotope ratio is increased and the mix ratio tends towards natural isotope ratio (R = 0.0508) after 100 days of contact; (ii) at 35° and 50°C the evolution and variations of the mix isotope ratio are similar and the temperature range has little effect on the surface reactivity. Beside, the study on calcite shows that the surface reactivity of this phase is dependent on the specific surface and ratio m/V. The mechanism controlling the equilibrium is (i) the type of dissolution / precipitation in the presence of a low surface area (~0.5 m^2/g) and (ii) isotope exchange-type in the presence of a high surface area (~10 m^2/g). In the latter case, the mix isotope ratio is close to the natural ratio (R = 0.310) after 100 days of contact.

The study of various components of the argillite has provided insight and understanding on the reactivity of Callovo Oxfordian argillite in the near-equilibrium conditions. We have shown that the argillite is a complex and dynamic system where mechanisms of dissolution/precipitation or isotope exchange mechanisms may control the equilibrium at the surface/solution interface.

1 ANDRA, *Dossier ANDRA argile: Evaluation de la faisabilité du stockage géologique en formation argileuse*, (2005), 239.

2 F. Bergaya, B. K. G. Theng and G. Lagaly, *Handbook of Clay Science, Developments in Clay Science*. Amsterdam Elsevier, (2006), 1246.

3 E. Gaucher, C. Robelin, J. M. Matray, G. Négrel, Y. Gros, J. F. Heitz, et al. (2004). ANDRA underground research laboratory: interpretation of the mineralogical and geochemical data acquired in the Callovian-Oxfordian formation by investigative drilling, *Physics and Chemistry of the Earth, Parts A/B/C*, 29 (1) 55-77.

4 T. Suzuki-Muresan, J. Vandenborre, A. Abdelouas and B. Grambow (2011). Solution controls for dissolved silica at 25, 50 and 90°C for quartz, Callovo-Oxfordian claystone, illite and MX80 bentonite, *Physics and Chemistry of the Earth, Parts A/B/C*, 36 (17-18) 1648-1660.

Effect of layer charge on the swelling of Na^+, K^+, and Ca^{2+} montmorillonites: DFT and molecular dynamics studies

Anniina Seppälä, Eini Puhakka, *Markus Olin*

VTT Technical Research Centre of Finland, P.O. Box 1000, FI-02044 VTT, Finland

Bentonite clay is an essential material component planned in the KBS-3 concept for safe disposal of spent nuclear fuel. The clay buffer's functions are to limit mass flow to and from the copper canister in order to prevent corrosion, retard transport of radionuclides to bedrock in the case of canister failure and protect the canister in the case of large dislocations of bedrock caused by e.g. tectonic movement. Bentonite consists mainly of montmorillonite which is its functional component, with the presence of some dissolved salts and accessory minerals. Montmorillonite is a swelling clay mineral that consists of 1 nm thick and approximately 200-400 nm wide negatively charged layers that form stacks, charge compensating cations between the layers and near the mineral surfaces. It has abilities to absorb water molecules into the interlayer space, which results in swelling of the mineral, and to change its cationic composition. Bentonite's beneficial macroscopic properties are based on nano level reactions and structures. Therefore, molecular level studies are needed regarding the long term performance assessment of spent nuclear fuel disposal.

The aim of this work was to study the effect of layer charge on montmorillonite's swelling properties. The work was carried out by using different molecular modelling techniques, quantum mechanics (QM) and molecular dynamics (MD). In the QM calculations with CASTEP code included into Materials Studio software (BIOVIA, former Accelrys Inc.), the total electronic energy and overall electronic density distribution are solved in order to define the energetically stable [1] montmorillonite-water structures with different cations, and sorption of cations and other species onto the montmorillonite surfaces. The MD method produces time evolution of a system, the trajectory, by solving Newton's equation of motion for the N-body system under the influence of specified forces. These calculations were used to evaluate equilibrium and transport properties that cannot be calculated analytically. The studied systems were significantly larger than those in the QM calculations, and the calculations were done using the molecular dynamics software LAMMPS [2] with the CLAYFF [3] interaction potential.

In order to perform reliable MD calculations, accurate crystal structures of pure montmorillonites are needed for starting points of the calculations. The structures were obtained from QM calculations, for which the starting point was the experimentally determined montmorillonite structures of Tsipursky et al. [4]. Based on the QM calculations, pure Na-, K- and Ca-montmorillonite structures were achieved, in which chemical composition and layer charges are controlled. Further, the water content of montmorillonites in the interlayer spaces was from 0-10 water molecules per a unit cell.

In the MD calculations, three different layer charges (-1.0 e/unit cell, -0.66 e/unit cell and -0.5 e/unit cell) were applied to three types of montmorillonite (Na, K, Ca). The water content ranged from 1-16 molecules per unit cell, (16 cases for each different montmorillonite) which means about 1-3 water layers in the interlayer space. The calculations were performed on a one layered montmorillonite particle in a periodic simulation box. The objective was to determine the interlayer thickness at equilibrium state in each case. These results were then compared to those from QM calculations. Swelling curves with respect to the water content (Figure 1 on the left) were determined for MD results on Na-montmorillonite. Comparisons were made to the sample system density (Figure 1 in the middle), with contribution only from the mineral layer and interlayer, and the number of interlayer water layers. The swelling curves obtained from both QM and MD calculations for Na-montmorillonite are presented in Figure 1 on the right.

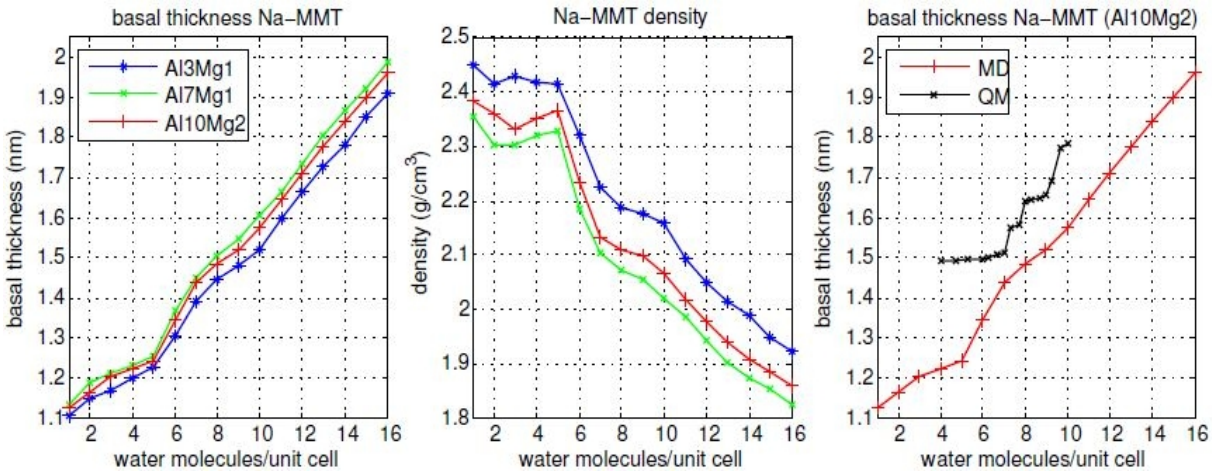


Figure 1 Swelling curves of Na-montmorillonite: basal thickness with respect to the water content (left), system density with respect to the water content (middle), and comparison of the swelling curves obtained from QM and MD calculations (right).

As was expected, smaller layer charge results in greater swelling, but also the type of cation present in the interlayer has an effect. However, these calculations consider only the equilibrium state of a montmorillonite system when water is ”forced” into the interlayer and the rate with which water is absorbed is not taken into account. Similarities between the MD and QM results can be detected, though the QM calculations predict the basal thickness larger than the MD calculations. Further, based on the MD calculations, the formation of water layers in the interlayer space of the montmorillonites can be predicted.

Acknowledgements

The authors wish to acknowledge funding received from Posiva Oy.

References

[1] A. R. Leach, Molecular Modelling, Principles and Applications, 2nd ed., Pearson Education Limited, Essex, (2001).
[2] R. T. Cygan, J.-J. Liang, and A. G. Kalinichev, Molecular Models of Hydroxide, Oxyhydroxide, and Clay Phases and the Development of a General Force Field, J. Phys. Chem. B, 108, 1255-1266 (2004).
[3] S. Plimpton, Fast Parallel Algorithms for Short-Range Molecular Dynamics, J. Comp. Phys., 117, 1-19 (1995). http://lammps.sandia.gov.
[4] S. I. Tsipursky, and V. A. Drits, The distribution of octahedral cations in the 2:1 layers of dioctahedral smectites studied by oblique-texture electron diffraction, Clay Minerals, 19, 177-193, (1984).

Geochemistry of Callovo-oxfordian argillite at 80°C: batch experiments and modeling

***H. Gailhanou*[1], S. Gaboreau[1], M. Debure[1], S. Grangeon[1], P. Blanc[1], N. Marty[1], J.M. Grenèche[2], B. Madé[3], S. Altmann[3], C. Tournassat[1].**

1. BRGM – 3 av. Claude Guillemin BP6009 45060 Orléans cedex 2, France (h.gailhanou@brgm.fr)
2. LUNAM –Université du Maine, Institut des Molécules et Matériaux du Mans, UMR CNRS 6283, 72085 Le Mans cedex (jean-marc.greneche@univ-lemans.fr)
3. Andra – Parc de la Croix Blanche, 1-7 rue Jean Monnet, 92298 Châtenay-Malabry Cedex (Benoit.Made@andra.fr) .

Introduction

A repository of high-level nuclear wastes in the Callovo-Oxfordian (COx) clay rock will lead to a temporary increase in temperature locally around the disposal cells, up to about 80°C. Thermally induced modifications of the pore-water chemistry of the clay rock must be assessed since the pore water chemistry can affect the rates of corrosion of metallic materials used in the disposal facility (Gaucher et al., 2009; Altmann, 2008). In the present study, carried out as part of a collaborative BRGM/Andra research program, the results of long-term batch experiments performed at 80°C, are compared with compositions predicted using a model based on the one developed for 25°C. These experiments include a previous study (Gailhanou et al., 2012) that is completed by recent long-term batch experiments in order to verify the reproductibility of results and better understand the reactivity of the COx rock-solution system at 80°C. In this aspect, selectivity coefficients for exchange reactions Na/K, Na/Ca, Na/Mg and Na/Sr in the clay-porewater system have been acquired at 80°C and have been considered to model the experiments.

Batch experiments

A first series of two experiments were performed with COx rock samples in contact with synthetic water, at 80°C, for durations at 6 and 20 months (Gailhanou et al., 2012). Few changes were detected in the mineralogy between initial and final solids. The only noticeable change was the formation of needles of nanocrystalline goethite on pyrite particles in the 20 months experiment (Gailhanou et al., 2012). A new series of experiments is being conducted to follow the reactivity of the clayrock-solution-gaz system at 80°C for durations from 20 months to 10 years. The results at 20 months are presented here and are compared with the previous ones. In addition, a last experiment was carried out with an initial $CO_2(g)$ partial pressure in the gaseous phase fixed at a higher value than the value predicted by modeling approach (log p_{CO2} = - 0.6 instead of -1.1). This new 20 months experiment aims at verifying that the carbonate system re-equilibrates or not with the whole system independently of the initial pH. All these experiments were prepared at 25°C under anoxic atmosphere in closed reactors, with solution compositions close to the predicted pore water composition (Gaucher et al., 2009). Afterwards, each system was heated at 80°C. p_{CO2} was monitored during the experiments. At the end of the experiments, the suspension was filtered at 0.1 μm at 80°C, under anoxic atmosphere. The pH was measured at 80°C; major cations (Ca, Mg, K, Na, Sr) and anions (notably Cl, SO4), TIC and minor and trace elements (notably Si, Al, Fe, Zn, Pb) were analysed.

In addition, selectivity coefficients were obtained for Na/K, Na/Ca, Na/Mg and Na/Sr cation exchange at 80°C on the clay fraction (< 2 μm).

Modelling of batch experiments

The predictive model of composition as a function of temperature was developed based on the model from Gaucher et al. (2009) and using the PHREEQC code and Thermoddem database (Blanc et al., 2012). Modelling prediction were in fairly good agreement with the results of the first series of experiments, at 6 and 20 months, if the following primary mineral assemblage was considered: quartz, pyrite, carbonates (calcite and dolomite), sulfates (celestite), aluminosilicates (chlorite and illite) and goethite (Fig. 1). This model differs from the model of Gaucher et al. (2009) at 25°C by the replacement of siderite by goethite (Fig. 1). This modification led to a noticeable improvement of the Fe concentration prediction. The introduction of goethite in the model instead of siderite, is in agreement with the presence of nanogoethite detected in the initial sample and in the solid after 20 months experiment .

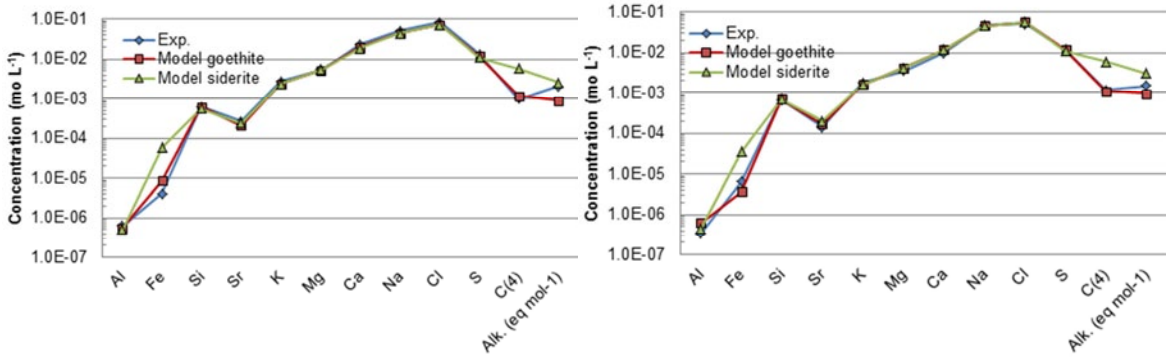


Fig 1. Results of the first series of experiments. Comparison between experimental and modeled concentrations (a) at 6 months at 80°C and (b) at 2 0 months at 80°C.

References

Altmann S. (2008) 'Geo'chemical research: a key building block for nuclear waste disposal safety cases. J. Contam. Hydrol. 102, 174–179.

Blanc P., Lassin A., Piantone P., Azaroual M., Jacquemet N., Fabbri A. and Gaucher E. C. (2012) Thermoddem: a geochemical database focused on low temperature water/rock interaction and waste materials. *Appl. Geochem.* 27, 2107–2116.

Gailhanou H., Tournassat C., Laperche V., Grangeon S., Blanc P., Marty N., Crouzet C., Henry B., Grenèche J.M., Kars M., Madé B., Altmann S. and Gaucher E.C. (2012) Influence of temperature on the geochemistry of Callovo-oxfordian argillite: batch experiments and modelling at 80°C. International meeting "Clays in Natural and Engineered Barriers for Radioactive Waste Confinement", Montpellier, France.

Gaucher E. C., Tournassat C., Pearson F. J., Blanc P., Crouzet C., Lerouge C., and Altmann S. (2009) A robust model for pore-water chemistry of clayrock: *Geochim. Cosmochim. Acta* **73**, 6470-6487.

HYDRATION SEQUENCE OF SWELLING CLAYS EXCHANGED WITH MIXED ALKALI/ALKALI-EARTH CATIONS

FABRICE SALLES[1], OLIVIER BILDSTEIN[2], JEAN-MARC DOUILLARD[1], BENEDICTE PRELOT[1], JERZY ZAJAC[1], HENRI VAN DAMME[3]

[1] *Institut Charles Gerhardt Montpellier, UMR CNRS 5253, UM2, ENSCM, Place E. Bataillon, 34095 Montpellier Cedex 05 France*
[2] *DEN/DTN/SMTM/LMTE, CEA Cadarache, 13108 Saint Paul Les Durance, France*
[3] *PPMD / ESPCI, 10 rue Vauquelin, 75231 Paris Cédex 5,France*

* *E-mail address presenting author fabrice.salles@univ-montp2.fr*

Swelling clays present a multi-scale structure and therefore a multi-scale porosity hierarchy: macroporosity between aggregates / inter-particle mesoporosity / microporosity in the interlayer spacing, as described by mercury intrusion porosimetry, nitrogen adsorption and XRD experiments respectively. In this work, XRD measurements, water adsorption and calorimetry[1], thermoporometry[2], and electrical conductivity results are coupled with electrostatic calculations to investigate (i) the hydration sequence occurring in alkali/alkali-earth cations exchanged montmorillonites, and (ii) the diffusion properties of the interlayer cations.[3]

The comparison between montmorillonites saturated with homoionic alkali or alkali-earth cations [4] and montmorillonite saturated with both alkali and alkali-earth cations leads us to elucidate the impact of the nature of cations and the possible interactions existing upon hydration.

Furthermore the determination of the driving forces for hydration in swelling clays as a function of the nature of the interlayer cations allows us to better capture the dynamics of ionic exchange in swelling clays.

1. F. Salles, J.M. Douillard, R. Denoyel, O. Bildstein, M. Jullien, I. Beurroies, H. Van Damme, Journal of Colloid and Interface Science, 2009, 333(2), 510-522
2. F. Salles, I. Beurroies, O.Bildstein, M. Jullien, J. Raynal, R. Denoyel, H. Van Damme, Applied Clay Science, 39(3-4), 186-201, 2008.
3. F. Salles, O. Bildstein, J.M. Douillard, B. Prélot, J. Zajac, H. Van Damme, submitted
4. F. Salles, O. Bildstein, J.M. Douillard, M. Jullien, J. Raynal, H. Van Damme, Langmuir, 2010, 26(7), 5028-5037

KEY WORDS: Hydration sequence, Cation diffusion, ionic exchange

Zn and Co sorption onto Na-illite – batch sorption study and modelling

V. Montoya [a], T. Kupcik[a], L. Van Laer[c], C. Bruggeman[c], M.A. Glaus[b], B. Baeyens[b], N. Maes[c], T. Schäfer[a], H. Geckeis [a]

[a] Institute for Nuclear Waste Disposal, Karlsruhe Institute for Technology, D-76021 Karlsruhe, Germany
[b] Laboratory for Waste Management, Paul Scherrer Institut, CH-5232 Villigen PSI, Switzerland
[c] Belgian Nuclear Research Centre SCK·CEN, Boeretang 200, 2400 Mol, Belgium

For highly sorbing species such as divalent cations, the coupled diffusion-sorption migration in clay rocks was found to be much more complex than expected (Altmann et al. 2012). The mobility of sorbing species seems to be significantly faster than the one predicted from coupling sorption models obtained in batch equilibrium systems with diffusion characteristics similar to water molecules. The overall objective of this work is to provide experimental evidences and the phenomenological understanding needed to justify the chemical and physical parameters for representing diffusion-driven transfer of actinides and other strongly-sorbing cationic species in clay rocks (see contribution of M.A. Glaus, *Surface diffusion effects for transition metals in compacted illite*).

As a collaboration between different research institutes (SCK·CEN, PSI-LES and KIT-INE) involved in the EC Euratom (FP7) Catclay project (www.catclay.org), sorption of the divalent metal ions Co and Zn onto Na-illite was studied under different experimental conditions (ionic strength and pH). The experimental results were quantitatively described with a sorption model taking into account cation exchange and surface complexation processes using the computer code PhreeqC 3.1. The final aim is to apply the sorption model together with the derived parameters, i.e. selectivity coefficients and surface complexation constants, to describe Co / Zn diffusion in illite.

Sorption experiments onto conditioned Na-illite (Puy-en-Velay, France) were performed both as sorption edges (sorption at trace metal ion concentrations as function of solution pH at a fixed ionic strength, I = 0.1 M) and isotherms (sorption as a function of metal concentration at fixed pH values (pH 5 and 9) and ionic strength, I = 0.1 M) All solutions were buffered to maintain a constant pH and the experiments were performed under controlled N_2 atmosphere (exclusion of CO_2).

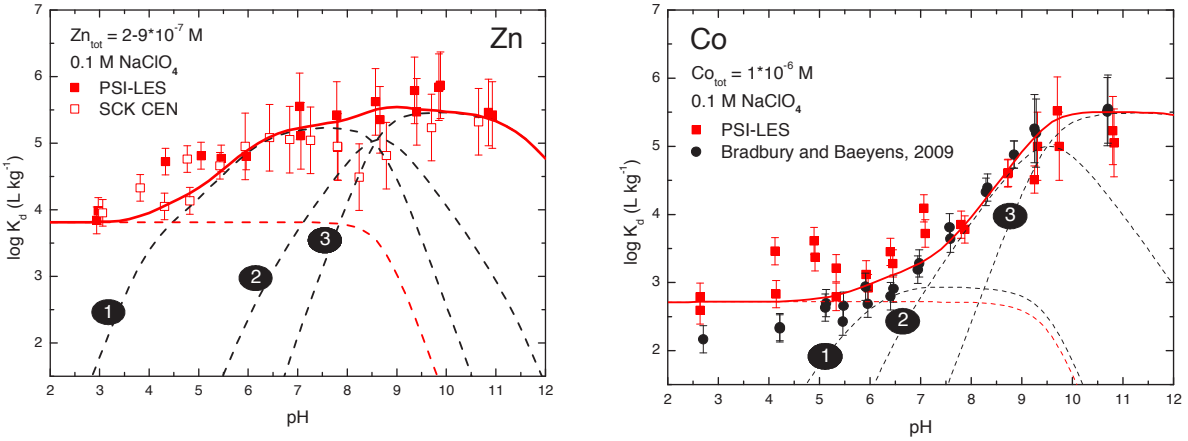


Fig. 1: Sorption edges for Zn (left) and Co (right) on Na-illite at low metal concentrations (Zn: 2-9x10^{-7} M; Co: 1x10^{-6} M) in 0.1M $NaClO_4$ recorded at SCK·CEN and PSI-LES together with literature data (Co only). The continuous curves and dashed lines were calculated using the 2SPNE SC/CE model (Bradbury and Baeyens, 1997).

The pH dependent sorption of Zn and Co onto Na-illite in 0.1M $NaClO_4$ is shown in Figure 1. The shape of the sorption edge differs remarkably for both elements, with a more distinct, typical "edge" shape for Co. For Zn, the flat shape differs significantly from Zn sorption edges measured on Na-montmorillonite (Baeyens and Bradbury, 1997), where logK_d varied over four orders of magnitude in

the pH range from ~5 to 9. The result on illite can be related to the presence of an accessory mineral with a high affinity towards Zn in the acid-to-neutral pH range, or a Zn selective sorption site, responsible for Zn uptake at trace concentrations. Thus, the red dashed curve in Fig. 1 left is rather reflecting Zn sorption onto the respective accessory mineral phase rather than cation exchange reactions.

For Co, two distinct pH regions are visible: constant $\log K_d$ values are observed at low pH ($pH \leq 6$), while $\log K_d$ increases steadily at higher pH. The present data show slightly higher K_d values compared to literature data (Bradbury and Baeyens, 2009), which can also be related to the influence of an accessory mineral phase on Co sorption at trace metal ion concentrations in the acid-to-neutral pH range. However, the general sorption behaviour is reproduced quite well.

A 2 Site Protolysis Non Electrostatic Surface Complexation and Cation Exchange (2SPNE SC/CE) sorption model similar to the one described in the literature for other divalent cations (Bradbury and Baeyens, 1997; Bradbury and Baeyens, 2009) was successfully applied (Fig. 1) using both cation exchange and surface complexation reactions. While cation exchange is the main uptake process for Co at low pH (≤ 6) and low background electrolyte concentrations (<0.1 M), specific inner-sphere complexation dominates Co sorption at higher pH values and ionic strengths. For Zn, the predominant sorption mechanism appears to be surface complexation over the whole pH range. The latter result is somehow remarkable, as literature data on Zn sorption onto Fithian Na-illite (Vermilion County, Illinois) (Gu and Evans, 2007), as well as the results for divalent Ni on conditioned Na-illite du Puy (Bradbury and Baeyens, 2009) show cation exchange mechanisms being present in Na-illite at lower pH.

Acknowledgement
The research leading to these results has received funding from the EURATOM 7th Framework Programme FP7/2007- 2011 under grant agreement n° 249624 (CATCLAY project). Additional funding was provided to SCK•CEN by ONDRAF/NIRAS, the Belgian Agency for Radioactive Waste and Fissile Materials.

References:

Altmann, S., Tournassat, C., Goutelard, F., Parneix, J. C.. Gimmi T., Maes N (2012). Diffusion driven transport in clayrock formations. Applied Geochemistry 27, 463–478

Baeyens, B., Bradbury, M. H. (1997). A mechanistic description of Ni and Zn sorption on Na-montmorillonite Part I: Titration and sorption measurements. J. Contam. Hydrology, 27, 199-222.

Bradbury, M.H., Baeyens, B. (1997). A mechanistic description of Ni and Zn sorption on Na-montmorillonite Part II: Modelling. J. Contam. Hydrol. 27, 223-248.

Bradbury, M.H., Baeyens, B. (2009). Sorption modelling on illite Part I: Titration measurements and the sorption of Ni, Co, Eu and Sn. Geochim. Cosmochim. Acta 73, 990–1003.

Gu, X., Evans, L.J. (2007). Modelling the adsorption of Cd(II), Cu(II), Ni(II), Pb(II), and Zn(II) onto Fithian illite. J. Colloid Interf. Sci. 307, 317-325.

Hoth, P., Wirth, H., Reinhold, K., Bräuer, V., Krull, P., Feldrappe, H., (2007). Endlagerung radioaktiver Abfälle in Deutschland. Untersuchung und Bewertung von Tongesteinsformationen. BGR-Bericht

Cs^+ adsorption on hydrated surfaces of illite, smectite, and interstratified illite/smectite clays: Molecular dynamics simulations to test the validity of the additive model

Andrey G. Kalinichev[1,*], **Narasimhan Loganathan**[1], **Brice F. Ngouana Wakou**[1], **Zongyuan Chen**[1], **Gilles Montavon**[1]

[1] Laboratoire SUBATECH (UMR 6457), Ecole des Mines de Nantes, 44307 Nantes Cedex 3, FRANCE

* Corresponding author: kalinich@subatech.in2p3.fr

Callovo-Oxfordian clay (COx) is under investigation as a host rock for long term nuclear waste repository in France. For that purpose, safety assessment models must account for interaction of radionuclides with repository materials over time- and distance- scales spanning many orders of magnitude. The clayey component of COx consists mostly of illite, smectite and interstratified illite/smectite (I/S) minerals, and the radionuclide sorption on COx is usually predicted considering an "additivity rule", e.g., averaging between their behavior with respect to illite and smectite separately.

Indeed, experimental studies of cation exchange indicate that in some cases I/S behaves more like a mixture of illite and smectite for the following reasons: (i) Cs^+ sorption on I/S can be quantitatively explained by two sub-models describing the sorption on illite and smectite; (ii) the measured value of I/S cation exchange capacity (CEC) is very close to the value calculated by the CECs of illite and smectite according to their ratio in I/S. However, this conclusion cannot be further verified because the cation exchange selectivity coefficients for illite and smectite are similar. Therefore, more detailed understanding and description of the adsorption and transport properties of radionuclides in I/S clay becomes a pressing issue.

We have applied molecular dynamics (MD) computer simulations in order to quantify the molecular scale mechanisms responsible for the adsorption of Cs^+ cations with the basal surfaces of illite, smectite, and I/S. A set of new structural models of illite, smectite have been constructed to more accurately account for the natural disorder in the structural isomorphic substitutions of Al/Si and Mg/Al substitutions in the tetrahedral and octahedral clay sheets, respectively. In addition, an atomistic structural model of I/S have been developed for the first time according to the atomic composition of the ISCz1 type of I/S. The newly developed models allowed us to identify several structurally different energetically favorable adsorption sites at the basal surfaces of all three clay substrates. Canonical ensemble (*NVT*) MD simulations were carried out by systematically constraining one Cs^+ cation at different distances from the clay surface (potential of mean force calculations using umbrella sampling algorithm). The results are quantitatively analyzed in terms of Cs^+ adsorption free energy profiles above each individual adsorption site on each clay surface. Cs^+ sorption properties for the three clay minerals, such as preferable sorption sites and their surface distributions, most stable adsorption distances, free energies of adsorption, are compared. The resulting equilibrium constants for surface adsorption and ion exchange are also compared with available experimental data.

Effect of pore structure of hardened cement paste on Cs^+ diffusion

D. Shitara[1], H. Takiya[1], M. Ito[1*], N. Watanabe[2], T. Kozaki[2]

[1]Division of Energy and Environmental Systems, Graduate School of Engineering, Hokkaido University, Kita 13 Nishi 8, Kita-ku, Sapporo, 060-8628, Japan [*]Currently at Mitsubishi Materials Corporation

[2]Division of Energy and Environmental Systems, Faculty of Engineering, Hokkaido University, Kita 13 Nishi 8, Kita-ku, Sapporo 060-8628, Japan

INTRODUCTION

Cementitious materials are used as an engineered barrier in geological disposal of low-level radioactive and TRU wastes in Japan. It is therefore important to understand migration behaviors of radionuclides in hardened cement paste (HCP), which is a major component of cementitious materials. Diffusion in fine pores, including capillary pores (10nm-1μm) and gel pores (up to 10nm), is generally considered to be the predominant migration process for radionuclides in HCP due to the low hydraulic conductivity. In this study, HCP specimens were prepared to have various capillary porosities by controlling water to cement (w/c) ratio and curing temperature. These specimens were used to determine apparent diffusion coefficients of Cs^+ in order to elucidate relationships between the HCP pore structure and the diffusivity of radionuclides.

EXPERIMENTAL

The HCP specimens were prepared by mixing ordinary Portland cement (Japan Cement Association) and deionized water at w/c ratio of 0.36, 0.45, 0.55, and 0.60. The mixtures were molded and solidified in cylindrical polyethylene containers (24.5 mm in diameter and 55 mm in height) for approximately 1 d. The solidified cement paste rods were removed from the molds and cured for 14 d at curing temperature of 283 K, 298 K, or 323 K in cement-equilibrated water. From the combination of various w/c ratios and curing temperature, the HCP specimens with different capillary porosities were obtained.

Capillary porosity was estimated from w/c ratio and degree of hydration. Degree of hydration of HCP was determined from the weight loss by ignition of a specimen. Several pieces of disks (5 mm in thickness) were cut from a cured HCP specimen with diamond blade. The pieces were dried in an oven at 333 K for over 7 d to remove water in pores. After oven-drying, the pieces were pulverized and ignited in an electric furnace at 1273 K for 3 h to determine the weight of ignition residue (m_r). Degree of hydration (α) was calculated by the following equation,

$$\alpha = \frac{m_c/m_s - L_{ig}}{(1-L_{ig}) \times b}$$

where m_s is the weight of specimen, m_c is the weight of water chemically bounded with hydrates ($=m_s$

$-m_r$), L_{ig} is the rate of the loss of cement powder mass by ignition in an electric furnace (6.2×10^{-3} for ordinary Portland cement used in this study), and b is the ratio of water consumed for complete hydration to 1 g of anhydrous cement (0.23) [1]. Capillary porosity (ε_{cap}) was estimated by the following equation [2].

$$\varepsilon_{cap}=\frac{w/c-0.36\alpha}{w/c+0.32}$$

Apparent diffusion coefficient (D_a) of Cs^+ in HCP was determined by the one-dimensional, non-steady diffusion method using a radiotracer of Cs-137. A small amount of Cs-137 tracer solution (1.0×10^{-5} dm^3) was applied to a flat surface of a HCP specimen, and two HCP specimens were placed together in contact. The HCP specimens were kept at temperature of 298 K during the diffusion experiment. After a prescribed period of diffusion, the specimens were sectioned from source surfaces by polishing with emery paper. The radioactivity of the powdered HCP was measured with a NaI scintillation counter, and was used to determine the concentration profiles of Cs^+ in HCP.

RESULTS AND DISCUSSION

Higher curing temperature enhanced hydration of the HCP, resulting in lower ε_{cap} at all of the w/c ratios. By controlling both curing temperature and w/c ratios, the HCP specimens were prepared to have ε_{cap} ranging from 17.6 to 43%. The values α and ε_{cap} of the HCP specimens are listed in Table 1.

The values of D_a of Cs^+ in the HCP specimens obtained in this study were on the order of 10^{-11} m^2 s^{-1}. The values of D_a increased as ε_{cap} increased, and can be expressed as a power function of ε_{cap}, which is a well-known empirical equation called "Archie's law" (Figure 1). This suggests the capillary pores can be the dominant diffusion pathway for Cs^+. Details of the diffusion process of Cs^+ in the HCP will be discussed together with the results of diffusion of HTO.

Table 1. Capillary porosity and degree of hydration of HCP prepared at different curing temperatures

w/c	283 [K]		298 [K]		323 [K]	
	α [%]	ε_{cap} [%]	α [%]	ε_{cap} [%]	α [%]	ε_{cap} [%]
0.36	54.6	24.0	60.6	20.9	66.7	17.6
0.45	52.5	33.9	66.7	27.3	73.5	24.1
0.55	54.5	40.1	70.6	34.0	——	——
0.60	56.9	43.0	72.4	36.9	78.1	34.7

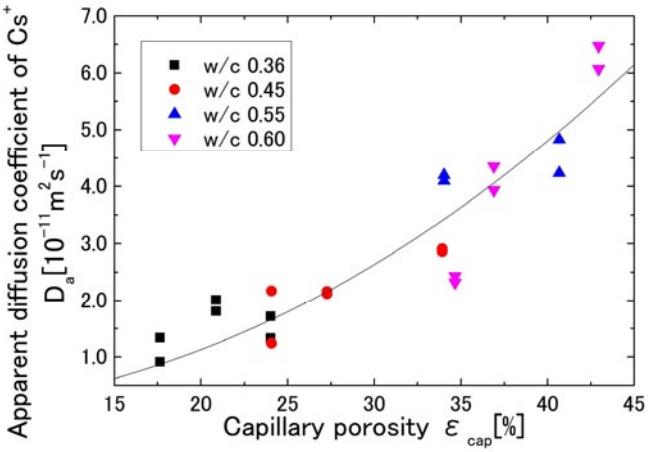


Figure 1. The dependence of apparent diffusion coefficient on capillary porosity of HCP

REFERENCE

[1] A.M. Neville, Properties of Concrete, 3rd Edn, ELBS with Longman, London (1981) 257-279.

[2] S. Mindess et al., Concrete, 2nd Edn, Prentice Hall (2003) 80-90.

Uranium adsorption onto bentonite with indigenous sulphate reducing bacteria

Seung Yeop Lee, **Jae Kwang Lee, Min Hoon Baik, Kyungsu Kim**

Korea Atomic Energy Research Institute (KAERI), Daejeon 305-353, Korea

The Korea Atomic Energy Research Institute (KAERI) has proposed a conceptual design of a geological disposal system for spent nuclear fuel (SNF), to be situated 500 m underground in granitic rock.[1] The purpose of a high-level radioactive waste (HLW) disposal system is to isolate the radioactive material and thus prevent it from contaminating the environment. In the Korean disposal concept, SNF will be put in metal canisters, which will be deposited in granitic bedrock and surrounded by bentonite. The surrounding bentonite will act as an adsorbent material to retard the migration of radionuclides (e.g., uranium) by electrostatically adsorbing them.

Therefore, the understanding of the interaction between radionuclides and the near-field materials is very important for assessing the safety of the repository site. There have been recent reports that indigenous sulfate-reducing bacteria (SRB) are present in commercial bentonite.[2,3] We, thus, tried to find out the microbial effect on the uranium(VI) adsorption by local granite and bentonite. The adsorption features of U(VI) by the near-field rock and minerals are important determinants of the mobility of U species in the HLW repository site.

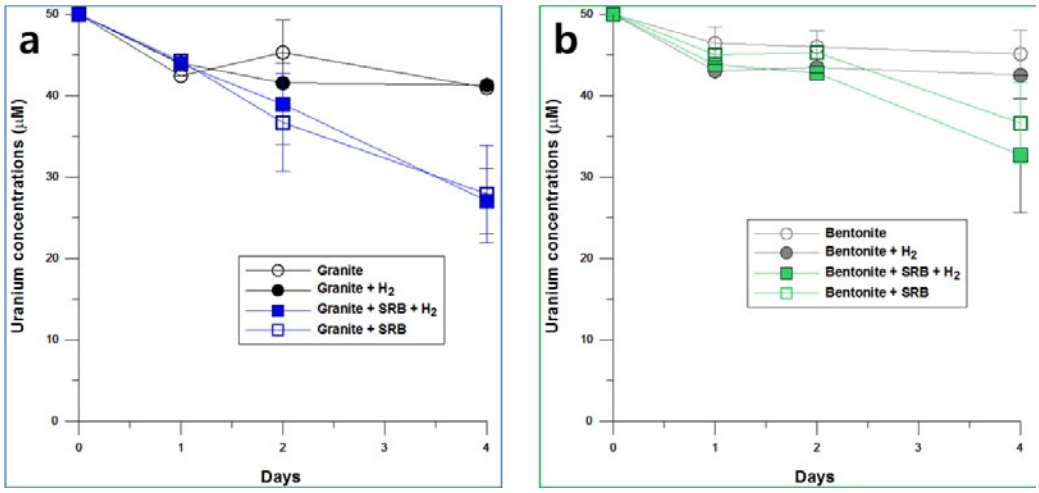


Fig. 1. The decrease patterns of aqueous uranium(VI) concentration by (a) granite and (b) bentonite, which were significantly affected by the added SRB or/and hydrogen gas.

In our experiment, two solid phases, granite and bentonite, were reacted with aqueous solutions of U(VI) in the addition of H_2 or/and SRB at neutral pH and anaerobic condition (Fig. 1). The aqueous U(VI) concentration (5×10^{-5} M) in a serum bottle gradually decreased to a certain level following the interaction between U(VI) and the adsorbents. The U(VI) adsorption onto granite was greater as the added SRB is gradually activated with time. The reason seems that the hexavalent uranium(VI) was

biologically reduced to tetravalent uranium(IV) or a portion of U(VI) would be adsorbed onto the suspending SRB. This shows that SRB can be an important agent to the U(VI) adsorption.

However, the U(VI) amount adsorbed by bentonite was slightly larger in the presence of H_2 gas regardless of the SRB addition. This means that there was a slight difference of U adsorption between 'bentonite alone' and 'bentonite + H_2 gas' conditions. In a condition of H_2 addition, the adsorbed U(VI) quantity by the bentonite increased more than 5~8% compared to that of H_2 absence. The difference of the U(VI) adsorption capacity between the two conditions may be attributed to the naturally surviving SRB in the bentonite, where SRB can be more activated by the provision of H_2. Therefore, the bentonite that has indigenous SRB seems to more effective in the adsorption of U(VI), if H_2 gas is diffused into it and plays a role of electron donor for the U(VI) reduction. This result could imply that if U(VI) is reacted with the bentonite in a repository, U(VI) migration would be retarded somewhat by the SRB surviving in the compacted bentonite buffer.

References

1) H. J. Choi, J. Y. Lee, J. W. Choi, Nucl. Eng. Technol. 45 (2013) 29.
2) P. Masurat, S. Eriksson, K. Pedersen, Appl. Clay Sci. 47 (2010) 51.
3) J. Y. Lee, S. Y. Lee, M. H. Baik, J. T. Jeong, J. Korean Radioact. Waste Soc. 11 (2013) 95.

Anion diffusion in low porosity argillaceous rocks

Cornelia Wigger, **Luc Van Loon, Thomas Gimmi**

Paul Scherrer Institut PSI, CH-5232 Villigen, Switzerland

The disposal of radioactive waste in clay rocks is considered in various countries. The reasons are the favourable properties of these rocks w.r.t. sorption, water flow and radionuclide transport. Due to the low hydraulic conductivity of compact clay, molecular diffusion is the major transport process for radionuclides released from the waste matrix into the host rock (Altmann et al., 2012).

Argillaceous rocks consist to a large part of clay particles composed by TOT-layers. They are negatively charged and these negative charges are compensated by cations in the pore solution such that a diffuse double layer forms. Anions are repulsed by the negative charges of the clay minerals and are excluded from the diffuse double layer (Figure 1). The latter process is well known as anion exclusion and has been observed in soils, clay rocks and compacted bentonite (Muurinen 1994, Bolt 1978, Van Loon 2014).

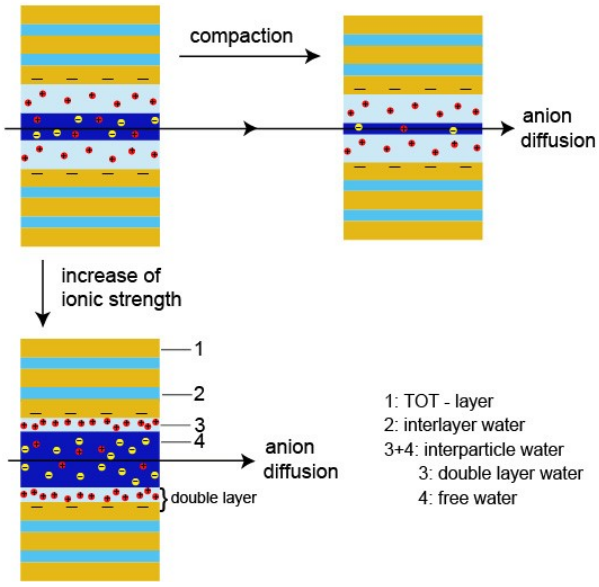


Figure 1: Schematic presentation of the pore space in compacted bentonite, illustrating the effects of ionic strength and mechanical compaction on the pore space.

For neutral and positively charged chemical species, the whole porosity of a clay rock (ε_{tot}) is available for transport. Anions, however, are partially excluded and the corresponding transport porosity, i.e. the anion accessible porosity (ε_{an}), is smaller than the total porosity. Earlier studies on compacted bentonite showed that both the mechanical compaction of bentonite and the composition of the pore water had an effect on the diffusion accessible porosity of anions (Van Loon et al., 2007). Compaction of bentonite resulted in a decreased anion accessible porosity. Increasing ionic strength of the pore water led to an increase in the anion accessible porosity (Figure 2). A similar dependence was expected for clay rocks such as Opalinus Clay, due to a similar structure. Recent measurements, however, did not confirm this (Van Loon, 2014).

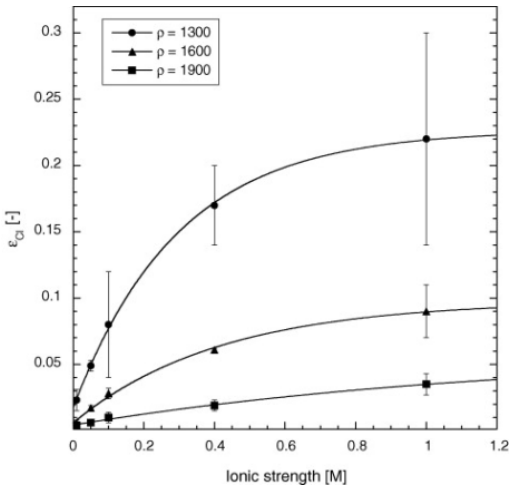


Figure 2: Effect of the ionic strength on the accessible porosity of bentonite for different degrees of compaction (Van Loon et al., 2007)

This study focuses on the anion diffusion behaviour in clay rocks as a function of the ionic strength of the pore water. The chosen clay rocks, Helvetic Marl and Opalinus Clay differ in mineral composition, specific surface area, cation exchange capacity (surface charge), bulk density and pore size distribution. Through-diffusion experiments with tritiated water (HTO) and chloride ($^{36}Cl^-$) were performed for assessing the total porosity (HTO) and the anion accessible porosity ($^{36}Cl^-$) for samples equilibrated with different compositions of the pore water ranging from 0.01 M – 2 M NaCl. These measurements give information on whether the anion behaviour observed for Helvetic Marl and Opalinus Clay is similar to the one observed for bentonite and whether a dual porosity model described in the literature (Van Loon et al., 2007; Tournassat and Appelo, 2011) is applicable for clay rocks.

The results contribute to a better understanding of the migration of anionic radionuclides in clay rocks and provide better constraints on the anion accessibility of the pore water. The latter is also important to characterise local *in-situ* pore water compositions of clay rocks.

References:

Altmann, S., Tournassat, C., Goutelard, F., Parneix, J.-C., Gimmi, T., Maes, N., (2012). Diffusion-driven transport in clayrock formations. Appl. Geochem. 27, 463-478.

Bolt, G.H. (1978). Adsorption of anions by soils. In: Bolt, G.H. and Bruggenwert, M.G.M. (Eds.) Soil Chemistry: A. Basic Elements. Elsevier Scientific Publishing Company, Amsterdam, Oxford, New York.

Muurinen, A. (1994). Diffusion of cations and anions in compacted sodium bentonite. VTT Publications 168, Technical Research Center of Finland, Espoo, Finland.

Tournassat, C. and Appelo C.A.J. (2011). Modelling approaches for anion-exclusion in compacted Na-bentonite. Geochim. Cosmochim. Acta 75, 3698-3710.

Van Loon, L.R., Glaus, M.A., Müller, W. (2007). Anion exclusion effects in compacted bentonites: Towards a better understanding of anion diffusion. Appl. Geochem. 22, 2536-2552.

Van Loon, L.R. (2014). Effective diffusion coefficients and porosity values for argillaceous rocks and bentonite: measured and estimated values for the provisional safety analyses for SGT-E2. Nagra Technical Report NTB 12-03, Nagra, Wettingen, Switzerland.

THE STRESS-STRAIN-PERMEABILITY BEHAVIOUR OF CLAY ROCK

Chun-Liang Zhang

Gesellschaft für Anlagen- und Reaktorsicherheit (GRS) mbH, 38122 Braunschweig, Germany
(chun-liang.zhang@grs.de)

For safety assessments of a repository in a clay host rock, the damage and recompaction behaviour of the clay rock under the impact of mining activities and the interactions with engineered barriers are very important. In particular, the resulting permeability evolution in the EDZ around the openings is the key factor influencing the performance of seal systems. Reliable prediction of the EDZ development and assessment of its impact on repository safety requires a robust database, a deep understanding, and an adequate modelling of the hydro-mechanical behaviour of the rock mass. The stress-strain-permeability behaviour of clay rock before and after damage has been extensively investigated in the framework of the European project DOPAS.

Triaxial compression tests were carried out on a large number of samples of the Callovo-Oxfordian clay rock including measurements of deformation, gas permeability, and wave velocity during loading. The samples were sequentially loaded by 1) hydrostatic pre-compaction to close up microcracks induced by coring and preparation; 2) deviatoric stressing to determine damage and permeability changes; and 3) recompression along different loading paths to examine reversibility of the damage. Based on the experiments, empirical models have been established for the prediction of permeability evolution of the clay rock with damage and recompaction.

First of all, the disturbed samples have to be pre-compacted for closing up the coring-induced microcracks. The lithostatic rock stress and even higher stresses have to be applied to achieve the natural undisturbed state with very low permeabilities below 10^{-20} m^2. The deviatoric stress-strain-permeability behaviour of the intact clay rock is characterized in Fig. 1. The clay rock is deforming elasto-plastically with increasing deviatoric stress. Volume compaction ε_v is dominating until dilatancy appears at stress σ_D. Subsequently, microcracks are created which propagate rapidly with loading. As a fracture network is being built up, the permeability k jumps up at stress σ_P called percolation threshold, very close to the peak break strength σ_B. From this point, the permeability increases dramatically by several orders of magnitude depending on the radial confining stress. The critical stresses at dilatancy, percolation, and peak failure increase with increasing confining stress.

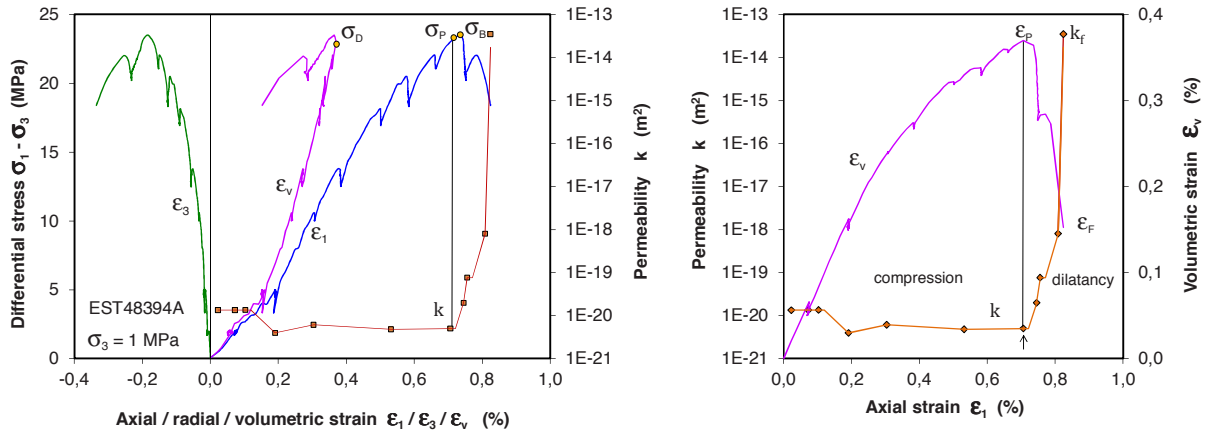


Fig. 1: Deviatoric stress-strain-permeability behaviour of the clay rock

The fracturing-induced permeability jump reflects the percolation behaviour due to interconnection of stressing-created cracks. Permeability can be expressed in a general form by $k = k_f \cdot P$, where k_f is the ultimate permeability of the fractured rock with perfectly interconnected cracks and P is the percolation probability defining the fraction of cracks belonging to the conducting part of a network. The ultimate fracture permeability increases with decreasing the minor principle stress σ_3 by $k_f = k_o \cdot \exp(-\gamma\sigma_3)$, where k_o is the permeability at zero minor stress and γ being a parameter characterizing the dilatability of the interconnected cracks. In addition, the percolation probability is assumed to be a function of crack dilatancy: $P = [1-\exp(-\Delta\varepsilon_D/\varepsilon_P)]$, where $\Delta\varepsilon_D = \varepsilon_v - \varepsilon_P$ is the volumetric dilatancy with reference to the volumetric strain ε_P at the percolation threshold. At $\varepsilon_v = \varepsilon_P$, $P = 0$, the connectivity of the cracks is zero. With increasing dilatancy the cracks tend to a full connection, $P \rightarrow 1$ as $\varepsilon_v \rightarrow \infty$. Fig. 2 compares the percolation model with the permeability data obtained during fracturing at different radial stresses. It is obvious that the evolution of permeability with the initial jump and the subsequent slowdown can be reasonably described by the model.

In contrast to the fracturing-induced permeability in intact clay rock, the permeability in fractured clay rock is mainly determined by the apertures of interconnected cracks. Thus, the cubic law is applied for describing the fracture permeability: $k = C \cdot (\varepsilon_R)^3$, where ε_R is the residual fracture void and C is the parameter characterising the final fractured state, $C = k_f / (\varepsilon_F)^3$. Fig. 3 compares the cubic law with the permeability evolution of the fractured clay rock during multi-step deviatoric stressing. A satisfactory agreement between the model and the data can be stated. However, more experiments are needed for the validation in the region of low fracture voids of □ 0.1 %, where disconnection of the fracture network may be allowed for.

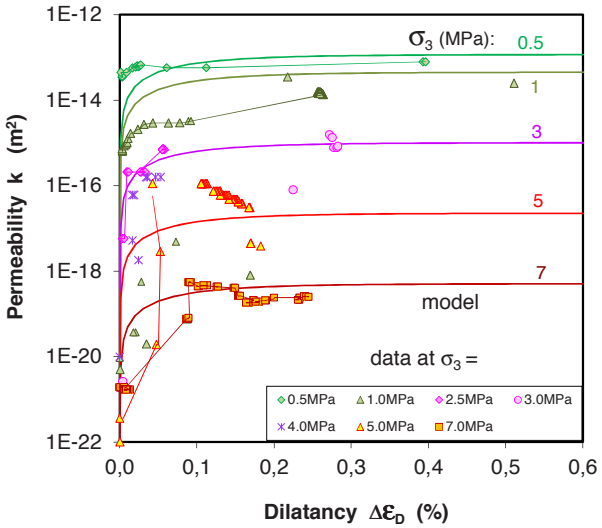


Fig. 2: Prediction of the fracturing-induced permeability in the intact clay rock using the percolation model

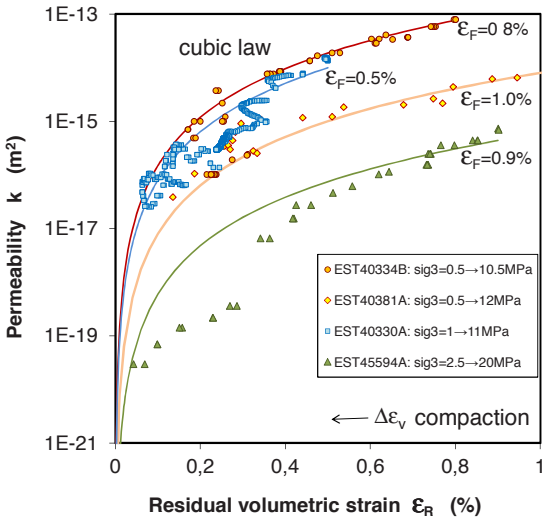


Fig. 3: Prediction of the compaction-reduced permeability in the fractured clay rock using the cubic law

Acknowledgements: The present work was co-funded by the German Federal Ministry of Economics and Technology (BMWi) under contract number 02E10377 and by the European Commission (EC) as the part of the Euratom's Seventh Framework Programme FP7/2007-2013 under grant agreement no. 323273 for the DOPAS project. The support from ANDRA for providing the test material and for the fruitful discussions is also gratefully acknowledged.

Laboratory and numerical investigation of the mechanical behaviour of the Tournemire argillite

G. Su[(1)], T.S. Nguyen[(1)], E. Haghighat[(2)], S.Pietruszczak[(2)], D. Labrie [(3)], J.D. Barnichon[(4)], H. Abdi[(5)]

(1) Canadian Nuclear Safety Commission (grant.su@cnsc-ccsn.gc.ca)
(2) McMaster University
(3) CANMET Mining and Mineral Sciences Laboratories, Natural Resources Canada
(4) Institut de Radioprotection et de Sûreté Nucléaire
(5) University of Ottawa

Argillaceous rock formations are being considered in Canada and other countries as host or cap rock formations for geological disposal of radioactive wastes. These formations were typically formed by deposition, and progressive consolidation and diagenesis of marine sediments. Consequently, they are characterized by the presence of bedding planes, resulting in anisotropy of their strength and deformation properties.

In order to better understand the ability of these rock formations to contain and isolate the wastes, and to develop a tool to independently assess the extent and characteristics of damage induced by excavation of a deep geological repository, the Canadian Nuclear Safety Commission (CNSC) has collaborated with different international research organizations and has access to Underground Research Laboratories (URL) worldwide. One of these URLs is situated in Tournemire, France, in an argillaceous rock.

In this investigation, both laboratory and numerical methods have been used to study the mechanical behaviour of the Tournemire Argillite. Eighty rock samples were obtained from the Tournemire URL. The laboratory testing program included the measurement of basic properties of the argillite, and uniaxial tests, triaxial tests, cyclic tests, and Brazilian tests with Acoustic Emission measurements. The laboratory tests were performed at different inclinations with respect to the bedding planes (θ=0°, 30°, 45°, and 60°, 90°) (Figure 1).

The laboratory testing results show that both strength and deformation of the argillite are direction-dependent. Failure occurs in a brittle manner with a sudden collapse of the material strength. The failure mode exhibits localization along distinct failure planes and also depends on the loading orientation (Figure 2). The experimental results of uniaxial and triaxial tests were used for numerical investigation of the anisotropic mechanical behaviour of the Tournemire argillite. The constitutive relation was developed to describe the stress-strain behavior of the argillite. A microstructure tensor approach was adopted in order to take into account the anisotropic behaviour of the argillite. The authors outline the identification procedure for material function and parameters and apply the model to simulate the set of triaxial tests performed at different levels of confinement pressure and orientation of the bedding planes. It is demonstrated that the model adequately reproduces the anisotropy, the pre-peak stress-strain response, and the onset of material collapse in those tests (Figure 3).

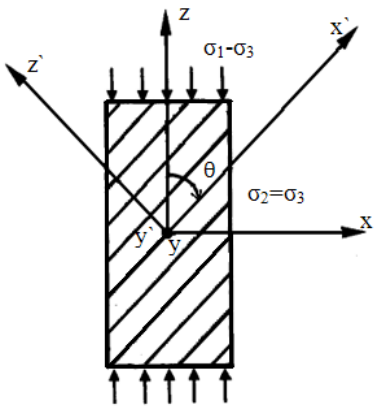


Figure 1. Loading direction with respect to beddings

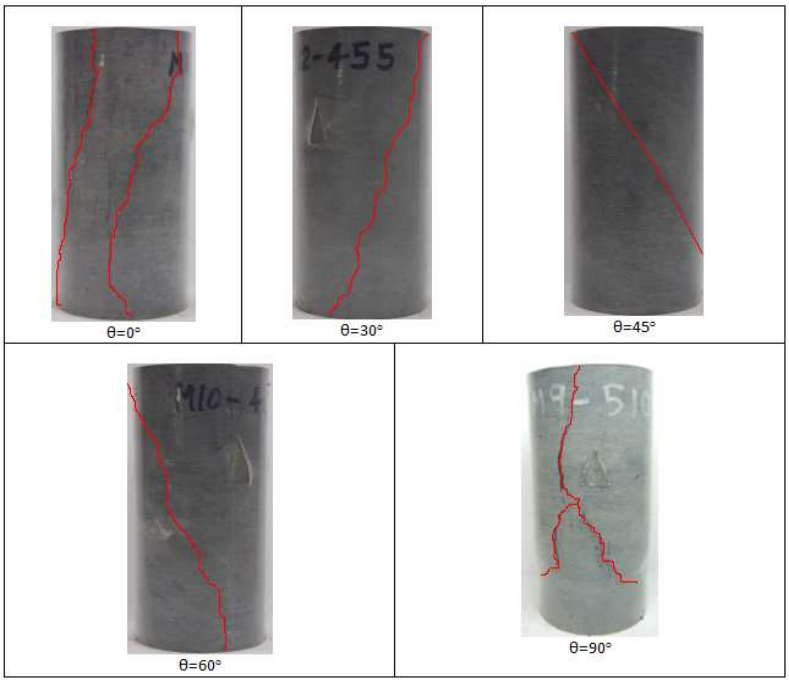


Figure 2. Failure modes of the Tournemire argilite under a different loading direction to the bedding planes

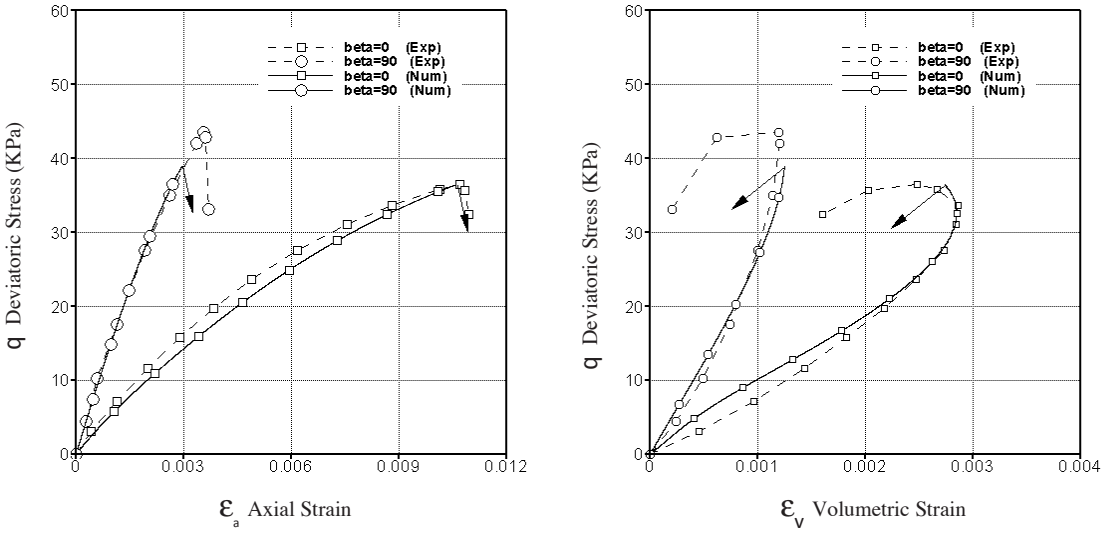


Figure 3. Numerical simulations of triaxial compression tests: deviatoric stress vs. axial and volume change characteristics corresponding to beta=90°

Constitutive behaviour of Opalinus Clay and workflow for simplified material laws for engineering purposes

Silvio B. Giger, ***Paul Marschall***

Nagra, National Cooperative for the Disposal of Radioactive Waste, CH-5430 Wettingen, Switzerland.
Tel.: +41 56 437 13 41, e-mail: silvio.giger@nagra.ch

Opalinus Clay is the designated host rock for high-level and a possible host rock for low- and intermediate level waste in Switzerland (BFE 2011). For the site selection process, the engineering feasibility of underground structures must be assessed for the host rock in different geological siting regions, in different tectonic regimes and covering potential repository depths from 300 to 900m below ground. In addition, long-term safety analysis must also evaluate hydro-mechanical processes in the host rock resulting from reduction in overburden due to erosion (i.e. in the uppermost 300m b.g.). The large range of different state conditions to be considered requires a comprehensive geomechanical characterization of the Opalinus Clay.

Core samples of Opalinus Clay were recently recovered from a depth of 830 to 950m b.g. in the geothermal well Schlattingen-1 in Northeastern Switzerland. The samples were geomechanically tested and characterized to complement the existing data bases of Opalinus Clay from more shallow depths, i.e. the URL Mont Terri (approximately 300 m b.g.) and the borehole Benken (540 to 650 m b.g.). The samples from all three locations show very similar mineralogical composition but differ in the overconsolidation ratios (i.e. the ratio of the maximum effective stress experienced in the past versus the contemporary in situ stress), ranging from values of approximately 1.5 to 5.0.

We present test results from the Schlattingen-1 core samples and synthesize the findings with the data bases from Mont Terri and Benken. Careful geotechnical characterization by index testing is considered crucial for comparison with empirical data bases of similar materials and hence as evidence to support laboratory test results. The grain size is dominated by the silt fraction and consequently Opalinus Clay classifies as a clayey (and sandy) siltstone. Based on the plasticity scheme (Atterberg limits), Opalinus Clay falls mostly into the category of lean clay with sand with minor silty clay with sand or silt with sand. Uniaxial consolidation and triaxial compression tests demonstrate stress-dependent and anisotropic stiffness and strength properties with a moderate swelling potential.

Critical state theory is considered a suitable conceptual framework to model the expected deformation behaviour during consolidation and shear in a predictive model. By combining a modified Cam-clay model (for compaction during normal consolidation) and Hvorslev limit state (for shear during over-consolidation) a complete state boundary surface is defined in a three dimensional space given by the effective mean stress (p'), the deviator stress (q) and a volumetric component (specific volume) (Fig. 1, *left*). The state boundary surface defines the possible states at the transition from elastic to plastic deformation (yielding) both during volumetric compaction and shear. A key aspect is that strength (expressed by the deviator stress q) increases with decreasing specific volume (or void ratio, porosity, water content). In its simple version the model does not take into account anisotropy, assumes that the material is saturated, that it deforms as a continuum and that it is not affected by creep.

The proposed constitutive model provides a holistic framework to evaluate the deformation behaviour of Opalinus Clay at a given stress state, but it is also very complex and somewhat cumbersome for custom-designed applications, especially when additional features such as anisotropic stiffness and strength properties are being considered. For instance for engineering purposes, a more practical and well accepted material law is desirable. The transversal isotropic, subiquitous joint model (SUBI) in FLAC^{3D} software is such a material model. It is based on a Mohr-Coulomb material law and accounts for hydro-mechanical coupling, stress and strength anisotropy, and it can be calibrated to reproduce

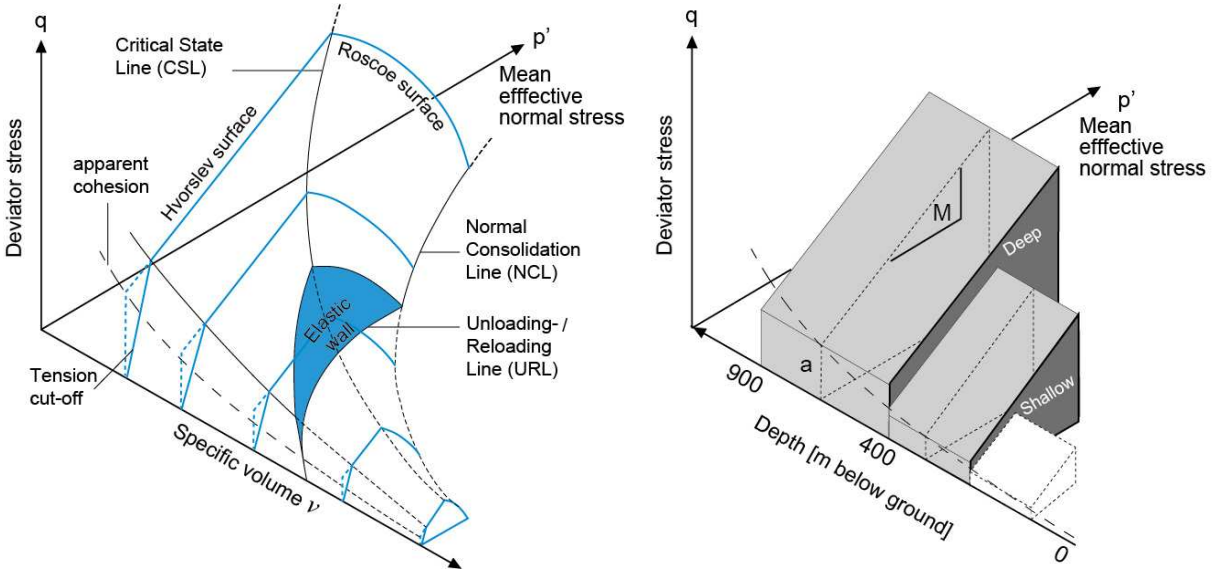


Fig.1: Schematic of complete state boundary surface (left) of Opalinus Clay and simplification for engineering purposes (right): an equivalent depth is calculated by the relationship of specific volume and effective stress. Two data sets with different physical and strength properties are formulated to honour strength dependence on specific volume: data set 'deep' for 400-900m and 'shallow' for < 400m. Specific volume and strength parameters (intersection *a* and slope *M*) are constant for the depth range specified for the two data sets. Only the Hvorslev surface is considered for plastic deformation in the simplification (i.e. no consolidation).

typical features of the stress-strain behaviour observed in shear tests (strain hardening and strain weakening).

In an abstraction process, the continuous state boundary surface of the full constitutive model is approximated by two data sets termed Opalinus Clay 'deep' and 'shallow' for the modelling using SUBI (Fig. 1, right). Both the specific volume and strength parameters (*a* and *M*, cf. Fig.1, right) are assumed constant within each of the two data sets. In this way, the dependence of strength on the specific volume is qualitatively honoured, although not in a continuous manner, but by two depth-dependent data sets. The strength parameters *a* and *M* can easily be converted in Mohr-Coulomb strength parameters of effective friction angle ($M = [6 \cdot \sin(\varphi')] \cdot [3 - \sin(\varphi')]^{-1}$) and effective cohesion ($a = C' \cdot [6 \cdot \cos(\varphi')] \cdot [3 - \sin(\varphi')]^{-1}$).

The focus in engineering feasibility calculations using SUBI is on cavern stability and the pattern of plastic deformation during and shortly after excavation. In a further step of the simplification process, consolidation (Roscoe surface in Fig 1, left) may hence be neglected as a relevant process. Only the Hvorslev surface is therefore considered.

Finally, to account for variable tectonic overprint in different geological siting areas, a number of rock models are formulated to mimic potential de-structuring of Opalinus Clay. The 'intact strength' is reduced (i.e. the parameters *a* and *M* are adjusted based on variability of laboratory data and comparison between peak and post-peak values) in a continuum, consistent with the constitutive model.

BFE (2011), Sachplan geologische Tiefenlager – Ergebnisbericht zu Etappe 1: Festlegungen und Objektblätter. Bundesamt für Energie BFE, Bern.

Development of a workflow for hydro-mechanical near-field studies – influence of the relative humidity

***Fabian DEDECKER*[1], Daniel BILLAUX[1], Alexandros PAPAFOTIOU[2], Paul MARSCHALL[3]**

1. ITASCA Consultants S.A.S., 64 Chemin des Mouilles, 69130 ECULLY, France
2. INTERA, Schloesslistrasse 12, 5408 Ennetbaden, Switzerland
3. NAGRA, Hardstrasse 73, 5430 Wettingen, Switzerland

Nagra is studying siting regions for the disposal of high-level waste (HLW) and long-lived intermediate level waste (ILW) within the Opalinus Clay formation in the Molasse Basin of Northern Switzerland. In this context, Nagra initiated generic modelling studies, aimed at analyzing possible scenarios of the hydro-mechanical evolution of the near-field after waste emplacement. The near-field comprises the waste matrix, the backfill and lining of the cavities and the Excavation Damage Zone (EDZ).

The phenomena and processes to be addressed include the unsaturated initial stage during the construction and operations phase, the repository re-saturation process, the consolidation of the backfill and the development of the EDZ. The impact of gas production and volume expansion of the corroding waste is also considered in a generic manner.

A 2D model is built using the two-dimensional explicit finite difference program *FLAC*. Two different cross sections are modelled, according to the waste type (Figure 1). Two-dimensional simulations are a pragmatic choice for these sections. The level of damage in the near-field material depends for a significant part on the excavation sequence, which is intrinsically 3D. We use a method akin to "convergence – confinement" to simulate the progressive release of stresses at each phase of the excavation process: instead of suppressing the zones to be excavated, the initial stresses they support are recorded and decreased progressively, allowing the gradual disappearance of the interaction between the excavated part and its surroundings.

Variations of saturation and pore pressures are a significant driving force during the early life of the cavern, with emplacement caverns open for decades, then backfilled at prescribed saturations (depending on the type of backfill), and finally re-saturated by converging flow. In fact, the suction processes at work in the vicinity of the cavern while it is open may have a strong positive effect on its stability. *FLAC* is not able to properly compute the transient desaturation (during opening) and re-saturation process in the near field, or the saturation process of the cavern materials themselves after closure. Although it is not possible to compute the saturation/pore pressure field with time, it is possible to take into account such a field.

Many studies have already been conducted by Nagra on the desaturation-resaturation process. For this study, the hydraulic evolution of the near-field and the cavern material with time are imported in *FLAC*, based on previous hydraulic simulations using TOUGH2. Such a method is slightly biased, since there is no "back-coupling" in the model from stress variations to saturation/pore pressures (for example, mechanical volume changes will not affect pore pressures). We show that in fact mechanical volume changes mainly appear during the excavation phase, which is short term behavior (only a few days), whereas saturation and pore pressures evolve for centuries. Because the clay has a low permeability, very little flow can occur during the short excavation phase. During this phase, "volume change" effects dominate, with a sharp pressure decrease around the opening. The volume change effect is instantaneous; it does not depend on the diffusion process inside the rock mass.

Thus, the evolution of this system can be separated in two phases: first, during the excavation phase, dominant hydro-mechanical processes are simulated using *FLAC*, without using flow simulations.

During this phase, the stabilizing effect of suction on the periphery of the cavity is not taken into account, since the system is considered as undrained. Once this phase has been simulated, the extension of the EDZ is evaluated by checking the size of the area that has undertaken plasticity. This extension is an input to TOUGH2, with larger permeabilities (and thus less suction effects) in the EDZ. The TOUGH2 simulation then proceeds from that state for the several following phases, and is then used to continue the *FLAC* simulation beyond the excavation phase. An automatic import/morphing procedure allows the use of the TOUGH2 results in the *FLAC* simulations.

In this paper, we mainly focus on the development of a modelling framework for the simulation of the hydro-mechanical response of the tunnel near-field on changes of suction and pore pressure, respectively. The simulations cover the excavation, the ventilation, the backfill emplacement and later times.

We show that ventilation variations and suction effects do have a significant influence on the transitory behavior of the near field, during the operational period and right after it.

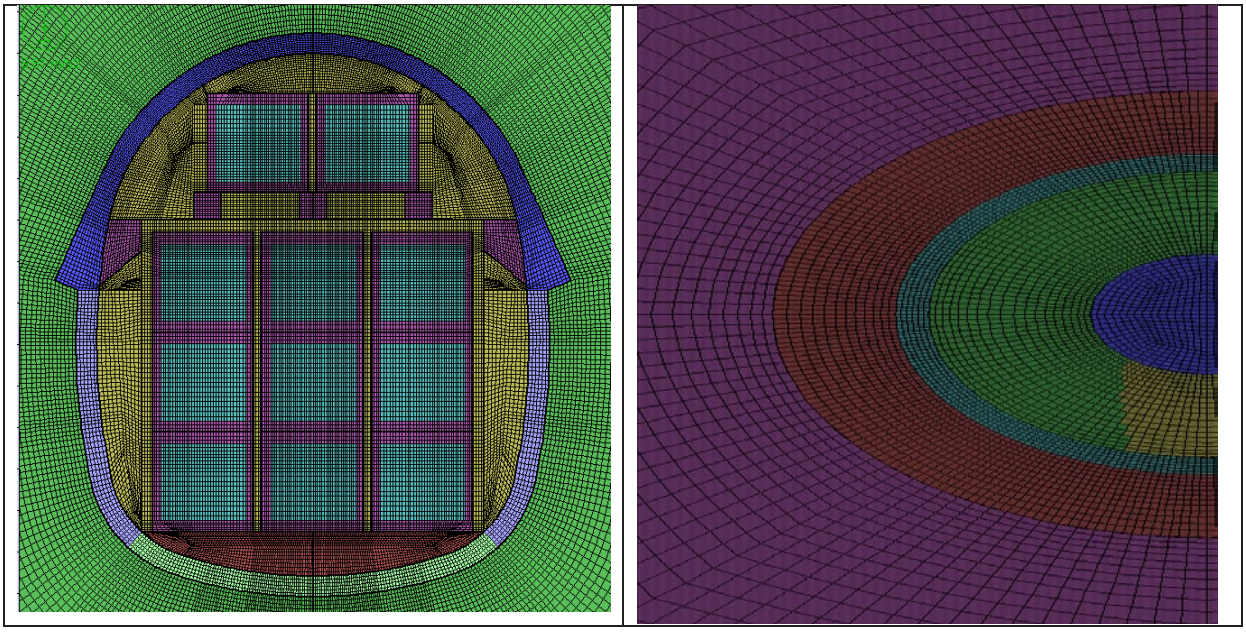


Figure 1 – Generic Layout of the a L/ILW cavern (on the left) and SF/HLW tunnel (on the right)

Influence of intrinsic material parameters on fluid pressure build-up and two-phase flow phenomena in a deep HLW repository in claystone

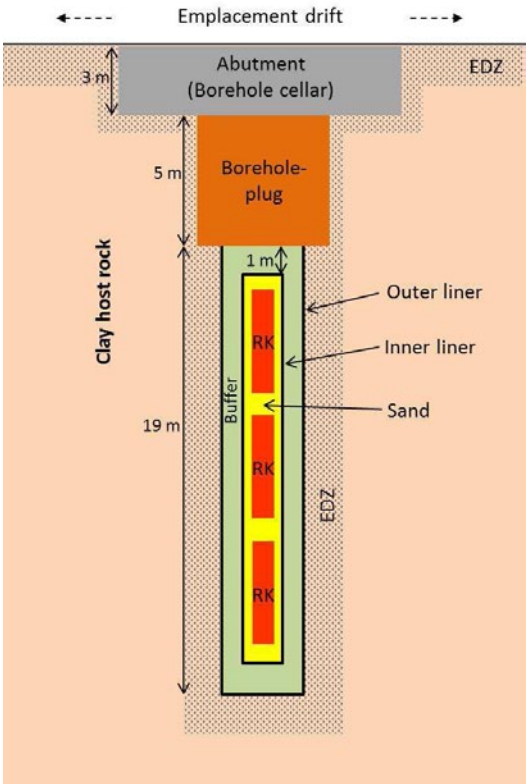
Victoria Shushakova, **Michael Jobmann, Johanna Wolf, Eric Kuate Simo**

DBE TECHNOLOGY GmbH, Eschenstraße 55, D-31224 Peine, Germany

Abstract

Within the framework of the R&D project "Methodological approach for a safety demonstration and verification concept for a HLW repository in claystone in Germany" ("AnSichT"), the repository concept takes into account a large amount of metal for canisters and liners. This leads to gas generation (where hydrogen is the main component) caused by the corrosion of the metal containers in the clay repository after closure of the facility. In the long-term safety assessment of deep HLW repositories in claystone, it is crucial to investigate the fluid pressure build-up at the drift and shaft seals. A suitable design of the sealing constructions is necessary to handle the fluid pressure evolution as a result of water inflow and gas production.

In the "AnSichT" concept, the repository comprises 32 emplacement fields. Each consists of 9 drifts with 12 or 13 sealed emplacement boreholes. In each borehole, three waste canisters and metal liners that contribute to the gas generation are emplaced (Fig. 1). The gas production rate for each borehole was estimated for two metal types: cast iron and stainless steel (GRS, 2014). In the present study, the model of one drift with 12 emplacement boreholes sealed with bentonite plugs and with a sealing plug at the end of the drift in one emplacement field was considered in order to determine the influence of the main material parameters on fluid pressure build-up.



Using the computer code TOUGH2 (Pruess, 1999), three-dimensional two-phase simulations were performed regarding model flow of water and hydrogen in the simplified drift model. The main goal was to quantify the fluid pressure build-up at the drift seal and the duration of water saturation of backfill in the drift with and without gas production under isothermal conditions. As a boundary condition, a fixed hydrostatic pressure was assumed at the upper and lower boundaries of the simulation model. The rock mass is completely saturated with water. Atmospheric pressure was considered in the drift, boreholes and in the sealing plugs. The influences of intrinsic parameters such as permeability and porosity of claystone, backfill, buffers, sealing plugs and gas entry pressure were systematically analysed by means of a sensitivity study.

Fig. 1: Concept for vertical borehole disposal

Two-phase flow modelling provides additional insight and clarification of the influences of the two-phase flow parameters of materials for flow of water and hydrogen. The results of the sensitivity study will help to understand the importance of each parameter for the flow and the pressure evolution in and around the repository with special regard to the design of the backfill and the sealing constructions.

References

GRS (2014) Personal communication

K. Pruess, C. Oldenburg, G. Moridis (1999) TOUGH2 User's Guide, Version 2.0, Report LBNL-43134, Lawrence Berkeley National Laboratory, Berkley, CA

Comparative modelling and simulation of selected in-situ measurements performed at URL Mont Terri using FLAC-TOUGH and CODE_BRIGHT

R. Seeska[1], O. Czaikowski[2], M. Komischke[2], K.-H. Lux[1], M. Rutenberg[1], K. Wieczorek[2]

[1] Clausthal University of Technology (TUC), Erzstraße 20, 38678 Clausthal-Zellerfeld, Germany (michael.rutenberg@tu-clausthal.de)
[2] Gesellschaft für Anlagen- und Reaktorsicherheit (GRS) mbH, Theodor-Heuss-Straße 4, 38122 Braunschweig, Germany (oliver.czaikowski@grs.de)

The international experience gained in the field of geological radioactive waste disposal indicates that coupling between thermal, hydraulic, mechanical, and chemical processes (THMC coupling) in claystone rock mass will be much more significant than in salt rock formations. The fabric components, saturation level, and pore water pressure determine the load-bearing behaviour of the claystone rock mass affected by the impact of excavation activity and aspects related to waste storage.

It is widely agreed that the overall detection of geohydraulic conditions and their changes due to geomechanical disturbances via in-situ measurements is one of the most relevant prerequisites for reliable physical modelling and numerical simulation of coupled processes. With respect to disposal in argillaceous formations, GRS therefore performs various experiments at URL Mont Terri. The main aim of the DM-B experiment is to observe and measure the mutual interaction of hydro-mechanical coupled processes over long time periods and under in-situ conditions, particularly the influence of borehole drilling on the time-dependent pore pressure distribution of the surrounding Opalinus clay and the resulting load-bearing behaviour of the rock mass.

Hydro-mechanical coupled numerical simulations have then been carried out calculating the mechanical induced change in pore pressure in the rock mass. To this end, a 2D cross-sectional combined borehole-drift model containing the actual in-situ properties of the Opalinus clay has been created, taking into consideration the initial pore pressure and stress states resulting from the excavation of the nearby Gallery 98 as well as desaturation effects due to suction at the gallery and borehole contours and thus two-phase fluid flow. For these simulations, a recently self-developed coupled simulator based on FLAC^{3D} (Itasca CG Inc., Minneapolis) and TOUGH2 (LBNL, Berkeley) has been used by TUC, whereas the software CODE_BRIGHT (UPC, Barcelona) has been applied by GRS. The outcomes of the simulations are presented in this work in comparison to each other and to the experimental findings.

References:

Czaikowski, O.; Komischke, M.; Wieczorek, K. (2014): Interpretative modelling of selected in situ measurements obtained at URL Mont Terri using CODE_BRIGHT. In: 6th Workshop of CODE_BRIGHT Users, UPC/CIMNE, May 13, 2014, Barcelona, Spain.

Lux, K.-H.; Rutenberg, M.; Seeska, R. (to appear 2015): Kopplung der Softwarecodes FLAC^{3D} und TOUGH2 in Verbindung mit in situ-, laborativen und numerischen Untersuchungen zum thermisch-hydraulisch-mechanisch gekoppelten Verhalten von Tongestein unter Endlagerbedingungen. Final report of the research project no. 02E11041 of the German Federal Ministry for Economic Affairs and Energy (BMWi).

Geomechanical modelling of the Dutch radioactive waste repository accounting for uncertainties.

P.J. Vardon[1], **P. Arnold**[1], **M. Milioritsas**[1], **M.A. Hicks**[1], **P.A. Fokker**[2], **J.H. Fokkens**[3]

1. Section of Geo-Engineering, TU Delft, PO Box 5048, 2600 GA Delft, The Netherlands
2. Earth, Environment and Life Sciences, TNO, PO Box 80015, 3508 TA Utrecht, The Netherlands
3. Department of Safety and Power, NRG, PO Box 25, 1755 ZG Petten, The Netherlands

The current generic disposal concept in the Netherlands is based upon the Belgian supercontainer concept and is designed to be situated in the Boom Clay stratum at approximately 500m depth (Verhoef et al., 2011). The location of such a repository has not been decided and as such the design contains many uncertainties. The impact of these uncertainties are important to the feasibility of the repository construction, with respect to both stability and consequential financial performance. In particular, the tunnel lining, initially estimated to be 0.5m thick (Verhoef et al., 2011), has been estimated to be up to 80% of the total repository construction costs (Barnichon et al., 2000).

An approach has been developed that utilises probabilistic methods to quantify uncertainties, that is by assigning probability distributions. These distributions are both based upon ranges of existing data from material tests and possible ranges, based upon engineering judgement. The statistical distributions of material properties, which include material property correlations where appropriate, link with a number of probabilistic tools to estimate the probability of repository performance. The choice of the probabilistic tool depends upon the computational cost of the individual analyses. Figure 1 illustrates the approach, where (a) shows a correlated statistical distribution of two parameters; (b) the response of a physical model (constitutive, numerical or analytical); (c) the performance of the system using the reliability method; (d) the sensitivity of the reliability to each varying parameter; (e) allows optimisation for both the range of expected behaviour and the impact of gaining more knowledge; and (f) is the impact upon the overall safety assessment.

For the stability of the adjacent tunnels in the repository, two failure criteria have been considered in this work: (i) the plastic radius, that is the radius where the clay rock is in the plastic (yield) part of the constitutive behaviour; and (ii) the liner collapse stress. The unsatisfactory performance of the tunnel and lining system is then defined as the probability of one of these criteria being met. Initially a new analytical axisymmetric solution has been developed and implemented within a Monte Carlo framework to gain insight into the variability and sensitivity of the solution to various model conditions. The model utilises an elasto-plastic strain-softening constitutive model and has been used to test probability distributions of material parameters with realistic, low and high mean estimates and coefficients of variation. More details are provided in Arnold et al. (2014a) and Arnold et al. (2014b - in prep.). Using this analytical solution additional investigation has been undertaken assessing the performance of approximate reliability-based methods in terms of accuracy and computational cost in comparison to the Monte Carlo solution. It has been seen that such approaches have been able to significantly reduce computational time (utilising ~10%) with only limited reductions in accuracy (~10%), but with the accuracy depending upon the non-linearity of the constitutive model and the type and order of the reliability method.

A commercial geotechnical numerical model (Plaxis, 2014) has been integrated into the reliability module developed. This enables the advantages of the Finite Element Method (FEM), that is, the ability to model non-regular geometries, staged analyses and complex material behaviour, to be incorporated in a reliability-based analysis. Material behaviour has been calibrated against limited laboratory test data on undisturbed Boom Clay, and 2D plane strain tunnel behaviour has been modelled and incorporated into the reliability assessment of the repository performance.

The reliability-based numerical tool has been utilised to give a more detailed insight into the ranges of parameters and material behaviour that need to be addressed, for instance, via site investigation, and further on the range of behaviours influencing most the design of a Dutch radioactive waste repository.

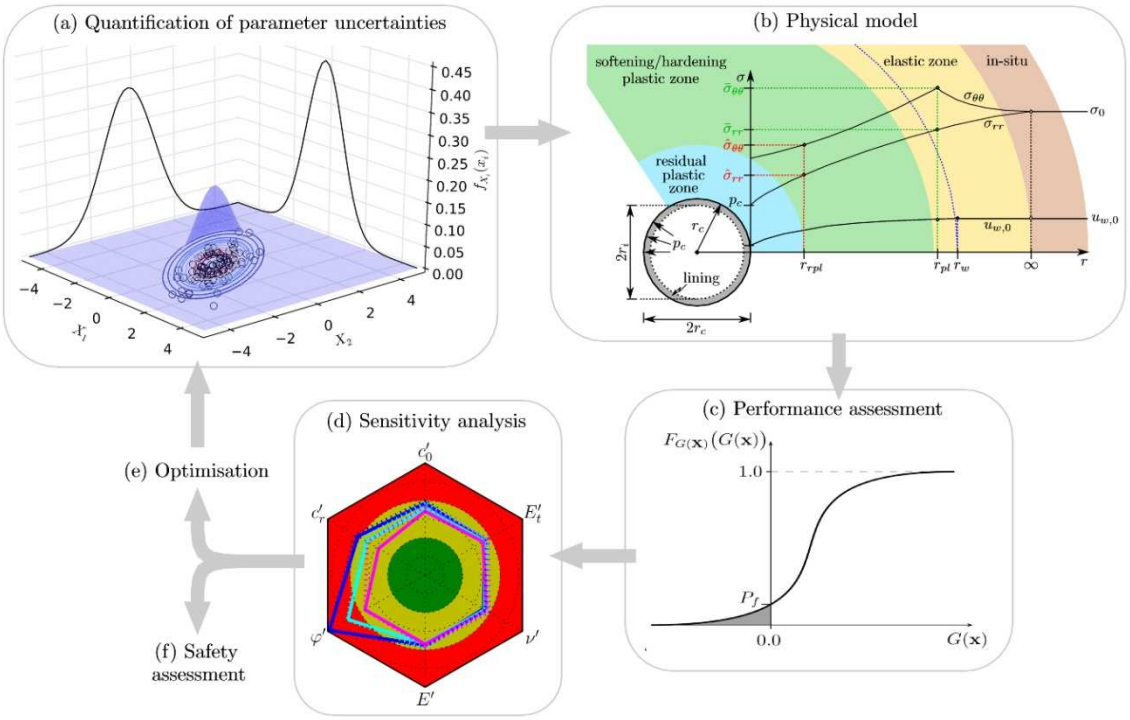


Figure 1. Probabilistic approach for the geomechanical modelling.

References

Arnold, P., Vardon, P.J., Hicks, M.A. (2014a) "Preliminary assessment of tunnel stability for a radioactive waste repository in Boom Clay", *Engineering Geology for Society and Territory – Volume 6*, Springer, 545-549.

Arnold, P., Vardon, P.J., Hicks, M.A., Fokkens, J., Fokker, P.A., Orlic, B. (2014b – in prep.) *A numerical and reliability-based investigation into the technical feasibility of a Dutch radioactive waste repository in Boom Clay*.

Barnichon, J.D., Neerdael, B., Grupa, J., Vervoort, A. (2000). *CORA Project TRUCK-II*. SCK·CEN., url: http://www.covra.nl/cms-file/get/iFileId/2477

Plaxis (2014) *PLAXIS 2D Anniversary Edition - Reference Manual*. PLAXIS B.V.

Verhoef, E., Neeft, E., Grupa, J., Poley, A. (2011) *Outline of a disposal concept in clay*. COVRA N.V., Report No. OPERA-PG-COV008.

Acknowledgements

The research leading to these results has received funding from the Dutch research programme on geological disposal, OPERA. OPERA is financed by the Dutch Ministry of Economic Affairs and the public limited liability company Elektriciteits-Produktiemaatschappij Zuid-Nederland (EPZ), and is coordinated by COVRA.

3D modeling of the mechanical behavior of liners (segments) placed around the gallery of nuclear waste repository

V. Renaud[1], *A. Poutrel*[2]

1. INERIS – Institut National de l'Environnement Industriel et des Risques, Campus ARTEM, Ecole des Mines de Nancy, CS 14234, F-54042 Nancy Cedex, France (vincent.renaud@ineris.fr)
2. Andra – Agence Nationale de gestion des Déchets Radioactifs, Direction de la Recherche et Développement / Mécanique des Fluides et des Solides, Parc de la Croix Blanche, 1/7 rue Jean Monnet, 92298 CHATENAY-MALABRY, France (adrien.poutrel@andra.fr)

Keywords: 3D numerical models, endo-viscoplasticity, creep, liner behavior, interface

Introduction

In 2005, Andra concluded that the feasibility of deep geological repository for high level (HLW) and intermediate level (ILW) long-lived waste was valid. Hence, Andra is now responsible for designing and implementing a repository disposal for HLW and ILW waste called: CIGEO (Geological Repository Project). A zone of interest for thorough exploration (ZIRA) was suggested in 2009. A simulation program is included to the CIGEO project.

One of the studied topics consists in the investigation of "the mechanical evolution of structures", and especially the analysis of the mechanical response of large underground galleries with concrete liner during the reversibility period (0 - 100 years) using the constitutive law (endoviscoplastic) with the lowest set of parameters. The main objective of this study is to know the impact of the use of this law (and various associated parameters) on the design of structures and to compare with the *in situ* experiment. The computations of this study allow us to understand the efforts in cementitious components (liner) subjected to claystone loading (with creep) and to analyze the mechanical response of this type of work on the reversibility period. Variability loading of concrete structures is studied using several cases: short-term variation parameters (threshold distortion, dilatancies) and long-term simulation of annular closure (claystone / lining segment) considering interfaces, the packing material, the concrete creep of the liner as well as the delay of applying the liner.

Context and methods

A numerical simulation program has been defined to assess the efforts in cementitious components (support and liner) subjected to claystone loading (due to creep). This program includes 11 endoviscoplastic 3D calculations performed with FLAC3D. The constitutive law used for these calculations is a model with viscoplastic damageable hardening (Hoek and Brown criterion). The input data concerning the mechanical behavior (perfect elastoplastic for concrete structures, endoviscoplastic for claystone, whether instantaneous or delayed).
For 4 of the 11 cases of calculation, the interfaces were defined between the liner and the packing material. The interface is a way of approaching the contact modeling of claystone with lining segment. Actually, there is a variable annular gap between the lining segment (reinforcement and corrosion are not considered) and the claystone rock mass in which a packing material (initially fluid) is poured. This material will make its hardening during the following 28 days (time modification of properties), time during which the massive claystone starts to creep and load the liner in areas where there is contact. The combined area of these contacts will gradually grow to a certain time when it can be assumed a contact without gap between the structure and the surrounding rock mass. This contact can, however, be considered as imperfect insofar the broken claystone (residual threshold exceeded) close to the wall does not transmit as many stresses as virgin claystone. If the numerical modeling assumes a perfect instant contact between the structure (highly stiff) and argillite / packing material (highly deformable), then the evolution speed of radial and orthoradial stresses is much overestimated. The use of the interface (mainly defined by its normal and tangential stiffness) avoids this bias.

Results and interpretation

The main conclusions that can be drawn from the results related to the loading of the liner following excavation of the large diameter gallery (carved into the claystone of Bure) are:
• the late setting up (a 12 m or 24 m installation from the front has been tested) of the liner limits its load and ultimately its yielding. This is the parameter that most influences the stresses, displacements and plastic extensions when no interface is considered;
• in accordance with the studied assumptions (no chemical degradation of concrete), the evolution of liner load (on the upper surface) correlates very well with a logarithmic regression, which facilitates predictions for creep time above 100 years. In the liner, radial stresses increase very fast: 75 % of the maximum 100-year-values are acquired from 1.5 years while double (3 years) is needed for orthoradial stresses;
• only the first radial mesh of the lower surface of the liner can reach the concrete failure criterion (Rc = 60 MPa) at the end of the study period (100 years). This occurs only when the gallery is oriented according to σ_h and if concrete interfaces (with low constant stiffness) are not taken into account. Lowering one or two threshold(s) of plastic shear strain (peak and / or residual) involves the increasing of post-peak plasticity and therefore viscoplastic strains of claystone. These then induce a stronger and faster loading on the concrete, that's why its yielding increases;
• interface presence restrict the liner loading, which is closer to the experimental findings. The interface role is all the more important as their characterizing stiffness is weak (lastingly). If stiffness increases in time up to 10 years (initial values x 10), calculated impacts on studied physical quantities are low (regarding low initial stiffness remaining constant on a period going from 0 to 100 years) and have less influence than a doubled installation time (without interface);
• the tested parameters set (lower) of behavior law does not significantly affect the radial strain of the liner, unlike orthoradial strain. However, these amplitudes remain low: radial strains reach 0.05 % maximum (in lower surface) while the orthoradial strains can assert to 0.16 % in the upper surface;
• orienting the gallery according to σ_H rather than σ_h is making vertical convergence drop by 56 % in the long term while horizontal convergences only increased by 8%: the ratio Cv/Ch is divided by 2.45 (it goes from 2.13 to 0.87).

In view of the assumptions considered, the parameters relating to the phasing (liner installation time, interface simulating the closing effect of the annular space) have a more significant influence on obtained stresses, strains, displacements and plastic extensions than parameters (tested in this study) relating to the viscoplastic behavior law (post-peak hardening parameter, residual and post-peak thresholds, concrete creep).

Hydraulic-mechanically coupled simulation of cyclic deformation processes investigated at the Mont Terri site

Ziefle, Gesa[1], **Maßmann, Jobst**[1]

[1] Bundesanstalt für Geowissenschaften und Rohstoffe, Stilleweg 2, 30655 Hannover, Germany

The investigation of potential host rocks for the storage of radioactive waste is subject of current research and scientific discussion. For the safety assessment of a repository, it is of great interest to understand the interacting thermal, hydraulic, mechanical and chemical processes in the storage area. Measurements of well defined experiments as well as numerical simulations lead to an increase of knowledge concerning the significance of various effects in the storage process.

Mainly due to its low permeability, sorption behavior and visco-plastic properties, clay formations serve as a potential host rock. Significant research concerning the characteristics of Opalinus clay is carried out at the Mont Terri site in Switzerland. Here, a great number of experiments investigates geological settings, material parameters, physical effects, and furthermore. The work presented here is motivated by observations performed in the framework of the "cyclic deformation" (CD) as well as the "long-term monitoring of pore pressures" (LP) experiment. Within these experiments the temperature and relative humidity as well as the convergence in an excavated niche are monitored. Special focus is laid on an existing joint and his deformation behavior due to the seasonal changes of temperature and relative humidity. Especially the interaction of such joints with shrinkage joints and the excavation disturbed zone is of significant interest for the understanding of the desaturation as well as a potential resaturation process.

Focusing on a numerical investigation of the hydraulic-mechanically coupled effects, a comparison of the modeling results with the measurements is conducted. Points of emphasis are placed on the question: Which effects are significant for the examined evolution of displacements in the niche? And furthermore: What happens with the existing joint? In a first step, the Opalinus clay is simulated as a homogeneous material – here, classical THM-calculations are carried out. Hereafter, the focus is laid

on the joint. Various model set-ups are compared due to their informative value concerning the measured data.

Concerning the coupled THM model, the initial conditions imply a fully saturated area of Opalinus clay. The excavation induces a stress redistribution coming along with a change of the pore water pressure according to the classical Terzaghi's approach applied for anisotropic material. Afterwards, seasonal changes of temperature and relative humidity influence the effects in the vicinity of the niche. Thermally induced strains are generated and a desaturation process takes place, which proceeds substantially in winter and implies changes of the pore water pressure and the deformation field. However, due to the characteristics of the clayey material, some additional mechanisms play an important role in the mentioned evolution process. Firstly, the material is characterized by hydraulic and mechanical transversal isotropic properties and additionally, swelling and shrinkage are induced by the changes of saturation. The significant impact of these effects on the deformation behavior can be illustrated by the numerical simulations. Finally, the convergence in the niche is characterized by seasonal changes which are superimposed by a trend, leading to a vertical convergence of the niche. This evolution is indicated by the measurements as well as the numerical simulation.

Concerning the evolution of the joint, two effects are essential. On the one side, the whole niche is characterized by a vertical convergence combined with a horizontal extension which influences the evolution of the joint. On the other side, the properties of the joint may change due to the changes in pore water pressure and the displacements. Both effects have an impact on the evolution of the joint which is a challenge for the simulation strategy.

Summarizing, the presented THM models picture the coupled behavior of the evolution process of the excavation disturbed zone with relevance to the swelling and shrinking behavior of the anisotropic clay. The results are interpreted concerning the measurements carried out at Mont Terri, Switzerland.

Acknowledgements:

We would like to thank Andreas Möri (swisstopo, Switzerland) and Jean Michel Matray (IRSN, France), who accompany and evaluate the measurements conducted within the former CD/LP experiments now gathered in a common experiment namely “long-term monitoring of pore parameters” LP-A at the Mont Terri site (CH).

Experimental study of the mechanical behavior of a steel casing in a 500 m deep clay formation based on in-situ experiments – Analysis of the scale effect

F. Bumbieler, J. Morel, N. Conil & G. Armand

Andra, Meuse / Haute-Marne Centre – Route Départementale 960 - 55290 Bure - France

Andra, the French national radioactive waste management agency, is in charge of the study on the possibility of disposal for High Level activity Wastes (HLW) in deep geological repositories. The concept of HLW cells consists of horizontal micro-tunnels (at least) 80 m long and about 0.7 m in diameter, equipped with a non-alloy steel casing to allow the emplacement and the retrieval of the waste containers during the reversibility period. Several in-situ experiments dedicated to the analysis of the short term mechanical behavior of the casing have been designed and set up in Andra's Underground Research Laboratory.

Reduced scale (1:5) in-situ experiments consisting of equipping boreholes parallel to the major horizontal stress (σ_H) with instrumented steel tubing, have been performed to analyze the mechanisms involved in the casing/rock interface. The main characteristics of the short term mechanical load applied by the rock have been determined from local strain and convergence measurements at different depths from the access drift. Although the radial stress applied by the rock is supposed to be isotropic for boreholes parallel to σ_H, measurements exhibit a strongly anisotropic load. This behavior, which is consistent with the convergence anisotropy measured on uncased full scale HLW cells having the same orientation with respect to the natural stress field, is directly related to the shape of the damaged zone around the cell. In the 1st loading step, the radial load is localized in the horizontal direction corresponding to the maximum extension of this damaged zone. This loading results in a radial bending of the casing and the circumferential stress can reach 350 MPa on the inner face. Once there is no more void between the tubing and the rock at least in the vertical direction, the mechanical load remains anisotropic with no impact on the tubing convergence. This 2nd loading step can be followed by a decrease of the load anisotropy (Figure 1).

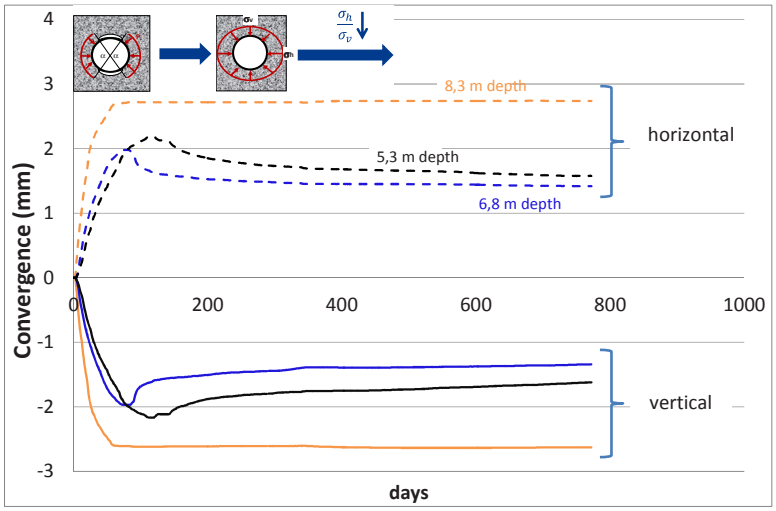


Figure 1 – Convergence of steel tubing at 3 different depths (thickness ≈ 0.02∅, initial annular space ≈0.03∅)

Tactile pressure sensors have also been wrapped around some tubing to determine the radial pressure distribution. First results show that the radial load remains significantly localized (even in the 2nd loading step), resulting in an almost horizontal maximum load axis (Figure 2, measurements performed at a depth of 7.3 m from the access drift). The maximum value of the mean radial stress over the axial width of the tactile sheet (almost 90 mm) reaches 2.5 MPa, some very localized loads reaching 5 MPa.

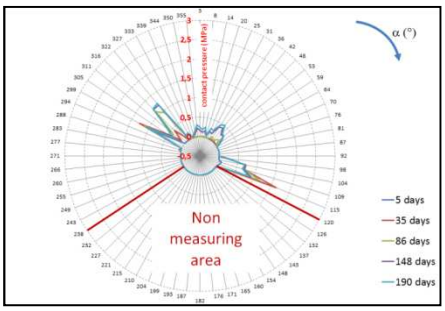


Figure 2 – Time evolution of the circumferential distribution of the mean radial stress applied over the width of the tactile sheet

A similar short term mechanical loading of the casing is observed also at the full scale. The casing of a 40 m long full scale HLW cell has been equipped with several displacement sensors and strain gauges to estimate the mechanical load applied by the rock. After 3 years of measurements, the convergence of the casing is not stabilized (Figure 3), which means that we are still in the 1st loading step with a much lower loading rate than for small scale experiments having the same theoretical initial annular space (0,03 ∅). This scale effect may be related to the presence of overbreaks at the cell vault, the partial filling of the annular space with rock cuttings during the drilling of the cell and the damaged zone stiffness difference between boreholes and full scale cells.

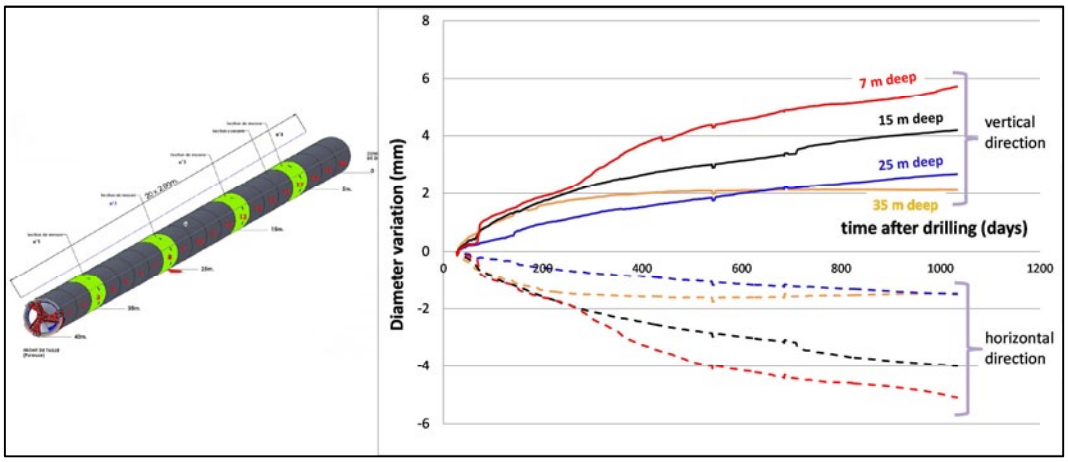


Figure 3 –Time evolution of the casing diameter of a 40 m long full scale cell (thickness ≈ 0.03∅, initial annular space ≈0.03∅)

In order to decrease the tensile stress level that can be reached in the casing (by limiting the radial bending), the feasibility of filling the annular space with a cement grout is under study. At reduced scale, the ability to block the ovalization of a tubing by injecting a cement-bentonite grout in an initial annular space of about 0.13 ∅ has been demonstrated. The 2nd loading step as defined previously has been reached in less than 10 days (i.e. 10 times faster than without injection).

A similar experiment has been performed at full scale using the same cement grout. The only difference is the size of the theoretical initial annular space which was about 0.04 ∅. In this case, the ovalization of the casing is not yet blocked (after 9 months of measurements) and the maximum load axis has rotated 90° in comparison with experiments without injection, resulting in a vertical convergence of the casing. Numerical simulations are currently being carried out to better understand the mechanical behavior of the system composed by the damaged rock, the cement grout and the casing and to explain this scale effect.

Long term behaviour of claystone and its interaction with steel casing – Comparison between continuum/discontinuum 3D models

Wenjie SHIU
ITASCA Consultants S.A.S., 64 chemin des Mouilles, 69130 ECULLY France
Marco CAMUSSO
ITASCA Consultants S.A.S., 64 chemin des Mouilles, 69130 ECULLY France
Daniel BILLAUX
ITASCA Consultants S.A.S., 64 chemin des Mouilles, 69130 ECULLY France
Adrien POUTREL
Andra, 1/7 rue Jean Monnet, 92298 CHATENAY-MALABRY Cedex, France

Plans are made in France in order to assess the feasibility of constructing a repository for radioactive waste at depth within a claystone layer. In this framework, the potential damage that may occur in the claystone surrounding a disposal gallery is of concern. First, it has been observed that excavation in such a material produces a pattern of fractures. Second, the radioactive waste has a much higher temperature than the surrounding claystone when it is installed inside the steel casing, and thus may induce non-negligible thermal strain on the claystone located near the cavity during creep. Finally, it is clear that the steel casing of any cavity built to store radioactive waste will eventually fail, albeit after a long period. The creep-prone claystone surrounding the cavity may then experience some damage. While initial fractures have been effectively observed, the long term behavior or the steel casing-claystone pair is both important and difficult to assess, one major question being how the excavation-induced fractures and the radioactive waste induced thermal strain affect the long term behavior.

Two 3D models are built using both continuum (*FLAC3D*) and discontinuum (*3DEC*) approaches. The 0.76m – diameter gallery is oriented along the major principal *in-situ* stress. In this study, two types of hollow steel cylinders are placed successively inside the gallery. First, a 25mm thick steel casing with 0.735m outside diameter is installed just after excavation. Then, an overpack, 65mm thick and 0.635m in outside diameter, is installed 10 years after excavation. This is the start of the heating process. The differences in diameters result in fully specified voids between the claystone, the steel casing, and the overpack. Bentonite-concrete type material is used to fill the void between claystone and steel casing, while the internal void is left open. Since the waste is not explicitly modeled, the maximum convergence of the overpack inner surface is monitored, in order to detect a potential contact between the overpack and the waste.

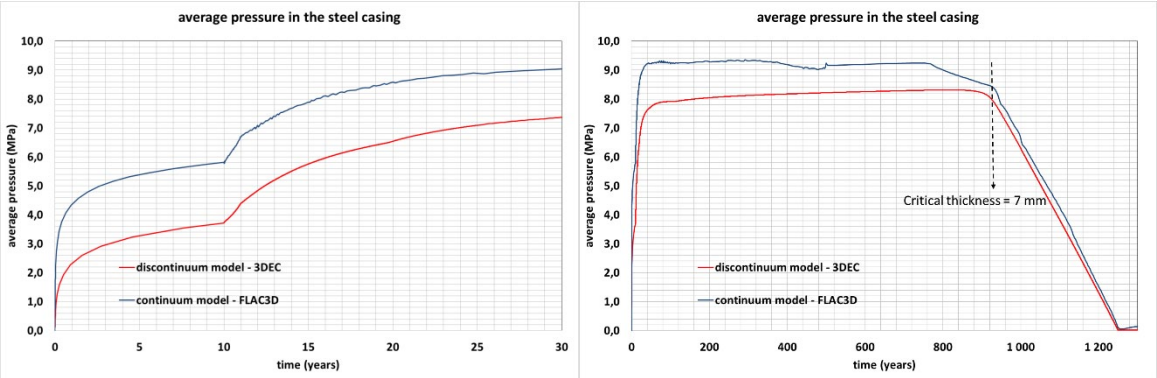
The excavation-induced fractures are explicitly introduced in the discontinuum model. In the continuum model, the initial damaged zone is represented by a macro block with smaller critical shear strain, thus forcing earlier strain softening.

The model reproduces the behavior of the claystone subjected to different unloading paths, depending on the damage scenario for the steel casing and the overpack, over a creep duration of several thousands of years. The instantaneous response of the material is represented by a hardening-softening Hoek-Brown law, where damage before peak strength is simulated by hardening in the framework of plasticity theory, while post-peak behavior is classically reproduced by softening. Time – dependent behavior is produced using a modified Lemaitre model, including a creep threshold and variation of the creep rate with damage. The steel casing and the overpack are considered as a Von-Mises material with strain hardening-softening. Moreover, corrosion effects are accounted for by reducing progressively the relevant steel properties, fitting a corrosion rate of 10 μm/year. Since the emphasis in this study is on the long term, no attempt is made to reproduce precisely the excavation stress path and the creation of the "instantaneous" fractures. From virgin stresses, the shape of the excavation is simply de-confined progressively before installing the steel casing and the filling. Creep starts after excavation, with the fractures (or the damaged zone block) already created in the claystone.

As expected, the load on the steel casing increases over the first 30 years, with contributions from creep and thermal strain both significant. Later, the load becomes fairly constant during a long period. It finally starts to decrease after approximately 900 years, for an average outside pressure of the order of 8 MPa. The continuum model predicts higher average pressures on the steel casing than the discontinuum model. This is due to partial dissipation of the load by joints sliding in the discontinuum model. The steel of the casing reaches its elastic limit where significant orthoradial stresses are observed. Plasticity then propagates towards the full casing thickness, on the entire perimeter.

The ground and steel casing behaviors are significantly impacted by the corrosion rate. The figure below illustrates the evolution of the average radial pressure applied by the claystone on the steel casing for the two models. For both continuum and discontinuum approaches, the numerical model predicts that the steel casing will be able to support a fairly constant load for approximately 900 years. After that time, the load drops linearly from 8 MPa to a quasi-zero value in about 350 years. Note that the 1250 years reached correspond to complete corrosion of the steel casing. The load will stay minimal while the casing converges until the overpack blocs its movement. During this period, the casing is still continuous, but it provides no resistance to the claystone pressure.

At 900 years, the maximum plastic shear strain in the steel casing was about 5%, far below the steel softening threshold (22%). This clearly indicates that the behavior of the steel casing is mainly dominated by corrosion, not by the hardening/softening properties of the steel. To quantify the effect of corrosion, we define a "critical thickness", as the minimum intact steel thickness necessary for the casing to withstand the pressure applied by the claystone. It is about 7 mm for both continuum and discontinuum models. Although a simplified representation of the fractured claystone is used in the continuum model, the numerical results in terms of average pressure on the steel casing are quite similar between the discontinuous and continuous approach.



Evolution of average pressure in the steel casing over the first 30 years (left) and 1300 years (right)

Full-scale test of dome plug (Domplu) - design, installation, predictions and results

Lennart Börgesson[1], Torbjörn Sandén[1], *Mattias Åkesson[1]*, Pär Grahm[2]

[1] Clay Technology AB, IDEON Science Park, Lund, Sweden
[2] Swedish Nuclear Fuel and Waste Management Co, Oskarshamn, Sweden

The deposition tunnels in a planned repository for spent nuclear fuel will be sealed with a plug at the end of the tunnels in order to withstand the swelling of the backfill and to seal off out-flowing ground water. The principle design of the plug consists of several components, among which the most important are the concrete dome, the bentonite seal and the filter. The water leakage past the plug has to be small enough in order to build up a water pressure inside the plug, and to keep eroding water from the tunnel at an acceptable level during the operational phase of the repository. The concrete part of the plug needs time (about 3 months) for hardening and contact grouting, and during that time the concrete section must be kept free from water. Wet tunnels therefore require a drainage system which can take care of the water coming from the inner parts of the tunnel.

These issues and demands have been addressed in the SKB project "System design of dome plug for deposition tunnels". The project aims to ensure that the reference configuration of the KBS-3V deposition tunnel end plug works as intended. By testing the design in a full-scale demonstration it is to be proven that the method for plugging of a deposition tunnel is feasible and controllable. The requirements on tightness of the plug are to be given a definite form. This presentation will give an overview of the full-scale test "Domplu" performed at 450 m depth at Äspö HRL in cooperation between SKB and Posiva. Monitoring and evaluation of Domplu are tasks included in the Euratom FP7 DOPAS project. The main goal of the Domplu test is to determine leakage through the plug, and through the contact surfaces between the rock and the concrete, at a stable water pressure of 4 MPa. Different lab tests and a design modeling have also been performed within the SKB project and these results are presented in an adjoining presentation[1].

The full-scale test consists of a number of components, each with its own purpose (Figure 1). The innermost component is a 1 m backfill zone which consists of a stack of bentonite blocks with a surrounding pellet filling. The next section is the filter which is composed of 0.3 m thick LECA-beams and a 0.3 m layer of gravel (2-4 mm). The filter section serves for drainage of groundwater during construction as well as for artificial wetting of the bentonite seal when the drainage is finally closed. The gravel and the bentonite seal are separated by a geo-textile which also facilitates distribution of water into the sealing. The bentonite seal consists of a 0.5 m stack of highly compacted MX-80 bentonite blocks with a surrounding MX-80 pellet filling closest to the rock. Finally, the restraining concrete structure is designed as an octagonal dome plug, casted in-situ by low-pH concrete (SKB recipe B200). The diameter of the concrete dome is 8.8 m while the concrete thickness is 1.79 m in the hub.

Besides extensive monitoring of the concrete dome structure, the inner plug components are instrumented with sensors for measurement of total pressure, pore pressure, relative humidity and displacements at several positions. The bentonite-based components and the filter were installed in January 2013. Pressurization by natural groundwater inflow began in October 2013. The artificial pressurization was increased stepwise to 4 MPa during the period from December 2013 to February 2014, and has been kept stable at this level until the submission of the abstract (September 2014). The measured leakage past the plug at that time was 2.9 liters per hour. Monitoring will continue at least until late 2016.

[1] "Dome plug for deposition tunnels – lab tests and design modeling" by Börgesson, Sandén and Åkesson

A blind prediction of the evolution of hydro-mechanical processes in the full-scale test was performed prior to the installation with a number of 2D axisymmetric Code_Bright models. The main results from the different numerical models have been the stress on plug, the displacement of the different components and the evolution of RH at different positions. A comparison of predicted and measured data will be presented at the conference.

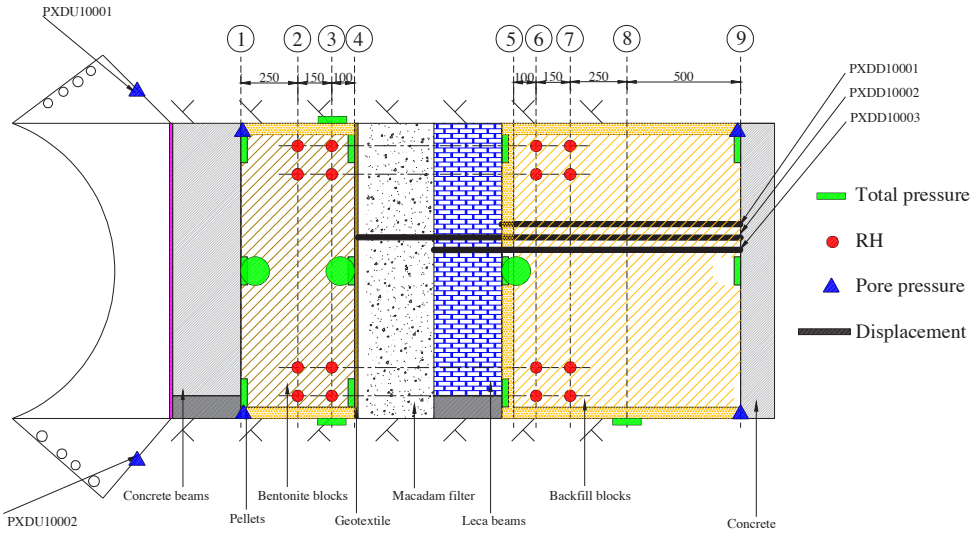


Figure 1. Schematic drawing showing the preliminary sensor position in bentonite sealing and backfill.



Figure 2. Emplacement of bentonite blocks in the sealing (left). Filter section (Leca-beam and macadam) together with geotextile, bentonite block and bentonite pellets (right).

The research leading to these results has received funding from the European Union's European Atomic Energy Community's (Euratom) Seventh Framework Programme FP7/2007-2013 under grant agreement no 323273, the DOPAS project.

Multiscale modeling of textural and mechanical properties of clays

Davoud Ebrahimi†, Andrew J. Whittle †, *Roland J.-M. Pellenq*†§‡

† Department of Civil and Environmental Engineering
Massachusetts Institute of Technology, Cambridge, MA 02139, USA

§ Centre Interdisciplinaire de Nanosciences de Marseille
Aix-Marseille Universit´ e, CNRS, Campus de Luminy, 13288 Marseille Cedex 09, France

‡ < MSE >2, UMI 3466
CNRS-MIT, Cambridge, MA 02139, USA

Engineered barriers usually made of highly compacted swelling clay are one of the options in covering canisters of radioactive waste embedded in deep geologic repositories. This research proposes a bottom up multiscale approach in studying change in macroscopic properties of clay during compaction based on atomic interaction at the atomic scale followed by interaction of clay platelets at the meso scale. By using this method we can characterize change in clay microstructure during compaction in parallel with the variation of mechanical properties.

The proposed method begins with full atomistic simulation of clay (Na-Wyoming montmorillonite)-water system using clayff force field for edge to edge and face to face interaction of two clay platelets. The change in free energy as a function of separation distance for these two basic configurations are used to calibrate Gay-Berne potential that represents each platelet as a single site ellipsoidal body. We have parameterized Gay-Berne potential for different platelet sizes and studied microstructural and mechanical evolution of systems composed of mono dispersed clay platelets. Systems of initially random oriented of clay platelets at mesocale under isothermal isobaric condition aggregate and form clay particles with 3-8 platelets per particle depending on the confining pressure and platelet size. Aggregate size increases with increase of platelet size. Scalar order parameter is used to study isotropy of the system. By increasing confining pressure aggregate size and ordering/anisotropy of the system increases until reaching to a maximum ordered state. Further increase of confining pressure results in decrease of aggregate size due to sliding of platelets against each other at a constant order parameter. The elastic mechanical properties of the system shows cubic symmetry and increases with increasing confining pressure. Results of the simulations are in good agreement with reported aggregate size (3-10) and nanoindentation results from experiment.

The research can be extended to study the effect of heterogeneity of platelet sizes and amount of isomorphous substitution on the microstructure and mechanical properties of the clay based materials.

Geomechanical characterization of the Opalinus Clay from an analysis of the FE Tunnel excavation at the Mont Terri URL

***R. Senger*[1], P. Marschall[2], S. Goodarzi[3], D. Walters[3], H.R. Müller[2], T. Vogt[2], B. Garitte[2]**

[1]INTERA Incorporated, Swiss Branch, CH-5408 Ennetbaden, Switzerland, (rsenger@intera.com)
[2]NAGRA, CH-5430 Wettingen, Switzerland (Paul.Marschall@nagra.ch)
[3]TAURUS Reservoir Solutions, Ltd, Calgary, Alberta, Canada

The Full-Scale Emplacement (FE) experiment at the Mont Terri underground research laboratory (URL) is designed to replicate the construction, emplacement, and early post-closure environment of an HLW underground repository (Müller et al. 2015). This involves the excavation of a 50 m long tunnel section, emplacement and backfilling of empty steel canisters, and heating of these canisters according to the expected heat generation rate from radioactive decay of the spent fuel waste. This study investigates the coupled hydro-mechanical (HM) phenomena associated with the excavation of the FE tunnel, during which pore pressures and strains were monitored in nearby borehole intervals as well as convergence of the tunnel wall. The excavation of the FE tunnel was in the Opalinus Clay, which is considered the host rock for a spent fuel / HLW repository. Understanding the geomechanical phenomena associated with the tunnel excavation is therefore important for the construction of underground repository systems in terms of engineering feasibility and the long-term safety assessment of the repository. Construction of underground tunnels in clay rocks causes excavation-induced stresses resulting in the development of an excavation-disturbed zone (EDZ) around the tunnel and distinct pore-pressure responses associated with the strongly non-linear elastic behaviour of the clay (Corkum and Martin, 2007).

Monitoring boreholes were drilled ahead of the excavation subparallel to the tunnel axis and were aligned parallel and perpendicular to bedding which dips at an angle of about 35 degrees (Fig. 1). Each borehole was equipped with a multi-packer system with six intervals at increasing distance from the tunnel mouth. The monitored pore pressures show distinct pressure responses, increasing ahead of the excavation front, followed by a sharp decline after the excavation front passed (Fig. 1), which are caused by the excavation-induced stress-strain response.

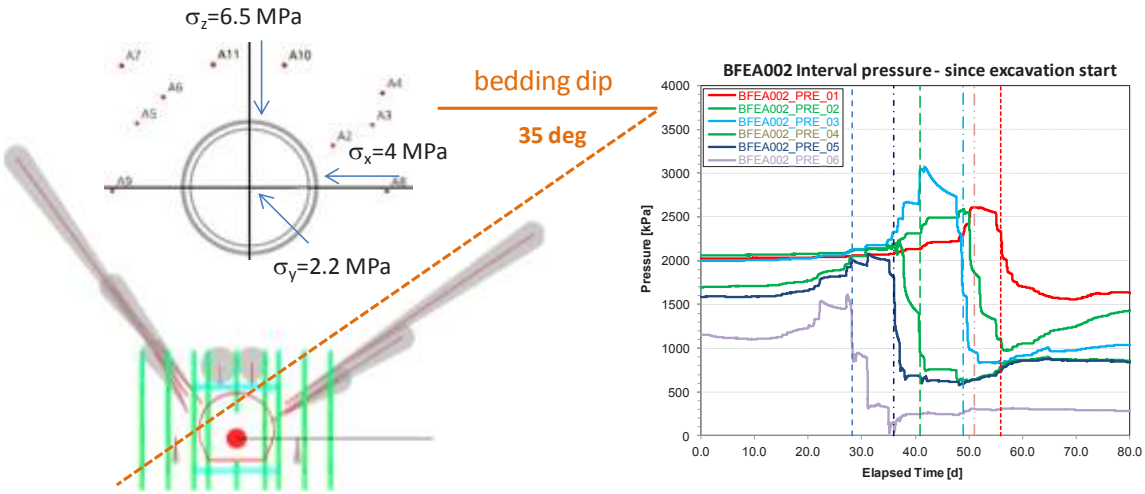


Figure 1. FE-Tunnel with borehole-locations (left) and pore pressure responses (right)

For the detailed assessment of the geomechanical phenomena, a 3D numerical model was developed to simulate the stress-strain changes associated with the tunnel excavation. For this, the coupled geomechanical code GEOSIM (Taurus Reservoir Solutions, Ltd.) is used. GEOSIM is a modelling system for coupled multiphase flow and heat transfer in porous media, and geomechanical (stress-strain) analysis. The focus is to examine the spatial evolution of stresses and corresponding pore-

pressure responses during the excavation advance and assess the convergences around the tunnel and associated strain in the near-field, using transversely isotropic elastic geomechanical properties.

The model represents a half-space with the left boundary representing a symmetry axis through the FE tunnel. To account for the excavation, the boundary conditions (or stress state) of the elements representing the tunnel were changed to model the material removal based on 2-m excavation steps. Following excavation the elements were assigned a "soft" and weak material to provide minimal support and allow tunnel convergence during stress rebalancing. The subsequent installation of the shotcrete liner and support structures were not considered. Accounting for the inclined layering and associated transversely isotropic geomechanical properties, the model geometry is rotated to align the rectangular grid to be parallel and perpendicular to bedding, which requires the rotation of the stress tensor according to: $\sigma'_{ij} = a_{im} a_{jn} \sigma_{mn}$.

For the comparison of the simulated stresses to the measured pore pressures, the change in the principal stresses ($\Delta\sigma_i$) is used, which can be related to the pore-pressure change (Δp) by: $\Delta p = B/3(\Delta\sigma_1+\Delta\sigma_2+\Delta\sigma_3)$, where B is the Skempton's parameter. By assuming a value of B=1, the estimated pore-pressure change corresponds to the maximum undrained response caused by the change in total average stress and corresponding change in strain and porosity. The results in Figure 2 are based on E-moduli parallel and perpendicular to bedding of 4.0 and 0.5 GPa, respectively. The computed Δp distribution indicates maximum changes ranging from about -1000kPa to +1000kPa. The pore-pressure responses in the different intervals in borehole A2 indicate pressure increases ahead of the excavation front but only minor decline afterwards, remaining mainly positive, which is different from the measured responses (Fig.1). However, at a nearby location, the simulated pressures are comparable to the measured responses. That is, a slight offset in the stress tensor could rotate the simulated stress field resulting in a better agreement with the measure pore pressures in the A2 borehole intervals. Similarly, the computed strains parallel and perpendicular to bedding are in the same range as the measured strains (Fig. 2), indicating the large anisotropy in elastic properties can produce significant convergence of the tunnel wall.

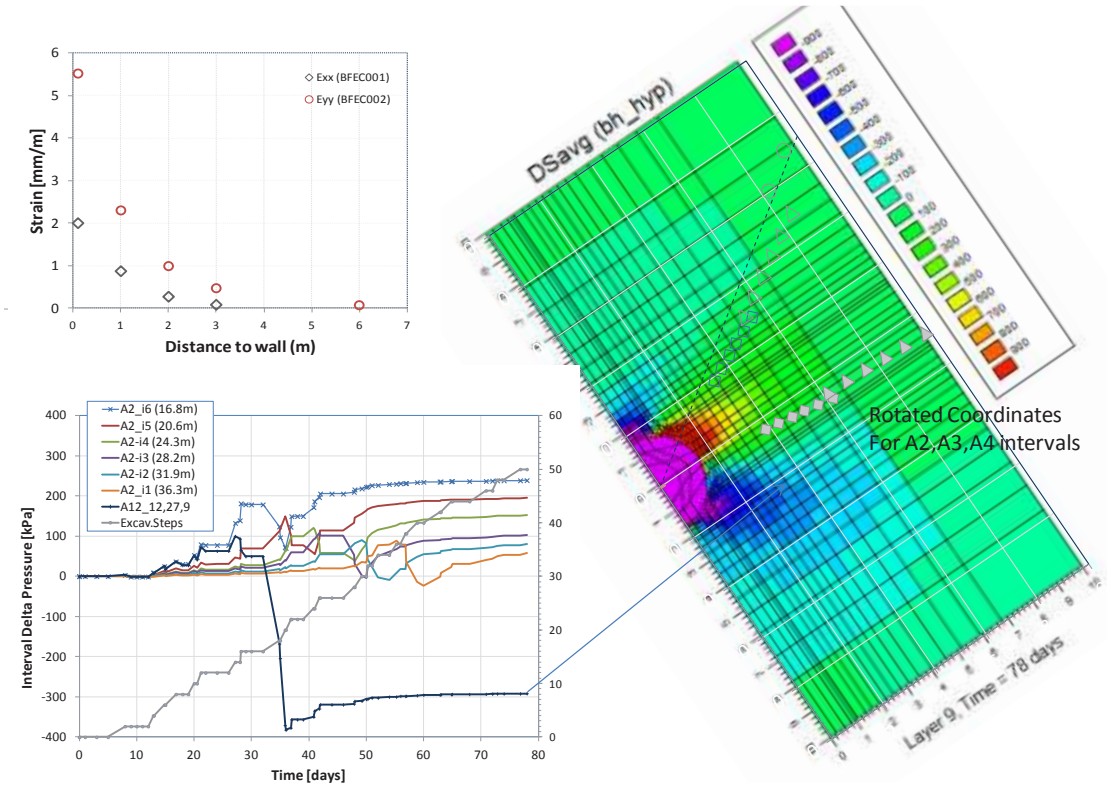


Figure 2. Simulation results with the pore pressure changes in the monitoring intervals in borehole A2 during the excavation steps (lower left), computed strain as a function of radial distance from the tunnel (upper left) and spatial distribution of total average stress changes at the approximate tunnel location of borehole interval A2_i6.

Characterization of the damage in Callovo-Orfordian claystone at two scales, strain localisation and micro cracks

***P. Bésuelle*[(1,2)], E. Andò[(1,2)], P. Lanatà[(1,2)], J. Desrues [(1,2)], G. Viggiani[(1,2)], S. Salager [(1,2)], P. Charrier[(1,2)]**

[(1)] Univ. Grenoble Alpes, Lab. 3SR, France
[(2)] CNRS, Lab 3SR, France

The principle of deep geological repositories for the disposal of radioactive waste relies among other things on the low permeability of the host rock. As the permeability is influenced by mechanical damage of the material, the characterization of damage mechanisms of the host rock (at several scales) is of outmost importance in the study of feasibility of radioactive waste repositories.

A first approach is developed to characterize the strain localisation at the scale of a laboratory specimen (a few centimeters). We present here new results obtained with a new true triaxial apparatus that allows observation of a rock specimen under loading. The strain field in the sample, and its evolution up to and beyond strain localisation, can be measured by digital image correlation (DIC) of photographs taken through a hard transparent window. Tests in plane strain compression have been performed, starting from isotropic stress states at several mean stress levels. Results of the time evolution of the pattern of localisation in the specimens are shown. Strain localisation appears to start well before the stress peak, sometime at about 50% of the stress peak, by very numerous parallel and conjugated shear bands. This early strain localisation, in the authors' knowledge, has never been observed before in rocks. Then, the number of active bands decreases progressively during subsequent loading, down to a very few bands at the peak and during strain softening. It is also possible to demonstrate how localization is influenced by confining pressure. The experimental results are systematically analysed in terms of fields of shear and volumetric strains.

The second approach focuses on a smaller scale, the scale of mineral inclusions embedded in a clay matrix where the inclusion size is a few microns. There is a challenge to study the mechanisms of deformation at this scale (clay cracking, de-cohesion of inclusions, etc…), which is the relevant scale for understanding the substantial evolution of some physical properties like fluid permeability. The aim of this study is to characterize the mechanisms of deformation at the small scale during loading experiments by combining of X-ray micro-tomography and DIC.
If the microstructure of the material is relatively well understood (Robinet et al, 2012), there are relatively few attempts to develop new experimental techniques to investigate the micro-scale mechanics of clay rocks in order to feed multi-scale numerical models. Optical microscopy was recently used by Wang et al. (2013). In this study, we have used 3D digital image correlation (3D-DIC) to measure the evolution of strain fields at the micro scale from X-ray microtomography images (with a spatial resolution of 0.7 microns) of specimens tested at ESRF (ID 19) (see Figure).

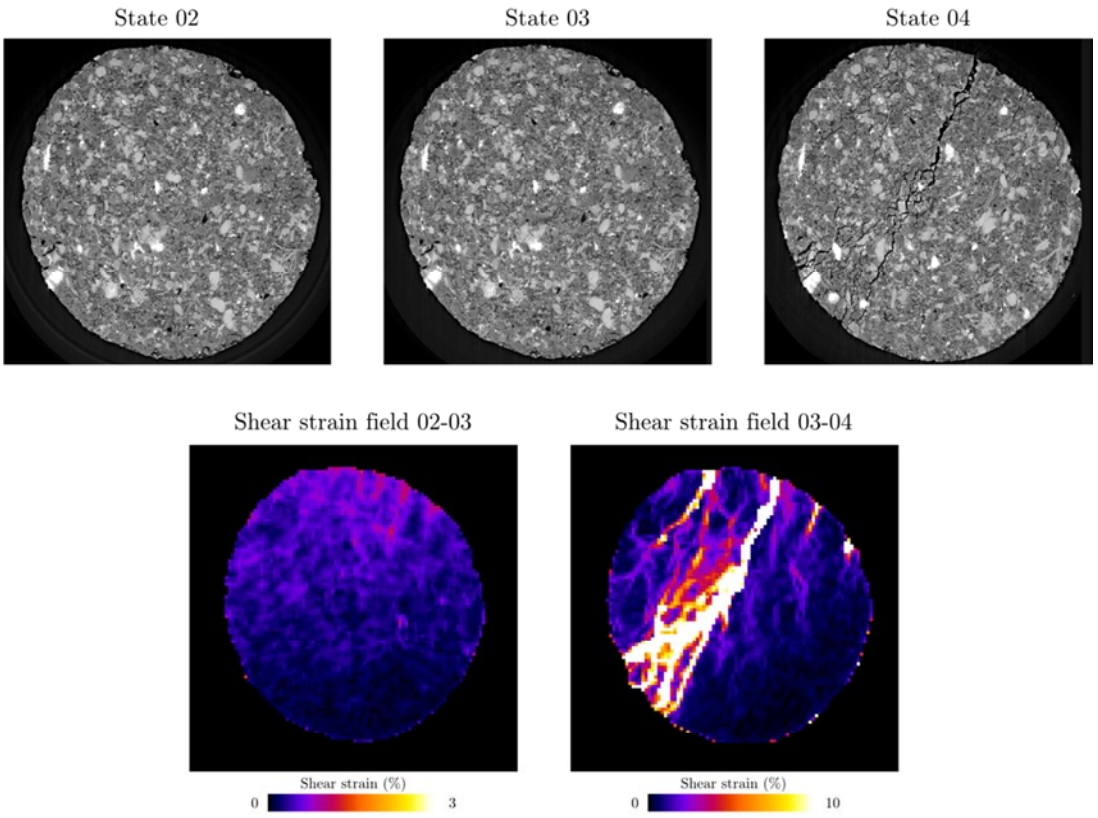


Figure 1: *Top: reconstructions (ID19) at different steps of loading of a clay-rock specimen (1mm diameter). Bottom: shear strain fields of the increments of loading, obtained by 3D-DIC*

Robinet J.-C., Sardini P., Coelho D., Pameix J.-C., Prêt D., Sammartino S., Boller E., Altmann S., 2010, Effect of mineral distribution at mesoscopic scale on solute diffusion in a clay-rich rock : Example of the Callovo-Oxfordian mudstone (Bure, France), Water Resources Res., vol. 48, W05554.

Wang LL., Bornert M., Chanchole S., Yang D.S., Héripré E., Tanguy A., 2013, Micro-scale experimental investigation of the swelling anisotropy of the Callovo-Oxfordian argillaceous rock, Clay Minerals 48-2, 391-402.

Numerical pre- and post-construction models of the geomechanical behaviour in the FE Experiment at the Mont Terri URL

Philippe Nater*, **Benoit Garitte****, **Sven Köhler****, **Herwig R. Müller****

*Pöyry Switzerland Ltd., Herostrasse 12, 8048 Zurich, Switzerland, philippe.nater@poyry.com
**Nagra, National Cooperative for the Disposal of Radioactive Waste, Hardstr. 73, 5430 Wettingen, Switzerland

For the Full-Scale Emplacement (FE) Experiment at the Mont Terri underground rock laboratory (URL) a circular tunnel was excavated in 2012 (see Müller et al. 2015). The tunnel is an elongation of the MB tunnel and situated in the shaly facies of the Opalinus Clay. The tunnel is 50 m long with a diameter of approx. 3 m, excavated by a road-header mounted on a small self-propelled carriage remotely controlled by an operator placed directly behind the rig. In order to reduce the convergence and to keep the excavation damage zone (EDZ) as small as possible, a slow advance rate of approx. 1 m / day and the placement of a stiff full ring support after every day including a sealing layer of min. 5 cm shotcrete and a structural layer of mesh reinforced shotcrete with min. 11 cm thickness was chosen. For encountering potential squeezing conditions, the usage of sliding elements in the springline was foreseen.

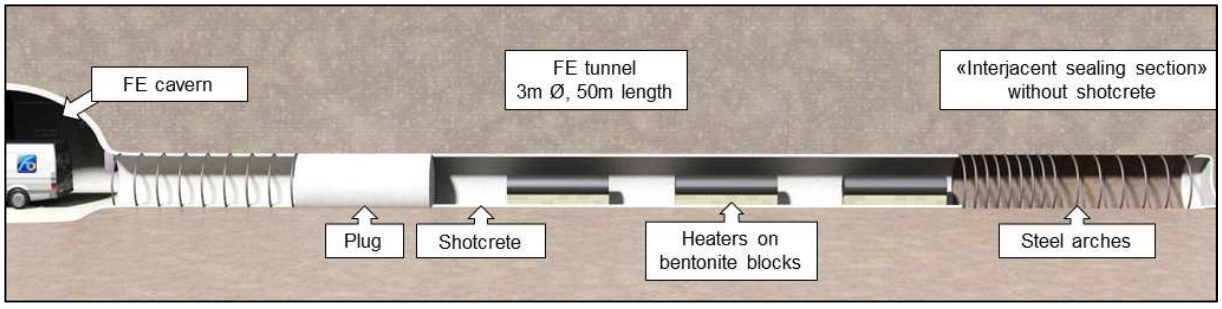


Figure 1: Visualization of the general experimental layout of the Full-Scale Emplacement (FE) experiment at the Mont Terri URL; sensors and bentonite backfill are not displayed.

As a guideline for the construction contractor predictive calculations of the potential displacements and the evolution of the EDZ were performed using 2D and 3D numerical calculations including hydro-mechanical coupling. Only limited displacements were predicted. The maximum value of e.g. head displacement was calculated to be 9 mm including the placement of a full ring lining and a drainage time of 2 years. This yields a relative closure of 0.6 %, which is stated to cause no squeezing problems according to the reference scale proposed by Aydan et al. (1993).

Most likely due to constructional issues and perhaps also as a results of a fault zone striking parallel to the tunnel axis (see Becker et al. 2015) the measured displacements exceeded the predictions significantly. As a consequence back-calculations were run which could partially allocate the additional displacements to the above-mentioned features.

The systems response of openings in comparable conditions (e.g. ED-B, EZ-A and MB test at Mont Terri URL) had been investigated by several authors and their research groups already; e.g. Corkum & Martin (2007), Popp et al. (2008) or Polster (2010). The geomechanical parameters have been partially reinterpreted by Bock (2008) and completed by later laboratory testing (Jahns, 2010). The numerical predictions and back calculations were performed with the codes FLAC2d and FLAC3d using the ubiquitous joints model incorporating hydro-mechanical coupling, plastic strain hardening / softening

and strength anisotropy. In addition, Corkum & Martin successfully applied a phenomenological-based stress dependent modulus approach (SDM).

Whereas shape and extension of the EDZ, as well as fluid pressure and displacements in the far field are well captured especially displacements in the near field are often underestimated. This yields towards a hypothesis that failure per se is adequately represented in the numerical models; still improvement can be achieved by introducing non-linearity and further stiffness degradation for the elastic parameters.

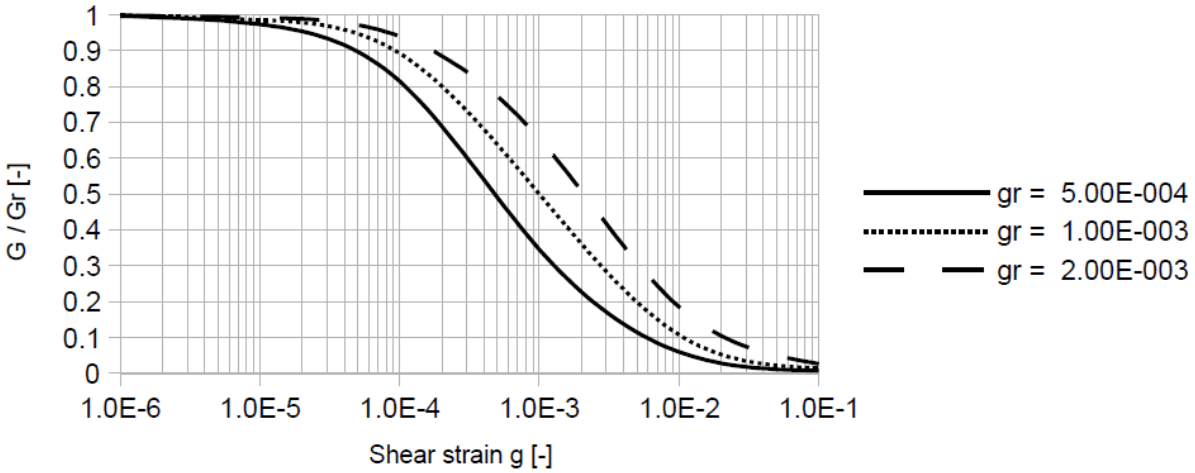


Figure 2: Shear modulus reduction curves after Stokoe et al. (2004) for different reference strains.

As an additional potential improvement to the SDM approach, a small strain stiffness function following Stokoe et al. (2004) was introduced degrading the shear stiffness with shear strain – with a significant impact on the near field displacements. The results of the calculations are compared to the ones elaborated with the standard procedure and with a previous parametric study, which also took into account effects of excavation shape accuracy and parameter variability.

References:

Aydan, Ö. et al. (1993): The squeezing potential of rock around tunnels: theory and prediction. Rock Mechanics and Rock Engineering. 2. pp. l37–163.
Becker et al. (2015): Synoptic structural geological analysis of the MB & FE tunnel excavation in the Mont Terri URL: Influences of pre-existing fractures on tunnel stability and EDZ characteristics. To be published @ CC2015.
Bock, H. (2008): RA Experiment: Updated Review of the Rock Mechanics Properties of the Opalinus Clay of the Mont Terri URL based on Laboratory and Field Testing. Technical Report. 2008-04.
Corkum, A.G. & Martin, C.D. (2007): Modelling a mine-by test at the Mont Terri rock laboratory, Switzerland. International Journal of Rock Mechanics & Mining Sciences. 44. pp. 846 - 859.
Jahns, E. (2010): RA-Experiment: Opalinus Clay Rock Characterisation. Technical Note. 2008-55.
Müller, H.R. et al. (2015): The Full-Scale Experiment – Implementation of a multiple heater experiment at the Mont Terri URL. To be published @ CC2015.
Popp, T. et al. (2008): Influence of bedding planes to EDZ-evolution and the coupled HM properties of Opalinus Clay. Physics and Chemistry of the Earth. 33. pp. 374 – 387.
Polster, M. (2010): Interpretive Modeling Results for Mine-by Test. MB Modeling Meeting. Unpublished presentation. DBE Technology.
Stokoe, K.H. et al. (2004): Development of a new family of normalized modulus reduction and material damping curves. International Workshop on Uncertainties in Nonlinear Soil Properties and their Impact on Modeling Dynamic Soil Response. UC Berkley. Ca. USA.

Insights into the response of a gallery sealing over the entire life of a deep repository

D.F. Ruiz[1], J. Vaunat[1*], A. Gens[1], M. Manica[1], and A. Pasteau[2]

1. Department of Geotechnical Engineering and Geosciences, Universitat Politècnica de Catalunya, E-08034 Barcelona, Spain (daniel.felipe.ruiz@upc.edu, jean vaunat@upc.edu).
2. Andra, agence nationale pour la gestion des déchets radioactifs, F. 92290 Châtenay-Malabry, France

(*) Corresponding author

The construction of a repository will involve the sinking of a number of access shafts, the excavation of a network of horizontal access drifts and the drilling of vertical boreholes or excavation of additional horizontal drifts for waste emplacement. Prior to closure, it will be necessary to seal and backfill access tunnels and shafts so that they do not become preferential radionuclide migration pathways. The issues concerning seal behaviour are similar to those arising in the design of engineered barriers, with the important difference that no high temperatures are expected.

A tentative configuration of the seal system for the connecting galleries, ramps and shaft consists of a central core built with swelling bentonite placed between two support concrete plugs. The plugs are in contact with the filling of the gallery, made with recompacted crushed argillaceous host rock (Figure 1). The performance of these systems relies on the reach of low permeability values in the bentonite and surrounding rock (particularly in the Excavation Damaged Zone) and low transmissivity values along possible discontinuities (contacts and eventual gaps).

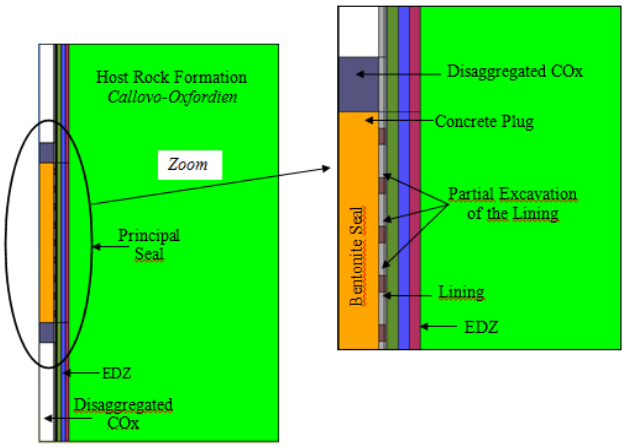


Figure 1. Geometry and materials includes in the basic 2D axisymmetric modelling

The paper describes the hydro-mechanical evolution of a sealing by the means of a fully coupled Hydro-Mechanical modelling of the configuration of the sealing system at the main horizontal gallery of a deep repository. The stress equilibrium and water mass continuity are solved simultaneously. The vapour flow and air flow are not taken into account. As a consequence, no diffusive fluxes exist. A two-dimensional and axisymmetric geometry around the axis of the gallery is considered and its features are as follows:

- Concrete in the support plugs and the lining is modelled by linear elasticity as a first approximation.
- Argillaceous Host Formation and EDZ are modelled by a visco-elastoplastic stress-strain relationship based on linear elasticity and Mohr-Coulomb yield criterion
- The response of the bentonite core and crushed argillaceous rock is computed by the modified version of the Barcelona Basic Model (BBM) (Alonso et al., 1990) with a dependency of the elastic parameters on the mean stress and suction. This model allows obtaining a gradual increment of swelling pressure in the hydration process.
- Concerning hydraulic phenomena, the retention curve, the variation of the intrinsic permeability with porosity and the variation of the relative hydraulic conductivity with degree of saturation are required.

- The contacts between the concrete support plugs and the lining are modelled with the joint elements implemented in finite element code (Zandarin 2010).

The computational domain has a width of 60 m and a length of 100.5 m. The diameter of the gallery is 9 m and the lining is composed of a 0.7 m thick support. The stages of the modelling includes the excavation of the gallery, the installation of the lining six month later, 100 years of operational phase, the sealing system installation and finally the hydration process generated by the host rock until that the initial water pressure (4.85 MPa) is recovered. The anisotropic initial stress state of the host rock was taken into account. The numerical results indicate that the full saturation and hydraulic initial conditions are reached at 1200 and 3000 years respectively (Figure 2). The modelling of contacts gives a realistic mechanical behaviour the system. The longitudinal effective stress decreases near to the concrete plugs due to their axial displacement. However, the radial component of the swelling pressure is constant along the bentonite core compressing the EDZ (Figure3). The evolution of stress around the gallery and additional load on the lining over the long time is obtained through the viscoplastic mechanism considered in the argillaceous host rocks.

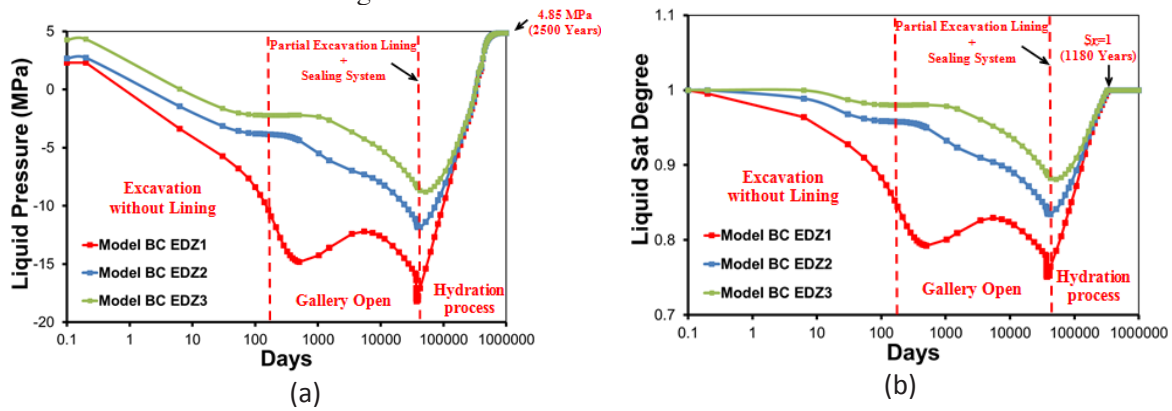


Figure 2: a) Time evolution of the liquid pressure at EDZ ; b) Time evolution the liquid saturation degree at EDZ

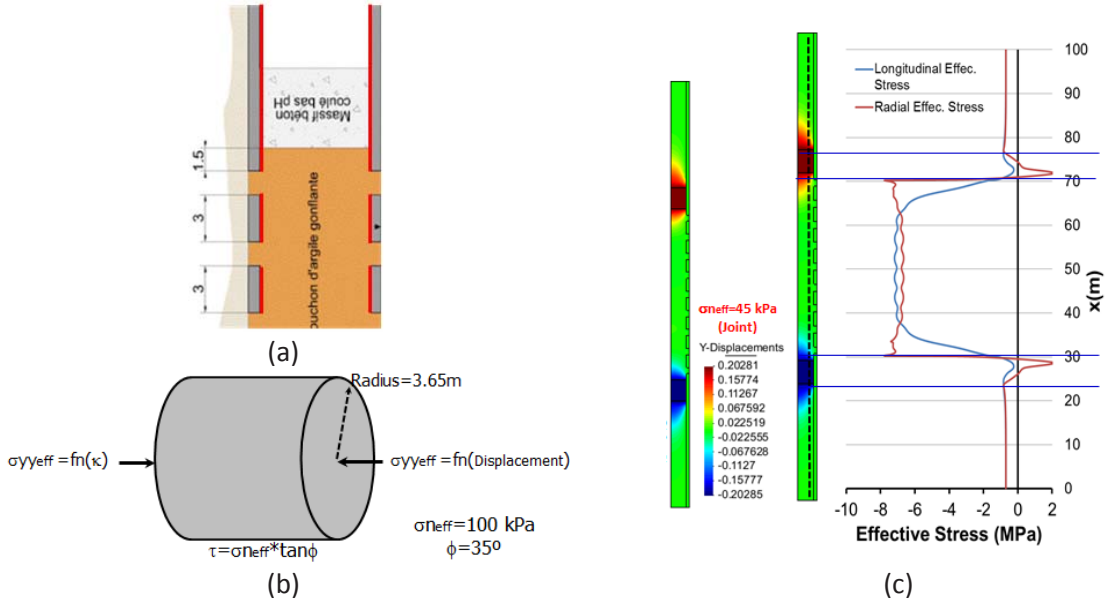


Figure 3: a) Location of joint elements; b) Forces at the concrete plug; b) Longitudinal and radial effective stress along the sealing system

References:

- Alonso, E.E. Gens, A. Josa, A. (1990). A constitutive model for partially saturated soils. Géotechnique 40, No. 3. 405-430
- Zandarin, M.T. (2010). "Thermo-Hydro-Mechanical analysis of joints - A theoretical and experimental study". PhD Thesis. Universitat Politécnica de Catalunya (UPC).

Numerical modelling of drifts excavated in stiff clays

M.A. Mánica[1], A. Gens[1*], J. Vaunat[1], D.F. Ruiz[1], D. Seyedi[2], G. Armand[3]

1. Department of Geotechnical Engineering and Geosciences, Universitat Politècnica de Catalunya, E-08034 Barcelona, Spain (miguel.angel.manica@estudiant.upc.edu, antonio.gens@upc.edu).
2. Andra, R&D Division, 92298 Chatenay-Malabery, France.
3. Andra, R&D Division, Meuse/Haute-Marne Underground Research Laboratory, 55290 Bure, France.

(*) Corresponding author

Stiff clay formations have shown great potential as possible geological host medium for radioactive waste. These materials have low permeability, significant retardation properties and they often exhibit a certain capacity of hydraulic self-sealing of fractures. In this context, the French national radioactive waste management agency (Andra) started in 2000 the construction of an underground research laboratory at Bure, in the Callovo-Oxfordian clay stone formation, to demonstrate the feasibility of this materials to host a radioactive waste repository (Andra, 2005). Several horizontal drifts have been excavated and monitored to characterize their short and long term behaviour, in conjunction with a comprehensive laboratory testing programme.

From the *in situ* measurements of the drifts, it is shown that the damage induced in the rock mass by the excavation process is one of the key issues affecting its short and long term behaviour. Damage is associated with the appearance of extensional and shear fracture networks, and its configuration is controlled by different factors as the initial stress state, local heterogeneities, material anisotropy and excavation geometry, among others. In the case of drifts orientated parallel to the minor horizontal stress, a larger extension of the damaged zone is observed in the vertical direction, together with larger vertical convergences. The latter seems to be mainly governed by the anisotropic stress state, since the damaged zone configuration can be numerically reproduced with a simple elasto-plastic model, without taking into account the anisotropy of the material properties. On the other hand, for drifts orientated parallel to the major horizontal stress, a nearly isotropic stress state is attained in the plane perpendicular to the drifts, which produces an damaged zone with a larger extension in the horizontal direction and with larger horizontal convergences. In this case, numerical results tend to show a nearly symmetric damaged zone, with similar convergences in the vertical and horizontal directions. This suggests a stronger influence of the anisotropy in the material properties.

From laboratory testing of small scale specimens, the short and long term behaviour of the clay stone have been characterized. In triaxial compression, important nonlinearities are identified prior peak strength, with a yield limit near to the 50% of the maximum deviatoric stress. The samples show a semi-brittle behaviour for the *in situ* stress range (i.e., about 12 MPa), with a significant strength loss in the softening branch of the stress-strain curve. Also a dependency of the stiffness with the confining pressure is possible in the elastic part of the response. In creep tests, increasing strain rates are observed for higher deviatoric stresses. For a given deviatoric stress, strain rates decrease with time in an exponential manner.

Based in the above-mentioned observations, an elasto-plastic constitutive model was developed to adequately reproduce the behaviour of the excavated drifts in the Callovo-Oxfordian clay stone. The model is an extension of an existing elasto-plastic formulation, in the framework of the computer program CODE_BRIGHT. The main model features are listed below:

- Cross-anisotropy form of the Hooke's law for the elastic part of the response.
- Linear dependency of the Young modulus with the confining pressure.
- The Mohr-Coulomb criterion for the yield and failure limits and its anisotropic extension.
- Non Associate flow rule.
- Nonlinear strain hardening/softening.

- Modified form of the Lemaitre law for visco-plastic strains.
- Exponential dependency of the intrinsic permeability with the damage variable.

The developed model was employed to simulate the laboratory tests, in order to verify its capabilities, and to calibrate the model parameters. Figure 1 shows the obtained results of triaxial compression and creep test, together with the laboratory data.

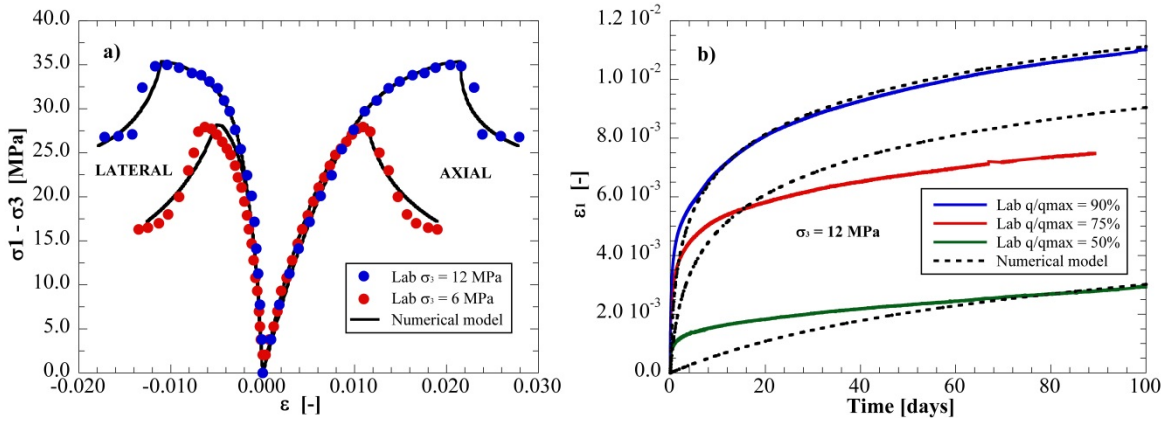


Figure 1. Simulation of (a) triaxial tests and (b) creep tests using the proposed model: comparison with the laboratory data.

Later, the model and the calibrated parameters were applied to the numerical simulations of the drifts. Figure 2 shows contour plots of the plastic multiplier obtained for drifts parallel to the minor and major horizontal stresses. In this model, the plastic multiplier is considered as the damage variable and therefore, the distribution of this variable is related with the configuration of the damaged zone. It can be observed that the model is able to reproduce qualitatively the observed configuration for both kinds of drifts, by taking into account the material anisotropy.

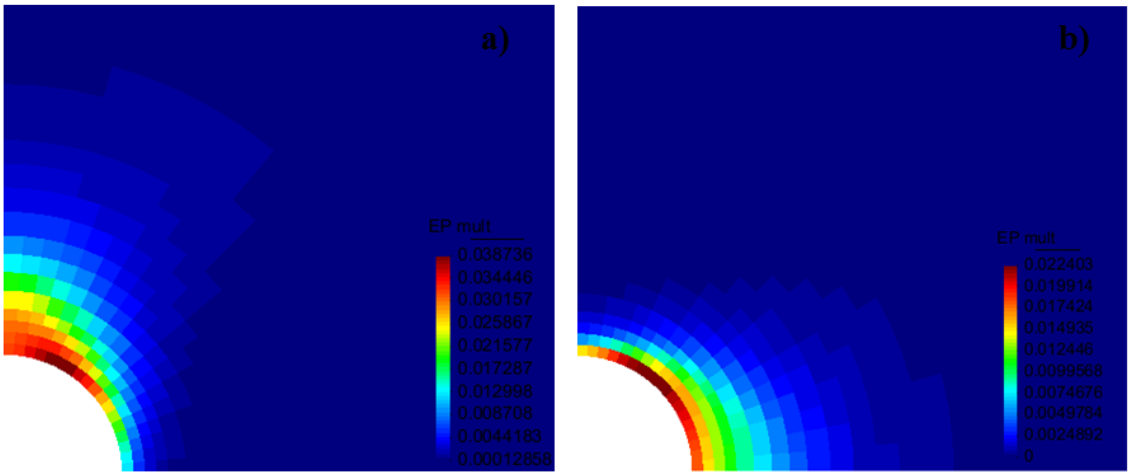


Figure 2. Configuration of the damaged zone obtained from the numerical simulations for drifts orientated parallel to the (a) minor and (b) major horizontal stresses.

References:

- ANDRA (2005). Dossier 2005 Argile. Evaluation de la faisabilité du stockage géologique en formation argileuse profonde. Rapport de synthèse. France: ANDRA; Juin 2005, (www.andra.fr).

Tunnel excavation in a claystone at 500 m deep: Road header under shield with segment emplacement experiment

Author(s)
Zghondi Jad
Carraretto Sébastien
Noiret Aurélien
Armand Gilles

Andra, Laboratoire Souterrain de Meuse/Haute-Marne, RD960, 55290 Bure, France

In 2005 Andra demonstrate the feasibility of a geological nuclear waste disposal in the Callovo Oxfordian claystone (COX). The research performed at the Meuse Haute Underground research laboratory through deep boreholes or from the drift and shaft were a significant contribution on the characterization of COX properties (Delay et al 2007)

The ongoing research program (started in 2006) is more dedicated to technologies improvement and demonstration issue of the different disposal systems, even if characterization studies are still ongoing. One of the main issues of this program is the development of construction methods and optimization of the structures of the disposal facility to improve the design. An important program was launch to study the impact of different excavation and support techniques. Parallel drifts far enough away from each other have been and are planned to be constructed to study the excavation induced fractured network for long term safety consideration, the hydromechanical behaviour of the Cox claystone and interaction in between the rock mass and the support.

Tunnel boring machines (TBM) are worldwide used in different type of rock and demonstrated their efficiency in many underground works. In the CIGEO repository, TBM could be an efficient construction technics due to length of the drifts. A full face TBM could not be easily used in the URL due to the small size of the shaft and the low capacity (in size and load) of the freight elevator. In spite of these conditions, a road header under shield was tested in 2013 with segments emplacement technique in a drift called GRD. Figure 1 shows the TBM.

The lining is composed of reinforced concrete segments of 45 cm thick. This method needs injection of backfill material in between the rock wall. Two type of filling mortar were injected: a classical mortar and a compressible mortar with polystyrene balls. The comparison among the two sections will help to understand of the interface behaviour and its role in the loading of the support. The main purpose of this drift is to follow the stress/strain evolution (at short and long term) in the lining. The drift is 80 meters long and is oriented along the major horizontal stress. The excavation took place without major difficulties and the pace (5 rings a week) provided was held. During manufacturing of concrete segments total pressure cells and vibrating wire extensometers have been casted in the concrete. Deformation could be followed during the drying of the concrete before delivery of the segment on site. Four rings of instrumented segments have been installed in the GRD drift (two per type of grouting material). One control segment is not in a ring but has been settle in the drift to try to correct measured deformation from thermal and drying effects.

When the ring in between the segment and the rock mass is fully filled of grounting material, meaning around 15 m behind the excavation front face, segment started to be loaded. The strain evolution differed from the location in the ring and at the inner or outer face of the segment. The strain field observe in the ring underline an anisotropic loading with a major load in the horizontal direction which is coherent with larger horizontal convergence (compared to vertical ones) already observed in drifts along this orientation (Armand et al 2014).



Figure 1- View of the TBM used: (a) road header, (b) segments emplacement



Figure 2- View of the GRD drift

Reference:

Carraretto S., Noiret A., Zghondi J. & Armand G., 2014, Excavation with a Tunnel Boring Machine at the Meuse/Haute-Marne Underground Research Laboratory, Aftes Conference, Lyon, 13-15 October

Delay, J., Vinsot, A., Krieguer, J.-M., Rebours, H. & Armand, G. (2007). Making of the underground scientific experimental programme at the Meuse/Haute-Marne underground research laboratory, northeastern France. Physics and Chemistry of the Earth, 32 (1/7): 2–18.

G. Armand, A. Noiret, J. Zghondi, D.M. Seyedi,2013, Short- and long-term behaviors of drifts in the Callovo-Oxfordian claystone at the Meuse/Haute-Marne Underground Research Laboratory, Journal of Rock Mechanics and Geotechnical Engineering 5,pp 221–230

A model benchmark exercise for numerical analysis of the Callovo-Oxfordian claystone hydromechanical response to excavation operations

D. Seyedi[1], G. Armand[2], P. Bésuelle[3], F. Collin[4], S. Cuvilliez[5], J. Desrues[3], G. Duveau[6], A.P. van den Eijnden[1][3], R. Fernandes[5], A. Gens[7], R. Giot[8], D. Hoxa[9], J.B. Kazmierczak[10], B. Pardoen[4], J.C. Robinet[11], J.F. Shao[6], M. Souley[10], T.H. Tran[11], J. Vaunat[7]

[1] Andra, R&D Division, 92298 Chatenay-Malabery, France (darius.seyedi@andra.fr)
[2] Andra, R&D Division, Meuse/Haute-Marne Underground Research Laboratory, 55290 Bure, France
[3] Univ. Grenoble Alpes – 3SR, F-38000 Grenoble, France
[4] ArGEnCo – Université de Liège, B-4000 Liège, Belgium
[5] EDF R&D, Clamart, France
[6] LML, UMR8107 CNRS, Cité Scientifique, 59655, Villeneuve d'Ascq, Fr
[7] Dep. of Geotechnical Eng. and Geosciences, Universitat Politècnica de Catalunya, E-08034 Barcelona, Spain
[8] GéoRessouces, University of Lorraine, Nancy, France
[9] PRISME, University of Orléans, Orléans, France
[10] INERIS, Nancy, France
[11] EuroGéoMat Consulting, Orléans, France

The Callovo-Oxfordian claystone (COx) is considered as a potential geological formation to host an industrial radioactive waste repository in France, thanks to its favorable characteristics for radioactive waste containment, as it has a very low hydraulic conductivity, small molecular diffusion and significant retention capacity for radionuclide. A deep understanding of the thermo-hydro-mechanical (THM) behavior of the COx is a key issue for design of different repository structures and the safety calculations of the project.

Several constitutive models have been developed/used in the framework of the R&D and simulation programs of Andra. These models aim to reproduce the THM behavior of COx under different repository situations and for different structures. A model benchmark exercise has been launched since 2012 to provide an overall view of the developed models, their basic assumptions, their mathematical descriptions, variables and parameters, and to investigate the consequences of these basic assumptions on the calculations results regarding to the experimental observations.

Three main constitutive model families are considered; namely, visco-elasto-plastic models, damage-mechanics based and computational homogenized (CHM) ones. Nine teams using different models have been participated to this benchmark exercise.

In this view, two series of test cases are defined. In the first one, simple stress paths close to those that can be produced during the excavation of the underground facilities are proposed. It consists of the stress paths, which differs to usually considered paths in the construction of the rock mechanics constitutive models (e.g., triaxial compression path). Extension/compression paths with or without remaining a constant mean stress and torsional stress cases are proposed in this step. The stress paths are applied to material points to avoid any structural effects on the response obtained by different models. The main goal of this first part was to investigate the effects of the basic assumptions on the simulated response.

The second series of the test cases consists in the numerical modeling of underground drifts oriented in two principal directions. Indeed, the most of the excavated drifts at the main level (i.e., -490 m) of the Meuse/Haute-Marne underground research laboratory follow directions of the *in situ* principal horizontal stresses. The major *in situ* principal stress is horizontal and the vertical and the smallest horizontal stresses are close to each other (Wileveau et al. 2007). Several drifts are instrumented to

measure drift convergence and the displacement induced in the rock mass around drifts due to the excavation (Armand et al., 2013) and to investigate the extent of the induced fractures around the drifts (Armand et al., 2014).

The main goal of this second series is to obtain a deep knowledge of the models and the obtained results considering realistic structures. A two-dimensional geometry is considered (Figure 1). The main tested features are:

- The effect of the support system on the rock behavior through considering two different support systems, i.e., a soft system and a completely rigid one
- The effect of hydromechanical coupling and creep behavior
- The role of stress and material anisotropies

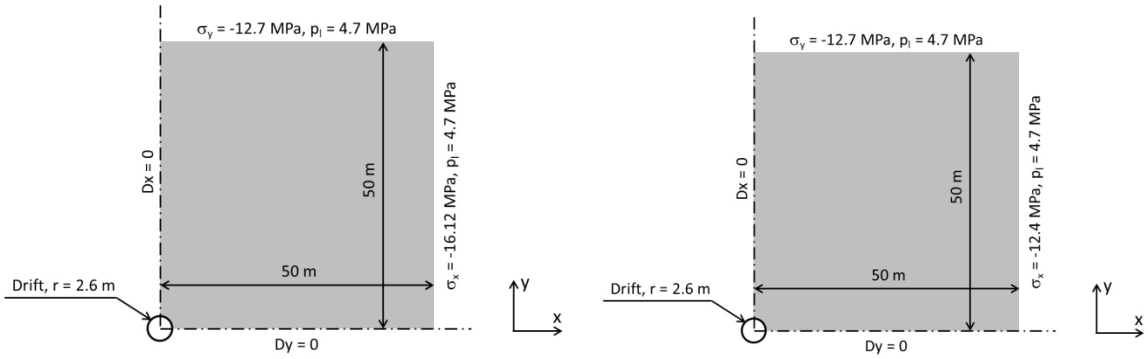


Figure 1: Considered geometry and applied boundary conditions: for a drift parallel to σ_h (left), for a drift parallel to σ_H (right).

Finally, the obtained results are compared especially in terms of the convergence measurements, the extent of the fractured/damaged zones and the pore pressure field evolution in the rock mass between models and with in situ observations.

References:

Armand, G., Noiret, A., Zghondi, J., & Seyedi, D.M. (2013). Short- and long-term behaviors of drifts in the Callovo-Oxfordian claystone at the Meuse/Haute-Marne Underground Research Laboratory. *J. Rock Mech. Geotech. Eng.*, 5, 221–230.

Armand, G., Leveau, F., Nussbaum, C., de La Vaissiere, R., Noiret, A., Jaeggi, D., Landrein, P. & Righini, C. (2014). Geometry and properties of the excavation induced fractures at the Meuse/Haute-Marne URL drifts. *Rock Mech. Rock Eng.*, 47, 21-41. doi:10.1007/s00603-012-0339-6.

Wileveau Y., Cornet F.H., Desroches J., Blumling P. (2007). Complete in situ stress determination in an argillite sedimentary formation. *Phys. Chem. Earth*, 32, 866–878.

Numerical analysis of the stiffness evolution of damaged zone around the drifts under mechanical loading/unloading cycles

M.N. Vu[(1,*)], **D. Seyedi**[(1)], **A. Noiret**[(2)], **R. de La Vaissière**[(2)], **G. Armand**[(2)]

[1]Andra R&D, 92298 Chatenay-Malabery, France
[2]Andra R&D, Meuse/Haute-Marne Underground Research Laboratory, 55290 Bure, France
[*]minh-ngoc.vu@andra.fr

The French National Radioactive Waste Management Agency (Andra) has been creating the Meuse Haute-Marne Underground Research Laboratory (M/H-M URL), which allows performing an in-situ multidisciplinary research program to demonstrate the feasibility of geological repository, in the Callovo-Oxfordian claystone. An important theme of this program is to study the behavior of the excavated damaged zone around the drifts induced by digging.

Within this framework, an experiment, called CDZ (compression of damaged zone) is dedicated to studying of the hydromechanical behavior of the fractured zone around drifts. As a part of this experiment, the effects of mechanical loading/unloading on the behavior of fractured are investigated. The experimental concept consists of a single end plate, with a cross section of 1 m^2, which is used to load the damaged zone at the drift wall. The 3D structure of the fracture network has been fully investigated. Extensometric measurements are performed to obtain displacements induced in the rock mass under the plate. Figure 1 present a 3D general view of this experiment.

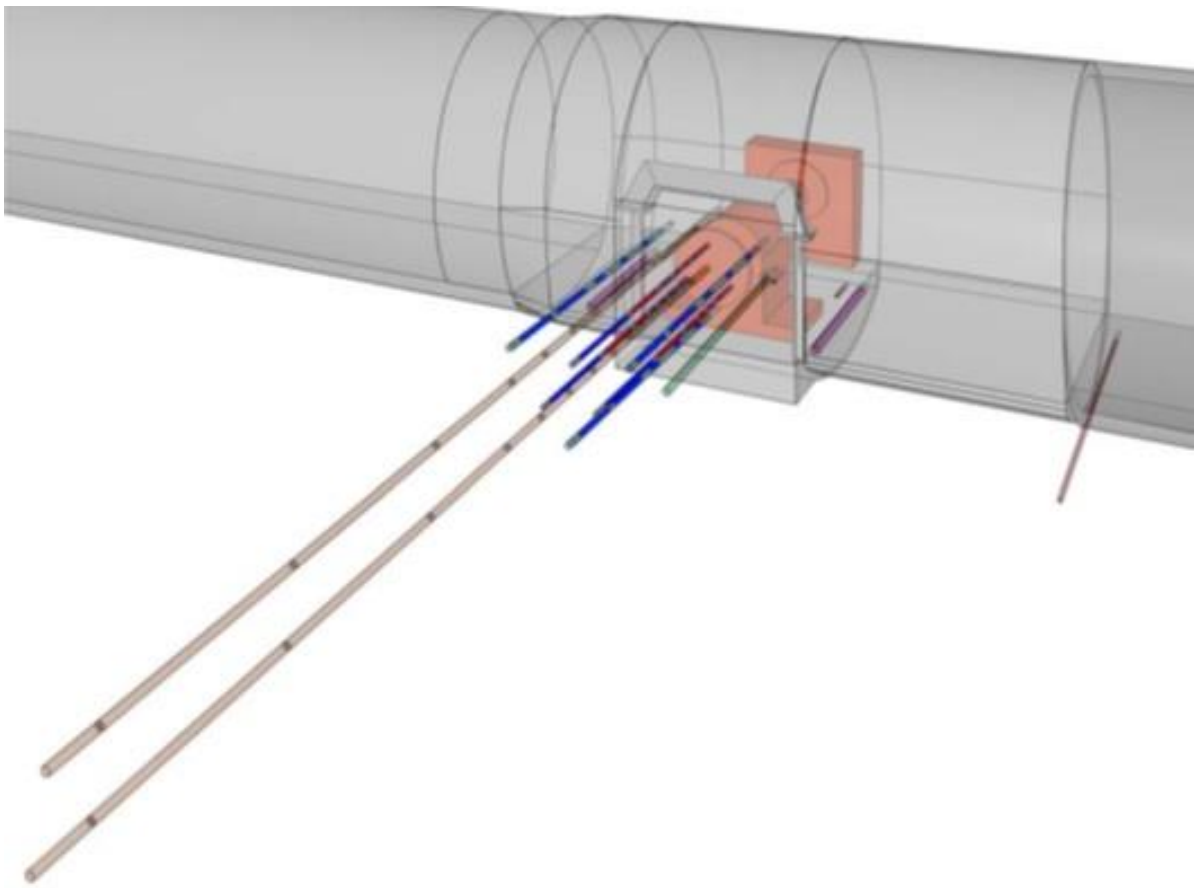


Figure 1: General view of CDZ experiment.

This study proposes a numerical scheme in order to back calculate stiffness of the fractured zone and its evolution undermechanical loading/unloading cycle. For this purpose, the damaged zone is split into three zones based on the observed fracture density around the drifts and the measured displacements (Figure 2). The stiffness of each zone is determined by using an inverse analysis scheme, which consists in a coupling between a finite element code and Non-Linear Least-Square Minimization algorithm. The stiffness values obtained by this work present a weak value within 0.5 m from the wall and then following an increase versus the depth towards the intact rock. The result shows also an increase of modulus of each zone as function of applied load and this increase is more pronounced for loading/unloading cycle compared to loading level (Figure 3).

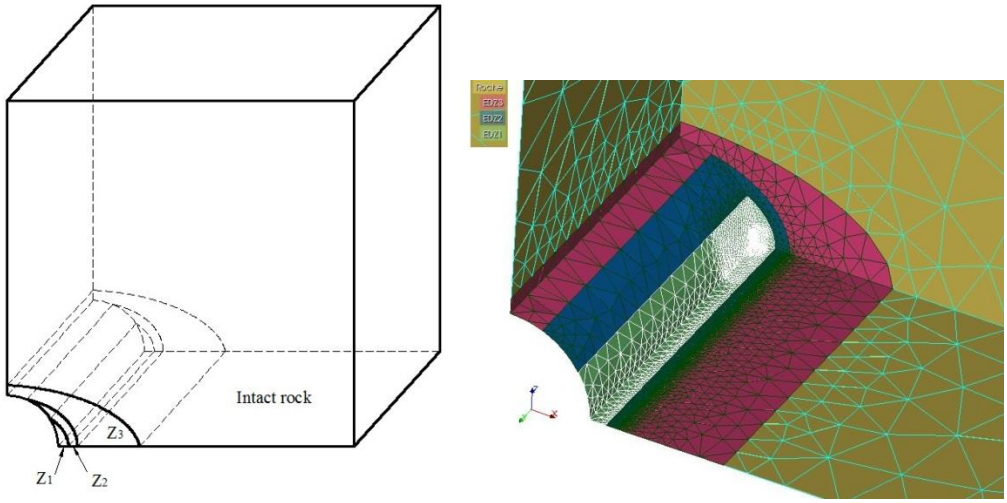


Figure 2: Geometric model and mesh using for finite element simulation.

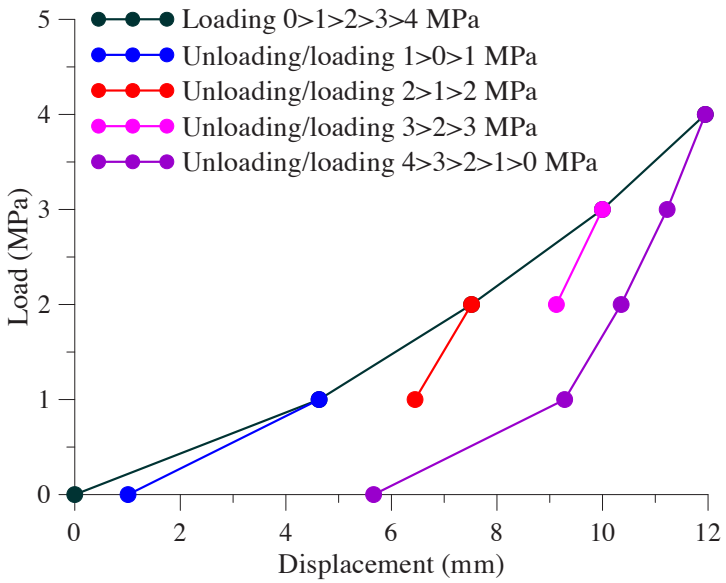


Figure 3: Displacement evolution versus loading levels and unloading/loading cycle.

Analytical solution of the post-closure behaviour of an underground cavity excavated in a viscoplastic rock mass

***T.A. Bui*[1*], H. Wong[1], F. Deleruyelle[2], D.K. Tran[3]**

[1]Université de Lyon, ENTPE/LGCB and LTDS UMR CNRS 5513, Vaulx-en-Velin, France
[2]IRSN, PRP-DGE, SEDRAN, BERIS, Fontenay-aux-Roses, France
[3]Université de Lyon and ECL, LTDS UMR CNRS 5513, Écully, France

[*]Corresponding author

In the context of radioactive waste disposal in a deep geological formation, a typical cylindrical gallery is supposed to go through a life cycle which can be simplified by a four-stage sequence (Figure1): (1) excavation; (2) cavity excavated but not yet supported; (3) cavity with lining during operation time; (4) post-closure after backfilling.

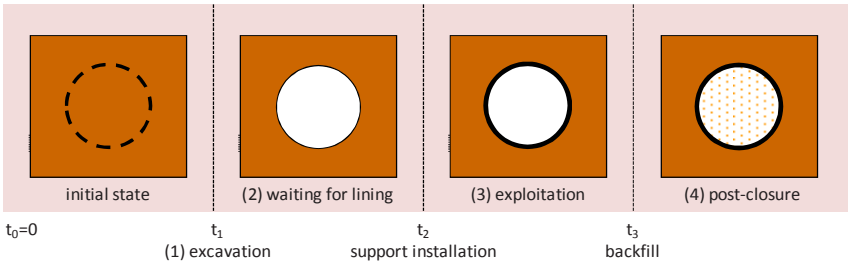


Figure 1. Simplified life cycle of a cavity

The behaviour of the gallery, especially during the post-closure phase, has to be accounted for in the safety assessment of the disposal. In a previous work, this issue has been analytically addressed by modelling different behaviours for the host rock, such as poro-elastic or poro-viscoelastic medium [1-3]. Recently, the influence of host rock creep has been accounted for in [4-5], in which the solution for the three first stages has been presented.

Following these results, this study presents a quasi-analytical solution for the last stage of the life cycle of the gallery excavated in a viscoplastic medium. The irreversible time-dependent rock behaviour is described by means of a simplified version of the Norton-Hoff's creep law. The Laplace Transform is used to transform partial differential equations to ordinary ones, which are subsequently solved in the transformed space. Numerical inversion by Stehfest's algorithm is then used to invert these complex analytic functions. Numerical applications and parametric studies are carried out to show the consistency and the utility of the solution, as well as the influence of some key parameters, such as rock viscosity and hydraulic conductivity.

The achieved results are devoted to constitute a useful benchmark for the validity of complex numerical simulations, or analyse *in situ* data (e.g. mine-by tests…). The utility of this quasi-analytical tool is not limited to the analysis and design of classic underground facilities, where mechanical stability and deformation are the main concerns, but can also contribute to assess whether creep-induced convergence in the host rock could induce divergent water flow, enhancing the transport of radioactive elements, which is of concern for the nuclear waste disposal design.

Keywords: Radioactive waste disposal, Hydro-mechanical coupling, Rock creep, Analytical solution, Laplace transform

References

[1] H. Wong, M. Morvan, F. Deleruyelle, C.J. Leo, 2008. Analytical study of mine closure behaviour in a poro-visco-elastic medium. *Int. J. Num. & Analy. Meth. Geomech*, n° 32, pp. 1737-1761.

[2] H. Wong, M. Morvan, F. Deleruyelle, C.J. Leo, 2008. Analytical study of mine closure behaviour in a poro-elastic medium. *Computers & Geotechnics*, Vol. 35, n° 5, pp. 645-654.
[3] N. Dufour, H. Wong, F. Deleruyelle, C.J. Leo, 2012. Hydromechanical Post-Closure Behaviour of a Deep Tunnel Taking into Account a Simplified Life Cycle. *International Journal of Geomechanics* Vol. 12, No. 5, pp. 1-11
[4] F. Deleruyelle, T.A. Bui, H. Wong, N. Dufour, 2014. Analytical modelling of a deep tunnel in a viscoplastic rock mass accounting for a simplified life cycle and extension to a particular case of porous media. *Geological Society, Special Publication series «Clays in Natural and Engineered Barriers for Radioactive Waste Confinement»*, Vol. 400, http://dx.doi.org/10.1144/SP400.14
[5] T.A. Bui, H. Wong, F. Deleruyelle, N. Dufour, C.J. Leo, 2014. Analytical modeling of a deep tunnel inside a poro-viscoplastic rock mass accounting for different stages of its life cycle. Computers and Geotechnics, Vol. 58, pp. 88-100, http://dx.doi.org/10.1016/j.compgeo.2013.11.004

Anisotropic convergence analysis in drifts of the Meuse/haute-Marne underground research laboratory

***Lina-María Guayacán-Carrillo*[1,2], Jean Sulem[2], Darius Seyedi[1], Siavash Ghabezloo[2], Aurelien Noiret[3], Gilles Armand[3]**

[1] Andra R&D, 92298 Chatenay-Malabry, France
[2] Université Paris-Est, Laboratoire Navier/CERMES, Ecole des Ponts ParisTech, IFSTTAR, CNRS, 77455 Marne la Vallée, France
[3] Andra R&D, Meuse/Haute-Marne Underground Research Laboratory, 55290 Bure, France

In 2000, the French National Radioactive Waste Management Agency (Andra) began the construction of the Meuse/haute-Marne Underground Research Laboratory (M/HM URL) with the main goal of demonstrating the feasibility of geological repository in Callovo-Oxfordian claystone. A network of experimental drifts have been excavated following the directions of the horizontal principal stresses and with variations on: excavation method, structure geometry and supports system. Note that, at the main level of M/HM URL (i.e., -490 m) the vertical stress is very close to the minor principal stress (≈ 12MPa), while the major principal horizontal stress is about 16MPa. Therefore, the initial stress state is quasi isotropic (in the plane of their section) for the drifts following the direction of the major horizontal principal stress, whereas the initial stress state for the drifts in the perpendicular direction presents a ratio σ_H/σ_v of about 1.3.

In each drift different sections have been instrumented to monitor the convergence evolution and the rock deformation. Continuous monitoring of the excavated zone around the drifts revealed the development of a fractured zone (extensional and shear fractures) induced by the excavation. The fracture distribution depends on both the drift orientation and the in-situ stress field (Armand et al., 2014) and has an important influence on the drifts deformation. Accordingly, convergence measurements showed an anisotropic closure, which is more pronounced for drifts excavated along the minor horizontal principal stress with a ratio of vertical to horizontal convergence of 4.0 while for drifts excavated along the major horizontal principal stress the ratio is about 0.5. (Armand et al., 2013).

The convergence measurements recorded for one representative drift (with a diameter of about 5m) in each direction is analyzed. The anisotropic character of the deformation is taken into account by assuming that the drifts section evolves following an elliptical shape. The characteristics of the deformed elliptical section are evaluated following the methodology proposed by Vu et al. (2013). Then, the evolution in time of the two axes of the ellipse is interpreted as the convergence of the drift wall along the two principal directions of deformation, and fitted using the semi-empirical law proposed by Sulem et al. (1987). This method allows to distinguish two effects: the face advance effect and the time-dependent behavior of the ground (Fig. 1).

The results for two drift orientations show very close values for the parameters describing the time-dependent properties of the ground, the distance of influence of the face, and the extension of the decompressed zone around the drift. Finally, the model is applied for a drift excavated in a small scale e.g. micro-tunnel of a diameter of about 0.7m. It is shown that the model can be applied for reliable predictions of the convergence evolution in the long term. Such a method can thus be used for the design of various types of support and the evaluation of its performance in the long term.

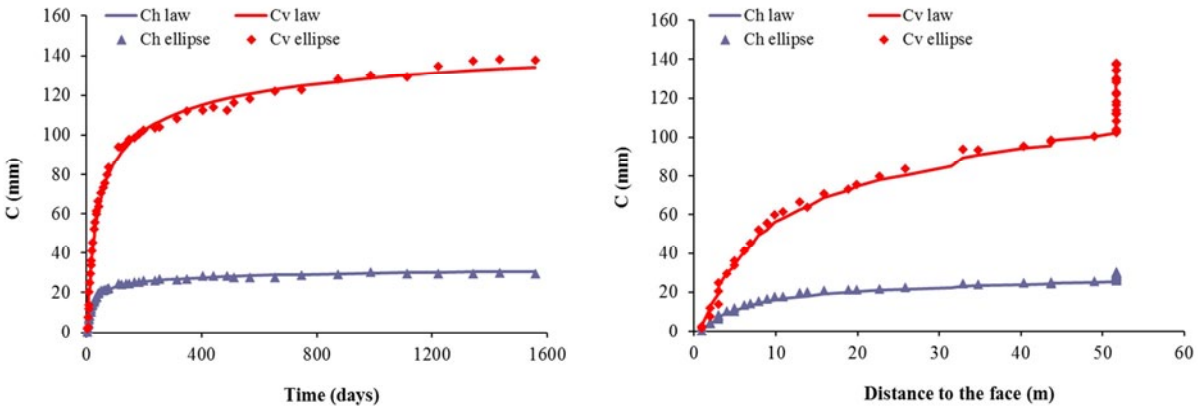


Fig.1. Convergence evolution in a drift section – Parallel to σ_h. (C_h = horizontal convergence; C_v = vertical convergence

References

Armand, G., Noiret, A., Zghondi, J., & Seyedi D.M. (2013). Short- and long-term behaviors of drifts in the Callovo-Oxfordian claystone at the Meuse/Haute-Marne Underground Research Laboratory. *J. Rock Mech. Geotech. Eng.*, *5*, 221–230.

Armand, G., Leveau, F., Nussbaum, C., de La Vaissiere, R., Noiret, A., Jaeggi, D., Landrein, P., & Righini, C. (2014). Geometry and properties of the excavation induced fractures at the Meuse/Haute-Marne URL drifts. *Rock Mech. Rock Eng.*, *47*, 21-41. doi:10.1007/s00603-012-0339-6.

Sulem, J., Panet, M., & Guenot, A. (1987). Closure analysis in deep tunnels. *Int J Rock Mech Min Sci Geomech Abstr* 24(3): 145–154. doi:10.1016/0148-9062(87)90522-5.

Vu, T.M., Sulem, J., Subrin, D., Monin, N., & Lascols, J. (2013). Anisotropic Closure in Squeezing Rocks: The Example of Saint-Martin-la-Porte Access Gallery. *Rock Mech Rock Eng* 46: 231–246. doi:10.1007/s00603-012-0320-4.

An anisotropic elastoplastic model for Boom Clay

Linh-Quyen DAO [1], *Jean-Michel PEREIRA* [1], Yu-Jun CUI [1], Anh-Minh TANG [1], Xiang-Ling LI [2], Xavier SILLEN [3]

[1] Université Paris-Est, Laboratoire Navier (UMR 8205), 6-8, av. Blaise Pascal, Cité Descartes, 77455 Marne-la-Vallée, France.
[2] European Underground Research Infrastructure for Disposal of nuclear waste in Clay Environment (EURIDICE, Mol, Belgium)
[3] Belgian Agency for Radioactive Waste and Enriched Fissile Materials (ONDRAF/NIRAS, Brussels, Belgium)

Several studies showed that Boom Clay at Mol (Belgium), a potential host rock for geological disposal of radioactive waste, is an anisotropic material due to the sedimentation process. However, there are few works on its anisotropic elastoplastic modelling. In this study, the isotropic model ACC-2 developed for Boom Clay by Hong (2013) was extended to an anisotropic model. This model was calibrated and then validated through several simulations of oedometer and drained triaxial tests on Boom Clay samples oriented differently: perpendicular, inclined at 45° and parallel to the bedding plane ($\theta = 0°, 45°, 90°$, respectively).

ANISOTROPIC MODEL

In the proposed model, the transverse isotropy is accounted for in both elastic and plastic parts. In the elastic part, the linear relationship of Hooke's law (equation (1)) is adopted with five independent elastic parameters: E_h, E_v, ν_{hh}, ν_{vh}, G_{hv} (equation (2)).

$$\{\varepsilon^e\} = [D_e]^{-1}\{\sigma^e\} \tag{1}$$

where $[D_e]$ is the elastic stiffness matrix. When $\theta = 0°$ (θ is the angle between the vector normal to the bedding plane and the direction of the major principal stress), the stress-strain relationship is given as follows:

$$\begin{pmatrix} \varepsilon_v^e \\ \varepsilon_h^e \\ \varepsilon_h^e \\ \gamma_{hv}^e \\ \gamma_{hv}^e \\ \gamma_{hh}^e \end{pmatrix} = \begin{pmatrix} 1/E_v & -\nu_{hv}/E_h & -\nu_{hv}/E_h & 0 & 0 & 0 \\ -\nu_{vh}/E_v & 1/E_h & -\nu_{hh}/E_h & 0 & 0 & 0 \\ -\nu_{vh}/E_v & -\nu_{hh}/E_h & 1/E_h & 0 & 0 & 0 \\ 0 & 0 & 0 & 1/G_{hv} & 0 & 0 \\ 0 & 0 & 0 & 0 & 1/G_{hv} & 0 \\ 0 & 0 & 0 & 0 & 0 & 1/G_{hh} \end{pmatrix} \begin{pmatrix} \sigma_v^e \\ \sigma_h^e \\ \sigma_h^e \\ \sigma_{hv}^e \\ \sigma_{hv}^e \\ \sigma_{hh}^e \end{pmatrix} \tag{2}$$

Note that in equation (2), $G_{hh} = E_h/[2(1+\nu_{hh})]$. When $\theta \neq 0°$, in order to define $[D_e]$ by the coordinate corresponding to the principal stress directions, this matrix needs to be rotated.

Regarding the plastic part, Boehler's theory (Boehler and Sawczuk, 1977) is used for formulating a transformed tensor $\hat{\sigma}_{ij}$ (equation (3)) that accounts for the structural anisotropy:

$$\left[\hat{\sigma}_{ij}\right] = (\alpha+\gamma-2\beta)(\hat{M}_{mn}\sigma_{mn})\hat{M}_{ij} + \gamma\sigma_{ij} + (\beta-\gamma)(\hat{M}_{ik}\sigma_{kj} + \sigma_{ik}\hat{M}_{kj}) \tag{3}$$

where M_{ij} is the structure tensor (defined as a tensor product of unit vector normal to the bedding plane); When $\theta \neq 0°$, M_{ij} has to be rotated and becomes $\hat{M}_{ij}$; α, β, γ are three anisotropic plastic parameters.

The anisotropic plastic strain is given by replacing the stress tensor with the transformed tensor in both yield and plastic potential functions of the two-surface plastic model ACC-2 for Boom Clay. In ACC-2, an Inner yield surface was added with a simple exponential law for a coefficient "r" that rescales the conventional yield pressure (equation (4)) in order to take into account the plastic behaviour inside the conventional Yield surface and thus simulate a smooth elastoplastic transition. When $r = 1$, the Inner yield surface coincides with the conventional Yield surface. The contribution of plastic shear strain during the evolution of the Inner yield surface is controlled through parameter A_d (equation (5)).

$$dr = \frac{(1+e_0)}{\lambda-\kappa} s(1-r)d\varepsilon_d^p \tag{4}$$

$$d\varepsilon_d^p = d\varepsilon_v^p + A_d d\varepsilon_s^p \tag{5}$$

where ε_v^p is the volumetric plastic strain, ε_v^p is the shear plastic strain and s is a material constant controlling the evolution of hardening modulus with strain.

After considering the transformed tensor due to inherent anisotropy, the new equations of hardening law (for the conventional Yield surface), and Inner yield surface f_I are:

$$d\hat{\bar{p}}'_c = \frac{1+e_0}{\lambda-\kappa}\hat{\bar{p}}'_c\, d\varepsilon_v^p \tag{6}$$

$$f_I = \hat{q}^2 + \frac{M_f^{\,2}}{1-k_f}\left(\frac{\hat{p}'}{r\hat{\bar{p}}'_c}\right)\left(r\hat{\bar{p}}'_c\right)^2 - \frac{M_f^{\,2}\hat{p}'^2}{1-k_f} \tag{7}$$

The new expression of plastic potential takes the same form as the yield surfaces. The modified plastic potential associated with the Inner yield surface reads:

$$g_I = \hat{q}^2 + \frac{M_g^{\,2}}{1-k_g}\left(\frac{\hat{p}'}{r\hat{\bar{p}}'_c}\right)\left(r\hat{\bar{p}}'_c\right)^2 - \frac{M_g^{\,2}\hat{p}'^2}{1-k_g} \tag{8}$$

SIMULATION OF OEDOMETER AND TRIAXIAL TESTS

The proposed anisotropic model ACC-2A has 18 parameters: 10 parameters of isotropic model ACC-2 (λ, κ, p'_{c0}, k_f , M_f, k_g, M_g, s, r_0, A_d), 5 parameters of anisotropic elasticity and 3 parameters of anisotropic plasticity. In this work, the 10 parameters of the original isotropic model were taken from the work of Hong (2013): $\lambda = 0.18$, $\kappa = 0.02$, $p'_{c0} = 6$ MPa, $k_f = 0.7$, $M_f = 0.67$, $k_g = 0.9$, $M_g = 0.67$, $s = 0.8$, $r_0 = 0.3$, $A_d = 0.1$. Based on the results from triaxial tests on Boom Clay specimens sampled in the directions perpendicular and parallel to the bedding plane, five elastic parameters were adopted $E_h = 500$ MPa, $E_v = 280$ MPa, $\nu_{hh} = 0.3$, $\nu_{vh} = 0.3$, $G_{hv} = 130$ MPa. Three plastic parameters ($\alpha = 0.85$, $\beta = 1.0$, $\gamma = 0.8$) were determined after calibrating this anisotropic model using the experimental results from a triaxial test under K_0 condition.

Figure 1 and 2 show the comparison between experimental data (oedometer and drained triaxial tests) and simulated results. The predictions by ACC-2A agree relatively well with the experimental results. Compared to MCC and ACC-2, ACC-2A provides better predictions for natural Boom Clay samples oriented differently under drained conditions.

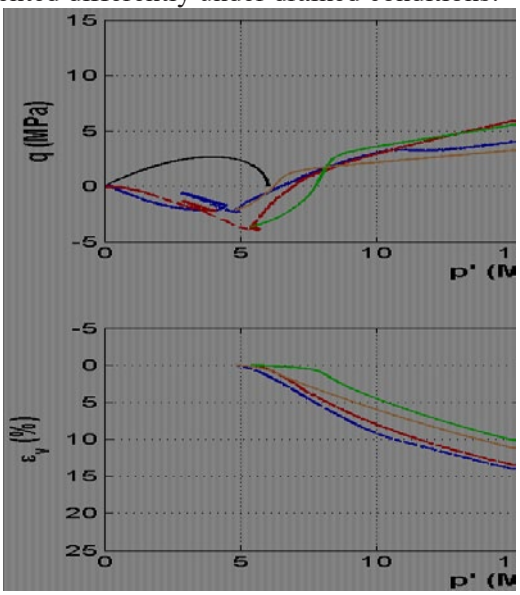


Figure 1: Simulation of oedometer tests.

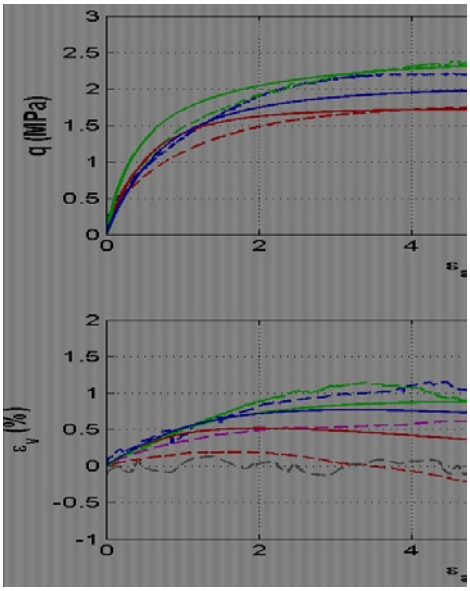


Figure 2: Simulation of triaxial tests.

REFERENCES

Boehler, J.P., Sawczuk, A., 1977. On yielding of oriented solids. Acta Mech. 27, 185–206.

Hong, P., 2013. Development and explicit integration of a thermo-mechanical model for saturated clays. PhD thesis. Université Paris-Est.

Le, T.T., 2008. Comportement thermo-hydro-mécanique de l'argile de Boom. PhD thesis. Ecole Nationale des Ponts et Chaussées.

Impact of excavation damage on the thermo-hydro-mechanical properties of natural Boom Clay

Linh-Quyen DAO [1], *Yu-Jun CUI* [1], Anh-Minh TANG [1], Jean-Michel PEREIRA [1], Pierre DELAGE, Xiang-Ling LI [2], Xavier SILLEN [3]

[1] Université Paris-Est, Laboratoire Navier (UMR 8205), 6-8, av. Blaise Pascal, Cité Descartes, 77455 Marne-la-Vallée, France.
[2] European Underground Research Infrastructure for Disposal of nuclear waste in Clay Environment (EURIDICE, Mol, Belgium)
[3] Belgian Agency for Radioactive Waste and Enriched Fissile Materials (ONDRAF/NIRAS, Brussels, Belgium)

Boom Clay has been considered as a potential host-rock for the geological disposal of heat-emitting radioactive waste in Belgium. In this context, it is important to well understand its thermo-hydro-mechanical behaviour around the disposal galleries. In this study, the effect of excavation damage on the thermo-hydro-mechanical properties of natural Boom Clay around the Connecting gallery (excavated in 2002) in the underground Research Laboratory HADES (High-Activity Disposal Experimental Site) was investigated. Several samples taken from a horizontal borehole drilled in July 2012 at Mol (borehole R66-67W) were tested. The thermal conductivity in three different orientations (perpendicular $\lambda_{\perp}$, parallel $\lambda_{//}$, and 45° λ_{45} to the bedding plane) was measured using the needle probe method. To further investigate the anisotropy behaviour, bender element tests were carried out under unconfined conditions to determine the small-strain shear modulus also in three different orientations. The investigations on the microstructure of several samples taken at different distances r from the axis of gallery by MIP and SEM methods were also carried out. An empirical damage model was then proposed based on the microstructural results. The relevance of this model was shown by comparisons between the predicted and experimental results in terms of thermal conductivity, small strain shear modulus and hydraulic conductivity.

EXPERIMENTAL RESULTS

The results of thermal conductivity measurements ($\lambda_{//}$, λ_{45}, $\lambda_{\perp}$) show a cross-anisotropy of natural Boom Clay with $\lambda_{//} > \lambda_{45} > \lambda_{\perp}$ (Figure 1). The measured values of $\lambda_{//}$ vary between 1.34 - 1.61 W/(m.K) whereas those of $\lambda_{\perp}$ vary between 0.82 – 1.06 W/(m.K). The value of $\lambda_{//}$ for $r > 4$ m is close to that found by Chen et al. (2011) by back analysis of an in situ test at the metre scale (1.65 W/(m.K)). An impact of the excavation damage on the thermal property of samples near the gallery was detected through a decrease of λ (in three directions) in the zone $r < 4$ m.

In terms of small-strain shear modulus measurements, the variations of G_{hv}, G_{h45}, G_{hh} with the distance r from the axis of gallery for each sample are presented in Figure 1. It appears that G_{hh} displays a clear trend with distance r. Although the trend of G_{hv}, G_{h45} with the distance r is less clear, the anisotropic behaviour of Boom Clay is still found: $G_{hh} > G_{hv}$. Moreover, the evolution of small-strain modulus with the distance r was found to be similar to that of thermal conductivity: the values in the zone near the gallery ($r < 4$ m) are lower than those at $r > 4$m. It is also found that the obtained values of G_{hv} and G_{hh} in the far field are in good agreement with those obtained by Lima (2011) under unconfined condition (G_{hh} =1483 MPa and G_{vh} = 1135 MPa).

From these experimental data, an extent of the excavation damaged zone (EDZ) of 4 m from the connecting gallery axis could be inferred. This is further supported by the results of MIP and SEM tests which showed several macro-pores of diameter > 5 µm identified in the Boom Clay samples near the connecting gallery.

APPROXIMATION OF THERMAL-HYDRO-MECHANICAL PROPERTIES

The identified macro-pores were related to the effect of excavation damage, and a damage variable was thus defined, allowing a damage model to be developed. A semi-empirical expression can be then proposed to estimate the effect of excavation damage on the properties of Boom Clay:

$$X = X_0(1 - b\exp(-a\frac{e}{e_M})) \quad (1)$$

where X_0 is the property of Boom Clay in the far field (intact zone), X is the property of Boom Clay in the near field (EDZ), e is the global void ratio, In this empirical equation, e_M voids ratio of macro-pores larger than 5 µm, $a > 0$ is a parameter depending on the material and b is a parameter depending on the property considered ($b > 0$ if the property of material decreases with the increase of macro-pores; $b < 0$ if the property of material increases with the increase of macro-pores).

The evolutions of small-strain modulus and thermal conductivity of Boom Clay were approximated with $a = 0.05$, $b = 0.5$. The field hydraulic conductivity (k) measurements of Boom Clay in 2004, 2005 (Yu et al., 2011) and 2012 (from the internal report of EURIDICE) were also used to verify this damage model with $a = 0.05$, $b = -0.5$. It is observed that the predicted results of k are closer to those of the measurements of 2012 as compared with the measurements of 2004 and 2005.The good agreement obtained between the model prediction and experimental data for the thermal conductivity, small-strain modulus (see Figure 1), and hydraulic conductivity shows that the damage variable defined based on the volume of macro-pores is relevant in predicting the effect of EDZ on the thermo-hydro-mechanical properties of natural Boom Clay.

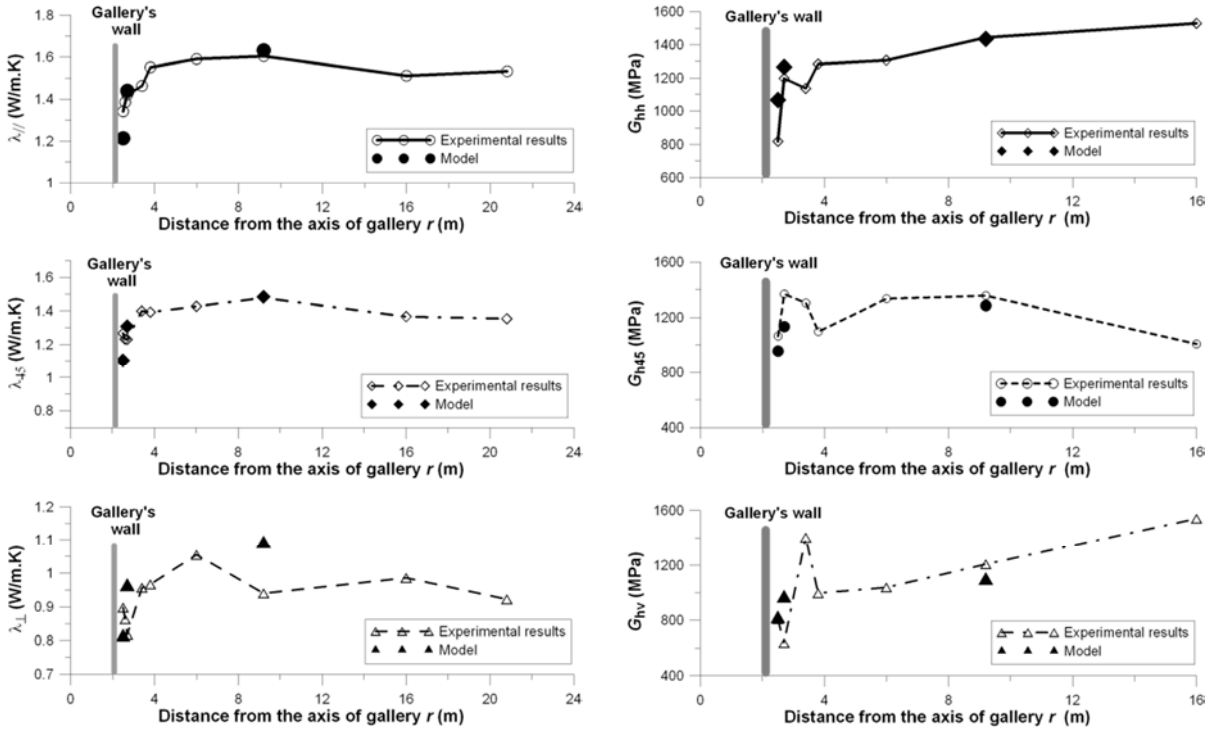


Figure 1: Comparisons between the experimental data (from thermal conductivity λ measurements and small-strain shear modulus G measurements) and simulated results using the damage model.

REFERENCES

Chen, G.J., Sillen, X., Verstricht, J., Li, X.L., 2011. ATLAS III in situ heating test in boom clay: Field data, observation and interpretation. Comput. Geotech. 38, 683–696.

Lima, A., 2011. Thermo-hydro-mechanical behaviour of two deep Belgian clay formations: Boom and Ypresian Clays. PhD thesis.Universitat Politècnica de Catalunya.

Yu, L., Gedeon, M., Wemaere, I., Marivoet, J., De Craen, M., 2011. Boom Clay hydraulic conductivity. A synthesis of 30 years of research. External report SCK-CEN, Mol (Belgium).

Temperature effect on the drained creep behavior of Boom clay

Z.Gong[1], *W.Z Chen*[1], Y.S Ma[1], H.D Yu[1], X.L Li[2], X. Sillen[3]

1. State Key laboratory of Geomechanics and Geotechnical Engineering, Institute of Rock and Soil Mechanics, Chinese Academy of Science, China
2. Euridice, SCK •CEN, Belgian Nuclear Research Centre, Mol 2400, Belgium
3. ONDRAF/NIRAS, 1210, Brussels, Belgium

Corresponding author email : wzchen@whrsm.ac.cn

Boom clay is a candidate host formation for nuclear waste disposal in Belgium. In the underground repositories, heat emitted from nuclear waste will induce coupled thermo-hydro- mechanical (THM) process in both near and far fileds for a long period of time. It is essential to better understand the temperature effect on the long-term hydro-mechanical behaviour of Boom clay in order to get a better assessment of its long term performance as a host formation.

The paper discusses the THM coupled creep behaviour of Boom clay with the focus on: (a). effect of temperature and time on creep rate; (b). volume change caused by temperature; (c). the reversibility of the creep behaviour of the Boom clay after cooling process.

Thermal-hydro-mechanical coupled triaxial creep tests have been conducted to understand the time-dependent behaviour of Boom clay. The test condition of these samples is listed in Table1. Specimens were trimmed to cylinders of 38 mm diameter and 76 mm in height and were first saturated under a confining pressure of 2.5MPa. The creep tests consider a cyclic temperature process which is similar with that expected in the real repository (40→60→80→60→40°C). Each creep phase lasted about one month.

The preliminary test results during the creep phase at different deviatoric stress levels and temperatures are presented in this paper. Fig.1 shows the creep curves, from which it can be observed that:

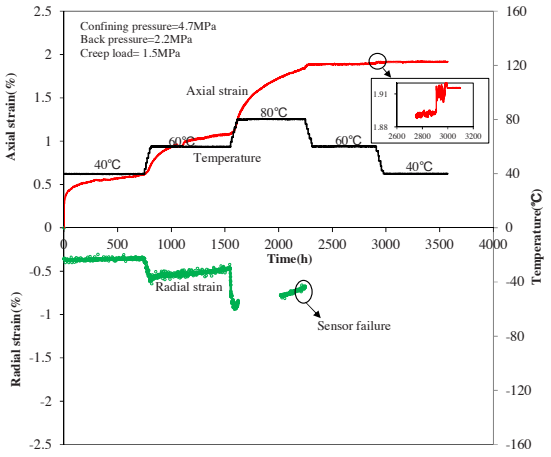
a) There was no significant phenomenon for creep behaviour when the deviatoric stress less than 1.0 MPa even when temperature reached up to 80°C. But the creep behaviour is remarkable under deviatoric stress 1.5MPa, except for the cooling process. It seems that there exists a threshold of deviatoric stress between 1~1.5MPa for creep behavior of Boom clay. Moreover, it seems that the creep rate depends also on the confining pressure (Fig. 2), a correlation between the creep rate and the confining pressure has been obtained from our laboratory tests.

b) Above the presumed deviatoric stress threshold, the creep rate (axial strain) increases with increasing of temperature. This confirms previous test results.

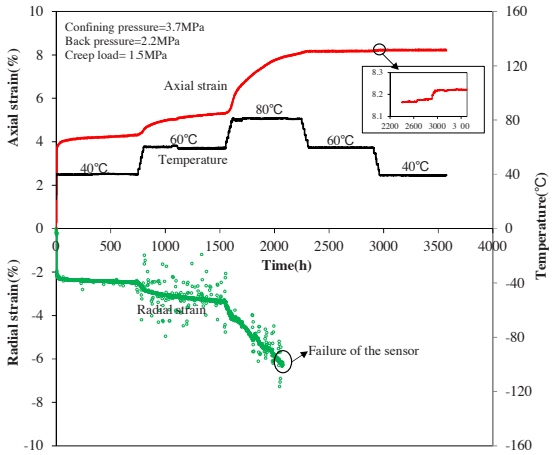
c) Under the stress paths applied in this study, cooling results in thermal compression (axial strain). No obvious creep appeared during the cooling process. More tests will be performed to further investigate this heating – cooling behaviour under different stress paths (different confining pressures and different deviatoric levels). This phenomenon suggests that the strength of Boom clay will not be further decreased due to the creep after cooling, as the creep tends to reduce the strength of a material.

Table.1 Testing condition

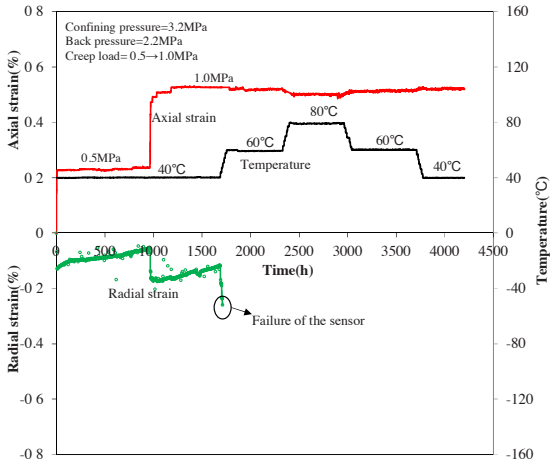
Specimen	Confining pressure (MPa)	Back pressure (MPa)	Creep stress level (MPa)
L-THM3.2-1	3.2	2.2	0.5~1
L-THM3.7-1	3.7	2.2	1.5
L-THM4.7-1	4.7	2.2	1.5



(a) L- THM-4.7-1

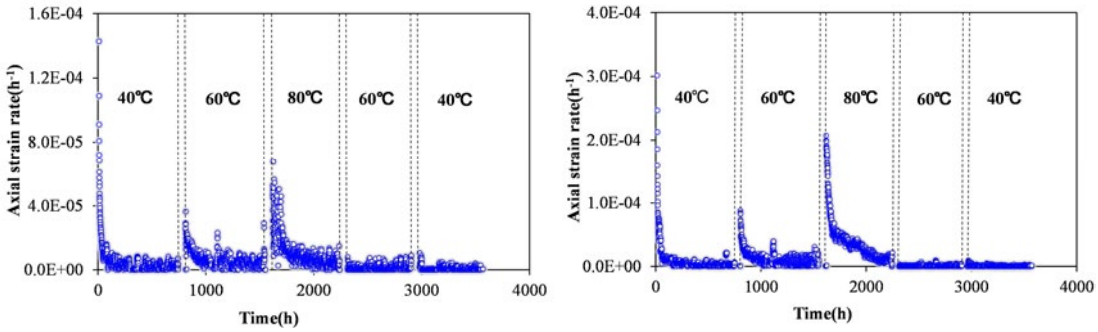


(b) L- THM-3.7-1



(c) L- THM-3.2-1

Fig.1 Creep behaviour of Boom clay during a cyclic temperature process



(a) L- THM-4.7-1 (b) L- THM-3.7-1

Fig.2 Axial creep rate of Boom clay with time and temperature.

Acknowledgements

Financial support of EURIDICE (Belgium) through the collaboration agreements with IRSM on ‘ Long-term Hydro-Mechanical behaviour of the Boom Clay’ (2008-2011) and on ‘Long term Thermo-hydro-mechanical behavior of the Boom clay’(2011-2015) and National Science Foundation for Distinguished Young Scholars(51225902) is greatly acknowledged.

Deformation mechanisms of Boom clay during long term consolidation test

H.D Yu[1], *W.Z Chen[1]*, D.S Yang[1], Z Gong[1], Y.S Ma[1], X.L Li[2], X. Sillen[3]

1.State Key laboratory of Geomechanics and Geotechnical Engineering, Institute of Rock and Soil Mechanics, Chinese Academy of Science, China
2. Euridice, SCK •CEN, Belgian Nuclear Research Centre, Mol 2400, Belgium
3. ONDRAF/NIRAS, 1210, Brussels, Belgium

Corresponding author email : wzchen@whrsm.ac.cn

The creep behavior of geomaterials is a crucial problem in geoenvironmental engineering. Especially the geomaterials surrounding nuclear radioactive waste disposal. For this reason, the long term mechanical behavior of the geomaterials must be studied with more attention. Within the context of the nuclear waste disposal at great depth in Belgium, particular attention has been paid to the long term mechanical behavior of Boom clay, one of the potential host formations Although the secondary consolidation behavior of soils has been widely investigated, there have been few long term consolidation tests performed on Boom clay, especially on the unloading path, which represents the situation of the soil in the vicinity of excavated galleries, and few studies on the microstructure variations under the long term loading. For this reason, the present work focuses on the creep behaviour of Boom clay under the mechanical loading and unloading from both macro- and micro- perspective. Several oedometer creep tests at controlled environmental temperatures were performed (lasting more than 1 year). The tests started with a standard oedometer tests, and then a long-term creep phase (2 month for each step), ended with an unloading phase (Fig. 1).

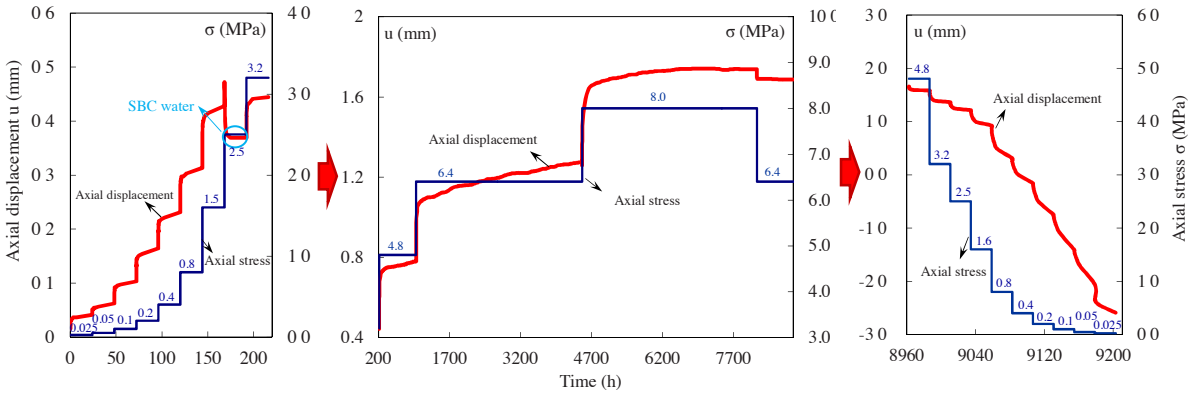


Fig.1 Oedometer creep test on sample TCP1

(Note: SBC water is the abbreviation for synthetic Boom clay water)

The test results confirm the high creep potential of Boom clay, and several interesting things are found at the same time.

a) Generally speaking, the creep behavior became more significant as the load increased. However, at load level (such as 8.0MPa), the creep rate was slightly weakened comparing to the load step(6.4MPa, 4.8MPa) as the increasing compression modulus due to the long-term load or the skeleton deformation due to the soil sliding or embedding.

b) The primary consolidation time for each loading step increased as the consolidation stress increased.

c) The creep rate (Fig. 2) was larger at the beginning of the tests and decreased a short time later. It tended to be stable on the order of approximately 10^{-6} ε/h for all the creep loading steps at last.

d) The rebound deformation of the Boom clay samples was not obvious as the action of the long term overconsolidated pressure.

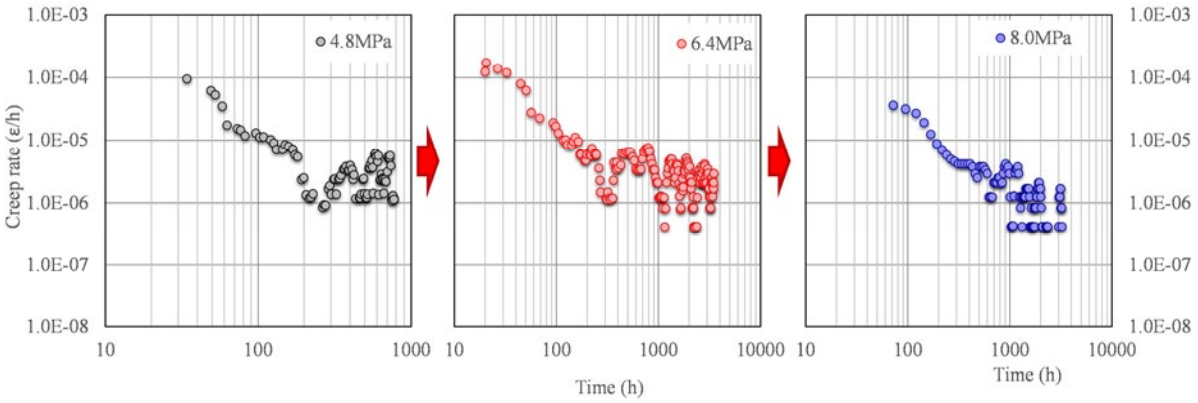
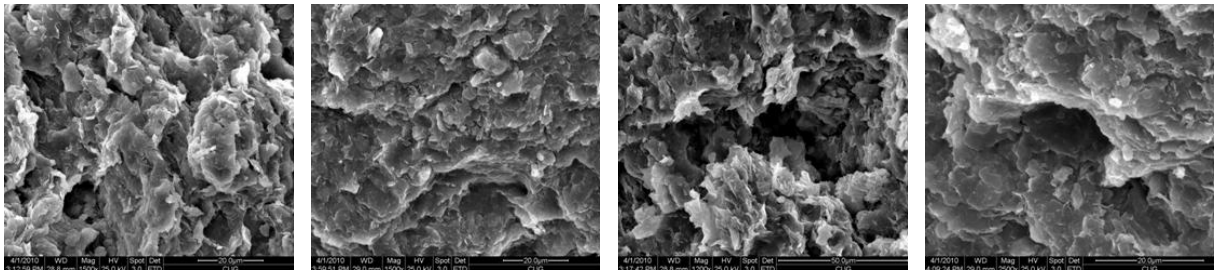


Fig.2 Axial creep rate variation for sample TCP1

e) The SEM tests show that the internal structure of Boom clay readjusted after suffering long-time axial load. The internal void diminished obviously with the rearrangement of clay particles.



(a) Before creep test (b) After creep test (c) Before creep test (d) After creep test

Fig.3 Micro structure variation of Boom clay before and after the oedometer creep test

Acknowledgements

Financial support of EURIDICE (Belgium) through the collaboration agreements with IRSM on ‘ Long-term Hydro-Mechanical behaviour of the Boom Clay’ (2008-2011) and on ‘Long term Thermo-hydro-mechanical behavior of the Boom clay’(2011-2015) and National Science Foundation for Distinguished Young Scholars(51225902) is greatly acknowledged.

Variation of the hydraulic conductivity of Boom clay under various thermal-hydro-mechanical conditions

Y.S Ma[1], *W.Z Chen[1]*, H.D Yu[1], D.S Yang[1], Z Gong[1], X.L Li[2]

1.State Key laboratory of Geomechanics and Geotechnical Engineering, Institute of Rock and Soil Mechanics, Chinese Academy of Science, China
2. Euridice, SCK •CEN, Belgian Nuclear Research Centre, Mol 2400, Belgium

Corresponding author email ： wzchen@whrsm.ac.cn

Boom clay is considered as a potential host formation for the deep geological disposal of high-level and heat emitting radioactive waste in Belgium. It will be subject to thermo-hydro-mechanical coupled perturbation after the installation of waste canisters, which in turn has effect on its permeability. To better understand this issue, fundamental data for intrinsic properties of Boom clay under different stresses and temperatures need to be well characterised. In this paper, an experimental study intended to identify (1) the anisotropy properties of permeability of Boom clay, (2) the effect of heating-cooling cycle and loading-unloading cycle on the hydraulic conductivity and intrinsic permeability of Boom clay, (3) the effect of the heating-cooling rate on the values of permeability is presented.

Constant head permeability tests were carried out in a temperature-controlled triaxial testing cell which was particularly designed for investigating the thermo-hydro-mechanical characteristics of Boom clay under various temperature, stress and pore water pressure conditions. In order to ensure a measurable flow in the dense plastic clay, smaller samples with standard diameter (38 mm) but reduced height (10 mm) were used. Taking into account the anisotropy of Boom clay, for each kind of test, two samples were trimmed manually with the axis parallel and perpendicular to the bedding, respectively. Samples resaturation has been done under in-situ effective stress before permeability test. The injection water is the synthetic Boom clay water (SBCW).

The test procedure, which is given below, involves eight stages: first of all, the samples were loaded isostatically to a confining pressure ($\sigma_1=\sigma_2=\sigma_3$=2.5 MPa). Then a heating-cooling cycle (23 (room temperature) →40→60→80→60→40→23 ℃) was applied. Afterwards, the samples were loaded from 2.5 MPa to 5.5 MPa, under which, another heating-cooling cycle same as previous one was applied. After that, samples were experienced three additional heating-cooling cycles (23→80→23 ℃) with different heating-cooling rates (1℃/h, 5℃/h, 20℃/h) . Finally, all samples were unloaded back to 2.5 MPa. At all steps of each stage of the test, permeability test was carried out.

The steady water flow characteristic through the Boom clay at different temperatures and confining pressures is presented in Fig. 1. The linear relationship between injected water flow and duration can be observed. And the inject water volume of the same duration increases with the increasing temperature. The intrinsic permeability was calculated considering the variation of water viscosity and density with temperature. The increase of hydraulic conductivity with temperature has been frequently considered resulting from the decrease of water viscosity and density with temperature. This increase was calculated for Boom clay with the permeability value at room temperature taking as a starting point.

The following results can be deduced from these experiments:

(1) The vertical (k_v) and horizontal (k_h) hydraulic conductivities are 1.73×10^{-12} m/s and 5.01×10^{-12} m/s, respectively, which are the same magnitude with the in situ measurements for hydraulic conductivity of Boom clay ($1.7–2.39\times10^{-12}$ m/s and $4.1–5.2\times10^{-12}$ m/s, respectively) (Yu et al. 2011).

(2) During heating-cooling cycle, there is a positive and reversible relationship between hydraulic conductivity and temperature. The hydraulic conductivity at 80℃ is about 2.4 times bigger than that of at room temperature (Fig. 2a). The increment of hydraulic conductivity with temperature is slightly lower than that predicted on the basis of water viscosity and density with temperature (Fig. 3). This confirms that the viscosity and density are the main driving factors on the variation of the hydraulic conductivity of Boom clay with temperature.
(3) The intrinsic permeability slightly decreases with the increasing temperature (Fig. 2b).
(4) During loading-unloading cycle, there is a negative and irreversible relationship between hydraulic conductivity and hydrostatic pressure (Fig. 4a). This will hold also for intrinsic permeability (Fig. 4b).
(5) The values of permeability basically unchanged with different heating/cooling rate (Fig. 5).

These experimental results provide additional information which will be useful for the assessment of the variation of hydraulic conductivity of Boom clay, one of the important repository performance assessment parameters, during the whole life of a repository: construction, heating and cooling phases.

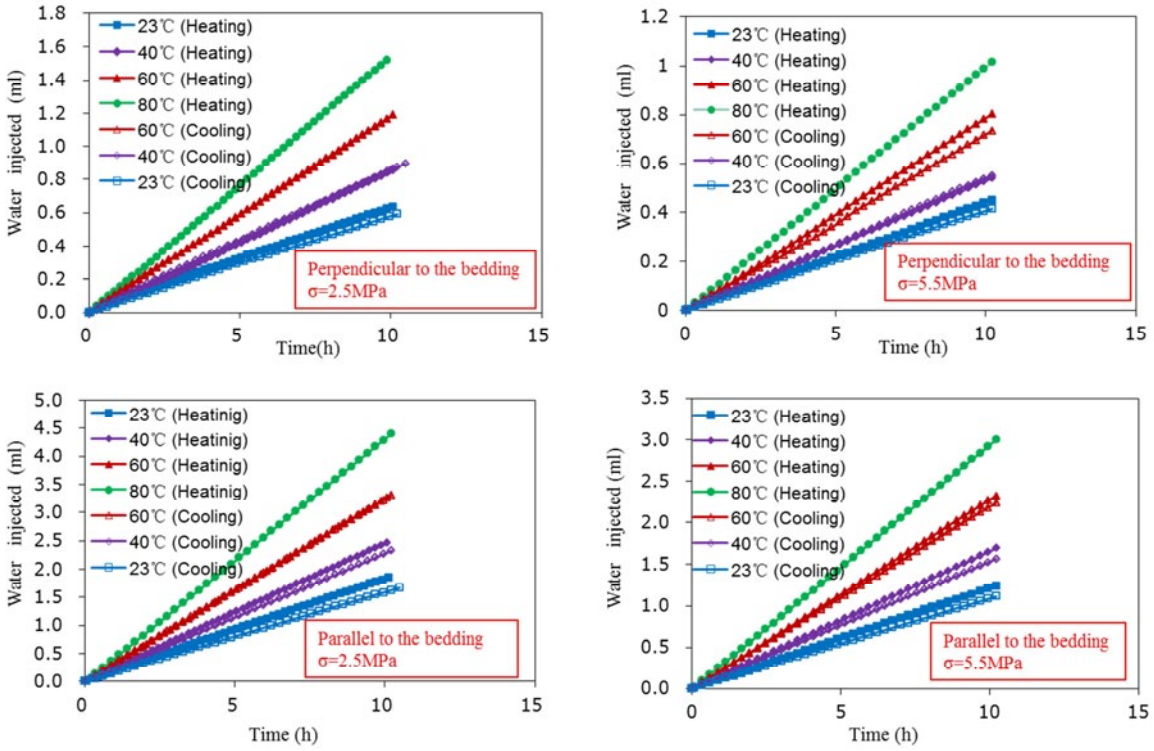
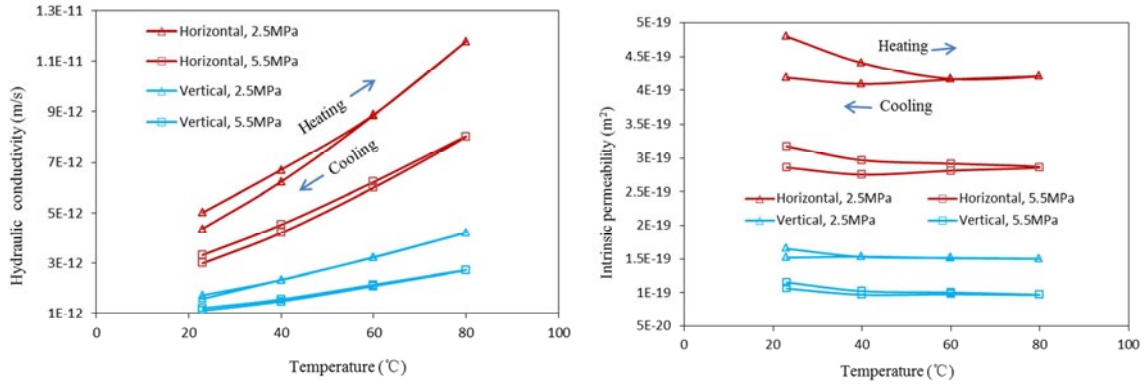
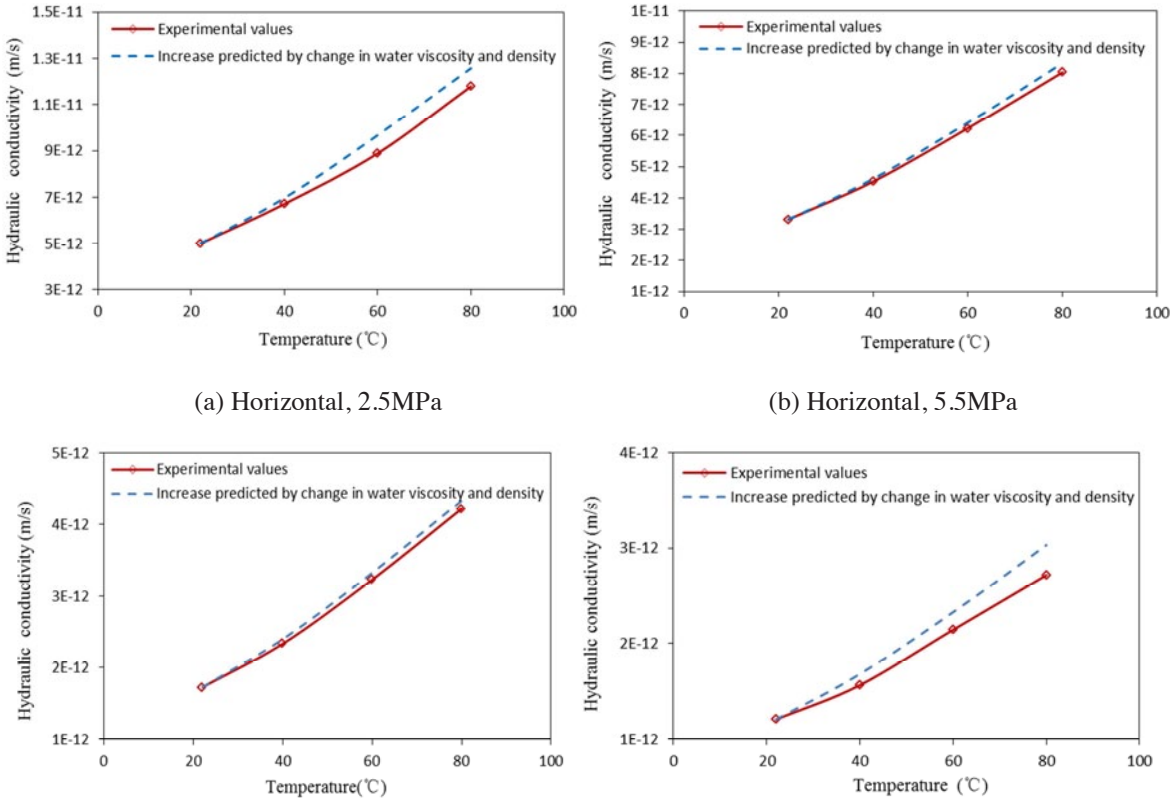


Fig.1 Injected water flow-time relationships of steady stage at different temperature and confining pressure



(a) Hydraulic conductivity (b) Intrinsic permeability

Fig.2 Variation of the hydraulic conductivity and intrinsic permeability during heating-cooling cycle



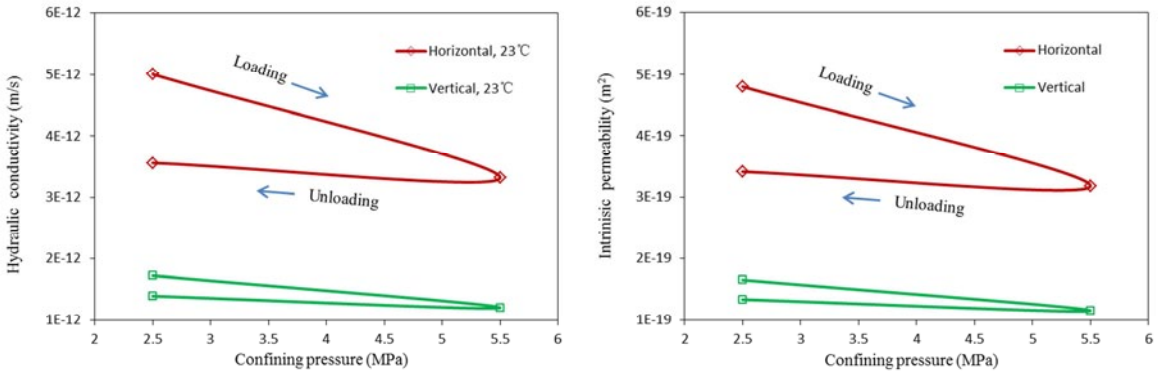
(a) Horizontal, 2.5MPa

(b) Horizontal, 5.5MPa

(c) Vertical, 2.5MPa

(d) Vertical, 5.5MPa

Fig.3 Comparison of hydraulic conductivity values determined experimentally and predicted on the basis of water viscosity and density change



(a) Hydraulic conductivity

(b) Intrinsic permeability

Fig.4 Variation of the hydraulic conductivity and intrinsic permeability at room temperature during loading-unloading cycle

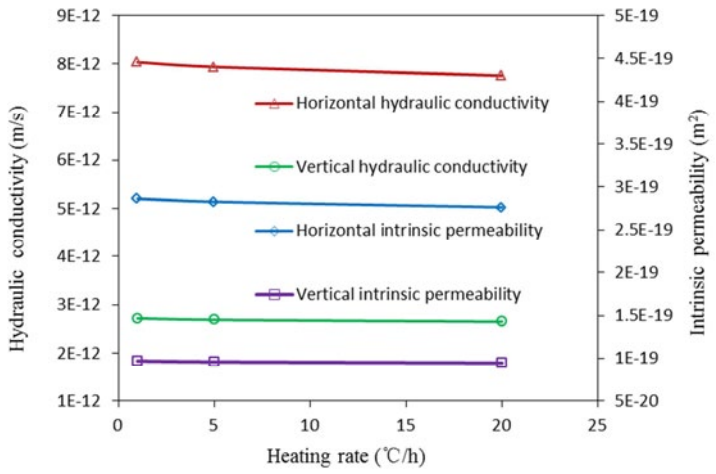


Fig.5 Variation of the hydraulic conductivity and intrinsic permeability at 80℃ with different heating rate

Reference:

Yu, L., Gedeon, M., Wemaere, I., Marivoet, J., De Craen, M., 2011. Boom Clay hydraulic conductivity. A synthesis of 30 years of research. External report SCK-CEN, Mol (Belgium).

Acknowledgements

Financial support of EURIDICE (Belgium) through the collaboration agreements with IRSM on ‘ Long-term Hydro-Mechanical behaviour of the Boom Clay’ (2008-2011) and on ‘Long term Thermo-hydro-mechanical behavior of the Boom clay’(2011-2015) and National Science Foundation for Distinguished Young Scholars(51225902) is greatly acknowledged.

X-Ray Computed Tomography Investigation of the Sandy Facies (Opalinus Clay, Mont Terri) Before and After Mechanical Testing

***Kaufhold, A.*[1], Gräsle, W.[1], Plischke, I.[1], Halisch, M.[2], Zacher, G.[3]**

[1]Federal Institute of Geosciences and Natural Recourses (BGR), Stilleweg 2, D-30655 Hannover,
e-mail: annette.kaufhold@bgr.de
[2] Leibniz Institute for Applied Geophysics (LIAG), Stilleweg 2; D-30655 Hannover
[3] GE Sensing & Inspection Technologies, Niels-Bohr-Str. 7, D-31515 Wunstorf

Introduction

In many countries, argillaceous formations are investigated as possible host rock in the field of geological disposal of radioactive waste. The favourable properties of claystone are low permeability, retention capacity for some radionuclides, and the ability to self-seal cracks, e.g. by swelling or time-dependent compaction creep. For the understanding of the long-term behaviour of clay host rocks, the interaction between mechanical behaviour, micro fabric, and mineral composition has to be understood (Bock et al., 2010). In the international research project Mont Terri (Switzerland) the Opalinus Clay (Jurassic Formation) is investigated in an underground rock laboratory (URL).
Yet the importance of the distribution of carbonates with respect to the mechanical strength was identified. Specifically, matrix carbonates increase the mechanical failure strength in contrast to coarse biogenic carbonates which generally reduce the mechanical strength (Kaufhold et al. 2013).
For understanding the deformation processes micro fabric investigation are required. In this case the non-destructive X-ray computed tomography was used for micro fabric investigations.
The Opalinus Clay specimen was first scanned with the v|tome|x L300 system at the GE facility in Wunstorf (Germany). The scan parameters were 270 KV and 0.3 mA and the scan duration was 145 min. With this system a spatial resolution of approx. 60 µm could be achieved.

Material

The specimen “file 13001” (drilling BLT-A6) was derived from the Underground Rock Laboratory (URL) Mont Terri (St. Ursanne, Switzerland) and belonged to the sandy facies of the Opalinus Clay (Kaufhold et al. 2013). The investigated core sample had a diameter of 100 mm and a length of 180 mm. The drilling was orientated perpendicular to the bedding. The material of the sandy facies in the URL Mont Terri consists of 20-40 wt.% carbonates, 30-50 wt.% quartz, and 15-25 wt.% clay minerals (< 5 wt.% swellable clay minerals). The natural water content of the specimen was preserved as good as possible,

Mechanical Testing

The claystone was tested by triaxial strength testing until a failure was developed. The test was executed in deformation controlled mode with a deformation rate of $d\varepsilon/dt=10^{-5}$ s^{-1} and carried out under undrained condition. After the mechanical testing the core was embedded in a resin to stabilize the specimen.

Large Scale and High Resolution X-ray CT Results

The CT results of the v|tome|x L300 show a spatial resolution down to ~60 µm for 10 cm sample width. As the highest power of this system is 0.5 kW, the contrast is not very high but still sufficient to detect different densities. Fractures and the delicate network can be nicely visualized (see figure 1).
The segmentation was performed in the central part of the sample, where one large horizontal crack originating from bedding plane disintegration ("discing") is intersected by a diagonal oriented crack system generated by the triaxial testing. Additionally, many cracks which are located close to the core surface and represent initial stages of drying cracks could be observed.



Figure 1: Transparent 3D view of the L300 CT result. Cracks are segmented (red colour).

Conclusions and Outlook

The analysis with X-ray CT based on v|tome|x L300 is suitable to give an overview of large core samples. The use of microfocus tubes can provide detailed images, which are necessary for special high resolution core analysis.

For the understanding of deformation processes during mechanical testing, detailed information before and after the mechanical testing are required. Thus, it is necessary to get micro fabric information of the undisturbed specimen, and after the mechanical test an overview of the deformed specimen. Using the overview scan it is possible to select regions of interest (ROI) which then can be analysed in more detail using high resolution CT devices. An example is given in Figure 2. The scan 3D data set was analysed and a suitable position for further micro plugging could be identified.

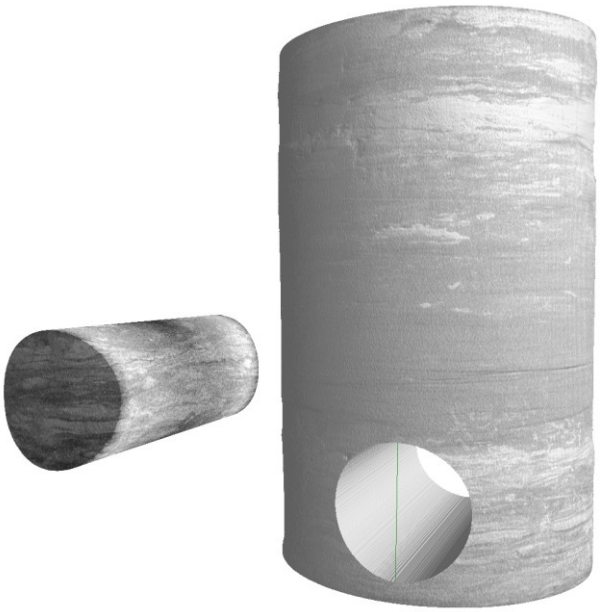


Figure 2: 3D view of the L300 CT result. The virtual plug has a typical diameter (~4 cm) used for additional experiments.

The selected area will be analysed using high-resolution CT techniques, as well as mineralogical and geochemical methods. The overall aim of the investigation of the Opalinus Clay (LT-A Project, Mont Terri) is to understand the rock deformation processes upon mechanical stresses. This behaviour is largely governed by microstructure. CT investigations, therefore, are a key method.

Additionally, chemical and mineralogical methods are used not only to characterize the stiffness of the matrix but also to identify homogeneous areas which can be considered representative of the entire rock. Hence, the CT information gathered from a small volume can be used to understand the mechanical processes of the entire rock.

References

Bock, H., Dehandschutter, B., Martin, C.D., Mazurek, M., de Haller, A., Skoczylas, F., Davy,C., 2010. Self-sealing of fractures in argillaceous formations in context with the geological disposal of radioactive waste. OECD/NEA Report 6184. OECD Nuclear Energy Agency, Paris, France. ISBN: 978-92-64-99095-1 (312 pp).

Kaufhold, A., Gräsle, W., Plischke, I., Dohrmann, R. Siegesmund, S. (2013). Influence of carbonate content and micro fabrics on the failure strength of the sandy facies of the Opalinus Clay from Mont Terri (Underground Rock Laboratory). Eng. Geology, 156, 111-118.

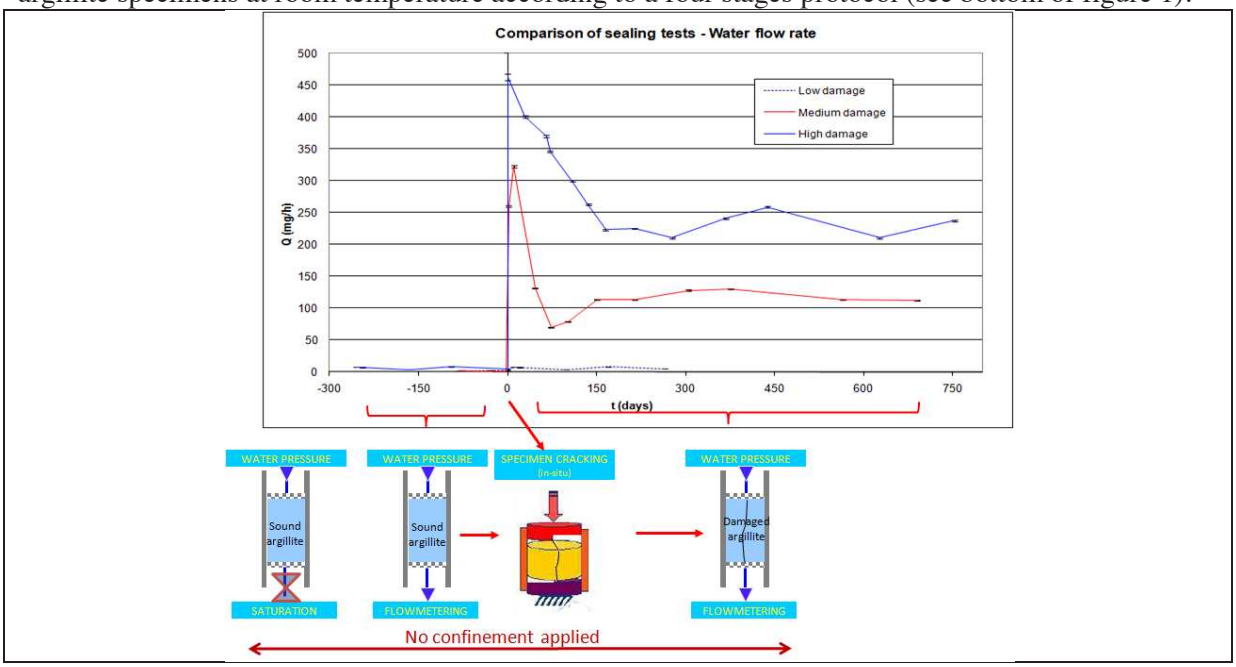
Hydraulic sealing experiments on Callovo-Oxfordian argillite

C. Imbert[(1)], *P. Sémété*[(2)], G. Touzé[(1)], J. Delorme[(2)], B. Février[(2)], P. Desgrée[(2)]

[(1)]CEA, Laboratory of Concrete and Clay Behaviour, DPC/SECR/LECBA
Commissariat à l'Energie Atomique, Centre de Saclay, 91191 Gif-sur-Yvette, France
[(2)]EDF R&D, Materials and Mechanics of Components Department,
Les Renardières, 77818 Moret-sur-Loing, France

Introduction.
The French National Radioactive Waste Management Agency (ANDRA) has chosen Callovo-Oxfordian (COx) claystone, an argillaceous formation in east of France, to sit the future deep geological disposal for intermediate and high level long-lived waste. The aim of the present study is to understand and quantify the sealing behaviour of both micro and macro cracks generated by the EDZ in Cox Claystone through experimental investigations. Therefore, two kinds of experiments were carried out on Callovo-Oxfordian samples. A first series of tests were conducted at EDF THEMHYS laboratory in order to study the possibility of hydraulic sealing in the case of macro-cracks or highly damaged samples. A second series of experiments were conducted by CEA and were devoted on the same kind of study but for the cases of micro-cracked material induced by thermal loadings.

Macro-cracks experiments.
The principle of these experiments consists in measuring Bure synthetic pore water flow through argillite specimens at room temperature according to a four stages protocol (see bottom of figure 1).



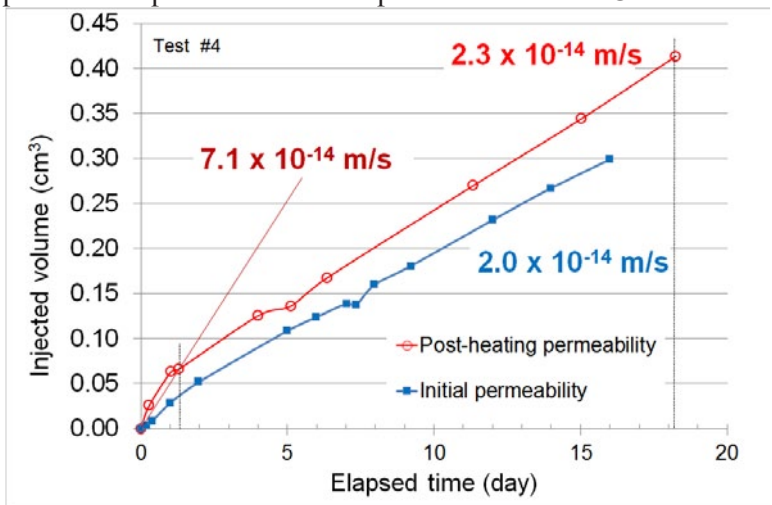
A first step of saturation is applied on a sound argillite specimen in a percolation cell, then permeability (water flow rate) measurement are made on this saturated material, after that, a mechanical cracking test is applied directly on sample inside the cell, and then permeability measurement are made on water saturated damaged argillite. It is important to note that no mechanical confinement is applied to the cell. Specimens (diameter/length ≈ 70/20 mm) are oriented in order to have their flat faces parallels to the bedding plan of the argillite. The flux of water percolating through the specimen has been determined under a pressure gradient of 10 bars (see results on figure 1). Argillite permeability can be derived according to the Darcy law. Mechanical damaging of the specimens was performed by applying shear stress directly inside the percolation cell in order to keep the same specimen during the whole experiment. Two samples were tested (on two different installations) with two damage levels for the first one (low and after, high damage) and an intermediate (medium) damage level was applied for the second test. The permeability of sound

samples is about 2 to 3.10^{-14} m/s and increases of two orders of magnitude (about 5 to 7.10^{-12} m/s) after high and medium damages (about 10^{-13} m/s after low damage). So a significant increase of water flow rate was obtained for the two higher damage levels and this is representative of EDZ situation. Then, a slow decrease of permeability is observed over 100-150 days and is followed by a stabilisation at around 1 to 3.10^{-12} m/s. The observed permeability decrease shows a hydraulic sealing or cracks closure due to material swelling. Two years after cracking, the sound material permeability is not reached and this is probably due to the lack of confinement, which is not representative of in-situ situation. Similar tests made with a confinement of 12 MPa allowed finding again the initial sound permeability level [1]. Possible chemical effect and leaching can also explain preferential flow paths.

Micro-cracks experiments

The principle of these experiments consists in comparing the permeability of either a sound specimen of argillite or a damaged specimen of argillite. Once saturated under confinement (with Bure synthetic pore water), the argillite is damaged through a rapid thermal solicitation and a partial release of the confinement pressure. Knowing that the thermal dilation coefficient of the claystone ($1.28\ 10^{-5}\ K^{-1}$) is lower than that of the water (from 2.0 to $8.0\ 10^{-4}\ K^{-1}$), a rapid heating of the saturated claystone may create over-pressures and may damage the sample. The hydraulic conductivity of the sound sample, measured before the heating phase, is considered as the reference value. After both the heating and cooling phases, the hydraulic conductivity of the sample is measured.

The Cox Claystone samples (diameter/length ≈ 57/26 mm) have undergone a saturation phase, during two months, in a special triaxial cell. A confining isotropic pressure (6 MPa) is maintained during the saturation phase. Concerning the thermal loading, different loading rates have been imposed, from 3°C per day to 0.45 °C per minute up to a maximal temperature about 115°C.



After the heating with a low thermal loading rate, the permeability of the sample is not different from the reference permeability (sound sample). By applying a rapid heating (0.45 °C.min^{-1}) up to 115°C and a partial release of the confinement pressure, the sample seems damaged. After complete cooling, the measurement shows an increase of the hydraulic conductivity (7×10^{-14} m/s to be compared to the reference value $2\ 10^{-14}$ m/s). But the hydraulic conductivity rapidly drops and the sample recovers its initial hydraulic property. The swelling of some minerals of the claystone may explain the drop of the hydraulic conductivity (Figure 2).

The two parts of this study show the same trend: when a sample of claystone is initially damaged through either a mechanical or a thermal solicitation, the percolation of water shows a decrease of the hydraulic conductivity towards the reference level, corresponding to the sound sample. In both cases, a process involving cracks closure is present.

Acknowledgment

The authors would like to thank ANDRA, CEA and EDF for supporting this work and all participants for fruitful discussions.

Bibliography

[1] C.A. Davy, F. Skoczylas, J.D. Barnichon, P. Lebon, Permeability of macro-cracked argillite under confinement: Gas and water testing, Physics and Chemistry of the Earth 32 (2007) 667-680

The initial damage/fractured excavation zone around deep underground facilities in Callovo-Oxfordian formation: modelling of fractures network using an anisotropic damage approach funded on shear and extension properties of argilites

R. Robinet[a] , F. Plas[b], C. Imbert[c] & J.C Robinet[d]

[a]Tractebel Engineering S.A. Groupe GDF-Suez, Brussels Belgium raphael.robinet@gdfsuez.com,

[b]Andra R&D Division, 92298 Chatenay Malabry France – frederic.plas@andra.fr.

[c]CEA, DPC/SECR/LECBA, Centre de recherche de Saclay, Gif sur Yvette christophe.imbert@cea.fr,

[d]Euro-Géomat-Consulting 45000 Orléans France robinet-jc@wanadoo.fr

Intensive effort has been spent by Andra in Bure URL to describe the initial damaged zone (DZ) in the Callovo-Oxfordian Formation (Argilites) and its short and medium terms mechanical behavior (Armand & al 2013). DZ is now well characterized: it is similar for all excavations tested in URL (borehole, drifts, small and large diameter…), as a fractured area with an anisotropic shape and divided in two distinct subzones from the wall of excavation, a 3D connected fractures zone then a discrete fractures zone. Characterization of fractures is showing that their origin is due to shear and/or extension mechanisms. Besides, observations are highlighting that the time-dependent mechanical behavior (convergence, strain and stresses) of the DZ is mainly controlled by fractures and blocks that are delimited.

To model convergence of clay rock and stresses applying on the underground structures (concrete liner, steel supports) from short to long terms, it is necessary firstly to represent the initial area of discontinuities (spatial distribution and number of fractures) created during excavation and then to implement hydro-mechanical mechanisms within this area (creep, swelling, plasticity…).

To achieve the first objective, a mechanical model, called SC2D, has been developed based on a competition between an anisotropic ductile behavior (directions of the subsidence's strain) and an anisotropic semi-fragile behavior (directions of the extension's strain). Theses behaviors are represented respectively by an elasto-plastic model characterized by a wide elastic range ($P_{consolidation}$ = 300 MPa) with a non-associative plasticity and negative hardening (Del Olmo & Huckel, 1996), and a hypo-elastic model with an anisotropic damage (Cordobois & Sidoroff 1982, Supartono & Sidoroff 1985) defined by a symmetric second order tensor (Mazars 1986).The creation of discontinuities in extension is associated with the values of the damage coefficients equal to the unity. Theirs orientations are perpendicular to the main directions of in situ stresses. The surfaces of discontinuities in shear domain correspond to the unit value of the shearing damage coefficients and theirs orientations correspond to the plane of maximum distortion. The model SC2D has been implemented in the fully coupled THM Finite Elements code CLEO.

Using experimental results from extension tests with constant medium-pressure and torsion tests (Robinet & al 1983-1989, Lee & al 2002) on Argilites and similar clay rock, numerical simulations were performed to represent EDZ around experimental drifts in the Andra's URL, GED drift oriented in the direction of the minor in situ stress and GCS and GCR drifts oriented in the direction of the major in situ stress (Armand & al 2013). A progressive unloading by 15 steps was used. Sensitive analysis, in particular of FE mesh, was also performed. Results show that the creation of discontinuities and the shape of damaged zone are well represented (see Figure 1): red lines represent the unit value of the damage coefficients in extension and the black lines the shearing-damage ones. Shape of damaged-fractured areas is elliptical with major axis about 8 m and minor axis about 6.4 m, in accordance to experimental measures.

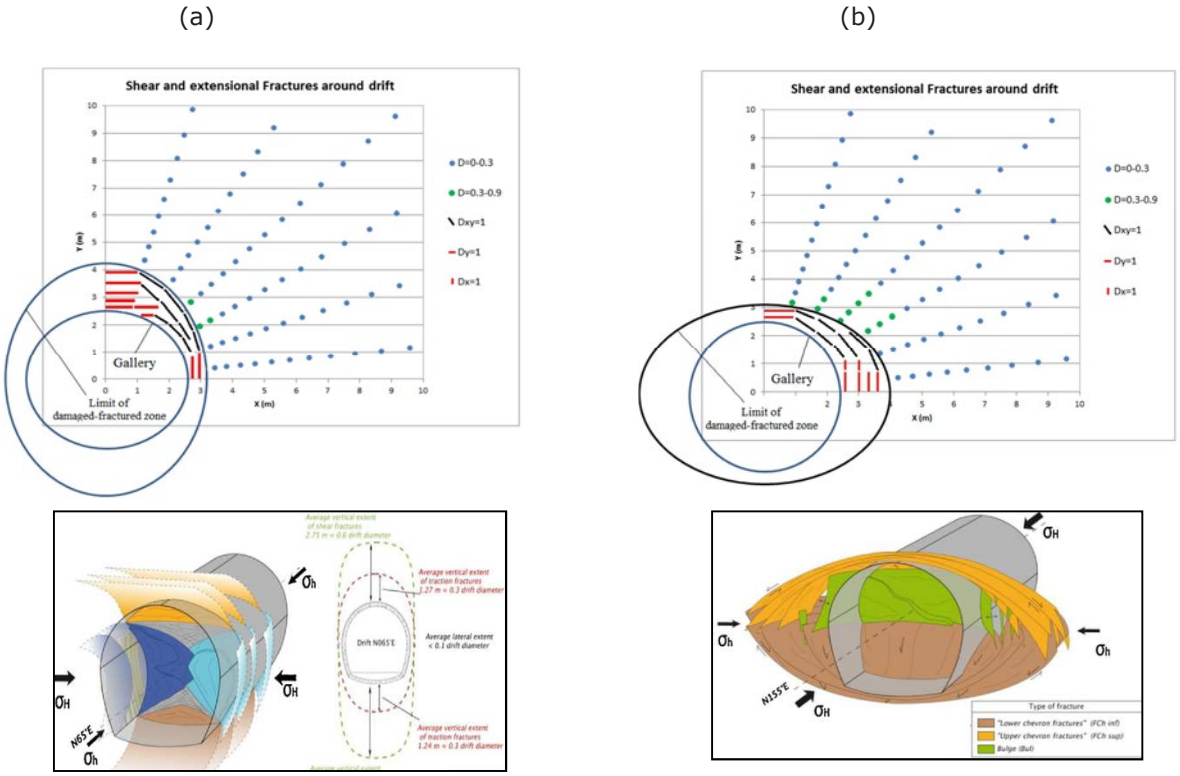


Figure 1 – Simulation of initial DZ around Andra's URL drifts (Armand & al 2013) (a) minor in situ stress σ_h and (b) major in situ stress σ_H

References

Armand G., Noiret A., Zghondi J., Seyedi D.M. (2013), Short- and long-term behaviors of drifts in the Callovo-Oxfordian claystone at the Meuse/Haute-Marne Underground Research Laboratory. J. of Rock Mechanics and Geotechnical Engineering 5 (2013), p.221-230

Cordebois J.P. & Sidoroff F. (1982). Damage induced elastic anisotropy, *Mechanical Behavior of Anisotropic Solids/Comportment Mécanique des Solides Anisotropes*, p.761-774, Springer Netherlands

Del Olmo C., Fioravante V., Gera F., Hueckel T., Mayor J.C., & Pellegrini R. (1996), Thermo-mechanical properties of deep argillaceous formations, Engineering Geology, 41(1), p. 87-102

Lee D.H., Hsein Juang C., Lin H.M. & Yeh S.H. (2002), Mechanical behaviour of Tien-Liao mudstone in hollow cylinder tests, Can. Geotech. J., p. 39 744-756

Mazars J. (1986), a description of micro- and macroscale damage of concrete structures, Engineering Fracture Mechanics 25, N° 5/6, p. 729-737

Robinet J.C., Golcheh Y., Deffayet M. & Fau D. (1983) Appareil de cisaillement des sols et des roches par torsion d'un cylindre creux, Cahier du groupe français de rhéologie (1983), p. 125-132

Robinet J.C, Chehade R. & Sharour I. (1989) Dilatance et potential de liquéfaction dans les essais triaxiaux et de torsion, 12th International Conf. On soil Mechanics and found. Eng., Rio de Janerio, p. 29-30

Supartono F. & Sidoroff F. (1985), Anisotropic Damage Modeling For Brittle Elastic-Materials. Archives of Mechanics, 37(4-5), 521-534.

Hydro-mechanical simulation in a deep excavation in Boom Clay

P. Y. Hong[a], ***F. Collin***[b], **Y. J. Cui**[a], **X.L. Li**[c], **X. Sillen**[d], **J. M. Pereira**[a], **A. M. Tang**[a]

[a]Université Paris-Est, Laboratoire Navier (UMR 8205), CNRS, ENPC, IFSTTAR, F-77455 Marne-la-Vallée, France (hongp@cermes.enpc fr)
[b]Department Argenco, University of Liège, Sart Tilman B52/3, Chemin des Chevreuils, 1, B-4000, Liege, Belgium (f.collin@ulg.ac.be)
[c]European Underground Research Infrastructure for Disposal of Nuclear Waste in Clay Environment, ESV EURIDICE GIE, Mol, Belgium
[d]ONDRAF/NIRAS, Belgium

In the Belgian program on the geological disposal of nuclear waste disposal, an experimental gallery (Praclay Gallery) was excavated in Boom Clay, tertiary plastic clay that hosts the underground research facility (HADES-URF) in Mol, Belgium [1]. The sensors installed around the excavated gallery in different directions allowed for a detailed description of the hydro-mechanical responses (pore pressure and displacement) of Boom Clay during and after excavation. In this context, finite element modeling has been carried out to understand and quantify the hydro-mechanical behavior perturbations of Boom Clay induced by the excavation.

The excavation of the Praclay Gallery (PG) is studied in a two-dimension (2D) plane strain assuming symmetry around the PG axis with the coupled hydro-mechanical behavior of the clay considered. The simple geometry of this model allows taking into account the anisotropy in 2D. As illustrated in Fig. 1 [2], this 2D plane strain model is 100 m wide and 100 m high. The external radius is equal to 1.25 m with a thickness of liner equal to 0.30 m. To compensate the convergence of the clay between its excavation and the installation of the concrete liner, an overexcavation was applied during the construction of the gallery, for the numerical simulation, a total overexcavation about 0.09m is assumed (Fig. 1). The real excavated radius is thus 1.34 m and the liner is supposed to be installed after a convergence of 0.09 m.

The hydro-mechanical conditions are represented in Fig .1. The gallery is situated at about 225 m depth and the underground water level is close to the ground surface. It is thus assumed that the clay is fully saturated. At this depth, the total vertical stress is around 4.5 MPa and the pore pressure is equal to 2.2 MPa, defining an effective stress of 2.3 MPa. A K_0 value (ratio of horizontal to vertical effective stresses) of 0.7 was adopted based on the laboratory and in situ investigations. The gravity is not considered in this modeling. X displacements are fixed on the boundaries FG and EF', and vertical displacements are fixed on the boundaries AB and B'C. All the boundaries are impervious except the boundary B'F' (excavated wall), which is considered in a drained condition during the excavation. The excavation sequence is simulated through a progressive relaxation of the external radial stress (σ_r) on the boundary B'F' till the boundary B'F' contact with the boundary BF due to the clay convergence.

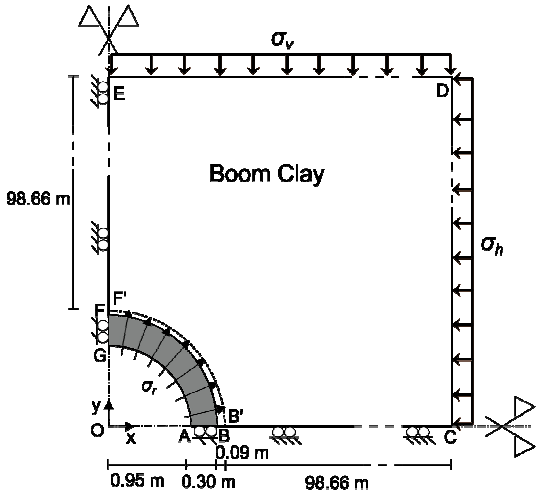


Fig. 1. *Schematic representation of the 2D plane strain modeling*

Conventional critical state models such as modified Cam Clay model (MCC) based on a simple elasto-plastic framework predicts a sharp elastic-plastic transition, which departs from the experimentally observed smooth elastic-plastic transition. Recently, Hong [3] has developed a two-surface model, namely ACC-2, with emphasis put on some important mechanical features of Boom Clay such as the limited elastic zone, smooth transition from elastic to plastic behavior. To investigate the sensitivity of the different elastoplastic constitutive models to the hydro-mechanical responses to excavation in Boom Clay, simulations of the gallery excavation are performed considering the classic MCC, a strain hardening Mohr-Coulomb model, and the ACC-2.

Fig. 2 compares the results of the finite element modeling with in-situ measurements along the horizontal profile (BC in Fig. 1). The pore pressure obtained with ACC-2 is quantitatively closer to the in-situ measurements than the results obtained with the MCC and Mohr-Coulomb models, indicating the importance to consider the smooth transition between elasto and plasticity with limited elastic zone of the clay.

The effects of the excavation duration, boundary condition and the anisotropy of the initial stress were also investigated, highlighting the necessity to account for the anisotropy of the initial stress state in Boom Clay.

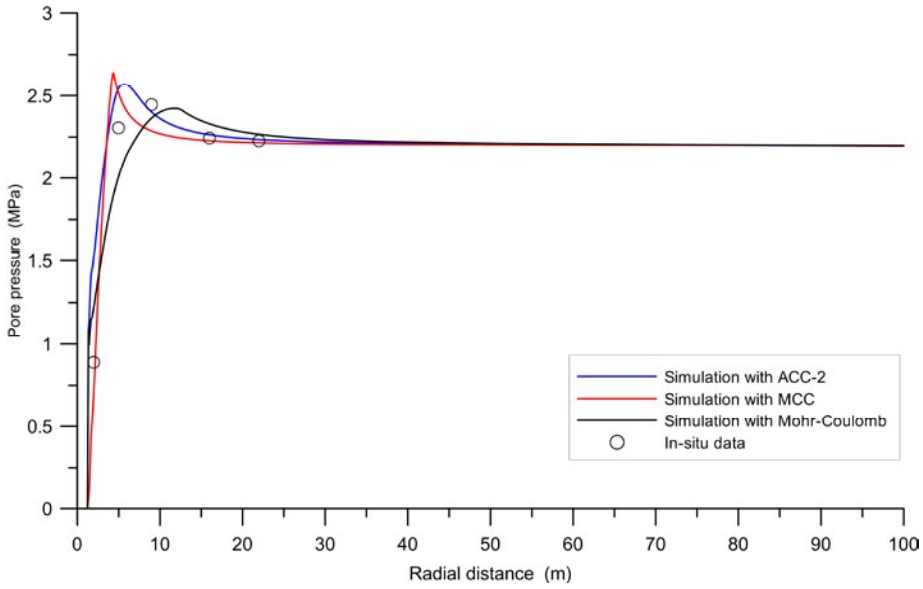


Fig. 1. *Comparison of the pore pressure along horizontal profile (BC) at the end of the excavation using ACC-2, MCC and Mohr-Coulomb*

References:

[1] P.Van Marcke, W.Bastiaens. Construction of the PRACLAY Experimental Gallery at the HADES URF. *In: Clays in Natural and Engineered Barriers for Radioactive Waste Confinement*, Nantes, France, P:7-18, 29 March - 1 April 2010.

[2] R. Charlier, R. Chambon, F. Collin, A. Dizier, S. Fauriel, B. François, J. Fokkens, B. Garitte, A. Gens, P. Gerard, et al. *Timodaz report: Deliverable d13–simulation of lab and in situ tests*. 2010.

[3] P.Y. Hong. Development and explicit integration of a thermo-mechanical model for saturated clays. *PhD Thesis*, Universite Paris-Est, France 2013.

Multi-scale investigation of the swelling clay material properties

L. Massat[1], O. Cuisinier[1], S. Gaboreau[2], F. Masrouri[1], M. Pelletier[3], I. Bihannic[3] and F. Claret[2]

1. LEMTA (UMR 7563 Université de Lorraine / CNRS), Vandœuvre-lès-Nancy, France
2. BRGM, Orléans, France
3. LIEC (UMR 7360 Université de Lorraine / CNRS), Vandœuvre-lès-Nancy, France

Introduction

Expansive clays are characterized by their sealing properties (low permeability, low porosity, high retention and high swelling potential) which make them of high interest for backfill materials in waste repositories. It is known that at constant volume, the swelling pressure of such smectites depends on different parameters such as relative humidity, interlayer cation, dry density, etc... Even if several studies focused on these parameters, the main difficulty is to establish simultaneously a link between porosity, particles' interaction and mechanical behaviour of expansive clays upon wetting. Therefore, a multi-scale investigation is mandatory to unravel the relationship between properties at both macro-, micro- and nano-scales during hydration.

The objectives of this work were on the one hand to continuously monitor the swelling pressures at constant volume of a specimen using a new designed specific oedometer and on the other hand to follow the evolution of its porosity at various scales. The tested sample was a specimen prepared from a purified Japanese sodic smectite (Kunipia G), hydrated with NaCl solutions at different ionic strengths.

Experimental method

The main objective was to characterize Kunipia G smectite from macro- to nano-scales to better correlate swelling pressure according to macro-porosity evolution from macro-pore size to interlayer pore access. Different types of oedometers were used to reach this goal.

A new tomographic cell was designed to monitor both swelling pressure and macro-porosity evolution using X-ray tomography. The specimen size was reduced to improve image resolution without disturbing the measurement of swelling pressure. This was validated by comparing the results obtained with this new cell with those obtained with conventional constant volume oedometrer. A cross comparison with data from the literature was also undertaken.

Example of results

The macroscopic properties (swelling pressure at equilibrium vs. dry density) obtained with the standard oedometers and the tomographic cell showed that Kunipia G behaviour is similar to other clay materials with high smectite content that were described in literature, MX 80, FEBEX or Bavaria bentonites (Schanz & Tripathy, 2009; Villar et al., 2012). The typical behaviour of such expansive clay is that swelling pressure rises when dry density is higher (Figure 1).

Figure 2 shows a set of results obtained with the tomographic cell: swelling pressure evolution vs. time as well as the tomography images recorded at various states of hydration. The

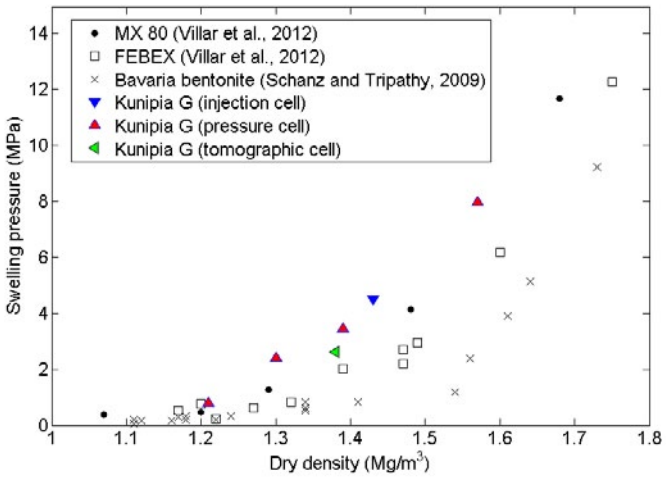


Figure 1: Swelling pressure at equilibrium versus dry density of Kunipia G compared to others swelling clay materials (MX-80, FEBEX, Bavaria bentonite)

swelling pressure was found to have two maxima: after an initial increase and the passage by a local maximum, the swelling pressure presents a trough before reaching equilibrium. X-ray tomography acquisitions at 4 different stages of the hydration process showed textural changes with a decrease of macro-pore volume over time until reaching a minimal volume at equilibrium at 26 days. Nevertheless, the decrease of porosity affected only the wetting part of the specimen under the hydration front. Such swelling pressure and porosity evolutions are also reported in literature (Villar et al., 2012; Wang et al., 2013). Therefore, swelling pressure variations are linked to macro-pore reorganisation (pore size > 5 μm) which could be due to particle expansion (hydration of interlayer spaces). Investigation at nano-scale should now try to explain the particle hydration to complete the study; thus an impregnation cell was also designed to keep the volume of the specimen unchanged after hydration with different aqueous solutions, impregnation by a resin and polymerisation.

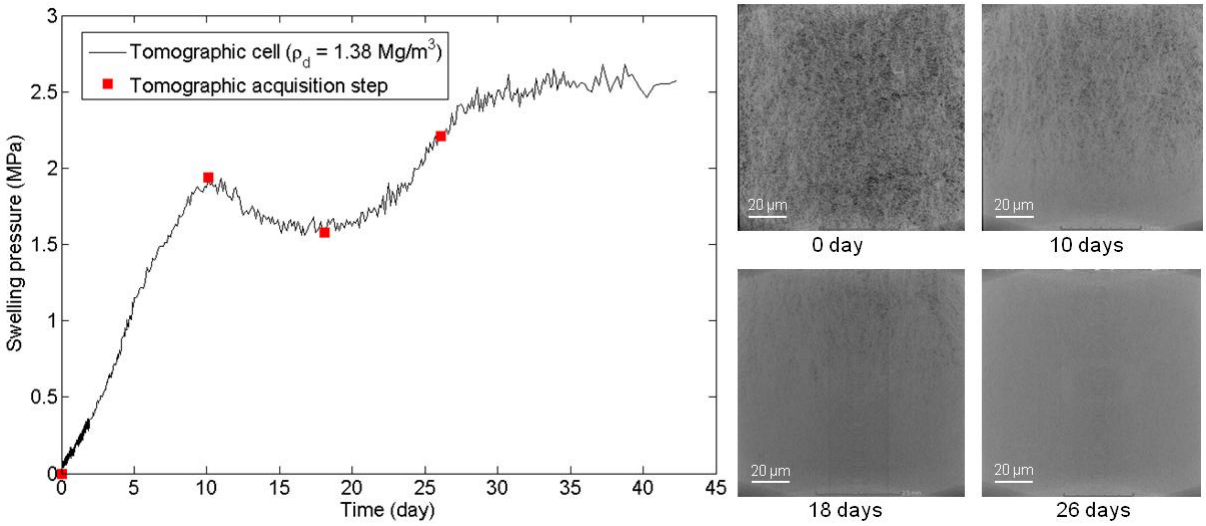


Figure 2: Simultaneous swelling pressure and tomographic acquisitions over wetting process. The red points refer to the tomographic acquisitions over time of experiment.

Conclusion and perspectives

The challenge of this work was to monitor simultaneously macro-porosity changes using X-ray tomography and swelling pressure. The results obtained with the designed tomographic cell were in good agreement with those obtained with standard oedometers. The correlation between swelling pressure and particles' reorganisation is currently studied by image processing to carefully quantify macro-pore changes (volume, connectivity, tortuosity, spatial distribution). Finally, the investigation should now be conducted at nano-scale to complete the study and better understand particle reorganisation upon hydration.

References

Schanz, T. & Tripathy, S. 2009. Swelling pressure of a divalent-rich bentonite: Diffuse double-layer theory revisited, *Water Resources Research* **45**, W00C12.

Villar, M. V. & Gómez-Espina, R. & Gutiérrez-Nebot, L. 2012. Basal spacings of smectite in compacted bentonite, *Applied Clay Science* **65–66**, 95-105.

Wang, Q. & Cui, Y.-J. & Tang, A. M. & Barnichon, J.-D. & Saba, S. & Ye, W.-M. 2013. Hydraulic conductivity and microstructure changes of compacted bentonite/sand mixture during hydration, *Engineering Geology* **164**, 67-76.

Study of the long term hydration of the FEBEX mock-up experiment considering four different coupled phenomena

***Marcelo Sánchez*[1], Antonio Gens[2], Fernando Aponte[1], Pedro Luis Martin[3], and Juan Carlos Mayor[4]**

[1]Zachry Department of Civil Engineering, Texas A&M University. Texas, US.
2Department of Geotechnical Engineering and Geosciences, Univ. Politècnica de Catalunya, Barcelona, Spain
3CIEMAT, Madrid, Spain
4ENRESA, Madrid, Spain

Abstract

The FEBEX mock-up test is being carried out in the CIEMAT facilities in Madrid. The experiment avoids many of the uncertainties arising from the natural system. This is achieved mainly due to the good control of the initial and boundary conditions of the experiment. Two electrical heaters (simulating canisters containing heat-emitting waste) are placed in the center of a steel cylinder 6 m long and with an inner diameter of 1.62 m. The space between the heaters and the steel cylinder is filled with a 0.64 m-thick engineered barrier made up from blocks of compacted bentonite. The barrier is hydrated uniformly from all around the cylinder with an applied water pressure of 0.55 MPa. Simultaneously, the barrier is heated maintaining a constant temperature of 100 ºC at the contact between heaters and bentonite. The test is intensely instrumented and it has provided the opportunity to study in detail the evolution of the main Thermo-Hydro-Mechanical (THM) variables over a long period of time. A complete description of the mock-up test can be found elsewhere (e.g. Sanchez et al., 2012).

Comprehensive laboratory tests carried out in the context of the FEBEX and NF-PRO projects allowed the identification of the main model parameters needed to describe the THM behavior of the compacted expansive clay. A conventional (single porosity) approach based on THM framework proposed by Olivella et al., (1996) was initially adopted to analyze the evolution of the experiment. Fig. 1.a) shows the comparisons between the experimental data (symbols) and the single porosity model (OBC, solid line) for a typical section involving heaters. It can be observed that the model is able to predict correctly the global THM behavior of the clay barrier in the short term (i.e. for times shorter than three years), but some model limitations can be detected concerning the prediction of the long-term hydration. The model predicts a much faster hydration of the clay barrier when it is compared against the experimental results. Note that this contribution presents updated results of the experimental data for a period of time of around 16 years, which perhaps represents the longer experimental data gathered from a large scale THM test.

With the aim of exploring the potential effect that some additional coupled phenomena (not included in the original THM formulation) may have on the long term hydration of the clay barrier, the numerical approach was upgraded to consider three additional coupled phenomena, as follows: i) presence of a threshold hydraulic gradient; ii) thermo-osmotic effects; and iii) evolution of the clay micro-fabric. The underline aim is to explore the hypothetical influence of these coupled phenomena on the final evolution of the mock-up test, and in particular to study their impact on the longer term model predictions.

The first additional coupled phenomenon (i) considered in this study is related to non-Darcy flow conditions. The presence of a threshold hydraulic gradient was included in the permeability model. Concepts based on the strong clay-water interactions have been suggested to explain the possible presence of this type of non-Darcy flow behavior in the clay barrier. Fig. 1.b) presents the model predictions using this model (ThG). It can be observed that the ThG model is able to reproduce a much slower rate of hydration, closer to the actual experimental one. It can also be seen that perhaps at advanced stages the hydration the hydration rate is even smaller than the observed one. This is particularly true in sections far from the heaters (not presented here). Similar tendencies are observed in other sections of the experiment.

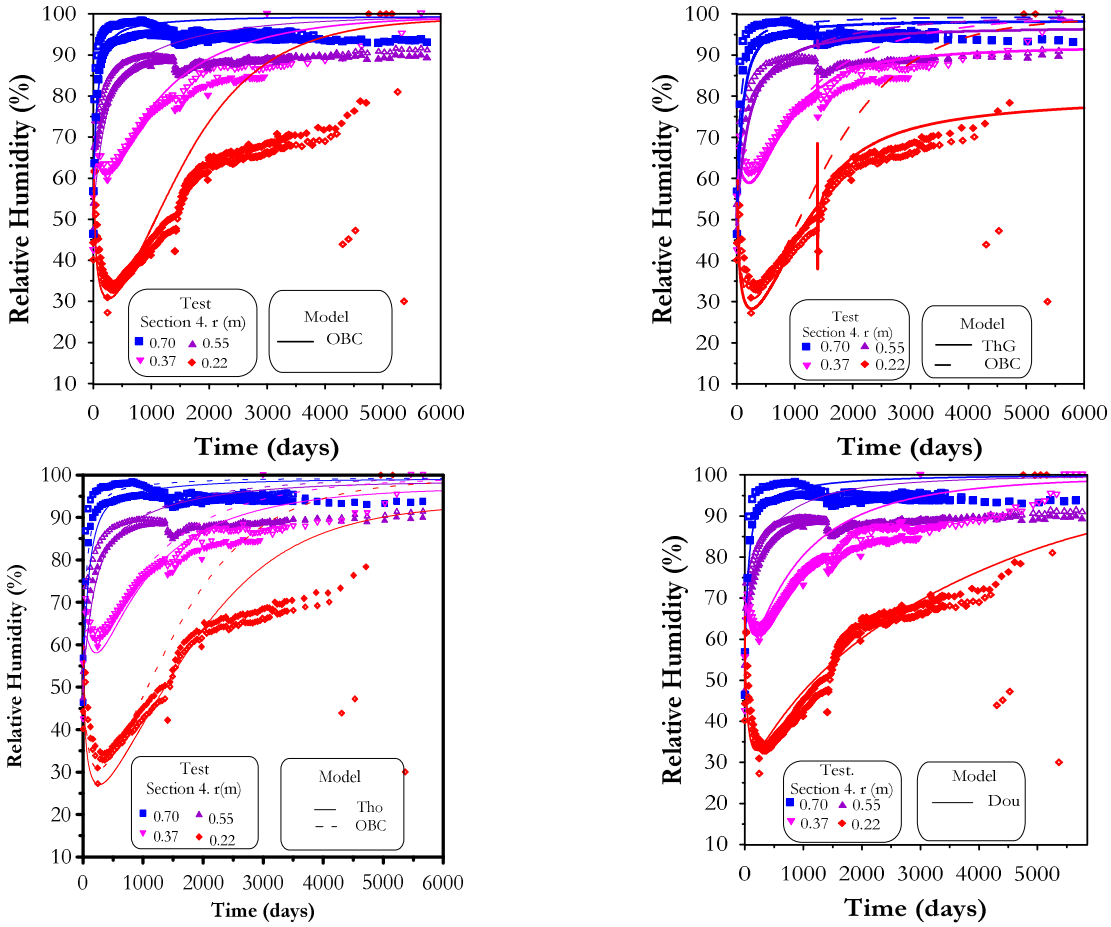


Figure 1. Evolution of relative humidity in the mock-up test in a typical section involving heaters, comparisons between experimental results and numerical models considering different phenomena: a) single porosity model, b) presence of a threshold hydraulic gradient; c) thermo-osmotic effects; and d) clay fabric effects modeled through a double structure model.

The second additional coupled phenomenon (ii) included in this study is related to thermo-osmotic effects. The hydraulic gradient is generally the main factor controlling the water transfer in soils. It is, however, not the only one. In non-isothermal conditions, a thermo-osmotic liquid flow associated with the thermal gradient may exist, inducing the movement of water from the hot zones (near the heater) to the cold areas (near the perimeter of the clay barrier). Fig. 1 (c) shows the model results (Tho) related to this phenomenon. It can be observed that the model is able to reduce the hydration rate; however the wetting is still quite slow when compared against the experiment, particularly near the heater.

The last coupled phenomena (iii) considered in this research, corresponds to the modeling of the clay micro-fabric evolution by means of a double structure model for expansive clays. The double structure model explicitly considers the two dominant pore levels that actually exist in the FEBEX bentonite, and it is able to account for their evolution during hydration. As shown in Fig 1.d), the simulation of the experiment using this enhanced model (Duo) provides a more satisfactory reproduction of the long-term experimental results. It also contributes to a better understanding of the observed test behavior and it provides a physically-based explanation for the very slow hydration of the barrier.

It is finally important to mention that all the phenomena discussed above can be interacting at the same time and influencing the final behavior of the clay barrier, as the presence of one of them do not necessarily exclude the other phenomena

References

Olivella S, Gens A, Carrera J. Alonso EE. Numerical formulation for a simulator (CODE-BRIGHT) for the coupled analysis of saline media. Engineering Computations 1996; 13(7): 87-112.

Sánchez M, Gens A, Olivella S. THM Analysis of a large scale heating test incorporating material fabric hanges. Int.Jnl for Numerical and Analytical Methods in Geomechanics 2012; 36 (4): 391-421.

Micro scale caracterisation of COX swelling and self-sealing behavior

S. Salager [1,2], D. Takano[3], P. Bésuelle[1,2], E. Andò[1,2], J. Desrues [1,2], G. Viggiani[1,2], P. Charrier[1,2]

[1] Univ. Grenoble Alpes, Lab. 3SR, France
[2] CNRS, Lab 3SR, France
[3] Port and Airport Research Institute, Japan

The process of swelling of clay rocks, an important concept for storage because it could contribute to the closure of large cracks (sealing and healing) induced by the galleries excavation, is still poorly understood. The aim of this study is to characterize the mechanisms of deformation at the small scale during swelling experiments (pore fluid saturation increasing) by the association of micro-tomography and digital image correlation (DIC). To achieve this goal the self-sealing of fractures in COX clay were observed and analysed.

Cylindrical specimens with 10 mm in diameter and 20 mm in height were prepared and for each of them a fracture parallel to the axis was created by modified Brazilian test. The specimens were wrapped with Teflon film and both ends were covered with grease to avoid the contact of the seepage flow with any part of the specimen except the fracture. They were then inserted into a tube of silicone paste and synthesized site water was used for seepage flow. Figure 1 present the schematic view of the experiment configuration.
The experiment was conducted through the following procedure: the first tomographic scan was made for initial conditions and then the fluid seepage was run. At different steps of the swelling the seepage was stopped and a scan was performed.

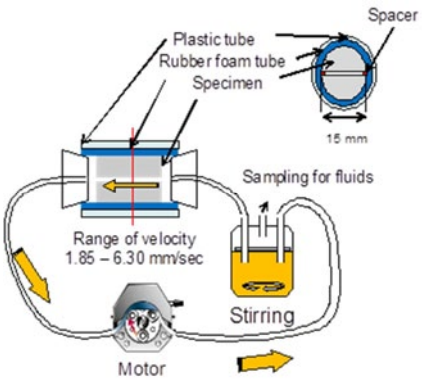


Figure 1: Schematic view of the experiment configuration

Figure 2 shows the reconstructed images, orthogonal to the axis of the specimen, at the different steps of the test, obtained from x-ray tomography. The re-closing the cracks can be observed from these images; (a) corresponds to the initial state, the sample before any swelling, (b), (c) and (d) correspond to 3 different states after 3h, 6h and 24h respectively. In addition it can be noticed that small secondary cracks are developed after 3h of seepage flow. At the end of the process the gap between the two walls rock is completely filled by the swelling of the clay.

DIC was applied to the experiment and figure 3 shows the incremental volumetric strain field in a vertical slice through the specimen. The maximum strain plotted in these figures equals 0.3. In the increment from initial to after 6 hours of seepage flow (Figure 3 (a)), the development of dilatant volumetric strain (swelling in the bulk) can be observed in top-left half of the specimen (yellow). Swelling can also be observed around the secondary open cracks. The red fringes (compaction) around fractures are most probably DIC artefacts due to crack edge displacements. The horizontal cut (Figure 3 (c)) shows that the swelling starts from the edges of the main fractures (yellow spot above the

crack). In the same cut, the contracting volumetric strain recorded at the ends of the fracture appears due to deformation of the spacer piles rather than of the rock itself. In the increment from 6 hours to 9 hours seepage flow, Figure 3 (b) and (d) show that swelling in the specimen starts developing extensively not only in the edge of the fracture but also inside the specimen. These incremental volumetric strain fields suggest that the argillaceous rocks start swelling after only a few hours of water injection, and then it develops extensively to inside the material.

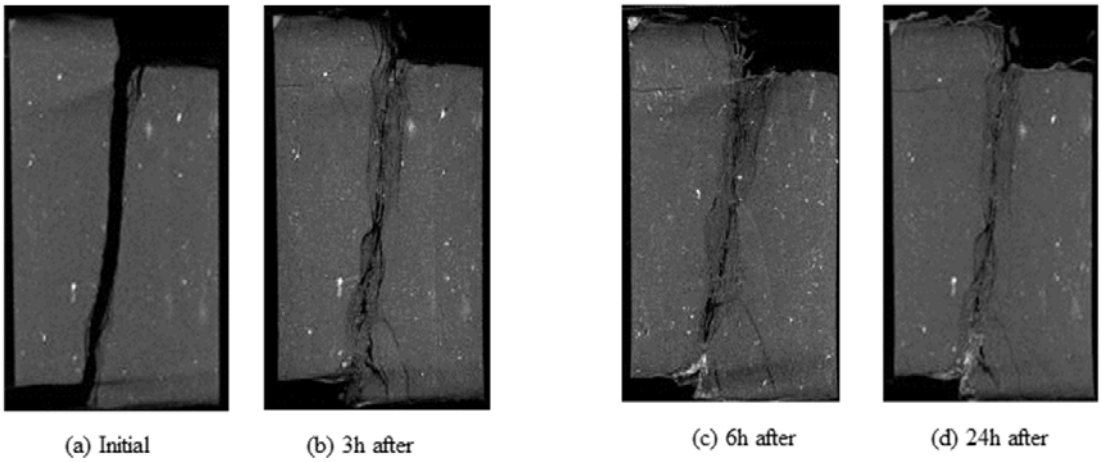


Figure 2: *Reconstructed images from x-ray tomography through cross section paralell to the axis of specimen. (a) initial condition, (b) 3h after the beginning of the swelling, (c) after 6h, (d) after 24h*

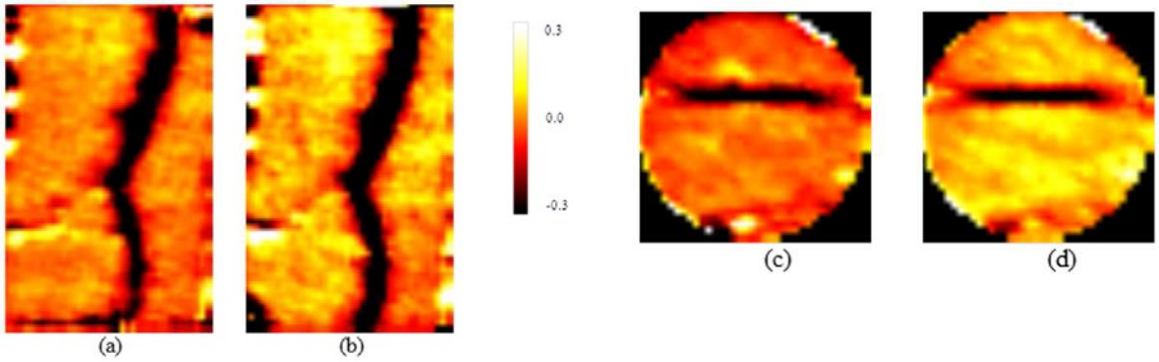


Figure 3: *Incremental volumetric strain determine from DIC. (a) vertical slice from initial to 6h, (b) vertical slice from 6h to 9h, (c) horizontal slice from initial to 6h, (c) horizontal slice from 6h to 9h.*

Ando E., Hall S., Viggiani G., Desrues J., Bésuelle P., 2012, Grain scale experimental investigation of localised deformation in sand: a discrete particle tracking approach, Acta Geotechnica vol.7-1, pp. 1-13.

Frey J., Chambon R., Dascalu C., 2012, A two-scale poromechanical model for cohesive rocks, Acta Geotechnica, doi 10.1007/s11440-012-0173-8.

Hall S., Bornert M., Desrues J., Pannier Yannick, Lenoir N., Viggiani G., Bésuelle P., 2010, Discrete and Continuum analysis of localised deformation in sand using X-ray micro CT and Volumetric Digital Image Correlation, Géotechnique vol.60-5, 315-322.

Robinet J.-C., Sardini P., Coelho D., Pameix J.-C., Prêt D., Sammartino S., Boller E., Altmann S., 2010, Effect of mineral distribution at mesoscopic scale on solute diffusion in a clay-rich rock : Example of the Callovo-Oxfordian mudstone (Bure, France), Water Resources Res., vol. 48, W05554.

Van den Eijnden B., Bésuelle P., Collin F, Chambon R., 2014, Doublescale modelling of hydromechanical coupling and anisotropy in localization problems, Int. Symp. Geomechanics from Micro to Macro, Cambridge, UK, 1-3 Sept 2014.

Wang LL., Bornert M., Chanchole S., Yang D.S., Héripré E., Tanguy A., 2013, Micro-scale experimental investigation of the swelling anisotropy of the Callovo-Oxfordian argillaceous rock, Clay Minerals 48-2, 391-402.

A two-surface viscoplastic model for saturated clays

P. Y. Hong[a], ***J. M. Pereira***[a], **Y. J. Cui**[a], **A. M. Tang**[a], **F. Collin**[b], **X.L. Li**[c], **X. Sillen**[d]

[a]Université Paris-Est, Laboratoire Navier (UMR 8205), CNRS, ENPC, IFSTTAR, F-77455 Marne-la-Vallée, France (hongp@cermes.enpc fr)
[b]Department Argenco, University of Liège, Sart Tilman B52/3, Chemin des Chevreuils, 1, B-4000, Liege, Belgium (jeanmichel.pereira@enpc.fr)
[c]European Underground Research Infrastructure for Disposal of Nuclear Waste in Clay Environment, ESV EURIDICE GIE, Mol, Belgium.
[d]ONDRAF/NIRAS, Belgium

Boom clay has been selected as one of the potential host material for nuclear waste disposal in Belgium. Experimental tests show that time dependent behavior is significant in Boom Clay [1]. It is therefore important to develop an appropriate model of viscoplasticity for Boom Clay to assess its impact on the long term evolution of the disposal facility.

In this study, an advanced viscoplastic model was developed for saturated clays in the framework of two-surface plasticity and isotach viscosity. Emphasis is not only put on the time effects on the mechanical behavior (viscosity), but also on some important features of natural clays evidenced experimentally such as the limited elastic zone, the smooth transition from elastic to viscoplastic behavior.

Based on the isotach concept, the yield surface accounting for strain rate effect on the preconsolidation pressure is introduced to reproduce the time dependent behavior [2]. The model adopts two yield surfaces (see Fig. 1): one Inner yield surface to predict the time dependent behavior inside the second yield surface namely Yield surface corresponding to the normal consolidated state (NC).

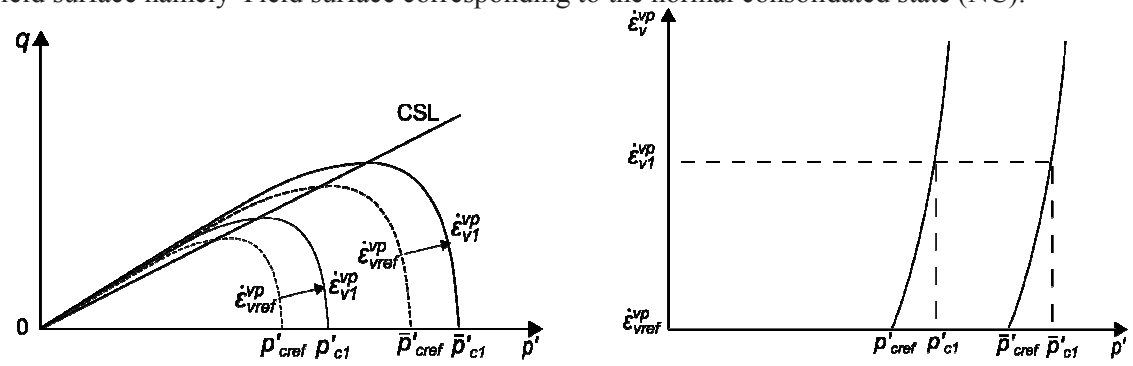


Fig. 1 Yield locus in (a): (p'- q) plane at two volumetric plastic strain rates (with $\dot{\varepsilon}_v^{vp} > \dot{\varepsilon}_{vref}^{vp}$); (b): (p'- $\dot{\varepsilon}_v^{vp}$) plane.

A generalized expression of Yield surface is adopted in (p'-q-$\dot{\varepsilon}_v^{vp}$) space as follows:

$$f_{YS} \equiv q^2 + \frac{M_f^{\,2}}{1-k_f}\left(\frac{p'}{\bar{p}'_c}\right)^{2/k_f} \bar{p}'^2_c - \frac{M_f^{\,2} p'^2}{1-k_f} = 0 \qquad (1)$$

with the preconsolidation pressure evolving with the plastic strain rate as follows [3]:

$$\bar{p}'_c = \bar{p}'_{cref}\left(\frac{\dot{\varepsilon}_v^{vp}}{\dot{\varepsilon}_{vref}^{vp}}\right)^{\alpha} \qquad (2)$$

where $\bar{p}'_{cref}$ and $\bar{p}'_c$ are defined as the apparent preconsolidation pressures at a reference volumetric plastic strain rate ($\dot{\varepsilon}_{vref}^{vp}$) and the actual volumetric plastic strain rate ($\dot{\varepsilon}_v^{vp}$), M_f and k_f are parameters to specify the shape of yield surface in (p', q) plane at a given volumetric plastic strain rate, α is a soil parameter depending on the soil type.

The Inner yield surface is homologous to the Yield surface with respect to the origin in (p', q) plane. A scalar r is defined by $r = p'_{cref} / \overline{p}'_{cref}$, giving the ratio of the size of a given Yield surface to that of the corresponding Inner yield surface. Parameters $\overline{p}'_{cref}$ and r are the hardening variables controlling the sizes of Yield surface and Inner yield surface, respectively. The internal variable increment $d\overline{p}'_{cref}$ depends on the volumetric viscoplastic strain increment:

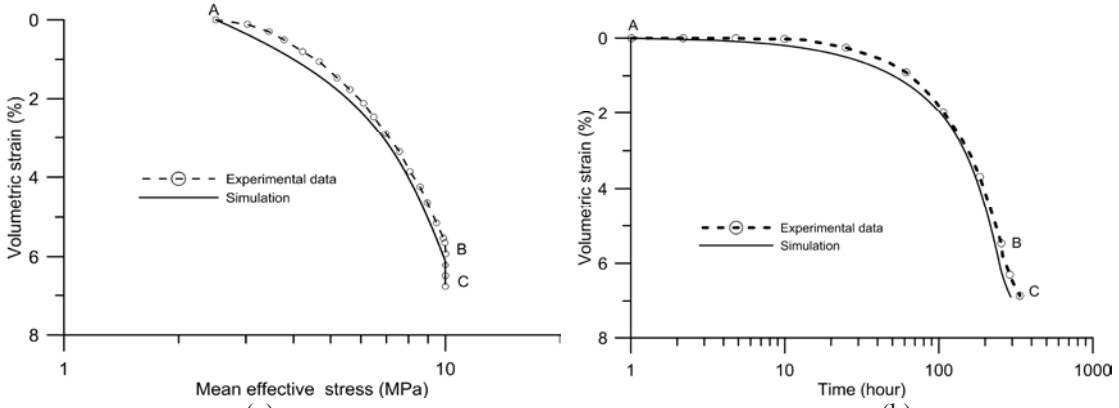
$$d\overline{p}'_{cref} = \frac{v_0}{\lambda - \kappa} \overline{p}'_c d\varepsilon_v^{vp} \tag{3}$$

where λ and κ represent the slopes, in (v, ln p') space, of normal (virgin) consolidation and swelling/recompression lines respectively, v_0 is the initial specific volume. To describe the viscoplastic modulus variation when Inner yield surface is activated, the following evolution law of r is adopted:

$$dr = \frac{v_0}{\lambda - \kappa} s(1-r) d\varepsilon_v^{vp} \tag{4}$$

where s is a material constant, which controls the rate at which the Inner yield surface approaches the Yield surface along loading paths, and thus describes the evolution of the slope of the stress-strain curve inside the Inner yield surface. To ensure that the critical state conditions are finally reached, the viscoplastic scalar multiplier is assumed constant on a given yield surface.

Using the proposed model, an isotropic test on Boom Clay was simulated and compared with the experimental results in Fig. 1. A creep stage (BC) under p' = 10 MPa is included after an isotropic mechanical loading (AB) with a constant rate of 0.5 kPa/min. As it can be observed, the simulation results fit the experimental data reasonably well in terms of isotropic loading and creep phase. Especially, the smooth elasto-viscoplastic behavior during the mechanical compression can be well described. The model is also well validated by simulating other experimental tests involving variable stress and/or strain rate conditions. Results show model's relevance in reproducing the general features of the time dependent behavior for saturated clays.



(a) (b)

Fig. 2 Isotropic compression tests on Boom Clay in terms of (a): Volumetric strain-Mean effective stress; (b): Volumetric strain-time

References:
[1] Y.J. Cui, T.T. Le, A.M.Tang, P. Delage, X.L. Li. Investigating the time dependent behaviour of Boom clay under thermo-mechanical loading. *Géotechnique*, 59 (4): 319-329, 2009.

[2] L. Šuklje. The analysis of the consolidation process by the isotache method. *In: Proc. 4th Int. Conf. on Soil Mech. and Found. Engng.*, London, vol. 1: 200–206,1957.

[3] V. De Gennaro, J.M. Pereira. A viscoplastic constitutive model for unsaturated geomaterials. *Computers and Geotechnics*, 54 (-): 143-151,2013.

Microseismicity induced by a gallery excavation in the Mont Terri underground rock laboratory

Y. Le Gonidec[1], J. Sarout[2], J. Wassermann[3], C. Nussbaum[4], P. Bossart[4]

[1] Géosciences Rennes, UMR6118-CNRS, Rennes, France
[2] CSIRO, Earth Science and Resource Engineering Perth, Perth, WA, Australia
[3] Géosciences et Environnement Cergy, Cergy-Pontoise, France
[4] Swisstopo, Swiss Geological Survey, Wabern, Switzerland

In 2008, a new gallery, called Ga08, was excavated in the Mont Terri to join a pre-existing end-face of an earlier gallery, called Ga04. The excavation method, using a particular excavation machine, hydraulic drum cutter Erkat ER 600, mounted on an excavator machine, allows for a smoother excavation that limits the extent of the induced damaged zone surrounding the final gallery.
This excavation operation was an opportunity for original geophysical field investigations to monitor of a fresh excavation Damage Zone.
In particular, acoustic experiments have been performed during and following the gallery excavation. Arrays of acoustic sensors have been specifically designed to be introduced, from the Ga04 end-face, in horizontal boreholes to monitor an argillaceous rock mass segment of 8 m in length. In the one hand, active experiments, called "seismic surveys", consisted in emitting high frequency pulses to sound the medium with a controlled acoustic source to highlight the P-wave velocity field. In the other hand, passive experiments, called "microseismicity", used the same acoustic arrays to detect acoustic emissions induced in the rock mass segment by stress redistribution around the freshly excavated gallery Ga08.
From the acoustic surveys, we highlight the transversely isotropic P-wave velocity field of the rock mass. We show that it can be used to efficiently locate the controlled acoustic sources and validate the location procedure. From the large data set of recorded acoustic emissions, we first identify only few stress-induced microseismic events (MSEs) with confidence by developing a restrictive but efficient multi-step filtering method. We then apply the location procedure to these MSEs and deduce their spatial distribution. We show an asymmetric geometry of the excavation damaged zone around the excavated gallery: no notable microseismic activity is observed in the sandy facies sidewall and a burst of MSEs locates in the shaly facies sidewall followed by two smaller bursts which occurred when the excavation procedure was stopped.
In a further step of the data analysis, we deduce the damage mechanisms associated to the last two bursts of MSEs, based on the determination of focal mechanisms. The first burst of microseismic activity, which locates ahead of the excavation front, is associated with a dominant double-couple component: a bedding plane reworking is suggested, that is, shear along bedding planes and associated wing-cracks. The second burst locates inside the shaly sidewall of the gallery and is associated to a dominant compensated linear vector dipole, suggesting extensional fracturing, that is, typical spalling damage in the vicinity of the stress concentration zone.
As a conclusion, this work allows identifying and discussing four major factors that seem to control the MSE source mechanisms: lithology, geometry of the geological features, gallery orientation and direction of the main compressive stress.

Swelling pressure behavior of compacted bentonites under controlled suction

Zemenu Geremew Yigzaw[1], *Olivier Cuisinier*[1], Farimah Masrouri[1vapor]

1. LEMTA (UMR 7563 Université de Lorrraine/CNRS), Vandœuvre –les-Nancy

Compacted bentonites and bentonite-aggregate mixtures have been considered as suitable backfilling materials for underground nuclear waste disposal systems because these materials should have swelling characteristics in order to seal and separate the waste from the surrounding environment. These sealing materials are expected to swell due to the high prospect of intrusion of water and saline solution from the host rock. Furthermore, it is expected that the development of the swelling pressure in the buffer materials would take place under near constant volume condition and in a gradual manner following suction reduction caused by the intrusion of water from the surrounding host rock. Consequently, laboratory experiments which allow investigating the development of swelling-pressure would be important to enhance the understanding of the performance of high-level radioactive waste disposal systems.

Laboratory swelling-pressure tests of compacted bentonite-based materials have been carried out by many researchers for the last several years. However, laboratory experiments showing the development of swelling pressure under controlled suction and constant volume conditions are scarce. However, several techniques exist for controlling suction of unsaturated soils: axis translation, vapour equilibrium and osmotic, of which the first two are the most widely used at present. Recently, few researchers have reported experimental test results showing the development of swelling pressure under confined condition using the vapour equilibrium and the axis translation technique to control suction in the high and low range respectively. However, it is reported that the axis translation technique has some limitations in its application particularly in samples which are at nearly saturated conditions[1]. The osmotic technique, on the other hand, better simulate the in-situ conditions of water suction, and it is reported that with the correct choice of semi-permeable membrane and solution, the osmotic technique can be used to perform controlled suction tests regardless of its duration[2]. In this context, the objectives of the research presented in this paper are focused, first, on the development of a constant volume swelling pressure measuring device which allows the control of suction over a wide range, from high to zero suction, using osmotic and vapour equilibrium techniques, and then, to study the swelling pressure evolution of a compacted bentonite under controlled suction.

To achieve the first objective, a new constant volume swelling pressure measuring experimental device is developed. The device allows controlling suction using either osmotic or vapor equilibrium techniques. A specially designed porous stainless steel allows the circulation of liquid (Polyethylene glycol (PEG) solution, water or vapour) all around the bottom of the sample. Its high resistance to deformation allows the measuring of high swelling pressure under constant volume condition without damage to the semi-permeable membrane. Suction in the range of 0 to 8.5MPa can be imposed to the specimen with the osmotic technique; higher suction values (as high as 300 MPa and more) could be imposed using the vapor equilibrium technique. Swelling pressure is continuously recorded using a pressure sensor placed inside the top part and directly in contact with the top surface of the soil specimen. For the study presented in this paper, only the osmotic technique is used.

To address the second objective, constant volume swelling pressure tests were performed on selected bentonites. The air dried bentonite was statically compacted to the target density directly inside the rigid steel mold of the constant volume device at hygrometric water content. Then, suction is reduced in stages under controlled conditions and the development of swelling pressure is monitored. Fig.1 shows the results obtained on a specimen of MX-80 statically compacted to an initial dry density of 1.40 Mg/m^3 (w%=10.7 %) and submitted to suction reduction in stages from as-compacted value to saturation under confined condition. Fig. 2 shows the stress paths in terms of suction against swelling

pressure of compacted MX-80 and Georgia bentonites specimens hydrated under controlled suction by osmotic technique.

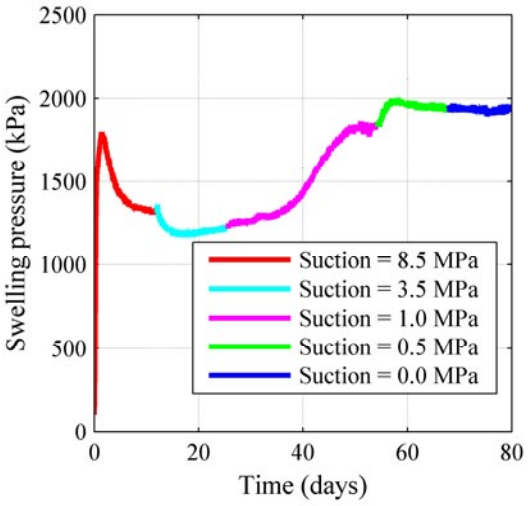


Fig.1. Swelling pressure development under confined condition and under controlled suction of compacted MX-80 bentonite

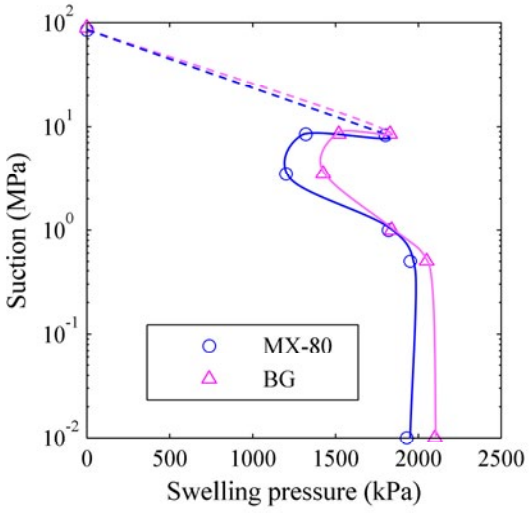


Fig.2. Stress paths in terms of suction against swelling pressure of compacted MX-80 bentonite and a bentonite from Georgia (BG)

Three stages of swelling pressure development are identified. In the first stage, following large suction reduction, the swelling pressure increases up to a peak value; then, in second stage, swelling pressure tends to decrease to a minimum value even though suction is reduced from 8.5 to 3.5 MPa; and finally, upon further suction reduction to low values, swelling pressure increases again and eventually stabilizes. A possible interpretation of this pattern is given, from microstructural perspective, by different authors [3], [4]. The initial transient increase of swelling pressure is attributed to the swelling of clay aggregates while they remain strongly held structural units. In the course of continued suction reduction (8.5 to 3.5MPa), the expansion of clay aggregates and the loss of shear strength in the contact regions of adjacent aggregates results a collapse of the macrostructure and hence a temporary drop in swelling pressure. Upon further suction reduction/saturation, the swelling pressure increase is associated with additional expansion of the clay microstructure while the clay is transformed from an aggregated to more homogeneous state.

Both MX-80 and Georgia bentonites show similar swelling pressure evolution pattern during wetting, though the structural collapse is more pronounced for MX-80. This may be attributed to differences in the initial microstructure of the bentonites. Similar results were obtained using vapour equilibrium technique for controlling suction during wetting.

In conclusion, the experimental results revealed that with the new device, the osmotic technique can be used to perform, in a satisfactory manner, suction controlled, volume constant swelling pressure tests. Forthcoming tests will try to verify the suitability of the technique to perform tests of long duration using different types of semi-permeable membranes.

References:

[1] P. Delage, E. Romero, and A. Tarantino, “Recent developments in the techniques of controlling and measuring suction in unsaturated soils,” in *First International Conference on Unsaturated Soils*, pp. 33–52, 1982.

[2] R. Monroy, a. Ridley, K. Dineen, and L. Zdravkovic, “The suitability of the osmotic technique for the long-term testing of partly saturated soils,” *Geotech. Test. J.*, vol. 30, no. 3, pp. 220–226, 2007.

[3] R. Pusch, “Mineral-water interactions and their influence on the physical behavior of highly compacted Na bentonite,” *Can. Geotech. J.*, vol. 19, pp. 381–387, 1982.

[4] P. Delage, “Microstructure Features in the Behaviour of Engineered Barriers for Nuclear Waste Disposal,” *Exp. Unsaturated Soil Mech.*, vol. 112, pp. 11–32, 2007.

A model for the swelling of bentonite by lowering salinity

Veli-Matti Pulkkanen

VTT Technical Research Centre of Finland, P.O. Box 1000, FI-02044 VTT, Finland
veli-matti.pulkkanen@vtt.fi

A model for the swelling of fully saturated bentonite by lowering salinity has been developed. In the model, the water in bentonite is divided conceptually to bound and unbound waters. The bound water is a part of the structure of bentonite adding to the volume of bentonite, whereas the unbound water fills pores without changing the volume. If a sample of bentonite is in contact with dilute water, the cations in the unbound water diffuse slowly out of the sample. Consequently, the activity of the unbound water increases and an activity imbalance between the waters develops. As a result, the unbound water tends to move into the bound water space increasing the volumetric strain of the material. If the sample volume is confined, the strain makes the stress increase until the activity difference is in balance with the developed stress. If the sample volume is not confined, the strain makes the sample to swell until local balances between the activity differences and the stress state are obtained. Describing this mathematically, the equations for the cation diffusion in the unbound water, the diffusion and increase of bound water, the unbound water decrease and the mechanical elasto-plastic behaviour are written. Simple experiments are simulated with the model to test its conceptual validity.

The model here is a part of a work aiming to model the erosion of bentonite by dilute water, a phenomenon which has been identified as a subject to research in the context of the disposal of spent nuclear fuel according to KBS-3 concept.

The research leading to these results has received funding from the European Atomic Energy Community's Seventh Framework Programme (FP7/2007-2011) under Grant Agreement n°295487, the BELBaR project

Elasto-plastic constitutive law based on evolving soil structure

Mohamed Oualmakran[1,2], ***Bertrand François***[1]

[1] Université Libre de Bruxelles, Avenue Franklin Roosevelt 50, 1050, Brussels, Belgium
[2] F.R.S.-FNRS, Rue d'Egmont 5, 1000, Brussels, Belgium
moualmak@ulb.ac.be, bertrand.francois@ulb.ac.be

Engineered barrier system for underground nuclear waste disposal involves compacted soil upon unsaturated conditions providing peculiar properties to the material linked to its double structure. Compaction at the dry side of optimum induces an aggregated structure to the soil (Delage et al. 1996). After closure of the disposal, this engineered barrier is submitted to a re-saturation process. At long term, and mainly close to the host rock, the material is fully re-saturated while the microstructure is still aggregated.

The objective of this work is to propose a new constitutive model for such a kind of aggregated soils based on the evolution of pore size distribution along mechanical loading. A physical significance of the structure variable is given by the tracking of the pore size distribution along different compression states. The soil is considered as fully structured when it exhibits a fully developed bi-modal pore size distribution while this structure variable vanishes when the pore size distribution shows a single mode of pore sizes. Particularly, in Figure 1 for a silty soil, different initial microstructures have been obtained from different compaction conditions (dry side of optimum, Fig. 1a; wet side of optimum, Fig 1b). Then, the subsequent loading affects the pore size distribution, mainly for the aggregated soils.

From a constitutive point of view, this evolving microstructure is taken into account through the structure variable that tends to unity when the microstructure passes from bi-modal pore size distribution to a uni-modal distribution. This structure degradation is linked to the generation of volumetric and deviatoric plastic strain.

Strictly speaking, the model is based on the ACMEG model developed for remoulded unsaturated soils (Francois and Laloui 2008) and extends it through the consideration of a structure variable. Irreversible strains are considered through two inter-connected plastic mechanisms. The isotropic mechanism is activated upon hydrostatic loadings while deviatoric mechanism is mobilised upon deviatoric stress states (Figure 2). The apparent preconsolidation pressure (p'c) is the link between both mechanisms. In addition to the conventional strain hardening, the structure variable modifies the apparent preconsolidation. Finally, progressive mobilisation of plasticity can also be activated inside the bounding surface in order to control the smooth transition between elastic and plastic responses. This is particularly well-appropriated for soil with a dispersed structure. The proposed model follows the main concept of the models for structured soils as developed previously by various authors (Kavvadas et Amorosi 2000, Nova et al. 2003, Liu et al. 2013, among others). The new ingredients are related to the double mechanism of plasticity that distinguishes structure degradation induced by deviatoric and isotropic loading.

This model is validated by comparison with experimental results (triaxial and oedometric compression tests (Figure 3)) obtained on re-saturated soils compacted at different moisture contents (in order to generate different microstructures). Also, triaxial tests on heavily overconsolidated soils were carried out to highlight the deviatoric behaviour of isotropically-destructured soils.

References

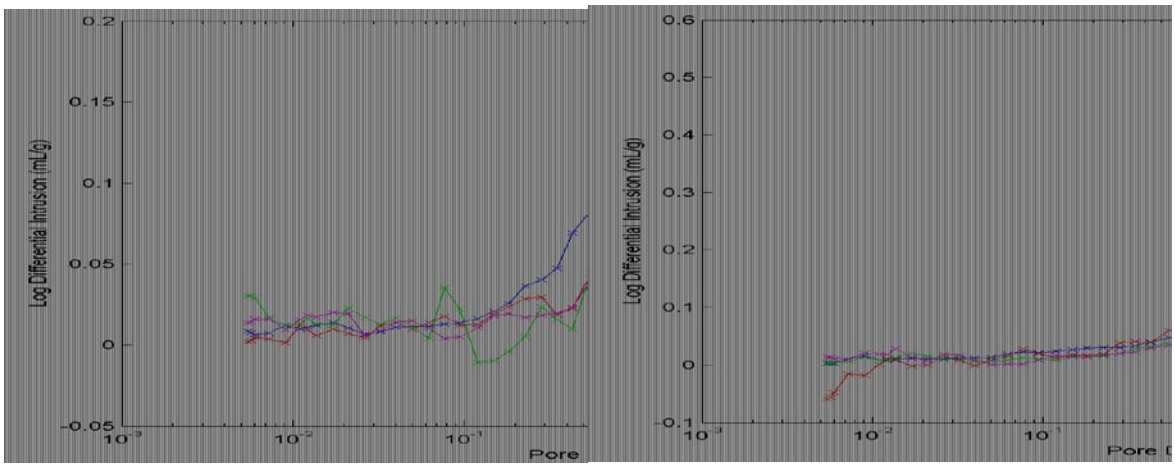
P. Delage, M. Audiguier, Y.J. Cui, M.D. Howat. 1996. Microstructure of a compacted silt. Can. Geotech. J. 33: 150-158.

B. François, L. Laloui. 2008. ACMEG-TS: A constitutive model for unsaturated soils under non-isothermal conditions. Int. J. Numer. Anal. Meth. Geomech. 32 : 1955-1988.

M. Kavvadas, A. Amorosi. 2000. A constitutive model for structured soils. Géotechnique 50(3): 263–273.

R. Nova, R. Castellanza, C. Tamagnini. 2003. A constitutive model for bonded geomaterials subject to mechanical and/or chemical degradation. Int. J. Numer. Anal. Meth. Geomech. 27: 705–732.
W. Liu, M. Shi, L. Miao, L. Xu, D. Zhang. 2013. Constitutive modeling of the destructuration and anisotropy of natural soft clay. Computers and Geotechnics: 24–41.

Illustrations



(a) (b)

Figure 1: Pore Size Distribution of soil: (a) structured soil, (b) unstructured soil. As-compacted state (blue), saturated (red) and loaded in an oedometer at 100 kPa (green) and 1600 kPa (magenta)

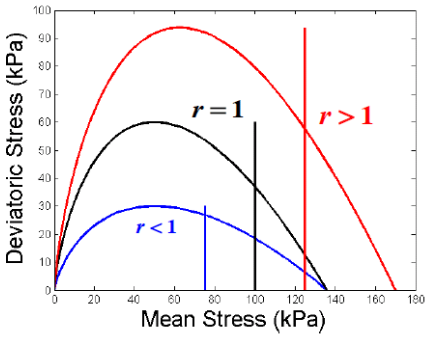


Figure 2: Elastic domain delimited by deviatoric and isotropic Yield Limit. r is the structure variable

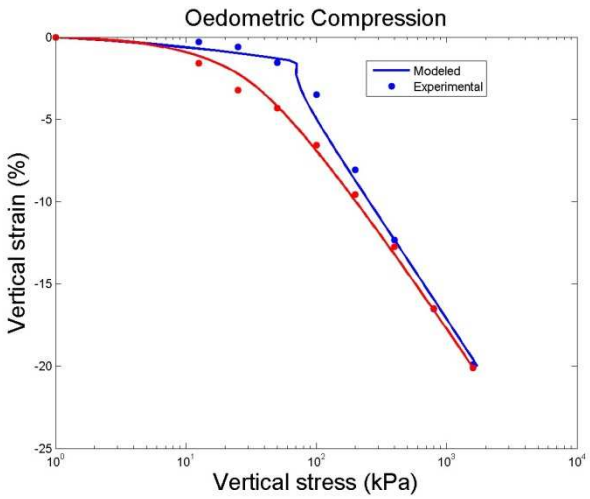


Figure 3: Modeling (solid line) of oedometric compression tests carried on structured (blue) and unstructured (red) soils

Small-strain shear stiffness of compacted MX-80 bentonite

E. Romero[1], J. Suriol[1], A. Lloret[1], X. Pintado[2]

[1] Department of Geotechnical Engineering and Geosciences, Universitat Politècnica de Catalunya, Barcelona, Spain. enrique.romero-morales@upc.edu
[2] B+TECH Oy, Helsinki, Finland

Introduction

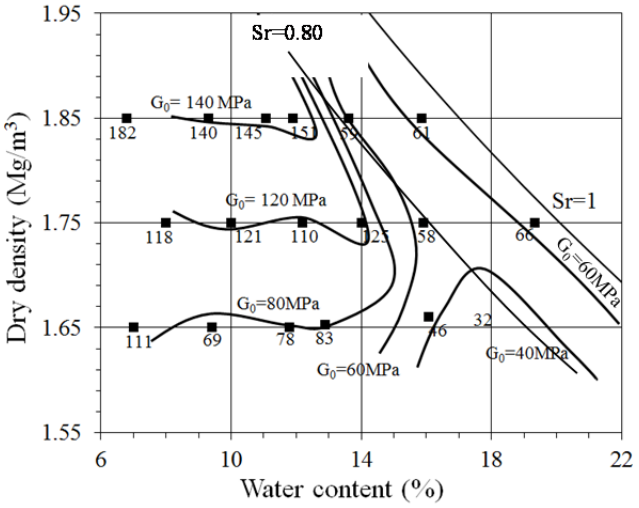
The small-strain shear modulus G_0 of compacted soils depends on void ratio, degree of saturation, overconsolidation ratio, current stress and suction state, and the way the microstructure (pore size distribution) is organised (see for instance, Suriol *et al*. 2014). All these dependencies make the small-strain shear stiffness particularly useful to verify the initial state of a compacted material for use in earthworks or engineered barrier systems. A large number of semi-empirical models have been proposed to predict this small-strain shear modulus, which have been recently extended to tackle with partially saturated (and compacted) states through the use of a generalised stress variable that include information on the degree of saturation, suction and the microstructural state of the sample (Alonso *et al*. 2013). Figure 1 shows the contour plots at constant small-strain shear modulus of compacted silty clay plotted in a Proctor plane. At constant water content (for example, w=12%) and low degrees of saturation S_r, the graph indicates an increase in the shear stiffness with increasing densification, but at certain point (S_r>0.80) the increasing trend is reverted due to the dominant effect of increasing S_r that induces the stiffness to reduce.

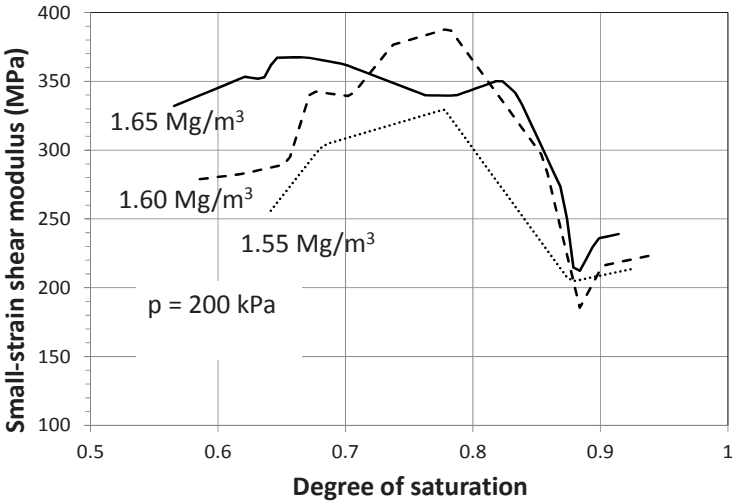
To better understand all these features in more active clays, an experimental study on statically compacted MX-80 bentonite was undertaken, in which the small-strain shear stiffness and damping ratios were systematically studied focusing on the effects of the initial state, the stress state and the microstructure set on compaction.

Experimental methods and results

Stiffness data at different isotropic stresses ranging from p=0.1 to 0.8 MPa were determined using a Stokoe-type resonant column under torsional mode of vibration. The Proctor plane was used to map different initial states, which covered a dry density range between 1.43 and 1.75 Mg/m^3 with degrees of saturation between S_r=0.51 and 0.96. Values of the small-strain shear moduli obtained for compacted MX80 bentonite were in agreement with those reported for compacted FEBEX bentonite (Pintado 2002; Huertas *et al*. 2006). The effect of mean stress p was quantified using the expression $G_0=G_{0.1}(p/0.1)^n$, where parameter $G_{0.1}$ is associated with the value of the small-strain shear modulus at reference mean stress p=0.1 MPa. The exponent n ranged between 0.08 and 0.26 with an average value around 0.2. Figure 2 shows the influence of S_r on G_0 for p=0.2 MPa and dry densities 1.55, 1.60 and 1.65 Mg/m^3. Despite some scattering of the results, it was possible to detect that shear moduli presented maximum values for degrees of saturation around 0.7 and 0.8 and rapidly declined towards a minimum at S_r around 0.9, following a similar behavioural trend to that observed in compacted silty clay (Figure 1). Figure 3 shows the evolution of the shear modulus at increasing shear strains and at p=0.8 MPa, which were fitted to the model proposed by Santos and Correia (2001): $G(\gamma) = G_0/(1+0.385\gamma/\gamma_{0.7})$. Parameter $\gamma_{0.7}$, which corresponds to the shear strain at which G=0.722G_0, displayed certain tendency to increase when the degree of saturation decreased. Damping ratios D increased exponentially with degree of saturation for S_r>0.75 (no important changes of D were detected for S_r between 0.5 and 0.75).

Test results on small-strain shear moduli were interpreted using well-established empirical expressions and a new microstructural framework, which used a generalised stress variable that included information on degree of saturation, suction and the microstructure set on compaction.





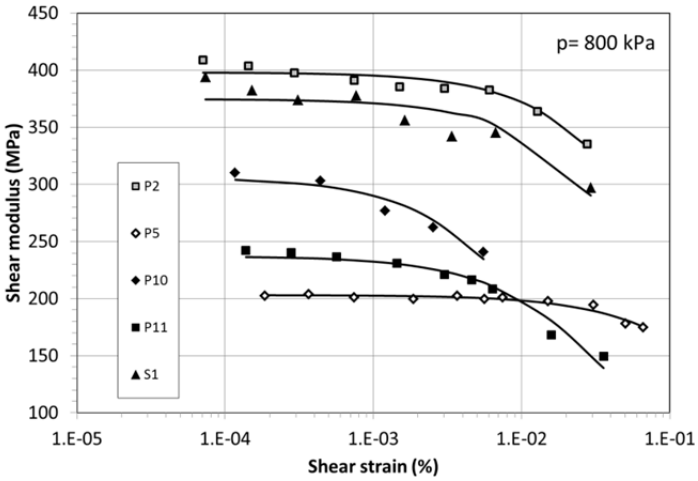


Figure 1 (top left). Contours of equal small-strain shear moduli at p=200 kPa on compacted silty clay (Suriol et al. 2014).
Figure 2 (top right). Evolution of the low-strain shear stiffness of compacted MX-80 with degree of saturation. Curves at different constant values of dry density.
Figure 3 (bottom). Evolution of the shear modulus with shear strain. Test results and predicted values using the small-strain stiffness model.

Acknowledgements
Financial support of POSIVA (Finland) through a collaboration agreement with B+TECH Oy and CIMNE (Spain) 'Small-strain stiffness of statically compacted MX-80 bentonite using resonant column tests' (2013-2014) is greatly acknowledged.

References

Alonso, E. E., Pinyol, N. M. and Gens, A.(2013). Compacted soil behaviour: initial state, structure and constitutive modelling. Géotechnique 63 (6): 463–478.
Huertas, F., Fariña, P., Farias, J., García-Siñeriz, J.L., Villar, M.V., Fernández, A.M., Martín, P.L., Elorza, F.J., Gens, A., Sánchez, M., Lloret, A., Samper, J. and Martínez, M.A. (2006). Full-scale Engineered Barriers Experiment. Updated Final Report 1994-2004. Publicación Técnica Enresa 05-0/2006.
Pintado, X. (2002). Caracterización del comportamiento termo-hidro-mecánico de arcillas expansivas. PhD Thesis, Universitat Politècnica de Catalunya.
Santos, J.A. and Correia, A.G. (2001) Reference threshold shear strain of soils, its application to obtain a unique strain-dependent shear modulus curve for soil. Proc. 15th Int. Conf. on Soil Mechanics and Geotechnical Engineering. Istanbul. Vol 1: 267-270.
Suriol, J., Romero, E., Lloret A. and Vaunat, J. (2014). Small-strain shear stiffness of compacted clays: Initial state and microstructural features. Proceedings of the 6th International Conference on Unsaturated Soils, Sydney, 2014. Unsaturated Soils: Research and Applications, Taylor & Francis Group, London, Vol.1: 769-775.

On the hydromechanical behaviour of Ypresian clays

Xuan-Phu NGUYEN[1,*], *Yu-Jun CUI*[1], *Anh-Minh TANG*[1], *Xiangling LI*[2], *Laurent WOUTERS*[3]

1. Laboratoire Navier (UMR 8205), CNRS, ENPC, IFSTTAR, Université Paris-Est, F-77455 Marne-la-Vallée, France (yujun.cui@enpc.fr; anhminh.tang@enpc.fr)
2. ESV EURIDICE GIE, Boeretang 200, BE-2400, MOL, Belgium (xli@euridice.be)
3. ONDRAF/NIRAS, Avenue des Arts, BE-1210, Brussels, Belgium (l.wouters@nirond.be)
*. Presently at CEA, DEN, DPC, SECR, LECBA, F-91191 Gif-sur-Yvette, France (phunguyenx@gmail.com)

The Ypresian clays are considered as a potential geological host formation in the Belgian radioactive waste disposal program. These marine clays were deposited during the Ypresian age between 55 and 49.6 Ma [1] in the North of Belgium and comprise the Kortrijk Formation (Members of Orchies, Roubaix and Aalbeke) and the Kortemark Member of the overlying Tielt Formation.
Geomechanical studies on Ypresian clays prior to SAFIR 2 [2] are scarce and scattered. In 1997 - 1998, ONDRAF/NIRAS, the Belgian agency for radioactive waste management, drilled a series of boreholes near the Doel NPP, for sedimentological, mineralogical and geochemical analyses with some thermal-hydro-mechanical (THM) characterisation [1]. Ten years later (2008 - 2009), another boreholes were drilled at Kallo, some 7 km to the south of Doel, enabling further thermo-hydro-mechano-chemical investigations [3], [4]. The present work gives an overview on the petrophysical properties and hydromechanical behaviour of Ypresian clays from the Doel and Kallo sites.

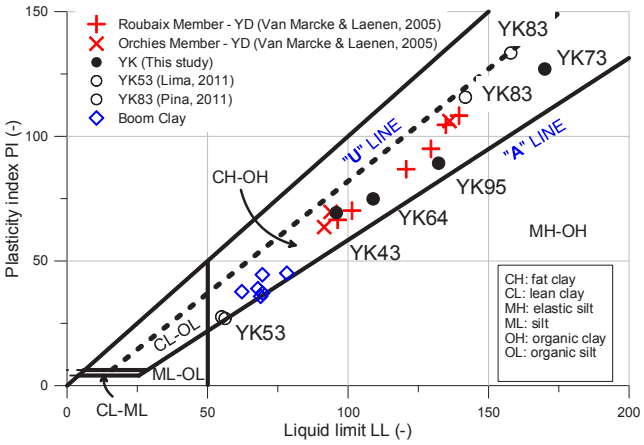


Figure 1: Classification of Ypresian clays at Doel and Kallo according to [5] and compared with Boom Clay

Core	YK43	YK64	YK73	YK95
G_s (-)	2.776	2.785	2.802	2.802
ρ_0 (Mg/m^3)	1.97	1.97	1.90	1.91
ρ_{d0} (Mg/m^3)	1.57	1.55	1.43	1.47
e_0 (-)	0.77	0.79	0.95	0.90
n_0 (%)	44	44	49	47
LL (-)	75.07	113.84	136.61	132.22
PL (-)	33.50	33.75	36.08	43.75
PI (-)	41.57	80.09	100.53	88.47
w_0 (%)	25.78	26.74	32.01	29.78
S_{r0} (%)	93	95	96	93
S_s (m^2/g)	83	149	275	267
VBS (g/100 g)	3.95	7.09	13.12	12.72
% $CaCO_3$ (g/100 g)	10.2	1.4	0.9	3.8

Table 1: Petrophysical properties of Ypresian clays

Petrophysical properties of Ypresian clays at Kallo for the four cores YK43, 64, 73 and 95 are presented in Table 1. It is observed that YK73 and 95 show higher void ratio e_0 and thus lower densities ρ_0, ρ_{d0} than the two lesser deep samples. The consistence limits w_L, w_P of Ypresian clays are significantly higher as compared to Boom Clay, which place them in the CH-OH group according to the ASTM soil classification [5] (Figure 1). Furthermore, w_L of YK73 and 95 are clearly higher than those of YK43 and 64. Microstructural analyses by SEM and MIP point out that YK73 and 95, due to large amount of clay and swelling clay minerals, present a matrix-type microstructure, while YK43 and 64 microstructures are more or less of the aggregate type. The $\%CaCO_3$ is quite low except for the YK43 depth.
Typical high-pressure œdometer compression curve of Ypresian clays (YK73) are presented in Figure 2 with parameters determination according to a conceptual model proposed in [6]. The yield stress σ'_y profile indicates that Ypresian clays are almost normally consolidated. The compression index C_c profile shows that the deeper samples YK73 and 95 are clearly more compressible than the two other samples. YK95 exhibits slightly lower C_c than YK73 which is related to its higher $\%CaCO_3$ given their similar clay mineralogy and thus Atterberg limits. The swelling pressure σ_s deduced from

œdometer tests (high- and low- pressure) with loading/unloading cycles in this study for the Kallo site are consistent with σ_s determined by common swelling test reported for the Doel site. Their profiles are in agreement with the consistence limits one. Vertical hydraulic conductivities k_v of Ypresian clays at Kallo (this study) and Doel [7] agree quite well (Figure 3) except for the YK43 level which is the coarsest one. The failure envelopes of Ypresian clays at Kallo determined from triaxial tests are presented in Figure 4 showing higher shearing strength of YK43 and 64 as compared to the two deeper samples that (dimensions ϕ38-H76) were more or less damaged during extraction upon coring and preparation in the laboratory. The shear strength of the adjacent core YK76 is situated however quite close to the envelope of YK64.

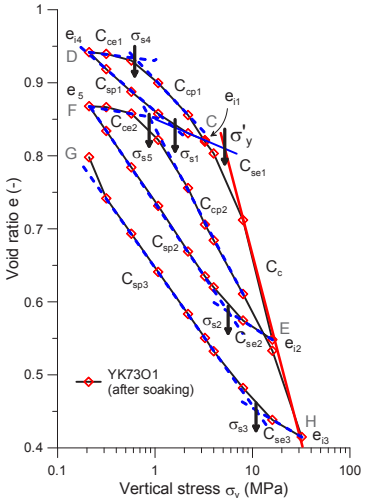


Figure 2: Typical œdometer compression curve of Ypresian clays and parameter determination

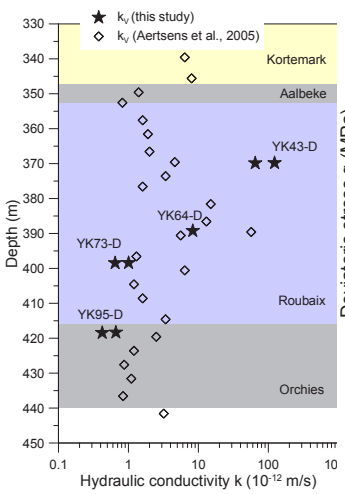


Figure 3: Hydraulic conductivity profile of Ypresian clays at Doel

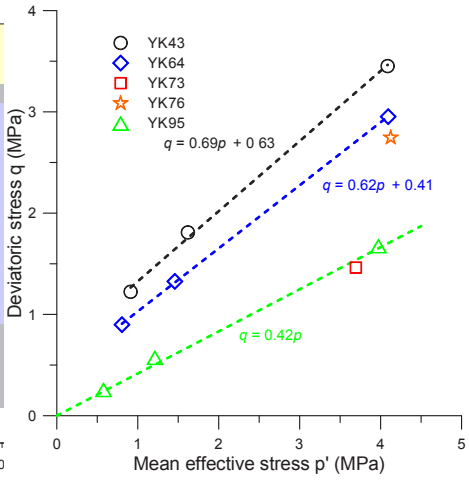


Figure 4: Failure envelope of Ypresian clays at Kallo

References

[1] P. Van Marcke and B. Laenen, "The Ypresian clay as possible host rock for radioactive waste disposal: An evaluation," ONDRAF, 2005.

[2] ONDRAF, "Safety Assessment and Feasibility Interim Report 2," ONDRAF, SAFIR2, Dec. 2001.

[3] A. Lima, "Themo-Hydro-Mechanical behaviour of two deep Belgian clay formations: Boom and Ypresian clays," Universitat Politècnica de Catalunya, Spain, 2011.

[4] X. P. Nguyen, "Étude du comportement chimico-hydro-mécanique des argiles raides dans le contexte du stockage géologique de déchets radioactifs," Ecole des Ponts ParisTech, 2013.

[5] ASTM, *Standard Practice for Classification of Soils for Engineering Purposes (Unified Soil Classification System). ASTM D 2487 - 06*. 2006.

[6] Y. J. Cui, X. P. Nguyen, A. M. Tang, and X. L. Li, "An insight into the unloading/reloading loops on the compression curve of saturated clays," *Applied Clay Science. Submitted*, 2013.

[7] M. Aertsens, A. Dierckx, M. Put, H. Moors, K. Janssen, L. Van Ravestyn, M. Van Gompel, M. Van Gompel, and P. De Cannière, "Determination of the hydraulic conductivity, IIR and the apparent diffusion coefficient on Ieper Clay and Boom Clay cores from the Doel-1 and Doel-2b drillings," Waste & Disposal Department, SCK-CEN, Boeretang 200, 2400 Mol, Belgium, Restricted contract report SCK-CEN-R-3589 02/MAe/P-9, Dec. 2005.

Preliminary comparative study on petrophysical and hydromechanical properties of Boom Clay and Ypresian clays

Xuan-Phu NGUYEN[1,*], *Yu-Jun CUI*[1], *Anh-Minh TANG*[1], *Yongfeng DENG*[2], *Xiangling LI*[3], *Laurent WOUTERS*[4]

1. Laboratoire Navier (UMR 8205), CNRS, ENPC, IFSTTAR, Université Paris-Est, F-77455 Marne-la-Vallée, France (yujun.cui@enpc.fr; anhminh.tang@enpc.fr)
2. Southeast University, Inst. of Geot. Engineering, Transportation College, Nanjing, China (noden@seu.edu.cn)
3. ESV EURIDICE GIE, Boeretang 200, BE-2400, MOL, Belgium (xli@euridice.be)
4. ONDRAF/NIRAS, Avenue des Arts, BE-1210, Brussels, Belgium (l.wouters@nirond.be)
*. Presently at CEA, DEN, DPC, SECR, LECBA, F-91191 Gif-sur-Yvette, France (phunguyenx@gmail.com)

The Boom Clay and Ypresian clays, two Belgian Palaeogene (some 30 and 50 Ma resp.) deposits in the southern part of the North Sea basin, are considered as potential host formations for geological radioactive waste disposal. While Boom Clay at Mol around the URL HADES (reference research site) has been extensively studied since several decades, geomechanical data on this formation at other sites and especially on Ypresian clays are much lesser reported, but mainly petrophysical ones. The present comparative study, based on laboratory tests on Boom Clay taken from Mol at the URL level - BM-URL (223 m depth) and five levels from Essen - BE75 (219 m), 83 (227 m), 96 (240 m), 104 (248 m) and 112 (245 m) - and four Ypresian clays cores from the ON-Kallo-1 borehole - YK43 (330 m), 64 (351 m), 73 (361 m) and 95 (382 m), features principal differences in terms of petrophysical and hydro-mechanical properties between these two geological host candidates. A tentative analysis of their inter-relationship was also made.

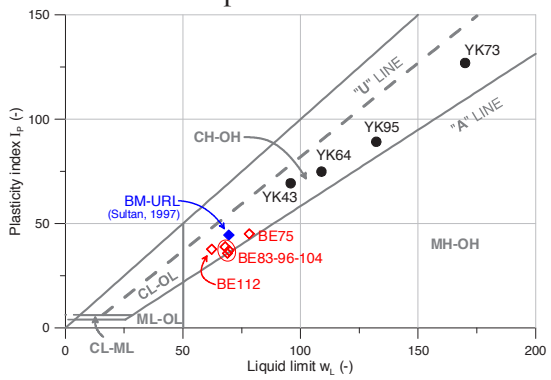


Figure 1: Classification of Boom Clay and Ypresian clays

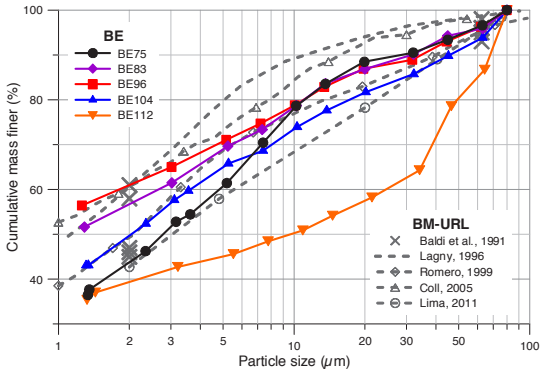


Figure 2: Particle-size distribution of Boom Clay

Amongst the five depths studied (218 - 256 m depth), BE shows a downward increase in quartz accompanied by a decrease in total clay mineral contents. The DRX semi-quantitative mineralogy of BE83 (about 60 % quartz and 40 % clay minerals) is similar to that of BM-URL. The consistence limits w_L, I_P (Figure 1), blue ethylene values *VBS* and specific surface S_s confirm these slight mineralogical differences. w_L, I_P, *VBS* and S_s of Ypresian clays suggest that this latter is significantly more plastic than Boom Clay, probably related to a higher swelling clay fraction, even with a clearly larger variability extent.

The particle-size distribution (PSD) curves of BM-URL found in the literature (all obtained with hydrometer method) exhibit considerable dispersion, suggesting some artefacts related to clay powder suspension preparation (Figure 2). The PSD curves of BE at the five depths are situated in this BM-URL's PSD range apart BE112, which shows coarser granulometry with a dominant particle size around 50 μm. The scanning electron microscopy (SEM) photos of BE112 confirm the dominance of this particle-size family, resulting in an aggregate-type microstructure. SEM photos of BE83 and 96 and that of BM-URL indicate matrix-inclusion type microstructure with preferential alignments of clay particles which is commonly reported in the literature for BM-URL. These two types of microstructure are also identified for the four studied YK samples with aggregate-type for YK43 and to some extent for YK64 while matrix-inclusion type for YK73 and 95. Furthermore, clay particle arrangement in Ypresian clays appears to be more dispersed than in Boom Clay, also suggesting a

higher smectite content in the former. Accordingly, the mercury intrusion porosimetry (MIP) of YK73 and 95 shows two dominant pore-size families (70 nm and 0.3 μm) with higher contribution of the micro-pore family (70 nm) w.r.t the meso-pore family (0.3 μm). This bimodality is quite particular compared to other deep sediments, including Boom Clay (BM-URL, BE83 and 96 with a sole dominant pore-size around 0.1 μm), which often exhibit mono-modal porosity.

The latter particular microstructural feature of Ypresian clays results macroscopically in higher void ratio e_0 than that of Boom Clay, despite their stronger compaction (some 100 m deeper location). This deeper location (higher *in situ* effective stress) and larger dominant pore-size (0.3 vs 0.1 μm) explain the measured unsaturated state of YK cores, which sustain difficultly the sampling-induced suction, while BE and BM-URL cores are almost fully saturated. The carbonates content $\%CaCO_3$ are quite low for BE75, 83, 96 and YK64, 73 (less than 1 %), slightly higher for BE104, 112 and YK95 (3-4 %), and quite high for YK43 (10 %), that have apparently an effect on their mechanical properties.

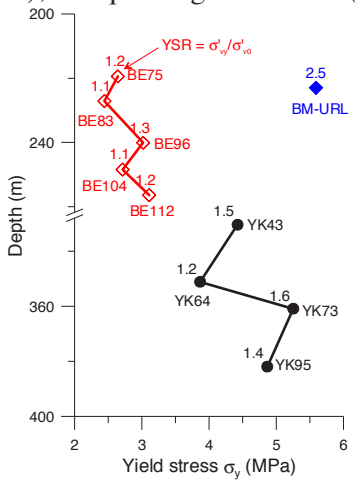


Figure 3: Yield stress of Boom and Ypresian clays

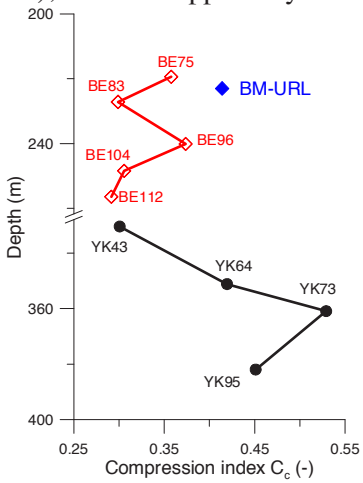


Figure 4: Compression index of Boom and Ypresian clays

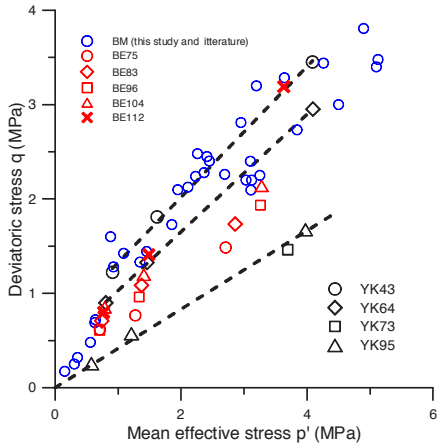


Figure 5: Failure envelopes of Boom and Ypresian clays

The yield stress ratio *YSR* (deduced from œdometer and isotropic compression tests) of both clays ranges from 1.1 to 1.6 except BM-URL which has higher *YSR* = 2.5 (Figure 3). Given the normally consolidated state of BM and limited diagenesis and tectonic activity in the Campine basin, different potential explanations have been raised, such as carbonate cementation effect, long term geochemical reaction, drying during sample storage… Due to this higher *YSR* value, BM-URL exhibits naturally higher compression index C_c than BE (Figure 4). C_c of YK appears to increase in the order YK43, 64 and 73 then to decrease to YK95, which is the same order as the consistence limits variations (Figure 1). Note that the $\%CaCO_3$ of YK95 is also higher than that of YK73.

On the deviatoric behaviour, BM presents the largest failure envelope, with a bi-linear shape that can be explained by the swelling effect under low confining pressure *p'* (Figure 5). BE112, YK43 and to some extent YK64 are also in the same range with BM thanks to their relatively coarse granulometry. BE112 exhibits the largest internal friction angle φ' which is related to its particularly coarser granulometry (Figure 2). As triaxial sample of YK73 and 95 are significantly damaged during preparation, their failure envelopes appear similar to those of reconstituted soils. The failure envelope of BE83 and 96 are quite close while that of BE75 is slightly below and BE114 a little above. Note that w_L of BE75 (Figure 1) and $\%CaCO_3$ of BE104 are higher than the corresponding values of BE83 and 96.

The common semi-logarithmically linear increase of permeability with void ratio for each core of Boom Clay and Ypresian clays is identified. Permeabilities of BE75, 83 and 96 are similar over a void ratio range e = 0.3-0.8, which are slightly lower than those of BM-URL and BE104. BE112 exhibits clearly higher permeability due to its coarser granulometry. Permeability of YK43 is even higher than that of BE112, while YK73 and 95' permeability is about one order lower than that of BE75. This latter feature emanated from the dominance of their micro-pore family, identified by MIP analyses, while water transport is mainly controlled by meso- and macro-pore families.

Acknowledgement

The financial support and soil core supply from ONDRAF/NIRAS and EURIDICE are greatly acknowledged. The views expressed in this paper are mainly based on experimental results and do not engage ONDRAF/NIRAS and EURIDICE in any matter.

Investigating the deviatoric behaviour of Boom Clay

Xuan-Phu NGUYEN[1,*], *Yu-Jun CUI*[1], *Anh-Minh TANG*[1], *Xiangling LI*[2]

1. Laboratoire Navier (UMR 8205), CNRS, ENPC, IFSTTAR, Université Paris-Est, F-77455 Marne-la-Vallée, France (yujun.cui@enpc.fr; anhminh.tang@enpc.fr)
2. ESV EURIDICE GIE, Boeretang 200, BE-2400, MOL, Belgium (xli@euridice.be)
*. Presently at CEA, DEN, DPC, SECR, LECBA, F-91191 Gif-sur-Yvette, France (phunguyenx@gmail.com)

Being considered as a potential host formation in the Belgian geological radioactive waste disposal RD&D program, Boom Clay has been extensively investigated since the seventies [1]. Most of deviatoric characterisations were carried out in traditional triaxial cells on small cylindrical samples (height and diameter of several centimetres with their ratio of about 2). The loading and strain responses of the sample were in general measured globally using, for example, Controller of Pressure/Volume (CPV) and/or displacement transducer installed on the piston outside the confining chamber. In some studies, Linear Variable Differential Transformer (LVDT) was installed directly in contact with sample so as to monitor the local displacement of the sample at the contact point. But due to the complexity of such installation in a small space, the number of measured local displacements is rather limited and hence the interpretation of local and global responses is sometimes quite difficult, given the "barrel" shape of the deformed sample and the shear band formation. Furthermore, the axial strain ε_{ag} determined by external displacement transducer has largely been reported to be overestimated, especially for hard soils and rocks, due to compliance of the contacts between pedestal - sample - top cap - piston, and consequently underestimating the (axial) Young modulus. In addition, few detailed investigations of the damage-induced Young modulus evolution of Boom Clay upon shearing and its behaviour during unloading-reloading loops have been reported so far [2], [3].

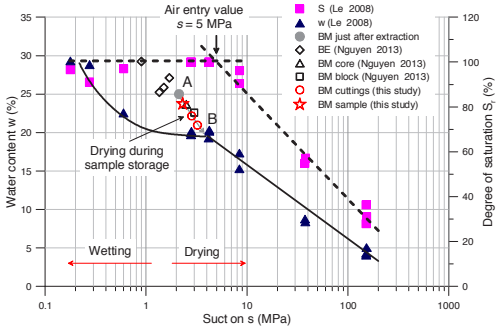


Figure 1: Initial hydric state of the sample

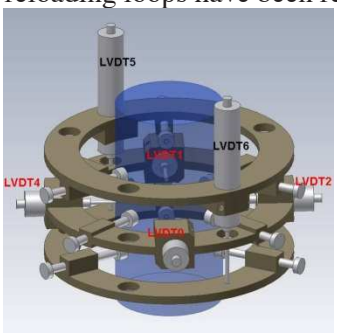


Figure 2: LVDTs' layout

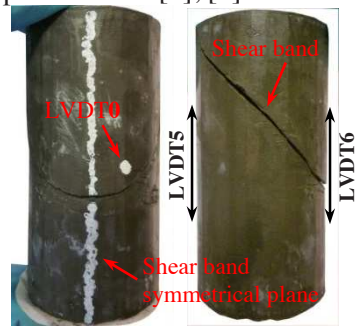


Figure 3: after-test sample

The present work highlights the local and global response of Boom Clay upon shearing with several unloading-reloading cycles by means of an advanced triaxial cell. This latter was equipped with (i) a global axial displacement transducer installed outside the cell on the piston; (ii) two axial LVDTs, numbered 5 and 6, in diametrical position, measuring the relative displacement between the top and bottom fixing rings spaced 30 mm apart (**Error! Reference source not found.**); (iii) four radial LVDTs, numbered 0, 1, 2 and 4, also in diametrical positions in two perpendicular directions installed at the sample's mid-height (**Error! Reference source not found.**); (iv) two force sensors at the two ends of the piston, inside and outside the cell, one in direct contact with the top cap while other blocked by a traverse; and (v) a back-pressure and a confining-pressure CPVs. Accordingly, the global axial strain ε_{ag} (only upon shearing), the local (mid- height) axial $\varepsilon_{a\ell}$, radial $\varepsilon_{r\ell}$ and volumetric $\varepsilon_{v\ell} = \varepsilon_{a\ell} + 2\varepsilon_{r\ell}$ strains, the global volumetric strains $\varepsilon_{vg\text{-}CP}$ and $\varepsilon_{vg\text{-}conf}$ respectively by back-pressure and confining-pressure CPVs, the interior F_{int} and exterior F_{ext} axial forces are monitored during a CD triaxial test with shearing at imposed axial displacement rate (1 μm/mn, corresponding to a strain rate of approx. 1.3×10^{-5} mn^{-1}).

The Boom Clay studied in this work was from a horizontally extracted core of 100 mm diameter and 800 mm length from the URL HADES at 223 m depth below ground level. The specimen was prepared by hand-trimming into a cylinder of 38 mm diameter and 76 mm height perpendicular to the bedding plane. The initial water content, density, void ratio and degree of saturation of the sample are respectively w_0 = 23.73 %, ρ_0 = 2.03 (Mg/m^3), e_0 = 0.63 and S_{r0} = 100 %. The initial water content w_0

and suction s_0 of the soil were also determined and reported in **Error! Reference source not found.** along with the water retention curve [4]. The initial suction of the sample was estimated at around s_0 = 2.3 MPa, which was still lower than the air entry value s = 5 MPa and quite close to the *in situ* effective stress. This suggests the fully saturated state of the sample.

The sample was stepwise isotropically consolidated up to a confining pressure equal to the *in situ* effective stress $p_{conf} = \sigma'_{v0}$ = 2.4 MPa. The drainage system was then saturated with Boom Clay synthetic water. After that, both p_{conf} and the back-pressure p_{CP} were stepwise increased in such a way that their difference was constant at $p'_c = p_{conf} - p_{CP} = \sigma'_{v0}$ till p_{CP} = 1 MPa. The sample was kept under these pressures for soil deformation stabilization. It is observed (Figure 4) that the averages of the two radial perpendicular diametrical couples' measures, 0-1 and 2-4, arre almost the same, indicating an isotropic behaviour of Boom Clay in the horizontal (bedding) plan, before and after soaking. Comparison of $\varepsilon_{a\ell}$ and $\varepsilon_{r\ell}$ shows that Boom Clay compression is almost isotropic, except at the beginning, under p_{conf} up to σ'_{v0} = 2.4 MPa without contact with water, while its swelling (happened even under $p'_c = \sigma'_{v0}$ = 2.4 MPa) is clearly orthotropic, in relation to the preferential alignment of clay particles along the bedding which was evidenced by various microstructural analyses.

The shearing stage, under $p'_c = \sigma'_{v0}$ = 2.4 MPa, with five pre-peak and one post-peak unloading-reloading loops, evidenced that the exterior load sensor cannot be used to compute the axial stress σ_a as the friction between the piston and the cover changes significantly when the displacement direction was inversed. The deviatoric curve q - ε_a indicated a maximum deviator stress q_{max} = 2.1 MPa and a residual value q_r = 1.3 MPa, defining a critical state coefficient M = 0.46, lower than those reported by [5] with M = 0.62 for the same depth (URL HADES) and *0.9* for 17 m deeper (Experimental Shaft).The yield state was also determined and compared with the existing data.

Six unloading-reloading hysteretic loops on each q - ε_{ag}, q - $\varepsilon_{a\ell}$, q - $\varepsilon_{r\ell}$ and p' - ε_{vg}, p' - $\varepsilon_{v\ell}$ curves were clearly observed, even at the beginning of shearing ($\varepsilon_{a\ell} < 5\times10^{-4}$). These hysteresis can be explained by: (i) two technical reasons, one related to the "loosening gear contact" in the press under low displacement rate when inversing the moving direction, and the other to the compliance of the piston - top cap - sample and sample - pedestal contacts; (ii) inherent competition between physicochemical and mechanical effects of the clayey material [6]; and the shear band.

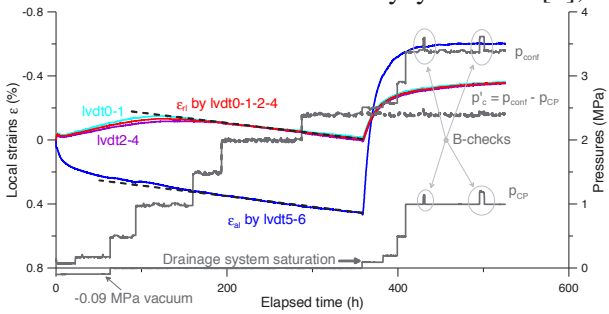


Figure 4: Local strains $\varepsilon_{a\ell}$ and $\varepsilon_{r\ell}$ during the consolidation stage

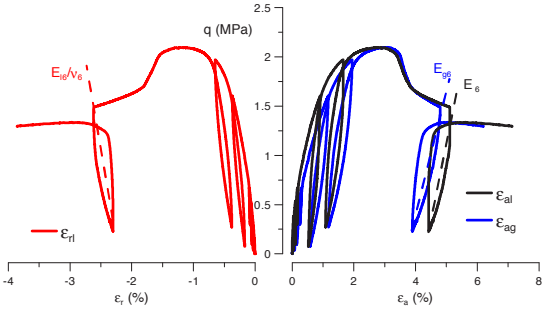


Figure 5: Deviator stress q versus radial $\varepsilon_{r\ell}$ and axial $\varepsilon_{a\ell}$, ε_{ag} strains during shearing

Luckily, the LVDT couple 0-1 was installed almost along the symmetrical plane of the shear band, while 2-4 perpendicular, and the two fixing points of the axial LVDT6 were in the two parts of the specimen separated by the shear band while those of the other axial LVDT5 were all in the lower part (Figures 2 and 3). This particular disposition allows following the initiation (opening upon (re)loading - closing upon unloading for the first loops under low deviator stress q < 0.2 MPa) and development (irreversible opening) of the shear band. As far as the volumetric behaviour is concerned, contrasting fashions were observed between local (mid-plane) $\varepsilon_{v\ell}$ and global ε_{vg} strains, especially in the beginning when the "barrel" form of the sample was developing. Decreases of Young modulus E and Poisson ratio ν with axial strain in power law were evidenced. Significant difference was identified between the locally measured Young modulus and globally measured one: $E_\ell > E_g$, suggesting that many reported values of Boom Clay Young modulus in the literature are underestimated.

Acknowledgement

The financial support and soil core supply from ONDRAF/NIRAS and EURIDICE are greatly acknowledged. The views expressed in this paper are that of the authors and do not engage ONDRAF/NIRAS and EURIDICE in any matter.

References

[1] ONDRAF, "Safety Assessment and Feasibility Interim Report 2," ONDRAF, SAFIR2, Dec. 2001.

[2] R. J. Mair, R. N. Taylor, and B. G. Clarke, "Repository tunnel construction in deep clay formations," Commision of the European Communities, Nuclear Science Technology, Report EUR 13964 EN, 1992.

[3] H. D. Yu, W. Z. Chen, X. L. Li, and X. Sillen, "A Transversely Isotropic Damage Model for Boom Clay," *Rock Mechanics and Rock Engineering*, vol. 47, no. 1, pp. 207–219, 2014.

[4] T. T. Le, "Comportement Thermo-Hydro-Mécanique de l'argile de Boom," Ecole des Ponts ParisTech, France, 2008.

[5] G. Baldi, A. Hueckel, A. Peano, and R. Pellegrini, "Developments in modelling of thermo-hydro-geomechanical behaviour of Boom clay and clay-based buffer materials," Commission of the European Communities, EUR 13964 EN, 1991.

[6] Y. J. Cui, X. P. Nguyen, A. M. Tang, and X. L. Li, "An insight into the unloading/reloading loops on the compression curve of natural stiff clays," *Applied Clay Science*, vol. 83–84, pp. 343 – 348, 2013.

The effects of suction and temperature on micro porosity variation in compacted bentonite based on a solid-solution geochemical model

Majid Sedighi **and Hywel R. Thomas**

Geoenvironmental Research Centre, School of Engineering, Cardiff University, The Queen's Buildings, Newport Road, Cardiff, CF24 3AA, UK
Email: SedighiM@cf.ac.uk; Tel. 0044 2920 874004

Abstract

A new approach to investigate the variation of microscopic porosity/pore water in compacted bentonite with suction and temperature is presented in this paper. The theoretical formulation is based on a geochemical modelling of the interlayer hydration/dehydration of smectite minerals using regular solid-solution reaction. The thermodynamic parameters of the model for the case of compacted FEBEX bentonite are presented. Using this approach the micro/macro-porosity evolutions with suction and temperature under retrained swelling conditions are discussed. The results provide an insight into the evolution of pore water in compacted bentonite with suction at different temperature values and quantify the distribution of water in micro and macro pores in the system. An application of the model in simulation of the flow of water and chloride in compacted FEBEX bentonite under non-isothermal water infiltration is described and the results are compared with the experimental data.

Modelling of large-scale *in situ* ventilation test in clayey rock

***B. Pardoen*[1,2], F. Collin[1], J. Talandier[3]**

[1] ArGEnCo Department, University of Liège, Liège, 4000, Belgium,
[2] FRIA, F.R.S.-FNRS scholarship holder. E-mail: b.pardoen@ulg.ac.be
[3] Andra, R&D Division, 92298 Chatenay-Malabery, France.

The underground long-term repository of radioactive waste in low permeability media needs a good understanding of the host formation behaviour. The desaturation of the clayey rock as well as of the damaged zone located around underground galleries is an important issue considering the safety function of the clay formation. A large-scale gallery ventilation test (SDZ) is performed by the French National Radioactive Waste Management Agency (Andra) in the Callovo-Oxfordian claystone in order to highlight ventilation effects on the host rock. *In situ* measurements indicate that drainage occurs in the rock mass and that desaturation can appear close to the gallery. To reproduce theses phenomenon, a two-dimensional plane strain state hydro-mechanical modelling of a gallery excavation and ventilation is performed (Lagamine code, ULg), taking into account the damaged zone development and the rock-atmosphere interaction.

The constitutive mechanical law used to model the clayey rock is an elasto-plastic model. The material plasticity is defined by a non-associated Van Eeckelen yield surface. A flow model is used to reproduce transfers in partially saturated porous media. The different parameters used in the model are obtained from the literature and from experimental data fitting.

To properly model the hydromechanical coupling occurring in the claystone, we model the damaged zone and its permeability variation. In fact, the drilling of underground galleries induces damage propagation in the surrounding medium and creates a damaged zone in which the material properties are modified (Blümling et al. 2007). The rock-atmosphere interaction is another crucial issue that conditions the drainage kinetics in the claystone. A nonclassical hydraulic boundary condition including water and vapour exchanges is used to model the hydraulic transfers between the cavity and the rock (Gerard et al. 2008). Once the permeability evolution and the rock-atmosphere interaction are well captured, the ventilation test is modelled and the numerical results are compared to *in situ* measurements.

The numerical results indicate that it is possible to calibrate the model to obtain a satisfactory reproduction of the in-situ experimental measurements and a better understanding of the fluid transfer around the gallery during the test. Concerning the damaged zone, the hydro-mechanical model exhibits a plastic zone extension similar to the in situ measurements.

References :

Blümling P, Bernier F, Lebon P, Martin CD (2007) The excavation damaged zone in clay formations time-dependent behaviour and influence on performance assessment. Phys Chem Earth 32(8–14):588–599

Gerard P, Charlier R, Chambon R, Collin F (2008) Influence of evaporation and seepage on the convergence of a ventilated cavity. Water Resour. Res., 44: W00C02. doi: 10.1029/2007WR006500

Steel corrosion effects on the thermo-hydro-mechanical process in an underground disposal tunnel for high-level wastes

Hanbing Bian[a], Yun Jia[b], Jianfu Shao[b], Adrien Poutrel[c]

a- LEM3 UMR CNRS 7239, Université de Lorraine, Ile du Saulcy, 57045 Metz Cedex 01, France
b-LML UMR CNRS 8107, Polytech'Lille, Cité Scientifique, 59655 Villeneuve d'Ascq, France
c-French National Radioactive Waste management Agency (ANDRA), 92298 Chatenay Malabry, France

In order to minimize the release of radionuclide to biosphere, the multi-barrier system is widely used in the design of underground repositories for high-level radioactive wastes (HLW). It involves the geological barrier and various engineered barriers, such as the waste matrix, the metallic container/over pack, the buffer material and the disposal liner. After the emplacement of waste packages, the engineered barriers are subjected to coupled thermal, hydraulic and mechanical (THM) processes, such as the decay heat of waste packages, the intrusion of groundwater from geological barrier, the stress changes due to the corrosion of steel components and the swelling of buffer material, etc…. On the other hand, the THM processes occurring in the engineered barriers interact also with the THM behaviour of the geological barrier in which it is constructed. These coupling processes may accelerate the movement of groundwater and radionuclide through the multi-barrier system. In view of this the long-term safety analysis of underground repository for HLW requires a good knowledge on the THM processes developed in the engineered barriers and geological barrier.

Numerous experimental programs simulating a multi-barrier system have been performed by different disposal organizations. However, an experimental design can incorporate only one multi-barrier system and its duration is much shorter than the real lifetime of underground repository. With recent developments in theoretic and computational techniques, the numerical simulation using a computer code becomes the most provocative and comprehensive approach to study the coupled THM processes occurring in the multi-barrier system on the long-term scale. However, the stress changes related to the corrosion of metallic components of engineered barrier system have not been detailed analyzed in previous studies. In the present study, the steel corrosion observed in the engineered barrier system will be incorporated in the numerical analysis of THM processes of underground repository for HLW, which is under construction in France. The numerical simulation will be realized by using the full coupled finite element calculation code THMPASA, which has been developed in the mechanical laboratory of Lille (LML) and has been applied to numerous applications in the underground radioactive waste disposal.

In France, the future underground repository for HLW is located in a stable geological formation, called Callovo-Oxfordian claystone. Based on the design concept defined by ANDRA (French National Radioactive Waste management Agency) during the period from 2004 to 2009, the primary package of HLW, delivered by the waste producers, is placed in a sealed unalloyed steel overpack. The total is then emplaced in a small diameter tunnel supported by a steel liner. The steel liner is to aid the emplacement and the retrievability of vitrified waste packages. In this configuration, the engineered barriers are the waste matrix, the steel overpack and the tunnel liner. In the underground structure of repository, the steel barriers may be corroded by the eventual contact with groundwater coming from the host rock. The major harmful effect of corrosion is the reduction of steel thickness leading to loss of mechanical strength and the failure of metallic barriers. In order to guarantee the retrievability of HLW and the long-term safety of underground repository, it is necessary to take into account the effect of steel corrosion for the analysis of the coupled THM processes in the disposal tunnel for HLW.

According to the numerical simulation of steel corrosion processes, three categories of numerical models have been formulated by ANDRA: semi-empirical models, mechanistic models and archaeological analysis approach. However, the validation of the semi-empirical and mechanistic

models is very difficult, especially on the long-term scale, because the duration of available laboratory tests is much shorter than the lifetime of underground repository. On the other hand, the archaeological analysis gives us some detailed information on steel corrosion for very long periods. However, the steel used for steel barriers of underground repository for HLW is quite different from typical archaeological materials which have been largely studied. Consequently, the archaeological results should be combined with theoretical calculations and available laboratory data obtained on the steel for HLW repository. In this study, the available archaeological results and laboratory tests obtained on the steel corrosion will be incorporated in the numerical analysis of THM processes in the disposal tunnel for HLW.

In this paper, after a general presentation of poroelastic model based on the non-linear poroelasticity theory of Coussy, the visco-elasto-plastic model particularly developed for the Callovo-Oxfordian Claystone is briefly introduced, and its performance is verified by simulating some laboratory tests. According to the steel components, its mechanical behaviour is described by an elastoplastic model of von-Mises type. The effects of steel corrosion are simulated quantitatively by a decrease of mechanical properties and a volumetric expansion related to corrosion products. Finally, a disposal tunnel for HLW is simulated and analyzed. The detailed geometry of the engineered barrier system is incorporated into the numerical calculation. The interpretation and discussion of numerical results can help the engineers to complete their understanding on the THM processes in the disposal tunnel and to evaluate the long-term safety of underground repository and the irretrievability of waste packages.

The concrete interface stability analysis during the hydro-mechanical process in an underground disposal tunnel

Hanbing Bian[a], **Yun Jia**[b], **Jianfu Shao**[b], **Antoine Pasteau**[c]

a- LEM3 UMR CNRS 7239, Université de Lorraine, Ile du Saulcy, 57045 Metz Cedex 01, France
b-LML UMR CNRS 8107, Polytech'Lille, Cité Scientifique, 59655 Villeneuve d'Ascq, France
c-French National Radioactive Waste management Agency (ANDRA), 92298 Chatenay Malabry, France

In order to minimize the release of radionuclide to biosphere, the multi-barrier system is widely used in the design of underground repositories for high-level radioactive wastes (HLW).It involves the geological barrier and various engineered barriers, such as the waste matrix, the metallic container/over pack, the buffer material and the disposal liner. After the emplacement of waste packages, the engineered barriers are subjected to coupled thermal, hydraulic and mechanical (THM) processes, such as the decay heat of waste packages, the intrusion of groundwater from geological barrier, and the stress changes due to the swelling of buffer material, etc…. On the other hand, the THM processes occurring in the engineered barriers interact also with the THM behaviour of the geological barrier in which it is constructed. These coupling processes may accelerate the movement of groundwater and radionuclide through the multi-barrier system. In view of this the long-term safety analysis of underground repository for HLW requires a good knowledge on the THM processes developed in the engineered barriers and geological barrier.

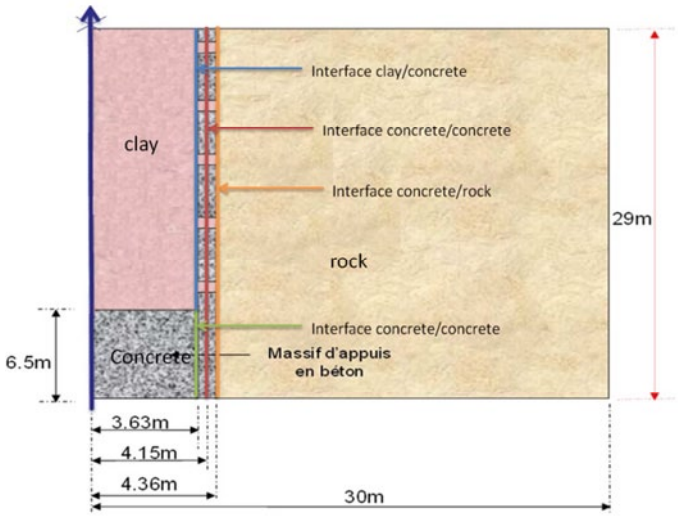


Fig. 1 Illustration of the selling of a underground radioactive disposal tunnel

One of most important points considered in this topic is the interfaces stability, as illustrated in the Fig. 1. In this configuration there are several interfaces, such as the interface clay/concrete, the interface concrete/rock and interface concrete/concrete. In fact, after the closure of the gallery, the water from the around rock penetrated into the swelling clay, and then the clay begin to "swelling" and push the massif concrete. As a results, the stability of the massif concrete is of a major concerns.

Based on the ancient work of Bandis, Barton, etc., we propose a constitutive model for the concrete interface, which taken into consideration not only the microstructure of joint surface, but also the degradation of mechanical behaviour of joint in function of time. The proposed model has several advantages. Firstly, because of the simplicity of its mathematical formulation, it is easy to implement in a calculation code. Secondly, it is based on physical considerations: the loading surface and plastic

potential defined from the microstructure of interface. By relating the regular asperities angle to the roughness coefficient of the interface, the proposed model initially for idealized concrete interface with a series saw-tooth is valid for all types of interface with different microstructure on the interface surface.

Traditionally, in the numerical simulation realized by means of finite element method, the interface is considered by using zero-thickness interface elements proposed by Goodman (Goodman et al., 1968). This special element is placed between neighbouring classical finite elements, along expected crack path. If the crack path is not known in advance, either remeshing is applied, or a sufficiently fine mesh must be used containing interface elements along all inter-element boundaries. The high number of elements may lead to substantial calculation times. Furthermore, a theoretically infinite dummy stiffness is usually required to keep the inactive interface element closed. The dummy stiffness might cause a poor conditioning of the system of equations and consequently inaccurate results. Based on partition of unity method, the XFEM (extended finite element) proposed by Moës and his colleagues (Möes et al., 1999), firstly as a method for analyzing crack growth without remeshing by using enrichment functions to simulate the discontinuous with a fixed mesh, has been successfully used for several years for the numerical simulation of cracked structures under statically and later under dynamically loading. It is now become an efficient way to reduce mesh dependency for macro-cracks growth analysis. This method has been adopted in the long term slope stability analysis of the concrete interface and its eventual propagation in the underground radioactive disposal tunnel.

The purpose of this paper is to propose a numerical model for predicting the long term stability of concrete interface, due to the push of the swelling clay and its eventual mechanical degradation of concrete. The proposed model and the XFEM has been incorporated into a full coupled calculation code. Firstly, the formulation of the model for interface is briefly recalled, and then, the crack initiation criteria and the crack direction criteria for the XFEM calculation are presented and discussed. And some validation examples have been presented and discussed. Finally, the proposed numerical approach has been applied to the concrete interface stability analysis during the hydro-mechanical process in an underground disposal tunnel.

Numerical investigation of damage and crack porosity closure effects on the soil-structure interaction around a deep drift at the Meuse/Haute-Marne URL

M. Souley[(1)], **D. Seyedi**[(2)], **G. Armand**[(3)], **M. Ghoreychi**[(4)]

[1] INERIS, Ecole des Mines, Campus ARTEM, 54042 Nancy, France (Mountaka.Souley@ineris.fr)
[2] Andra R&D, 92298 Chatenay-Malabry, France
[3] Andra R&D, Meuse/Haute-Marne Underground Research Laboratory, 55290 Bure, France
[4] INERIS, BP 2, 60550 Verneuil-en-Halatte, France

Since 2000, the French National Radioactive Waste Management Agency (Andra) has been constructing an Underground Research Laboratory (URL) at Bure to perform experiments in order to obtain the *in situ* data necessary to demonstrate the feasibility of a geological repository in the Callovo-Oxfordian claystone (COx) formation. The excavation of galleries at the main level of the laboratory showed a significant fracturing induced by the excavation. One can distinguish a connected fractured zone (with extensional and shear fractures) and a zone of discrete fracturing. The extent of the fractured zones depends on the orientation of the drift with respect to the initial stress state (Armand *et al*. 2014). The short and long terms hydromechanical behavior is closely related to the behavior of the induced fractured zone as indicated by the *in situ* strain measurements. Similarly, the nature and extent of these fractured zones directly act on the magnitude of loading transferred to the concrete supporting elements. Hence it is necessary to account for the damage induced by the excavation in order to understand the long-term behavior of the couple COx – structural supports. Indeed, the loading-unloading of the plate test carried out at the wall of the GET gallery (parallel to the major horizontal stress) shows a change in the stiffness of the fractured zone as a function of the load (Vu et al., 2015). The increase of the rigidity can be explained by the mechanical closure of the induced fractures under compressive loading. This phenomenon is similar to those observed in the mechanics of rock joints or the re-closure of initial gap observed at the beginning of triaxial tests on soft rocks or soils. The evolution of the stiffness of the fractured zone, i.e., stiffness degradation due to excavation and partial stiffness recovery due to fracture closure affect the loads transferred to structural elements. The main goal of the present paper is to provide insights on the role of this stiffness change and its effect for a more accurate design of different repository structures.

In the framework of a scientific collaboration between Andra and INERIS, a macroscopic isotropic visco-elastoplastic model, which accounts for the impact of induced damage (modeled through a plastic hardening function) on the viscoplastic strain rates, has been developed (Souley et al. 2011) and used in several design and predicting studies of the mechanical and hydromechanical behavior around the Meuse/Haute-Marne URL structures. The results of tests performed on claystone samples showed that after the peak strength, the post-peak phase is characterized by development of damage and localized strain area which leading to the creation of a shear failure plane in compression or a transverse plane of failure in extension. It can therefore reasonably link the fractured zone to the extent of zones where the mechanical behavior enters in post peak or residual phase. The previous visco-plastic model is then improved by incorporating "a stiffness degradation part" in the post-peak region. The Young modulus varies linearly between E_0 and E_{min} according to an internal damage variable defined as: $d=\min(\gamma/\gamma^{ult}, 1)$, where γ is the plastic shear strain, γ^{ult} is the ultimate strain beyond which the macro-fractures occur in the sample. For instance, a simple form of damage variable as a function of plastic strain is considered unlike more frequent expressions encountered in the literature of the continuum damage mechanics, in order to investigate the role of this stiffness change on the structural behavior.

Once a rigid liner is installed, the creep of the surrounding rocks combined to the rigid boundary provided by the liner can produce a progressive closure of some of cracks or fracturing resulting to a partial stiffness recovery of the fractured zone. A progressive closure of cracks porosity with the volumetric strain

relationship is considered to model this phenomenon. First, a linear variation (increase from E_{min} to E_{reload}) of the Young modulus according to the variation of the compressive mean stress ($<\Delta P_{mean}>$-) is considered. The mass conservation allows then to express the Young's modulus of re-loading as a function of the total porosity of the micro-fractured element. In a second times, a nonlinear evolution (Bourgeois et al. 2005) of E with respect to ($<\Delta P_{mean}>$-) was also used.

The two macroscopic mechanisms (damage induced by the excavation and the stiffening due to reconfinement of fractured zone) were incorporated into the previous model and implemented in FLAC^{3D}. As an application, a gallery of large diameter (ϕ= 10.82 m) oriented in the direction of the minor horizontal stress was simulated in 2D following the convergence-confinement method. A very rigid liner (with 5.1 and 4.3 m outer and inner radii respectively) was set up, and a soft packing material is used to fill gap between the converged gallery and the support. The duration of the simulation is 100 years. Three cases are discussed: (a) a simulation that does not take into account the damage induced the excavation, $E = E_0$; (b) a case where only the induced damage is considered, $E = E_D$; (c) a simulation integrating both the induced damage and module restoration, $E = E_{D+Closure}$. Figure 1 (a)-(c) shows the magnitude of the displacement in the support after 100 years. In the first case ($E = E_0$), there is very little convergence of roof and drift walls compared to the floor convergence. This results in a vertical compression of the support leading to its ovalization in the horizontal direction. In contrary, in two other cases, an overall vertical movement of the rigid structure occurs, and as the viscoplastic strain rates are higher in the sides of the drift than at the floor-roof, the support crushing occurs in horizontal direction. The restoration of modules ($E_{D+Closure}$) tends to reduce the displacement transmitted to the structure. This analysis is in agreement with the predicted orthoradial stresses illustrated in Figure 1 (d)-(f). Finally, the present study opens an opportunity in understanding the complex mechanism of interaction between the supports and the long term behavior of the fractured zone.

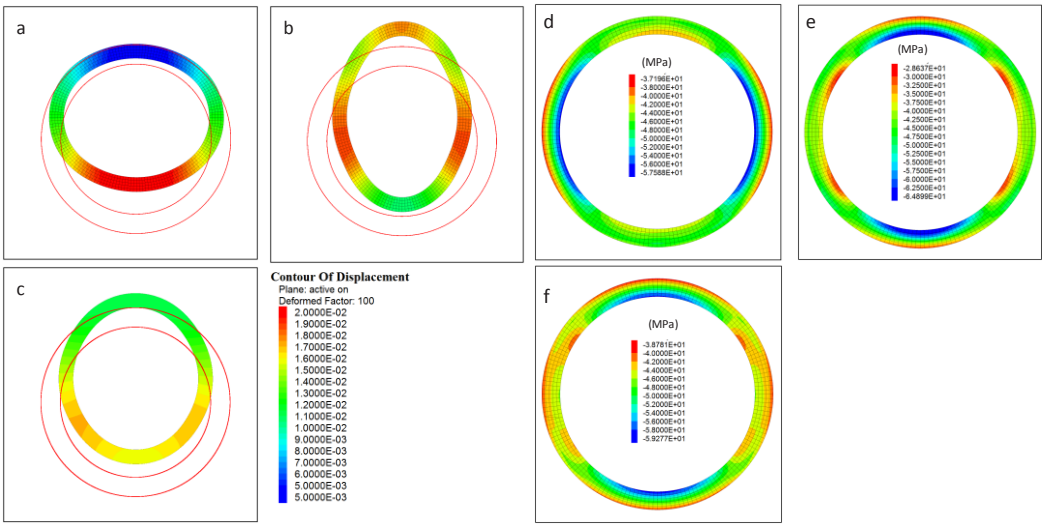


Figure 1: Contours of : displacements (a) case E_0, (b) damage only, (c) damage and cracks porosity closure; orthoradial stress (d) case E_0, (e) damage only, (f) damage and cracks porosity closure.

References:

Armand, G., Leveau, F., Nussbaum, C., de La Vaissiere, R., Noiret, A., Jaeggi, D., Landrein, P. & Righini, C. (2014), Geometry and properties of the excavation induced fractures at the Meuse/Haute-Marne URL drifts, Rock Mech. Rock Eng. 47 , p. 21-41

Bourgeois E., Coquillay S., Mestat P. (2005). Exemples d'utilisation d'un modèle élastoplastique avec élasticité non linéaire pour la modélisation d'ouvrages géotechniques. Bulletin des Laboratoires des Ponts et Chaussées, vol. 256/257, p. 67-84.

Souley M, Armand G, Su K, Ghoreychi M. (2011). Modelling of the viscoplastic behaviour including damage for deep argillaceous rocks. Physics and Chemistry of the Earth 2011;36:1949–59.

Vu MN., Seyedi D., Noiret A., de La Vaissière R., Armand G. (2015) Numerical analysis of the stiffness evolution of damaged zone around the drifts under mechanical loading/unloading cycles, paper submitted to 6th International Clay Conference.

Numerical modeling of in situ "PRACLAY seal test"

Guangjing Chen[1], **Xiangling Li**[1], **Jan Verstricht**[1], **Xavier Sillen**[2]

1. European Underground Research Infrastructure for Disposal of Nuclear Waste in Clay Environment (EURIDICE), Mol, Belgium
2. Belgian Agency for Nuclear Waste and Fissile Materials (ONDRAF/NIRAS), Brussels, Belgium

To study the response of Boom Clay to a thermal transient due to the disposal of heat-emitting radioactive waste, the PRACLAY Heater Test is operated in the PRACLAY gallery (PG) in the HADES underground research facility in Mol, Belgium. By installing a hydraulic seal at the intersection between the heated and the nonheated part of PG, and backfilling the heated PG with water-saturated highly permeable sand, the PRACLAY Heater Test will impose nearly-undrained conditions which are more penalizing than those prevailing in a real repository in terms of Thermo-Hydro-Mechanical (THM) evolution.

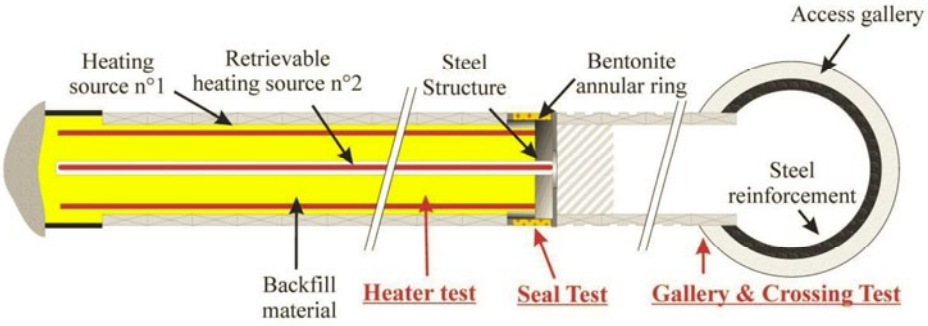


Figure 1: Schematic view of PRACLAY gallery, heater test and seal test

The seal is located at 10 m from the access gallery to limit the mutual interaction between the heater test and the access gallery. The seal does not only have to close the heated part of the PG, but it also has to hydraulically cut off the potentially preferential hydraulic pathway to the main gallery through the excavation disturbed zone (EDZ) around the gallery. MX 80 bentonite was chosen for the seal material due to its high swelling capacity and low intrinsic permeability when compacted to an appropriate dry density.

Fig. 2 shows a schematic view of the layout of the seal. Highly compacted bentonite blocks fill the major space encompassed by the Boom Clay, the steel structure (steel cylinder and two flanges) and the four steel ribs. There are two initial technological voids (each about 1 cm wide) in the seal, which inevitably result from the installation of the different bentonite blocks and instrumentation in the bentonite.

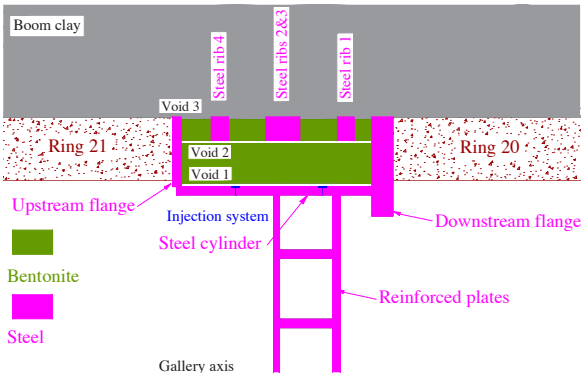


Fig. 2. Schematic view of Praclay seal

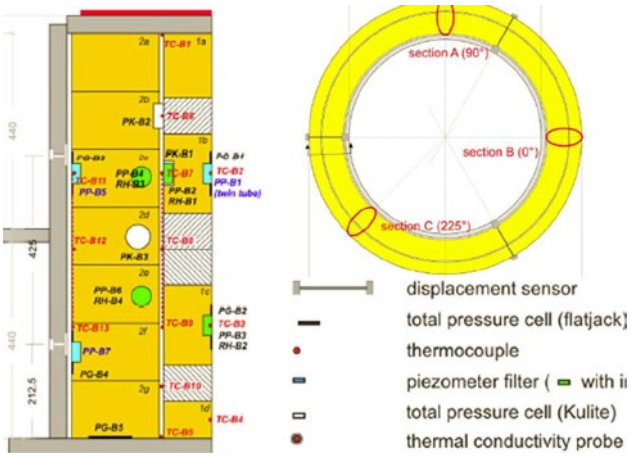


Fig. 3: Instrumented sections and section B detail

To monitor the THM behaviour of the seal, a large number of sensors measure the pore water pressures, displacements, total stresses, temperatures etc. in and around the bentonite. Most sensors were installed at three sections (see Fig. 3). This study focuses on the coupled THM modelling of the PRACLAY seal test using the finite element code "CODE_BRIGHT" developed by Technical University of Catalonia (UPC).

In order to simulate well the bentonite hydration, all interfering components are considered in the numerical model. These mainly include unsaturated bentonite, Boom Clay, concrete lining of the PG, steel and backfill sand. The THM parameter values of these materials are determined based on literature review, laboratory tests, in-situ measurements etc. The actual test evolution, including gallery construction, drainage, unlocking of steel ribs, seal installation, injection of water into seal, backfilling and pressurization of the PG, is simulated as realistically as possible. With the parameter values obtained before heating, we predict the seal behaviour during the heating phase (about 10.5 years).

Three dimensional (3D) coupled THM modelling considering an unsaturated bentonite is very time consuming. Therefore, three other coupled THM models (one dimensional (1D), two dimensional (2D) plane strain considering anisotropy, and 2D axisymmetric) are adopted in the simulation of the seal test. These three models allow to make the sensitivity analysis and identify the key factors controlling the seal behavior.

As an example, Figure 4 presents the modelled total swelling pressure at the "bentonite/Boom Clay" interface at section A and section B (see Figure 3) by means of a 2D plane strain model. The modelling results are in good agreement with the measured data before heating.

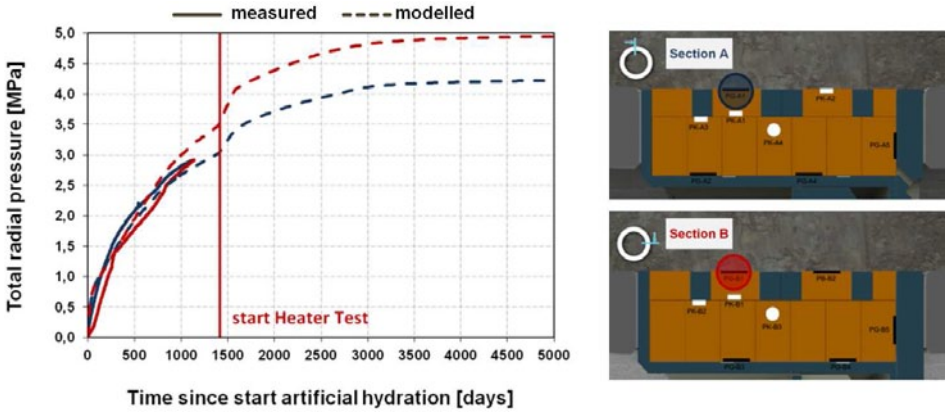


Fig. 4: Measured and modeled total swelling pressure at interface "bentonite/Boom Clay"

Material parameters, test procedures, main assumptions, models and their mutual validation, more comparison between measurement and modelling, interpretation, and prediction for the THM behaviour of the seal during the heating phase will be given in a full paper intended for publication.

Underground storage and its caprock: the good cap / bad cap principle

C. Dietl, **H. Baumgartner, E. Jahns**

Gesteinslabor Dr. Eberhard Jahns, Hospitalstr. 13, 37308 Heiligenstadt, Germany

Underground gas storage (UGS) in porous rock plays a decisive role for the reliability of energy supply in modern societies. For safety reasons, both the permeability and the porosity of the future storage itself as well as the hydraulic and mechanical integrity of the caprock have to be proven. The permeability, the threshold pressure, the frac pressure and the geomechanical properties of the caprock have to be determined to find out if the geomaterial – generally a claystone, siltstone or marlstone – is a suitable barrier.
In this study we focus on two topics: a) brine permeability and threshold pressure of claystone and marlstone; b) geomechanical properties of intensely laminated claystone (i.e. claystone with "weak bedding planes"). Gesteinslabor Dr. Eberhard Jahns is specialised in geomechanical testing of typical caprocks, as well as in the investigation of brine permeability and threshold pressure of claystone.
By definition, the threshold pressure is the pressure difference between the injected gas phase and the water phase in the caprock. This pressure is needed to overcome the capillary forces to initiate a flow into the caprock (Egermann et al. 2006).
Threshold pressure and brine permeability of typical caprock were determined with one of the very few laboratory devices in the world that allows carrying out these experiments under reservoir conditions. The measurements follow the slightly modified continuous injection method by Meyn (1999). Our tests indicate a weak negative power law correlation between brine permeability k_B and threshold pressure P_T:

$$P_T = 4.1 * 10^{-2} * k^{-0.362}$$

This is in good accordance with k_B- P_T correlations observed by Ibrahim et al. (1970) and Davis (1991). Moreover, a weak positive logarithmic correlation exists between threshold pressure P_T and overburden pressure P_O following the equation

$$P_T = 0.317 * {P_O}^{0.087}$$

From the observed correlations it can be inferred that P_T decreases dramatically with decreasing P_O and k_B.
Geomechanical key parameters such as peak and residual strength, Young's modulus and Poisson's ratio for these peculiar rocks were determined using triaxial cells suitable for high pressure testing (up to 2 kbars). Our geomechanical investigations show the dependency of most geomechanical parameters on the orientation of the bedding planes in relation to the principal compressive stress σ_1. Bedding planes are weak when oriented 30-60° to σ_1.
With all achieved rock physical and geomechanical data we constructed a geomechanical model for a UGS in the Vienna basin and its silty caprock based on the centroid concept. This was done to roughly estimate the potential of damage due to fracturing by a too high reservoir gas pressure. The centroid concept described by Finkbeiner et al. (2001) is a mighty tool to describe the pore pressure state in a reservoir and in its caprock. It is helpful in understanding at which height within the hydrocarbon column the reservoir pore pressure exceeds the pore pressure within the caprock. The level at which the pore fluid pressure within the reservoir equals the caprock pore pressure is labelled centroid. In case we have information about the stress state within the caprock or at least data about its geomechanical behaviour we can even model the risk of hydro-fracturing or (re)activation of a fault adjacent to the reservoir (Finkbeiner et al. 2001). Instead of pore pressures we calculated with the maximum planned operating pressures and the capillary pressure of the caprock (initial gas pressure in the reservoir + threshold pressure of the caprock). The minimum horizontal stress (basically σ_3) was calculated from the friction angles of the caprock. Those were derived from the Mohr-Coulomb

criteria based on UCS and multi-stage triaxial compressive strength tests for the claystone in question. From the relation between σ_1 (with the overburden assuming to represent the principal vertical stress), σ3 and φ

$$\sigma_3 = \frac{\sigma_1 * (1 - \sin\varphi)}{1 + \sin\varphi}$$

we achieved minimal horizontal stresses for the caprock.
Our calculations show that the reservoir gas pressure never exceeds the caprock capillary pressure and would reach the frictional limit of the caprock (i.e. its minimum horizontal stress) at a shallow depth well above the reservoir. Consequently, we can conclude that the caprock in question fulfils all criteria necessary to call it a "good cap". Nevertheless, only minor changes in some of the assumptions have to be made to change the picture: a slight increase of the maximum reservoir gas pressure or a little bit more stiffness of the caprock (leading to a higher angle of internal friction) would shift the intersection of gas pressure and the frictional limit of the caprock towards the depth. This in turn would gas fracturing of the caprock make more probable at the top of the actual UGS.
In conclusion we so far did not yet have reason to classify any of the investigated caprocks as „bad cap." Nevertheless, they all have their bad facets and need to be handled with care. Our investigations show that in particular the caprock of shallow UGS oriented with an unfavourable angle to the principle compressive stress should be treated carefully and investigated in detail.

Literature

Ibrahim, M.A., Tek, M.R., Katz, D.L., Threshold pressure in gas storage, American Gas Association, Inc., Arlington, Virginia (1970).
Davies, P.B., Evaluation of the role of threshold pressure in controlling flow of waste-generated gas into bedded salt at the Waste Isolation Pilot Plant (WIPP), Sandia Report, SAND 90-3246, 62 pp.. (1991).
Egermann, P., Lombard, J. M., Bretonnier, P., A fast and accurate method to measure threshold capillary pressures under representative conditions, SCA A46, In: SCA International Symposium, Trondheim (2006).
Meyn, V., Die Bedeutung des Sperrdruckes (threshold pressure) für den Fluidtransport in niedrigstpermeablen Gesteinen: Experimentelle und theoretische Aspekte, DGMK-Tagungsbericht 9901, 255-264 (1999).
Finkbeiner, T., Zoback, M.D., Flemings, P., Stump, B. (2001): Stress, pore pressure and dynamically-constrained hydrocarbon column heights in the south Eugene Island 330 field, Gulf of Mexico. American Association of Petroleum Geologists Bulletin, 85, 1007-1031.

Geomechanical model based on the complete description of an UGS caprock: an integrative laboratory study

C. Dietl[1], R. Braun[2], H. Baumgartner[1], E. Jahns[1]

1) Gesteinslabor Dr. Eberhard Jahns, Hospitalstr. 13, 37308 Heiligenstadt, Germany;
2) Dr. Roland Braun Consultancy in Rock Mechanics, Caputh, Schmerberger Weg 113, 14548 Schwielowsee, Germany

A well constrained geomechanical model is the base for successful hydraulic fracturing of an unconventional reservoir, but also necessary for any safety prediction for underground gas storage. In this study we present a complete geomechanical description of a marlstone which serves as caprock for a pore-space store in south-eastern Europe. Our approach combines:

- brine permeability measurements and direct threshold pressure determination in a climate chamber under in situ conditions;
- measurement and calculation of the geomechanical characteristics of the caprock by rock strength testing (Brazilian tests, UCS testing, multi-stage compression and extension experiments);
- identification of the 3D rock anisotropy and in situ stresses from ultrasonic measurements on samples from the drill core with RACOS® analyses (Rock Anisotropy Characterization On Samples).

The core samples come from a grey marlstone taken at a vertical depth of about 2000 m and with a porosity of about 4-6% and a density of 2.5-2.6 g/cm^3. The brine permeability and threshold pressure measurements show that the marlstone is fairly tight to act as caprock: Permeability ranges at 10^{-21} m^2 and threshold pressure in the range of 20 MPa.
The investigated rock material has a (for marlstone typical) low to intermediate uniaxial strength. The axial compressive load-carrying capacity at failure only increases slightly with increasing confining pressure. The strength analysis also indicates brittle behaviour at low confining pressure, which transforms relatively quickly into a ductile state. Strength value evaluation based on Mohr-Coulomb analysis reveals low to intermediate angles of (internal) friction between 11 and 45° (peak conditions) and 12 and 33° (residual conditions).
From the measured direction-dependent wave velocities a horizontal bedding and N-S and E-W striking in situ structures are derived. Moreover, the spatial pore pressure effectiveness (Biot's coefficient in 3D) was determined, which is a significant factor for the evaluation of rock properties, as well as for the tensorial linking of effective and total stresses. Values of about 0.45 are relatively small as is typical of rocks with low porosity and permeability. The least component can also be an indication of the preferred flow direction. However, in this case only a very small spatial anisotropy was found.
The in situ stress state at the time of coring can be described as a normal faulting regime ($S_V > S_{Hmax} > S_{hmin}$). There are only small differences in the magnitudes of the horizontal stresses. The larger horizontal component (which is significant for the propagation of hydraulic fractures) is oriented NNE-SSW. The determined stress data correspond with data from the world stress map in this region.
With all our rock physical and geomechanical data we were able to develop a geomechanical model based on the centroid concept (Finkbeiner et al. 2001). Our model shows, that hydraulic fracturing and leakage of the storage site due to a too high gas entry pressure are improbable. However, reactivation of faults seems to be possible based on the relatively low friction angle retrieved from uniaxial and triaxial testing.

Literature

Finkbeiner, T., Zoback, M.D., Flemings, P., Stump, B. (2001): Stress, pore pressure and dynamically-constrained hydrocarbon column heights in the south Eugene Island 330 field, Gulf of Mexico. American Association of Petroleum Geologists Bulletin, 85, 1007-1031.

Hydromechanical behaviour of technological voids and interfaces: finite element formulation and application

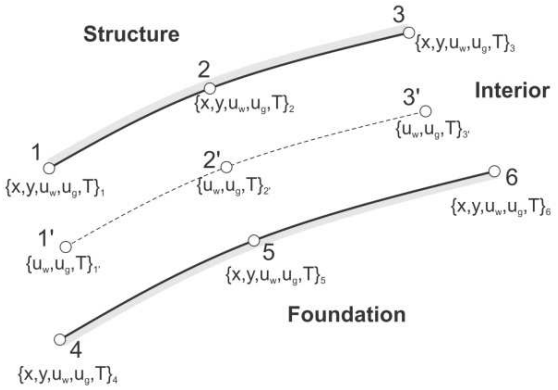
A.C. Dieudonne[1,2], **B. Cerfontaine**[1], **J.P. Radu**[1], **F. Collin**[1] **and R. Charlier**[1]

[1] University of Liege, ArGEnCo Department, Chemin des Chevreuils 1, 4000 Liege, Belgium (ac.dieudonne@ulg.ac.be)
[2] F.R.I.A., Fonds de la Recherche Scientifique – FNRS, Rue d'Egmont 5, 1000 Brussels, Belgium

In recent years, particular attention has been paid to the behaviour of bentonite-based materials in relation to their use as engineered barriers in deep geological repositories for nuclear waste. In this context, the engineered barrier aims at creating a zone of low permeability that is able to reduce water flow coming from the host rock, hence the release of radionuclides into the environment. Therefore bentonite-based materials have generally been selected for their high swelling capacity, their low permeability and their important radionuclides retardation capacities.

However, the placement of a bentonite buffer within a gallery involves unavoidable technological voids between the engineered barrier and the host rock. While most researches have traditionally focused on the behaviour of the buffer and the host rock separately, little attention has been paid to the role and influence of technological voids and interfaces between materials. In numerical modelling, the existence of technological voids is generally neglected and perfect contact is assumed between the different materials. This strong hypothesis assumes continuity of both mechanical displacements and pore pressures between materials, which is not true, especially during the first years of the disposal life. Therefore the behaviour of interfaces should be considered and special numerical tools should be developed. Therefore the behaviour of interfaces should be considered for at least two reasons: (1) interfaces significantly affect the transient saturation process of the buffer and (2) they may act as preferential pathways for the migration of radionuclides.

In this paper, the finite element formulation of a coupled hydromechanical interface element, implemented in the finite element code Lagamine, is presented. The interface element FAIF2 (Figure 2) is an isoparametric element for two-dimensional analysis. In order to describe the flow not only through the interface, but also within the interface, a three-node formulation is adopted. The finite element FAIF2 uses 2 or 3 nodes on each side of the interface (structure and foundation), as well as 2 or 3 additional nodes inside the interface (interior). The nodes of the structure and the foundation are characterized by 5 degrees of freedom (2 mechanical displacements, water pressure, gas pressure and temperature), while the ones of the interior have only 3 degrees of freedom (water pressure, gas pressure and temperature) and have the same coordinates as the nodes on the structure side of the element.



Finally, in order to highlight the influence of interfaces and technological voids on the hydration kinetics of bentonite plugs, one-dimensional and two-dimensional academic examples are presented and analysed in details.

Experimental evidence and constitutive modelling of desiccation cracks in clayey materials

Pierre Gerard[1], Ian Murray[2], Alessandro Tarantino[2]

[1] Université libre de Bruxelles (ULB), Batir department, Laboratory of Geomechanics, Av. F. Roosevelt 50 – CPI 194/02, 1050 – Bruxelles, Belgium – Email: piergera@ulb.ac.be
[2] University of Strathclyde, UK

Predicting the time and location of desiccation cracks in clayey geostructures is a challenging problem in many engineering applications, and especially in radioactive waste repository where the significant changes induced by desiccation cracks in the mechanical and hydraulic behaviours of the host rock alter the long-term integrity of such solutions. Desiccation cracking has been investigated for a number of years (Konrad and Ayad, 1997; Tang et al 2011). Despite this the mechanism for crack initiation is not yet well understood. Experimental evidence relating to desiccation cracking indicates that crack initiation occurs in Mode I (i.e. opening mode), suggesting that crack initiation occurs as a result of the mobilisation of soil tensile strength (Corte and Higashi, 1960; Hu et al, 2006; Peron et al, 2006). However, this mechanistic model disregards the cohesionless, effective stress-dependent frictional behaviour of fine-grained soils (Shin and Santamarina, 2011). Recent findings in the literature (Thusyanthan et al., 2007) suggest that cracking is associated with failure in shear.

Our contribution investigates the mechanism of desiccation crack initiation and makes an attempt to model the onset of cracking in simple clay forms exposed to desaturation by air drying. Constrained drying laboratory tests are first performed on initially saturated clay forms in a temperature and relative humidity controlled environment. Displacement field and crack formation in proximity of the evaporating surface are monitored using high definition web cameras and laser scanning. To better localize and characterize these features, high deviatoric stresses/strains are generated on different geometries of clay forms by imposing non-uniform hydraulic boundary conditions (evaporation only being allowed through a portion of the boundary) and mechanical boundary conditions (displacements restrained only along a portion of the boundary) with different clay forms.

Cracking is then tentatively modelled using a coupled hydro-mechanical model based on the assumption that cracking is associated with failure in shear (Thusyanthan et al, 2007). The comparison of numerical simulations with experimental results in terms of cracks location and time of cracking make it possible to assess this assumption of failure in shear. These first results are coupled with the re-analysis under the assumption of shear failure of previous experimental data investigating the desiccation cracks (Rodriguez et al., 2007).

REFERENCES

Corte, A., Higashi, A. 1960. Experimental Research on Desiccation Cracks in Soil, Research Report 66: U.S. Army Snow Ice and Permafrost Research Establishment, Wilmette, Illinois.

Hu, L, Peron, H, Hueckel, T, Laloui, L. 2006. Numerical and phenomenological study of desiccation of soil. In: Advances in unsaturated soil, seepage, and environmental geotechnics. ASCE gotechnical special publication 148, p. 166–73

Konrad, J.M., Ayad, R. 1997. An idealized framework for the analysis of cohesive soils undergoing desiccation. *Canadian Geotechnical Journal* 34: 477- 488.

Peron, H., Laloui, L., Hueckel, T., Hu, L.B. 2006, Experimental study of desiccation of soil. In: Miller et al., editors. UNSAT, ASCE geotechnical special publication 147, p. 1073–84.

Rodriguez, R., Sánchez, M., Ledesma, A., Lloret, A. 2007. Experimental and numerical analysis of desiccation of a mining waste. *Canadian Geotechnical Journal* 44: 644-658.

Shin, H., Santamarina, J.C. 2011. Desiccation cracks in fine-grained soils: particle level phenomena and effective stress analysis, *Geotechnique* 61(11): 961-972.

Tang, C.S., Shi, B., Liu, C., Suo, W.-B., Gao, L. 2011. Experimental characterization of shrinkage and desiccation cracking in thin clay layer, Applied Clay Science 52: 69-77.

Thusyanthan, N.I., Take, W.A., Madabhushi, S.P.G., Bolton, M.D. 2007. Crack initiation in clay observed in beam bending, *Geotechnique* 57(7): 581–594.

On the thermo-mechanical behaviour of the Callovo-Oxfordian claystone

MENACEUR[1] H., *DELAGE[1] P.*, TANG[1] A.M. and CONIL[2] N.

[1] Ecole des ponts ParisTech, Navier/CERMES, France
[2] ANDRA, Bure, France

The Callovo-Oxfordian (COx) claystone is considered as a potential host rock in the French concept of high level radioactive waste disposal at great depth. To better understand and to complement existing published data on the thermo-hydro-mechanical behaviour of the COx claystone, an experimental program was carried out by using a hollow cylinder triaxial device specially developed for low permeability materials. Special care was devoted to the saturation of the specimens that was made under stress conditions close to in-situ, and to conditions ensuring full drainage, with a reduced drainage length and low shear rate. Tests were carried out under in-situ, half to in-situ and twice the Terzaghi mean effective in-situ stress at 25°C and 80°C to investigate the effects in the close field of the temperature elevation due to the exothermic nature of the wastes. Some radial permeability tests were conducted at various temperatures. The data obtained showed that there is little effect of temperature on the elastic parameters determined, whereas a tendency to a decrease in shear strength was noted, compatible with the few published data. Temperature also appeared to have little effect on the intrinsic permeability, with higher flows mainly due to the decrease in water viscosity.

A microstructure investigation of the compression-swelling behaviour of the Callovo-Oxfordian claystone

MENACEUR[1] H., *DELAGE[1] P.*, TANG[1] A.M. and TALANDIER[2] J.

[1] Ecole des ponts ParisTech, Navier/CERMES, France
[2] ANDRA, Châtenay-Malabry, France

This work following a previous one (Mohajerani et al. 2011) carried out in high stress oedometers on the compressibility/swelling behaviour of the Callovo-Oxfordian (COx) claystone, a potential host rock for high activity radioactive waste disposal at great depth in France. An investigation of the changes in microstructure of the COx claystone during compression and swelling was carried out by investigating the microstructure (by means of Scanning Electron Microscope and mercury intrusion porosimetry) on specimens i) at initial (unsaturated) state, ii) after saturation with no volume change, iii) after compression (56 and 113 MPa) and stress release at constant water content and iv) after compression and swelling. The idea was to confirm previous findings about coupling between swelling and damage. MIP and SEM observation carried out on freeze-dried specimens confirmed that swelling was related to the development in the clay matrix of large cracks parallel to bedding. It seems indeed that, as suggested by Mohajerani et al. (2011), the higher the compression stress, the larger the damage and the resulting swelling. The stress release at constant water content of saturated specimens resulted in some swelling due to an internal transfer of water molecules from the inter-platelets porosity (30 nm average diameter) to the inter-layer spaces within the interstratified illite-smectite platelets (smaller then 5.5 nm, the lower limit of MIP), confirming recent observations of Delage et al. (2014). The detailed analysis of the pore size distribution curve allows investigate the relative importance of the compression and collapse of the inter-platelets pores with respect to the volume changes resulting from the changes in inter-layer spacing within the smectite minerals included in the illite-smectite interstratified minerals.

References

Mohajerani M, Delage P, Monfared M, Sulem J, Tang A.M. and Gatmiri B. 2011. Oedometer compression and swelling behaviour of the Callovo-Oxfordian argillite, *International Journal of Rock Mechanics and Mining Sciences*, 48 (4), 606-615.
Delage P., Menaceur H., Tang A.M. and Talandier J. 2014. Suction effects in deep Callovo-Oxfordian claystone. *Géotechnique Letters*, accepted.

A poroelastic investigation of the Callovo-Oxfordian claystone

M. Belmokhtar[1], P. Delage[1], S. Ghabezloo[1], H. Menaceur[1], J. Talandier[2]

[1] Ecole des ponts ParisTech, Navier/CERMES, France
[2] Andra, Châtenay-Malabry, France

A new system based on an isotropic compression cell with high precision measurement of both axial and radial strains by means of LVDTs was developed to determine the poroelastic parameters of the Callovo-Oxfordian (COx) claystone on specimen of 38 mm in diameter and 10 mm in height. High precision strain measurements were made with direct contact of the LVDT with the specimen through the membrane, providing a 0.1 µm precision in displacement (0.001% in volumetric strain). The tests carried out included an undrained compression, a drained compression and, finally, an unjacketed compression test (carried out with same increase in total stress and pore pressure). The drained bulk modulus (K_d), undrained compression modulus (K_u) and unjacketed modulus (K_s) were carefully determined so as to allow calculate the Biot's coefficient b. The poroelastic parameters obtained were in good mutual compatibility, providing with satisfactory reliability a *b* value of 0.84 for a COx specimen with a porosity of 19% extracted in the Meuse/Haute Marne Underground Research Laboratory at -490m where clay content is maximum.

Criteria for demonstrating the integrity of the geological barriers in claystone in Germany

***Jobmann*[1], *M.*, Maßmann[2], J., Meleshyn[3], A., Polster[1], M.**

DBE TECHNOLOGY GmbH, Eschenstraße 55, D-31224, Peine, Germany.
Bundesanstalt für Geowissenschaften und Rohstoffe (BGR), Stilleweg 2, D-30655 Hannover
Gesellschaft für Anlagen- und Reaktorsicherheit mbH (GRS), Theodor-Heuss-Straße 4, D-38122 Braunschweig

Abstract

Within the framework of the R&D project "ANSICHT", DBE TECHNOLOGY GmbH, BGR, and GRS are developing an integrated methodology to demonstrate the safety of a HLW repository in claystone in Germany.

In recent years, the methodology of safety demonstration has been substantially improved. For a long time, meeting a radiological release limit demonstrated by long-term calculations was the main component of the safety demonstration. Currently, these calculations are seen as one part of a line of arguments belonging to an integrated methodology (Safety Case) where the key element is to demonstrate the integrity of the geologic and geotechnical barriers. The strength of this integrated methodology lies in the strong link between legal and geologic boundary conditions, disposal and closure concept, demonstration of barrier integrity, and long-term analysis of probable and less probable repository evolutions.

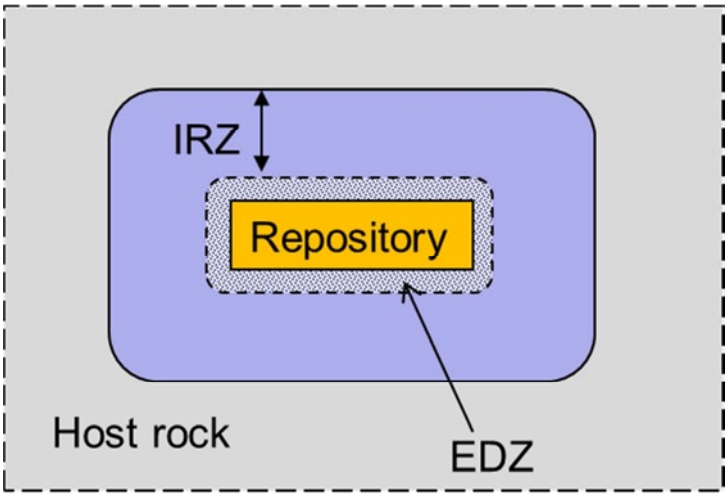


Fig. 1: Sketch of the isolating rock zone (IRZ) around the repository

A key element of this concept is the demonstration of the integrity of the geologic barrier, in particular of the so-called "isolating rock zone" (IRZ) (Fig. 1). The legal basis are the safety requirements of the regulating body (BMU, 2010) which stipulate that for the normal evolution of the repository (reference scenario), the integrity of the IRZ within the host rock has to be demonstrated for a period of 1 million years. For this reason, the necessary spatial extension of the IRZ has to be defined and – taking into account the retention effects of the geotechnical barriers – it has to be demonstrated that

- the transport of radionuclides by advection through the IRZ is at best comparable with the transport by diffusion (**advection criterion**)
- the expected mechanical load does not exceed the dilatancy strength of the host rock and of the IRZ. The excavative damaged zone (EDZ) is not part of the IRZ and is therefore to be excluded (**dilatancy criterion**).
- the expected fluid pressures do not exceed the load bearing capacity of the IRZ. This is to avoid any enhanced ingress of water into the IRZ (**fluid pressure criterion**).
- the barrier effect of the IRZ is not compromised by temperature impulses resulting from HLW emplacement (**temperature criterion**).

In view of the practical implementation of these qualitative regulatory requirements, it is necessary to concretize these criteria in such a way that a demonstration by mathematical calculations will be possible in the framework of the new safety demonstration concept. This means that precise limit values have to be defined so that the integrity of the IRZ can be demonstrated by means of these calculations.

This presentation explains the derivation of these values and explicitly defines the four integrity criteria in a quantitative manner.

References

BMU (2010). Safety Requirements Governing the Final Disposal of Heat-Generating Radioactive Waste. Bundesministerium für Umwelt, Naturschutz und Reaktorsicherheit (BMU), Berlin.

Jobmann, M., Maßmann, J., Meleshyn, A., Polster, M. (2014). Quantification of criteria for integrity demonstration, Technical Report, DBE TECHNOLOGY, GmbH, Peine, Germany (in preparation).

Quantitative characterisation of EDZ fracture network in the Meuse/Haute-Marne Underground Research Laboratory - In situ experiment and numerical interpretation of helium injection test -

Shao, Hua[1]; Göthling, Sebastian[1]; Liu, Wenting[1]; Hesser, Jürgen[1]; Morel, Jacques[2] & Sönnke, Jürgen[1,*]

1. Federal Institute for Geosciences and Natural Resources (BGR), 30655 Hannover, Germany
2. French National Agency for Radioactive Waste Management (Andra), 55290 Bure, France

* Contact person: Corresponding author (e-mail: juergen.soennke@bgr.de)

Abstract

After excavation in the underground facility fractures can exist in the near-field of the opening. In the underground laboratory Meuse/Haute-Marne (Bure, France), different fracture systems have been intensively investigated. Three main features can be observed in the Galleries parallel to the main principle stress: subvertical 'oblique' fractures to the tunnel axis, chevron-type fracture and unloading joints (Nussbaum, 2007). Within a cooperation project between BGR and Andra, geophysical measurements and borehole gas tests have been conducted in three well-designed boreholes in the Gallery GRM to characterise the fracture structure and to determine the gas tracer velocity along the fracture network. In this paper special attention was paid on the in situ helium test and the numerical interpretation of the experiment.

On the basis of seismic measurements and nitrogen gas interference tests, helium was injected into an interval of borehole OHZ3003, where both chevron fracture and tensile fracture are characterised. The injection took place in the form of a ten minute 'pulse' with an injection pressure of 2 bar. The other two boreholes, OHZ3002, where an upper part of chevron fracture dominates, and OHZ3001, where unloaded fractures exist, served as observation holes (Figure 1). To keep up the pressure gradient between injection hole and observation holes, nitrogen gas was flushed into the injection hole afterwards. Two breakthroughs and developments of helium concentration in the two observation holes were continuously monitored using two helium leakage detectors PHOENIX L300i.

To interpret the measured pressure and concentration data, two modules, gas flow and mass transport, of the numerical code OpenGeoSys (Kolditz et. al, 2014) were used in a coupled manner. A two-dimensional model was constructed to simulate the fracture system. The experimental procedure and the volume of the injection borehole were numerically reproduced. Using the calibrated transport parameter data for helium tracer from the previous experiments in the Mont Terri Rock Laboratory, especially the effective porosity and (longitudinal and transversal) dispersion length for the saturated clay rock, the measured breakthrough curves can be very well modelled by variation of permeability of fractures (Figure 2). The determined permeability from the tracer test agrees well with those from the nitrogen gas tests.

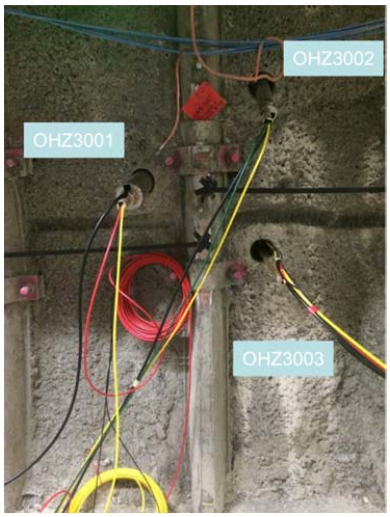


Figure 1: Layout of boreholes

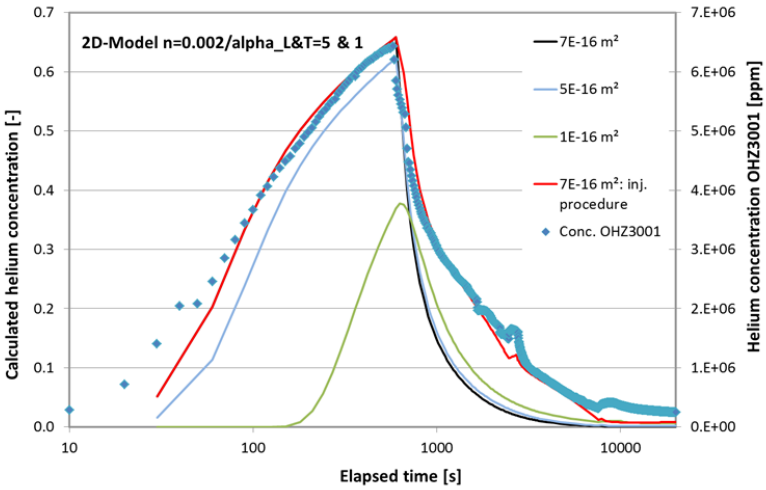


Figure 2: Measured and modelled breakthrough curves.

Reference

Nussbaum, C., Wileveau, Y., Bossart, P., Möri, A. and Armand, G. (2007): Why are the geometries of the EDZ fracture networks different in the Mont Terri and Meuse/Haute-Marne rock laboratories? Structural approach, in International meeting on Clays in Natural and Engineered Barriers for radioactive waste confinement, Sept. 17 – 18 2007, Lille, France

Kolditz, O., Bauer, S., Bilke, L., Böttcher, N., Delfs, J.O., Fischer, T., Görke, U.J.,Kalbacher, T., Kosakowski, G., McDermott, C.I., Park, C.H., Radu, F., Rink, K., Shao, H., Shao, H.B., Sun, F., Sun, Y.Y., Singh, A.K., Taron, J., Walther, M., Wang, W.,Watanabe, N., Wu, Y., Xie, M., Xu, W., Zehner, B. (2012): OpenGeoSys: an open-source initiative for numerical simulation of thermo-hydro-mechanical/chemical (THM/C) processes in porous media, Environ. Earth Sci. http://dx.doi.org/10.1007/s12665-012-1546-x

Shao, H., Schuster, K., Sönnke, J. & Bräuer, V. (2008): EDZ development in indurated clay formations - In-situ borehole measurements and coupled HM-modelling, Physics and Chemistry of the Earth, 2008; Elsevier , doi: 10.1016 / j.pce.2008.10.031

Yildizdag, K., Shao, H., Hesser, J., Noiret, A. and Soennke, J. (2014): Coupled hydromechanical modelling of the mine-by experiment at Meuse/Haute-Marne underground rock laboratory France; Geological Society, London, June, 16, 2014, doi 10.1144/SP400.42

Synoptic structural geological analysis of the MB & FE tunnel excavation in the Mont Terri URL: Influences of pre-existing fractures on tunnel stability and EDZ characteristics

J.K. Becker[1*], **D. Jaeggi**[2], **D., A.Lisjak**[3], **H. Madritsch**[1], **S. Schefer**[4], **H.R. Müller**[1], **T. Vietor**

[1] NAGRA, Hardstrasse 73, 5430 Wettingen, Switzerland, * jens.becker@nagra.ch
[2] Mont Terri Consortium, Swisstopo, Rue de la gare 63, CH-2882 St-Ursanne
[3] Geomechanica Inc., 90 Adelaide St. W., Suite 300, Toronto, Canada
[4] Geoexplorers Ltd., Wasserturmplatz 1, CH-4410 Liestal

Between 2008 and 2012, several niches and tunnels were excavated within the Opalinus Clay of the Mont Terri underground research laboratory (URL) (see Fig. 1). During the excavation phases each newly-excavated section was geologically mapped in detail. The mapping focused on the orientation of the bedding and on the inventory of structural features, including fractures of the excavation damaged zone (EDZ). Based on this data and additional information (such as fracture kinematics), a structural analysis of these underground openings is presented. This analysis also yields insights into the anatomy of fault zones. Consideration of breakout phenomena and in-situ stress conditions help to illustrate the influence of minor natural, pre-existing fracture systems on the rock mass stability and EDZ characteristics.

During the excavation of the MB tunnel (i.e., the first niche to be excavated) the most important structural features mapped were: (1) sedimentary structures, such as accumulations of biodetritus or quartz, (2) tectonic faults, and (3) excavation-induced fractures. Bedding consistently strikes parallel to the tunnel axis and dips moderately (20-48°) to the SSE. As a consequence, the excavation proceeded slightly stratigraphically downward. Nevertheless, hardly any lithological variations became evident. The excavated rock mass consisted of laminated claystone belonging to the shaly facies of the Opalinus Clay. Faults that formed prior to the tilting of the sedimentary stack, which is related to the formation of the Late Cenozoic Mont-Terri anticline, can be classified as pre-excavation features. Three main sets of such discontinuities were recognized. (i) roughly N-S striking normal faults that dip moderately towards the E. These faults mark an E-W extension and are suspected to be related to the Eo-Oligocene formation of the European Cenozoic rift system (ii) E-W striking, sub-horizontal reverse faults that indicate N-S contraction and are interpreted to be related to the formation of the Jura fold-and-thrust belt. These faults apparently formed during an early stage of folding and were rotated during the formation of the Mont Terri Anticline (iii) E-W striking moderately SSE dipping normal faults oriented sub-parallel to the bedding. These findings are roughly in line with those of Nussbaum et al. (2011).

The excavation of the MB tunnel was later followed by the excavation of the so-called FE-A niche (Fig. 1) which is also located in the shaly facies of the Opalinus Clay. Bedding here is still dipping at an average of 35° trending towards 150° (i.e., sub-parallel to the MB tunnel axis). However, in contrast to the MB tunnel, only moderately SSE-dipping reverse faults and low-angle SW-dipping faults were mapped. The N-NNE-striking, sinistral strike-slip faults reported by Nussbaum et al. (2011) were not observed. The EDZ mapped in the FE-A niche was greatly influenced by the previous excavation of the MB tunnel. A similar observation is valid for the first few meters of the FE tunnel, a 50 m long tunnel with a diameter of approx. 3 m excavated from the FE-A niche. Here, the EDZ was mainly oriented parallel to the advancing tunnel face. Apart from these EDZ fractures and the three

main pre-excavation discontinuity sets described above, the main tectonic feature of the FE tunnel is a well-developed fault zone that emerges after 15 m in the tunnel floor and continues until the end of the tunnel where it is situated approximately in the middle part of the tunnel face. This fault zone was not visible in the FE-A niche or MB tunnel as it is probably located below them. The orientation of this fault zone is sub-parallel to the tunnel axis and dips about 50° to SSE.

The age of the three different sets of faults is poorly constrained. It is suspected that they formed during the folding of the anticline and were partly reactivated during the excavation as part of the EDZ. The EDZ fractures consist of sub-vertical, rough-faced fractures which developed in extensional mode.

The stability of the excavations was found to be closely related to the structural framework, which tended to control the localization of systematic excavation instabilities. For example, during the excavation of the MB tunnel, small breakouts and continuous cracks, oriented parallel to the tunnel axis, formed sub-parallel to the bedding, especially in the upper left (southern) corner of the tunnel. Breakouts occurred in the form of sub-vertical EDZ-fractures. Pre-existing, sub-horizontal and gently dipping faults acted as upper and lower boundaries of rock flakes developing from the central tunnel face. The close spacing of these fault-sets significantly limited the maximum breakout size. Larger, slide-like breakouts occasionally occurred along E-dipping normal faults.

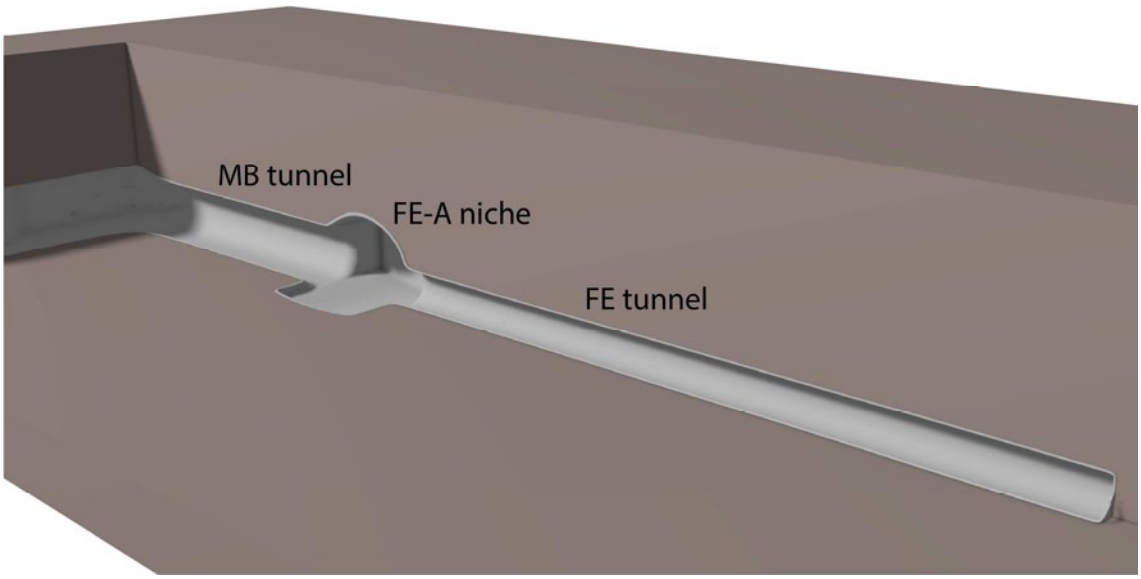


Fig. 1: 3D view of the tunnels and niche excavated between 2008 and 2012.

References:

Nussbaum, C., Bossart, P., Amann, F., & Aubourg, C. (2011): Analysis of tectonic structures and excavation induced fractures in the Opalinus Clay, Mont Terri underground rock laboratory (Switzerland). Swiss Journal of Geosciences, 104: 187-210. DOI 10.1007/s00015-011-0070-4.

Ultrasonic and geoelectrical characterization of tunnel near field features within the FE-E experiment (Mont Terri RL)

Kristof Schuster[1], *Markus Furche*[1], *Jens Becker*[2], *Friedhelm Schulte*[1], *Hendrik Albers*[1], *Christoph Czora*[1], *Torsten Tietz*[1]

[1] BGR, Stilleweg 2, 30655 Hannover, Germany
[2] NAGRA, Hardstrasse 73, 5430 Wettingen, Switzerland

Within the Full-scale Emplacement (FE) experiment a sub experiment (FE-E) deals with the determination of tunnel near-field features, including the characterization of Excavation Damaged/disturbed Zones (ED/dZ). Geophysical measurements were performed in summer 2013 and winter 2014 in the Mont Terri Rock Laboratory in the shaly facies of the Opalinus Clay. In an unlined and a lined section of the 50 m long FE-gallery (diameter of 2.7 m) six boreholes with lengths between 6 and 12 m were used for the investigations. As a consequence of the relatively strong convergences of the gallery the status of the ED/dZ as well as small scale geo-mechanical important features in the vicinity of the gallery are of special interest.

High resolution geophysical in-situ-borehole methods like ultrasonic and geoelectrical methods were applied in six single boreholes with diameters of 86 mm and between several of these boreholes. For an assessment of borehole walls and their evolution, borehole cameras and borehole photography were applied additionally. For the ultrasonic measurements, a BGR mini sonic probe with 3 emitters and 7 receivers was used. The spacing between the piezo-electric transducers was 5 cm. The measurement steps range between 5 cm for the single hole measurements and 10 to 20 cm for the cross hole measurements. For the geoelectrical measurements, a BGR geoelectrical borehole probe with 50 electrodes with a spacing of 1.5 cm was used in single boreholes for classical Wenner-alpha profiling and a 32/32 electrode system (electrode spacing 10 cm) for resistivity tomography measurements between boreholes.

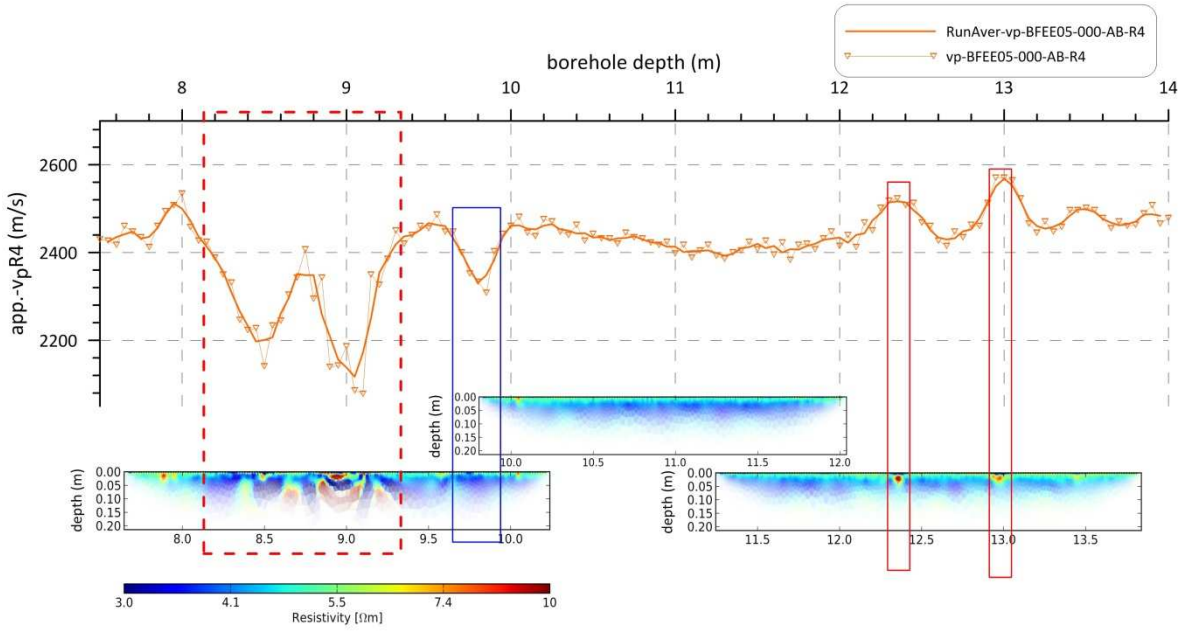


Figure 1: Comparison of seismic P-wave velocity and electrical resistivity distribution along a 6 m long borehole section.

Major results are first of all the pronounced small scale variability of all derived geophysical parameters in a centimeter range and a good correlation between these parameters. Figure 1 shows an example from a 6 m long section. Seismic P-wave velocities (app v_p) are derived from ultrasonic interval velocity measurements along the borehole at one orientation. Exemplarily the apparent v_p distribution for receiver 4 at a distance of 20 cm from the emitter is compared with the spatial resistivity distribution as a results from the geoelectrical borehole measurements in the same borehole and same orientation.

Between 10 m and 12 m, the parameters point to a relatively smooth rock. But outside of this section the parameter variations indicate several pronounced changes of rock properties. All v_p deviations correlate very well with changes in electrical resistivity. For example, both v_p peaks at 12.35 m and 13.0 m correlate with increased electrical resistivities. A higher carbonate content could be the reason for this locally terminated anomaly. The v_p decrease at 9.8 m allows to presume a higher clay content of the Opalinus clay, whereas the v_p variations between 8.1 m and 9.3 m and the related resistivity distributions seem to be more complex, especially when parameters like seismic amplitudes and the elasto-dynamic Young's modulus are taken into account. A tectonically disturbed zone could be a reason.

All 3 geoelectrical sub-sections show a small rim with higher electrical resistivities which reflect a several centimeter thick borehole disturbed zone (BdZ) caused by the drilling process. Comparable BdZ signatures are derived from ultrasonic interval velocity measurements. The degree and extent of BdZ as well as the evolution with time can be captured with repetition measurements.

Furthermore, several geophysical parameters which were derived from cross hole measurements reflect the remarkable anisotropy of the Opalinus Clay.

Further BGR investigations in the FE-E experiment performed in parallel, like gas permeability measurements, are presented at this conference.

High resolution geoelectrical and ultrasonic investigations of EDZ features at the URL Meuse / Haute-Marne

Markus Furche[1], *Kristof Schuster*[1], *Jacques Morel*[2], *Jürgen Sönnke*[1], *Hendrik Albers*[1], *Friedhelm Schulte*[1], *Christoph Czora*[1], *Torsten Tietz*[1]

[1] BGR, Stilleweg 2, 30655 Hannover, Germany
[2] Andra, Meuse Haute Marne Center, 55290 Bure, France

Within the framework of the BGR-Andra collaboration, and as part of different joint experiments started in 2001 and continued in 2009 (phase II) several seismic / ultrasonic borehole measurements at different locations and at different depth levels were performed by BGR at the Meuse / Haute-Marne URL (F). In spring 2009 at several locations of the early GRM drift at the 490 m level ultrasonic measurements were performed. In the later extended drift BGR investigations were resumed. Three boreholes at the side wall of the drift with diameters of 86 mm and lengths of 6 m were used in May 2014 for high resolution geoelectrical and ultrasonic measurements in the Callovo-Oxfordian claystone (COX). Beside the continuously enhanced BGR ultrasonic borehole tools, a new BGR geoelectrical borehole probe/system was used. Measurements were performed in single boreholes and between boreholes. For an assessment of borehole walls and their evolution borehole cameras and borehole photography was applied additionally.
For the ultrasonic measurements a BGR mini sonic probe with 3 emitters and 7 receivers was used. The spacing between the piezo-electric transducers was 5 cm. The measurement steps range between 5 cm for the single hole measurements and 20 cm for the cross hole measurements. For the geoelectrical measurements a BGR geoelectrical borehole probe with 50 electrodes and a spacing of 1.5 cm was used in single boreholes for classical Wenner-alpha profiling and a 32/32 electrode system (electrode distance 10 cm) for resistivity tomography measurements between boreholes.
Geophysical investigations aimed at the determination of tunnel near-field features like the characterization of Excavation Damaged/disturbed Zones (ED/dZ), small scale variations of geophysical parameters in the vicinity of the gallery and BdZ features (Borehole disturbed Zone).

Small scale variations in several geophysical parameters along the borehole were observed. Even the BdZ varied remarkable. Figures 1 and 2 show examples of both methods from a 6 m long borehole.

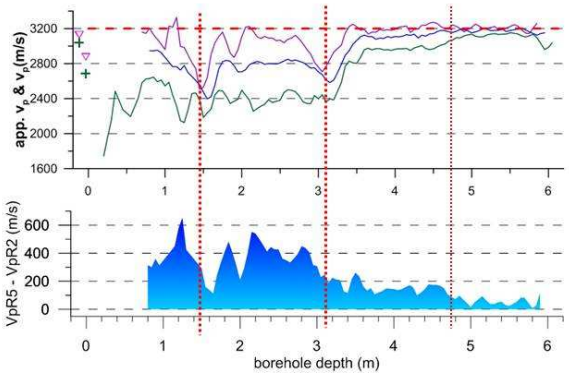


Figure 1: Top: Derived app. v_p (green: R2, blue: R5) and BdZ corrected v_p (pink). Below: v_{pR5}-v_{pR2} difference indicates qualitatively the extent of the BdZ.

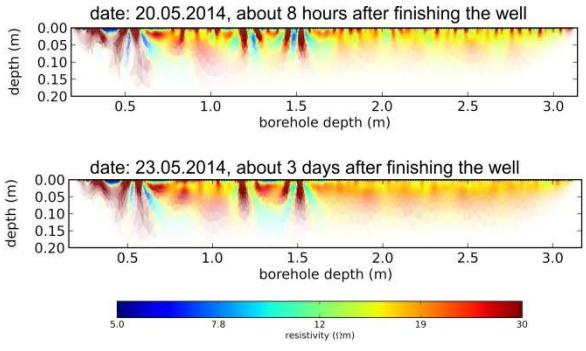


Figure 2: Spatial electrical resistivity distribution along the borehole at two different time steps.

Apparent seismic P-wave velocities (app v_p) are derived from ultrasonic interval velocity measurements along the borehole at one orientation. Exemplarily the app v_p distribution for receivers 2 and 5 at distances of 10 cm and 30 cm from the emitter are displayed. The app v_p distribution is used

for the calculation of a BdZ corrected v_p (pink graph in Figure 1). A v_p of 3200 m/s is assumed to indicate an undisturbed COX. This v_p is reached at 3.5 m. Obviously at 1.5 m and 3.1 m the vp drops locally limited. Taking additionally the seismic amplitudes into account this points to remarkable anomalies. The v_p and BdZ distribution implies a separation of the 6 m long borehole into 4 different sections as indicated by the red dashed lines in Figure 1.

As a main result the high resolution geoelectrical single hole measurements resolve a temporal change of BdZ structures in specific regions. The resistivity distributions as a result of a measurement performed about 8 hours after finishing the well show a high variable zone up to 1.5 m and a lower variable zone from 1.5 m to about 3.3 m (Figure 2 top). For higher depth only small resistivity variations are visible. 3 days later the resistivity distribution changes remarkable. While the resistivity structures in the first zone become stable and partly more distinct, respectively, the variations seen in the second zone between 1.5 m and 3.3 m are almost disappeared (Figure 2 below). This implies, that the BdZ structures seen directly after finishing the borehole are partly degenerated within 3 days at this region.
The geoelectrical results confirm the separation of the borehole indicated by the seismic measurements in the front region. Only the last transition (indicated by the third red dashed line in Figure 1) is not visible in the geoelectrical data.

Furthermore, several geophysical parameters which were derived from ultrasonic cross hole measurements support the findings from single hole measurements.

Further BGR investigations in these boreholes like gas permeability measurements are presented at this conference.

SELF-SEALING OF FRACTURES IN CLAY ROCK

Chun-Liang Zhang

Gesellschaft für Anlagen- und Reaktorsicherheit (GRS) mbH, 38122 Braunschweig, Germany
(chun-liang.zhang@grs.de)

Excavation of an underground repository for disposal of radioactive waste in clay formations generates fractures around the openings, which may act as pathways for water transport and radionuclides migration. Because of the favourable properties of the clay rocks such as the rheological deformability and swelling capability, a recovery process of the excavation damaged zone (EDZ) can be expected due to the combined impact of rock compression, backfill resistance, and clay swelling during the post-closure phase. Another important issue is the impact of gases produced from anoxic corrosion of waste containers and other metallic components within the repository. The EDZ may act as a conduit for preferential gas flow, depending on the extent of the recovery process. For the safety assessment of a repository, the self-sealing behaviour and impact on water and gas transport through the EDZ have to be characterized, understood, and predicted.

During the last decade, GRS has extensively investigated these important issues with various kinds of laboratory and in situ experiments under relevant repository conditions [1-5]. Test samples were taken from the Callovo-Oxfordian argillite at Bure in France and the Opalinus clay (shaly facies) at Mont Terri in Switzerland. Major findings are summarized as follows.

As observed in laboratory and in situ, the gas permeabilities of the claystones increase with stress-induced damage by several orders of magnitude from the impermeable state up to high levels of 10^{-12}–10^{-13} m^2. When hydrostatic confining stress is applied and increased, the fractures in the claystones tend to close up, leading to a decrease in gas permeability down to different levels of 10^{-16}–10^{-21} m^2 at stresses in a range of 10 to 20 MPa.

As water enters and flows through fractures, the clay matrix can take up a great amount of the water and expand into the interstices. Consequently, the hydraulic conductivity decreases dramatically by several orders of magnitude down to very low levels of 10^{-19} to 10^{-21} m^2 even at low confining stresses of 2-4 MPa within short periods of months to years, compared with the long post-closure phase of tens of thousands of years. The very low water permeabilities reached are the same order as that of the intact claystones, indicating that the fractures in the claystones can be completely resealed.

The very low water permeabilities do not change significantly during heating and cooling within a temperature range between 20°C and 90°C. This suggests no negative thermal impact on the sealing of the fractures.

Before water saturation, the fractures act as conduits for preferential gas flow. However, after water saturation, gas entry and penetration into the resealed fractures in claystone needs certain driving forces to overcome the capillary thresholds. The gas entry/breakthrough pressure is determined by the sealing intensity of the fractures and the confining stress. The gas tests carried out on the highly-resealed claystones show that the gas breakthrough pressures increase with confining stress from low levels of 0.2-1.0 MPa at a low stress of 2 MPa up to 8.3-11.3 MPa at high stresses of 12.5-16.0 MPa corresponding to the rock stress state at a depth of ~500 m. It is obvious that the breakthrough pressures are still below the applied confining stresses. This important finding implies that the EDZ, even when highly-resealed, will still have the capacity for gas migration with moderate pressures and thus contribute to avoid high pressure build up for fracturing the host rock.

Generally speaking, the significant sealing capacities of the claystones hinder water transport and thus radionuclides migration through the fractures, but allow gas migration at moderate pressures without

fracturing the host rock. These significant advantages guarantee the long-term integrity and barrier function of the host rock.

References:

[1] Zhang C.L., Rothfuchs T., Dittrich J., Müller J.: Investigations on self-sealing of indurated clay – part of the EC NFPRO project, GRS-230, 2008.

[2] Zhang C.L., Czaikowski O., Rothfuchs T.: Thermo-Hydro-Mechanical Behaviour of the Callovo-Oxfordian Clay Rock – Final report of the BURE-HAUPT/TIMODAZ project, GRS-266, 2010.

[3] Zhang C.L.: Experimental evidence for self-sealing of fractures in claystone, Physics and Chemistry of the Earth, Vol. 36 (2011), 1972-1980.

[4] Zhang C.L., Czaikowski O., Rothfuchs T., Wieczorek K.: Thermo-Hydro-Mechanical Processes in the Nearfield around a HLW Repository in Argillaceous Formations, Project Report THM-TON, GRS-312, 2013.

[5] Zhang C.L.: Investigation on Gas Migration in Damaged and Resealed Claystone, In the Proceedings of Gas Generation and Migration in Radioactive Waste Repositories (accepted for publication 2014).

Strain localization modelling around an underground gallery in Mol with an analysis of the contact pressure on the lining

Fatemeh Salehnia[1], *Arnaud Dizier*[2], *Xiangling Li*[2], *Xavier Sillen*[3], *Robert Charlier*[1]

[1] Department ArGEnCo, Université de Liège, Chemin des Chevreuils, 4000 Liège, Belgium
[2] European Underground Research Infrastructure for Disposal of Nuclear Waste in Clay Environment (EIG EURIDICE), Mol, Belgium
[3] Belgian Agency for Nuclear Waste and Fissile Materials (ONDRAF/NIRAS), Avenue des arts 14, 1210 Brussels, Belgium

Abstract

There is an international consensus on the advisability of storing high-level nuclear waste in deep geological repositories. In potential host rocks, water flow rate must be very low to ensure limited radionuclide release rates in the event of a loss of containment due to the degradation of the engineered barrier system. Hence, clay formations are considered to be well-suited for hosting radioactive waste repositories in a number of European countries considering their low hydraulic conductivity. Boom Clay, a thick deposit of marine clay is considered as a possible host rock for geological disposal of radioactive waste because of its low permeability, large retention (sorption) capacity for many radionuclides and its self-sealing capacity.

Should a repository be constructed in Boom Clay, the stress redistribution induced by the excavations will create a zone with significant irreversible deformations and changes of hydro-mechanical and geo-chemical host rock's properties. This zone which is called as Excavation Damaged Zone (EDZ) is characterized by the macro and micro-fracturing induced by a rearrangement of the rock microstructure. As a consequence of the rock damage and the creation of the crack network, some preferential flow paths depending on the network connectivity may be constituted. As a result, they could locally alter the original flow and transport properties in the rock mass, which could be of importance for later flow and transport processes. Hence, the coupled hydro-mechanical behaviour of Boom clay, the numerical simulation of fracturing and the extension of EDZ during a gallery excavation and their evolution over long-term as the issues of particular interest will be the focuse of this study. The studied gallery is the Connecting Gallery (CG) in the underground research facility (HADES), located at a depth of about 225 m, close to the mid-plane of Boom clay formation in Mol, Belgium.

During the construction of Connecting Gallery, the fracture pattern which was observed around the gallery was found to be similar to that observed in several in situ and lab experiments at different scales (Bastiaens et al., 2003, Mertens et al., 2004, Bésuelle et al. 2014, Lenoir et al. 2007). This suggests that this fracture pattern mainly depends on the intrinsic mechanical properties and the local stress field of Boom Clay. To better understand the mechanisms leading to this fractures' network, we propose to analyse the EDZ and its extension around the Connecting Gallery by numerical modelling, in the framework of a strain localization approach. Numerical modeling of strain localization needs a specific approach to overcome the practical problem of mesh size dependency within the framework of classical finite elements. Therefore, an enhanced technique introducing an internal length scale is needed to address this problem. Among the different regularization methods, the second gradient model is used in this study in which the continuum is enriched by the microstructure effects (Germain 1973, Chambon et al. 1998 & 2001, Collin et al. 2006). In the proposed approach, the kinematics includes microkinematics as well as macrokinematics.

Firstly, the extension of the EDZ and the structure of shear bands of localization during the excavation of Connecting Gallery is studied through the numerical modelling of a quarter of the gallery in plane strain conditions, under the initial anisotropic in situ stress state and considering material anisotropy (see Figure 1). Then, considering the concrete lining on the gallery's wall, the evolution of the contact between the clay mass and the lining is studied during the gallery's construction. The link between the distribution of the contact pressure on the lining and the shear bands pattern around the gallery is analysed.

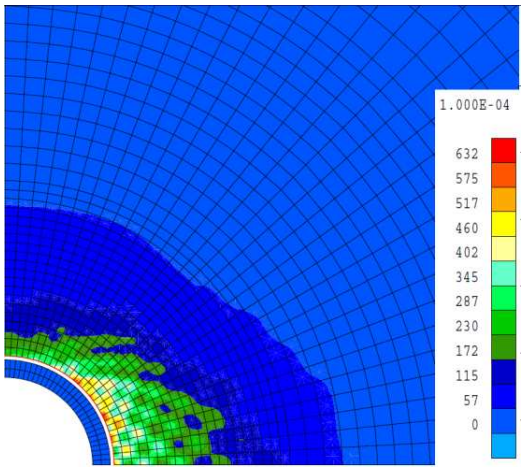


Figure 1: Extension of the localized zone in terms of plastic deviatoric strain around the Connecting gallery at the end of excavation

References

Bastiaens, W., Bernier, F., Buyens, M., Demarche, M., Li, X.L., Linotte, J.M. and Verstricht, J., [2003] The Connecting Gallery - the extension of the HADES underground research facility at Mol, Belgium. EURIDICE report 03-294. Mol: ESV EURIDICE.

Bésuelle, P., Viggiani, G., Desrues, J., Coll, C., and Charrier, P. [2014] A Laboratory Experimental Study of the Hydromechanical Behavior of Boom Clay. Rock Mechanics and Rock Engineering, 47(1), 143-155.Chambon, R., Caillerie, D. and El Hassan, N. [1998] One-dimensional localisation studied with a second grade model. Eur. J. Mech. A/Solids, 17(4), 637-656.

Chambon, R., Caillerie, D. and Matsushima, T. [2001] Plastic continuum with microstructure, local second gradient theories for geomaterials: localization studies. International Journal of Solids and Structures, 38, 8503-8527.

Collin, F., Chambon, R. and Charlier, R. [2006] A finite element method for poro mechanical modelling of geotechnical problems using local second gradient models. Int. J. Numer. Meth. Eng., 65(11), 1749-1772.

Germain, P. [1973] The method of virtual power in continuum mechanics. Part 2: Microstructure. SIAM J. Appl. Math, 25, 556–575.

Lenoir, N., Bornert, M., Desrues, J., Bésuelle, P. and Viggiani, G. [2007] Volumetric digital image correlation applied to X-ray microtomography images for triaxial compression tests on argillaceous rock. Strain, **43**(3), 193–205.

Mertens, J., Bastiaens, W., Dehandschutter, B., [2004] Characterisation of induced discontinuities in the Boom Clay around the underground excavations (URF, Mol, Belgium). Appl. Clay Sci. 26, 413–428.

Feedback on methods of characterization of damage around underground structures in argillites by analyzing wave propagation

Cyrille Balland[1], **Philippe Côte**[2], **Jacques Morel**[3]
(1) INERIS – School of mines – Nancy (France)
(2) IFSTTAR – Bouguenais (France)
(3) Andra – Meuse/Haute-Marne Center– Bure (France)
cyrille.balland@ineris.fr, philippe.cote@ifsttar.fr, jacques.morel@andra.fr

The Callovo-Oxfordian claystones were chosen for their low permeability. This feature marked by the clay content of the rock is inevitably accompanied by a low tensile strength. This generates the development of an excavation damaged zone. Seismic elastic wave propagation analysis methods are potentially valuable for the characterization of the damaged zone. These methods are more or less adapted to clay environment mainly due to the strong wave attenuation.

The easiest seismic method to implement is probably the seismic refraction. It is used from the surface of the wall. It involves analyzing the waves refracted at the interface between the fractured zone and the bedrock. Sato et al. (2003) showed with this method the influence of excavation mode on the extension of the damaged zone in the underground laboratory in Japan Tono (sedimentary clay rock). Similarly, Lagarde et al. (2006) used the method in the Callovo-Oxfordian claystone. The application of seismic refraction in this context is at the limit of resolution because it assumes a multilayer tabular model without velocity reverse and the error on the arrival time measured is very close to time variations due to the damaged zone.

The analysis of the surface waves is based on the dispersive property of these waves. They have the particularity to propagate at different depths depending on their frequency. The objective is therefore to measure the dispersion curve of the wave model and find the velocity profile that best matches. This method called MASW (Multi-Channel Acquisition of Surface Waves) is typically used to find the velocity profile of a tabular field where the inversion is simplified. As part of the thesis of Lagarde (2007), the MASW method was extended to the concave geometry of deep underground excavations to characterize the velocity profile in the damaged zone. It makes it possible to reveal any velocity profile including those with one or more velocity reverse. This method was used at the Meuse Haute Marne URL to characterize the damaged zone at the bottom of a drift.

Seismic methods can also be implemented in borehole, for example ultrasonic logs. They are well suited to the scale of the damaged zone and numerous surveys in deep underground excavations. In the Meuse Haute Marne URL, this method has been used on numerous occasions (Schuster et al, 2001) during the different phases of the excavation of shafts and galleries. These velocity measurements are used to describe both the evolution of the gradient of damage / deconfinement from gallery wall and isolated fractures at greater depth.

Acoustic emissions (AE) occur during initiation and expansion of cracks. Quantifying and locating those AE can bring information in determining the initiation and expansion of the damaged zone. Monitoring these AE has been successfully applied around structures in very resistant rock under high stresses such as granite host rocks of the Lac du Bonnet, Manitoba (Meglis et al, 2005). In claystones, however, the strong wave attenuation make them almost undetectable. The only opportunity to detect them is to place acoustic sensors in close proximity to sources. Forney (1999) developed a compact device capable of recording AE reflecting the creation of the damaged zone during the excavation of a gallery in Mont Terri.

Claystones might show a natural variability that must be taken into account in the analysis of velocity variations induced by damage. A solution to overcome this problem is to measure the velocity of the waves in the rock before it was damaged and monitor its evolution during the excavation of the build. This technique called "velocity survey" has been implemented several times during the excavation of shafts (Balland et al, 2009), galleries or slots. It allowed characterizing the intensity and extension of the damaged zone, as well as the phenomena occurring during sealing or reconfinement of a fractured rock

vicinity. Using a specifically designed 3D device with S and P waves back analysis in the stiffness matrix changes.

A summary of seismic methods for the characterization of the damaged zone in claystones is given in the table below with the main assets, limits, drawbacks and expected results. Some improvement points would concern the power source while increasing the frequency of the waves eventually improves resolution. The frequency sweep is a solution which has already been tested in the Meuse Haute Marne URL and has showed some experimental improvement. Another line would be to connect wave propagation parameters to the dynamic mechanical characteristics of the rock damaged.

Methods	Assets	Limits and drawbacks	Results
Seismic refraction	-	Relies on a simplistic model, resolution limit	Thickness of the damaged zone
MASW	Reflects reversal velocity	Inversion difficulties because of the gallery concavity	Simplified profile of the damaged zone
Ultrasonic logging	Very good spatial resolution, low sensitivity to attenuation	measurement in itself disturbed borehole	Profile of the damaged zone, detection of fractures
Tomography	Good 2D spatial coverage, determination and consideration of the anisotropy	data processing rather long, medium resolution	Image of the damaged zone, velocity anisotropy
Velocity survey	Very good noise immunity, easy integration time component, 3D spatial coverage	Getting complicated work, sensible to damping	Evolution of the EDZ, preferred orientation of the fracturing
AE monitoring	Testifies directly fracturing mechanisms	Very sensitive to damping, records only the events near the sensors	Type of fractures and mechanisms, location and extension of the damaged zone

Balland, C., Morel, J., Armand, G., Pettitt, W., 2009, Ultrasonic velocity survey in Callovo-Oxfordian argillaceous rock during shaft excavation, International Journal of Rock Mechanics and Mining Sciences, Volume 46, Issue 1, Pages 69-79.

Côte, P., Magnin, O., 2008, Mesures tomographiques sur le pilier des galeries scientifiques, Rapport Final TOMO N°1 (RFT1), D RP 1LCP 07 002 / B.

Forney, F., 1999, Caractérisation par méthodes ultrasoniques de la zone endommagée induite par le creusement d'un tunnel en milieu argileux: Cas d'étude au tunnel du Mont Terri, Thèse INPL.

Lagarde, J., Abraham, O., Laguerre, L.., Côte, P., Piguet, J-P., Balland, C., Armand, G., 2006, Cement and Concrete Composites, Volume 28, Issue 4, April 2006, Pages 337-348.

Meglis, I.L., Chow, T., Martin, C.D., Young, R.P., 2005, , International Journal of Rock Mechanics and Mining Sciences, Volume 42, Issue 1, Pages 25-34.

Schuster, K., Alheid, H.-J., and Böddener, D., 2001, Seismic Investigation of the EDZ in Opalinus Clay, Engineering Geology 61, 189-197.

Sato, T., Kikuchi, T. and Sugihara, K., 2000, In-situ experiments on an excavation disturbed zone induced by mechanical excavation in Neogene sedimentary rock at Tono mine, central Japan, volume 181, April, Pages 97-108.

EDF contribution to the ANDRA benchmark exercise: "numerical analysis of the Callovo-Oxfordian claystone hydromechanical response to excavation operations"

S. Cuvilliez[(1)], **R. Fernandes**[(1),(2)], **S. Raude**[(3)]

[1] EDF R&D, 1 avenue du Général de Gaulle, 92140 Clamart, France. (sam.cuvilliez@edf.fr)
[2] LaMSID - UMR EDF/CNRS/CEA 8193, 1 avenue du Général de Gaulle, 92140 Clamart, France.
[3] EDF, CIH, Savoie Technolac, 73373 Le Bourget-du-Lac, France.

R&D studies are today led by EDF to better understand the behaviour of excavations in deep geological formation such as the Callovo-Oxfordian claystone (Cox), which is considered as a potential host for nuclear waste storage in France. In this context, EDF has developed ([1], [2]) a specific visco-elasto-plastic constitutive model which is used in the finite element software *Code_Aster* [5] to describe the Cox behaviour in Thermo-Hydro-Mechanical computations for safety analysis. The main features of this model are summarized as follows:

- yield surfaces are written on a generalized Hoek-Brown criterion;
- the elastoplastic part of the model is first described by an isotropic strain hardening, and then by an isotropic strain softening;
- the viscoplastic part of the model is described by the overstress concept of Perzyna;
- a specific non-associated flow rule allows to take into account the evolution of the dilatancy with respect to the stress state;
- a coupling between instantaneous and delayed mechanisms may occur depending on the stress state.

The purpose of this paper is to present the results of EDF contribution to a numerical benchmark exercise that has been launched since 2012 by ANDRA. A full description of this benchmark is given in the abstract [4] submitted to Clay Conference by ANDRA and the nine participating teams. The first step of this benchmark consists in an evaluation (at the material point level) of the constitutive model response to simple stress paths. The second step is dedicated to the application of the model to finite element analysis at the structure scale, which corresponds to realistic configurations of the ANDRA underground research laboratory of Bure (France).

Given a set of material parameters that has been calibrated on laboratory elementary tests, we will focus in this paper on the second step of the benchmark and present the simulation results of two types of underground galleries: galleries that are parallel to the minor *in situ* principal horizontal stress, and galleries that are parallel to the major *in situ* principal horizontal stress.

- On the first type of galleries, the influence of the support structure stiffness is studied as well as the effect of hydro-mechanical coupling. In order to prevent localisation issues related to strain softening, a second gradient regularisation technique [3] has been used.
- On the second type of galleries, a comparison is made between numerical simulations and *in situ* observations provided by ANDRA (convergence measurements, displacement and pore pressure measurements in the rock mass).

References:

[1] Kleine A. 2007. Modélisation numérique du comportement des ouvrages souterrains par une approche viscoplastique. PhD Thesis, Inst. Nat. Polytech. Lorraine.
[2] Raude S., Laigle F., Giot R., Fernandes R. A unified thermo-plastic/viscoplastic constitutive model for geomaterials. Submitted to Clay Conference Brussels 2015.

[3] Fernandes R., Chavant C., Chambon R. 2008. A simplified second gradient model for dilatant materials: Theory and numerical implementation. Int. J. of Solids and Strucutres, 45: 5289-5307.

[4] D. Seyedi *et al*., A model benchmark exercise for numerical analysis of the Callovo-Oxfordian claystone hydromechanical response to excavation operations, submitted for oral presentation to Clay Conference Brussels 2015.

[5] Code_Aster, EDF R&D, finite element software (GNU GPL licence). http://www.code-aster.org

On the Thermo-Hydro-Mechanical behaviour of a sheared Callovo-Oxfordian claystone sample with respect to the EDZ behaviour

MENACEUR[1] H., *DELAGE[1] P.*, TANG[1] A.M. and CONIL[2] N.

[1] Ecole des ponts ParisTech, Navier/CERMES, France
[2] ANDRA, Bure, France

To better understand the impact of temperature elevation on the response of the excavation damaged zone around repository cells and galleries for radioactive waste disposal, the combined effects of shear and temperature elevation were investigated in the laboratory on the Callovo-Oxfordian claystone. To do so, a hollow cylinder thermal triaxial cell with short drainage path specifically developed for low permeability rocks was used. Once properly saturated under stress conditions close to in-situ, the specimen was sheared along a constant effective mean stress path mimicking the stress path followed during gallery excavation. The shear stress was afterwards released and an undrained heating test was performed on the sheared specimen. It was observed that the temperature increase under undrained conditions led to a thermal increase in pore water pressure resulting in a decrease in mean effective stress that brought back the sheared specimen to failure, evidencing a thermally induced failure. Steady state radial permeability tests performed at various stages of the test demonstrated that the overall permeability of the sheared specimen was comparable to that before shearing, confirming the excellent self-sealing properties of the Callovo-Oxfordian claystone. This shows that, in spite of being possibly remobilized by temperature elevation, the EDZ will return to an overall permeability constant equal to that of the massive rock, reaching the same isolation properties.

The HE-E experiment (Mont Terri): modelling a large in situ heating test

B. Garitte[2], A. Gens[1*], R. B. de Vasconcelos[1], J. Vaunat[1] and I. Gaus[2]

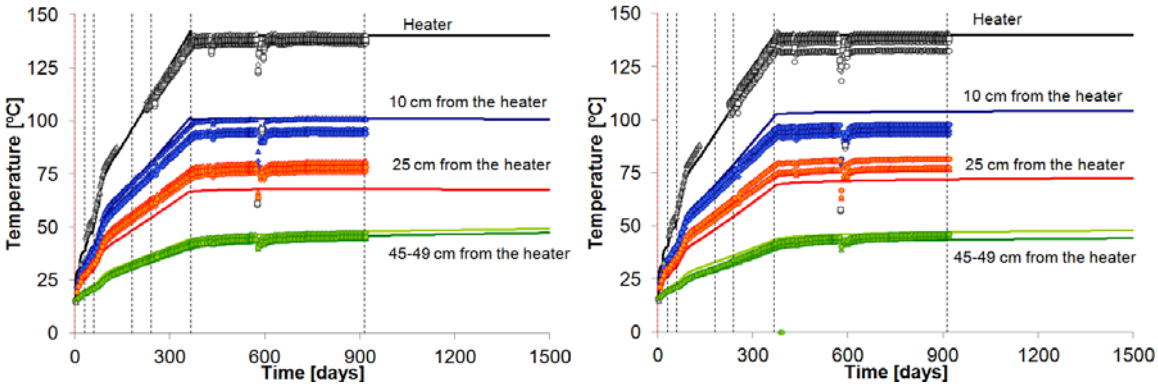
1. Department of Geotechnical Engineering and Geosciences, Universitat Politècnica de Catalunya, E-08034 Barcelona, Spain (antonio.gens@upc.edu).
2. NAGRA, Hardstrasse 73, 5430 Wettingen, Switzerland

(*) Corresponding author

The HE-E experiment is an in situ heating experiment in the Mont Terri underground rock laboratory. It consists of the installation of two 4m-long heaters with a diameter of 30cm in the microtunnel (past location of the Ventilation Experiment) surrounded by a bentonite buffer. The microtunnel has a diameter of 1.3m. The temperature at heater-bentonite interface increased from July 2011 reaching 140º after one year. After that, the temperature has been kept constant. The experiment configuration and the instrumentation system are described in Gaus et al. (2012). The experiment layout is divided in two parts: in the first one the buffer is composed by pure MX-80 bentonite pellets whereas the second one is composed of pellets of a mixture of sand and bentonite (50%-50%). The heaters simulating the canisters rest on a pedestal made up of compacted bentonite. 2D THM axisymmetric computations were used to analyse the buffer and rock response. The analyses have been extended until 917 days after the switching on of the heaters; the experiment is however continuing. The following stages have been considered in the modelling:

- Excavation of the tunnel 4450 days before the emplacement of the test. Afterwards a simplified scheme of the ventilation history is applied in order to achieve a suction/pore pressure distribution in the rock consistent with observations
- Emplacement of the barrier and construction of the concrete barrier
- Switching on the heaters 76 days after emplacement.
- Application of the power to the two heaters for a year
- After reaching a temperature of 140ºC, temperature is kept constant

The comparisons between computed and observed temperatures are shown in Figure 1 for the first 917 days of heating. The satisfactory agreement that is achieved requires a good characterization of the variation of thermal conductivity with degree of saturation.



a) b)

Fig. 1. Measured (dots) and simulated (full lines) temperature evolution in the centre of a) bentonite pellest section and b) the granular sand-bentonite section

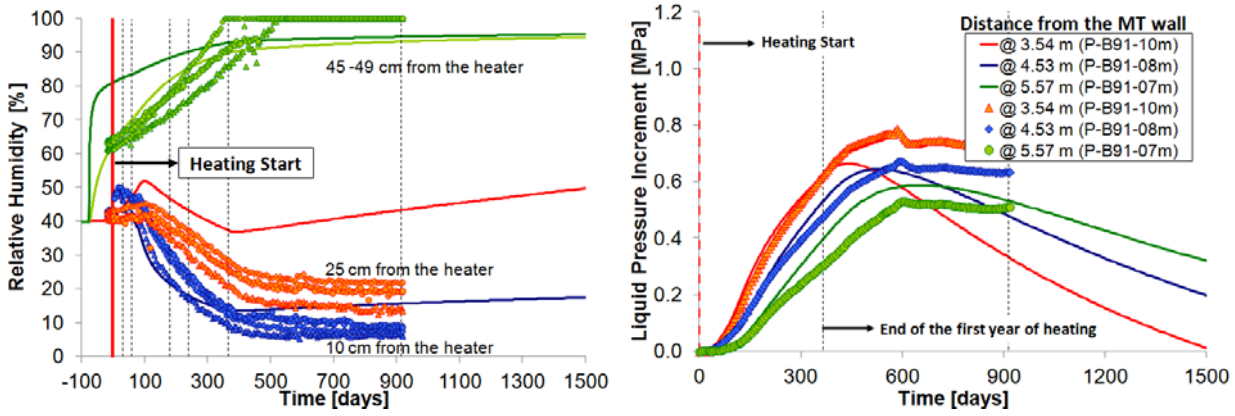
The most remarkable feature to be observed is the high thermal gradient inside the buffer due to heating. After the first year of the experiment the temperature reaches about 140ºC close to the heater-buffer interface and a value around 40ºC near the buffer-rock interface Indeed, 18 months after the end of the first heating only the innermost 5-10 cm of the bentonite buffer exceeds a temperature of 100ºC. The

difference in thermal conductivities of the buffers (thermal conductivity for the bentonite-sand mixture is lower than the bentonite pellets one) also explains why the power required for applying/maintaining a similar temperature in both heaters is lower in the GRS section

The evolution of relative humidity (RH) in the buffer at different distances from the heater is illustrated in Fig. 2a. Measurements from other buffer sections showed a very consistent response with the one depicted here. Sensors near the heater register first an increase of RH that is attributed to vapour diffusion coming from the zone between the sensor and the heater were liquid water evaporates as a consequence of the high temperature. Water evaporation and diffusion towards colder zone dries the material near the heater and results in a decrease of the RH. Near the rock, most of the increase of RH is attributed to water intake from Opalinus Clay. The simulated RH reproduces quite well the observed trend. The RH evolution was found to be very sensitive to the retention curve and to the dependency of water permeability on the degree of saturation.

Measurements show that liquid pressures increase in saturated Opalinus Clay (Fig 2b). Gens et al. (2007) showed that the increase of pore water pressure was mainly due to the differential thermal expansion of the water and the pores in combination with the relatively low water permeability that prevents full drainage of the generated overpressure. Using the same parameters as those from Gens et al. (2007), the measured pore water pressure increments are reproduced satisfactorily. In the full paper, measurements will be available until day 500, which will allow the correct evaluation of the predicted pore water pressure peak.

Although the mechanical response of the EBS is simulated using an elastoplastic model that incorporates the effects of suction and temperature in its formulation (the swelling potential of the bentonite is also considered) and despite the fact that the overall THM behavior is correctly simulated, the analysis overestimates the rate of hydration close to the heater in the early stages of the test. This fact may suggest the need to consider more advanced numerical formulations that incorporate explicitly the microstructure of the bentonite and its evolution during the process of hydration.



a) b)

Fig. 2. Measured (dots) and simulated (full lines) a) relative humidity evolution in the EBS and b) pore water pressure increments in the Opalinus Clay at various distances from the buffer-rock interface.

References:

Gaus I., K. Wieczorek, K. Schuster, J.-C. Mayor, T. Trick, J.-L. Garcià Siñeriz, O. Czaikowski, U. Kuhlmann, B. Garitte, S.-P. Teodori, P. Marshall. 2012. EBS behaviour immediately after repository closure in a clay host rock: the HE-E experiment (Mont Terri RL). Clays in Natural and Engineered Barriers for Radioactive Waste Confinement, Montpellier.

Gens, A., Vaunat, J., Garitte, B. & Wileveau, Y., 2007. In situ behaviour of a stiff layered clay subject to thermal loading. Observations and interpretation. Géotechnique, vol. 57, no 2, pp. 207-228.

Displacement of heater in the THMC China-Mock-up test

Y.M. Liu[1,2*], S.F. Cao[1,2], J Wang[1,2], J.L. Xie[1,2], L.K. Ma[1,2], X.G. Zhao[1,2], L. CHEN[1,2]

1. Beijing Research Institute of Uranium Geology (BRIUG), 2. CNNC Key Laboratory on Geological Disposal of High-level Radioactive Waste, 10, Xiao-Guan-Dong-Li, P.O. Box 9818, 100029, Beijing, China

* Corresponding author: liuyuemiao@163.com Tel: +86 13621105011

1. Description of the experimental infrastructure

In accordance with the current disposal concept of High-level Radioactive Waste (HLW) disposal in China, the large scale China-Mock-up test is designed as a vertical cylindrical tank(Φ900×H2200mm), filled with compacted GMZ-bentonite (Fig.1). An electrical heater, which could move vertically to simulate the HLW canister(Φ300×H1600mm, weight:1 ton), is placed inside the compacted bentonite blocks, with water content of 8.7% and dry density of 1710 kg/m^3. The installed hydration system on the exterior surface simulates the supply of groundwater. A layer of geotextile is placed between the tank and compacted GMZ bentonite. The gaps between the tank and heater with the bentonite blocks are filled with crushed pellets, with an averaged dry density of 1300 kg/cm^3.

More than 160 sensors have been installed within the experiment to measure the important parameters, including the temperature, relative humidity, hydraulic pressure, the total pressure in the bentonite and displacement of heater. The sensors are distributed in 7 sections in vertical direction to investigate the behavior of buffer material under THMC complex coupling condition.

According to the reference concept of HLW disposal in China, the canister is completely supported by the surrounding buffer material. Therefore, the mechanical performance of buffer material may influence the overall stability of the canister. In order to evaluate this potential influence, six LVDT sensors are installed on the top and bottom of the heater to monitor its vertical displacement.

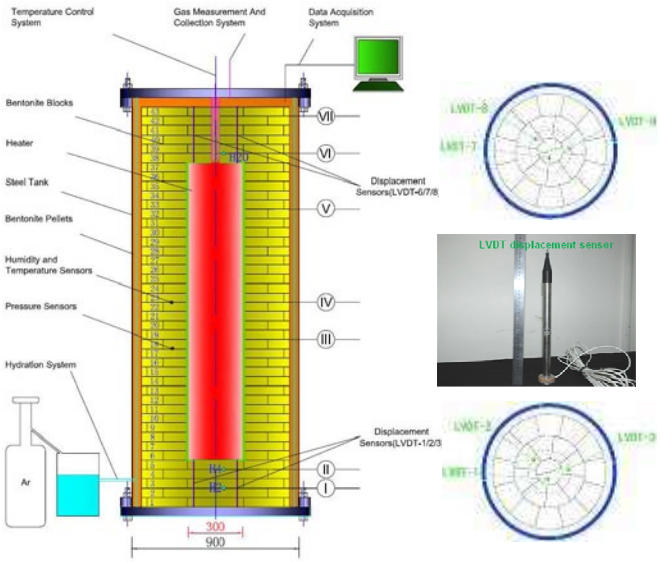


Figure 1 Sketch of the China-Mock-up facility (unit: mm).

2. Mock-up operation

The China-Mock-up experiment was assembled completely on 10th September 2010. The real-time

data acquisition and monitoring system has recorded all the measurement data from January 1st 2011. The THMC experiment was commenced on July 8th 2011.

The power supply to the heater has been made in three phases. First, the temperature of the heater was increased to 30°C and maintained constant to verify the reliability of the installed sensors. Then, the temperature was increased progressively to 90°C which is the maximum temperature expected on the canister surface according the current disposal concept in China. Finally, the system was switched to the constant temperature control mode at 90°C on the surface of the heater.

In order to avoid potential damage to the sensors, the hydration was initially controlled by a water injection rate which was increased gradually from 400g/day to 1500 g/day in the first stage. Then the injection was controlled by a constant pressure which be increased gradually from 0.2Mpa since August 25th 2013. As planned, a constant pressure of 2MPa is to be applied when the pellets become fully saturated.

3. Analysis of Displacement of the heater

Fig. 2 presents the evolution of displacement and temperature of the heater, as well as the relative humidity (RH) at the bottom and top of the heater. An upward displacement 7.5mm of the heater was recorded. It can be noticed that, the increase rate of displacement could be separated three phase.

The first stage, the displacement is mainly controlled by thermal expansion due to the increase of the temperature. Especially, when the temperature of the heater increased from 30°C to 90°C, the displacement of the heater increased quickly.

The second stage, the displacement is mainly related to the saturation and swelling process of bentonite at the bottom of heater. With the relative humidity of the bentonite (H2 and H4) increase quickly, the bentonite swelled and pushed the heater upward quickly. When the bentonite nearly saturated, the bentonite swelled slowly and the heater moved upward slowly.

The last stage, the displacement is mainly related to the saturation and swelling process of bentonite at the top of heater. With the relative humidity of the bentonite (H20) increased and the bentonite swelled, the heater moved upward gradually.

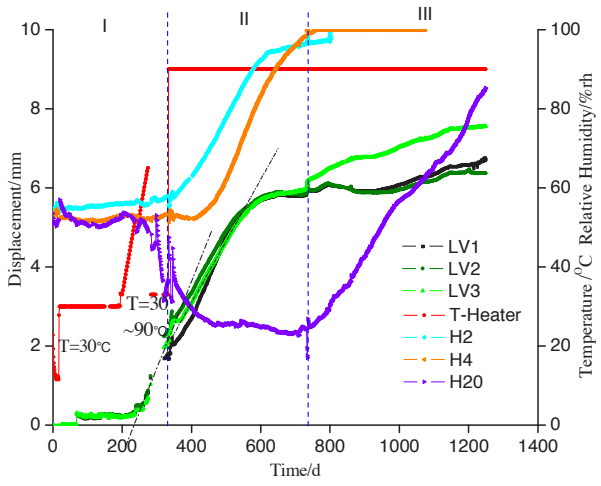


Fig. 2 Evolution of displacement and temperature of the heater with the relative humidity (RH).

4. Conclusion

As a milestone for the buffer material study in China, the China-Mock-up test is considered as a source of valuable data to investigate the THM behavior of GMZ bentonite under relevant repository

condition and to improve the knowledge of the THMC process in the EBS.
For China-mock-up test the upward displacement of the heater suggests that the thermal expansion and saturation process of the buffer material may influence the stability of canister in the long-term, which should be considered in the design of the repository.

Results from hydro-mechanical and geochemical analyses of the retrieved buffer material from the Prototype Repository at Äspö Hard Rock Laboratory

Lars-Erik Johannesson, Pär Grahm, Anders Sjöland
SKB Sweden

Introduction

Prototype Repository is a full-scale trial of the KBS-3V system, installed at the Äspö Hard Rock Laboratory in 2001-2003. The trial consists of six full-scale deposition holes in a TBM-tunnel at a depth of 450 metres in crystalline rock. Each deposition hole was installed with bentonite buffer (MX-80) and full-scale canisters, equipped with heaters to simulate residual heat from spent fuel. The deposition tunnel was backfilled with a mixture of crushed rock and bentonite (30 % bentonite). The design of the trial includes two sections separated by a concrete dome plug. The inner section, which still is in operation, consists of four deposition holes. The outer section with two deposition holes was opened and retrieved during 2011. The dimensions of the tunnel and the deposition holes are shown in Figure 1.

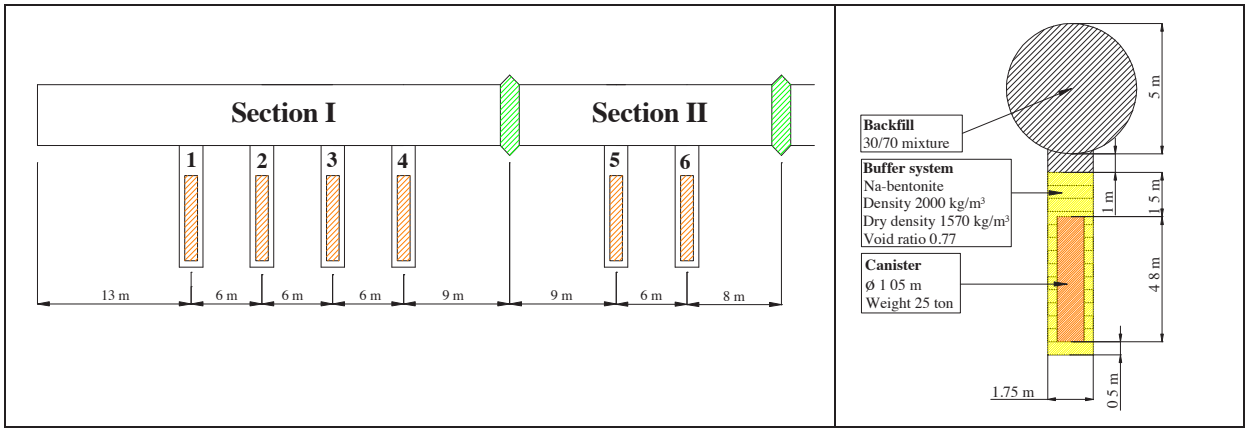


Figure 1. *Schematic layout of the deposition tunnel and the deposition holes of the Prototype Repository.*

The buffer and backfill of the outer section (Section II) has been wetted by the naturally inflowing groundwater until the end of year 2010 when the outer plug was breached. 900 tons of backfill, 40 tons of buffer and two canisters were retrieved during 2011. Laboratory examinations were then carried out until summer 2013.

Determinations of buffer density and water content

After almost 8 years of wetting, none of the two buffers was homogeneous and large variations in water saturation existed, both between the deposition holes, between blocks from the same hole, and also within one and the same block. Results from about 4000 determinations of density and water content in each buffer are now available.

Laboratory examinations

At the retrieval of the buffer, samples were also taken for laboratory examinations concerning both hydro-mechanical, chemical and mineralogical characterisation. Examinations were performed on both field exposed material and on reference samples, saved at the manufacturing of the buffer blocks. The purpose of this procedure was to study possible changes in the buffer material after almost 8 years of exposure to elevated temperature and saturation of water from the surrounding rock. The maximum temperature had never exceeded ~85ºC during the test period and higher temperature had been maintained for a longer time in deposition hole 5 than in deposition hole 6.

Results from hydro-mechanical and geochemical examinations of the buffer material
Hydro-mechanical tests were performed on samples from one radial profile from the warmest part of each buffer and included determinations of hydraulic conductivity, swelling pressure, unconfined compression strength, and shear strength.

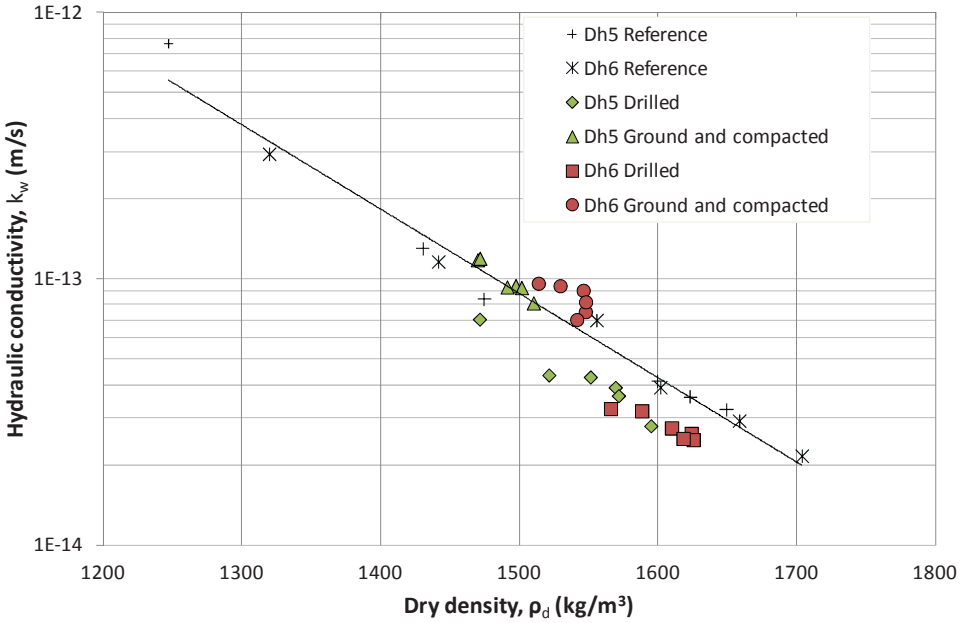


***Figure 2**. The determined hydraulic conductivity as a function of the dry density of samples from deposition holes 5 and 6. Black points denote references.*

The conclusions from the hydro mechanical investigations are:

- the measurements of the swelling pressure and hydraulic conductivity show no large differences in swelling pressure between the reference specimens and the specimens with field-exposed material,
- the stress at failure, measured in unconfined compression tests, increased with increasing dry density but no large differences in strength between the reference specimens and the specimens with field exposed material could be seen. The field exposed material was somewhat more brittle than the reference specimens.

Chemical-mineralogical analyses were carried on four radial profiles from three blocks with variable water content. The analyses included determinations of water-soluble salts, chemical composition, cation exchange capacity, exchangeable cations, and mineralogy. The results from the analyses show that:

- the chloride concentration in the three saturated profiles had increased 3 to 6-fold. Soluble accessory minerals in the bentonite, mainly gypsum but also calcite, had been redistributed and re-precipitated close to the canister,
- the major change in the exchangeable cation pool was a small but general loss in magnesium relative to the reference concentration, in the outer and middle parts of all profiles investigated,
- non-exchangeable magnesium had increased relative the reference level close to the canister, suggesting a transfer of magnesium along the thermal gradient, and accumulation in the warmest part of the buffer,
- the bentonite from the buffer tended to have somewhat lower cation exchange capacity than the references,
- the FTIR-and XRD-characteristics, the calculated structural smectite formulae, and the CEC of the <0.5 µm fraction provided no significant evidence of any structural changes in the montmorillonite.

Hydraulic response of Opalinus Clay during excavation and ventilation phases of the 1:1 scale FE Experiment

Tobias Vogt[1], **Herwig R. Müller**[1], **Benoit Garitte**[1], **Toshihiro Sakaki**[1], **Niels Giroud**[1], **Tim Vietor**[1]

[1] Nagra, Hardstr. 73, 5430 Wettingen, Switzerland (tobias.vogt@nagra.ch)

The Full-Scale Emplacement (FE) Experiment at the Mont Terri underground research laboratory in Switzerland is a 1:1 scale multiple heater test in a clay-rich formation (Opalinus Clay). Based on the Swiss repository concept it simulates the construction, emplacement, backfilling, and post-closure thermo-hydro-mechanical (THM) evolution of a spent fuel (SF) / vitrified high-level waste (HLW) repository tunnel in a realistic manner. The main aim of this experiment is to investigate SF / HLW repository-induced THM coupled effects mainly in the host rock but also in the engineered barrier system (EBS), which consists of bentonite pellets and blocks. Further aims are to gather experience with full-scale tunnel construction and canister/buffer emplacement as well as investigation of hydro-mechanical (HM) processes in the host rock during excavation and ventilation phases.

The entire experiment implementation (in a 50 m long gallery with approx. 3 m diameter) as well as the post-closure THM evolution will be monitored using a network of several hundred sensors (state-of-the-art sensors and measurement systems as well as novel fiber-optic sensor technologies). The sensors are distributed in the host rock near- and far-fields, the tunnel lining, the EBS, and on the heaters.

The hydro-mechanic instrumentation concept and rationale as well as the first monitoring results of the excavation and ventilation phase are presented. During excavation a strong hydraulic response in the host rock was observed. In this context the spatiotemporal evolution of porewater-pressure time series was analyzed to get a better understanding of HM coupled processes during and after the excavation phase as well as the signature of the anisotropic geomechanic and hydraulic properties of the clay-rich formation onto the measured system response. Excavation related investigations included also inclinometer and extensometer data as well as convergence measurements to characterize the non-elastic and time-dependent deformations. In addition, the effect of drainage, suction and desaturation processes during the ventilation phase on the pressure distribution in the host rock was evaluated. The investigations were completed by a hydraulic testing campaign for the characterization of hydraulic conductivity in the host rock near- and far-field. The results give detailed spatiotemporal insights into the anisotropic HM behavior on 1:1 scale, namely stronger pressure variations and deformation perpendicular to the bedding. In addition, a deeper desaturation zone in the unlined tunnel section is observed during the ventilation phase compared to the lined tunnel section. Based on these results the conceptual models of large scale HM processes including the hydraulic behavior of this clay-rich formation during excavation and ventilation phases were improved. The collected data serve as a basis for several ongoing numerical modelling projects.

THM modeling of the compacted GMZ bentonite in the China-Mock-up test

Liang CHEN,
corresponding author: Liang Chen; Tel: +86-13466678227; E-mail: liangchencn@yahoo.cn..

Address(es) :
Beijing Research Institute of Uranium(BRIUG), Beijing, 100029,China

Abstract :
The China-Mock-up test is installed to evaluate the performance of the compacted Gaomiaozi (GMZ) bentonite under coupled thermo-hydro-mechanical (THM) conditions in deep geological disposal. Numerical studies of the test are carried out in this paper.

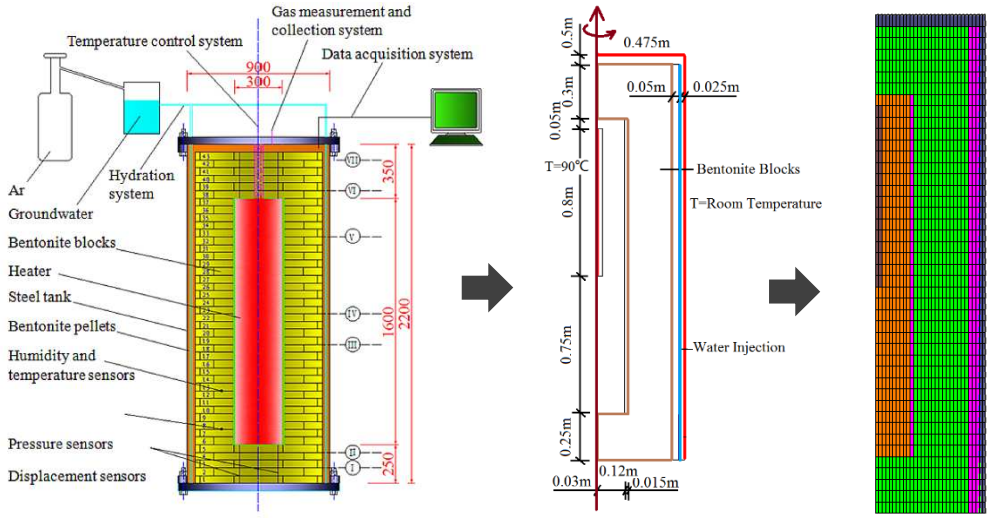


Fig.1 The numerical study of China-Mock-up test

A THM model is proposed to reproduce the complex physic-mechanical behaviors of the bentonite. The Barcelona basic model is incorporated to reproduce the mechanical behavior of the GMZ bentonite under unsaturated conditions. With the presented model, a 2D-axisymetric finite element simulation of the China-Mock-up test is realized with the help of LAGAMINE. Five materials are included in the simulation: the compacted GMZ bentonite, pallets, steel tank, electrical heater and the steel can of the heater. Also, there are two temperature boundary conditions and a water injection boundary condition which is simulated by a highly permeable material. The system is initially at room temperature.

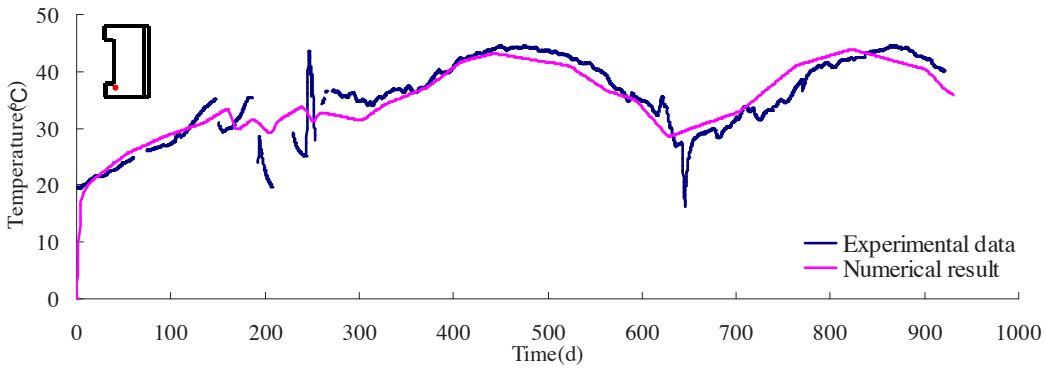


Fig.2 Simulation results of the lower part in China-Mock-up

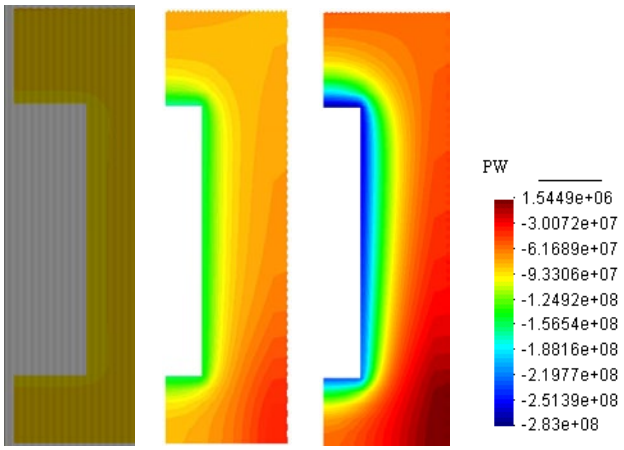


Fig.3 The evolution of water pressure with time

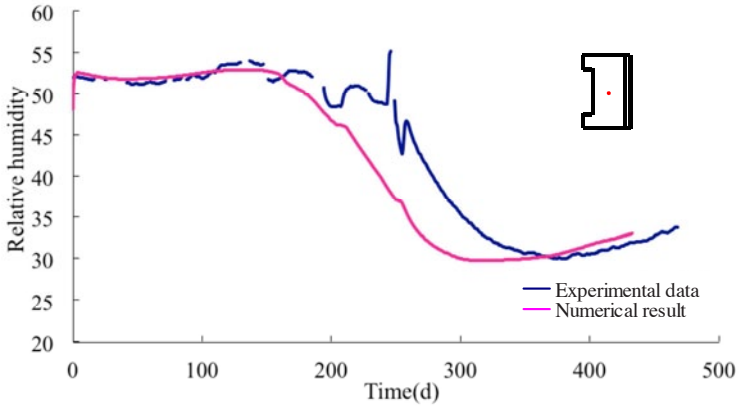


Fig.4 Simulation result of water pressure

Compared to the experimental data, the time variations associated with the temperature, degree of saturation, suction, relative humidity and swelling pressure are studied. It can be noticed that the experimental process can be well simulated with the proposed model, especially for the desaturation-saturation process in the area that near the heater. This phenomenon can be attributed to the evaporation, generated by high temperature of the electrical heater. The results suggest that the numerical method is able to simulate the behavior of the GMZ bentonite, and to predict moisture motion under coupled THM conditions.

Stability of compacted bentonite blocks and block pedestals under changing climatic conditions in tunnels and long-term loads

Benoit Garitte, Florian Kober, Herwig R. Müller, Sven Köhler, Hanspeter Weber and Ingo Blechschmidt

NAGRA, National Cooperative for the Disposal of Radioactive Waste, Hardstrasse 73, CH-5430 Wettingen, Switzerland, benoit.garitte@nagra.ch

Introduction

The BeLLT (Bentonite Large scale Load Test) and the BLL (Bentonite Long term Load) experiments aim at investigating the stability of compacted bentonite blocks under climatic and mechanical loads. They are satellite experiments of the FE experiment (Müller et al., 2015) and were designed to optimize the production parameters of the FE bentonite blocks (Garitte et al., 2015) and the design of the bentonite block pedestals of the FE experiment that must sustain the 5 ton heaters. Both experiments were performed at Grimsel Test Site (GTS) and were associated with a series of mechanical laboratory experiments run at CEA on blocks produced at different compaction pressures and different water contents aiming at investigating the influence of ambient relative humidity on block stability.

BLL experiment

The set-up of the BLL experiment consists of 4 groups of 2 blocks that were produced at different water content and different compaction pressure. Each of the groups is loaded at a pressure equivalent to the weight of a FE heater on a bentonite block pedestals and exposed to the ambient relative humidity at GTS (varying between 50% and 90%). The correlation between the BLL experiment results (summarized in figure 1) and the laboratory tests run at CEA are depicted in the paper.

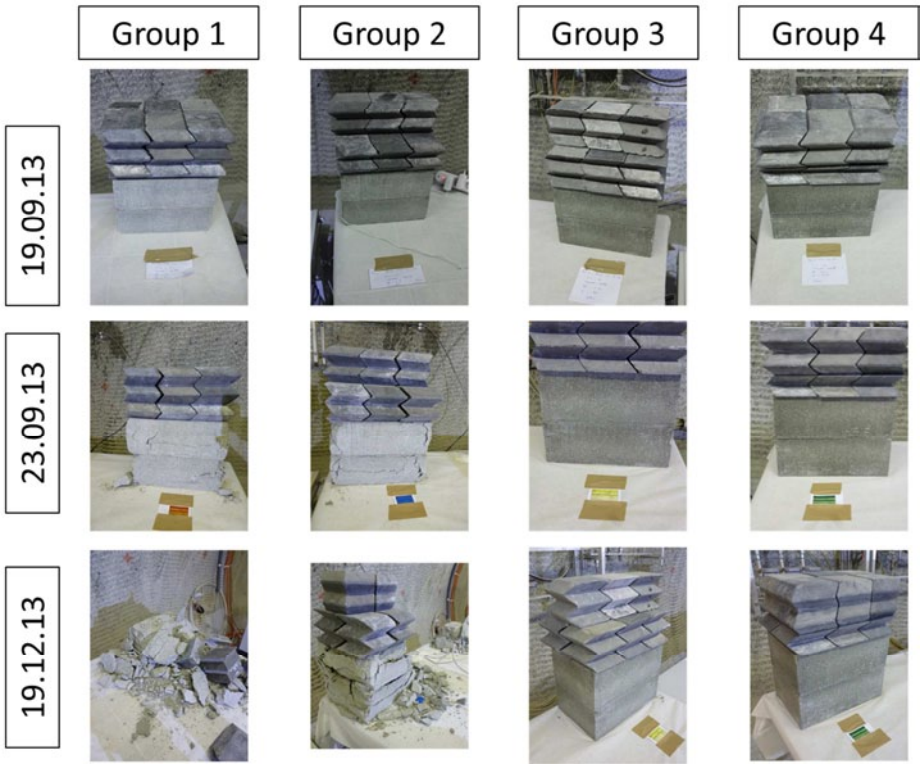


Figure 1: *Resistance of compacted bentonite blocks to exposition time to ambient relative humidity as a function to the production parameters (water content and compaction pressure are different for each of the 4 groups).*

BeLLT experiment

The BeLLT experiment aims at assessing the safety factor in terms of short term load capacity of a canister pedestal built from bentonite blocks to ensure a safe emplacement of the heaters in the FE experiment. To this purpose, a 80cm long bentonite block pedestal characterized by the same sectional dimensions as those of the FE experiment were built below a loading frame built for the experiment (figure 2, left). Two tests were performed (figure 2, right) to investigate the influence of reinforcement elements. The paper describes the experimental results and a qualitative comparison with FeM-DeM modelling results using parameters determined in the laboratory.

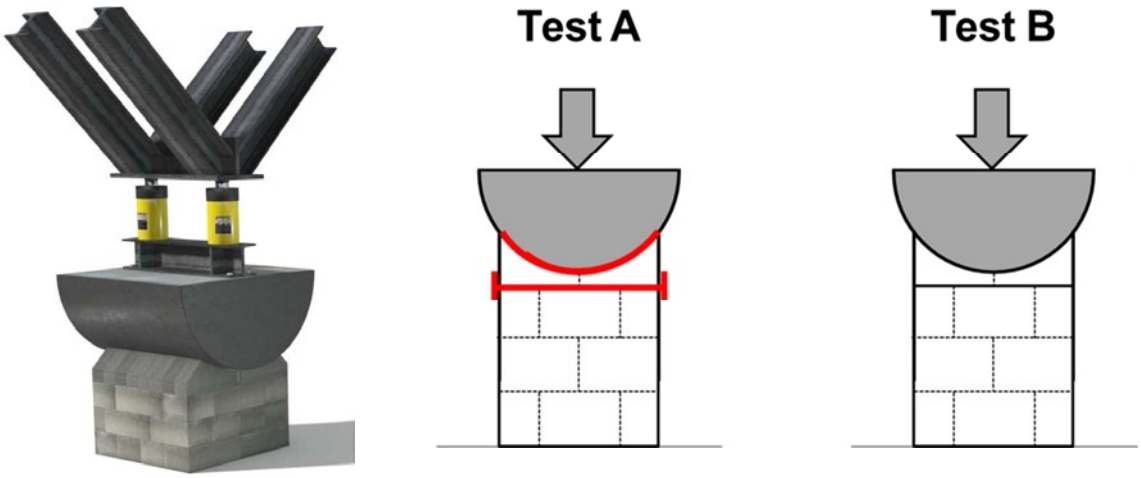


Figure 2: *Set-up of the BeLLT experiment (left) and two different test runs (right)*

References

Müller H. R., Vogt T., Garitte B., Köhler S., Sakaki T., Weber H., Vietor T. The Full-Scale Emplacement Experiment – Implementation of a multiple heater experiment at the Mont Terri URL. Conference companion paper.

Garitte B., Müller H. R. and Weber W. FE experiment: Production of bentonite based backfill materials. Conference companion paper.

FE experiment/LUCOEX: Production of bentonite based backfill materials

Benoit Garitte, Herwig R. Müller and Hanspeter Weber

NAGRA, National Cooperative for the Disposal of Radioactive Waste, Hardstrasse 73, CH-5430 Wettingen, Switzerland, benoit.garitte@nagra.ch

Introduction

The Full-Scale Emplacement (FE) Experiment at the Mont Terri underground research laboratory is a full-scale heater test with three heaters in a clay-rich formation ('Opalinus Clay'). The general lay-out and experimental aims are described in a companion paper (Müller et al., 2015). This paper focusses on the optimisation of the bentonite buffer material production, one of the objectives of the FE experiment. A natural (non-activated) sodium bentonite from Wyoming was used. The production of approx. 3,000 bentonite blocks (70 tons) in a high pressure press and of approx. 350 tons (highly compacted) granulated bentonite mixture, (hc)GBM, is described in terms of design parameters and production quality control. The bentonite blocks will be used in the FE experiment to backfill a 2m long tunnel section in direct contact with the rock and to build pedestals that will support the heaters. The hcGBM will be used to backfill the remaining open volume of the tunnel (around and between the heaters).

Bentonite Blocks

The bentonite blocks were produced at a rate of one block per minute. The average characteristics of the blocks are given in table 1. The control parameters during the production are the compaction pressure, weight of each block and water content of the raw material. The compaction pressure and water content were determined in two pre-productions aiming at producing blocks as insensitive as possible to relative humidity variations. A relatively high compaction pressure (130 MPa) and relatively high water content (18%) were found necessary to produce almost saturated blocks resistant to changes of relative humidity below 75%. The compaction pressure and water content lead to an average dry density of 1.78 g/cm^3, characterizing the compaction at the wet side of Proctor's optimum. Production requirements on dimensions and density were a tolerance of 0.85mm or 0.02g/cm^3, respectively, relative to the average dimensions and density of the first 100 blocks. Figure 1 illustrates the variation of the block density throughout production. Only a small number of blocks had to be rejected.

Table 1: *Average production parameters and characteristics of the 2500 rectangular bentonite blocks*

	Compaction pressure [Mpa]	Weight [g]	Length [mm]	Width [mm]	Height [mm]	Density [g/cm^3]	Measured water content [%]
Average	129.6	24,517	401.3	200.6	145.3	2.096	18.00
Std dev.	0.4	93	0.2	0.2	0.3	0.007	0.67
Min	128.7	23,920	400.5	199.9	143.9	2.061	17.27
Max	131.5	25,000	402.1	201.7	146.5	2.119	19.74

Highly compacted Granulated Bentonite Mixture (hcGBM)

The 350 tons were produced in a three step process consisting of:

- Adjustment of the grain size distribution and water content of the raw material
- Compaction of the raw material into pellets
- Mixing of the pellets to adjust the grain size distribution of the to be emplaced hcGBM

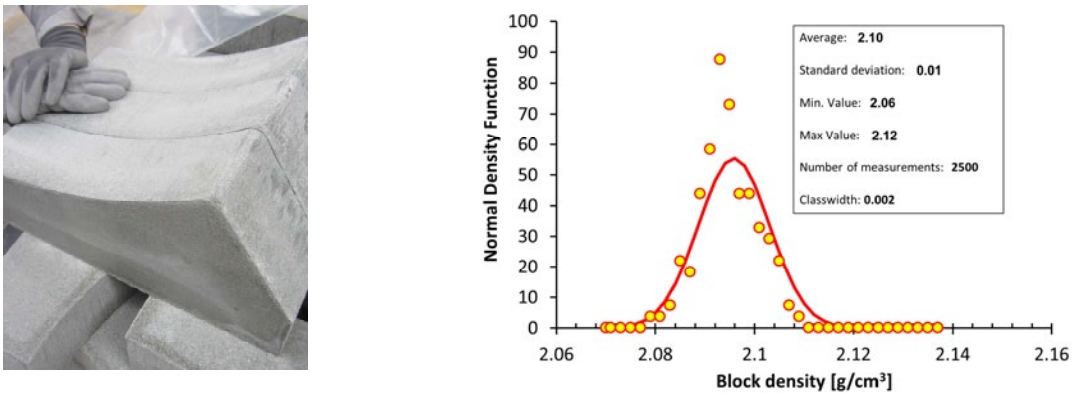


Figure 1: *Curved blocks to be used for the top layer of the pedestal supporting the heaters (left) and statistic about the density of the blocks throughout production (right).*

The final aim of this three step procedure was to obtain a mixture constituted by high dry density pellets with the lowest possible porosity between the pellets considering that those two parameters control the final mixture dry density as:

$$\rho_{mixture} = (1 - \varphi_{inter-pel})\rho_{dry\ pel} \quad (1)$$

where $\varphi_{inter\text{-}pel}$ is the porosity between the pellets and $\rho_{dry\ pel}$ is the pellet dry density. Equation 1 is illustrated in figure 2 where the target emplacement dry density and target production dry density are indicated. The pellet dry density measured in samples taken every ton during the first 100 tons was 2.18 g/cm^3 on average and had a very small standard deviation (see figure 2, right). The pellet dry density falls thus well inside the production target range. The inter-pellet porosity of the mixture could not be measured on a regular QC basis during the production and the mixture grain size distribution and mixture pouring density were used as QC parameters instead.

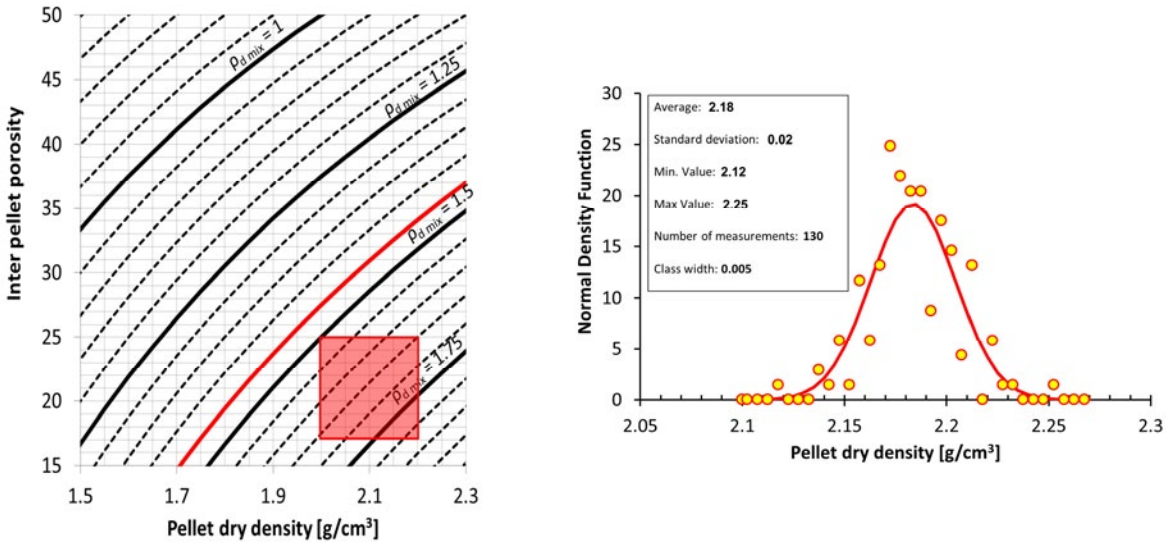


Figure 2: *Theoretical dependency of mixture dry density on pellet dry density and inter pellet porosity (left, target emplacement dry density for FE is indicated by red isoline and target production mixture dry density is indicated by red rectangle) and statistic about the pellet dry density measured in the first 130 produced tons (right).*

References

Müller H. R., Vogt T., Garitte B., Köhler S., Sakaki T., Weber H., Vietor T. The Full-Scale Emplacement Experiment – Implementation of a multiple heater experiment at the Mont Terri URL. Conference companion paper.

FE experiment: THM modelling, predictions, observations and interpretation

Benoit Garitte, Kate Thatcher, Tobias Vogt, Herwig R. Müller and Tim Vietor

NAGRA, National Cooperative for the Disposal of Radioactive Waste, Hardstrasse 73, CH-5430 Wettingen, Switzerland, benoit.garitte@nagra.ch

Introduction

The Full-Scale Emplacement (FE) Experiment at the Mont Terri underground research laboratory (URL) is a full-scale heater test in a clay-rich formation ('Opalinus Clay'). The general lay-out and experimental aims are described in a companion paper (Müller et al., 2015). This paper focusses on the Thermo-Hydro-Mechanical modelling work done in the framework of the FE experiment to:

- Help the instrumentation lay-out
- Design the heating strategy
- Interpret the first observations

At the time of writing this abstract, the heaters and bentonite backfill of the FE experiment are about to be emplaced and the interpretation of the first observations is thus not described in here, but will be included in the final paper.

Modelling features and results

Modelling was performed in steps of increased complexity. In a first step, the best fitting function for the thermal conductivity dependency on the degree of saturation was determined to reproduce the temperature measurements in the GBM (granulated bentonite mixture) buffer of the HE-E experiment accounting for some laboratory measurements of the thermal conductivity (figure 1). One of the challenges here was that laboratory measurements of GBM thermal conductivity are scarce in the literature and only found for low degree of saturation. In the high degree of saturation range, the function used in this work is lower than the laboratory measurements on compacted bentonite (at the same dry density).

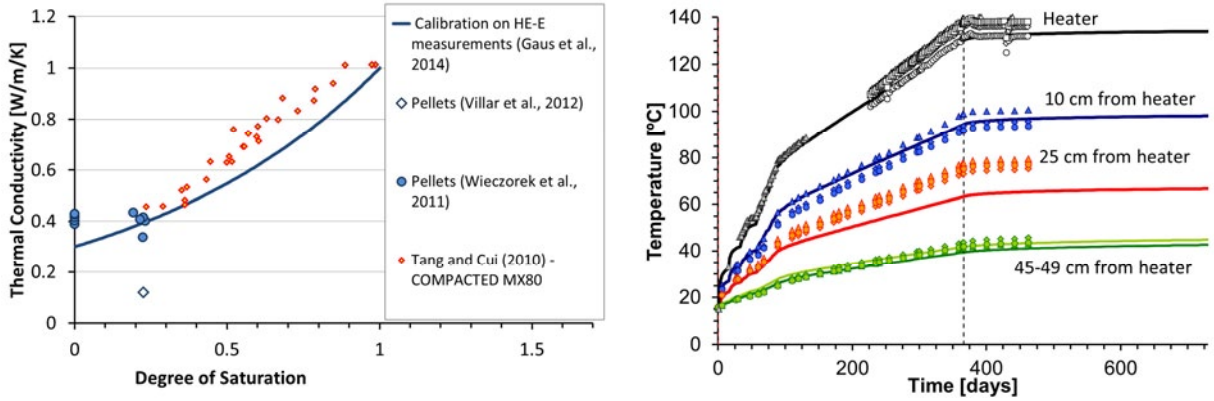


Figure 1: *Thermal conductivity as a function of degree of saturation for GBGM (left) and reproduction of the temperature evolution in the HE-E buffer using this function (right).*

The calibrated thermal conductivity function was then used in two axisymmetric models developed independently by two of the authors to predict the temperature evolution, RH evolution in the buffer, pore water pressure and deformation in the rock using the decaying heating power of radioactive waste canisters (figure 2, left). The two axisymmetric models give very similar results (figure 2, right). The temperature evolution at rock-buffer interface was shown to be relatively independent of the buffer properties. A full 3D model was then developed to account for 1) the rock anisotropy, 2) the presence of high conductive blocks below the heater element and 3) the presence of the canister in the computation (figure 3). According to the THM temperature predictions of the FE experiment and considering the parameters calibrated on the HE-E emplaced material (dry density about 1.4g/cm3,

Gaus et al. 2014) a temperature of 170°C or more might thus be expected. Nevertheless, this temperature will not be allowed in the FE experiment because such a high temperature might damage the emplaced sensors. Two possible scenarios are envisaged: 1) the emplaced GBM in the FE experiment will have a higher dry density than that of the HE-E one, which will result in a slightly higher thermal conductivity and the peak temperature might still be lower than 150°C (maximum temperature allowed by the sensors) using the power input given in figure 2, left or 2) the temperature increase will be too high and the power input will have to be reduced.

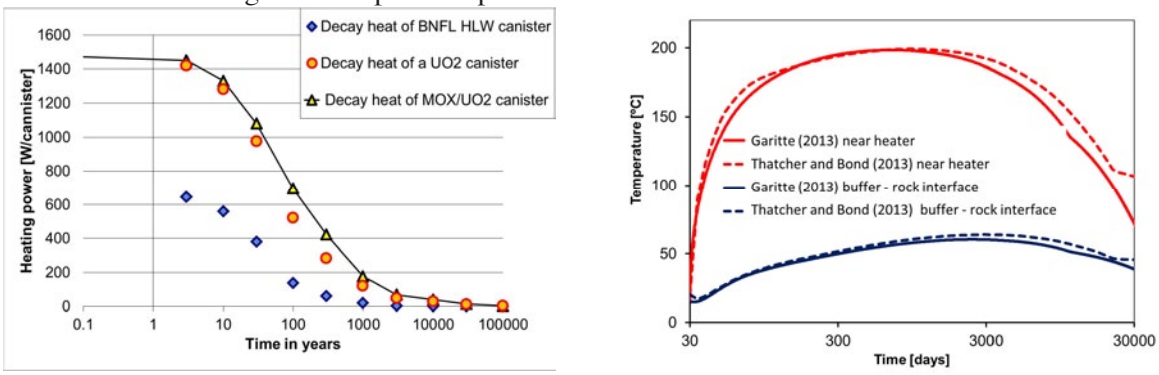


Figure 2: *Applied heating power per heater in the FE experiment as foreseen for Swiss high level waste canister (Johnson et al., 2002) (left) and predicted temperature evolution at heater surface and rock-buffer interface by two modellers (right).*

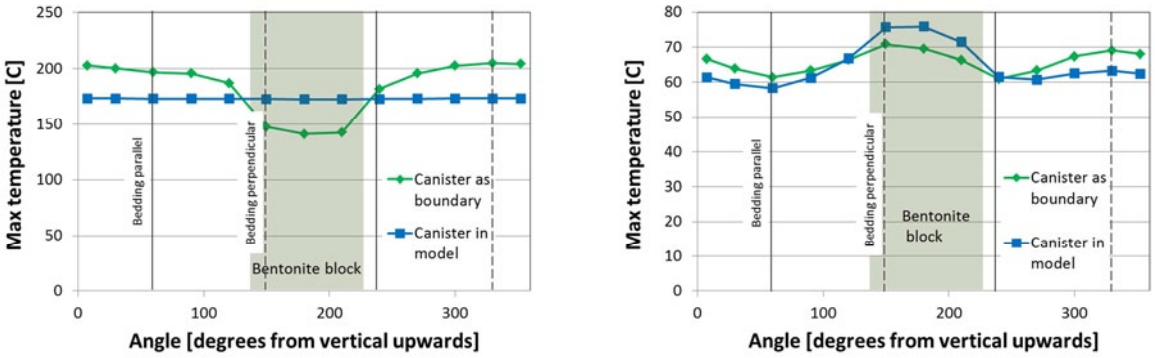


Figure 3: *Predicted peak temperature reached at heater surface (left) and rock-buffer-interface (right) in a model where the heater element is represented as boundary condition (green curves) and a second model where the heater element is explicitly taken into account.*

References

Gaus I., Wieczorek K., Schuster K., Garitte B., Senger R., Vasconcelos R., Mayor J.C. 2014. EBS behaviour immediately after repository closure in a clay host rock: HE-E experiment (Mont Terri URL). Journal of the Geological Society (Impact Factor: 2.58). 03/2014; DOI:10.1144/SP400.11

Johnson, L.H., Niemeyer, M., Klubertanz, G., Siegel, P. & Gribi, P. (2002): Calculations of the temperature evolution of a repository for spent fuel, vitrified high-level waste and intermediate level waste in Opalinus Clay. Nagra Tech. Rep. NTB 01-04.

Müller H. R., Vogt T., Garitte B., Köhler S., Sakaki T., Weber H., Vietor T. The Full-Scale Emplacement Experiment – Implementation of a multiple heater experiment at the Mont Terri URL. Conference companion paper.

Villar M.V., Martín P.L., Gómez-Espina R., Romero F.J., Barcala J.M.. 2012. THM cells for the HE-E test: setup and first results. PEBS Report D2.2.7a. CIEMAT Technical Report CIEMAT/DMA/2G210/02/2012. Madrid, 34 pp.

Wieczorek, K., Miehe, R., Garitte, B. (2011): Measurement of Thermal Parameters of the HE-E Buffer Materials. PEBS Deliverable D2.2-5.

Tang, A.M. and Cui, Y.J. (2010). Effects of mineralogy on thermo-hydro-mechanical parameters of MX80 bentonite. Journal of Rock Mechanics and Geotechnical Engineering, 2 (1): 91–96.

3D Numerical simulation on thermo-hydro-mechanical coupled behavior of Boom clay in PPRACLAY heating experiment

***W.Z Chen*[1], Z Gong[1], X.L Li[2], G.J Chen [2], X. Sillen[3], H.D Yu[1]**

1. State Key laboratory of Geomechanics and Geotechnical Engineering, Institute of Rock and Soil Mechanics, Chinese Academy of Science, China
2. Euridice, SCK •CEN, Belgian Nuclear Research Centre, Mol 2400, Belgium
3. ONDRAF/NIRAS, 1210, Brussels, Belgium

Corresponding author email ：wzchen@whrsm.ac.cn

The main goal of the PRACLAY experiment is to perform a large-scale in-situ Heater Test to examine the effect of the thermal load generated by the heat-emitting waste on the Boom Clay, considered as one of potential host rocks in the Belgian R&D programme for geological disposal. The Heater Test will be hosted in the PRACLAY gallery in the underground laboratory HADES, excavated perpendicular to the existing connecting gallery. The PRACLAY gallery is 45 m long and has an external diameter of 2.5 m. the heated part is 10 m away from the Connecting galley and closed by a seal. On the one hand, it is known that Boom Clay presents anisotropy, on the other hand, the PRACLAY Heater Test will last at least 10 years, during which the Connecting gallery stays open and serves as a drained hydraulic boundary condition. Conseqently, Praclay heater test is a 3D problem. It is important to investigate this 3D effect including the influence of the Connecting gallery on the PRACLAY Heater test over such a long period. The 3D numerical model has been thus built based on the real dimensions of the experimental set-up (Fig.1).

The 3D numerical simulation used a transversely isotropic thermo-mechanical coupled elasto-plastic-damage constitutive model with consideration of self-sealing. The constitutive model was firstly developed based on the intensive laboratory tests performed in the IRSM and further calibrated by back-analysis of the in situ measurements around Connecting gallery, especially, the parameters related to the self-sealing (excavation induced permeability variation and its subsequent evolution) were obtained by back-analysis of the in situ pore water pressure evolution. The model was further extended to consider the evolution of permeability, Young's modulus and strength of Boom clay with temperature on the basis of dedicated laboratory test results. Numerical simulation considered all consecutive experimental phases: excavation of Connecting gallery, drainage of Connecting gallery, excavation of Praclay gallery, installation of Praclay seal, backfilling and pressurization of Praclay gallery and 10 years of heating. Numerical results provided valuable information on the time and spacial evolution of the temperature, pore water pressure, effective stress and damaged zone in the coming 10 years and highlighted the following aspects:

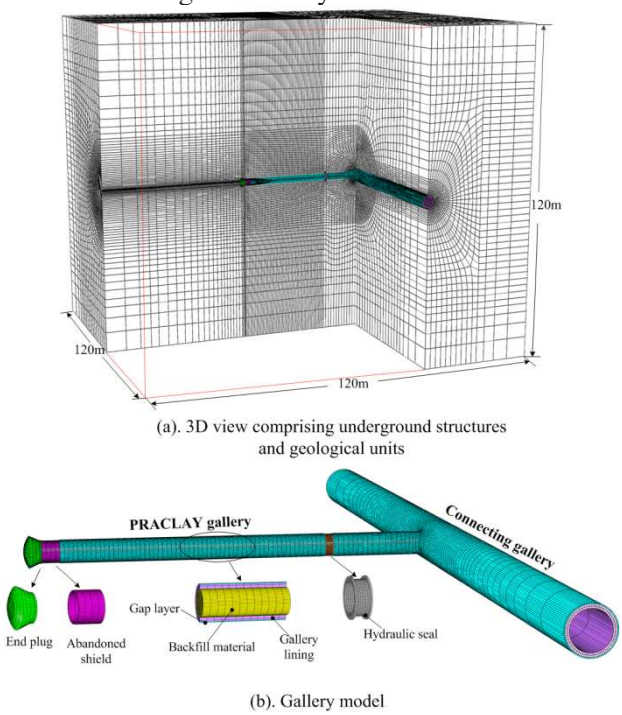
a) Pore pressure increases significantly at the beginning of the heating phase due to the different thermal expansion coefficient of water and clay skeleton. With the considered constitutive model, the maximum pore pressure at the Praclay gallery wall reaches up to 2.97 MPa after heating for 0.5 years, then, the excessive pore pressure will gradually dissipate in the latter period.

b) The increasing of pore pressure results in the decreasing of effective stress , but no tensile stress appears during heating according to the simulated results (Fig. 2).

c) The damaged zone around PRACLAY gallery is mainly induced by excavation. during heating phase, it will be extended slightly due to strength weakening of clay by temperature according to numerical results.

d) Despite of the length of Connecting gallery, the effect of Connecting gallery on the Praclay heater test becomes visible with time. The peak of pore water pressure moves slowly towards the end of Praclay gallery (Fig.3).

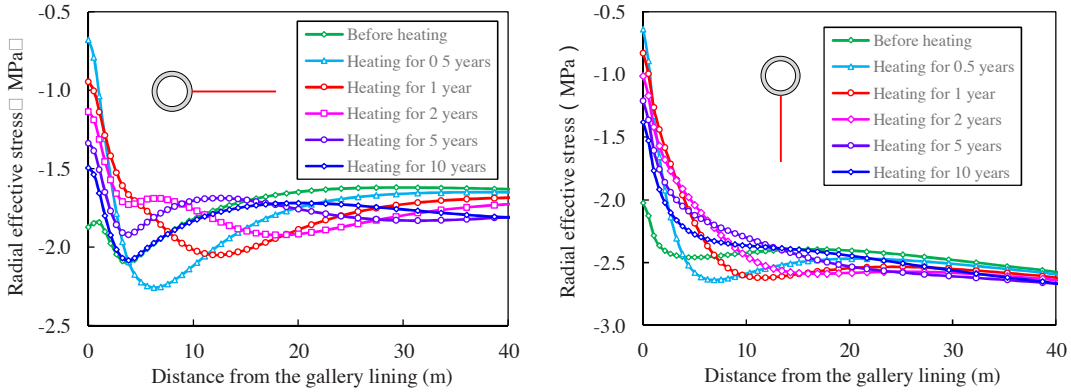
The numerical results from the 3D numerical simulation will be and helpful for the interpretation of test results and thus important to steering the Praclay heater test .



(a). 3D view comprising underground structures and geological units

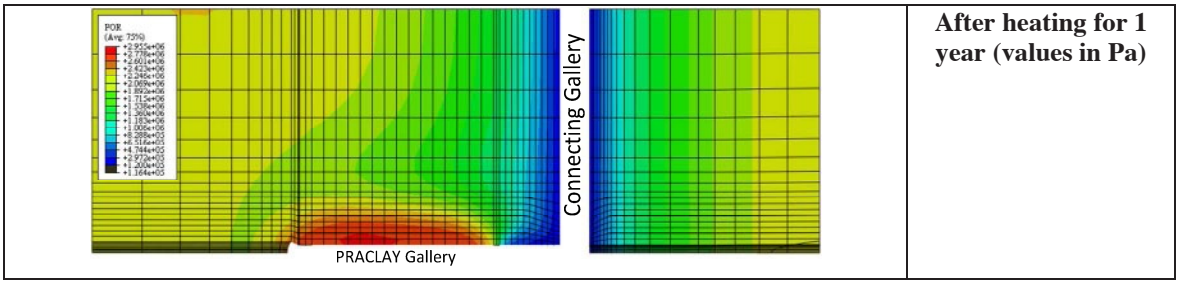
(b). Gallery model

Fig 1. 3D FEM mesh in the modelling of PPRACLAY in situ experiment



(a). Horizontal profile (b).Vertical profile

Fig 2.Radial effective stress around PRACLAY gallery at different time (profile at mid-plane of Praclay gallery)



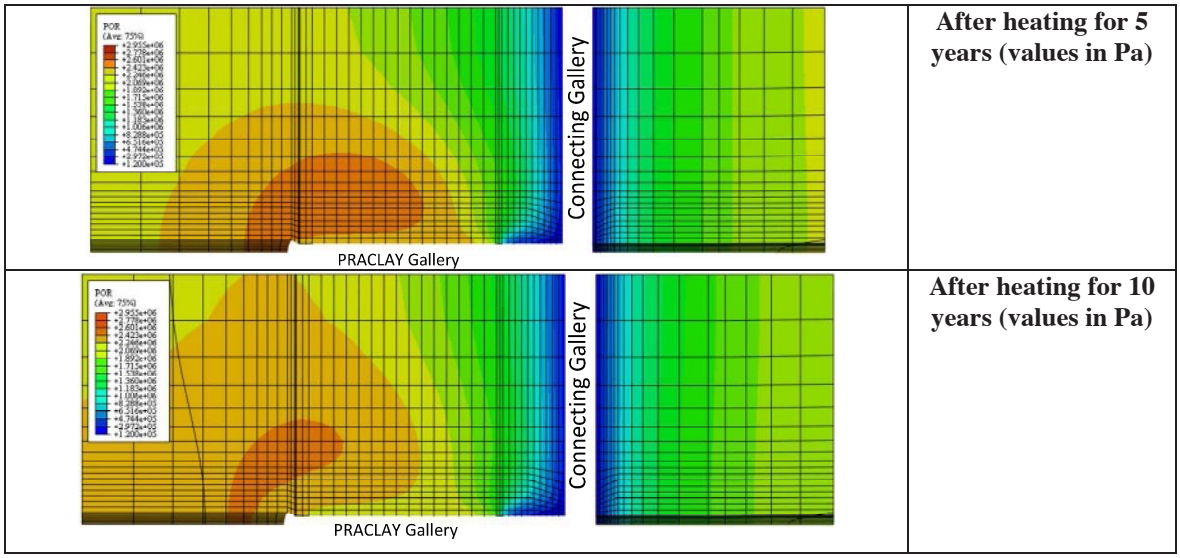


Fig. 4 Distribution of pore pressure around PRACLAY gallery (Horizontal plane) (unit:

Acknowledgements

Financial support of EURIDICE (Belgium) through the collaboration agreements with IRSM on ' Long-term Hydro-Mechanical behaviour of the Boom Clay' (2008-2011) and on 'Long term Thermo-hydro-mechanical behavior of the Boom clay'(2011-2015) and National Science Foundation for Distinguished Young Scholars(51225902) is greatly acknowledged.

Medium scale ATLAS IV in-situ heating test in Boom Clay

Guangjing Chen[1], **Xiangling Li**[1], **Jan Verstricht**[1], **Xavier Sillen**[2]

1. European Underground Research Infrastructure for Disposal of Nuclear Waste in Clay Environment (EURIDICE), Mol, Belgium
2. Belgian Agency for Nuclear Waste and Fissile Materials (ONDRAF/NIRAS), Brussels, Belgium

The medium scale in-situ ATLAS (Admissible Thermal Loading for Argillaceous Storage) tests have been run in the HADES underground research facility in Mol, Belgium to assess the Thermo-Hydro-Mechanical (THM) effects of a thermal transient on the host Boom Clay. Four test campaigns – ATLAS I to IV – have taken place since 1993. These different ATLAS tests allowed us to improve our knowledge on the THM behaviour in a stepwise way.

The initial ATLAS test setup (used for the ATLAS I and II tests) consisted of a heater borehole (AT89E) and two observation boreholes (AT85E, AT93E), all in one horizontal plane. For the third test (ATLAS III), two instrumented boreholes were added (Figure 1): the horizontal AT98E to measure pore water pressure (PWP) and temperature at larger distances, and the downward sloping borehole AT97E with only temperature sensors to investigate the Boom Clay thermal anisotropy. Through in-situ measurements and numerical modeling, this test has highlighted the anisotropic THM behaviour of Boom Clay, and yielded a set of THM parameter values. By introducing the anisotropic mechanical properties, numerical modeling could well reproduce the general evolution of the temperatures and pore water pressures (PWP) around the heater but also more subtle features of the experiment behaviour, such as an instantaneous but temporary PWP decrease (increase) in the horizontal plane following a power increase (cooling).

To get more confidence in the anisotropic THM behaviour and further validate the corresponding Boom Clay parameter values, an upward borehole AT90IU allowing temperature and PWP measurements in the vertical plane above the heater has been installed in 2010 (Figure 2). The fourth test (ATLAS IV) adopted the same heating strategy as ATLAS III to facilitate the comparison between the two tests. The heating started from mid October 2011 for about 13.5 months. The measurements from the five observation boreholes represent, to some extent, the far field behaviour of the host formation.

For the four existing boreholes of both tests, ATLAS IV gave almost the same measured data as ATLAS III, confirming recoverable THM responses (e.g. no irreversible effects) in the far field. The newly installed AT90IU borehole delivered new data on temperature and PWP responses in the vertical plane. Some interesting observations and predictions are confirmed by ATLAS IV: (1) the Boom Clay thermal anisotropy is directly confirmed by comparing the AT98E5 and AT90IU-3 temperature sensors (Figure 3), which are at almost the same distance from the heater center but in orthogonal directions (horizontal vs. vertical); (2) the instantaneous but temporary PWP decrease (increase) after each power increase step (cooling) is again observed at the three instrumented boreholes in the horizontal plane (AT85E, AT93E and AT98E); (3) in the upward borehole AT90IU, as predicted during ATLAS III, the measured PWP increases (decreases) more rapidly after increasing power (cooling) in contrast to observations in the horizontal plane (Figure 4). This validates and builds up our confidence in the hypotheses about anisotropy.

A three dimensional (3D) THM coupling model using the THM parameter values yielded from ATLAS III could very well reproduce the temperature and PWP measured in the four boreholes (AT85E, AT93E, AT97E and AT98E), while the measured temperature and PWP in borehole AT90IU display moderate deviations from the model prediction. Besides, some parameter values, such as the thermal expansion coefficient of the pore water, the thermal expansion coefficient of the Boom Clay solid phase, and the Boom Clay hydraulic conductivity, have recently been improved based on literature review, laboratory tests and in-situ permeability measurements. These improved values are being used in the new modelling of ATLAS IV, which allows us to further refine the whole set of THM parameter values of the Boom Clay. The numerical results of ATLAS IV, together with the refined THM parameter values will be presented in this paper.

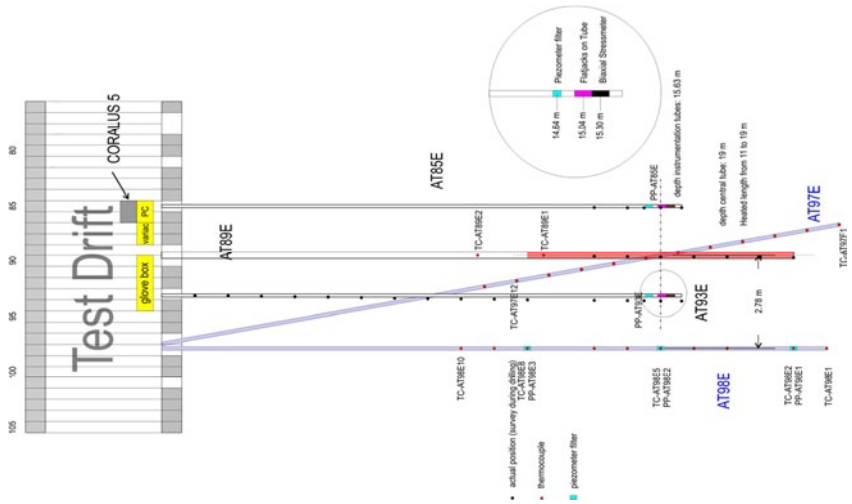


Figure 1. Schematic plan view of small scale in-situ ATLAS test (without upward borehole)

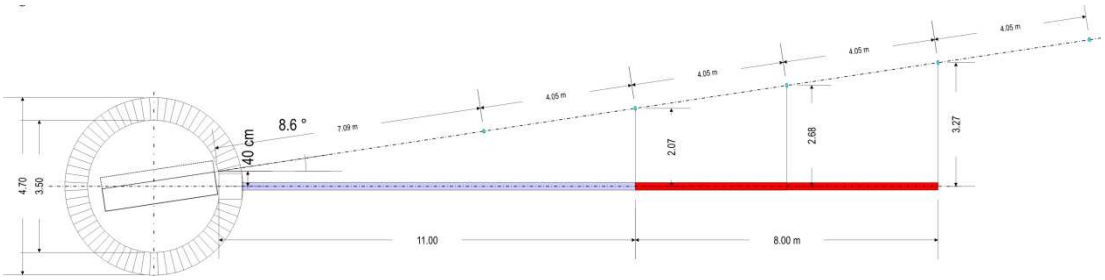


Figure 2: Upward borehole AT90IU above heater drilled for ATLAS IV (side elevation view)

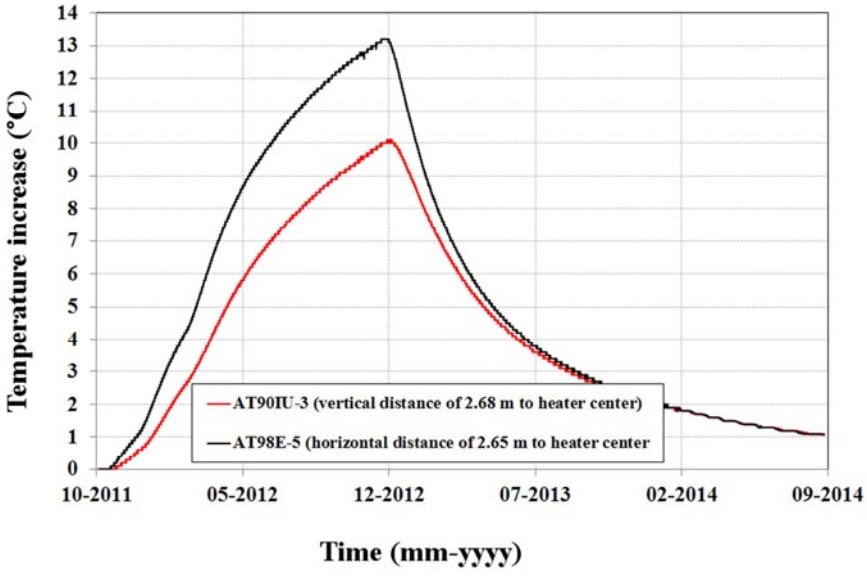


Figure 3: Measured temperature in horizontal borehole AT98E-5 and upward borehole AT90IU-3

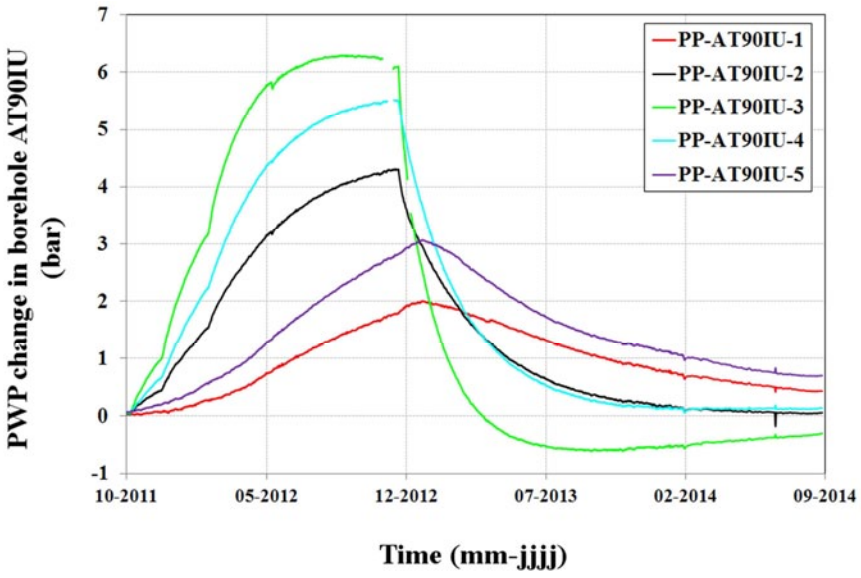


Figure 4: Measured PWP in upward borehole AT90IU

Consequences of water inflow and early water uptake in deposition holes (EVA-project)

Lennart Börgesson
Torbjörn Sandén
Ann Dueck
Linus Andersson
Viktor Jensen
Ulf Nilsson
Siv Olsson
Mattias Åkesson
Ola Kristensson
Clay Technology AB
Ideon
SE-223 70 Lund
Sweden

Urban Svensson
Computer-aided Fluid Engineering AB

Jan Hernelind
5T Engineering AB

Bentonite is an excellent sealing material after full water saturation when the high swelling pressure and low hydraulic conductivity can hinder water from flowing through the deposition holes. However, before the bentonite has produced a high swelling pressure that acts on the rock surface, which may take many years, it cannot prevent water inflow due to the very high water pressure that will be produced in the water bearing fracture at repository depth. If the water inflow is stopped the water pressure will rise in the fracture and since the pellet filling in the slots between the bentonite blocks and the rock cannot resist this pressure water will break the seal and force its way through the pellet filling.

The goals of the EVA- project have been to understand and develop models for critical processes at an early stage and to find bases for leakage criteria of the end plug in the deposition tunnel.

The project has included study of the following processes:

1. Erosion
2. Piping
3. Water flow in pellet filled slots
4. Ability to stop piping
5. Water absorption of the bentonite blocks
6. Formation of water or gel pockets in a pellet filled slot
7. Outflow of bentonite gel
8. Self-sealing of cracks by eroding water
9. Buffer swelling before placement of backfill
10. Self-sealing of erosion channels

In addition the study has included modelling. The following modelling work has been done:

1. Formulation of mathematical and conceptual models of some of the processes
2. Modelling of the expected inflow distribution in the Forsmark Repository
3. Modelling of water absorption of the buffer at different inflow situations

Finally a scenario description has been made. It has included the evolution of the hydraulic and mechanical processes in the bentonite in a deposition tunnel, with deposition holes and an end plug, in the time period from the installation until the end plug takes all the water pressure in the rock. All possible inflow combinations according to the inflow modelling have been considered. The results have been used to compile bases for a decision on how tight the plug needs to be in order to prevent erosion from being damageable for the sealing ability of the buffer and the backfill.

The analyses have led to a number of preliminary conclusions regarding damages on the buffer and backfill. These conclusions have also been used as bases for the scenario analyses:

- The erosion follows Equation 1 with β=0.2 for the buffer and β=2.0 for the backfill as upper limits. The upper limits have been used in the analyses.

$$m_s = \beta \times (m_w)^{\alpha} \quad (1)$$

where
m_s= accumulated mass of eroded bentonite (g)
m_w= accumulated mass of eroding water (g)

- Piping and subsequent erosion will occur and be maintained until the water pressure gradient is located at the plug and the flow rate out from the backfill is lower than 10^{-4} L/min. This flow rate is chosen since the process studies show that at lower flow rates the flow channels will be self-sealed and piping and erosion will stop. This means that piping and erosion may continue at least during the life time of the plug i.e. 100 years, since the plug is not expected to have a lower leakage rate.
- Self-sealing of cracks in the plug or the rock will occur but cannot be considered in the analyses. This is a pessimistic conclusion based on that no real proof of that sealing of cracks always will take place has been derived.
- Erosion channels with limited radial extension (1-2 cm) will be sufficiently healed, in order not to have a major influence on the hydraulic properties of the bentonite, when stagnant water pressure has been established.
- Formation of water or gel pockets in the bentonite pellet part may occur at low inflow rates but have not been considered in the scenario analyses.

Since a leakage through the plug and the rock is inevitable such scenarios have also been studied. The scenario analyses have yielded the following conclusions regarding the demands on water inflow distribution into deposition holes and deposition tunnel at different magnitudes of leakage through the plug and the rock, based on the estimated loss of bentonite caused by erosion:

- At a leakage less than 0.1 L/min all combinations of inflow rates into deposition holes and tunnel are acceptable for the buffer if the inflow rate into separate deposition holes are less than 10 % of the inflow into the deposition tunnel.
- At a theoretical leakage less than 1.0 L/min all combinations of inflow rates into the deposition holes and tunnel are acceptable if the inflow rate into separate deposition holes are less than 10 % of the inflow into the deposition tunnel except for if the inflow rate into the hole is higher than 0.01 L/min.
- At a plug leakage higher than 0.1 L/min there may be too large erosion damages in the backfill.

Some scenarios with a non-functioning plug have also been studied. The conclusions of these studies are that there are cases when no requirements on the plug tightness are needed but that it depends largely on the time to fill up the repository with water.

Modelling of bentonite swelling in complex geometries

Lennart Börgesson
Ann Dueck
Reza Goudarzi
Clay Technology AB
Ideon
SE-223 70 Lund
Sweden

Jan Hernelind
5T Engineering AB

Swelling of the buffer blocks and buffer homogenization are important functions to guarantee the requirements of the buffer in a deposition hole after full water saturation. It is important to understand and be able to predict the final condition of the buffer after the swelling and homogenization, which occurs both during the initial saturation and after possible loss of bentonite caused by for example erosion.

Presently a SKB project is running with the objectives to increase the knowledge of the homogenisation processes. The project consists of four parts; theoretical studies, fundamental laboratory tests, laboratory study of the influence of friction and medium scale tests of the scenario involving loss of bentonite. Laboratory tests from the latter part are described in another contribution to this conference.

A material model that can be used for simulating the swelling process by finite element simulations has been derived and implemented into the finite element code Abaqus. It is an elastic plastic cap model with a failure surface, a yield surface and a non-associated flow surface. It reminds of the Cam-clay model but has some substantial differences that make it more suitable for swelling bentonite.

The model has been applied on laboratory tests with pure radial and pure axial swelling of bentonite in a confined cell with measurement of swelling pressure at different positions and careful sampling after finished tests. The material parameters in the model could be adapted to yield good agreement both regarding pressure evolution and density distribution for pure radial swelling and were then checked and validated for pure axial swelling with good agreement between modelled and measured results without changing the parameters.

A medium scale laboratory experiment with very stiff and confined boundaries and a high density bentonite block has been used to simulate the loss of bentonite in a part of a deposition hole. The block has a diameter of 30 cm and a height of 10 cm. Two irregular voids of 35x50x70 mm were cut in the block before installation and measurements of the homogenisation process were done both during the test time (swelling pressure and RH at different locations) and after the test with careful sampling and determination of density distribution. This test has also been modelled with a predictive modelling before start of the test.

The article will present the material model and the results of the modelling and also comparisons between modelled results and measured results.

Figure 1 shows example of modelled and measured results at radial swelling. Figure 2 shows the finite element model of the medium scale test and modelled void ratio distribution after homogenisation.

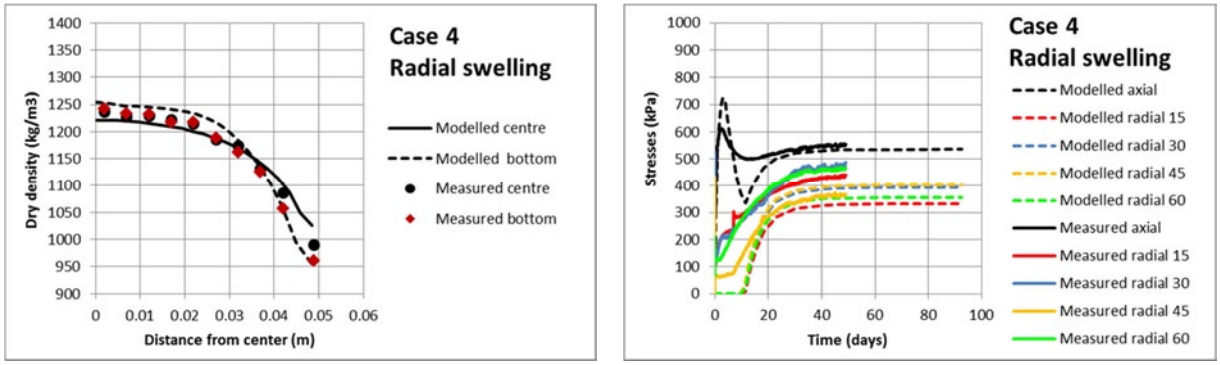


Figure 1. Modelled and measured stresses and density distribution during and after radial swelling

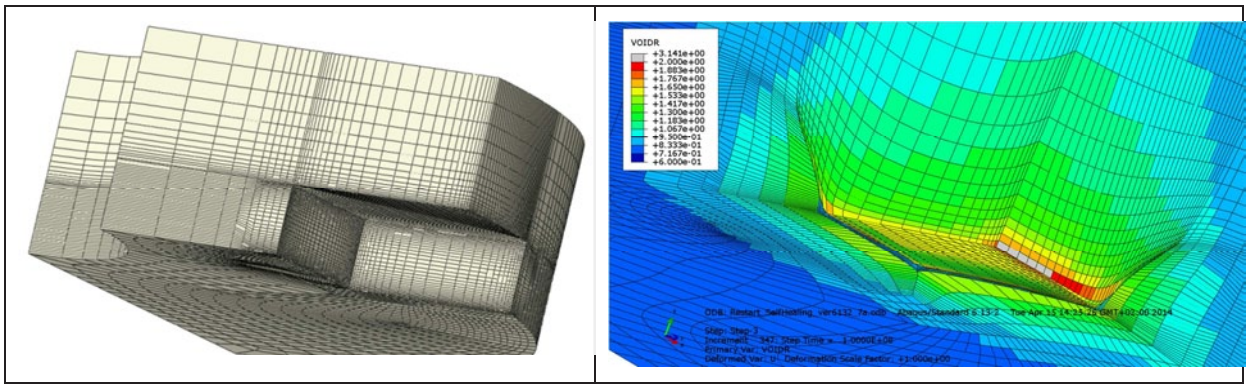


Figure 2. Element mesh of an 1/8:th of the bentonite block with initial void (left) and void ratio distribution after modelled homogenisation

Column tests on pellets-based barrier material: analysis and interpretation

A. Gens[1*], R. B. de Vasconcelos[1], M.V. Villar[2], J.C. Mayor[3] and P.L. Martín[2]

1. Department of Geotechnical Engineering and Geosciences, Universitat Politècnica de Catalunya, E-08034 Barcelona, Spain (antonio.gens@upc.edu).
2. CIEMAT, Av Complutense, 40, 28040 Madrid
3. ENRESA, Emilio Vargas, 7, 28043 Madrid

(*) corresponding author

Expansive clays (bentonite) are adopted as the main material for these barriers because of their low hydraulic conductivity, high retention capacity and its ability to fill and seal irregularities, gaps and fractures. In order to fulfil the safety functions of the engineered barrier, the material has to exhibit a sufficient expansion capacity that it is usually characterized in terms of swelling pressure. Swelling pressure developed during saturation is in turn closely related to the dry density of the material; a minimum value to be achieved during installation is usually specified in the design. Pellets-based materials have become an attractive solution for forming engineered barriers and seals. Because of the very high density of the pellets, adequate average dry densities may be obtained even with minimal or no compaction effort.

Thermo-hydraulic column tests have been performed in the CIEMAT laboratory in Madrid on a granular assemble of pellets made up of pure MX-80 bentonite, a material that is being used in the HE-E heating test in the Mont Terri laboratory (Gaus et al. 2014) The test considered in this contribution is being performed in a cylindrical cell (Figure 1a) with an internal diameter of 7 cm and a length of 50 cm. Teflon cell walls are used to limit the amount of lateral heat dissipation. A heater is placed at the bottom boundary of the cell whereas hydration is performed from the upper boundary. The thermal condition of the upper boundary is controlled by water circulation at constant temperature. To provide thermal insulation the cells were laterally surrounded by a layer of dense foam 5-mm thick replaced later by insulation wool. Temperature and relative humidity were measured at three different elevations along the column. In addition, heater power and axial stress were also monitored. Figure 1b shows the appearance of the material tested. The initial state of the sample was as follows: the dry density achieved was 1.53 g/cm^3, porosity 0.444, water content 6.4 % and the overall degree of saturation 22%. No compaction was required to achieve the desired dry density value.



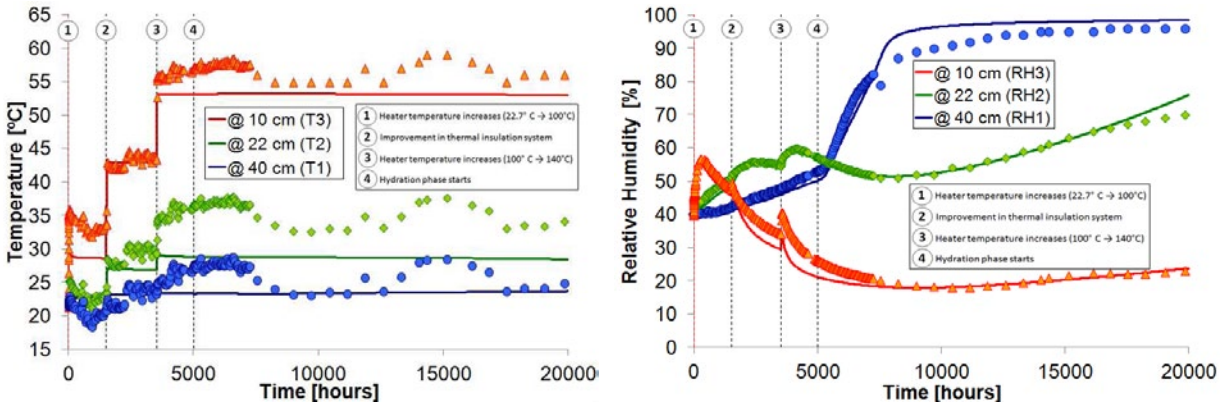
a) b)

Figure 1. a) Appearance of the material tested: MX-80 pellets, b) Column cell tests in operation (Villar et al. 2012)

A fully coupled THM analysis has been performed taking advantage of the axisymmetric geometry of the problem. The analyses followed closely the various stages of the real experiment:

- Construction of the column and emplacement of the isolation material
- Temperature increase until reaching the 100ºC mark (in 33 minutes), kept constant afterwards
- Reinforcement of the isolation system 1518 hours after the start of heating.
- 3527 hours after the first temperature increase, temperature in the heater is raised to 140ºC (in 17 minutes) and kept constant afterwards.
- Controlled hydration of the bentonite cell. Hydration started 5015 hours after the start of heating. A constant liquid pressure of 0.01 MPa (0.1 bar) was applied to the upper horizontal boundary of the column simulating the hydration process of the cell. This condition has been kept unchanged until the end of the simulations.

The computed evolution of temperatures and relative humidly at different locations along the column are plotted in Figure 2 where they are also compared to the experimental observations. It can be noted that a good agreement is obtained throughout the analysed duration of the test. In the thermal stage without hydration, it is apparent that heating brings about water vapour generation at the bottom part of the pellet column. Condensation takes place closer to the top of the bentonite cell where the water vapour (coming from the hot zones by diffusion mechanism) condensates. Vapour condensation leads to an increment of humidity (and consequently, an increase in degree of saturation) in the cooler zones inside the cell as indicated in the RH measurements and model computations for the two sensors further away from the heater. In contrast, after the first RH increase, the degree of saturation decreases near the heater during the heating experiment as recorded by the sensor RH3. Once hydration starts, relative humidity values tend to increase in all sensors but at different rates, the sensor close to the hydration boundary showing near full saturation. Again the observations are closely tracked by the results of the analysis.



a) b)

Fig. 2. a) Observed and computed temperatures at different points of the column b) Observed and computed relative humidity at different points of the column

References:

Gaus, I., Garitte, B., Senger, R., Gens, A., Vasconcelos, R., Garcia-Sineriz, J.L., Trick, T., Wieczorek, K., Czaikowski, O., Schuster, K., Mayor, J.C., Velasco, M., Kuhlmann, U., Villar, M.V. 2014. The HE-E Experiment: Lay out, Interpretation and THM Modelling. Arbeitsbericht NAB 14-53. NAGRA, Wettingen.

Villar M.V., Martin, P.L. Gómez-Espina, R., Romero, F.J., Barcala, J.M. 2013. *THM cells for the HE-E test: setup ad first results*. PEBS report D2.2.7a. CIEMAT Technical Report CIEMAT/DMA/2G210/02/2012. Madrid.

Buffer homogenization after loss of bentonite – medium scale laboratory test

***Ann Dueck*, Reza Goudarzi, Lennart Börgesson**
Clay Technology AB, IDEON Science Park, SE-223 70 LUND, SWEDEN

Swelling of the buffer blocks and buffer homogenization are important functions to guarantee the requirements of the buffer in a deposition hole after full water saturation. It is important to understand and be able to predict the final condition of the buffer after the swelling and homogenization, which occurs both during the initial saturation and after possible loss of bentonite caused by for example erosion.

Presently a SKB project is running with the objectives to increase the knowledge of the homogenization processes. The project consists of four parts; theoretical studies, fundamental laboratory tests, laboratory study of the influence of friction and medium scale tests of the scenario involving loss of bentonite. Results from the latter of the four parts are presented in this contribution to the conference. Material models have been developed and verified with some of the laboratory test results from this project and modelling of the swelling bentonite are described in another contribution.

Buffer homogenization involving loss of bentonite have been studied by two medium scale laboratory tests. The two tests, SH1 and SH2, having almost the same boundary conditions were started in December 2012 and while the non-instrumented SH2 was finished and dismantled in May 2014 the instrumented SH1 is still ongoing.

In each of the set-ups cylindrical bentonite blocks with diameter 300 mm and height 100 mm were made with uniaxial compression of MX-80 bentonite with the initial water content 23.6%. A simulated canister with the diameter 100 mm was included in the centre. A stiff filter was mounted to the inside of the very stiff cylinder with the purpose to provide water to the bentonit. The set-up of SH1 is shown in Figure 1. In both bentonite blocks cavities were cut in two diametrical positions. The dimensions of the cavities cut in SH1 was 35x50x70 mm^3, shown in Figure 2. The cavities cut in the bentonite block SH2 were slightly larger.



Figure 1. *Set-up of one of the tests (SH1) used in the study.*

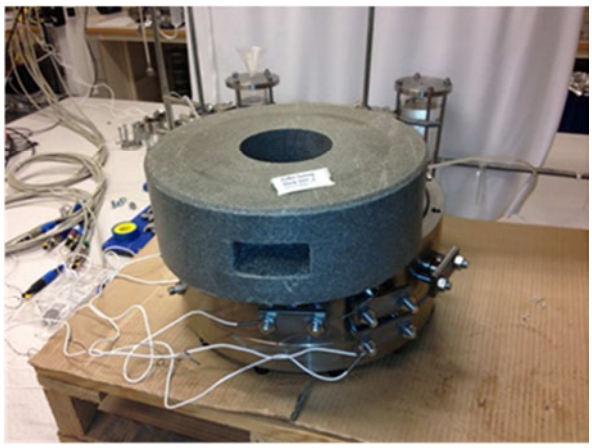


Figure 2. *The cylindrical bentonite block used in one of the tests (SH1) with a cut cavity. In the diametrical position another cavity was cut.*

After mounting of bentonite rings, lids and transducers the tests were started by filling the filters and the cavities with water and applying a low water pressure (10 kPa). Each ring is equipped with four water inlet positioned on each side of the cavities. Two of them were used for water supply. These inlets were used regularly, for flushing the filters in order to eliminate air bubbles that may be collected in the filters.

In the instrumented test SH1 the swelling pressure are measured at nine positions, Figure 3. Six of the pressure transducers are unique (P1-P6) while three are placed in mirrored positions (P33, P55 and P66) for repeatability reasons. The maximum values (blue lines) and minimum values (green lines) are all measured from the outside and at the middle height of the cylinder ring but when the minimum values are measured in the center of the cavities the maximum values are measured well outside of the cavities. Test results after dismantling of the non-instrumented test SH2 are shown in Figure 4 where a plan and section of the benonite block are also shown. The initial dry density of the block was approximately 1650 kg/m^3. The results show the difference in density in the upper part of the bentonite block as a function of the radial distance and in different directions. The lowest values (yellow points) and the highest values (red points) were seen in the directions coinciding with and perpendicular to the direction of the cavity respectively. The test has been modelled as described in another contribution.

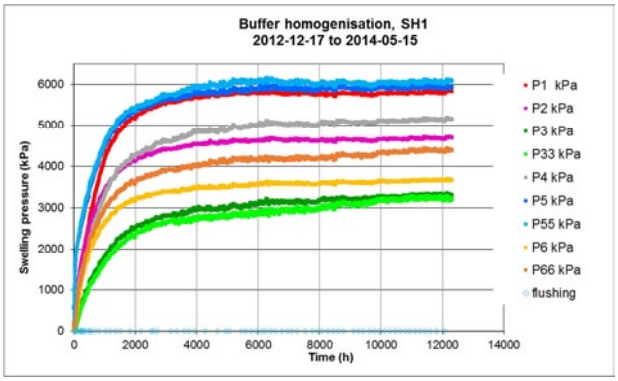


Figure 3. *Resulting swelling pressure from SH1.*

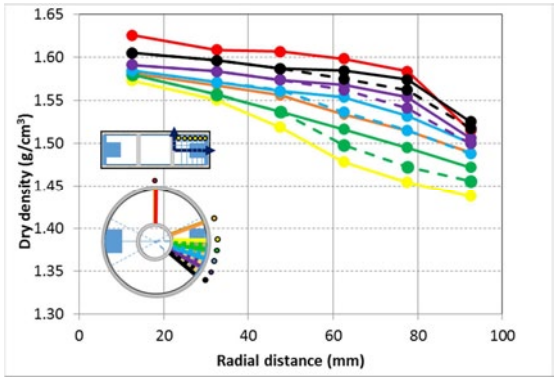


Figure 4*. Difference in density measured at the upper part in different directions after dismantling of SH2.*

References

Dueck A., Goudarzi R., Börgesson L., 2011. Buffer homogenisation, status report. SKB Technical Report TR-12-02. Svenska Kärnbränslehantering AB.

Dueck A., Goudarzi R., Börgesson L., 2014. Buffer homogenisation, status report 2. SKB report in progress.

Theoretical Studies with Density Functional Theory on Ca/ Na Montmorillonite: Structure, Forces and Swelling Properties

Guomin Yang, *Longcheng Liu*, Ivars Neretnieks, Luis Moreno
Department of Chemical Engineering and Technology
Royal Institute of Technology, KTH
SE 100 44, Stockholm, Sweden.

Within the framework of density functional theory (DFT), a self-consistent weighted correlation approach (SC-WCA) is developed to study the structural and thermodynamic properties of electric double layers. The results facilitate better understanding of the structure, interaction and swelling behaviours of e.g. the Ca/Na montmorillonite particles, the main component of the bentonite clay used for an engineering barrier in nuclear waste repositories of the KBS-3V type in Sweden and Finland.

Using the restricted primitive model, which corresponds to charged hard sphere ions and a continuum solvent, the advantage of the SC-WCA over the weighted correlation approach[1] (WCA) and other conventional DFT methods[2] is that it exactly complies with the surface thermodynamic consistency by means of the contact theorem. In essence, it combines two sets of WCA with two weighted pair correlation functions to take the ion-ion correlations into account, i.e. to evaluate the change of the single-particle direct correlation function of the clay-water system relative to that of a reference state[1].

Although the SC-WCA can, in principle, be applied to any inhomogeneous, charged hard-sphere fluid, we focus in this paper specifically on the studies of the interaction of counterion-only electric double layers for a Ca/Na montmorillonite system in equilibrium with distilled water. To the best of our knowledge, no DFT methods have been used previously to predict the ionic density profiles and the osmotic pressures of such a counterion-only system, due mainly to the fact that no electrolytes are involved in the bulk fluid and therefore it cannot be chosen as the reference state. To tackle this problem, we define the local state of the ions at the mid-plane between the clay particles as the reference instead. The application of SC-WCA against the Monte Carlo (MC) simulations in a wide range of surface charge densities, particle separations, and combinations of mono- and di-valent counterions shows that it is capable of capturing the fine features of the structural properties of the counterion-only electric double layers and that it can well predict the change of the osmotic pressures under a variety of conditions.

In particular, it is found that in the case when counterions are only monovalent, the SC-WCA always predict a considerable repulsive forces between montmorillonite particles, as shown in figure 1, which are in excellent agreement with MC simulations. When counterions are only divalent, however, attractive forces can be obtained in cases where the surface charge density is larger than 0.08 C/m^2, with a minmum eshibiting at an aqueous layer between the clay platelets of about 1nm, as can be seen in Figure 2. This explains why the sheets of montmorillonite tend to aggregate in stacks forming larger particles in calcium systems (such particles may have up to tens of sheets, separated by about 1 nm), but nearly completely separated in sodium systems, as the consequence of ion-ion correlations due to the ion size effect[5]. Such correlatins between ions also favor divalent counterions in a situatiojn with a competition with monovalent ones. As shown in Figure 3, only when the fraction of surface charge neutralized by the Na^+ counterions is larger than 20-30%, the osmotic pressure as a function of particle separation becomes monotonic, which indicates that the sodium dominated bentonite would then behave more like the purified and fully Na-exchanged montmorillonite to readily release particles, forming a expansive gel, when dispersed in distilled water.

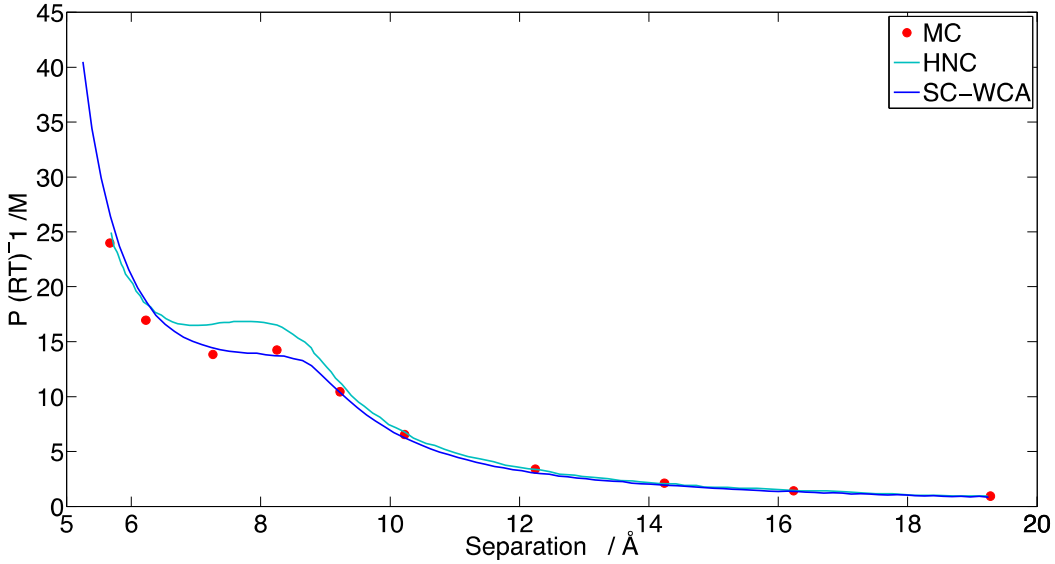


Figure 1 The osmotic pressure between two charged surfaces (σ = 0.267 C m^{-2}) for a system with only monovalent ions. The bulk solution consists of pure water. The solid light blue line is from the HNC [3], the solid circles are Monte Carlo data [3].

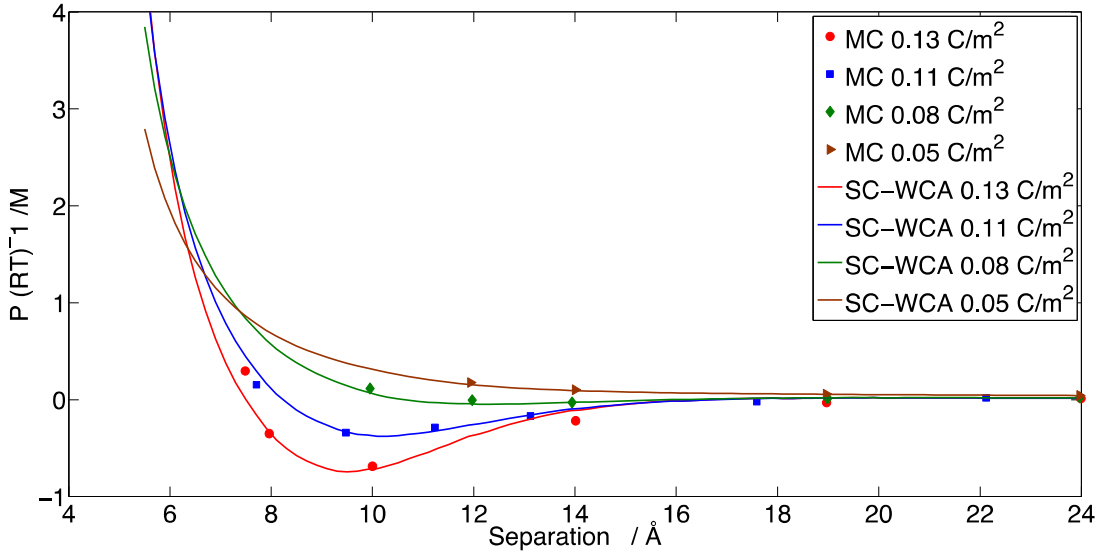


Figure 2 The osmotic pressure as a function of separation for a system with only divalent counterions. The bulk solution consists of pure water and the surface charge density is indicated in the figure. The solid circles are Monte Carlo data [4].

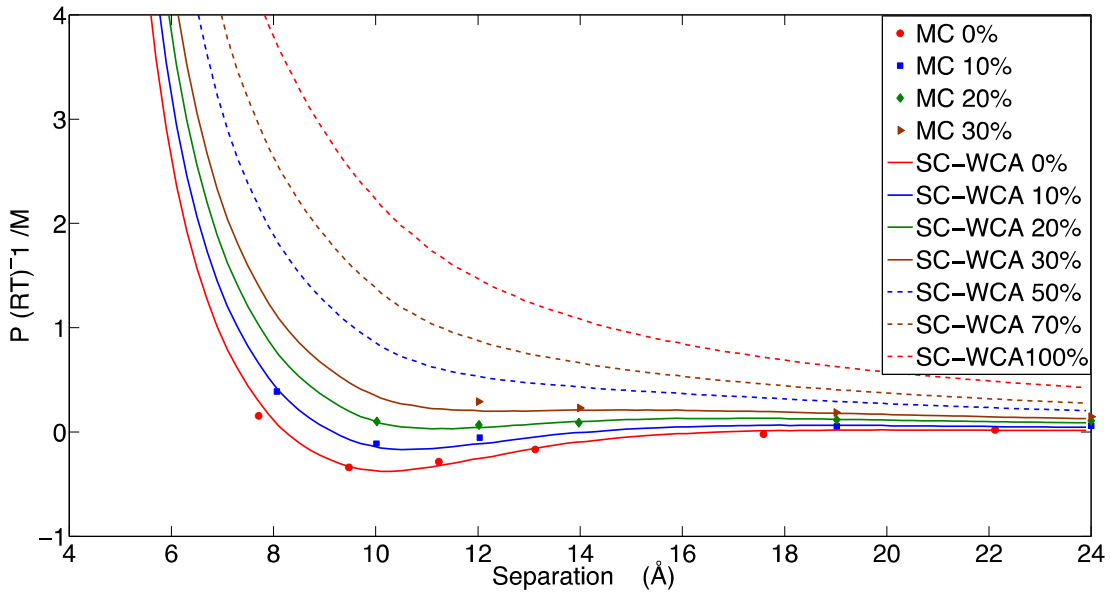


Figure 3 The double layer net osmotic pressure as a function of separation. The system is in equilibrium with pure water and the amount of monovalent /divalent counterions has been varied. The fraction of surface charge neutralized by monovalent counterions is indicated in the figure. The surface charge density is -0.11 C m^{-2}. The solid circles are Monte Carlo data [4].

References

1 Z. Wang, L. Liu and I. Neretnieks. J. Phys.: Condens. Matter, 2011, 23(17), 175002.

2 Hansen J-P and McDonald I R 2006 *Theory of Simple Fluid* (London: Academic).

3 R. Kjellander, T. Åkesson, Bo Jönsson and S. Marcelja. J Chem. Phys., 1992, 97(2), 1424-1431.

4 M. Segad, Bo Jönsson, T. Åkesson and B. Cabane. Langmuir, 2010, 26(8), 5782-5790.

5 L. Liu, M. Luis and I. Neretnieks. Langmuit, 2009, 25(2), 679-687.

Different conceptual models for bentonite re-saturation leading to similar mathematical process descriptions

Klaus-Peter Kröhn

Gesellschaft für Anlagen- und Reaktorsicherheit (GRS), Theodor-Heuss-Straße 4, 38122 Braunschweig, Germany

In most countries compacted air-dry bentonite is favoured for engineered barriers in final repositories for nuclear waste. The process of re-saturation, however, is still not fully understood although modelling of this process is nevertheless done since the early 1980s.

In the beginning an **empirical approach** (approach 1) was used that looked formally like Fick's second law with the water content as the primary variable. Only a so-called "diffusion coefficient" was required whose value proved to be constant in time and space. Additionally, all published uptake tests indicated a very narrow bandwidth for this constant (e.g. [1]).

After a while the limitations of this method became apparent. Increased hydraulic pressure as well as non-isothermal conditions could not be captured. One decade later the **two-phase flow approach** (approach 2) known from soil science was thus introduced and formed the hydraulic part of the thermo-hydraulic-mechanically coupled (THM-)codes as we know them today. This solved the problems that the former approach had run into and THM-codes were successfully applied to a number of different problems. But some inconsistencies between the macroscopic conceptual model and the processes taking place at microscopic level were not reconciled. Usually, no difference between hydrated water in the interlamellar space and free water in the pore space is allowed in the framework of two-phase flow, the retention curve represents suction and not capillary forces and the concept of relative permeability developed for rigid porous media does not apply to re-saturating bentonite.

For these reasons the alternative **extended vapour diffusion approach** (approach 3) was developed at GRS shortly after the turn of the century. It is restricted to confined conditions and involves only vapour diffusion in the pore space, hydration and diffusion of hydrated water in the interlamellar space. As it turned out this model was also able to reproduce re-saturation under repository relevant conditions [2].

Of interest here is what evolves mathematically from these three different concepts. On the face of it three rather different looking equations are solved either for the water content w (eq. (1): empirical approach) or for liquid saturation S_l or liquid pressure p_l (eq. (2): two-phase flow approach) or for the vapour partial density ρ_v (eq. (3): extended vapour diffusion approach):

$$\frac{\partial w}{\partial t} - \tilde{D}\Delta w = 0 \qquad (1)$$

$$\frac{\partial(\rho_l \Phi S_l)}{\partial t} - \nabla \cdot \left(\rho_l \frac{k_{rl}}{\eta_l} \mathbf{k} \cdot (\nabla p_l - \rho_l \mathbf{g}) \right) = 0 \qquad (2)$$

$$f_1 \frac{\partial \rho_v}{\partial t} + f_2 \frac{\partial T}{\partial t} + f_3 \Delta \rho_v + f_4 \cdot \nabla \rho_v + f_5 \rho_v + f_6 \nabla T + f_7 \Delta T = 0 \qquad (3)$$

The terms f_1 to f_7 in eq. (3) contain all required parameters for the extended vapour diffusion model as well as differential operators for secondary variables and particularly temperature. Details can be found in [2]. A not too long list of simplifications, however, allows transforming of all three mathematical models into the form

$$\frac{\partial S}{\partial t} - D\Delta S = 0 \qquad (4)$$

which can be interpreted as one form of the Richards equation since D depends on the degree of saturation S. A comparison of the three mathematical models can hence be reduced to a comparison of the coefficients $\tilde{D}$, $\hat{D}$, and $\overline{D}$ that follow from approaches 1 to 3 and replace D in eq. (4).

The basis of such a comparison is formed by

- published data on the empirical „diffusion coefficient“ $\tilde{D}$ for MX-80,
- two-phase flow parameters for MX-80 from a benchmark exercise based on essentially one-dimensional and non-isothermal laboratory experiments by ANDRA [3] as well as the subsequent exercise on the Canister Retrieval Test of SKB at the Hard Rock Laboratory at Äspö, and
- a theoretical as well as numerical evaluation of the terms in eq. (3) also based on the above mentioned benchmarks.

Several aspects in Figure 1 showing the resulting curves for the three “diffusion coefficients” $\tilde{D}$, $\hat{D}$, and $\overline{D}$ are worth mentioning. The bandwidth of the coefficients D is about one order of magnitude for each model. There is a slight increase of D with the degree of saturation (except, of course, for the empirical diffusion model). But most striking is the agreement of all curves in the range of saturations above 20 % which is the most relevant range for all practical purposes. Further investigations have shown that the influence of bentonite dry density and of temperature on $\hat{D}$ and $\overline{D}$ leads to a little less good agreement of the resulting curves but certainly not to the extent that the conclusions from Figure 1 are invalidated.

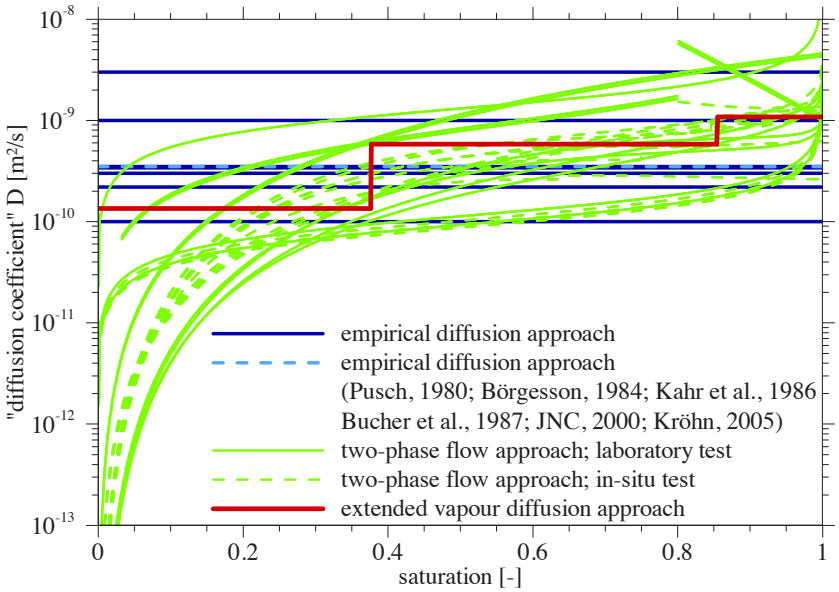


Figure 1: Comparison of “diffusion coefficients” $\tilde{D}$, $\hat{D}$, and $\overline{D}$.

It thus appears that physically quite different approaches for the hydraulics during bentonite re-saturation lead eventually to similar mathematical descriptions indicating basically a diffusion-like process. While bentonite re-saturation may have been well reproduced by one model or another the invers conclusion from the successful model to the underlying physics is therefore presently highly debatable.

References

[1] Kröhn, K.-P., Modelling the re-saturation of bentonite in final repositories in crystalline rock. Final report, FKZ 02 E 9430 (BMWA), Gesellschaft für Anlagen- und Reaktorsicherheit (GRS) mbH, GRS-199, Köln (2004)
[2] Kröhn, K.-P., Code VIPER - Theory and Current Status. Status report, FKZ 02 E 10548 (BMWi), Gesellschaft für Anlagen- und Reaktorsicherheit (GRS) mbH, GRS-269, Köln (2011)
[3] Gens, A.: Task Force on Engineered Barrier System (EBS), TASK 1: LABORATORY TESTS. Svensk Kärnbränslehantering (SKB), Stockholm. (to be published)

An extended vapour diffusion model for modelling non-isothermal re-saturation of bentonite buffers

Klaus-Peter Kröhn

Gesellschaft für Anlagen- und Reaktorsicherheit (GRS), Theodor-Heuss-Straße 4, 38122 Braunschweig, Germany

In most countries compacted air-dry bentonite is favoured for engineered barriers in final repositories for nuclear waste. The process of re-saturation, however, is still not fully understood yet. Established codes for modelling the re-saturation of compacted bentonite like CODE_BRIGHT, ABAQUS or GeoSys/ROCKFLOW are based on the assumption that the hydraulic processes can be described as a two-phase flow of liquid water and air. Success in many cases seems to confirm the coupled thermo-hydro-mechanical (THM) approach to re-saturation. But not all hydraulic phenomena occurring on microscale during re-saturation are properly represented by this macroscopic description. A different physical concept for the re-saturation of compacted bentonite was thus developed and also successfully tested.

Key to the consistency between micro- and macroscopical descriptions is a microscopical view of the clay grains (see Fig. 1). Water propagates within the space formed by the macro-pores between the clay grains and also migrates from the macro-pores into the intragranular micro-pores. From here the water is further drawn into the interlamellar space of the clay particles. This process applies to liquid water as well as to water vapour and is called hydration here. The particles act as local sinks for pore water irrespectively of its phase state and swell at the same time reducing under confined conditions the available pore space accordingly. This hydration is usually not considered in the THM-codes.

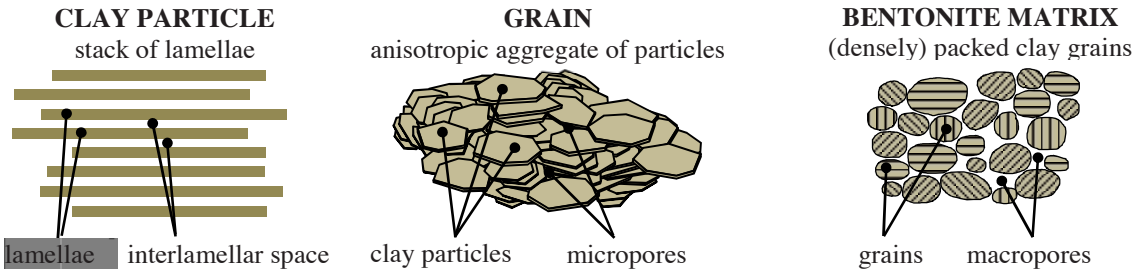


Figure 1: Structure of bentonite at different levels of observation.

Experiments and related modelling indicated that compacted bentonite in contact with liquid water may not re-saturate via the liquid water phase but mainly by evaporation in the pore space and subsequent vapour diffusion [1]. The related conceptual model as depicted in Fig. 2 is based on the idea that a narrow and fully water-saturated zone develops very fast in the bentonite where it comes into contact with liquid water. The extremely low permeability of bentonite at full saturation impedes liquid water flow in that narrow zone to the extent that the amount of liquid water entering the bentonite balances the amount of water evaporating at the water-air interface inside the bentonite. This interface does therefore not proceed into the bentonite but instead

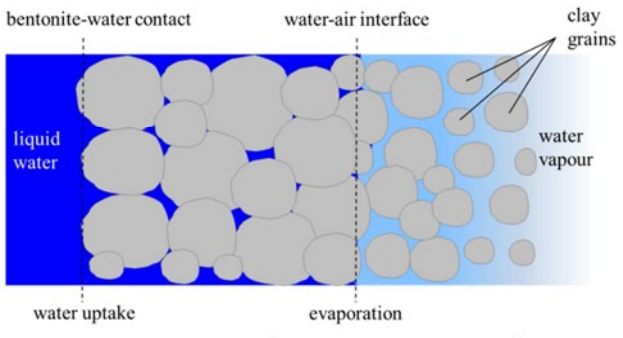


Figure 2: Conditions and processes at the bentonite-water contact zone.

provides a locally more or less fixed boundary for water evaporation and subsequent vapour diffusion into the pore space.

Additional investigations indicated furthermore that hydrated water may not be immobile. Instead, it appears to be migrating in a diffusion-like manner analogously to the observed self-diffusion of interlamellar water (e.g. [2]). Ignoring this difference between free and hydrated water in the clay as well as the related different migration processes is a major inconsistency between the hydraulic processes occurring on a microscopic scale and the macroscopic conceptual THM-model.

Two balance equations - one for water vapour in the pore space and one for hydrated water in the interlamellar space - were formulated and coupled by sink/source terms representing the process of hydration. The result was a double continuum formulation which is solved numerically with the finite element code VIPER (Vapour transport In Partially saturated bentonite as Engineered barrier for Repositories). The theoretical basis as well as the complete set of assumptions underlying the model can be found in [3]. This alternative model is restricted to re-saturation under constant volume conditions as this type of problem does not require a coupling of hydraulics to the mechanics. Whether the coupling of hydraulics to heat transport can also be neglected is still to be investigated.

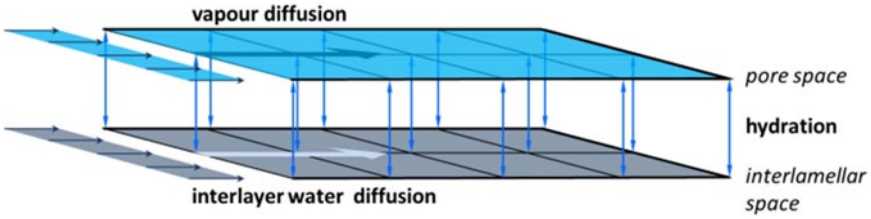


Figure 3: Double continuum approach for the extended vapour diffusion model.

The vapour diffusion model was tested step by step against uptake experiments with a physically increasing complexity: beginning with tests under ambient conditions, continuing with water uptake under an increased hydraulic pressure and finally modelling re-saturation under non-isothermal conditions. Switching from laboratory to in-situ tests was also successful. This step included the simulation of a re-saturating bentonite-sand buffer. The related work is summarised in [3].

A particularly appealing aspect of this approach is the fact that most material data and relations required by the model are already well established. Very few quantities are not exactly known but they can vary only within very limited boundaries. Under these stringent conditions the observed good agreement between measurements and numerical simulations provides strong evidence for a conceptual model that may represent an alternative to the common THM-approach.

Considering the fact that the equations of state used in the classic THM-codes describe re-saturation basically as a two-phase flow process the conceptual model of VIPER appears to be physically better justified. Both models have nevertheless been successfully shown to model complex non-isothermal problems. This highlights the notion that advective water flow in the re-saturating bentonite as assumed in the THM-codes is debatable and that vapour diffusion could play an important if not a key role for the re-saturation of bentonite.

References

[1] Kröhn, K.-P., Modelling the re-saturation of bentonite in final repositories in crystalline rock. Final report, FKZ 02 E 9430 (BMWA), Gesellschaft für Anlagen- und Reaktorsicherheit (GRS) mbH, GRS-199, Köln (2004)
[2] Skipper, N.T., Lock, P.A., Titiloye, J.O., Swenson, J., Mirza, Z.A., Howells, W.S., Fernandez-Alonso, F., The structure and dynamics of 2-dimensional fluids in swelling clays, Chemical Geology 230, 182-196, (2006)
[3] Kröhn, K.-P., Code VIPER - Theory and Current Status. Status report, FKZ 02 E 10548 (BMWi), Gesellschaft für Anlagen- und Reaktorsicherheit (GRS) mbH, GRS-269, Köln (2011)

Wetting Behavior of Bentonite Pellets

Jari Martikainen[1], **Timothy Schatz**[1], **Noora Kanerva**[1] **and Kari Koskinen**[2]

1. B+TECH, FI-00420 Helsinki, Finland (jari.martikainen@btech.fi)
2. POSIVA, FI-27160 Olkiluoto, Finland

In the repository for spent nuclear fuel at Olkiluoto, pellet filling of gaps is a likely design feature of both the buffer and backfill systems (Figure 1). During initial saturation periods, it is reasonable to assume that, given their proximity to the host rock, such pellet-filling materials will be in the most direct contact with saturation interfaces. As the wetting behavior of bentonite pellets affects water distribution and possible channel formation, it is a key factor in determining buffer and backfill performance.

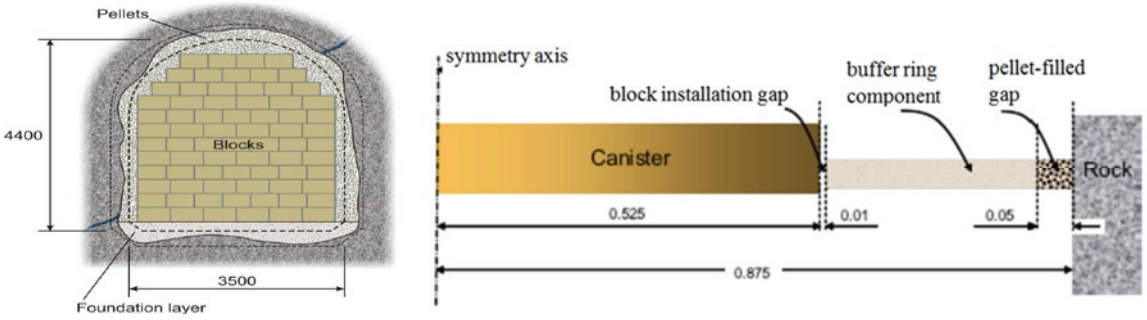


Figure 1. *Schematic illustrations showing the pellet-filling in a backfilled deposition tunnel (left) and a buffer emplaced deposition hole (right) (Keto et al. 2013 and SKB 2008).*

In order to examine the initial, saturation behavior in pellet-filled gaps, a series of laboratory tests (called infiltration tests) were conducted on discrete volumes of pellets material to which inflow was introduced and the distribution of inflowing water and heaving response of the system were studied as a function of time.

Infiltration tests are performed using two pellet box configurations. One box, for testing buffer pellet filling, features a gap size of 50 mm and the other, for testing backfill pellet filling, has a gap size of 250 mm. Both of the pellet boxes are two meters long and one meter high (see Figure 2). Steel support frames around the boxes are used to prevent increases in width due to strain.

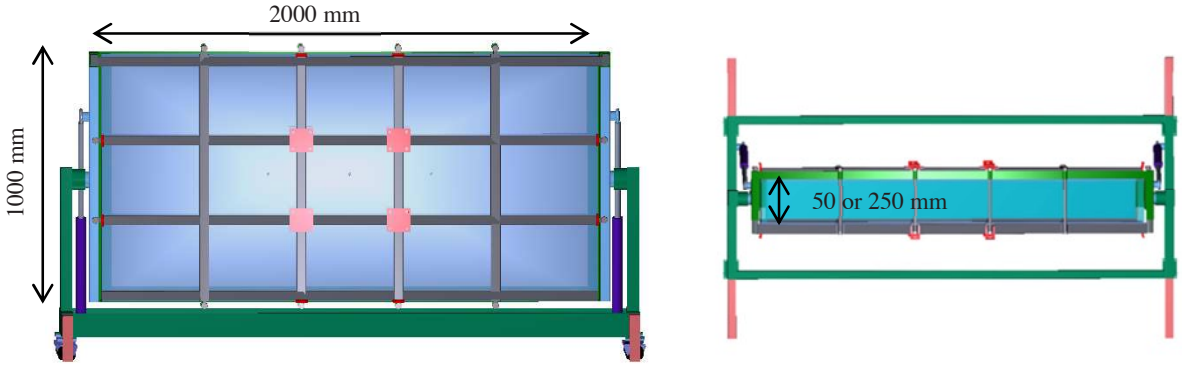


Figure 2*. Schematic illustrations of the pellet box configuration from face (left) and top (right) perspectives.*

Pellet materials (Cebogel or MX-80 pellets) are installed manually in the pellet boxes. Solution inflow is pumped (at flow rates of interest) into the pellet boxes through ports varying in type, number and location. Inflow rates and pressures were monitored continuously throughout the tests. Vertical displacement of the pellet filling and changes in box width are periodically measured over the course

of the tests. In addition, visual observations of wetting patterns and flow path formation are recorded by digital photography. After stopping the tests, the setups were dismantled and samples collected for water ratio determinations.

For tests on buffer pellet filling in a 1 meter long pellet box, wetting behavior was clearly influenced by inflow rate (see Figure 3). At 0.1 L/min the inflowing solution evenly filled the available void volume in the pellet box in a bottom-up manner and post-mortem analyses indicate rather uniform water ratio distributions. At 0.01 L/min the inflowing solution also fills the available void volume in the pellet box in a bottom-up manner but somewhat less evenly than at 0.1 L/min and post-mortem analyses indicate non-uniform water ratio distributions. At 0.002 L/min the inflowing solution progressively fills the system faster upwards than downwards and post-mortem analyses indicate non-uniform water ratio distributions, symmetric about the inlet port location, but with more wetting above the inlet port than below. Higher inflow pressures were observed with decreases in inflow rate and increases in pellet box volume. However, maximum observed pressures were on the order of 100 kPa indicating rather modest levels of resistance.

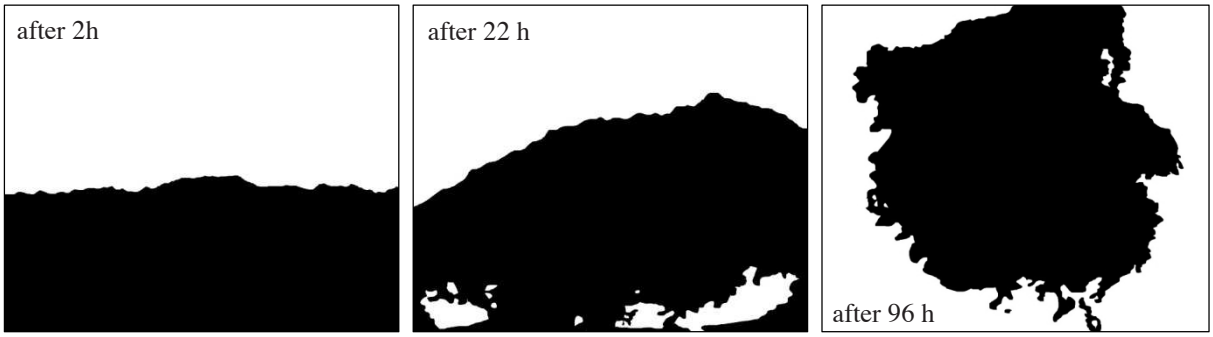


Figure 3. *Qualitative wetting pattern threshold images for infiltration tests at inflow rates of 100, 10 and 2 ml/min from left to right, respectively. Cumulative inflow volume into the pellet boxes is approximately the same in each test at the given time. Inflow ports are located in the center of the pellet boxes.*

The vertical displacement of the top of the pellet filling showed a regular pattern of behaviour with an early slump below initial levels followed by a later rise above in each test.

Infiltration test results for both buffer and backfill pellet filling, with respect to inflow rate, inflow port type and number as well as pellet filling material, will be presented and discussed.

References

Keto, P., Hassan, M., Karttunen, P., Kiviranta, L., Kumpulainen, S., Korkiala-Tanttu, L., Koskinen, V., Jalonen, T., Koho, P. & Sievänen, U. 2013. Design, production and initial state of the deposition tunnel backfill and plug. Posiva Report 2012-18. Posiva Oy, Olkiluoto.

SKB 2008 Äspö Hard Rock Laboratory – Annual report 2007. SKB TR-08-10. Svensk Kärnbränslehantering AB.

Testing Backfill Performance in a Pilot-Scale Deposition Tunnel

Jari Martikainen[1], **Timothy Schatz**[1], **Jorma Autio**[1] , **Pieti Marjavaara**[1] **and Kari Koskinen**[2]

1. B+TECH, FI-00420 Helsinki, Finland (jari.martikainen@btech.fi)
2. POSIVA, FI-27160 Olkiluoto, Finland

The deposition tunnels in the repository for spent nuclear fuel at Olkiluoto will be backfilled using, three, clay-based components: a foundation layer, compacted blocks, and pellet filling (Figure 1).

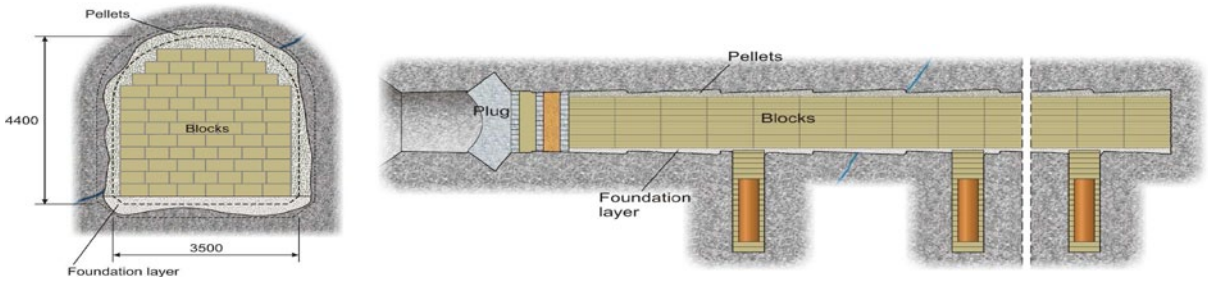


Figure 1. *Schematic figure showing the backfill components (foundation layer, backfill blocks and pellets) in a deposition tunnel from both facing (left) and side (right) cross-sectional perspectives [Keto et al. 2013].*

In order to ensure the safety and performance of the backfill design, the key processes occurring during saturation of the system must be determined and defined. These processes involve water transport characteristics and specifically, saturation time, susceptibility to erosion and density homogenization are of interest. In order to examine the initial, saturation behavior of a backfilled deposition tunnel, infiltration tests are performed using a pilot-scale, deposition tunnel test device (Figure 2) with solution inflow (corresponding in composition and rate to expected repository conditions) introduced into the system at a specific location and geometry.

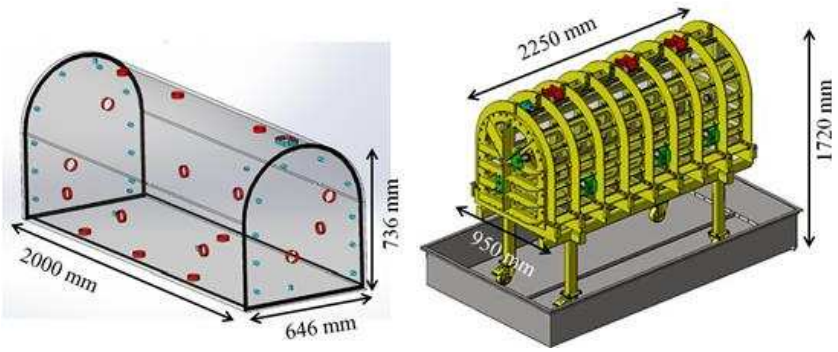


Figure 2. *Schematic illustrations of the pilot-scale, deposition tunnel test system. The device is comprised of two different units; an inner, acrylic tunnel (left) and an outer, steel support casing (right) with dimensions as indicated. The red and blue circles indicate locations for pressure sensors and solution inlet/outlet ports, respectively.*

Reflecting current repository backfill design propositions, three components are used in the tests: a foundation layer, compacted blocks and pellet-filling (see Figure 3). All material installation is performed manually in three stages. In stage one, a 150 mm thick foundation layer is put down. In stage two, 64 compacted blocks are placed on top of the foundation layer. In stage three, the remaining tunnel space is filled with pellets.

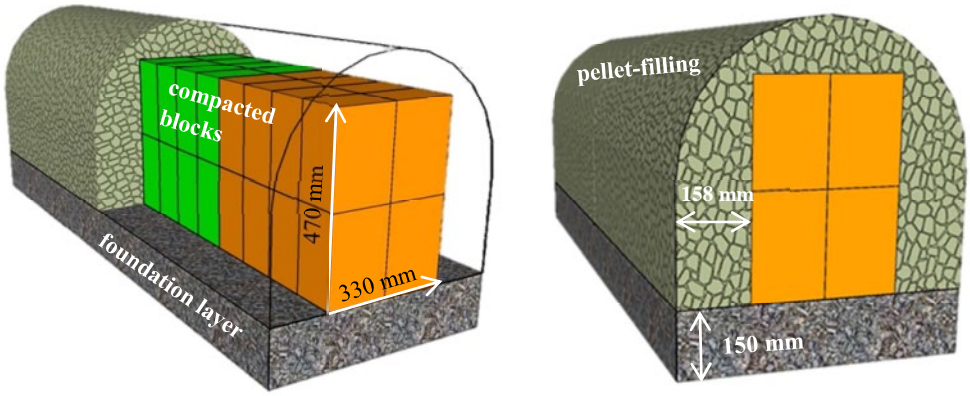


***Figure 3**. Schematic illustrations of the pilot-scale, deposition tunnel test system showing installed material dimensions.*

The total inner volume of the pilot-scale, deposition tunnel test system is 951 dm^3. After backfilling, the test system is calculated to contain 1500 kg of material at an average dry density of approximately 1400 kg/m^3 leaving 300 dm^3 void volume before saturation.

In the pilot-scale deposition tunnel tests, constant inflow is provided into the test system through the middle point of one of the side walls. Pressure evolution is measured at numerous locations over the course of the tests. In addition, visual observations, e.g., wetting patterns, flow path formation, are recorded by digital photography. Effluent solids contents are also analyzed for the presence of eroded material. Strains and displacement of the pilot-scale deposition tunnel test system are measured at external locations on both the acrylic and steel components. The tests are stopped if, the internal design pressure threshold 500 kPa for the system is reached or the distribution of inflowing water and pressure response of the test system are determined to be at relatively steady-state conditions. Upon dismantling, samples are acquired from numerous locations over all of the installed components for water content determination.

A set of results from the first pilot-scale, deposition tunnel test will be presented and discussed.

References

Keto, P., Hassan, M., Karttunen, P., Kiviranta, L., Kumpulainen, S., Korkiala-Tanttu, L., Koskinen, V., Jalonen, T., Koho, P. & Sievänen, U. 2013. Design, production and initial state of the deposition tunnel backfill and plug. Posiva Report 2012-18. Posiva Oy, Olkiluoto.

Hydraulic Sealing Ability of Bentonite Pellets at Small, Contact Apertures

Jari Martikainen[1], **Timothy Schatz**[1], **and Kari Koskinen**[2]

1. B+TECH, FI-00420 Helsinki, Finland (jari.martikainen@btech.fi)
2. POSIVA, FI-27160 Olkiluoto, Finland

Saturation of the clay-based, barrier components in the repository for spent nuclear fuel at Olkiluoto will be governed by the hydrogeological conditions in the surrounding bedrock and the hydraulic properties of the components themselves, and may result in the formation of channels or pipes through the buffer or backfill material, and possibly erosion thereof, inside the deposition tunnels.

Ideally, after the available void volume inside the deposition tunnel has been filled, the water pressure gradient will be transferred from the initial inflow point to the tunnel plug (see Figure 1), the inflow will effectively cease and homogenization will take place. However, leakage may occur at a variety of downstream interfaces, e.g., other fractures, fissures, or joints, as well as the deposition tunnel plug itself leading to undesired water flow and the possible preservation of advective transport pathways.

Insofar as any deposition tunnel material may be able to seal leakages due to a "self-grouting" or "self-filtration" effect, such outflow may be stopped altogether. Given the heterogeneous design of the tunnel backfill installations, it is reasonable to assume that the material in most direct contact with possible leakage interfaces will be the outermost foundation layer material, pellet-filling materials and plug components.

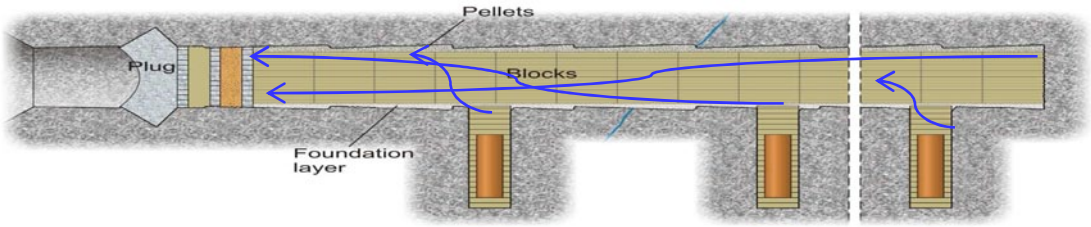


Figure 1. *Schematic figure showing a deposition tunnel and various saturation inflow scenarios (Keto et al. 2013).*

In order to evaluate the sealing potential of bentonite pellet material at small leakage apertures, a series of laboratory experiments were performed in which MX-80 pellet material was placed into contact with a small, contact leakage slit (Figure 2) and tested against solution salinity, inflow rate and aperture size. Additionally, threshold conditions for channel formation through the pellet volume were examined as well.

For MX-80, roller-compacted, pillow-shaped pellets at a dry density of ~920 kg/m^3, material extrusion into a 0.05 mm leakage slit routinely occurred after the saturation front reached the aperture. Complete sealing of leakage flow was never observed up to the maximum inflow pressure of 4000 kPa. However, periodic inflow, lower inflow rates, possible buildup of accessory minerals in the leakage slit, higher initial dry density of the pellets and smaller aperture size were observed to enhance the sealing ability, i.e., resulted in higher inflow pressures to maintain leakage outflow.

Immediately after the available void volumes were filled, distinct and sustained flow channels were formed at 0.01 L/min inflow rate and higher with 10 g/L TDS solution (Figure 3, column C). At flow rates of 0.1 ml/min and down to 0.0055 ml/min in tests against 10 g/L solution channel formation was not observed (Figure 3, column B). At similar inflow rates against tap water solution, water pocket formation was observed and the systems were "sealed" to the permeability of the pellet medium (Figure 3, column A).

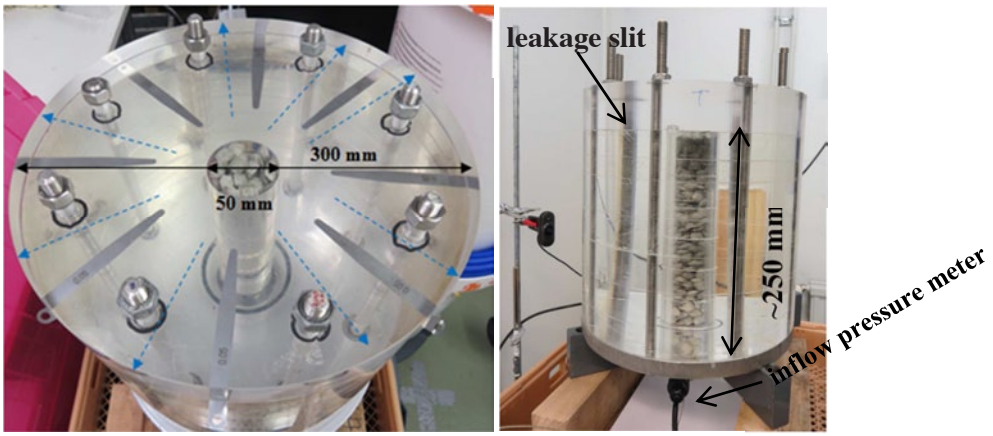


Figure 2. *Photographic images of the sealing test system. Overhead (left) and facing (right) images of the test setup after material installation. Blues dashed arrows show the direction of leakage outflow.*

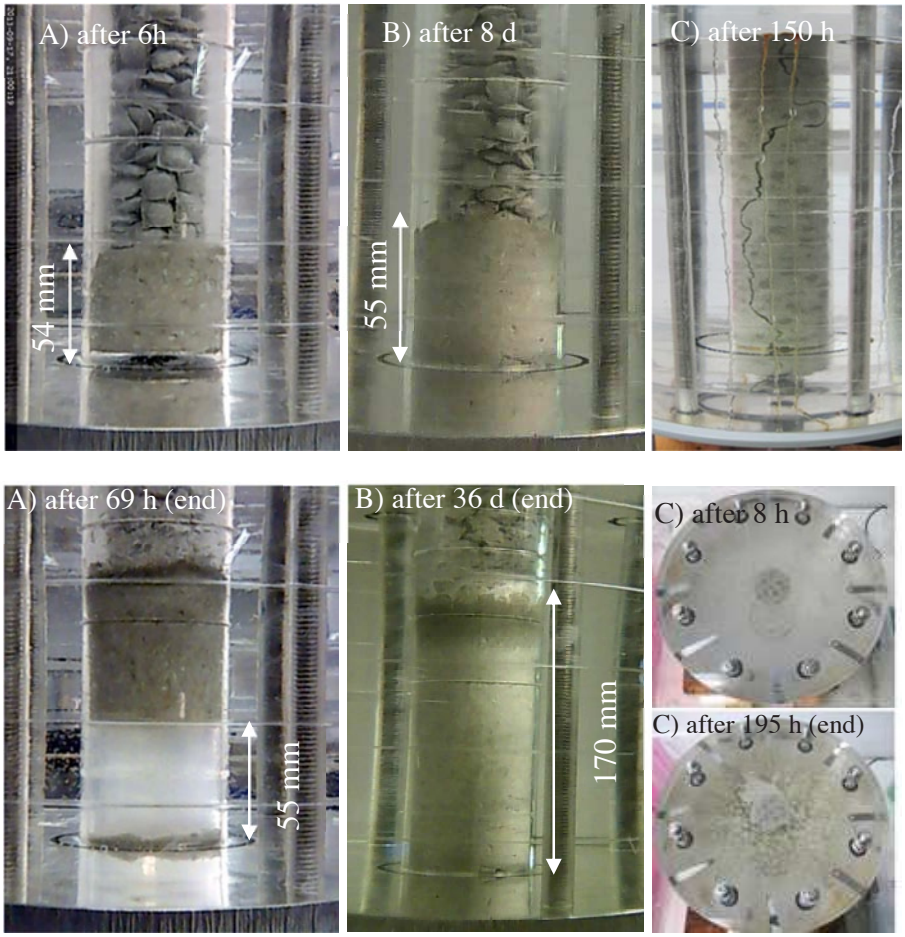


Figure 3. *Photographic images of three sealing tests: Column A - inflow rate = 0.1 ml/min with tap water, Column B - inflow rate = 0.0055 ml/min with 10 g/L TDS solution, Column C - inflow rate = 10 ml/min with 10 g/L TDS solution.*

References

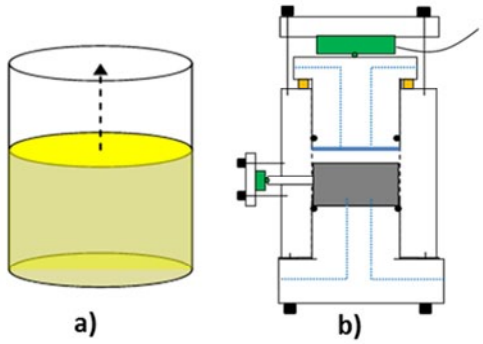
Keto, P., Hassan, M., Karttunen, P., Kiviranta,, L., Kumpulainen, S., Korkiala-Tanttu, L., Koskinen, V., Jalonen, T., Koho, P. & Sievänen, U. 2013. Design, production and initial state of the deposition tunnel backfill and plug. Posiva Report 2012-18. Posiva Oy, Olkiluoto.

Axial Homogenization of Bentonite: Experiments and Modelling

Md.Mamunul Hassan[1], Jari Martikainen[1] and Kari Koskinen[2]
1. B+TECH Oy, FI-00420 Helsinki, Finland (mdmamunul.hassan@btech.fi)
2. Posiva Oy, FI-27160 Eurajoki, Finland

Initial heterogeneous design of buffer due to installation procedure and possible local mass loss during hydration by mechanical erosion and/or glacial erosion demand buffer to swell and homogenize in order to fulfill the performance requirement of nuclear spent fuel repository. In the Task force for Engineering Barrier Systems (EBS TF – homogenization task, Börgesson et al. [2014]) various homogenization experiments and related modelling efforts have been performed. This abstract briefly presents the axial density homogenization experiments, modeling and comparison of the test results.

A series of axial homogenization tests were performed with MX-80 bentonite material (see Figure 1). Test A-1, A-2 and A-3 featured 3, 5 and 8 mm of axial free swelling space, respectively and test durations of 36 days. To study the effect of time on density homogenization a long-term test A-LT (173 days) was performed and the other conditions remained the same as in Test A-2.The target, initial dry densities of the samples in these tests were 1590 kg/m^3 with dimensions of 20 and 50 mm, height and diameter, respectively. The samples were compacted directly into the test cells (see Figure 1).



Sample ID	Initial h/ø [mm]	Free swelling space	Swelling $\Delta V/V_0$ [%]	Time [Day]
A-1	20/50	3 mm above	15	36
A-2	20/50	5 mm above	25	36
A-3	20/50	8 mm above	40	36
A-LT	20/50	5 mm above	25	173

c)

***Figure 1**. a) Illustration of the limited, axial free swelling case (Börgesson et al. 2014), where the yellowcylinder represents the initial volume of the saturated sample, b) Schematic illustration of the axial swelling test device, c) Test Matrix: Sample ID, initial sample dimensions (height/diameter), limited free swelling space, volumetric swelling (%) and test duration.*

All axial density homogenization tests were performed using well-defined geometries and consisted of two distinct experimental phases: an initial saturation phase with a confined sample volume and a limited, free swelling phase following an increase in axial head space. After relatively, steady state swelling pressure conditions were observed during the initial phase (in both axial and radial directions), additional head space was provided by pulling the axial pistons upwards. The resulting head space voids were then filled with saturating solution. Thereafter, solution was supplied into the test cells at pressures of 15-20 kPa through the both top and bottom circuits of the cells over the course of the limited, free swelling phases. After completion of the limited, free swelling phases, i.e., relatively constant swelling pressures were established, the test cells were dismantled and visual observations were performed. The samples were then sectioned for water content and bulk density determinations.

The Barcelona Expansive Model (BExM) [Alonso et al. 1990, 1999 and Gens & Alonso 1992] implemented in the finite element code "CODE BRIGHT v4.2" [Olivella et al. 1996] was used to model the axial swelling and subsequent homogenization process. The 'gap model' was chosen to simulate the equivalent void/gap length. The significant properties of the 'gap model' are that it is mechanically soft enough that it will not impede the displacement and deformation of the buffer elements, and that it is hydraulically permeable enough that it will not impede the flow of water to the buffer.

Figure 1 and 2 present comparisons of the measured and modelled swelling pressures and dry density evolutions for axial homogenization tests A-1, A-2, A-3 and A-LT. During the limited, free swelling phases, i.e., homogenization, the modelled cases shows a slight delay in swelling pressure development compared to the experimental results (Figure 1 and 2). Generally, the modelled swelling pressures slightly overestimate the measured pressures (Figure 1 and 2). Density homogenization was routinely observed, but significant density gradients persist over the sample heights in each test. For the test with the largest head space, A-3, the modelled dry density distribution over the height of the sample is more homogenized than that observed experimentally (see Figure 1). The modelled dry density closely follows the measured results for test A-LT (Figure 2). Figure 2 also shows that no significant density homogenization was observed when A-2 and A-LT tests were compared though approximately five times longer test duration was allowed.

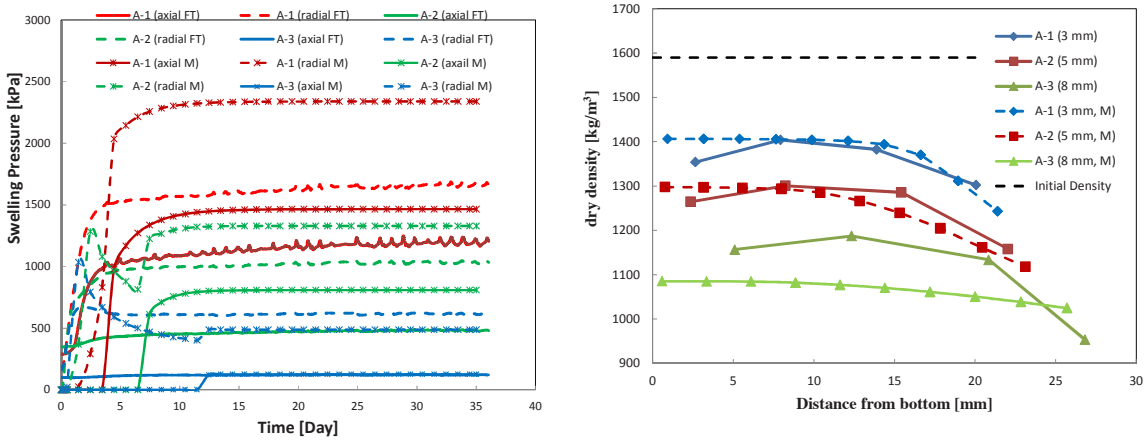


Figure 1. *Comparison of measured and modelled (M refers to model result) swelling pressure and dry density distributions of Test A-1, A-2 and A-3.*

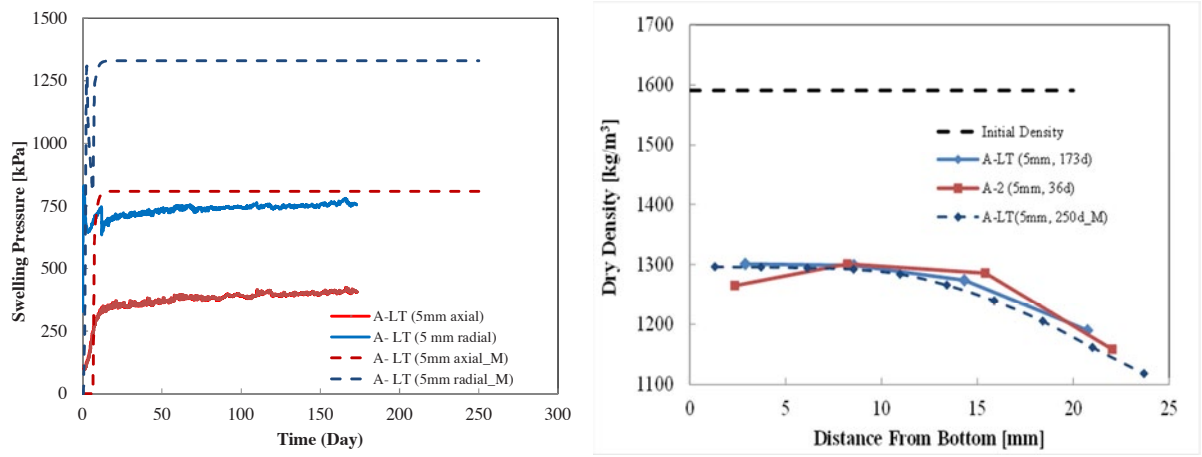


Figure 2. *Comparison of the measured and modelled (M refers to model result) swelling pressure for long-term test (A-LT) and dry density distribution of test A-LT, A-2 and modelled result.*

References

Alonso, E. E., Gens, A., & Josa, A. (1990). A constitutive model for partially saturated soils. Géotechnique 40(3): 405–430.

Alonso, E. E., Vaunat, J., Gens, A. (1999). Modelling the mechanical behaviour of expansive clays. Engineering Geology 54: 173–183.

Börgesson, L., Dueck, A., Goudarzi, R. & Hernelind, J. (2014). Status of Swelling and homogenisation of bentonite buffer and backfill . TF EBS 22/5 2014, Tokyo, Japan.

Gens, A. & Alonso, E. (1992). A framework for the behavior of unsaturated expansive clays. Canadian Geotechnical Journal, 29(6): 761-773.

Olivella, S., Gens, A., Carrera, J., Alonso, E.E., (1996). Numerical formulation for a simulator (CODE-BRIGHT) for the coupled analysis of saline media. Eng. Comput. 1: 87– 112.

The bentonite rock interaction experiment (BRIE) - results from the bentonite parcels

***Mattias Åkesson*[1], Åsa Fransson[2] and Anders Sjöland[3]**

[1] Clay Technology AB, IDEON Science Park, Lund, Sweden
[2] Division of GeoEngineering, Chalmers University of Technology, Gothenburg, Sweden
[3] Swedish Nuclear Fuel and Waste Management Co, Stockholm, Sweden

Introduction

The Bentonite Rock Interaction Experiment (BRIE) is a field experiment which addresses the hydraulic interaction between the system components of compacted bentonite and near-field host rock composed of hard and fractured crystalline bedrock. This experiment is also addressed in a joint modelling task (Task 8) of the SKB Task forces on Engineered Barrier Systems (EBS) and on Groundwater Flow and Transport of Solutes (GWFTS). The objective of BRIE, and Task 8 as a whole, is to enable: i) an enhanced understanding of the exchange of water across the bentonite-rock interface; ii) better predictions of the hydration of the bentonite buffer; and iii) better characterization methods of the deposition holes. The experiment is performed in the TASO tunnel located at a depth of 420 m at Äspö Hard Rock Laboratory in Sweden, and is subdivided into two main parts: i) the selection and characterization of a test site and two central boreholes; and ii) the installation, hydration and dismantling of two bentonite parcels. This presentation gives an overview of the experiment with the main emphasis on the results from the bentonite parcels.

Rock characterization

Investigation boreholes have been central for the characterization of the rock, which was divided in three phases: the site selection, the site characterization; and the characterization of two central boreholes. Five primary boreholes (Ø76 mm and approximately 3 m deep) were drilled in the tunnel floor during the site selection, whereas 14 additional vertical boreholes and four horizontal holes were drilled during the site characterization. Two of the primary boreholes (17G01 and 18G01) were finally enlarged to Ø300 mm, and the depth of one of holes (17G01) was increased to approximately 3.5 m. The core drillings have shown that the main rock type is diorite, and that two types of granite (Ävrö granite and fine-grained granite) also can be found. The five primary boreholes and the two Ø300 mm *test holes* were characterized through BIPS (borehole image processing system) imaging and core mapping. These measurements have resulted in information concerning depth and orientation of individual fractures intersecting the boreholes. The *hydraulic characterization* has consisted of different types of measurements. Inflow measurements were performed as: i) pump tests in different packed-off sections in the primary boreholes as well as in the test holes; ii) Posiva flow log (PFL) measurements; iii) nappy tests, in which the rock surface of the test holes was covered with diapers during a defined time period, and subsequently removed and analyzed with respect to water content; and iv) with sorbing mats which were used in a similar way as the diapers but on the tunnel floor. Pressure measurements were performed in packed-off sections in all the Ø76 mm boreholes. Transient hydraulic tests were performed for quantification of properties for individual fractures. In addition to this, characterization of the rock matrix was performed in the laboratory (hydraulic conductivity, porosity, water retention curve and measurements of relative humidity in rock blocks).

Bentonite parcels

Two bentonite parcels (denoted Hole 17 and 18) were installed in two Ø300 mm core-drilled test holes in September 2012. The lengths of the parcels were 3.5 and 3.0 m, respectively, and were put together with compacted blocks of MX-80 bentonite (Ø298 mm and height 100 mm) which were threaded on a central tube (Ø40 mm), and confined with steel plates in the bottom and the top. The blocks had a dry density value slightly higher than the target dry density value (corresponding to a void ratio of 0.78), since the blocks would swell and fill the 1 mm slot between the blocks and the borehole wall. The water content of the blocks was 11.6 ± 0.2 %.

Each bentonite parcel was instrumented at two sections: one wet section dominated by flow from a main fracture of interest in each hole, and one dry section potentially dominated by matrix flow. These sections consisted, in turn, by two blocks which were instrumented with sensors for measurement of relative humidity, total pressure and pore pressure. The installed sensors subsequently displayed data on the evolution of the analysed variables at the different sensor positions and therefore reflected the hydration of the bentonite. This monitoring was performed during a period of 419 days for Hole 17 and 515 days for Hole 18. Data from Hole 17 showed a clear response from sensors in the wet section, whereas the corresponding response in the dry section was very slow. Data from Hole 18 indicated less difference between the wet and dry sections.

The bentonite parcels were dismantled during the winter of 2013/2014. The dismantling operation followed a procedure of stitch-drilling of cylindrical rock pillars with a diameter of 0.7 m which was cut in the lower end through wire sawing. Since the rock cover around the bentonite parcels was cracked, however, both bentonite parcels were finally pulled out directly from the test holes without any rock cover. The parcels were subsequently documented, partitioned, sampled and analyzed with respect to water content and density. In addition, the sensors were salvaged and the function of the RH sensors was checked. Photographs of the parcel surfaces displayed traces of the main fractures of interest as well as previously uncharted fractures (especially for Hole 18). These traces were in many cases correlated with measured water content distribution. The results from the water content measurements were consistent with the recorded RH data: the contrasts between the wet and dry section were more pronounced in Hole 17 than in Hole 18. The photographs of the parcel surfaces were used to evaluate the positions of the main fractures of interest. An in-situ retention curve was evaluated by relating the last reading from each RH sensor with the analysed water contents in bentonite samples most closely located to the sensors.

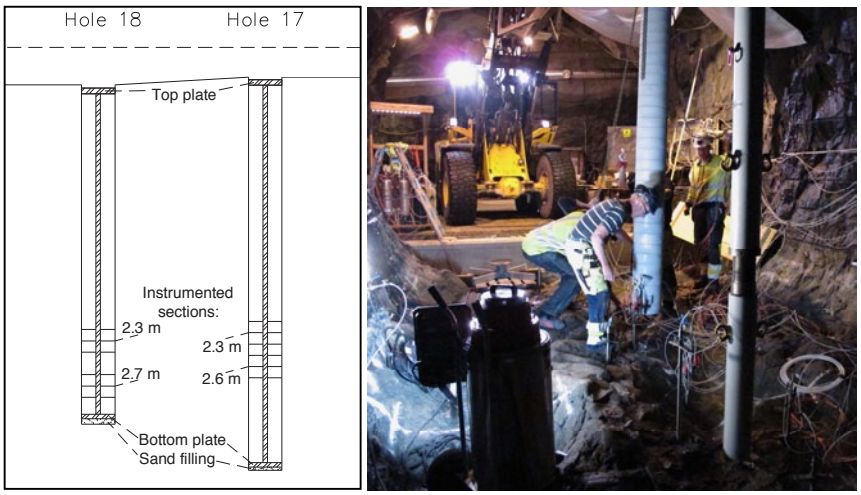


Figure 1. *Outline of bentonite parcel (left). Photograph shows the lowering of the parcel in Hole 17 and the retaining pillar for Hole 18 (right).*

Dome plug for deposition tunnels – lab tests and design modeling

Lennart Börgesson, Torbjörn Sandén, *Mattias Åkesson*

Clay Technology AB, IDEON Science Park, Lund, Sweden

The deposition tunnels in a planned repository for spent nuclear fuel will be sealed with a plug at the end of the tunnels in order to withstand the swelling of the backfill and to seal off out-flowing ground water. The principle design of the plug consists of several components, among which the most important are the concrete dome, the bentonite seal and the filter. The water leakage past the plug has to be small enough in order to build up a water pressure inside the plug, and to keep eroding water from the tunnel at an acceptable level during the operational phase of the repository. The concrete part of the plug needs time (about 3 months) for hardening and contact grouting, and during that time the concrete section must be kept free from water. Wet tunnels therefore require a drainage system which can take care of the water coming from the inner parts of the tunnel.

These issues and demands have been addressed in the SKB project "System design of dome plug for deposition tunnels". The project aims to ensure that the reference configuration of the KBS-3V deposition tunnel end plug works as intended. By testing the design in a full-scale demonstration it is to be proven that the method for plugging of a deposition tunnel is feasible and controllable. The requirements on tightness of the plug are to be given a definite form. This presentation will give an overview of the different activities within the sub-project denoted "Laboratory tests and modeling". The full-scale experiment is presented in an adjoining presentation[1].

Several *laboratory tests of the sealing materials* have been performed: i) compaction tests of sealing blocks; ii) strength tests of sealing blocks; iii) oedometer tests of MX-80 bentonite in the dry density range of 1300 – 1500 kg/m^3; iv) swelling pressure and hydraulic conductivity measurements on specimen which had been compacted to a high degree of saturation; v) tests of self sealing of artificial fractures; vi) tests of sealing of initial slots.

Several *laboratory tests of the drainage components* have been performed with the goal to determine the hydraulic conductivity and the compression properties. Three *geological* draining materials were tested; a mix of stone dust and macadam with grain sizes 0-5 mm, a natural sand/gravel with grain sizes 0-4 mm and finally pure macadam with grain sizes 2-4 mm. Two qualities of the needle felted *geotextile* were tested; 1000 and 1200 g/m^2. Two stiff *draining material candidates* were tested: lightweight concrete and LECA.

Scale tests of the sealing and draining function, in a radial scale of 1:20, have been designed in order to demonstrate the functions of the plug (Figure 2). A total of six laboratory model tests have been implemented with the following main purposes: i) to demonstrate the function of the draining components (LECA and macadam filter); ii) to demonstrate that the bentonite sealing can withstand a water pressure of 5 MPa without leakage; iii) to investigate if a bentonite sealing is needed when using grouted concrete beams; iv) to investigate the bentonite sealing function against grouted and non-grouted concrete beams; v) to investigate how the sealing function is influenced by the void space size between the concrete beams; vi) to study how fast and how soon a water pressure can be applied to the sealing after water filling of the filter.

Hydro-mechanical modeling of the tunnel plug. This work has basically been two-parted: i) dimensioning calculations of the general plug design, and this has mainly consisted of analytical calculations of dimensions for different plug components in different configurations; ii) predictions of the hydro-

[1] "Full-scale test of dome plug (Domplu) – design, installation, prediction and results" by Börgesson, Sandén, Åkesson and Grahm.

mechanical processes in the planned full-scale test, and this has been performed stepwise during the course of the project. The dimensioning calculations were performed with the aim to limit the swelling pressure on the concrete dome to 2 MPa. The swelling pressure in the backfill may however reach significantly higher levels (~ 6 MPa). This has initiated the development of a transition zone, which provides a component in which the stresses along the tunnel axis can be "geared down" due to friction along the rock wall (Figure 1 right).

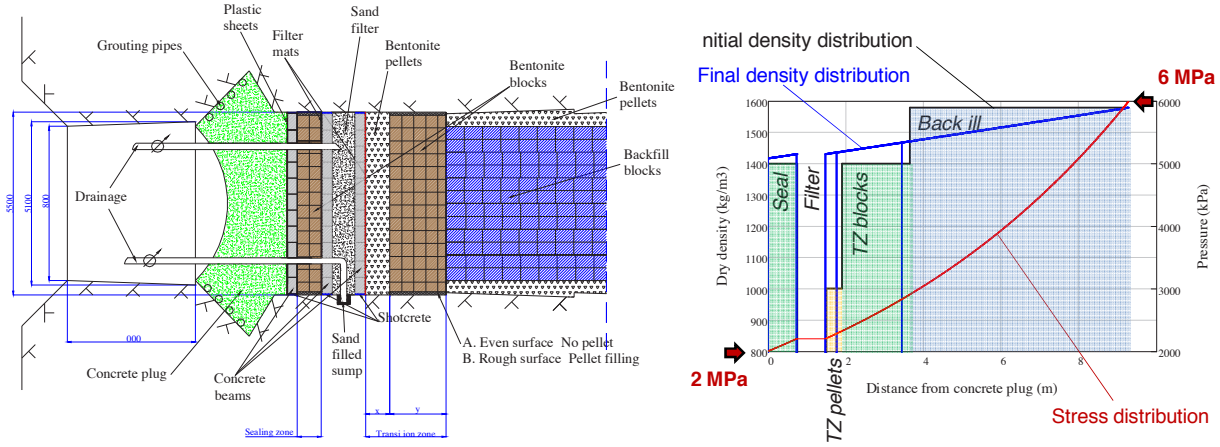


Figure 1. Illustration of main components of plug design (left). Calculated stress and dry density distributions along the tunnel/plug design (right).

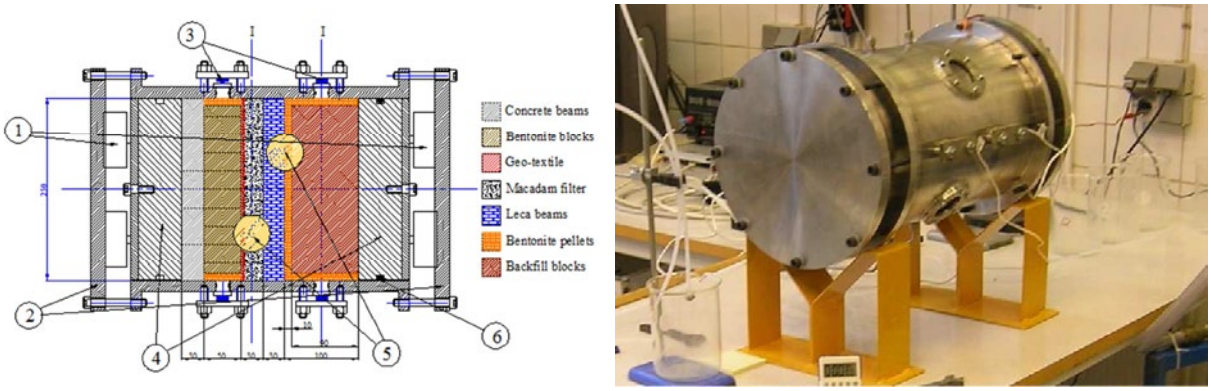


Figure 2. Cross section sketch (left) and photo (right) of the equipment for the scale tests.

The distribution of buffer saturation times in the planned Forsmark Repository

Author(s)
***Daniel Malmberg*[1], c**
[1]Clay Technology AB, IDEON Science Park, S-223 70, Lund, Sweden

The Forsmark site is the planned location for final storage of the Swedish spent nuclear fuel. The repository will consist of more than 6000 vertical deposition holes positioned in more than 200 horisontal deposition tunnels. Each deposition hole, which is 7 m deep and 1.75 m in diameter, will contain a spent-fuel canister embedded in a bentonite-clay buffer. The deposition tunnels will be backfilled with bentonite blocks and pellets, whereafter they are sealed using concrete plugs. Once all the nuclear waste has been deposited the access tunnels will be backfilled and the repository sealed.

The purpose of the bentonite in the deposition-hole buffer, and the tunnel backfill, is to act as a safety barrier, protecting the canisters mechanically and preventing radioactive particles from leaving the repository, and enter the groundwater system. At installation, the buffer is dry, with a water content between 10% and 17%. After installation it will take up water from the host rock, through fracture and matrix flow, untill it is fully saturated.

An important aspect when analysing the safety function of the buffer and backfill is to understand how soon after installation it will reach full saturation. This is a complex question, as the inflow into the individual depsition holes in the repository can vary greately; deposition holes that are intersected by water bearing fractures may be saturated within a few decades, while deposition holes with no intersecting fractures could remain dry for many thousand years.

We have used groundwater models of the Forsmark repository (Joyce et al. 2013) which simulated the period after excavation but before installation of the buffer (hence the inflows are measured during atmospheric conditions). From the models we have, for example, analysed the fraction of deposition holes that is intersected by fractures, the fracture inflows and the distance from each deposition hole to nearby tunnel-intersecting fractures.

The groundwater fracture statistics have been combined with numerical Code_Bright models of the saturation process of both the tunnel backfill and the deposition-hole buffer. The saturation time of each deposition hole was calculated according to the following algorithm:

1) Each deposition hole was checked for intersecting fractures; if any was found the open-repository inflow was measured and the saturation time, t_{S_DHF}, was calculated using a Code_Bright model of a single deposition hole intersected by a single fracture with the measured inflow (see also chapter 3 of Åkesson et al. 2010).
2) Then, the saturation time in the pellets just above the deposition hole, $t_{S_TF}(x_{DH})$, was analysed using Code_Bright models of the saturation process in the tunnel backfill due to water inflow from fractures (see also chapter 2 of Åkesson et al. 2010).
3) The saturation time of the deposition hole was then taken as $t_S = \min(t_{S_DHF}, t_{S_TF})$; hence assuming that 1) a deposition hole will be saturated shortly after the pellet above it reach full saturation, and 2) that the saturation time at any point within this pellet volume is not altered significantly by the presence of the deposition holes.
4) If no fractures intersect the tunnel or the deposition hole, the saturation time was set equal to infinity.

The analysed saturation times were then compiled into a distribution of saturation times, which is shown as the grey line in Figure 1. As can be seen, this analysis indicates that many deposition holes will remain unsaturated for a very long time (for example, after 10 000 years only about 70% of all deposition holes have reached full saturation).

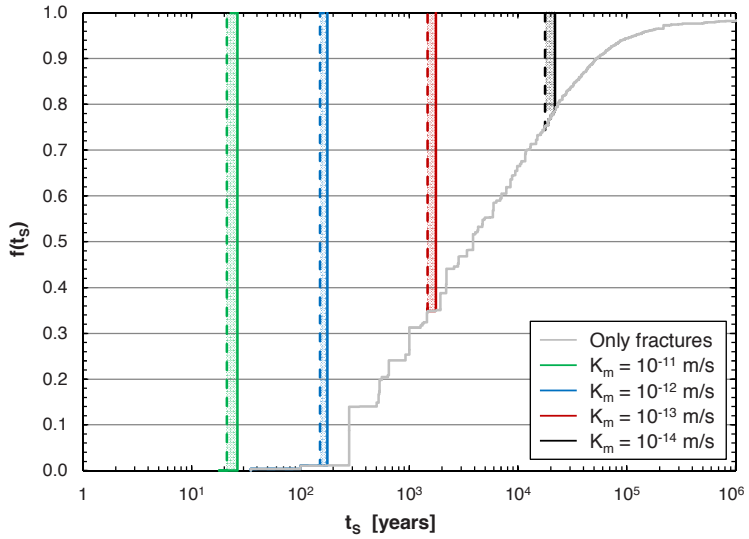


Figure 1. *The solid grey line identifies the cumulative distribution of saturation times, $f(t_S)$, for the planned Forsmark repository when not assuming matrix flow. The colored lines identify the time interval within which all deposition holes will reach full saturation if matrix flow is included and the matrix hydraulic conductivity, K_m, has the value 10^{-11}, 10^{-12}, 10^{-13}, or 10^{-14} m/s.*

One important feature, however, has so far been neglected in this discussion: the matrix flow. The matrix flow is here defined as the flow through very small and connected fractures, which are below the cut-off limit in the DFN models. Measurements of the hydraulic conductivity, K_m, of the matrix in Forsmark (Vilks 2007) suggest a range of $5 \cdot 10^{-12} - 4 \cdot 10^{-14}$ m/s on the decimetre scale.

The time until saturation when only considering matrix flow has been evaluated using Code_Bright models with varying values of K_m. The results from these models are shown as coloured zones in Figure 1 (the width of the zones corresponds to the uncertainty in the models caused by the simplification that mechanical processes were not explicitly modelled). The interpretation of these zones is best explained using two examples:

- If $K_m = 10^{-11}$ m/s (green zone) all deposition holes will become saturated within 30 years after installation and fracture flow will be of no importance.
- If $K_m = 10^{-14}$ m/s (black zone) about 75% of deposition holes will be saturated through fracture flow, and the remaining 25% will be saturated through matrix flow on a time-scale of about 20 000 years.

Given the range of matrix conductivities suggested by experimental measurements ($K_m = 5 \cdot 10^{-12} - 4 \cdot 10^{-14}$ m/s) the present analysis thus indicates a strong possibility that a considerable fraction of deposition holes will remain unsaturated for thousands of years, even when accounting for the transport of water through the rock matrix.

References

Joyce S, Swan D, Hartley L. 2013 Calculation of open repository inflows for Forsmark, SKB R-13-21, Svensk Kärnbränslehantering AB

Vilks P 2007. Forsmark site investigation – Rock matrix permeability measurements on core samples from borehole KFM01D. SKB P-07-162, Svensk Kärnbränslehantering AB

Åkesson M, Kristensson O, Börgesson L, Dueck A, Hernelind J, 2010b. THM modeling of buffer, backfill and other system components – Critical processes and scenarios. SKB TR-10-11. Svensk Kärnbränslehantering AB

Coupled hydro-mechanical modelling of bentonite resaturation and swelling for DECOVALEX-2015

KE Thatcher[1], AE Bond[1], C McDermott[2], AP Fraser-Harris[2] and S Norris[3]

[1] Quintessa Limited, 633/635 Birchwood Boulevard, Warrington, UK.
[2] University of Edinburgh, Grant Institute, The King's Buildings, West Mains Road, Edinburgh, UK.
[3] Radioactive Waste Management Limited, Building 587, Curie Avenue, Didcot, UK.

The long term performance of clay based sealing systems is being studied in the SEALEX experiments at the Tournemire Underground Rock Laboratory (URL). One of the SEALEX experiments, involving a 70/30 mixture of MX80 bentonite and sand, has been chosen as the focus of a coupled-modelling task in DECOVALEX-2015 (www.decovalex.org). The ultimate aim of the task is to represent the coupled hydro-mechanical behaviour of the chosen SEALEX experiment, but this task has been broken down into a number of smaller stages to enable models to be built and calibrated against simpler data sets. The work discussed here has been carried out by a team working for Radioactive Waste Management Limited (RWM) and represents the work of just one of the teams participating in this DECOVALEX-2015 task.

The first of these stages was to build models capable of reproducing oedometer test data on samples of the MX80 bentonite sand mixture and suction curves for both swelling and confined conditions. A number of different approaches were taken to build a range of models. These include approaches based on the Modified Cam Clay (MCC) model, the Barcelona Basic Model (BBM), a non-linear elasticity and a new model called the Internal Limit Model (ILM), which aims to relate the mechanical and hydraulic parameterisation more closely to reduce the overall number of free parameters in the model. All of these models were capable of representing the oedometer data provided (Figure 1), but the models make different assumptions about the type of deformation that has occurred in the experiment and about the amount and distribution of water that has been taken into the sample.

The models were then used to predict the outcome of a 1/10th scale mock-up of the SEALEX experiment in an oedometer test cell (Figure 2). The mock-up is simpler than the full experiment as there is no interaction with host rock, but the mock-up does include the complex behaviour associated with the initial open annulus (‘technological void’) around the circumference of the sample. Some models were used to provide true blind predictions of the outcome of this experiment, whilst others were calibrated to the results of the experiment. Whilst the MCC, BBM and ILM models provided good matches to the data available, they made significantly different predictions about radial stresses and the distribution of water in the sample, but there was insufficient data to distinguish between the models.

The work is on-going, with further modelling to be conducted on the full-scale test, but the results so far demonstrate that we have a range of models that are capable of reproducing some or all of the observations in the laboratory experiments. However, the models do not provide unique predictions of the processes that are controlling the resaturation and swelling of the bentonite.

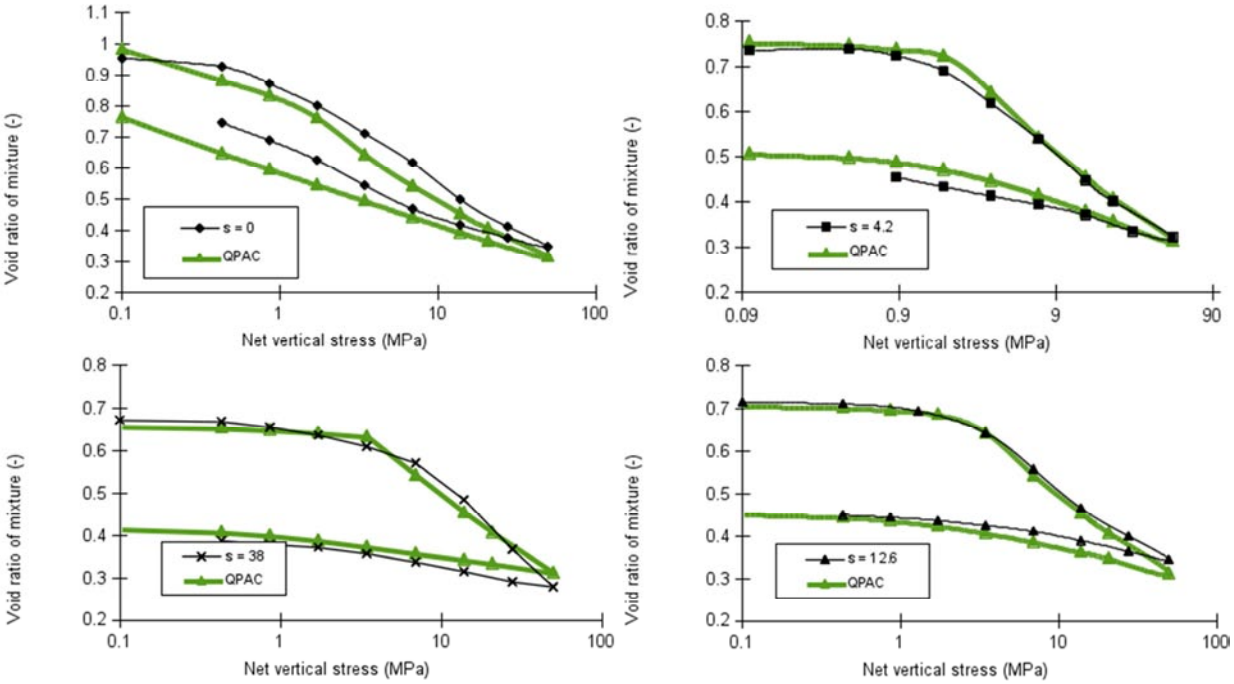


Figure 1: Oedometer test data for experiments at four different suctions and the corresponding modelled void ratio using the ILM model.

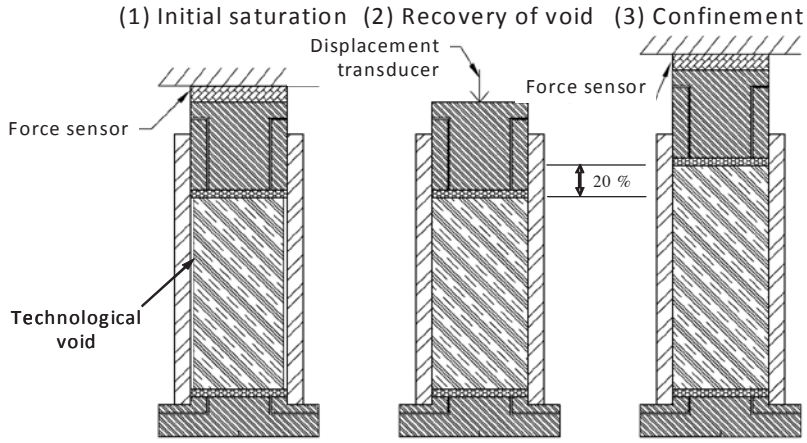


Figure 2: The 1/10th scale mock-up test with three stages of the experiment, all of which were modelled.

Model Development for Thermohydrological-Mechanical (THM) Behavior of Bentonite

Randall Fedors,[1] Chandrika Manepally,[2] Stuart Stothoff,[2] Goodluck Ofoegbu,[2] and Biswajit Dasgupta[2]

[1]U.S. Nuclear Regulatory Commission (NRC)
Washington, DC

[2]Center for Nuclear Waste Regulatory Analyses® (CNWRA®)
Southwest Research Institute®
San Antonio, Texas, USA

Understanding the swelling behavior of bentonite used in buffers and seals for radioactive waste disposal is important for assessing their barrier capability. To a lesser extent, the shrink/swell processes in certain argillite host rocks may also be important in the system's response to excavation damage and ventilation of emplacement drifts or boreholes. Several international radioactive waste disposal programs are actively researching appropriate methods for incorporating the complex coupled thermohydrological (TH) and mechanical processes (M) responsible for the swelling behavior in numerical simulators. This paper discusses NRC's efforts to develop a numerical code to model swelling clays. Once developed, the code is expected to be used for scenario analysis that encompasses different bentonites in a range of engineered barrier designs and thermal loads in a generic repository environment. At this stage, the numerical development work is described in the context of NRC's involvement in the DEvelopment of COupled Models and Their VALidation against EXperiments (DECOVALEX) project. The objectives of the DECOVALEX project are to increase understanding of coupled processes and validate models by simulating laboratory or field experiments. Two of the tasks in the current phase, DECOVALEX-2015, incorporate laboratory and field experiments to address coupled processes for bentonite buffer and seals in argillite host rocks. In general, the process is to simulate laboratory experiments and simplified field experiments as preparatory to simulating large, complex field experiments.

The NRC model development approach couples two existing simulators, *xFlo* (which models TH processes) and FLAC® (which models mechanical processes). To address expansive porous media, constitutive models are needed for (i) hydromechanical behavior for unsaturated conditions, and (ii) hydrologic properties for permeability and unsaturated relationships between water retention and relative permeability as the pore space evolves during shrinking or swelling.

The hydromechanical constitutive user-defined module for unsaturated expansive porous media (e.g., bentonite) developed for part of the FLAC® computations uses the Bishop principle to evaluate suction contributions to the effective stress, and incorporates hardening due to suction and compaction. Stresses due to suction and external loading are combined using the principle of effective stress. Stress strain relationships are derived based on elastoplasticity theory. The effects of thermal load and physicochemical swelling due to moisture absorption are also accounted for in the model. FLAC® and the user-defined module were able to represent swelling and shrinkage that resulted from varying moisture conditions or external stresses in different laboratory experiments for bentonite modeled as part of the DECOVALEX-2015 tasks.

To evaluate the adequacy of hydrological constitutive relations implemented in the current version of *xFlo*, a nonsiothermal infiltration test using granular bentonite was simulated. Constant permeability and the standard van Genuchten-Mualem relations for water retention and relative permeability were implemented in the *xFlo* model. The laboratory column test selected for the DECOVALEX-2015 task was designed to study THM conditions for a vertical column of buffer consisting of granular bentonite. The column test features a heater at the bottom (simulating heat from emplaced waste) and both a cooling bath and a source for rewetting (simulating moisture from host rock) at the top. The heater was held at 100 °C [212 °F] and 140 °C [284 °F] in successive stages, followed by the hydration stage where the bentonite was wetted via an injection tube at the top of the cell with the heater held at 140 °C [284 °F]. Comparing the measured and calculated axial pressure indicates that the mechanical model adequately represents the mechanical response. Comparisons of measured temperature and relative humidity at three probe locations with model results indicated that *xFlo,* in general, is able to represent the evolution of the moisture redistribution in response to heat. Comparions of simulated and measured water intake illustrated the need to account for evolving porosity. Based on how the pore space evolves during wetting (and drying) of bentonite, as described below, an approach and basis for modifying the permeability, water retention, and relative permeability constitutive relations was developed. This approach considers the micro- and macro-porosity, and evolution thereof, as moisture conditions change during wetting and drying.

To improve the constitutive relationships implemented in *xFlo*, the effect on hydraulic properties should consider (i) characteristic pore scales such as inter-layer, intra-aggregate, inter-aggregate, and inter-granule, (ii) loss of the inter-granule pore scales after rewetting, and (iii) irreversible pore structure rearrangement. Techniques such as mercury intrusion porosity reveal pores at one to three distinct scales in swelling materials commonly proposed for buffers, in addition to the inter-layer pores within clay grains that are too small to observe. These distinct pore scales range from the nanometer to the millimeter scale. Some thermohydrologic processes are strongly affected by changes to pore sizes. Electrostatic forces drive swelling at the nanometer scale between mineral layers in clay particles; electrostatic forces respond to bulk changes in capillary pressure, electrolyte composition, and applied stresses. Changes in clay particle geometry and orientation due to inter-layer expansion and contraction within the clay particles induce a cascade of changes at the larger pore scales. Laboratory and field tests suggest that rewetting of some media proposed for buffers, including MX–80 and FEBEX bentonite, may induce irreversible pore structure rearrangement as the clay particles rearrange. For example, the macropore space between dried bentonite granules may irreversibly close during rewetting and measured initial wetting and drying retention curves often differ in clayey materials. With this background in the pore structure of expansive clays, recent constitutive models for swelling media in the literature are beginning to (i) link bulk thermohydrologic properties to characteristic pore scales and (ii) link changes in pore structure across scales. Such models show promise, but are typically limited to two characteristic pore scales. We discuss progress using the same general approach to develop bulk constitutive relationships suitable for numerical simulators in order to represent thermohydrologic processes in granular bentonite, which features (i) up to four characteristic pore scales on emplacement (inter-layer, intra-aggregate, inter-aggregate, and inter-granule), (ii) loss of the inter-granule pore scales after rewetting, and (iii) irreversible pore structure rearrangement. An equivalent continuum approach that considers multimodal pore-size distributions and their response to swelling offers promise of consistently accounting for processes active over the range of pore scales.

The NRC staff views expressed herein are preliminary and do not constitute a final judgment or determination of the matters addressed or of the acceptability of any licensing action that may be under consideration at the NRC.

Characterisation of the volumetric behaviour of MX-80 aggregates using water retention data

Vicente Navarro[a], Laura Asensio[a], Ángel Yustres[a], Xavier Pintado[b]

[a] University of Castilla-La Mancha. Civil Engineering Department. Avda. Camilo José Cela s/n, 13071 Ciudad Real, Spain

[b] B+Tech Oy. Laulukuja 4, 00420 Helsinki, Finland

The results from Dueck and Nilsson (2010), Wadsö et al. (2004) and Kahr et al. (1990) plotted in Fig. 1 have been analysed. The total soil water content has been assumed to be the sum of the water that partially fills the intra-aggregate voids ("macrostructural" water) and the water stored inside the inter-aggregate porosity ("microstructural" water) (see, among others, Alonso et al. 2011, Della Vecchia et al. 2013 and Casini et al 2012). According to Tuller and Or (2005), it was accepted that capillary contributions due to the water held in the macropores dominate at the wetter range of the water retention curve. In turn, it was admitted that adsorptive contributions dominate at the dryer range of the curve, when the water is mainly in the micropores. Results from Or and Tuller (1999) indicate that, for a wide range of soil textures, capillary contributions become negligible for matric suction values higher than 10 MPa. Romero et al. (2011) identified the suction corresponding to empty macropores and fully saturated micropores as 25 MPa for the FEBEX bentonite. Jacinto et al. (2009) confirmed that, for an MX-80 bentonite, the dry density influences the water retention capacity at suctions lower than 30 MPa. This indicates a region dominated by adsorptive storage mechanisms (Romero et al. 2011). This work assumes that, for suction values higher than 20 MPa, the water content values in Fig. 1 are related to intra-aggregate water.

In very dry conditions, the hydration was assumed to be linked to crystalline swelling, which is practically complete when suction reaches around 44 MPa (72% RH at 20ºC) (Cases et al. 1992). When suction is lower, the hydration dynamics changes, as osmotic swelling processes become more relevant. For this reason, the microstructural water content was w_m defined as:

[1] $$w_m = w_{mC} + \Delta w_{mO}$$

where w_{mC} corresponds to crystalline water and Δw_{mO} is the increment of microstructural water due to osmotic swelling. If we suppose that, from the dry state, the increment of microstructural void space is equal to the increment of microstructural water, the following relationship holds:

[2] $$e_m = G_S \cdot w_m$$

where G_S is the specific gravity of soil particles ($G_S = \rho_S / \rho_W$, where ρ_S is the density of mineral particles and ρw is the water density), and e_m is the microstructural void ratio (= volume of voids in the microstructure per volume of clay mineral). This way, the definition of microstructural water content implies a model of the microstructural porosity and vice versa. Equation 1 can be expressed in terms of the microstructural void ratio:

[3] $$e_m = e_{mC} + \Delta e_{mO}$$

A Van Genuchten (1980) model was used to calculate e_{mC}:

[4] $$e_{mC} = \frac{e_{mCMAX}}{\left(1 + (\alpha_m \cdot s_m)^{n_m}\right)^{m_m}}$$

The osmotic term was computed as:

[5] $$\Delta e_{mO} = -\kappa_m \cdot \mathrm{Ln}\left(\frac{s_m + P_{ATM}}{s_{mO} + P_{ATM}}\right)$$

This expression was used, for instance, by Sánchez et al. (2005), Alonso and Navarro (2005), Alonso et al. (2011) or Gens et al. (2011) to define the volumetric behaviour of microstructure. In Eq. 5, κ_m is a microstructural stiffness parameter, for which an optimal value of 0.04 was identified. In addition, the values α_m=0.018 y m_m=0.612 (Eq. 4) were identified. The relationship n_m=1/(1-m_m) (Van

Genuchten 1980) was assumed, and, for Eq. 5, s_{mO}=40 MPa was taken. These parameters yield the satisfactory fit depicted in Fig 2.

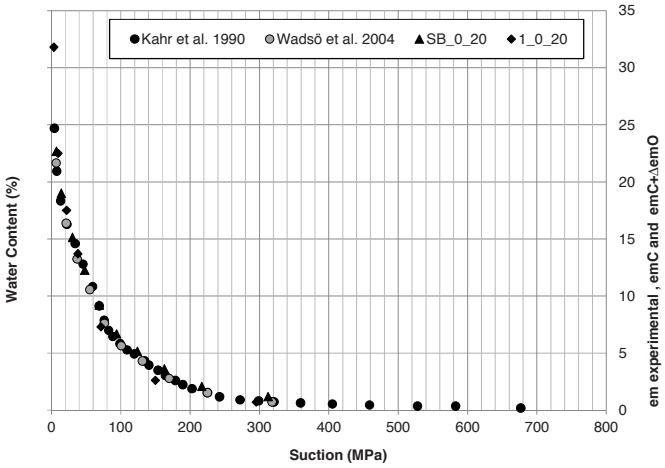


Fig 1.

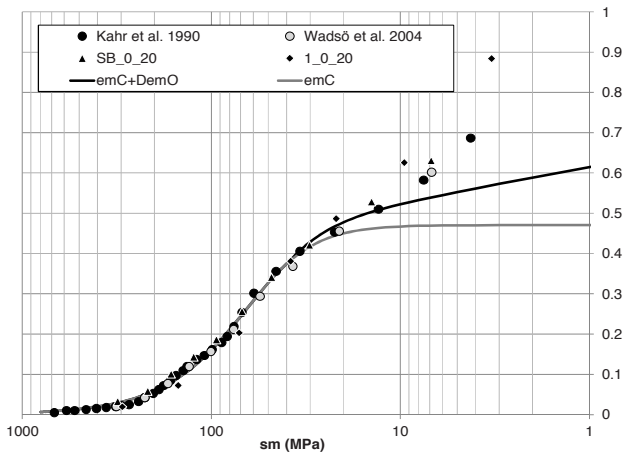


Fig. 2

REFERENCES

Alonso E. E., Navarro V., 2005. Microstructural model for delayed deformation of clay: loading history effects. Canadian Geotechnical Journal, 42, 2, 381-392.

Alonso E. E., Romero E. and Hoffmann C. 2011. Hydromechanical behaviour of compacted granular expansive mixtures: experimental and constitutive study. Géotechnique 61, 4, 329–344.

Cases J. M., Bérend I., Besson G, François M., Uriot J. P., Thomas F. and Poirier J. E. 1992. Mechanism of Adsorption and Desorption of Water Vapor by Homoionic Montmorillonite. 1. The Sodium-Exchanged Form. Langmuir, 8, 2730-2739.

Casini F., Vaunat J., Romero E. and Desideri, A. 2012. Consequences on water retention properties of double-porosity features in a compacted silt. Acta Geotechnica, 7:139–150.

Della Vecchia G., Jommi C. and Romero E. 2013. A fully coupled elastic–plastic hydromechanical model for compacted soils accounting for clay activity. International Journal for Numerical and Analytical Methods in Geomechanics, 37, 5, 503–535.

Dueck A. and Nilsson U. 2010. Thermo-Hydro-Mechanical properties of MX-80. Results from advanced laboratory tests. Clay Technology AB.

Gens A., Valleján B., Sánchez M., Imbert C., Villar M.V.and Van Geet M. 2011. Hydromechanical behaviour of a heterogeneous compacted soil: experimental observations and modelling. Géotechnique 61, 5, 367-386.

Jacinto A.C., Villar M.V., Gómez-Espina R. and Ledesma A. 2009. Adaptation of the van Genuchten expression to the effects of temperature and density for compacted bentonites. Applied Clay Science, 42, 575–582.

Kahr G, Kraehenbuehl F, Stoeckli H F and Müller-Vonmoos M. 1990. Study of the water-bentonite system by vapour adsorption, immersion calorimetry and X-ray techniques: II. Heats of immersion, swelling pressures and thermodynamic properties. Clay Minerals, 25, 499–506.

Or D. and Tuller M. 1999. Liquid retention and interfacial area in variably saturated porous media: Upscaling from single-pore to sample-scale model, Water Resour. Res., 35, 12, 3591– 3606.

Romero E., Della Vecchia G. and Jommi C. An insight into the water retention properties of compacted clayey soils. Géotechnique, 61, 4, 313–328.

Sánchez M., Gens A., Guimarães L. do N. and Olivella S. 2005. A double structure generalized plasticity model for expansive materials. Int. J. Numer. Anal. Methods Geomech. 29, 8, 751–787.

Tuller m. and Or D. 2005. Water films and scaling of soil characteristic curves at low water contents. Water Resources Research, 41, W09403, doi:10.1029/2005WR004142.

Van Genuchten M. T. 1980. A closed-form equation for predicting the hydraulic conductivity of unsaturated soils. Soil Sci. Soc. Am. J. 44, 5, 892–898.

Wadsö L, Svennberg K, Dueck A, 2004. An experimentally simple method for measuring sorption isotherms. Drying Technology, 22, 2427–2440.

Variations in unconfined strength results of highly compacted bentonite blocks with respect to various aspects of testing procedures and specimen characteristics

***Radek Vasicek*, Marketa Levorova, Zbynek Kaisr**

Czech Technical University in Prague, Faculty of Civil Engineering, Centre of Experimental Geotechnics, Thakurova 7, 166 29 Praha 6, Czech Republic (radek.vasicek@fsv.cvut.cz)

The highly compacted Ca-Mg bentonite blocks are to be used in the Czech deep geological disposal concept. The engineered barrier must provide such properties to withstand all the adverse effects that may occur underground for up to hundreds thousands years. Thus the effect of long-term mechanical loading on prefabricates can play important role. Naturally, the conditions inside bentonite barrier will change during the lifetime of the repository. Initially the bentonite blocks will have relatively low water content favourable for their best compaction. After that the blocks will gradually intake water from host rock until full saturation. The blocks will have to transmit vertical load caused by weight of canister with the high level waste (hundreds of kPa) in all those phases of engineering barrier. Inhomogeneous swelling of the buffer will create additiona load on some blocks inside the buffer. Therefore knowledge on bentonite blocks response to load under various condition is necessary.
Several standards and recommendations for compression strength testing exist and may be apllied (e. g. CSN CEN ISO/ TS 17892-7 - Test for unconfined compressive strength for fine-grained soils [1]; CSN EN 1926 - Natural stone testing methods - Determination of compressive strength [2]; International Society for Rock Mechanics on Determination of the uniaxial Compressive Strength Rock of Materials [3]).
Specimen characteristics (size, shape, aspect ratio…) of the samples can vary according to the standard requirements. The aspect ratio is required most often between 2 and 3but, for example, CSN EN 1926 requires value of 1. Non uniform requirements on specimens can lead to different test results. Moreover samples extracted from in-situ experiments must not have sufficient size (or shape) to follow standard requirements. Therefore the paper shows effect of various factors (size, shape, aspect ratio) on the unconfined compressive strength results of highly compacted blocks. Effect of water content and velocity of samples compaction during manufacturing is also demonstrated.
General principles of mechanical behaviour of specimens during test are well known for several civil engineering construction materials. One of the important issues is relation of “short term” and “long term” properties (decrease in unconfined strength for this case). The response of bentonite blocks under long-term uni-axial constant load is another issue described in the contribution.
The difference among the test standards for the testing of natural stone and soils is primarily in the shape and size of the tested samples. The CSN EN 1926 was used for testing of highly compacted bentonite blocks as a default procedure at Centre of Experimental Geotechnics. Variations of specimen characteristics and procedure were as follows:

- Aspect ratio - the blocks were made by compaction of powder dry bentonite (Czech Ca-Mg) with the aspect ratio from 0.2 to 2 to demonstrate the influence of aspect ratio on the final compressive strength value.
- Degree of saturation - compacted bentonite samples with different degrees of saturation were produced to show water content and compression strength relation.
- Velocity of compaction - for determination influence of velocity during compaction of samples blocks were prefabricated with 6 different strain rates from 2.5 to 100 mm/min.
- Long-term behaviour - the compacted bentonite cubes were loaded by value equal to one third of their “short term” compression strength until sample strain change was stabilized. After that next loading step (increase load) was applied on the samples and procedure was repeated until sample failure.

Results show how the measured values of strength exponentially increase with decreasing aspect ratio (decreasing of sample height) as an effect of contact stresses between sample and pressing machine. Naturally, the Aspect ratio significantly affects the measured forces at failure. For aspect ratio between one and two some difference about 20% remains.

The effect of the shape of the sample (cylinder/ cube) was also investigated. Use of sample effective area for strength calculation is recommended to gain comparable results.
The effect of velocity of compaction did not show significant effect on final compression strength. Dispersion of strength results were mostly in the same range as the effect of velocity of compaction.
Relevant impact on final values of compression strength has various degree of saturation of samples. The unconfined strength of saturated blocks was twice lower then samples with natural water content.
Bentonite blocks under long-term constant uni-axial load presented compression strength (samples failed) at value in range of 78 to 85 % of "short-term" compression strength. The value is independent on degree of compaction (dry densities from 1350 to 1650 kg/m^3).

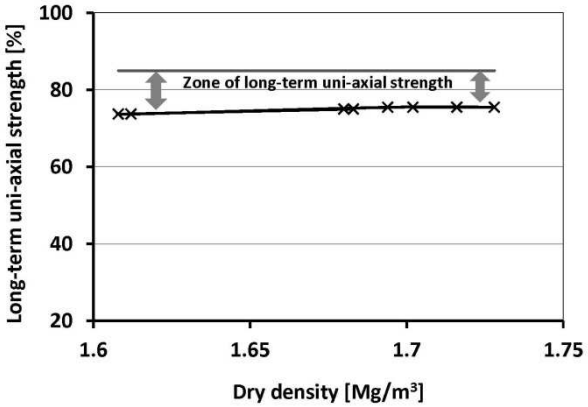


Figure 1 –Long term uni-axial strength capacity as a percentage of the "short" term (standard) value

LITERATURE

[1] *ČSN CEN ISO/ TS 17892-7. /Geotechnical investigation and testing - Laboratory testing of soil: Part 7: Unconfined compression test on fine-grained soil/. Český normalizační institut, 2005.*
[2] *ČSN EN 1926. /Natural stone test methods - Determination of uniaxial compressive strength/. Český normalizační institu, 2007.*
[3] *INTERNATIONAL SOCIETY FOR ROCK MECHANICS. /Suggested Methods for Determining the Uniaxial Compressive Strength and Deformability of Rock Materials: Part 1 - SM for Determination of the Uniaxial Compressive Strength of Rock Materials./1979.*
[4] *INTERNATIONAL SOCIETY FOR ROCK MECHANICS. /Suggested Methods for Determining the Uniaxial Compressive Strength and Deformability of Rock Materials: Part 2 - SM for Determining Deformability of Rock Materials in Uniaxial Compression/. 1979*

Development of Safety Assessment Scenarios for Gas Behavior in the Bentonite Barrier for TRU Waste Disposal Concept in Japan

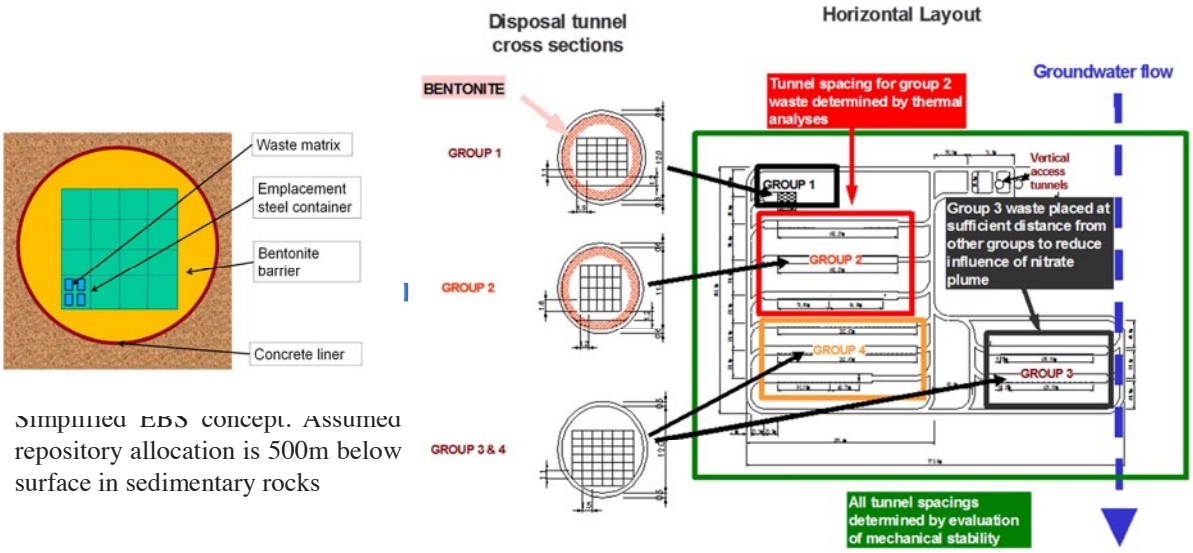
Hideki Kawamura[1*], Kazumasa Koga[2], Hitoshi Owada[2]

1. Obayashi Corporation; Intercity- B, Konan 2-15-2, Minato-ku, Tokyo 108-8502, JAPAN
2. Radioactive Waste Management Funding and Research Center (RWMC)

* Corresponding author, E-mail; kawamura.hideki@obayashi.co.jp

Abstract

In the reference geological disposal concept for "group-2" TRU waste [1)] (hulls and ends), which includes a low permeability bentonite clay barrier (Fig.1) and relatively high amount of steel material, gas is one of the key issues for long-term safety assessment[2)]. Especially, concerns include the impact of gas breakthrough on longevity of the barrier safety functions and resultant radionuclide release from the engineered barrier system (EBS). Although gas generation and transport are almost certain to occur, gas scenarios have been treated to date as perturbations of the basic groundwater release scenario [2)].



Simplified EBS concept. Assumed repository allocation is 500m below surface in sedimentary rocks

Fig-1 TRU waste repository concept (right)[1)] and Engineered Barrier System of Group-2 (left)

Last 6 years, we have developed a method for describing gas scenarios that consider the temporal and spatial evolution of the EBS within specific surrounding geological conditions[3)]. This method is as called a "hybrid" approach combining "top-down" and "bottom-up" (Fig.2), based on understanding EBS system evolution in each assessment time range, i.e.: construction and operation, closure and re-saturation, during the assured safety functions of the clay barrier, after it loses such functions. In each time range, we specify integrated, safety-related FEP groups that cover all expected gas behavior in the EBS and radionuclide release phenomena.

Using integrated gas FEPs and their associated knowledge bases, we specified "Super FEP" and constructed Super FEP correlation map (Fig.3).

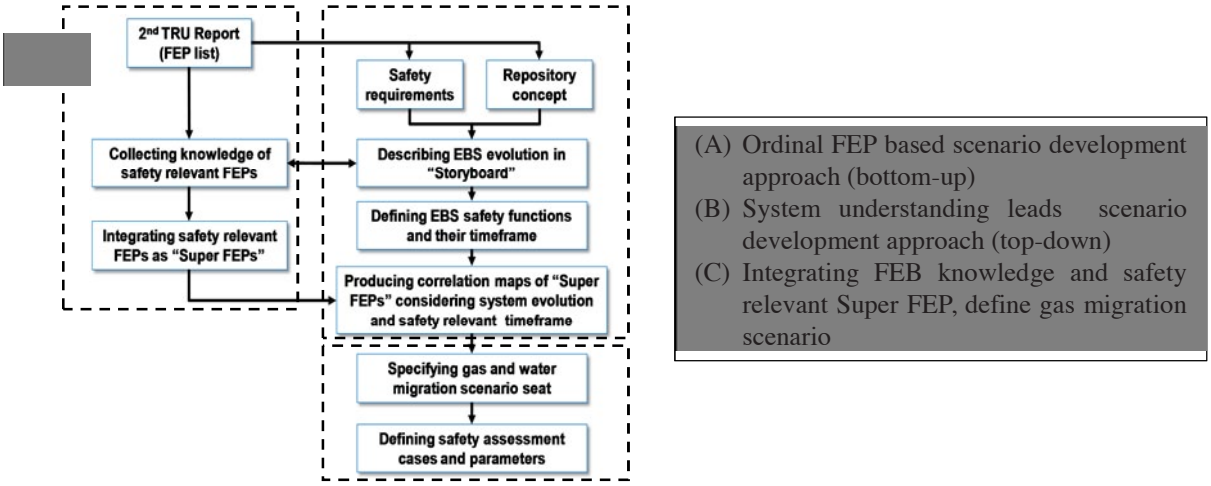
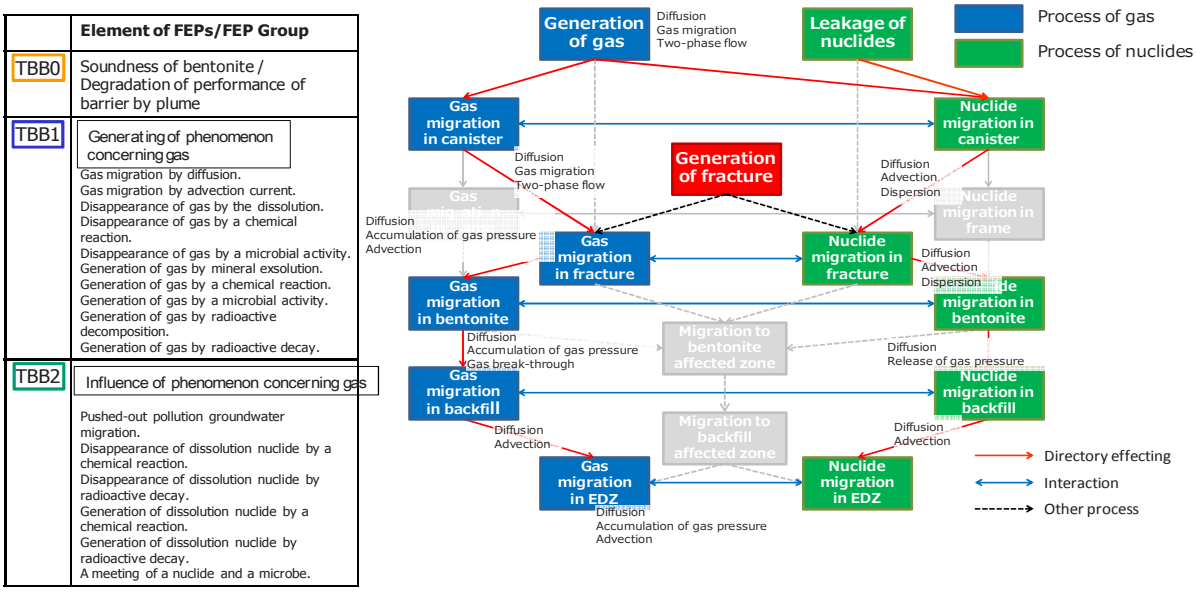


Fig. 2 Hybrid scenario development method for defining Gas Migration in EBS

Based on these correlation maps in different assessment time ranges, we defined "basic (most likely), "perturbed" and "very unlikely" scenarios together with associated uncertainties in each time range. These scenarios could be grouped according to gas generation rate and extent of clay barrier alternation caused by cement rich pore water. Thus gas breakthrough phenomena are included in a "gas basic scenario", when key safety functions of clay barrier are assured (low permeable and self-healing properties). If gas breakthrough causes failure of such functions, gas breakthrough is described within "disturbed" or "very unlikely" scenarios and thus, in safety assessments, we will assess them use risk-informed dose standards[2].

Fig.3 Integrated Super FEPs list and correlation map of Super FEPs in bentonite assuring safety function

This study have been conducted under a grant from the Agency of Natural Resources and Energy, the Ministry of



Economy Trade and Industry of Japan

1) Japan Atomic Energy Agency (JAEA) and the Federation of Electric Power Companies of Japan, "Second Progress Report on Research and Development for TRU Waste Disposal in Japan - Repository Design, Safety Assessment and Means of Implementation in the Generic Phase," (2007)
2) Nuclear Safety Commission (in Japan), the fundamental view of licensing safety review about burial project of the radioactive waste of second kind, (2011, in Japanese)
3) Radioactive Waste Management Funding and Research Center (RWMC), "Development of the technique for the evaluation of long team performance of EBS" (2007-2012)

Gas migration through a pre-compacted bentonite blocks: in-situ demonstration of a gas breakthrough

de La Vaissière Rémi[1],**Talandier Jean**[2]

[1] Andra, Laboratoire Souterrain de Meuse/Haute-Marne, RD960, 55290 Bure, France
[2] Andra, Siège, 1-7 rue Jean-Monnet 92298 Châtenay-Malabry

Several field scale experiments have been designed by the French national Agency for the management of radioactive waste (Andra) to understand: (i) the mechanisms controlling gas entry and gas migration in the Callovo-Oxfordian (COX) clay (PGZ1 experiment), the proposed host rock of the french deep geological repository, (ii) the interaction between gas and bentonite seals use to close the tunnels within the repository (PGZ2 experiments).

PGZ2 experiment is a set of a five horizontal boreholes drilled between two galleries to allow access from both sides and to avoid sensor equipment through the bentonite plugs. Two kind of materials have been tested: (i) pre-compacted bentonite plugs made with a mixture of MX80 and sand (70%/30% in mass), dry density about 1.8 g/cm^3 (boreholes PGZ1011, PGZ1012 and PGZ1013) (ii) pellets/powder mixture made with MX80 directly built in place (borehole PGZ1021), dry density about 1,54 g/cm^3. The resaturation of the bentonite plugs was only done by natural water from the host rock without any kind of water injection. In each borehole multiple pore pressure and total pressure sensors have been installed to follow as best as possible swelling pressure evolution and water saturation.

The bentonite-sand mixture in the borehole PGZ1013 was installed in February 2010 and the seal started to hydrate immediately. Pore pressure and total pressure increased and reached equilibrium after 16 months. At this stage, the seal is supposed to have reached full saturation. In October 2011, the hydraulic conductivity of the seal was measured and it is closed to 2-4 10^{-13} m/s. The swelling pressure (total pressure minus pore pressure) measured axially is about 4.6 to 5 MPa. This value is slightly lower than the target swelling pressure (7 MPa). This is due certainly to the drilling which leads locally to larger borehole diameter. The volume offer to bentonite swelling is then miscalculated.

In April 2014, a gas test was performed to evaluate the efficiency of the seal and the surrounding claystone. For this purpose, before starting gas injection, water pressure (~ 3 MPa) was lowered in one side of the seal (GEX side: -0.5 MPa) creating a pressure gradient between the two sides of the seal (GMR ~ 3 MPa and GEX ~2.5 MPa). This pressure gradient was imposed during all the testing period and the extracting flow rate at GEX side was monitored.
Then, a gas mixture (nitrogen 95% and helium 5 %) was injected at constant pressure at GMR side in two steps.

- First, the gas was injected at 3.05 MPa during 6 days. Only dissolved gas was observed in the extraction line at GEX side.
- Secondly, gas pressure was increased at 4 MPa and then a gas breakthrough was observed mainly 24 h after increasing gas pressure.

During the gas test, helium concentration was also recorded at the extraction line (GEX side).

This gas breakthrough occurred at a pressure level between 0.5 to 1.5 MPa above hydrostatic pressure and well below the swelling pressure of the seal measured axially. Many authors have shown, in bentonite samples that the gas breakthrough is closed to the swelling pressure or could be higher. They also showed that the interface is probably the location of gas pathway. In contrast, several authors have shown that in damaged claystone even if self-sealing occurs, the gas entry pressure can be significantly lower than for sound claystone even with confining stress.

Our results show that the most probable location of the gas pathway is the interface between bentonite plug and claystone or the borehole damaged zone itself.
The consequences of those results at the repository scale are that gas could be released through the interface and damaged zone along the repository drifts without any disturbance of the seal. Many arguments now seem to show that gas breakthrough pressure in those zones is much lower than in intact claystone or in bentonite plug.

Key Achievements of the FORGE Project

R.P. Shaw

British Geological Survey, Keyworth, Nottingham, NG12 5GG, UK

In the framework of the safety assessment of a geological disposal, one of the issues of concern is the impact of gases produced within the facility, notably in terms of possible perturbations which may decrease the containment capability of the disposal system and geosphere. The integrated, multi-disciplinary FORGE project addressed this key research area so as to provide new insights into the processes and mechanisms governing gas generation and migration.
Work undertaken in the FORGE project will benefit a range of users, e.g. implementers, regulators, industry and academia, via the provision of new information and understanding into gas-relevant FEPs, including mechanisms governing gas generation and migration, for consideration in the safety case. FORGE has also provided high-quality data that could be used for future activities such as benchmarking and validation of numerical codes for the quantitative prediction of gas flow, the development of HM (Hydrogeological – Mechanical) models for the prediction of EDZ and near-field processes and to assist in the assessment of the long-term evolution of the potential geological barriers. Key findings are noted here.

Gas generation

Overall, gas generation processes are generally well-understood for different types of metals, including how generation rates are globally affected by changes in experimental conditions/conditions in repository. The effects of higher short-term gas production rates need to be checked for the specific EBS design and hydraulic boundary conditions.

Engineered barrier systems

For Bentonite-based barriers:

- 2-phase flow is the dominating transport mechanism in unsaturated or partially saturated bentonite (also for saturated sand-bentonite mixtures if the sand content is sufficiently high);
- Classical 2-phase flow models cannot correctly represent gas migration in a compacted saturated bentonite;
- High gas pressure may significantly delay the saturation of the bentonite;
- If the gas pressure reaches a higher value than the pressure in the bentonite a mechanical interaction will occur, leading to either consolidation of the bentonite; and/or formation of dilatant pathways (allowing gas mobility);
- Dilatant pathways exhibit spatio-temporal evolution - localised outflows during gas breakthrough and no measurable desaturation in any test samples.
- A detailed stress analysis is required to capture the transition from consolidation to dilatant pathway formation; effect is clearly geometry dependent, but other factors may be involved (e.g. when the gas pressure reaches the sample pressure, as seen in LASGIT).
- Self-sealing of bentonite always occurs after a gas migration event.

For concrete barriers:

- For other materials studied in FORGE, the deformation of the solid phase is less important and therefore 2-phase flow can be considered as the main mechanism for gas flow even near water saturation. Improved database and process understanding has been gained for gas permeability in concrete under different conditions and how carbonation, will affect the permeability of concrete.

Gas migration in interfaces

- Gas will generally move along the interface between the clay and another material in a saturated system (because gas entry pressure in the interface is generally lower than in the surrounding materials);
- Interfacial flow depends on surface roughness, geomechanical properties, wettability, etc of the materials;

- In a saturated system bentonite/bentonite interfaces will seal (or heal - as demonstrated by the development of cohesion) and there will not be preferential pathways for gas. Gas pressure induced re-opening of healed interfaces is not observed;
- Shear displacement in the contact zone due to pressurisation of a plug will not result in mechanically-induced pathways because the saturated bentonite behaves plastically.

Disturbed host rock formations

Our understanding of fundamental processes governing gas flow in the EDZ has significantly improved as a result of FORGE. Relevant mechanisms affecting gas transport properties include stress and pore pressure conditions, stress history, orientation of EDZ fractures to the stress field, strains and hydro-chemical porewater-rock interactions (e.g. swelling, precipitation, filtration, erosion).

- Gas flow is initially focussed within the repository EDZ, the network of discrete EDZ fractures acting as a preferential pathway. Flow in EDZ highly localised along the largest EDZ fractures, exhibiting a complex inter-dependence between fracture transmissivity and the distribution of radial stress around tunnel;
- Tests show temporal evolution of flow behaviour;
- The evolution of the EDZ as a gas transport path is controlled by a variety of features, events and processes, such as the connectedness of EDZ fracture network, the resaturation of the repository near field, pore pressure recovery, build-up of swelling pressures in the clay-bearing EBS, rock creep in response to the local stress field and by the nature of the actual gas source term;
- Generic modelling studies emphasised the relevance of the spatial variability of rock properties in gas transport simulations. The inclusion of small-scale variability of certain rock properties (strength, permeability) enabled models to better simulate gas flow localisation.

Undisturbed host rock formations

- Major experimental challenges for undisturbed clay host rock have been identified and considered in improved test protocols;
- Difficult to create a gas flow into an intact clay host rock as the gas entry pressure and water retention is very high;
- Both laboratory and in situ experiments show that very little water is displaced by gas phase flow through undisturbed clay;
- Evidence for hydro-mechanical coupling and pathway dilatancy found as gas transport mechanism in very carefully-performed laboratory experiments in which all mechanical and hydraulic boundary conditions are well controlled and sample is near water saturation (or saturated);
- As its gas entry pressure is generally lower, free gas will preferentially flow through the EDZ rather than in intact rock in a clay host rock;
- Implicit and explicit formulations have been tested to introduce hydromechanical coupling in gas transport simulations
    - Implicit formulations are based on an extension of classical 2- phase flow codes to cope with fluid flow and gas transport processes in deformable media. Successful applications are reported for gas permeability tests, associated with low and moderate volumetric strains in response to the gas pressure build-up;
    - Explicit formulations (fully coupled HM modeling) were needed in other cases to reproduce the main features of the experimental results;
- Measuring the water retention curves of an indurated clay (e.g. Opalinus clay) reveals new issues to be addressed in a future research programme:
    - No significant difference was noted between applying matrix or total suction, suggesting that osmotic suction (i.e. porewater chemistry) has only a minor impact on gas transport.
    - Increasing mechanical stress seems to further increase the capillary strength value which in any case is already high (6 to 34 MPa).

Acknowledgements

This abstract is based on summary reports prepared by each FORGE work package and the Work Package leaders who prepared these reports and the authors that contributed to them are thanked for their contributions which have been used here. All organisations participating in FORGE and their personnel are thanked for their scientific contribution to the project. The European Commission is acknowledged for its funding of this pan-European project which has received funding from the European Atomic Energy Community's Seventh Framework Programme (FP7/2007-2011) under Grant Agreement no 230357.

Gas-Permeable Seal Tests at Various Scales at Grimsel Test Site (GTS)

Niels Giroud, **Thomas Spillmann, Paul Marschall, Stratis Vomvoris**

Nagra, Hardstrasse 73, 5430 Wettingen, Switzerland
niels.giroud@nagra.ch

The aim of a gas permeable seal in a L/ILW repository is to increase the capacity of the backfilled underground structures to transport gas so that no undue gas overpressures are created nor any hydraulic barrier function is compromised. The Gas Permeable Seal Test (GAST) was constructed at the Grimsel Test Site (GTS) to (i) experimentally demonstrate the effective functioning of the gas-permeable seal concept under realistic boundary conditions, (ii) determine large-scale water and gas permeabilities. A mock-up experiment at ~1:6 scale aims at validating and improving the current conceptual models for the saturation and gas invasion processes. We present the experimental layout of both experiments and review the acquired data.

The GAST in situ experiment was emplaced in 2011/2012 as a partner project with Nagra, Andra, KORAD (formerly KRMC) and NWMO. The experiment features a compacted sand/bentonite (S/B) (80/20%) body (3.00 m diameter, 8 m length) [Figure 1] which is confined by two highly permeable gravel filter elements at both ends. The body is encased in pure bentonite to prevent preferential water and/or gas flow along the S/B-granite interface or into the formation. The few water conducting features in the surrounding granite were sealed artificially and the excavation damage zone is known to be negligible, thus enabling water injection at pressures similar to those expected for a L/ILW repository seal at 300 – 500 m depth, i.e. 3-5 MPa. After an initial hydration phase when water was injected with low rates (3 to 6 ml/min), the injection started with the full rate of ~33 ml/min in May 2013. More than 150 sensors that are distributed among 15 cross sections continuously monitor pore pressures, humidity, saturation and mechanical pressures within the S/B body and at the interfaces. Pore pressure observations during this transient phase indicate a heterogeneous saturation with higher pressures in the lower layers.

The Mock-up experiment started as part of WP3 of the FORGE project. It consists of a 62 cm long and 51 cm diameter S/B (80/20%) cylinder emplaced between two porous filters in a stainless steel housing. To simulate the interface between the S/B repository seal and the porous mortar backfill the filters are made of porous mortar. This will allow improving the understanding of reactions occurring at the interface between the two types of materials and the effect on the gas transport properties of the repository seal. Similarly to the GAST project, a layer of pure bentonite minimises the risk of preferential flow path along the S/B and cylinder wall interface.
Water was injected with pressures up to 2 MPa between October 2010 and October 2013. Gas injection was initiated on the 5 June 2014. The gas injection system is designed to control rate injection at low flow rates (> 1 mlN/min) in the porous filter after flushing out the water by gas. The primary gas for used for the injection is N_2, at first pure, but after the breakthrough to be switched to a mixture of 0.5% He, Ar, Xe and SF_6 in 98% N_2. Tracer outflow will be monitored online with a quadrupole mass-spectrometer.
Following the gas injection and gas tracer test, a dismantling phase will allow analysing the interface between cementitious material and S/B, and the saturation, density and bentonite content of the S/B. This post-mortem analysis will provide information on the localisation of the gas flow path, on the saturation and desaturation processes, and provide as well data for numerical model calibration.

An extended set of laboratory experiments and modelling tasks complete the two experiments of the GTS to validate the selection of materials and evaluate the scaling potential of this type of experiments.

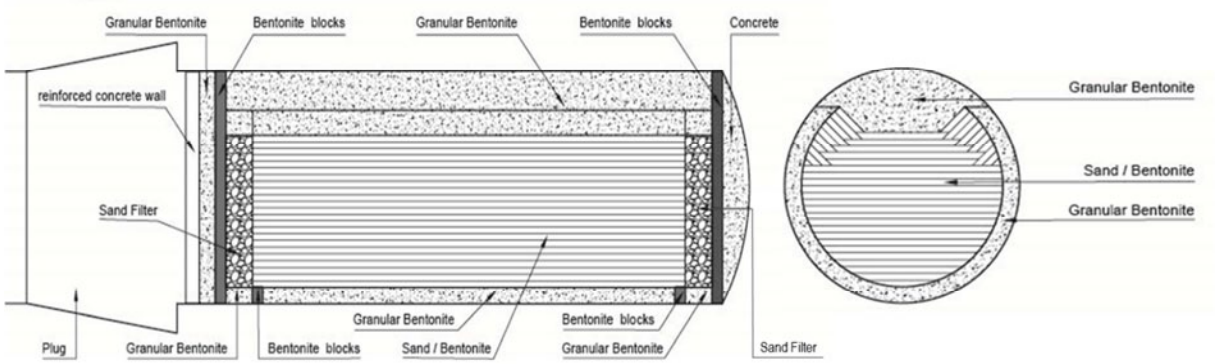


Figure 1. Transversal and cross section of the GAST experiment.

The visualisation of gas pathways in clay-rich materials; initial results from the Fracture Visualisation Rig.

***Andrew Wiseall*, Robert Cuss, Caroline Graham, Jon Harrington**

Corresponding author e-mail: andyw@bgs.ac.uk

British Geological Survey, Keyworth, Nottingham, NG12 5GG

The visualisation of flow pathways, be they for water and/or gas, in clay-rich low permeability materials is a considerably challenging aspect of experimentation. The current state of knowledge and understanding is based upon non-invasive observations during laboratory and field experiments. Recent technological advances have meant that this knowledge base has increased; techniques such as x-ray Computed Tomography (CT) scanning and synchrotron x-ray imaging have the potential to identify localised flow pathways in low-permeability materials. These techniques along with the experimental work have led to the current understanding of how gas and water flow through clay-rich materials. However, the dimensions of the flow pathways and the necessity to perform experiments at *in situ* stresses within steel pressure vessels means that x-ray based imaging has limitations.

As technology and experimental techniques have developed the theories of how gas and water flow through clay-rich materials have improved. Several theories for the flow of gas and water through clay-rich low permeability materials have been proposed. The current understanding is that flow occurs via localised dilatant pathways within the material (e.g. Cuss *et al*., 2014).

Several methodologies have been established at the British Geological Survey which have been used to visualise flow pathways. These methods include the use of fluorescein stained water (Cuss *et al*., 2011), radiologically tagged gas and nano-particles (Harrington *et al*., 2012) that are transported by gas into the clay and subsequently imaged. These methods have gone to further support the theory that flow occurs in localised dilatant pathways. The disadvantages of these methods, however, are that the pathways cannot be observed *in-situ* or in real time, as the analysis can only occur post-test; this also risks damage to the sample material in preparation for imaging.

These factors have resulted in the development of a new apparatus with the aim of being able to visualise flow pathways in real time under a normal load. A thin clay paste is confined between two large steel platens, with a thick fused-silica glass plate embedded into the top platen, which acts as a viewing window. A normal load of up to 3 MPa can be applied through 12 torqued bolts. Gas or water can be injected into the central base of the clay paste by means of a high precision ISCO/Teledyne syringe pump, allowing full control and monitoring of pore pressure. A Nikon DSLR camera captured images every three-seconds, with images combined to create a time-lapse video of each test. This enables imaging in real-time of pathway development and propagation in clay rich materials.

Early tests have been carried out on fully saturated kaolinite paste, injecting either helium or water. Figure 1 shows the development of a network of pathways throughout the course of a test on kaolinite paste. The first image can be said to be the time at which gas entry first occurred, after this the pathways developed from those initial entry points. It can be seen that some pathways develop preferentially compared to others.

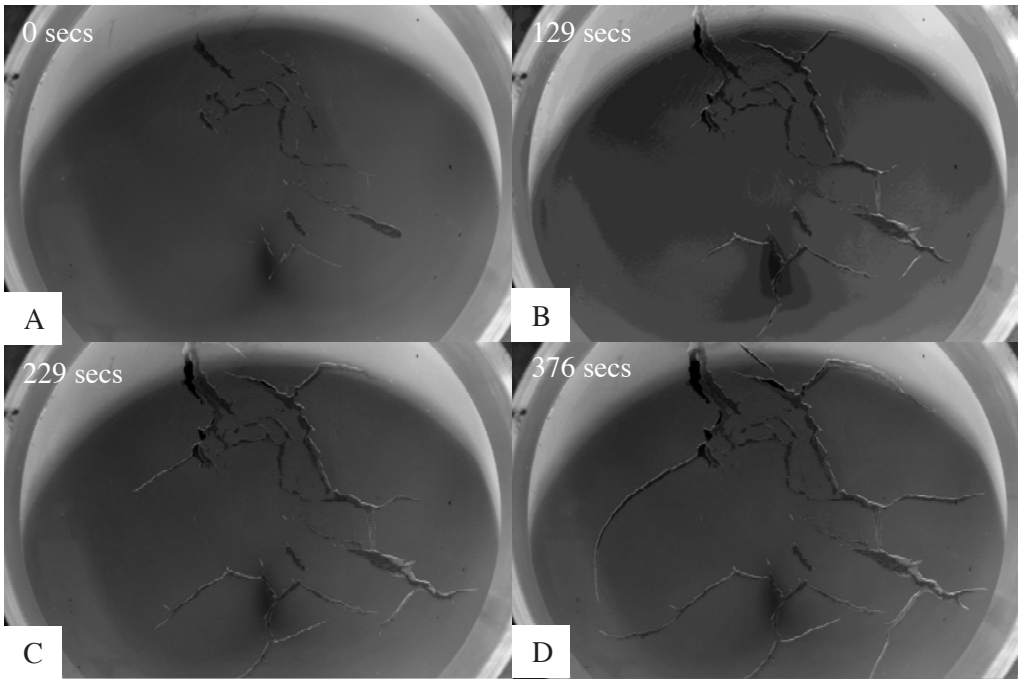


Figure 1: Images showing development of gas pathways through a kaolinite clay paste. (a) Initial gas entry into paste, (b) pathways begin to development, (c) further development shows preferential pathways beginning to form, (d) complex flow pathway network with large and small pathways

Testing has shown de-watering occurred along the flow pathways. This occurred as compaction took place in the paste surrounding the dilating flow pathways, resulting in water expulsion; this supports the theory of dilatant flow pathways migration. Furthermore, testing has showed that once pathways reach the edge of the apparatus a preferential pathway formed; this can be likened to the gas breakthrough pressure for the material. Once breakthrough occurred a reduction in gas pressure within the pathway resulted in the closure and self-sealing of some features.

The combination of flowpath visualisation with other imaging techniques mentioned above, such as nano particle injection, have greatly increased our understanding of the hydro-mechanical controls on gas and water flow through clay-rich materials.

Cuss, R.J., Milodowski, A., and Harrington, J.F. (2011) Fracture transmissivity as a function of normal and shear stress: first results in Opalinus clay. Physics and Chemistry of the Earth. 36, pp.1960-1971.

Cuss, R.J., Harrington, J., Giot, R., and Auvray, C. (2014) Experimental observations of mechanical dilation at the onset of gas flow in Callovo-Oxfordian claystone. Clays in Natural and Engineered Barriers for Radioactive Waste Confinement. 400: Geological Society Special Publications: London, United Kingdom, Geological Society of London

Harrington, J.F., Milodowski, A.E., Graham, C.C., Rushton, J.C., and Cuss, R.J. (2012) Evidence for gas-induced pathways in clay using a nanoparticle injection technique. Mineralogical Magazine. December 2012, Vol. 76(8), pp.3327-3336.

Evaluation of gas transport phenomena in support of the Full-Scale Emplacement Experiment at the Mont Terri URL

A. Pappafotiou[1], *R. Senger[1]*, P. Marschall[2], B. Garitte[2], H. R. Müller[2]

[1]INTERA Incorporated, Swiss Branch, CH-5408 Ennetbaden, Switzerland, (rsenger@intera.com)
[2] NAGRA, CH-5430 Wettingen, Switzerland (Paul.Marschall@nagra.ch)

The Full-Scale Emplacement (FE) experiment at the Mont Terri underground research laboratory (URL) involves the excavation of a 50 m long tunnel section, emplacement and backfilling of replicated spent fuel (SF) canisters, and heating of these canisters according to the expected heat generation rate from radioactive decay of the SF. For this purpose three canisters with heater elements will be emplaced on bentonite blocks in the tunnel and backfilled with granular bentonite according to Nagra's high-level waste emplacement concept. The tunnel will be closed by a concrete plug and heated for 20 years. The evolution of important state parameters of the disposal system such as temperature, pore-water pressure, water saturation, and stress and strain are being monitored. For details about the general set-up, the experimental aims, and the different working steps see Müller et al. (2015) in this compendium.

Following the emplacement of the canisters in the bentonite buffer material complex THM-C conditions develop. Associated with it gas transport phenomena will take place due to the corrosion of the waste canister and liner reinforcement and consumption of oxygen (O_2) and generation of hydrogen (H_2) gas. In the sealed emplacement tunnel, corrosion occurs under aerobic conditions until the oxygen in the air in the partially saturated pore space of the bentonite buffer is consumed, which is followed then by anaerobic corrosion. Aerobic corrosion typically occurs at a significantly higher rate than anaerobic corrosion. Aerobic conditions can be extended by diffusive transport of oxygen from the operations/access tunnel system through the cavern seal. When the oxygen is consumed and corrosion continues under anaerobic conditions, hydrogen is produced which slowly increases the pressure in the bentonite backfill creating a pressure gradient for gas flow from the emplacement tunnel through the tunnel seal to the operations tunnel. In addition to corrosion, other O_2 consumption processes may occur associated with mineral or microbial reactions in the bentonite or in the surrounding Opalinus Clay. The relevant gas transport phenomena are schematically summarized in Figure 1.

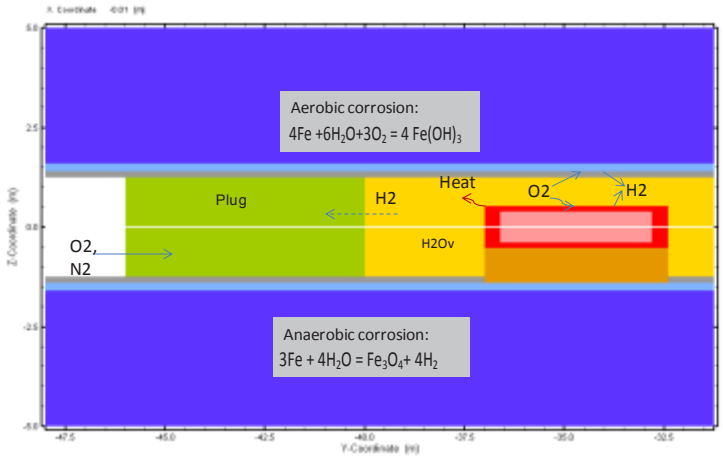


Figure 1: Transport/consumption phenomena from corrosion

Scoping calculations of the relevant TH phenomena in the FE experiment are performed with focus on the gas transport phenomena associated with corrosion and consumption of O_2 and H_2O and generation of H2 gas. The modeling of the different phases of the FE experiment include (a) the excavation and the consequent ventilation of the tunnel, (b) the emplacement of the canisters (heater) and buffer material and (c) a subsequent heating phase.

The transport of the different gas components was simulated with the TMVOC code (Pruess and Batistelli, 2003) which can account for multiple non-condensable gases (NCGs). For this particular study, the H_2 gas component had to be added to the list of NCGs in the TMVOC code, in terms of

specifying the corresponding thermodynamic laws. In addition, the consumption of specific components (i.e., H_2O and O_2) had to be implemented in the code. The geometric configuration of the FE tunnel and different components were implemented in a 3D integrated finite difference (IFD) mesh (Fig. 2)

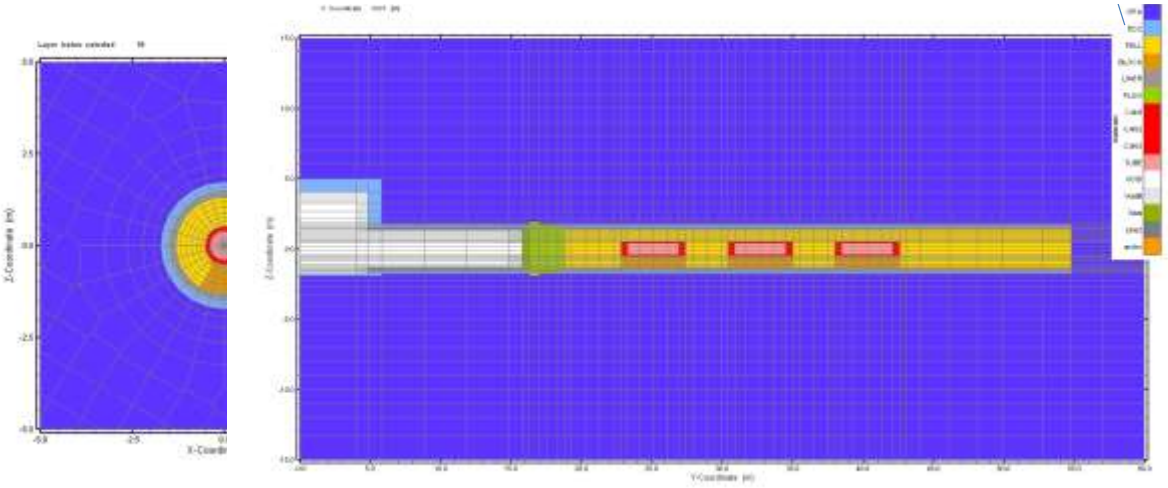


Figure 2: XZ- and YZ cross-sections of the FE tunnel with the different materials.

The results of the gas transport simulations show that aerobic corrosion and associated O_2 consumption can significantly reduce the O_2 concentration in the tunnel backfill provided diffusive transport of O2 is reduced through the plug, either having high water saturation in the plug or using a "seal" on the plug with reduced diffusivity (Fig. 3). Under these conditions, anaerobic conditions occur within several months, leading to anaerobic corrosion and associated H_2 generation. However, the accumulation of H_2 is relatively small and does not produce a noticeable pressure increase in the buffer over the projected 10-15 year duration of the FE experiment. At the same time, the water saturation in the plug will decrease due to drying from ventilation of the access tunnel and diffusive transport of O_2 through the plug will increase (in case of no explicit seal on the plug) and O_2 concentration in the buffer would increase.

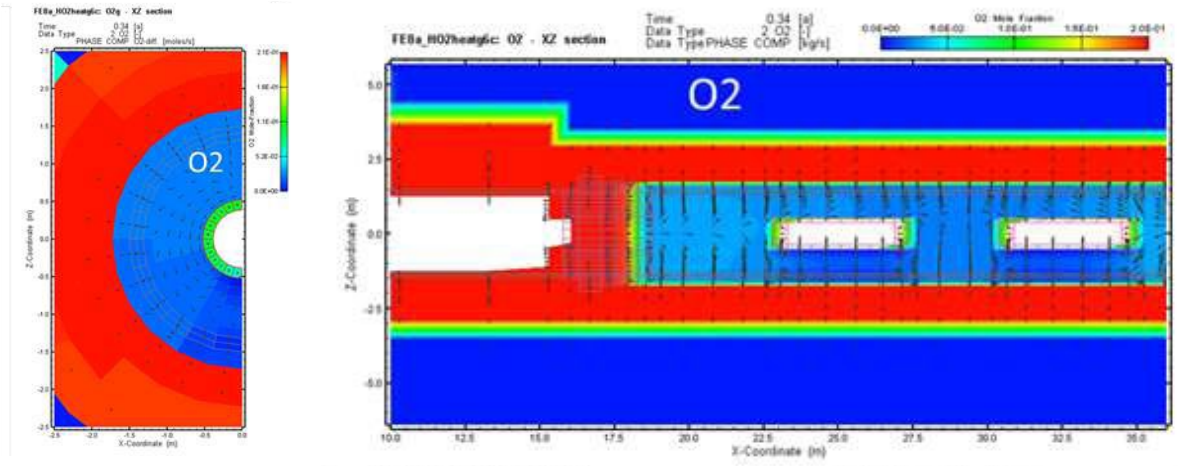


Figure 3: Simulated O_2 concentrations after 0.33 yrs for orientation perpendicular (left) and parallel to tunnel axis (right).

Pruess, K. and Battistelli, A., 2002, TMVOC, A Numerical Simulator for Three-Phase Non-isothermal Flows of Multicomponent Hydrocarbon Mixtures in Saturated-Unsaturated Heterogeneous Media. Lawrence Berkeley National Laboratory, Report LBNL-49375, Berkeley, CA, U.S.A.

Müller, H.R., Vogt, T., Garitte, B., Köhler, S., Sakaki, T., Weber, H.P., Vietor, T. (2015): The Full-Scale Emplacement Experiment – Implementation of a multiple heater experiment at the Mont Terri URL. Abstract, Clay Conference Brussels 2015.

The gas permeability and self-healing ability of Czech Ca-Mg bentonite

Jan Smutek, **Lucie Hausmannova, Jiri Svoboda**

Czech Technical University in Prague, Faculty of Civil Engineering, Centre of Experimental Geotechnics, Thakurova 7, Prague, Czech Republic; jan.smutek@fsv.cvut.cz

The gas permeability and self-healing ability of Czech bentonites is being investigated in the context of a research project being conducted for the Czech Science Foundation (GA14-19655S). The aim of the project is to determine the key characteristics of the migration of gases through clays in connection with the safety of landfill sites and the disposal of radioactive waste.
The primary objective is to study the gas breakthrough pressures of saturated bentonite samples in comparison with both the material's dry density and hydraulic conductivity following saturation. It is intended that repeated gas injection and re-saturation cycles will serve for the investigation of the self-healing ability of bentonite. One of the secondary objectives of the project is to study the gas permeability of unsaturated samples (with original moisture content values).
It is planned that three different types of bentonite will be used in the research. B75 bentonite, a Czech calcium-magnesium bentonite with a montmorillonite content of between 65 and 80%, was chosen for the pilot phase. This low-activated bentonite is produced by the Keramost a.s. company in powder form. All the various material characteristics investigated will be dependent on the material's dry density; therefore, samples of several different dry density values will always be tested. In addition, so as to allow the study of the influence of sample geometry, different sample heights (between 5 and 20mm) will be employed. Inhomogeneous samples will also be tested in the later phases of the project.
The testing procedure involves the powder material, with an initial moisture content of around 5%, being compacted into a special steel cylindrical cell 30mm in diameter which can be connected either to a water permeameter or gas injection system. The samples are unable to expand (zero volumetric change). The water permeameters are used for the saturation of the material and the subsequent measurement of hydraulic conductivity and swelling pressure in each cycle/stage. The gas properties of each sample are investigated in several stages employing two types of injection system both of which use compressed air as the injection medium.
The first sample testing stage includes the performance of gas injection tests on unsaturated samples using a mobile measuring station. The testing procedure consists of an ascending cycle of step-by-step increases in gas pressure followed by a corresponding descending cycle. The lowest testing pressure level is 5bar and the maximum pressure is dependent on and limited by a maximum applied gas flow rate of 5Nl/min (normal litres per minute). Varying injection pressures and flow rates enable the study of the dependence of calculated gas conductivity on injection pressure. Once these tests have been completed, the sample is saturated by means of the water permeameter.
The later stages consist of the performance of the gas breakthrough test and re-saturation in cycles. The aim of the breakthrough test is to create a preferential path by means of a gas fracturing mechanism and then to verify whether subsequent re-saturation fully heals the sample. Each cycle is accompanied by the measurement of hydraulic conductivity during the (re-)saturation phase. One cycle typically lasts several weeks.
Breakthrough testing involves two types of test, the first of which employs a step-by-step increase in the injection gas pressure by 5 or 10 bar every 15 minutes up to a maximum pressure level of 12MPa which is then maintained until gas breakthrough is achieved. The second type of test consists of the constant load test wherein the saturated sample is loaded directly by a constant level of gas pressure slightly exceeding its swelling pressure; the time required to attain breakthrough is then recorded.
Results to date of tests on unsaturated samples revealed that no rapid changes in gas conductivity values occurred as the result of the application of different injection pressures (Fig. 1). However, the dependence of gas conductivity on injection pressure exhibits a slightly decreasing trend. Registered flow rates ranged from tenths of normal litres per minute (Nl/min) up to 5 Nl/min. Maximum achieved pressures for maximum applied flow rates ranged from 1MPa (1250Kg/m3) to 4MPa (1600Kg/m3).

Interestingly, much lower changes in permeability according to dry density were detected compared to the results of the testing of FEBEX bentonite with similar dry densities (Villar et al, 2012). An increase in density from 1200 to 1600kg /m3 causes a decrease in permeability by a mere two orders of magnitude as opposed to the four orders of magnitude detected in experiments on FEBEX bentonite (Villar et al, 2012) in which, admittedly, significantly lower injection pressures were applied (up to 8 bar).
Initial tests on the saturated samples revealed that no breakthrough occurred during the step-by-step increase-in-pressure phase of the gas breakthrough test (which lasts 3 or 6 hours). Results to date indicate that gas breakthrough is achieved no earlier than after several days of sample loading with gas pressure even if the gas pressure exceeds several times swelling pressure.

References:
VILLAR, M.V., V. GUTIÉRREZ-RODRIGO, P.L. MARTÍN and J.M. BARCALA. *Results of the tests on bentonite (Part 2)*. CIEMAT Technical Report CIEMAT/DMA/2G207/07/12 (FORGE Report D3.27). 2012

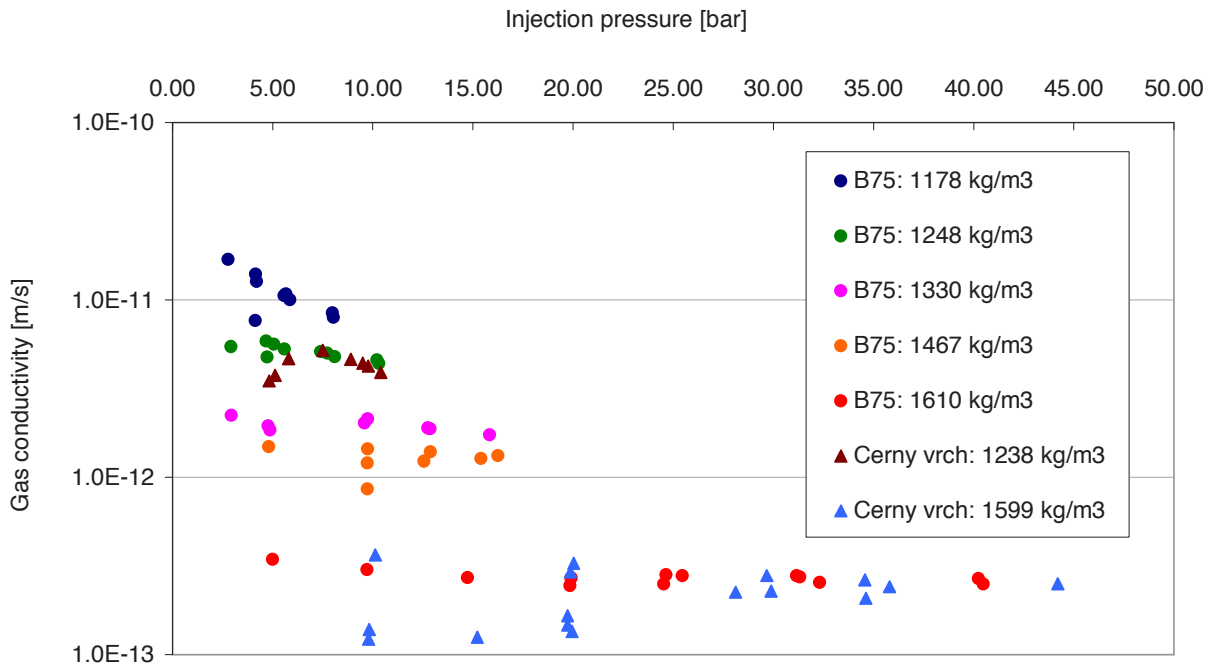


Fig. 1 - Results of gas tests on unsaturated samples

Scoping calculations of hydrogen generation, transport and consumption in bentonite and Opalinus clay

A. Idiart[1], G. Román Ross[1], O. Silva[1], F. Grandia[1], *L. Duro*[1], M. Sentís[2]

Amphos 21 Consulting S.L., Passeig Garcia I Faria, 49-51, 1st floor, 08019, Barcelona, Spain (lara.duro@amphos21.com)
Swiss Federal Nuclear Safety Inspectorate ENSI, Industriestrasse 19 CH-5200 Brugg, Switzerland

In the Swiss concept for a deep geological disposal facility of high level radioactive waste, the assessment of the effects of hydrogen gas generation due to the steel corrosion process depends not only on the gas generation rates for each type of waste and the detailed repository design, but also on the hydrogen (dissolved and gas) transport properties and consumption rates of the bentonite barrier and surrounding clay rock. The anaerobic corrosion of Fe-containing material is considered to be the major contributor of repository gases and leads to considerable amounts of hydrogen. The generation, accumulation and release of gases from the disposal facility may significantly influence the long-term radiological safety of the repository via a number of processes (Nuclear Energy Agency, 2001).

As anoxic corrosion proceeds, H_2 will be generated and dissolved hydrogen will diffuse out through the porewater of the bentonite barrier towards the Opalinus clay formation at a rate that is given by the effective diffusion coefficient of each porous domain. As long as the dissolved hydrogen concentration remains below the solubility limit at a given pressure and temperature, no free gas phase will form. The competition between the generation of dissolved H_2 from the corrosion process and the escape of dissolved H_2 via a diffusive flux in the bentonite porewater will determine when a free gas phase will form. As corrosion proceeds hydrogen will keep accumulating as a free gas phase, which will cause a gas pressure build-up near the canister surface. These elevated pressures may affect the safety of the repository by e.g. creating preferential pathways for radionuclides to escape.

The bentonite porewater will gradually be consumed by the corrosion reactions. If water supply by the surrounding porous medium were not fast enough, the availability of water for corrosion would be compromised and therefore the corrosion rate itself could be limited by the water flow towards the canister. Part of the hydrogen might in turn be consumed within the bentonite and the Opalinus clay formation as a result of chemical reactions such as microbial activity, mineral transformation (reduction of pyrite and sulphate), and adsorption on the existing clays.

The present work focuses on the above mentioned processes (hydrogen generation, consumption, diffusion, and water availability) under initially fully water saturated conditions, i.e. before a free gas phase is formed. The results of a set of scoping simulations aimed at estimating the effect of chemical reactions such as pyrite to pyrrhotite reduction, H_2 adsorption onto bentonite and H_2 consumption by microbial activity on the reactive transport of dissolved hydrogen in the bentonite and Opalinus clay are presented. The scoping calculations are based on a 1D reactive transport model with a setup that corresponds to the Swiss concept for a deep geological repository. In addition, the time needed to form a free gas phase due to the competition of the corrosion rate and the diffusive flux of hydrogen has been estimated taking into account the effect of different temperatures. Finally, the availability of water for the corrosion reaction before a free hydrogen gas phase is formed has also been assessed.

From the results obtained for a series of sensitivity cases, the relevance of chemical reactions in hydrogen consumption has been evaluated assuming the most likely evolution of the physico-chemical conditions over time.

The simulations of the dissolved gas diffusion indicate that the time needed to form a free gas phase in the present setup is roughly proportional to $(1/r_c^2)$, where r_c is the corrosion rate (μm/year). With regard to the availability of water, it is shown that the consumption of water by the corrosion process does not induce a decrease of the liquid degree of saturation in the bentonite porewater, at least before

a free hydrogen gas phase is formed. Instead, only a decrease of the pore pressure is observed initially around the steel canister.

References

Nuclear Energy Agency, 2001. Gas generation and migration in radiactive waste disposal: safety relevant issues. Organisation for Economic Cooperation and Development, 192 pp.

Anisotropic diffusion of dissolved gases in Boom Clay

E. Jacops [1,2,3], N. Maes [1], A. Grade [1], J. Govaerts [1], E. Weetjens [1]

[1] SCK•CEN Institute for Environment, Health and Safety, Boeretang 200, 2400 Mol, Belgium
[2] KU Leuven, Earth and Environmental Sciences, Celestijnenlaan 200E, 3001 Heverlee, Belgium
[3] Institute of Geology and Geochemistry of Petroleum and Coal, RWTH Aachen University, Lochnerstr. 4-20, 52056 Aachen, Germany

Boom Clay has been studied since 1974 as a potential host formation for the disposal of high and intermediate level long-lived radioactive waste in Belgium. In a geological repository system, gas generation is unavoidable. To evaluate its impact, it is important to make a correct evaluation of the balance between gas generation and gas dissipation processes. Gas dissolution in pore water and transport of dissolved gas is one of the possible dissipation mechanisms. As solute transport through Boom Clay is dominated by diffusion, reliable diffusion coefficients for dissolved gases are therefore essential. In addition to providing values of parameters to be used in transport models, diffusion experiments can also be used to characterize some microstructural properties of the porous material like the tortuosity of the pore network and the anisotropy of its connectivity. Up to now these parameters have been derived mainly from diffusion experiments with non-sorbing tracers such as iodide (I^-) and HTO. By measuring the diffusion coefficient for a suite of gases (He, Ne, H_2, Ar, CH_4, Xe, C_2H_6) a larger dataset becomes available to evaluate these microstructural properties. Moreover, as these gasses all have a different size, such measurements will potentially allow for more insight into the diffusive process and the porous microstructure. Since the proposed technique does not disturb the sample, it creates also a major advantage compared to destructive techniques (for instance MIP, FIB-SEM,…) used for microstructural characterisation.

Jacops et al. (2013) described a new method to measure diffusion coefficients of dissolved gases in porous rocks. The diffusion coefficients of a suite of (dissolved) gases (He, Ne, H_2, Ar, CH_4, Xe, C_2H_6) are measured on two Boom Clay samples (originating from the Mol-1 borehole). In the test with sample 84b the sample is oriented so that diffusion occurs in the direction perpendicular to the bedding planes, and in the test with sample 127b, diffusion occurs in the direction parallel to the bedding planes. In order to compare the diffusion of the dissolved gases to the diffusion of water in the samples, experiments with HTO are performed.

Table 1: diffusion characteristics in pure water and results obtained for diffusion through Boom Clay

Gas	Kin ø (1) (10^{-10}m)	D_0 (2) (10^{-9} m²/s)	Sample 84b ⊥ D_{eff} (10^{-11} m²/s)	Sample 127b // D_{eff} (10^{-11} m²/s)	Sample 84b τ^2 (3)	Sample 127b τ^2	Anisotropy ratio (4)
He	2.58	7.28	43.7	71.8	6.17	3.75	1.64
Ne	2.79	4.03	18.9	23.4	7.90	6.38	1.24
H_2	2.97	5.11	/	55.1	/	3.43	/
Ar	3.42	2.44	7.47	15.3	12.08	5.91	2.04
CH_4	3.82	1.84	8.29	14.2	8.21	4.78	1.72
Xe	4.06	1.47	5.96	7.22	9.13	7.54	1.21
C_2H_6	4.42	1.38	4.55	6.14	11.22	8.31	1.35
HTO	2.75	2.44	12.0	/	7.53	/	/

[1] (Hirschfelder et al., 1964)
[2] (Boudreau, 1996)
[3] $\tau^2 = D_0 / D_{eff} * \eta$ with η the diffusion accessible porosity (set at 0.37 for Boom Clay)
[4] Anisotropy ratio = D_{eff} sample 127b / D_{eff} sample 84b

For both samples, an exponential relationship can be found between the kinetic diameter of the gas and the effective diffusion coefficient D_{eff} (Fig.1 left). The relationship for sample 84b is given by $D_{eff} = 4.93\ 10^{-9}\ e^{-1.09x}$ m^2/s and for sample 127b $D_{eff} = 1.40\ 10^{-8}\ e^{-1.25x}$ m^2/s with the kinetic diameter x in 10^{-10} m. For D_0 (diffusion coefficient of gas in free water), a similar relation is found $D_0 = 6.23\ 10^{-8}\ e^{-0.90x}$ m^2/s.

When plotting the tortuosity value as function of the gas kinetic diameter (Fig. 1 right) an increasing trend is observed but with quite some scatter. This indicates that the larger the molecule, the less access it has to the smaller pores. Thus larger gas molecules have access to a smaller interconnected pore network and are more affected in their movement. We can conclude that tortuosity values for diffusing gas molecules are function of the molecular size of the gas.

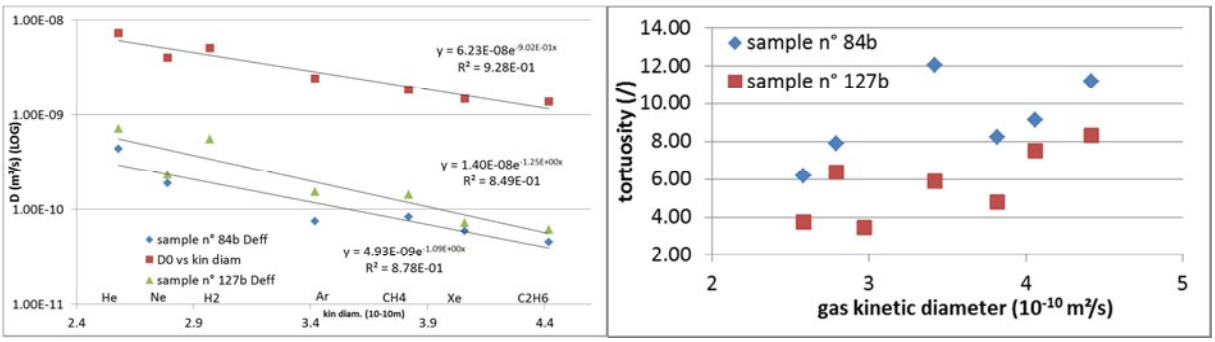


Figure 1: Left: relation between D_{eff} and D_0 and kinetic diameter. Right: gas kinetic diameter vs. tortuosity for both samples.

It is generally observed in Boom Clay that solute diffusion rates are higher in the direction parallel to the bedding plane compared to the direction perpendicular to the bedding plane, due to the layered structure of clay. This is confirmed by the results shown in Table 1: D_{eff} values measured in sample 127b are higher than those measured in sample 84b and consequently, the tortuosity values for sample 127b are lower. Anisotropy ratios for the gases studied vary between 1.2 and 2.0 with an average anisotropy ratio of 1.5. One might expect that larger molecules would benefit more from the advantageous orientation of sample 127b, leading to a higher anisotropy ratio for higher kinetic diameter but the data suggest no relation between the anisotropy ratio and the kinetic diameter. The gas anisotropy values are lower than the available anisotropy ratios reported for HTO (2 – 3) and Iodide (2.7) (Bruggeman et al., 2010).

Boudreau, B., 1996. The diffusive tortuosity of fine-grained unlithified sediments. Geochimica Et Cosmochimica Acta, 60(16): 3139-3142.
Bruggeman, C., Aertsens, M., Maes, N., Salah, S., 2010. Iodine retention and migration behaviour in Boom Clay – Topical report, First Full Draft. SCK-CEN ER-119, Mol, Belgium.
Hirschfelder, J., Curtiss, C., Bird, R., 1964. Molecular Theory of Gases and Liquids Nueva York, EUA : Wiley.
Jacops, E., Volckaert, G., Maes, N., Weetjens, E., Govaerts, J., 2013. Determination of gas diffusion coefficients in saturated porous media: He and CH4 diffusion in Boom Clay. Applied Clay Science, 83-84(0): 217-223.

Measuring the diffusion coefficient of helium in clay formations envisaged for geological disposal of radioactive waste (Boom Clay, Opalinus Clay and Callovo-Oxfordian Clay)

Arno Grade, **Elke Jacops, Norbert Maes, Joan Govaerts**

SCK•CEN, Institute for Environment, Health and Safety, Boeretang 200, B-2400 Mol, Belgium

Boom Clay, Opalinus Clay and Callovo-Oxfordian Clay are studied as potential host formations for the deep geological disposal of long-lived, radioactive waste respectively in Belgium, Switzerland and France. Knowledge of the diffusion coefficient of helium dissolved in the pore water is important for performance assessment for two reasons.

Firstly, diffusion coefficients are used to determine the dissipation rate of gases generated in situ by anaerobic corrosion of the waste and packaging, microbial degradation of organic material present in the host rock and radiolysis. These gases, of which hydrogen is the most important, dissolve in the pore water and are transported away from the repository by diffusion as dissolved species. However, if the gas generation rate is larger than the diffusive flux, a free gas phase is formed and gas flow may occur. Helium is often used as a proxy for hydrogen to avoid experimental difficulties like methanogenesis and explosion hazards.

Secondly, diffusion coefficients are used in natural tracer profile studies. Interpretation of natural tracer profiles provides information on transport processes in host rocks on a large spatial and temporal scale. Helium is one such natural tracer and accurate He transport parameters obtained on small scale samples help with a more trustworthy interpretation of these profiles.

At the moment, data for helium diffusion coefficients in these three host formations in literature are scarce and have varying degrees of uncertainty, as is shown in Table 1.

Table 1: Results summary of He diffusion experiments on Boom, Opalinus and Callovo-Oxfordian Clay (COx) found in literature as described in (Jacops et al., 2013)

	Reference	Measured D^* (m^2/s)	Remark
Boom Clay	Volckaert et al., 1994	n/a	Only H_2
Opalinus Clay	Gómez-Hernández, 2000	$D_{eff} = 2.1*10^{-10}$	estimated porosity of 30%
Opalinus Clay	Rübel, et al., 2002	$D_p = 3.5*10^{-11}$	overly simplified model
COx	Bigler et al., 2005	$D_p = 2.4*10^{-10}$	Large uncertainty ($0.8\text{-}7.2*10^{-10}$ m^2/s)
COx	Rebour et al., 1997	$D_p = 5\pm1*10^{-11}$	

* The effective (D_{eff}) and pore (D_p) diffusion coefficients are proportional to the diffusion coefficient in pure water (D_0), following the relationship $D_{eff} = \varepsilon D_p = \varepsilon D_0 \delta/\tau^2$, with ε the porosity and δ/τ^2 a geometry factor specific to the clay.

In order to obtain reliable diffusion coefficients of dissolved gases, a new cross-through diffusion experiment was designed at SCK•CEN as described by (Jacops et al., 2013). A clay core is embedded in a stainless steel diffusion cell, which is connected at both sides to a vessel filled with water and gas at equal pressure to avoid advective transport. Due to a concentration gradient the dissolved gas

diffuses through the clay core. The diffusive flux is quantified by analyzing the gas phase composition on the opposite side of the clay by gas chromatography.
Fick's law of diffusion is solved numerically in COMSOL Multiphysics. A least squares fit of the outlet concentration versus the experimental data allows to determine the effective diffusion coefficient D_{eff}.

In the framework of the research programmes on geological disposal, carried out by ONDRAF/NIRAS and ANDRA, diffusion experiments on respectively Boom Clay and Callovo-Oxfordian clay are performed at SCK•CEN. For the Swiss research programme on "Natural Tracers", a helium diffusion experiment was performed in cooperation with the Institute of Geological Sciences in Bern on an Opalinus Clay sample. Diffusion was measured in the direction perpendicular to the bedding plane.

Table 2: Results overview of helium diffusion experiments on Boom, Opalinus and Callovo-Oxfordian Clay (The experiment on COx is currently ongoing.)

Clay	Origin	K (m/s)	ε (%)	D_{eff} (m^2/s)	2σ(%)
Boom	Mol (B)	$3.3*10^{-12}$	37	$4.5*10^{-10}$	5
Opalinus	Schlattingen (CH)	$1.8*10^{-13}$	9.6	$5.2*10^{-11}$	4
COx	Bure (F)	$2.6*10^{-13}$	TBD	TBD	TBD

The parameters as shown in Table 2 were determined with high precision and can now be used for their respective goals: gas perturbation studies and modeling of natural tracer profiles.

SCK•CEN would like to thank ONDRAF/NIRAS, the Institute of Geological Sciences in Bern and ANDRA for providing the clay samples and for their intellectual and financial contributions to these projects.

Bigler, T., Ilhy, B., Lehmann, B., Waber, H., 2005. Helium Production and Transport in the Low-Permeability Callovo-Oxfordian Shale at the Site Meuse/Haute Marne, France, Helium Production and Transport in the Low-Permeability Callovo-Oxfordian Shale at the Site Meuse/Haute Marne, France. NAGRA, Wettingen.

Gómez-Hernández, J. J. (2000). Mont Terri Project Technical Note 2000-40. Valencia, Spain: Technical University of Valencia.

Jacops, E., Volckaert, G., Maes, N., Weetjens, E., Govaerts, J., 2013. Determination of gas diffusion coefficients in saturated porous media: He and CH4 diffusion in Boom Clay. Applied Clay Science, 83-84(0): 217-223.

Rebour, V., Billiotte, J., Deveughele, M., Jambon, A., le Guen, C., 1997. Molecular diffusion in water-saturated rocks: A new experimental method. Journal of Contaminant Hydrology, 28: 71-93.

Rübel, A. P., Sonntag, C., Lippmann, J., Pearson, F., & Gautschi, A. (2002). Solute transport in formations of very low permeability: Profiles of stable isotope and dissolved noble gas contents of pore water in the Opalinus Clay, Mont Terri, Switzerland. Geochimica et Cosmochimica Acta, 66(8), 1311-1321.

Volckaert, G. et al., 1994. MEGAS Modelling and experiments on gas migration in repository host rocks. Final Report Phase 1. EUR16235, Luxembourg.

Investigating the consequences of uncertainties on gas generation and dissipation for the design and performance of a repository

Yu Li [a], **Weetjens Eef** [a], **Manuel Capouet** [b] **and Xavier Sillen**[b]

[a] Belgian Nuclear Research Centre (SCK•CEN), Boeretang 200, 2400 Mol, Belgium
[b] Belgian Agency for Radioactive Waste and Enriched Fissile Materials (ONDRAF/NIRAS), Avenue des Arts 14, 1210 Brussels, Belgium

In a deep geological repository for radioactive waste, formation of gas – whether by anaerobic metal corrosion, (bio-)chemical degradation of wastes or radiolysis – might be unavoidable. In a disposal system saturated with groundwater or close to saturation, (part of) the gas will be evacuated by dissolution and diffusion. If the amount of gas generated exceeds the removal capacity by diffusion as a dissolved species, a pressurized gas phase is formed. Laboratory and in situ experiments have shown that pressurized gas transport in Boom Clay samples occurs via discrete pathways (Volckaert et al, 1997; Harrington et al, 2012). As this transport mode is associated with the dilation of pathways through the porous media and may lead to the reactivation excavation-induced fractures or the development of new fractures in the damaged zone around the repository, it may affect the properties of the geological barrier.

Exploratory calculations have been carried out to evaluate whether the diffusive removal capacity of gas through Boom Clay would be sufficient or not to evacuate the gas generated by different waste classes and engineered barrier system (EBS) materials. Four categories of waste have been considered, together with their corresponding EBS configurations: vitrified high-level waste (VHLW), spent fuel (SF), bituminized waste (Eurobitum), and compacted waste (CSD-C) which includes the compacted claddings and structural elements of the fuel assemblies.

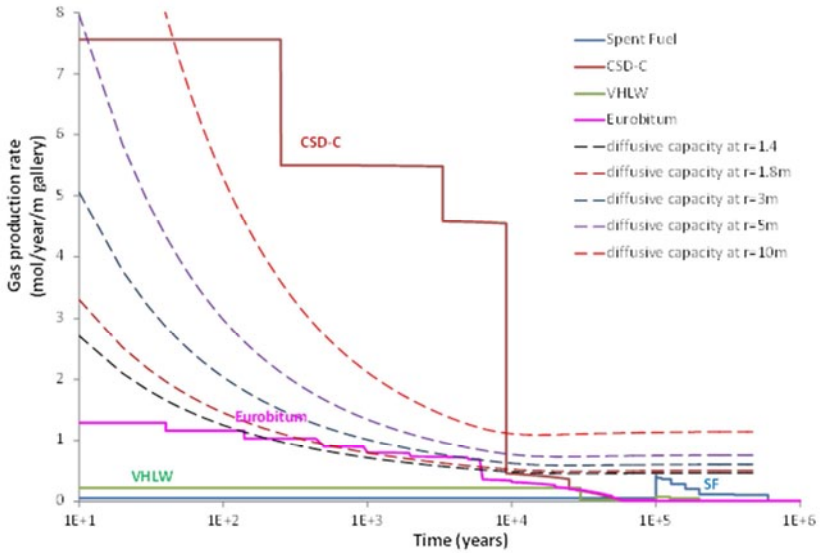


Fig. 1: Comparisons between gas production from four types of waste (conservative estimates) and potential gas dissipation rate by dissolution and diffusion through Boom Clay porewater at increasing radii from the axis of a disposal gallery.

Fig. 1 compares the gas production rate of the different types of waste considering the current reference engineered barrier design based on cement with the potential capacity for diffusive removal through the host rock (Yu and Weetjens, 2012). Key assumptions are:

- the gas generation source term considers only the hydrogen production from the corrosion of the metals contained in the waste and used for their packaging (other sources are negligible except in the case of Eurobitum);

- the gas production rate is based on the maximum values of metal corrosion in highly alkaline environment, although some corrosion rates are known to decrease with time because of passivation;
- each potential removal capacity shown in the picture is calculated assuming that the concentration of hydrogen is kept equal to its solubility under repository condition at the given radial distance from the gallery axis; this capacity progressively decreases with time because as the dissolved gas diffuses and accumulates into the host formation, the concentration gradient decreases.

Results show that diffusive removal is expected to be sufficient to evacuate all the gas produced in VHLW and SF disposal galleries, while the occurrence of a pressurized gas phase in the repository cannot be ruled out for Eurobitum and CSD-C. The uncertainty on gas diffusive rates is relatively small. Uncertainties on corrosion rates could be reduced by further R&D but demonstrating very low rates can be difficult. Progress in the characterisation of the propagation of a gas phase through Boom Clay might allow to better estimate its impact in terms of actual effects on the properties of the geological barrier, but given the complexity of some of the processes and features involved, such as damage propagation and pathways instability, this endeavour may face irreducible uncertainties.

Alternative design strategies are another way to tackle phenomenological uncertainties. In this study, sensitivity analyses have been carried out to investigate possible adaptations of the EBS. The aim is to organise the storage of the excessive amount of gas produced and its subsequent removal. Indeed, next to the reduction of the metal amount in the waste and packaging, enlarging the pore volume of the concrete backfill in the gallery to supply sufficient space for temporary gas storage might be an adequate design measure. Moreover, should the backfill have a sufficiently low gas entry value and a high enough hydraulic conductivity, gas flow could occur preferentially along the engineered barriers (essentially the backfill) and the shaft under moderate pressure. The dimension of the backfill required for an adequate hydrogen storage were estimated considering two cases in the calculations:

- Case 1 – It is conservatively assumed that the galleries are fully saturated at all time. It follows that the volume of water displaced due to the pressurisation exactly equals the volume of excess gas produced. This should be regarded as a limiting case.
- Case 2 – It is assumed that after part of the pore water initially available in the backfill is displaced by gas, a continuous gas passage in the gallery is formed which allows for the remaining excessive gas to flow.

The implications of each case in terms of repository design parameters and overall repository performance have been evaluated and will be discussed.

References

Davy, C., Skoczylas, F., Willemetz, M.-C. (2011) Experimental characterization of mechanical performance, water retention and gas relative permeability of a SCK•CEN concrete. Laboratoire de Mecanique de Lille, UMR CNRS 8107.

Harrington, J. F., A. E. Milodowski, C. C. Graham, J. C. Rushton, and R. J. Cuss (2012) "Evidence for Gas-Induced Pathways in Clay Using a Nanoparticle Injection Technique." Mineralogical Magazine 76 (8): 3327–36. doi:10.1180/minmag.2012.076.8.45.

Jacops E. (2013) Results and interpretation of the gas migration tests in concrete. FORGE report D3 26.

Volckaert, G., Ortiz, L., De Cannière, P., Put, M., Horseman, S.T., Harrington, J.F., Fioravante, V., Impey, M. (1994). "MEGAS Modelling and Experiments on Gas Migration in Repository Host Rocks. Final Report Phase 1". EUR16235 EN, Luxembourg.

Weetjens E. and Govaerts J. (2012) Preparative Safety Assessments in the Framework of SFC 1: Reference case (Version 3) model calculations for compacted waste (CSD-C). SCK•CEN-R-5413.

Yu L. & Weetjens E.(2012) Estimation of the gas source term for spent fuel, vitrified high-level waste, compacted waste and MOSAIK waste. SCK•CEN-ER-162.

Compressibility properties on loading and on air injection of two deep claystone formations

E. Romero[1], P. Marschall[2], L. González[1], R. Gómez[1]
[1] Department of Geotechnical Engineering and Geosciences, Universitat Politècnica de Catalunya, Barcelona, Spain. enrique.romero-morales@upc.edu
[2] NAGRA Science and Technology, Switzerland

Introduction

The paper presents selected results of an experimental investigation aimed at characterising the volume change properties along loading/unloading and air injection/dissipation of two deep claystone formations from a Mesozoic sequence in Northern Switzerland, considered as candidate host rocks in the Swiss program for deep geological disposal of radioactive waste (Opalinus Clay and 'Brauner Dogger'). The experimental program intends to analyse the phenomena that control the migration of air through initially water saturated claystone, paying particular attention to the volume change response of the material along this process (Romero *et al*. 2012, Senger *et al*. 2014).

Material and experimental methods

Four core samples were retrieved from a deep geothermal well near Schlattingen in the Molasse Basin of North-eastern Switzerland. Two of them were recovered from a clay-rich sequence at depths 777 and 782 m bg, called 'Brauner Dogger' (strata of the Upper Dogger). The two remaining cores were taken from the Opalinus Clay formation at depths 880 and 936 m bg. Initial conditions of the samples are summarised in Table 1. Mercury intrusion porosimetry (MIP) tests revealed mono-modal pore size density functions with decreasing dominant entrance pore sizes –and increasing air-entry values– at increasing depths, as indicated in the table. Samples displayed high initial suctions (between 4 and 44 MPa), despite being nearly saturated, due to stress relief disturbances.

An experimental program on very stiff oedometer cells was initially carried out to determine the constrained moduli of the materials on loading/unloading and to compare these results with the stiffness observed during air injection and dissipation experiments at constant total mean (isotropic) stress. Samples with bedding planes orthogonal to vertical axis (50 mm in diameter and 20 mm high) were initially loaded under oedometer conditions to σ_v=12 MPa at constant water content and then put in contact with artificial pore water at u_w=0.5 MPa. Some swelling was recorded on pore water equalisation (between 0.10% and 0.47%). Saturated samples were then loaded (up to σ_v=25 MPa) and unloaded at constant water back-pressure (u_w=0.5 MPa). Adequate controlled-stress rates were used to ensure drained conditions.

Controlled-volume rate air injection experiments (2 and 100 mL/min), followed by shut-in and dissipation stages were performed under constant isotropic stress conditions (total mean stresses p=15 MPa and 19 MPa) in a high-pressure isotropic cell (samples 50 mm in diameter and 25 mm high). The protocol included: a) isotropic loading to p=12 MPa at constant water content; b) application of water pressure at upstream and downstream caps (u_w=5.5 and 0.5 MPa, respectively) and measurement of water permeability; c) isotropic drained loading to p=15 MPa or 19 MPa at u_w=0.5 MPa ; and d) controlled-rate air injection at upstream/bottom cap from u_a=3 to 14 MPa (or 18 MPa), followed by shut-in and recovery phases at constant p.

Experimental results and interpretation

Figure 1 shows loading and unloading oedometer results on two samples, as well as constrained moduli $\Delta(\sigma_v\text{-}u_w)/\Delta\varepsilon_a$ on both paths followed (L: loading, U: unloading, ε_a: axial strain). Opalinus Clay displayed a higher compressibility on loading/unloading compared to 'Brauner Dogger'. Figure 2 presents the evolution of axial strain with constitutive stress (p minus air pressure u_a at the bottom injection point) along the air injection and dissipation stages of selected tests on 'Brauner Dogger' and Opalinus Clay. In this case, changes in porosity are a consequence of changes in fluid pressure, since tests were carried out at constant p. During the air injection stage (A to B in the figures); samples

underwent approximately the same small expansion, in which no appreciable differences were observed between both volume injection rates (figure on the left). After shut-in (B in the figure), expansion continued as a consequence of the air pressure front propagation into the sample, which induced the fluid pressure to increase and the constitutive stress to decrease. Lower rates are currently being considered to study their influence on the evolution of expansion during air injection and the early stage after shut-in. Maximum expansions on pore pressure increase were observed on Opalinus Clay, consistent with compressibility results on loading/unloading. Some elapsed time after shut-in, the air injection pressure started to decrease along the dissipation stage towards point C, which induced sample compression during constitutive stress increase. Axial stiffness values $\Delta(p\text{-}u_a)/\Delta\varepsilon_a$ have been reported in the figure for Opalinus Clay, which are in agreement with loading/unloading results. A lower compressibility of 'Brauner Dogger' has been also observed during this dissipation stage, which is still running.

Formation	Brauner Dogger		Opalinus Clay	
Depth (m)	777	782	880	936
Density (Mg/m^3)	2.51	2.55	2.53	2.53
Water content (%)	4.34 – 5.43	4.78	4.30 - 4.70	4.79
Density of solids (Mg/m^3)	2.69	2.69	2.69	2.69
Void ratio, e	0.116 – 0.130	0.090	0.107 – 0.112	0.110
Porosity, n	0.104 – 0.115	0.080	0.097 – 0.101	0.100
Degree of saturation, S_r	1.0	0.95 - 1.0	1.0	0.98 - 1.0
Dominant pore mode from MIP (nm)	20	22	16	< 8
Air-entry value from MIP (MPa)	14	13	18	> 36
Liquid limit, w_L (%)	28	24	-	29
Plastic limit, w_P (%)	18	17	-	18

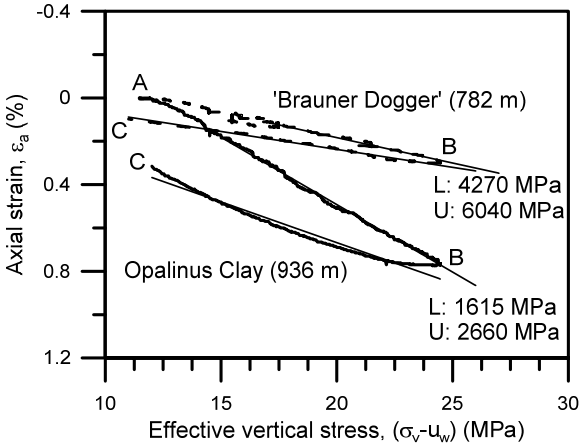


Table 1. (Left) Initial conditions of tested samples 'Brauner Dogger' and Opalinus Clay.
Figure 1. (Right) Loading/unloading curves under oedometer conditions. Drained constrained moduli.

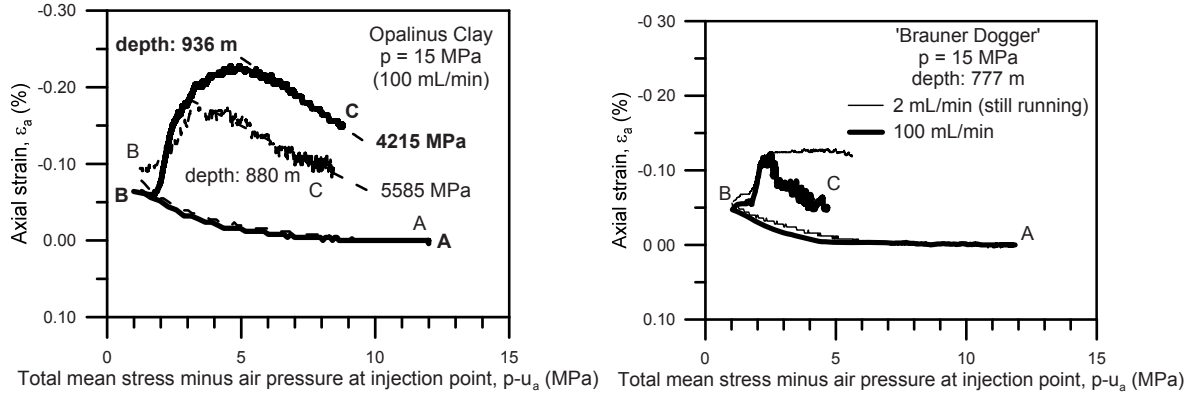


Figure 2. Evolution of volumetric strains during air injection (A to B) and dissipation (B to C) stages on Opalinus Clay (left) and 'Brauner Dogger' (right).

Acknowledgements
Financial support provided by NAGRA (Switzerland) through a collaboration agreement with CIMNE (Spain) 'Experimental study on deep core samples from Schlattingen SLA-1 Borehole' (2012-2014) is greatly acknowledged.

References

.Romero E., Senger R., Marschall P., Gómez R. 2012. Air tests on low-permeability claystone formations. Experimental results and simulations. In: Multiphysical Testing of Soils and Shales. L. Laloui and A. Ferrari (eds.). Springer Series in Geomechanics and Geoengineering. Springer, Heidelberg: 69-83.

Senger, R., Romero, E., Ferrari, A., Marschall, P. 2014. Characterization of gas flow through low-permeability claystone: laboratory experiments and two-phase flow analyses. In: Special Publications 2014, v.400. Geological Society, London: 531-543.

On the role of "surface diffusion" and competing cations for diffusion of transition metal ions in Opalinus Clay

L.R. Van Loon, W. Pfingsten
Paul Scherrer Institut, CH-5232 Villigen PSI

Diffusion of radionuclides in clay rocks has been studied intensively during the last 10 - 15 years in small scale laboratory experiments (Van Loon et al., 2003; Aertsens et al., 2004; Descostes et al., 2010), in field experiments (Gimmi et al., 2014) and by analysing natural tracer profiles (Mazurek et al., 2012). Although some progress in process understanding has been obtained for non-sorbing, weakly sorbing and anionic radionuclides, the diffusion of strongly sorbing elements such as transition metals, lanthanides and actinides is still poorly understood (Altmann et al., 2011), maybe due to too simplified model concepts for non- and weakly sorbing cationic and anionic elements.

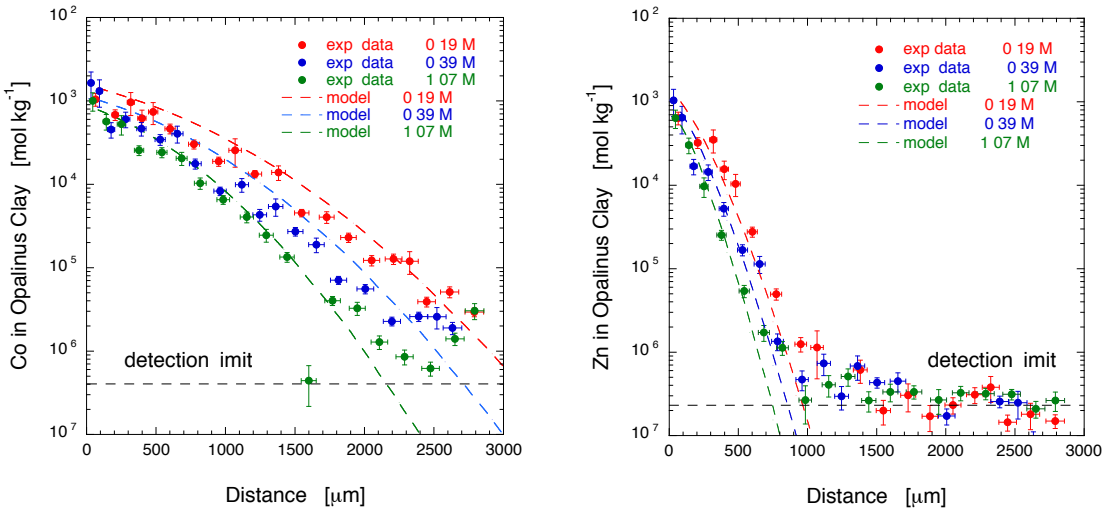


Fig. 1: Diffusion profiles for Co(II) (left) and Zn(II) (right) in Opalinus Clay as a function of the ionic strength of the pore solution. Symbols represent experimental data, dashed lines are calculated by the single species model.

In the framework of the EU 7 FP CatClay project, the diffusion of Co(II) and Zn(II) was studied using a modified version of the combined in-diffusion/abrasive peeling technique (Van Loon and Müller, 2014). The diffusion of both cations was found to depend on the ionic strength, i.e. the composition of the pore water: a low ionic strength promotes diffusion resulting in a larger diffusion distance whereas for high ionic strength pore waters the diffusion profiles are more shallow (Figure 1), if sample heterogeneity could be excluded. Such behaviour has been described recently for alkaline and earth-alkaline metals by Gimmi and Kosakowski (2011) who called it "surface enhanced diffusion". Diffusion of Zn(II) was less pronounced compared to Co(II) what can be easily explained by a stronger sorption of Zn(II) on OPA as observed in accompanying batch sorption studies.
The diffusion profiles for both Co(II) and Zn(II) could be reproduced by a simple single species diffusion model characterised by an effective diffusion coefficient (D_e) and a linear sorption coefficient (K_d), which are only valid parameters for the experimental conditions here. Although Bradbury and Baeyens (2011) proposed two sorption sites in Opalinus Clay - a strong and a weak site - based on batch sorption studies on illite, the successful K_d approach is equivalent to a single sorption site and one may conclude that strong sites must have been occupied by trace elements that are omnipresent in nature. It is known from pore water analysis that elements such as Fe(II), Mn(II) and several lanthanides are present in Opalinus Clay pore water at concentrations high enough to fully saturate the strong sorption sites (Bossart, 1998). Unfortunately, these elements were not measured in the experiments. Modelling with multicomponent diffusion models in which the sorption model of Bradbury and Baeyens (2011) was implemented, showed that "surface diffusion" or diffusion in the

electric double layer has to be assumed in order to describe the effect of ionic strength on the diffusion profile, whereas a similar modelling, where sorption competition of Co(II) and Zn(II) with Fe(II) and Mn(II) has been taken into account, reproduced the measured profiles well but without the assumption of "surface diffusion" (Figure 2), both indicating the need for a better system understanding.

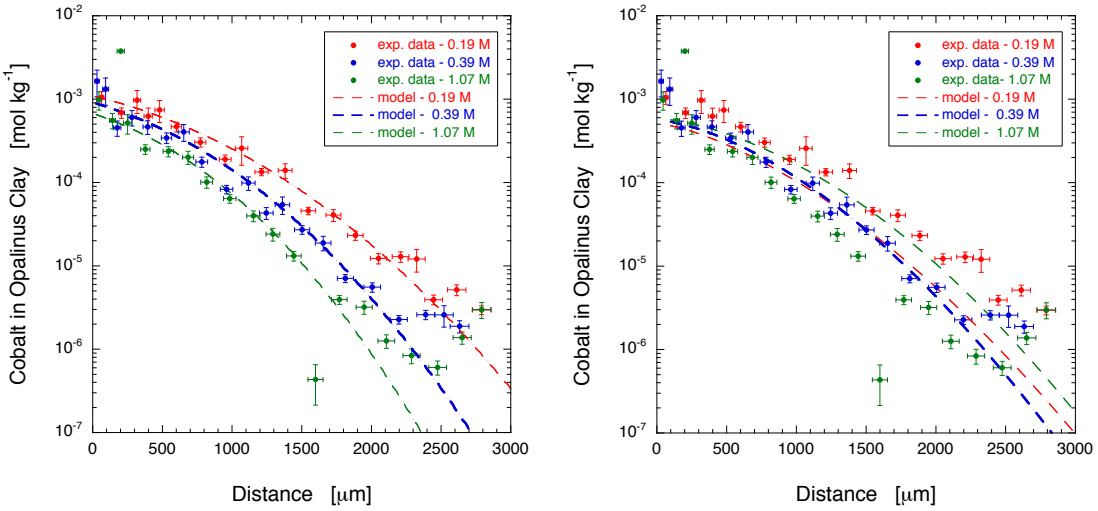


Fig. 2: Diffusion profile of Co(II) in Opalinus Clay modelled with a multicomponent diffusion model with diffusion in the electric double layer, two sorption sites and sorption competition (left) and without diffusion in the electric double layer, two sorption sites and sorption competition (right).

References

Aertsens, M., Wemaere, I., Wouters, L. (2004). Spatial variability of transport parameters in the Boom Clay. Appl. Clay Sci. 26, 37-45.

Altman, S., Tournassat, C., Goutelard, F., Parneix, J.-C., Gimmi, T., Maes, N. (2012). Diffusion-driven transport in clayrock formations. Appl. Geochem. 27, 463-478.

Bossart, P. (1998). Basic geochemical data from water sampling (WS) experiments, Phases 1 and 2. Technical Report TR97-02, Mont Terri, St. Ursanne, Switzerland.

Bradbury, M.H., Baeyens, B. (2011). Predictive sorption modelling of Ni(II), Co(II), Eu(III), Th(IV) and U(VI) on MX-80 bentonite and Opalinus Clay: A "bottom-up" approach. Appl. Clay Sci. 52, 27-33.

Descostes, M., Blin, V., Bazer-Bachi, F., Meier, P., Grenut, B., Radwan, J., Schlegel, M.L., Buschaert, S., Coelho, D., Tevissen, E. (2008). Diffusion of anionic species in Callovo-Oxfordian argillites and Oxfordian limestones (Meuse/Haute-Marne, France). Appl. Geochem. 23, 655-677.

Gimmi, T., Leupin, O.X., Eikenberg, J., Glaus, M.A., Van Loon, L.R., Waber, H.N., Wersin, P., Wang, H.A.O., Grolimund, D., Borca, C., Dewonck, S., Wittebroodt, C. (2014). Anisotropic diffusion at the field scale in a 4-year multi-tracer diffusion and retention experiment – I: Insights from the experimental data. Geochim. Cosmochim. Acta 125, 373-393.

Gimmi, T., Kosakowski, G. (2011). How mobile are sorbed cations in clays and clay rocks? Environ. Sci. Technol. 45, 1443-1449.

Mazurek, M., Alt-Epping, P., Bath, A., Gimmi, T., Waber, H.N., Buschaert, S., De Cannière, P., De Craene, M., Gautschi, A., Savoye, S., Vinsot, A., Wemaere, I., Wouters, L. (2011). Natural tracer profiles across argillaceous formations. Appl. Geochem. 26, 1035-1064.

Van Loon, L.R., Soler, J.M., Bradbury, M.H. (2003a). Diffusion of HTO, $^{36}Cl^-$ and $^{125}I^-$ in Opalinus Clay from Mont Terri: Effect of confining pressure. J. Contam. Hydrol. 61, 73-83.

Van Loon, L.R., Müller, W. (2014). A modified version of the combined in-diffusion/abrasivepeeling technique for measuring diffusion of strongly sorbing radionuclides in argillaceous rocks: A test study on the diffusion of caesium in Opalinus Clay. Appl. Radiat. Isot. 90, 197-202.

Multispecies random walk simulations in radial symmetry – model concept, benchmark and application to HTO, ^{22}Na & ^{36}Cl diffusion in clay

Shuo Meng & *Wilfried Pfingsten*
Paul Scherrer Institut, 5232 Villigen-PSI, Switzerland

Introduction

The modelling of radionuclide transport in clay often can be simplified by use of radial symmetry of the laboratory experimental setup or due to the cylindrical shape of the underground nuclear waste storage installations. Especially, if the complex geochemical system with a lot of species, chemical (sorption) reactions and minerals has to be taken into account, one-dimensional simulations in radial geometry would allow modelling radionuclide migration in such systems within reasonable computational time. Here we present an extension of the multispecies reactive transport code MCOTAC (Pfingsten 1996, 2002, 2011) to applications with radial symmetry. The advantage of the random walk approach over other numerical schemes is that negative species concentrations are excluded during transport calculations, which generates numerical problems if transport and geochemical equilibrium-kinetic modules are directly coupled. Since there is no direct procedure available describing one-dimensional random walk of particle in radial symmetry, two-dimensional random walk of particles has been reduced to a single radial coordinate for geochemical equilibrium-kinetic calculations to save computer memory and computational time. In the following we present the model concept, a benchmark with COMSOL Multiphysics and applications to laboratory experiments.

Model Concept

The simulations were performed using a multi-grid approach. Random walk transport simulations were performed on a 2D equidistant grid as described in Pfingsten, 2002, whereas the calculations of chemical equilibrium were performed in 1D using radial symmetry, reducing a lot the calculation time. Independent random walk in x and y direction is mapped onto the radial coordinate r (= sqrt(x^2+y^2)). The radial symmetry is taken into account via the area S(r) at radius r with a ring width dr given by , with ring index i.
This ring area/volume is taken into account when calculating species concentrations in individual rings from the sum over all particle/species masses present in the individual ring after a transport step.

Benchmark

In order to verify this new random walk approach for radial symmetry, we compared MCOTAC radial symmetrical calculations for single species diffusion in clay with results from a COMSOL Multyphysics calculation for the same system shown in Figure 1. The agreement is very good and allows to apply MCOTAC with the new radial symmetric transport module to radial symmetric systems but with complex geochemistry, which is not possible with COMSOL Multiphysics.

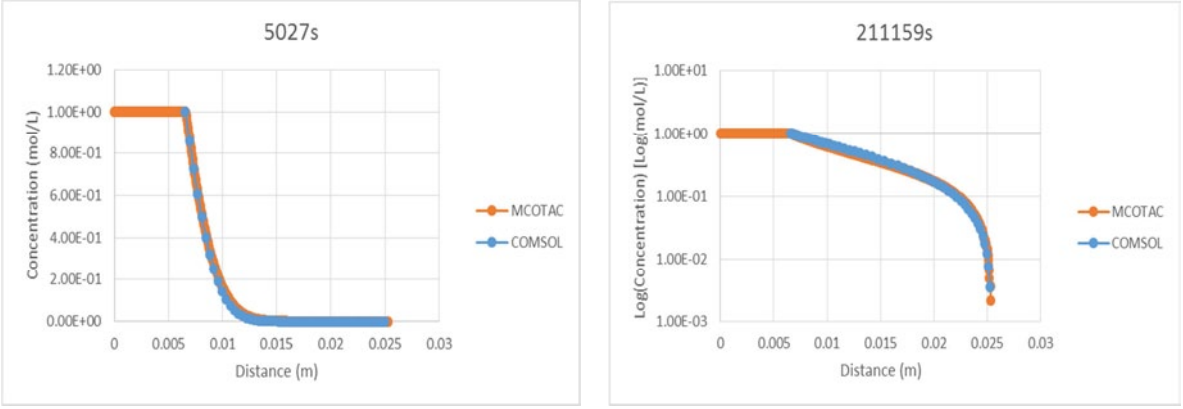


Figure 1: Comparison of MCOTAC and COMSOL profiles calculated for single species diffusion into a cylindrical clay sample at 5027 s and 211159 s.

Application

The new model is applied to laboratory through diffusion experiments performed with HTO, ^{22}Na and ^{36}Cl in clay reported in the literature (Van Loon et al., 2004), where their modelling did not include differentiation between transport parameters for filters and sample; single parameter values identical for filters and sample were used and constant concentration boundary conditions for the tracers as well. Here we performed a more detailed modelling of the experiments, taking into account different transport parameters for filters and sample explicitly, e.g. porosities of 0.418, 0.15 and 0.367 respectively and related the different effective diffusion coefficients $D_e=D_p*\square$ (D_p is the pore diffusion coefficient in m^2/s and $\square$ is the porosity). We also take into account the decreasing tracer concentration in the "high concentration reservoir" with time due to tracer in-diffusion into the clay and compare the results with those where mean and constant transport parameters were used to deduce these parameters for the clay sample. For the HTO experiment with a small volume at the high concentration side we deduced by chance the same best fit transport parameters as reported in the literature where mean parameters identical for sample and filters and a constant HTO concentration at the high concentration side was assumed. For the HTO experiment with the large volume reservoir it was not necessary to take into account a decreasing HTO concentration in the reservoir – the same best fir parameters were deduced. For ^{22}Na we got different best fit parameters for D_e and K_d (Figure 2) when using our more detailed modelling setup compared to the modelling with mean and identical parameters for filters and clay sample as reported in the literature; and for ^{36}Cl we got slightly different ones. From these results we conclude that it is important to include as much information as possible from the experiments within the modelling in order to deduce sample transport parameters carefully, as for example done in (Jakob et al., 2009), and not getting by chance – using identical mean values for filters and sample and a not appropriate constant concentration boundary – the same transport parameters as for the more detailed modelling of the HTO experiment. In case of the diffusion experiment with sorbing ^{22}Na, different transport parameters were deduced, since here no-sorption on the filters and sorption on the clay sample cannot be replaced in the modelling by using mean transport parameters identical for both.

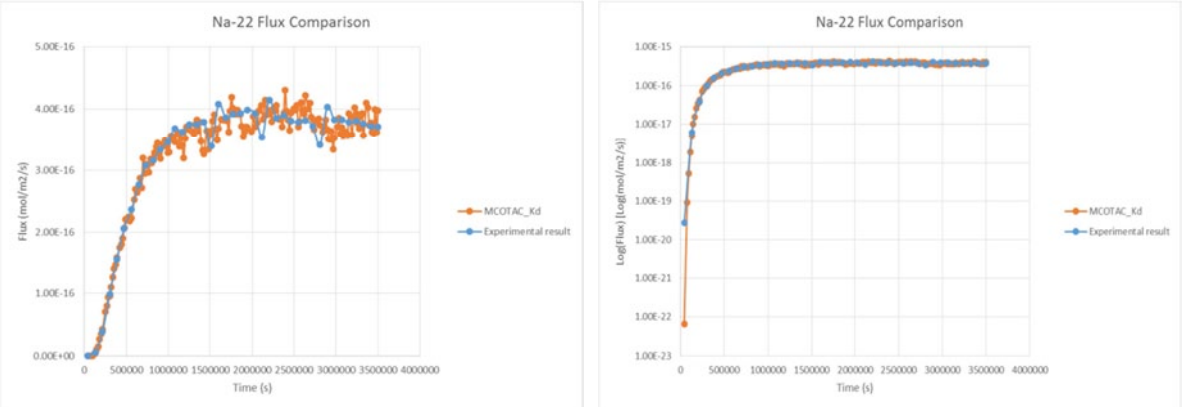


Figure 2: Measured and calculated flux for radial ^{22}Na diffusion through a clay sample.

References

COMSOL Multiphysics. http://www.comsol.com/comsol-multiphysics.

Jakob, A., Pfingsten, W., Van Loon, L. (2009). "Effects of sorption competition on caesium diffusion through compacted argillaceous rock." Geochimica et Cosmochimica Acta 73(9): 2441-2456.

Pfingsten, W. (1996). "Efficient Modeling of Reactive Transport Phenomena by a Multispecies Random Walk Coupled to Chemical Equilibrium." Nuclear Technology 116(2): 208-221.

Pfingsten, W. (2002). "Experimental and modeling indications for self-sealing of a cementitious L&ILW repository by calcite precipitation." Nuclear Technology 140(1): 63-82.

Pfingsten, W., Bradbury, M.H., Baeyens, B. (2011). "The influence of Fe(II) competition on the sorption and migration of Ni(ii) in MX-80 bentonite." Applied Geochemistry 26(8): 1414-1422.

Van Loon, L. R., Soler, J.M., Mueller, W., Bradbury, M.H. (2004). "Anisotropic diffusion in layered argillaceous rocks: A case study with Opalinus Clay." Environ. Sci. Technol. 38: 5721-5728.

Influence of the ionic strength on the diffusion in clay rocks of three sorbing cations: Sr^{2+}, Zn(II) and Eu(III)

Sébastien Savoye, **Jean-Luc Lacour, Bernard Grenut and Agnès Fayette**

CEA, DEN, DPC, Gif/ sur Yvette, France. (sebastien.savoye@cea.fr)

It is now well established that the transport properties of solutes in clayrocks, *i.e.* parameter values for Fick's law, are mainly governed by the negatively charged clay mineral surface. While a good understanding of the diffusive behaviour of non-reactive anionic and neutral species is now achieved, much effort has to be placed on improving understanding of coupled sorption–diffusion phenomena for sorbing cations. Indeed, several cations known to form highly stable surface complexes with sites on mineral surfaces, migrate more deeply into clayrock than expected (Altmann *et al.*, 2012).

The study reported in this paper aimed at investigating the influence of ionic strength on the diffusion of three cations in the Callovo-Oxfordian claystones. The cation species have been chosen for covering a representative range of cation families: from a moderately sorbing cation, the strontium, to strongly sorbing cations, one being divalent, the zinc and the other being trivalent, the europium. For that purpose, batch and diffusion experiments were performed. Diffusion cells with ionic strength varying from 0.085 Eq/L (corresponding to the equilibrated pore-water) to 0.58 Eq/L were setup for carrying out successively the through-diffusion method for strontium, and in-diffusion method with zinc and europium. In a first step, diffusion of tritiated water (HTO) was studied in order to compare the diffusive behaviour of the three cations with a water tracer.

The Figure 1 shows the comparison of the ^{85}Sr results obtained during the through-diffusion experiments for the three ionic strengths. The increase of the ionic strength leads to a less pronounced activity decrease in the upstream reservoir, while the flux decreases in the downstream reservoir. The associated modelling indicates that, when the ionic strength increases, the effective diffusion coefficient (D_e) and the diffusivity (D_e/D_{bulk}) values show a decrease with the same extent as the decrease of the rock capacity factor and the K_d values (Figure 2).

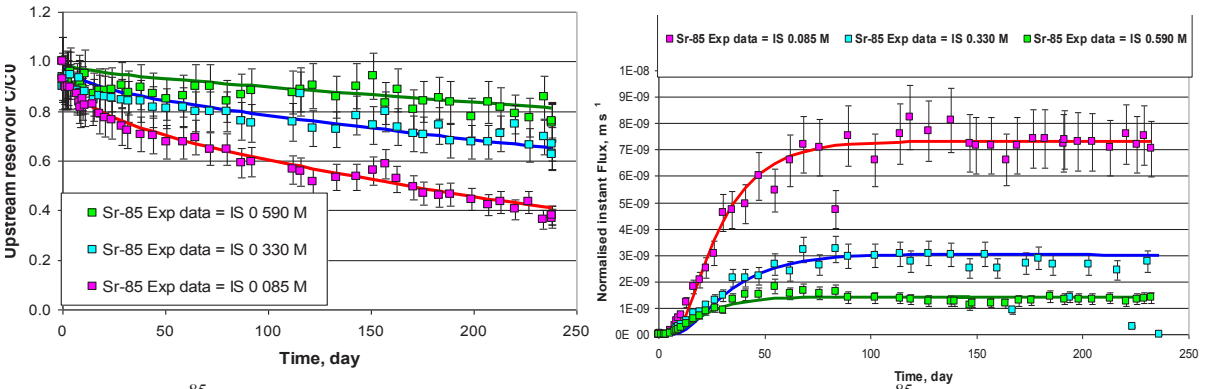


Figure 1. (left) ^{85}Sr activity evolution in the upstream reservoir and (right) ^{85}Sr flux in the downstream reservoir as a function of time in the 0.085 Eq/L cell, the 0.330 Eq/L cell and the 0.590 Eq/L cell with the associated modelling

The same tendency was observed for zinc. At an ionic strength of 0.085 Eq/L, we observed an enhancement of their diffusion with an extent of the same order of magnitude for both cations, compared to HTO (diffusivity Sr or Zn ~ 4 x diffusivity HTO). While at the highest ionic strength, the diffusivity becomes very close to that of the water tracer (Figure 2), suggesting an inhibition of the surface diffusion mechanism.

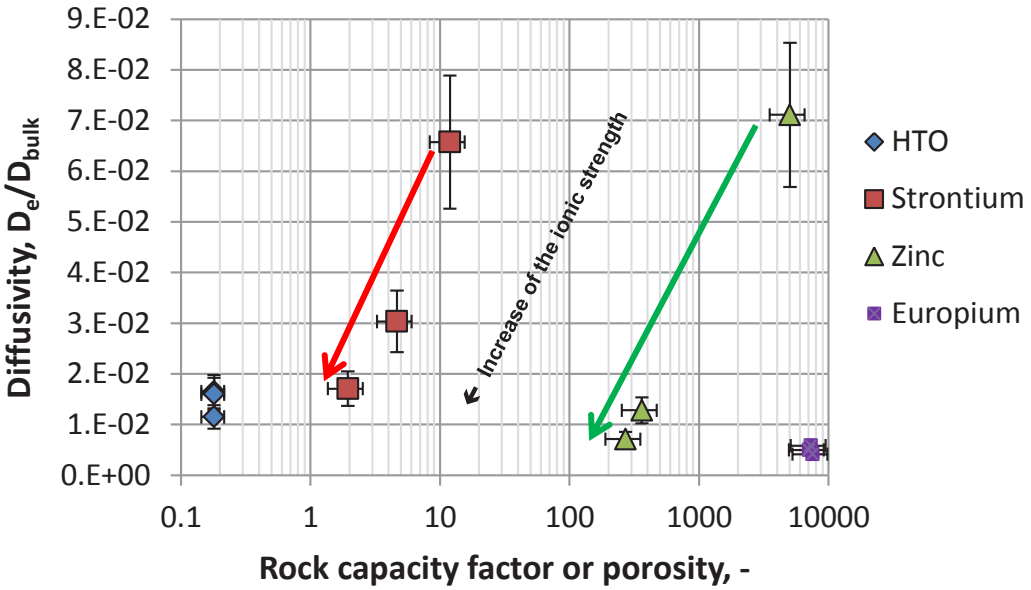


Figure 2. Evolution of the diffusivity as a function of the rock capacity factor or porosity for HTO, strontium, zinc and europium with the increase of the ionic strength

On the other hand, the diffusion of europium was not seen to be impacted by the change of ionic strength, based on the unique set of diffusive parameters derived from the three experiments. In this case, the europium diffusivity values are very close to those determined for HTO (Figure 2), indicating that the surface diffusion component would be negligible for this cation. However, the non-uniform diffusion profile of radioactive Eu in the rock, derived from one of these cells suggests that the diffusion process is much more complicated, likely involving the contribution of several Eu species. Eu diffusion would be more governed by its chemistry in solution than by some enhanced diffusion processes.

Lastly, simulations by means of a chemical-transport code (Savoye *et al*., 2012) were carried out for assessing its capability of reproducing this dataset showing the distinct diffusive behaviour of three cations.

Acknowledgements

The research leading to these results has received funding from the European Union's European Atomic Energy Community's (Euratom) Seventh Framework Programme FP7/2007-2011 under grant agreement n° 249624 (CATCLAY project). The authors also thank Andra for providing the rock samples used in this study.

References

Altmann, S., Tournassat, C., Goutelard, F., Parneix, J.C., Gimmi, T., Maes, N., 2012. Diffusion-driven transport in clayrock formations. *Appl. Geochem*. 27, 463-478.

Savoye S., Beaucaire C., Fayette A., Herbette M., Coelho D., 2012. Mobility of Cesium through the Callovo-Oxfordian Claystones under Partially Saturated Conditions. *Environ. Sci Techno*. 46, 2633-2641.

Re-saturation and THMC behaviour of bentonite buffers: modelling capabilities, uncertainties and developments

D.G. Bennett[1*], S.J. Benbow [2], A.E. Bond[3], M. Shibata[4], K. Ozone[5] and H. Takase[5]

[1]TerraSalus, Orchard House, Church Lane, Bisbrooke, Oakham, Rutland, LE15 9EL, United Kingdom.
[2]Quintessa, The Hub, 14 Station Road, Henley-on-Thames, Oxfordshire, RG9 1AY, United Kingdom.
[3]Quintessa, 633/635 Birchwood Boulevard, Warrington, WA3 7QU, United Kingdom.
[4]Japan Atomic Energy Agency, 4-33 Muramatsu, Tokai, Ibaraki, 319-1194 Japan.
[5]Quintessa Japan, Queen's Tower A 7-077, 2-3-1 Minatomirai, Nishi-ku, Yokohama, 220-6007 Japan.

* corresponding author: DavidBennett@TerraSalus.co.uk

Bentonite clay is commonly included in concepts for the disposal of high-level radioactive waste (HLW) and / or spent fuel (SF). In such concepts, bentonite-based materials are used to form an engineered barrier known as the 'buffer' that surrounds the waste containers, as well as being used as backfill. Bentonite clay is a natural material that has properties that make it a potentially very effective barrier to water flow. Over time, a wide range of thermal, hydraulic, mechanical, chemical (THMC) and other (e.g. radiological, biological) processes will occur in disposal facilities for HLW and /or SF, and these may affect the performance of the engineered barriers, including the buffer.

In order to develop a convincing safety case for radioactive waste disposal, it is necessary to develop and demonstrate sufficient understanding of the possible behaviour and evolution of the disposal system, including the evolution from its 'as-emplaced' state to its target state and into the long-term. This requires understanding of the engineered barriers and the materials from which they are formed. Bentonite clays are complex materials and although much progress has been made in understanding and modelling their behaviour, a complete constitutive THMC model of their behaviour is not yet available.

This paper reviews and discusses the status of understanding of buffer re-saturation and THMC behaviour, based on findings from key experimental and modelling studies that have been made on bentonite-based buffers under conditions as close as possible to those expected in waste repositories, and at relevant spatial scales. The paper discusses the current state of the art in terms of the capability to model re-saturation and THMC processes in bentonite materials, and identifies issues that could be investigated further to improve the current level of understanding.

The paper focuses on re-saturation and the associated early phase THMC processes, rather than on microbiological or radioactive decay processes for example, because the processes operating early in the evolution of the disposal system have significant potential to affect safety.

Construction licence applications that are currently under review in some countries are proposing 'exchangeability' of the bentonite materials in the design in order to accommodate future materials supply uncertainties. The large-scale experiments and associated modelling studies that were reviewed considered a range of bentonites with varying Na:Ca ratios and composition. Observations of bentonite buffer re-saturation from the experiments suggest a wide envelope of values for the relevant bentonite properties such as suction and swelling capacity, which exert a strong control on rates of re-saturation. In addition to reviews of previous studies, further modelling studies were undertaken of the Swedish Canister Retrieval Test (CRT) using the QPAC code to investigate the level of modelling capability that existed at the start of the study and identify remaining uncertainties.

The CRT was a 5-year, full-scale test managed by SKB at the Äspö Hard Rock Laboratory in Sweden. The THM behaviour of the CRT has been modelled by SKB using CODE_BRIGHT and by Quintessa using the QPAC code, amongst other groups. Both models indicate similar trends in terms of

gradually increasing saturation with time (e.g. over a few hundred years), but it is apparent both from these results and other sensitivity studies, that the models are very sensitive to assumptions made regarding buffer properties and homogenisation, and that many model parameters show high sensitivity to the values of saturation obtained.

A notable feature is that water inflows to the CRT gradually reduced with time and only increased again once the water pressure applied at the outer edge of the buffer was increased. It is not clear whether this is an artefact of the experiment or an intrinsic property of the system, but it may suggest that, under some circumstances, re-saturation of the outer part of the buffer may effectively limit or prevent full re-saturation of the inner parts of the buffer. In addition, even under conditions which were supposed to increase the rate of buffer re-saturation, several large-scale tests suggest that buffer re-saturation may be spatially heterogeneous and slow in some locations. In a repository, the buffer may remain in a partially-saturated state for several thousand years which could affect the safety functions of the buffer that assume full saturation.

Other authors have suggested the use of non-Darcian models to represent flows into bentonite as it resaturates. Modelling has been conducted to test these ideas by using a non-Darcian pressure gradient threshold flow model and representing the supply of water to the buffer via a channelled fracture in the host rock. Example 2D results are shown in Figure 1. The non-Darcian flow model reproduces some of the self-limiting type behaviour of the bentonite and appears to better represent the types of spatial heterogeneity observed in some large-scale experiments.

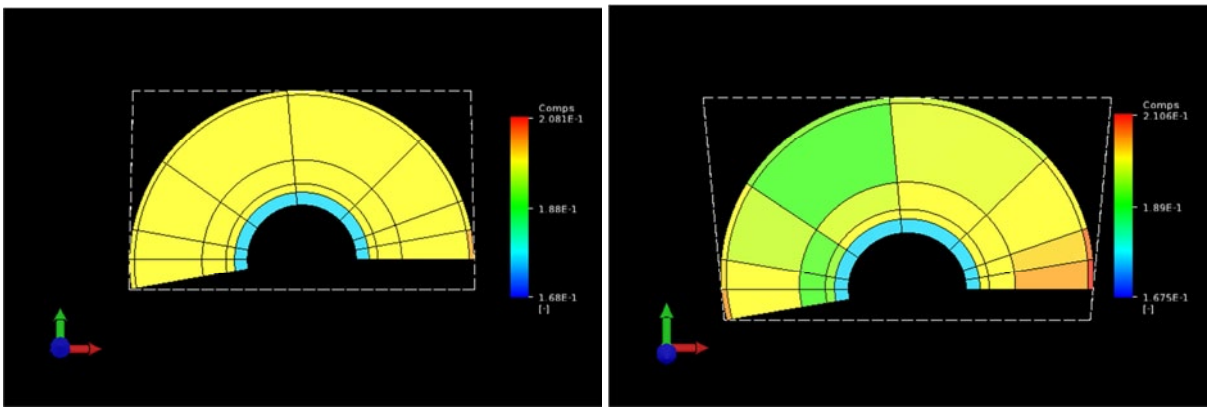


Figure 1 Comparison of the calculated water contents of a bentonite buffer (2D cross-section) after 100 years of re-saturation by water flowing from a fracture intersecting the waste deposition hole. The model on the left uses a Darcian flow model and shows more rapid and homogeneous re-saturation. The model on the right uses a non-Darcian pressure gradient threshold model. The non-Darcian model appears to better reproduce the types of spatial heterogeneity observed in some large-scale experiments.

Exploring the quantification of groundwater fluxes in the aquifers surrounding a clay host rock

***B. Rogiers*[1*], M. Gedeon, S. Labat, K. Vandersteen, B. Leterme, K. Beerten, M. De Craen**

[1]Institute for Environment, Health and Safety, Belgian Nuclear Research Centre (SCK•CEN), Boeretang 200, BE-2400 Mol, Belgium
*Corresponding author: bart.rogiers@sckcen.be

The current generation of numerical groundwater flow and solute transport models developed at SCK•CEN in the framework of radioactive waste disposal studies for ONDRAF/NIRAS solely uses groundwater heads as quantitative state variable observations of the hydrogeological system (Gedeon 2008, Gedeon *et al*. 2011, Vandersteen *et al*. 2012, Rogiers *et al*. 2014). Additionally, some hydrochemical analyses are used to validate the underlying conceptual models qualitatively (Mallants *et al*. 2011). The limited amount of quantitative inverse conditioning data makes the rather detailed models not very well constrained and subject to considerable prediction uncertainties.
Considerable progress has been made recently on material parameter characterization and direct conditioning of the models (Rogiers 2013, Vandersteen *et al*. 2014, Bennett 2014), but still only groundwater heads and/or derived values are being used. This creates kind of an unbalance (see Figure 1), and makes that the available state variable observations can hardly differentiate between different model parameterizations.
Additional state variable observations, and especially the ones carrying information on groundwater fluxes, would greatly improve the knowledge on the hydrogeological systems relevant to geological disposal. Moreover, the estimates on the fate of solutes released from a host rock to the adjacent aquifers would benefit considerably from such data. Together with available groundwater heads, such additional state variable observations would provide multiple lines of evidence for the groundwater flow regimes within the aquifers. Moreover, it would restore the balance between material parameter characterization and state variable observations, which would allow to develop and validate more complex and realistic hydrogeological models.
In addition to on-going developments concerning the quantitative use of hydrochemistry (Vandersteen & Leterme 2014), the integration of overland flow and surface water components with the groundwater flow models (which would enable the use of river gauge data; Leterme *et al*. 2013 Vandersteen *et al*. 2012), and attempts in unlocking the palaeohydrological archive (Leterme & Beerten 2013, Beerten *et al*. 2014) the current work explores the following approaches to quantify groundwater fluxes in the aquifers surrounding a clay host rock:

- Single well tracer tests using solute and heat tracers (very relevant in the framework of minimally invasive site characterization),
- and the large-scale use of heat as a passive groundwater tracer (very relevant in terms of understanding the hydrogeological system as a whole).

The obtained groundwater fluxes can be used directly as inverse conditioning data for groundwater flow models. The vertical temperature log data at different locations is used indirectly through the simulation of forced heat convection. The performed tests and modelling are performed in the framework of validating the Neogene

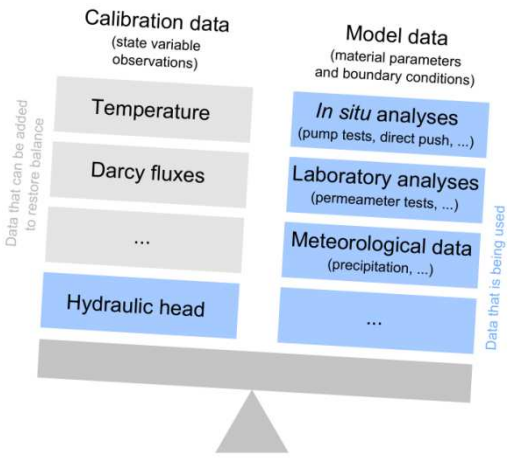


Figure 1 The unbalance that currently exists, and the elements that could be added to resolve this.

Aquifer Model (Gedeon 2008), in order to guide future updates of the model.
The first tests indicate that applications of the classical Point Dilution Method (Drost *et al*. 1968) lead to groundwater fluxes in the same order of magnitude as predicted by the existing models, and that a regional collection of temperature logs is consistent with the conceptual hydrogeological models used (see also Rogiers 2014).

References

Beerten K, Van Nieuland J, Vandenberghe D, Deforce K, Rogiers B. 2014. Fluvial development of the Nete valley during the Late Weichselian and early Holocene: new data from a cross-section south of Kasterlee (NE-Belgium). Geophysical Research Abstracts, Vol. 16, EGU2014-5301, EGU General Assembly 2014

Bennett G. 2014. Integration of detailed borehole core measurements and pump test data from the aquifers below the Boom Clay in a groundwater flow model. Unpublished MSc thesis, Faculty of Engineering, Vrije Universiteit Brussel, 78 pp.

Drost W, Klotz D, Moser H, Neumaler, F. 1968. Point dilution methods of investigating ground water flow by means of radioisotopes. Water Resources Research, 4(1), 125–146.

Gedeon M. 2008. Neogene Aquifer Model, SCK•CEN-ER-48 (p. 110). Mol.

Gedeon M, Mallants D, Vandersteen K, Rogiers B, Laloy E. 2011. Hydrogeological modelling of the Dessel site. Overview report. Project near surface disposal of category A waste at Dessel, NIROND-TR 2008-15 E V2, 227 pp.

Leterme B, Beerten K. 2013. HYDRUS 2-D water balance simulations in a changing drift sand landscape: a realistic case from the last millennium in the Campine area, northern Belgium. Geophysical Research Abstracts, Vol. 15, EGU2013-8323, EGU General Assembly 2013

Leterme B, Gedeon M, Jacques D. 2013. Groundwater Recharge Modeling of the Nete Catchment (Belgium) Using the HYDRUS-1D – MODFLOW Package. Conference paper: Hydrus Software Applications to Subsurface Flow and Contaminant Transport Problems, Prague, Czech Republic, 21-22/03/2013.

Mallants D, Beerten K, Wemaere I, Gedeon M, Rogiers B, Labat S. 2011. Integration of major ion chemistry and stable isotope data with hydrogeological modelling to infer groundwater pathways. Geophysical Research Abstracts 13: EGU2011-7223. EGU General Assembly 2011, Vienna, 3-7 May 2011.

Rogiers B. 2013. Multi-scale aquifer characterization: from outcrop analogue, direct-push and borehole investigations towards improved groundwater flow models. PhD thesis, Faculty of Science, KU Leuven, 234 pp. - ISBN 978-90-8649-672-3 - D/2013/10.705/87 - ISSN 0250-7803

Rogiers B. 2014. Exploratory temperature logging in the upper part of the Neogene aquifer at Mol-Dessel-Retie. SCKCEN external report ER-258. Tech. rep., pp. 1–34 (cit. on p. 26)

Rogiers B, Vienken T, Gedeon M, Batelaan O, Mallants D, Huysmans M, Dassargues A. 2014. Multi-scale aquifer characterization and groundwater flow model parameterization using direct push technologies. Environmental Earth Sciences 72(5): 1303–1324.

Vandersteen K, Gedeon M, Rogiers B. 2012. Transient model of the confined aquifers below the Boom Clay: 2011 update. Regional Hydrogeological Modelling of the Mol Site. External Report, SCK•CEN-ER-199. - ISSN 1782-2335.

Vandersteen K, Leterme B, Gedeon M. 2012. Modelling of surface hydrology in the Nete catchment. Update of the Neogene Aquifer Model. RESTRICTED CONTRACT REPORT, SCK•CEN-R-5408.

Vandersteen K, Leterme B. 2014. Regional aquifer geochemistry below the Boom Clay (NE-Belgium): data analysis and modelling. Geophysical Research Abstracts, Vol. 16, EGU2014-3279, EGU General Assembly 2014

Vandersteen K, Gedeon M, Beerten, K. 2014. A synthesis of hydraulic conductivity measurements of the subsurface in Northeastern Belgium. GEOLOGICA BELGICA (2014) 17/3-4: 196-210

Detailed characterisation of borehole cores from deep aquifers surrounding a potential clay host formation, using air permeameter measurements.

***B. Rogiers*[1*], K.Vandersteen[1], L. Potums[2] and G. Bennett[3,4]**

[1]Institute for Environment, Health and Safety, Belgian Nuclear Research Centre (SCK•CEN), Boeretang 200, BE-2400 Mol, Belgium
[2]University of Leuven, Faculty of Sciences, Department of Earth and Environmental Sciences, Celestijnenlaan 200E BE-3001, Leuven-Heverlee, Belgium
[3]University of Brussels, Interuniversity Programme in Physical Land Resources, Pleinlaan 2, BE-1050 Brussels
[4]University of Dodoma, College of Earth Sciences, School of Mines and Petroleum Engineering, Department of Mining and Mineral Processing, P.o.Box 259, Dodoma, Tanzania
*Corresponding author: bart.rogiers@sckcen.be

In order to quantitatively describe groundwater flow, the hydraulic properties of sediments, such as hydraulic conductivity and storage coefficients, are necessary input parameters for the groundwater flow equation. The most important parameter from a perspective of modelling groundwater flow is the (saturated) hydraulic conductivity K_s [LT^{-1}], since this parameter together with the hydraulic gradient allows quantifying groundwater flow according to Darcy's Law. Furthermore, the heterogeneity in this parameter can have a large effect on groundwater flow and solute transport.
SCK•CEN has been collecting hydrogeological data in the Campine (NE-Belgium) for more than 30 years in the framework of radioactive waste disposal studies. Recently, it has been shown by Rogiers *et al*. (2014) that the hand-held air permeameter is a very efficient cost-effective tool to obtain high-resolution information on variability of K_s from borehole core slabs. In this study, high-resolution hydraulic conductivity measurements on 6 deep borehole core sections in the vicinity of the Boom Clay were performed using air permeametry. The measurements are compared to classical laboratory permeameter measurements.
Air permeameter measurements are non-destructive small-scale measurements used to assess the air permeability of porous media, such as soils and sediments, which can be transformed into K_s using well-defined transfer functions (Rogiers *et al*., 2013). Amongst others, the most important prerequisite is that the water content should be small enough to allow air being sucked from the porous medium into the permeameter. The method is not representative of large sediment volumes. However, when applied to high-resolution sampling grids, it can provide a good measure of the heterogeneity of the porous material, and upscaling might be performed in order to obtain K_s values representative for larger support volumes.

In this study, use was made of the Tinyperm II air permeameter (New England Engineering 2011) (

Figure 1), which consists of a vacuum cylinder, pressure transducer, handle and plunger, and a microprocessor and control unit. Basically, the apparatus monitors the recovery of air pressure inside the vacuum cylinder, while air is being sucked into the device through the porous medium.
Detailed measurements (if possible every 5 cm) were done on the Dessel-5, Essen-1, Kallo-1, Kallo-2, Herenthout-1 and Herenthout-2 core slabs (Beerten et al., 2010, Labat et al., 2008a, Labat et al., 2008b, Labat et al., 2012). For the Dessel-5 borehole, measurements were done on Neogene sediments (Diest, Dessel, Berchem, Voort and Eigenbilzen



Figure 1: Two students performing air permeameter measurements on borehole cores, with the TinyPerm II Portable Permeameter.

Sands). For the other boreholes, deeper sediments were measured (Formations of Boom, Zelzate, Maldegem, Lede, Gent and Tielt). The obtained K_s data for the Herenthout-1 borehole are displayed in Figure 2a illustrating the amount of detail obtained from this kind of characterization.
A comparison was made between values measured with the air permeameter method and with classical permeameter laboratory measurements. This is shown for the Herenthout-1 and -2 boreholes in Figure 2b. The laboratory measurements are in all cases clearly lower than the values obtained using air permeametry. This is probably due to the difference in decompaction (not experienced in previous work on shallow aquifers) between the samples used for classical permeameter measurements and the sediments in the borehole core slabs, as well as the different support volumes. Also the presence of clay in the sediments can play a role: hand-held air permeametry is not very practical for very low-permeable sediments such as clays, and the air-tightness of the permeameter represents a hard lower boundary. Figure 2b shows a linear relationship between the log-transformed values of both measurement methods.

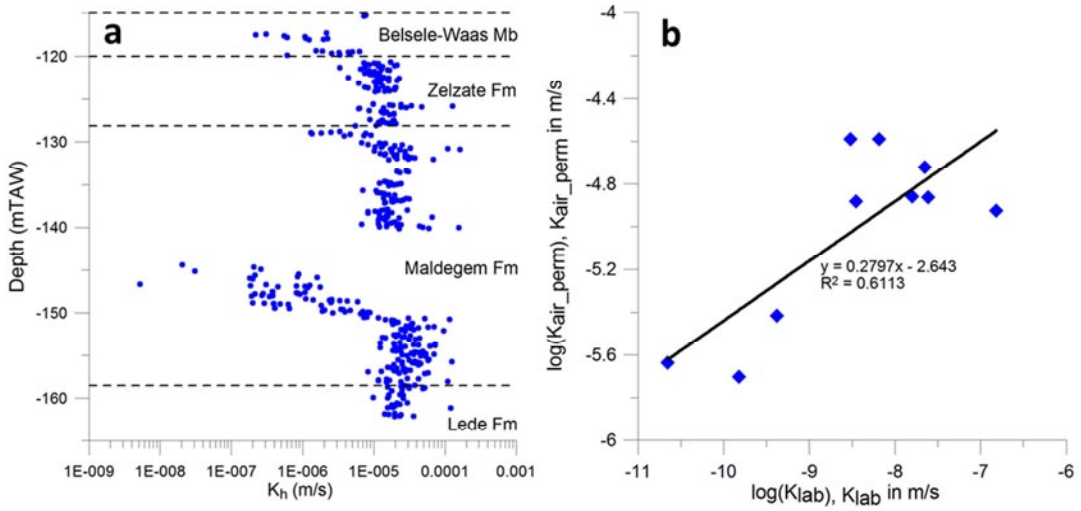


Figure 2. Overview of raw K_h data for the Herenthout-1 borehole (a) and comparison between conductivity values measured with air permeametry (using the Iversen et al. (2003) equation) and a classical laboratory permeameter for the Herenthout-1 and -2 borehole (b).

Despite these drawbacks in using an air permeameter for deep sediment characterization, the revealed small-scale heterogeneity contains a wealth of information, and allows to delineate (hydro-)geological sub-units, quantify spatial covariance and detect potential cyclicity (*e.g.* in the Boom Belsele-Waas Member in the Essen-1 borehole) in sedimentary deposits.

References

Beerten, K., Wemaere, I., Gedeon, M., Labat, S., Rogiers, B., Mallants, D., Salah, S. and Leterme, B., 2010. Geological, hydrogeological and hydrological data for the Dessel disposal site. Project near surface disposal of category A waste at Dessel – Version 1.- Brussels, Belgium: ONDRAF/NIRAS, 2010.- 273 p.- NIROND–TR 2009–05 E V1.

Labat, S., Marivoet, J., Wemaere, I., Maes, T., 2008a. *Essen-1 borehole of the hydro/05neb campaign: technical aspects and hydrogeological investigations*. SCK•CEN-ER-68, 35p.

Labat, S., Wemaere, I., Marivoet, J., Maes, T., 2008b. *Herenthout-1 and Herenthout-2 borehole of the hydro/05neb campaign: technical aspects and hydrogeological investigations*. SCK•CEN-ER-59, 27 p.

Labat, S., Marivoet, J., and T. Maes. *Kallo boreholes: technical aspects and hydrogeological investigations*. SCK•CEN-ER-224, in prep.

New England Research & Vindum Engineering, 2013. TinyPerm II Portable Air Permeameter, User□s Manual. Retrieved from http://www.vindum.com/TinyPermManual.pdf on 5-10-2013.

Rogiers, B., Beerten, K., Smeekens, T., Mallants, D., Gedeon, M., Huysmans, M., Batelaan, O. & Dassargues, A., 2013. *Derivation of flow and transport parameters from outcropping sediments of the Neogene aquifer*. Geologica Belgica 16(3): 129-147.

Rogiers, B., Winters, P., Huysmans, M., Beerten, K., Mallants, D., Gedeon, M., Batelaan, O. & Dassargues, A., 2014. *High resolution hydraulic conductivity logging of borehole cores using air permeability measurements*. Hydrogeology Journal. DOI 10.1007/s10040-014-1144-y

A synthesis of NE-Belgium hydrogeology

K.Vandersteen*, M.Gedeon, B. Leterme and B. Rogiers

Institute Environment-Health-Safety, Belgian Nuclear Research Centre (SCK•CEN), Boeretang 200, 2400 Mol, Belgium
*Corresponding author: katrijn.vandersteen@sckcen.be

The knowledge on the hydrogeological system in NE-Belgium (Campine region) has been evolving during more than 30 years of hydrogeological research in the framework of the Belgian nuclear waste disposal programme currently managed by ONDRAF/NIRAS.
Over this time, a considerable dataset of hydraulic parameters, geochemical composition and groundwater heads of the NE-Belgium underground has been collected. This data was integrated into stepwise improving hydrogeological models. The accumulated knowledge on the hydrogeology of NE-Belgium, along with data obtained from external sources (Flemish Environmental Agency, Belgian universities, Geological Survey of Belgium among others), is presented in this summary study.

An important step in the conceptual understanding of the Campine hydrogeological system was the recognition of two different aquifer systems, each with its own characteristics: the shallow and the deep aquifer systems, above and below the Boom Clay, respectively. The shallow aquifer system is driven by surficial processes including topography effects, rivers and infiltration. In contrast, the confined deep aquifer system is mainly influenced by groundwater extractions.

These two aquifer systems considerably differ in their respective boundaries. The shallow aquifer system is laterally bounded by river catchment divides. In a larger lateral context, other natural boundaries can be considered (Scheldt River, Boom Clay outcrop). Vertically, the shallow aquifer system is bounded by the Boom Clay, which can be considered relatively impermeable considering the shallow aquifer system. The deep aquifer system boundaries are much more uncertain; until now it is not entirely clear how to put its bottom limit. Also in the lateral direction, uncertainties about the deep aquifer system boundaries are reflected in models, particularly concerning the hydraulic function of the faults related to the Roer Valley Graben system (east of the Campine).

The available measured hydraulic properties of each hydrogeological layer, from the Quaternary until the Palaeozoic Basement, are summarized. For the Neogene Aquifer system, numerous hydraulic property data are collected in the vicinity of the Mol-Dessel nuclear site. However, at a regional scale, less data is available so far. Also, in the deep aquifer system located below the Boom Clay, data scarcity grows with depth. For the very deep aquifers below the Ypresian Aquitard, few data are available, while for the Oligocene and Ledo-Paniselian-Brusselian Aquifer Systems, more data with a good spatial spread are available in the Campine region. Based on these data, a relationship of conductivity versus depth was suggested for the latter aquifer.

An analysis of piezometric measurements combined with results from groundwater modelling offers insight into regional and local trends of groundwater level dynamics and flow directions. In the shallow aquifer system, both seasonal and multi-year oscillations are visible in the piezometric data. However, the latter are tempered by the hydraulic connection of the aquifers to rivers. The role of the Pliocene Clayey layer in the shallow groundwater system is explained through the analysis of double piezometer measurements, leading to a conceptual model for the local groundwater flow in the shallow aquifer system.

The transient nature of the deep aquifer system piezometry was investigated using a trend analysis on the available measurements. It was found that the groundwater extractions in the Oligocene Aquifer System trigger only local effects on groundwater heads. Hence, the regional effects (constant decrease of groundwater heads) present in the Oligocene Aquifer System are presumably caused by pumping in

the Ledo-Paniselian-Brusselian Aquifer System, whereby the magnitude of this influence is governed by the hydraulically isolating Bartonian Aquitard System.

For the piezometers located in the Ledo-Paniselian-Brusselian Aquifer System, we see that although the pumping is concentrated in the south, it causes the water level to decrease far northwards, which implies a higher transmissivity of this aquifer than that of the Oligocene Aquifer System. Only a few piezometers are documenting the evolution of groundwater heads in the deeper aquifers (Paleocene, Cretaceous and Basement). However, the available trend analysis mostly indicates a behaviour similar to the Ledo-Paniselian-Brusselian Aquifer System.

The hydraulic gradient over the aquitards in the deep aquifer system shows areas of upward and downward flow. Currently, the gradients in the deep aquifer system are considerably influenced by pumping. This is particularly true for the southern Campine, where the groundwater flow, which is generally west to north-west under natural conditions, is bended towards the south under the influence of pumping. In the northern Campine, the pumping influence on groundwater flow is much smaller. For the deeper aquifers, too few data are available to draw any conclusions about the groundwater flow. However, regional effects of pumping (decreasing groundwater heads) are visible in the north of the Campine in the Paleocene and Cretaceous aquifer.

On a regional scale, the groundwater flow direction in the shallow aquifer system is mainly NW-wards, originating from the major SE recharge area on the Campine Plateau, which coincides with the Meuse-Nete (Scheldt) catchment divide towards the northwest. The cuesta of the Campine Clay-Sand Complex in the north (Meuse – Scheldt catchment divide) causes the general regional groundwater flow direction to bend from a northern to a western direction. In general, the discharge areas are located at the rivers, while recharge areas are located in between them.

Water balance calculations for the shallow aquifer system suggest that 80 to 90% of the infiltrating water discharges into rivers and drains. The proportion of pumping is estimated between 10% and 15%. Water balance calculations for the deep aquifer system show a large influence of pumping. In the assumed natural situation (without pumping), we deal with a virtually closed hydraulic system. The absence of groundwater outlet from the confined deep aquifer system causes almost all groundwater that enters the deep aquifer system through the Boom Clay to return up to the shallow aquifer system. Under current excessive pumping conditions the hydraulic system is open, where the pumping wells remove water that infiltrates the confined deep groundwater circulation domain. Additional recharge comes from the shallow groundwater circulation domain through the outcrops of the deep aquifers.

Regarding the aquifer geochemistry, the groundwater in the shallow aquifer system is in non-equilibrium (undersaturation) due to the unconfined conditions and fresh water recharge. The aquifer is well flushed with fresh water, and pH, alkalinity and mineralization generally increase in the direction of groundwater flow. Most of the groundwater above the Boom Clay is of the $CaHCO_3$-type, although more detailed variations are observed (e.g. eastern, decalcified part vs. western, still calcified part). In the deep aquifer system below the Boom Clay, groundwater is generally of the $NaHCO_3$- to NaCl-type and generally re-equilibration with the host formations occurs. Major cation/anion and stable isotope analyses indicate a mixture between saline water and fresh water end members for the Oligocene Aquifer System and the Ledo-Paniselian-Brusselian Aquifer System.

This analysis and extensive summary of the hydrogeological knowledge in NE-Belgium not only improved our general understanding of the hydrogeological system as a whole, but in revealing several knowledge gaps it is also a helpful tool in directing future hydrogeological research in the framework of radioactive waste disposal.

Overview of more than 30 years of hydrogeological research in the Belgian nuclear waste disposal programme

K.Vandersteen* **and M.Gedeon**

Institute Environment-Health-Safety, Belgian Nuclear Research Centre (SCK•CEN), Boeretang 200, 2400 Mol, Belgium
*Corresponding author: katrijn.vandersteen@sckcen.be

In NE-Belgium, the Boom Clay (Figure 1) is considered as a potential host rock for the geological disposal of radioactive waste. The possible extent of the contamination reaching the biosphere – via well or river exposure pathways - is evaluated by studying the migration of radionuclides from the disposal system through the hydrogeological system to the biosphere entry point. This implies a good understanding of the hydrogeological system and of the radionuclide transport phenomena.

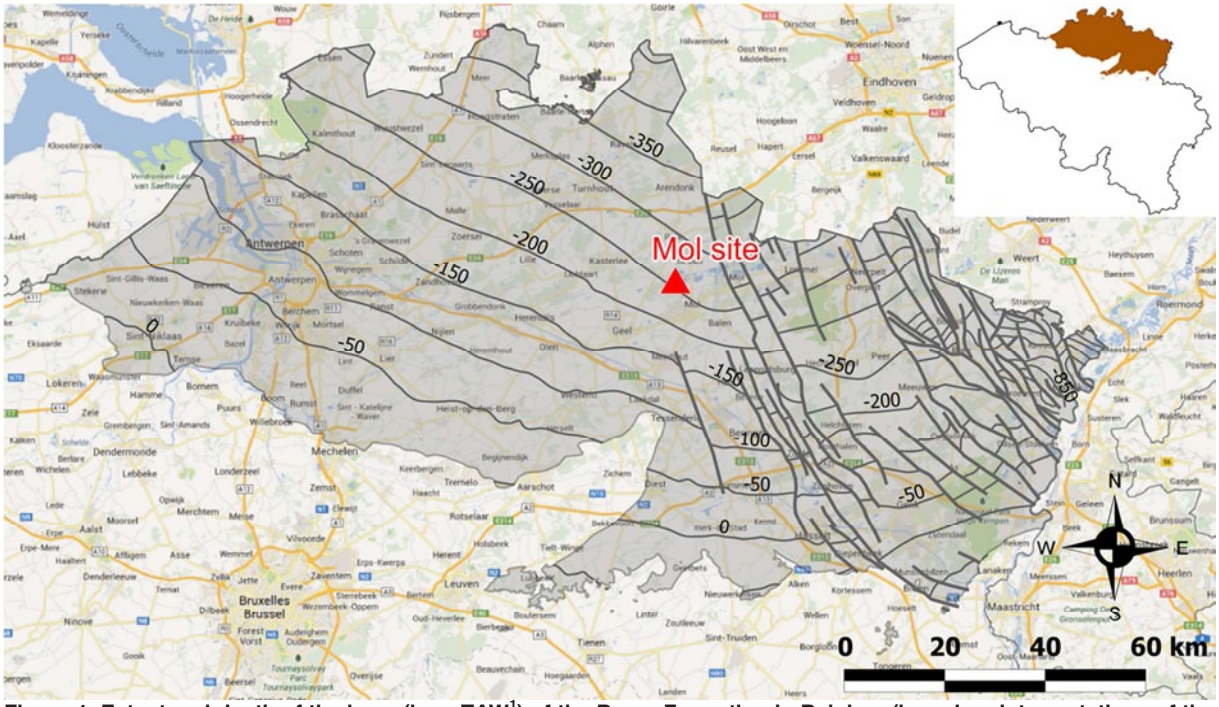


Figure 1. Extent and depth of the base (in m TAW[1]) of the Boom Formation in Belgium (based on interpretations of the Geological Survey of Belgium; Vancampenhout, 2004). Faults cross-cutting the Boom Formation are shown by NW-SE trending lines; they belong to the Roer Valley Graben system. A map of Belgium with the location of the Boom Formation is shown in the upper right corner.

SCK•CEN has been investigating the hydrogeology of NE-Belgium for more than 30 years. In this period, most effort has been put to characterizing the groundwater flow using piezometric measurements, collecting measurements of hydraulic properties and groundwater geochemistry, defining the hydro-stratigraphy and updating our knowledge on groundwater flow by means of groundwater flow modelling. A regional piezometric network for supporting the regional modelling has been set up since 1983, covering NE-Belgium. In this network, measurements are collected from the Neogene Aquifer above the Boom Clay as well as from deeper aquifers below the Boom Clay.

From the very start of the hydrogeological investigations in 1985, the focus was put to the Mol site (Figure 1), i.e. the location of the underground research facility HADES. The first data on aquifers located above the Boom Clay were collected during construction of the first access shaft. Later on, the

[1] Tweede Algemene Waterpassing

hydrogeological data were mainly collected from boreholes at or located close to the Mol site. Consecutive groundwater modelling exercises revealed knowledge gaps, resulting in several additional measurement campaigns dating from the eighties until now. In contrast to the earlier investigation campaigns, the latter covered the whole Campine region (NE-Belgium). This iterative research cycle between groundwater modelling and data collection allowed increasing our level of knowledge and decreasing the level of uncertainty on the prediction of necessary indicators related to the aquifer systems.

Groundwater modelling has been performed at various scales from the regional scale extending beyond NE-Belgium, to local scale supplying transport models with a spatially detailed groundwater flow solution. The regional models are needed to thoroughly understand and represent the flow mechanisms on a regional scale. From these regional models, sub-regional models and finally local models were derived, which describe the hydrogeology with more detail. Groundwater modelling at SCK•CEN started around 1985 with the first regional hydrogeological model. For about 15 years, attempts were made in modelling the regional hydrogeology in NE-Belgium. Around 2000, the first sub-regional model around Mol (for the deep disposal program of category B&C waste) and subsequent local model (for the surface disposal program of category A waste) were built in order to provide the detailed flow field for the transport calculations, which were focused on the Mol site. More recently, the regional modelling increasingly used the natural boundaries of the system, whereby the position of the Mol site within the model became less centred. This evolution is not in contradiction with the evolution of the geological disposal program, in which siting comes only after the necessary strategic decisions and the successful completion of a Safety and Feasibility Case (e.g. SFC1) and Mol represents merely a reference site.

References

Vancampenhout, P., 2004. Isohypse maps of the Tertiary in Flanders. Geological Survey of Belgium.

A new multiscale approach to modelling the fully coupled hydraulic and thermal evolution of a whole repository throughout its lifetime

Bond AE[1], **Thatcher KE**[1], **Towler GH**[1] **and J Wendling**[2]

[1] Quintessa Limited, 633/635 Birchwood Boulevard, Warrington, Cheshire, WA3 7QU, UK.
[2] Andra, 1-7, rue Jean-Monnet - 92298 Châtenay-Malabry cedex, France.

Understanding the evolution of a whole radioactive waste disposal facility in terms of its hydraulic and thermal performance is a key input to the demonstration of post-closure safety. Representation of such systems become more complex in low-permeability, diffusive dominated host rocks where the process couplings can be significant to safety performance over extended periods of time, for example in the detailed behaviour of gas generation through metal corrosion. As such, major aspects of the performance of a facility can become dependent on the representation of these key features and associated coupled processes, which often operate only at very small spatial scales in comparison with the whole facility.

With these issues in mind a whole repository model based on the Andra 2009 reference design (Figure 1) was constructed considering a mixture of waste (French 'MA-VL', 'HA' and 'C0-CU3' waste) each with differing heat sources and hydrogen gas generation rates, with the impacts of coupling of gas generation rates to fluid saturation and temperature also to be assessed. The objective was to develop a model which captures, as well as possible, all relevant hydraulic and thermal behaviours at all relevant spatial scales within a single model until the system returns to equilibrium. Thus the approach adopted had to minimise the impacts of errors arising to due spatial homogenisation and should avoid any attempt to separate the domain into separate models that are not fully coupled.

A novel modelling approach was developed using the Quintessa code QPAC, which involved embedding detailed sub-models of individual MA-VL vaults and HA cells within a model of the entire repository. This approach enabled very small (cm) scale features, such as voids and interfaces around waste packages / containers that significantly influence the coupled thermo-hydraulic evolution to be represented explicitly in a model with a >50 km^2 areal domain. These sub-models were fully coupled into the solve using a monolithic approach, and did not rely on a split-operator or partially decoupled techniques. The approach relied on the expectation that many of the MA-VL vaults and HA cells will behave similarly, and therefore their behaviour can be approximated by representation of a small number of individual vaults or cells. This approach results in a small loss of information through spatial averaging, however when performed carefully, this was considered to be insignificant when compared with the additional detailed information retained at the vault and cell scale compared with conventional upscaling techniques.

Confidence in the new approach was developed by:

- systematically developing the approach using models of increasing complexity utilising known benchmark results from the FORGE project, WP1;
- undertaking global and local mass balance checks;
- grid refinement testing;
- comparison of results against models using conventional upscaling techniques; and
- examining and comparing the results of a number of sensitivity and alternative conceptualisation cases.

The developed models were found to be numerically stable, with negligible mass imbalance, even for relatively coarse grids where there are large contrasts in material properties and hydraulic conditions. Run times for the cases were manageable on a single threaded desktop computer and hence there was no need for recourse to high performance computing methods.

The work demonstrated that for the design and conceptual process model used, the key control on migration of gas within the repository is migration in the EDZ past sealing structures. This occurred because the EDZ may become partially desaturated during the operational phase, resulting in an open gas pathway past seals during the early part of the post-closure period. As the EDZ resaturates this gas pathway is closed. As a result, migration of gas in the tunnel network becomes sensitive to the locations of the seals, since the spatial location of the seal controls whether the seal EDZ resaturates before free gas generated from the waste migrates to the position of the seal. It was also shown that migration of gas (air) in tunnels during the early part of the post-closure period can influence the long term evolution. Therefore, for the system modelled in this study, it is important to model the operational phase in order to obtain the correct conditions at closure. Modelling the operational phase was the most numerically challenging part of the simulation and accounted for approximately half of the run time.

For the system that was modelled in this study, it was found that the majority of gas generated from the waste migrates into the EDZ and dissolves in the porewater. Subsequent migration of dissolved gas is via diffusion with almost all gas generated from the waste entering the rock. Only a small amount of gas migrates through the tunnels in the repository and there is very limited migration of gas up the shaft, well and associated EDZs. However the dominance of the diffusion did result in gas and fluid pressures rising approximately 3 MPa above hydrostatic values in and around the facility.

This sub-modelling approach could also be applied to other key components of the repository within the whole repository model, for example detailed sub-models of individual tunnel seals. However, the new approach is most advantageous when a large number of repeat features need to modelled in detail. Nested sub-models could also potentially be developed and more complex interactions between sub-models are also a possibility for future applications.

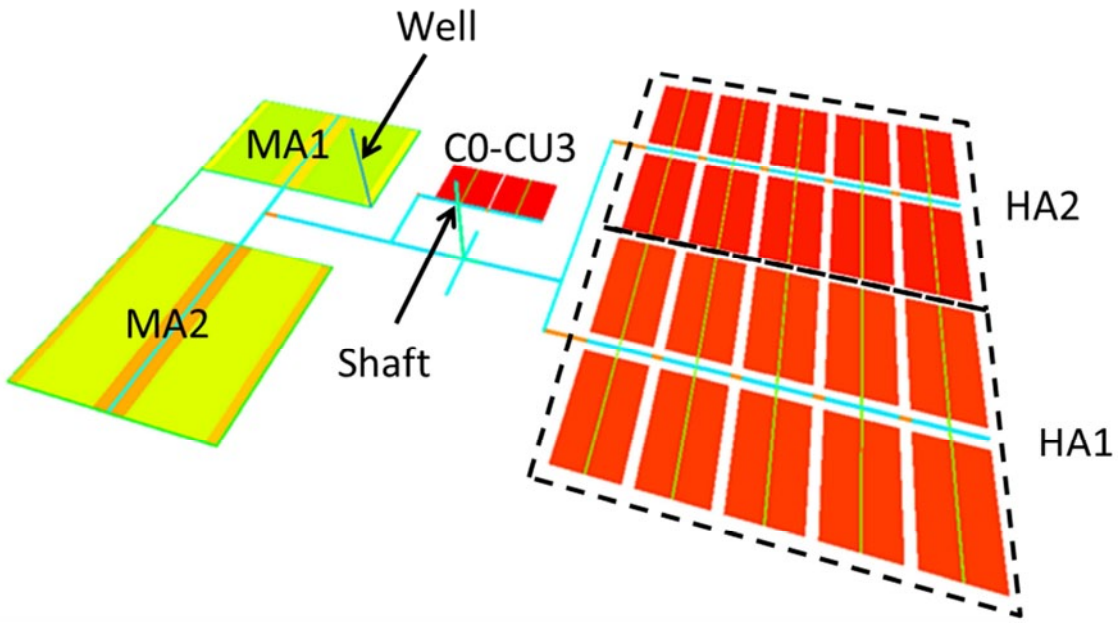


Figure 1. High-level geometry of the repository layout considered in the study with the surrounding geology made invisible. Labels indicate different waste zones (MA-VL, HA and C0-CU3) and other major engineering features, including vault and tunnel seals (yellow, orange) and shaft seals (green).

Surface diffusion effects for transition metals in compacted illite

M.A. Glaus [a], M. Aertsens [b], C.A.J. Appelo [c], T. Kupcik [d], N. Maes [b], L. Van Laer [b], L.R. Van Loon [a]

[a] Laboratory for Waste Management, Paul Scherrer Institut, CH-5232 Villigen PSI, Switzerland
[b] Belgian Nuclear Research Centre (SCK•CEN), Expert Group Waste & Disposal, 2400 Mol, Belgium
[c] Hydrochemical Consultant, 1071 MB Amsterdam, The Netherlands
[d] Institute for Nuclear Waste Disposal, Karlsruhe Institute for Technology, D-76021 Karlsruhe, Germany

Despite the large efforts invested in the past to measure, understand and model diffusion-driven transfer of radioactive elements in saturated natural or engineered low-permeability porous argillaceous media, the predictive capacity of our system understanding is still limited. In particular the role of surface diffusion (defined here as the enhancement of mass transfer rates induced by a concentration enrichment of the diffusing species in the clay phase) for different types of metal cations has not been unambiguously clarified. While such effects have been thoroughly investigated for representatives of the alkali and earth alkaline groups (Glaus et al., 2007), little is known regarding transition metals, lanthanides or actinides, mostly because of the short-comings in the experimental techniques which have so far been used to measure the diffusion of such metal cations. The purpose of the current work is: (i) to develop experimental techniques to measure the diffusion of such species, (ii) to measure their diffusivity under different conditions relevant for radionuclide transport in the geosphere and (iii) to test various conceptual models. The models were not only tested for their ability to represent the experimental data in a pure parameter fitting exercise, but checked for their consistency with respect to the equilibrium distribution of surface and solution species calculated for the different chemical conditions of the experiments.

Within the frame of the EC Euratom (FP7) Catclay project, we studied the diffusion of Sr^{2+}, Co(II) and Zn(II) in compacted illite in the pH range between 5 and 9, at background electrolyte concentrations between 0.01 and 1.0 mol/l and in the presence and absence of inorganic and organic carbon. The experiments were complemented by batch sorption studies under similar chemical conditions. The main reason behind the choice of these conditions was to study diffusion at varying fractional occupancies of the different binding sites, viz. the planar cation exchange sites and the more specific surface complexation sites. The chosen cations tend to be present as exchanged species in the lower pH range, while at higher pH they are bound to specific sorption sites. In addition, this distribution is influenced by the background electrolyte concentration. Sr^{2+} forms mainly exchanged species, while the two transition metals tend to form surface complex species (Bradbury and Baeyens, 2009). It has been demonstrated in previous work that those cations undergoing cation exchange may predominantly exhibit surface diffusion effects (Glaus et al., 2007). This phenomenon is not only restricted to smectites in which the interlayer space is accessible to cations , but also applies to illites (Glaus et al., 2010) in which the interlayer space is occupied by dehydrated potassium cations and therefore inaccessible to other cations.

Different techniques were used in the diffusion experiments in view of the potential difficulties anticipated in the measurements e.g. short penetration depths, high tracer fluxes leading to dominant resistances of the confining filters or sorption of the tracers on the equipment. Conventional in- and through-diffusion experiments were carried out using compacted clay cores with dimensions in the cm range. These were enclosed in stainless steel cells equipped either with an advectively flushed filter system or with filters in which the solution was stagnant. New types of diffusion cells made from PEEK were developed for clay cores with diameters in the mm range. The clay core was separated from the solution by a thin polymeric membrane only, which largely eliminated the problems typically encountered when using porous stainless steel filters.

Fig. 1 shows the results for the in-diffusion of Co(II) in Illite du Puy (acid washed, conditioned to the Na^+ form) measured using the membrane confined diffusion cells. The experiments were carried out at pH 5 and various concentrations of the background electrolyte ($NaClO_4$) in the absence of added

inorganic carbon. No significant effect of inorganic carbon at concentrations relevant for representative rock pore waters was found for all cations tested.

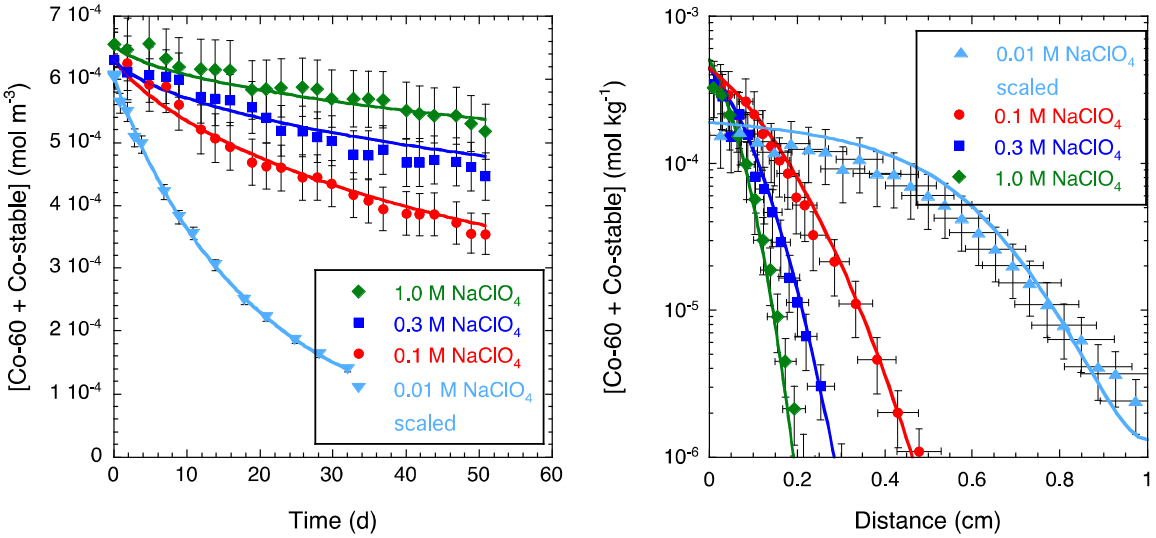


Figure 1. In-diffusion experiments with ^{60}Co(II) at pH 5 showing the total element concentration in the reservoir solution (left) and the profile in the clay obtained after termination of the experiment (right). The fitted curves were obtained using a single-species model assuming constant sorption distribution values.

Fitting the data using a single-species model resulted in sorption distribution values exhibiting a relatively weak dependency on the background electrolyte concentration. The corresponding dependence of the effective diffusion coefficients was, however, much stronger. The correlation between the sorption distribution values and the effective diffusion coefficients was thus rather poor for Co(II) and Zn(II). The two parameters were, however, strongly correlated in the case of the diffusion of Sr^{2+}. A conventional pore diffusion model can be ruled out in all cases due to the observed dependence of the effective diffusion coefficients on the background electrolyte concentration and the fact that the measured effective diffusion coefficients were much larger than the respective scaled diffusion coefficients of a neutral tracer (tritiated water). Surface diffusion is concluded to be the main transport process for Sr^{2+} in compacted illite. The situation for Co(II) and Zn(II) is more complex: A surface species present at low fractional occupancies appears to undergo surface diffusion, while dominant surfaces species such as the specific surface complexes do not significantly contribute to the overall diffusive transport. Such a conceptual model approach was confirmed by speciation calculations performed with Phreeqc (Appelo and Wersin, 2007) in which the mobile surface species is assumed to be enriched in the electrical double layer of the negatively charged clay surface.

As a general conclusion a reliable prediction of the diffusive fluxes of transition metals (and probably also lanthanides and actinides) depends thus on an adequate knowledge of the equilibrium distribution of the various surface species and their specific molecular mobility.

Acknowledgment: We thank Nagra, PSI and NIRAS for the partial financial support. The research leading to these results has further received funding from the European Atomic Energy Community's Seventh Framework Programme (FP7/2007-2011) under grant agreement n° 249624.

References:

Appelo, A., Wersin, P., 2007. Multicomponent diffusion modeling in clay systems with application to the diffusion of tritium, iodide, and sodium in Opalinus Clay. Environ. Sci. Technol. 41, 5002–5007.

Bradbury, M.H., Baeyens, B., 2009. Sorption modelling on illite Part I: Titration measurments and the sorption of Ni, Co, Eu and Sn. Geochim. Cosmochim. Acta 73, 990–1003.

Glaus, M.A., Baeyens, B., Bradbury, M.H., Jakob, A., Van Loon, L.R., Yaroshchuk, A., 2007. Diffusion of ^{22}Na and ^{85}Sr in montmorillonite: Evidence of interlayer diffusion being the dominant pathway at high compaction. Environ. Sci. Technol. 41, 478–485.

Glaus, M.A., Frick, S., Rossé, R., Van Loon, L.R., 2010. Comparative study of tracer diffusion of HTO, $^{22}Na^{+}$ and $^{36}Cl^{-}$ in compacted kaolinite, illite and montmorillonite. Geochim. Cosmochim. Acta 74, 1999–2010.

Pore network model of electrokinetic transport through charged porous media

A. Obliger[1,2,3], M. Jardat[2,3], D. Coelho[1], S. Békri[4], *B. Rotenberg*[2,3]
[1] *Andra, Châtenay-Malabry, France*
[2] *Sorbonne Universités, UPMC Univ. Paris 06, UMR 8234 PHENIX, Paris, France*
[3] *CNRS, UMR 8234 PHENIX, Paris, France*
[4] *IFP Energies nouvelles, Rueil-Malmaison, France*

We introduce a method for the numerical determination of the steady-state response of complex charged porous media to pressure, salt concentration and electric potential gradients. The macroscopic fluxes of solvent, salt and charge are computed within the framework of a Pore Network Model (PNM) [1], which describes the pore structure of the samples as networks of pores connected to each other by channels. The PNM approach is used to capture the couplings between solvent and ionic flows which arise from the charge of the solid surfaces. The microscopic transport coefficients on the channel scale, taken here of a simple analytical form obtained previously by solving the Poisson-Nernst-Planck and Stokes equations in a cylindrical channel [2], are upscaled for a given network by imposing conservation laws for each pores, when macroscopic gradients are applied to the sample. The complex pore structure of the material is captured by the distribution of channel diameters. We investigate the combined effects of this complex geometry, the surface charge and the salt concentration on the macroscopic transport coefficients. The upscaled numerical model preserves the Onsager relations between the latter, as expected [3]. The calculated macroscopic coefficients behave qualitatively like their microscopic counterparts, except for the permeability (see Fig. 1) and the electro-osmotic coupling coefficient when the electrokinetic effects are strong. Quantitatively, the electrokinetic couplings increase the difference between the macroscopic coefficients and the microscopic ones for a single channel of average diameter [4].

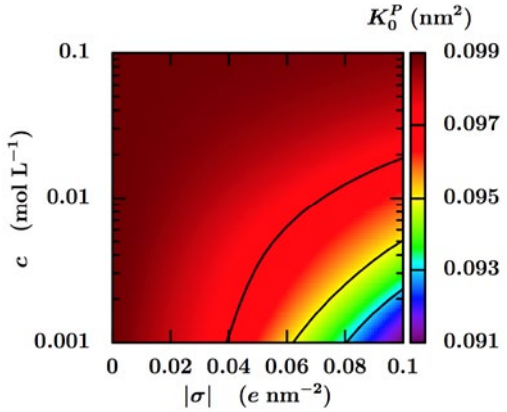


Fig. 1 Macroscopic permeability K_0^P (in nm^2) as a function of the salt concentration c in the reservoirs in equilibrium with the charged porous material, and of the surface charge density σ of the channels.

References

1. S. Békri, C. Laroche, O. Vizika. *International Symposium of the Society of Core Analysts* (2005)
2. A. Obliger, M. Duvail, M. Jardat, D. Coelho, S. Békri, B. Rotenberg, *Phys. Rev.E* **88**, 013019(2013)
3. E. Brunet, A. Ajdari, *Phys. Rev. E* **69**, 016306 (2004)
4. A. Obliger, M. Jardat, D. Coelho, S. Békri, B. Rotenberg, *Phys. Rev.E* **89**, 043013 (2014)

Nature of water diffusion in montmorillonite at different scales: Combination of experimental and modelling approaches

Churakov S.V.[a], **Gimmi T.**[a,b], **Van Loon L.R.**[a], **Juranyi F.**[a]

[a] Paul Scherrer Institute, CH-5232 Villigen, Switzerland
[b] University of Bern, Institute of Geological Sciences, CH-3012 Bern, Switzerland

Quantitative description of water and ion transport in clays and clay minerals is known to be challenging due to a tangled hierarchy of transport pathways and complex interactions between water, the surface of clay minerals, and aqueous cations. Smectites form particles composed of stacks of quasi two-dimensional TOT-layers, which themselves are formed by a sheet of octahedrally coordinated cations confined by two sheets of tetrahedrally coordinated cations [1]. The interlayer space between TOT layers is occupied by hydrated cations which compensate the permanent charge of the TOT layer. The interlayer space is typically varying from one to three water pseudo-layers depending on the TOT layer charge, the composition of the interlayer cations, the water chemical potential and the water to solid ratio. In compacted rocks, smectites form aggregates with 5–20 TOT layers [2]. A typical radial size of these particles is of the order of 0.01 to 1 μm. The pore space between smectite particles is referred to as interparticle porosity. Depending on the degree of compaction, the inter-particle porosity contributes from ~0 % to 30% of the total water accessible pore space ([3], and refs. therein).

Due to disparity of the transport scales in different types of porosity of clays distinct numerical simulation techniques and experimental methods have to be applied to allow a description of transport processes at all relevant scales. Recently, we combined Molecular Dynamic (MD) simulations of montmorillonite (Mt) and Random Walk (RW) simulations based on a simplified representation of pore space in Mt to estimate the influence of mineral surfaces charge and the effect of the arrangement of Mt particles on the meso- to macroscopic diffusivity of water in montmorillonite clay (Figure 1). The developed pore scale model for poly-mineral clays reflect the preferred orientation, size and aspect ratio of clay minerals in the rocks as well as relations between interlayer and inter particle porosity. These theoretical calculations were complemented with quasielastic neutron scattering (QENS) measurements of water diffusion in Mt with two pseudo-layers of water performed at four significantly different energy resolutions (i.e. observation times).

Our simulations [4] show that the size of the interlayer and the size of Mt particles are two characteristic dimensions which determine the time dependent behaviour of water diffusion in Mt. MD simulations suggest that at very short time (~ ps) scales water dynamics has the characteristic features of an oscillatory motion in the cage formed by neighbors in the first coordination shell. At longer time scales (10-100 ps), the interaction of water with the surface determines the water dynamics, and the effect of confinement on the overall water mobility within the interlayer becomes evident. At time scales corresponding to an average water displacement equivalent to the average size of Mt particles, the effects of tortuosity are observed in the meso- to macroscopic pore scale simulations. Consistent with the picture obtained in the simulations, the QENS data can be described using a (local) 3D diffusion at short observation times, whereas at sufficiently long observation times a 2D diffusive motion, as confined by interlayer surfaces, is clearly observed. The effects of tortuosity measured in macroscopic tracer diffusion experiments are in qualitative agreement with RW simulations. By using experimental data to calibrate molecular and mesoscopic theoretical models, a consistent description of water mobility in clay minerals from the molecular to the macroscopic scale can be achieved. In turn, simulations help in choosing optimal conditions for the experimental measurements and the data.

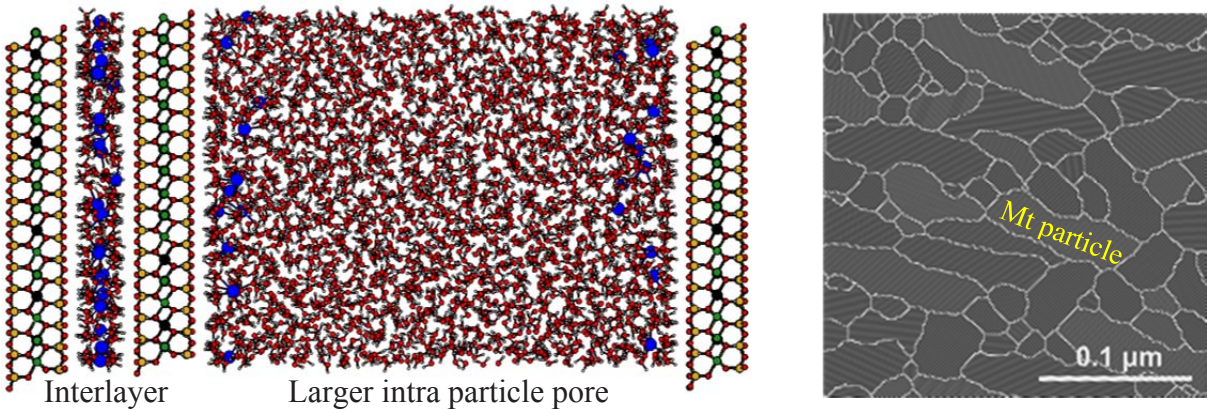


Figure 1. Left: A snapshot from molecular dynamic simulations of Na-Mt with an interlayer and a larger intra particle pore. Na-ions are shown as blue spheres. Right: A fragment of 2D model for pore network in the Mt rock used for random walk simulations of water transport. Mt-particles include interlayer pores parallel to the major grain axis.

References:

[1] Brigatti, M.F., Galan, E., Theng, B.K.G., 2006. Structures and mineralogy of clay minerals. In: Bergaya, F., Theng, B.K.G., Lagaly, G. (Eds.), Handbook of Clay Science. Elsevier, pp. 19–86.
[2] Segad, M., Jonsson, B., Akesson, T., Cabane, B., 2010. Ca/Na montmorillonite: structure, forces and swelling properties. Langmuir 26, 5782–5790.
[3] Holmboe, M., Wold, S., Jonsson, M., 2012. Porosity investigation of compacted bentonite using XRD profile modeling. J. Contam. Hydrol. 128, 19–32.
[4] Churakov, S. V., Gimmi, T., Unruh, T.,Van Loon, L.R., Juranyi, F. (2014). "Resolving diffusion in clay minerals at different time scales: Combination of experimental and modeling approaches." Appl. Clay Sci.. 96, 36-44.

Piping and erosion in 1:6 scale tests simulating the saturation of the bentonite buffer in Olkiluoto KBS-3V repository

Teemu Laurila[1], **Elisa Rautioaho**[1], **Petri Sane**[1], **Xavier Pintado**[1], **Kari Koskinen**[2]

[1] B+Tech Oy, Laulukuja 4, 00420 Helsinki, Finland
[2] Posiva Oy, Olkiluoto, Finland
correspondence: teemu.laurila@btech.fi

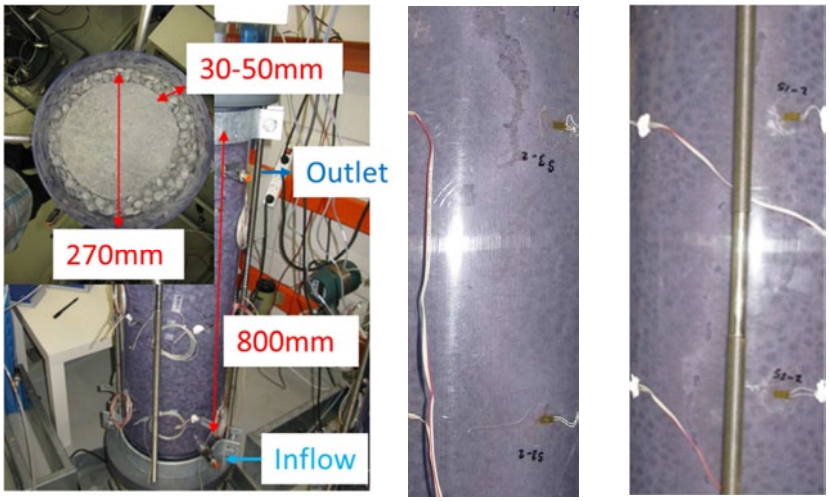


Figure 1. Picture of the test setup (transparent cell), and visual observations of piping channels within the pellet filling. Left hand side piping channel is at 10 g/l salinity and right hand side at 1 g/l.

Laboratory tests are performed to simulate the beginning of the saturation phase of the bentonite buffer in a KBS-3V deposition hole in Olkiluoto. Inflow is from a point-like inlet and the rate corresponds to the highest flow allowed in one deposition hole for Olkiluoto KBS-3V (**0.1 l/min**). Piping and erosion are observed in all tests. The water pressure required to maintain the flow is in the range of 10-100 kPa, while the measured radial swelling pressure range is an order of magnitude higher (Bendito 2014). The erosion rate is measured as clay content of the outflow by sampling the flow and oven drying. The measured erosion rate is found to have large scatter, but the average remains a constant that does not depend on time as saturation progresses, properties of the pellet filling, or salinity of the inflow (Figure 2). An outflow solid content of **0.2 ± 0.1 g/l** is obtained. The data is adequately explained by the normal distribution, which justifies taking the average over measurements at different times and different tests (Figure 3).

Cylindrical MX-80 blocks (dry density 1.8 ± 0.1 g/cm^3, water content 16.5 ± 0.5%) are used to simulate buffer blocks. Tests are performed in steel cells of diameter 350mm and transparent plastic cells of diameter 270mm. The gap around the blocks is filled with two different types of MX-80 pillow pellets, or left unfilled. Salinity of the inflow is varied using Posiva reference solutions for Olkiluoto (1 g/l and 10 g/l TDS, with NaCl : $CaCl_2$ mass ratio of 5.1:1 and 1.8:1, respectively). The tests are tabulated in Table 1, and reported in detail in (Pintado 2012).

A markedly constant erosion rate is observed between tests (Table 1) and the erosion keeps constant as the saturation progresses in time (Figure 2). By visual observation, piping channels at higher salinity tend to be wider and contain more detritus material (Figure 1). In the test without pellets, the channel is also wider. Interestingly the changes in channel morphology are not seen to affect the erosion rate.

The process of measuring clay in the outflow is prone to scatter because the samples contain overwhelmingly more salt than clay, and the sum of salt and clay is obtained by drying the sample. The salt is subtracted by taking a reference sample from the inflow.

Table 1. List of the tests and conditions. Average measured erosion for each test is given.

test type	duration (h)	pellet slot (mm)	pellets	inflow salinity (g/l)	average erosion (g/l)
transparent	678	29,5	SKB pillow	1	0.18±0.03
transparent	3143	29,5	SKB pillow	10	0.16±0.05
transparent	2726	29,5	None	1	0.14±0.02
transparent	2664	49,5	Posiva pillow	1	0.23±0.02
transparent	2736	49,5	Posiva pillow	10	0.19±0.04
steel cell	4690	30	SKB pillow	10	0.17±0.05
steel cell	4690	30	SKB pillow	1	0.18±0.09

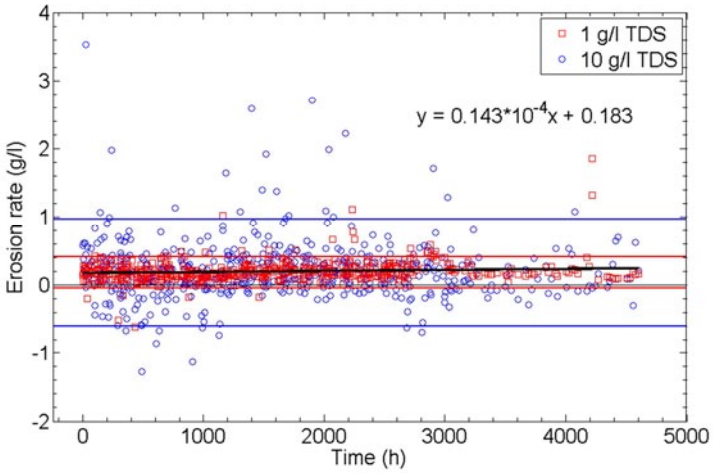


Figure 2. Measured erosion rate as outflow solid concentration in all 7 tests. The average is shown as the black line. Outlier limits for 10 g/l and 1 g/l inflow salinities are shown as coloured lines.

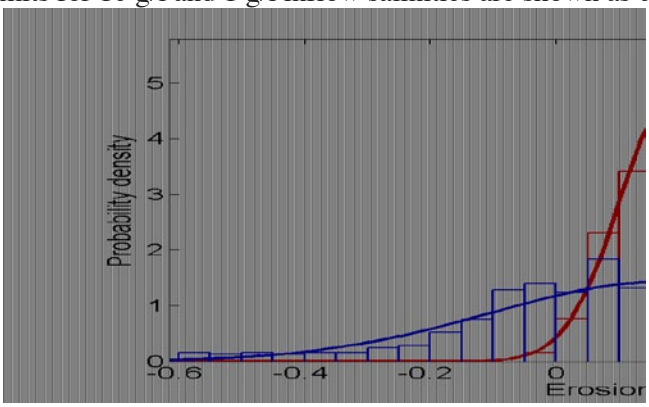


Figure 3. Probability distribution histograms for the erosion rates for the two salinities. Outliers are excluded and normal distributions are fitted.

Outliers are identified with 1.5 times the interquartile range. With outliers excluded, the erosion data for each inflow salinity is adequately fit by the normal distribution (Figure 3). Outliers in the erosion data are more frequent than the normal distribution predicts. It is not known whether this long tail reflects the reality of the erosion process, or is caused by the method of measuring.

Piping erosion rate in pellets without the blocks has been observed to decrease in time (Sanden 2010). The constant erosion in our tests could be caused by the saturation and swelling of the compacted block maintaining local bentonite density near the piping channel.

References

Bendito E., Pintado X. Env. Geotech. **2014** (in review) *Swelling pressure determination in plastic cells*
Pintado X. et al. Posiva Working Report **2012**-100. *Downscaled Tests on Buffer Behaviour*
Sandén T., Börgesson L. SKB Report **2010**-70. *Early effects of water inflow intoa deposition hole*

THE IMPACT OF GLACIAL FLUID INVASION ON VERTICAL ADVECTIVE AND DIFFUSIVE PROCESSES IN THE THICK ORDOVICIAN LIMESTONES AND SHALES OF THE EASTERN MICHIGAN BASIN

Omar A. Khader and Kent Novakowski*

Civil Engineering Department, Queen's University, Ellis Hall, Kingston, ON, K7L 3N6, Canada
* Corresponding Author (kent.novakowski@queensu.ca)

In several recent studies of glacial impact on the sedimentary basins of North America, lateral migration of glacial fluid in the permeable horizons of the stratigraphy at the basin margins has been recognised as a potentially significant process in the redistribution of fresher water into primarily saline formations (Wittrup and Kyser, 1990; Grasby et al., 2000; Person et al., 2012). This process is driven by the massive hydraulic gradients imparted via wet-based ice sheets through surface exposure of the permeable units. In conjunction with substantial loading from the weight of the ice sheet, complex and potentially repetitive geochemical signatures are applied to the upper and lower boundaries of intervening aquitards in the stratigraphic sequence.

In this study we use numerical simulations of the $\delta^{18}O$ and $\delta^{2}H$ profiles collected during the characterization of the proposed Bruce Deep Geological Repository site on the eastern edge of the Michigan Basin to explore the impact of glacial fluid migration and glacial loading on thick Ordovician shale and limestone sequence of very low hydraulic conductivity bounded above and below by permeable features. The entire sedimentary sequence has a thickness of 860 m at this location and the permeable horizons that bound the shale/limestone are identified in a Cambrian aquifer at the Precambrian contact, and in the Guelph formation at a depth of 320 m. Hydraulic conductivity in the limestone/shale sequence ranges from 8×10^{-15} m/s to 5×10^{-12} m/s. Porosity ranges from <1% to approximately 11%, with the majority of units in the 1-3% range. Notably, present day environmental head measurements indicate a significant underpressure of -350 m in the centre of the low permeability limestone/shale, and an artesian environmental head in excess of +100 m in the underlying Cambrian sandstone aquifer. The development of these pressures has been explained by hydromechanical modeling of the glacial loading cycles (Khader and Novakowski, 2014a).

To conduct the simulation of the isotope profiles, a three-dimensional FE model, *HydroGeoSphere*, was used. The solution domain was constructed as a 3-D column having 1 m by 1 m elements, 10 by 10 on a side in the horizontal plane with each layer 1 m in thickness to a depth of 860 m. Considerable effort was expended to ensure that the discretization and time steps utilized produced accurate and representative results. To explore the origin and evolution of the resident fluids, we performed a series of pure-diffusion and advection-diffusion simulations using a variety of concentration boundary conditions for solute transport. The measured environmental heads were used as the driving force for advection. In order to match the observed profiles, initial conditions were established and specific combinations of boundary conditions applied over 5-100 Ma. The boundary conditions were

applied at the permeable formations and were intended to simulate changes in water origin at specific times relating to potential glacial fluid intrusion. Four end members for mixing were applied including compositions representing present day meteoric water, deep basin brine, Precambrian brine, and glacial water.

The results show that under the flow gradients observed at the present time, advection cannot be neglected as a solute transport process. The advection term improves the fit of the model results to the measured natural isotope compositions primarily adjacent to the highly-permeable Cambrian aquifer and the discrete horizons in the Silurian formations. The simulations also substantiate the hypotheses that younger fluids likely driven by glacial pressures have invaded all of the permeable horizons over the last 2.5 Ma and in particular the upper formations during the last 100 ka. In the Cambrian aquifer the direction of flow of this fluid has reversed and older fluid began migrating back towards the basin margin at 50 ka. These results have been substantiated by independent density-dependent simulations of solute transport conducted using a full-basin model (Khader and Novakowski, 2014b).

References

Grasby, S.E. and Betcher, R., 2000. Pleistocene recharge and flow reversal in the Williston basin, central North America. Journal of Geochemical Exploration, 69-70: 403-407.

Khader, O. and Novakowski, K., 2014a. Impacts of Pleistocene glacial loading on abnormal porewater pressure in the eastern Michigan Basin. Geofluids (2014), doi: 10.1111/gfl.12074.

Khader, O. A., and Novakowski, K., 2014b. Resolving the Timing of Freshwater Invasion in the Michigan Basin as Identified Using Natural Tracers: Building the Safety Case for the Deep Geological Repository in the Bruce Peninsula. Canadian Nuclear Safety Commission Report Con. #87055-12-0320, 42 pp.

Person, M., Bense, V., Cohen, D., and Banerjee, A., 2012. Models of ice-sheet hydrogeologic interactions: a review. Geofluids (2012) 12: 58–78.

Wittrup, M.B. and Kyser, T.K., 1990. The petrogenesis of brines in Devonian potash deposits of western Canada. Chemical Geology, 82: 103-128.

Modelling radionuclide transport through a layered porous medium: Analytical analysis to guide simplifications

Mohamed Hayek[1], **Gerhard Mayer**[1], **Andreas Poller**[2]

[1]AF-Consult Switzerland Ltd, Baden, Switzerland
[2]National Cooperative for the Disposal of Radioactive Waste (Nagra), Wettingen, Switzerland

In Switzerland, the Nuclear Energy Act requires the disposal of all radioactive waste in deep geological repositories. In a first stage of the Swiss site selection process, Nagra proposed several geological siting regions for different repository types based on criteria relating to long-term safety and engineering feasibility.

The geological barrier has a layered structure in most of the geological siting regions. For the purpose of radionuclide transport modelling, layering on a small scale is usually conceptualized as an alternating sequence of different porous materials, each having homogeneous transport properties. If the modelling of each member of that sequence results in an overly detailed radionuclide transport model, the alternating sequence of materials may be re-arranged to form a single sequence.

In order not to underestimate radiological consequences, a general condition is derived for a single radionuclide to evaluate which order of materials in the rearranged single sequence yields the largest maximum radionuclide flux. The derived condition depends on key transport properties of the individual materials with respect to the considered radionuclide (accessible porosity, diffusion/dispersion coefficients and sorption coefficient). The condition is generalized for a fractured system with matrix diffusion. In this case, the condition depends on key transport parameters of both the fractures and the matrices, as well as on the decay constant of the radionuclide.

An improved model for through-diffusion experiments: application to Sr diffusion in Boom Clay and compacted illite

M. Aertsens, **L. Van Laer, N. Maes, J. Govaerts**

Institute for Environment, Health and Safety, Belgian Nuclear Research Centre, SCK•CEN, Boeretang 200, B-2400 Mol, Belgium (marc.aertsens@sckcen.be)

In Belgium, clay formations are studied as potential host formations for final disposal of high-level and/or long-lived radioactive waste. In Boom Clay, transport is dominated by diffusion. In order to evaluate the performance of the Boom Clay as a barrier, the values of the parameters determining the diffusive flux in clay are needed: (1) the capacity factor ηR, which is the product of the diffusion accessible porosity η and the retardation factor R, and (2) the apparent diffusion coefficient D_{app}.

Several types of experiments exist to determine these transport parameters in clay (Aertsens et al., 2008). For this paper, through-diffusion experiments were performed to measure the Sr transport parameters in Boom Clay and compacted, purified Na-illite which serves as model component for Boom Clay. In a through-diffusion experiment, a clay core is confined between two well mixed water compartments. Initially, tracer is added to the inlet compartment, from where it diffuses through the clay towards the outlet compartment. Between the clay and both water compartments, confining filters are needed to prevent the swelling and disintegration of the clay core.

Originally, through-diffusion experiments were performed while maintaining a constant tracer concentration in the inlet compartment and a zero concentration outlet compartment (e.g. by regularly replacing both reservoirs). In this way, a steady state can be reached, allowing to determine with simple mathematical expressions the migration parameters (Takeda et al., 2008). Maintaining a constant tracer concentration (CC) is experimentally cumbersome, and therefore this method, called CC-CC (Constant Concentration inlet, CC outlet, Takeda et al., 2008) has become obsolete. It is also possible to extract the transport parameters, by using variable concentration (VC) conditions (Takeda et al., 2008). In the VC-VC setup, in both water compartments the concentration changes according to the diffusive flux into (inlet) or out of (outlet) the clay. Hybrid forms of these set-ups are possible as well: (*i*) a variable inlet concentration with a zero outlet concentration (VC-CC), and (*ii*) a constant inlet concentration with a variable outlet concentration (CC-VC). The analytical solutions for these four cases are summarized in (Takeda et al., 2008).

Apart from one VC-VC experiment, the through-diffusion experiments discussed in this paper are an intermediate between the VC-CC and the VC-VC types. The concentration in the inlet compartment decreases according to the diffusive flux into the clay, and the outlet compartment is regularly replaced by a zero concentration solution. Although, at the end of a measurement, the concentration in the outlet compartment is sometimes too high (with respect to the inlet concentration) to be approximated by a constant zero concentration. Therefore, a new model was developed (*i*) taking explicitly into account the concentration increase at the outlet during a measurement, and (*ii*) after each measurement, the outlet concentration is put to zero again (see Figure 1). This model is numerically solved with the COMSOL package.

In line with previous percolation experiments (Aertsens et al., 2009), the apparent diffusion coefficients for Sr in Boom Clay are in the range 7×10^{-12} to 1.1×10^{-11} m^2/s. In illite, these values are similar (average 1.2×10^{-11} m^2/s). The capacity factor ηR typically lies between 100 and 200 in illite. In Boom Clay, higher values are obtained (900 to 7000).

Because model predictions are valid only if the basic assumptions of the model are correct, a new Through-Diffusion model was developed. This model is generally valid, but needs to be used in case

the measured/predicted outlet concentrations are not negligible with respect to the inlet concentrations. The parameter values predicted by the new model are consistent with previously measured values in other types of experiments.

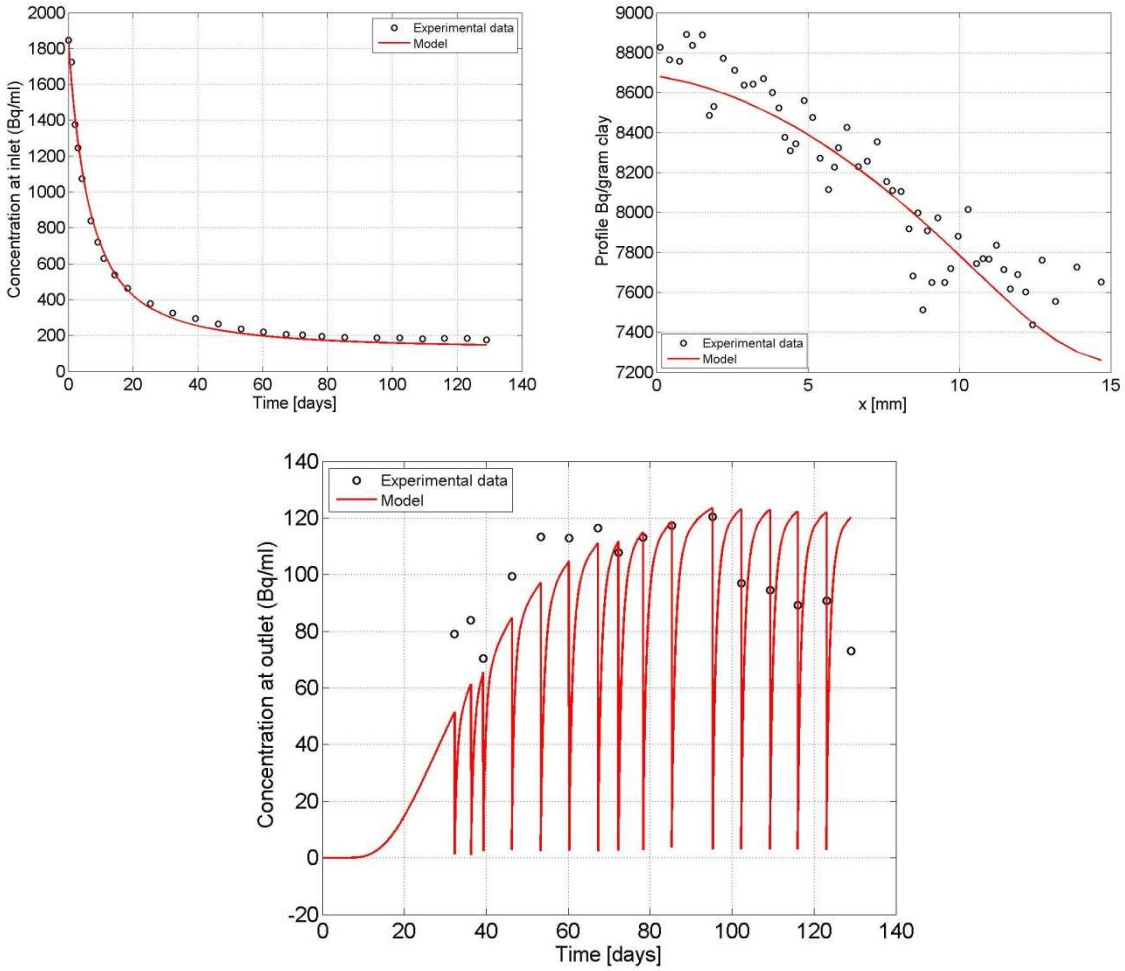


Figure 1: Experimental data and model prediction of Sr diffusion in illite ($NaClO_4$ 0.1 M – pH 7) obtained by fitting simultaneously (*i*) the evolution of the inlet concentration (left above), (*ii*) the evolution of the outlet concentration (below), and (*iii*) the tracer profile in the clay core (right above, note that the y-axis starts at 7200 Bq/g clay).

Acknowledgement

The research leading to these results has received funding from the EURATOM 7th Framework Programme FP7/2007- 2011 under grant agreement n° 249624 (CATCLAY project) and from ONDRAF/NIRAS, the Belgian Agency for Radioactive Waste and Fissile Materials.

References

Aertsens M., De Cannière P., Lemmens K., Maes N., Moors H., Overview and consistency of migration experiments in Clay, Phys. Chem. of the Earth, Vol. 33, p. 1019-1025, 2008.

Aertsens M., Maes N., Van Gompel M., Consistency of the strontium transport parameters in Boom Clay obtained from different types of migration experiments, in Scientific Basis for Nuclear Waste Management, ed. Burakov B., Aloy A., Mat. Res. Soc. Sump. Proc., Vol. 1193, p. 421-428, 2009.

Takeda M., Nakajima H., Zhang M., Hiratshuka T., Laboratory longitudinal diffusion tests: 1. Dimensionless formulations and validity of simplified solutions, J. Cont. Hydrology, Vol. 97, p. 117-134, 2008.

Study of ^{85}Sr transport through a column filled with crushed granite in presence of bentonite colloids

K. Videnská[1,2], **R. Červinka**[1], **V. Havlová**[1]

1. ÚJV Řež, a. s., Fuel Cycle Chemistry Department, Hlavní 130, Řež, 250 68 Husinec, Czech Republic (katerina.videnska@ujv.cz)
2. Department of Analytical Chemistry, Institute of Chemical Technology, Prague 6, 166 28 Prague, Czech Republic

The formation and stability of clay colloids, being form with engineered barrier system of deep geological repository for radioactive waste may have a direct impact on safety due two main aspects: generation of colloids may degrade the engineered barrier and colloid transport of radionuclides may reduce the efficiency of the natural barrier.

The presented work is focused on study of strontium ^{85}Sr transport through crushed granite column in presence of bentonite colloids under dynamic arrangement. The main aim of the experiments was to compare the strontium behaviour itself and strontium + colloids behaviour passing through crushed granite column and quantification the effect of bentonite colloids presence on tracer migration (mobilization/immobilization).

The migration experiments were investigated under aerobic conditions in the column set-up. The granite used for column infill originated from the depth 97.5-98.7 m (Melechov massif, Czech Republic). The rock was crushed and sieved into defined fractions. The fraction 0.125-0.63 mm was used for presented experiments. The crushed granite was placed into 5 cm^3 plastic columns.

First the column properties were evaluated by non-sorbing tracer ^{3}H. Then column experiment with bentonite colloids only was performed. Followed migration of ^{85}Sr solution was studied. Finally the very last experiment was focused on the transport of strontiun all together with bentonite colloids suspension (radiocolloidal form). The inlet of liquid phase into column was continuous with constant colloid concentration, strontium concentration and flow rate of liquid phase. Defined volumes of liquid phase were sampled in periodic time intervals at the column outlet for the measurement of colloids concentration and strontium activity. The transport of studied tracers through crushed granite was finnally drawn out as breakthrough curves.

The following solutions were used as liquid phase in the experiments: the bentonite colloid suspension (c = 100 mg/l), the $SrCl_2$ solution ($c = 10^{-6}$ mol/l) spiked by ^{85}Sr in distilled water and the radiocolloid suspension, consisting of bentonite colloids (c = 100 mg/l) and $SrCl_2$ solution ($c = 1 \cdot 10^{-6}$ mol/l) spiked by ^{85}Sr. The purified commercial bentonite product "Bentonite 75", denoted as B75 in Na^+ form, was used for clay colloid preparation. Initially the mean hydrodynamic size of bentonite particles in suspension was about 500 nm (measured by photon cross correlation spectroscopy).

The results of dynamic experiments showed totally different behaviour of strontium and colloid particles during transport through crushed granite. The breakthrough curves are displayed in Fig. 1. The experimental breakthrough curves were fitted by CXTFIT Code (STANMODE, version 2.08). The input parameters were flow velocity v, dispersion coefficient D and retardation coefficient R. For initial estimate we used their experimental values and the values of v and D were fitted by CXTFIT Code.

The number of pore volume n_{PV} is on x-axis, the relative concentration (activity) c_{rel}, A_{rel} measured at outlet of column is on y-axis. The transport of colloids (×) was fast, without retardation, being comparable with behaviour of conservative, non sorbing tracer ^{3}H (▲). The column experiment with strontium without presence of bentonite colloids showed strong strontium sorption on granite, reaching break through after almost two months (-). Experiment with radiocolloid suspension showed that the bentonite colloids (■) passed through crushed granite during first 24 hours and left the strontium sorbed in the rock column (♦). The most probable reason is that the sorption potential of granite material was higher than the interaction forces between strontium and bentonite colloids (ion

exchange). The observed retention of strontium on granite suggests higher affinity of strontium towards granitic rock than towards bentonite colloids and showed the reversibility of the sorption of strontium on bentonite colloids. However, the strontium transport in presence of colloids was faster (20 days) than without the bentonite colloids (compare ♦ and -).

Affinity of granite towards strontium was studied in additional static batch experiments. The aim of static experiments was to estimate the extent of strontium sorption on individual minerals (especially mica mineral muscovite) of crushed granite. The crushed granitic rock itself and segregated muscovite were used as solid phases. The experiments were carried out with 10^{-6} mol/l solution of $SrCl_2$ spiked by ^{85}Sr in distilled water. The muscovite was considered as a possible dominant sorbent of strontium in granitic material. However this assumption was not confirmed, the results showed higher sorption of strontium on granite (K_d = 30 ml/g) than on muscovite (K_d = 20 ml/g).

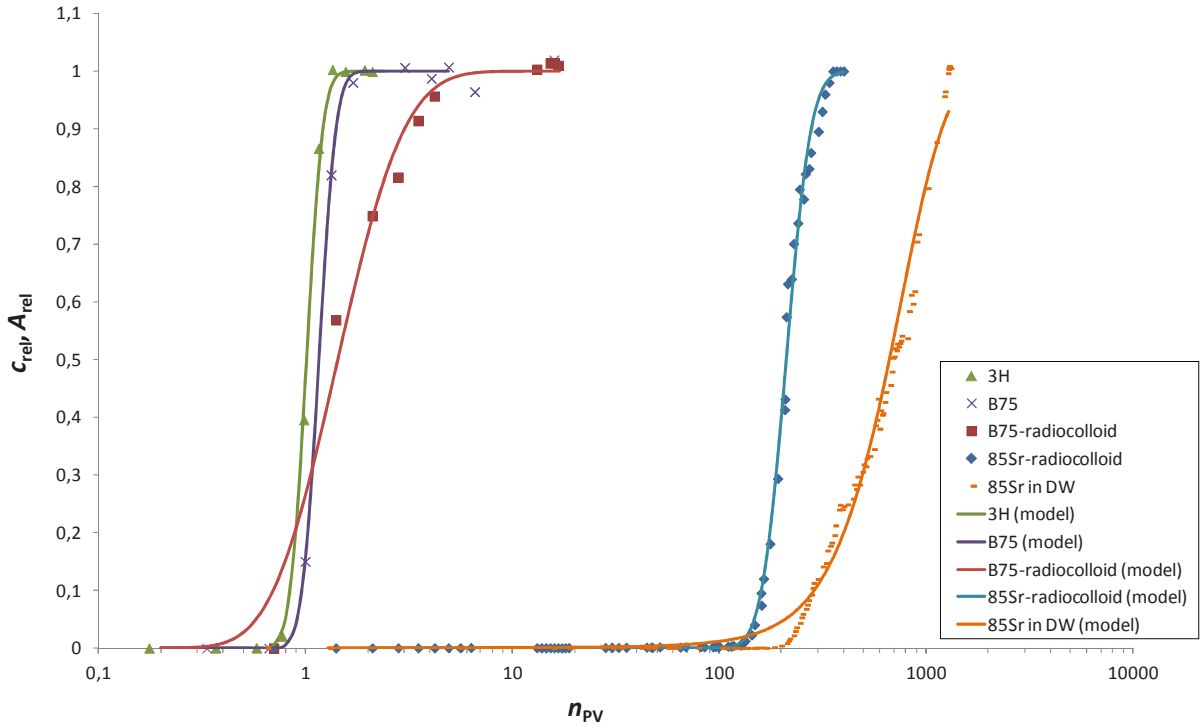


Fig. 1. The experimental (points) and theoretical (lines) breakthrough curves of strontium transport through crushed granite under different conditions (see explanation in the text).

Acknowledgment:

The research leading to these results has received funding by the European Atomic Energy Community's Seventh Framework Programme (FP7/2007-2011) under grant agreement 295487 – project BELBaR and by SÚRAO (CZ).

References:

Toride N., Leij F.J., van Genuchten M.Th. (1995). The CXTFIT Code for Estimating Transport Parameters from Laboratory or Field Tracer Experiments, version 2.0. Research Report No. 137, U.S. Department of Agriculture, Riverside, California.

U(VI) diffusion as a function of bentonite bulk density: Results from a 6-year study

C. Joseph[1], **J. Mibus**[2*], **P. Trepte**[2§], **C. Müller**[2], **V. Brendler**[2], **A.B. Kersting**[1], **M. Zavarin**[1]

[1] Glenn T. Seaborg Institute, Physical & Life Sciences Directorate, Lawrence Livermore National Laboratory, L-231, P.O. Box 808, Livermore, CA 94550, USA (corresponding author: joseph20@llnl.gov)
[2] Helmholtz-Zentrum Dresden-Rossendorf e.V., Institute of Resource Ecology, P.O. Box 510119, 01314 Dresden, Germany
[*] present address: Nagra, Hardstrasse 73, CH-5430 Wettingen, Switzerland
[§] present address: LSI Sachsen GmbH & Co. KG, BioInnovationsZentrum Dresden, Tatzberg 47, 01307 Dresden, Germany

To guarantee the safe enclosure of high-level nuclear waste in a repository in deep geological formations, a complex barrier system is proposed to keep the waste isolated from the surrounding biosphere. The argillaceous rock, bentonite, has been discussed as potential backfill material which can have different densities in a repository depending on the level of confinement. Uranium in the form of spent nuclear fuel will represent a main component of the stored high-level radioactive waste. For safety assessment it is essential to investigate how uranium that is ultimately released from the nuclear waste interacts with the backfill material. Besides the process of sorption, molecular diffusion will be important in the retardation of uranium. The bentonite density affects the diffusion-accessible pore space or effective porosity, ε_{eff}, of a migrating radioactive species. The ε_{eff} is also influenced by the properties of the diffusing species (charge, size) and the background electrolyte (degree of salinity, type of ions). Thus, bentonite bulk density can have a significant influence on the diffusive transport of species in a repository.

In this study, over a six year period we investigated the diffusion of $^{238}U(VI)$ (c_0 = 1×10^{-6} M) in bentonite (MX-80) at three different bulk densities: 1.3 g/cm^3, 1.6 g/cm^3, and 1.9 g/cm^3. The experiment was conducted under aerobic conditions at room temperature using a well-known set-up developed by Van Loon and Soler (2004). The background electrolyte was a synthetized model pore water (Van Loon et al., 2005). Its composition differed slightly depending on clay density (pH 8, I = 0.3 M). After stopping the experiments, the uranium diffusion profiles were determined applying the abrasive peeling technique (Van Loon and Eikenberg, 2005). Within six years the added $^{238}U(VI)$ diffused between 2 mm (at 1.3 g/cm^3) and 0.8 mm (at 1.9 g/cm^3) deep in the clay. Based on the profiles, the diffusion parameters (effective diffusion coefficient, D_e; distribution coefficient, K_d; apparent diffusion coefficient, D_a) were determined using the CrunchFlow reactive flow and transport code (Steefel, 2011) and the PEST optimization code (Doherty, 2003).

Speciation calculations showed that the $Ca_2UO_2(CO_3)_3(aq)$ complex is the dominant species in solution (71-87%, depending on the bulk density). This complex is quite large as shown by extended X-ray absorption fine-structure spectroscopy (Bernhard et al., 2001). Possibly, the interlayers of the montmorillonite fraction in bentonite are not accessible for this complex as the diffusing species in contrast to diffusing HTO. It is supposed that $\varepsilon_{eff}(Ca_2UO_2(CO_3)_3(aq))$ is smaller than $\varepsilon_{eff}(HTO)$. In addition, previous U(VI) sorption experiments on Opalinus Clay showed the low sorption affinity of $Ca_2UO_2(CO_3)_3(aq)$ towards clay (Joseph et al., 2011). In this study, the K_d values determined by modelling the uranium diffusion profiles were lower compared to the majority of literature values (Torstenfelt and Allard, 1986, Wang et al., 2005) and decreased slightly with increasing density from $(5.8 \pm 0.6)\times10^{-3}$ m^3/kg at 1.3 g/cm^3 to $(2.6 \pm 0.8)\times10^{-3}$ m^3/kg at 1.9 g/cm^3. This behaviour could be attributed to changes in the U(VI) speciation (1.3 g/cm^3: $Ca_2UO_2(CO_3)_3(aq)$ (84%) and $UO_2(CO_3)_3^{4-}$ (13%); 1.9 g/cm^3: $Ca_2UO_2(CO_3)_3(aq)$ (71%) and $UO_2(CO_3)_3^{4-}$ (26%)). At 1.9 g/cm^3, a slightly higher fraction of $UO_2(CO_3)_3^{4-}$ was present, which does not sorb on the negatively charged clay.

The modelled D_e values decreased with increasing density. By using these values and the modelled K_d values, D_a values were calculated. Compared to literature D_a values of "short-term" experiments (most

of them were conducted for less than one year), the D_a values obtained from this long-term experiment are by two orders of magnitude lower (cf. Figure 1). Bentonite contains natural uranium (~13 ppm in these experiments). As a result, U(VI) was also detected in the receiving reservoir. The modelling of this U(VI) outflow led to D_a values which agree well with literature values (cf. Figure 1). What is the reason for these substantial different results for the inflow and outflow of U(VI)? An aging or redox process in the clay may have occurred which would hinder the further migration of uranium over time. Changes in porosity or pore connectivity within the clay could also be an explanation. Additional numerical and experimental analyses have to be performed to answer this question.

This study shows that in particular the long-term behaviour of U(VI) should be further investigated. However, it shows the excellent retention capacity of bentonite for weakly sorbing U(VI) species, since molecular diffusion is the decisive retardation process compared to sorption.

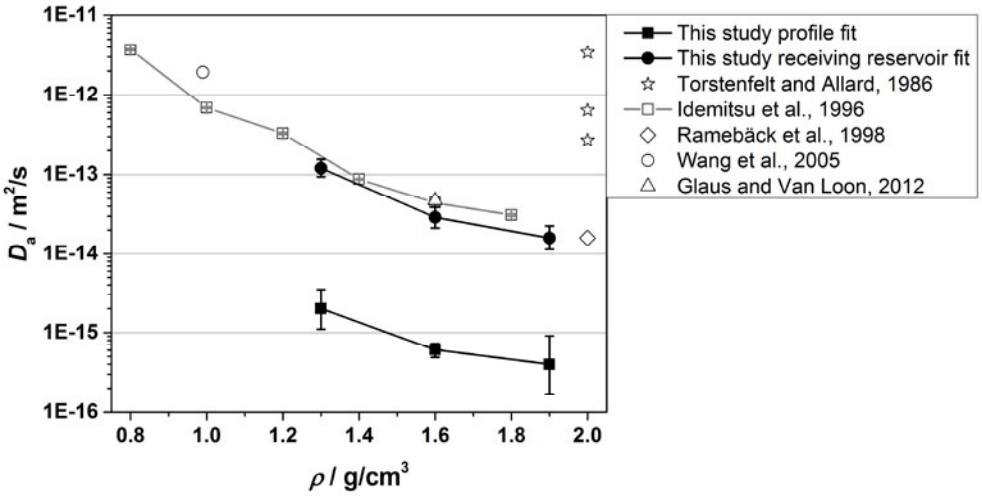


Figure 1: Comparison of apparent diffusion coefficient values (D_a) obtained in this study with literature values for the uranium diffusion in bentonite/montmorillonite in dependence on bulk density (ρ).

References:

Bernhard, G., Geipel, G., Reich, T., Brendler, V., Amayri, S., Nitsche, H. 2001. *Radiochim. Acta* 89(8), 511-518.
Doherty, J. 2003. PEST. Model-independent parameter estimation and uncertainty analysis.
Glaus, M.A., Van Loon, L.R. In Proceedings: *Clays in Natural & Engineered Barriers for Radioactive Waste Confinement - 5th International Meeting*, 22.-25.10.2012, Montpellier, Andra, 885-886.
Idemitsu, K., Tachi, Y., Furuya, H., Inagaki, Y., Arima, T. 1996. *Mater. Res. Soc. Symp. Proc.* 412(Scientific Basis for Nuclear Waste Management XIX), 683-690.
Joseph, C., Schmeide, K., Sachs, S., Brendler, V., Geipel, G., Bernhard, G. 2011. *Chem. Geol.* 284(3-4), 240-250.
Ramebäck, H., Skålberg, M., Eklund, U.B., Kjellberg, L., Werme, L. 1998. *Radiochim. Acta* 82, 167-171.
Steefel, C. 2011. CrunchFlow. Software for modeling multicomponent reactive flow and transport.
Torstenfelt, B., Allard, B. 1986. *SKB Technical Report 86-14*. Swedish nuclear fuel and waste management CO, Stockholm.
Van Loon, L.R., Eikenberg, J. 2005. *Appl. Radiat. Isot.* 63, 11-21.
Van Loon, L.R., Müller, W., Glaus, M.A., Baeyens, B., Bradbury, M.H. 2005. *NF-Pro Progress Report January 2004 – June 2005*. Paul Scherrer Institut, Villigen PSI.
Van Loon, L.R., Soler, J.M. 2004. *PSI-Bericht 04-03*. Paul Scherrer Institut, Villigen PSI.
Wang, X.K., Chen, C.L., Zhou, X., Tan, X.L., Hu, W.P. 2005. *Radiochim. Acta* 93(5), 273-278.

LLNL-ABS-659903. Prepared by LLNL under Contract DE-AC52-07NA27344. This work was supported by the Used Fuel Disposition Campaign of the Department of Energy's Nuclear Energy Program and the U. S. DOE Office of Biological & Environmental Sciences, Subsurface Biogeochemistry Research Program. Funding by the European Commission (Project NF-PRO under contract C2-ST-C-01) is gratefully acknowledged by HZDR.

Helium and argon vertical distribution in porewaters of the Eastern Paris Basin (Bure/Haute-Marne) : constraints on transport processes through the sedimentary sequence

P. Jean-Baptiste[1], **B. Lavielle**[2], **E. Fourré**[1], **T. Smith**[2], **M. Pagel**[3]

[1] LSCE, CEA-Saclay, Gif-sur-Yvette (France)
[2] CENBG, CNRS-Université de Bordeaux, Gradignan (France)
[3] IDES, CNRS-Université Paris-Sud, Orsay (France)

In 2008, as part of the ongoing project of high activity long-lived radioactive waste repository, a 2000-m deep borehole was drilled by the French Nuclear Waste Agency (Andra) in the Eastern Paris Basin, with the aim of gaining deeper insight into hydrogeological processes controlling solute transport through this sedimentary sequence of alternating aquitards and aquifers. In this context, geochemical tracers are powerful tools : the measured vertical chloride distribution was simulated with a 2-D advection-diffusion model [1] showing that, in addition to vertical diffusion, lateral advection in the aquifers plays a major role in transporting chlorine away from the study area. Helium concentrations have also been measured in porewaters along the borehole [2, 3]. Because helium input function (helium is produced by the radioactive decay of U and Th series) is chiefly different from that of chlorine, it represents an excellent alternative tracer to further constrain transport characteristics.

In the present study, we applied Rebeix et al.'s advection-diffusion model [1] to the case of helium with the appropriate source term for ^{4}He based on U-Th measured concentrations. $^{40}Ar/^{36}Ar$ data, which are available along the whole sequence, were also simulated, taking into account the high retentivity of the rocks with respect to argon.

Modelled and measured ^{4}He profiles are in good agreement, indicating that the transport parameters (groundwater residence time in the aquifers, formulation of the diffusion coefficient as a function of porosity, ...) used for the chlorine simulations are robust. $^{40}Ar/^{36}Ar$ simulations also give coherent results and confirm that most of the radiogenic ^{40}Ar remains trapped in the rock matrix.

In our presentation, we will show helium and argon results and give a detailed account of the modelling work.

[1] Rebeix R. et al. (2013). Chlorine transport processes through a 2000 m aquifer/aquitard system. Marine and Petroleum Geology 53, 102-116.

[2] Waber H.N. and Vinsot A. (2010). Unraveling solute fluxes across the aquitard-aquifer sequence in the Eastern Paris Basin: pore water tracer data from borehole EST433. In: Clays in Natural and Engineered barriers for radioactive waste confinement, 4th Int. Conf., 353-354 (abstract).

[3] Battani A. et al. (2011). Contribution of logging tools to understanding helium porewater data across the Mesozoic sequence of the East of the Paris Basin. Geochim. Cosmochim. Acta 75, 7566-7584.

THM Modelling of Onkalo - Radioactive Waste Disposal Project

Erdem Toprak[1], Sebastia Olivella[1], Xavier Pintado[2]

1 Escola de Camins, UPC, Barcelona, Spain 2 B+TECH Oy, Finland

The preliminary analyses of coupled THM processes in ONKALO have been published by POSIVA Oy (Toprak et al. 2013). In that report, the time required for the buffer to reach full saturation, the maximum temperature reached in buffer, deformations at the buffer-backfill interface and the buffer and backfill homogenization were analyzed.

In this paper, an additional modelling work on the backfill material is included. The backfill material refers to granular material used to fill the drift mainly. At present, Friedland clay is considered as one of the candidates. In order to investigate the hydro-mechanical behavior of Friedland clay, a series of laboratory tests are in progress at B+TECH laboratories. Two types of tests have been performed: oedometer tests and infiltration tests. These tests have been simulated using the finite element code Code_Bright using the constitutive model BBM (Alonso et al., 1990).

With regard to the hydraulic part of the analyses, the time required for full saturation is sensitive to vapor diffusion, advective water flow which depends on intrinsic permeability and retention curve of the various elements. Another fundamental issue is to determine relevant hydraulic boundary conditions at boundaries that are not far enough. This is also de case of temperature which was already identified in the previous simulations. In short, both temperature and liquid pressure cannot be fixed on relatively close boundaries.

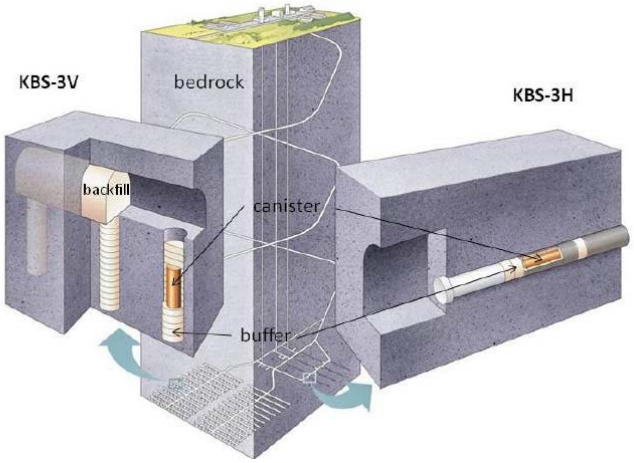


Figure 1-A. Alternative designs of the KBS-3 concept for the nuclear spent fuel disposal(In this study, it has been modeled vertical concept, KBS-3V)

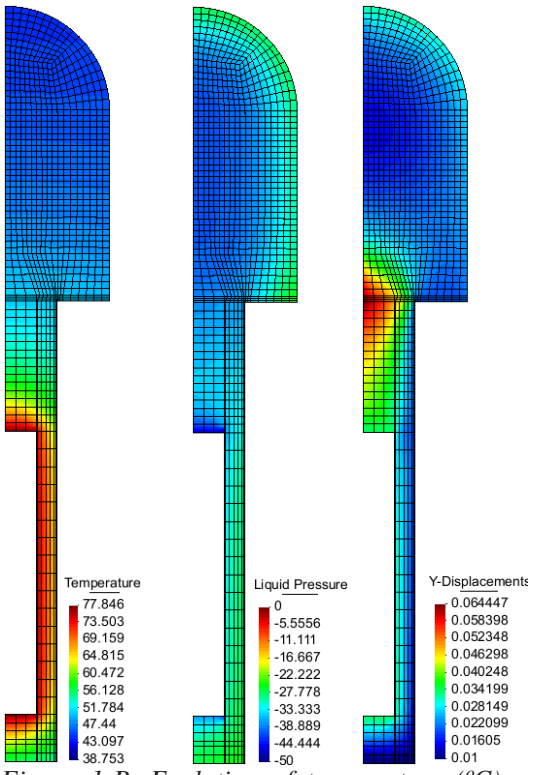


Figure 1-B. Evolution of temperature (ºC) (30 years), liquid pressure(MPa) (3 years) and vertical displacements (m) (100 years)

The study presented in this paper consists of the simulation of a disposal scheme which includes several clay based components of the EBS as it is shown in Figure 1-A. These components are referred to as: buffer components (bentonite blocks and pellets), backfill (several types of components), host rock and interfaces. The complete understanding of the THM response of the system requires calibration of the most appropriate constitutive equations for each of the components. These constitutive equations should cover not only mechanical effects but also hydraulic and thermal effects. For instance, an air gap between the canister (heat source) and the clay buffer may require the inclusion of the thermal radiation term as this element is initially full of air which has very low thermal conductivity. Double structure concept will be necessary to accurately model the clay based elements but these elements have different nature. In addition, the response to changes in water salinity should be taken into account.

Distribution of temperature, liquid pressure and vertical displacement are shown in Figure 1-B. The modeling process of buffer-backfill interface is an important part of tunnel backfill design. The calculations will aim to find out deformations at this intersection whose behavior is important for the buffer swelling. In order to investigate the hydro-mechanical behavior of MX-80 bentonite (buffer material), a series of laboratory tests are in progress at the laboratories of B+Tech Oy (Pintado et al., 2013) and modelling results of these tests have been given in Pintado and Rautioaho (2013) and Toprak et al. (2013). According to new data for backfill and pellets, the THM results achieved for buffer will be updated. To evaluate the influence of different parameters over system components, sensitivity analysis will be performed. Other analysis in KBS-3V concept can be found in Åkesson et al. (2010).

It should be noted that this study includes some assumptions and simplifications, such as 2D axisymmetric modeling. There are several alternatives for the engineered materials (bentonite blocks, granular material and pellets) that are going to be considered in the repository. Therefore, some parameters of these materials should keep handling through sensitivity analyses as a future work.

References

Åkesson, M., Börgesson, L., Kristensson, O. (2010). THM modelling of buffer, backfill and other system components. Updated 2013-12. SKB TR-10-44. Stockholm. Sweden.

Alonso E.E., Gens A and Josa A, 1990."A constitutive model for partially saturated soils". Géotechnique, 40(3): 405-430

Hokmark. Harald. October 2003. Hydration of the bentonite buffer in a KBS-3 repository. Clay Technology AB, Ideon Research Centre, 223 70 Lund, Sweden

Ikonen, Kari. June 2003. Thermal Analyses of Spent Nuclear Fuel Repository

Pintado, X., Rautioaho, E. (2013). Thermo-Hydraulic Modelling of Buffer and Backfill. Posiva Report 2012-48. Eurajoki. Finland.

Pintado, X., Hassan, Md, Martikainen, J. (2013). Thermo-Hydro-Mechanical Tests of Buffer Material. Posiva Report 2012-49. Eurajoki. Finland.

Toprak Erdem, Nadia Mokni, Sebastia Olivella, August 2013. POSIVA 2012-47: Thermo-Hydro-Mechanical Modelling of Buffer, Synthesis Report

Perturbing a field diffusion experiment: The DR-A test at the Mont Terri Underground Rock Laboratory (Switzerland)

T. Gimmi[1,2], O.X. Leupin[3], J.M. Soler[4], L.R. Van Loon[1], J. Eikenberg[1], M.A. Glaus[1], H.N. Waber[2], W. Pfingsten[1], M. Xie[5], K.U. Mayer[5], C.A.J. Appelo[6], C.I. Steefel[7]

[1] Paul Scherrer Institut, CH-5232 Villigen, Switzerland
[2] Institute of Geological Sciences, University of Bern, CH-3012 Bern, Switzerland
[3] Nagra, CH-5430 Wettingen, Switzerland
[4] IDAEA-CSIC, E-08034 Barcelona, Spain
[5] University of British Columbia, Earth, Ocean and Atmospheric Sciences, Vancouver, BC V6T 1Z4, Canada
[6] Valeriusstraat 11, 11071 MB Amsterdam, The Netherlands
[7] Lawrence Berkeley National Laboratory, Berkeley, CA 94720, USA

Diffusion and sorption parameters for cations, anions and neutral tracers are important when assessing the performance of engineered or natural clay barriers. These parameters are mostly obtained in small-scale laboratory experiments and then verified in larger-scale field experiments. For both types of experiments, the rock is brought into contact with an artificial pore water (APW) that contains a tracer cocktail. In most experimental setups, one tries to match the artificial pore water as closely as possible—regarding the concentrations of the main ions—with the estimated composition of the *in situ* pore water. Under these conditions, the diffusion of individual tracers can be observed in the absence of any significant gradients in the pore water chemistry (e.g., Palut et al. 2003; Wersin et al., 2008; Gimmi et al., 2014). While this approach is suited for obtaining sets of well-defined parameters, it does not allow for testing the predictive capabilities of reactive transport codes that can simulate the inherently coupled transport of different ions. The latter can only be done if the pore water chemistry varies in time and space, for instance as a result of an external perturbation.

The field diffusion and retention experiment DR-A in the Mont Terry Underground Rock Laboratory (Switzerland) was performed with this idea in mind. The DR-A experiment aimed at providing insight into the coupled transport and sorption processes of cations and anions and at testing the capabilities of reactive transport models. The design of the experiment was based on established setups. An artificial pore water containing a suite of tracers was circulated through a 1-m screened borehole interval (injection interval) from where the tracers diffused into the rock. The tracers included HTO, I^-, Br^-, Cs^+, $^{85}Sr^{2+}$, $^{60}Co^{2+}$ and Eu^{3+}. The initial composition of the APW was chosen to match the local *in situ* geochemical conditions as closely as possible. After 6 months of tracer diffusion, the APW was exchanged by a high-salinity solution containing the tracers at the same concentrations as measured just before the exchange. The ionic strength of the new APW was about three times higher compared to the original one and contained an increased fraction of K^+. The strong geochemical perturbation was expected to provoke responses in the pore water concentrations that could be observed within the circulated borehole solution, as well as in the exchanger composition on the rock surfaces. The time evolution of the tracer concentrations within the circulated solution was determined by regular sampling. After 2 years, the experiment was stopped and the injection interval was overcored. The concentrations of tracers and other ions were determined along several radial profiles.

The first 6 months of the experiment were characterized by a decrease of the various tracers in the circulated injection solution resulting from both diffusion and sorption processes, as expected based on similar earlier experiments. Following the high ionic strength perturbation and the increase in the K^+ content, the Cs^+ concentration within the circulated injection solution increased sharply before decreasing again. Concentrations of Ca^{2+}, Mg^{2+} and Sr^{2+} increased and later decreased more slowly, whereas Na^+ remained about constant and K^+ and Cl^- steadily decreased (Figure 1). The observations are interpreted as being the result of a displacement of Cs^+ and bivalent cations from the exchanger mainly by K^+. The interpretation is supported by the observed radial profiles of total cation concentrations, showing an increase in K^+ and a decrease in Ca^{2+} and Mg^{2+} towards the borehole

interface. Anions like I^- and Br^- appeared to decrease slightly faster in the circulated solution after the change in ionic strength as compared to the first six months. This may be related to an increase in the anion accessible porosity owing to the decrease of the DDL (diffuse double layer) thickness on the clay surface as the ionic strength of the pore water increases. But because HTO showed a similar trend, other reasons have to be considered as well.

The data are being modelled by different groups using codes with different functionalities. Step-wise comparisons starting with pre-defined parameter sets were performed to check the comparability of codes and model assumptions. Problems encountered are, among others, the conceptualization of the injection interval, notably of the small gap initially present between rock and installation equipment, and the coupling of anion and cation diffusion. Final simulations of the experiment, performed once the complete data will be available, will allow obtaining and verifying parameter sets for the different ions and tracers.

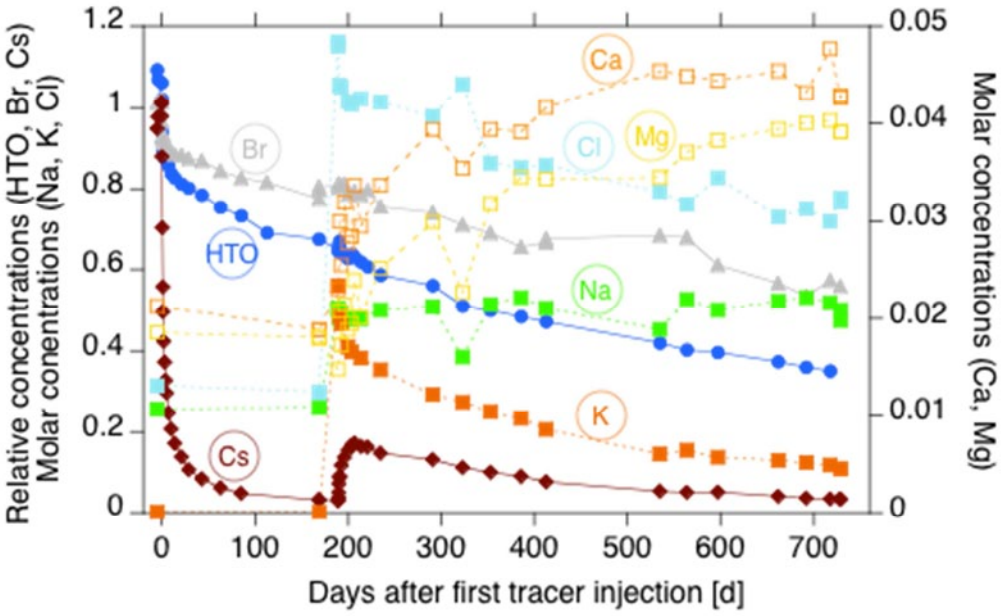


Figure 1. Time evolution of the relative concentrations of some of the tracers (HTO, Br^-, Cs^+), and of molar concentrations of some ions (Na^+, K^+, Cl^-, Mg^{2+}, Ca^{2+}) within the circulated solution (estimated uncertainties ±5 to ±10%).

References

Gimmi, T., Leupin, O.X., Eikenberg, J., Glaus, M., Van Loon, L.R., Waber, H.N., Wersin, P., Wang, H.A.O., Grolimund, D., Borca, C.N., Dewonck, S., Wittebroodt, C. (2014). Anisotropic diffusion at the field scale in a four-year multi-tracer diffusion and retention experiment - I: Insights from the experimental data. Geochimica et Cosmochimica Acta, 2014, 125, 373-393.

Palut J. M., Montarnal P., Gautschi A., Tevissen E. and Mouche E. (2003). Characterisation of HTO diffusion properties by an in situ tracer experiment in Opalinus clay at Mont Terri. J. Contam. Hydrol. 61, 203–218.

Wersin P., Soler J.M., Van Loon L., Eikenberg J., Baeyens B., Grolimund D., Gimmi T. and Dewonck S. (2008). Diffusion of HTO, Br□, I□, Cs+, Sr-85(2+) and Co-60(2+) in a clay formation: results and modelling from an in situ experiment in Opalinus Clay. Appl. Geochem. 23, 678–691.

Possibility of using bentonite clay and red clay as a barrier material for sealing of radioactive waste

Wioleta Olszewska, Agnieszka Miśkiewicz, Grażyna Zakrzewska – Kołtuniewicz

Institute of Nuclear Chemistry and Technology, Dorodna 16 03-195 Warsaw

Safety of radioactive waste is associated with their ability to isolate[1] radioactive materials and limiting[2] the entry of harmful pollutants into the biosphere. Each of radioactive waste repository is equipped with the system of barriers, which reduces the possibility of radionuclides release from the storage. Security systems may differ from each other depending on the type of repository. They consist of the natural geological barrier provided by the repository host rocks and its surrounding and an engineered barrier structure (EBS) [1].The overall concept of the construction of repository involves placing immobilized (solidified) waste in metal or concrete, chemically resistant canisters which are the first engineered barrier. Canisters are covered with a layer of clay (e.g. bentonite) and placed in a concrete construction site. Its closure is created with a multi-layer cover, which aims to reduce the migration of water, slowing the corrosion phenomena packaging and leaching of radioactive substances. Natural protective barrier is the geological structure of the area. This barrier determines the choice of the location of the landfill site. The suitable geological and hydrogeological conditions are intended to prevent the spread of radionuclides in soil and their penetration into the groundwater and surface water.

It is assumed that the metal canisters and the system of barriers adequately isolate the deposited waste from the biosphere. Even in the case of a leak, the layer of bentonite, due to its sorption and permeation properties is capable to stop the transport of radionuclides into the environment. Despite this, in the reason of long-term storage safety and long-term evaluation of its effectiveness, the most pessimistic scenarios are taken into consideration (e.g. gaping vessels and the release of radionuclides, which could migrate into the environment).

Natural sorbents (e.g. clay, bentonite or zeolites) are known as effective barriers that reduce the migration of radionuclides from radioactive waste repositories and contaminated sites. They could be used as buffer, backfill and sealing materials in the repository, and their presence in the host rock and the surrounding geological formations increases the retention properties of the strata [3]. Clay materials have a number of favourable properties, such as: low water permeability, homogeneity, ability to plastic deformation as well as self-sealing of fractures by swelling, and ability to retarding the migration of radionuclides[4].

In turn, the EBS may itself comprise a variety of sub-systems or components, such as waste forms, canisters, buffers, backfills, seals and plugs. The EBS plays a major role in providing the required disposal system performance[1].

The evaluation of the multi-barrier system is carried out after detailed tests to determine its parameters and after analysis, including mathematical modelling of contaminant migration.

Multi-barrier system and mathematical codes should be considered as a whole for assessing the safety of the repository. These two factors are the protection against the various black scenarios such as gaping tanks or the release of radionuclides to the environment.

It is important to prepare the relevant data necessary to formulate the initial and boundary conditions and to determine the values of the model coefficients. On the basis of information on the medium geometry, physico-chemical characteristics of fluid, it is possible to estimate the values of some coefficients (eg. resistance factor of water movement, mass dispersion coefficient, the speed of a chemical or physical processes). However, a sufficiently precise definition of these factors can be difficult. In such situations, it is necessary to conduct research in order to obtain results adequate to reality. The correct definition and evaluation of mechanisms affecting the migration of radionuclides is essential to carry out accurate calculations and estimates determining long-term safety of the planned repositories.

This paper describes research on the application of such argillaceous media as bentonite and red clay as potential host rocks for the radioactive waste disposal. Compacted bentonite or other clay-based material may additionally form part of the engineered barrier. A cycle of studies on the sorption

of aqueous solutions of cobalt ions on the bentonite clay and red clay have been performed. Namely, the kinetics of sorption of Co^{2+} ions in these sorbents as well as sorption isotherm were determined. Moreover, the effect of pH, reagent ratio and ionic strength on rate of the ions removal was examined. Additionally, the stability of cobalt ions sorption was examined by eluting samples of sorbent with water. Results indicate that kinetic of cobalt ion sorption on two considered materials is relatively fast e.g. in case of red clay, equilibrium state is reached after only a few minutes, and in case of bentonite after one hour. Results also show that the reagent ratio has great influence on the efficiency of the cobalt sorption on bentonite and red clay, as well.
In the next stage, in order to simulate transport of radioactive cobalt (^{60}Co) in the system consisted of bentonite and red clay barrier, a model described as a system of partial differential equations will be applied with using results achieved from laboratory tests.

References.

[1] Nuclear Energy Agency organisation for economic co-operation and development (2003); Engineered Barrier Systems and the Safety of Deep Geological Repositories, ISBN 92-64-18498-8,9
[2] Environment Agency (2010); Understanding controls on the performance of engineered barrier systems in repositories for high-level radioactive waste and spent fuel, ISBN 978-1-84911-199-7,2
[3] I.G.Stefanova (1784); Natural Sorbents As Barriers Against Migration Of Radionuclides From Radioactive Waste Repositories
[4] S.Norris (2014); Clays in Natural and Engineered Barriers for RadioactiveWaste Confinement: an introduction, The Geological Society of London

MIGRATION OF CALCIUM AND BICARBONATE IONS IN WATER-SATURATED COMPACTED MONTMORILLONITE UNDER ELECTRICAL POTENTIAL GRADIENT

S. Tanaka[1*], M. Mizuto[1,2], N. Watanabe[1], *T. Kozaki*[1]

1. Division of Energy and Environmental Systems, Faculty of Engineering, Hokkaido University, Kita 13 Nish 8, Sapporo 060-8628, Japan (tanaka-shingo@eng.hokudai.ac.jp)
2. Tokyo Nuclear Services Co., Ltd.

Introduction

Long-term evaluation of interactions between bentonite and cementitious materials, including calcite precipitation, is important in geological disposal of radioactive waste. However, experimental study on calcite precipitation in bentonite is difficult due to slow transport of reactants and/or low reaction rate. Electrokinetic methods have a potential to accelerate the transport of reactants and to enhance the chemical reaction rate of calcite precipitation. Under electrical potential gradient, anions and cations migrate to opposite directions even in compacted montmorillonite that has quite low permeability. In our previous study, electrokinetic method was used to study the migration of Na^+ and Cl^- in compacted montmorillonite to obtain electrokinetic parameters of simple ions in montmorillonite(1). In the present study, the same method was applied to $^{45}Ca^{2+}$ and $H^{14}CO_3^-$ to obtain electromigration parameters in water saturated compacted montmorillonite to discuss the possibility of calcite precipitation.

Experimental

Na-montmorillonite and Ca-montmorillonite were prepared by homoionization of Kunipia-F (Kunimine industries Co., Ltd., Japan). The clay powder was dried and compacted into pellets (20 mm in diameter and 20 mm in length) to have designated dry densities between 0.8 and 1.6 Mg/m^3. A pellet was placed between two sintered stainless-steel filters in an acrylic cell. The cells were immersed in $CaCl_2$ or $NaHCO_3$ solution at concentrations varying from 0 to 1.0 M for 30 days to complete saturation. Figure 1 shows the experimental setup for electromigration. A slight amount of radiotracers ($H^{14}CO_3^-$ or $^{45}Ca^{2+}$) was applied to one contact surface between the specimens. A constant current between 5 mA and 50 mA was applied at 298 K to a series of the pellets that have different. Electric potential differences were measured using two reference Ag/AgCl electrodes in each compartment. After electromigration, motmorilonite samples were sliced and the racdioactivity of each specimen was measured to obtain concentration profiles of radiotracers in the montmorillonite.

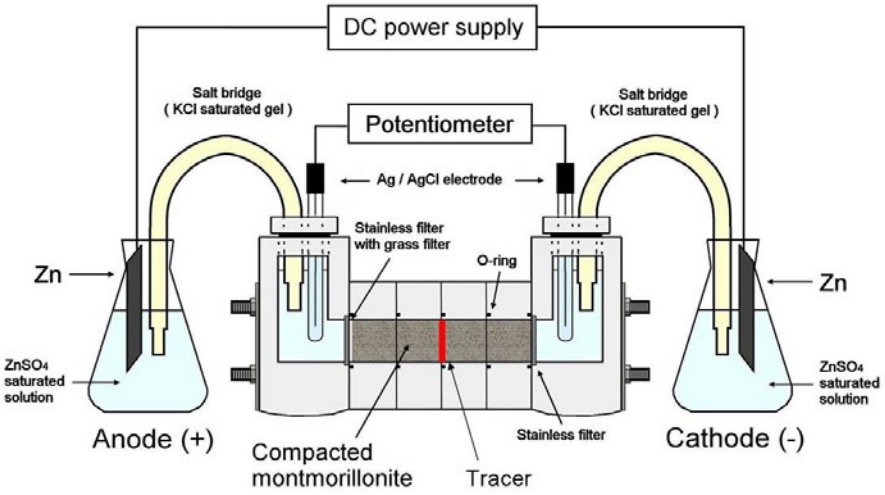


Fig. 1 Electromigration experimental setup

Results and Discussion

The profiles of species *i* can be described by the solution of the advection-dispersion type equation,

$$C^i = \frac{M^i}{2\sqrt{\pi D_h{}^i t}} \exp\left\{-\frac{\left(x - V_a{}^i t\right)^2}{4 D_h{}^i t}\right\} \quad (1)$$

where x is the distance from the initial position of the tracer, t is the time after the current was applied, C^i and M^i are the concentration and the amount of chemical species i, respectively, $D_h{}^i$ is the hydrodynamic dispersion coefficient and $V_a{}^i$ is the apparent migration velocity of chemical species i. The apparent migration velocities are proportional to the electric potential gradient E,

$$V_a{}^i = u_a{}^i E \quad (2)$$

The relative mobility must be taken into account when the water as migration medium moves. Therefore, apparent electromigration mobility of species i , $u_{em}{}^i$, can be obtained from the relation[(2)],

$$u_{\mathrm{em}}{}^i = u_a{}^i - u_a{}^{\mathrm{HTO}} \quad (3)$$

where $u_a{}^i$ is the apparent mobility of species I and $u_a{}^{\mathrm{HTO}}$ is the apparent mobility of water.

Figure 2 shows the concentration profiles of $^{45}Ca^{2+}$ and $H^{14}CO_3^-$ ions after electromigration. Figure 2 (a) shows that the $^{45}Ca^{2+}$ ions migrate to the direction of the Cathode side (right side). On the other hand, $H^{14}CO_3^-$ ions seem to stay in the initial position, although they spread to both directions by diffusion. This may be due to the effect of electro-osmotic water flow to the cathode side, which compensated the migration of $H^{14}CO_3^-$ ions to the direction of the anode side (left side). In the Eq. (3) for $H^{14}CO_3^-$ ions, the value of u_a is close to zero resulting in the u_{em} value to be nearly equal to $-u_a{}^{\mathrm{HTO}}$. The significant difference of V_a between $H^{14}CO_3^-$ ions and $^{45}Ca^{2+}$ ions suggests a possibility of electromigrating the two ions to opposite directions to meet in water-saturated montmorillonite. Preliminary experiments succeeded in the formation of calcite in compacted montmorillonite sample, suggesting that the activity product of CO_3^{2-} ions and Ca^{2+} ions exceeds the solubility product of calcite in the montmorillonite. Detailed experimental data and conditions of the calcite precipitation is discussed in this study.

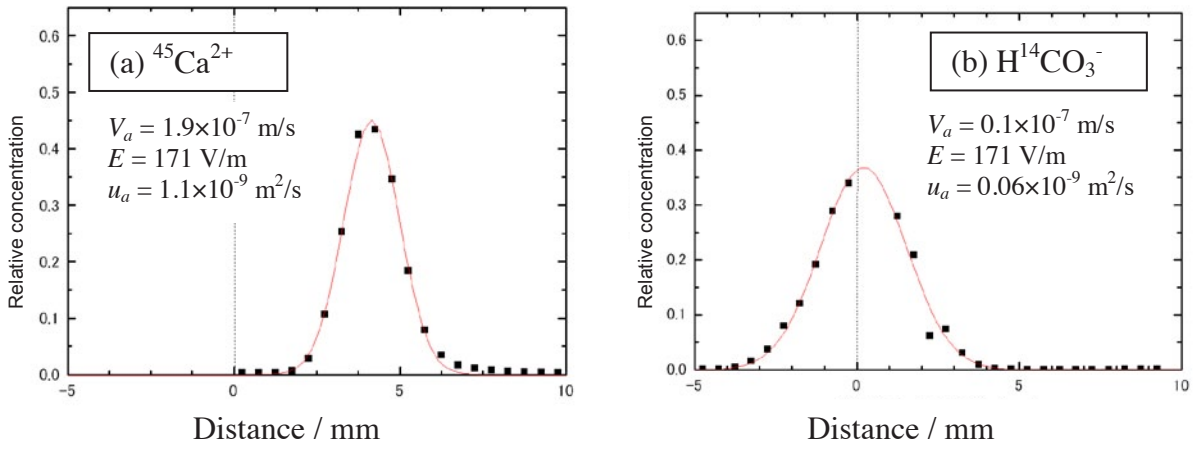


Fig. 2. Concentration profiles of (a) Ca^{2+} ions, and (b) HCO_3^- ions.
(Dry density; 1.2 Mg/m^3, Salinity; 0 M (deionized water) , Current; 15 mA, Time; 21,600 sec.)

References

(1) Tanaka, S., et al., 2011. Journal of Nuclear Science and Technology 48[3], 454-462.
(2) Maes, N., *et al.*, 1999. Journal of Contaminant Hydrology 36, 231-247.

Influence of hydraulic gradient on the transport of Dissolved Organic Matter in Boom Clay

***D.Durce*[(1)], C.Bruggeman[(1)] and N.Maes[(1)]**

[(1)] Belgian Nuclear Research Centre (SCK.CEN), Expert Group Waste&Disposal, Boeretang 200, B-2400 Mol, Belgium

Deep geological disposal of nuclear waste in clay formations is based on low mobility of radionuclides (RN) resulting from low water permeability and retention phenomena. However, transport of solutes in these formations is also subject to the presence of dissolved organic matter (DOM) which is ubiquitous in natural environments. The Boom Clay, one of the potential host formations under study in Belgium, contains relative high amounts of DOM (50-150 mgC/L). The mobility of DOM in Boom Clay and its influence on multivalent lanthanide/actinide transport has been demonstrated in many occasions [1-6]. However, the transport of DOM was observed to be limited by natural filtration[1-5]. Organic species with molecular weights (MW) larger than what can be defined as a rock cut-off are irreversibly trapped in the pore network of the non-disturbed rock. They remain immobile unless a fractionation of the molecules occurs. The Boom Clay rock cut-off was estimated as corresponding to a MW of 10-20 kDa [4,5] and equivalent to a hydrodynamic radius of 2.8 nm. The organic species displaying lower MW are expected to be, at least partly, mobile along the Boom Clay. It was however evidenced that the so-called "mobile" fraction is heterogeneous and present various mobility according to the MW distribution. The larger MW, the larger is the capacity factor, or the product □R (with □ the porosity and R the retardation factor) [2,5] .
In low permeable media, such as Boom Clay, percolation experiments are one of the reference methods for the determination of solute transport parameters. In such experimental set-ups, a hydraulic gradient ensures the transport of the solute through the rock sample. This approach allows to significantly reduce experimental times compared to traditional pure diffusion experiments. However, the effect of the hydraulic gradient on both the solute and the rock sample is still not fully understood. In the case of DOM, the influence of flow rate on the DOM recovery was studied by Maes et al., 2006 [1]. They observed a higher recovery when using higher Darcy velocity. Ionescu et al., (2007) [6] modelled these experiments by coupling the classical advection-diffusion equation with colloid attachment theory. However, the authors did not discriminate the mobile DOM in several fractions and considered it as one entity. It was previously reported that in a percolation experiment at 10 bars, the mobile fraction could be divided into three sub-fractions [5]. DOM species smaller than 0.7 kDa were observed to be fully recovered while 96% of DOM with MW between 0.7 and 3.5 kDa and only 38 % of the fraction 3.5 < MW <20 kDa was recovered after 500 days. A similar observation was reported by Martens et al. (2010) [4] on an *in situ* migration experiment. They indeed observed a lower recovery of the DOM fraction 1-10 kDa compared to the fraction < 1 kDa. The transport parameters for each fraction were however not determined and mobile DOM was once more seen as one species. Although the influence of pressure gradient on the transport of DOM in Boom Clay has already been partly treated, a complete approach coupling hydraulic gradient to size effects is therefore still missing.

In this presentation, we will discuss the transport of natural DOM in Boom Clay as a function of hydraulic gradient. Results from pure diffusion and percolation experiments performed with pressures of 5, 10 and 20 bars will be presented. The size distribution of the eluting mobile DOM is measured over time in each experiment using size exclusion chromatography and the DOM concentration is monitored by UV-Vis spectroscopy and TOC analyses. In a first step, the indigenous DOM is leached out by synthetic clay water solution. The influence of the pressure gradient on the accessible porosity of the Boom Clay is then investigated by injection of the tracers HTO and I125. Following these phases, DOM present in the pore water collected *in situ via* a piezometer is percolated in each set-up. The diffusion and breakthrough curves are modelled using a 1D reactive transport including if necessary colloid filtration theory.

The first results obtained from the leaching of the indigenous DOM as a function of hydraulic gradient are presented in Figure 1. The decrease of absorbance (λ=280nm), i.e DOM concentration, in the outlet is similar for all the set-ups. At this stage no significant influence of hydraulic gradient on the mobility of indigenous DOM is observed.

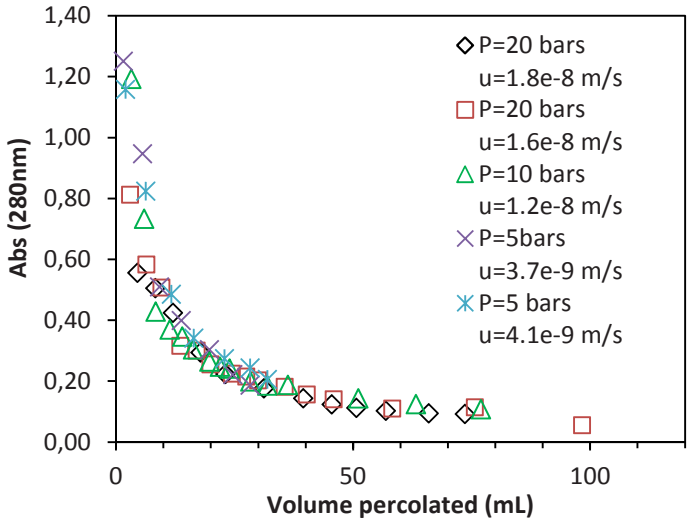


Figure 1. Evolution of the absorbance of the outlet solution during migration of indigenous DOM in percolation experiments performed with various pressures (P) and Darcy velocities (u). Inlet solution= synthetic clay water solution

[1] Maes, N., Wang, L., Hicks, T., Bennett ,D., Warwick, P., Hall, P., Walker, G., Dierckx, A., (2006). *The role of natural organic matter in the migration behaviour of americium in the Boom Clay-Part 1: migration experiments*. Physics and Chemistry of the Earth, 31, 541-547

[2] Put, M. J., Dierckx, A., Aertsens, M., and De Canniere, P., (1998). *Mobility of the dissolved organic matter through intact boom clay cores*. Radiochim. Acta 82, 375-378.

[3] Put, M. J., Monsecour, M., and Fonteyne, A., 1992. *mobility of the dissolved organic material in the interstitial boom clay water*. Radiochim. Acta 58-9, 315-317.

[4] Martens, E., Maes, N., Weetjens, E.,Van Gompel, M. and Van Ravestyn, L., 2010. *Modelling of a large-scale in-situ migration experiement with labelled natural organic matter in Boom Clay* . Radiochim. Acta 98, 695-701

[5] Durce, D., Maes, N., Bruggeman, C., 2010. *Dissolved organic matter transport in Boom Clay: size effects* . Personal communication, Migration conference 2013, Brighton, UK

[6] Maes, N., Bruggeman, C., Govaerts, J., Martens, E., Salah, S., and van Gompel, M., 2010. *A consistent phenomenological model for natural organic matter linked migration of Tc(IV), Cm(III), Np(IV), Pu(III,IV) and Pa(V) in Boom Clay*. Physics and Chemistry of the earth, 36, 1590-1599

[7] Ionescu, A., Maes, N., Mallants, D., 2007. *Modelling transport of 14C-labelled natural organic matter (NOM) in Boom Clay*. Sci. Basis Nucl. Waste Manage. XXXI, 629-636

Acknowledgements
This work is undertaken in close co-operation with, and also with the financial support of ONDRAF/NIRAS, the Belgian Agency for the Management of Radioactive Waste and Enriched Fissile Materials, as part of its programme on the geological disposal of long-lived radioactive waste.

Extrusion and Erosion of Bentonite Buffer Material in Sloped Fracture Environments

Timothy Schatz **& Nora Akemati**

B+Tech Oy, Laulukuja 4, 00420 Helsinki, Finland (tim.schatz@btech.fi)

One scenario of interest for the long-term safety assessment of a spent nuclear fuel repository involves the loss of bentonite buffer material through contact with dilute groundwater at a transmissive fracture interface [SKB 2011, Posiva 2012]. Analysis of such mass loss has, both experimentally and theoretically, been largely confined to consideration of interaction with horizontal fractures. However, taking into account the likelihood that the majority of fractures in the repository bedrock will be inclined at greater than 0°, and the heightened relevance of such inclined fractures as possible mass loss pathways for horizontal deposition (e.g., KBS-3H method), it is clear that the extrusion and erosion behaviour of clay materials in these environments must be examined.

In order to simulate the potential extrusion/erosion behaviour of bentonite buffer material in inclined fracture environments, a series of small-scale, flow-through, artificial fracture experiments were conducted in fractures positioned at steep slope angles (Figure 1). Extrusion/erosion effects were analysed against solution chemistry (salt concentration and composition), material composition (sodium montmorillonite, calcium/sodium montmorillonite mixtures, as-received bentonites), flow velocity, flow direction, fracture aperture and surface roughness.

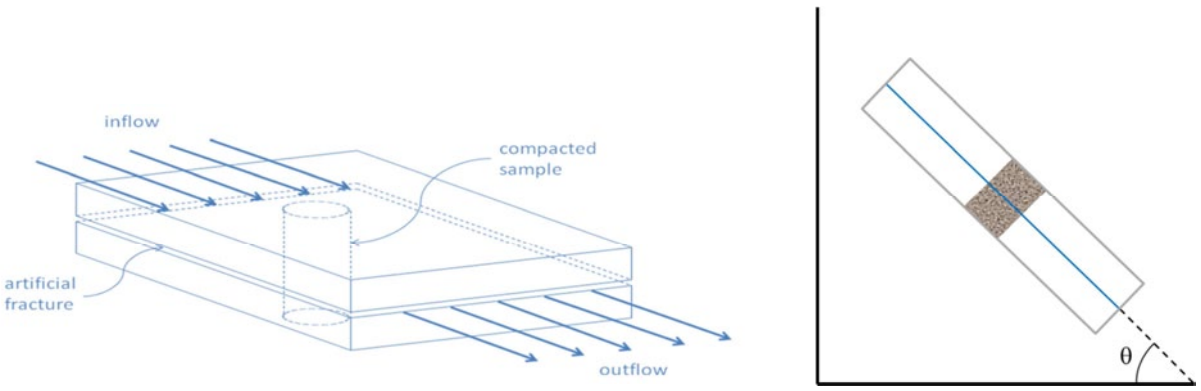


Figure 1. *Conceptual representation of the flow-through, artificial fracture test system (left) and diagram showing the test system positioned at steep slope angles ($\theta \geq 45°$).*

In artificial fracture tests conducted at steep slope angles, clay mass is lost from the extruded source material via a predominantly sedimentary process (Figure 2). This behaviour lies in sharp contrast to that observed in horizontal fracture environments where the mass release is dispersive in nature [Schatz et al. 2012]. It is also the case, as opposed to horizontal fractures, that steady-state extrusion distances are not established in tests at steep slope angles, i.e., extrusion distances recede with mass loss over time. Moreover, the shapes of the extruded zones become somewhat ovate with only one axis of symmetry remaining as more mass is lost from the lower halves of the extrudates than the tops.

Average mass loss rates in the sloped fractures were always larger than those of the corresponding horizontal cases. Moreover, increased slope angles generally resulted in increased mass loss rates as well. Sedimentary-type mass loss was observed in sloped fractures under stagnant (no) flow as well as flow-through conditions. An increase in flow velocity down the fractures from zero (stagnant) to

~10^{-6} m/s produced a 3-fold increase in mass loss whereas a further increase in flow velocity by roughly two orders of magnitude yields only a 15% additional increase in mass loss. By contrast, a similar, two order of magnitude flow velocity increase in horizontal fracture systems leads to an 80% increase in mass loss.

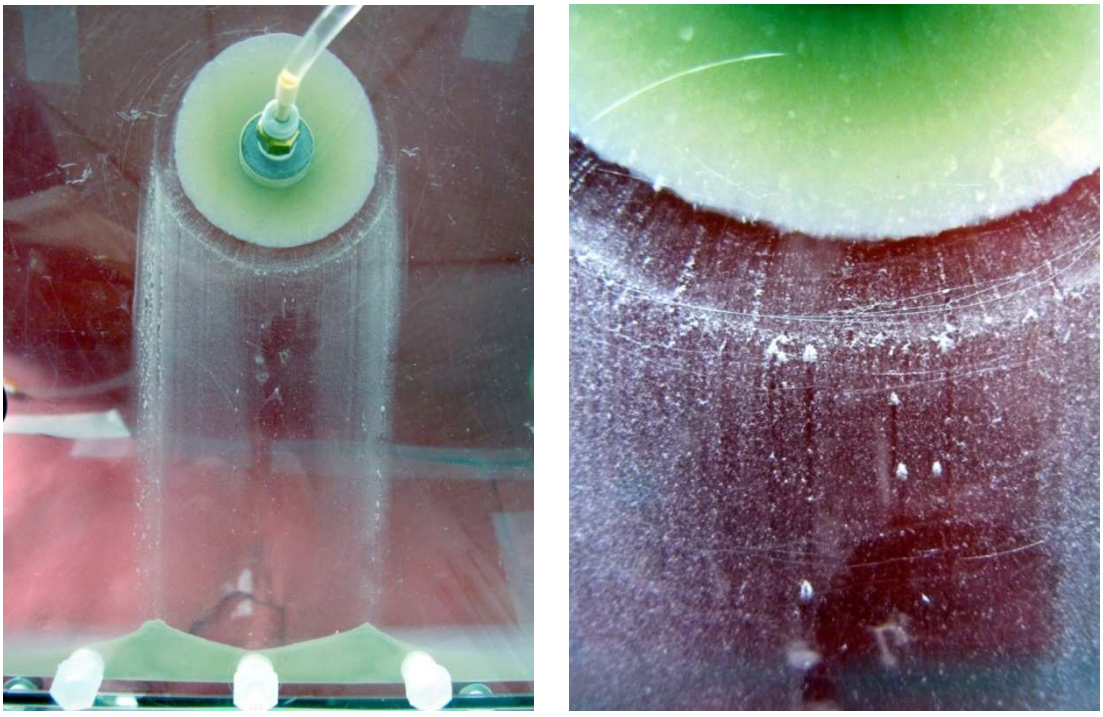


Figure 2. Front *facing image (left) of a test with 50/50 calcium/sodium montmorillonite in contact with a Grimsel groundwater simulant at an average flow rate of 0.09 ml/min down a 1 mm aperture artificial fracture system positioned at a 45° slope angle and close-up view (right) of the solid/liquid (erosion) interface.*

Erosion data from artificial fracture tests can be applied to determine bounding estimates of mass loss due to sloped, saturated fractures intersecting deposition holes (vertical) or drifts (horizontal). Assuming the measured erosion rates scale with sample (or deposition hole or drift) diameter and that the extrusion distances themselves behave and scale similarly, upscaled erosion rates on the order of 2 to 10 kg/yr can be calculated.

References

Posiva 2012. Performance Assessment Report. Posiva Report 2012. Posiva Oy.

SKB. 2011. Long-Term Safety for the Final Repository for Spent Nuclear Fuel at Forsmark. Main Report of the SR-Site Project. Volume II. SKB Technical Report. TR-11-01. Svensk Kärnbränslehantering AB.

Schatz, T., Kanerva, N., Martikainen, J., Sane, P., Olin, M., Seppälä, A. & Koskinen, K. 2013. Buffer Erosion in Dilute Groundwater. Posiva Report. 2012-44. Posiva Oy.

The Ypresian clays as a potential host rock for radioactive waste disposal in Belgium: knowledge gaps in the hydrogeology

Author(s) *Pieter Jan Haest*[1*], Yves Meyus[1], Hervé Van Baelen[2], Laurent Wouters[2]

1. A.G.T. n.v., Kontichsesteenweg 38, 2630 Aartselaar, Belgium. *corresponding author: pieterjan.haest@agt.be
2. ONDRAF /NIRAS, Kunstlaan 14, 1210 Brussels, Belgium

1. Introduction

The Ypresian clays are considered as a potential host rock for radioactive waste disposal in Belgium. The nuclear site at Doel is the reference site for research purposes of the Ypresian clays, similar to the Mol-Dessel site for the Boom Clay (Figure 1). Contrary to the research for the Boom Clay that started more than 30 years ago with the excavation of HADES-URF, the research for the Ypresian clays started in the second half of the nineties. Data are still being gathered to define the spatial extent of the different units in the Ypresian Aquitardsystem, in addition to hydraulic parameters of this system and its adjacent aquifers. Van Marcke and Laenen (2005) thoroughly discuss the knowledge from the previous decades regarding the properties of the Ypresian clays. Nevertheless, Vandenbohede et al. (2011) conclude from their hydrogeological model of the Doel region that the uncertainty regarding the hydraulic parameters should be further reduced to be able to approximate the well head observations. Furthermore, Olsthoorn (2011) points out that more knowledge is required regarding the boundary conditions of the hydrogeological setting for an eventual safety assessment. As such, this study summarizes the knowledge gaps for a hydrogeological model that are present today in order to assess the potential of the Ypresian clays as potential host rock for radioactive waste disposal in Belgium.

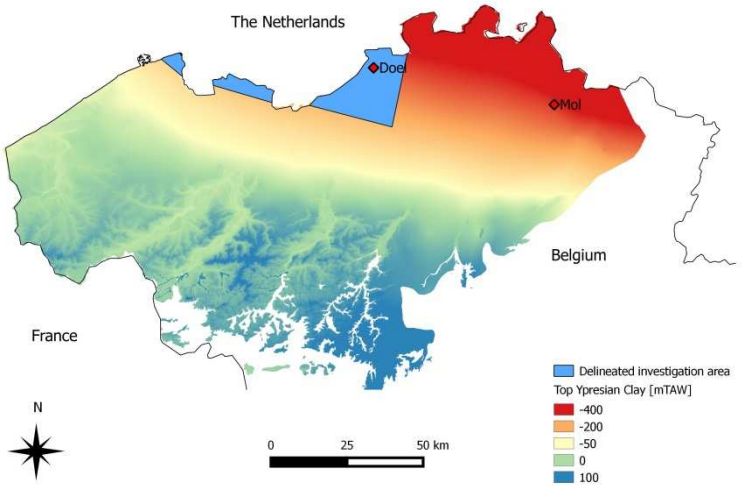


Figure 1: The extent of the Ypresian Clays in Belgium and the delineated investigation area according to SAFIR2 (ONDRAF/NIRAS 2001) for geological disposal (Van Marcke and Laenen ,2005).

2. Hydrogeological conceptual model

Data are being gathered from different actors that study the Ypresian clays and are used in a conceptual hydrogeological model to evaluate the knowledge gaps that remain. Four major factors of uncertainty are discerned in this research: (a) the delineation of the Ypresian clays and its adjacent aquifers, (b) the hydraulic properties of the porous media at the depth of >200 m-bgs near Doel, (c) the boundary conditions of the hydrogeological model and (d) the potential for density driven flow.

a) The Ypresian clays comprise the Kortrijk Formation and the overlying Kortemark Member of the Tielt Formation. Two digital resources are currently available to delineate the Ypresian clays in Belgium: the HCOV mapping (Meyus et al., 2000) and the geological 3D model (Matthijs et al., 2013). They show a differing vertical delineation of the Ypresian clays up to several meters, indicating the uncertainty related to a discrete classification of the subsoil layers. Another uncertainty related to the vertical delination of the Ypresian clays is the definition of its boundaries: A recent mapping of the Ypresian clays by the Geological

Survey of Belgium proposes to extend the Ypresian clays up to the informal Egemkapel Member of the Tielt Formation (Walstra et al. , 2014). Finallly, the delineated investigation area is at the border with The Netherlands. However, the Ypresian clays are not mapped in the Province of Noord-Brabant impeding the development of a regional hydrogeological model.

b) Point data of hydraulic properties of the Ypresian clays and the adjacent aquifers corroborate the conclusion by Vandenbohede et al. (2011) that more measurements are required. The limited amount of measurements that are available for the hydraulic conductivity of the Ypresian clays at a depth > 200 m-bgs show a large variation that cannot be readily approximated by empirical formulas. The heterogeneity of the Ypresian clays has been reported by Huysmans and Dassargues (2006) to reduce the flux of radionuclides to the overlying Egem member by 40% and increase the flux to the underlying Tienen Formation by 59% compared to a homogeneous layer. The effect in a regional hydrogeological model remains to be validated.

c) The regional stratification suggests a general North-Northwestern groundwater flow in the aquifers above and below the Ypresian clays, following the dipping bottom boundaries towards the center of the North Sea Basin. However, excessive pumping of the Chalk, Paleocene and Ledo-Paniselian-Brusselian Aquifersystems regionally influences the water heads below/above the Ypresian clays (Dassargues & Walraevens, 2014). Unfortunately, accurate pumping data are scarce. In addition, the model boundaries in the East and North are formed by fault zones of which the potential occlusion for groundwater flow is currently debated.

d) The pore water density varies laterally and vertically around and in the Ypresian clays. The limited data are used to evaluate the driving force ratio for density driven flow across the Ypresian clays and in the adjacent aquifers.

3. Conclusion

This research points to the need for a good definition of the extent of the Ypresian clays as potential host rock, in addition to more data on hydraulic and physical properties of the potential host rock. The limited amount of information at the large considered depth requires all available knowledge, crossing national borders, in order to accurately define a hydrogeological model.

References

Dassargues, A., & Walraevens, K. (2014). *Watervoerende Lagen en Grondwater in België - Aquifères et Eaux Souterraines en Belgique* (p. 455). Gent, Belgium: Academic Press.

Huysmans, M., & Dassargues, A. (2006). Hydrogeological modeling of radionuclide transport in low permeability media: a comparison between Boom Clay and Ypresian Clay. *Environmental Geology*, *50*(1), 122–131.

Matthijs, J., Lanckacker, T., De Koninck, R., Deckers, J., Lagrou, D., & Broothaers, M. (2013). *In Dutch: Geologisch 3D lagenmodel van Vlaanderen en het Brussels Hoofdstedelijk Gewest – versie 2, G3Dv2* (p. 21).

Meyus, Y., Batelaan, O., & De Smedt, F. (2000). *In Dutch: Technisch concept van het VGM Hydrogeologische Codering van de Ondergrond van Vlaanderen (HCOV)* (p. 58).

Olsthoorn, T. N. (2011). *Geologische Berging van Radioactief Afval in België: Mogelijke Gevolgen voor Nederland* (p. 107).

ONDRAF/NIRAS, 2001. *SAFIR 2 – Safety Assessment and Feasibility Interim Report 2*. ONDRAF/NIRAS report NIROND 2001-06E

Van Marcke, P., & Laenen, B. (2005). *The Ypresian Clays as Possible Host Rock for Radioactive Waste Disposal: An Evaluation* (p. NIROND TR–2005–01).

Vandenbohede, A., Lebbe, L., & Courtens, C. (2011). *Een hydrogeologisch model in de streek rond Doel (Beveren)* (pp. NIROND–TR 2011–65).

Walstra, J., Dusar, M., & De Ceukelaire, M. (2014). *Geological model of the Ypresian Clay* (p. 77).

Effect of confining pressure on diffusion coefficients: Ordovician shale and limestone, southwest Ontario, Canada and Opalinus clay, Switzerland

Yan Xiang and *Tom Al

Department of Earth Sciences, University of New Brunswick, Fredericton, New Brunswick, Canada, E3B 5A3
* now at University of Ottawa, Department of Earth Sciences, ARC 410, Office: 613-562-5800 ext. 6966, Cell: 343-540-8665, E-mail: Tom.Al@uOttawa.ca

The effect of confining pressure (CP) on the diffusion of tritiated water (HTO) and iodide (I^-) tracers through Upper Ordovician rock samples from the Michigan Basin, southwestern Ontario, Canada, and through Opalinus Clay samples from Schlattingen, Switzerland was investigated at the laboratory scale. Samples representing different formations and lithologies in the Michigan Basin were studied: one from each of the Queenston Formation shale, the Georgian Bay Formation shale, the Cobourg Formation limestone and the Cobourg Formation argillaceous limestone. These samples were retrieved from cores between 472 and 681 meters below ground surface with estimated in-situ vertical pressures of 12.0 to 17.4 MPa. Effective diffusion coefficients (D_e) were determined in through-diffusion experiments with CP ranging from ambient laboratory pressure (AP) to 17.4 MPa. With HTO tracer (Figure 1), increasing CP resulted in decreases in D_e from 4.9×10^{-12} to 4.2×10^{-12} $m^2\cdot s^{-1}$ (-14%) for the Queenston Formation shale (CP = 12 MPa); from 4.1×10^{-12} to 2.8×10^{-12} $m^2\cdot s^{-1}$ (-32%) for the Georgian Bay Formation shale (CP = 15 MPa); from 3.5×10^{-13} to 2.3×10^{-13} $m^2\cdot s^{-1}$ (-34%) for the limestone (CP = 17.4 MPa); and from 7.0×10^{-13} to 4.8×10^{-13} $m^2\cdot s^{-1}$ (-31%) for the argillaceous limestone (CP = 17.4 MPa). With I^- tracer, larger decreases in D_e values were observed for the shale samples: 2.9×10^{-12} to 2.4×10^{-12} $m^2\cdot s^{-1}$ (-17%) for the Queenston shale and 2.5×10^{-12} to 1.4×10^{-12} $m^2\cdot s^{-1}$ (-44%) for the Georgian Bay shale, suggesting that anion exclusion effects are enhanced with increasing CP. No significant difference was observed between D_e values for HTO and I^- for the limestone samples. The effect of confining pressure on D_e in two Opalinus Clay samples was tested in the pressure range from 0.3 to 15.0 MPa. With increasing pressure, measured D_{eHTO} values for two samples decreased from 1.4×10^{-11} to 7.4×10^{-12} m^2/s (-47%) and from 1.2×10^{-11} to 6.7×10^{-12} m^2/s (-44%). Similar to the shale samples from the Michigan Basin, the effect of confining pressure on D_e for the Opalinus samples is greater for the iodide tracer. At low pressure (0.3 MPa) D_{eI} values of 3.1×10^{-12} m^2/s and 2.7×10^{-12} m^2/s were obtained, and at 15.0 MPa the D_{eI} values decreased respectively to 1.1×10^{-12} m^2/s and 1.0×10^{-12} m^2/s for overall decreases of 65% and 63%.

Experiments on samples from southern Ontario investigated the reversibility of the confining pressure influence on D_e. The sequence of experimental pressure changes started at maximum CP, decreased to AP and then returned to maximum CP. Data from the Queenston and Georgian Bay fm. shale samples (Figures 1a,b) indicate that, within error, the D_e changes are reversible. In contrast, confining-pressure induced changes in D_e for the limestone and argillaceous limestone are not reversible (Figure 1c).

The results of these experiments demonstrate that D_e varies with confining pressure for each of the rock types with the maximum effect observed for anionic tracers in compressible, clay-rich rocks.

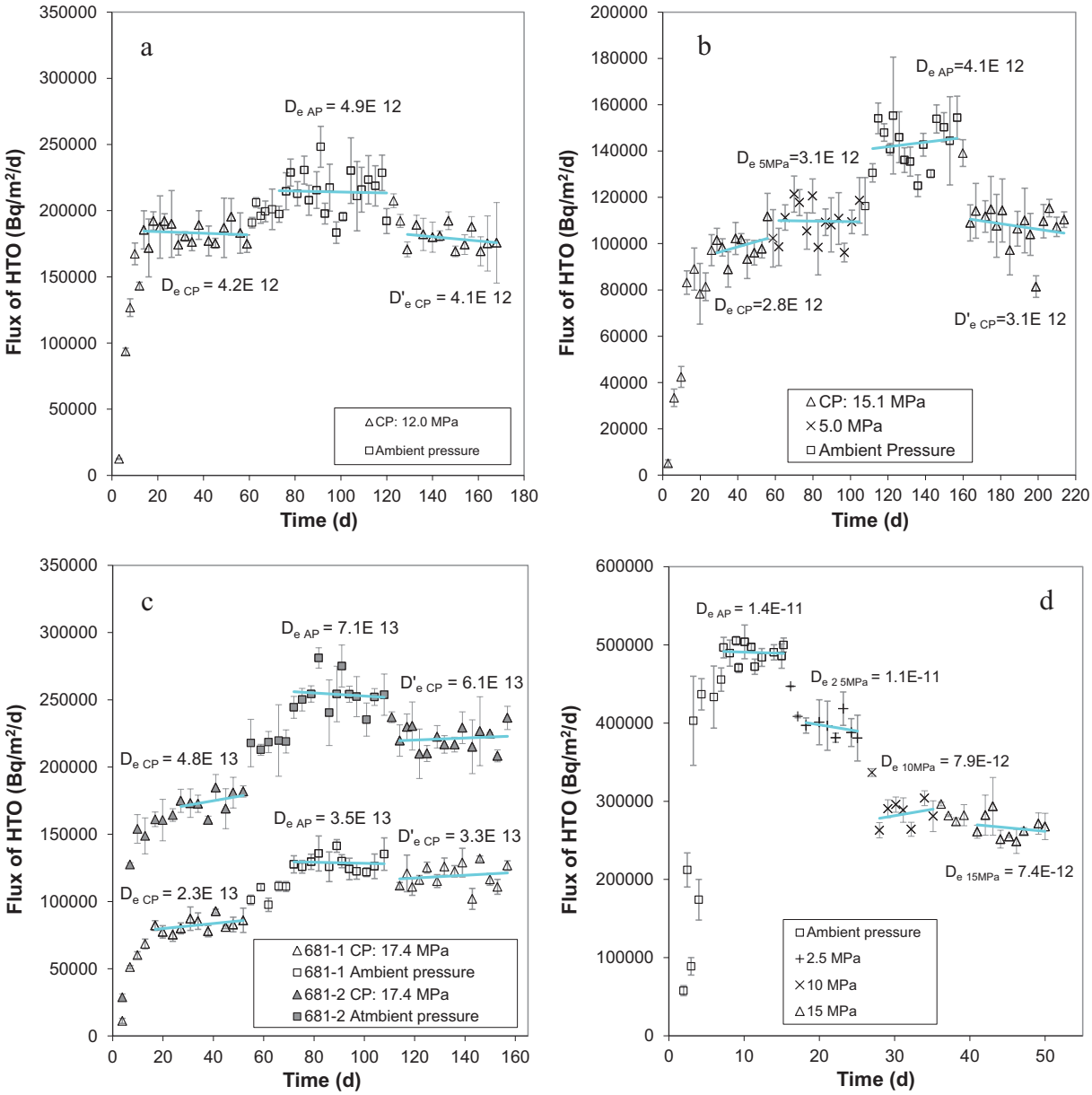


Figure 1. Diffusive flux of HTO across samples of: a) Queenston Formation shale, b) Georgian Bay Formation shale, c) Cobourg Formation limestone (DGR3-681-1) and argillaceous limestone (DGR3-681-2), and d) Opalinus clay from Schlattingen, Switzerland (SLA-857).

Diffusion and Sorption of Sr in Compacted Sodium Montmorillonite: Multispecies Modeling

Yukio Tachi, Kenji Yotsuji, Tsuyoshi Ito, Tadahiro Suyama

Sector of Decommissioning and Radioactive Waste Management, Japan Atomic Energy Agency, Muramatsu 4-33, Tokai, Ibaraki, 319-1194, Japan (tachi.yukio@jaea.go.jp)

Sorption and diffusion of radionuclides in compacted montmorillonite are the key processes in the safe geological disposal of radioactive waste. To set reliable parameters under various geochemical conditions relevant to performance assessment, it is necessary to understand detailed processes of diffusion and sorption, and to develop mechanistic models, which describe them. The integrated sorption and diffusion (ISD) model has been developed and applied for sorption and diffusion data of various radionuclides such as cations (Cs^+, Na^+, Sr^{2+}), anions (I^-), and actinide species (Np(V), Am(III), U(VI)) as functions of porewater salinity and dry density (Tachi et al., 2010; 2014, Tachi and Yotsuji, 2012; 2014). Key challenges for enhancing the applicability of the ISD model are extending the model from single species systems to multispecies systems. In this study, the diffusion and sorption behaviors of multispecies Sr (divalent cation Sr^{2+}, neutral $SrSO_4$ (aq)) in compacted montmorillonite as a function of porewater salinity were investigated by experimental and multispecies modeling approaches.

Effective diffusion coefficients (D_e) and distribution coefficients (K_d) of Sr in purified Na-type montmorillonite (Kunipia F®) compacted to a dry density of 800 kg/m^3 were measured under aerobic conditions at room temperature. Three types of Na_2SO_4 solution (0.05, 0.1, 0.5M) were used to investigate the effect of coexisting multispecies and porewater salinity on diffusion and sorption in the compacted montmorillonite. The diffusion tests were conducted by the through-diffusion method with variable concentrations in the inlet and outlet reservoirs coupled with depth profile measurement in compacted samples (Tachi and Yotsuji, 2014). Then, D_e and K_d values were derived by multiple curve analysis as shown in Figure 1. The D_e and K_d values decreased drastically with increasing porewater salinity (Figure 2a and 2b). Based on the thermodynamic calculation, two species, Sr^{2+} and $SrSO_4$(aq) are coexisting at almost equal concentration at 0.5 M Na_2SO_4 solution (Figure 2c). As a result of coexisting of $SrSO_4$(aq), the D_e and K_d values decreased those measured for single species (Sr^{2+}) in NaCl solutions (Tachi and Yotsuji, 2012).

These sorption and diffusion behaviors were interpreted based on the ISD model by coupling the thermodynamic aqueous speciation (Tachi and Yotsuji, 2014). The thermodynamic sorption model (TSM) was based on a simple 1-site ion exchange model in the case of Sr. The diffusion model based on a simplified pore structure and the electrical double layer (EDL) theory, describes the change of ionic concentration and viscoelectric effects caused by the electrostatic interaction with negatively charged clay surfaces. As shown in Figure 2a, the D_e values of Sr^{2+} decreased as salinity increased, although those of $SrSO_4$(aq) were mostly independent of salinity. The D_e for multispecies Sr was determined as the harmonic weight-average considering the two species distribution and their log D_e values at each condition. This averaging method was validated through the comparing with reactive-transport calculations using the PHREEQC code and the different D_e values for each species predicted by the ISD model (Figure 1). As a result, the D_e trend could be quantitatively explained by the ISD model considering multispecies contributions (Figure 2a). The thermodynamic sorption model considering ion exchange reactions could provide reasonable account of Sr sorption trends as functions of salinity (Figure 2b). From these results, the ISD model can be basically applicable in predicting multispecies diffusion and sorption behaviors, however is further needed to test for more complex multispecies systems such as actinide series.

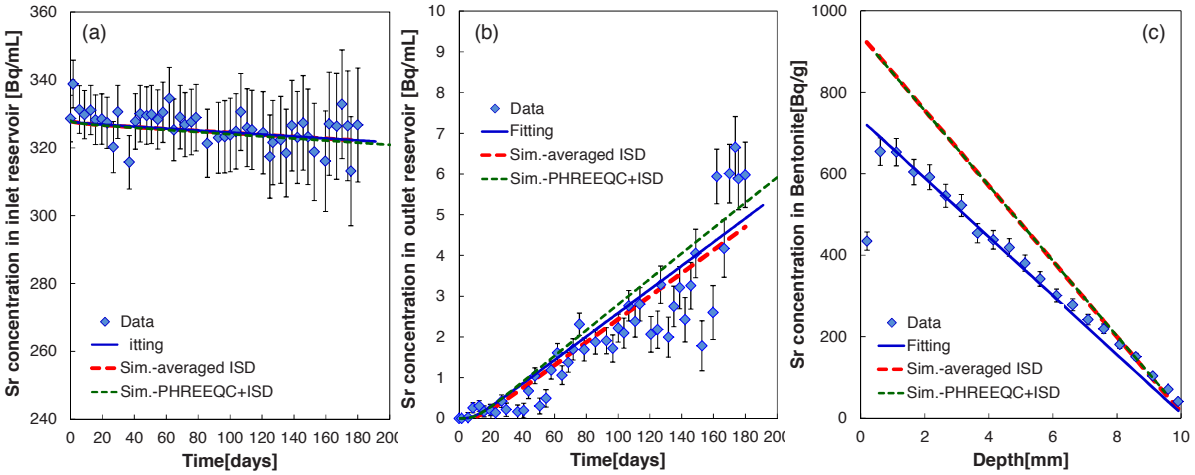


Figure 1. **Typical results of through-diffusion experiments for Sr: (a) reservoir-depletion curve, (b) breakthrough curve and (c) depth profile in montmorillonite sample, for porewater salinity of 0.5M Na_2SO_4. Solid lines were obtained by simultaneous fitting of analytical solution of the diffusion equation. Dashed lines are simulated results by the harmonic weight-averaged D_e values and the reactive-transport calculation by PHREEQC, respectively.**

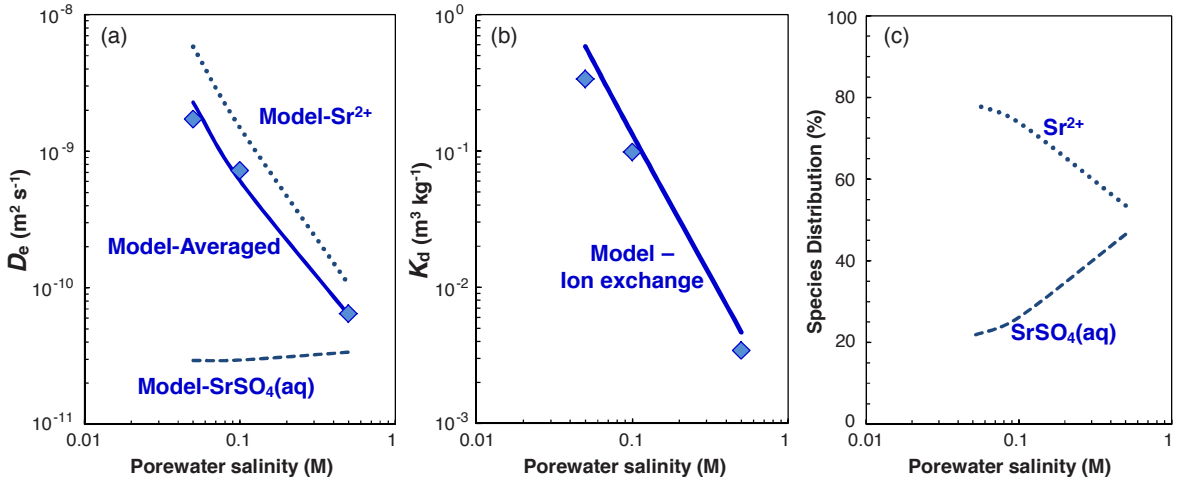


Figure 2. **Comparison between measured and modelled results for multispecies Sr: (a) D_e values and modeling result based on the harmonic weight-average of those for each species, (b) K_d values and modeling result by the ion exchange model, (c) two Sr species distribution by the thermodynamic calculations.**

*This study was partly funded by the Ministry of Economy, Trade and Industry of Japan. The authors greatly appreciate the contributions from Tokyo Nuclear Service Inc. for experimental work.

References:

Tachi, Y. et al. 2010. Diffusion and sorption of neptunium(V) in compacted montmorillonite: effects of carbonate and salinity. Radiochim. Acta 98, 711–718.

Tachi, Y. and Yotsuji, K. 2012. Diffusion and sorption of Sr^{2+} in compacted sodium montmorillonite as a function of porewater salinity. Clays in Natural and Engineered Barriers for Radioactive Waste Confinement. 5th International meeting. Abstract P/MT/DP/20.

Tachi, Y. and Yotsuji, K. 2014. Diffusion and sorption of Cs^+, Na^+, I^- and HTO in compacted sodium montmorillonite as a function of porewater salinity : Integrated sorption and diffusion model". Geochim. Cosmochim. Acta 132, 75–93.

Tachi, Y. et al. 2014. Integrated sorption and diffusion model for bentonite. Part 2: porewater chemistry, sorption and diffusion modeling in compacted systems. J. Nucl. Sci. Technol. 51(10), 1191-1204.

The possibility of salt accumulation due to coupled localized inflow and vapour transport in a KBS-3 repository

Martin Birgersson, **Reza Goudarzi**

Clay Technology AB, Ideon Science Park, S-223 70 Lund, Sweden

It has long been recognized that salt accumulation may occur in a KBS-3 repository as a consequence of vaporization of incoming saturating ground water in the presence of temperature gradients under unsaturated conditions (Karnland, 1995; Karnland et al., 2000). Significant salt accumulation may, in turn, influence the chemical evolution under the saturated stage and e.g. contribute to increasing canister corrosion rates. A "worst case" scenario for this type of salt accumulation process is schematically pictured in Figure 1: In the case of a rock section with very few water bearing fractures, the situation may arise that a larger part of the repository is saturated from a single fracture located in the lower part of a deposition hole. Should vaporization of the incoming water occur, huge salt accumulation is conceivable simply as a consequence of the large water volume required for saturation.

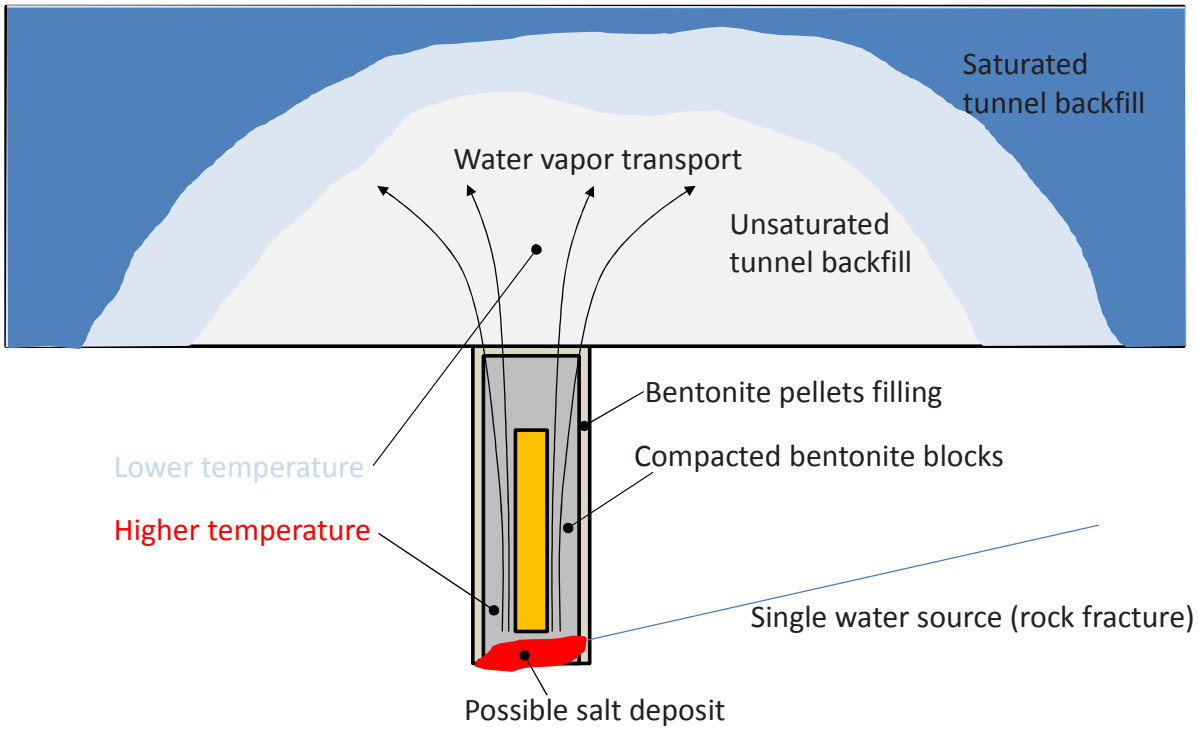


Figure 1: Schematic illustration of the possible problem of major salt accumulation near a cansiter due to localized inflow and otherwise dry conditions in a KBS-3 repository.

This work discusses the involved physicochemical principles behind this type of salt accumulation process in bentonite as well as reporting laboratory test made on how vapour interacts with different bentonite components. The interaction between water vapour and e.g. compacted bentonite blocks or bentonite pellets, and the ability of these components to seal off the system due to water uptake and swelling under the prescribed conditions is a key mechanism for quantifying possible salt accumulation.
Figure 2 shows water consumption in tests where water vapour where led through a sample of bentonite pellets under two different conditions: 1) the pellet sample where allowed to swell upwards (labelled "room2" in figure 2) 2) volume constrained pellets sample ("room4"). Figure 2 shows both

the total amount of water consumed water as well as the amount of water taken up by the pellets. The difference between these quantities consequently equals the amount of water lost to the environment.

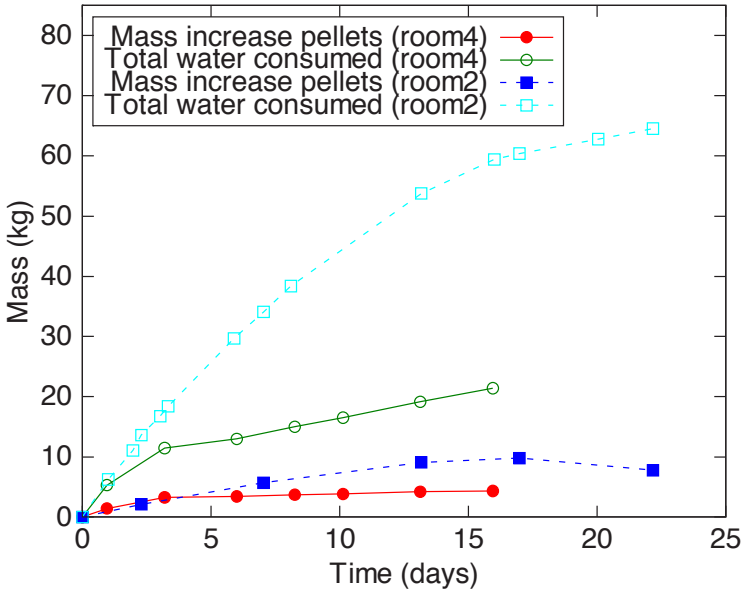


Figure 2: Water consumption in two tests where water vapor were led through a sample of bentonite pellets (Birgersson and Goudarzi, 2013). In the test lablelled "room2" the pellets was allowed to swell upwards, in the test labelled "room4" no volume expansion was allowed.

From the picture it is obvious that the volume constrained pellet sample seal of the system much more effectively than the sample which were allowed to swell upwards. However, the decreasing rate of total consumed water, demonstrates that also the swelling sample (room2) increased its sealing ability with time.

References:

Birgersson, M., Goudarzi, R., 2013. Studies of vapor transport from buffer to tunnel backfill (Sauna effects) (R-13-42) SKB.

Karnland, O., 1995. Salt redistribution and enrichment in compacted bentonite exposed to a thermal gradient — results from laboratory tests (AR-95-31). SKB.

Karnland, O., Sandén, T., Johannesson, L.-E., Eriksen, T.E., Jansson, M., Wold, S., Pedersen, K., Motamedi, M., Rosborg, B., 2000. Long term test of buffer material - final report on the pilot parcels (TR-00-22) SKB.

Swelling and erosion of bentonite/montmorillonite in dilute aqueous solutions

Magnus Hedström[1], **Emelie Hansen**[1*], **Noora Kanerva**[2], ***Timothy Schatz***[2]

1. Clay Technology AB, Ideon Science Park, SE-223 70 Lund, Sweden, (mh@claytech.se)
2. B+Tech Oy, 00420 Helsinki, Finland (tim.schatz@btech.fi)
* Present address: BASF A/S, DK-2300 Copenhagen, Denmark

One scenario of interest for the long-term safety assessment of a spent nuclear fuel repository involves the loss of bentonite buffer material through contact with dilute groundwater at a transmissive fracture interface [SKB 2011, Posiva 2012]. In dilute water, sodium dominated montmorillonite is known to form a colloidal sol which would easily be transported away with flow. For montmorillonite dominated by divalent cations (Ca^{2+} or Mg^{2+}) the sol phase is absent. However, as little as 10-20% sodium content of exchangeable cations in a mixed Ca/Na-montmorillonite results in dispersion and erosion behaviour similar to pure Na-montmorillonite in deionized (DI) water (Birgersson et al. 2009). In the study by Birgersson et al. it was also found that water with cation content higher than 2–4 mM charge equivalents prevent erosion through porous frits in swelling pressure cell set-ups, provided that the calcium content in the montmorillonite is above 20%. Partial confirmation of this results was provided in flow-through artificial fracture tests (Figure 1), where the observed erosion of a 50/50 Ca/Na-montmorillonite in 4 mM NaCl was found to be significantly lower than in any other system at the same flow velocity (Schatz et al. 2013). Even if these experiments have contributed to narrow down the concentration range where erosion due to sol formation need be taken into account in the safety assessment (SKB 2011, Posiva 2012), it is at the same time clear that this process cannot be fully ruled out especially after glaciations. Thus further experimental characterisation, both qualitative and quantitave, of the erosion process is needed.

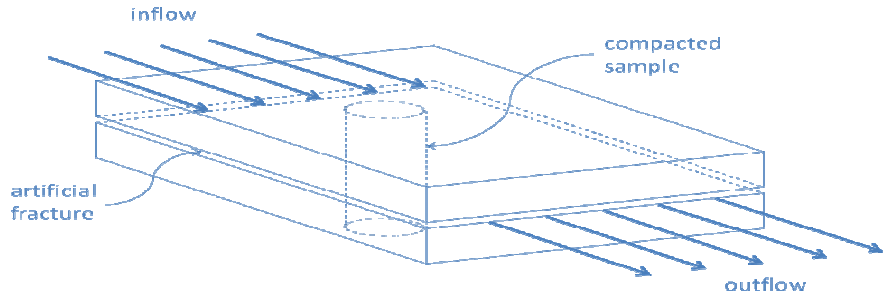


Figure 1: Schematic representation of the flow-through, artificial fracture test system design basis.

The aim of this study is to provide a synthesis of results obtained at two different laboratories, Claytech and B+Tech. In order to simulate the potential extrusion/erosion behaviour of bentonite buffer material under dilute water conditions, a series of small-scale, flow-through, artificial fracture experiments were performed in which swelling clay material could extrude/erode into a well-defined system (Figure 1). The lateral dimensions of the fracture are ~20 cm × 20 cm and the aperture (a) range from 0.1 to 1 mm. The compacted sample dimensions were 2 cm (height) × 2 cm (diameter) (B+Tech) and 1 cm × 3.5 cm (Claytech). Extrusion/erosion effects were analysed against solution chemistry (salt concentration and composition), material composition (sodium montmorillonite and admixtures with calcium montmorillonite), and flow velocity. The montmorillonite dry density in the compacted sample ranges from 1250 to 1430 kg/m^3.

To facilitate comparison between different tests and set-ups we define a unit erosion rate as eroded mass/(time*area), where the area is given by rim surface area of the eroding clay, $2\pi ra$, r being the average radius of the extruded clay (compacted region included). For Na-montmorillonite obtained from MX-80 (Wy-Na), the unit erosion rate was found to be 110 kg/m^2/yr in the case of a 0.12 mm aperture and 5 mM NaCl (aq) at a high flow velocity of 2.0×10^{-4} m/s (Claytech). A test performed with 4.3 mM NaCl at similar flow velocity (1.9×10^{-4} m/s) but with 1 mm aperture gave an almost

identical result 102 kg/m^2/yr (B+Tech). These two tests at high flow velocity gave similar unit erosion rates independent of aperture. On the other hand the extrusion radii differed significantly in the two tests. Results at a an order of magnitude lower flow velocity (1.5×10^{-5} m/s) suggest lower unit erosion rates with 0.24 mm aperture than with 0.12 mm. The comparison is unfortunately not straightforward as the swelling in the fracture with 0.24 mm aperture deviated from being radially symmetric.

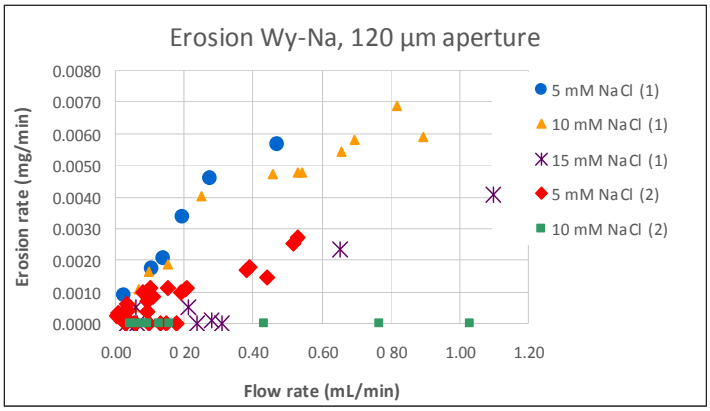


Figure 2: Erosion rates vs. flow rate for the case where first the NaCl concentration in the flowing solution was increasing (1). After reaching 20 mM where erosion stopped NaCl the concentration in the flowing solution was decreased (2). Evidently there is a strong hysteresis related to the ionic strength changes.

Another finding is the strong hysteresis effect related to the attractive gel formation above the critical coagulation concentration. For a given NaCl concentration erosion rates are lower at the dilution phase compared to the values obtained under increasing NaCl concentrations (Figure 2). Similarly Wy-Na montmorillonite under gradient elution conditions (0.5, 0.25, 0.125 g/L NaCl and finally DI water) at an average flow rate of 2.76 ml/min through the artificial fracture system showed limited erosion (effluent solid concentration) as long as the NaCl concentration was finite, while DI water led to a drastic increase in erosion (Schatz et al. 2013). Furthermore, during the elution the extrution radius continued to increase, indicating a certain strength of the extruded clay paste, until contacted with DI water. At that point the significant erosion caused the radius to change from 70 to 10 mm. The erosion dependence on aqueous history could be of importance for the safety assessment, as in the repository dilute groundwater may only reach repository depth after long periods of saline conditions far above the critical concentration for attractive gel formation.

The research leading to these results has received funding from the European Atomic Energy Community's Seventh Framework Programme (FP7/2007-2011) under Grant Agreement N° 295487, the BELBaR project.

References

Birgersson M., Börgesson L., Hedström M., Karnland O., Nilsson U. 2009. Bentonite erosion – Final report. SKB Technical Report, TR-09-34, SKB Stockholm.

Posiva 2012. Safety Case for the Disposal of Spent Nuclear Fuel at Olkiluoto – Performance Assessment 2012. Posiva Report 2012-4. Posiva Oy.

Schatz T, Kanerva N, Martikainen J, Sane P, Olin M, Seppälä A, Koskinen K, 2013. Buffer erosion in dilute groundwater. POSIVA 2012-44. Posiva Oy, Olkiluoto, Finland.

SKB. 2011. Long-Term Safety for the Final Repository for Spent Nuclear Fuel at Forsmark. Main Report of the SR-Site Project. Volume II. SKB Technical Report. TR-11-01. Svensk Kärnbränslehantering AB.

Homogenisation of a dual density bentonite interface

***Caroline C. Graham*[1], Jon F. Harrington[1], Robert, J. Cuss[1], Patrik Sellin[2]**

[1]British Geological Survey, Keyworth, Nottingham NG12 5GG, UK.
[2]Svensk Kärnbränslehantering AB, Stockholm, Sweden.

Swedish plans for an Engineered Barrier System (EBS) involve surrounding the waste canister with rings of pre-compacted bentonite and filling the void space between the blocks and the deposition wall with bentonite pellets. As a consequence, a notable density contrast within the bentonite is expected to exist close to the rock wall , and to the canister, as its hydration state matures. Such a dual-density bentonite/bentonite interface has the potential to persist for significant timescales and observations at the field-scale Lasgit experiment in Äspö, indicate the potential significance for this interface to play a role in fluid migration ([1];[2]). We present results from a laboratory experiment designed to investigate the influence of such an interface on the hydration phase, the associated stress development and the transience/degree of permanency of such an interface.

The test apparatus reproduces key features of the EBS, including the constant volume condition provided by the granodiorite rock wall and a constant hydration condition, as provided by conductive fractures in the host rock. The pressure vessel comprises a stainless-steel steel, dual-closure vessel (Figure 1, *left*). A filter in both the top and bottom end-closures and three additional radial filter arrays provide a flexible geometry with which to hydrate or independently monitoring local changes in pore fluid pressure. Five total stress sensors allow the resulting evolution in radial and axial stresses to be monitored during clay swelling. The vessel also includes two injection rods, allowing water or gas to be introduced directly into either the top or the bottom of the test sample (Figure 1, *right*). Testing was conducted using Mx80 bentonite in powder form and as pre-compacted blocks, made to meet the reference specifications for the Swedish national programme. Pre-compacted bentonite was placed in the lower 60% of the pressure vessel, before the remaining chamber space was filled with bentonite powder (Fig. 1, *right*). The injection rods were positioned such that fluid could be injected directly into either the lower or the higher density clay.

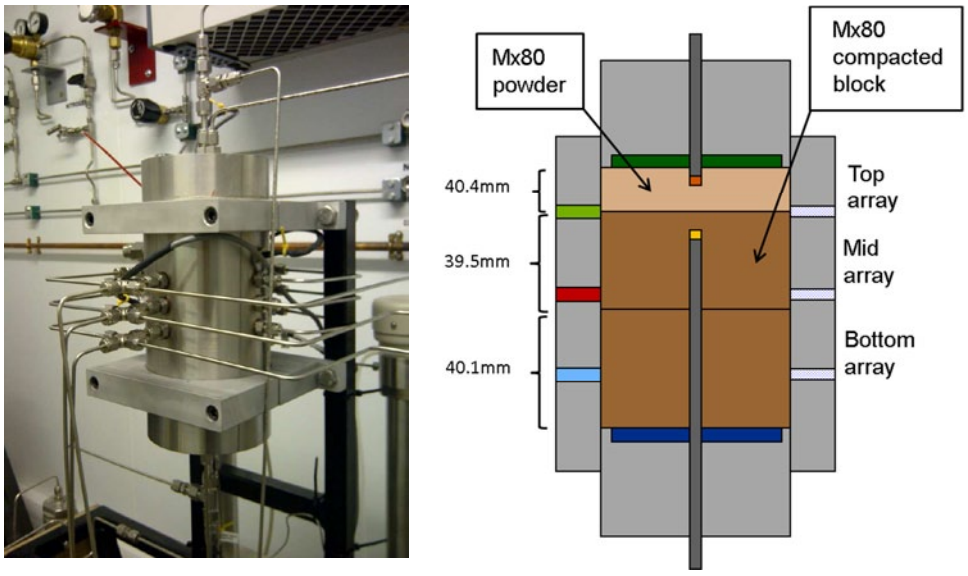


Figure 11 – The Interface Constant Volume Radial Flow apparatus (ICVRF). The schematic includes top and bottom injection rods (filters are coloured orange and yellow), the end closure filters (top and bottom axial filters are dark green and dark blue respectively) and the three filter arrays (top = light green, mid = red and bottom = light blue).

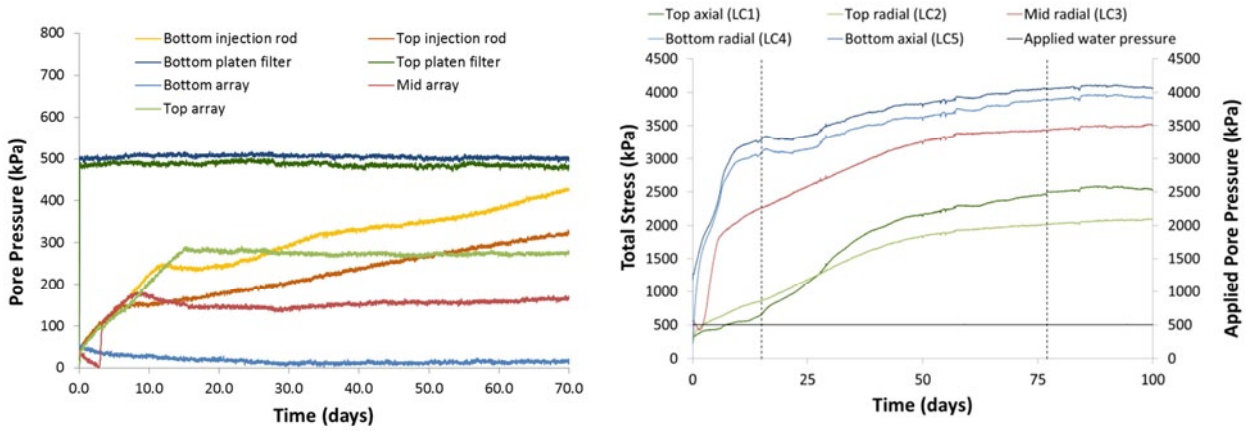


Figure 22 – Initial hydration of the dual density bentonite sample at a constant applied water pressure of 500kPa. Evolution of pore pressure (*left*) and generated total stress (*right*). Colours are used to denote location, as highlighted in Fig. 1.

Hydration of the clay was initiated by applying a constant water pressure through the top and bottom end-closure filters for a period of just over 75 days, whilst the resulting pore-pressure development was independently monitored through all other filters. Figure 2 (*right*) shows the pore-pressure evolution during saturation of the bentonite and highlights the exceptionally slow rate at which this occured. This may partly be caused by localised saturation occurring in the vicinity of the injection filters; in essence leading to a 'skin' effect, which inhibits the penetration of water into the remaining body of the sample. Nevertheless, further testing is required to investigate this hypothesis.

Despite a marked drop-off in the rate of water inflow by the second month of hydration, local pore pressure observations continued to indicate that substantial regions of the bentonite were yet to equilibrate. Observations also highlight the potential for bentonite to maintain substantial heterogeneity in the local pore-pressure distribution. This hetereogeneity was not insignificant, with unexpectedly large pressure gradients being sustained for several months. The hydration process was seen to occur in a staggered fashion, favouring different regions of the sample over time. Declining local pore pressures were also apparent at times, as hydration of other regions of the clay was favoured. In spite of this continued regional evolution of the clay, the resultant inflow curve appears suprisingly insensitive to local fluctuations and is perhaps less suitable for assessing sample hydration state than local pore-pressure measurements. Stress generation resulting from swelling of the clay also appears to be reasonably insensitive to the observed localised fluctuations in pore pressure, with the majority of stress development occurring in the early stages of bentonite hydration, though this may be the result of side-wall friction. Whilst the stresses generated by the low density slurry registered significantly lower values than those in contact with the pre-compacted bentonite blocks, this stress gradient was observed to continue for a substantial period of time. Even with this small clay volume (sample diamter=60mm, length=125mm), the stress gradient generated by the contrast in clay density was seen to persist for more than a year and half with no significant signs of homogenisation.

Findings highlight the complexity of the hydration process in pure Mx80 bentonite and suggest that variations in the rate of inflow and measurement of evolving stress distributions may not be as clear an indicator of the maturity of the clay saturation state as previously expected. Stress development and pore-pressure evolution are not uniform and evolve in an inconstant manner. Evolution of the clay on hydration exhibited several behaviours remarkably similar to those seen at the much larger, multi-component system, at the Lasgit field test (Cuss et al. 2010; 2011; 2012). The findings highlight the value of laboratory data to inform field-scale observations and confirmation expected/untested behaviours. Observations also demonstrate the complexity of the processes involved, even at a laboratory scale.

[1] Cuss, R.J., Harrington, J.F., Noy, D.J., Wikman, A., and Sellin, P., 2011. Large scale gas injection test (Lasgit): Results from two gas injection tests. Physics and Chemistry of the Earth, 36, 17-18, 1729-1742.
[2] Cuss, R.J., Harrington, J.F., Noy, D.J., and Graham, C.C., 2012. Final Report of FORGE WP3.1.1: The large scale gas injection test (Lasgit) performed at the Äspö Hard Rock Laboratory. British Geological Survey Commissioned Report, CR/12/141. 32pp.

Inflow characterization and predicting the TH evolution of a full-scale repository test in Olkiluoto

Xavier Pintado, Elisa Rautioaho*

B+Tech Oy, Laulukuja 4, 00420 Helsinki, Finland
*correspondence: elisa.rautioaho@btech.fi

The thermo-hydro-mechanical processes taking place in the buffer and backfill components are to be studied in a full-scale demonstration test in the ONKALO underground rock characterization facility in Olkiluoto, Finland (Posiva 2013), following Posiva's KBS-3V repository concept for spent nuclear fuel. One aspect of the test is the integration of thermo-hydraulic numerical modelling to improve understanding of the various processes and to provide a prediction for the saturation and temperature development of the clay components. In addition, the modelling work aims to propose a strategy for implementing hydrogeological conditions and properties in large-scale continuum models. As part of this implementation, the data from the host rock is assessed by hydrogeologists in cooperation with modellers.

The ONKALO facility is located some 420 m below ground level and comprises several demonstration tunnels, one of which will accommodate the full-scale repository test. The experiment is to include a small number of filled deposition holes, each containing a heater surrounded by bentonite material. The tunnel will be backfilled with clay materials, and the entrance will be closed by a concrete plug. The numerical model geometry comprises the main features of the demonstration test as well as the near-by tunnels, as they may interfere with the test proceedings during the proposed several years of operation time. The analyses are performed with the finite-element code CODE_BRIGHT (Olivella et al. 1994, 1996).

In the first stage of the modelling, the sensitivity of liquid pressure, saturation and temperature evolution to information regarding the host rock hydraulic conductivity and fracture matrix, and to the implementation method of the outer boundary conditions, was investigated. As shown in Figure 1, the saturation time of the buffer is highly dependent on the overall intrinsic permeability of the rock. However, the differences in tested boundary conditions did not in general significantly affect the saturation of the buffer within the simulation period of 15 years, although the liquid pressure distribution in the rock could be notably altered (see Figure 2).

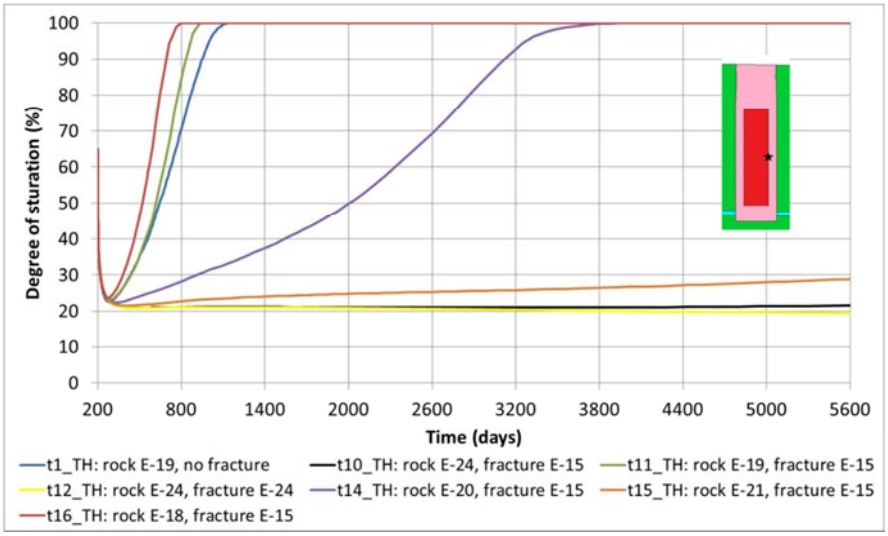


Figure 1. Sensitivity analyses of rock intrinsic permeability (m^2), depicting the degree of saturation over time (d) at the buffer – heater interface at heater mid-height.

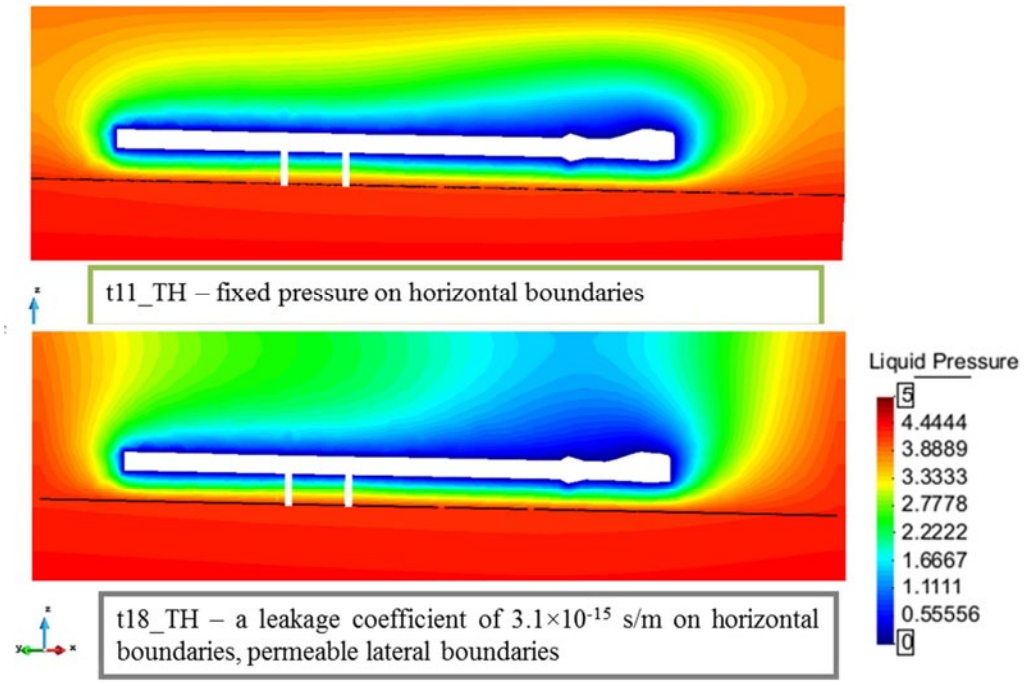


Figure 2. Liquid pressure (MPa) in the rock on a vertical cross-section of the demonstration tunnel and deposition holes after 5400 days of heating. The cases differ in terms of outer boundary conditions. The black line indicates a fracture intersecting the deposition holes.

The maximum temperature differences between the cases remained below 10 °C in the buffer. Overall, the sensitivity analyses composed of best-estimate hydrogeological cases demonstrated that a lack of information regarding rock properties, such as fracture locations and intrinsic permeability, is likely to result in a numerical estimation that is not sufficiently accurate, with regard to the wetting behaviour of the buffer and the temperature evolution in the near-field (Pintado et al. 2014).

Based on the preliminary analyses, the numerical model is updated with more detailed and more thoroughly evaluated rock-characterization data, including inflow measurements from a number of fractures intersecting the tunnel and the deposition holes, in order to obtain a reasonable thermo-hydraulic prediction of the full-scale repository experiment. Furthermore, the increased level of detail in the updated model is made possible by the new developments in 2D-fracture implementation in the finite-element program CODE_BRIGHT.

References

Olivella, S., Carrera, J., Gens, A., Alonso, E. E. (1994). Non-isothermal Multiphase Flow of Brine and Gas through Saline media. Transport in Porous Media, 15: 271-293.

Olivella, S., Gens, A., Carrera, J., Alonso, E.E. (1996). Numerical formulation for a simulator (CODE-BRIGHT) for the coupled analysis of saline media. Eng. Comput. 1: 87– 112.

Pintado, X., Rautioaho, E., Olivella, S. (2014). Preliminary TH modelling of two deposition holes in Demonstration tunnel 2. Posiva Working Report, *in review*.

Posiva (2013). YJH-2012. Nuclear Waste Management at Olkiluoto and Loviisa Power Plants: Review of Current Status and Future Plans for 2013-2015. Posiva Oy, Eurajoki, Finland.

Size distribution of bentonite colloids upon fast disaggregation in lower ionic strength waters

Natalia Mayordomo[1], Claude Degueldre[2], Ursula Alonso[1], Tiziana Missana[1]

[1]CIEMAT Avenida Complutense, 40, 28040 Madrid (Spain)
[2]Paul Scherrer Institute, 5232 Villigen-PSI (Switzerland)

Compacted bentonite is used in nuclear waste repositories to avoid radionuclide release to the environment after corrosion of canisters had taken place. Bentonite is a suitable material to take part of geochemical barriers because of its low permeability, good swelling properties and its permanent negative charge, which allows it to retain cationic pollutants on its surface. Bentonite erosion is of concern since colloids released to water flows can act as contaminant vehicles when radionuclide-colloid bond occurs and if colloids are stable, i.e. particles are not aggregated.
Several bentonite colloid stability studies have been carried out, analysing aggregation behaviour taking into account factors such as pH, electrolyte type and ionic strength **[1]**, or kinetics of generation and sedimentation pseudo-equilibrium **[2,3]**. It is known that low ionic strength (I ~ $1 \cdot 10^{-3}$ M), little presence of bivalent cations and neutral-alkaline conditions favour colloid stability and mobility.
Nevertheless, to the best of our knowledge, studies on colloid disaggregation when ionic strength is changed from high to lower values are scarce. This scenario could be the consequence of mixing high saline water, which prevents colloid stability and mobility, with diluted water from different origin (a lake, a glacier, a river or the rain). The intrusion of low saline water would decrease ionic strength that favours consequently disaggregation of bentonite particles. The size and stability recovered by these disaggregated particles would condition their further transport.
The aim of the present work is to study the disaggregation behaviour of bentonite colloid suspensions after changing electrolyte background and ionic strength. Samples were analysed by measuring their size distribution by Single Particle Counter (SPC) technique. SPC technique has different channels to detect particles in diluted samples with size range from 50 to 5000 nm.
In this technique, colloidal sample is into an ultrapure deionised water main stream, at high water flow (500 mL/min), which promotes high sample dilution during measurement time (up to 20 minutes). Therefore, the own SPC configuration allows analysing whether fast particle disaggregation occurs.

In this study, an initial bentonite colloids suspension at $5 \cdot 10^{-4}$ M $NaClO_4$ was considered as reference stable suspension (*mom*). This sample was aggregated by increasing ionic strength to 0.1 M with $NaClO_4$ electrolyte (*agr*). Aliquots of *agr* were diluted into different salinity environments: $NaClO_4$ or NaCl-$CaCl_2$ mixed water, whose ionic strengths values were $1 \cdot 10^{-2}$ M, $1 \cdot 10^{-3}$ M and $5 \cdot 10^{-4}$ M. These represent samples of intermediate stage dilutions, useful to compare their disaggregation to that of aggregated (*agr*) or initial *mom* sample.

The initial *mom* suspension decreased the ionic strength during SPC measurements to $3.3 \cdot 10^{-6}$ M, what lead to a stable suspension where up to 99% of particles have a size lower than 200 nm.
When aggregated sample (0.1 M $NaClO_4$ electrolyte) is subjected to a fast ionic strength decrease during SPC measurements (to $6.6 \cdot 10^{-4}$ M), 76% of measured particles recovered size < 200 nm, indicating that particles are disaggregated but the initial stable stage is not fully recovered. In the intermediate diluted samples, SPC measurements showed that population related to the lowest size channels (size < 200 nm) is higher when $NaClO_4$ is used to dissolve the suspension, whilst particle concentration in higher size channels (size > 200 nm) is higher when mixed water is used as electrolyte background. Figure 1 presents the normalized concentration associated to different size channels obtained by SPC measurements of the different diluted suspensions in NaClO4 or mixed electrolyte.

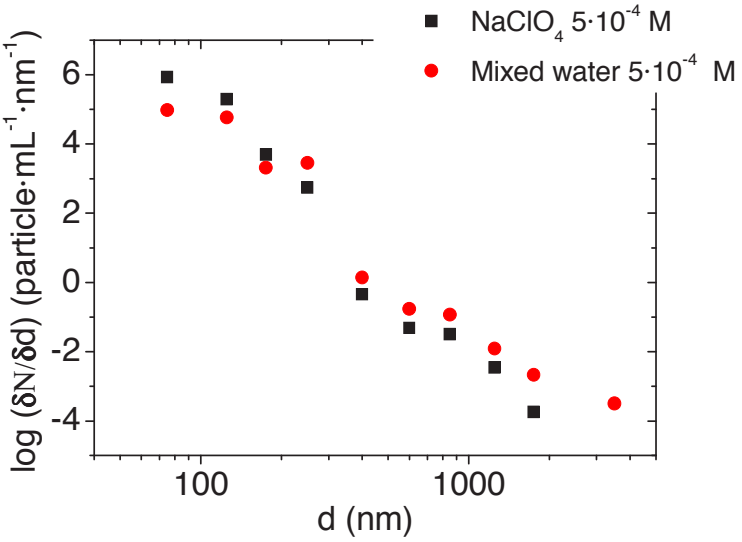


Figure 1. Normalized concentration associated to different size values obtained by SPC measurements on unshaken suspensions at the lowest ionic strength 24 hours after starting experiments.

References

[1] Missana, T., Alonso, U., Turrero, M.J., **2003**. Generation and stability of bentonite colloids at the bentonite/granite interface of a deep geological radioactive waste repository. *J. Contam. Hydrol*. 61, 17–31.

[2] García-García, S., Degueldre, C., Wold, S., Frick, S., **2009**. Determining pseudo-equilibrium of montmorillonite colloids in generation and sedimentation experiments as a function of ionic strength, cationic form, and elevation. *J. Colloid Interface Sci*. 335, 54–61.

[3] Albarran, N., Degueldre, C., Missana, T., Alonso, U., García-Gutiérrez, M., López, T., **2014**. Size distribution analysis of colloid generated from compacted bentonite in low ionic strength aqueous solutions. *Appl. Clay Sci*. 95, 284–293.

Acknowledgement

This work has been supported by NANOBAG Ministry of Economy and Competitiveness project. N.M acknowledges FPI BES-2012-056603 grant from MINECO (Spain).

Bentonite erosion and stability of formed colloids

P. Hölttä, V. Suorsa, S. Niemiaho and J. Lehto

University of Helsinki, Department of Chemistry, Laboratory of Radiochemistry, PO Box 55, FI-00014 University of Helsinki, Finland (pirkko.holtta@helsinki.fi)

In Finland, the repository for spent nuclear fuel will be excavated at a depth of about 500 meters in the fractured crystalline bedrock in Olkiluoto at Eurajoki, the site proposed by Posiva Oy. The spent uranium fuel placed in the final disposal tunnels in copper iron canisters will be surrounded with bentonite clay, which is assumed to be a potential source of colloids due to bentonite erosion. Colloids may effect on the migration of radionuclides and colloid-facilitated transport may be significant to the long-term performance of a spent nuclear fuel repository. The potential relevance of colloids for radionuclide transport is highly dependent on the release and stability of colloids in different chemical environments and their interaction with radionuclides. The objective of this work was to determine the bentonite erosion and stability of colloids formed from MX-80 type bentonite clay, which mainly consists of montmorillonite.

In the experiments, MX-80 Volclay powdered bentonite or bentonite pellets were used. In the case of powdered material, 1 g of powder was weighed in a sample tube and 45 mL of solution was added. Diluted OLSO reference groundwater, which simulates the current saline groundwater in Olkiluoto in oxic conditions, and electrolyte solutions, NaCl (I = 1 M – 1 10^{-7} M) and $CaCl_2$ (I = 3 M – 3 10^{-7} M) were used as solutions. The samples were then mixed and left to equilibrate, stored for the sampling and the samples have been taken from the top of the liquid phase. In the case of bentonite pellets, two pellets were put in a sample tube and 50 mL of solution was added. Allard, low salinity granitic (I = 4.2 10^{-3} M) and OLSO (I = 0.517 M) reference groundwater and 1 mM NaCl and $CaCl_2$ were used. The samples were stored and bentonite erosion was followed without and with gentle agitation. The formation and stability of bentonite colloids was followed as a function of time by analysing particle size distribution, particle concentration and zeta potential applying the photon correlation spectroscopy method and zeta potential applying the dynamic electrophoretic mobility (Malvern Zetasizer Nano ZS).

Formation of bentonite colloids in diluted OLSO reference groundwater as a function of ionic strength (I = 0.001–0.03 M) is shown in Figure 1. A noticeable colloid concentration can be seen only in the most diluted (1 and 5 mM) solutions. A thin layer between bentonite suspension and colloidal fraction is a result of bentonite erosion via gel formation.

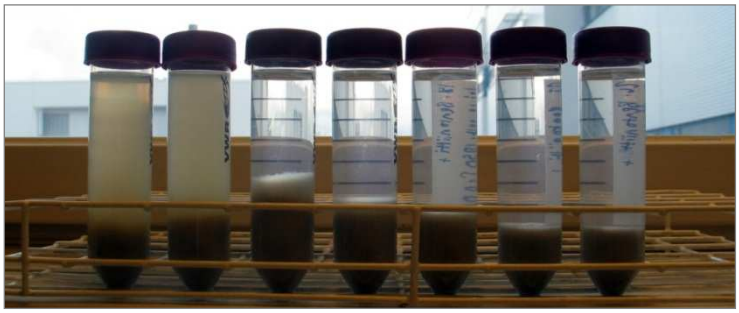
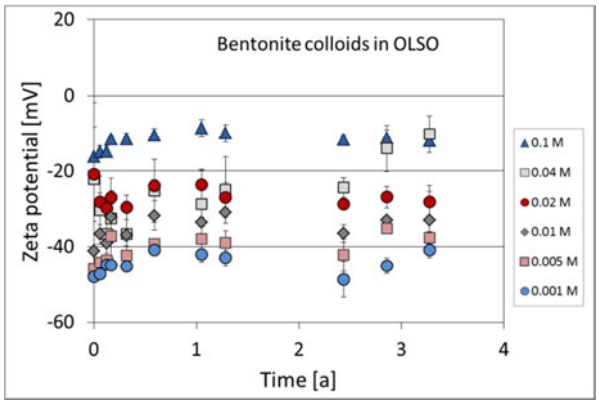


Figure. 1. The formation of bentonite colloids in diluted OLSO reference groundwater. Ionic strength from the left 0.001-0.03 M.

Mean zeta potential of colloids formed from bentonite powder in OLSO is presented as a function of time in Figure 2 and the estimated particle concentration in Figure 3. Estimated particle concentration of colloids formed from bentonite pellets in OLSO, Allard, NaCl and $CaCl_2$ solutions without agitation is presented in Figure 4 and with gentle agitation in Figure 5. In low salinity solutions, high negative zeta potential values, lower than -30 mV, indicated the existence of stable colloid dispersion. In more

saline solutions, zeta potential values were near zero indicating particle aggregation and instable colloids. There has been no notable change in the stability of colloids during the experiment.



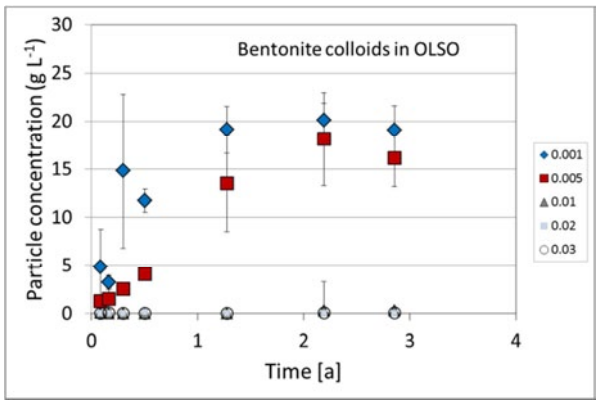
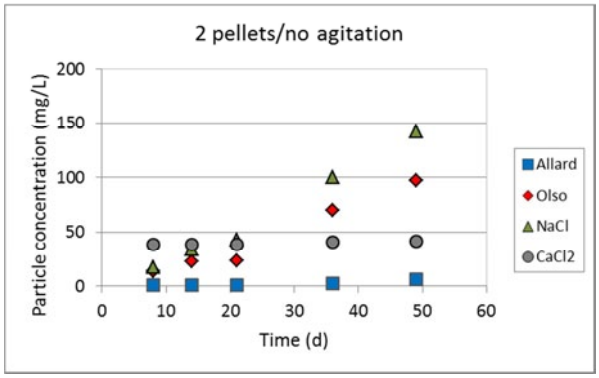


Figure 2 (left). Mean zeta potential of colloids formed from bentonite powder in OLSO.

Figure 3 (right). Estimated particle concentration of colloids formed from bentonite powder in OLSO.



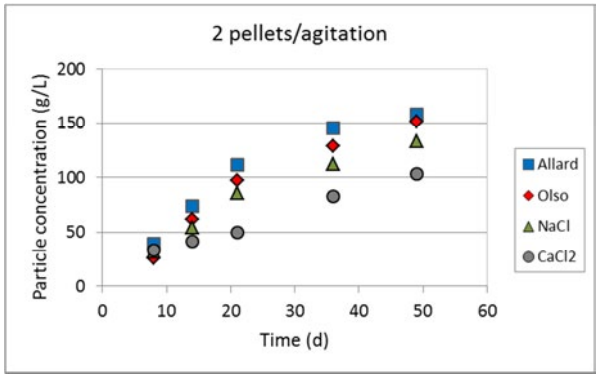


Figure 4 (left). Estimated particle concentration of colloids formed from bentonite pellets in OLSO, Allard, and NaCl and $CaCl_2$ solutions without agitation.

Figure 5 (right). Estimated particle concentration of colloids formed from bentonite bentonite pellets in in OLSO, Allard, and NaCl and $CaCl_2$ solutions with gentle agitation.

The erosion and stability of bentonite colloids depend strongly on the ionic strength of the medium and the valence of the cation. The stability colloids formed from the bentonite powder in dilute solutions did not change substantially during three years. Noticeable colloid erosion occurred only in the most diluted solutions. The bentonite erosion was significantly increased with the slow agitation. At current conditions in Olkiluoto, the ionic strength of the groundwater is around 0.5 M and the colloids released from the bentonite barrier are aggregated and unstable do not have an influence on the migration of radionuclides. However, this knowledge and understanding of bentonite erosion in colloidal form can be utilized in the estimation performance of the bentonite barrier. The possibility of a future glacial period and subsequent post-glacial phase when the infiltration of fresh, glacial melt water dilutes groundwater, implies that dilute groundwater conditions cannot be excluded and the influence of bentonite and other colloids has to take into consideration.

The research leading to these results has received funding from the European Atomic Energy Community's Seventh Framework Programme (FP7/2007-2011) under grant agreement n° 295487. Finnish Research Programme on Nuclear Waste Management and funding from the State Nuclear Waste Management Fund is also acknowledged.

Sorption and diffusion behavior of Cs in illite-added compacted montmorillonite

T. Ishidera[1], S. Kurosawa[2], M. Hayashi[2], K. Uchikoshi[2] and H. Beppu[2]

1. Japan Atomic Energy Agency (JAEA), 4-33, Muramatsu, Tokai, Ibaraki, 319-1194, Japan
2. Inspection Development Company Ltd., 3129-37, Hibara, Muramatsu, Tokai, Ibaraki, 319-1112, Japan

Introduction

Compacted bentonite is planned to be used as a component of engineered barrier system for the geological disposal of radioactive waste. The diffusivity of radionuclides in compacted bentonite is evaluated by the effective diffusion coefficient (D_e), so that a large number of D_e has been obtained experimentally. The D_e of cationic species has been sometimes found to be larger than those of neutral and anionic species. The increase of D_e has been explained by the surface diffusion: the cationic species sorbing on the bentonite are considered to have ability to diffuse along the bentonite surface, and as a result the diffusive flux is increased. This surface diffusion might be especially significant for the bentonite with high sorption capacity. Therefore, although the high sorption capacity is generally an advantage for the retardation of radionuclides, there is a possibility that the diffusivity of radionuclides is increased due to the sorption.

Illite is known to have high sorption capacity to Cs. The illite content might be increased by the hydrothermal alteration of montmorillonite, which is the main component of bentonite, caused by the decay heat of radioactive waste. The illite content in compacted bentonite possibly increases the diffusivity of radioactive Cs due to the surface diffusion. In fact, the increase of Na^+ diffusivity in compacted illite has been found and explained by surface diffusion (Glaus et al., 2010). However, the difference of dominant sorption site between Cs^+ and Na^+ on illite is considered to affect the surface diffusion. In this study, the sorption and diffusion behavior of Cs in illite-added compacted montmorillonite was investigated by through-diffusion experiment to clarify the effect of surface diffusion of Cs on illite surface in compacted montmorillonite.

Experimental method

Kunipia F (Kunimine Industries, Japan), which consists of over 98% of Na-montmorillonite and accessory minerals such as quartz and calcite, was used for the momtmorillonite material. The montmorillonite was compacted to the diffusion cells with 5% illite (Rochestsr, USA, Nichika Inc.) and 45% silica sand at a dry density of 1.2 Mg/m^3. The compacted montmorillonite with 50% silica sand without illite were prepared for comparison. The compacted montmorillonite with 5% biotite (Pradesh, India, Nichika Inc.) and 45% silica sand were also prepared for comparison, as the sorption sites of biotite is considered to be similar as illite. Membrane filters and porous plastic filters were placed at both ends of the compacted montmorillonite in the diffusion cell to prevent leaching of montmorillonite. The cell was connected to two reservoirs by tubes. The solution in the reservoirs was circulated through the filters in the diffusion cell. The solution containing Cs-137 tracer flew through the filter on one side of compacted montmorillonite (high-concentration side). A tracer-free solution flew through the filter on the other side (low-concentration side). The diffusion experiment was started by spiking Cs-137 to the high-concentration side reservoir at the concentration of around 7×10^{-11} mol/dm^3 after the saturation of compacted montmorillonite by 0.5 mol/dm^3 NaCl solution. The tracer concentrations in both reservoirs were periodically measured. The low-concentration side reservoir was replaced by new tracer-free 0.5 mol/dm^3 NaCl solution at regular intervals to keep the Cs concentration lower than around 5% of high-concentration side Cs concentration. The D_e was determined from the flux and the concentration of Cs in the high-concentration side reservoir at the steady state. The compacted montmorillonite was cut into sections to obtain the Cs concentration

profile in compacted montmorillonite at the end of the experiment. The distribution coefficient (K_d) was determined from the concentration profile.

Results and discussion

Figure 1 shows the diffusive flux of Cs. The fluxes were normalized by the Cs concentration in the high-concentration side reservoirs. For the compacted montmorillonite with 5% illite, almost no flux was observed up to 40 days. The flaxes of the other compacted montmorillonite increased immediately after the beginning of experiment. Thus, strong retardation of Cs was found in compacted montmorillonite with 5% illite. The fluxes reached constant after a certain periods. The D_es determined from the constant fluxes were $(4.2 \pm 0.2) \times 10^{-10}$, $(4.9 \pm 0.8) \times 10^{-10}$ and $(6.0 \pm 0.6) \times 10^{-10}$ m^2/s for compacted montmorillonite with 5% illite, 5% biotite and 50% silica sand, respectively. Figure 2 shows the concentration profiles of Cs in compacted montmorillonite. The concentration of Cs in compacted montmorillonite with 5% illite was obviously higher than those of the other montmorillonites. The K_d calculated from the concentration profiles were 0.27, 0.12 and 0.070 for the compacted montmorillonite with 5% illite, 5% biotite and 50% silica sand, respectively. The K_ds for the compacted montmorillonite with 5% illite and 5% biotite were several times larger than that for the montmorillonite with 50% silica sand. However, no increases of D_e were found for the compacted montmorillonites with 5% illite and 5% biotite compared to the montmorillonite with 50% silica sand. The dominant sorption site of Cs on illite is considered to be the frayed edge site (FES) considering the Cs concentration in this experiment (Bradbury et al., 2000). Therefore, the surface diffusion of Cs sorbing on the FES on illite surface was considered to be negligible in compacted montmorillonite. The surface diffusion on the biotite, which is considered to have similar sorption sites as illite, was also negligible in this experiment.

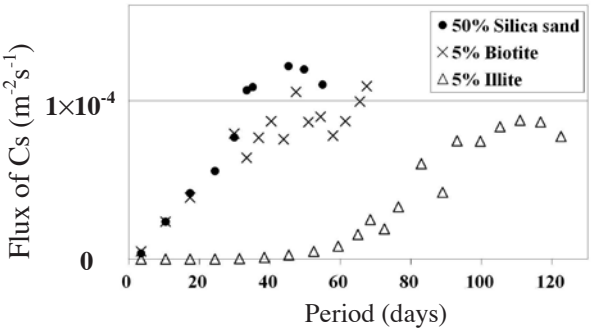


Figure 1 Fluxes of Cs for compacted montmorillonites with 5% illite, 5% biotite and 50% silica sand

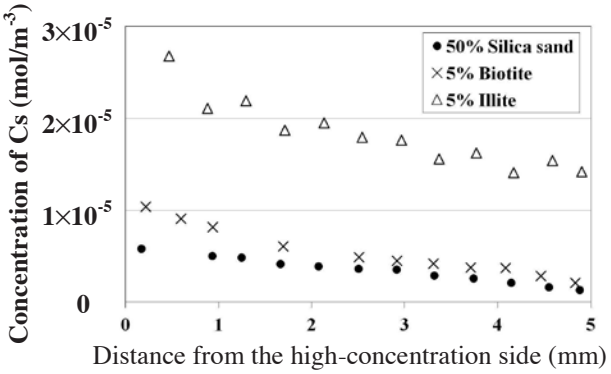


Figure 2 Concentratino profiles of Cs in compacted montmorillonites with 5% illite, 5% biotite and 50% silica sand

References:

Bradbury, M. H., Baeyens, B., 2000. A generalised sorption model for theconcentration dependent uptake of caesium by argillaceous rocks. *J. Contam. Hydrol.*, 42, 141-163.

Glaus, M. A., Frick, S., Rosse, R. and Van Loon, L. R., 2010. Comparative study of tracer diffusion of HTO, $^{22}Na^+$ and $^{36}Cl^-$ in compacted kaolinite, illite and montmorillonite, *Geochim. Cosmochim. Acta*, 74 1999-2010.

Models for ionic diffusion in compacted bentonite. Application to the ABM field test at the Äspö Hard Rock Laboratory

Andrés Idiart[1], **Marek Pękala**[1], **Patrik Sellin**[2]

[1]Amphos 21 Consulting S.L., Passeig Garcia I Faria, 49-51, 1º1º, 08019, Barcelona, Spain (andres.idiart@amphos21.com)
[2]SKB, Svensk Kärnbränslehantering AB, Stockholm, BOX 5864, S-102 40 Stockholm, Sweden

The KBS-3V concept of deep geological repositories for spent fuel in Sweden and Finland relies to a large extent upon the performance of compacted bentonite, a material that will be used as buffer surrounding the copper canisters. The suitability of compacted bentonite is based on their confining properties, i.e. an elevated swelling capacity, a very low permeability, and a large sorption capacity for certain species. Under these conditions, solute transport in water saturated clays occurs almost exclusively by diffusion, thus limiting the release of radionuclides in the event of a failure of the canister. Even though diffusion in compacted clay and bentonite has been intensively studied during the last three decades, there remain at present a number of controversial issues regarding a mechanistic representation of the underlying phenomena. These issues result, in most of the cases, from a lack of a well-establish and widely accepted nano-/micro-structural conceptual model of compacted bentonite at different dry densities and salinities. The applicability of currently available characterization techniques for the porosity distribution and nanostructure of compacted bentonite is limited as they often perturb the structure of the water saturated bentonite. As a result, reliable experimental results are difficult to come by and indirect evidence must be relied on to a large extent. In these systems, the validity of the fickian diffusion approach has been questioned in some cases, as it is shown to not correctly represent the diffusion of cations, anions and neutral species simultaneously. More complex mechanistic models have been proposed in the literature to explain experimental data, based on different conceptualizations of the pore space.

In this work, the results of the Alternative Buffer Material (ABM) field test at Äspö Hard Rock Laboratory in Sweden [1] have been used to evaluate the applicability of different models to explain experimental observations. In particular, available data on the cation exchanger composition and chloride concentrations in the different blocks have been used to evaluate the following models:

1) Single bulk porosity coupled to cation exchange reactions [2]
2) Single interlayer porosity Donnan equilibrium model [3]
3) Multi-porosity (interlayer, double layer, and free) model [4]

The models consider the effects of the high temperature conditions of the test and groundwater composition used for the artificial saturation of the column, as well as the block-specific physical and chemical characterization data (30 blocks of 11 different compacted bentonites were randomly distributed in the column). The results obtained confirm that the classical Fickian diffusion approach using a single total (bulk) porosity fails to predict the concentration of anions in the bentonite blocks (in this case chloride). On the other hand, this simple approach, if coupled to cation exchange reactions, explains fairly accurately the evolution of the cation exchanger composition of the different blocks.

The single interlayer porosity Donnan equilibrium model and the multi-porosity (three porosity types, assuming complete anion exclusion from the interlayer and double layer porewater) are both able to explain the observed chloride concentrations in the different bentonite blocks. On the other hand, the Donnan equilibrium model largely overestimates in all cases the calcium occupancy of the exchanger at the expense of underestimating the sodium and magnesium fractions.

In addition, scoping calculations of a theoretical setup relevant to the Performance Assessment calculations of radionuclide migration in the KVS-3V concept have been repeated using different diffusion models. The goal is to compare the diffusive fluxes of different models when using a best-

guess parameterization approach. In this case, different diffusion coefficients have been typically used for different species, depending on the charge of the ions (e.g. [5]). Despite their conceptual differences, the results indicate that the diffusive fluxes obtained with the different models compare relatively well, especially for anions, and to a lesser extent for cations.

References

[1] Svensson D. et al., 2011. Alternative Buffer Material – Status of the ongoing laboratory investigation of reference materials and test package 1. SKB TR-11-06.
[2] Pękala M, Idiart A, Arcos D, 2012. Reactive transport modeling of the ABM experiment with Comsol multiphysics, Clays in Natural and Engineered Barriers for Radioactive Waste Confinement, pp. 905-906, Montpellier, France, October 22-25, 2012.
[3] Birgersson M, Karnland O, 2009. Ion equilibrium between montmorillonite interlayer space and an external solution – Consequences for diffusional transport. Geochimica et Cosmochimica Acta, 73, 1908–1923.
[4] Appelo C A J, 2013. A Review of Porosity and Diffusion in Bentonite. Posiva Report WR 2013-29.
[5] Ochs M, Talerico C, 2004. SR-Can. Data and uncertainty assessment. Migration parameters for the bentonite buffer in the KBS-3 concept. SKB TR-04-18.

PhreeqcRM: A reaction engine for flow and transport simulators based on the geochemical modelling framework PHREEQC

Laurin Wissmeier[1], **David L. Parkhurst**[2]

[1]AF-Consult Switzerland Ltd, Groundwater Protection and Waste Disposal, Taefernstrasse 26, CH-5405 Baden, Switzerland
[2]U.S. Geological Survey, Box 25046, MS 413, Denver Federal Center, Denver, CO, 80225, USA

During the past decade, one of the main driving forces in reactive-transport modelling has been the ongoing global search for strategies for safe disposal of radioactive waste. Governmental agencies are taking great efforts to manage radioactive waste and to assess the risks of different disposal schemes. Reactive-transport modelling is of interest because of (1) its potential to predict the evolution of contaminant plumes over long time scales, and (2) its capabilities to simulate near-field processes to improve safety in the design of confining structures and containers.

PhreeqcRM (PHREEQC Reaction Module) is a high-level programming interface, based on the well-known geochemical modelling framework PHREEQC, that is specifically designed to be coupled with existing transport simulators. Thus, by using PhreeqcRM, many codes for THM (thermo-hydro-mechanical) processes in the domain of radioactive waste disposal could be enhanced with the simulation of detailed geochemistry. Designed as a wrapper class, PhreeqcRM provides access to the full set of equilibrium capabilities of PHREEQC, including reactions with minerals, ion exchangers, surface complexers, a gas phase, and solid solutions. In addition, PHREEQC's powerful kinetic rate integrator for the calculation of time-dependent reactions with user-defined rates can be used to simulate kinetic mineral reactions, biological transformations, or any other kinetic reactions. PhreeqcRM can be coupled to transport simulators by using a sequential operator-splitting approach that alternates transport and reaction steps. Between the reaction steps, PhreeqcRM retains the compositions of all reactants, which eliminates the need to exchange compositions of any reactants (other than solutions) with the host transport simulator. Furthermore, PhreeqcRM encapsulates efficient parallelization using either multi-threading with OpenMP on shared memory systems or multi-processing with MPI on distributed memory systems. PhreeqcRM exposes high-level API's for C++, its native language, as well as C and Fortran (Fortran90 or newer).

PhreeqcRM has the functionality to define geochemical solutions in terms of elements and charge imbalance, which allows for efficient geochemical transport when species-independent transport properties can be assumed. However, PhreeqcRM also provides the necessary methods to define the aqueous solutions in terms of chemical species, which facilitates couplings with species-dependent transport equations (i.e., Nernst-Planck equation).

FEFLOW is a finite element (FE) subsurface flow (FLOW) and transport model that is routinely used by state authorities and industry to assess mass-transport related issues of radioactive waste disposal. A new reaction module using PhreeqcRM is implemented as a plugin for the FEFLOW host application based on the FEFLOW interface manager (IFM). Validation of the FEFLOW plugin is presented using an analytical solution of 3D transport with a first-order decay chain. Additional code verification is provided by a detailed simulation of the MoMaS (Modeling, Mathematics and numerical Simulations related to nuclear waste management problems) reactive transport benchmark, which is specifically designed for reactive transport problems in the context of radioactive waste disposal. Figures show selected concentrations of dissolved constituents (X2 and X3), surface species (S), and precipitated solids (CP1) for easy, medium, and hard benchmark simulations using FEFLOW.

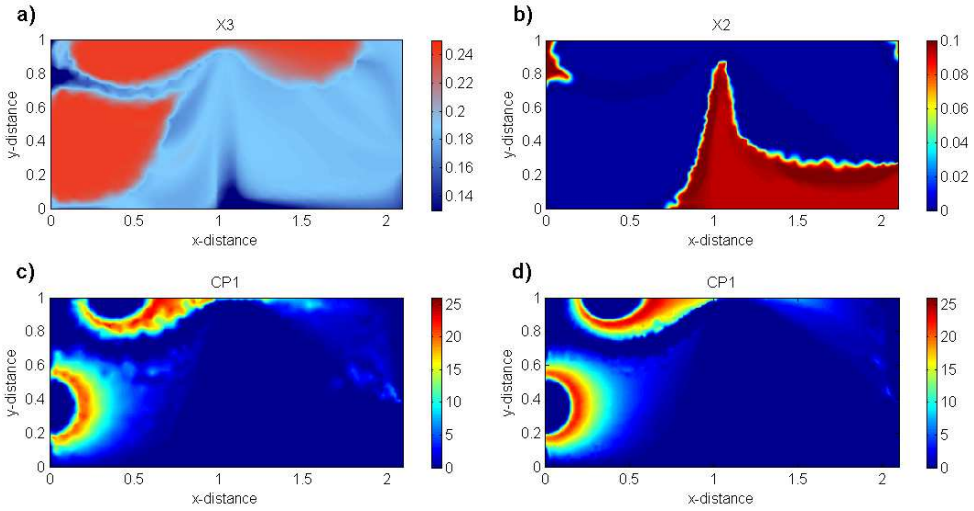


Figure 1: MoMaS results from 2D advective cases: (a) X3, easy case at time 1000; (b) X2, medium case at time 1000; (c) CP1, hard case at time 2000; (d) same as (c) but calculated with refined mesh.

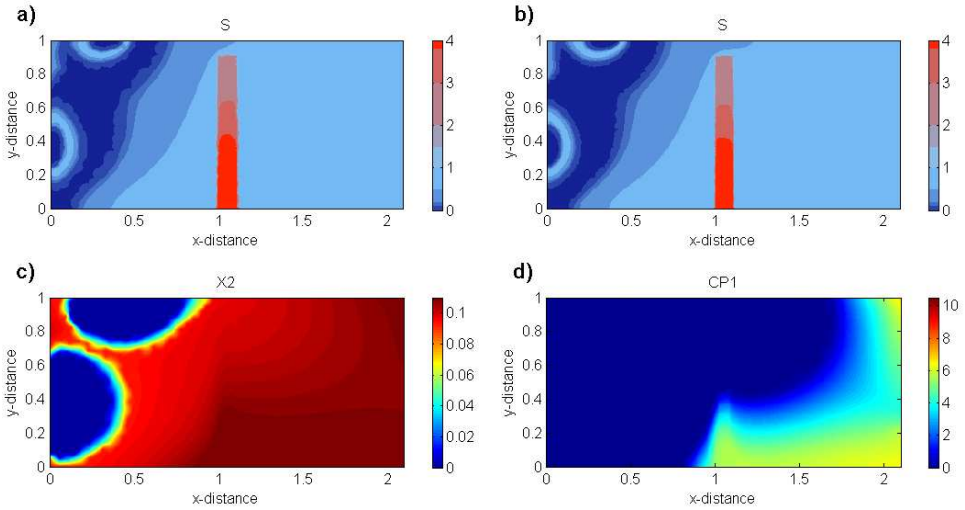


Figure 2: MoMaS results from 2D dispersive cases: (a) and (b) S, easy case at time 10 with coarse and fine mesh, respectively; (b) X2, medium case at time 1000; (c) CP1, hard case at time 2000.

Large-scale meshing for safety calculations for the planned deep geological repository and its surrounding geological environment in France

***Nicolas Hubschwerlen*[1], Jean Roger[2], Laurent Tacher[3], Bernard Vialay[2]**

[1] AF-Consult Switzerland Ltd, Groundwater Protection and Waste Disposal, Taefernstrasse 26, CH-5405 Baden, Switzerland, *Nicolas.Hubschwerlen@afconsult.com*
[2] Andra, 1-7 rue Jean Monnet, F-92298 Châtenay-Malabry Cedex, France
[3] Terre+, Chemin de Closel 9, CH-2022 Bevaix, Switzerland

Safety calculations for a deep geological repository for radioactive waste are particularly challenging because the involved spatial scales span over many magnitudes. The repository itself consists of tunnels with a length of up to a few kilometres which contain features below the meter-scale whereas the geological environment that needs to be considered expands over several kilometers horizontally and several hundred meters vertically. Furthermore, the relevant geological entities and the topography vary in space which requires that, e.g., disappearing geological layers and small-scale features have to be taken care of. Covering all these spatial scales by adapting a spatial discretization at the scale of the smallest represented detail would lead to meshes which are incompatible with the computing capacities of the simulators used for safety calculations.

A common approach for working around this difficulty is to establish local models with a limited spatial extent where a high level of detail is required (i.e. in the repository) and perform simulations on those limited zones, which are then stepwise nested into coarser larger scale models until the regional scale is reached. The impact of the nested models is taken into account by assigning specific inner boundary conditions in the larger scale model. This approach however *de facto* creates some discontinuities. Moreover it is not suitable for representing precisely some coupled processes likely to occur between different model scales. That is why Andra desires to perform some reference safety calculations on a model of the repository including all scales from the largest regional level to the waste cell detail level.

Hence we have developed sophisticated meshing tools and techniques that allow representing efficiently a geological model spanning over a regional scale together with a geological repository composed of a number of drifts, shafts and an access ramp in a limited number of mesh cells. These techniques based on a modular strategy offer a high level of flexibility for easily implemented variations of the repository's layout and of the level of detail to be modeled. The resulting meshes are designed to be used for calculations using a Finite Volume numerical technique with Porflow. It is conforming and its elements are mostly hexahedral, completed by some prisms with a triangular base. The mesh can also be exploited with a Mixed-Hybrid Finite Element code such as Andra's code Traces for numerical comparison purposes. For the mesh generation, particular care is taken to avoid numerically unfavourable element sizes and shapes.

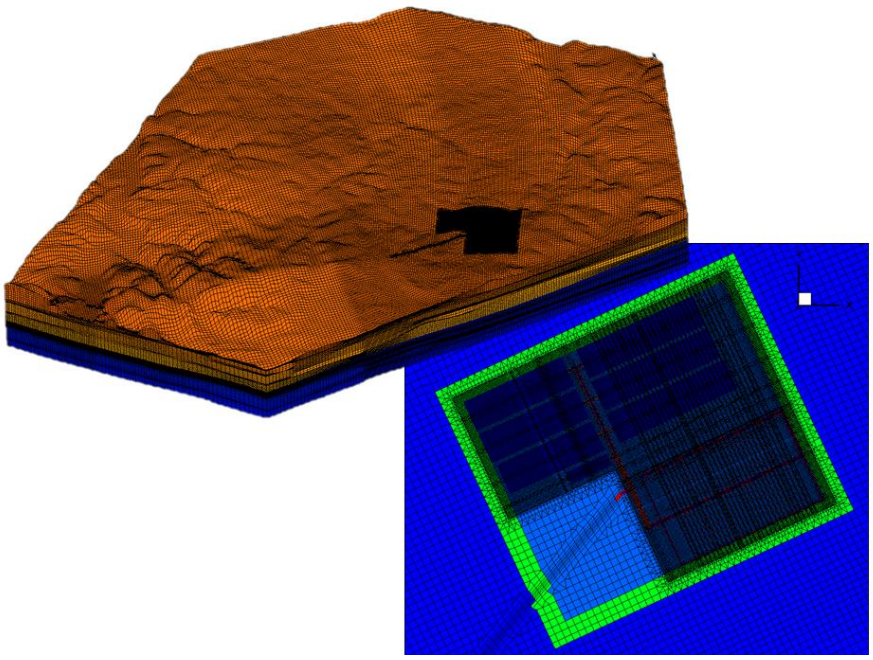
The meshing strategy consists of creating a multilayer mesh of the geological environment, based on some horizontally smoothed macro element boxes meshed with hexahedrons. Those are cut to fit the domain's borders, also resulting in a few triangle based prism elements which are exclusively located on the boundaries. The mesh layers follow precisely the limits of the geological layers and the vertical discretization within the geological layers is carefully chosen to ensure a progressivity of the discretization length and to take into account the hydrogeological properties. The horizontal extension of the repository zone is entirely meshed by hexahedrons having an orthogonal base with strictly regular dimensions. Those regular elements are oriented along the repository layout's main directions. The repository is constructed as a local structured mesh with a high resolution. Particular attention is paid to the regularity and the progressivity of the size of the elements around the most finely meshed

zones, corresponding to details such as some potentially damaged waste containers and the extension limits of some drifts and their damaged zones. This results in two independent meshes with different scales. In order to assemble them into a unique conforming mesh, some layers of transition elements are automatically built around the fine repository mesh to progressively increase its boundary element size. This progressive mesh coarsening involves a combination of different macro elements constituted of triangle based prisms and hexahedrons. They allow the progressivity in element size while ensuring that quality properties such as element skewness remain close to optimal. Once the boundary of the repository and its envelope of transition elements have reached the discretization length of the regular part of the geological mesh, it is straightforward to replace this regular part by the repository mesh.

Particularly challenging is the insertion of the repository access ramp into the geological mesh because of its length of over 4 km, its orientation, and its inclination. The construction methodology consists of creating a structured two-dimensional mesh of the drift, the surrounding damaged zone and some additional transition layers for ensuring progressivity of the cell sizes. This mesh is repeated for all mesh layers. Vertically, the ramp and its damaged zone are approximated by a stair formed by all cells on the real trajectory of the ramp from the surface to the repository level. Within the stair pattern all neighbouring cells are in contact by one face. Elements of the geological mesh crossed by the trace of the access ramp are replaced, and conform linking between the ramp and the geological mesh is completed with triangle-based prisms and hexahedrons where necessary.

The developed tools have been applied to build some representations of the French deep geological repository which is planned to be constructed in a Callovo-Oxfordian clay host-rock layer located approximately 500 m below surface. The model extends over approximately 660 km^2 and is bounded by an irregular polygon fitting into a 30 km sided square. Vertically, it ranges from the surface down to the bottom of the Dogger at a depth of more than 1000 m below surface. The extension of the waste storage zone itself is about 4 km by 6 km. An average element has a 100 m side length in horizontal direction within the geological mesh whereas the smallest repository elements are less than 10 x 10 m in size.

Some first Finite Volume simulations have been performed with the new meshes. They have shown that the flow and transport results match with the computation results obtained with models on different scales. Moreover, the developed meshes lead to a good numerical convergence. Not least, the resulting computation times remain reasonable regarding the extension and the level of detail of the model.



Groundwater and thermohaline modelling in the Paris Basin, considering the past geodynamic evolution

J. Holmén[1], H. Benabderrahmane[2]

[1] Golder Associates P.O. Box 20127, Östgötagatan 12, 104 60, Stockholm, Sweden (johan_holmen@golder.se)
2 Andra, 1/7 rue Jean Monnet, 92298 Châtenay-Malabry, Cedex, France (hakim.benabderrahmane@andra.fr)

Modelling of transport of natural tracers on the scale of the Paris Basin is part of a phenomenological analyzes of the hydrogeological functioning of the Meuse/Haute-Marne aquifer system (*de Hoyos et al.*). Indeed, modelling of the sources of these tracers, and especially the migration mechanisms in the aquifer system provides insight into the past hydrogeological evolution: and the past hydrogeological evolution influences present and future groundwater flows. It also defines the elements used for the study of future hydrogeology. The major objectives of Andra's Cigéo project is to build a consistent concept of the hydrogeology of the future Radwaste site, and to support the performance assessment hydrogeological model which includes the present situation and the future hydrogeological evolution through the next million of years. The modelling of groundwater and thermohaline on the scale of the Paris Basin aims to understand the effect of the past geodynamic evolution on the present time salinity distribution in the multi-layered aquifer and especially on the Dogger and Oxfordian layers embedding the Calovo-Oxfordian clay formation. Such modelling will also indicate the hydrogeological role of the regional faults.

The construction of the conceptual model of the Paris Basin multi-layered aquifer system and its evolution through the past 20 Million of years includes the present time hydrogeological model (*Holmén et al. 2011)* and the past tectonic uplift and erosion modelling results (*Andra 2013*). A fully coupled three-dimensional groundwater flow and transport model (salinity and heat with density effects) has been developed. It takes into account the hydro-mechanical effect resulting from the erosion of the geological layers. The model covers the entire Paris Basin and is focused on the Meuse/Haute-Marne Sector area including the repository site. The properties of the model are based on the conceptual and calibrated model of the Paris Basin (present situation) (*Andra 2009*). The past geodynamic evolution describes the deformation of the geological layers induced by tectonic uplift and erosion processes during 20 million years before the present. Simulations are performed by GEOAN computer code based on the finite difference numerical method. The multi-layered aquifer system was discretized into over 14 million active cells and simulations were run for a time period of more than 20 million of years. A number of different simulations have been carried out testing different aspects of the system studied; demonstrating the importance of e.g. initial condition for head and salt and other aspects of the transport phenomenon studied, tectonic uplift and erosion, hydro-mechanical effects, permeability of fault zones and low-permeable layers.

The simulations demonstrate that when considering the time scale studied (20 Ma) the geodynamic evolution of the basin is of importance for the development of groundwater heads and concentrations, both for surface near layers and at great depths. The geometry of the basin 20 Ma before the present included larger extensions of surface near layers of Cretaceous age and also a flatter topography; for such a situation the groundwater flows magnitude will be less than for the present situation. It was also demonstrate that the time scale for the salt migration is very larger than 20 Ma for the central part of the basin. The present day conceptual model geometry will tend to overestimate the past advective transport, which can be of significant importance for the simulated concentrations in aquifers. In the model the tectonic uplift and the erosion of surface near layers will together create a tendency for overpressures in confined layers, also at great depths; these overpressures are not balanced by hydro-mechanical effects.

References

Amélie de Hoyos, Pascal Viennot, Emmanuel Ledoux, Jean-Michel Matray, Muriel Rocher, Catherine Certes (2012 Influence of thermohaline effects on groundwater modelling – Application to the Paris sedimentary Basin. *Journal of Hydrology 464-465 (2012) 12-26*.

Holmén J, Benabderrahmane H, Buoro A, Brulhet J (2011) Modelling of permafrost freezing and melting and the impact of a climatic cycle on groundwater flow at the Meuse/Haute-Marne site. *Phys. Chem. Earth 36, 1531-1538*.

Acquisition of a permeability profile through the Opalinus Clay at the Mont Terri rock laboratory from a petrophysics-related Poiseuille type law applied to BDB-1 borehole samples

Matray, Jean-Michel[1], **Ould-Bouya, Lamine**[1,2], **Yu,Catherine**[1]

[1]IRSN, BP17, 92262 - Fontenay-aux-Roses cedex, France
[2]University of Paris-Sud 11, Faculté des Sciences, 91405 – Orsay Cedex, France

Modelling coupled fluid and solute transport processes require both the acquisition of phenomenological parameters and of their force gradients (P,T,C). For fluid flow occurring in clayey aquitards, where membrane behavior plays an important role, the phenomenological transport parameters are all permeability dependent. In the context of a Deep Geological repository of HL-ILLL radioactive wastes, the way by which most mobile radionuclides (Cl, Se and I) may potentially migrate through a host rock when canisters are leaking is of major importance for its performance assessment. The relative importance of coupled fluid flow to diffusion in the RN transfer through a clayey geological barrier is not yet fully understood especially when transient transport processes are involved. The Mont Terri rock laboratory now offers the opportunity to answer this puzzling problem through the recent drilling of a 250m deep inclined borehole called BDB-1 through the Opalinus Clay. This 130m thick clayrock is known for hosting a recent transient flow of water and solutes evidenced by a Quaternary-dated input of meteoric waters in the Lower and Middle Jurassic. The borehole BDB-1 was 45° inclined for providing core samples normal to the bedding and yielded excellent material especially to assess the spatial distribution of petrophysics, mineralogy, porewater geochemistry and to constrain stratigraphy and facies limits. The lithostratigraphic sequence crossed by the borehole was successively composed of carbonates (Hauptrogenstein, 0-37m) and marls (Passwang Fm., 37-106m) in the upper part followed by the different facies (sandy, shaly and carbonate-rich) composing the Opalinus clay (106-237.5m), and finished in the lower part by the marly Staffelegg Fm., Gross Wolf- and Rietheim members (237.5-247.5m). Right after drilling and logging, the borehole was equipped with a multi-level packer system isolating seven test sections for acquiring the pressure and temperature profiles and performing hydraulic tests after recovery of the initial pore pressure and

temperature, which still is in progress. The profile of intrinsic permeability was computed across the Opalinus Clay as a function of petrophysical parameters acquired on core samples every 10meters through the Kozeny-Carman equation. It is a Poiseuille type law based on a plane-parallel geometry for pores, likely convenient for compacted clayrocks. The Kozeny-Carman relation links the half-pore size (nm) to the formation factor of Achie's law. The half-pore size was deduced from petrophysical parameters and fits quite well with those estimated from the pore size distribution obtained with the BJH method. Total porosity, grain density, degree of saturation and specific surface area were determined respectively by combining i) total apparent densities by density measurements in oil and by water content measurements performed at 105°C, ii) grain density by He pycnometry at 105°C, iii) porewater density calculated from porewater salinities deduced from out diffusion experiments and iv) specific surface areas by coupling BET and BJH methods. The formation factor was deduced from the Archie's law that links the physical porosity to the cementation factor obtained by fitting permeability estimates to porosity data.

The preliminary results on the Opalinus Clay indicate that the samples were fully saturated at the bottom hole and partially (down to 90%) desaturated in its upper part. They also surprisingly indicate, whatever the facies, porosities in the order of 14±1% which is lower than the 18% usually considered at the gallery level. The petrophysical parameters and permeability profiles fit very well mineralogy deduced from XRD measurements on the bulk rock. Estimates of intrinsic permeability and hydraulic conductivity depend on the cementation factor considered. For the Opalinus clay, the average values for intrinsic permeability range between 2E-20 and 6E-23 m^2 and for hydraulic conductivities between 2E-13 and 5E-16m/s when the cementation factor varies from 2 to 5, respectively. The comparison of hydraulic conductivities deduced from hydraulic tests to those estimated from petrophysical measurements will enable us to obtain a better estimate of the cementation factor and improve our permeability profiles in prevision of our future fluid flow modelling.

oooooooooooo

Acknowledgements:Authors would like to warmly thank all the Mont Terri Partners of the DB and DB-A experiments for their financial and technical support. This includes: swisstopo and Nagra (CH); BGR and GRS (D), NWMO (Ca) and IRSN (France).

Process based modelling of Cs transport in Boom Clay

Norbert Maes, **L. Muthwill, L. Van Laer, S. Liu, C. Bruggeman**

SCK•CEN, Belgian Nuclear Research Centre, Institute for Environment, Health and Safety,
Boeretang 200, B-2400 Mol, Belgium, (nmaes@sckcen.be)

The long-term safety of geological disposal of high-level waste and spent fuel in argillaceous formations relies very much on the capability of the host formation to delay and attenuation the release of radionuclides. Sorption and ion-exchange processes are important mechanisms that ensure this delay and attenuation function in clay formations.

Sorption of Cs onto clays has been extensively studied and Bradbury and Baeyens (2000) developed a generalised 3-site cation exchange model that is able to describe the Cs sorption onto several host rocks studied in the field of geological disposal (OPA, COx, Boom Clay). This "simplified" model is based on illite as unique model component representing the host formation.

In a previous study on the retention of Cs in Boom Clay (Maes *et al*., 2008), batch sorption data were interpreted with the generalised 3-site cation exchange model. This model was then incorporated into a coupled geochemical transport model (PhreeqC2.13) in order to interpret a Cs column migration experiment that lasted 13.7 years. Modelling results showed that experimental Cs diffusion was faster than expected and could not be predicted by the transport model. Two reasons were put forward and tested: not all sorption sites are available in compacted state (resulting in a lower retardation compared to batch sorption data), or so-called "surface diffusion", with effective diffusion coefficients (D_{eff}) for Cs being (much) higher than effective diffusion coefficients for HTO. Later on, it was proven that compaction has no effect on the availability of sorption sites (Van Loon *et al*., 2009; Altmann *et al*., 2012), hence the discrepancy of the experiment with the model was attributed to "surface diffusion". Appelo *et al*. (2010), proposed a multicomponent diffusion model that was able to describe the transport of, a.o., Cs in Opalinus clay. This model distinguishes 3 types of porewater, hence 3 domains where tracers can be transported: free water (interparticle pores), DDL water (water in the electric double layer on outer clay planes & edges) and IL water (interlayer water present in overlapping double layers between clay plates in smectite clays). Due to ion-exchange, cations like Cs become enriched in the DDL and IL, resulting in a local increase in concentration gradient, and hence in a higher flux. This can lead to a higher overall D_{eff}. The "surface diffusion" effect, or better stated the "double layer diffusion" has been extensively investigated in the EC project Catclay (www.catclay.org).

Based on the current state of the art, the Cs sorption and diffusion data in Boom Clay are revisited. First, experimental Cs sorption data were obtained on Boom Clay samples, on which the relative proportions of clay minerals (illite, muscovite, smectite, interstratified illite-smectite (ISS)) were quantified (core 116 Mol-1). The Cs sorption model for Boom Clay based on illite (Ill) was extended by including Montmorillonite (MoMo) as an extra ion-exchanging phase. Adding MoMo was necessary in order to achieve a better description of Cs sorption at higher concentration (Figure 1 left, dashed line). The experiment was modelled using 2 mixing proportions of Illite and Montmorillonite. The 15/28 mix represents the ratio of illite+muscovite/smectite+ISS while for the 24/15 mix, the ISS fraction is divided over Illite and Smectite. Chen *et al*. (2014) modelled Cs sorption on COx samples, and they stated that the ISS did not contribute to the Frayed Edge Sites (FES) that are typical Cs sorption sites on illite. In our case, both models provide good matches to the experimental data (fig. 1 left, filled circles) with a slightly better match for the mix where it is considered that the ISS fraction contributes to the FES sites. However, more samples need to be investigated to conclude on this (on-going).

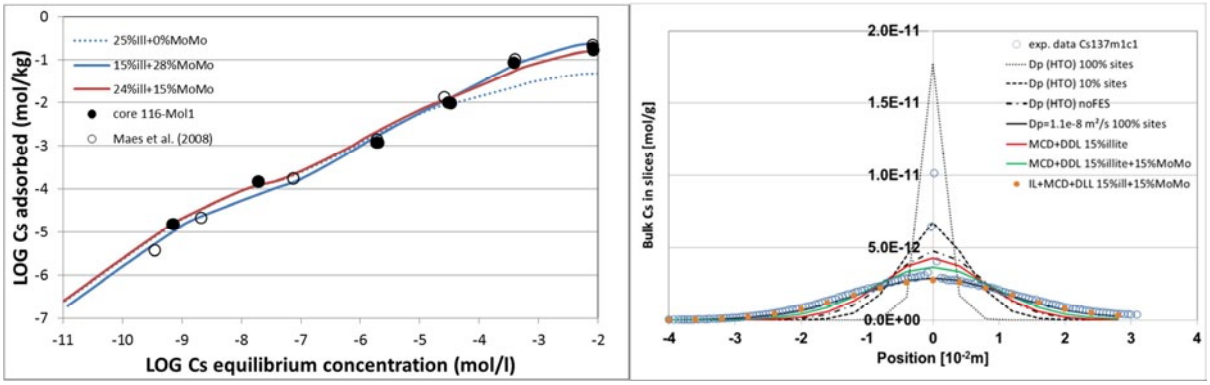


Figure 1: Left: Cs sorption isotherms on BC samples and respective modelling using different mineral mixtures. Right: Cs column migration experiment in Boom Clay (duration 13.7 yrs.) and coupled geochemical transport model simulations (PhreeqCi-3).

Finally, the Cs transport experiment published in Maes *et al*. (2008) was remodelled by incorporating the sorption model for illite (Bradbury & Baeyens, 2000) and montmorillonite (Bradbury & Baeyens, 2010) in a coupled geochemical transport code (PhreeqCi-3) allowing multicomponent diffusion and introducing diffusion in the DDL and IL (Appelo *et al*., 2010). In figure 1 (right), the evolution in the model approach is shown. In Maes *et al*. (2008) the experiment was modelled assuming that the Boom Clay sample consists of 20% illite. By decreasing the number of sites (results for 10% sites or no FES are shown) the model curve tends towards the experiment. When considering all sites available, only a good match is obtained when the D_{pore} was increased to a value much higher than the D_{pore} of HTO. In the resumed model, first multi-component diffusion and diffusion in the double layer is introduced by assuming that the sample consists of 15% illite or a mix of 15% illite and 15% MoMo. By allowing also IL diffusion in the MoMo, a good match to the experimental curve is achieved. No dead-end pores had to be assumed in the model, contrary to results obtained on Opalinus Clay (Appelo *et al*., 2010).

The transport of Cs in Boom Clay can be adequately described by considering the underlying processes of sorption via ion-exchange on illite (3 sites) and MoMo (1 site), using well established sorption models (site capacities, selectivity coefficients) and accounting for enrichment in DDL and IL creating extra diffusive fluxes.

Acknowledgement: This work is performed in close cooperation and with financial support of ONDRAF/NIRAS.

References

Altmann S., Tournassat C., Goutelard F., Parneix J.C., Gimmi T., Maes N. (2012) Applied Geochemistry 27, 463-478.

Appello, CAJ., Van Loon L., Wersin P. (2010) Geochimica et Cosmochimica Acta 74, 1201-1219.

Bradbury M., Baeyens B. (2000) Journal of Contaminant Hydrology 42, 141–163.

Bradbury M., Baeyens B. (2010) Comparison of the reference Opalinus Clay and MX-80 bentonite sorption data bases used in the Entsorgungsnachweis with sorption data bases predicted from sorption measurements on illite and montmorillonite. PSI Bericht Nr 10-09, PSI, Switzerland.

Chen Z., Montavon G., Ribet S., Guo Z., Robinet J.C., David K., Tournassat C., Grambow B., Landesman C. (2014) Chemical Geology 387, 47-58.

Maes N., Salah S., Jacques D., Aertsens M., Van Gompel M., De Cannière P., Velitchkova N. (2008) Physics and Chemistry of the Earth 33, S149-S155.

Van Loon L., Baeyens B., Bradbury B. (2009) Applied Geochemistry 24/5, 999-1004.

Origin of halides (Cl^- and Br^-) and of their stable isotopes ($\delta^{37}Cl$ and $\delta^{81}Br$) at the Tournemire clayrock URL (France) - Experimental and numerical approach

N. BACHIR-BEY[1-2], *J.-M. MATRAY*[1]

[1-2]IRSN – Institut de Radioprotection et de Sûreté Nucléaire, BP 17, 92262 Fontenay-aux-Roses, France
[2]Université Paris-Sud 11, Bât. 504, Orsay Campus, France. (bachirbey.nassim@hotmail.fr)

This work is part of research conducted by the Institute of Radiological and Nuclear Safety (IRSN) on the geological disposal of High-Level and Intermediate-Level Long-Lived (HL-ILLL) radioactive waste in deep clayrocks. In France, the choice of the potential host rock for the geological storage is focused on the Callovian-Oxfordian (COx) of Meuse/Haute-Marne from its low permeability, capacity for self- sealing, high sorption and ability to radionuclide (RN) transport by diffusion, whose studies are driven mainly by the ANDRA (Agence Nationale pour la gestion des Déchets RAdioactifs). IRSN, which plays an expert role for ASN (l'Autorité de Sûreté Nucléaire), has its own underground research laboratory in a clayrock which has strong analogies to the COx. This is the Toarcian/Domerian clayrock located at Tournemire in southern Aveyron in France.

The purpose of this study was to assess the transfer of RN in the Tournemire clayrock through the study of halides contents and of their stable isotopes (Cl^-, Br^-, Cl^-/Br^-, $\delta^{37}Cl$, $\delta^{81}Br$). The approach used was multiple and consisted for halides to: 1) Assess their stock in different fractions of the rock by applying several techniques including i) alkaline fusion for their total stock, ii) leaching to access their stock in porewater and to mineral phases sensitive to dissolution iii) cubic diffusion for their stock in porewater, 2) Get their diffusive transport parameters of a selection of samples from the upper Toarcian by cubic diffusion experiments modelled using the Hytec transport code developed by Mines ParisTech and 3) Model their transport after palaeohydrogeological known changes of the Tournemire massif.

The experimental approach, conducted at the LAME lab (Laboratoire d'Analyses et des Moyens Expérimentaux, France), did not lead to an operational protocol for the alkaline fusion due to an incomplete rock dissolution. Leaching was used to characterize the concentrations of halides in the fractions of pore water and of minerals sensitive to dissolution. The results show levels of halides much higher than those of pore water with very low Cl/Br ratios likely resulting from the dissolution of mineral species. The cubic diffusion produced the pore diffusion coefficients for Cl and Br as well as their concentration in the porewater. Cubic diffusion also allowed to estimate a Cl to Br pore diffusion coefficient ratio, necessary to calculate the profiles of Cl/Br. These estimates have required the use of the transport code Hytec i) for dimensioning and implementing the experiment in a time frame compatible with the work period, ii) for analysing the sensitiveness of the model to the accessible porosity and to the diffusion coefficient which act respectively to the steady phase and transient phase of the experiments, and finally, iii) for adjusting the pore diffusion coefficients of Cl and Br to an accessible porosity of 3-4% as shown in Fig.1 below.

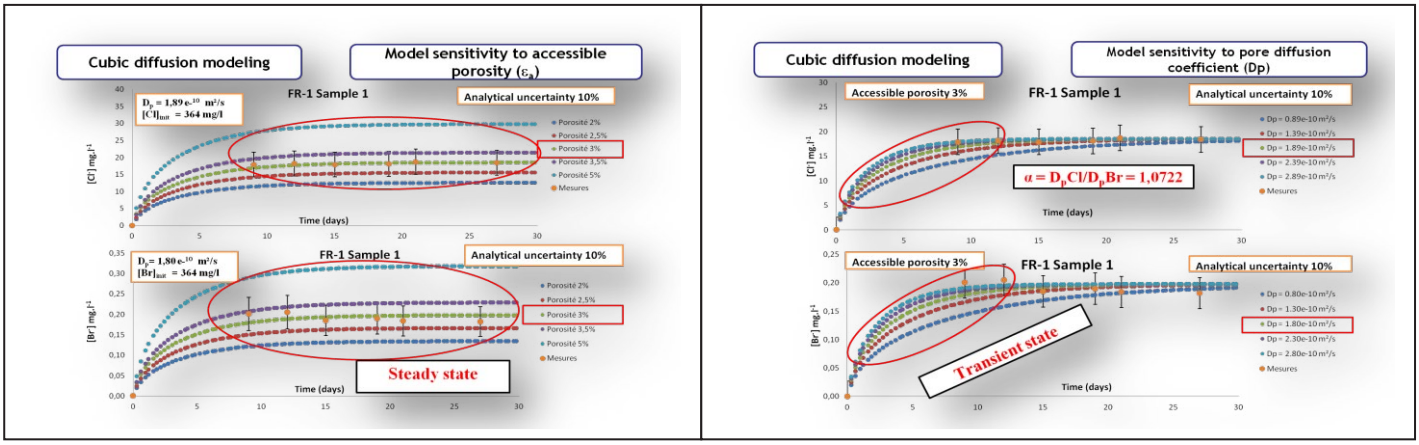


Fig.1: Sensitivity of the model to accessible porosity (left) and diffusion coefficient (right)

The Hytec code was then used to check the consistency of the current profiles of chlorides, bromides, ^{35}Cl , ^{37}Cl , $\delta^{37}Cl$, Cl/Br in 1D, a fake drilling assumed crossing the entire clayrock. The assumption is that halides have undergone a diffusive transport between seawater trapped during sedimentation and meteoric waters infiltrated at different times to domain boundaries. Four scenarios were tested according to the paleohydrogeological history of the massif. All tracers and scenarios are consistent with a unique marine source of halides more or less diluted by meteoric waters. The duration of the diffusive exchange initially suggested 85 ± 10 Ma (Bensenouci, 2010) is never contradicted despite uncertainties related to changes in boundary conditions; as shown in Fig 2 . This body of evidence would suggest that molecular diffusion is the transport process which has affected and still affect the Tournemire clayrock, outside of fault zones. The $\delta^{37}Cl$ results expected on the surrounding carbonated aquifers, leachates and fracture waters (including $\delta^{81}Br$ values; data processing in progress) should help to refine the models and the results.

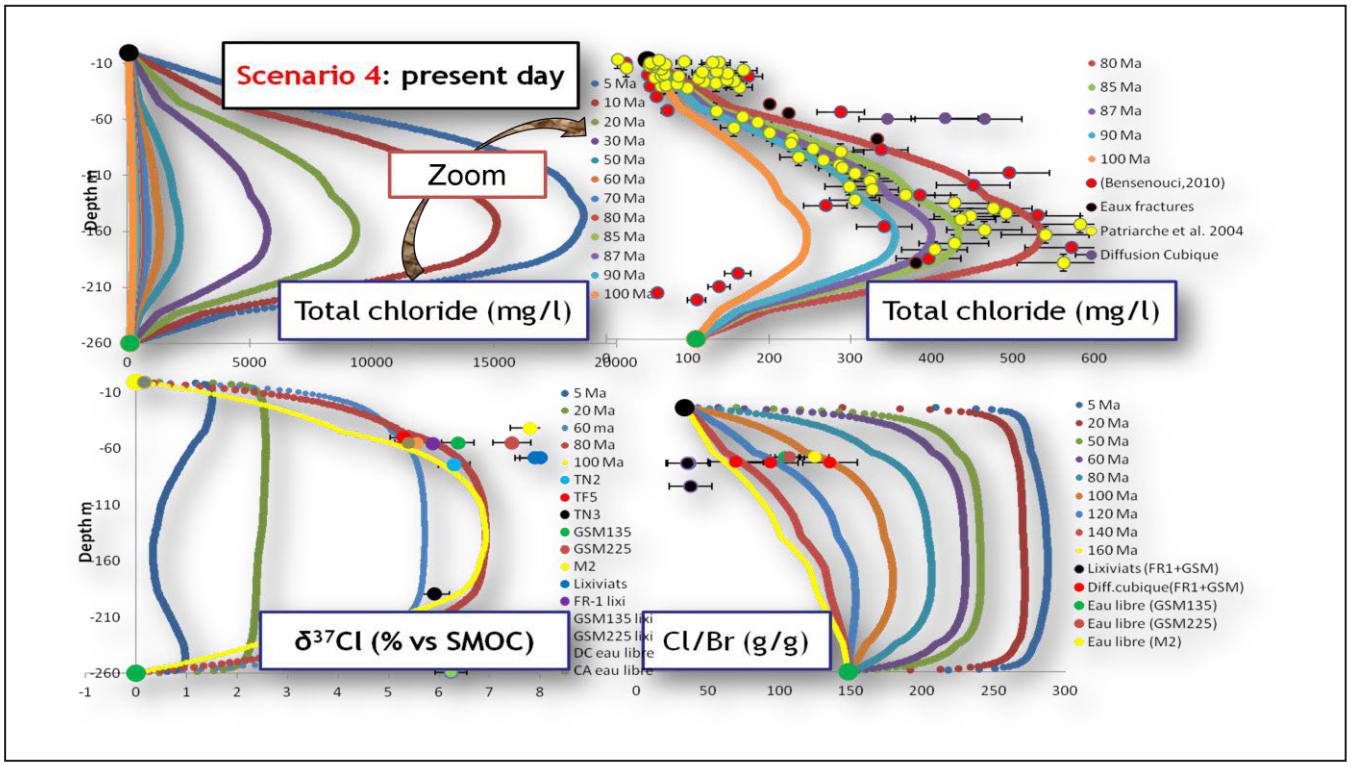


Fig.2: Total chloride, $\delta^{37}Cl$, and the ratio Cl/Br simulations compared to measurements

With this abstract, we wish to participate in the 6th International CLAY Conference in Brussels (Belgium) in March 2015, in Geochemistry and Mass transfer topics, to make both an oral presentation and a poster to show the results obtained in this study for the first time in this field and hope to be selected to propose a full paper to be published as a special editions of scientific journals.

Geochemical evolution and reactive transport of radionuclides in the near-field of a disposal cell for high-level vitrified waste in the Callovo-Oxfordian claystone: the impact of coupled processes on radionuclides retardation

Marek Pękala[1], **Orlando Silva**[1], **David García**[1], **Jorge Molinero**[1], **Mireia Grivé**[1], **Andrés Idiart**[1], **Isabelle Munier**[2], **Nicolas Michau**[2], **Eric Giffaut**[2] **and Benoit Cochepin**[2]

[1]AMPHOS 21 CONSULTING S.L., Paseo de García Faria, 49-51 08019 Barcelona, Spain (marek.pekala@amphos21.com)
[2]Agence Nationale pour la Gestion des Déchets Radioactifs (Andra), 1-7, rue Jean-Monnet - 92298 Châtenay-Malabry cedex, France

Andra (the French national agency for management of radioactive waste) studies the disposal of high-level vitrified waste in a deep-underground geological facility engineered in the Callovo-Oxfordian clay formation [1]. Quantitative calculations of radionuclide release and migration are necessary to evaluate the safety of the disposal concept. Physical and chemical processes taking place within the Engineered Barrier System (EBS) and in its immediate vicinity (adjacent parts of host-rock) define the radionuclide source term to the far-field and the possible radiological impact.

Large amounts of information regarding the properties and the expected future evolution of both the host-rock (Callovo-Oxfordian claystone) and the different elements in the EBS have been amassed over the years through a combination of experimental and theoretical work [e.g. 2, 3, 4, 5]. Due to the high complexity of the disposal system and long times to consider (tens to hundreds of thousands of years or more), until recently calculations of interactions within the EBS have been performed in a simplified manner (e.g. using one dimensional models, focusing on a selected portion of the disposal system or employing simplified chemical reaction models…). However, it is known that many key processes (such as temperature evolution due to heat generation, glass dissolution, steel corrosion, concrete degradation, porosity changes due to minerals dissolution or precipitation, and radionuclides retardation during migration…) are closely coupled. Moreover, the geometry of the system can result in complex patterns of dilution and preferential transport paths. Therefore, there has been an increasing need for integrating experimental information within a modelling framework capable of representing the coupling of relevant chemical and transport processes, while at the same time accurately representing geometrical details of the engineered design.

Here we present results obtained from a state-of-the-art reactive transport model for a vitrified-waste disposal cell, implemented in iCP [6] (a software interface developed in-house by Amphos 21 that couples the capability of PHREEQC [7] and COMSOL Multiphysics [8]) and calculated over a period of 100,000 years. The model reproduces details of design geometry on the centimetric scale, implements a range of chemical interactions resulting from the chemically complex system of multiple materials (glass, steel, concrete, compacted bentonite and claystone), and couples that reactivity to diffusive transport in a 2D axisymmetric domain over a longitudinal distance of ca. 10 meters. Chemical reactions are temperature-dependent and the impact of porosity change due to dissolution and precipitation reactions is also included. The coupled model makes it possible to evaluate the effects of interconnected-processes (e.g. temperature evolution and mineral solubility or mineral dissolution/precipitation and diffusion), and to assess the relative importance of various radionuclide retardation processes (surface complexation, cation exchange and mineral dissolution/precipitation) during transport throughout the disposal system and its near-field. A number of deterministic sensitivity and alternative cases were considered to test the effect of major assumptions, uncertainties and engineering design on radionuclide release and transfer to the near-field.

References:

[1] Andra (2005). Dossier 2005. Andra research on the geological disposal of high-level long-lived radioactive waste.
[2] Gaucher E., Robelin C., Matray J. M., Négrel G., Gros Y., Heitz J. F., Vinsot A., Rebours H., Cassagnabère and Bouchet A. (2004). ANDRA underground research laboratory: interpretation of the mineralogical and geochemical data acquired in the Callovian–Oxfordian formation by investigative drilling. Physics and Chemistry of the Earth 29, 55-77.
[3] Gaucher E. C., Tournassat C., Pearson F. J., Blanc P., Crouzet C., Lerouge C. and Altmann S. (2009). A robust model for pore-water chemistry of clayrock. Geochimica et Cosmochimica Acta 73, 6470-6487.
[4] Altmann S. (2008). 'Geo'chemical research: A key building block for nuclear waste disposal safety cases. Journal of Contaminant Hydrology 102, 174-179.
[5] Altmann S., Tournassat C., Goutelard F., Parneix J.-C., Gimmi T. and Maes N. (2012). Diffusion-driven transport in clayrock formations. Applied Geochemistry 27, 463-478.
[6] Nardi A., Idiart A., Trinchero P., de Vries L. M. and Molinero J. (2014). Interface COMSOL-PHREEQC (iCP), an efficient numerical framework for the solution of coupled multiphysics and geochemistry. Computers & Geoscience 69, 10-21.
[7] Charlton, S. R. and Parkhurst, D. L (2011). Modules based on the geochemical model PHREEQC for use in scripting and programming languages. Computers & Geoscience 37, 1653–1663.
[8] COMSOL, 2013. COMSOL Multiphysics.Version4.3a, Available from: www.comsol.com.

Numerical computation of relative permeabilities of argillaceous porous media using Lattice Boltzmann Models and X-ray tomography images

Seifallah Ben Hadj Hassine [1], **Magdalena Dymitrowska** [1], **Valérie Pot** [2], **Alain Genty** [3].
[1] IRSN, PRP-DGE/SEDRAN/BERIS, BP17, Fontenay-aux-Roses, France,
[2] INRA, AgroParisTech, UMR EGC 1091, Thiverval-Grignon, France,
[3] CEA Saclay, DEN/DM2S/SFME/MTMS, Saclay, France.

One of the key issues in the context of waste geological disposal is the management of the production and transport of hydrogen within the facilities and the host rock. Indeed, anaerobic corrosion of metallic materials like the waste canisters is expected to produce a significant amount of hydrogen. The induced two-phase flow may increase several potential risks such as early gas breakthrough leading to the degradation of confinement properties. Experimental characterization of fluids transport properties, like relative permeabilities, suffers from inaccurate measures when facing low-permeability media like argillaceous materials especially when approaching the full water saturation. However it has been seen in numerical simulations that relative permeabilities are key parameters for two-phase flow models.
To address these specific questions, a numerical tool is developed to study the transport phenomena at the pore scale and computations are performed in order to better understand and characterize gas-water flow inside an undeformable poral matrix. The present study propose to simulate two-phase flow with a pore scale model based on the lattice Boltzmann approach using 3D reconstructed images of the porosity of real samples of the Mont Terri (Switzerland) Opalinus clay, obtained by X-ray tomography at fine resolution (0.7 μm).

The implemented Lattice Boltzmann Model (LBM) is based on the Rothmann and Keller (RK) approach [1] using a Two Relaxation Time (TRT) scheme [2, 3]. Part of the novelty of this tool is the implementation of the model on Graphical Processing Unit (GPU) [4] enabling a significant increase of the computation performances (~70 times faster than Central Processing Unit (CPU) computations).

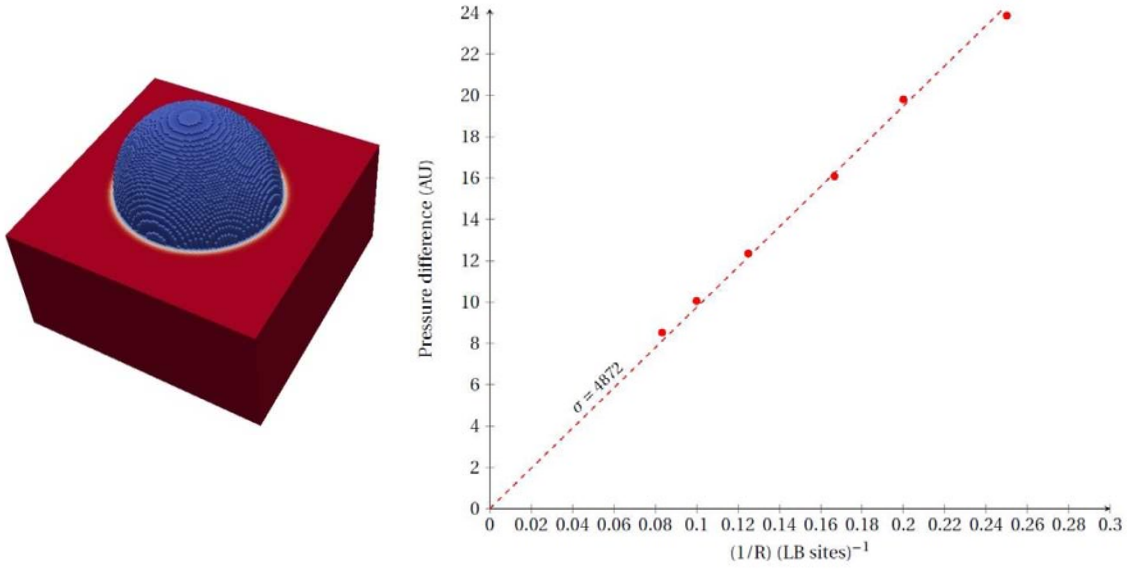


Figure 1: Young-Laplace equation validation (a gas bubble immersed in water)

A dimensional analysis is presented to fit the LBM parameters in order to respect the real hydrodynamics defined by characteristic numbers of Reynolds, Bond, capillarity and by mobility ratio [3, 5]. In order to better control the minimal sufficient space resolution as well as to optimize the algorithm for permeability calculations, the two-phase flow has been simulated using classical geometries like Poiseuille and Venturi. It was tested against classical static and dynamic two-phase flow analytic problems (ex: Young-Laplace equation (Figure1)). Finally, we performed two-phase flow computations inside real 3D connected porosity obtained from X-ray tomography images (Figure 2). Using these simulations, we were able to obtain relative permeability curves.

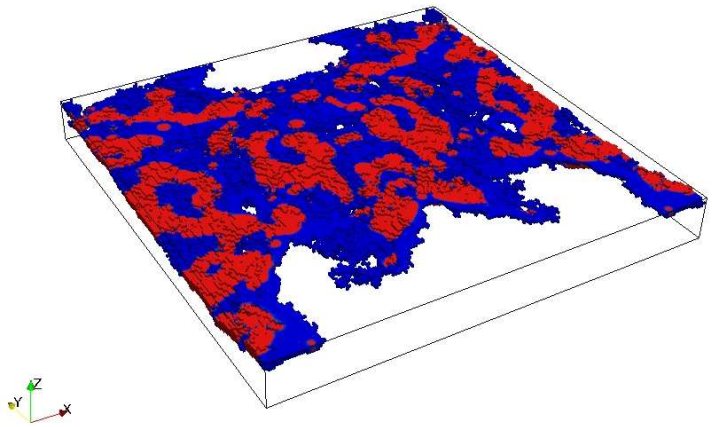


Figure 2: Two-phase flow in a 3D fracture (water is blue as gas is red)

References:

1. Gunstensen, A.K., Rothman, D.H., Zaleski, S., Zanetti, G.: Lattice Boltzmann model of immiscible fluids, Physical Review, Vol. 43, N. 8, 1991.
2. Ginzburg, I., Verhaeghe, F., d'Humières, D.: Two-relaxation time lattice Boltzmann scheme: about parametrization, velocity, pressure and mixed boundary conditions. Commun. Comput. Phys. 3, 427–478 (2008a).
3. Genty, A., Pot, V.: Numerical Simulation of 3D Liquid–Gas Distribution in Porous Media by a Two-Phase TRT Lattice Boltzmann Method, Transport in Porous Media 96, 271–294 (2013)
4. Obrecht, C., Kuznik, F., Tourancheau, B., Roux, J.-J.: Multi-GPU implementation of the lattice Boltzmann method, Computers & Mathematics with Applications 65, Issue 2 (2013)
5. Dou, Z., Zhou, Z.-F.: Numerical study of non-uniqueness of the factors influencing relative permeability in heterogeneous porous media by lattice Boltzmann method, International Journal of Heat and Fluid Flow 42, 23-32 (2013)

The scaling properties of Neretnieks' model for glacial erosion

Markus Olin, Veli-Matti Pulkkanen

VTT Technical Research Centre of Finland, P.O. Box 1000, FI-02044 VTT, Finland

Mass losses caused by dilute post glacial groundwater pulse are considered an important issue in KBS-3 safety case both in Sweden and Finland. Much experimental and modelling work is going on the subject, but the only commonly used model is given by Neretnieks (Neretnieks et al.,2009). Our modelling is based on Neretnieks' equations, which are however considerably simplified for the present purposes (Olin, 2014): 1) the complex functional dependencies have been replaced by piecewise polynomial interpolants to achieve better convergence when solving the model numerically; 2) whole system is kept at constant salinity meaning exclusion of one transport equation; 3) parameter values outside physically relevant values are chosen to enable effective numerical computation and 4) the dependence of bentonite gel viscosity on the bentonite volume fraction has been limited to values below 700 and 45 000 times the lowest value.

All computations were carried out by COMSOL Multiphysics 4.4 in Dell T3500 workstations of 24 GB of memory, which enabled use of about 300 000 mesh elements. The basic geometry is shown in Figure 1. Most of the modelling was done at constant salinity of 0.1 mM, but groundwater flow velocity v and system size R was varied as given in Table 1.

The erosion mass flux Q was able to formula $Q \sim (vR)^n$ in cases of low and high viscosity limit between, the flow velocity, and the radius of the bentonite source R; the exponent was fitted to be 0.45 (data for that case shown in Table 1) and 0.31 in the low and high limit cases, respectively.

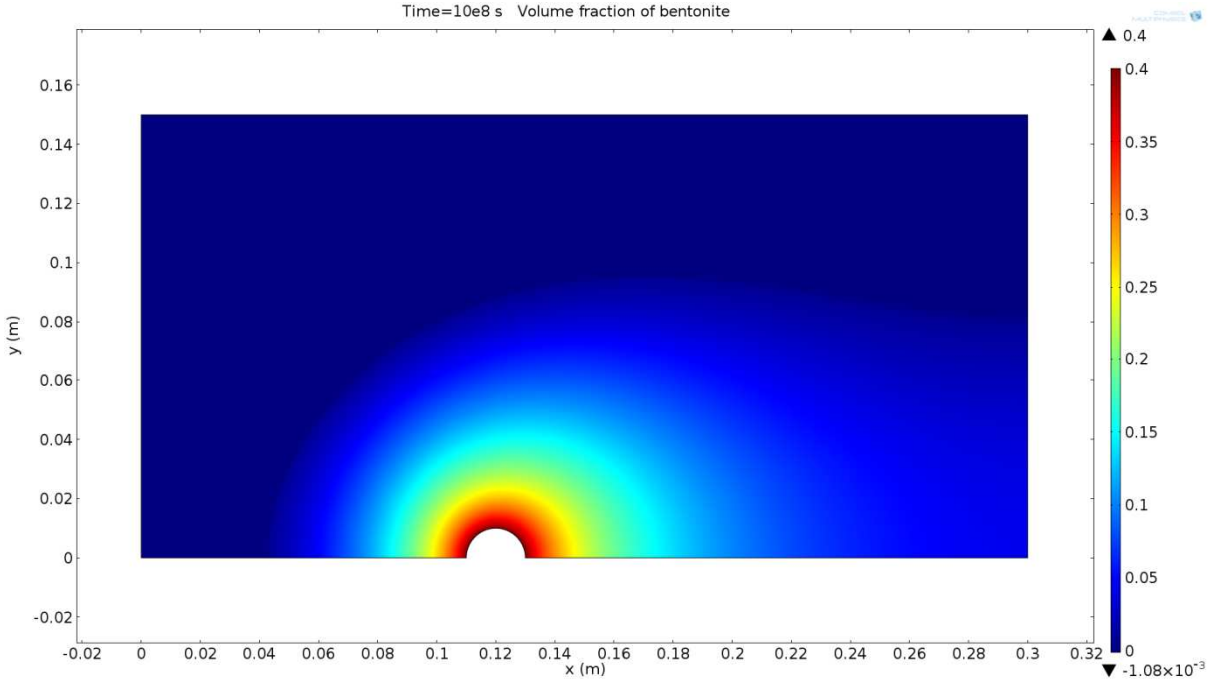


Figure 1. The basic geometry: water flows from left to right; the radius of the bottom circle is R. The volume fraction of bentonite for case of R = 0.01 m and v = 6 000 m/a is shown at the final time (10^9 s) as colour map.

Table 1. Total erosion mass flux Q (μg/s ≈ 30 g/a) as function the system size, R, and groundwater flow velocity, v.

			v (m/a)		
R (m)	0.6	6	60	600	6000
0.01	n.c.	0.17	0.8	2.1	5.8
0.02	n.c.	0.24	1.1	2.8	8.0
0.05	n.c.	0.48	1.6	4.2	12.4
0.10	0.22	0.75	2.1	5.8	17.0
0.30	0.43	1.21	3.4	9.7	28.4
0.90	0.81	1.98	5.5	16.2	50.1
2.70	1.3	3.15	9.2	27.7	84.9

n.c. = not computed

For system of v = 6000 m/a and R = 0.01 m, the salinity was varied from 0.1 mM to 100 mM. Qualitatively observing, the salinity of water seems to have a smaller effect on the swelling behaviour of bentonite in the model than in experiments; note, only one case was studied this far. Moreover, the shape of the swollen bentonite in the model differs significantly from the shape in the slit erosion experiments. When reviewing the results, the difficulties in reaching convergent numerical solutions caused by the extremely steep gradients in parameters built in the model should be kept in mind.

Acknowledgements

The research leading to these results has received funding from the European Atomic Energy Community's Seventh Framework Programme (FP7/2007-2011) under Grant Agreement no295487, the BELBaR project.

References

Neretnieks, I., Liu, L., Moreno, L. (2009). Mechanisms and Models for Bentonite Erosion. Report SKB TR-09-35, Svensk Kärnbränslehantering AB, Stockholm, Sweden

Olin, M (2014). Tunnel Backfill Erosion by Dilute Water. Posiva Working Report 2014-07, Posiva Oy, Olkiluoto, Finland

Multitracer (HTO, ^{36}Cl, ^{85}Sr) diffusion in compacted $Cu(en)_2^{2+}$-illite and -montmorillonite

T. Kupcik [a], M.A. Glaus[b], L.R Van Loon[b], B. Baeyens[b], Th. Schäfer[a], H. Geckeis [a]

[a] Institute for Nuclear Waste Disposal, Karlsruhe Institute for Technology, D-76021 Karlsruhe, Germany
[b] Laboratory for Waste Management, Paul Scherrer Institut, CH-5232 Villigen PSI, Switzerland

Clay rich sedimentary formations are currently considered in Germany as potential host rocks for a radioactive waste repository (Hoth et al., 2007). In argillaceous rocks, fine-grained porous materials composed of clay minerals (illite, smectite, kaolinite) together with accessory mineral phases and organic matter, diffusion is the main transport mechanism for solute contaminants. The diffusive transport (i.e. the effective diffusion coefficient D_e) for neutral and charged tracers was observed to decrease for cations > neutral species > anions (Van Loon et al., 2007, Glaus et al., 2007, 2010). The reduced diffusivity of anionic compared to neutral species is well understood and can be related to a repulsive interaction of anions with the negatively charged clay surfaces leading to a reduced accessibility of the total pore space (anion exclusion). Cationic species, being electrostatically attracted to the negatively charged clay surfaces, retain their mobility and the higher D_e compared to HTO can be related to their enrichment in the interlayer (surface enhanced diffusion). Values for D_e were observed to decrease for cationic and increase for anionic tracers with increasing ionic strength (Glaus et al., 2007, 2010), thus indicating that an electrostatic shielding of the surface charge (induced by an increase in ionic strength) is affecting the diffusion properties of charged solutes. The negative surface charge on the planar surfaces of clay minerals can be effectively blocked by high selective transition metal-organic ligand complexes such as copper-ethylenediamine $Cu(en)_2^{2+}$, leading to a reduced access of alkaline and alkaline-earth metals to these exchange sites (Maes et al., 1977). Within the framework of the EC Euratom (FP7) Catclay project we studied the multi-tracer (HTO, $^{36}Cl^-$ and $^{85}Sr^{2+}$) diffusion in $Cu(en)_2^{2+}$ exchanged montmorillonite and illite, the former representing low-charged clay mineral capable of swelling whereas the latter is taken as a model for high-charged clay minerals with collapsed interlayers which are not accessible for solutes.

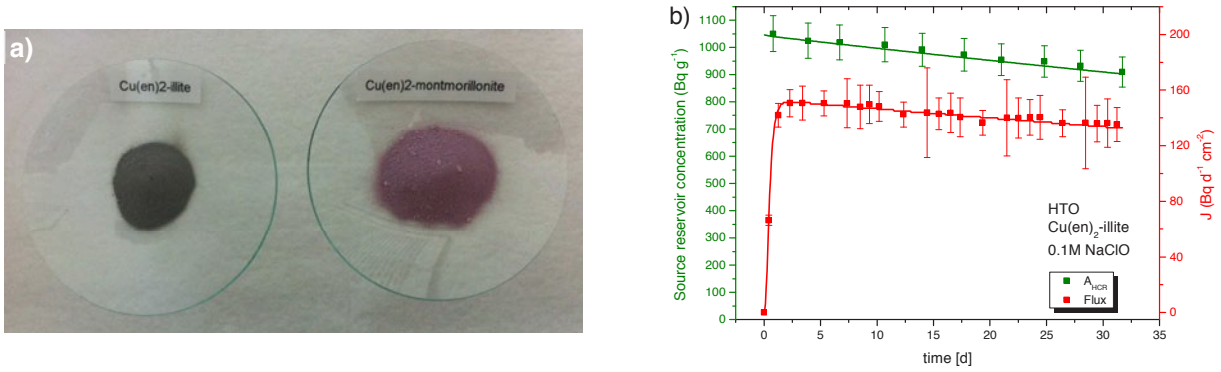
Diffusion experiments with compacted $Cu(en)_2^{2+}$-illite and -montmorillonite (dimensions in the cm range, bulk dry density 1700 kg m^{-3}) were performed in conventional through-diffusion experiments (Glaus et al., 2010) using stainless steel cells equipped with an advectively flushed filter system (Glaus et al., 2013). Fig. 1 shows the results for HTO (a), $^{36}Cl^-$ (b) and $^{85}Sr^{2+}$ (c) diffusion through $Cu(en)_2^{2+}$-illite, both as flux and evolution of activity in the high concentration reservoir. The data are also representative for $Cu(en)_2^{2+}$-montmorillonite. For HTO and $^{36}Cl^-$, a steady state situation (indicated by a constant flux) is reached after short time whereas the flux for $^{85}Sr^{2+}$ is still increasing after 32 days. The observation time was, however, sufficient in all cases to determine the best fit parameter values, D_e and the rock capacity factor α, using the Comsol Multiphysics computer code.

For HTO the values for D_e and α for both $Cu(en)_2^{2+}$-illite and -montmorillonite are in good agreement with literature data on the Na^+-exchanged clays (Glaus et al. 2010), indicating that the geometrical properties (i.e. tortuosity, constrictivity) were not altered by $Cu(en)_2^{2+}$-exchange.

In the case of $Cu(en)_2^{2+}$-montmorillonite D_e as well as the porosity for ^{36}Cl are significantly higher compared to the Na-form, indicating that anions are no longer repelled form the vicinity of the clay surface. However, this effect is not observed in the case of $Cu(en)_2^{2+}$-illite. This dissimilarity can be understood in the context of the different types of pore space available in both clay minerals. While interlayer pores are present in Na-montmorillonite, these are not accessible in illite because of the intercalation of dehydrated K^+-cations. A similar situation is encountered in $Cu(en)_2^{2+}$-montmorillonite as evidenced by X-ray diffraction (Maes et al., 1977). The interlayer spacing is largely collapsed due to intercalation of $Cu(en)_2^{2+}$ complexes and the available porosity can be assumed to exhibit the character of interparticle porosity. The conversion of interlayer porosity to interparticle porosity induced by $Cu(en)_2^{2+}$ has thus a significant effect on anion diffusion in montmorillonite, while the

effect of the modification of external surfaces by the presence of $Cu(en)_2^{2+}$ complexes in illite appears to be less.

For cationic ^{85}Sr both D_e and α decrease by $Cu(en)_2^{2+}$-exchange compared to the Na^+-form in case of illite and montmorillonite, pointing thus to the fact that Sr^{2+} enrichment near the charged surfaces (a pre-requisite for the enhanced mass transfer compared to HTO) is reduced due to a local neutralization of the negative surface charge. The diffusive behaviour of Sr^{2+} in the $Cu(en)_2^{2+}$ modified clay minerals is, however, clearly distinct from the one of HTO indicating that charge effects near the interparticle surfaces are still effective.



c)

Tracer	$Cu(en)_2^{2+}$-illite		Na-illite		$Cu(en)_2^{2+}$-mnt.		Na-mnt.	
	D_e (10^{-10} m² s⁻¹)	α (-)	D_e (10^{-10} m² s⁻¹)	α (-)	D_e (10^{-11} m² s⁻¹)	α (-)	D_e (10^{-11} m² s⁻¹)	α (-)
HTO	1.76±0.19	0.44±0.13	2.0±0.2[a]	0.43±0.20[a]	3.35	0.39	3.1±0.7[b]	0.39[b]
^{36}Cl	0.65±0.09	0.32±0.10	0.67±0.04[a]	0.18[a]	0.98	0.14	0.0072±0.0008[c]	0.019±0.002[c]
^{85}Sr	1.56±0.61	40.9±20.0	9.6[a]	90[a]	9.66±0.55	20.3±15.8	310±220[d]	330±120[d]

[a]: this work ; [b]: rescaled (Archies law) from (Glaus et al., 2013), ρ_{db} = 1564 kg m^{-3}, salinity 1.0 M $NaClO_4$; [c]: (Glaus et al., 2010); ρ_{db} = 1900 kg m^{-3}, salinity 0.1 M $NaClO_4$; [d]: personal communication M.A. Glaus, recalculated from ρ_{db} = 1600 kg m^{-3}, salinity 0.1 M $NaClO_4$.

Fig. 1: $Cu(en)_2^{2+}$-illite and -montmorillonite (a). Diffusion of HTO through compacted $Cu(en)_2^{2+}$-illite (background electrolyte 0.1 M $NaClO_4$) as mass flux in the low concentration reservoir (J) and evolution of the source reservoir concentration. The solid lines are obtained from the best fit parameter values (b). De and α values for HTO, ^{36}Cl and ^{85}Sr in $Cu(en)_2^{2+}$-illite and -montmorillonite at a bulk dry density (ρ_{db}) of 1700 kg m^{-3}, together with literature data for the Na-exchanged clays (c).

Acknowledgement

The research leading to these results has received funding from the EURATOM 7th Framework Programme FP7/2007- 2011 under grant agreement n° 249624 (CATCLAY project).

References:

Glaus, M.A., Baeyens, B., Bradbury, M.H., Jakob, A., Van Loon, L.R., Yaroshchuk, A., 2007. Diffusion of ^{22}Na and ^{85}Sr in montmorillonite: Evidence of interlayer diffusion being the dominant pathway at high compaction. Environ. Sci. Technol. 41, 478–485.

Glaus, M.A., Frick, S., Rossé, R., Van Loon, L.R., 2010. Comparative study of tracer diffusion of HTO, $^{22}Na^+$ and $^{36}Cl^-$ in compacted kaolinite, illite and montmorillonite. Geochim. Cosmochim. Acta 74, 1999–2010.

Glaus, M.A., Birgersson, M., Karnland, O., Van Loon, L.R., 2013. Seeming Steady-State Uphill Diffusion of $^{22}Na^+$ in Compacted Montmorillonite. Environ. Sci. Technol. 47(20), 11522–11527.

Hoth, P., Wirth, H., Reinhold, K., Bräuer, V., Krull, P., Feldrappe, H., 2007. Endlagerung radioaktiver Abfälle in Deutschland. Untersuchung und Bewertung von Tongesteinsformationen. BGR-Bericht

Maes, A., Peigneur, P., Cremers, A. (1977). Stability of metal uncharged ligand complexes in ion exchangers. Part 2.-The Copper-Ethylenediamine Complex in Montmorillonite and Sulphonic Acid Resin. J. Chem. Soc. Farad. T1 74(0), 182–189.

Van Loon, L.R., Glaus, M. A., Müller, W. (2007). Anion exclusion effects in compacted bentonites: Towards a better understanding of anion diffusion. Appl.Geochem. 22, 2536–2552.

Internal structures of fault zones in low permeability formations and their relationship with fluid flow: insights from the Tournemire URL

P. Dick[1], C. Courbet[1], C. Wittebroodt[1], A. Dauzeres[1] & J-M. Matray[1]

1. IRSN- Institut de Radioprotection et de Sûreté Nucléaire, BP 17, F-92262 Fontenay-aux-Roses, France (pierre.dick@irsn.fr; christelle.courbet@irsn.fr, charles.wittebroodt@irsn.fr; alexandre.dauzeres@irsn.fr, jean-michel@irsn.fr)

Context

In order to assess the safety of a geological disposal facility for high-level waste, IRSN (French Institute for Radiological Protection and Nuclear Safety) conducts its own studies related to the confining properties of compacted argillaceous sequences at the Tournemire Underground Research Laboratory (URL). Located on the western border of the Mesozoic sedimentary Causses Basin (SW France), the URL crosses a thick Toarcian shale formation (≈250 m) and is interbedded between two aquiferous limestone units. In addition to the 250 m thick overlying limestones, the geotechnical and hydrogeological characteristics of this site exhibit similarities with those measured by the French National Agency for Radioactive Waste Management (Andra) in the Callovo-Oxfordian formation of Bure (Meuse/Haute Marne, France).

Past research programs carried out at Tournemire (Matray *et al.*, 2007) have shown that fluid circulations in the undisturbed matrix are very slow (hydraulic conductivity of 10^{-14} to 10^{-15} $m.s^{-1}$). However, recent work related to the occurrence of small scale fault zones indicate that fluid circulations may have been significantly modified in the vicinity of such features (Courbet *et al.*, 2013).

In the present study we aim to integrate the division of fault zones from drilling, imaging logging, petrophysical, structural and mineralogical data to qualitatively classify and append internal fault architectures with *in situ* hydraulic conductivity measurement within a clay-rich fault zone.

Field results

The studied fault zone corresponds to a N-S trending sub-vertical strike-slip fault that affects not only the shale formation but also the over and underlying limestone units. The fault zone in the shale formation is 10-20 thick and consists of a complex array of anastomosed fault surfaces. Whereas, in the upper limestone units, the fault zone widens and fracturing becomes more scattered. Field evidence from well-developed slickenlines mainly indicates sinistral to sinistral-normal offsets. The estimated amount of slip along strike is assessed to be between 15-30 meters while slip perpendicular to strike is approximately 4-6 meters. The fault zone is characterised by two major components: a damage zone and a fault core. The fault core consists of a heterogeneous brittle to cataclastic zone where localised slip occurs along thin (0.5 - 2 cm thick) anastomosing shear bands and pre-existing sedimentary and tectonic structures are erased by cataclastic flow. The total thickness of the fault core varies from 0 to 1.5 meters along and perpendicular to strike. The damaged zones includes brittle fault-related deformation structures such small as faults, veins, fractures, cleavage as well as sub-millimetric clay-smears along brittle deformation bands. Strain within the damage zone is considerable lower than in the fault core, hence bedding surfaces and inherited structural fabric are commonly preserved.

Surprisingly, petrophysical results indicate in general higher porosity values in the fault core (≈20%) than in the damaged and undisturbed zone (≈10%). However, due to localised grain crushing and fluid flow shear bands within the fault core presents extremely low porosity values (<4%). Thus, owing to the variability in thickness and intrinsic architecture for any given location, the fault core may either behave as a conduit or barrier to fluid flow.

In situ results

As part of this study, Modular Mini-Packer System (MMPS) hydraulic testing was conducted in multiple boreholes to characterize hydraulic conductivities within the formation. Pressure data

collected during the hydraulic tests were analysed using the nSIGHTS (n-dimensional Statistical Inverse Graphical Hydraulic Test Simulator; Roberts *et al*. 2012) code to estimate hydraulic conductivity and formation pressures of the tested intervals in order to identify whether the hydraulic properties of the fractured clay materials differ statistically from that of the undamaged formation.
Preliminary pulse tests performed in the fault zone indicate hydraulic conductivities of 5.10^{-12} $m.s^{-1}$ in the fault core and overlapping damaged zone and 10^{-14} $m.s^{-1}$ in the adjacent undisturbed shale. These results are coherent with those derived from petrophysical, structural and mineralogical data. However, diagnostic plots revealed that the late-time pressure derivatives never stabilize at a constant value in the tested intervals, suggesting that no stable flow dimension seems to be reached during the tests. The volume of fractured rock tested through different pulses in the same interval tends to exhibit heterogeneity that cannot be represented by a single flow dimension. As shown by many authors (Beauheim *et al*., 2004), no unique hydraulic properties can be inferred analytically in that case.

In this study we show that the hydraulic conductivity in the fault core appears to be enhanced with respect to the adjacent damaged and undamaged zone by up to two orders of magnitude. However, it is recognized that the uncertainty associated with the in situ pulse test results also means that the scale of the in situ test might not be suited to determine with exactitude the hydraulic properties of a heterogeneous fault core. Moreover, coupled flow processes may be of great significance in fractured shale formations; in particular, the measured heads may result from hydraulic effects coupled with mechanical deformations.

References

Beauheim, R.L., R.M. Roberts, and J.D. Avis (2004) Well testing in fractured media: Flow dimensions and diagnostic plots, Journal of Hydraulic Research, Vol. 42, pp. 69-76.

Courbet, C., Dick, P., Lefèvre, M., Wittebroodt, C., Matray, J. and Barnichon, J. (2013) Estimating Hydraulic Conductivities in a Fractured Shale Formation from Pressure Pulse Testing and 3d Modelling, American Geophysical Union, Fall Meeting 2013.

Matray, J.-M., Savoye, S., Cabrera, J. (2007). Desaturation and structure relationships around drifts excavated in the well-compacted Tournemire's argillite (Aveyron, France). *Eng. Geol*. 90, 1-16.

Roberts R.M., Beauheim R.L, Avis J., Barnhart K., Kuhlman K. (2012) n-dimensional Statistical Inverse Graphical Hydraulic Test Simulator, Open Source Software package available at the following URL: http://nsights.github.com/nSIGHTS, United States Department of Energy, Sandia National Laboratories.

Characterisation of diffusive transport parameters associated with a secondary fault cross in the Upper Toarcian argillite: FRACTEX project

C. Wittebroodt[1], J.-M. Matray[1], P. Dick[1], J. Cabrera[1], J.-D. Barnichon[1]

1. IRSN, PRP-DGE/SRTG/LETIS, BP17, F-92262 Fontenay-aux-Roses Cedex (charles.wittebroodt@irsn.fr)

Context and motivations

Because of their favourable transport and retention properties, argillaceous rocks are considered as a potential host rock for radioactive waste repositories. At the request of the French Authority of Nuclear Safety (ASN), the French Institute for Radioprotection and Nuclear Safety (IRSN) is in charge of an independent expertise of the French industrial (Andra's) project. Therefore, IRSN develops experimental research programs in such geological formations at the Tournemire Underground Research Laboratory (URL) (Aveyron, France). One of the objectives of this project is to evaluate the occurrence and the driving processes controlling the radionuclide migration through an argillaceous formation (argillite) similar to the Callovo-Oxfordian formation studied by Andra. Since undisturbed argillaceous rocks display very low values for both hydraulic conductivity (K_h) and water content (θ_e) (Matray *et al.*, 2007), diffusion is considered to be the main transport mechanism governing radionuclide migration through the argillite. On the other hand, in the presence of fractures in the argillaceous formation, the flux of water through this preferential pathway could dramatically accelerate the migration of the radionuclides (Savoye *et al.*, 2003). Thus, the implementation of a radwaste disposal facility requires a precise sedimentary and structural characterization of the pre-selected site to guarantee the presence of a soundand homogenous clay layer over a large area.
Since small-scale faults cannot be detected in the argillaceous layer during the site characterization, it is crucial to determine transport properties associated with such structures if they are intersected during excavation operations. Hence, parallel to in situ pulse tests performed to measure hydraulic conductivities of a fault zone, IRSN carried out through diffusion experiments in order to assess the diffusive transport parameters associated with different states of the rock mass (damaged, disturbed and undisturbed argillite).

Experimental

Through diffusion experiments were performed on core samples collected from a horizontal air-drilled borehole (diameter 101 mm) which intersects a hectometer-sized subvertical strike-slip fault displaying a 4-6 m vertical offset in the Upper Toarcian argillite of the Tournemire URL. Geological mapping and borehole logging permited us to select representative samples of the damaged, disturbed and undisturbed argillite. Mineralogical and petrophysical characterizations of the rock have been performed on samples taken in the immediate vicinity of those selected for the through diffusion experiments. All core samples were sealed in aluminium-coated plastic bags under a nitrogen atmosphere to limit both oxidation of pyrite and dehydration.
Each sample was sliced into 1-cm-thick cylindrical pieces of 3-cm diameter using a wire saw (no lubricating fluid was used) and was then placed in a through diffusion cell. Firstly, each diffusion cell was filled with a synthetic pore water solution in order to apply an equilibration step to the rock sample to re-saturate them and to limit chemical and osmotic disruption during the diffusion experiment. After this equilibration step was achieved (~7 weeks), a first diffusion stage was applied to the diffusion cells by adding a water radiotracer (HTO) and an anionic radiotracer ($^{36}Cl^-$) to the upstream reservoirs solution. Then, a second diffusion stage was applied to the cells by adding HTO and a cationic radiotracer ($^{22}Na^+$) to the upstream reservoirs solution.

Results

The comparison between the effective diffusion coefficient (D_e) and diffusion accessible porosity (ε_a) values calculated for HTO during the first and the second diffusion stage allowed us to check that these values are stable during the two experiments and, consequently, that the argillite samples have not been perturbed during this period. The comparison between the diffusive parameters (D_e and ε_a) obtained for HTO and those obtained for $^{36}Cl^-$ enabled to confirm the existence of the anionic exclusion phenomenon. Furthermore, the comparison between the $^{22}Na^+$ rock capacity factor (α) and the HTO diffusion accessible porosity allowed us to highlight the retention of the sodium onto the rock and to calculate its distribution ratio (R_D). Moreover, the comparison between the effective diffusion coefficient values calculated for these two radiotracers showed that the diffusion of sodium is apparently accelerated with regard to the HTO's one.
The comparison between the diffusive transport parameters obtained for the different cells shows that the diffusion process associated to the damaged fault zone and at its vicinity is more rapid with regards of those from the undisturbed zones.
Finally, these results will be discussed with those obtained during the *in situ* hydraulic characterizations. The comparison between the time required to propagate a perturbation by advection and diffusion (estimation of a Peclet number, Tremosa *et al.*, 2011) will allow to assess the relative significance of transport properties for the different states of the rock (damaged, disturbed and undisturbed argillite). Data obtained within this project will supply numerical simulation tools for a better understanding of fluid flow in fractured shale formation.

References

Matray, J.-M., Savoye, S., Cabrera, J. (2007). Desaturation and structure relationships around drifts excavated in the well-compacted Tournemire's argillite (Aveyron, France). *Eng. Geol.* 90, 1-16.

Savoye, S., Cabrera, J., Matray, J.-M. (2003). Different hydraulic properties of single fracture in argillaceous médium: the case of the IRSN Tournemire site (France). In: *Krasny, J., Hrkal, Z., Bruthans, J. (Eds), Groundwaters in Fractured Rocks, IHP-VI, series on groundwater*, No.7, 383-384.

Tremosa, J., Gonçalves, J., Matray, J.-M. (2011). Natural conditions for more limited osmotic abnormal fluid pressure in sedimentary basins. *Submitted in Water Resour. Res.*

Influence of surface conductivity on the apparent zeta potential of homoionic montmorillonite particles

Philippe Leroy[1*], Nicolas Devau[1], Christophe Tournassat[1], Olivier Bernard[2], and Mohamed Azaroual[1]

[1] BRGM, French Geological Survey, 3 Avenue C. Guillemin, 45060 Orléans, France.

[2] PHENIX, CNRS, UMR 8234, Pierre and Marie Curie University, 75252 Paris, France.

[*]E-mail: p.leroy@brgm.fr

Zeta potential is a physicochemical parameter of particular importance in describing ion adsorption and double layer interactions between charged particles [1]. However, for clay particles, the conversion of electrophoretic mobility measurements into zeta potentials is difficult. This is due to their lamellar form, their anisotropic surface charge density distribution, but above all to their very high surface electrical conductivity, which is inversely proportional to the sizes of the particles [2]. When surface conductivity is similar to or higher than the electrical conductivity of bulk water, it can significantly lower the electrophoretic mobility of the particles. It follows that the magnitude of the intrinsic zeta potential can be grossly underestimated if surface conductivity is not considered in the calculation of the zeta potential, in particularly when the aqueous solution is diluted (ionic strength typically < 0.1 M; [3]).

We use a basic Stern model to describe the electrochemical properties and to calculate the intrinsic zeta potential of the basal planes of homoionic montmorillonites particles immersed in respectively NaCl, $CaCl_2$ and $MgCl_2$ aqueous solutions (10^{-5} to 1 M) (Fig. 1). Only the equilibrium constant of adsorption of Na^+ ions on the basal plane of montmorillonite is adjusted by cation exchange capacity and electrophoretic mobility measurements [4] at fixed pH (pH = 6.5) and high salinity (1 M). Electrophoretic mobilities are then calculated by coupling our electrostatic surface complexation model with Henry's electrophoretic mobility model that considers (1) the retardation force associated with surface conductivity of the Stern and diffuse layers and (2) the internal conductivity of the clay aggregate. Our electrophoretic mobility model is also not restricted to low zeta potentials because the electrical potential distribution at the surface of the particle is calculated by numerically solving the non-linear Poisson-Boltzmann equation. The very good agreement of calculated and measured electrophoretic mobilities confirms that the true zeta potential of the basal plane of montmorillonite particles may correspond to the electrical potential at the onset of the diffuse layer, i.e., at the outer Helmholtz plane (Fig. 2).

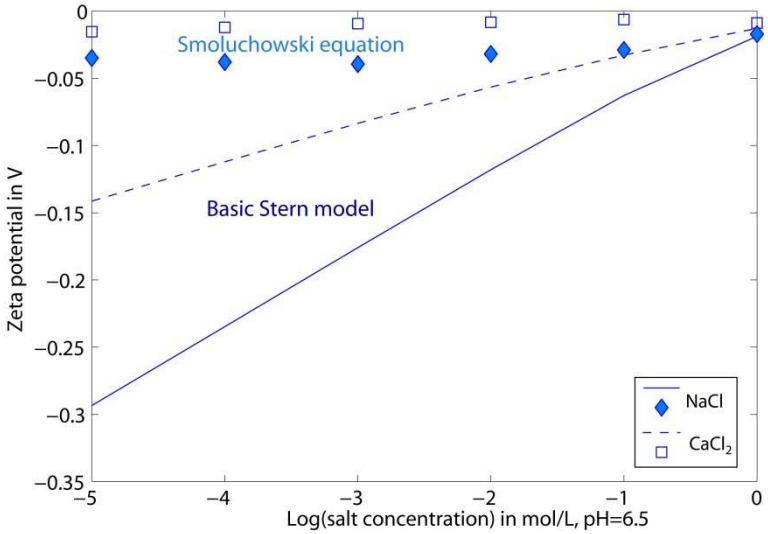


Fig. 1. Measured apparent zeta potentials (symbols) and calculated intrinsic zeta potentials (lines) of homoionic montmorillonite particles in NaCl or $CaCl_2$ aqueous solutions (experimental data from Sondi et al. [4]).

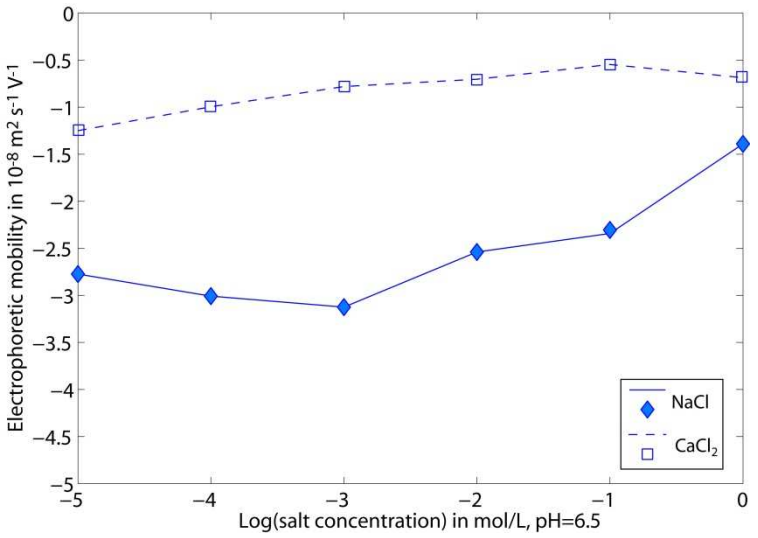


Fig. 2. Measured (symbols) and modelled (lines) electrophoretic mobilities of homoionic montmorillonite particles in NaCl or $CaCl_2$ aqueous solutions (experimental data from Sondi et al. [4]).

References

[1] P. Leroy et al., Journal of Colloid and Interface Science, 410 (2013), 81-93.
[2] P. Leroy, A. Revil, Journal of Colloid and Interface Science, (2004), 371-380.
[3] P. Leroy et al., Journal of Colloid and Interface Science, 356 (2011), 442-453.
[4] Sondi et al., Journal of Colloid and Interface Science, 178 (1996), 514-522.

Application of electromigration technique to study radionuclide transport in compacted bentonite

Eva Hofmanová[1,2], Norbert Maes[3]

[1]Department of Nuclear Chemistry, Czech Technical University in Prague, CZ-11519 Prague, Czech Republic
[2]Fuel Cycle Chemistry Department, ÚJV Řež, a. s., CZ-25068 Husinec - Řež, Czech Republic
(hofmanova.eva@gmail.com)
[3]Expert Group Waste & Disposal, Belgian Nuclear Research Centre, SCK•CEN, BE-2400 Mol, Belgium

Classical migration experiments (especially with sorbing tracers) require long experimental time periods in order to obtain diffusion parameters. Electromigration (EM) technique uses an electrical gradient as driving force for transport of ionic species. Hence the experimental time can be reduced to a few hours or days. This technique was applied to determine diffusive properties for different radionuclides in Boom Clay (e.g. Maes et al. (1999), Maes et al. (2002), Beauwens et al. (2005), and thereafter extended for use on compacted sodium montmorillonite by e.g. Higashihara et al. (2004), Tanaka et al. (2008), and in crystalline rocks by Löfgren and Neretnieks (2006).

This study presents original results of the electromigration technique applied to compacted Czech commercial bentonite B75 performed in newly developed EM cells at SCK•CEN. This cell represents a modular system consisting of two or three bentonite plugs in series and in between an aliquot of studied tracer is spiked. The bentonite specimen is separated by glass filters from the reservoirs filled with an electrolyte in which electrodes are immersed to provide an electrical field over the specimen. A solution of 0.033 M $CaCl_2$ was used as working electrolyte to suppress the swelling of bentonite. After the test, the bentonite was sliced and tracer activity in each slice was measured. Experimental profiles were fitted by an analytical solution (Eq. 10, Maes et al., 1999) in terms of the apparent dispersion velocity V_c and the apparent dispersion coefficient D. By performing a series of experiments at different electrical field, one obtains a linear relationship between V_c and D, from which the apparent diffusion coefficient D_a^{EM} can be evaluated by extrapolating to zero V_c. In order to demonstrate that the EM technique provides comparable values as classical diffusion tests, through-diffusion experiments were performed in parallel. Therefore, only non-sorbing tracers (e.g. iodide) or slight sorbing (e.g. sulphate) tracers and a bentonite dry density of 1300 kg/m^3 were used in this study.

In case of iodide, EM revealed that the purchased ^{125}I spiking solution was not pure in terms of a single speciation (Fig. 1), namely I^- (iodide) as announced on the specification sheets provided by the producer. This was not evident from classical diffusion experiments. EM profiles were deconvoluted in order to determine V_c, D and also the proportion of iodide to total initial ^{125}I activity in the spiking solution. Thereafter, results of through-diffusion experiments were interpreted taking into account the presence of two iodine species and an iodide apparent diffusion coefficient $D_a^{DIF} = (3.0 \pm 0.5) \cdot 10^{-10}$ m^2/s was determined. In order to remove less mobile iodine species (probably iodate), a reductive treatment of ^{125}I spiking solution with $Na_2S_2O_3$ under acidic conditions was carried out. Only faster iodine species (iodide) was indentified in the EM profiles after the treatment (Fig. 2). From a series of iodide EM experiments, an apparent diffusion coefficient $D_a^{EM} = (2.6 \pm 1.2) \cdot 10^{-10}$ m^2/s was determined which is in line with the value obtained from through diffusion experiments.

Subsequent to a monovalent anion, a set of EM experiments with a bivalent anion was performed. Sulphate $^{35}SO_4^{2-}$ (surrogate for selenate) was chosen for this purpose. An EM sulphate profile is displayed on Fig. 2. It can be seen that sulphate is less mobile than iodide which corresponds to a lower sulphate diffusivity in free water (by factor of two). However, the obtained sulphate apparent diffusion coefficient $D_a^{EM} = (2.5 \pm 1.8) \cdot 10^{-11}$ m^2/s is one order of magnitude lower than for iodide. This is probably caused by a slight retardation on the bentonite which was considered in the

evaluation of diffusion experiments. A value of $D_a^{DIF} = (3.2 \pm 1.3) \cdot 10^{-11}$ m^2/s was determined from through-diffusion experiments which is in good agreement with results from EM experiments.

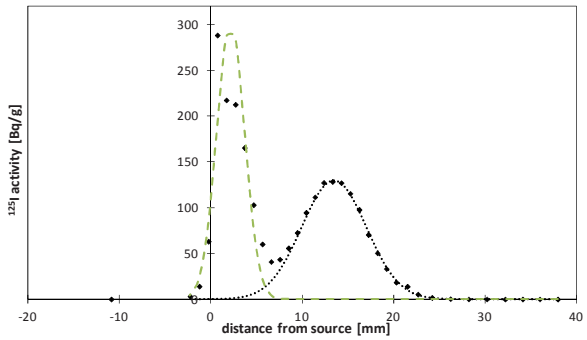


Fig. 1:
^{125}I activity profile and its deconvolution; obtained after 4 h of EM experiment with fixed current at 18 mA and equilibrium potential of 80 V.

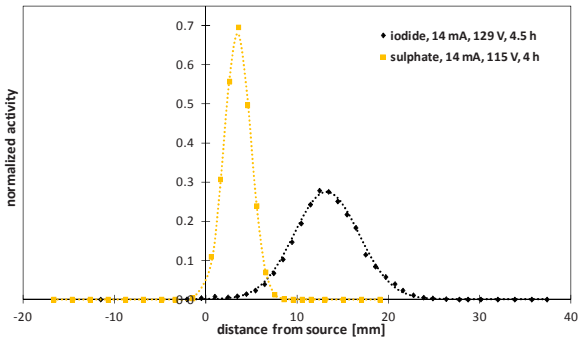


Fig. 2:
EM profiles for iodide (after reductive treatment) and sulphate under similar experimental conditions and their corresponding best fits.

The EM technique (with new cell design) was successfully applied to study radionuclide transport in compacted bentonite. The relatively large uncertainty on the obtained D_a^{EM} values is the result of a limited number of experiments which might be reduced by carrying out more experiments. However, the data are in line with data obtained by classical diffusion technique. The results confirmed that the EM technique represents a fast method for obtaining reliable apparent diffusion coefficients. Therefore, the EM technique will be used for future migration studies of critical radionuclides at higher bentonite densities to be used in the framework of a deep geological repository.

References:
Beauwens et al., Eng. Geol. 77, 285 (2005).
Higashihara et al., Appl. Clay Sci. 26, 91 (2004).
Löfgren and Neretnieks, J. Cont. Hydrol. 87, 237 (2006).
Maes et al., J. Cont. Hydrol., 36, 231 (1999).
Maes et al., Radiochim. Acta, 90, 741 (2002).
Tanaka et al., Phys. Chem. Earth, 33, S163 (2008).

Critical insight into methodology of through-diffusion experiments and their evaluation

Eva Hofmanová[1,2], **Dušan Vopálka**[1], **Aleš Vetešník**[1]

[1]Department of Nuclear Chemistry, Czech Technical University in Prague, CZ-11519 Prague, Czech Republic (hofmanova.eva@gmail.com)
[2]Fuel Cycle Chemistry Department, ÚJV Řež, a. s., CZ-25068 Husinec - Řež, Czech Republic

The diffusion of radionuclides in clay (bentonite buffer and argillaceous host rock) is an important process that needs to be precisely described with the aim to correctly model the radionuclide transport in the near- and far-field of the proposed final disposal of radioactive waste. Despite an extensive research in the area of radionuclide diffusion through clayey materials, the question of real ranges of diffusion coefficients needed for performance assessment studies is, however, debatable. By comparing the results of different laboratories it is difficult to assess whether presented results do not differ due to some discrepancies in methodology and/or evaluation methods of the experimental data.

The literature review showed that, e.g., full saturation of clay sample is rarely checked and data on separating filters are often missing and/or not taken into account. Also despite the fact that the tracer concentration in the source reservoir decreased, the "essentially" constant concentration is declared. In order to evaluate diffusion experiments, usually a simple evaluation procedure based on the analytical solution of diffusion equation derived for the specific initial and boundary conditions is applied even though these conditions are not fully accomplished. Although number of new evaluation approaches which make an effort to simulate the real diffusion experiments using own codes (e.g. Tachi and Yotsuji, 2014) grows, analytical solution (or its simplified variants) of 1-D diffusion equation still dominates in the evaluation (e.g. Shackelford and Moore, 2013). Therefore, this study aims to characterize systematic errors in the determination of apparent and effective diffusion coefficients that might occur from the inappropriate evaluation. The novelty of this study further consists in an innovative procedure of through-diffusion experiment on compacted bentonite.

Often, only the break-through curve is considered in the evaluation (alternatively with subsequent out-diffusion experiment data) without taking into account the presence of filters. As can be deduced from formulation of the diffusion equations in homogeneous porous medium, it is a two parametric problem (from the mathematical point of view) obviously fully determined by D_e and the rock capacity factor α, which is for non-sorbing species equal to effective porosity ε_{eff} (Shackelford and Moore, 2013). In order to determine these two parameters, or other two, from which the mentioned parameters could be computed, an effective two-parametric fitting method is needed. When steady-state is reached, D_e and α can be effortlessly calculated from the slope and intercept, respectively, of the linear regression between total amount of tracer diffused through the clay boundary and time.

In the field of radionuclide diffusion in porous media, some improvements of experimental procedure and evaluation of diffusion experiments were performed in our laboratory. The first results of these attempts (Vopálka et al., 2006) showed that the new evaluation program realized in the GoldSim environment enabled to take into account the diffusion in filters separating clay specimen from the liquid phase. This module can also respect real concentration changes in both reservoirs and thus eliminates the need to replace the target reservoirs (to keep the concentration close to zero) and/or to have a big source reservoir (to keep "essentially" constant concentration) and thus results in reduction of laboratory radioactive waste. The next upgrade of the module consisted in making possible to simulate diffusion in the layer with heterogeneous porosity profile. The model, named EVALDIFF, was thoroughly tested and successfully verified against the results of analytical solutions for specific boundary conditions.

In order to demonstrate the effect of filters, HTO and ReO_4^- concentration evolution in both reservoirs in time for GMZ bentonite at 1600 kg/m^3 were simulated without and with presence of filters, see Fig.1

(according experimental set-up described in Wu et al. 2014; Wu et al., 2012, i.e. $d = 2.54$ cm, $L = 0.86$ cm, $V_{in} = 0.2$ l, $V_{out} = 0.02$ l, $\varepsilon_f = 0.3$, $L_f = 0.158$ cm). It can be seen that the HTO concentration cannot be considered to be "essentially" constant in the source reservoir and that there is statistically significant difference in diffusion with and without filters. When filters are not taken into account in the evaluation of diffusion of tracers entering the total pore space, a systematic error in diffusion coefficient determination up to 50% may arise (depending on the dry density, see Vopálka et al., 2006). On the other hand, the effect of filters on anionic conservative tracers is negligibly small and can be neglected at high dry densities.

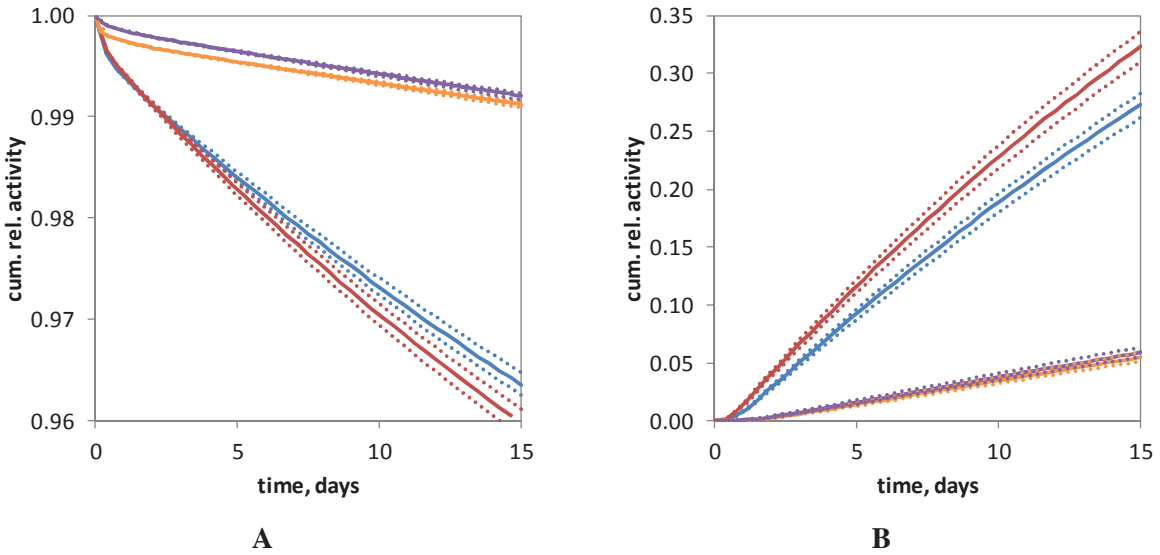


Fig. 1: Concentration evolution in the source (A) and target (B) reservoir in time simulated by the module EVALDIFF; HTO: $\varepsilon = 0.40 \pm 0.02$, $D_e = (11.2 \pm 0.6) \cdot 10^{-11}$ m^2/s, no filters (—), with filters (—) and ReO_4^-: $\alpha = 0.18 \pm 0.01$, $D_e = (1.8 \pm 0.1) \cdot 10^{-11}$ m^2/s) , no filters (—), with filters (—). Dotted line represents the uncertainty on the simulated curve.

In our methodology, we take into account all experimental outputs, i.e. concentration evolution in both reservoirs in time and a tracer concentration profile in the sample layer determined after the termination of through-diffusion experiment. Procedure for obtaining concentration profiles enables to determine a value of grain density, dry density and total porosity for each experiment. In case of non-sorbing tracers, also rock capacity factor can be determined independently from the break-through curve fitting. In addition, apparent filter length could be discussed from HTO concentration profiles. However, still three (for non-sorbing tracers) or four (for sorbing tracers which comply with linear sorption isotherm) parameters remain generally unknown. Therefore, we make an effort to develop a multi-parametric regression program that would enable, with the help of prepared module EVALDIFF, to determine simultaneously all unknown parameters by fitting of all types of output datasets. Developing this procedure we keep in mind the possible reduction of parameters number by the independent determination of filter parameters (e.g. Glaus et al., 2008, Aldaba et al., 2014) that would simplify the fitting procedure under development.
The present work revealed some discrepancies in methodology of through-diffusion experiments and their evaluation that may lead to a systematic shift in the values of the diffusion coefficients and provides guidelines on their solution.

References:

Aldaba et al, Radiochim. Acta, 102, 8, 723 (2014).
Glaus et al., Clay. Clay. Miner., 56, 6, 677 (2008).
Shackelford and Moore, Eng. Geol., 152, 133 (2013).
Tachi and Yotsuji, Geochim. Cosmochim. Ac., 132, 75 (2014).
Vopálka et al., Mat. Res. Soc. Symp. Proc., 932, 983 (2006).
Wu et al., Appl. Clay. Sci., in press, http://dx.doi.org/10.1016/j.clay.2014.07.028 (2014).
Wu et al., J. Radioanal. Nucl. Chem., 292, 853 (2012).

Monte-Carlo-based uncertainty propagation in an up-scaled model of solute diffusion in clays

Francesco Cadini[a], **Enrico Zio**[a,b]

[a]Dipartimento di Energia – Politecnico di Milano, via Ponzio 34/3 20133 Milano, Italy.
[b]Chair on Systems Science and the Energetic challenge, European Foundation for New Energy- Électricité de France, Ecole Centrale Paris and Supelec.

Under the growing international pressure on the definitive disposal of high-level radioactive wastes, much effort has been placed on improving the understanding of diffusion-driven transport in clays and clayrocks. To this aim, both experimental and modeling efforts have been undertaken. In particular, compacted clays, such as bentonite, are largely considered as having the properties required for the engineered barriers of the disposal facility, whereas natural clay rocks, i.e. fine grained, porous materials containing a significant proportion of clay minerals, are envisaged in many countries as potential host rock formations. The most interesting properties of these materials are the extremely low permeabilities and their large sorption capabilities of cationic species by the negatively charged clay structures.
Bentonite is essentially composed of montmorillonite, which is a smectite-type clay mineral, whereas clay minerals in clay rocks are in general made up of both illite- and smectite-type minerals in different amounts. Both minerals are made up of platelets of positive charge deficient alumino-silicate layers stacked one above the other. The resulting net negative charge is balanced by cations located in the interlayer pore space and attached to the external aggregate surfaces. In smectites, differently from illites, interlayer cations and their associated hydration water can exchange with cations and water in the pore solution, thus providing these minerals with the capability of swelling in the presence of water. As a consequence, smectite-type minerals exhibit in general extremely low permeabilities, and molecular diffusion can be assumed as the dominant mass transport process.
The diffusion of water or solute particles in smectite-type minerals is thus strongly influenced by the geometrical layout of the complex microstructure of these clays, often described in literature as a dense 'house of cards' arrangement of clay platelets, which are in turn composed of stacks of clay layers. At the same time, in smectites water can be found in two different physico-chemical states: the free water in the pore space between the edges of the clay platelets, whose properties are similar to those of bulk water, and the interlayer water present between the clay layers, whose properties are influenced by the counter balancing cations. Thus, in general these materials behave as double-porosity media, wherein water particles can migrate in the macropores filled of free water and the nanopores of the interlayer water, with different diffusive properties; as the level of compaction increases, however, macropores tend to reduce their volume and interlayer diffusion seems to become the dominant pathway. It is worth noticing that the high density of negative surface charge, especially in compacted clays, allows diffusion of only neutral and cationic species in the interlayer water, whereas anions are excluded due to the strong electrostatic repulsion of the clay layer surfaces. Finally, the diffusion of cations is further influenced by the chemical interactions with the surfaces of the solid phase, generally due to the combined effect of ion exchange and surface complexation reactions.
Despite the large availability of diffusion data and models, many issues are still open to investigation because of: i) the still poor understanding of the phenomena involved in the diffusion process of charged particles (cation surface diffusion, for example), ii) the need to improve the numerical models in order to account for these phenomena within the complex geometrical structures of clays and iii) the need for up-scaling the local scale numerical models for the prediction of mass transport on larger scales and longer times.
In practice, the complexity and incomplete knowledge of the phenomena involved, give rise to uncertainties in the modeling of the future occurrences of events which may severely affect the functionality of the disposal facility barriers, in the values of the model input parameters and/or in the hypotheses supporting the model structure itself.

A proper treatment of these uncertainties is then a necessary task for the quantitative assessment of the potential risk associated to a radioactive waste disposal facility. Within a probabilistic framework, a typical approach for this issue is Monte Carlo (MC) simulation, whereby several realizations (or simulations) of the system evolution are generated by, first, random sampling from suitable probability distributions and, then, by evaluating the analytical/numerical models used to represent the physical behavior of the system, so to estimate the distributions of the outcomes of interest by statistical analysis.

In this work, we propose to resort to a MC-based strategy in order to study how the geometrical and physical uncertainties of the diffusion models at the structure map scale are affected by the up-scaling procedures needed to model the radionuclide migration at the repository scale.

The uncertainty analysis is shown with reference to a case study of diffusion within compacted clay samples made up of montmorillonite or pyrophillite, where realizations of the two-dimensional, uncertain structure map are obtained by building a 'network' of connected, one-dimensional domains with stochastic lengths and orientations, representing both the interlayers and the pore spaces between edges. The solute diffusion within a single realization of the medium geometry is then solved by a particle tracking-based approach presented in a previous work of the authors, alternative to the classical random walk method, for modeling solute transport in clay minerals at the pore structure map scale. The approach is based on an original extension of the Kolmogorov-Dmitriev (KD) stochastic branching model applied to the transport of contaminants in groundwater. The model aims at describing the stochastic transport of the populations of solute particles in the clay pore spaces by means of a discrete-states, continuous-time Markov process based on transition probability distribution functions defined on the basis of physical reasonings. Partial differential equations, known as the Forward Kolmogorov Equations (FKEs), are then derived for the expected values of the different particles' populations, which are proportional to the solute concentrations. The FKEs are then solved by a particle tracking (PT) algorithm which can be simply derived from the underlying Markovian formalism. The resulting Kolmogorov-Dmitriev-based particle tracking (KDPT) algorithm allows to straightforwardly account for the complex geometrical structure of the clay particles, as the classical random walk method, and, at the same time, also for the nonequilibrium dynamics of the chemical interactions between the dissolved species and the surface.

An up-scaled compartment modeling strategy based on discrete-states, continuous-time Markov processes is adopted to represent the radionuclide migration at the repository scale.

FE Experiment: Monitoring of water content in Opalinus Clay using a moisture profile probe and a customized TDR sonde

Toshihiro Sakaki[1)], Tobias Vogt[1)], Herwig R. Müller[1)] and Holger Wörsching[2)]

[1)] Nagra, Hardstrasse 73, 5430 Wettingen, Switzerland,
[2)] Solexperts AG, Mettlenbachstrasse 25, 8617 Mönchaltorf, Switzerland

1. Introduction

For the safety assessment in spent fuel (SF) and high-level radioactive waste (HLW) disposal programs, it is essential to understand and predict coupled thermal, hydraulic, mechanical and (bio)chemical (THM(B)C) processes in the host rock around a repository tunnel. The host rock in the Swiss disposal concept for SF/HLW is a clay-rich formation called Opalinus Clay. To better understand the THM effects of a SF/HLW repository tunnel on the host rock on a large scale, a 1:1 scale multi-heater test, the so-called Full-Scale Emplacement Experiment (FE Experiment) is being implemented in the Mont Terri Underground Research Laboratory (URL) located in north-western Switzerland.

The entire experiment is located in a tunnel (length = 50 m, diameter = 3 m) and the THM(B)C evolution of the experiment will be monitored using a network of several hundred sensors. Because rock water content controls and affects all THM(B)C properties of the rock, it is one of the most important quantities to be measured. However, measuring water content in partially saturated clay-rich high-salinity rock is very challenging. The focus of this study was on application of two dielectric tools for monitoring water content in Opalinus Clay.

2. Material and methods

2.1 Commercial moisture profile probe

One of the dielectric tools examined in this study is a commercial moisture profile probe shown in **Figure 1** originally developed for agricultural and soil science applications. As this sensor is *not* designed to resist high temperature for a long time, it was only installed in "cold" sections that are far from the heaters or between the heaters. The profile probe used in this study is 1 m long and has six sensors at depths of 5, 15, 25, 35, 55 and 95 cm. In general, each sensor is known to sense about 6-10 cm into the material as illustrated in **Figure 1**.

The profile probe requires a plastic access tube to be first installed into the rock. A total of 6 access tubes were installed in cold sections; 4 (BFEC006 – 008 and BFEB051) in unlined section without shotcrete and 2 (BFEB049 - 050) in the lined section with shotcrete. Unlike the soils for which the sensors were originally designed, it requires significantly more effort to install them properly on rock to achieve a good contact with the tube and rock.

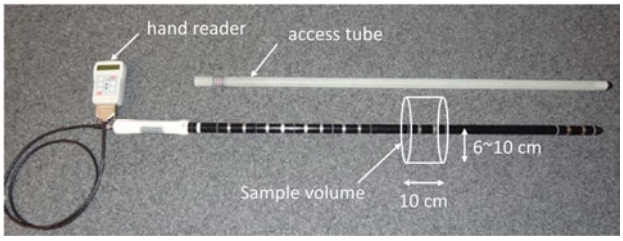


Figure 1. Moisture profile probe

The access tubes were grouted based on the findings of Sakaki et al. (2013), where different access tube installation methods were tested and compared. Grouting resulted in the best coupling with the rock and the access tube while maintaining a high accuracy of data.

For calibrating the profile probe, a "hybrid" procedure was adopted. An access tube was installed on a block of Opalinus Clay with an initial saturation of 0.54. The water content of the block was decreased in steps and a measurement was taken at each step. This was repeated until the block was oven-dried. On the other hand, the field rock mass where the access tubes were installed can be considered to be fully saturated. A combination of the readings from the sensors installed in the field at full saturation and readings from the block at lower saturations allowed us to develop a calibration to which a cubic function was fitted.

2.2 Customized TDR sonde

The second type of sensor was designed specifically for Opalinus Clay in the "hot" sections of the FE tunnel. To withstand long-term use under high temperatures, time domain reflectometry (TDR) was selected because the sensor can be designed so that all vulnerable electric parts/devices can be outside the test tunnel. Four pairs of copper strips (width = 5 mm, spacing = 5 cm) were installed on a temp-resistant cylinder (diameter = 99 mm) with a 25 cm separation (**Figure 2** left). The clay-rich rock with saline porewater has a high electrical conductivity (EC) which is known to cause significant adverse effects on the TDR signals. To circumvent such effects, the electrodes were coated with a thin film.



Figure 2. Left) Customized TDR sonde (Solexperts AG, Switzerland). Copper strip electrodes are coated with a thin film. Right) Grout return confirmed during installation.

Following the successful application of the grouting method for the PR2 probe, the TDR sonde was designed to have a 1 mm annulus to be grouted. Six sondes with a total of 24 TDR sensors were produced for two hot sections at two heaters, with three installed in each section in an inverted Y-shape configuration. The boreholes (BFEB017-022, diameter = 101 mm, length = ~120 cm) were drilled immediately before the installation. **Figure 2** (right) shows the grout return at one of the downward boreholes. For the vertical upward boreholes, a grout return line was used instead.
For calibrating the TDR sensor, a hybrid procedure similar to that for the profile probe was employed. A separate single TDR sensor was installed on an Opalinus Clay block and acquisition of data at different saturations is currently underway. Data from the sensors installed in the field (saturated rock) will be combined with those from the block and a calibration function will be developed.

3. Preliminary results

The first set of profile probes was installed in the FE tunnel at the Mont Terri URL in December 2012. The measured data collected to date indicate that, in the shotcrete-lined section of the FE tunnel, the Opalinus Clay behind the lining is fully saturated. In the unlined sections, the first ~50 cm of the rock is somewhat desaturated and seasonal variations can be detected near the rock surface.
A total of six TDR sondes (24 sensors) were installed in the FE tunnel in February 2014 and connected to a TDR100 system (Campbell Scientific, Inc.) via a low-loss coaxial cable. For the first few weeks, the hardening of the grout was observable in the data; this has now stabilized. The data acquisition unit has been temporarily removed from the site to avoid possible damage to the system during the bentonite emplacement. The measurement will be resumed after the emplacement is completed.
In summary, the profile probes were successfully installed in cold sections in the field and, together with the hybrid calibration, they seem to be generating reasonable data on water content in Opalinus Clay. For the customized TDR, it was confirmed that the installation was successful with the grouting method, calibration is underway and data acquisition will be resumed in the fall.

Acknowledgments

The laboratory calibration data were obtained at Okayama University, Japan.

References

Sakaki, T., et al. (2013), Monitoring water content in Opalinus Clay in the FE-experiment: Test application of a dielectric water content sensor, The 46th AGU annual Fall Meeting.
Müller et al. (2015), The Full-Scale Emplacement Experiment – Implementation of a multiple heater experiment at the Mont Terri URL, this conference.

Seismic long-term monitoring in the heater experiment HE-E

Kristof Schuster

BGR, Stilleweg 2, 30655 Hannover, Germany

Within the 1:2 scale heater experiment (HE-E), which was part of the EC PEBS project (Long-term Performance of Engineered Barrier Systems), seismic methods were used for the characterization of the backfill and the surrounding rock. In the shaly facies of the Opalinus Clay (OPA) at the Mont Terri RL in one part of the HE-E test section a sand-bentonite (Almeria, Spain) mixture (65/35) was used as backfill material.

The seismic experiment started in March 2011 several weeks before the test section was closed off and the heater was switched on. A seismic array consisting of 15 piezoelectric transducers was installed in 3 boreholes which were used before for seismic investigations in the preceding EC project Ventilation Experiment (VE). According to the experiences from this experiment the focus was laid on the first meter of the rock. Seismic transmission measurements were conducted on a daily bases each night.

Major results are first of all the pronounced variations of the derived seismic parameters with time as a consequence of the installation work (ventilation), backfill emplacement, closure and heating. Not all of these seismic parameter changes are fully understood and were not interpreted completely up to now, especially the v_p decreases in the OPA after one year.

Exemplarily the normalized velocity distributions for ray paths running through the backfill (Figure 1, left) and approximately parallel to the bedding in the OPA (Figure 1, right) are shown. Immediately after the emplacement of the backfill and closure of the test section (day 50) the consolidation / saturation of the backfill started. The heaters were switched on at day 109. It seems that the saturation / consolidation of the backfill within the first 553 days occur with different intensities and a phase without progress in consolidation / saturation took place (days 200 – 300). The notch in the graph at day 538 is related to an interruption of the heating due to a power breakdown. This demonstrates as a side effect the high sensibility of the method.
In the OPA at different distances from the interface EDZ features (creation of micro cracks) could be responsible for the v_p decreases until days 70 to 140. Afterwards the closure of micro cracks leads to gradual v_p increases. The v_p decreases from days 350 on are difficult to explain (approaching vapor front?). For the travel path orientations normal and 45° to bedding the v_p distributions are comparable.

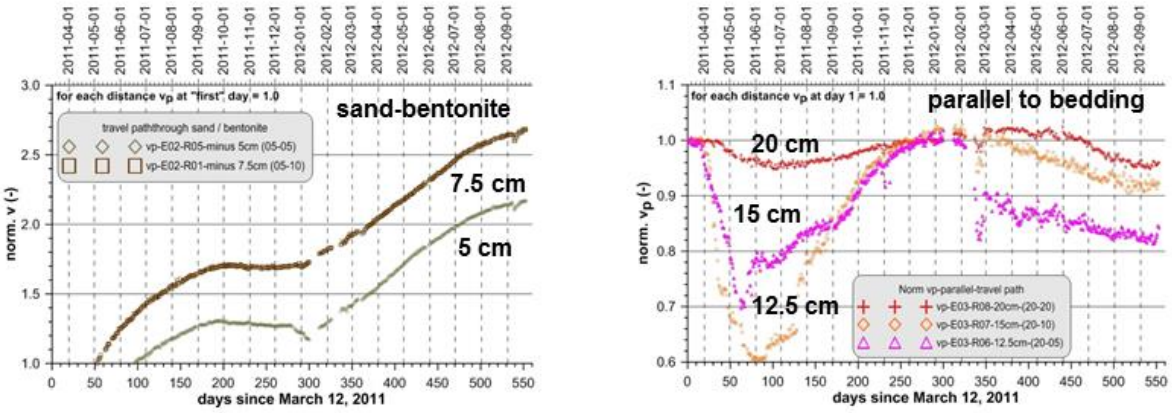


Figure 1: 15 months of seismic velocity evolution at different locations in and around the HE-E EBS. Values from day 1 were used for the velocity normalization. Left: seismic travel paths within the backfill. Right: seismic travel paths in the OPA with an approximately parallel orientation to the bedding.

The seismic experiment is still running, meanwhile in the fourth year and since July 2014 as the HE-E experiment in the Mont Terri Project.

Seismic long-term monitoring - characterisation of the 12 years lasting Engineered Barrier Emplacement Experiment (EB/PEBS)

Kristof Schuster

BGR, Stilleweg 2, 30655 Hannover, Germany

The EC Engineered Barrier emplacement experiment (EB) started in 2001 in the Mont Terri RL (CH). In a 1:1 situation a dummy canister was emplaced. The demonstration of the emplacement and the understanding of related hydro-mechanical aspects were the main targets. In the follow up EC PEBS project (Long-term Performance of Engineered Barrier Systems) which started in 2010 the activities continued. The project ended in 2013 with a complete dismantling. Several geophysical measurements and two seismic long-term monitoring phases were conducted by BGR. The seismic experiments aimed at the determination, characterization and monitoring of the evolution of the backfill material (FEBEX bentonite, Almería, Spain) as well as the surrounding Opalinus Clay (OPA).

Main results from seismic / ultrasonic measurements can be summarized as follows:

1) Immediately after the excavation of the EB emplacement niche (L = 6 m, D = 3 m) in spring 2001 and several months later different seismic measurements were performed. The extent and degree of the ED/dZ (Excavation Damaged/disturbed Zone), several small scale anomalies and the seismic anisotropy behavior of the OPA were determined.
2) Results from phase 1 of the seismic long-term monitoring (April 2002 – Nov. 2003) show a clear consolidation of the backfill material and a trend of closure of the previously created micro cracks. Furthermore, a good correlation with total pressure data was observed.
3) In summer 2011 two pilot boreholes were drilled by BGR into the saturated backfill. Results from ultrasonic interval velocity measurements show a rather homogeneous pattern but an eggshell like borehole wall, most probably as a result of the drilling (inverse v_p distribution).
4) Phase 2 of the long-term monitoring started in July 2012, several months before the dismantling of the EB niche. The resumption after 8.6 years shows clear jumps in v_p between 5 % and 15 % depending on the distance from the interface backfill / OPA.
5) As a consequence of the dismantling v_p decreases were observed with different intensities depending on the distance to the interface backfill / OPA. It indicates a recreation of the ED/dZ.

In Figure 1 results from 3 depth levels of both phases of the long-term monitoring are summarized.

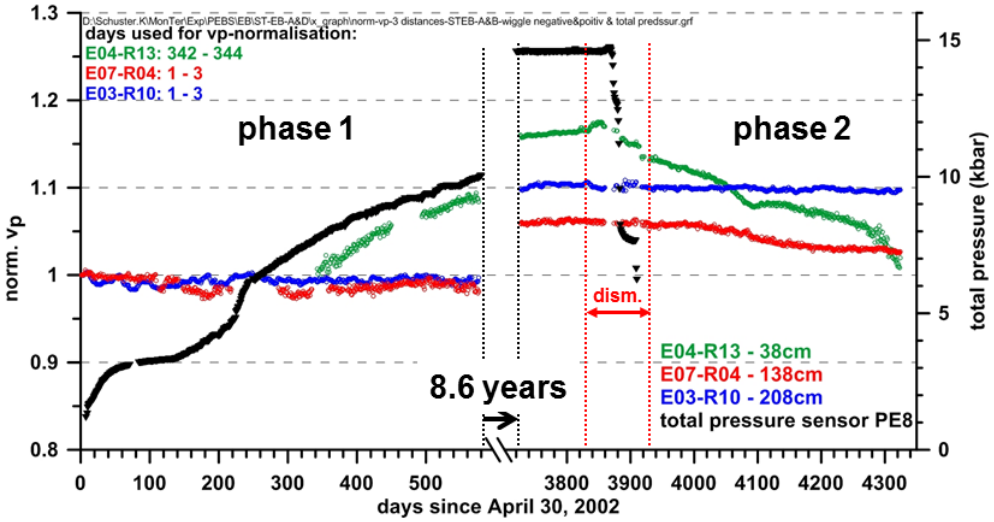


Figure 1: Evolution of normalized seismic P-wave velocities between April 2002 and February 2014. Note the v_p jumps after 8.6 years and the different v_p decreases during and after dismantling.

Monitoring system design for Intermediate level long lived radioactive waste cells – Feedback obtained and future demonstrator in Andra's underground laboratory

R. FARHOUD, S. DELEPINE-LESOILLE, S. BUSCHAERT, G. HERMAND

Andra, 1-7 rue Jean Monnet 92298 Chatenay-Malabry, France

The monitoring of underground radioactive waste disposal is a very big challenge because of a secular operational period, poor access for maintenance and harsh conditions for sensors. Limited feedback on instrumentation such environment involves demonstrators' uses in order to assess and validate chosen solutions. For intermediate level long lived (ILLL) disposal cells, a first demonstrator of a tunnel monitoring section was performed in 2011 in the Andra's underground research laboratory (URL). It consists of a tunnel of 4.3m in diameter poured in the GCR ("Galerie de Conception Rigide") gallery, according to the major horizontal stress and already provides useful information. One of these results is the clays' displacements around the galley measured by inductive extensometers in boreholes and compared with convergences measured by Invar wire system. Other interesting results are linked to the temperatures measured, along the whole borehole, by optical fiber cables. It provides the thermal diffusion profile in the rock around the gallery according to the depth.
The next step, in 2015, consists on improving knowledge obtained in GCR gallery on implementation procedures (like 3D fiber optics cable in borehole for strain measurements), data treatments and testing new sensors and transmissions (like wireless pore water pressure senor) in the frame work of a new demonstrator. This demonstrator will be performed in the URL in the GER gallery ("Galerie d'Essais des Revêtements")**, excavated according to the minor stress field. It aims to validate results obtained in the first demonstrator and to provide more data in order to provide inputs for models and data fusion process.**

Cigéo, the French underground disposal for radioactive waste (in project), would be constructed in a clay rock, at about 500m under the surface, in the north east of France. The French concept of cells, for ILLL wastes, consists of tunnels made by concrete with about 8m in diameter. A concept of the monitoring of these cells, for thermo-hydro-mechanical characterizations, was tested in 2011 in the URL and could be considered as the first one to one scale monitoring demonstrator [1] in the Andra's URL. The instrumentation was composed of sensors already used for decades for the monitoring of tunnels, damns or nuclear power plants like vibrating wire extensometers or platinum probes (Pt) or innovative and promising sensors like optical fiber sensors (OFS) [2]. Several lessons were obtained on installation procedures, localisation of sensors in the target environment and robustness of selected sensors. The data acquired with the in situ sensors are compared with the expected behaviours of the structure and the host rock obtained by the mathematical models [3]. These models are improved by the measurements obtained in situ in an iterative process.

In order to improve knowledge obtained and validate results and lessons acquired in the framework of the first demonstrator, Andra planned to instrument a similar gallery, according to the minor horizontal stress field, in the URL in 2015 in the GER gallery. Firstly, chosen sensors to be installed are those intended to be qualified for the monitoring of Cigéo. As an example extensometers in borehole single rod multipoint are preferred to those multimode because the sensing's electronics are installed in the part of the sensor close to the gallery, so exposed to gamma ray. Secondly, tested cables in gallery GCR based on optic fiber sensors will be installed in the gallery GER in order to measure strains and temperatures in clay and concrete. Finally, the location of sensors will be adapted to this new configuration where several section tests will be instrumented in order to compare data.

The instrumentation planned to be installed in gallery GCR consists of, firstly a "classical" extensometer in borehole which will be compared to optical fiber cable for displacement measurements of the host rock. The boreholes will be equipped by one or two technologies in parallel

boreholes. Secondly, 2 technologies of transmission of pore water pressure sensors, based on vibrating wire extensometers, will be tested, classical sensor communicating with wires and wireless sensors. The borehole dedicated to wireless sensors will be equipped with 3 sensors in order to provide a profile of the pore water pressure around the gallery at 3 different depths. Finally, other methods and sensors in the concrete will be tested like a pulse sensors for permeability measurements, the TDR (time domain Reflectometry) for the water content measurements, optical fiber sensors for strains and temperatures measurements and vibrating wire extensometers for strains measurements.

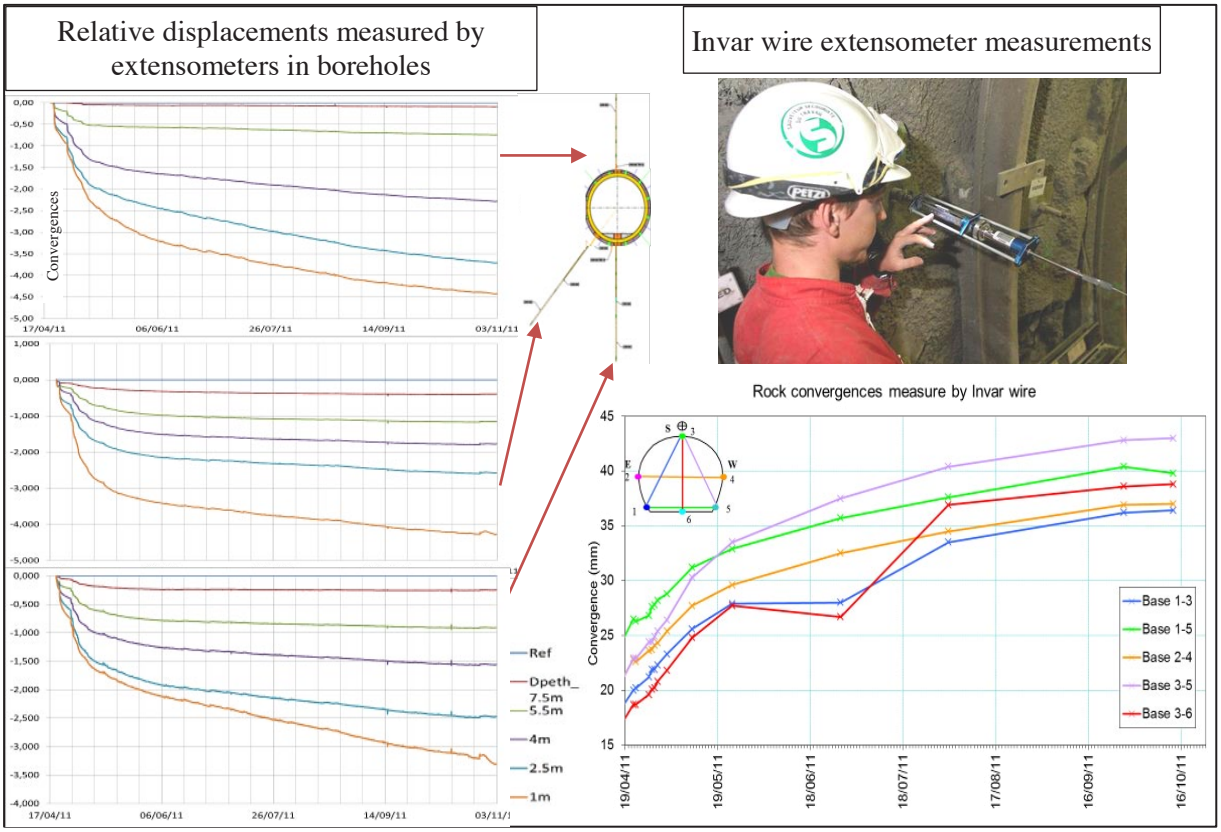


Figure 1: Comparison between displacements measured by Invar wire system and inductive extensometers in boreholes in the gallery GCR in Andra's URL

Tested sensors, in the frame work of this demonstrator in the Andra's URL since 2011, show a very good survival rate of sensors after about 4 years, of 95%. The comparison between technologies used indicates a good correlation and justify their installation in the future demonstrator in GER galley. Also, new configurations and sensors will be tested and promise interesting data.

References

[1] R. Farhoud et al "Full scale in situ monitoring section test in the Andra's Underground Research Laboratory", 1st Technical Innovation in Nuclear Civil Engineering conference October 28 – 31, 2013, Paris, France.

[2] S. Delepine-Lesoille et al "Industrial Qualification Process for Optical Fibers Distributed Strain and Temperature Sensing in Nuclear Waste Repositories", Journal of Sensors 01/2012.

[3] R. Farhoud et al "Monitoring system design of underground repository for radioactive wastes – in situ demonstrator", 3rd International Conference on Civil Engineering and Architecture July 30-August 01, 2014, Campinas, Brazil.

Downscaled deposition hole simulation in four setups: Transparent, Rigid, Heated and Large scale

Xavier Pintado[1], **Kari Koskinen**[2]

[1] B+Tech Oy, Laulukuja 4, 00420 Helsinki, Finland
[2] Posiva Oy, Olkiluoto, Finland
Correspondence: xavier.pintado@btech.fi

The design development process for the Engineered Barrier Systems (EBS) in future repository in Finland needs the calibration of the models which reproduce the buffer behaviour and to study the complex processes which take place in it. The small scale tests give the parameters for the models but it is also necessary to use tests in larger scale for improving the knowledge of such processes in buffer and the models calibration. Downscaled tests have been carried out in Finland with transparent and rigid cells fully instrumented for studying the buffer behaviour as part of the integration THM-experimental work and modelling (Pintado et al., 2010).

Four different downscaled tests setups have been developed for measuring the swelling pressure evolution, the saturation evolution and the density distribution with time and the mechanical erosion. The tests were done in blocks with lower diameter than the test setup and the gap was filled with rod or pillow pellets or was kept void at the beginning of the test. The initial gap thickness was 30 and 50 mm.

The transparent setup is showed in Figure 1a. It is a 270 mm inner diameter PVC (polyvinyl chloride) cell. The height of the sample is 800 mm (four blocks of 200 mm thickness). The axial swelling load is measured with a load cell on top and the radial swelling pressure is measured with three 9 mm diameter sensors in different sections. The circumferential strains are measured with strain gauges. It is possible to transform such strains to inner swelling pressure but it is necessary to make some assumptions and the PVC shows creep, so it could disturb the measures. A wireless system for measuring the relative humidity evolution with capacitive hygrometers can be used (Figure 2b). The radio waves can move through the plastic walls. The rigid setup is showed in Figure 1c. It is a 350 mm inner diameter carbon steel cell coated for protection against corrosion. The height of the sample is also 800 mm (four blocks of 200 mm thickness). The cell wall thickness is 20 mm with three sections indented (Figure 1d) with 5 mm thickness for measuring the strains because of the swelling pressure development. The axial load is measured with a load cell and the radial swelling pressure is measured in four sections with 6 load cells each one. The load cells are connected with 20 mm diameter pistons which are pushed by the sample during the saturation process. This test has the option of heating (Figure 1d). These two tests are extensively described in Pintado et al., 2013.

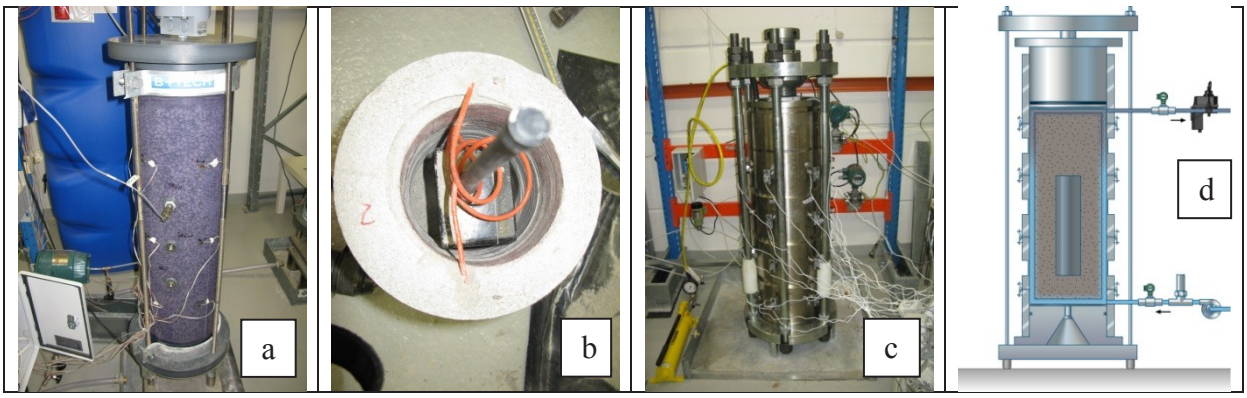


Figure 1. *Transparent setup (a). Wireless system in transparent setup (b). Rigid setup (c). Rigid setup schematic image (d) with an optional heater inside.*

The transparent test setup has been modified and a heating system has been implemented. The heater has 780 mm length and 0.8 mm diameter (Figure 2a). The temperature is kept constant at 95ºC and the temperature on the surface of the PVC tube and on the top piston is measured as well.

The large scale test setup (Figure 2b) is a modular system of tubes manufactured from acrylic (PMMA) plastic reinforced with metal bands made in carbon steel painted for protection against corrosion. The inner diameter is 800 mm and the height is 2000 mm (ten blocks 200 mm thickness). The axial swelling load is measured with a load cell on top and the radial swelling pressure is measured with pressure sensors with a diameter of 50 mm. There are six sensors in two sections. The test setup has five transmitters which send the signal from three total pressure sensors and three capacitive hygrometers each other (Figure 2c). The position of the sections with wireless data transmission is in Figure 2d. Some strain gauges are glued in the plastic tubes and in the metal bands for checking the correct behaviour of the reinforcement.

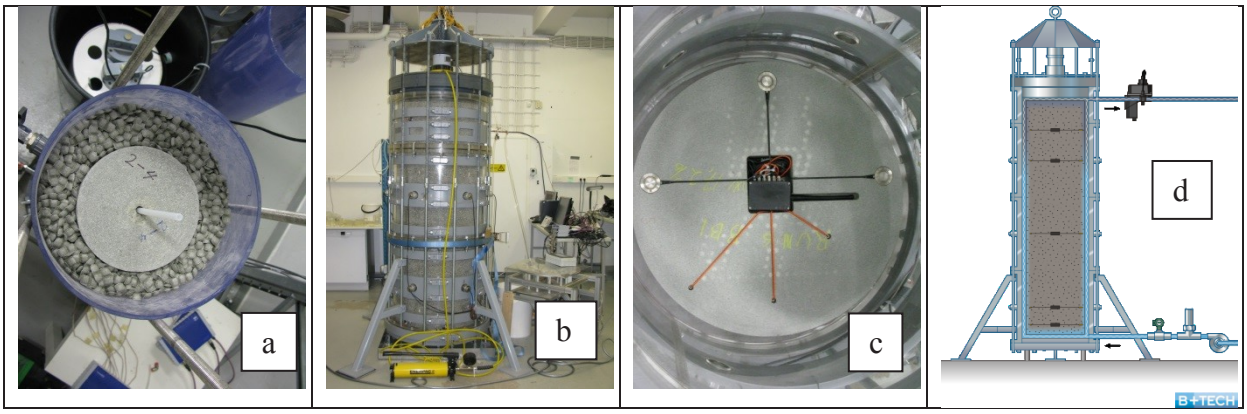


Figure 2. *Heated setup with the resistance at the middle (a). Large scale setup (b). Wireless system in large scale setup (b). Wireless system in large scale setup (c). Large scale setup schematic image (d).*

All tests were done pumping water at flow rate of 0.1 L/min through a water inlet at the bottom of the cell. The water flows out through a water outlet at the top of the cell. The effluent is collected in flasks for measuring the content of effluents and calculates the erosion rate. Tests are done with tap water (TDS, total dissolved solids content of 0.0345 g/L) but tests with higher TDS have been done: 1 g/L and 10 g/L. The test periods were some months and after the test, a post-mortem analysis was done measuring the final water content and the final bulk density. The dry density distribution and the degree of saturation can be calculated from these measures. The suction in these samples was also measured with a chilled-mirror dew point psychrometer.

References

Pintado, X., Autio, J., Koskinen, K. (2010). Integration of THM-experimental work and modelling to design. Proceedings of the Meeting “Nantes 2010”. Clay in Natural and Engineered Barriers for Radioactive Waste Confinement. Andra. France

Pintado X., Adesola, F., Turtiainen, M. (2013). Downscaled Tests on Buffer Behaviour. Posiva Working Report 2012-100. Eurajoki. Finland

Geoelectrical monitoring of dismantling operation within the Engineered Barrier Emplacement Experiment (Mont Terri RL)

Markus Furche, *Kristof Schuster, Christoph Czora, Hendrik Albers*

BGR, Stilleweg 2, 30655 Hannover, Germany

The Engineered Barrier Emplacement Experiment in Opalinus Clay "EB" Experiment aimed at the demonstration of a new concept for the construction of HLW repositories in horizontal drifts, in competent clay formations. The principle of the new construction method was based on the combined use of a lower bed made of compacted bentonite blocks, and an upper buffer made of granular bentonite material (GBM). The project consisted on a real scale isothermal simulation of this construction method in the Opalinus Clay formation at the Mont Terri underground laboratory in Switzerland. A steel dummy canister, with the same dimensions and weight as the Spanish reference canister, was placed on top of a bed of bentonite blocks, and then the upper part of the drift was buffered with the GBM made of bentonite pellets. The drift was sealed with a concrete plug having a concrete retaining wall between the plug and the GBM. To investigate the rock resistivity in the EB niche two circular profiles in the drift cross section and one horizontal profile along the drift axis were installed in 2001 before emplacement of the canister. After sealing the niche in 2002 the resistivity distribution was measured in two additional campaigns between November 2002 and November 2003. In July 2012 test measurements using these electrode arrays were performed successful. One of the circular profiles was used for a monitoring of the dismantling operation based on daily measurements between September 27th 2012 and May 24th 2013. The result is the two dimensional resistivity distribution of the electrode profile section for every day.

The results have to be distinguished in two parts: The first part is the period where the niche is filled before the dismantling front reached the geoelectrical section. In this situation most of the current field distributes in the backfill material but not in the clay, so these measurements can be used to characterize the niches interior. In the second part the niche is open after dismantling, the whole current flows in the Opalinus Clay around the drift, so this type of measurement is appropriate to characterize the near field features of the drift wall.

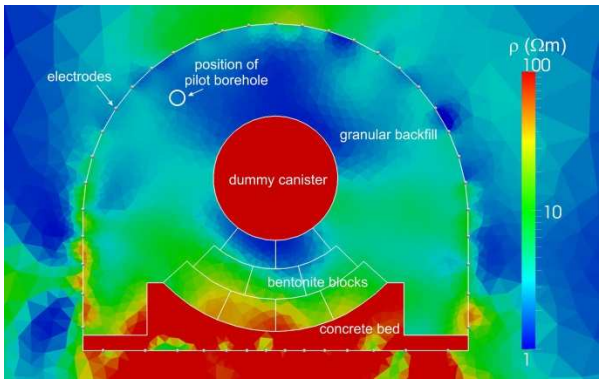


Figure 1: Resistivity distribution of the filled niche in front of the dismantling procedure

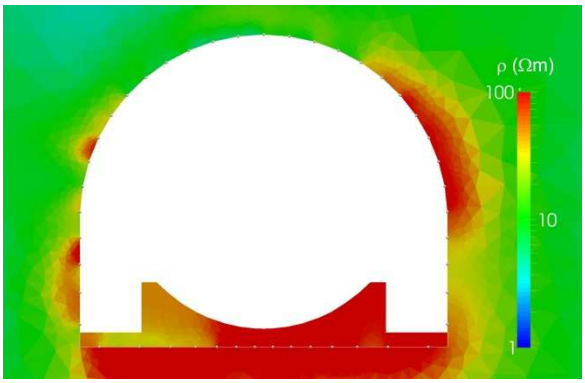


Figure 2: Resistivity distribution of the OPA around the EB niche 3 month after finished dismantling procedure

In the filled case (see Figure 1) the concrete floor as well as the concrete bed are resolved as high resistive structures with more than 100 Ωm as expected, also the dummy canister is reconstructed as a high resistive area (>> 100 Ωm), because of the isolation effect of a lacquer coat and the textile membrane that surrounds the canister. The lowest resistivities (below 3 Ωm) are displayed above and

directly below the canister. There is only a small variability of resistivity seen in the horizontal direction within the bentonite, but there is obviously a vertical gradient present with higher resistivities (~ 10 Ωm) at the floor. It is remarkable that no contrast can be seen at the border between the bentonite blocks and the granular material. Results from high resolution borehole measurements performed in a pilot borehole in 2011 confirm the resistivity values for this region. In comparison to water content measurements performed for samples while dismantling there exists a positive correlation of resistivity and water content so the resistivity pattern gives a qualitative image of the water distribution. Additional laboratory analysis of bentonite samples confirm this special behaviour.

In the dismantled case the region around the drift is characterized by resistivities of about 10 Ωm, except of two regions (right top and left wall down) where higher resistivities (>40 Ωm) are visible. Three month later these regions increase in extension as well as in resistivity contrast (see Figure 2). These results can be compared with spatial stress distribution as a result of a stress analysis of the EB niche before emplacement. There exist broad areas of low confining stress at the left top and the bottom of the niche. But remarkable are the two zones indicating areas of high deviatoric stress exactly at the same positions where the geoelectrical measurements show the enhanced resistivities. After the stress relaxation further to dismantling the niche this high deviatoric stress could enforce the formation of micro cracks in the Opalinus Clay. These cracks may lead to higher drying out at this positions and results finally in a higher electrical resistivity.

High resolution fibre-optic monitoring system for the FE Experiment in Mont Terri

K. Kishida[1], **T. Vogt**[2], **A. Guzik**[1], **H.R. Müller**[2], **B. Frieg**[2], **B. Knüpfer**[3]

[1] Neubrex Co., Sakae-machi 1-1-24, Kobe, Hyogo 650-0023, Japan (kishida@neubrex.jp)
[2] Nagra, Hardstrasse 73, Postfach 280, 5430 Wettingen, Switzerland
[3] Brugg Kabel AG, Klosterzelgstrasse 28, 5201 Brugg, Switzerland

The Full-Scale Emplacement (FE) Experiment at the Mont Terri underground research laboratory in Switzerland is a 1:1-scale multiple heater test in a clay-rich formation (Opalinus Clay). The main aim of this experiment is to investigate spent fuel / vitrified high-level waste repository-induced thermo-hydro-mechanical (THM) coupled effects mainly in the host rock but also in the engineered barrier system (EBS), which consists of bentonite pellets and blocks. This objective implies requirements for long term monitoring. For this experiment the monitoring has to provide information on the deformation of the tunnel in which the heaters are to be emplaced as well as on the THM behaviour of the EBS. Therefore, 3D snapshots of THM tunnel properties could considerably improve the monitoring levels. The high resolution distributed fibre optics (FO) monitoring system installed in the FE Experiment addresses all these requirements and needs.

The system is designed to provide distributed measurements of temperature, strain, and displacements (overall tunnel deformation) over many years of continuous monitoring in a non-accessible location. Furthermore, the Distributed Acoustic Sensing (DAS) can be added to enhance the system capabilities and range of available data.

One of the most critical aspects of long term monitoring of THM problems is the design and installation of the fibre-optical cables. New sensing cables were developed for the purpose of the FE experiment. They are capable of sustaining temperatures of 85° C for a prolonged period of time. The design and materials ensure repeatability of measurements and lack of hysteresis (after heating up and cooling down), typically observed for many generic fibre cables. Cables were calibrated prior to installation to determine the strain-frequency and temperature-frequency coefficients and to eliminate the effect of thermal expansion of the coating from the measurement results. Additionally, optical fibres were installed on four plastic (POM) rods, creating so called "smart rods", used to measure displacements and thus overall tunnel deformations. In order to improve the quality and durability of the installation on rods, the plasma surface activation process was employed. Moreover, all the fibre-optic cables were installed without any connectors inside the tunnel, reducing the number of possible points-of-failure.

The core element of the system is the hybrid Brillouin-Rayleigh backscattering instrument (NeubreScope NBX-7020) offering 2-cm spatial resolution. The hybrid technology is capable of separating strain from temperature in single-mode (SM) fibre. This feature is especially important in FE Experiment as non-uniform and time-varying temperature gradients are expected. The measurements of pure strain with high resolution allow to detect the deformation of the smart rods and to calculate deformation of the tunnel. The paper presents the deformation calculations procedure and its error analysis. Moreover, the strain evolution during the tunnel backfill operation with bentonite will be reported.

The monitoring system is designed to be controlled and operated remotely. The measurement results are processed and stored by a customized database-backend application, allowing easy trend analysis and reporting. Additionally, for the purposes of FE Experiment the measurements are exported and feed into an existing database gathering data from the vast number of point sensors installed in the FE underground laboratory.

FE Experiment: The instrumentation and monitoring concept of a 1:1-scale heater experiment at the Mont Terri URL

Tobias Vogt, **Herwig R. Müller, Toshihiro Sakaki, Marian Hertrich, Thomas Spillmann, Benoit Garitte, Niels Giroud, Tim Vietor**

Nagra, Hardstr. 73, 5430 Wettingen, Switzerland (tobias.vogt@nagra.ch)

The Full-Scale Emplacement (FE) Experiment at the Mont Terri underground research laboratory (URL) is a full-scale heater test in a clay-rich formation ('Opalinus Clay'). Based on the Swiss repository concept it simulates the construction, emplacement, backfilling and post-closure thermo-hydro-mechanical (THM) evolution of a spent fuel (SF) / vitrified high-level waste (HLW) repository tunnel in a realistic manner. One of the main aims of this experiment is to investigate SF/HLW repository-induced THM coupled effects mainly on the host rock but also in the engineered barrier system (EBS) and to validate existing coupled THM models. The entire experiment implementation (in a 50 m long tunnel with a diameter of approx. 3 m) as well as the post-closure THM(C) evolution will be monitored using a network of several hundreds of sensors. The sensors are distributed in the rock near- & far-field, the tunnel lining, the EBS, and on the heaters.

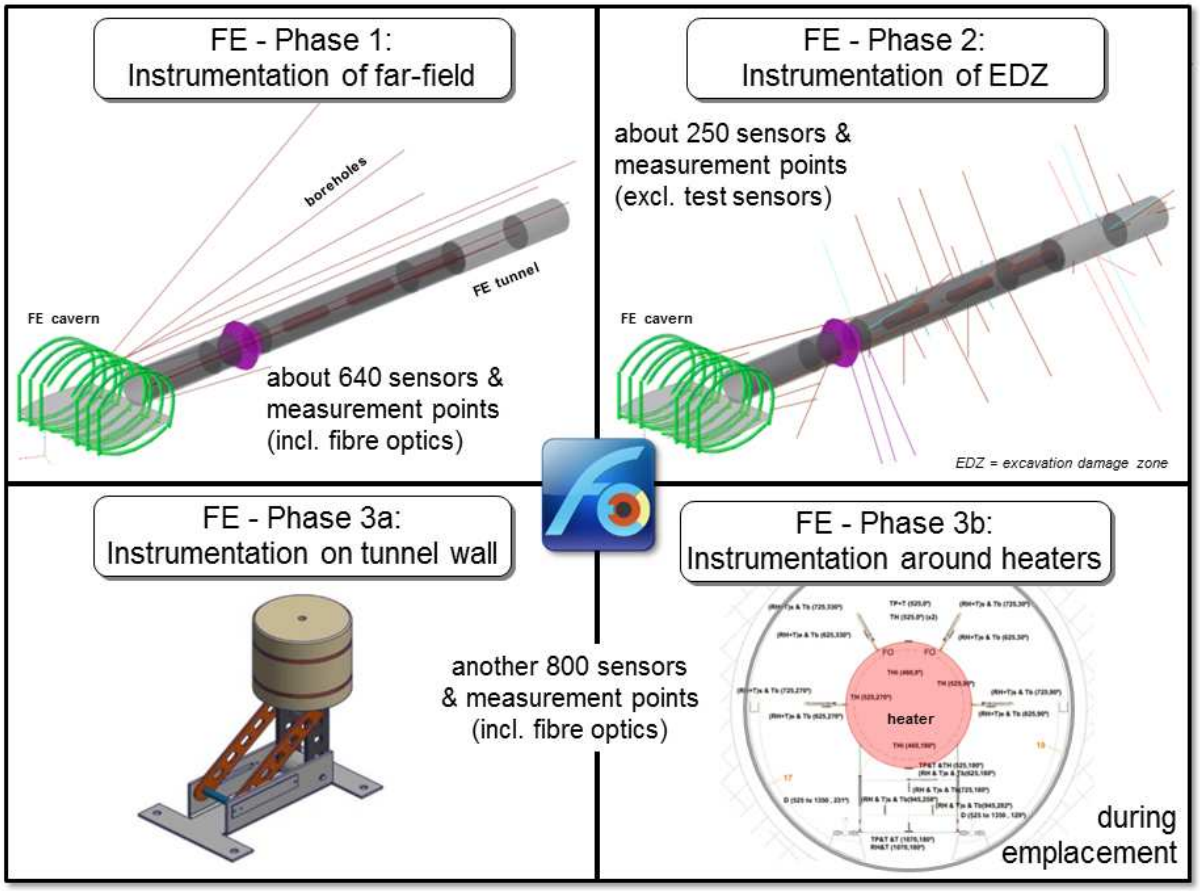


Figure 1: *Overview showing the main instrumentation phases of the FE Experiment at the Mont Terri URL as well as the approximate 3D arrangement of the longitudinal and radial boreholes.*

The rock in the 'far-field' was instrumented with up to 50 m long boreholes drilled from the FE cavern; this instrumentation was completed in April 2012 before the FE tunnel was built and therefore allowed a 'mine-by' observation of the later tunnel construction. Until February 2014 the 'excavation damage zone' (EDZ) was instrumented with radial boreholes drilled from the FE tunnel (see upper

right square in *Figure 1*). In June 2014 the instrumentation of the tunnel wall was completed for future monitoring of the bentonite buffer; here also many fiber optical cables for distributed temperature and deformation monitoring were installed. More sensors for monitoring the EBS close to the heaters will be brought in together with the heaters. The sensors on the tunnel wall, in the EBS and on the heaters have to be installed on erectable sensor holders due to the space conflict with the newly developed prototype machine for backfilling the FE tunnel with granular bentonite (cf. MÜLLER et. al. in this issue).

The main parameters to be monitored are temperature, pressure, deformation, and humidity/water content but also geophysical and gas related monitoring will be performed.

- Water pressure in rock: 6 boreholes with multi-packer systems and 6 intervals each, 8 boreholes with multi-packer systems and 2 intervals each, 13 boreholes with single-packer systems and 1 interval each.
- Rock deformation: 5 boreholes with standard rod extensometer and 6 boreholes with specially designed long-term rod extensometer. 2 boreholes with inclinometer-chains, 40 segments each, two measurement axes. 7 boreholes with fiber-optic strain sensors (SOFO).
- Water content in rock: 29 boreholes with water content (TDR/FDR) and relative humidity sensors
- Rock temperature: All boreholes are equipped with in total 320 temperature sensors (PT1000 and thermocouples). In addition, 360 m of fiber-optical cable on the inclinometer casing and 250 m at tunnel wall for distributed temperature sensing are installed. A heatable fiber-optic cable is installed as well for determination of water content distribution.
- Tunnel climate during ventilation phase: 12 climate sensors (RH & temperature, wind speed, air pressure) during ventilation phase.
- Heater monitoring (sensors per heater): 6 internal temperature sensors, 44 temperature sensors on heater surface (thermocouples and fiber-optic FBG sensors), 7 displacement sensors (LVDT and fiber-optic FBG sensors) to track heater movement, 2 total pressure cells on heater surface, polished areas at heaters to investigate corrosion after future dismantling.
- Bentonite (EBS) monitoring: 105 conventional temperature sensors (thermocouples and PT1000), approx. 430 m of fiber-optic cables for distributed temperature and strain sensing, 99 RH sensors, 15 water content (TDR/FDR) sensors, 27 total pressure cells at shotcrete - bentonite interface to monitor swelling pressures, 12 thermal conductivity sensors.
- Gas monitoring in the EBS: 14 in-situ H2 sensors and 5 in-situ O2 sensors as well as 9 sampling lines.
- Geophysical monitoring of the EBS: 7 permanently installed seismic transmitters and receivers as well as monitoring pipes that penetrate into the EBS to run temporary seismic, radar and other geophysical logging tool.

The monitoring environment is challenging. Temperatures of up to 150°C in the bentonite buffer and of up to 60-80°C in the rock are expected. In addition, saline pore water will cause corrosion in the rock and in the humid / (partially) water saturated areas close to the tunnel wall. So although some state-of-the-art sensors and measurement systems could be installed, also prototype measurement systems were developed especially regarding the choice of material with respect to corrosion and thermal conductivity. Naturally novel fiber optical sensor technology was also heavily used.

Safety Indicators and Demonstrators

J.B (Jacques) Grupa
E. (Ecaterina) Rosca-Bocancea

NRG
Westerduinweg 3, 1755 LE PETTEN
P.O. Box 25, 1755 ZG PETTEN
THE NETHERLAND

The DOPAS project (Full-Scale Demonstration of Plugs and Seals) aims at improving the adequacy, consistency and industrial feasibility of the plugs and seals to be used in disposal facilities for radioactive waste across a range of different geological environments (http://www.posiva.fi/dopas). Plugs and seals contribute to maintaining a very-low-water-flow condition and a favourable chemical environment around waste canisters. As such, they fulfil an important role in supporting the high level *safety function* 'isolation of the waste'.

As part of our task in the DOPAS project, we reviewed the list of endpoints of the performance assessment calculations. These endpoints are often addressed as Safety and Performance Indicators. Most of these indicators are based on calculated future radionuclide fluxes and concentrations in various parts of the disposal system. There are two important limitations of these indicators: 1) Even in case of poor performance, radionuclide migration may not occur until e.g. 1000 years after emplacement, and 2) In a multi-barrier system, the performance of the second, and subsequent barriers can only be evaluated by nuclide-based indicators if the inner barriers are assumed to fail. As a result this type of indicators is not applicable to the outer components of the EBS, such as plugs and seals, during the demonstration and operation period.

However, a particular class of indicators, the so-called *Safety Function Indicators*, introduced by SKB and POSIVA in their safety studies, stands out as these indicators do not relate to nuclide migration. "A S*afety Function Indicator* is a measurable or calculable property of a repository component that indicates the extent to which a *safety function* is fulfilled." We noted that these *Safety Function Indicators* are treated mainly as technical requirements, and are not explicitly addressed in the performance assessments. As part of our contribution to DOPAS we are developing a method, through which these indicators will have a more important role in the Performance Assessment.

An example of a *Safety Function Indicator* is the buffer hydraulic conductivity. If the hydraulic conductivity is sufficiently low the system develops according to the (favourable) Normal Evolution Scenario, while if the buffer hydraulic conductivity is too high a less favourable altered evolution may occur: advective transport may in the long term lead to alteration of the chemical environment, which may lead to increased corrosion rates of the

waste package, and faster migration of nuclides that may escape from the waste package. The threshold for the buffer hydraulic conductivity is design and site specific.

To use this Safety Function Indicator in a generic performance assessment methodology (i.e. not specific for a site or disposal concept), we propose to translate hydraulic conductivity into a Péclet number. The Péclet number of saturated bentonite system reflects the ratio between the rate of advective and of diffusion driven transport. All evolutions of the bentonite system where the Péclet number is less than one are considered to be part of the Normal Evolution Scenario (because diffusive transport in bentonite is unavoidable). This allows us to formulate a generic threshold: if the Péclet number is less than one, the bentonite or clay system develops in accordance with the Normal Evolution Scenario, if the Péclet number is more than one, a potential for development into a less a less favourable Altered Evolution Scenario emerges.

In this paper it will be explained in more depth how this approach is applied to the DOMPLU demonstrator: the Dome Plug Experiment. This is a full-scale deposition tunnel end plug demonstration at Äspö Hard Rock Laboratory conducted by SKB and Posiva. The monitoring part of the Experiment belongs to the DOPAS project. This demonstrator is used to show a disposal gallery containing the waste canister, the bentonite buffer and the bentonite backfill (as in the KBS-3 disposal concept) can be adequately closed by the concrete dome-shaped plug. DOMPLU includes the end plug and a part of the backfill. The concrete part of the DOMPLU plug is equipped with 56 sensors; the filter and seal layers with backfill include 47 sensors. An estimate of the hydraulic conductivity of the bentonite can be derived from the measurements - to derive the Péclet number additional estimates about the hydro-geological environment of the disposal site have to be included.

Eventually we aim at identifying more indicators and approaches to all demonstrators in the DOPAS project, and to give the demonstrator results a place in the safety and performance assessment component of the safety case. In this way we hope to achieve a better/ more direct coupling between the work on EBS and demonstrators on the one hand and the performance assessment and the safety case on the other hand.

The research leading to these results has received funding from the European Union's European Atomic Energy Community's (Euratom) Seventh Framework Programme FP7/2007-2013 under grant agreement no 323273, the DOPAS project and from the Dutch research programme on geological disposal OPERA.

Electromagnetic techniques for Callovo-Oxfordian Clay Rockwater content measurements

Sylvie Delepine-Lesoille, Thierry Bore, Jean-Charles Robinet, Daniel Coelho, Norman Wagner, Gonzague Six, Frederic Taillade

French National Radioactive Waste Management Agency (Andra), France
French Institute of Science and Technology for Transport, Development and Networks, Universite Paris Est, France
Institute of Material Research and Testing, Bauhaus-University WeimarCoudraystr. 4, 99423 Weimar, Germany

Water content is a key parameter to monitor in nuclear waste repositories, to evaluate saturation process in host clay rock, backfill material or coverage structure. TDR (Time domain reflectometry) sensing chains are commonly used in agriculture to optimize watering. However, adaptation to clay materials requires caution since variation ranges are smaller and empirical calibration equations for soils fail for clay-rock. We evaluated the impact of water content on the electromagnetic property of callovo-oxfordian clay rock, in a water saturation range from 0.16 to nearly saturation. We observed clay is a dispersive material on the electromagnetic point of view which calls for evolution towards Frequency Domain Reflectometry techniques. We demonstrated empirical calibration based on re-compacted materials are not valid.

Time Domain Reflectometry (TDR) probes are commonly used in agricultures to optimize watering. Andra tested this technology in a 1 to 1 scale demonstrator of covering structure. Among 4 tested methods, only TDRs have provided expected measurements over the past 20years. This is why Andra decided to adapt these commercial sensors to radioactive waste repository monitoring, more precisely to the host material of the Cigéo project, the Callovo-Oxfordian (COx) hard clay.

TDR probes actually provide indirect measurement of water content. A major difficulty to face is the link between the performed permittivity measurements with host material water content to sense. Various empirical models are used for soil ([1][2]).Yet it is well known they are not valid for clays ([3][4]). Another solution is to rely on laboratory calibrations. However, it encounters opposite specifications (i) need for large samples to place the TDR probes and respect interaction field (ii) duration of water content forced variations. We developed a new laboratory dielectric measurement device, consisting of a coaxial transmission line and a network analyzer, enabling characterization of intact clayrock permittivity over the 50 MHz - 1 GHz frequency range. We performed dielectric characterization of non-crushed clay rock, as a function of their water content, in a water saturation range from 0.16 to nearly saturation.

Clay samples were extracted form the Andra Underground Research Laboratory (URL). Four core samples (∅ = 80 mm) were extracted at different depths within the COx layer:S1, S2,S3 and S4 were taken at -506m, -450m, -503m and -496m, respectively. S1, S3, S4 belong to the same geological unit, characterized by a high clay content (~ 50 %) and little variations of mineralogy and petro-physical properties. S2 was extracted from the carbonate silt unit which is characterized by a lower clay content (20 - 40%).

The selected method requires the rock sample under test to be carefully drilled and machined to precisely fit in a holder. For each material, that is to say each “Sx”, 18 specimens were produced : three for each relative humidity (RH=11%, 33%, 58%, 75%, 90% and nearly 100%) to evaluate reproducibility. The samples were controlled by daily weighing until the equilibrium was reached. The apparent density ρ (mass of the cylinder/volume of the cylinder),porosity n and the degree of saturation S_w were measured.

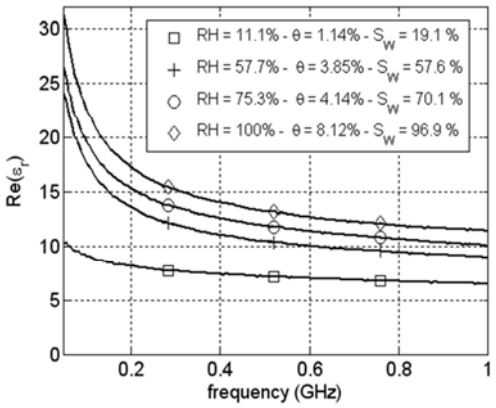


Fig. 1: For one serie, influence of working frequency on the permittivity, for four water contents

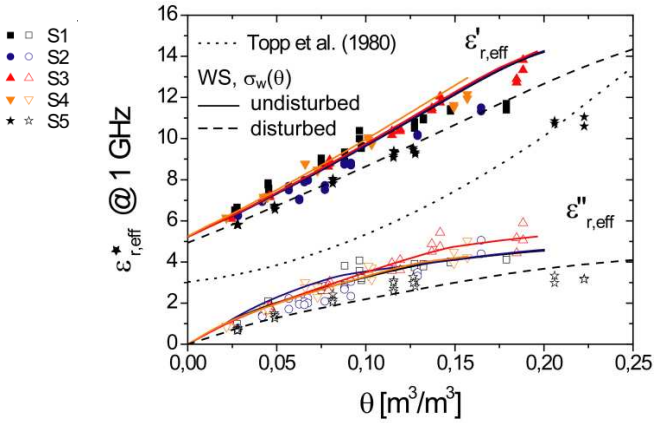


Fig. 2: Real $\varepsilon'_{r,eff}$ and imaginary part $\varepsilon''_{r,eff}$ of thecomplex relative effective permittivity as a function of water content for the four series

As expected, the complex permittivity of clayrock increases with water content. However, we also observe a strong dependence on frequency on both real and imaginary part (see for instance fig. 1), for all the samples. Such dispersive behavior is attributed to porosity, specific surface area and cation exchange capacity: the state of porous water is influenced by different surface bonding forces due to interface process [5]. TDR sensing chain makes use of a broadband (MHz-GHz) short pulse in the time domain, whose propagation time is measured. As a consequence, the TDR signal is strongly distorted and attenuated. Hence, this conventional approach is not suited to dispersive materials such as COx clay rock. We must turn towards frequency-domain methods.

We compared the obtained calibration to the empirical relationship between volumetric water content and effective permittivity according to the empirical Topp-equation. Fig.2 illustrates the result for 1 GHz frequency. It clearly demonstrated this simple empirical model does not apply in case of this clay rock due to the inability to consider the real rock-structure, i.e. porosity and pore size distribution. We developed a novel hydraulic-mechanical-electromagnetic coupling approach. This approach enables modeling of the complex permittivity as a function of water content in the frequency range of TDR applications around 1 GHz in reasonable agreement with experimental data [5].

It is worth noting the four tested clay materials result similar. This is promising for future underground repository application. Finally, we also evaluated the difference between disturbed (S5 serie) and undisturbed samples. As illustrated in Fig.2, it turned out to be important. It further implies the inability to perform an empirical calibration for the electromagnetic method with re-compacted material.

Perspective is to evaluate temperature and density influences on these calibrations, then to develop the adapted FDR approach for water content measurement.

REFERENCES

[1] G.C. Topp, *et al*,"Electromagnetic determination of soil water content: Measurement in coaxial transmission lines ",*Water Resources Research*, 16(3), 574-582 (1980)

[2] M.C. Dobson, *et al*, "Microwave dielectric behavior of wet soils – Part II : Dielectric mixing models", *IEEE Trans.on Geoscience and Remote Sensing*, GE-23(1),pp. 35 – 46 (1985).

[3] D. Robinson, *et al*,"Evaluation of a capacitance probe frequency response model accounting for bulk electrical conductivity comparison with TDR and network analyser measurement", *Vadoze Zone Journal*, 4(4), 992 – 1003 (2005)

[4] N. Wagner, *et al*, "Determination of the spatial TDR-sensor characteristics in strong dispersive subsoil using 3D-FEM frequency domain simulations in combination with microwave dielectric spectroscopy", *Meas. Sc. Tech.*, 18(4), 1137 – 1146 (2007).

[5] N. Wagner et al. Dielectric relaxation behaviour of Callovo-Oxfordian clay-rock", J. Geophys. research: Solid earth, 118, 1–16, 2013

Ultrasonic monitoring of the concrete block support of a sealing core in Callovo-Oxfordian argilites

Cyrille Balland[1], **Jacques Morel**[2], **Rémi de La Vaissière**[2]
(1) INERIS – School of mines – Nancy (France)
(2) Andra –Meuse/Haute-Marne Center – Bure (France)
cyrille.balland@ineris.fr, jacques.morel@andra.fr, remi.delavaissiere@andra.fr

The French concept of drift sealing in the framework of a IL/HL-LL waste underground disposal consists of a swelling clay based core confined between two concrete blocks. The resaturation of the core generates a swelling pressure against the drift wall that induces a compaction of the EDZ and achieves a low permeability of the system (up to 10^{-11}m/s). The concrete blocks function is to ensure a mechanical confinement of the swelling clay core, thus orienting the swelling pressure radially. The concrete block will therefore be subject to high stresses.
A specific in-situ experiment (NSC, for Sealing Core) has been designed and is currently carried out in the Meuse Haute Marne URL, to test the performance of such a sealing. The core, 5 m long and near 5 m in diameter, is confined by a concrete block 2.5 m thick.
The concrete block has been designed to withstand the swelling stress of the sealing core with its own weight, the induced friction between the block, the gallery and the key. This anchoring consists of a concrete key inside the surexcavated gallery called "tooth". Its diameter is that of the gallery with 4.6 m in its narrowest part and 5.6 m in its surexcavated part. One of the challenges is to check whether the in situ high pressure generated by the sealing core can damage the concrete block and if so to what extent.

An ultrasonic monitoring has been designed and installed to monitor the damage in concrete and rock vicinity. A portion of the device has been initially installed in the block volume prior to concreting and a second wall portion after concrete formwork. A 3D velocity model has been designed taking into account the P-wave velocity of the concrete (4293 m/s: average of all raypaths), in the argilites (2500 m/s: estimated from previous EDZ ultrasonic tomography) and bentonite (1000 m/s estimated from Tisato et Marelli, 2013). This model was validated with the location of the emitted pulses from the sensors and simulation of AE in argillite and bentonite (Figure 1). The error in the localization is of the order of 5 centimeters in the concrete.

The large number of triggers on changes in the level of ultrasonic noise shows variations of activities that can be linked to the preliminary solicitation of the sealing core. Only a few AE have been recorded by the device. Two of them were located, they are in areas that are expected to be pressurized by the swelling of the sealing core: near the concrete raft of the gallery and key inking of the rock mass. The few AE are used to test the analysis of focal mechanisms.

P-wave velocity increases on the majority of rays with a daily average of 0.2 m / s. These changes are related to the concrete hardening process. Given the large number of raypath on which the P-wave velocity is measured (over a hundred), it is intended to a volume tomography of the concrete block to see the most stressed zone and potentially with time the damaged areas.

A preliminary analysis of the energy recorded in the sensors according to the length of the raypath shows that wave attenuation is relatively low and therefore that the quality factor Q of the concrete block is high (147) confirming its good mechanical characteristics which continue to improve with time (due to the drying process). Daily monitoring of the averaged quality factor is possibly a good indicator of the overall progress of the block physical properties in the short and medium term. Finally, to make operational monitoring, automatic processing of data coupled with a web-page has been developed. It will detect the AE highest energy and abnormal variations in the velocity of P waves. This system will enable the operator to quickly have information on the health of the concrete block.

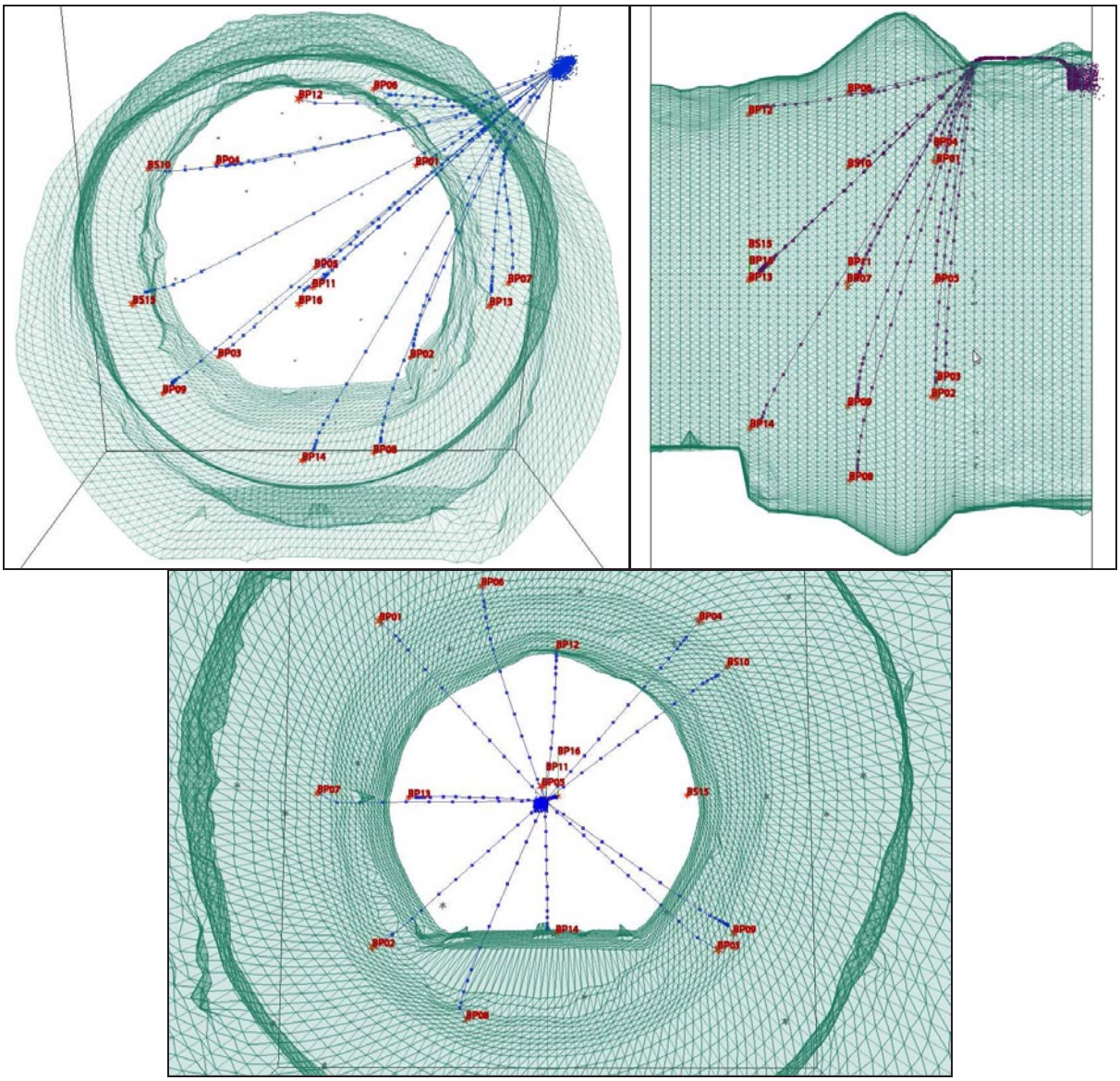


Figure 1 : Simulation of AE in argillites rear view (top left) in the bentonite sectional view (top right) and locating a pulse from the sensor in the central concrete block front view (bottom)

De La Vaissière R., Conil N., Morel J., Leveau F., Gatabin C., Garcia-Sineriz J.L, Habos H., Rey M., Piedevache M., Helminger B., Balland C., 2014, Design and construction of a large-scale sand-bentonite seal in in the Meuse/Haute Marne underground research laboratory: NSC experiment, International Conference on the Performance of Engineered Barriers, Hannover (Germany), February 6-7.

Tisato N., Marelli S., 2013, Laboratory measurements of the longitudinal and transverse wave velocities of compacted bentonite as a function of water content, temperature, and confining pressure, Journal of Geophysical Research: Solid Earth, Volume 118, Issue 7, pages 3380–3393

Data Mining Approach for heavily instrumented repository cells

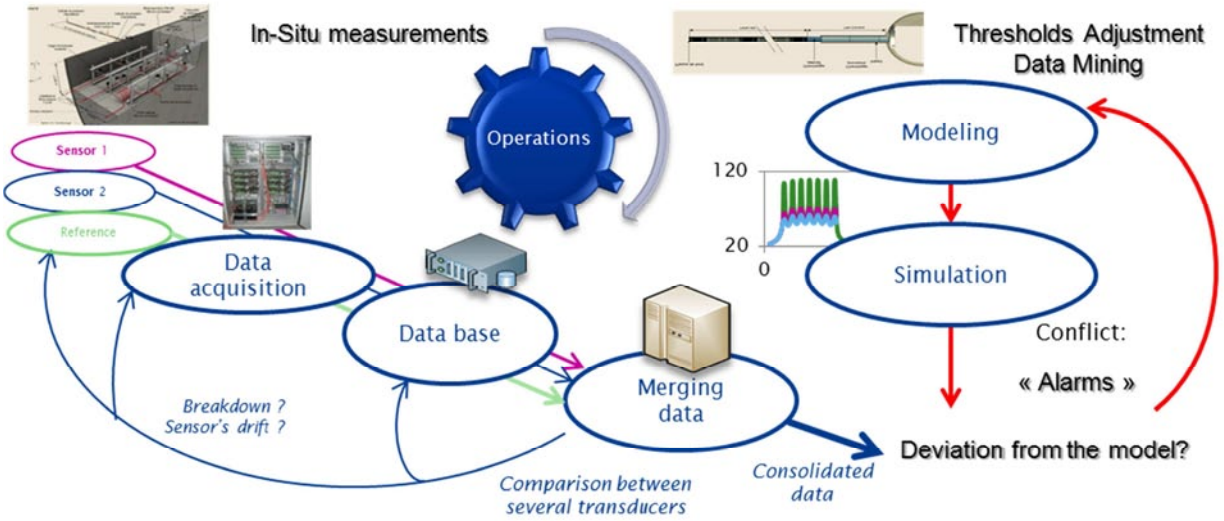
G. Hermand, N. Gilardi, S. Buschaert, A. Chabiron, N. Stoffels

Andra, 1-7 rue Jean Monnet 92298 Chatenay-Malabry, France

Data mining for structural health monitoring is an emergent field of studies, not only because of the buzz around the theme of big data but also because numerous civil engineering industries have to deal with aging and instrumented structures [1]. Andra's project of a monitored deep geological repository (Cigéo) has to anticipate the strategy of data mining. The main issue will be: how to deal with the continuous flow of thousands of sensors measurements over several decades without the help of hundreds of experts checking regularly the data? Anticipating the data mining will not only verify that the design of the repository fulfils its functionalities, but it will also help to position adequately all the instruments.

In order to insure operational safety and long term safety, several tens of thousands of sensors generating roughly a hundred of thousands of measure points will be progressively installed in HL waste and ILL waste repository cells. Potentially this process could produce more than 3 million of data every day. In Cigéo project, the design of the ILL waste repository cell is a circular concrete liner which shares similarities with more common concrete structures (such as subway galleries, for instance). Structural health monitoring field (SHM) shows currently a high interest in R&D pressed by a growing number of aging structures.
Regarding Andra's needs in term of decision tools to analyse phenomenological processes, long-term safety and waste package retrievability, the methodologies for the sensor measurement analyses in disposal cells must be anticipated. This preliminary work should provide optimization of the instrumentation in terms of positioning and redundancy.
This approach is hence reinforced by the need of semi-automatic or automatic analysis of data and comparison to modelling such as multi-parameters physical models, meta-models or statistical models sometimes obtained by machine learning methods.

Overview of the approach
This approach is conducted in the framework of Andra policy of data traceability (cf. ISIS project [2]). A strategy to manage the measurements has been developed and is synthetized by the following diagram.



The diagram is composed of three main parts:

- The left side is the acquisition and management of repository monitoring data, future version of a data acquisition system, like "SAGD", currently deployed in Andra Underground Research Laboratory (URL) with about 10 000 functioning measurement points .
- At the top right is the modeling of systems (such as THM structures of steel and concrete, rock, and interfaces) providing expected values.
- Both domains meet by data fusion and comparison with expected values.

At the end, the iterations of each system, provides the necessary information for decision making.
The choice of the consolidated data is determined by the kind of results we can obtain by simulations.

First results and current studies

Inspired by methodologies used in automation, predictive simulation methods have been tested thanks to *in situ* demonstrators. Preliminary work has been done using Auto-Regressive-Moving-Average with eXternal input (ARMAX) and Principal Component Analysis (PCA).
ARMAX is a predictive model based on a parameter of influence. It needs a certain time to learn the behaviour of the system. It has been applied on a real case: a vibrating wire extensometer installed in the concrete liner of the URL main shaft. Results, cf. [3], show that using ambient temperature measured near the shaft can provide a coherent predictive model of the normal behaviour of the system (sensors on the concrete). After the learning period (i.e. 2 years in our case), a gap or a deviation between the sensor's measurements and the predictive model indicate a fault[1] in the system. In order to size the gap or deviation related to an event we want to detect, a threshold is determined according to the results from multiple tests using a simulated fault in a real signal.
The advantage of this method relies on the fact that we do not need to understand physically how the temperature affects the sensors and the concrete liner. On the other hand, this method cannot distinguish a sensor failure from a fault in the structure (such as a crack in the concrete).
PCA methods help to determine accurately correlations between many variables. The application of these methods to SHM, and especially taking into account the variety of Cigéo instrumentation, is a work in progress [4]. It should offer a solution to automatically identify a sensor failure by comparing to the results of the nearest other sensors.
In parallel with further work outlined above, physical models will be developed for creating indicators. The aim of the data fusion consists in reducing the number of data to monitor. This will be done considering the design of the instrumentation of the repository cells. To illustrate this point, we consider four groups of four extensometers in an annular section of concrete. Each group of sensors will participate to the evaluation of an indicator (e.g. only one value) regarding the load applied by the rock on the concrete liner (to confirm the phenomenology parameters), the deformation of the ring (to insure that the waste package will not be stuck), and the health of the structure including the detection of cracks or the limit of rupture in the concrete. These tasks involve a good knowledge of the physical properties of the mediums (concrete, rocks …). In the preliminary tasks, thermal parameters will be separated from mechanical and from hydration phenomena in order to build meta-models.

Conclusion

The challenge to process such a flow of data for SHM is unique and will be achieved thanks to work prepared today. It should be functional at the start of Cigéo excavation. We show how to proceed with current methods and how to decrease the number of data to look at, without losing information. These will provide a great support for credibility of information using a large variety of measurements with various sensitive elements.

References

[1] A.S. Kiremidjian, "Structural Health Monitoring for Civil Infrastructure – From instrumentation to Decision support", p27 in Structural health Monitoring 2011 – Volume1

[1] A "fault" in this document refers to a defect in a machine or a functional system.

[2] A. Chabiron & al. "The scientific knowledge management at Andra: a new approach of the data traceability (ISIS project)", 6th Clay in Natural and Engineered Barriers for Radioactive Waste Confinement Conference, March 23-26, 2015, Brussels
[3] V. Sircoulomb & al. "Optimal tuning for an abrupt change detection algorithm: Application to an underground gallery structure health monitoring", Systol 2013, 2nd International Conference on Control and Fault-Tolerant Systems, October 9-11, 2013, Nice, France
[4] N. Stoffels & al. "Principal Component Analysis for Fault Detection and Structure Health Monitoring", EWSHM 2014, 7th European Workshop on Structural Health Monitoring, July 8-11, 2014, Nantes, France

The optimum bentonite for the disposal of high level radioactive waste

Kaufhold S.[a,*], Dohrmann, R.[a,b]

[a]BGR, Bundesanstalt für Geowissenschaften und Rohstoffe, Stilleweg 2, D-30655 Hannover, Germany
[b]LBEG, Landesamt für Bergbau, Energie und Geologie, Stilleweg 2, D-30655 Hannover, Germany

presentation: Oral
topic of scientific programme: Alteration processes
full paper: No (already submitted)

Abstract

Most of the concepts for the safe storage of high level radioactive waste (HLRW) consider bentonite to improve the barrier performance. Different research organisations of different countries gained appreciable experience in handling a specific type of bentonites over the last decades. Bentonites and their properties, however, vary from deposit to deposit and sometimes even within one deposit or mining area. The bentonite industry, therefore, established a set of quality determining parameters (QDP) for each type of product to provide constant quality to the customer. Using bentonites for encapsulation of HLRW, however, is a new industrial application and widely accepted quality determining parameters for the production do not yet exist. Within almost 14 years of research on a significant set of bentonite samples from all over the world, a preliminary set of quality determining parameters could be identified based on several laboratory tests (Kaufhold & Dohrmann, 2014). First, 10 desired and/or required properties of the bentonite were identified determining the quality of the bentonite. Their relative importance may not be equal but differs from one concept to another and, therefore, no attempt to weigh them was made. The 10 key properties are: 1) sealing capacity (based on swelling properties), 2) stability against extensive drying, 3) stability against cement pore water, 4) stability against unaerobically corroding iron, 5) stability against eroding water, 6) stability against saline water, 7) large capacity for the retention of radionuclides, 8) mechanical resistance against canister displacement (mechanical integrity), 9) large thermal conductivity, and 10) stability against nuclear radiation.
The first quality determining parameter (QDP) concerns reactive and/or soluble components as C- and S-phases (organics, sulphides, sulphates, and carbonates) which should be absent. The second QDP concerns the type of interlayer cation, either Ca/Mg or Na. Na-bentonites have a larger swelling capacity in the uncompacted state. In the presence of water they may form soft gels and hence reduce permeability. However, HLRW bentonites are commonly compacted to dry densities at which the swelling capacity of both types of bentonites is similar. On the other hand, Na-bentonites tend to liberate colloidal particles, e.g. at the outer part of the barrier. Therefore, Ca/Mg-bentonites should be preferred (unless other indispensable properties of Na-bentonites are found). Thirdly, the Fe-content of the bentonites should be low because Fe-smectites are known to be less stable with respect to thermal load, against solutions, and even against nuclear radiation. As electron donor and/or acceptor they may also induce unwanted reactions. Finally, medium to high charged smectites should be preferred because low charged smectites were found to be more aggressive towards iron than high charged ones. These specifications may have to be adjusted to special features of a specific repository and will be complemented based on further research but they are the first which were identified by investigation of all relevant parameters.
Bentonite may also be used as backfill material, to seal tunnels and shafts. The specifications for this material, however, are believed to be less important because of less relevant concentration- and temperature-gradients in the backfill compared to the material encasing the canister.
Notably, using a bentonite not fulfilling the four given QDPs will not lead to an unsecure barrier system but the failure probability could possibly be larger.

Kaufhold, S., Dohrmann, R. (2014) The optimum high level radioactive waste bentonite. – submitted to Earth Science Reviews, June, 2014.

Full-Scale Shaft Seal in Granite: Status after 6 Years (2009-2014) of Natural Evolution

D.A. Dixon[1], D.G. Priyanto[2], S. Stroes-Gascoyne[2], P. Korkeakoski[3] and R. Farhoud[4]

[1] Corresponding Author, Golder Associates Limited, Winnipeg, Canada (david_dixon@golder.com)

[2] Atomic Energy of Canada Limited, Pinawa, Canada (priynantd@aecl.ca; stroesgascoynes@aecl.ca)

[3] Posiva Oy, Olkiluoto, Finland (petri.korkeakoski@posiva.fi)

[4] Agence Nationale pour la gestion des Dechets Radioactifs ANDRA, Paris (Radwan.FARHOUD@andra.fr)

ABSTRACT

A full-scale shaft seal was designed and installed in the 5-m-diameter access shaft at Atomic Energy of Canada's (AECL's) Underground Research Laboratory (URL) in 2009, as part of Canada's Nuclear Legacies Liability Program. A 6-m-thick bentonite-based component was sandwiched between 3-m-thick, keyed upper and lower concrete components (Figure 1). The seal is located at the point where the main shaft intersects an ancient water-bearing, low-angle thrust fault at a depth of ~275 m in granitic rock. The bentonite-based component spans the fracture zone and extends approximately 1 m beyond the maximum identified extent of the fracture. In addition to the main shaft seal, a smaller diameter sealing having similar configuration and design was installed at the point where the vent raise intersects the fracture zone (Figure 1). This design was adopted in order to limit the mixing of groundwater from the deeper, saline regions with the fresher, near-surface groundwater regime. The concrete components provide the mechanical confinement and the bentonite component, an in situ compacted 40/60 (dry mass) mixture of bentonite clay and quartz/feldspar sand, provides the sealing component. The lower concrete is reinforced with rebar while the upper is not.

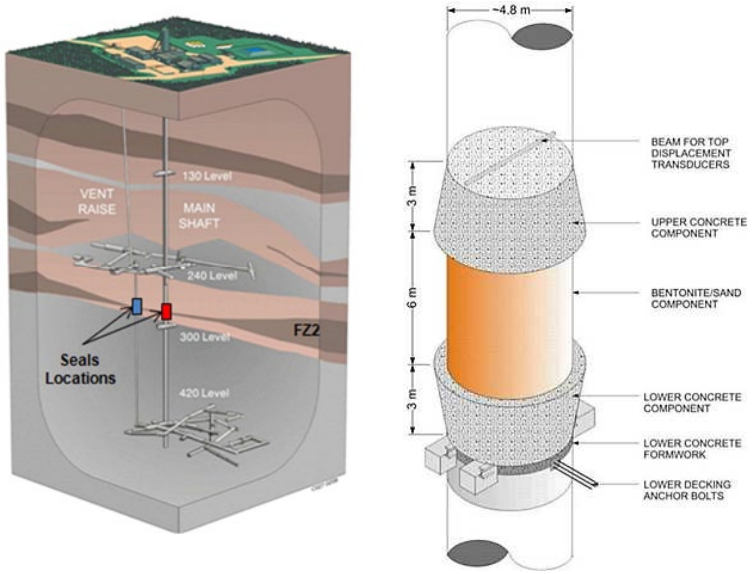


Figure 1: Location and Geometry of Shaft Seal

In addition to accomplishing the permanent closure of the URL, the construction of this seal provides a unique opportunity to monitor the evolution of a full-scale shaft seal as recovery of the regional

groundwater regime occurs during passive flooding of the region above this installation. A jointly-funded monitoring project, called the Enhanced Sealing Project (ESP), was developed by AECL (Canada) and funded by NWMO (Canada), SKB (Sweden), Posiva Oy (Finland) and ANDRA (France). Due to the very slow ongoing evolution/saturation of the seal and its surroundings, and the pending removal of the surface facilities associated with the URL decommissioning, monitoring has now evolved to a stand-alone, lower frequency data collection program. The ongoing monitoring is now being supported by AECL, ANDRA and Posiva Oy.

The seal installed in the main shaft of the former URL is still evolving. The performance of the seal and the ESP instrumentation system can be summarized as follows:

- The majority (~75%) of the sensors whose functionality was originally desired for ongoing monitoring are still functioning. These sensors have cables that run 275m vertically through a now partially-flooded shaft to a surface-based monitoring system, an extremely severe condition for monitoring.
- Recovery of the local groundwater table from the drawdown conditions induced by the URL opening is slowly progressing. Current regional hydraulic pressure monitoring results indicates that the recovery of the local groundwater table is still in the early stages.
- Groundwater inflow into the shaft segment above the seal is now estimated to be 6-8 m^3/ day, based on the data collected up to mid 2014. As of September 2014, the standing water level is approximately 6.9 m above the floor of the 240 Level horizontal excavations (Figure 2). Increasing rate of head development indicates that the horizontal excavations have now been filled with water. Rapid hydraulic head development will now occur as the water level quickly rises in the small volume shafts.
- A substantial hydraulic pressure differential continues to be observed across the 6 m-thick clay seal (Figure 2). This is attributed to the effectiveness (very low permeability) of the clay seal and its ability to limit mass (water) transport across it.
- Associated with rapid shaft flooding should be a reversal in the direction of the pressure-differential across the seal, a further opportunity to examine the effectiveness of the seal.

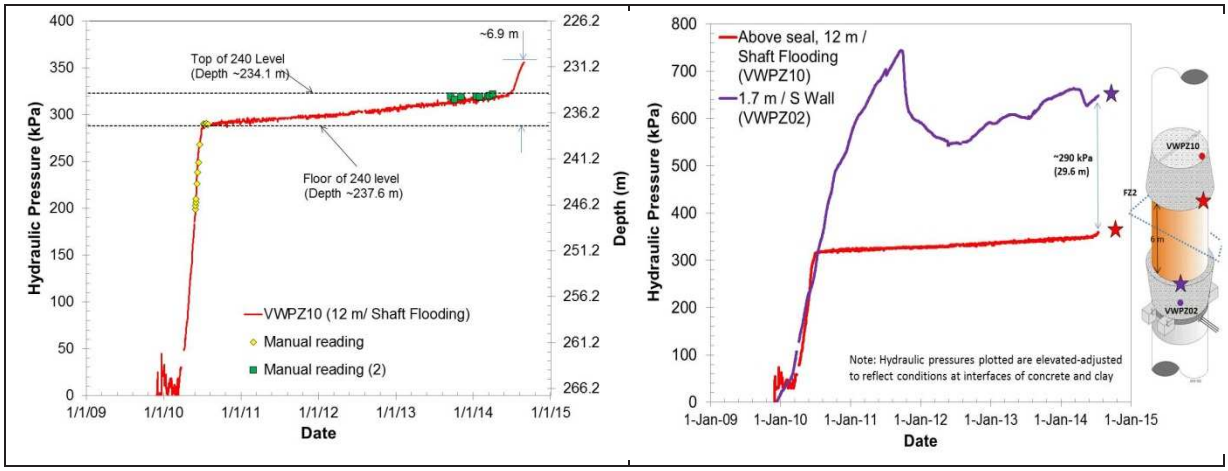


Figure 2. Development of hydraulic head above and comparison to pressure below the shaft seal

The ESP continues to supply valuable information on the field-scale evolution and performance of a shaft seal of the type that could be used in a repository environment. Information gained from monitoring the ESP can also be used to aid in the development of non-vertical (room and tunnel) seals in granitic or alternative geological media and to gain confidence in their performance.

Perspective of clay-salt slimes using as a sorbent of radionuclide and for safety disposal of radioactive waste

L. N. Maskalchuk*, A. A. Baklay, T. G. Leontieva, D. K. Stralenka
Joint Institute for Power and Nuclear Research, Sosny, NAS of Belarus, A.K. Krasin str., 99, 220109, Minsk, Belarus; E-mail: leonmosk@tut.by

In recent decades significant amounts of radioactive waste, accumulated in result of NPP and other nuclear facilities operation, as well as problems of rehabilitation of soils, which were radioactively contaminated resulting the Chernobyl and "Fukushima-1" accidents, represent a serious danger to human health and environment.

Investigation of effective and low cost sorption materials for radionuclide (^{137}Cs, ^{90}Sr) immobilization and for rehabilitation of radioactive contaminated soils currently has special relevance due to the urgent need to solve a range of technological and environmental problems associated with treatment, storage and disposal of NPP's radioactive waste and prevention of further radionuclide migration in the environment.

In order to solve NPP's technological problems on radioactive waste immobilization, it's safe storage and disposal, as well as ecological problems on the protection of the environment in case of NPP accident, supposed to use waste of potassium industry (clay-salt slimes - CSS) as a source material to produce powder and granular sorbents of radionuclide and soil amendments with specified physicochemical and sorption properties.

Clay-salt slimes are waste of potassium industry formed in result of sylvinite ore recycling. Annually in result of mining and processing of sylvinite ore at JSC "Belaruskali" (Soligorsk, Belarus) 2.0-2.5 million tons clay-salt slimes (CSS) are supplied in slime repositories, to date has accumulated more than 99 million tons.

CSS are complex formations, the main components of which are calcium and magnesium carbonates, calcium sulfates, alumosilicates, potassium and sodium chlorides. The insoluble rest (i. r.) of CSS prevails over the content of soluble salts: i. r. – 65–70%, NaCl – 20–25% and KCl – 13–15%. Clay-salt slimes have a range of important specific properties: high dispersion of particles, swellability and ion exchange capacity, considerable hydrophilicity. The specific composition of clay-salt slimes causes a possibility for their further modification and obtaining sorbents of radionuclide with specified sorption properties.

To assess the prospects of obtaining radionuclide sorbents (powder, granular) based on CSS, comprehensive studies of their physicochemical and sorption properties were carried out. CSS samples selected from 3rd mine factory of JSC "Belaruskali" were used as the research objects: the initial sample (CSS-1) and modified samples (CSS-2 and CSS-3).

The samples were analyzed with use of the following equipment: scanning electron microscope JEOL JSM – 6380 LA with X-ray spectral microanalizator JED 2300 - morphology and the elemental composition; diffractometer with a rotating anode Rigaku D/MAX 2500X-ray (CuK_{α}) - phase composition, laser microprobe particle size Analysette 22 - dispersion.

According to the obtained data, the samples of CSS are characterized by lamellar structure, which is typical for clay minerals. It was pointed out that the elemental composition of the native sample CSS-1 represented as a following, wt. %: O – 40,05; Na – 2,22; Mg – 4,84; Al – 5,97; Si – 18,7; S – 1,08; Cl – 3,95; K – 6,33; Ca – 9,27; Ti – 0,6; Fe – 5,09; Cu – 1,08; Zn – 0,81. Compound composition of CSS-1 sample is represented in the Table 1.

Table 1: Compound composition of the native sample CSS-1

Compound Composition, mass %											
SiO_2	CaO	K_2O	FeO	Cl	Al_2O_3	MgO	Na_2O	SO_3	CuO	ZnO	TiO_2
27,35	19,84	13,21	9,72	7,66	7,53	5,26	2,86	2,01	1,99	1,49	1,07

From the ratio of the basic elements in the individual points of the sample CSS-1 was evaluated its mineral composition, comprising a wide range of mineral phases: thin grains and aggregates of K-feldspar, quartz, biotite, clay minerals and silicates of Ca and Mg. According to X-ray phase analysis, the dominant mineral phases of the CSS samples are montmorillonite, illite and quartz.

It is established that in modified samples percentage of particles with sizes ranging from 0.1 to 3 microns is greatly increased (in comparison with the native sample CSS-1, 11,4%): 58,9% for CSS-2 and 93,7% for CSS-3.

Study of ^{137}Cs sorption on the sample CSS-1 was conducted under static conditions at a ratio of the solid (S) and the liquid (L) phases equal (S : L = 0.1g : 50 ml) with t = 20±2 °C. It was determined that the proportion of water-soluble, exchange and fixed forms of ^{137}Cs in the system CSS-1 – solution makes accordingly 0,4%, 17,5% and 82,7%; the degree of sorption – 99,6%; $K_d = 1,2 \cdot 10^5$ l/kg [1].

Radiocaesium Interception Potentials RIP(K) for CSS-1 defined by the Wauters J. method [2] are: RIP(K) = 6343±1120 mmol/kg (Russia) and RIP(K) = 6631±216 mmol/kg (Belgium).

It was determined that the main sorption-active minerals (relatively to ^{137}Cs) in CSS-1 are illite and montmorillonite. It was shown that used method of enrichment allow to increase their content in the sample CSS-3 by 3,5 times (in comparison with the sample CSS-1). Thus RIP(K) for the sample CSS-3 perhaps amount to 22000 mmol/kg.

The received data allow us to speak about possibilities of CSS use for obtaining powder and granular sorbents for radionuclide immobilization, as well as for rehabilitation of radioactive contaminated soils. On the base of CSS granular composite sorbent with polyacrylamide as a binder was synthesized and possibility of its use for ^{137}Cs immobilization has been shown [3].

The authors are grateful for collaboration in carrying out preliminary research of CSS samples to Dr. L. R. Van Loon (Paul Scherrer Institut, Switzerland), Dr. R. Dohrmann (Bundesanstalt für Geowissenschaften und Rohstoffe, Germany), Prof. S. N. Kalmykov (Moscow State University), Shinichiro Uematsu (SCK·CEN, Mol, Belgium), Dr. S. S. Vetohin (BSTU, Minsk, Belarus).

It is required further and detailed investigations of CSS samples from various mine factories (slime repositories) of JSC "Belaruskali" to verify methods of their modification and obtaining sorbents of ^{137}Cs with specified physicochemical and sorption properties.

References:

1. Baklai A.A., Maskalchuk L.N., Kapustina I.B., Pozylova N.M., Hololovich M.E., Stromsky A.S., Method of radiocesium fixation: Pat. Rep. of Belarus # 11011 dated 20.03.2007.

2. Wauters J.,D Elsen A., Cremers A., Konoplev A.V., Bulgakov A.A., Comans R.N.J. Prediction of solid/liquid distribution coefficients of radiocaesium in soils and sediments. Part one: A simplified procedure for the solid phase characterization // *Applied Geochemistry*. 1996. Vol. 11, № 4, 589-594.

3. Maskalchuk L.N., Baklay A.A., Leontieva T.G., 2012. Synthesis and Properties of the Composite Sorbents on the Basis of Alumosilicates Separated From the Clay-salt slimes. *Journal of Environmental Science and Engineering*. Vol. 1, № 12, 1356-1361.

A Study on the Seismic Response of an Engineered Barrier System

S. Sato[1], Y. Yamamoto[2], S. Suzuki[2], K. Ito[1]

1. Obayashi Corporation, Minato-ku, Tokyo 108-8502, Japan (sato.shin.ro@obayashi.co.jp)
2. Nuclear Waste Management Organization of Japan, Minato-ku, Tokyo 108-0014, Japan

INTRODUCTION

The 2011 off the Pacific coast of Tohoku Earthquake caused extensive damage to Japan. A seismic study aiming to confirm the effect of the large-scale earthquake on an engineered barrier was conducted by using the seismic waves observed during this earthquake. In the light of the developments on the numerical analysis techniques in the geotechnical field; it was decided to evaluate the mechanical stability by the latest methods. The behaviour of a buffer material is simulated with the effective stress method. The three-dimensional elastic-plastic seismic response analysis was then performed.

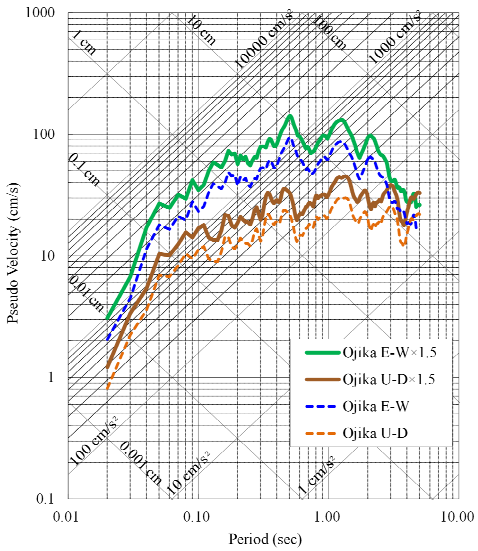


Figure 1 Response spectrum of Ojika

GROUND MOTION CONSIDERATIONS

The input ground motion was searched by using the recorded data in K-NET, KiK-net strong motion observation networks of National Research Institute for Earth Science and Disaster in Japan. The selection criteria were as follows; maximum acceleration to be more than 500 Gal and seismic waves that have been observed in the high rigidity ground with V_s=2000m/s or more.

As a result, the ground motion observed in Ojika in the Miyagi Prefecture during 2011 off the Pacific coast of Tohoku Earthquake was selected. Response spectrum of the selected ground motion is shown in Figure 1. In order to perform a conservative analysis, the input ground motion was set to be 1.5 times the velocity amplitude of the original waveform.

ANALYSIS CONDITIONS

In this study, long term post-closure state of the engineered barrier, in particular a state that the buffer material was saturated with the groundwater, while the corrosion expansion of the overpack did not occur, was targeted.

An assumed soft rock ground model consists of sandstone (0m bgl to 300m bgl), mudstone (300m bgl to 700m bgl) and sandstone (700m bgl to 1200m bgl) was simulated.

Host rock, buffer, overpack and waste were modelled in the analysis. The waste was modelled using elastic and other materials with the elastoplastic constitutive laws. Elastaplastic constitutive laws were selected as Von Mises for the overpack and Drucker – Prager model for the host rock. The subloading model proposed by Hashihiguchi et. al. (1998), which is an elastoplastic model depending on cyclic loading, was utilised for buffer material. In Figure 2, relationship between subloading surface and normal-yield surface of subloading model is shown in p'-q plane. Material properties used in the analysis were set according to H12 Project to Establish Technical Basis for HLW Disposal

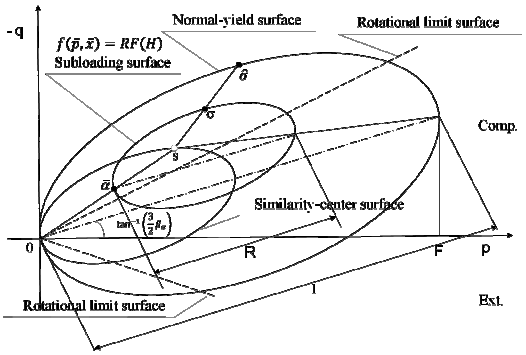


Figure 2 Normal-yield and subloading surface with a rotational hardening illustrated in the axisymmetric stress state in the (p,q)plane.(Hashiguchi, 1998)

in Japan (JNC, 1999). For buffer material, cyclic shear stress ratio and number of repetitions of undrained cyclic shear test history for cohesive soil were set as reproducible parameters.

RESULTS OF ANALYSIS

A comparison of the horizontal displacement time history of host rock, buffer and waste at the same depth determined by the analysis, is given in Figure 3. This comparison showed that the amount of displacement and the phase were consistent for each material, resulting in the surrounding rock and the engineered barrier vibrating as a unit during an earthquake.

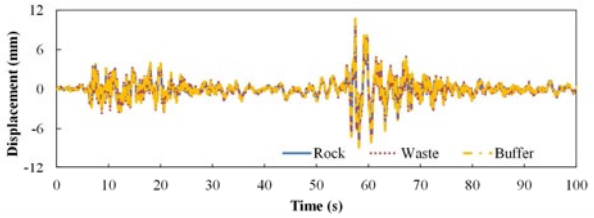
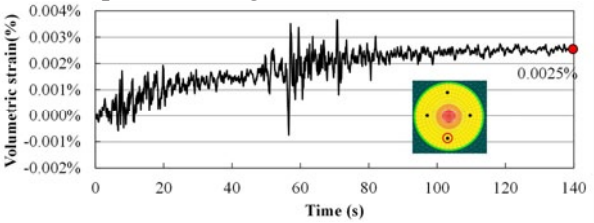
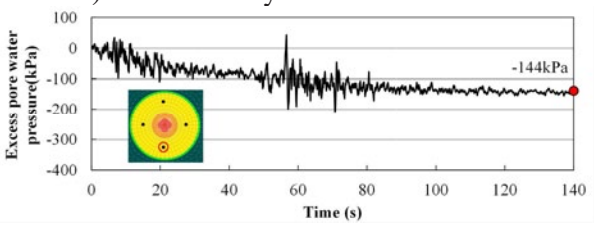


Figure 3 Time history of Horizontal displacement compare with engineered barrier and rock

The volumetric strain and the excess pore water pressure time history responses of the buffer were shown in Figure 4. During vibration, volumetric strain gradually accumulated to the volume expansion side until reaching a residual state; meanwhile negative pore water pressure was developed in a similar manner. The generation of the negative pore water pressure, acts in the direction of increasing the reaction stress of soil skeleton, hence the presence of pore water will result in a strength increase. In other words, when the buffer material is saturated, it will be in a state that a decrease in the effective stress is difficult to occur as a result of a ground motion due to the interaction of soil skeleton and the pore water. Therefore, it is important to treat the seismic analysis of the engineered barrier as a two-phase problem.



a) Time histroy of volumetric strain



b) Time history of excess pore water pressure

Figure 4 Time history of buffer material

Effective stress path in the bottom centre of the buffer material is given in Figure 5. The value in parentheses represents the percentage of maximum effective stress ratio during ground motion for a limit state stress ratio of M = 0.63. Even the maximum value was observed to be less than 10% of the limit state stress ratio, hence it can be concluded that the buffer material that formed the engineered barrier was robust enough to withstand the ground motion.

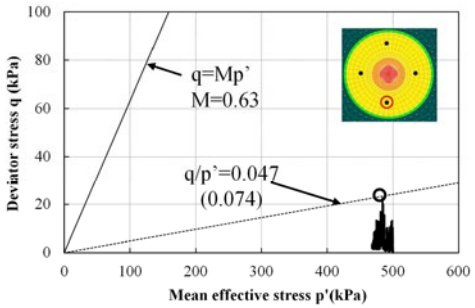


Figure 5 Effective stress path of buffer

On the earthquake-resistance of overpack, the occurred stress was observed to be 1/164 of the yield stress, hence showing that the overpack was also robust enough.

CONCLUSIONS

In this study, a seismic stability analysis of an engineered barrier was performed by utilising the ground motion that has been observed in the 2011 off the Pacific coast of Tohoku Earthquake. Depending on the analysis results, it is concluded that the engineered barrier vibrated as a unit with surrounding rock and it is robust enough that occurrence of the stress fracture was not observed. From the above results, it was confirmed that a decrease in the mechanical stability of the engineered barrier due to ground motion is unlikely.

References :

K.Hashiguchi and Z. –P. Chen(1998) : Elastoplastic constitutive equation of soils with the subloading surface and the rotational hardening, International journal for numerical and analytical methods in geomechanics, vol. 22, 197-227

JNC (1999) : H12 Project to Establish Technical Basis for HLW Disposal in Japan

SEALEX In-Situ Experiments-Performance Tests Of Repository Seals: Experimental observations and modelling

N. Mokni, **and J-D. Barnichon**

Institute for Radiation Protection and Nuclear Safety, IRSN, France.

The SEALEX project was built with specific focus on long-term hydraulic performance of sealing systems as part of the overall IRSN R&D program that provides the bases for scientific expertise on disposal safety. SEALEX is dedicated to *(i)* test the long-term hydraulic performance of sealing systems in normal conditions for different core compositions (pure MX80 or sand/MX80 mixtures) and conditionings (pre-compacted blocks or in-situ compacted), *(ii)* quantify the impact of intra core geometry (construction joints) on the hydraulic properties of sealing systems, and *(iii)* quantify the effect of altered conditions (decrease of the swelling pressure caused by the failure of the concrete confining plugs) on the performance of the sealing system. The SEALEX experiments are emplaced in the Tournemire Underground Research Laboratory (Toarcian argillites) via horizontal boreholes (diameter 60 cm) excavated from recent drift (2008). Each experiment (Figure 1) consists of a bentonite based core mechanically confined at both ends, which represents a generic seal mock-up except for the artificial saturation system (porous filters located at both core ends) (Barnichon et *al.*, 2011). A number of materials are being considered as seals; the current work focuses on clay cores built of pre-compacted disks composed of bentonite/sand mixture. In such layout, an annular technological void exists between the clay core disks and the surrounding host-rock. This gap with variable thickness is technically needed to facilitate the emplacement of the clay core into the borehole. This paper examines the coupled hydromechanical behaviour of the first SEALEX in-situ test (PT-N1). The clay seal of test PT-N1 is made of 8 monolithic pre-compacted disks of 70/30 MX80 bentonite/sand mixture with an initial dry density of 1.97 Mg/m^3 and initial water content around 11%. The annular technological void is estimated to 14% (volume of void/volume of borehole). A coupled analysis has been performed using a 3-D model that includes the clay core, the air-filled gap with variable thickness and the surrounding host-rock. The numerical analysis has been carried out using

the finite element code CODE_BRIGHT (Olivella et al., 1996). A key feature in the simulation lies in the appropriate modeling of the bentonite-sand mixture hydro-mechanical behavior. A fundamental property of this material is the multimodal nature its porous network which influences its hydraulic and mechanical properties. The double structure model proposed by Gens et *al*. (2011) is used to analyse the coupled HM behaviour of the heterogeneous mixture. The modeling results are compared to the field observations. The models predict reasonably well the evolution of liquid saturation and axial swelling pressure at different points of the clay core. Differences are observed between the model predictions and the measurements in terms of radial swelling pressures evolution, related to the non-uniformity of the initial air-gap in the SEALEX experiment.

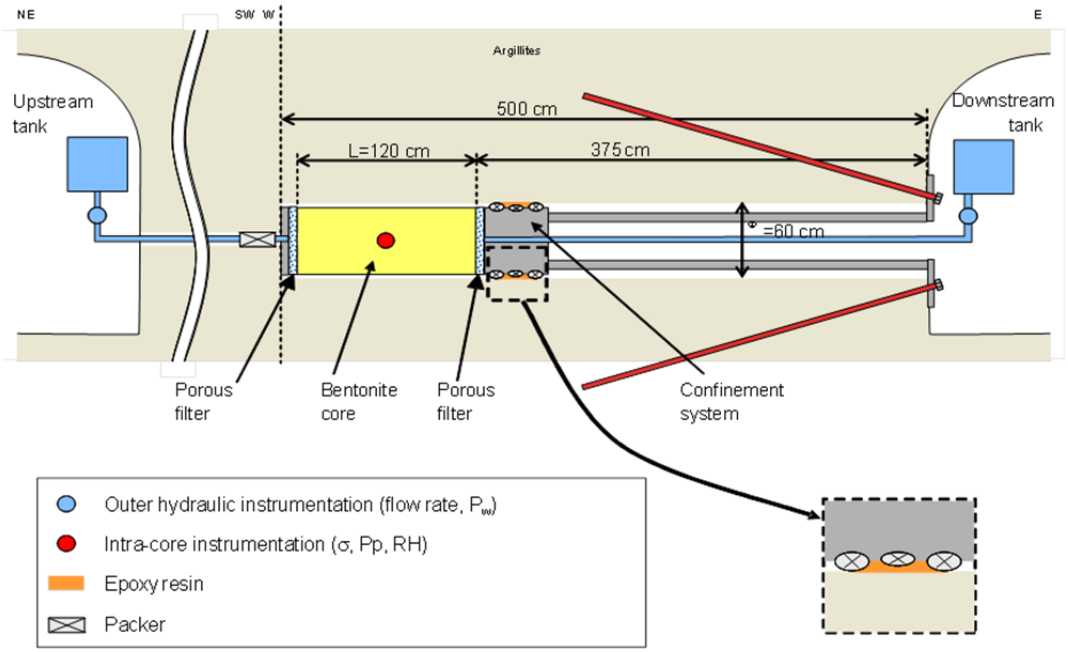


Figure 1. Layout of SEALEX in-situ tests

References

Barnichon J.D., & Dick P., &Bauer C. (2011). The SEALEX in situ experiments: Performance tests of repository seals. In: Harmonising Rock Engineering and the Environment – Qian & Zhou (eds) © 2012 Taylor & Francis Group, London, ISBN 978-0-415-80444-8, pp. 1391-1394.

Olivella S., Gens A., Carrera J, and Alonso EE. (1996). Numerical formulation for a simulator (CODE_BRIGHT) for the coupled analysis of saline media. Engineering Computations 13 (7), 87-112

Gens A., Valleján B., Sanchez M., Imbert C., Villar M.V., and Van Geet M.(2011).Hydromechanical behavior of a heterogeneous compacted soil :experimental observations and modelling. Géotechnique 61, No. 5, 367-386.

Disposal facility for solid low and intermediate level radioactive waste (LILW) intended to be constructed in clay deposits

A. Barinov, A. Tkachenko, S. Speshilov.

Russia, Moscow, The Federal State Unitary Enterprise "National Operator for Radioactive waste management" (FSUE "NO RWM")

It is planned to construct disposal facility for final placement of low and intermediate level radioactive waste (LILW) at the depth about one hundred meters without an intention of the waste retrieval and ensure radiation safety for workers, the public and the environment for a period of potential hazard of disposed radioactive waste .

In accordance with the universally accepted concept of radioactive waste management the countries with nuclear power facilities should develop disposal facilities for conditioned radioactive waste.

It is internationally recognized that the final solution for the newly formed and accumulated low and intermediate level radioactive waste is to placed them conditioned for the entire period of their potential hazard in the near-surface disposal facilities equipped with engineering barriers system at the depth of 30-100 m in appropriate geological conditions.

Only radioactive waste corresponding with the acceptance criteria established for disposal facilities are accepted for disposal.

RW packages reception for disposal in near-surface disposal facilities type is carried out on the basis of the following criteria:

- radioactive waste acceptance criteria;
- radiation parameters;
- physico-chemical characteristics of the waste form;
- chemical waste form;
- radioactive waste packages (containers) acceptance criteria.

There was developed non-return protective container made of composite materials on the basis of reinforced concrete for long-term storage and radioactive waste disposal. The container is designed for four drums volume of 0.2 m^3 each, or 1.5 m^3 of solid or solidified intermediate level radioactive waste placement. The container is designed taking into account the regulatory requirements for stages of long-term storage, transportation and disposal.

In the designed containers there was used concrete with a density of $2{,}4\times10^3$ kg/m^3 as a structural material. With a wall thickness of 150 mm the dose rate at the surface is 2.0 mSv/h at a distance of 1 m - 0.1 mSv/h, which ensures the safety of the staff without the use of remote schemes for waste disposal from the activity of up to 10^7 Bq/kg, which corresponds to the upper boundary of intermediate level radioactive waste containing beta-emitting radionuclides (except tritium) and alpha-emitting nuclides (including transuranic).

The site is complicated because of thickness of Paleogene and Neogene sediments overlain by Quaternary Formations up to 30 m at an angle of 3-8 °. Paleogene is presented by clay formations, among which is a thick layer of clay Maikop formation. According to the engineering-geological survey of a scale 1: 25,000 Maikop clays are located for many kilometers. Maikop clays are well explored by boreholes and mine workings.

Deposits of Maikop are dark gray clay and dark green clay having a massive visual texture. In fact deposits generally hidden-layered. Clay in the main part is not completely saturated with water, so in the case of water flow through fractures much of it can be fixed with clay, which has swollen (swelling pressure 0,45-1,2 MPa), will close the fractures and prevent further movement of water from surface aquifers . There were explored several structural boreholes with a depth of more than 450 m and exploration-operating mine, including vertical wellbore and horizontal mine working at a depth of 467 m.

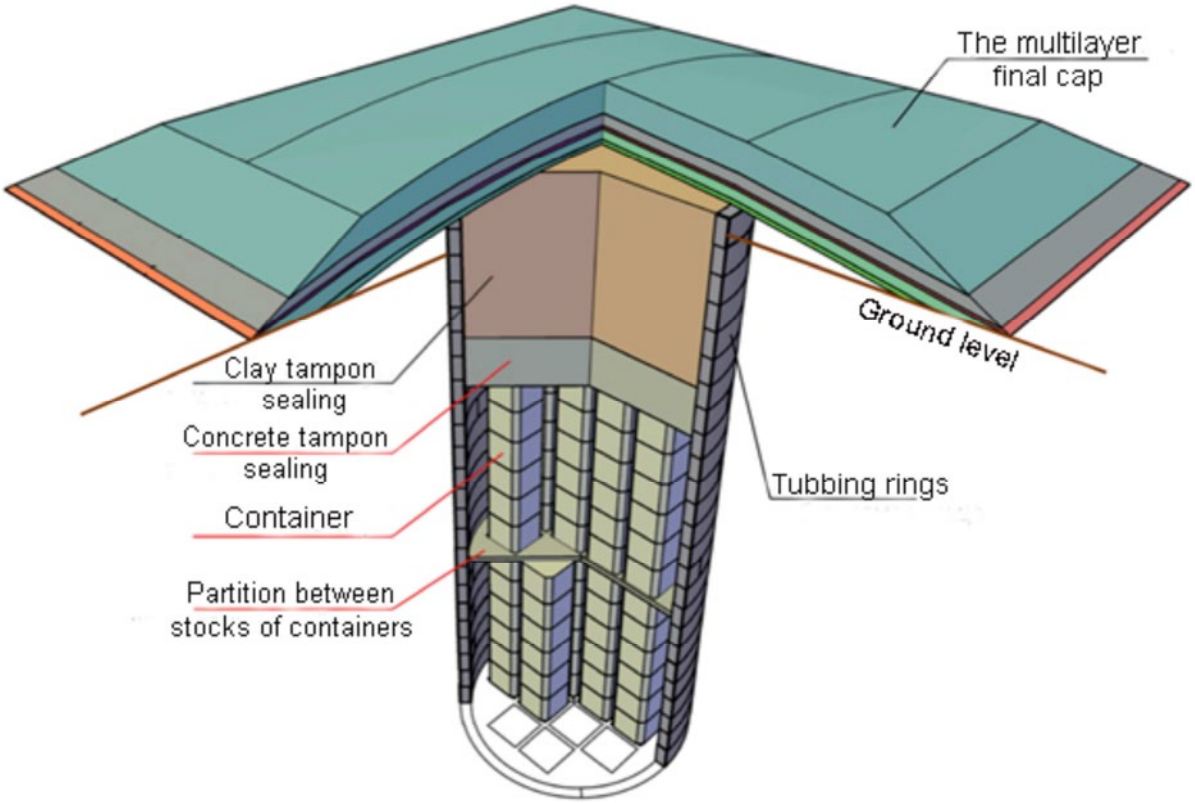


Fig. 1 Conceptual model of borehole type disposal facility

A feature of the Maikop clays is their fine hydromica montmorilonitovy composition and the absence of fractures in natural occurrence. The ability of clay «to heal» fractures in the rock mass due to swelling when wet ensures their high water resistance, the absence of watering and flows in the tectonic fractures, which in combination with good sorption properties and a small diffusion coefficient is a guarantee against the migration of nuclides from disposal.

In addition, the arid climate of the territory is a positive factor, significantly limiting the possibility of migration of contamination in the operational period and after its conservation, preservation of radionuclides during their potential danger.

One of the main exception conditions radionuclide release outside the working volume of disposal facility is to apply the principle of multi-barrier protection, consisting of three main elements:

- Geological environment having low filtration and high sorption properties;
- Created in the construction engineering barriers, having comparable with the terms of the potential danger of short-lived radionuclides lifetimes;
- Package of radioactive waste ensuring radiation safety.

DOPAS EPSP experiment

Jiří Svoboda[1], Jaroslav Pacovský[1], Markéta Dvořáková[2], Irena Hanusová[2], Petr Večerník[3], Dagmar Trpkošová[3]

[1] Czech Technical University in Prague, Centre of Experimental Geotechnics, Thákurova 7, Prague, Czech Republic; svobodaj@fsv.cvut.cz
[2] SÚRAO, Dlážděná 6, Prague, Czech Republic
[3] ÚJV Řež, a. s.; Hlavní 130; 250 68 Husinec - Řež; Czech Republic

The international DOPAS project (Demonstration of Plugs and Seals), which involves the participation of 14 European organisations (Posiva, ANDRA, DBE-TEC, GRS, Nagra, RWA, SÚRAO, SKB, CTU, NRG, GSL, BTECH, VTT, ÚJV Řež), is concerned with the structural solution for sealing plugs to be used in deep geological radioactive waste repositories. The project is funded by the 7th framework programme – EURATOM. The Czech contribution to the DOPAS project (the EPSP experiment – Experimental Pressure and Sealing Plug) consists of an experiment which is being conducted at the Josef Regional Underground Research Centre (Josef URC, Čelina-Mokrsko). The aims of the EPSP experiment are to develop, monitor and verify the functionality of such plug and to determine a detailed characterisation of the materials from which the plug is constructed. The EPSP experiment is being conducted by a Czech consortium made up of SÚRAO, CTU and ÚJV Řež, a. s. The technical design of the plug was the responsibility of the Centre of Experimental Geotechnics of the Czech Technical University (CTU), Prague and was based on a structural proposal contained in Reference Design 2011.

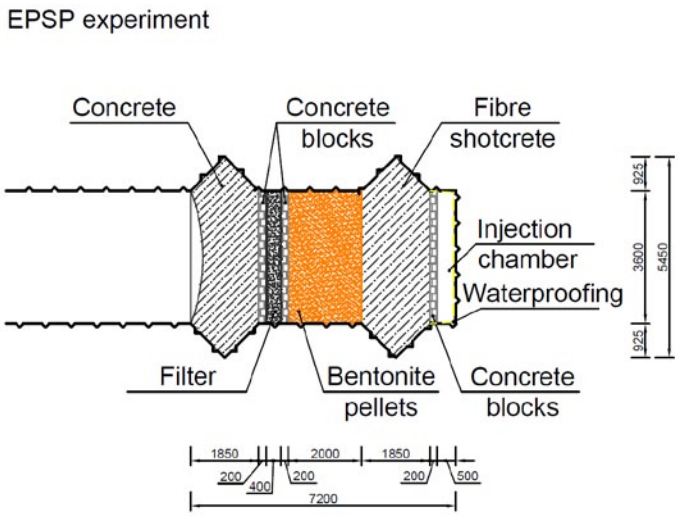


Fig. 1 - The EPSP cross section

The EPSP plug has the following main components: a pressurisation chamber, the inner glass fibre-reinforced shotcrete plug, bentonite sealing material, a filter, an external concrete plug and the host rock environment. The experiment also comprises a number of auxiliary structures such as porous concrete walls, an extensive monitoring system and service centre.
The pressurising media will consist of air, water and a bentonite suspension. The pressurising medium will be transported to the pressurisation chamber via 23m-long connecting boreholes from the neighbouring service centre niche. The chamber is enclosed by a porous concrete wall which will during the construction serve as support to the one of the main elements of the EPSP – the inner glass fibre-reinforced concrete plug.

The inner plug makes up one of the key components of the experiment and verifying that it works efficiently makes up one of the main objectives of the project. It has two basic functions: static and hydraulic which means primarily that it must ensure the mechanical stability of the entire system even under high pressure conditions and, at the same time, must restrict flow through the plug so that the bentonite sealing is not damaged through the creation of an erosion channel in the period in which the bentonite sealing zone is undergoing, but has not yet reached, full saturation.
A further major component of the EPSP is the bentonite sealant, the purpose of which is to hydraulically separate/seal the experimental the plug. Owing to its exceptional swelling properties (and consequent self-healing capacity) and very low permeability, bentonite is particularly suitable for fulfilling this function. However, its sealing properties depend, in addition to its mineralogical composition, principally on its density. Therefore, in order to achieve the required density level, bentonite will be used in the form of highly-compressed pellets. The EPSP experiment also includes the testing of bentonite installation technology, for example the use of the shot clay method.
The filter has been designed principally for the monitoring of seepage through the plug. Nevertheless, it is connected through the afore-mentioned boreholes to the service centre niche and can be used, if required, as an alternative pressurising chamber. The design of the experiment even provides for alternative testing scenarios in which the filter can be used as the pressurising chamber enabling the forced saturation of the bentonite sealant, the testing of reverse flow (first by bentonite then by the inner concrete plug) and the testing of the outer concrete plug.
The EPSP is enclosed by an outer concrete plug and the function of which is to mechanically stabilise the entire block.
The EPSP experiment run is divided into 4 stages. The first stage primarily concerned the laboratory verification of the suitability of the materials to be used for plug construction, namely bentonite and a concrete mixture, the quality and detailed characteristics of which received particular attention during work on the design of the plug. Part of this research are laboratory scale physical models which were constructed at ÚJV Řež's laboratories. Two type of models were constructed. The objective of the first one was to obtain data to be used for the calibration of numerical models of the saturation of bentonite. The second type is focused on laboratory simulation of the interection processes in materials, mainly on the concrete-bentonite interface which occur in demonstration plug
The second stage of EPSP consisted of the construction of the in-situ experiment which commenced in 2013 with grouting and drilling work in the experimental gallery niche. This was followed by the construction of the plug itself, including the full instrumentation of the experiment and its immediate surroundings.
The third stage consists of pressurisation by saturation media (air, water and a bentonite suspension) during which the plug will be exposed to pressure of up to 7MPa. The experiment and the technology employed will be monitored constantly throughout this period of the experiment.
The final stage of the experiment will concentrate on the evaluation of the data and knowledge obtained from both the in-situ and laboratory experiments using numerical analysis techniques and modelling. The final output will consist of the verification of the operational safety of the various structural elements of plugs to be used in DGRs and detailed recommendations for the future design and construction of such plugs.

The research is being funded from the European Union European Atomic Energy Community (Euratom) Seventh Framework Programme FP7 (2007-2013) according to grant agreement no. 323273, the DOPAS project. The project is also supported by the Czech Republic via funding provided by the Ministry of Education, Youth and Sports – institutional support grant no. 7G13002.

Inflow handling during the emplacement of the backfill in the KBS-3 concept

Ville Koskinen[1], Torbjörn Sandén[2]
1. Fortum Power and Heat Oy, Espoo, POB 100, FI-00048 Fortum, Finland
2. Clay Technology AB, IDEON research center, S-22370, Lund, Sweden

The conclusions and the viewpoints presented in the abstract are those of the authors and do not necessarily coincide with those of SKB and Posiva

ABSTRACT

The work described in this abstract has been done on behalf of SKB and Posiva.
This paper describes a research project regarding the usage of geotextiles for distribution of inflowing water during the installation of backfill. The objective of the research was to develope a technical method to distribute inflowing water more evenly in the backfill in order to increase the water storing capacity of the outermost bentonite pellet filling. Inflowing water may affect the stability of the backfill installation and also cause erosion of the backfill. The suggested method will decrease the risk for inflowing water to reach the backfill installation front and will thereby increase the flexibility of the backfill installation process. The method is assessed to be suitable for inflow rates between 0.5 to 1 l/min.
The method developed and tested during the project should be functional as long as the deposition tunnel is open. The method's adverse effect on the long term safety of the SNF repository should be minimal. Also other methods than water distribution with geotextiles (for example long steel or glass pipes along the tunnel) were considered, but discarded based on the potentially adverse effects on the long term safety.
The test-program was divided into three parts:

1. Laboratory scale test
2. ½-scale steel tunnel tests
3. Fastening tests at the Loviisa L/ILW repository

The purpose of the laboratory scale tests was to verify the potential of the geotextile fabrics in distributing the inflowing water between the rock and the bentonite pellets. Three different types of geotextile fabrics were tested. In the laboratory scale the rock surface was replaced with a Plexiglass tube (diameter 100 mm and length 1 000 mm). The evaluation of the laboratory scale test results was done based on evolution of the inflow water pressure and on visual differences between tests.
According to the results, geotextiles seemed to provide significant advantages for the water distribution capabilities of the bentonite pellet front. No major differences between different types of geotextiles were observed in the laboratory scale.
Based on the laboratory scale tests, a typical polypropylene geotextile was used in the ½-scale steel tunnel tests, since it was easily available. However, a polypropylene geotextile is not a preferred type of geotextile to be used in the deposition tunnels due to the potentially adverse long term safety effects because of its organic content.
Three separate tests were done in a ½-scale steel tunnel:

- Reference test 0.25 l/min pointwise inflow, without geotextile.
- The first test with geotextile 0.25 l/min pointwise inflow.
- The second test with geotextile 0.5 l/min pointwise inflow.

Compared to the reference test, the geotextile seems to function well. The differences can be seen in Table 1. Due to practical reasons related to the installation, some changes (fine particles were sieved

out of the pellets, and the geotextile was moved 20cm backwards) were made to the test setup for the last test, and therefore the results are not fully comparable with the other tests.

Table 1. *Results from the ½-scale steel tunnel tests*

Test, no.	Geotextile	Inflow rate [l/min]	Time to first outflow, [h]	Water stored before outflow, liters	Amount of available void space used before outflow, %
Reference test	no	0.25	30.4	460	18.4
The first test	yes	0.25	39.5	588	23.5
The second test	yes	0.5	53.3	1600	64.0

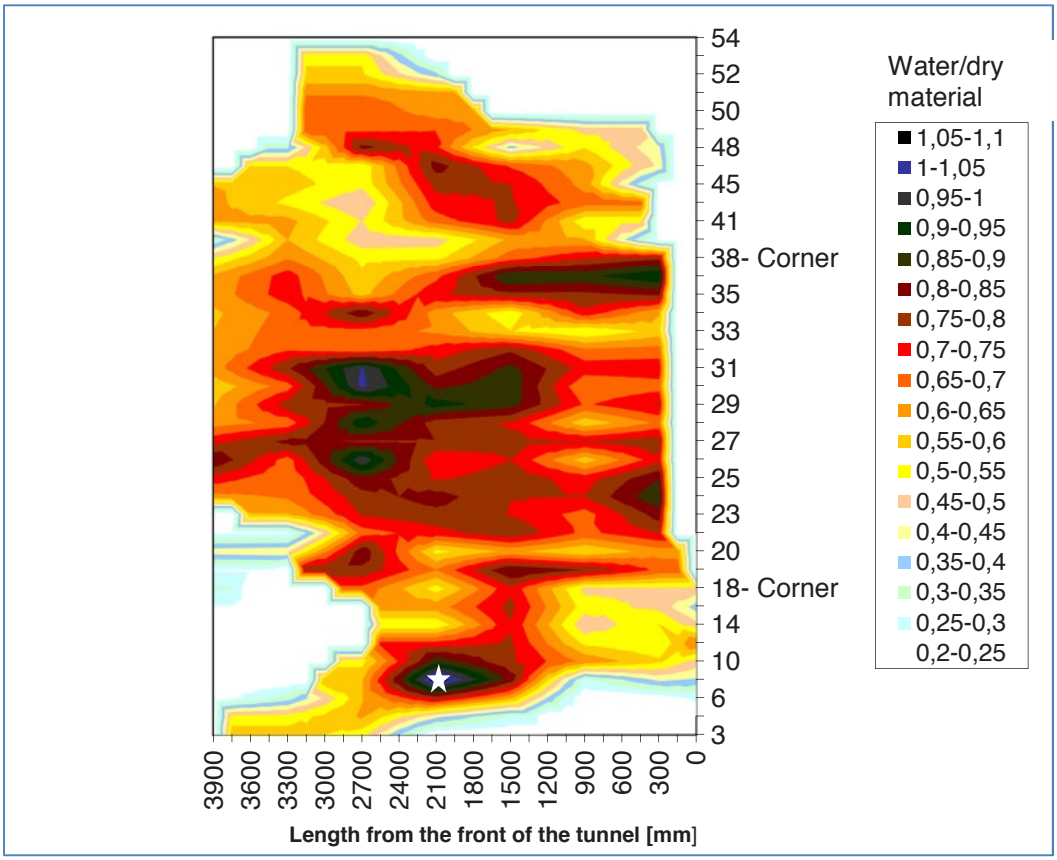


Figure 1. *Wetting pattern of the pellet filling in the second test. The picture shows a top view of the roof with the left tunnel side downwards. The star marks the place of the inflow point.*

Fastening onto rock wall was tested independently from the laboratory scale and ½-scale steel tunnel tests. Fastening tests were done at Loviisa NPP's L/ILW repository in order to mimic the real SNF-repository conditions. The tested methods for fastening were express nails, two different types of glues and concrete. Out of those three, the most promising method was the fastening with express nails, although it still needs detailed specifications.
During 2014-2016 there will be a new SKB-Posiva joint research project continuing the water handling method development. Focus will be on the development of new methods to handle larger inflow rates, but some additional testing with geotextiles is likely to be done.

Refernces:
Koskinen V., Sandén T., System Design of Backfill. Distribution of inflowing water by using geotextile. SKB R-14-10 (in preparation)

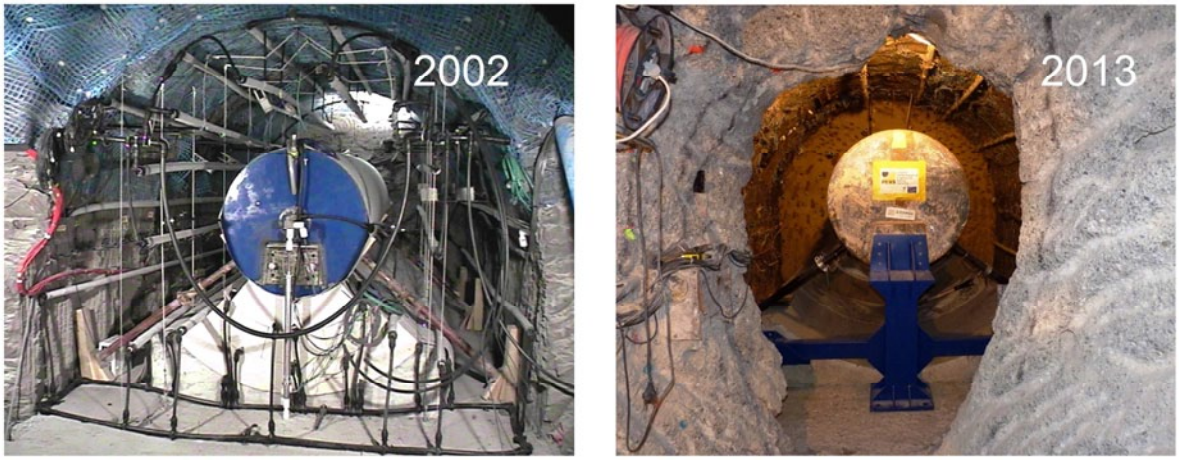
EB Experiment: from design to dismantling

Authors: María Rey Mazón[1], *José Luis García-Siñeriz[1], Beatriz Palacios[1] and Juan Carlos Mayor[2]*
[1] AITEMIN Asociación para la Investigación y Desarrollo Industrial de los Recursos Naturales. c/ Margarita Salas, 14, E-28916 Leganés (Madrid), SPAIN;
[2] ENRESA Empresa Nacional de Residuos Radioactivos, S.A. Emilio Vargas, 7, E-28043 Madrid, SPAIN

The "EB Experiment" aimed the "in situ" demonstration of a new emplacement technique for HLW canisters in horizontal drifts excavated in consolidated clay formations, by using highly compacted bentonite blocks to support the canister and granular mix as backfill material (granular buffer material, GBM) to filling-in the remaining volume of the drift. This full-scale test was carried out in a drift specially excavated in the Opalinus clay formation at the Mont Terri underground laboratory: A dummy canister –with the same dimensions and weight as the reference HLW canister– was placed on top of a pedestal of bentonite blocks which lay over a concrete bed. The remaining volume of the drift was backfilled with a granular material made from bentonite pellets. The drift was sealed with a concrete plug, and the evolution of the different Hydro-Mechanical parameters, both in the barrier and the rock (especially in the EDZ), was monitored. Due to the short amount of free water available in this formation, an artificial hydration system was installed to accelerate the hydration process in the backfill.

To asses that this backfilling technique is feasible, it had to be first demonstrated that the final values of the key parameters of the clay buffer that may be achieved with this method, such as dry density, swelling pressure and permeability are suitable within the limits considered in the Performance Analysis of the repository concept, and this was precisely the objective of the EB experiment.

After almost 12 years of the experiment running, and having the evidence that the buffer was fully saturated, the experiment was dismantled to assess the real status of the GBM used: degree of saturation, permeability, density, aspect, homogeneity, etc. It was also important to check the status of the bentonite blocks that support the canister, the rock in contact with the buffer with especial interest in the EDZ, and the degree of saturation of the concrete in the vicinity of the buffer (plug and blocks support). Therefore, the activities of the dismantling were coordinated with a sampling program intended to analyse the parameters of interest in the laboratories of the different involved organizations as well as on site.



From installation to dismantling

Design and installation phases: The 15 m long EB niche (9 m of service area and the 6 m long test section) was excavated in April to June 2001. A road header was used for the test section, to obtain a smooth surface (profile tolerance of ±5 cm). Following, "in situ" geophysical and hydraulic measurements were performed, to characterize the EDZ. From these field surveys, it was concluded that the EDZ reaches a depth of about 0.7 m in the roof of the test section, while at the sidewalls it only extends to 0.1 m depth. The instrumentation to monitor the rock and barrier behaviour during the hydration: 16 hygrometers, 20 piezometers, 8 pressure cells, 7 extensometers, seismic sensors and electrode chains was installed from end 2001 to mid 2002, as well as the concrete bed; the bed of bentonite blocks (3 layers) and the artificial hydration system (tubing and geotextile mats). Finally, the GBM was emplaced. The hydration of the buffer started in May 2002.

Monitoring phase: The monitoring of all parameters was carried on from May 2002 to January 2013.

Dismantling and sampling operation: The operation started in the last semester of 2012 with the partial dismantling of the concrete plug, followed by the sampling and bentonite removal (GBM and blocks), which were coordinated in order to reach even sections and to alter as minimum as possible the sampling areas. The dismantling operation ended with the removal of the Data Acquisition System (DAS): the monitoring of the test was kept running during the whole dismantling process.

Almost 500 samples were taken; around 210 of them were analysed on site and the rest were packed and sent to the different partners´ laboratories. Two main parameters were determined on site: water content and dry density.

The aim of the proposed paper is to synthesise the main facts of the experiment, including design, installation, monitoring, dismantling and sampling operations as well as to record the most relevant outcome in relation with the HLW underground storage concepts.

Numerical Modelling of 6 Years Natural Saturation of a Full-Scale Shaft Seal in Granite (2009-2014)

D.G. Priyanto[1], D.A. Dixon[2], P. Korkeakoski[3] and R. Farhoud[4]

[1] Corresponding Author, Atomic Energy of Canada Limited, Pinawa, Canada (priyantd@aecl.ca)

[2] Golder Associates Limited, Winnipeg, Canada (david_dixon@golder.com)

[3] Posiva Oy, Olkiluoto, Finland (petri.korkeakoski@posiva.fi)

[4] Agence Nationale pour la gestion des Dechets Radioactifs, ANDRA, Paris (Radwan.FARHOUD@andra.fr)

ABSTRACT

A full-scale shaft seal was installed at the intersection of the 5-m-diameter access shaft of the Atomic Energy of Canada Limited (AECL)'s Underground Research Laboratory (URL) with a major, moderately dipping fracture zone (FZ) located at approximately 273 m depth below the surface. The shaft seal consists of a 6-m-thick clay component that was sandwiched between 3-m-thick upper and lower concrete components. The clay component was an in situ compacted 40/60 (dry mass) mixture of bentonite clay and quartz/feldspar sand with dry density of approximately1.87 Mg/m^3 and designed to provide the hydraulic sealing function. The concrete components were designed to provide mechanical confinement and have no hydraulic isolation role, especially at the concrete-rock interface.

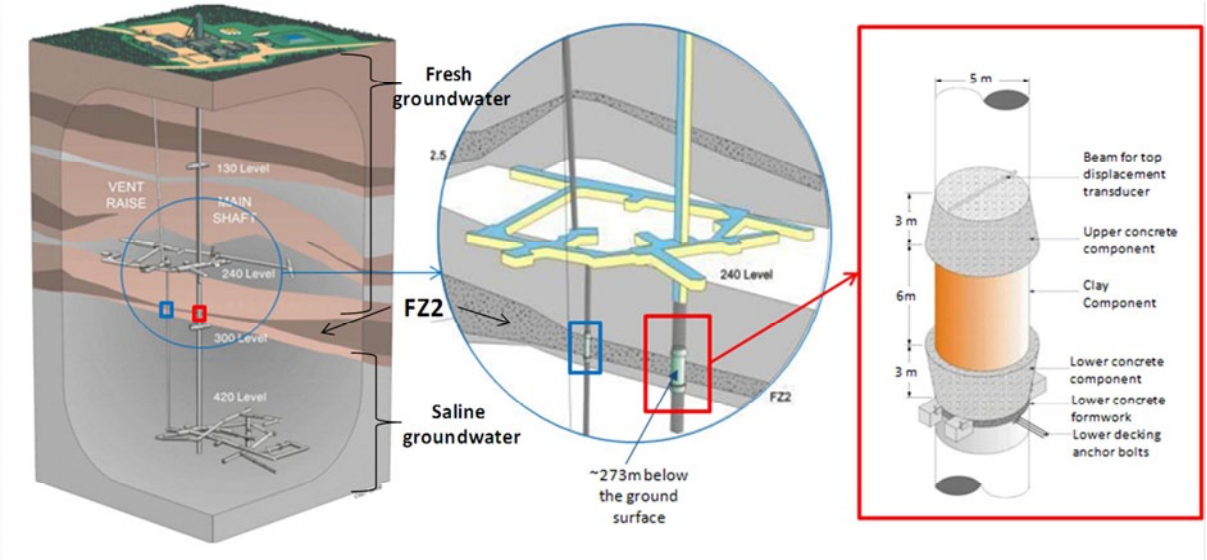


Figure 1. Location and Geometry of the Shaft Seal

Construction of the shaft seal was done as part of Canada's Nuclear Legacy Liability Program (NLLP). The construction of this seal has provided an opportunity to monitor the evolution of a full-scale shaft seal as recovery of the regional groundwater regime occurs. The Enhanced Sealing Project (ESP) was developed by AECL (Canada) and funded by NWMO (Canada), SKB (Sweden), Posiva Oy (Finland) and ANDRA (France) in order to monitor the initial evolution of the shaft seal (2009 to 2013). In the course of the very slow ongoing evolution/saturation of the seal and its surroundings, the

removal of the surface facilities associated with the URL has resulted in evolution of the monitoring system to a stand-alone, lower frequency data collection system. This ongoing monitoring program is now being supported by AECL, ANDRA and Posiva Oy. The current data collection systems continue to supply valuable information on the field-scale evolution and performance of a shaft seal.

Preliminary numerical modelling of the ESP shaft seal was undertaken by Priyanto et al. (2014), but only limited comparison to the field measurements were possible at that time. Comprehensive comparison of the numerical modelling results with the results of ESP monitoring can improve understanding the functionality of the shaft seal. This paper shows the results of 2D-axisymetric geometry models using a finite element code (i.e., COMSOL Multiphysics). They simulate 6-years of natural saturation of the shaft seal. Two different stages were considered in this numerical modelling. The first stage of modelling simulates evolution of the groundwater level in the surrounding rock after 20 years of URL operation, and prior to the seal installation. The second stage uses the final results of the first stage model as the initial condition and simulates 6-years of seal and surrounding host rock evolution after seal installation. The geometry used for the second stage is illustrated in Figure 2. Comparison of the 6-years ESP monitoring and the results of the numerical modelling are used to assess the functionality of the shaft seal.

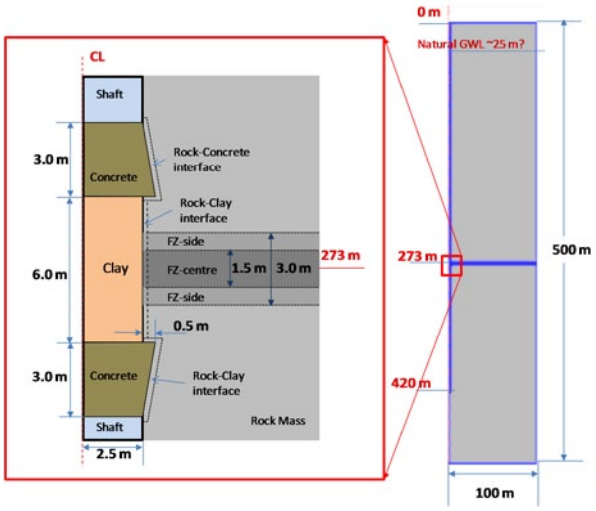


Figure 2. 2D-Axisymmetric Geometry for Numerical Modelling of Shaft Seal

Reference

D.G. Priyanto, D.A. Dixon, C-S.Kim, P. Korkeakoski and J.E. Vilagran. 2014. Preliminary modelling of the saturation of a full-sized clay and concrete shaft seal. From: Norris, S., Bruno, J., Cathelineau, M., Delage, P., Fairhurst, C., Gaucher, E. C., H□hn , E. H., Kalinichev, A., Lalieux, P. & Sellin, P. (eds). Clays in Natural and Engineered Barriers for Radioactive Waste Confinement. Geological Society, London, Special Publications, 400, http://dx.doi.org/10.1144/SP400.38

Geo-scientific Information System Upgrade

M. Gedeon[1], H. De Soete[1], A. Berckmans[2]

1. Belgian Nuclear Research Institute, SCK•CEN, B-2400 Mol, Belgium (mgedeon@sckcen.be)
2. Belgian National Agency for Radioactive Waste and enriched Fissile Material, ONDRAF/NIRAS, B-1210 Brussels Belgium (a.berckmans@nirond.be)

In the framework of the geological disposal of high level radioactive waste, the characterization of the Boom Clay and its environment has been going on for more than 35 years. This research has resulted in a great quantity of data. In order to be able to manage this valuable data properly, a geo-scientific information system was built. The aim was to create a central place where all types of data could be looked up for further analyses and interpretation. The data stored in this system had to be geographically referenced.
The GSIS database was created using PostgreSQL database with PostGIS spatial extension. It offers many modern features: complex queries, foreign keys, triggers, views, transactional integrity and multi-version concurrency control. PostGIS is an extension to the PostgreSQL object-relational database system which allows GIS (Geographic Information Systems) objects to be stored in the database.

The initial GSIS concept, design and use.
The initial structure of the GSIS database splitted the objects with geographic information and data into two separate main tables with a number sub-tables. Consecutive changes to the design requiring inclusion of metadata rendered this structure rather complex. During the use of the database system it became necessary to redesign the GSIS database to allow more flexibility and faster response for the users. Furthermore, the original aim to only store and retrieve data changed towards a more interactive use to allow validation of the data, link interpretations and documents, geographical retrieval of data, a coherent workflow of the management of cores and the integration of results of calculations on real 3D grids instead of the use of 2D points with Z as an auxiliary variabele with accompanying interactive visualisation. This required a major overhaul of the system.

The new design of the GSIS.
The redesign of the GSIS system started in 2012. More flexibility was introduced through merging the object and data into a single table defining their hierarchy and of the use of a metadata master table. The faster response towards the end user was realised by producing a xml output from the database upon a user request, rendered using xslt stylesheets.

The GSIS database has now 2 major parts defined being 'Objects' linked to each other in a hierarchical manner and 'Metadata' which are linked to one or more 'Object(s)'.
'Objects' are devided into 2 sub-groups:

a) Physical objects with defined 2D or 3D geometry
   Examples: galleries, boreholes, cores, sensors, piezometers, ground sample locations, filters, etc.
a) Data linked to the physical objects
   Examples: Analysis, Time series, Geophysical logs

The objects (2) are organised in a hierarchical structure using an adjacency list model with three principal parts:

- the HADES underground research facility data with 3D geometry;
- the regional boreholes (2D geometry) including data bound to the drilling program, such as piezometers, cores and related data.
- the surface objects (2D geometry) including different measurement points located at ground surface (climatic stations, gauges, but also direct push prospection).

Data linked to objects are organised in measurements (time series), analyses (set of measured values) or logs (measurements along a spatial axis).
The metadata linked to the objects represent addition information on objects:

- validation flag (data quality check) and linked projects;
- attached files, images; and a stratigraphic and hydrostratigraphic interpretation;
- spatial grids.

Besides the objects and metadata, GSIS database contains a number of auxiliary tables, mostly with lists of authorized data that can be entered in specific fields of the main tables (e.g. the list of parameters, list of available units, etc.). The existence of lists helps to assure referential integrity of the database and optimal storage of data.

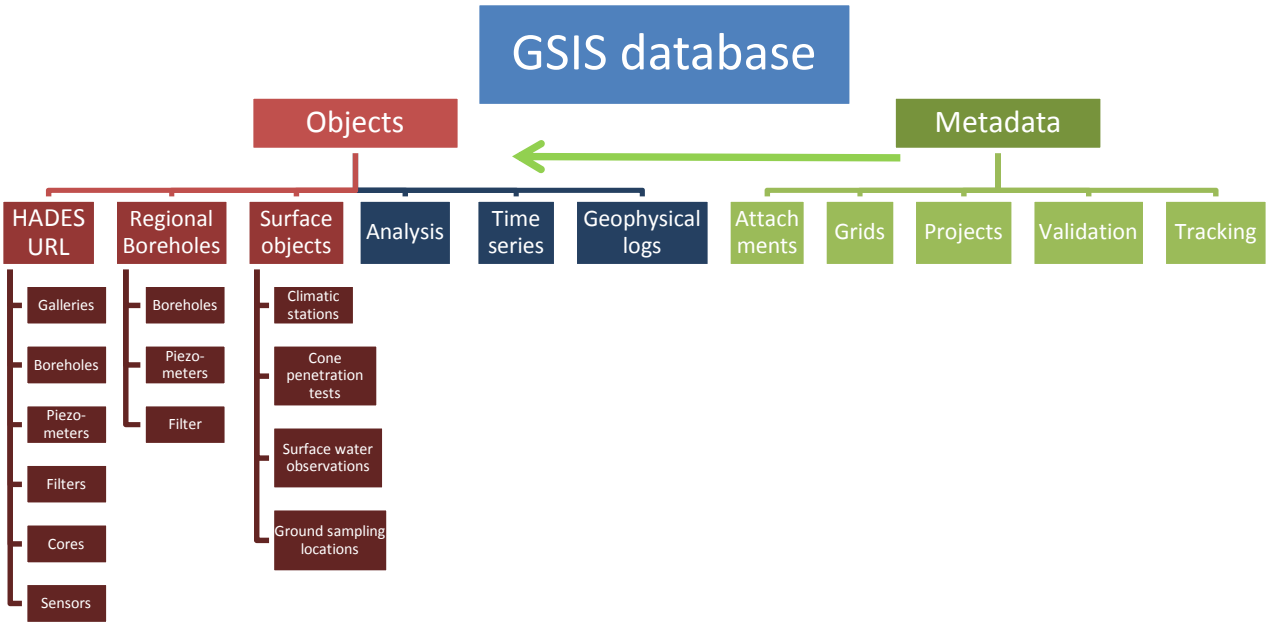


Figure 2: Schematic overview of the main components of the new GSIS database system

The users access the GSIS database system runs via a web-based user interface. This interface allows for lookup of the records using geographical and classical query tools. The selection can be saved and used for further search or export.

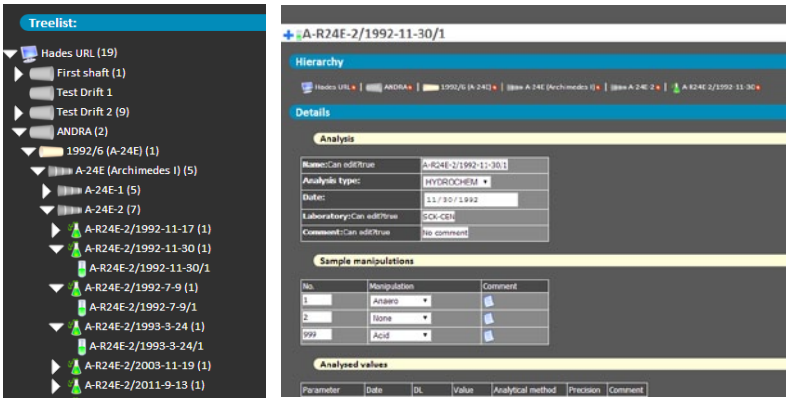


Figure 3: Screen shot showing the web-based user interface to GSIS

This work is performed in close cooperation with, and with the financial support of ONDRAF/NIRAS, the Belgian Agency for Radioactive Waste and Fissile Materials, as part of the programme on geological disposal of high-level/long-lived radioactive waste that is carried out by ONDRAF/NIRAS.

KBS-3H Multi-Purpose test

Xavier Pintado[1], **Jorma Autio**[1], **José Luis García-Siñeriz**[2], **Magnus Kronberg**[3]

[1] B+Tech Oy, Laulukuja 4, 00420 Helsinki, Finland
[2] Aitemin. Madrid, Spain
[3] SKB AB, Oskarshamn, Sweden
Correspondence: xavier.pintado@btech.fi

The Multi Purpose Test (MPT) is an in situ full scale test of the KBS-3H repository system which is currently carried out at Äspö Hard Rock Laboratory in Sweden. It is part of the System Design phase of KBS-3H Project (SKB, 2012) and of the Euratom LucoeX project. KBS-3H project is led by SKB in Sweden and Posiva in Finland. The main objective of the MPT is to demonstrate the manufacturing, transport and handling of the full scale KBS-3H components. Additional objective is to follow the behaviour of engineered barrier system after installation, and the test is therefore instrumented with 220 THM sensors. In addition to using conventional wired data acquisition system, a novel wireless system developed by AITEMIN in Spain is used. The MPT test set up is presented in Figure 1. The distance blocks, transitions blocks and filling components show in Figure 1 are made of high density bentonite. The spent fuel canister and adjoining buffer blocks are embedded in a metal Supercontainer and the complete set-up is confined with a metal plug, for additional information see (SKB, 2012).

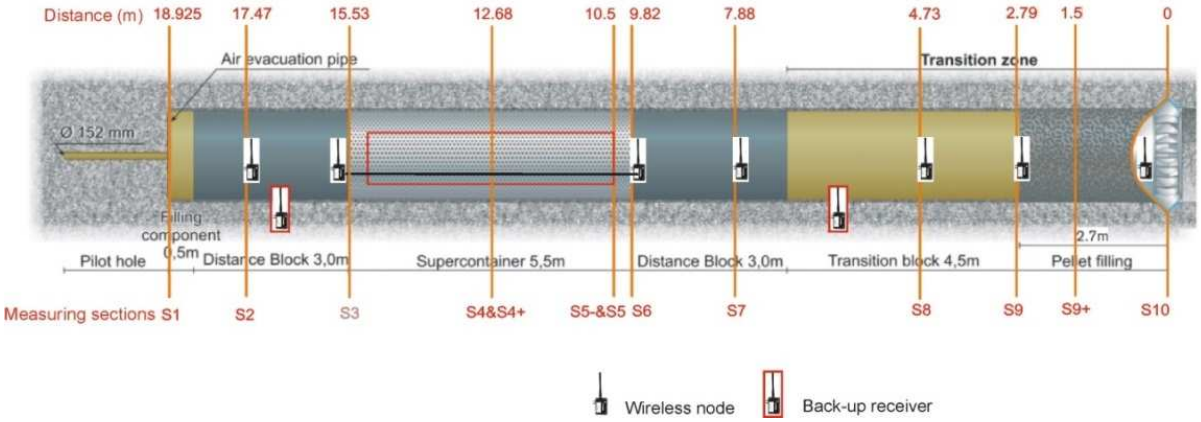


Figure 1. *The MPT test set-up, instrumented sections and positions of the wireless transmitters and redundant receivers which are parts of the wireless data acquisition system.*

Sensors were installed in the distance and transition blocks (Figure 2a), Supercontainer plug and rock. The sensors installed in the distance and transition blocks were piezo-resistive total pressure sensors, capacitive hygrometers for measuring relative humidity evolution in relatively dry conditions, thermocouple psychrometers for measuring suction evolution near saturation conditions, piezo-resistive pore pressure sensors for measuring the positive pressure once the blocks are saturated, frequency domain reflectometers for measuring the volumetric water content and LVDTs and inclinometers for measuring the movements of the blocks and the Supercontainer. Sensors were installed on the metal plug (Figure 2b). The sensors were strain gauges, LVDTs and a flow meter. Sensors were also installed in rock (Figure 2c). The sensors installed in rock were vibrating wire total pressure sensors and hydraulic pressure sensors coupled to multipacker systems for measuring the evolution of the pore pressure in rock. In addition strain gauges were installed on the Supercontainer.

The test started on 7th December 2013 filling the system with water. The water was pressurized to 200 kPa pressure approximately.



Figure 2. *Block with the sensors (a) inside the Supercontainer. Plug instrumentation: LVDTs and strain gauges (b). Total pressure sensors in the rock wall (c).*

The saturation process is followed with different sensors. The evolution of relative humidity and the volumetric water content are presented as example in Figure 3. The sections reference is in Figure 1.

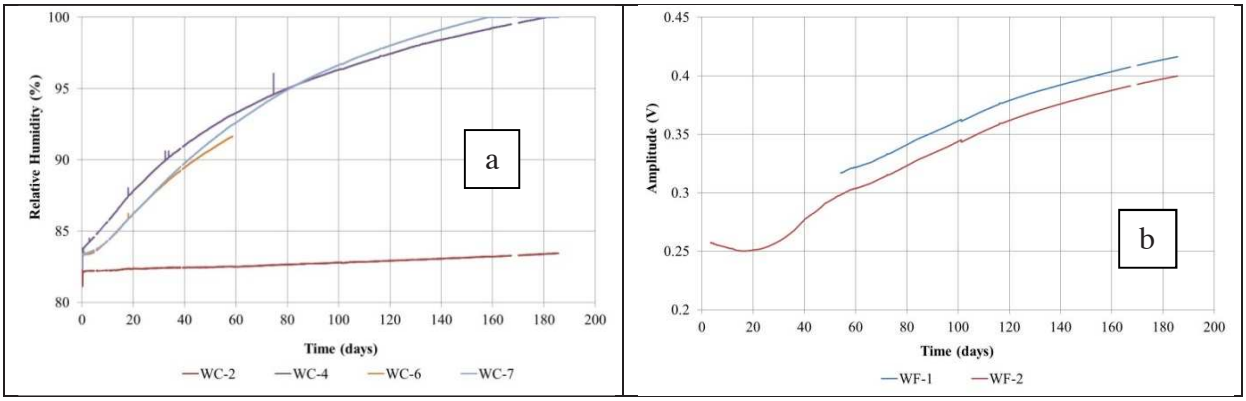


Figure 3. *Relative humidity evolution in section 8 (a). The WC-2 is near the drift axis and the WC.4, WC-5 and WC-6 are near the border of the block. Frequency Domain Reflectometers signal evolution in section 2 (b). The sensors are near the border of the block. The WF-1 is on the bottom and WF-2 on top.*

The evolution of the total pressure in rock is presented in Figure 3a. It is important to discriminate such measure of the evolution of the water pressure in order to calculate the swelling pressure against the rock. The evolution of the strain gauges is presented in Figure 3b. Although the plug has 40 mm thickness, it is possible to measure the effect of the pressure against it.

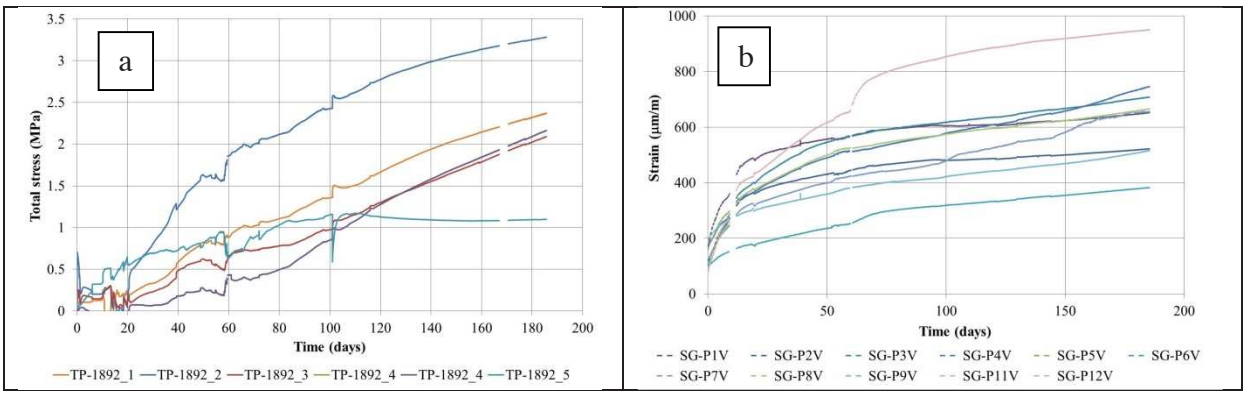


Figure 4. *Total pressure evolution drift front (section 1, see Figure1) (a). Strain gauges evolution in different parts of the plug (b).*

References

SKB (2012). KBS-3H Complementary Studies 2008-2010. SKB TR-12-01. Stockholm. Sweden

DOPAS- Full-Scale Demonstration Of Plugs And Seals

Johanna Hansen

Posiva Oy, Olkiluoto, 27160 Eurajoki, Finland

The DOPAS Full-Scale Demonstration Of Plugs And Seals (DOPAS) project aims to improve the adequacy, consistency and industrial feasibility of the plugs and seals to be used in disposal facilities for radioactive waste across a range of different geological environments. The data and modelling results from five plug and seal full-scale demonstration experiments, laboratory tests and performance assessment studies will be compiled and reported within the project and the knowledge and experience gained will be shared via several dissemination events.
The DOPAS project team, consisting of fourteen beneficiaries from eight European countries, brings forward important demonstration activities in plugging and sealing, which are required ahead of repository construction in order to build confidence in their implementability and performance. These demonstration activities are also a part of each participant's long-term research, development and demonstration (RD&D) programmes and the need for these experiments, and the use of the data generated, have been identified in these RD&D programmes. Only those parts of the activities that are needed for integration of the results and for sharing of the experiences are undertaken within DOPAS. However, the broader aspects of the work are included within published reports from the project. In some cases, the use of results is connected to licensing applications expected to commence soon, or to development of underpinning evidence that will be used for building public confidence and supporting future license applications.
Demonstration experiments which will be partially or wholly implemented during the DOPAS project are a full-scale seal (FSS) implemented on the surface in Saint-Dizier, France, an experimental pressure sealing plug (EPSP) underground in the Josef Gallery in Czech Republic, a deposition tunnel dome plug (DOMPLU) in the Äspö Hard Rock Laboratory in Sweden, a deposition tunnel wedge plug (POPLU) in the underground rock characterisation facility ONKALO (future spent fuel repository) in Finland, and components of a shaft sealing system (ELSA) in Germany.

- Full-scale seal (FSS) by Andra and Nagra is a technological demonstration of swelling clay core construction with low pH concrete containment walls, inside a lined drift model having full-scale dimensions. FSS Experiment includes the construction of the FSS test box (drift model), experiment design, material formulation and laboratory and field characterization of low pH self compacting concrete (SCC) and shotcrete for plugs and bentonite for swelling clay core. Emplacement activities have been performed successfully, despite the unexpected delays to the original schedule.

- Experimental pressure sealing plug (EPSP) by SURAO, CTU and UJV will evaluate the pneumatic emplacement methods for a repository plug for Czech bentonite-based mixtures and low pH concrete developed for repository plug. The material studies and modelling work is progressing and the field work and emplacement actions run simultaneously.

- Deposition tunnel dome plug (DOMPLU) by SKB and Posiva demonstrates the monitoring and pressurising of a deposition tunnel end plug consisting of an arched low-pH concrete dome, a bentonite seal, filter materials and delimiters. In the DOMPLU design many technical challenges have been considered related to the practical implementation of plugs, including issues like the Excavation Damaged Zone (EDZ) in the tunnel; plug -backfill interactions with

pressure conditions at repository depth; and smoothness of surfaces required for controlled concrete fitting. The plug was emplaced in Spring 2013 and currently the pressurisation of the plug is followed by monitoring activities.

- Deposition tunnel wedge plug (POPLU) by Posiva, VTT, BTECH and SKB aims to be the first underground full-scale engineered barrier system (EBS) component construction and demonstration at Posiva's future repository site. Confirming POPLU experiment site location, the design of different parts of the plug with laboratory work and mechanical modelling and plans for monitoring have been the basis for the full scale implementation of POPLU Experiment.

- Shaft seal (ELSA) by DBE TECH and GRS in Germany prepares in-situ demonstration test for shaft sealing components. The work has been initiated with process level modelling activities to increase process understanding. In parallel a couple of laboratory test will be performed which addresses sealing materials planned to be utilised in the shaft seals. The programme aims at providing experimental data needed for the theoretical analysis of the long-term behaviour of MgO and cement based salt concrete in interaction with the host rock and fluids. The data gained will be needed to show the long-term preservation of the required permeability of the seals.

DOPAS Experiments and their status will be presented more detailed in the poster.

The research is being funded from the European Union European Atomic Energy Community (Euratom) Seventh Framework Programme FP7 (2007-2013) according to grant agreement no. 323273, the DOPAS project.

Large-scale sealing experiment in the Meuse/Haute Marne Underground Research Laboratory

Author(s)
de La Vaissière Rémi
Conil Nathalie
Leveau François
Armand Gilles

Andra, Laboratoire Souterrain de Meuse/Haute-Marne, RD960, 55290 Bure, France

During the excavation of a shaft or drift, the rock properties around the underground openings could be altered due to the level of the ratio in situ stresses over strength of the rock. And even in some case, the rock mass could be fractured. One concern regarding waste disposal is that the associated disturbance and damage created in this area around these excavations, called excavation damaged zone (EDZ), might change the favorable properties of such formations and thus negatively impact the repository performance. To limit radionuclides migration along drifts and through the EDZ, seals will be implemented in drifts and shafts. These seals will be composed of swelling clay (mainly bentonite) core in between two concrete plugs. Bentonite is used because in fully saturated state (due to natural hydration from the surrounding rock mass) its hydraulic conductivity is low which avoid radionuclides migration in the access drifts and shaft and , it will swell and apply radial pressure against the drift wall in order to reduce hydraulic conductivity of the EDZ .

In this context, Andra designs and implements a large scale sealing experiment which is called NSC (French acronym for Noyau de SCellement). The main objective is to back analyze the equivalent permeability of the seal in place in order to check the efficiency of such seal. Before to reach this ambitious goal, numerous output will be provided by this experiment on the effect of the hydration of the seal: evolution of the permeability (at the interface seal/claystone and in the surrounding rock mainly the damaged zone), the pressure build up on the concrete plug. In a nuclear waste repository in a claystone like the Callovo Oxfordian (COX), fully saturation of access drift seal will take a long time mainly due the low permeability of the COX(meaning low inflow of water) and the size of the drift (≈10 m in diameter). This duration is not compatible with a reasonable experiment timescale. That implies that properties and geometry of the seal experiment has to be designed to get results over a reasonable timescale and could not be fully representative of the forecast seal. The main ideas are to have an artificial hydration in the bentonite seal itself with geotextile pad, and to select a sand/bentonite mixture, as seal core material, in order to get a not so low hydraulic conductivity of the seal core.

This seal is implemented in a drift of 5 m long and 4.6 m of diameter into a dead-end drift between two concrete plugs. The chosen material is a mixture of Sand/Bentonite (MX80) in proportion 60% and 40% respectively in the form of brick (300 x 200 x 100 mm). With this S/B mixture, the target permeability will be closed to 10^{-11} m/s. The experiment is composed of 4 zones (figure 1): injection chamber (zone 1), seal (zone 2), concrete plug (zone 3) and water thigh drift (zone 4). The injection chamber will be the upstream part during the performance test and the concrete plug will be the downstream part. To avoid leakage between the two faces of the seal, all instruments installed within the S/B sealing (sensors, hydration membranes and surrounding boreholes) must to be wired towards the injection chamber passing through the concrete plug in 2 tubes system that guarantees the test tightness. All the wires pass through 6 “instrumentation” boreholes between injection chamber and NRM niche.

In terms of instrumentations, the monitoring instruments are divided in different cross sections. In the seal and at the interface with the concrete plugs (upstream and downstream), is composed of 319 sensors (humidity sensors: 64 capacitives, 64 psychrometers and 16 FDR; pore pressure sensors: 99; total pressure sensors: 76) and 6 hydration membranes. Between each hydration membrane, the thickness of the S/B seal is 1 m. The maximal distance inside the S/B mixture from hydration membrane is therefore equal to 50 cm. Moreover, 23 boreholes were drilled to monitor pore pressure with multi-packers systems and deformation with extensometers of the rock in the vicinity of the seal. Into the multi-packers boreholes, hydraulic tests will be repeated to see the evolution of the hydraulic conductivity around the seal in respect to the swell of the S/B mixture.

The GES drift was excavated in 2012 and all the instrumentation inside GES drift and S/B mixture was installed during 2013. During the construction of the S/B seal, volume and mass of the S/B mixture was controlled. Those measurements were used to estimate the dry density of clay material in the seal and therefore estimate the swelling pressure. The estimated dry density of clay material and swelling pressure are closed to 1.45 kg/m3 and 2.5 to 6.4 MPa respectively.

The artificial hydration started in January 2014. A sequential hydration of the seal was preferred rather than a simultaneous hydration on all hydration membranes. The hydration membrane at the interface between injection chamber was first flooded with water at constant flowrate and then the others membranes inside the seal was progressively flooded.

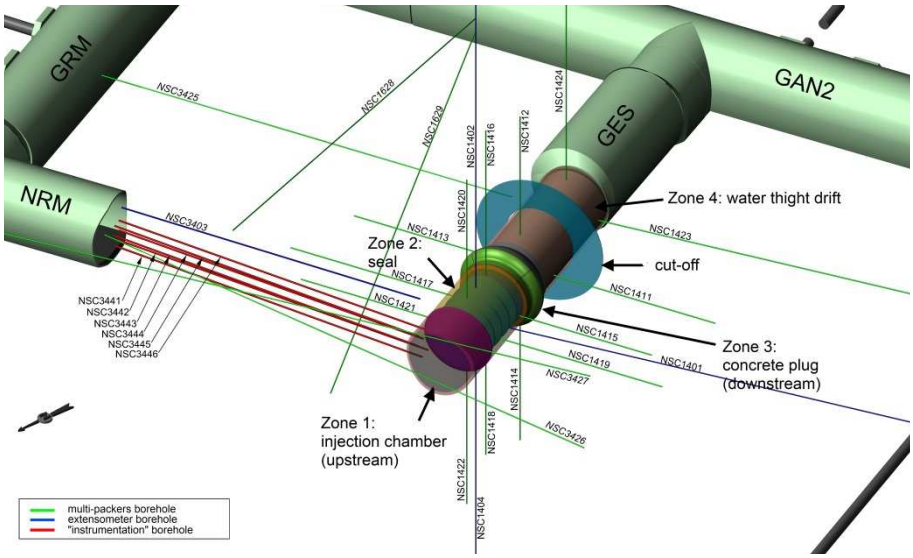


Figure 1 : General layout of the NSC experiment in the Andra's URL

Material characterisation and laboratory models for EPSP experiment in DOPAS project

Petr Večerník[1], **Dagmar Trpkošová**[1], **Jenny Gondolli**[1], **Jiří Svoboda**[2], **Markéta Dvořáková**[3], **Václava Havlová**[1]

[1] ÚJV Řež, a. s.; Hlavní 130; 250 68 Husinec - Řež; Czech Republic; petr.vecernik@ujv.cz
[2] Centre of Experimental Geotechnics; Czech Technical University in Prague; Thákurova 7; Prague; Czech Republic
[3] SÚRAO; Dlážděná 6; Prague; Czech Republic

The Czech contribution to the DOPAS project (Demonstration of Plugs and Seals) has been based on , the EPSP experiment – Experimental Pressure and Sealing Plug. The experiment has being realised at the Josef Regional Underground Research Centre (URC Josef). The objectives of the EPSP experiment are following: to develop, monitor and verify the functionality of constructed experimental plug to determine and describe in detail the materials which are used for experimental plug construction. The EPSP experiment has been prepared namely by SÚRAO and Czech Technical University in Prague, both being supported by ÚJV Řež, a. s. The demonstration plug has three main construction components: inner concrete part, bentonite sealing part, outer concrete part. For EPSP design (see FIG 1) glass fibre shotcrete with low-pH leachate and bentonite pellets were proposed as construction materials. Local Czech materials are used for EPSP construction.

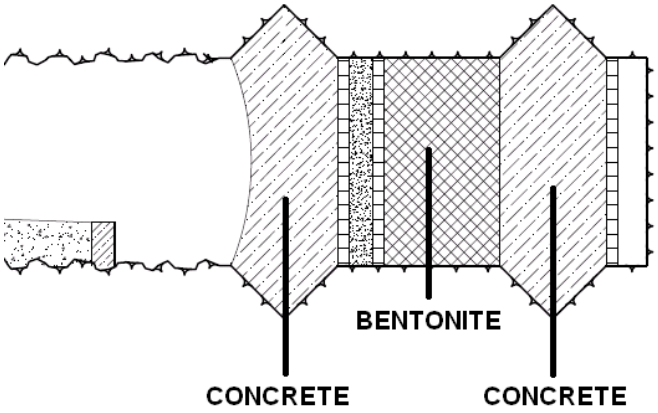


FIG 1: The EPSP construction design.

Materials, used for construction of the plug, has to be characterised prior, during and after the experiments. Moreover, their properties and performance has to be confirm. One of possible way how to do that is to compare the experimental in-situ results with laboratory mid-scale physical models and with mathematical models. The following paper presents an overview of plug performance transfer into laboratory scale.

The bentonite material, labelled as B75_2013, was selected for the EPSP sealing. B75 Bentonite is a Czech Ca-Mg industrially milled and sifted non-activated bentonite, produced by Keramost, Plc. The material was supplied in 2013. The laboratory tests were performed with two forms of bentonite material (powder, pellets) in order to verify their properties. Two types of water (distilled and/ or SGW - synthetic granitic water) were used during the laboratory tests. The distilled water has been used either when required by the standard testing methods or when results comparable to former ones were desirable. Laboratory prepared synthetic granitic water SGW (Havlová et al., 2010), based on a statistical evaluation of Czech granitic massif groundwaters (depths 20-200 meters) had been used in laboratory tests in case that as realistic conditions to the real in-situ experiment as possible are needed. Moreover, large volumes of solution with defined composition are desired to be prepared repeatedly and reproducibly.

The supporting laboratory experiments has been aimed to study chemical and mineralogical composition of the bentonite itself and also to determine leachate composition. The determination of bentonite B75_2013 ion-exchange capacity of was also performed and compared with the results of previous analyses on same type of material (B75_2010).
Two types of independent laboratory scale physical models has been constructed in ÚJV laboratories. The main goal of the first type is to obtain data which will be used for the calibration of numerical models of the bentonite saturation. The second one is focused on laboratory simulation of the interaction processes that could occur in the demonstration plug. Those considered are namely processes on concrete-bentonite interface. The main reason for performing such an experiment in lab is the lack of information from in-situ as EPSP experiment will not be dismantled during the course of the DOPAS project.
The physical models consist of defined number of cylindrical shape stainless steel chambers of 5 cm in length and 8 cm in diameter each that are equipped with sensors in order to record the distribution of water content and pore water pressure within the bentonite material. Bentonite powder was pressed into the nine test chambers in order to reach bulk density of 1.4 g/cm^3 (the identical bulk density as assumed for the EPSP experiment) and gradually saturated with water under pressure. The maximum SGW pressure up to 20 MPa is applied in laboratory tests. At the end of the experiment samples of the bentonite material will be dismantled and divided into layers with an estimated thickness of 1cm. The water content in each layer then will be determined. It is assumed the duration of the experiment with approximately 1 year (45 cm layers of compacted bentonite powder). In parallel experiments with bentonite pellets are ongoing, using different length configurations in order to describe saturation processes, material homogenization and water distribution.
An interaction laboratory model consists of a bentonite part, 5 cm thick, surrounded by 5 cm thick blocks of low-pH concrete from both sides. In order to approach the real plug set-up, the concrete blocks has been sealed in steel chambers using grouting materials, the same as used for grouting the host rock in situ. The SGW under the pressure up to 20 MPa is then infiltrating one side of the experimental cell, sealed with concrete, in order to simulate the same procedure of pressure loading in EPSP.
Both saturation and interaction experiments will be dismantled after approximately 1 year. Bentonite material saturation and water distribution will be determined and so as the mutual interaction of bentonite and low-pH concrete.

References:
Havlová V., Holeček J., Vejsada J., Večerník P., Červinka R. (2010): Příprava syntetické podzemní vody pro laboratorní experimentální práce (Preparation of synthetic ground water for experimental laboratory work). Technical report of Ministry of Industry and Trade of the Czech Republic project no. FR-TI1/367 (in Czech).

The research leading to these results has received funding from the European Union's European Atomic Energy Community's (Euratom) Seventh Framework Programme FP7/2007-2011 under grant agreement no 323273, the DOPAS project.

Approaches to Evaluate and Underpin the Technical Feasibility of the Belgian Disposal Concept

S. Doudou[1], **E.J. Harvey**[1], **P.J. Richardson**[1], **S.M. Wickham**[1] **and P. Van Marcke**[2]

1 Galson Sciences Ltd, 5 Grosvenor House, Melton Road, Oakham, LE15 6AX, United Kingdom
2 ONDRAF/NIRAS, Avenue des Arts 14, 1210 Brussels, Belgium

In 2009, ONDRAF/NIRAS, the Belgian Agency for Radioactive Waste and Enriched Fissile Materials, established a six-year research, development and demonstration (RD&D) programme to explore the feasibility of its concept for the geological disposal of category B&C radioactive waste in Belgium. This programme, generally referred to as "Project B&C Techno", aims to acquire evidence and build arguments in order to demonstrate that the proposed disposal system can be constructed, operated and progressively closed, taking into account long-term safety requirements and operational safety requirements, at a cost that is commensurate with available funding. In particular, it aims to demonstrate that there are no fundamental flaws or "showstoppers" relating to plans for construction and operation of the disposal facilities. The developments in understanding gained through the programme will support ONDRAF/NIRAS' first Safety and Feasibility Case (SFC1).

Galson Sciences Ltd has been supporting coordination of activities under Project B&C Techno. This support has included synthesis of research outputs and development of various tools and methods to demonstrate that the Belgian geological disposal concept is feasible to implement. RD&D activities undertaken to substantiate feasibility focus on issues of particular relevance to the Belgian concept, and aim to avoid repeating work where transferable evidence is available from elsewhere.

Two examples of tools developed by Galson Sciences Ltd for ONDRAF/NIRAS under Project B&C Techno to substantiate feasibility are:

- A review of other national geological disposal concepts to identify transferable experience relating to the feasibility of constructing and assembling comparable disposal system components. This enables identification of key gaps in knowledge, and hence, prioritisation of ONDRAF/NIRAS' ongoing RD&D activities.
- Development of a storyboard illustrating the steps involved in disposing of category B&C waste, from retrieval from interim storage, through transport to the disposal site, to backfilling and closure of the repository.

This paper describes the outcomes from development of both substantiation tools.

Review of Disposal Concepts

The objective of this study was to review the designs and concepts for geological disposal under consideration by waste management organisations in nine countries, and focus on the engineering and technical feasibility of fabricating or constructing components similar to those envisaged in the Belgian geological disposal concept for category B&C wastes, with a view to identifying the extent to which RD&D work in those countries helps to substantiate the feasibility of implementing the Belgian concept.

Disposal concepts in the following nine countries have been reviewed: Canada, Finland, France, Germany, Japan, Sweden, Switzerland, the UK and the US. The specific components of the disposal concepts covered are: the Spent Nuclear Fuel (SNF) canister, SNF overpack insert, overpack, concrete container for Long-Lived Low and Intermediate-Level Waste (LILW-LL – equivalent to category B

waste in Belgium), repository layout, waste transport methods, ventilation approach, backfilling concept, and sealing method.

The study concluded that transferrable experience from the countries reviewed can be used for all the disposal concept components considered, except for the backfilling concept used in Belgium for category C waste. No other country reviewed uses cement-based materials for backfilling High-Level Waste (HLW) and SNF disposal galleries. However, many countries use such materials for backfilling LILW-LL disposal galleries.

Storyboard

A series of diagrams, referred to as the "B&C Techno Storyboard", have been produced illustrating, at a high level, the sequence of activities involved in constructing and operating a repository for category B&C waste, from the initial retrieval of the wastes from interim storage through transport and emplacement in the repository, through to final closure of the repository. The following steps have been considered to-date in producing the storyboard diagrams:

- Retrieval of primary waste packages from interim storage off-site.
- Emplacement of primary waste packages into transport container.
- Emplacement of transport container into transport vehicle.
- Transport of primary waste containers from interim storage facilities to disposal site.
- Removal of primary waste packages from transport container at disposal site
- Fabrication of monolith B caisson and lid.
- Transfer of monolith B caisson and lid to post-conditioning facility.
- Insertion of primary waste packages into the monolith B caisson.
- Pouring mortar into the monolith B caisson.
- Emplacement of the monolith B lid.
- Transfer of completed monolith B to intermediate store prior to transfer underground.
- Retrieval of completed monolith B from interim store and transport to waste shaft.
- Transport of monolith B down waste shaft on transport cart.
- Transport underground of monolith B to disposal gallery.
- Emplacement of monolith B in final disposal location and backfilling of disposal gallery.

The storyboard provides a completeness check on activities under Project B&C Techno, informs consideration of operational safety, highlights any remaining open questions, and also acts as a communication tool.

Bentonite buffer design and recognition of risks for Finnish KBS-3V concept

Juvankoski, M.[1], Holt. E.[1], Niemeläinen, E.[1], Rantamäki, P.[2]

1) VTT Technical Research Centre of Finland, Espoo, Finland
2) Posiva, Eurajoki, Finland

Introduction

The KBS-3V method is a design line of a repository for spent nuclear fuel and high level waste disposal in Finland. This method is a multi-barrier system including single copper canisters containing spent nuclear fuel which are emplaced in individual vertical boreholes drilled in the floor of deposition tunnels in bedrock at about 420 m depth below ground level. The canisters are surrounded by bentonite blocks and pellets. Disk type bentonite blocks are installed at the bottom of the hole and on the top of the disposal canister. Ring type bentonite blocks surround the canisters. The outer gap between the blocks and the walls of the deposition hole is filled with bentonite pellets. The tunnels and shafts are also filled with backfill blocks made of bentonite.

Geotechnical design of bentonite blocks and pellets forms an essential part of barrier planning. Behavior of the bentonite blocks is depended on the change of water saturation and resulting swelling. The saturated density of the bentonite is the key parameter related to performance targets of the buffer. When estimating the saturated density range the different sources of variability and uncertainty have to be taken into account. The bulk density of the bentonite blocks and pellets and their volume are the only possible factors to control at the design phase. Final properties of the bentonite components are determined iteratively, taking into account the requirements set for the buffer system, the properties of the deposition hole, and the manufacturing and installation processes of the buffer components.

Performance targets for buffer

The main safety targets for bentonite buffer are to contribute the mechanical, geochemical and hydrogeological conditions that are predictable and favorable to the fuel canister. The buffer protects the canister from external processes that could jeopardize the function of complete containment of the spent nuclear fuel and associated radionuclides. The buffer system also limits and retards radionuclide releases in the event of canister failure.

The capability to swell and be self-healing when exposed to water is the most substantial reason to use bentonite clay for buffer material. It must be also be plastic enough to attenuate the impact of rock shear to the canister and at the same time be stiff to support the weight of canister. The density and permeability must also be sufficient to prevent the microbial and corrosive activity and retain the access of water to the canister surface. Slow diffusion is the only allowed migration mechanism for groundwater movement and possible radionuclide release thorough bentonite buffer [1]. The efficient heat transferring capability is needed for keeping the buffer temperature below 100 °C. The gaps between the canister and buffer and buffer blocks and rock walls should be made as narrow as possible without compromising the future performance of the buffer.

Design specifications

The reference buffer material being considered in Finland is MX 80 type bentonite, containing mainly mineral montmorillonite including sulphurs or organic material less than 1 wt %. It is also acceptable to use some other bentonite type containing montmorillonite 75–90% which fulfills all the performance targets of the buffer. The capability of the buffer to maintain the safety functions depends

on its swelling pressure, density, porosity, hydraulic conductivity, stiffness and content of substances that may be harmful for the other barriers.

The water content of the reference bentonite material used for the disk blocks, for the ring shaped blocks and for the pellets is 17 % ±1 %. In order to conform to the density range given in all sections of the deposition hole, the ring shaped blocks surrounding the canister and the disk blocks must be compacted to different densities. The target density of the saturated buffer is 2000 kg/m^3 ±50 kg/m^3 in a deposition hole with a diameter of 1750 mm -5/+50 mm. The pellet filled gap width between the blocks and rock wall is 50 mm ±25 mm. The tolerances are evaluated based on the production techniques of the blocks and pellets and the deposition hole. The tolerance of the saturated density is based on mutually competing requirements on what buffer shall be able to do in different circumstances: stiff enough for example to prevent microbiological action (lower limit) and elastic enough to protect the canister against potential rock shear[1]. The tolerances were used in probability calculations to check that the saturated density stays in the allowable interval. In the probability calculation also it was also checked that the swelling pressure is not too high for the canister in case of calcium exchanged sodium bentonite in dilute ground waters and not too small for ground waters with high salt content.

The design targets are iterated during the demonstration phase, based on achievable values during construction and emplacement trials. The iterative calculation process included the clearing how the rate of unsaturated (bulk) density affects to the final saturated density taking the tolerances into account. When the volume of blocks changes the unsaturated density must be recalculated.

The design parameters for the Finnish reference bentonite materials in a certain size are presented in Table 1[2].

Design parameter	Design value	Allowed deviation
Disk blocks		
Water content of disk blocks	17 %	±1 %-unit
Bulk density of disk blocks	1990 kg/m^3	±20 kg/m^3
Disk block outer diameter	1650 mm	±2 mm
Disk block height	400 - 800 mm	±1 mm
Parallelism block bottom / top		< 1 mm/1750 mm
Ring blocks		
Water content of ring blocks	17 %	±1 %-unit
Bulk density of ring blocks	2050 kg/m^3	±20 kg/m^3
Ring block outer diameter	1650 mm	±2 mm
Hole diameter in ring blocks	1070 mm	±1 mm
Ring block height	875 - 960 mm	+2 mm
Pellets		
Bulk density of separate pellets	1850 ±70 kg/m^3	±70 kg/m^3
Dimensions	11 x 11 x 5 mm	-
Bulk density of pellets	1075 kg/m^3	±50 kg/m^3
Water content of pellets	17 %	±1 %-unit

Conclusions

Final properties of the different buffer components to be installed have to be designed iteratively taking into account the design targets and requirements set for the buffer, different scenarios, other engineered barriers and the manufacturing and installation processes of the buffer components. In estimation of the saturated density range obtainable in buffer, also different sources of variability and uncertainty of the buffer components themselves have been taken into account. The reference design material chosen for the buffer is MX-80 bentonite, with a montmorillonite content of 75-90 %. The buffer consists of buffer components with a water content of 17 % and with the bulk density of disk blocks 1990 kg/m^3, ring blocks 2050 kg/m^3 and pellets 1075 kg/m^3 at installation phase. These properties result in a saturated density of 2000 kg/m^3 ±50 kg/m^3 in the final buffer.

References

1. Juvankoski, M., Ikonen, K. & Jalonen, T. 2012. Buffer Production Line 2012 – Design, Production and Initial State of the Buffer. POSIVA 2012-17. Posiva Oy, Eurajoki. ISBN 978-951-652-198-8.
2. Juvankoski, M., 2012. Buffer Design 2012. POSIVA 2012-14. Posiva Oy, Eurajoki

Development of subsurface disposal facility for radioactive wastes in North-West region of Russian Federation (condition and prospects)

Authors
A.V. Demin, V.T. Sorokin, V.V. Kascheev, D.I. Pavlov, V.U. Petrov

Address
JSC "ATOMPROEKT"
Russian Federation, Saint-Petersburg, Savushkina steet, 82

Abstracts

The report presents the legislative, regulatory and technical aspects of the subsurface disposal facilities for low and intermediate level radioactive wastes.

Considered backgrounds for the construction of this facility in the Leningrad region. Main of this backgrounds are significant amounts of radioactive waste, stored in surface storage and the existence of large clays deposits, suitable for underground construction. The geological structure of the region allows to create subsurface disposal facility in blue clay Cambrian horizon and laminarite clay of Kotlin horizon (Vendian deposits).

In the report discusses the construction and transport-technological scheme for the treatment of waste casks in the subsurface disposal facilities.

The monuments of a new kind

Cécile Massart

Artist - Researcher

My approach to facilities designed to host high-level nuclear waste in a clay barrier system may appear idealistic and full of respect for the work of researchers.

I call them *monuments of the future* because they are designed by experts after long international multidisciplinary research. They will be invisible at the surface and in order to ensure safety they will have to be revealed by a kind of speech or picture. All my artistic work is based on this issue.

Given the level of danger that characterizes those monuments, unprecedented attention must be drawn to them.

Today we are faced with a challenge: building a "cathedral" in clay rock for the most intriguing waste that will characterize the 21st century for a very long time.

The industrial structure of this monument lies at the heart of scientific studies, but it is interesting to develop images of the clay barrier and of its alteration in contact with high-level radioactive waste.
Invisible in the land chosen by the authorities to dispose it, the "monument" already scares us although it is still under investigation.
We are immersed in a visual culture and if we want to understand what happens we need an image. The general lack of information brings us back to our fears; we may become disillusioned and we may loose the confidence that this issue will be properly treated.

Perhaps some humans in 3015 will be the custodians of this large clay monument. At the heart of this underground argillaceous barrier, the radioactive energy will continue to characterize it. Its transformation under the action of heat must be monitored continuously.

It is our responsibility to provide a space in the present time to promote knowledge in the site area and to generate interest in this topic. The new consequent scientific discoveries will be precious for the living world.

As an artist I work on developing this vision by devising a shape made of clay around the industrial structure. As a result, ceramic works of small dimension will invite us to reflect on the transformation of the monument over time.
Though invisible at the surface, this large sculptural group will be identified and it has to find its way into the set of strategies devised for the preservation of the living world.

Andra's scientific knowledge management: an integrated and structured approach to improve data traceability (ISIS project)

Authors: ***A. Chabiron***, **E. Huret & M. Garcia**

Address: Andra, 1-7 rue Jean Monnet, 92290 CHATENAY-MALABRY- France

The French radioactive waste management organization (Andra) is in charge of the long-term management of all radioactive waste generated in France. Its missions include R&D activities on a reversible deep geological repository for high level and long lived, intermediate level radioactive wastes; industrial operations of the disposal facilities for short lived, low and intermediate level radioactive waste and duty of information.

For 20 years, Andra has collected and stored in different database a large amount and diversity of data on the different sites and projects and on complementary aspects (clay medium, waste packages, material behaviour, repository design and reversibility studies, analysis of the long-term behaviour of the repository and safety analyses).

To ensure a rigorous management and use of scientific data and to justify the selection of the data to be used in various calculations (e.g. calculation of performance, safety assessment of the repository…), Andra has developed a quality method of traceability of its scientific data and knowledge. This approach is called ISIS for Integration and StructurIng of Scientific data and aims to:

- Trace the different stages of data processing from the acquisition to the use of data in various applications;
- Ensure a rigorous and justified scientific data processing;
- Provide a quick and easy access to all data.

A first phase of the ISIS project consisted to improve data categorization according to the entire processing chain of data, from acquisition in the field to the use of the data.

ISIS distinguishes four main categories of data (figure 1):

- Primary data ("Basic data" under Andra terminology)are acquired using different methods during surveys, observations, experiments, etc. and have not been subjected to processing or any other manipulation. These basic data play a very critical role in the research methodology for the definition and understanding of the studied objects;
- Reference data are obtained after verification and validation of basic data using quality assurance methods. Reference data must be representative of the assessed environment and/or behaviour;
- Structured data are the result of the critical analysis of the reference data. A focus is made on variability and uncertainties of the data. They are inputs for the definition of integrated data used in the conceptual models that finally support the design and the performance assessment and safety analysis. As such, ISIS provides the reference dataset and associated uncertainties including statistical analysis;
- Integrated data correspond to the choice of value according to the use (phenomenological calculation, safety calculation) or results of evaluations.

ISIS approach also aims to improve and systematize the traceability process of the different stages of data treatment from one category of data to another. Initially, the project focused on the data and parameters that characterize the geological environment and was tested for two years. The ISIS approach is now completely integrated in the daily analytical work on Andra's scientific data. The ISIS project just entered its second phase. This second phase aims to generalize this approach to all storage projects of Andra (surface disposals) and to the data characterizing the environment, materials and storage structures.

Along with the ISIS approach, Andra tries to adapt and improve databases, knowledge bases and tools to make available the data. For this purpose, Andra has developed a set of databases for the different levels of data analysis and integration:

- Measurements of experiments are recorded automatically or manually depending on their nature and acquisition frequency, by a Geo-scientific Data Acquisition System (Geoscientific D.A.S.) which has been developed by Andra over the past ten years;
- A database is dedicated to primary data capitalization and reference data;
- Structured data are recorded in a specific knowledge base, in form of summaries with ranges of values and uncertainties in function of the application. These syntheses are made available in an accessible portal for each type of data and critical analysis related to files. This ensures an easy update of the files when new data are acquired.

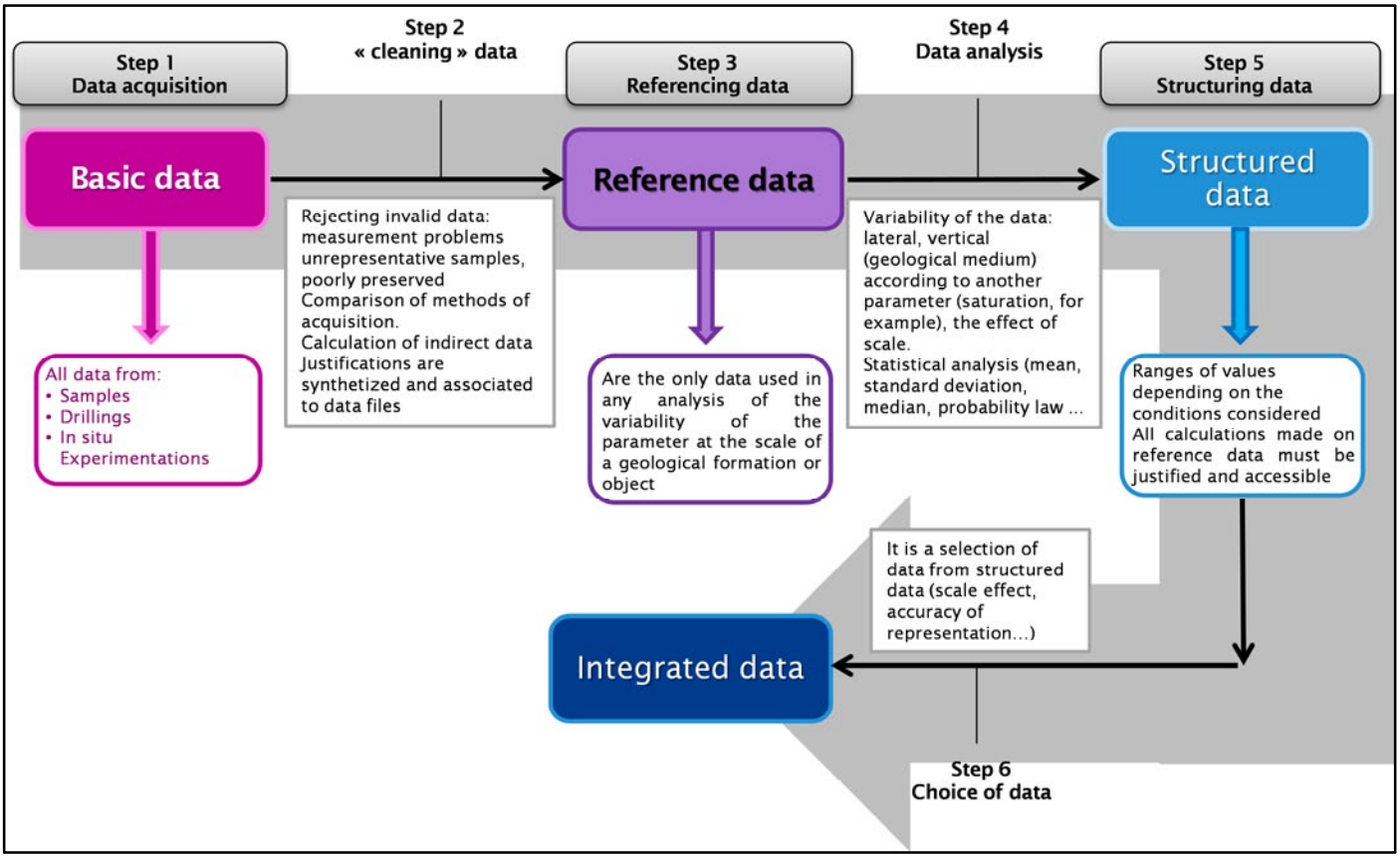


Figure 1 *The four categories of data and the different stages of their treatment*

Development and application of a safety assessment methodology in preparation for a safety case

Capouet M.[1], **Depaus C.**[1], **Weetjens E.**[2], **Govaerts J.**[2] **and Smith P.**[3]

[1]ONDRAF/NIRAS, Avenue des Arts 14, 1210 Brussels, Belgium
[2]Belgian Nuclear Research Centre (SCK•CEN), Boeretang 200, 2400 Mol, Belgium
[3]Safety Assessment Management (Switzerland) GmbH, Klingnau, Switzerland

In addition to its role in supporting the safety case by demonstrating compliance with safety requirements, safety assessments provide key information that helps focus the broader repository development programme, especially site characterisation and RD&D (scientific research, engineering design and testing). Conversely, these aspects of repository development produce data that support a high quality safety assessment. Carrying out a safety assessment thus requires significant interaction and iteration between those engaged in the safety assessment itself and those involved in the above-mentioned aspects of repository development (NEA, 2012). In the Belgian program, *the so-called preparatory safety assessments* fulfil this role by ensuring that the necessary internal interaction and iteration takes place in the programme to develop an adequate repository design, concept and safety case.

Preparatory safety assessments are conducted continuously and repeatedly, on the basis of phenomenological evidence from the assessment basis, and in parallel with system development. Formal satety assessment, on the other hand, are conducted only at the main project milestones. In the preparatory safety assessments, the iterative development of the reference case plays an important role. The reference case, in ONDRAF/NIRAS terminology, is a realisation of a reference scenario in which the system is assumed to be implemented according to design specifications and safety functions are provided over the timeframes specified in the safety concept (ONDRAF/NIRAS, 2013). The reference case also, however, entails a conservative set of parameter values and modelling choices as a means of handling uncertainties in system evolution within the reference scenario. The results of working versions of the reference case developed during preparatory safety assessments provide a snapshot of the minimum level of safety that the current results of the site characterisation and the RD&D programme can support, as well as guiding these programmes and informing expert discussions. It is ensured that the conservatism of the working versions of the reference case is appropriate for evaluating the degree to which compliance with the main regulatory criteria can currently be supported. As the reference case is iteratively developed and amended and eventually confirmed through successive iterations, a list of uncertainties that are less amenable to reduction, and also phenomena that have the potential to perturb the safety functions detrimentally, is developed as the basis for alternative scenarios and assessment cases.

Three versions of the reference case have been developed since the beginning of the SFC1 preparatory assessment phase. The knowledge from the previous formal safety assessments reported in SAFIR2 (ONDRAF/NIRAS, 2001), combined with a new EBS design, were the basis for developing the first working version of the reference case in 2009. The hypotheses of this first working version were in some instances highly conservative, due to the limited knowledge available in some fields (e.g. EBS environment) and to the lack of adequate characterisation of some phenomenological uncertainties. Additional RD&D results allowed many conservative assumptions to be relaxed in the second (and subsequent) version(s) of the reference case, especially those related to the waste matrix, containment lifetime and the retardation processes in clay. The development of the current version 3 reference case has been motivated by the need to assess the potential importance of retention processes in a concrete environment. In particular, analysis of the current reference case gives indications of the potential benefits that could result from accounting for such retention processes in safety assessment modelling (Weetjens et al., 2012). Future studies on retention processes in cement will either confirm the assumptions and model abstractions currently made in this case, or allow them to be refined.

The uncertainties in the safety parameters in successive versions of the reference case were quantified in terms of intervals of possible or expected values, an approach is inspired by the principles of fuzzy set theory, rather than, for example, in terms of PDFs. When deriving such intervals, the safety assessors, in collaboration with phenomenological experts, attempts to capture the phenomenological uncertainties affecting a parameter in terms of two different ranges values, taking into account the hypotheses that define the scenario at hand (ONDRAF/NIRAS, 2014):

- The expert range is the range within which the parameter value is expected to lie considering current knowledge.
- The source range is the range outside of which the parameter value is expected to lie considering current knowledge.

Since the reference case aims to provide a conservative (but not excessively conservative) representation of repository evolution within the reference scenario, the most pessimistic values from the expert ranges were selected for the reference case parameter values. These can be either maximum or minimum values within the ranges, depending on the parameter in question.

In preparation of the next version of the reference case (version 4), detailed analysis have been carried out to test the assumption of monotonic dependency of consequences on individual parameter values; an assumption on which the selection of parameter values by the above methodology rests. Weetjens and Govaerts (2013) and Smith (2014) reported several instances of non-monotonic behaviour: one is related to the ratio instant release fraction/matrix fraction in combination with a certain matrix dissolution time (spent fuel); another is related to the ingrowth of daughter nuclides in actinide chains (all waste) and a final instance is associated with the interplay between the concentration of organic matter in clay and its diffusion coefficient. These effects have limited impacts on the calculated releases of contaminants from the repository system, but will nevertheless be accounted for in the next version of the reference case.

References

NEA, Methods for Safety Assessment of Geological Disposal Facilities for Radioactive Waste, Outcomes of the NEA MeSA initiative, NEA Report No. 6923, OECD/NEA, Paris, 2012.

ONDRAF/NIRAS, SAFIR2 – Safety Assessment and Feasibility Interim Report 2, ONDRAF/NIRAS, report NIROND 2001-06E, 2001.

ONDRAF/NIRAS, Research, Development and Demonstration (RD&D) Plan for the geological disposal of high-level and/or long-lived radioactive waste including irradiated fuel if considered as waste, State-of-the-art report as of December 2012, ONDRAF/NIRAS, report NIROND-TR 2013-12 E, 2013.

ONDRAF/NIRAS, Management Strategy and Management System for SFC1, ONDRAF/NIRAS, report NIROND-TR, in preparation, 2014.

Smith, P., Near field and geosphere parameter sensitivity analyses for the Reference Scenario in support of SFC1, Nagra, Project Report NPB 14-12, 2014.

Weetjens, E., Marivoet J. and Govaerts, J., Preparatory Safety Assessment, SCK•CEN, report ER-215, 2012.

Weetjens E. and Govaerts J., Non-monotonicity in Safety Assessment calculations for a hypothetical geological repository in Boom Clay, SCK•CEN, report R-5499, 2013.

FE Experiment / LUCOEX: Development of a prototype machine for backfilling horizontal emplacement tunnels with granulated bentonite

Heinz Jenni[1], *Sven Köhler*[2], Herwig R. Müller[2]

1: ROWA, Rowa Tunnelling Logistics AG, Leuholz 15, CH-8855 Wangen, h.jenni@rowa-ag.ch
2: NAGRA, National Cooperative for the Disposal of Radioactive Waste, Hardstrasse 73, CH-5430 Wettingen, Switzerland, sven.koehler@nagra.ch

The Full-Scale Emplacement (FE) Experiment at the Mont Terri underground research laboratory (URL) is a full-scale heater test in a clay-rich formation. It simulates the construction, waste emplacement and backfilling of a spent fuel (SF) / vitrified high-level waste (HLW) repository tunnel as realistically as possible. One of the main aims of the FE experiment, which is also Nagra's participation in the EC co-funded 'Large Underground COncept EXperiments' (LUCOEX) project, is the investigation of backfilling procedures for underground conditions. An overview about the FE experiment in general is given by Müller et al. (2015; to be found in this compendium).

Based on the experiences from ESDRED (Plötze & Weber, 2007), a new prototype backfilling machine with five horizontal auger conveyors was developed for the FE experiment (see *Figure 1*). This prototype will be used to backfill a horizontal tunnel with a diameter of 2.5-3 m with dry granulated bentonite material as tightly as possible. According to the Swiss high-level waste disposal concept, this material had to be emplaced with an overall bulk dry density of at least 1'450 kg/m^3.

For the FE experiment about 350 tons of a granulated bentonite mixture (GBM) with an average "pellet" dry density of 2.18 g/cm^3 and with a very broad "pellet" size distribution (a so-called Fuller-type distribution) were produced. This material will be delivered to the prototype machine in big bags. After emptying the big bags into a hopper, the prototype machine transports, emplaces and compresses the GBM into the tunnel using five auger conveyors simultaneously.



Figure 1: *The prototype machine with five auger conveyors (to be seen on the left side) developed for backfilling the horizontal FE tunnel with granulated bentonite as tightly as possible. The longest auger is 8.5 m long, bringing the machine length with the big bag transport trolley to 17 m in total.*

During the backfilling procedure all augers are filled up to 100% (see *Figure 2, left*) and remain in the GBM slope in order to build up a backfilling pressure. This pressure pushes the material up to 70 cm

upwards after leaving the augers, filling gaps and overbreaks in the tunnel ceiling. During this process the prototype is held in place by hydraulic breaks which have to hold a force of up to approx. 32 kN. With sophisticated controls, many parameters such as the auger force & rotation speed and the push-back resp. breaking force and therefore the backfilling speed resp. the bulk emplaced density can be controlled and steered (see *Figure 2, right*).



Figure 2: *The front end of one auger conveyor filled with a fuller-type granulated bentonite mixture (GBM) is shown on the left; the screw diameter is approx. 25 cm. The control panel for steering various machine parameters such as the screw turning speed & the break force is shown on the right.*

With several, partially even 1:1-scale pre- and mock-up-tests (one shown in *Figure 3*) the prototype was tested and found to be functioning as planned and anticipated. An average bulk emplaced dry density was achieved that clearly exceeded the target dry density. The advantage of this method is its flexibility regarding tunnel shape and obstacles (such as the canisters). Together with the Fuller-type GBM which does not need special care during handling (except of keeping it dry) this method is – once developed – robust and fairly easy to use. Further optimizations and developments are possible and will in the coming years perfect this backfilling method.



Figure 3: *The newly developed backfilling machine being tested in a 1:1-scale tunnel model in an off-site workshop. The 1 m diameter dummy heater can be seen in between the augers.*

Acknowledgment
The engineering and demonstration components of the FE experiment are part of Nagra's participation in the EC co-funded 'Large Underground COncept EXperiments' (LUCOEX) project and therefore receive funding from the European Atomic Energy Community's Seventh Framework Programme (FP7) under grant agreement n269905.

References:

Herwig R. Müller, Tobias Vogt, Benoit Garitte, Sven Köhler, Toshihiro Sakaki, Hanspeter Weber, Tim Vietor (2015): The Full-Scale Emplacement Experiment – Implementation of a multiple heater experiment at the Mont Terri URL. Clay Conference 2015, Brüssels.

Plötze, M.; Weber, H. (2007): ESDRED Emplacement tests with granular bentonite MX-80 – Laboratory results from ETH Zürich. Nagra Arbeitsbericht NAB 07-24

Support Design of a Large Diameter Gallery for Mid-level Nuclear Waste in Cigéo Project

PLASSART Roland, **LAIGLE François**

EDF – Centre d'Ingénierie Hydraulique, Savoie Technolac, 73370 Le Bourget-du-Lac

SAITTA Adrien, SUZAC Gonzalo

EGIS Tunnels, 35 Les Pléiades – Park Nord Annecy, 74370 Pringy

MARTIN François, JANUTOLO Michele

BG Ingénieurs-conseils, 13 Rue des Emeraudes, 69006 Lyon

The storage of nuclear waste gives rise to a lot of innovative issues for underground space technologies. The nuclear activity of the waste generates temperature effects on both the lining and the surrounding rock mass. In order to avoid these unfavorable effects, the number of waste containers is controlled in the gallery section. The galleries section has consequently ranged from a diameter of 4 to 6 meters.

However, for mid level nuclear waste, due to the lower temperature, the number of containers in a cross section of a gallery can safely be increased. In spite of some technical difficulties, a large diameter gallery (typically 12m excavated) seems to be more cost effective. This paper aims at demonstrating the feasibility of such a gallery in the specific context of the Cigéo project.

The COx argillite is modeled thanks to a constitutive law including a creep mechanism. The safety support (bolts and shotcrete) is installed immediately after excavation, whereas the lining is set one year after. With a usual support, the modeling results have shown excessive stresses in the shotcrete, which needs to be thickened. The total thickness of the lining eventually exceeds 1.3m.

With proven experience of such a case, elements of high deformable concrete (like HiDCon®) have then been set between the shotcrete segments of the immediate support. The orthoradial stresses are so reduced. The definitive concrete lining has to be thickened but the total thickness remains at a reasonable and cost effective value of 85cm.

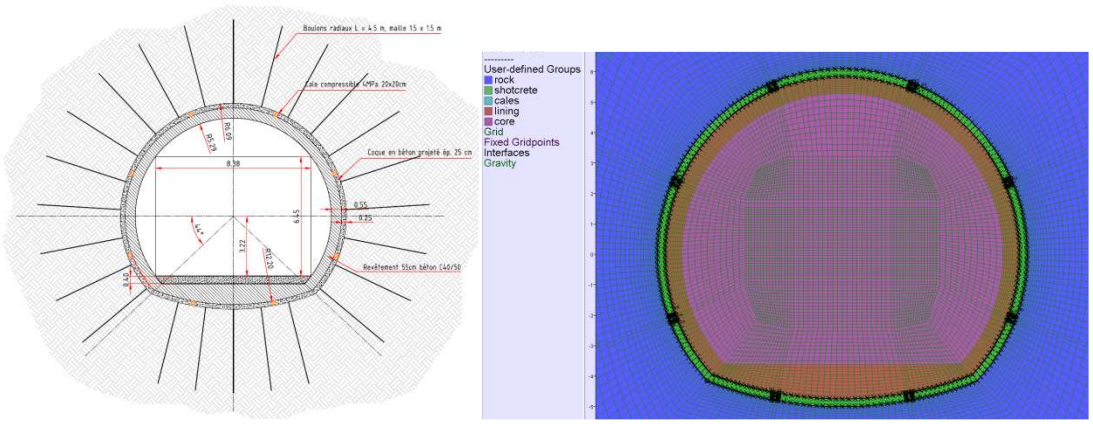


Figure: Support design (including shotcrete and HiDCon type elements) of a large diameter gallery

Swiss backfilling concept – Requirements and Approaches for Optimization of the Bentonite Barrier around SF/HLW Disposal Canisters

Authors: *Sven Köhler*, Thomas Fries, Herwig R. Müller, Irina Gaus

NAGRA, National Cooperative for the Disposal of Radioactive Waste, Hardstrasse 73, CH-5430 Wettingen, Switzerland

Introduction to the Swiss reference repository concept

The Swiss reference repository concept for spent fuel / high level radioactive waste (SF/HLW) (fig. 1) is based on a multi barrier system. Besides the natural geological barrier (Opalinus Clay), it comprises several engineered barriers, such as the disposal canister, backfill surrounding the canister and several tunnel seals.

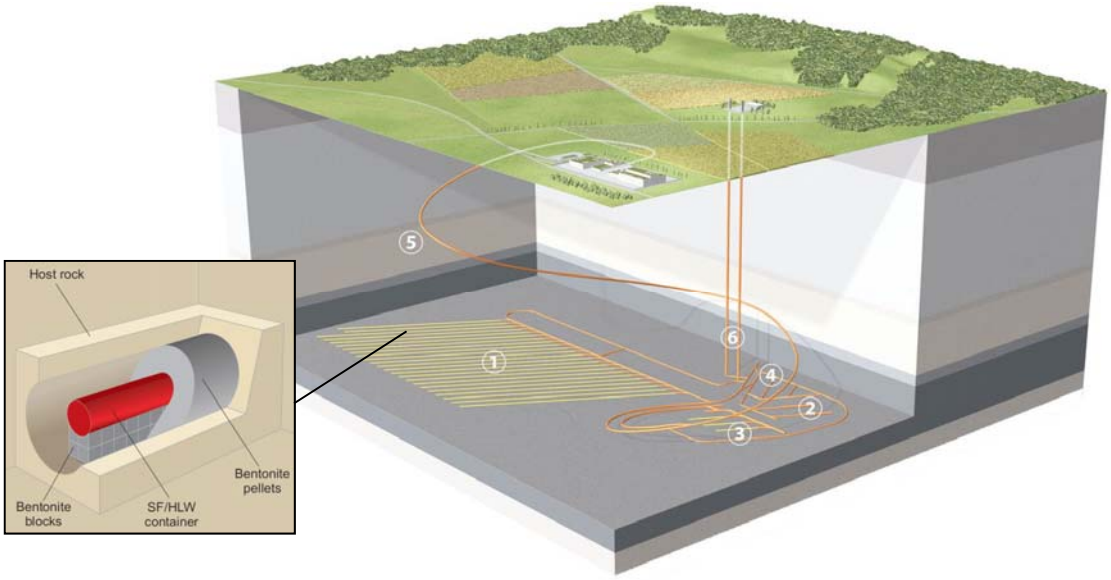


Fig. 1: Swiss reference repository concept for spent fuel / high level waste (SF/HLW). ① SF/HLW repository (Emplacement tunnels); ② ILW repository; ③ Pilot facility; ④ Test facility; ⑤ Access tunnel; ⑥ Construction shaft and ventilation shaft

Bentonite backfill

According to the current reference concept, SF/HLW will be emplaced in disposal tunnels (inner diameter of 2.8m). Each disposal canister will be embedded in a suitable buffer material that is made of bentonite blocks and of (highly compacted) granulated bentonite mixture (GBM). The tunnel will be backfilled with GBM after emplacement of each disposal canister. The bentonite material as well as the backfilling procedure have to fulfill several requirements regarding long term safety (Leupin & Johnson, 2013) and technical feasibility.

Long-term safety requirements

Final saturated density is considered the key property to ensure adequate long-term performance of the bentonite based backfill material in a repository since it directly influences the safety relevant attributes such as swelling pressure, gas- and water permeability, porosity and suppression of microbial activity. Suppression of microbial activity sets perhaps the most stringent density

requirement. Stroes-Gascoyne (2011) reported that microbial activity is clearly suppressed in highly compacted bentonite. Leupin & Johnson (2013) concluded that a saturated density of 1.90 t/m^3 (corresponding to a dry density of 1.45 t/m^3) for bentonite MX-80 is a desirable target as it may decrease the likelihood of microbial induced corrosion.

Design requirements

Hence, for the Swiss reference concept, a dry density of 1.45 t/m^3 is regarded as a target design requirement in the emplacement tunnels for SF/HLW. This value has proven to be achievable in terms of technical feasibility (Plötze & Weber, 2007; Gaus et al., 2011).

Regarding the backfilling method, the major requirements are attributed to the complete backfilling of the SF/HLW emplacement tunnels around, before and behind each disposal canister allowing for

- a target dry density of 1.45 t/m^3 or higher for the entire bentonite backfill. This includes the necessity of a high content of swelling minerals (i.e. basically montmorillonite).
- a homogeneous distribution of the backfilled GBM and the target dry density.

Moreover, in choosing an appropriate backfilling method, the following aspects have to be considered:

- Continuous backfilling process in a retreating mode for each disposal canister with high reliability and availability
- Iteration with the emplacement of disposal canister units incorporating pedestals made of highly compacted bentonite blocks
- Accurate backfilling quality for varying tunnel radius due to gallery excavation deviations and support elements (e.g. shotcrete lining, steel ribs etc.)

Prototype backfilling machine

A prototype backfilling machine (fig. 2) has been designed and fabricated in the framework of the Full-scale Emplacement (FE) Experiment that has been implemented at the Mont Terri Rock Laboratory (Müller et al. 2015; Jenni et al. 2015). This backfilling machine is based on screw conveyance methodology exhibiting five horizontal augers. The overall dry density target of the backfilled granulated bentonite mixture was clearly met. However, there is still some potential for further improvement of backfilling quality in terms material homogeneity, since some segregation effects were observed.



Fig. 2: Prototype backfilling machine fabricated for the Fullscale Emplacement (FE) Experiment. (Side note: The pictured feeding device containing bigbags does not exhibit any prototype character.)

Outlook

Current and future work focuses on the estimation and analysis of local dry density variations (Sakaki et al. 2015a and Sakaki et al. 2015b), as well as on its mitigation by innovative process engineering.

Acknowledgment

The engineering and demonstration components of the FE experiment are part of Nagra's participation in the EC co-funded 'Large Underground COncept EXperiments' (LUCOEX) project and therefore receive funding from the European Atomic Energy Community's Seventh Framework Programme (FP7) under grant agreement n269905.

References

Gaus, I., Köhler S., Teodori, S., Weber, H., Rösli, U.; Steiner, P., Trick, T., Siñeriz, J-L., Nussbaum, C., Czaikowski, O., Wieczorek, K.; Schuster, K., Kuhlmann, K., Garitte, B., Gens, A., Mayor J. C. (2011): Long Term performance of Engineered Barrier Systems (PEBS). Mont Terri HE-E experiment: detailed design. Nagra Arbeitsbericht NAB 11-01

Jenni , H., Köhler, S., Oberberger, A.;Battisti, L., Müller, H.R.: FE Experiment / LUCOEX (2015): Development of a prototype machine for backfilling horizontal tunnels with granulated bentonite. Conference companion paper

Leupin, O.X., Johnson, L.H. (2013): Buffer Requirements for a SF/HLW Repository in Opalinus Clay. Nagra Arbeitsbericht NAB 13-46

Müller H.R., Vogt T., Garitte B., Köhler, S., Sakaki, T., Weber H., Vietor, T. (2015): The Full-Scale Emplacement Experiment – Implementation of a multiple heater experiment at the Mont Terri URL. Conference companion paper.

Nagra (2002a): Projekt Opalinuston: Konzept für die Anlage und den Betrieb eines geologischen Tiefenlagers: Entsorgungsnachweis für abgebrannte Brennelemente, verglaste hochaktive sowie langlebige mittelaktive Abfälle. Nagra Technical Report NTB 02-02.

Plötze, M.; Weber, H. (2007): ESDRED Emplacement tests with granular bentonite MX-80 – Laboratory results from ETH Zürich. Nagra Arbeitsbericht NAB 07-24

Sakaki, T., Köhler, S., Müller, H.R. (2015a): FE Experiment: Density measurement of granulated bentonite mixture in a 2D pre-test using a dielectric moisture profile probe. Conference companion paper

Sakaki, T., Köhler, S., Hertrich, M., Müller, H.R. (2015b): FE Experiment: Density measurement of granulated bentonite mixture in a 3D 1:1 scale mockup test using dielectric tools. Conference companion paper

Stroes-Gascoyne, S. (2011), Atomic Energy of Canada Limited AECL: Microbiological Characteristics of Compacted Bentonite at a dry density of 1450 kg/m3 – A Literature Review. Nagra Arbeitsbericht NAB 11-05

IGD-TP main achievements to date and role in implementing the European policy on radioactive waste

Author(s): *Jacques Delay*[1], Raymond Kowe[2], Marie Garcia[3]

Address(es)
1, Andra, Centre de Meuse / Haute-Marne - Route Départementale 960 - BP 9 - 55290 Bure, France
2, RWM, Radioactive Waste Management, Building 587, Curie Avenue, Harwell Oxford, Didcot, OX11 0RH, United Kingdom
3, Andra, 1-7 rue Jean Monnet, Parc de la Croix Blanche, 92298, Châtenay –Malabry, France

Abstract

The Implementing Geological Disposal of Radioactive Waste Technology Platform (IGD-TP) was launched on November 12, 2009. This Technology Platform has 120 members sharing the vision that "by 2025, the first geological disposal facilities for spent fuel, high-level waste and other long-lived radioactive waste will be operating safely in Europe".
The platform is led by eleven European organizations in charge of radioactive waste management in their respective countries (WMO). They have produced a Strategic Research Agenda (SRA) and a Deployment Plan to implement the remaining Research, Development and Demonstration (RD&D) issues through technical projects and cross-cutting activities. The Deployment Plan was published in 2012 and had its second annual update in 2014.
Five years after its inception, the IGD-TP is a key actor for the coordination at the European level of the RD&D in radioactive waste geological disposal programmes.
Currently there are eight on-going European projects which were initiated by the IGD-TP that are aligned with the objectives of the SRA. An additional four technical proposals supported by the IGD-TP have been submitted in the framework of the first H2020 Euratom call.
Alongside these technical projects, the IGD-TP is engaged in collaborative work with other European technical platforms or projects to identify future technical priorities arising from the evolution of reactor technologies and to comply with the regulators needs for safety assessment.
In addition, two specific actions are supported by the IGD-TP's Secretariat to address the needs of the new Member States which are identified within the platform as "less advanced programmes". The first one is support for networking, structuring and developing RD&D competences in countries with less advanced geological disposal programmes. This action will develop guidelines to help the RD&D in these countries to meet the requirements of the European "Waste Directive". The second action is a support for the development, implementation and coordination of Competence Maintenance, Education and Training (CMET) activities in geological disposal in Europe. It aims to facilitate the access to expertise and technology and to maintain competence in Member States.
In 2014 the IGD-TP prepared the setting up of a "Joint Programming on Radioactive Waste Disposal" which is aimed at coordinating at the European level, national research programmes and the associated R&D activities on geological disposal for high activity long lived radioactive waste. This action will help to maintain and develop the EU leadership in knowledge and expertise for innovative radioactive waste management solutions that match public expectations. Moreover, it will reinforce the interaction at EU level more effective between WMOs, TSOs (Technical support organisations), industry, policy makers and research organisations.